Wind and Seismic Effects

Proceedings of the 24th Joint Meeting

NIST SP 843

NAT'L INST. OF STAND & TECH R.I.C.
A11103 809306

NIST
PUBLICATIONS

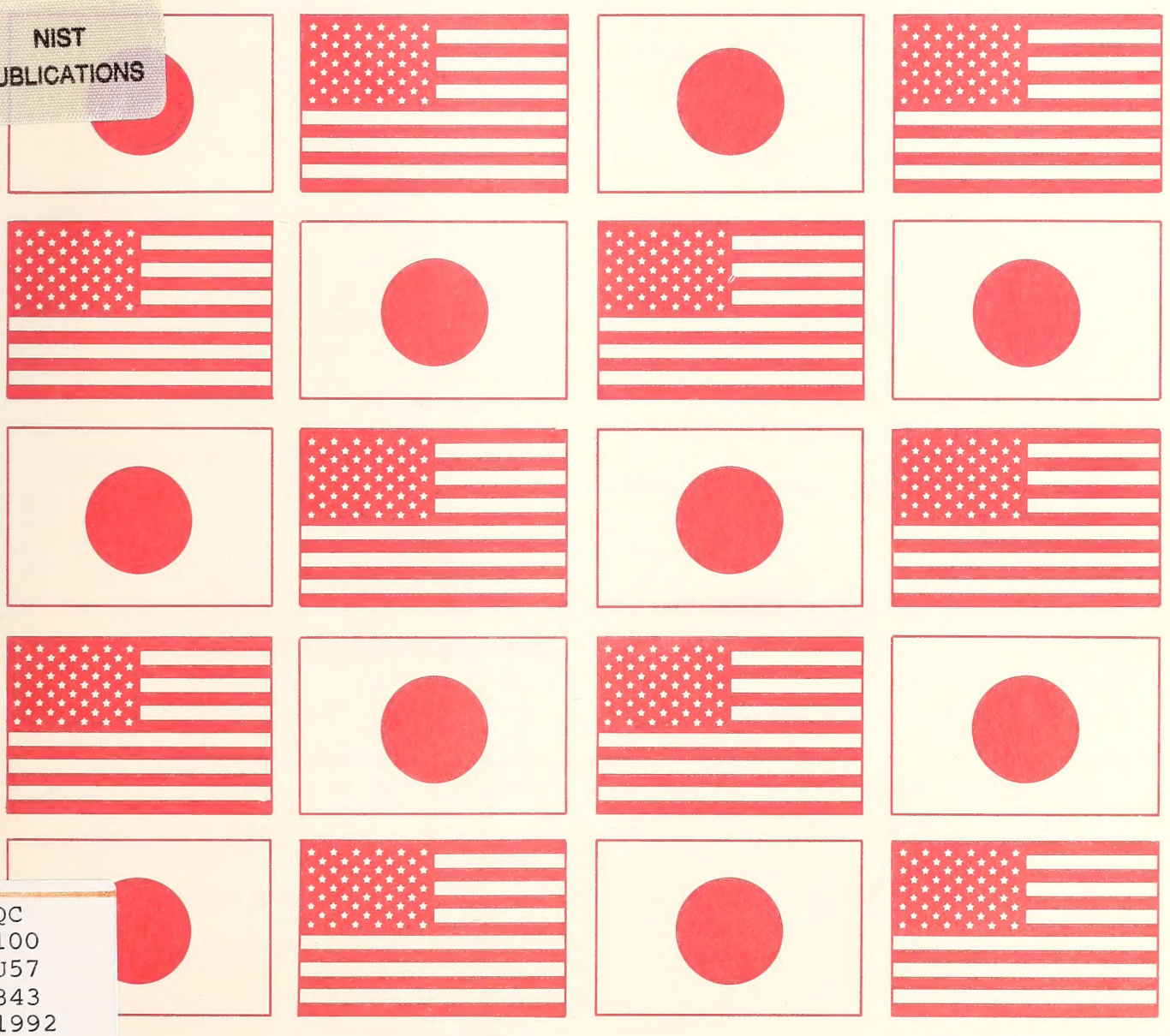

QC
100
.U57
843
1992

U.S. DEPARTMENT OF COMMERCE
Technology Administration
National Institute of Standards and Technology

The National Institute of Standards and Technology was established in 1988 by Congress to "assist industry in the development of technology . . . needed to improve product quality, to modernize manufacturing processes, to ensure product reliability . . . and to facilitate rapid commercialization . . . of products based on new scientific discoveries."

NIST, originally founded as the National Bureau of Standards in 1901, works to strengthen U.S. industry's competitiveness; advance science and engineering; and improve public health, safety, and the environment. One of the agency's basic functions is to develop, maintain, and retain custody of the national standards of measurement, and provide the means and methods for comparing standards used in science, engineering, manufacturing, commerce, industry, and education with the standards adopted or recognized by the Federal Government.

As an agency of the U.S. Commerce Department's Technology Administration, NIST conducts basic and applied research in the physical sciences and engineering and performs related services. The Institute does generic and precompetitive work on new and advanced technologies. NIST's research facilities are located at Gaithersburg, MD 20899, and at Boulder, CO 80303. Major technical operating units and their principal activities are listed below. For more information contact the Public Inquiries Desk, 301-975-3058.

Technology Services
- Manufacturing Technology Centers Program
- Standards Services
- Technology Commercialization
- Measurement Services
- Technology Evaluation and Assessment
- Information Services

Electronics and Electrical Engineering Laboratory
- Microelectronics
- Law Enforcement Standards
- Electricity
- Semiconductor Electronics
- Electromagnetic Fields[1]
- Electromagnetic Technology[1]

Chemical Science and Technology Laboratory
- Biotechnology
- Chemical Engineering[1]
- Chemical Kinetics and Thermodynamics
- Inorganic Analytical Research
- Organic Analytical Research
- Process Measurements
- Surface and Microanalysis Science
- Thermophysics[2]

Physics Laboratory
- Electron and Optical Physics
- Atomic Physics
- Molecular Physics
- Radiometric Physics
- Quantum Metrology
- Ionizing Radiation
- Time and Frequency[1]
- Quantum Physics[1]

Manufacturing Engineering Laboratory
- Precision Engineering
- Automated Production Technology
- Robot Systems
- Factory Automation
- Fabrication Technology

Materials Science and Engineering Laboratory
- Intelligent Processing of Materials
- Ceramics
- Materials Reliability[1]
- Polymers
- Metallurgy
- Reactor Radiation

Building and Fire Research Laboratory
- Structures
- Building Materials
- Building Environment
- Fire Science and Engineering
- Fire Measurement and Research

Computer Systems Laboratory
- Information Systems Engineering
- Systems and Software Technology
- Computer Security
- Systems and Network Architecture
- Advanced Systems

Computing and Applied Mathematics Laboratory
- Applied and Computational Mathematics[2]
- Statistical Engineering[2]
- Scientific Computing Environments[2]
- Computer Services[2]
- Computer Systems and Communications[2]
- Information Systems

[1] At Boulder, CO 80303.
[2] Some elements at Boulder, CO 80303.

QC 100
.U57
843
1992
c.2

Wind and Seismic Effects

NIST SP 843

PROCEEDINGS OF
THE 24TH JOINT
MEETING OF
THE U.S.-JAPAN
COOPERATIVE PROGRAM
IN NATURAL RESOURCES
PANEL ON WIND AND
SEISMIC EFFECTS

Issued September 1992

Noel J. Raufaste,
EDITOR

Building and Fire Research Laboratory
National Institute of Standards and Technology
Gaithersburg, MD 20899

U.S. DEPARTMENT OF COMMERCE
Barbara Hackman Franklin, Secretary

TECHNOLOGY ADMINISTRATION
Robert M. White, Under Secretary for Technology

National Institute of Standards and Technology
John W. Lyons, Director

National Institute of Standards and Technology Special Publication 843
Natl. Inst. Stand. Technol. Spec. Publ. 843, 594 pages (Sept. 1992)
CODEN: NSPUE2

U.S. GOVERNMENT PRINTING OFFICE
WASHINGTON: 1992

For sale by the Superintendent of Documents, U.S. Government Printing Office, Washington, DC 20402-9325

PREFACE

BACKGROUND

The U.S.-JAPAN Cooperative Program in Natural Resources (UJNR) was created in January 1964. It is part of the U.S.-JAPAN Cooperative Science Program. The objective of UJNR is to exchange information on research results and exchange scientists and engineers in the area of natural resources for the benefit of both countries. The UJNR is composed of 17 Panels each responsible for specific technical subjects.

The Panel on Wind and Seismic Effects was established in 1969. Seventeen U.S. and six Japanese agencies participated with representatives of private sector organizations, to develop and exchange technologies aimed at reducing damage from high winds, earthquakes, storm surge, and tsunamis. This work is produced through collaboration between U.S. and Japanese member researchers working in 11 task committees. Each committee focuses on specific technical issues, e.g., earthquake strong motion data. The Panel provides the vehicle to exchange technical data and information on design and construction of civil engineering lifelines, buildings, and water front structures, and to exchange high wind and seismic measurement records. Annual meetings alternate between JAPAN and the United States (odd numbered years in JAPAN; even numbered years in the U.S.). These 1-week technical meetings provide the forum to discuss ongoing research and research results; 1-week technical study tours follow the meetings.

The National Institute of Standards and Technology (NIST) provides the U.S.-side chairman and secretariat. The Public Works Research Institute (PWRI), JAPAN, provides the JAPAN-side chairman and secretariat.

Cooperative research is performed through formal Panel Programs. In 1981, cooperative research in Large-Scale Testing was started under the auspices of the Panel. Also in 1981, joint research on Reinforced Concrete Structures was initiated. Full-scale testing was performed at the Building Research Institute (BRI), one of the six Japanese member organizations, with supporting tests in JAPAN and in the United States. Two years later a joint research program on Steel Structures was initiated. Full-scale testing again was led by BRI with supporting tests in the United States and JAPAN. The U.S.-JAPAN coordinated program for Masonry Building Research was started in 1985. A U.S.-JAPAN coordinated program on Precast Seismic Structural Systems was initiated in 1991.

Task Committee meetings, exchanges of data and information through technical presentations at annual Panel meetings, exchanges of guest researchers, visits to respective research laboratories and informal interactions between Panel meetings, joint workshops and seminars, and joint cooperative research programs all contribute to the development and effective delivery of knowledge that has influenced design and construction practices in both countries.

Direct communication between counterpart country organizations is the cornerstone of the Panel. Effective information exchanges and exchanges of personnel and equipment have strengthened domestic programs of both countries. There are opportunities for experts in various technical fields to get to know their foreign counterparts, conduct informal exchanges, bring their respective views to the frontiers of knowledge, and advance knowledge of their specialties.

The Panel's results have supported improvements in practices in both countries. They have:

1. created and exchanged digitized earthquake records for use as the basis of research for Japanese and U.S. geotechnics and structures;

2. produced data that advanced U.S. design and construction of bridge columns;

3. produced large-scale testing data that advanced seismic design standards for buildings;

4. created a database comparing Japanese and U.S. standard penetration tests to improve seismic design criteria for soil liquefaction;

5. created databases on storm surge and shore line interaction and on tsunamis and tsunami warning systems for use by designers to verify mathematical models of tsunamis and storm surge.

HIGHLIGHTS OF THE 24th JOINT PANEL MEETING

Thirty-six papers were presented at the joint meeting (45 papers were authored), organized into five themes: wind engineering, storm surge and tsunamis, joint cooperative research program, earthquake engineering, and four reports on the Panel's Task Committee workshops of the past year.

Highlights include:

- Technical presentations:

  - highlighted important work by the United States and Japan. U.S. research in wind engineering is enhanced by links to the extensive research performed by Japan's Public Works Research Institute. Wind hazard mitigation efforts lag seismic in both Japan and the United States.

  - important knowledge was exchanged for research and practice, e.g., wind tunnel and analytical modeling for coupled torsional and flexural response of suspension bridges, field and analytical studies of the performance of pile groups, large scale finite element modeling of storm surges validated with historical data.

  - information was gained about extensive Japan and U.S. public works projects and civil engineering research and their applications into practice.

- Base isolation systems and high performance concrete: Excellent work is being performed by both sides. Panel participants advance their competence by becoming more familiar with these research projects and through direct participation in appropriate research.

- Seismic strengthening: Studies of assessment, research, design, and construction for seismic retrofit of buildings and highway structures provide for private and public sector, U.S. and Japanese collaborations in making seismic retrofit more cost effective.

- Recent earthquakes: Report on reconnaissance of the Erzincan Turkey Earthquake of March 13, 1992 shows again the need to address the vulnerability of nonductile concrete and masonry buildings.

- Publications:

  - Each-side of the Panel published a catalog, *List of Publications 1969–1991 Panel on Wind and Seismic Effects.* The NIST Special Publication 835, April 1992, contains titles, keywords, and author index of over 1200 Panel papers published during its 23-year life. Over 1000 copies will be distributed to developing countries in support of the International Decade for Natural Disaster Reduction (IDNDR).

  - NIST published a two-volume series, *Earthquake Resistant Construction Using Base Isolation,* NIST SP 832-1 and 832-2, April 1992; the text was translated from Japanese.

TECHNICAL SITE VISITS

The second week (23–29 May), was devoted to technical reviews of laboratories, public works projects, and construction sites. In addition to the 36 papers presented during the first week; eight papers continued the Panel's technical presentation during the second week. These presentations were equally divided between the U.S. and Japan-sides. Three of the four U.S. papers are included in these Proceedings. The four Japan-side presentations and one U.S. presentation were specially prepared for two technical site visits and are not part of the Proceedings.

Eight sites were visited:

1. LEHIGH UNIVERSITY, ADVANCED TECHNOLOGY FOR LARGE STRUCTURAL SYSTEMS (ATLSS) MULTIDIRECTIONAL EXPERIMENTAL LABORATORY

The delegation visited, and discussed in detail, work on evaluating the yield strength of high strength structural steel and crack propagation in ship hulls to examine fatigue crack growth behavior in large scale box sections of high strength low-alloy grade 80 steel. Also, work was observed in fatigue strength of HSLA 80 welded steel to evaluate its characteristics in double hulled ships. Some work is underway in base isolation for buildings and bridges.

Presentations by ATLSS staff and Japan-side Panel members addressed a variety of topics: ATLSS's work in developing consistent design methods and models for precast concrete connections for unified connection design based on codification and rules for knowledge-based systems used to integrate different countries' rules into structural models. Japanese presentations centered on reviewing their base isolation and active controls work including applications for buildings and bridges and on Japanese structural engineering facilities. The Japan-side identified a variety of field experiments used to reduce seismic loads using mass damping, rubber bearings, viscous oil dampers, springs, sliding isolators, etc.

The ATLSS laboratory can accommodate three-dimensional testing of large structures. Its main bay is 91 m (300 ft) long with a test floor of 31×12 m (102×40 ft); its buttress wall is 15 m (50 ft) high. The large-scale multi-directional facility has a capacity of applying 22.2 MN (5M lbs) in compression. The pumps are located outside the facility to reduce noise.

2. STENNIS SPACE CENTER

The delegation viewed the three massive ground rocket engine propulsion test facilities. The largest stand that houses the main rocket engines during test firing is 122 m (400 ft) high and is fastened to the ground by 49 m (160 ft)-long anchors. This impressive construction project illustrated technologies used to solve a major civil engineering challenge. Testing of advanced solid rocket motors will begin in 1994. The stands are linked by 12.1 km (7.5 mi) of canals used to transport the rocket stages and propellants. High pressure water from a 242 m^3 (64 M gal) tank cools the stands during rocket engine test firings.

The Stennis Space Center's mission is to support the testing of the Space Shuttle main engine and large propulsion systems; conduct research in land and oceanographic remote sensing, and manage the 5.3 K ha (13 K acre) Stennis facility and provide support services to the 19 Federal and state agencies occupying the site.

3. CORPS NEW ORLEANS DISTRICT HEADQUARTERS

An introductory briefing provided background on the Corps' New Orleans District's mission to mitigate floods in the lower Mississippi Valley through flood control systems as: levees for containment; floodway channel improvements and stabilization for passage of excess waters; tributary basin improvement for major drainage and flood control through dams and reservoirs, pumping plants, auxiliary channels, environmental enhancements; wetland protection; and providing technical support to

appropriate public and private sector organizations. Since 1879 the Corps has had lead responsibilities in flood and navigation control in this region – the largest drainage basin in the U.S. The Corps has developed a planned defense system to contain a flow of 84 K m^3/s (3 M ft^3/s). Soon, the Corps will undertake a new mission assignment to provide program management and technologies to assist EPA perform toxic waste cleanup in this region.

During the morning, three technical presentations were made; two by the U.S.-side and one by the Japan-side. The first, a Corps paper discussed physical model test programs and computer models under development that improve prediction of beach profile change during storms and cross-shore sand transport processes. The second, also a Corps paper addressed the importance of non-linear response to seismic loading of concrete gravity dams. The Japan-side presentation addressed mitigating wave damage in harbors using innovative wave dissipators. A variety of dissipators are being tested and new concepts are being modeled to identify their most favorable performance attributes.

The Japan-side presentation was specially prepared for this meeting; it is not part of the Proceedings. Several related papers on dissipating wave energy using breakwater structures are found in past Proceedings of the Panel on Wind and Seismic Effects.

A Corps boat provided the delegation with a river tour to allow a direct review of the technologies and projects for flood control and safe and efficient navigation. The trip down the Mississippi River and two connecting waterways showed many public works projects including the Algiers and Harvey Locks (sector and miter gates), spill way projects, levees and flood control structures and pumping stations, shallow draft channels, docks and waterfront structures.

4. MINERAL MANAGEMENT SERVICES AND FREEPORT-MCMORAN GLOBAL RESOURCE COMPANIES

MMS is responsible for leasing land for mineral exploration and for regulating environmental and human safety for oil/gas/mining. MMS performs this work in the Gulf of Mexico using 60 field inspectors and 12 helicopters. MMS adopts American Petroleum Institute's Standards, if practical, and at times further strengthens API's Standards with MMS' Standards. MMS works closely with other Federal agencies in performing its mission such as: EPA in the assessment of discharges of contamination into water and on land; the Coast Guard for ensuring safety of personnel associated with offshore operations; and the Corps who issues permits for certain pipelines and for abandoning platforms.

After these discussions a helicopter transported the delegation about 160 km (100 mi) to the Freeport-McMoRan Offshore Sulfur Platform. The Complex is composed of 14 platforms extending for 1.8 km (1.1 miles), tip-to-tip. It is the largest sulphur mine in the U.S; reserves total 68B kg (75M tons). The design and construction costs of these huge platforms exceeded $750M. They are designed for a 40 year life. The complex sets on top of a salt dome located about 670 m (2200 ft) below water level. Sulphur is under the dome and natural gas and oil reserves surround the 3.2 km (2 mi) diameter dome.

The main product of this production platform is sulphur. Sulphur is mined using superheated water at 157 °C (315 °F) injected into the sulfur bed, forcing it out and into transport tubes to two large storage tanks on its own platform where it is prepared for barging to the mainland. The storage tanks hold a four-day supply of the liquid sulphur. Oil and gas also are mined at this site. They are transported by underwater pipe to shore. Another platform contains the living quarters for 150 persons, the boiler plant platform has daily production capability to generate 38 K m^3 (10 M gal) of fresh water and 17 mW of electricity. The plant went into operation in April 1992; sulfur production is expected to reach 5Mkg (5.5k tons) per day using 30 wells.

The platform substructures are about 70m (230 ft) in length. They were constructed horizontally, transported to the site, and slid off transport barges into the water. Their 2.1 m (84 in) outer legs and 1.2 m (48 in) central legs were flooded bringing the platform into a vertical position. Stability pilings, 107 m (350 ft) in length, were sunk into the sea bed through the center and outer platform legs. The outer pilings are 1.8 m (72 in) in diameter; the center pilings are 1.5 m (60 in). Thirteen bridges connect the 14 towers. Over 90.7 M kg (100 K tons) of fabricated steel were used to fabricate the complex. The two sulphur production platforms will be moved every 10 years to drill for new supplies as the seafloor will subside approximately 9.1 m (30 ft) due to removing the minerals from the earth.

The platforms are designed for 40 year life based on API RP 2A Recommended Practice. They are designed for the North Sea environment (safety index of 3.6). Its environmental criteria are based on 1000 year storm with 20 m (67 ft) waves. Even waves from a 5000-year storm will not reach the base of the 34 m (110 ft) high platform. Subsidence consideration included designing for heavy loads which used specially designed joints and bearings to accommodate expansions and contractions. Design for vertical waves included probability-based design load, design for soil subsidence, 80 year fatigue life, 445 k Nm^2 (100 ksi) steel in piles, nonlinear pile analysis, vertical wave fatigue analysis, post-sleeve jacking system, adjustable boat landing and barge bumpers, and very long bridges. Their corrosion safety factor considers 6.4 to 9.5 mm (1/4 to 3/8 in) scaling.

5. CALIFORNIA DEPARTMENT OF TRANSPORTATION (CALTRANS)

CALTRANS is reinforcing bridges designed prior to the 1971 San Fernando Earthquake to improve their ability to withstand future shaking as experienced in 1971 and the 1989 Loma Prieta earthquakes. CALTRANS sponsors some research with the University of California at San Diego and at Berkeley. For the latter, the Civil Engineering Department is testing retrofit methods for double level bridges and column bents. After the 1987 Whittier earthquake, analysis showed that attention must be focused on retrofitting bridge columns since many suffered shear failures. CALTRANS is retrofitting those structures that pose the greatest risk to damage from another earthquake. Their end goal is to retrofit 750 bridges between 1989 and 1994.

A site visit was made to the Southern Freeway viaduct (Route 280 near Alemany), San Francisco. This bridge experienced damage during the Loma Prieta earthquake. This portion of the viaduct was closed to vehicles following the earthquake. Its columns are being replaced; work involves shoring the upper deck, cutting the column at its cap and installing a new reinforced concrete column structure. Some column footings are being replaced, others are being strengthened with new footings. Piles will be used to withstand high tension loads and compression loads in anticipation of similar future loads as experienced during the Loma Prieta earthquake. Several techniques are being explored and five companies were contacted to learn about their new innovations and construction techniques to meet the design load criteria for pilings. There is much public pressure to complete this job by the end of 1992. CALTRANS hopes single lane traffic will be possible by December 1992, with full highway use by May 1993.

6. LAWRENCE BERKELEY LABORATORY AND UNIVERSITY OF CALIFORNIA, BERKELEY (UCB)

The U.S.-side presented two papers: the first was on scale models of buildings to help visualize structural behavior during an earthquake; the second addressed developing a seismic safety program for research laboratory facilities. These oral presentations well illustrate the need for effective earthquake technology translation for use by practitioners. Following these presentations, several LBL and UCB buildings were visited:

Advanced Light Source (ALS). The ALS is nearing completion for use in performing advanced studies of materials, surface sciences in atomic and molecular physics and fabrication technologies, and characterization for micro- and nanostructures. The delegation viewed the installation of electron storage rings, several electron beam ports, and the facility's thick shielded walls. The central radial area has been made earthquake resistant. The ALS is in a 0.8 ha (2 acre) building.

UCB, Structural Test Laboratory. Here research is underway on evaluating the expected performance of bridge retrofits, design criteria, and detailing. CALTRANS sponsors research on performing proof of concept. A brief discussion on seismic retrofit of two LBL buildings was provided. A review of this subject is published as "Safety and Economic Benefits Realized From Upgrading the Lawrence Berkeley Laboratory," Wind and Seismic Effects Proceedings of the 23rd Joint Meeting, NIST SP 820, September 1991, pp. 225–237.

Seismic Retrofit of University Hall. A tour was made of the seismic retrofit of the 61 × 21m (200 × 70 ft), seven-story University Hall. Symmetrically arranged X-braced steel frames were placed in the building's bays. This approach was selected because it permitted building occupants to continue working during the construction and the cost for this approach was the lowest. The X-braced frames are attached to the columns transferring the seismic loads through an innovative system from the bracing and vertical steel down to the strengthened concrete columns.

UCB, Richmond Field Station. This off campus facility houses the Earthquake Engineering Research Center (EERC) and its information center that for more than 20 years has served the earthquake engineering community with technologies. The library offers on-line data base research and rationales, *EERC News*, etc.

The Station is upgrading its shake table for three-dimensional accelerations. The shake-table was constructed in 1972. Its dimensions are 6.1 × 6.1 m (20 × 20 ft) with a 45.4 K kg (50 ton) capacity. The Station closely works with the UC Berkeley, Department of Civil Engineering.

The delegation visited one of the Station's laboratories performing research in base isolation. This project is a three-story 6 m × 10 m (20 × 33 ft) reinforced concrete residence hall at the Tohoku University campus, Sendai. The research budget is funded by Shimizu Corporation. Work involves performing vertical and horizontal 1.5 g acceleration of light models and 0.8 g for heavy models. The models are of 1/2.5 scale reinforced concrete building. The work involves performing low-level earthquake tests of the model using three different base isolation systems; performing high level earthquake tests of the scale-model using one base isolation system; conducting analytical studies of structures using linear and non-linear techniques; and performing mechanical tests of the three different base isolators.

7. FORELL/ELSESSER ENGINEERS, INC.

This consulting engineering firm specializes in structural and earthquake engineering. Three principals discussed their analyses, options, and recommendations for rehabilitating historic buildings damaged by the Loma Prieta earthquake: the San Francisco City Hall, Stanford University Green Library-West, and the Oakland City Hall. A fourth building, Lawrence Livermore National Laboratory, Building 111, which was retrofitted in the late 1980s, was briefly discussed.

Analyses performed on the historic buildings and the several options for seismic strengthening were discussed. For the first and third buildings, base isolators were selected as the prime method to protect the buildings from future earthquake loads. The second building was repaired using reinforced concrete structural walls. Each building repair and strengthening must have a complete lateral load-resisting system transferring loads into the foundations. New materials, seismic force levels, and construction must comply with the latest building standards and codes.

San Francisco City Hall. A five story building of plan dimensions about 91 × 122 m (300 × 400 ft) has a dome about 91 m (300 ft) high. The building was constructed in 1916. There is much ornate finish within the building; light courts are on the second floor. The building's structure is steel frame with reinforced concrete slabs. Exterior granite walls and light court walls are unreinforced brick masonry and infill partition walls are hollow clay masonry tiles. These areas suffered the majority of the earthquake damage. The structural steel frame was undamaged; no structural instabilities or collapse were

observed. Over 500 base isolators are proposed for installation to reduce loads; some shear-resisting elements are required to strengthen and stiffen the superstructure. A new ground floor of steel framing concrete/metal deck will be located above the isolators.

Stanford Green Library-West. The library was constructed in 1917, in the neo-classical style; a four-story building of 70 × 55 m (230 × 180 ft). It is designed around four light courts and central rotunda. Reinforced concrete spread footings beneath the interior steel columns and perimeter wall footings form the foundation. The building has a moment resisting steel frame encased in concrete. Its exterior unreinforced brick masonry walls and hollow clay tile partitions were severely damaged. The building has little ductility; it experienced significant earthquake damage. It lost 40–60 percent of its lateral strength due to the large number of wall openings.

The design team recommended using new reinforced concrete structural walls 0.3–0.4 m (12–16 in) in thickness, new reinforced concrete floors to reduce adding new concrete walls and to complete the load path, new foundation for the wall loads, and strengthening the masonry piers. Base isolators are not practical because the library would lose its basement.

Oakland City Hall. It has plan dimensions of about 38 × 56 m (125 × 185 ft) and a highly decorated clocktower rising to 99 m (325 ft). When completed in 1914, this building was the tallest in the western U.S. Large interior cavities within the steel frame were enclosed by unreinforced brick masonry, unreinforced concrete, and hollow clay tile. Its foundation is a 0.7 m (2 foot 3 in) reinforced concrete mat over the entire basement area. The earthquake loading was resisted by a combination of the building's flexible steel moment frame encased in brick masonry, unreinforced brick walls, and hollow clay tile walls. The City Hall suffered much damage from the Loma Prieta earthquake. Ground motion was estimated at about 10% g.

Its irregular vertical structure consisting of several setbacks contributed to whipping action producing cracks in the clock tower. An interesting side light; information was uncovered that accelerometers had been installed in the building providing data from the earthquakes on 22 March 1957. This was valuable information used in the redesign of the City Hall.

The City of Oakland recognizes this building as a historical landmark; accordingly, it wanted as few surface changes as possible to preserve the building's interior and exterior walls. Over 110 elastomeric bearing base isolators will be installed below the first floor girders under the perimeter columns in conjunction with the concrete shearwalls. The superstructure will be strengthened to resist maximum forces above the isolators. Top portion will be braced to resist lateral loads and shear walls and braces in walls are expected to prevent overturning. The building will be decoupled from its base isolators to accommodate an upward 6mm (1/4 in) unloading.

Repair and strengthening of the City Hall provided the City with the opportunity to perform a much needed exterior cleaning, spruce up its interiors, modify its HVAC systems, add new carpeting, etc.

Lawrence Livermore National Laboratory, Building 111. This building was built in the early-1960s with a reinforced concrete non-ductile frame. After the 1980 earthquake the design team had added two buttress towers on piers. Now forces are transferred from the building to the buttresses. Steel elements were constructed on either side of the floor beams. Elements were bolted and epoxied to the floor beams with cast-in-place end caps in buttress.

8. SAN FRANCISCO BAY-DELTA TIDAL APPROACH MODEL

The Corps of Engineers constructed this 0.4 ha (1 acre) hydraulic model basin to simulate water levels, flow patterns, and salinity in the San Francisco Bay and Delta. The model is a scaled representation of the bay; 27 km (17 mi) into the Pacific Ocean; 27 km (17 mi) east toward Sacramento; and 51 km (32 mi) south of Stockton. The model provided similitudes for the dominant forces. It is distorted by a factor of 10 in the vertical scale. Copper strips are used throughout to correct distortion of the hydraulic efficiency of the flow. The model is 98 × 122 m (320 × 400 ft).

The model predicts the impact of deepening and realigning navigation channels, varying flows, small changes from planned construction projects. Results help better determine salinity changes from deepening navigation channels, failure of levees and delta island flooding, and proposed water transfer projects; sediment disposal sites, breakwaters, and municipal approved discharge projects; and emergency cleanup procedures in the event of an oil spill.

Both dynamic and steady-state testing are performed. Computers control tides and check on boundary conditions. Tides are generated by a valve control. The model was designed and constructed in conjunction with WES.

ACKNOWLEDGMENTS

The preparation of this publication was made possible by the Department of Army, Corps of Engineers; Department of Commerce, National Oceanographic and Atmospheric Administration and the National Institute of Standards and Technology; Department of Energy; Department of Interior, Mineral Management Services; Department of Navy, Naval Civil Engineering Laboratory; Department of State, and the Federal Emergency Management Agency; the National Science Foundation; and the Nuclear Regulatory Commission.

Noel J. Raufaste, Secretary
U.S.-Side Panel on Wind and Seismic Effects

ABSTRACT

This publication is the proceedings of the 24th Joint Meeting of the U.S.-Japan Panel on Wind and Seismic Effects. The meeting was held at the National Institute of Standards and Technology, Gaithersburg, Maryland, during May 19–22, 1992. The proceedings include the program, list of members, panel resolutions, task committee reports, and 45 technical papers.

The papers were presented under five themes: (I)—Wind Engineering, (II)—Storm Surge and Tsunamis, (III)—Joint Cooperative Research Program, (IV)—Earthquake Engineering, (V)—Summaries of Task Committee Workshop Reports (oral presentations only).

KEYWORDS: accelerograph; bridges; building technology; concrete; design criteria; disasters; disaster reduction; earthquakes; geotechnical engineering; ground failures; lifelines; liquefaction; masonry; repair and retrofit; risk assessment; seismic; soils; standards; storm surge; structural engineering; tsunamis; and wind loads.

CONTENTS

PAGE

PREFACE iii

ABSTRACT xi

AGENDA FOR 24TH JOINT UJNR MEETING xvii

LIST OF PANEL MEMBERS xxv

LIST OF TASK COMMITTEE MEMBERS XLI

RESOLUTIONS XLIV

IDNDR PRESENTATION

U.S. Federal Agency Role in the International Decade for Natural Disaster Reduction and UJST Workshops for Natural Disaster Reduction 3
Paul Kilho Park

THEME I: Wind Engineering

Flutter Characteristics of Super Long-Span Suspension Bridge 13
Koichi Yokoyama, Tokida Kanazaki, and Masahiko Yasuda

Predicting Wind Forces Using Computer Simulation of Air Flow Around Bridges 25
Okey Onyemelukwe and Harold Bosch

THEME II: Storm Surge and Tsunamis

A Numerical Simulation of the Tsunami Generated by Landslide of Mt. Mayuyama in 1792 41
Chiaki Goto and Tomotsuka Takayama

Empirical Simulation of Storm Histories for Coastal Design 45
Martin C. Miller and Robin D. Reinhard

THEME III: Joint Cooperative Research Program

The Japan-PRESSS Program—Analytical Tools in Japan 57
T. Okoshi and S. Nakata

U.S. Japan Cooperative Research in Precast Seismic Structural Systems (PRESSS) Program—Status Report 69
Nigel Priestly and H. S. Lew

CONTENTS

PAGE

Seismic Response Control of Highway Bridges by Variable Damper 71
Kazuhiko Kawashima, Shigeki Unjoh, and Hideyuki Shimizu

THEME IV: Earthquake Engineering

Seismic Design Considerations for Jordanelle Dam 87
John A. Wilson, Perry J. Hensley, William O. Engemoen, and Francis G. McLean

An Evaluation of Seismic Forces Acting on Embankment Dams and Its Simplified Prediction Procedure 101
Tadahiko Fujisawa, Nario Yasuda, Norihisa Matsumoto, and Kenji Yamabe

Resolving Uncertainties in Seismic Hazard Models 115
J. K. Kimball

Earthquake Alert System Feasibility Study 127
Philip E. Harben

Guidelines for Seismic Design Methods of Large Underground Structures 143
Hajime Asakura, Kazuhiko Kawashima, and Hideki Sugita

Seismic Vulnerability and Impact of Disruption of Lifelines in the Conterminous United States—An Overview 159
William S. Bivins

Design Criteria for Base Isolation of Buildings 165
Harry W. Shenton, III

Manual for Menshin Design of Highway Bridges 173
Kazuhiko Kawashima, Kinji Hasegawa, and Hiroyuki Nagashima

Friction Controllable Bearings for Sliding Base Isolation Systems 189
Maria Qing Feng and Masanobu Shinozuka

State-of-the-Arts on Building Structures With Structural Response-Control System in Japan 199
Yosikazu Kitagawa and Mitsumasa Midorikawa

Status of NSF Structural Control Research Programs 215
S. C. Liu, H. J. Lagorio, and K. P. Chong

Significant Results From Standardization Work on Rubber Bearings for Base-Isolation Buildings 225
Yuji Ohashi and Hiroyuki Yamanouchi

CONTENTS

PAGE

Effect of Temperature on the Dynamic Behavior of Base-Isolated Bearings 233
Osamu Nakano, Hideyuki Taniguchi, and Hiroaki Nishi

Dynamic Centrifugal Model Tests of Embankments on Liquefiable Ground (Part 2) 241
Yasuyuki Koga, Jun-ichi Koseki, and Akihiro Takahashi

Earthquake-Induced Landslides in the Santa Cruz Mountains 253
M. E. Hynes and M. Hudson

Study on Prediction of Lateral Ground Flow by Soil Liquefaction and Its Influence on Piles 271
Ken-ichi Tokida, Hideo Matsumoto, Ikuo Towhata, and Yasushi Sasaki

Horizontal Bearing Capacity of Pile Foundations Based on Horizontal Loading Tests 285
Minoru Fujiwara, Michio Okahara, Shoichi Nakatani,Yoshitomi Kimura, and Shitgeru Takagi

Seismic Effects on Port and Harbour Structures 301
Hajime Tsuchida and Setsuo Noda

Implementation of Executive Order 12699, "Seismic Safety of Federal and Federally Assisted or Regulated New Building Construction 311
Richard N. Wright

U.S. Army Corps of Engineers Earthquake Engineering Research Program 317
W. D. Roper, M. E. Hynes, and R. F. Davidson

A Progress Report on the Worldwide Earthquake Risk Management (WWERM) Program 329
S. T. Algermissen, Walter W. Hays, and Paul R. Krumpe

Development of Advanced Reinforced Concrete Buildings Using High-Strength Concrete and Reinforcement Researches on Structural Performance Conducted in 1991 337
Tatsuo Murota, Hisahiro Hiraishi, Takashi Kaminosono, Masaomi Teshigawara, Hitoshi Shiohara, and Hideo Fujitani

Dynamic Testing of Reinforced Concrete Frames 359
Pamalee Brady and Steven C. Sweeny

Shaking Table Collapse Tests of RC Columns 371
Chikahiro Minowa, Nobuyuki Ogawa, Tadashi Mikoshiba, and Norio Oyagi

A Hollow Clay Tile Wall Seismic Performance Program Overview 383
J. E. Beavers, W. D. Jones, and W. C. T. Stoddart

CONTENTS

PAGE

The Valuation and Designation Systems for Structural Calculation Programs in Building Engineering 393
Keiichi Ohtani

Highlights of the 13 March 1992 Erzincan (Turkey) Earthquake 397
Mehmet Celebi

Beach Profile Response to Storm Surge and Waves 411
Nicholas C. Kraus, Magnus Larson, Bruce A. Ebersole, and Jane McKee Smith

Developing a Seismic Safety Program 427
Donald G. Eagling

Desk-Top Model Buildings for Dynamic Earthquake Response Demonstrations 435
A. Gerald Brady

Manuscripts Authored for Panel Meeting but Not Presented Orally

Determination of Windborne Missile Design Parameters 447
James R. McDonald

Advances in Wood Engineering and Construction Research 459
Erwin L. Schaffer

The Impacts of Siting Lifelines in Close Proximity Upon Their Earthquake Vulnerability 491
William Bivens

Nonlinear Research Needs for Concrete Gravity Dams 495
Robert L. Hall and Wayne G. Johnson

Seismic Risk Assessment Methodology for Water Systems 507
Craig E. Taylor and Stuart D. Werner

Bridge Scour/An Element of Bridge Management 513
J. Sterling Jones and Stanley R. Davis

U.S. Coordinated Program for Masonry Building Research—Seventh Year Status 521
James L. Noland

Appendix: Task Committees A–K Reports 529

AGENDA FOR 24TH JOINT UJNR MEETING

Tuesday 19 May

1000 **OPENING CEREMONIES**
(Lecture Room B, Administration Building)

Call to order by Noel RAUFASTE, Secretary-General U.S. Side, UJNR Panel

Opening remarks by John LYONS, Director, National Institute of Standards and Technology

Remarks by Yukihide HAYASHI, Counsellor for Science and Technology, Embassy of JAPAN

Remarks by Richard N. WRIGHT, Chairman U.S.-Side, Panel on Wind and Seismic Effects, Director, Building and Fire Research Laboratory

Remarks by Yukihiko SUMIYOSHI, Chairman JAPAN-Side, Panel on Wind and Seismic Effects, Director-General, Public Works Research Institute

Introduction of U.S. Members by U.S. Panel Chairman

Introduction of JAPAN Members by Japan Panel Chairman

Elect Joint Meeting Chairman

Adopt Agenda

Adjourn

1115 Group Photograph

1130 **Lunch**: Hosted by the National Institute of Standards and Technology, John LYONS, Director

IDNDR

1230–1300 IDNDR, U.S. Federal Agency Role in IDNDR, Kilho PARK*, NOAA

1300–1310 Discussion

THEME—WIND ENGINEERING

1310–1410 **Technical Session—Wind Engineering**
Chairman: Yukihiko SUMIYOSHI

1310–1330 Flutter Characteristics of a Super Long-Span Suspension Bridge, Koichi YOKOYAMA*, Tokida KANAZAKI, and M. YASUDA, PWRI

1330–1350 Predicting Wind Forces Using Computer Simulation of Air Flow Around Bridges, Okey U. ONYEMELUKWE* and Harold R. BOSCH, FHWA

1350–1410 Discussion

1410–1430 Break

TASK COMMITTEE MEETINGS

1430–1700 **T/C Meetings**

T/C A Strong Motion Instrumentation Arrarys and Data (Brady/ Noda) Employees Lounge

T/C C&D Repair and Retrofit of Existing Structures and Evaluation of Structural Performance (Chong- Fuller/Yamanouchi) Lec. Rm. B

T/C E Ground Motion and Seismic Design Forces (Algermissen/ Kawashima) Conference Room, B111

T/C H Soil Behavior and Stability During Earthquakes (Franklin/ Yokoyama) Conference Room B113

T/C J Wind and Earthquake Engineering for Transportation Systems (Cooper/ Fujiwara) BFRL Conference Room, Bldg 226, Rm. B221

1700 Conclusion of day 1

Wednesday 20 May

THEME – STORM SURGE AND TSUNAMIS

0830–0930 **Technical Session – Storm Surge and Tsunamis**
Chairman: Richard WRIGHT

0830–0850 A Numerical Simulation of the Tsunami Generated by Landslide of Mt. Mayuyama in 1792, C. GOTO and Tomotsuka TAKAYAMA, PHRI (Presented by Setuo NODA)

0850–0910 Empirical Simulation of Storm Histories for Coastal Design, Martin C. MILLER* and Robin D. REINHARD, WES

0910–0930 Discussion

0930–0950 Break

THEME – JOINT COOPERATIVE RESEARCH PROGRAM

0950–1050 **Technical Session – Joint Cooperative Research**
Chairman: Richard WRIGHT

0950–1010 Development of Precast Seismic Structural System – Interim report, Tastuo MUROTA, Shinsuke NAKATA, M. TESHIGAWARA, H. SHIOHARA, BRI (Presented by Hiroyuki YAMANOUCHI)

1010–1030 U.S. Japan Cooperative Research in Precast Seismic Structural Systems (PRESSS) Program – Status Report, Nigel Priestly, UCSD and H. S. LEW*, NIST

* Identifies oral presenters.

1030–1050 Seismic Response Control of Highway Bridges by Variable Damper, Kazuhiko KAWASHIMA*, S. UNJON, H. SHIMIZU, PWRI

1050–1110 Discussion

THEME – EARTHQUAKE ENGINEERING – PART I

1110–1230 **Technical Session – Earthquake Engineering – Part I**
Chairman: Richard WRIGHT

1110–1130 Seismic Design Considerations for Jordanelle Dam, John WILSON*, Perry HENSLEY, William ENGEMOEN, and Francis MCLEAN, BUREC

1130–1150 Considerations on Evaluation of Seismic Force Acting on Embankment Dams and Its Simplified Prediction Procedure, Tadahiko FUJISAWA, N. YASUDA, N. MATSUMOTO, and K. YAMABE, PWRI (Presented by Yoshikazu YAMAGUCHI)

1150–1210 Resolving Uncertainties in Seismic Hazard Models, Jeffrey K. KIMBALL*, DOE

1210–1230 Discussion

1230–1330 **Lunch**: Hosted by National Science Foundation, Dr. Dov JARON, Director, Biological and Critical Systems Division

1330–1450 **Technical Session – Earthquake Engineering – Part I Cont.**
Chairman: Richard WRIGHT

1330–1350 Earthquake Alert System Feasibility Study, Philip HARBEN*, LLNL-DOE

1350–1410 Guideline for Seismic Design of Large Underground Structures (Draft), Hajime ASAKURA*, Kazuhiko KAWASHIMA, and H. SUGITA, ACTC

1410–1430 ATC-25 Vulnerability of Lifelines, William BIVINS*, FEMA

1430–1450 Discussion

1450–1500 Break

TASK COMMITTEE MEETINGS

1500–1700 **Task Committee Meetings**

T/C B Large Scale Testing Programs (Lew/ Ohtani) BFRL Conference Room, Bldg. 226, Rm. B221

T/C F Disaster Prevention Methods for Lifeline Systems (Dikkers/ Kawashima) Employees Lounge

T/C G Passive, Active, and Hybrid Control Systems (Liu/ Kitagawa) Lecture Room B

T/C I Storm Surge and Tsunamis (Meyers/Yokoyama) Conference Room B113

---

* Identifies oral presenters.

T/C K Wind and Earthquake Engineering for Marine Facilities (Smith/ Noda) Conference Room B111

1700 Conclusion of day 2

Thursday 21 May

THEME – EARTHQUAKE ENGINEERING – PART II

0815–1110 **Technical Session – Earthquake Engineering – Part II**
Chairman: Yukihiko SUMIYOSHI

0815–0835 Design Criteria for Base Isolation of Buildings, H. Tripp SHENTON*, NIST

0835–0855 Menshin Design Manual for Highway Bridges (Draft), Kazuhiko KAWASHIMA*, K. HASEGAWA, and H. NAGASHIMA, PWRI

0855–0915 Friction Controllable Bearings for Sliding Base Isolation Systems, Maria Q. FENG, Princeton University and Masanobu SHINOZUKA*, NCEER

0915–0935 Discussion

0935–0950 Break

0950–1010 State-of-Art and Building Structure with Seismic Response Control System in Japan, Yosikazu KITAGAWA* and M. MIDORIKAWA, BRI

1010–1030 Status of NSF Structural Control Research Programs, S. C. LIU*, Ken CHONG, and Henry LAGORIO, NSF

1030–1050 Significant Results from Standardization Work on Rubber Bearings for Base-Isolated Buildings, U. OHASHI and Hiroyuki YAMANOUCHI*, BRI

1050–1110 Effect of Temperature on Dynamic Behavior of a Base-Isolated Bridge, Osamu NAKANO*, H. TANIGUCHI, and H. NISHI, HDB

1110–1130 Discussion

1130–1230 **Lunch**: Hosted by U.S. Army Corps of Engineers, Dr. Robert OSWALD, Director of Research and Development

1230–1630 **Technical Session – Earthquake Engineering – Part II Cont.**
Chairman: Yukihiko SUMIYOSHI

1230–1250 Dynamic Centrifugal Model Tests of Embankments on Liquefiable Ground, Yoshikazu KOGA, Jun-ichi KOSEKI*, and A. TAKAHASHI, PWRI

1250–1310 Santa Cruz Landslide, Mary Ellen HAYNES*, WES

1310–1330 Study on Estimation of Lateral Ground Flow by Soil Liquefaction and Its Influence on Piles, Ken-ichi TOKIDA, H. MATSUMOTO, I. TOWHATA, and Yasushi SASAKI, PWRI (Presented by Jun-ichi KOSEKI)

---

* Identifies oral presenters.

1330–1350 Discussion

1350–1410 Break

1410–1430 Horizontal Bearing Capacity of Pile Foundations Based on Horizontal Loading Tests, Michio OKAHARA, S. NAKATANI, Y. KIMURA, and S. TAKAGI, PWRI (Presented by Minoru FUJIWARA)

1430–1450 Seismic Requalification of Offshore Structures, Charles SMITH*, MMS

1450–1510 Analysis of Seismic Effects on Quay Walls, S. IAI, T. KAMEOKA, and Setsuo NODA*, PHRI

1510–1530 Discussion

1530–1550 Implementation of Executive Order 12699, "Seismic Safety of Federal and Federally Assisted or Regulated New Building Construction," Richard WRIGHT*, NIST

1550–1610 CORPS Earthquake Engineering Research Program, William ROPER*, CORPS

1610–1630 Worldwide Seismic Risk Management Program—Progress Report, Ted ALGERMISSEN*, U.S.GS

1630–1650 Discussion

1650 Conclusion of day 3

Friday 22 May

THEME—EARTHQUAKE ENGINEERING—PART III

0830–1110 **Technical Session—Earthquake Engineering—Part III**
Chairman: Richard N. WRIGHT

0830–0850 Seismic Performance of Reinforced Concrete Structures Utilizing High-Strength Materials, Tastuo MUROTA, H. HIRAISHI, T. KAMINOSONO, H. SHIOHARA, and H. FUJITANI, BRI (Presented by Yosikazu KITAGAWA)

0850–0910 Dynamic Testing of Nonductile Concrete Frame Systems, P. A. BRADY and S. SWEENY*, CERL

0910–0930 Shaking Table Collapse Tests of Reinforced Concrete Columns, N. OYAGI, Nobuyuki OGAWA*, C. MINOWA, and T. MIKOSHIBA, NIED

0930–0950 Discussion

0950–1010 A Hollow Clay Tile Wall Seismic Performance Program Overview, J. E. BEAVERS*, W. D. JONES, and W. C. T. STODDART, MMES-DOE

1010–1030 The Valuation and Designation Systems for Structural Calculation Program in Building Engineering, Keiichi OHTANI*, NIED

---

* Identifies oral presenters.

1030–1050 Preliminary Report on Reconnaissance of Turkish Earthquake, Mehmet CELEBI*, U.S.GS

1050–1110 Discussions

1110–1125 Break

THEME – T/C WORKSHOP REPORTS

1125–1220 **Technical Session – Summary T/C Workshop Reports**
Chairman: Yukihiko SUMIYOSHI

1125–1135 T/C "E" *Ground Motion and Seismic Design Forces*, May 27–30, 1991, Tsukuba (Presented by T. ALGERMISSEN)

1135–1145 T/C "F" *Disaster Prevention for Lifeline Systems*, August 19–21, 1991, Los Angeles (Presented by R. DIKKERS)

1145–1155 T/C "G" *Passive, Active, and Hybrid Control Systems*, September 4–5, 1991, Buffalo (Presented by K. KAWASHIMA)

1155–1205 T/C "J" 8th *Bridge* Workshop, May 11–15, 1992, Chicago area (Presented by J. COOPER)

1205–1220 Discussion

1220–1320 **Lunch**: Hosted by U.S. Geological Survey, Dr. Robert WESSON, Chief, Office of Earthquakes, Volcanoes, and Engineering

TASK COMMITTEE REPORTS AND RESOLUTIONS

1320–1510 **Task Committee Reports**
Chairman: Richard N. WRIGHT

T/C A Strong Motion Instrumentation Arrays and Data

T/C B Large-Scale Testing Programs

T/C C Repair and Retrofit of Existing Structures

T/C D Evaluation of Structural Performance

T/C E Ground Motion and Seismic Design Forces Programs

T/C F Disaster Prevention Methods for Lifeline Systems

T/C G Passive, Active, and Hybrid Control Systems

T/C H Soil Behavior and Stability During Earthquakes

T/C I Storm Surge and Tsunamis

T/C J Wind and Earthquake Engineering for Transportation Systems

T/C K Wind and Earthquake Engineering for Offshore and Coastal Facilities

---

* Identifies oral presenters.

1510–1610 **Adoption of Final Resolutions**

1610–1620 Break

CLOSING CEREMONIES

1620 Call to Order by Noel J. RAUFASTE, Secretary-General, U.S.-Side Panel

Closing Remarks by Yukihiko SUMIYOSHI, Chairman JAPAN-Side Panel

Closing Remarks by Richard N. WRIGHT, Chairman U.S.-Side Panel

1645 Conclusion of Joint Meeting

LIST OF PANEL MEMBERS

UNITED STATES-SIDE PANEL ON WIND AND SEISMIC EFFECTS
MEMBERSHIP LIST
1992

Dr. Richard N. Wright
Chairman
Director, Building and Fire Research Laboratory
National Institute of Standards and Technology
U.S. Department of Commerce
Gaithersburg, MD 20899
301.975.5900 FTS 879.5900 FAX 301.975.4032

Mr. Noel J. Raufaste
Secretary-General
Head, Cooperative Research Programs
Building and Fire Research Laboratory
National Institute of Standards and Technology
U.S. Department of Commerce
Gaithersburg, MD 20899
301.975.5905 FTS 879.5904 FAX 301.975.4032

Dr. Kharaiti L. Abrol
Acting Director
Structural Engineering Service (088C1)
Department of Veterans Affairs
810 Vermont Avenue, NW
Washington, DC 20420
202.233.2864 FAX 202.233.2115

Dr. S. T. Algermissen
Research Geophysicist
Hazard and Risk Assessment Group
MS 966, POB 25046
Denver Federal Center
Geological Survey
U.S. Department of the Interior
Denver, CO 80225
303.273.8557 FTS 776.1611 FAX 303.236.0618

Mr. Charles E. Anderson
P.O. Box 25007 (D-3130)
Bureau of Reclamation
U.S. Department of the Interior
Denver, CO 80225
303.236.9114 FTS 776.9114 FAX 303.236.6763

Dr. Celso S. Barrientos
Supervisory Physical Scientist
NOAA/NESDIS-E/RA28
National Oceanic and Atmospheric Administration
U.S. Department of Commerce
5200 Auth Road
Camp Springs, MD 20746
301.763.8102 FAX 301.763.8108

Dr. Eddie N. Bernard
Director, Pacific Marine Environmental Laboratory
National Oceanic and Atmospheric Administration
U.S. Department of Commerce
7600 Sand Point Way, NE
BIN C15700/Building 3
Seattle, WA 98115-0070
206.526.6239 FTS 392.6800 FAX 206.526.6815

Dr. Roger D. Borcherdt
Branch of Engineering Seismology and Geology
Geological Survey
U.S. Department of the Interior
345 Middlefield Road, MS 977
Menlo Park, CA 94025
415.329.5619 FTS 459.5619 FAX 415.329.5163

Dr. A. Gerald Brady
Research Civil Engineer
Branch of Engineering Seismology and Geology
Geological Survey
U.S. Department of the Interior
345 Middlefield Road, MS 977
Menlo Park, CA 94025
415.329.5664 FTS 459.5664 FAX 415.329.5163

Mr. H. Lee Butler
Chief, Research Division
Coastal Engineering Research Center
U.S. Army Engineer Waterways Experiment Station
Office CEWES-CR
P.O. Box 631
Vicksburg, MS 39180-0631
601.634.2405 FTS 542.2405 FAX 601.634.4314

Dr. Ken P. Chong
Program Director, Structural Systems and Construction Processes
Directorate of Engineering
National Science Foundation
1800 G Street, N.W., Room 1108
Washington, DC 20550
202.357.9542 FAX 202.357.0167

Dr. Riley Chung
Group Leader, Earthquake Engineering
Structures Division
Building and Fire Research Laboratory
National Institute of Standards and Technology
U.S. Department of Commerce
Gaithersburg, MD 20899
301.975.6056 FTS 879.5863 FAX 301.975.4032

Mr. James D. Cooper
Deputy Chief, Structures Division, HNR-10
Federal Highway Administration
U.S. Department of Transportation
6300 Georgetown Pike
McLean, VA 22101
703.285.2447 FAX 703.285.2379

Dr. A. G. Franklin
Chief, Earthquake Engineering & Geophysics Division
CEWES-GH Geotechnical Laboratory
U.S. Army Engineer Waterways Experiment Station
3909 Halls Ferry Road
Vicksburg, MS 39180-3909
601.634.2658 FTS 542.2658 FAX 601.634.4134

Mr. G. Robert Fuller
Acting Director, Manufactured Housing and Construction
Standards Division
Room 9152 HSMM
U.S. Department of Housing and Urban Development
Washington, DC 20410-8000
202.708.2210 FAX 202.708.0299

Mr. James H. Gates
Caltrans - Structures
P. O. Box 942874
Sacramento, CA 94274
916.445.1439 FAX 916.323.2259

Mr. Peter E. Gurvin
Director, Building Design and Engineering Division
Foreign Building Operations
Building SA-6, Room 335
U.S. Department of State
Washington, DC 20520
703.875.6117 FAX 703.875.6204

Dr. Walter W. Hays
Deputy for Research Applications
Office of Earthquake, Volcanoes and Engineering
905 National Center
Geological Survey
U.S. Department of the Interior
Reston, VA 22092
703.648.6711 FTS 959.6717 FAX 703.648.6717

Mr. James R. Hill
Manager, Natural Hazards Mitigation Programs
Office of Safety, Health and Quality Assurance
U.S. Department of Energy
Washington, DC 20545
301.903.4508 FAX 301.903.5285

Mr. Larry C. Hultengren
Senior Structural Engineer
Office of Civil/Structural Engineering
Foreign Building Operations
U.S. Department of State
Washington, DC 20520
703.875.6194 FAX 703.875.6204

Dr. Dov Jaron
Director
Division of Biological and Critical Systems
National Science Foundation
1800 G Street, NW
Washington, DC 20550
202.357.9500 FAX 202.357.7636

Dr. William B. Joyner
Geophysicist
Branch of Ground Motion & Faulting
Geological Survey
U.S. Department of the Interior
345 Middlefield Road, MS 977
Menlo Park, CA 94025
415.329.5640 FTS 459.5640 FAX 415.329.5163

Dr. Michael G. Katona
Chief Scientist
Air Force Civil Engineering Laboratory
Headquarters Air Force Civil Engineering
Support Agency
Tyndall AFB, FL 32403-6001
904.283.6274 FAX 904.283.6064

Mr. Roger M. Kenneally
Structural Engineer
Structural and Seismic Engineering Branch
Seismic Section
Office of Nuclear Regulatory Research
U.S. Nuclear Regulatory Commission
Washington, DC 20555
301.492.3893 FAX 301.443.7836

Dr. Henry J. Lagorio
Program Director, Architectural and Mechanical Systems
Division of Biological and Critical Systems
National Science Foundation
1800 G Street, N.W.
Washington, DC 20550
202.357.9780 FAX 202.357.9803

Dr. H.S. Lew
Chief, Structures Division
Building and Fire Research Laboratory
National Institute of Standards and Technology
U.S. Department of Commerce
Gaithersburg, MD 20899
301.975.6061 FTS 879.6061 FAX 301.975.4032

Dr. Shih-Chi Liu
Program Director, Structural Systems
Division of Biological and Critical Systems
National Science Foundation
1800 G Street, N.W., Room 1132
Washington, DC 20550
202.357.9780 FAX 202.357.7636

Mr. Robert B. MacDonald
Manager, Geology Branch
Engineering and Research, Code D-3610 A
Bureau of Reclamation
U.S. Department of the Interior
Building 67, Denver Federal Center
Denver, CO 80225
303.236.6904 FTS 776.8643 FAX 303.236.6763

Dr. Wayne N. Marchant
Chief, Research and Laboratory Services Division
P. O. Box 25007, Denver Federal Center
Code D-3700
Bureau of Reclamation
U.S. Department of the Interior
Denver, CO 80225
303.236.5983 FTS 776.5983 FAX 303.236.7664

Dr. Francis G. McLean
Chief, Geotechnical Engineering and Embankment
Dams Branch
P.O. Box 25007
Bureau of Reclamation
U.S. Department of the Interior
Denver, CO 80225
303.236.3854 FTS 776.3854 FAX 303.236.6763

Mr. Herbert Meyers
Chief, Earth Geophysics
National Geophysical Data Center
National Oceanic and Atmospheric Administration
U.S. Department of Commerce
325 Broadway
Boulder, CO 80303-3328
303.497.6521 FTS 320.6521 FAX 303.497.6513

Mr. Ugo Morelli
Policy Manager for Seismology
Federal Emergency Management Agency
500 C Street, SW
Washington, DC 20472
202.646.2810 FAX 202.646.3041

Mr. Howard D. Nickerson
Earthquake Engineering and Weapons Specialist
Naval Facilities Engineering Command
Hoffman Building #2, Room 12S63, Code 04B2
200 Stovall Street
Alexandria, VA 22332
703.325.0044 FAX 703.325.1916

Dr. William E. Roper
Assistant Director
Research and Development (Civil Works)
U.S. Army Corps of Engineers
20 Massachusetts Avenue, N.W
Washington, DC 20314-1000
202.272.0257 FAX 202.272.0907

Dr. Erwin L. Schaffer
Assistant Director, Wood Products Research
Forest Products Laboratory
Forest Service
U.S. Department of Agriculture
One Gifford Pinchot Drive
Madison, WI 53705-2398
608.231.9272 FTS 364.5672 FAX 608.231.9592

Mr. Charles E. Smith
Research Program Manager
Offshore Minerals Management
Technology Assessment and Research Branch
Minerals Management Service
U.S. Department of the Interior
381 Elden Street, MS 4800
Herndon, VA 22070-4817
703.787.1559 FAX 703.787.1010

Dr. T. T. Soong
Samuel P. Capen Professor
Department of Civil Engineering
National Center for Earthquake Engineering Research
State University of New York at Buffalo
212 Ketter Hall
Buffalo, NY 14260
716.636.2469 FAX 716.636.3733

ALTERNATE MEMBERS

Dr. Clifford J. Astill
Program Director
Division of Biological and Critical Systems
National Science Foundation
1800 G Street, N.W.
Washington, DC 20550
202.357.9500 FAX 202.357.9803

Dr. Mehmet K. Celebi
Research Civil Engineer
Branch of Engineering Seismology and Geology
Geological Survey
U.S. Department of the Interior
345 Middlefield Road, MS 977
Menlo Park, CA 94025
415.329.5623 FTS 459.5623 FAX 415.329.5163

Mr. Michael Changery
Chief, Global Analysis Branch
National Climatic Data Center
National Oceanic and Atmospheric Administration
U. S. Department of Commerce
Federal Building
Ashville, NC 28801
704.259.0765 FTS 672.0765 FAX 704.259.0246

Mr. C.Y. Chen
Senior Civil/Geotechnical Engineer
Foreign Building Operations
A/FBO/PE/CSB, SA-6, Rm. 327
Washington, DC 20520
703.875.6207 FAX 703.875.6204

Mr. Vincent P. Chiarito
Research Structural Engineer
Structural Mechanics Division
Structures Laboratory
U.S. Army Engineer Waterways Experiment Station
3909 Halls Ferry Road
Vicksburg, MS 39180-6199
601.634.2714 FAX 601.634.3412

Dr. James F. Costello
Senior Structural Engineer
Structural and Seismic Engineering Branch
Structural Section
Office of Nuclear Regulatory Research
U.S. Nuclear Regulatory Commission
Mail Stop 007NL
Washington, DC 20555
301.492.3818 FAX 301.492.3696

Mr. Lucian G. Guthrie
Structural Engineer
Office of Chief of Engineers
HQUSACE (CEEC-ED)
U.S. Department of the Army
20 Massachusetts Avenue, N.W.
Washington, DC 20314-1000
202.272.8673 FAX 202.272.1485

Dr. James R. Houston
Chief, Coastal Engineering Research Center
US Army Engineer Waterways Experiment Station
3909 Halls Ferry Road
Vicksburg, MS 39180-6199
601.634.2000 FAX 601.634.2655

Mr. James Lander
Geophysicist
Cooperative Institute for Research in
  Environmental Sciences
University of Colorado
Campus Box 449, Room 152 RL3
3100 Marine Street
Boulder, CO 80309
303.497.6446 FTS 320.6446 FAX 303-497.6513

Mr. Robert R. Ledzian
Senior Staff Assistant for Research
Office of Liaison - Engineering Research, Code 3020
Bureau of Reclamation
U.S. Department of the Interior
1849 C Street, N.W.
Washington, DC 20240
202.208.3432 FAX 202.208.6252

Mr. Tingley K. Lew
Research Structural Engineer
Structures Division, Code L51, Bldg. 560, Rm. 278B
Naval Civil Engineering Laboratory
Port Hueneme, CA 93043
805.982.1234 FAX 805.982.1418

Mr. Michael Mahoney
Physical Scientist
Federal Emergency Management Administration
500 C Street, SW
Washington, DC 20472
202-646-2810 FAX 202-646-3041

Dr. J. Eleonora Sabadell
Director, Natural and Manmade Hazards Mitigation Program
Directorate of Engineering
National Science Foundation
1800 G Street, N.W.
Washington, DC 20550
202.357.9780 FAX 202.357.9803

Dr. John B. Scalzi
Program Director, Structures and Building Systems
National Science Foundation
1800 G Street, N.W.
Washington, DC 20550
202.357.9542 FAX 202.357.7636

JAPAN-SIDE PANEL ON WIND AND SEISMIC EFFECTS
MEMBERSHIP LIST
May 1992

Mr. Yukihiko Sumiyoshi
Chairman
Director-General
Public Works Research Institute
Ministry of Construction
1, Asahi, Tsukuba-shi,
Ibaraki-ken 305
Tel. 0298-64-2211

Dr. Takashi Iijima
Secretary-General
Assistant Director General
Public Works Research Institute
Ministry of Construction
1, Asahi, Tsukuba-shi,
Ibaraki-ken 305
Tel. 0298-64-2211

Mr. Tadahiko Fujisawa
Head, Fill Type Dam Division
Dam Department
Public Works Research Institute
1, Asahi, Tsukuba-shi,
Ibaraki-ken 305
Tel. 0298-64-2211

Mr. Tokunosuke Fujitani
Chief, The Second Research Laboratory
Applied Meteorology Research Division
Meteorological Research Institute
Japan Meteorological Agency
1-1 Nagamine, Tsukuba-shi,
Ibaraki-ken 305
Tel. 0298-51-7111

Mr. Minoru Fujiwara
Director, Structure and Bridge Department
Public Works Research Institute
Ministry of Construction
1, Asahi, Tsukuba-shi,
Ibaraki-ken 305
Tel. 0298-64-2211

Mr. Tadao Hoya
Director, Geographic Department
Geographical Survey Institute
Ministry of Construction
1, Kitazato, Tsukuba-shi
Ibaraki-ken 305

Dr. Kazuhiko Kawashima
Secretary, Japan-Side Panel
Head, Earthquake Engineering Division
Earthquake Disaster Prevention Department
Public Works Research Institute
Ministry of Construction
1, Asahi, Tsukuba-shi,
Ibaraki-ken 305
Tel. 0298-64-2211

Dr. Yoshikazu Kitagawa
Director, International Institute of
Seismology and Earthquake Engineering
Building Research Institute
1, Tatehara, Tsukuba-shi,
Ibaraki-ken 305
Tel. 0298-64-2151

Dr. Yasuyuki Koga
Head, Soil Dynamics Division
Construction Method and Equipment Department
Public Works Research Institute
Ministry of Construction
1, Asahi, Tsukuba-shi,
Ibaraki-ken 305
Tel. 0298-64-2211

Dr. Hatsukazu Mizuno
Head, Large Scale Structure
  Testing Division
Building Research Institute
Ministry of Construction
1, Tatehara, Tsukuba-shi
Ibaraki-ken 305

Mr. Tastuo Murota
Director, Structural Engineering Department
Building Research Institute
Ministry of Construction
1, Tatehara, Tsukuba-shi,
Ibaraki-ken 305
Tel. 0298-64-2151

Dr. Shinsuke Nakata
Associate Director for Composite
Structures Research
Structural Engineering Department
Building Research Institute
Ministry of Construction
1, Tatehara, Tsukuba-shi,
Ibaraki-ken 305
Tel. 0298-64-2151

Mr. Kazuhiro Nishikawa
Head, Bridge Division
Structure and Bridge Department
Public Works Research Institute
Ministry of Construction
1, Asahi, Tsukuba-shi,
Ibaraki-ken 305
Tel. 0298-64-2211

Dr. Setuo Noda
Director, Structural Engineering Division
Port and Harbour Research Institute
Ministry of Transport
3-1-1, Nagase, Yokosuka,
Kanagawa-ken 239
Tel. 0468-44-5029

Dr. Nobuyuki Ogawa
Head, Earthquake Engineering Laboratory
National Research Institute for Earth
Science and Disaster Prevention
Science and Technology Agency
3-1, Tennodai, Tsukuba-shi
Ibaraki-ken 305

Mr. Keiichi Ohtani
Director, Disaster Prevention Research Division
National Research Institute for Earth
  Science and Disaster Prevention
Science and Technology Agency
3-1, Tennodai, Tsukuba-shi,
Ibaraki-ken 305
Tel. 0298-51-1611

Dr. Michio Okahara
Head, Foundation Engineering Division
Structure and Bridge Department
Public Works Research Institute
Ministry of Construction
1, Asahi, Tsukuba-shi
Ibaraki-ken 305
Tel. 0298-64-2211

Dr. Shin Okamoto
Director General
Building Research Institute
Ministry of Construction
1, Tatehata, Tsukuba-shi,
Ibaraki-ken 305
Tel. 0298-64-2151

Mr. Shin Otsuka
Head, Typhoon Research Division
Meteorological Research Institute
Japan Meteorological Agency
1-1, Nagamine, Tsukuba-shi
Ibaraki-ken 305
Tel. 0298-51-7111

Dr. Yasushi Sasaki
Director, Earthquake Disaster
  Prevention Department
Public Works Research Institute
Ministry of Construction
1, Asahi, Tsukuba-shi,
Ibaraki-ken 305
Tel. 0298-64-2211

Dr. Masaaki Seino
Head, Seismology and Volcanology
Research Division
Meteorological Research Institute
Japan Meteorological Agency
1-1, Nagamine, Tsukuba-shi
Ibaraki-ken 305
Tel. 0298-51-7111

Dr. Tomotsuka Takayama
Director, Hydraulic Engineering Division
Port and Harbour Research Institute
Ministry of Transport
3-1-1, Nagase, Yokosuka,
Kanagawa-ken 239
Tel. 0468-41-5410

Mr. Ken-ichi Tokida
Head, Ground Vibration Division
Earthquake Disaster Prevention Department
Public Works Research Institute
Ministry of Construction
1, Asahi, Tsukuba-shi,
Ibaraki-ken 305
Tel. 0298-64-2211

Dr. Takaaki Uda
Head, Coastal Engineering Division
River Department
Public Works Research Institute
Ministry of Construction
1, Asahi, Tsukuba-shi,
Ibaraki-ken 305
Tel. 0298-64-2211

Dr. Tatsuo Uwabe
Chief, Disaster Prevention Laboratory
Structural Engineering Division
Port and Harbour Research Institute
Ministry of Transport
3-1-1, Nagase, Yokosuka-shi
Kanagawa-ken 239
Tel. 0468-44-5030

Dr. Hiroyuki Yamanouchi
Special Researcher for International
Standard, Research Planning
and Information Department
Building Research Institute
Ministry of Construction
1, Tatehara, Tsukuba-shi,
Ibaraki-ken 305
Tel. 0298-64-2151

Dr. Yutaka Yamazaki
Director, Production Department
Building Research Institute
Ministry of Construction
1, Tatehara, Tsukuba-shi,
Ibaraki-ken 305
Tel. 0298-64-2151

Dr. Koichi Yokoyama
Secretary, Japan-Side
Head, Structure Division
Structure and Bridge Department
Public Works Research Institute
Ministry of Construction
1, Asahi, Tsukuba-shi,
Ibaraki-ken 305
Tel. 0298-64-2211

July 1992

LIST OF TASK COMMITTEE MEMBERS
1992

Task Committee	US Side	Japanese Side
A. Strong-Motion Instrumentation Arrays and Data	A.G. Brady* C.J. Astill R.D. Borcherdt M.K. Celebi A.G. Franklin W.B. Joyner R.B. MacDonald F.G. McLean H. Meyers J.R. Hill	S. Noda* Y. Kitagawa K. Ohtani M. Seino K. Tokida H. Yamanouchi
B. Large-Scale Testing Programs	H.S. Lew* V.P. Chiarito J.E. Sabadell C.E. Smith J. Beavers S. Sweeney	K. Ohtani* Y. Koga H. Mizuno S. Noda Y. Yamazaki K. Yokoyama
C. Repair and Retrofit of Existing Structures	K.P. Chong* P.A. Brady G.E. Freeland J.O. Jirsa H.J. Lagorio H.S. Lew T.K. Lew H.D. Nickerson D.H. Oh M.A. Phipps J.B. Scalzi D. Jones D. Eagling S. Woodson	S. Nakata* M. Fujiwara S. Okamoto Y. Sasaki
D. Evaluation of Structural Performance	J.B. Scalzi* S.A. Asar M.K. Celebi G.R. Fuller E.L. Schaffer R.L. Hall J.R. Hill D. Eagling J. Hunt D. Ellsworth	Y. Yamazaki* T. Fujitani M. Fujiwara T. Murota M. Okahara S. Ohtsuka H. Yamanouchi K. Yokoyama

Task Committee	US Side	Japanese Side
E. Ground Motion and Seismic Design Forces Programs	S.T. Algermissen* C.S. Barrientos R.D. Borcherdt A.G. Brady G.R. Fuller J.R. Hill J. Hunt W.B. Joyner J. Kimball T.K. Lew	K. Kawashima* T. Hoya Y. Kitagawa Y. Sasaki T. Uwabe H. Mizuno K. Ohtani
F. Disaster Prevention Methods for Lifeline Systems	R.M. Chung* C.J. Astill M.K. Celebi J.D. Cooper G. Al-Chaar T.K. Lew J.B. Scalzi J.S. Spencer S. Wu	Y. Sasaki* K. Kawashima T. Murota N. Ogawa K. Tokida T. Uwabe
G. Passive, Active, and Hybrid Control Systems	S.C. Liu* V.P. Chiarito K.P. Chong J.R. Hayes L.C. Hultengren H.J. Lagorio T.T. Soong	Y. Kitagawa* K. Kawashima N. Ogawa H. Yamanouchi K. Yokoyama
H. Soil Behavior and Stability During Earthquakes	A.G. Franklin* C.J. Astill R.D. Borcherdt C.Y. Chen F.G. McLean C.E. Smith	K. Tokida* T. Fujisawa Y. Koga S. Noda M. Okahara Y. Sasaki H. Mizuno
I. Storm Surge and Tsunamis	H. Meyers* C.J. Astill C.S. Barrientos E.N. Bernard L. Butler C.F. Jelesnianski J. Lander W.E. Roper	T. Uda* S. Ohtsuka T. Takayama M. Seino

Task Committee	US Side	Japanese Side
J. Wind and Earthquake Engineering for Transportation Systems	J.D. Cooper* A.G. Franklin J.H. Gates J.B. Scalzi H.S. Lew	M. Fujiwara* T. Fujitani K. Kazuhiko K. Nishikawa M. Okahara Y. Sasaki K. Tokida K. Yokoyama
K. Wind and Earthquake Engineering for Offshore and Coastal Facilities	C.E. Smith* C.S. Barrientos W.E. Roper J.E. Sabadell M.C. Miller M.K. Celebi	T. Urabe* T. Fujitani T. Murota S. Noda M. Okahara

*Chairman

RESOLUTIONS OF THE TWENTY-FOURTH JOINT MEETING U.S.-JAPAN PANEL ON WIND AND SEISMIC EFFECTS (UJNR)

National Institute of Standards and Technology
Gaithersburg, MD 20899
May 19-22, 1992

The following resolutions are hereby adopted:

1. The Twenty-Fourth Joint Panel Meeting provided an opportunity to exchange valuable technical information which was beneficial to both countries. In view of the importance of cooperative programs on the subject of wind and seismic effects, the continuation of Joint Panel Meetings is considered essential.

2. The following activities have been conducted since the Twenty-Third Joint Meeting:

   a. Researchers were exchanged from both countries to promote and conduct research that advanced the state of earthquake and wind engineering.

   b. Technical documents, research reports, and proceedings of workshops were exchanged.

   c. Both sides published a List of Panel Publications 1969-1991 for distribution to U.S. and to Japan domestic organizations and to international organizations, especially those in the less developed countries.

   d. Five significant conferences were held:

      a) The First Workshop on Hazard/Risk Assessment and Design Earthquake Loading, Task Committee (E), Tsukuba, May 28-29, 1991.

      b) The Fourth Workshop on Earthquake Disaster Prevention for Lifeline Systems, Task Committee (F), at Los Angeles, CA, August 19-21, 1991.

      c) Workshop on Earthquake Protective Systems of Bridges, Task Committee (G), at Buffalo, NY, September 4-5, 1991.

      d) The Second U.S.-Japan Joint Technical Coordinating Committee on PRESSS, Task Committee (B), at Tsukuba, Japan, October 1991.

      e) The Eighth Bridge Workshop, Task Committee (J), at Chicago, IL, May 11-15, 1992.

3. A one day International Symposium on the International Decade for National Disaster Reduction was held in Gifu City on May 20, 1991, to increase the awareness of the people of Japan about the disastrous effects from strong winds and earthquakes. This Panel provided three of the five presentations. More than 600 persons attended.

4. The Panel will continue to seek methods to contribute to the International Decade of Natural Disaster Reduction (IDNDR) such as exchanging Proceedings of joint Panel Meetings and Task Committee Workshops with their respective Country's National Committees of IDNDR.

5. The Panel recognizes the importance of the work by both sides in the U.S.-Japan Joint Research Program on Precast Seismic Structural Systems (PRESSS).

6. The Panel accepts each Task Committee's report developed during the Twenty-Fourth Joint Meeting. Each report presents objectives, scope of work, accomplishments, future plans, information exchange, impacts, and barriers.

7. The Panel endorses the following proposed Task Committee Workshops during the coming year.

   a. Task Committee (B) plans a workshop on Hybrid Structural Systems, September 1992, San Francisco, CA.

   b. Task Committee (E) plans a 2nd workshop on Ground Motion and Seismic Design Forces, May 1993, Tsukuba.

   c. Task Committee (F) plans a 5th workshop on Earthquake Disaster Prevention for Lifeline Systems, October 26-27, 1992, Tsukuba.

   d. Task Committee (G) plans a 2nd workshop on Earthquake Protective Systems of Bridges, December 1992, Tsukuba.

   e. Task Committee (G) plans a workshop on Smart and High Performance Material and Systems, May 1993, Japan.

   f. Task Committee (J) plans a 9th Bridge Workshop before the 25th Joint Meeting, Japan.

   g. Task Committee (K) plans a Workshop on Wind and Earthquake Engineering for Offshore and Coastal Facilities, May 1993, Yokosuka.

   In addition, three Task Committees have scheduled workshops after the 25th Joint Panel Meeting:

   a) Task Committee (A) has scheduled a workshop on Digital Recording Technologies, Fall 1993, Hawaii.

   b) Task Committee (H) has scheduled a workshop on Remedial Treatment of Potentially Liquefiable Soils, October 1993, Japan.

   c) Task Committee (I) has scheduled the 3rd Workshop on Storm Surge and Tsunamis, August 19-20, 1993, Japan.

   Scheduling for the workshops shall be performed by the U.S. and Japan Chairmen of the respective Task Committee with concurrence of the Joint Panel Chairmen. Results of each activity conducted before the 25th Joint Meeting shall be presented at the 25th Joint Meeting.

8. In the spirit of celebrating the 25th Anniversary of the Panel on Wind and Seismic Effects, a special event will be conducted during the 25th Joint Panel Meeting to mark this occasion. Both

sides' Secretaries will identify an appropriate method that celebrates the Panel's activities and facilitates the transfer of the Panel's technologies into practice, e.g., special symposium, publication, joint activity. The Secretarys' suggestions will be discussed at the respective sides' early fall 1992 domestic meetings to begin scheduling and arranging this event during mid-fall 1992.

9. The Panel recognizes the importance of continued exchange of personnel, technical information, research results, and recorded data that lead to mitigating losses from strong winds and earthquakes. The Panel also recognizes the importance of using available large-scale testing facilities in both countries. Thus, these activities should continue to be strengthened and expanded and, as appropriate, share Task Committee activities at other meetings that have technical interests in the Task Committee activities. To facilitate these exchanges, the Panel will provide official endorsement.

10. The Twenty-Fifth Joint Meeting of the UJNR Panel on Wind and Seismic Effects will be held at PWRI, Tsukuba, Japan, May 1993. Specific dates, program, and itinerary will be proposed by the Japan-Side Panel with concurrence of the U.S.-Side Panel.

IDNDR Presentation

U.S. Federal Agency Role in the International Decade for Natural Disaster Reduction and UJST Workshops for Natural Disaster Reduction

by

Paul Kilho Park*

ABSTRACT

Under auspices of the UJST (US-Japan Science and Technology) Agreement of 1988, annual UJST workshops for natural disaster reduction have been going on since March 1990 as part of the International Decade for Natural Disaster Reduction (IDNDR) activities of the U.S. and Japan. Two workshops held have resulted in formulation of pilot projects and identification of future thrusts, such as joint database establishment and improvement of hazard mapping via Geographic Information System (GIS). The third workshop is planned at Mt. Hood, 7-11 September 1992. The first UJST panel was formed in 1991; it is the UJST Panel on Volcanic Disaster Prevention.

KEYWORDS: earthquake; GIS (Geographic Information System); hazard mapping; human health; IDNDR (International Decade for Natural Disaster Reduction); landslides; severe storms; socioeconomics; UJST (US-Japan Science and Technology Agreement); volcano.

1. INTRODUCTION

Broad interdisciplinary cooperative agreement between the two heads of the state in 1988 initiated the U.S.-Japan Science and Technology Agreement (UJST). The seven main areas of cooperation agreed on are as follows: life science, including biotechnology; information science and technology; manufacturing technology; automation and process control; global geoscience and environment; joint database development; and advanced materials, including superconductors.

Almost at the same time the 42nd UN General Assembly in December 1987 unanimously adopted a resolution designating the 1990s as the "International Decade for Natural Disaster Reduction (IDNDR)." The 44th UN General Assembly in December 1989 unanimously adopted a resolution establishing the international framework for action by the UN and proclaimed the IDNDR beginning on 1 January 1990 ending 31 December 1999.

Within the United States, in 1988, the Federal Government's IDNDR effort was vested on the Federal Coordinating Council for Science, Engineering and Technology (FCCSET), headed by the President's Science Advisor. Within the FCCSET, the Committee on Earth and Environment Sciences (CEES) established the Subcommittee for Natural Disaster Reduction (SNDR) to directly deal with and contribute to the IDNDR activities (Bergner, 1991). Concurrently, non-governmental National Committee was established, and Professor Walter R. Lynn, Dean of the University Faculty at Cornell University, is its current chairman. The FCCSET, CEES, and SNDR are headed by Drs. D. Allan Bromley, Frederick Bernthal and William H. Hooke, respectively.

In Japan, Japanese Government Headquarters for the IDNDR, headed by the Prime Minister with the Disaster Prevention Bureau of the National Land Agency, Prime Minister's Office, acting as secretariat, was established by a decision of the Cabinet in May 1989. In August 1990, Japanese National Committee for the IDNDR was organized by the private sector, which includes the academia, industry, the Japanese Red Cross Society. Professor Jiro Kondo is the Chairman of Japan National Committee for the IDNDR. Both the U.S. and Japan have had similar organizational evolution heretofore.

Vigorous national and international activities to enhance the IDNDR effort have commenced,

---

* NOAA Office of the Chief Scientist
1825 Connecticut Avenue, NW (Room 625)
Washington, DC 20235-0001

especially in Japan and the U.S. The IDNDR International Conference 1990 Japan was held in Yokohama and Kagoshima, 27 September-3 October 1990. About 1300 participants from 43 countries and 16 international organizations attended the 1990 meeting. Similar turnout was repeated at the IDNDR Summit Conference on Earthquake and Natural Disaster Countermeasures 1991 Japan, Tokyo, 8 - 11 October 1991.

On 9 January 1992, Prime Minister Miyazawa and President Bush jointly announced the Global Partnership Plan of Action in Tokyo, in which the two heads of the state agreed to "cooperate to reduce natural hazards, in accordance with the International Decade for Natural Disaster Reduction and the U.S-Japan Science and Technology Agreement, by assisting developing counties to prepare disaster reduction plans, including hazard mapping, risk assessment and the establishment of joint databases;..." Much staff work is going on to follow up this accord, especially to get ready for Prime Minister Miyazawa's planned visit to the U.S. of summer, 1992.

Between the U.S. and Japan two UJST workshops for natural disaster reduction have been held. The first workshop was at Hilo and Punalu'u, Hawaii, 26 - 30 March 1990, and the second at Karuizawa, Japan, 23 - 27 September 1991; the third workshop is planned to be held at Mt. Hood Timberline Lodge, 7 - 11 September 1992. This report describes the details of the Karuizawa workshop. Both the first and second workshops have been chaired by Drs. Yukio Hagiwara, Director-General, National Research Institute for Earth Science and Disaster Prevention (NIED), Science and Technology Agency (STA), and William H. Hooke, Chairman, Subcommittee for Natural Disaster Reduction (SNDR). In Japan, Science and Technology Agency belongs to the Prime Minister's Office, as so does the National Land Agency.

Both Japan and the U.S. dispatch disaster relief teams. When a 635-year-dormant volcano, Pinatubo, exploded in 1991, both Japan and the U.S. dispatched their teams to help the Philippines cope with the devastation. Their onsight activities were highlighted at the Karuizawa workshop to understand the casual relationship on the disaster impact upon humanity. The U.S. effort was greatly enhanced by the Office of Foreign Disaster Assistance (OFDA) in the Department of State, and the Japanese effort by Japan International Cooperation Agency (JICA).

The JICA's fiscal year (FY) 1990 budget was 133 billion yen (about one billion dollars), some of which was earmarked for emergency disaster relief. The JICA is in charge of dispatching Japan Disaster Relief Team (JDR) and providing equipment and materials needed for disaster relief and restoration activities. The JDR carries out search and rescue, emergency medical care (as of August 1989, a total of 350 doctors and nurses are registered), and emergency measurers (prevention of secondary disasters) and restoration. Stock-piled relief goods are located at Narita (Japan), Singapore, Italy and Mexico. Japanese medical and rescue teams have been dispatched to Iran (earthquake) on 21 June 1990 and to the Philippines (earthquake) on 16 July 1990. The JICA also sent an engineering team for reconstruction to the Philippines (earthquake) on 16 July 1990 and to Saudi Arabia (petroleum over Gulf) on 3 March 1991.

Although the UJST workshop for natural disaster reduction continues to focus mainly on the cutting edge of understanding of the physical processes leading to natural hazards, resulting in improved prediction, especially during the IDNDR period, 1 January 1990 - 31 December 1999, we are to cooperate with all the concurrent IDNDR activities so that we contribute not only at the scientific frontier but also to facilitate other bilateral and multilateral activities. A prominent example is to cooperate with various U.S.-Japan Natural Resources (UJNR) activities especially with the UJNR Panel on Wind and Seismic Effects. Another example is that Japan-U.S. Symposium on Snow Avalanche, Landslide, Debris Flow Prediction and Control (JUSSLDPC) was held at Tsukuba, Japan, 30 September - 5 October 1991. This effort has been ongoing since 1980. The third UJST Workshop for Natural Disaster Reduction, Mt. Hood, Oregon, 7-11 September 1992, will enhance the JUSSLDPC effort by working together with them. Similarly the non-governmental U.S. National Committee for IDNDR is planning to have a U.S.-Japan earthquake symposium to formulate pilot projects between the two countries in the near future, to be carried out by non-governmental

resources. It is a commendable effort, and when there occurs much mutually enhancing confluence between the non-governmental organization (NGO) effort and government-to-government bilateral pilot project formulation (such as via UJNR and UJST), the true spirit of the IDNDR cooperation blossoms.

I especially wish to single out that there are very active ongoing bilateral disaster-mitigation activities under the umbrella of U.S. - Japan Natural Resources (UJNR) accord for over 20 years. The original agreement was signed off by Japanese Foreign Minister and U.S. Secretary of State. Two significant panels within UJNR for disaster mitigation are that of earthquake and severe storm mitigation technology as well as forest fire. Furthermore, at working level the two countries' Geological Surveys continue to have a functioning sister relationship; there also is much cooperation between Japan Land Agency, Ministry of Construction and the U.S. Federal Emergency Management Agency. All of these ongoing activities will be enhanced by the new thrust the UJST pursues in consort with IDNDR in the 1990s.

2. THE FIRST UJST WORKSHOP, 26-30 MARCH 1990

Under the auspices of the Earth Science and Environmental Task Group of the UJST Agreement, the first workshop had a running start from initial planning in January 1990 to its execution in March 1990. The workshop was effective and successful due to the high priority attached to the work by both sides and the desire to make a substantive start. Unsung heros include Chris Newhall, Will Prescott, and Dick Janda of USGS and Shoichiro Katayama, Yukio Hagiwara and Masayuki Watanabe of Japan. Sixteen Japanese and Nineteen Americans participated in the workshop. This workshop provided an initial opportunity to define cooperative activities in disaster reduction with emphasis on knowledge, and described specific U.S.-Japan projects that complement the ongoing activities. Three broad goals thus generated are as follows:

1. Better understanding of the physical processes leading to natural hazards, resulting in improved prediction.
2. Translation of scientific advance into improvement in the human condition, through better application of scientific knowledge to disaster reduction.
3. Better scientific understanding of the effect of global change on the frequency and severity of natural hazards.

The workshop developed specific recommendations for cooperative projects in the following four specialist groups:

Earthquake prediction
Volcanic eruption prediction
Typhoon prediction
Landslide prediction

The final report of the workshop has been reprinted by the Science and Technology Agency of Japan; I shall be delighted to supply you it upon request.

3. THE SECOND UJST WORKSHOP 23-27 SEPTEMBER 1991

Formulation of cooperative pilot projects attainable by 31 December 1999, the end of the IDNDR, was one of the major objectives for the second workshop. Also an added-on objective was the establishment of joint database for disaster reduction in cooperation with the Joint Database Development Task Group of the UJST Agreement. Thirty-six Japanese and seventeen U.S. scientists participated in the workshop at Karuizawa.

To flesh out the second goal of the general recommendations generated by the first workshop, which is "translation of scientific advance into improvement in the human condition, through better application of scientific knowledge to disaster reduction", the second workshop added two new groups of socioeconomics and human health, in addition to earthquakes, volcanoes, typhoons and landslide groups. Keynote addresses were given in socioeconomics and human health as well as on climatic change and its impact on natural disasters that requires innovative extensions to current natural disaster research. Furthermore, the typhoon group was renamed "severe weather

phenomena" group to include mecoscale storms as well as locally heavy rainfall. Four comprehensive recommendations were generated by the workshop. They are as follows:

1. Better understanding of the physical processes leading to natural hazards, resulting in improved prediction. Better understanding of the opportunities for reducing natural disasters through socioeconomic and medical sciences.
2. Translation of advances in science and technology into improvement in the human condition through exchange of information and better application of knowledge to disaster reduction.
3. Better scientific understanding of the effect of global change on the frequency and intensity of natural hazards.
4. To enhance progress toward [1]-[3] above, endeavor to develop joint databases and improve capabilities for information exchange.

During the intercessional period between April 1990 and August 1991, several prominent natural disasters have occurred (earthquakes in Iran and the Philippine in 1990; volcanic eruptions at Mt. Unzen in Japan and Mt. Pinatubo in the Philippines in 1991, and a cyclone disaster in Bangladesh in 1991). Both the U.S. and Japan dispatched medical, rescue, and engineering teams for reconstruction for the Iranian and Philippines disasters. Mt. Pinatubo volcano eruption was scientifically studied by both countries; thus resulting in having a special session to compare the scientific understanding of the volcanic eruptions at Mt. Unzen and Mt. Pinatubo at the second workshop. Though painful each natural disaster is a gigantic natural laboratory for us to understand the physical processes leading to the disaster and during the disaster, and post-disaster processes.

Also during the intercessional period, the UJST Agreement has established "volcanic panel" to specialize in volcanic hazard mitigation. The panel will start its own independent deliberation in near future; at the same time it will continue to contribute to the forum such as the joint database establishment, hazard mapping through geographical information system (GIS), and advancing its close tie with landslide and earthquake prediction groups. Furthermore, snow avalanche and landslide group too plans to establish its own UJST panel to sharpen its focus on its respective specialty; it will be a cumulative product of the group's U.S.-Japan cooperation that began in 1980.

To facilitate the second workshop we issued a 411-page preprint collection at the workshop, so that the workshop does not become mere a scientific symposium where the bulk of time was spent on oral presentations. We plan to follow similar format to facilitate the third workshop, Mt. Hood, Oregon, 7-11 September 1992. The workshop preprint collection has been reprinted by the Science and Technology Agency of Japan (Japan international Science and Technology Exchange Center, 1992).

Each individual group's reports are summarized and given in Section 5. Pilot projects recommended are listed and explained in the workshop proceedings. The workshop recommends that UJST secure necessary funds to carry out the pilot projects, so that our effort does not become a mere paper exercise. For example, two projects have given the magnitude of the fund needed to carry out the pilot projects; they are a cultural and cross-hazard study for earthquake and typhoon (hurricane) in Japan and the U.S., and the Tsunami Inundation Modeling Exchange (TIME) project at Tohoku University. As Goethe said: "Until one is committed, there is hesitancy, the chance to draw back, always ineffectiveness, ... boldness has genius, power and magic in it." Political commitment has been made by the two heads of the state of Japan and the U.S. How we would implement the pilot projects the workshop generated by our governments can learn a lesson from the recent successful 7-year Kuroshio Projects Japan and China have executed under the leadership of Science and Technology Agency with timely funding.

4. THE THIRD UJST WORKSHOP 7-11 SEPTEMBER 1992

Mt. Hood Timberline Lodge in Oregon is the venue of the third workshop for natural disaster reduction; it provides a natural laboratory to study volcanic activities, snow avalanche and landslide countermeasurers. Much intercessional, preparatory activities are going on to carry out the

workshop effectively. A core of the executive committee has been established to prepare for the workshop. Drs. Richard Janda of USGS Cascades Volcano Laboratory (established in 1980 following the eruption of Mt. St. Helens) and Fred Swanson of the U.S. Forest Service in Oregon are the local co-chairmen. Professor Dennis Mileti of Colorado State University and I comprise the rest of the executive committee.

The second workshop has recommended sharing of hazard mapping techniques used and planned to be implemented as a common third workshop theme among individual groups. Geographical Information System (GIS) applied within disaster reduction and elsewhere will be scrutinized; a plan is made to invite an expert to give a keynote speech on this regard. Interestingly, the IDNDR International Conference 1990 Japan, 27 September - 30 October 1990, too pointed out that some major work must be done "to prepare hazard maps and formulate land use plan which incorporates the viewpoint of disaster prevention." On the hazard mapping an attention is being made to invite practioners to the UJST working groups.

An additional common theme to be surfaced at the third workshop is the universality of hydrologic factors that induce natural disasters. The Pinatubo volcano calamity was magnified by an onslaught of a typhoon over the volcano, which produced much volcanic ash-mud flow upon the anthrosposhere The typhoon energy was converted into damaging mud flow of phenomenal size. Snow avalanche and ice disasters also share common hydrologic factors. Receding glaciers due to global warming too can be considered an aspect of future disaster mitigation concerns.

A field trip is planned to study ecological means to combat landslides at the Andrews Experimental Forest in Oregon. It relies on soft engineering means in contract to commonly seen hard engineering practice where dams and concrete walls are built to protect human habitat. Ecological recovery at the site of Mt. St. Helens volcanic eruption too will be visited.

Since each UJST workshop for disaster reduction is a precious opportunity to advance our knowledge to mitigate natural disasters, pertinent private sector participation, especially from the academic and the user communities, is warranted so that both Japan and the U.S. go forward to make significant progress on preparedness issues.

5. PRODUCTS OF THE SECOND WORKSHOP

For the 2nd workshop two new working groups were added based on the 1st workshop recommendation (socioeconomics and human health groups). Thus the workshop spent the bulk of its time discussing progress toward the achievement of the workshop goals by the following six working groups:

Volcanic eruptions
Earthquakes
Severe weather phenomena
Landslides
Socioeconomics
Human health

In addition the workshop was charges by the UJST liaison and working levels meetings, Tokyo, 16-19 July 1991, to work on the joint database establishment between Japan and the U.S.

Three keynote addresses were given at the onset of the workshop to broaden and integrate the group deliberations. The topics covered are the casual relationship between the global change and natural hazards, socioeconomic issues in natural disaster reduction, and the role of epidemiology in natural disaster reduction.

Data management initiatives were developed by each of the working groups. In particular, participants identified the need for improved GIS capabilities.

5.1 Volcano group

The volcano group proposes 10 projects that are current, practical to start within the next few years. They are (1) volcanic hazard and risk mapping; (2) low-frequency volcanic earthquakes and volcanic tremor; (3) processes leading to volcanic eruptions; (4) quantitative characterization of eruptions in progress; (5) dynamics of dome building and related pyroclastic flows; (6) data acquisition system for volcano-genetic vibration; (7) observation and monitoring of submarine volcanoes; (8) volcanically induced melting of snow

and ice; (9) joint observation of selected Japanese and U.S. volcanoes; and (10) coordinated assistance to developing countries.

The volcano group is to become the first UJST scientific panel entitled Volcanic Disaster Prevention Panel; the new panel's charge includes dissemination and application of volcanic hazard information in addition to basic investigations of processes, both volcanic and volcano-hydrologic, contributing to volcanic disasters. The volcano group featured a special session to discuss the findings of the recent Mt. Unzen and Pinatubo eruptions. At the 3rd workshop, the volcano group will devote mainly on the substantive reports of new methods to elucidate the processes toward disaster prevention and hazard mapping by GIS.

5.2 Earthquake group

The earthquakes group covers both earthquakes and tsunamis; the group also gives recommendations in mitigation policy, for the advancement of scientific frontier must put into good use. On earthquakes, the detection of crustal movements is now greatly enhanced by space-based geodetic systems, such as Global Positioning System (GPS), Very Long Baseline Interferometry (VLBI) and Satellite Laser Ranging (SLR). Also continuous monitoring for deformation is essential to detect short-term precursors of earthquakes and volcanic eruptions, which must be coupled with evaluations of anomalies in continuous observations. Deep drilling and borehole measurements, both geophysical and geochemical, in seismically active areas is warranted to supplant the ongoing surface observations.

Tsunami is a Japanese word for destructive, large ocean waves caused by underwater earthquakes or volcanic eruption and it propagates ocean-wide. Much theoretical works, such as numerical models for forecasting fare-field tsunami as well as the Tsunami Inundation Modeling Exchange (TIME) project, which Japan has been developing, are recommended to be pursued in consort with both the field measurements of tsunami initial profile for submarine earthquakes and the development of common database and maps of tsunami disasters; the working group strongly endorses to establish a satellite communication system, both voice and data channels, to transmit seismic waveform data to strategically located ground stations in an around the Pacific basin, and to use the PEACESAT system of the U.S. for this purpose.

To mitigate the loss of life and property from natural disasters by the judicious use of scientific knowledge emerging, a comparison of current mitigation policy and programs between Japan and U.S. is recommended to be carried out in the areas of (1) education and awareness; (2) preparedness and response; (3) seismic construction provisions for new and existing buildings; and (4) land-use planning practice. The earthquake group strongly feels that both Japan and the U.S. serve the world community through this bilateral agreement by joint research and monitoring activities in the third world countries, upholding the spirit of the International Decade for Natural Disaster Reduction (IDNDR), 1990-1999, transcending national boundaries, for big earthquakes happen at many places in the world and all of these events must be scrutinized scientifically and their impacts upon humanity minimized.

5.3 Severe storms group

The typhoon group was renamed "Severe Weather Phenomena Including Typhoon and Local Heavy Rains Group" (Severe storms group from now on). The group now encompasses severe local storms including heavy rainfall, floods, and hydrological aspects as well as disaster preparedness. Hydrological studies interlink volcano, landslide, and severe storms in reference to physical process studies. For instance when Mt. Pinatubo erupted a typhoon passed over, thus causing much damages to the communities nearby by volcanic ash flow. The predictive skill of the typhoon is gradually improving on the basis of the advancement in observing systems, data processing systems and numerical prediction models. Further improvement will be accelerated by cooperation between two countries through exchange of technical information in numerical modeling, ongoing and future satellite observations including new measurement missions of the TRMM (Tropical Rainfall Measurement Mission). Basic typhoon research projects proposed includes the development of diagnostics schemes for determining horizontal wind distribution in tropical cyclone intensity; understanding the mechanisms of typhoon movement in relation to asymmetric typhoon structure and environmentally large-scale

flow, and developing a more sophisticated convention parameterization scheme for moist convection. The possibility of a change in the numbers and intensities of tropical cyclones due to global climate change is of great concern to many coastal and sea-going nations. Research should be undertaken to investigate the effect of global climate change on tropical cyclone activity using a sophisticated numerical model.

Severe local storms including heavy rainfall and floods are affecting both countries continually. On account of recent technological advances in atmospheric and hydrospheric measurements, we can now link our emerging technological knowledge to assess and mitigate hazardous hydrologic disasters such as floods, flash floods, storm surges, heavy snow, freezing rain, lightening. The group recommends that joint efforts be undertaken to incorporate new measurements by satellite remote sensing, new lightening detection system, high-resolution rain-gauge networks, and polarization measurements of hydrometer particle electric fields. They greatly help improve hydrometerological model to better prediction of severe local storms and floods.

As other working groups recommend, the severe storms group considers disaster preparedness issue essential, continual and evolutionary; the public use of and reaction to severe storms warning must be timely and effective. The group as a first step in the continuing dialogue and cooperation between Japan and U.S. recommended a meeting of severe weather experts in Norman, Oklahoma, during the STORM-Fronts Experiment Systems Test (STORM-FEST), 1 February - 15 March 1992, to observe and work with the novel instrumentation and experimental systems deployed, which include NEXRAD Doppler radars, profiler network, new automated surface observation network, research aircraft and special soundings. This meeting was held during 8-10 March 1992 to plan for the 3rd UJST workshop for natural disaster reduction, Mt. Hood, Oregon, 7-11 September 1992.

5.4 Landslide group

The landslide research communities of both Japan and the U.S. have been working together since 1980. Japan is a recognized leader in research facility utilization, and the U.S has the unequalled natural laboratories. Ongoing cooperation include simulation and field observations of slope processes of snow avalanches, landslides, debris flow and stream channel processes. Physical process studies jointly undertaken are slope failures and sediment transport, rainstorms that trigger landslides and debris flow, and that associate with extensive volcanic cones.

The UJST separately supported a Japan-U.S. symposium on snow avalanche management, landslide prediction and control under the old UJST agreement at Tsukuba, Japan, 30 September -5 October 1991, where the snow avalanche and landslide specialists of the two countries exchanged their most up-to-date research efforts. Comprehensive future collaboration plans itemized in the landslide group report encompasses (1) landslide hazard assessment and information exchange assisted by experimental study of mechanism of landslide initiation and GIS (Geographic Information System) technology to overlay stability attributes; (2) landslide hazard mitigation by monitoring triggering mechanism and preparing hazard maps; (3) mechanism studies on the transformation of landslides to debris flows; (4) debris-flow hazard assessment and mitigation by better understanding of physics of flow and by preparion of hazard maps; (5) initiation of movement and mobility by snow and ice by studying its dynamics in both laboratory and field settings; (6) research on subaqueous mass movement; (7) flood hazards arising from landslide dams and sedimentation within by exchanging data on well-documented cases and educating public officials and population to long-term hazards; (8) elucidating the mechanism of earthquake-induced landslide; and (9) impact of the climatic change on landslides, including receding glaciers triggering new landslides.

5.5. Socioeconomic group

The socioeconomic group recommends the adoption of a cross-cultural approach to socioeconomic studies of natural disasters that will enhance both robustness and efficiency of our societal disaster prevention system worldwide. The group recommends a pilot project between the two countries; it is a cross-cultural and cross-hazard comparison for earthquake and typhoon disasters. Already considerable amount of data exists in both countries. Since the ultimate goals of social scientific investigations of natural disasters is to produce knowledge to enhance the adoption of effective countermeasures, such as mitigation and preparedness, by people at all levels of human aggregation, including individuals, families,

governments, and businesses, factors considered include elements of culture, experience, risk communication, conditions and perceptions that collectively form risk perception. All of these factors then are fed to the ultimate risk management for both mitigation and preparedness. The group proposes to obtain representative samples of 500 to 600 respondents via telephone interviews from four study sites, Tokyo, Nobi Plain in Aichi-ken, northern or southern California and South Carolina. A planning meeting for the pilot project in 1992 will construct the interview schedule and standardized coding procedures. The project proposed has a duration of two years.

5.6 Human health group

The human health group has had the benefit of working together in the third world countries providing medical and health reliefs following natural disasters. Japan and the U.S. have shown leadership and cooperation to improve disaster medicine preparedness and response. Sixteen recommendations prepared by the group fall under the three categories of (1) improved disaster preparedness; (2) response and operation cooperation, and; (3) disaster medicine research. Specific recommendations include the development of disaster medicine and disaster epidemiology centers at academic institutions; development of their curricula and practical textbook on disaster medicine based on the expertise and experience of the two countries; development of methods of rapid and accurate health needs assessment in disaster situations; development of standardized triage system; conducting joint workshops on focused topics, such as trauma surgery; tropical medicine, and epidemiology of disasters; cooperative research in crush syndrome and infectious diseases; joint database development; human health technology transfer to developing countries; taking a leadership role in carrying out the five priority demonstration projects recommended by the IDNDR Scientific and Technical Committee, which include improved hospital disaster planning in hurricane-prone regions and health hazard mapping. It is also important to consider the linkage between climate change and human health recognizing that climate change would alter the ecosystems of many disease-carrying vectors and agents, such as viruses, bacteria, parasites, plants, mosquitoes, snails, and increased heat-related illnesses such as heat stroke and death and injuries from coastal flooding.

6. CONCLUSIONS

Much progress has been made by the two workshops of 1990 and 1991. As the third year of IDNDR goes on now, execution, rather than planning of pilot projects; specific cooperation, rather than general; knowledge synthesis and application of emerging knowledge to prepare for and mitigate natural disasters loom and guide the two countries' joint endeavor. The third workshop at Mt. Hood, Oregon, 7-11 September 1992, will focus on hazard mapping by the use of GIS (Geographic Information System) and other means to chart various hydrologic factors, earthquakes and volcanic eruption prediction pattern to prepare for natural disasters yet to happen. Defense never rests, and the best of two countries' academic and public talent and government agencies continue to work together for the welfare of humanity; both UJNR and UJST efforts are to enhance our collective quest to reduce natural disaster damages the best way we can.

7. ACKNOWLEDGEMENTS

The bulk of my text came from the executive summary and the introduction I was asked to write by the 2nd UJST workshop to prepare its proceedings. I am responsible for interpreting and summarizing adequately the six group-deliberations the 53 workshop participants at Karuizawa laboriously developed. Mr. Keiji Doi of the Science and Technology Agency has been my constant co-worker to issue the 2nd workshop proceedings; I am most grateful.

8. REFERENCES

1. Bergner, T.A. (1991). "United States Federal Subcommittee for Natural Disaster Reduction, History and Perspective." Preprints for the Second Workshop on Natural Disaster Reduction under U.S.-Japan Science and Technology Agreement, Karuizawa, Nagano, Japan, 23-27 September 1991, Science and Technology Agency, Prime Minster's Office, Tokyo, pages 211-220.

2. Japan International Science and Technology Exchange Center (1992). "Proceedings of the Second Workshop for Natural Disaster Reduction, Japan-United States Science and Technology Agreement, Karuizawa, Nagano, Japan, 23-27 September 1992", Science and Technology Agency, Tokyo, 520 pages.

Theme I

Wind Engineering

Flutter Characteristics of Super Long-Span Suspension Bridge

by

Koichi Yokoyama[1], Tokida Kanazaki[2], and Masahiko Yasuda[3]

Abstract

Since the collapse of the old Tacoma Narrows Bridge, aerodynamic stability has been verified through wind tunnel tests at the design stage of flexible bridge structures. In Japan verification of aerodynamic stability of suspension bridges has generally been carried out through spring-mounted rigid model tests using a section model (section model tests). As for the test conditions of a section model test, primary torsional oscillation is selected as well as vertical bending oscillation, whose mode shape is similar to that of torsion. This wind tunnel testing method is based on the fact derived by F.Bleich that oscillation of a three-dimensional structure like a long-span suspension bridge can be treated as that of a rigid section model under the assumption that wind force is uniform along to the longitudinal direction and that both mode shapes for vertical bending and torsion are almost the same.

However, the coupled flutter observed in the full bridge model wind tunnel tests of the Akashi Kaikyo Bridge is entirely different from the general concept and the mode shape of vertical bending motion was very much complicated. This phenomenon implies that there is a limitation for the verification method of the aerodynamic stability through section model tests.

This paper shows characteristics of the coupled flutter observed in a smooth flow test and discusses problems of the current verification method.

Keywords : Aerodynamic stability,
Suspension bridge, Coupled flutter,
Full bridge model test, Wind tunnel test

1. Introduction

The Akashi Kaikyo Bridge is now under construction between Kobe-city and the Awaji Island. The bridge is a super long-span suspension bridge with total length of 3,910 meters. The main span length of 1,990 meters is far beyond that of the current world longest suspension bridge, the Humber Bridge. General view of the Akashi Kaikyo Bridge is shown in Figure-1.

The relation between span length of suspension bridges and principal frequencies or lateral deformation during a design storm is illustrated in Figure-2. The longer span length becomes, the lower frequencies become and the bigger deformation becomes. Therefore, it should be recognized that it is far more difficult to secure the aerodynamic stability of the Akashi Kaikyo Bridge than that of ordinary suspension bridge and that it is important to estimate the deformation by wind load more accurately than ever.

There are three kinds of wind tunnel testing methods to verify aerodynamic stability of a suspension bridge, ① section model test, ② taut strip model test, and ③ full bridge model test. It is said that full bridge model tests are most reliable if models are well simulated not only in shape but also in dynamic properties.

Accordingly, wind tunnel tests using a full bridge model of the Akashi Kaikyo Bridge were planed and are now in progress at the large wind tunnel in PWRI. The main purpose of the test is to verify the safety more accurately. Therefore, it is required that shape and elasticity of the model should be similar to the prototype bridge as much as possible.

Tests of completed bridge in a smooth flow and in a boundary layer turbulent flow have already been completed, and tests for different wind direction and for an erection stage are in progress .

This paper shows that the aerodynamic stability of super long-span bridges cannot be estimated through spring-mounted rigid model tests only, focusing on the coupled flutter observed in the smooth flow test.

1) Dr.Engrg., Head, Structure Division, Structure and Bridge Department, Public Works Research Institute, Ministry of Construction
2) Ms.Engrg., Senior Research Engineer, ditto
3) Ms.Engrg., Head, First Design Division, Design Department, Honshu-Shikoku Bridge Authority

A series of tests are being carried out as "A cooperative research on wind resistant design method for super long-span suspension bridges" between the Public Works Research Institute and the Honshu-Shikoku Bridge Authority.

2. Purpose of the study

In Japan, spring-mounted rigid model tests are generally carried out to verify the aerodynamic stability of a long-span suspension bridge. The fact that oscillation of three-dimensional structures like a suspension bridge can be treated as that of rigid section model was derived by F.Bleich[1] under the assumption that wind force is uniform along to the longitudinal direction and that both mode shapes for vertical bending and torsion are almost the same. This assumption is said to be adequate to completed suspension bridges except such a suspension bridge as partially installed with sound-barrier. This assumption is a base that the aerodynamic stability of completed suspension bridges can be verified through spring-mounted rigid model tests, in which the lowest torsional and vertical bending frequencies are simulated. The modes for both oscillation are usually first symmetric.

In the results of full bridge model wind tunnel tests of the Akashi Kaikyo Bridge, however, counter-evidence against the assumption is clearly recognized.

Here, summarized are analysis of the results and problems of existing estimation method through the section model test.

3. Test conditions

The general layout of the large wind tunnel facility is shown in Figure-3.

Properties of a smooth flow in this wind tunnel (width: 41 meters x height: 4 meters) were measured as follows,

a)Turbulence intensity : less than 0.5 %

b)Variation in mean speed : less than 3 %

Consequently, uniformity of the flow is sufficiently satisfied.

The full bridge model was fabricated with a geometrical scale of 1/100, having a total length of 40 meters. The model is shown in Figure-4. As design considerations were reported last year[2], Table-1 shows natural frequencies of the model comparing with the required values.

Froude number similitude has to be satisfied in wind tunnel tests of the full suspension bridge model, because gravitational effects are dominant. This means that ten times of wind velocity in the wind tunnel is that for prototype bridge and that the required natural frequencies are ten times of those of prototype. Natural frequencies measured at dynamic tests of the model have a good agreement with the required values, which shows that the model was fabricated with good accuracy.

4. Results of full bridge model tests

The followings are results of full bridge model tests of basic design with a cross section of a stiffening girder shown in Figure-5. The results are reported with those of section model tests.

4.1 Static torsional deformation

Relation between wind velocity and static torsional deformation at the mid-point of center span is shown in Figure-6. At wind velocity of 6 m/s, that is equivalent to design wind speed of 60 m/s for the prototype bridge, torsional deformation of -2 degrees was observed. This deformation was far beyond that of ordinary suspension bridge. Aerodynamic sensitivity of this cross section to the attack angle was well understood through the section model tests that had already been carried out. These facts indicate that the first assumption by Bleich is not yet applicable to this model.

In addition, through the tests and analysis, it reveals that major cause of torsional deformation is not the aerodynamic moment but torque from inclined suspender rope tension caused by the difference of lateral deflections between cables and a stiffening truss (see Figure-7).

In Figure-6, there is a difference between the torsional deformation of the model and analytical value of the prototype bridge. The difference is mainly due to restrictions in fabrication of the model. For example, ① longitudinal stiffness of towers cannot be simulated, ② apparent fixing points of suspender ropes are higher than analytical model because of the stiffness of fixing device, and ③ torsional stiffness declines when V-shape springs to simulate the stiffness of a stiffening girder are deformed by lateral deflection.

The aerodynamic performance of the model should be modified considering the difference of torsional deformation in flutter analysis.

4.2 Flutter characteristics

1) Change of damping

Relation between wind speed and logarithmic decrement is shown in Figure-8. The damping of torsional mode was settled up until wind speed of 7 m/s, and it declined drastically beyond 7 m/s. Wind speed of 8.5 m/s (85 m/s for prototype) was flutter onset velocity, where damping changed from positive to negative. Here, the torsional oscillation was not pure torsion observed in windless condition, but coupled oscillation with vertical bending mode, which was observed from comparatively low wind speed.

Damping of pure vertical bending motion increased drastically along wind speed.

In case of the section model test of the attack angle of 0 degree, damping decrease was observed from wind speed of 2 m/s, and flutter occurred at 6 m/s.

In wind tunnel tests of suspension bridges, onset velocity of flutter is most noticed. The onset velocity of the section model test and full bridge model test cannot be compared directly because of the effect of torsional deformation of the full bridge model, so disagreement of onset velocity obtained from each test is a matter of course.

2) Change of natural frequency

Change of natural frequencies by aerodynamic force along with wind speed is shown in Figure-9. Frequency of torsion was decreasing as wind speed became higher, and at onset velocity the frequency became 90 % comparing with that in windless condition. On the other hand, frequencies of bending motion were scarcely decreasing.

This tendency of natural frequencies is almost same as that of section model tests.

3) Movement of rotation center

On the flutter motion at the wind speed of 8.5 m/s, movements of rotation center were calculated from amplitude of windward and leeward cords. Figure-10 illustrates the position of rotation center measured along bridge axis. The rotation center lay on the windward side at the midspan, on the leeward side at quarter point of center span, and on the windward side again at the middle of side spans. Movement of rotation center must be uniform along the bridge axis according to the assumption by Bleich, but it clearly varied.

Flutter which was observed in the section model test was also bending-torsion coupled one in which the rotation center lay on the windward side, and the behavior was almost similar to that of the midspan.

4) Modes of flutter

Torsional and vertical bending response at every 1/8 natural period are illustrated in Figure-11. In the same figure, torsional and vertical modes in windless condition are also indicated. As for the torsion, flutter mode was the same as the first symmetric one in windless condition. As for the vertical bending, however, flutter mode did not agree with any single mode in windless condition, but very complicated.

Moreover, there was a phase angle difference of 20 degrees between the vertical and torsional component of the motion at midspan. This difference of phase angle agrees with the fact that rotation center lay on the windward side at the midspan or at side spans.

Rotation center lay inside of girder width at the midspan because torsional motion was dominant, but lay outside of the girder width at side spans because vertical motion was dominant there.

At around quarter point of center span, however, a difference of phase angle was approaching to 180 degrees. Though this agrees with the fact that the rotation center lay on the leeward side, variety in movement of rotation center is opposed to the assumption by Bleich.

5. Comments on verification method of aerodynamic safety

The full bridge model wind tunnel tests of the Akashi Kaikyo Bridge provided counter-evidence contrary to the Bleich's assumption that aerodynamic stability of three dimensional line-like structures such as suspension bridges can be predicted by spring-mounted rigid model test using a section model, which has only two-degree-of-freedom. For example, torsional mode during flutter is the same as the first symmetric mode in windless condition, but vertical mode is similar to neither the torsional mode nor the first symmetric vertical mode in windless condition. Vertical mode during flutter is very much complicated. By this reason, it is probable that flutter onset velocity of the prototype bridge cannot be predicted well from section model tests.

Next, the causes of this complicated coupled flutter are discussed referring to the assumption by Bleich.

(1) The assumption, that aerodynamic force is uniform along to the bridge axis, is seriously disturbed by large torsional deformation. In other words, relative angle of attack is largely varied along the bridge axis by the static deformation.

In case of ordinary suspension bridges, which have a center span of about 1,000 meters, static torsional deformation was negligibly small to estimate the aerodynamic stability of the bridge. By the test and analysis, however, the possibility to induce a bigger deformation than ever is indicated in case of a super long-span bridge, which has center span of about 2,000 meters. Therefore, the effects of torsional deformation on the aerodynamic stability must be sufficiently considered.

(2) The assumption, that the torsional and vertical mode in windless condition are almost similar, is applicable to the center span, but is not to side spans as shown in Figure-11. Torsional component is small at side spans comparing to vertical component.

These two factors are thought to be causes that coupled flutter of the full bridge model was different from that expected through section model tests, and vertical motion was complicated along the bridge axis.

In addition, it was major cause of difference between test results that the flutter of the Akashi Kaikyo Bridge was not a stall flutter (single-degree-of-freedom flutter of torsion), which is observed for ordinary truss stiffened suspension bridge, but a coupled flutter.

Hereafter, planed is recently proposed flutter analysis using measured flutter derivatives and some vertical modes with primary torsional mode in windless condition. By analysing the cause of difference between the test results and by understanding the effects of each cause, limitation of the section model test will be made clear, and it will become possible to predict aerodynamic stability of super long-span bridge more precisely than ever.

6. Concluding remarks

In the results of wind tunnel tests using a full bridge model of the Akashi Kaikyo Bridge, coupled flutter of complex mode shape was observed. Such flutter has never been predicted from section model tests and onset velocities obtained from both tests do not agree well.

The results implies that it is difficult to predict onset velocity of flutter for super long-span bridges only through the section model test. In this sense, the meanings of full bridge model tests are significant.

The causes of a complex mode flutter are thought to be as follows:

(1) Aerodynamic force acting on the girder is not uniform along bridge axis because of big torsional deformation of the girder.

(2) The difference in primary mode shape between torsion and vertical bending is comparatively big.

All of these factors originate in the span length of the Akashi Kaikyo Bridge.

Hereafter, the estimation method of the aerodynamic stability for super long-span bridge will be proposed by establishing the theory to explain the flutter performance of the full bridge model.

References

1) Bleich F., et al.: The Mathematical Theory of Vibration in Suspension Bridge, Dept. of Commerce, U.S. Gov. Print Office, 1950

2) Yokoyama K., Kanazaki T. and Yasuda M., Boundary Layer Wind Tunnel Study on Full Aeroelastic Long Span Bridge Model, Proc. 23rd Joint Panel Meeting on Wind and Seismic Effects, UJNR, 1991.

3) Miyata T.,Yokoyama K.,Yasuda M.,Hikami Y. Akashi Kaikyo Bridge:Wind effects and full model wind tunnel tests, Proc. of the first international symposium on aerodynamics of large bridges, Copenhagen, 1992

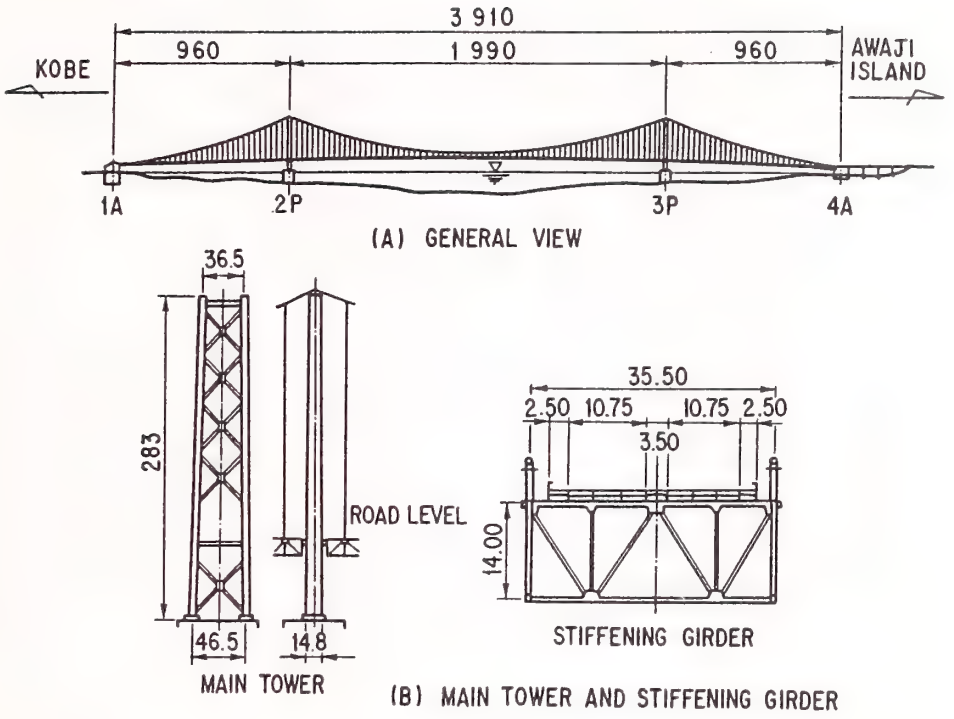

Figure—1 General veiw of the Akashi Kaikyo Bridge (unit:m)

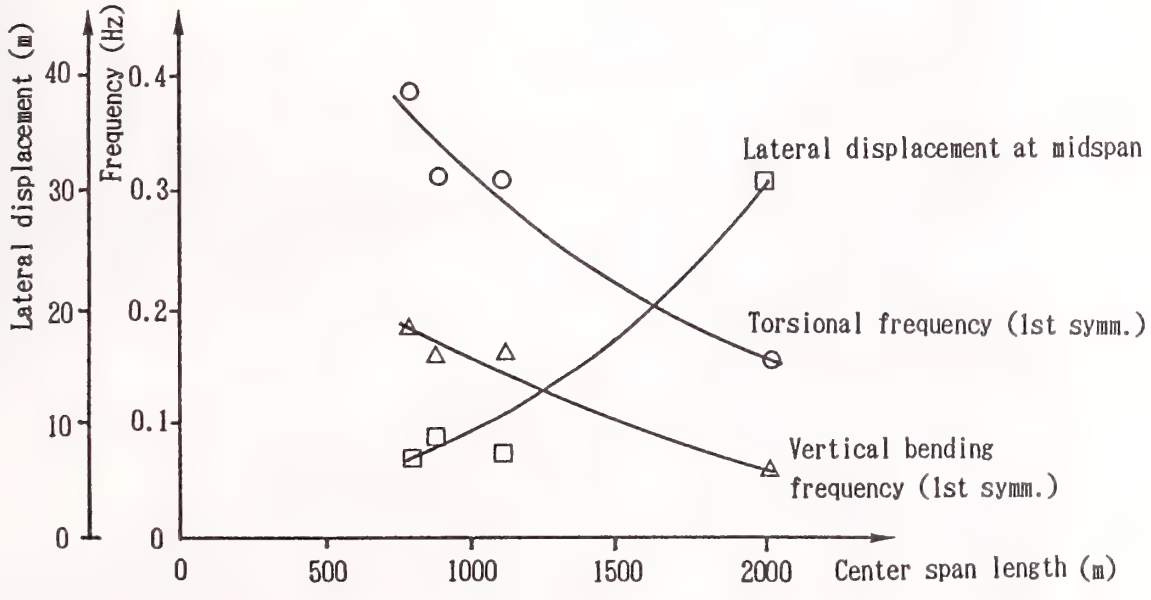

Figure—2 Structural properties of long-span bridges

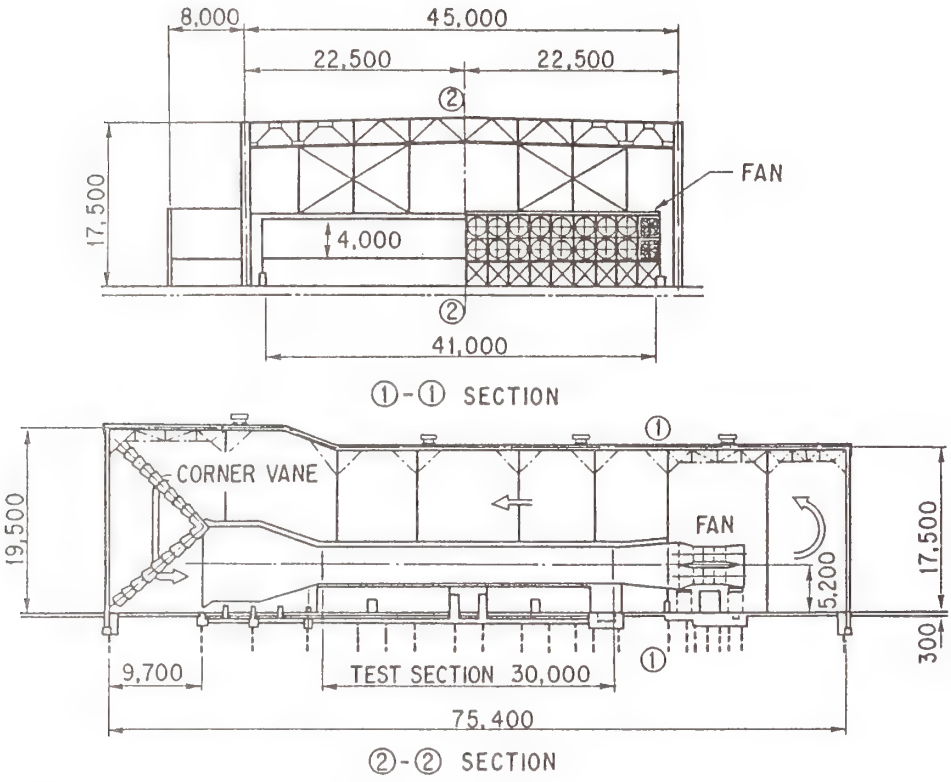

Figure—3 General layout of
large boundary layer wind tunnel (unit:mm)

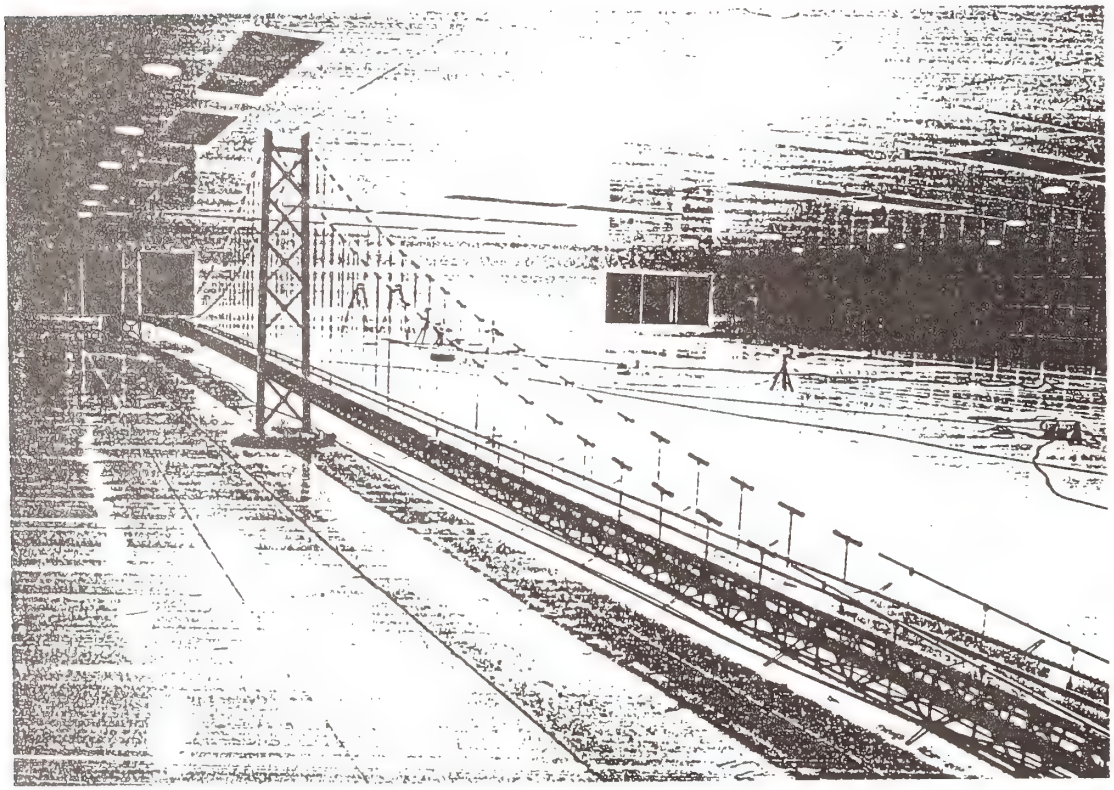

Figure—4 Full bridge model of the Akashi Kaikyo Bridge

Table—1 Natural frequency of the full bridge model

No.	Mode	frequency	
		required	full model
1	1st symm. bending 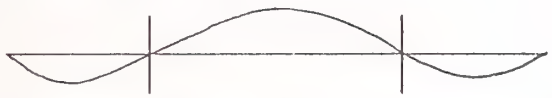	0.638 Hz	0.647 Hz
2	1st anti-symm. bending	0.745 Hz	0.757 Hz
3	2nd anti-symm. bending 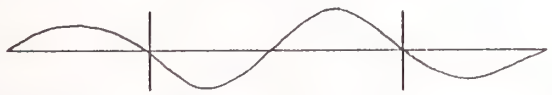	0.835 Hz	0.855 Hz
4	2nd symm. bending	1.213 Hz	1.245 Hz
5	1st symm. torsion	1.497 Hz	1.557 Hz
6	1st anti-symm. torsion	2.077 Hz	2.075 Hz
7	1st symm. lateral	0.387 Hz	0.391 Hz
8	1st anti-symm. lateral 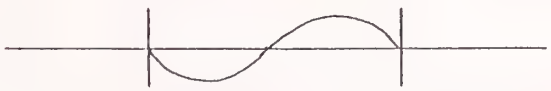	0.775 Hz	0.781 Hz

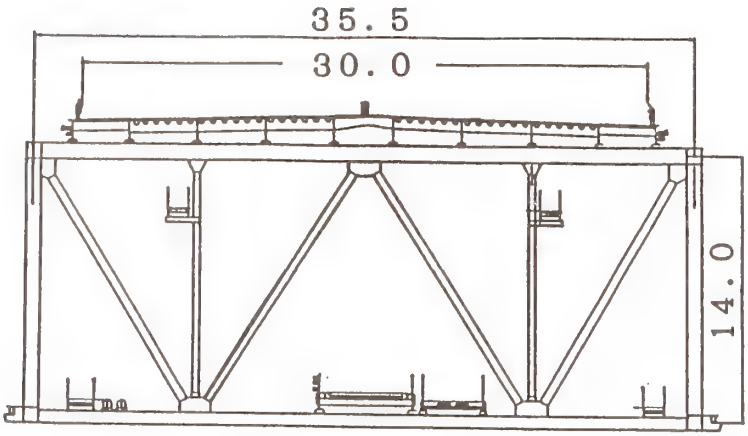

Figure—5 Cross section of truss stiffening girder (unit:cm)

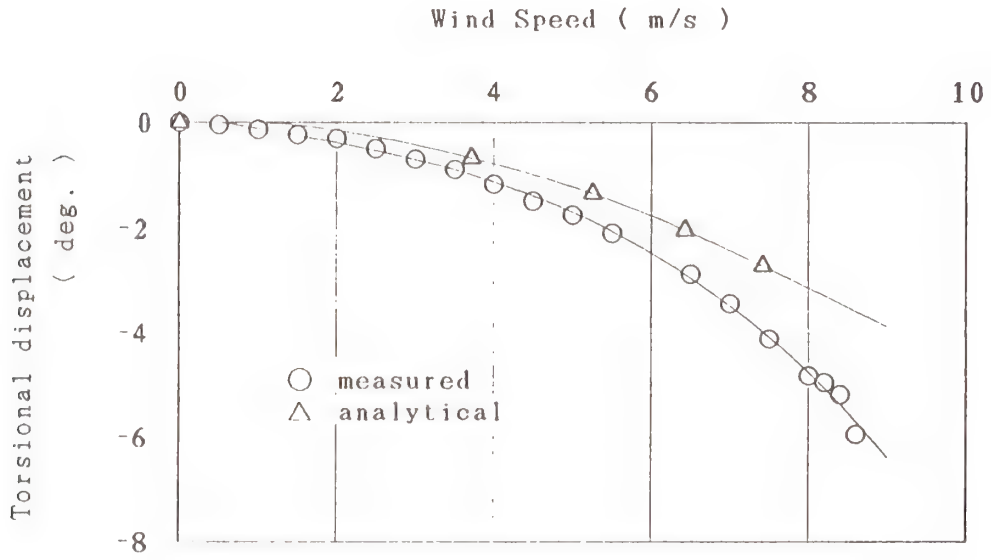

Figure—6 Torsional deformation by wind (midspan)

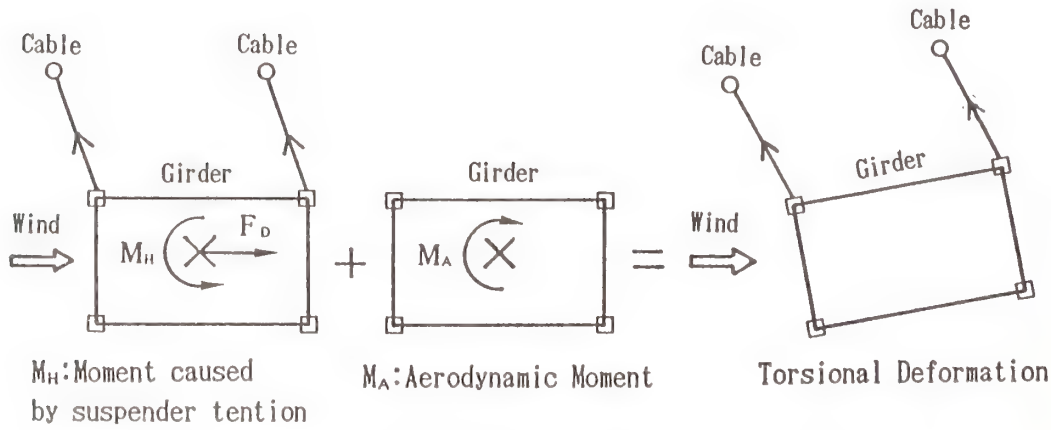

Figure—7 Moment caused by lateral deflection

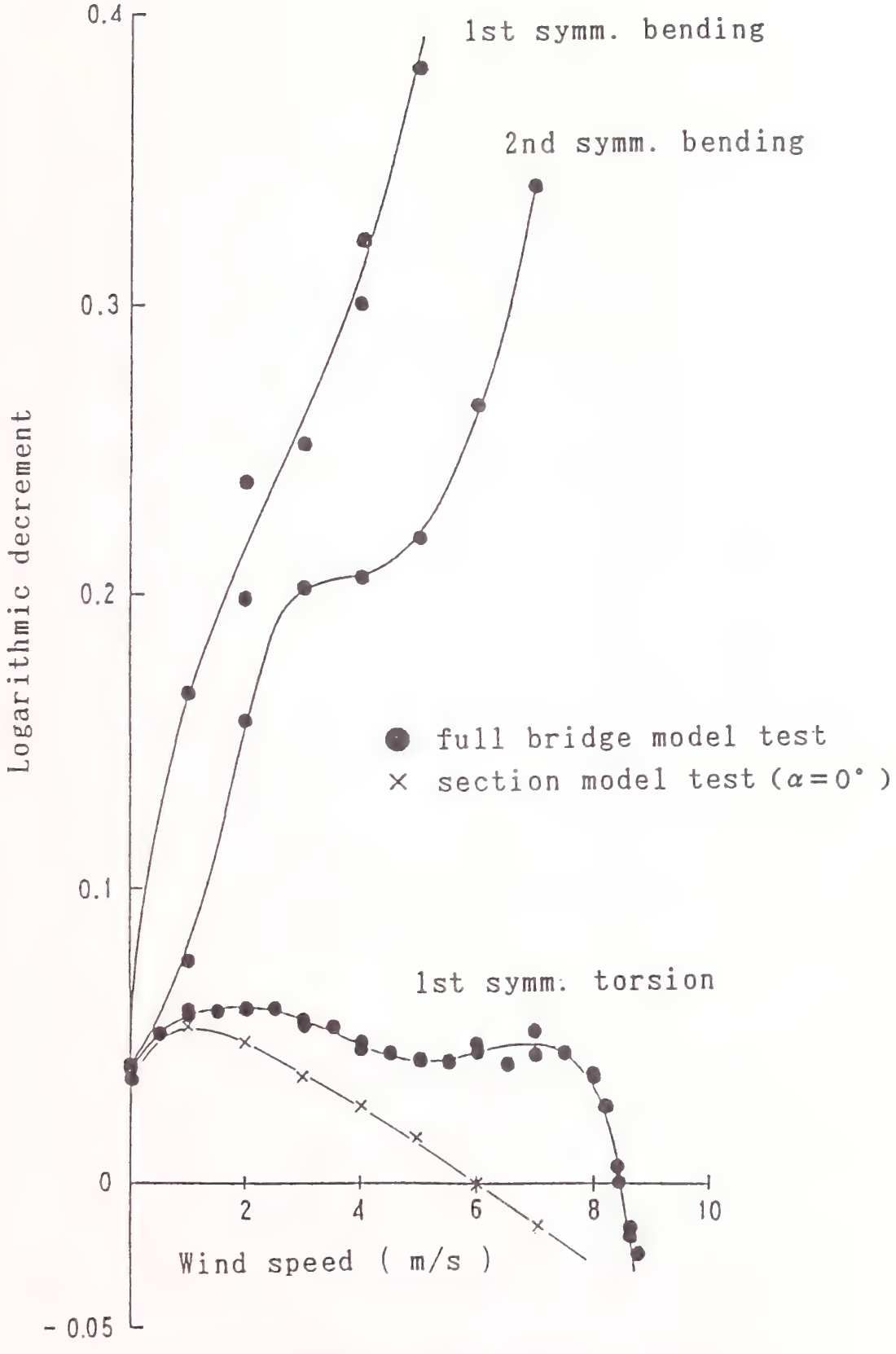

Figure—8 Change of aerodynamic damping

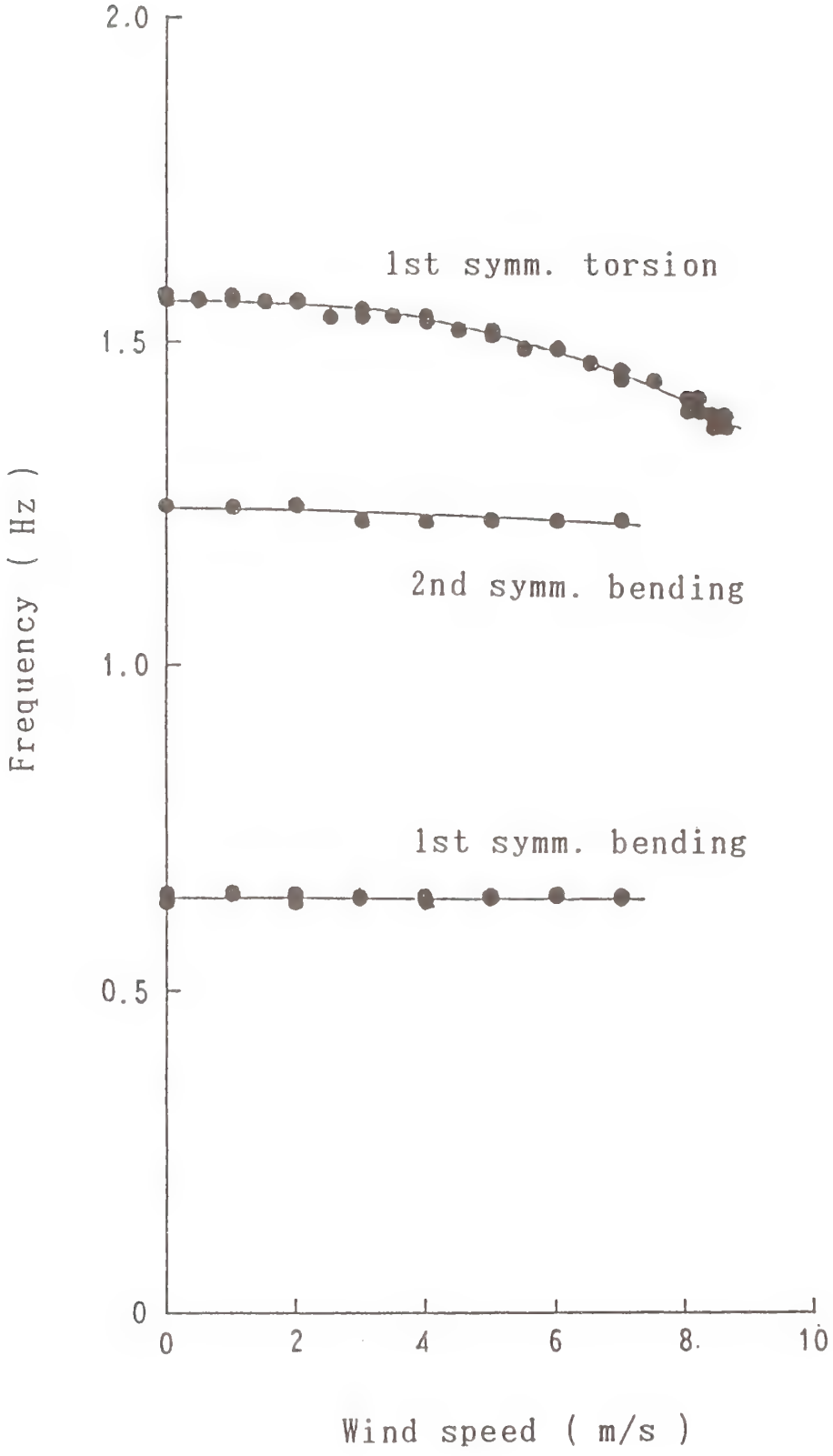

Figure—9 Change of response frequency

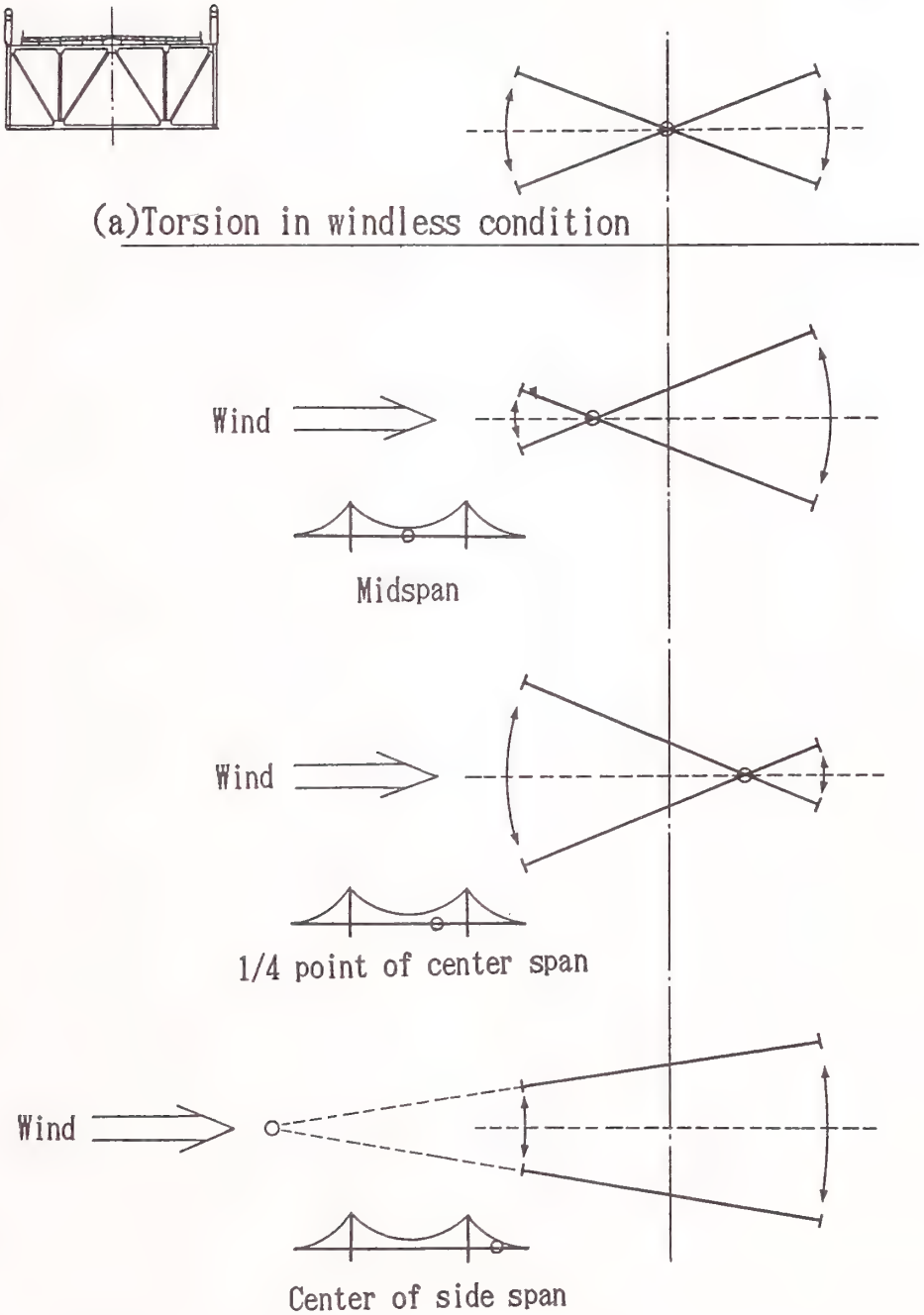

Figure−10 Movement of rotation center

(a) 1st symm. torsion

(b) 1st symm. bending

(1) Mode shapes in windless condition

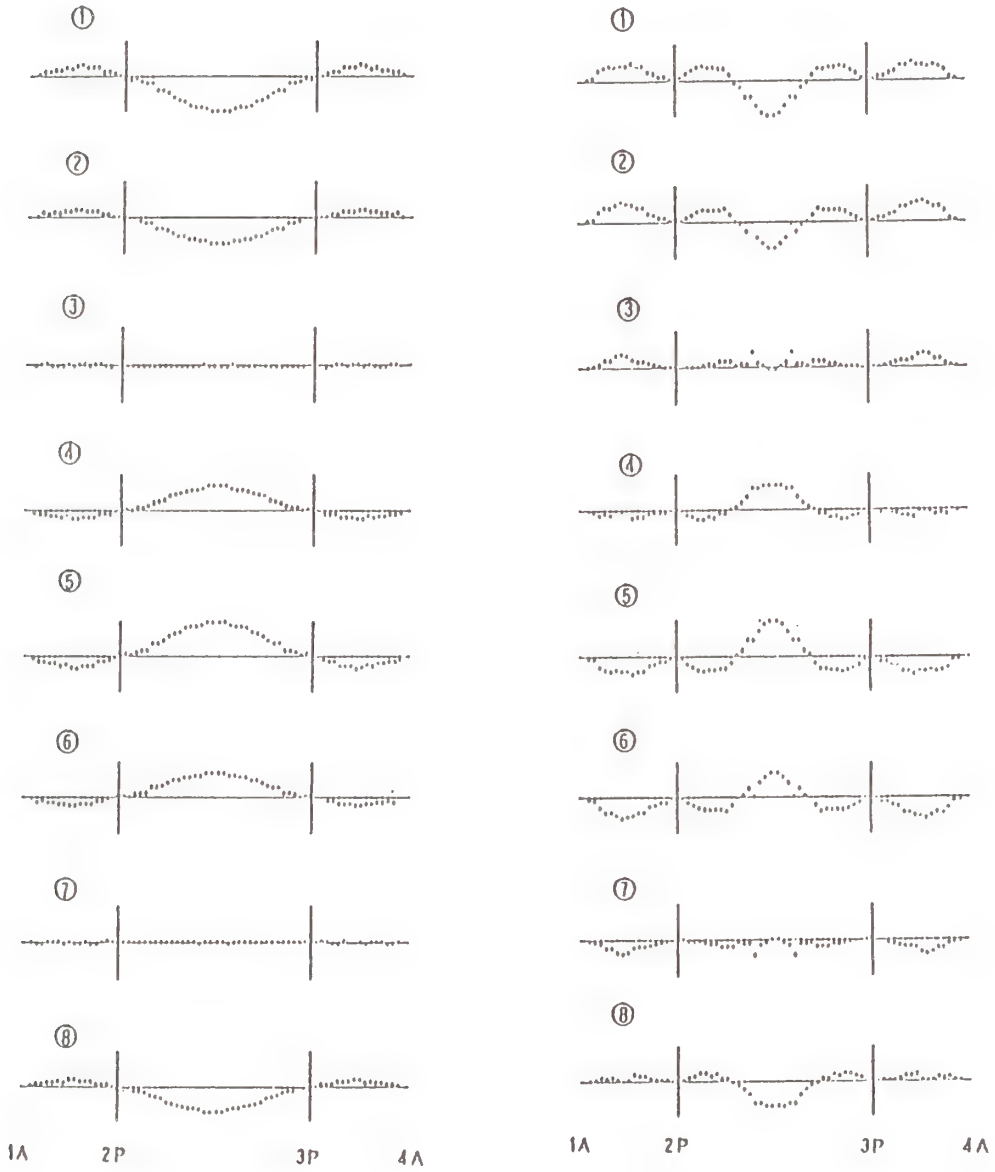

(a) torsion

(b) vertical bending

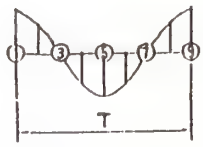

one cycle

(2) Response during flutter

Figure—11 Response of girder in one cycle during flutter

Predicting Wind Forces Using Computer Simulation of Air Flow Around Bridges

by

Okey Onyemelukwe* and Harold Bosch**

ABSTRACT

The finite-difference procedure has been used to solve the non-conservative form of the two-dimensional, unsteady, incompressible, laminar, Navier-Stokes equations in a body-fitted curvilinear coordinate system. In order to avoid stringent numerical stability restrictions that lead to excessive computation time, an implicit solution scheme was employed. The finite-difference mesh was generated by using an automatic grid generation technique, based on the boundary-fitted curvilinear coordinate system suggested by Thompson et al. (1977). The advantage of using the boundary-fitted coordinates being that the irregular body geometries inherent in bridge shapes can be handled more generically, than by the use of the more familiar rectangular cartesian coordinates. Solving the primitive variable form of the Navier-Stokes equations directly yields the values of the velocity components and pressure. The resulting pressure coefficients are then integrated along the body surface to obtain the desired values of the force coefficients, drag, lift, and pitching moment. Application to various bluff shapes and bridge components, show excellent prediction of the wind flow patterns around the body, especially the vortex shedding phenomenon. The fluctuating pressure coefficients obtained are good qualitatively, but sufficient time history record is required in order to compute the mean values.

KEYWORDS: Numerical Simulation; Wind Simulation; Flow Simulation; Bridges; Bluff Bodies; Aerodynamic Stability.

1. INTRODUCTION

For many years, wind tunnel testing and full scale measurements have been the primary means of obtaining the fluctuating wind forces on bridge structures. The George Vincent Memorial Aerodynamics Laboratory of the Federal Highway Administration (FHWA), Mclean, Virginia, remains one of the few facilities in the United States dedicated to conducting wind related research studies, solely focusing on bridge structures and its components. In recent years, however, due to the ever increasing availability of fast, efficient and relatively inexpensive computers, coupled with the successful implementation in the aeronautical field, numerical simulation of wind effects on bridges has become a viable research area for Wind Engineers. In this regard, Computer Simulation Software is currently being developed at the FHWA Aerodynamics Laboratory, to numerically predict the wind flow patterns and wind induced forces on bridge structures. When evaluating wind forces on a bridge structure, it is generally assumed that the critical wind direction is perpendicular to the longitudinal axis of the bridge. In other words, it is the 2-D Navier-Stokes equations that are solved. Although the natural wind is highly turbulent and random in nature, this phase of the research, as a start, solves the flow equations of motion assuming laminar flow conditions.

* Graduate Research Fellow, Federal Highway Administration, Turner-Fairbank Research Center, Mclean, Virginia 22101.

** Research Structural Engineer, Federal Highway Administration, Turner-Fairbank Research Center, Mclean, Virginia 22101.

The numerical scheme used, employs the finite-difference procedure in solving the governing 2-D, unsteady, incompressible, laminar, Navier-Stokes equations, in a body-fitted curvilinear coordinate system. This paper discusses the grid generation technique used, the governing equations both in the physical and the transformed planes, the finite-difference scheme, and the results from application of this numerical scheme to various bridge elements.

2. GRID GENERATION TECHNIQUE

The body-fitted curvilinear coordinate system is one in which, at least one coordinate line coincides with the boundary surface of the body in the flow field. This automatically eliminates the need for interpolation in the finite-difference implementation of boundary conditions for an irregularly shaped body. This grid generation technique involves the solution of an elliptic partial differential system in the physical plane. To solve the system of equations, a coordinate transformation from the physical plane (x,y), to a uniform rectangular computational plane (ξ,η) is necessary. Mathematically, this transformation is stated as,

$$\begin{aligned} \xi &= \xi(x,y) \\ \eta &= \eta(x,y) \end{aligned} \qquad (1)$$

where the transformed coordinates (ξ,η) are the independent variables, and the physical coordinates (x,y) are the dependent variables. The elliptic system of equations solved are either of the Laplace type or the Poisson type, which are both stated below:

Laplace Equation-

$$\begin{aligned} \nabla^2 \xi &= 0 \\ \nabla^2 \eta &= 0 \end{aligned} \qquad (2)$$

Poisson Equation-

$$\begin{aligned} \nabla^2 \xi &= P(\xi,\eta) \\ \nabla^2 \eta &= Q(\xi,\eta) \end{aligned} \qquad (3)$$

After transformation of these equations to the computational plane by using the chain rule of differentiation, the resulting form of the Laplace equation that is actually solved for the grid point values are,

$$\begin{aligned} a x_{\xi\xi} - 2b x_{\xi\eta} + c x_{\eta\eta} &= 0 \\ a y_{\xi\xi} - 2b y_{\xi\eta} + c y_{\eta\eta} &= 0 \end{aligned} \qquad (4)$$

Dirichlet boundary conditions consisting of the physical coordinates of the body geometry, and the outer flow boundary must be specified, before the solution can proceed. The coefficients a, b, c, are transformation metrics given in terms of the following difference expressions,

$$\begin{aligned} a &= x_\eta^2 + y_\eta^2 \\ b &= x_\xi x_\eta + y_\xi y_\eta \\ c &= x_\xi^2 + y_\xi^2 \end{aligned} \qquad (5)$$

The functions $P(\xi,\eta)$ and $Q(\xi,\eta)$ in the Poisson equation are chosen to enable the control of the grid lines within the flow field. Thus the grid lines can be clustered towards the body surface where high flow gradients exist. Figures 1a. and 7a. show the finite-difference grid network generated by this procedure, around a square cylinder and a typical bridge deck cross-section respectively. Note that the grid lines are packed close to the body surface.

3. FLOW EQUATIONS

3.1 Physical Plane

In the physical plane, the governing flow equations are the 2-dimensional, incompressible, laminar momentum equations, and the continuity equation. The dimensional form of the flow equations are usually non-dimensionalized with respect to the flow parameters of the undisturbed flow region. The primitive variable form of the

non-dimensional flow equations are :

$$u_x + v_y = 0$$
$$u_t + uu_x + vu_y = -p_x + \frac{\nabla^2 u}{Re} \quad (6)$$
$$v_t + uv_x + vv_y = -p_y + \frac{\nabla^2 v}{Re}$$

Instead of solving the continuity equation, a new poisson equation in pressure form is solved. The need for the poisson pressure equation is to eliminate the pressure-velocity coupling that exist between the momentum and continuity equations. Also, the elliptic nature of this poisson type pressure equation allows for the elliptic characteristic of the physical flow to be introduced into the model. Again in the physical plane, the poisson pressure equation solved is:

$$\nabla^2 p = S_p - D_t \quad (7)$$

where,

$$S_p = -(u_x)^2 - 2v_x u_y - (v_y)^2$$

$$D = u_x + v_y$$

The derivation of this pressure equation ensures the satisfaction of the continuity requirement. However, the temporal D term is purposely not set to zero according to Harlow and Welch (1965), to avoid numerical instabilities that would otherwise occur.

3.2 Transformed Equations

Before the flow equations can be solved in the computational plane, a similar transformation procedure stated earlier must be applied. After introducing the applicable transformation metrics for the equations, the form of the transformed momentum equations solved are :

u-momentum-

$$u_t + \frac{u(y_\eta u_\xi - y_\xi u_\eta)}{J} + \frac{v(x_\xi u_\eta - x_\eta u_\xi)}{J} = -\frac{y_\eta p_\xi}{J} + \frac{y_\xi p_\eta}{J} + \frac{(au_{\xi\xi} - 2bu_{\xi\eta} + cu_{\eta\eta} + du_\eta + eu_\xi)}{ReJ^2} \quad (8)$$

v-momentum-

$$v_t + \frac{u(y_\eta v_\xi - y_\xi v_\eta)}{J} + \frac{v(x_\xi v_\eta - x_\eta v_\xi)}{J} = -\frac{x_\xi p_\eta}{J} + \frac{x_\eta p_\xi}{J} + \frac{(av_{\xi\xi} - 2bv_{\xi\eta} + cv_{\eta\eta} + dv_\eta + ev_\xi)}{ReJ^2} \quad (9)$$

Pressure Equation-

$$\nabla^2 p = S_p - D_t \quad (10)$$

where,

$$\nabla^2 p = \frac{(ap_{\xi\xi} - 2bp_{\xi\eta} + cp_{\eta\eta} + dp_\eta + ep_\xi)}{J^2}$$

$$S_p = -\frac{(y_\eta u_\xi - y_\xi u_\eta)^2}{J^2} - \frac{(x_\xi v_\eta - x_\eta v_\xi)^2}{J^2} - \frac{2(y_\eta v_\xi - y_\xi v_\eta)(x_\xi u_\eta - x_\eta u_\xi)}{J^2}$$

$$D = \frac{(y_\eta u_\xi - y_\xi u_\eta - x_\eta v_\xi + x_\xi v_\eta)}{J}$$

a, b, c, d, e, x_ξ, x_η, y_ξ, y_η are all transformation scale factors or metrics, while J is the Jacobian of transformation and Re is the flow Reynolds number.

3.3 Boundary Conditions

The boundary conditions used for the momentum equation are the no-slip boundary conditions i.e. $u=0$, $v=0$. For the pressure equation, a Neumann type boundary condition is used at the wall surface $\partial p/\partial n$, and $p=0$ is specified at the outer boundary. Note that the pressure being referred to is the non-dimensional pressure, hence, setting the outer boundary value which occurs far away from the body in the undisturbed flow region to zero is satisfactory. In the computational plane, periodicity was employed in implementing the boundary conditions along the ξ coordinate in the numerical solution routines.

4. FINITE-DIFFERENCE SCHEME

The finite-difference formulation is based on an Upwind-Implicit scheme. A backward difference is used in time, and central difference expressions used for the space derivatives. Due to numerical instability resulting from using a central difference for the first derivative convection terms, the transformed form of a third order upwind difference expression suggested by Kawamura and Kuwahara (1984) is used instead. For the u-velocity convection term in the transformed momentum equations, the finite-difference expression used is :

$$\left(\hat{u}\frac{\partial u}{\partial \xi}\right)_i = \hat{u}_i \frac{-u_{i+2} + 8(u_{i+1} - u_{i-1}) + u_{i-2}}{12\Delta\xi} + |u_i| \frac{u_{i+2} - 4u_{i+1} + 6u_i - 4u_{i-1} + u_{i-2}}{4\Delta\xi} \qquad (11)$$

The $\hat{u}_i$ refers to the transformed form of the non-linear velocity term in the flow equations of motion.

5. SOFTWARE APPLICATION

The simulation software developed in this study has been applied to a square cylinder, a rectangular cylinder with depth to width ratio of 0.5, and to a typical bridge deck cross-section. In each case, the flow was impulsively started, using the results from a potential flow simulation as the initial iteration guess. A Reynolds number of 1×10^5 was used for all the flow problems. This value is considered typical for the physical flow regime in which most bridge structures exist. The outer boundary for the flow around a square cylinder was placed at 10 times the body length. Figure 1 show a portion of the mesh in the physical plane, and also plots of the flow streamlines, velocity vectors and pressure contours at the Instantaneous non-dimensional time (NDT= $u_\infty t/L$) of 50. The computed pressure coefficient C_p is given by the non-dimensional expression:

$$C_p = \frac{p - p_\infty}{\frac{1}{2}\rho u_\infty^2} \qquad (12)$$

The variables with ∞ represent the flow parameters of the undisturbed flow region far from the body. In Figures 2 and 3, the fluctuating nature of the wall surface pressure distribution is depicted for non-dimensional times of 50 and 75. In both cases, negative suction pressures exist on the top, bottom, and leeward sides as expected. On the windward side, the pressures are characteristically positive i.e. pressures directed into the wall. An illustration of the vortex shedding phenomenon is shown in Figure 4, for flow around a rectangular cylinder of depth to width ratio of 0.5. The distribution of pressure on the body surface of this rectangular cylinder at non-dimensional time of 75 is shown in Figure 5. The instantaneous flow streamlines and wall surface pressure distribution on both a square cylinder, and a rectangular cylinder computed by Inamuro and Saito (1985), using the discrete vortex method are shown in Figure 6a. In Figure 6b, they show a comparison of their calculated mean pressures to experimental values from the work of Otsuki et al. (1974, 1978 & 1980). Note that their pressure plots are for values of pressure coefficients times -1, i.e ($-C_p$). The values of instantaneous pressure in Figures 2, 3, and 5 are in qualitative agreement with those in Figure 6. Finally, the results from

application to a bridge deck section are shown in Figures 7 and 8. Figure 7 shows the clustered grid used, the instantaneous flow streamlines, velocity vectors, and pressure contours at a non-dimensional time of 20. The wall surface pressure distribution is plotted in Figure 8. Again these values are qualitatively acceptable.

6. CONCLUSION

The computer flow visualization plots of the flow streamlines, show excellent prediction of the wind flow patterns around the various bodies. On the other hand, the resulting pressure coefficients are qualitatively acceptable at this time. Sufficient time history record is required in order to compute representative mean values, that can be directly compared with mean values from wind tunnel experiments.

7. ACKNOWLEDGMENTS

Much of this work is from the first author's PhD dissertation. The study was supported by a Federal Highway Administration grant.

8. REFERENCES

1. Thompson, J. F., Thames, F. C., and Mastin, C. W., (1977). "Boundary-Fitted Curvilinear Coordinate Systems for the Solution of Partial Differential Equations on fields containing any number of Arbitrary Two-Dimensional Bodies." NASA CR-2729.

2. Harlow, F. H. and Welch, J. E., (1965). "Numerical Calculation of Time-Dependent Viscous Incompressible Flow of Fluid with Free Surface." Physics of Fluids, Vol. 8, pp. 2182-2189.

3. Kawamura, T. and Kuwahara, K., (1984). "Computation of High Reynolds Number Flow around a Circular Cylinder with Surface Roughness." AIAA Paper, 84-0340.

4. Inamuro, T. and Saito, T., (1985). "A Numerical Analysis of Unsteady Separated Flow by Discrete Vortex Method." Proc. 5th U.S. National Conf. Wind Engineering, Nov. 6-8, Lubbock, Texas, pp. 5B-17 - 5B-24.

5. Otsuki, Y., Fujii, K., Washizu, K. and Ohya, A., (1974). "A Note on the Aeroelastic Instability of a Prismatic Bar with Square Section." Journal of Sound and Vibration, Vol.34, part 2, pp. 233-248.

6. Otsuki, Y., Fujii, K., Washizu, K. and Ohya, A., (1978, 1980). "Wind Tunnel Experiments on Aerodynamic Forces and Pressure Distributions of Rectangular Cylinders in a Uniform Flow (Part 1, 2) (in Japanese)." Proc. 5th and 6th Symp. Wind Effects on Structures, Tokyo, pp. 169-175, 1978, pp. 153-160, 1980.

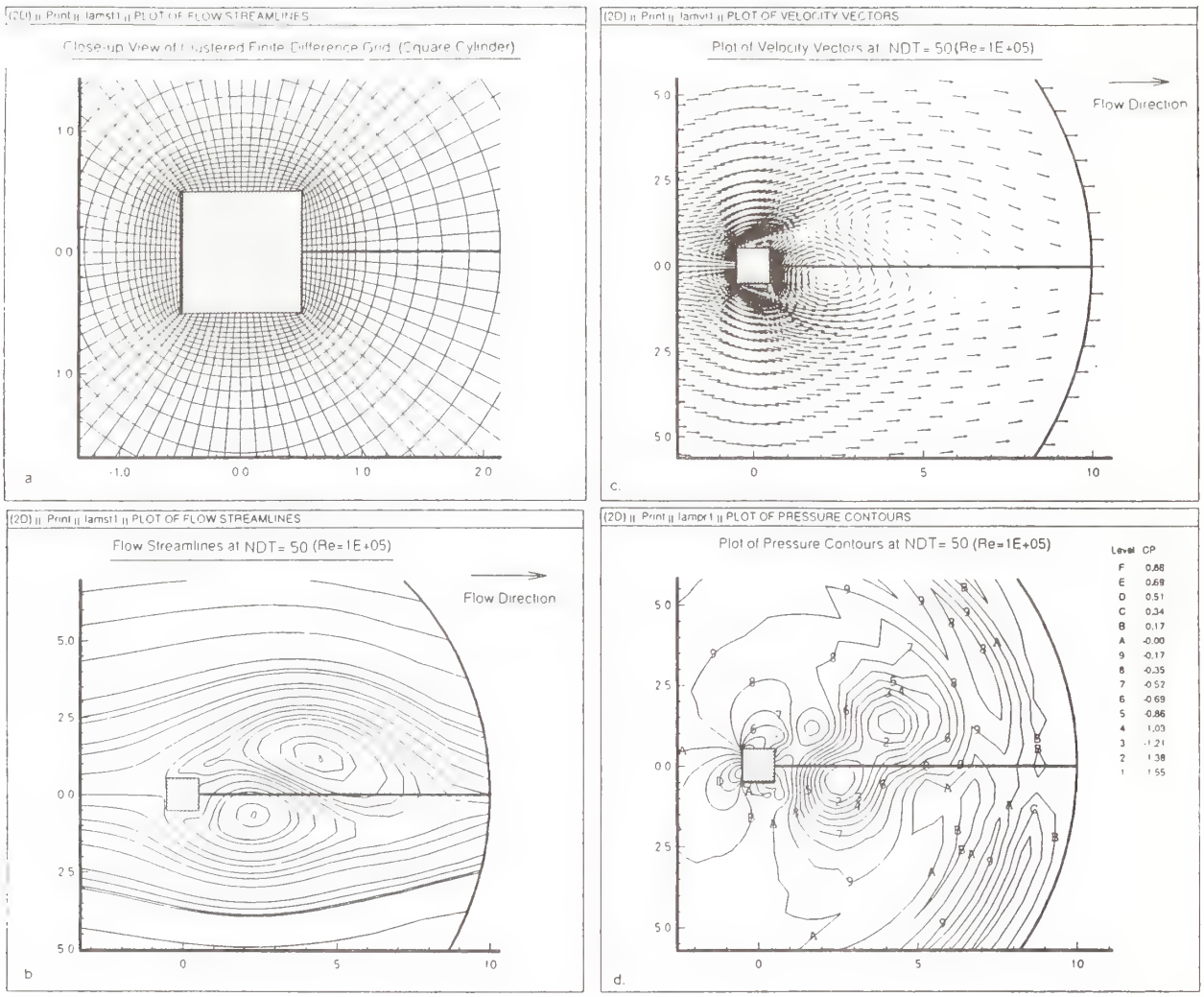

Figure 1. Instantaneous Flow around a Square Cylinder at NDT= $u_\infty t/L$ = 50

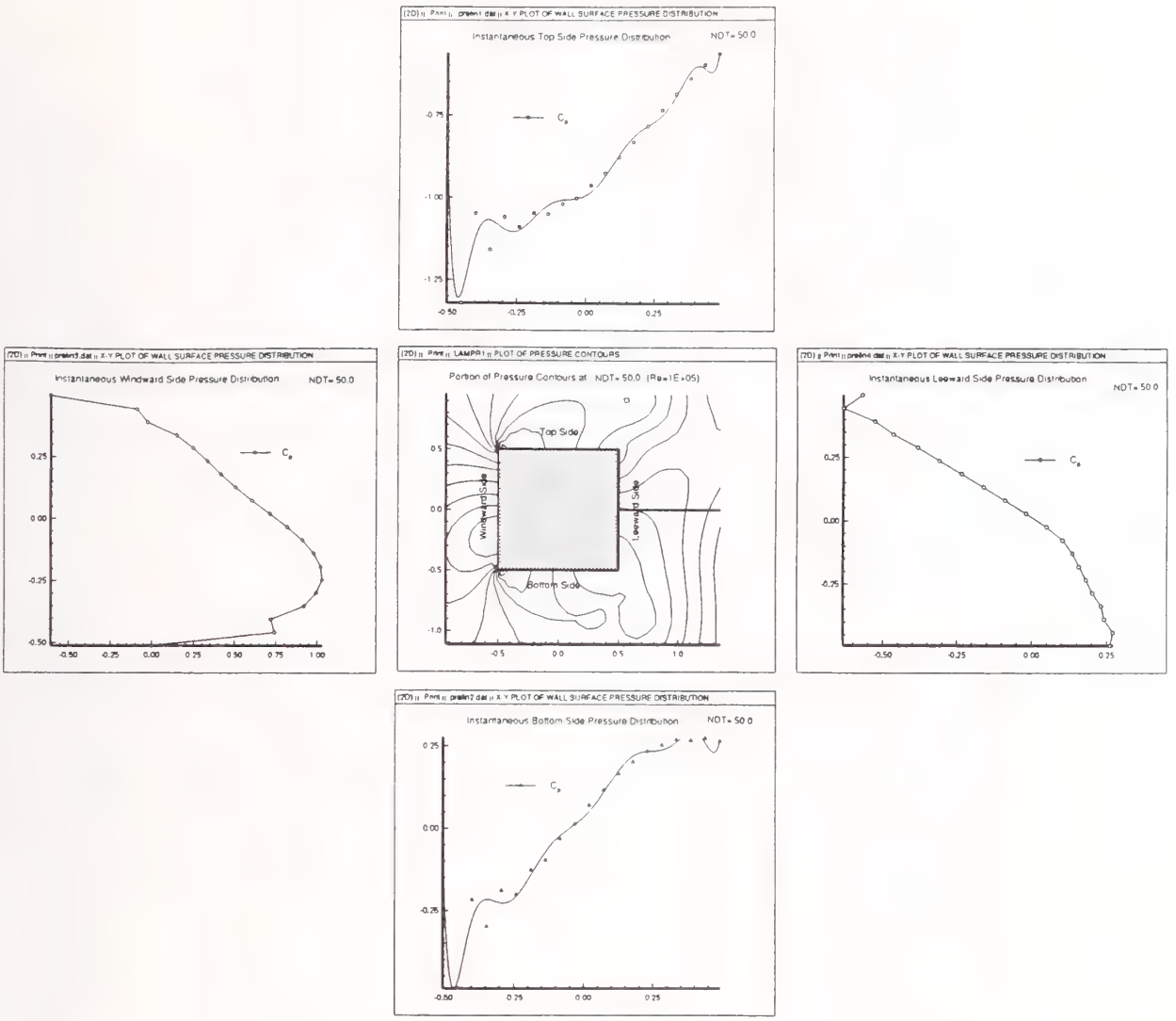

Figure 2. Instantaneous Body Surface Pressure Distribution around a Sqaure Cylinder at NDT= $u_\infty t/L$ = 50

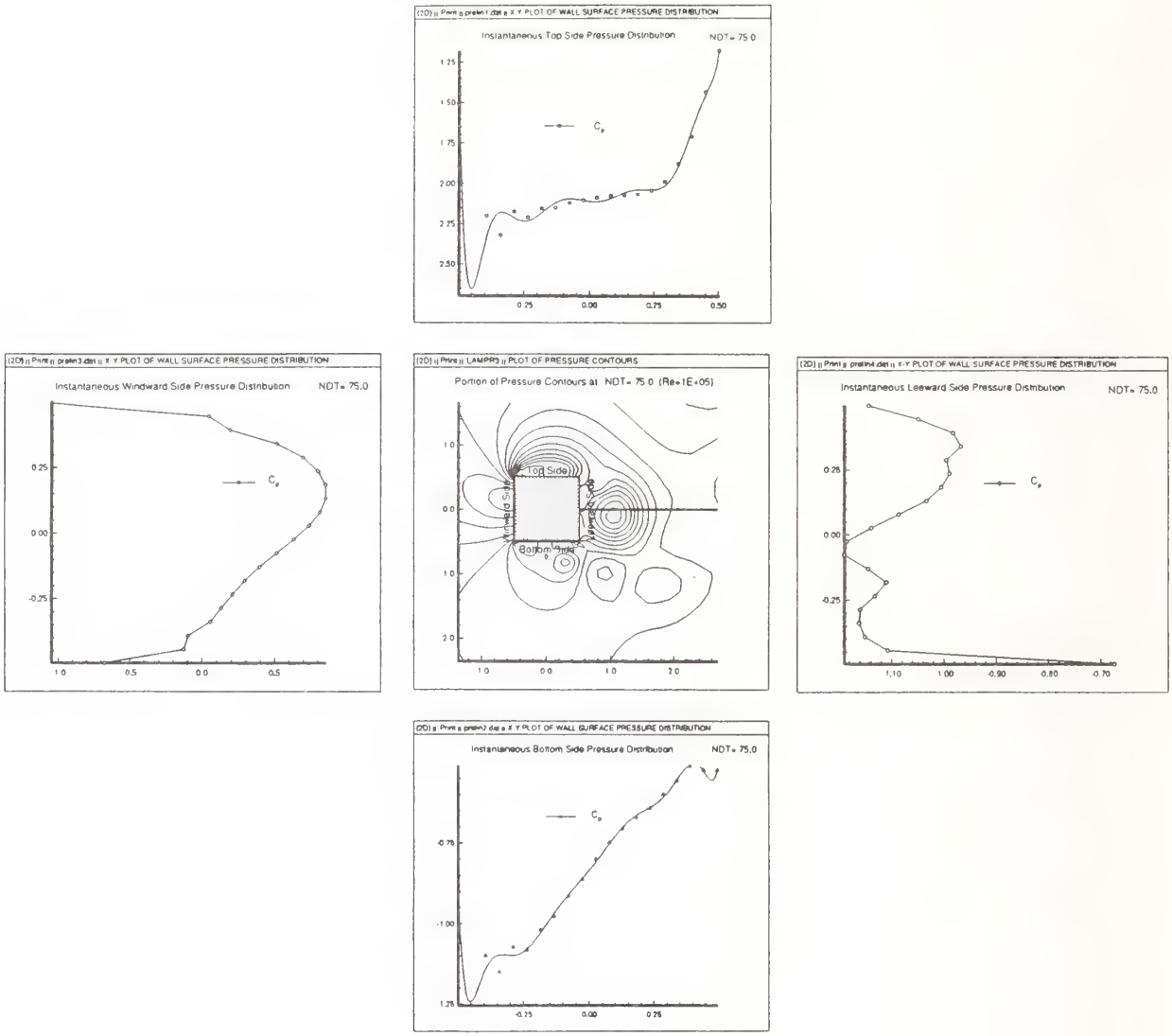

Figure 3. Instantaneous Body Surface Pressure Distribution around a Sqaure Cylinder at NDT= $u_\infty t/L = 75$

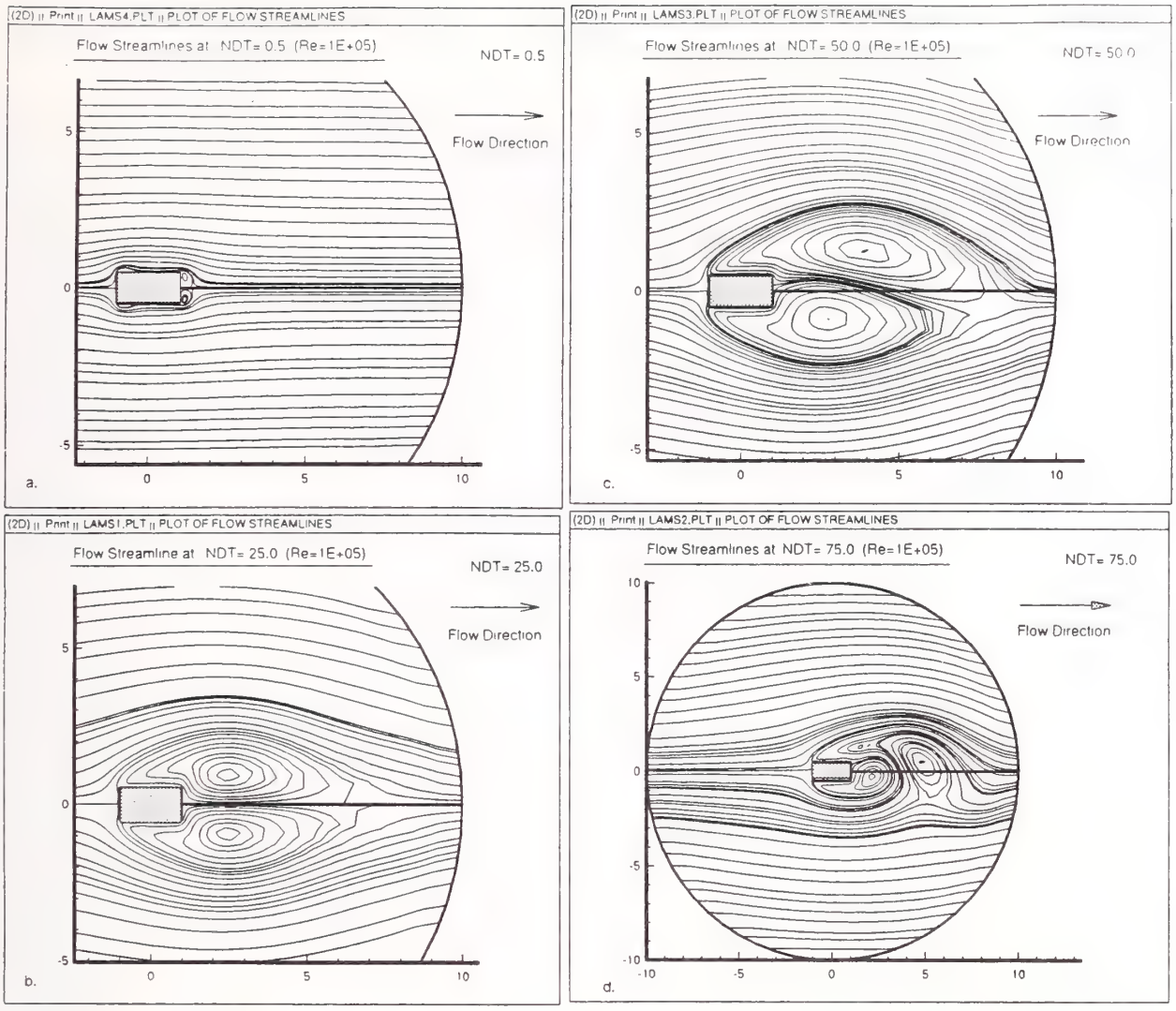

Figure 4. Time History of Flow around a Rectangular Cylinder (d/w=0.5)

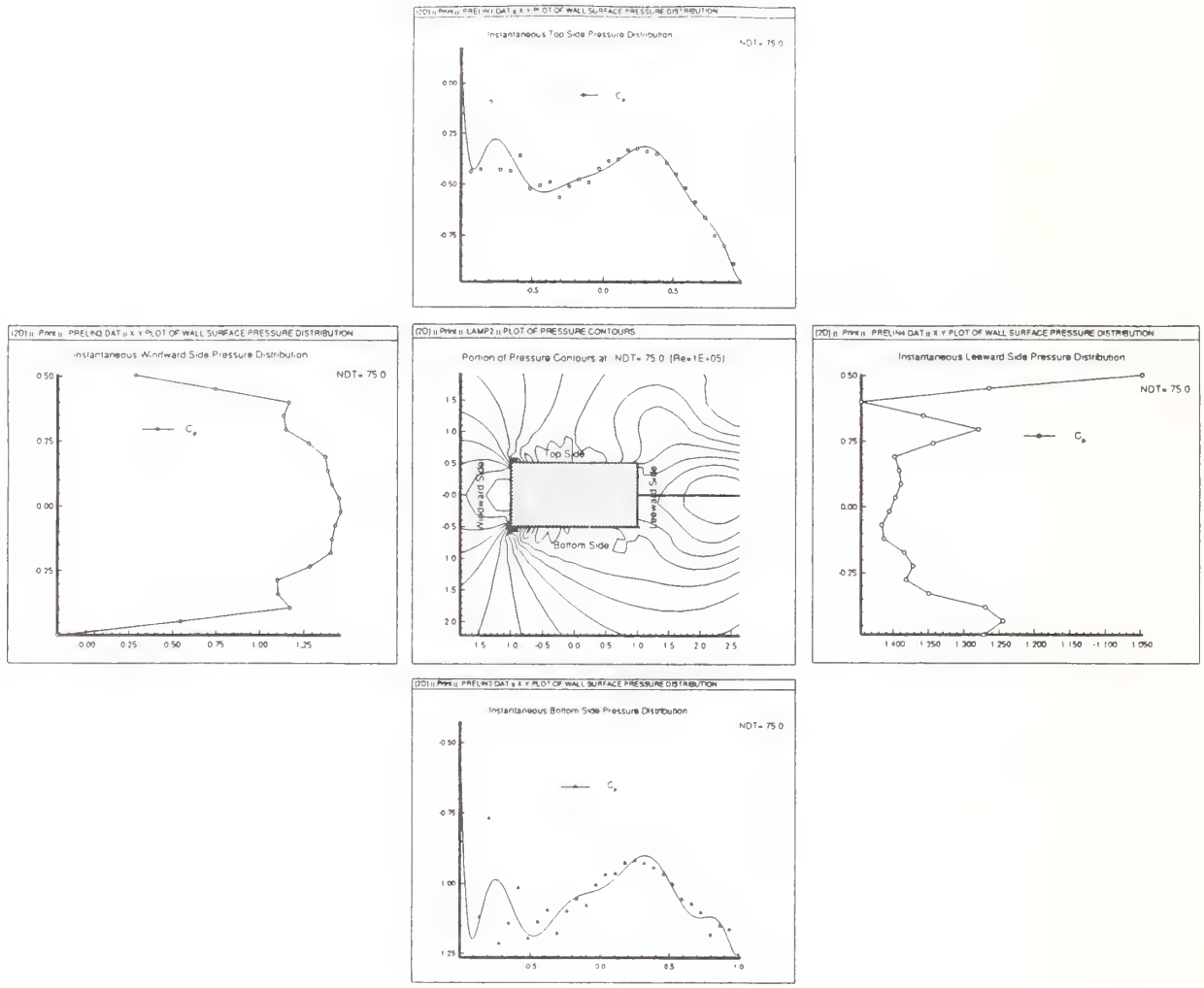

Figure 5. Instantaneous Body Surface Pressure Distribution around a Rectangular Cylinder (d/w=0.5) at NDT= $u_\infty t/L$ = 20

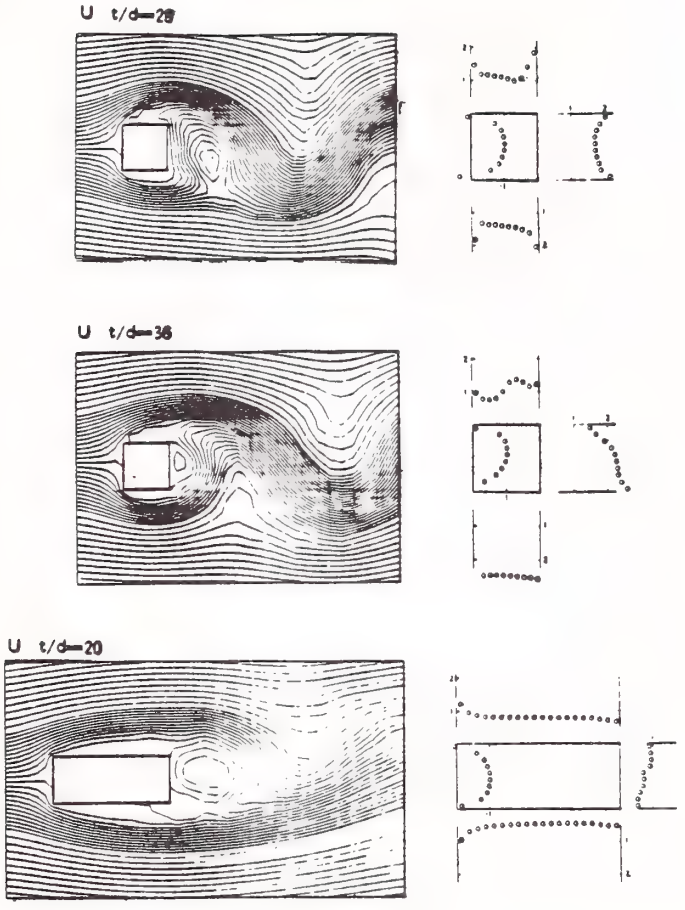

Figure 6a. Instantaneous Flow Streamlines and Pressure Distribution ($-C_p$) Using Discrete Vortex Method

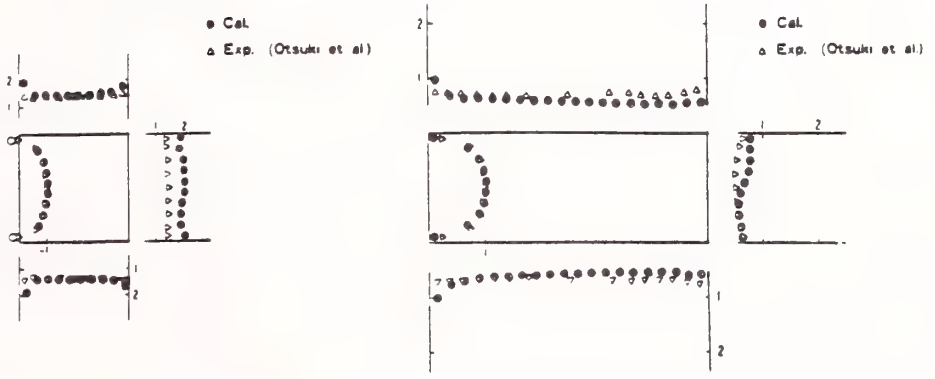

Figure 6b. Mean Pressure Distribution from Discrete Vortex Method and Wind Tunnel Experiment

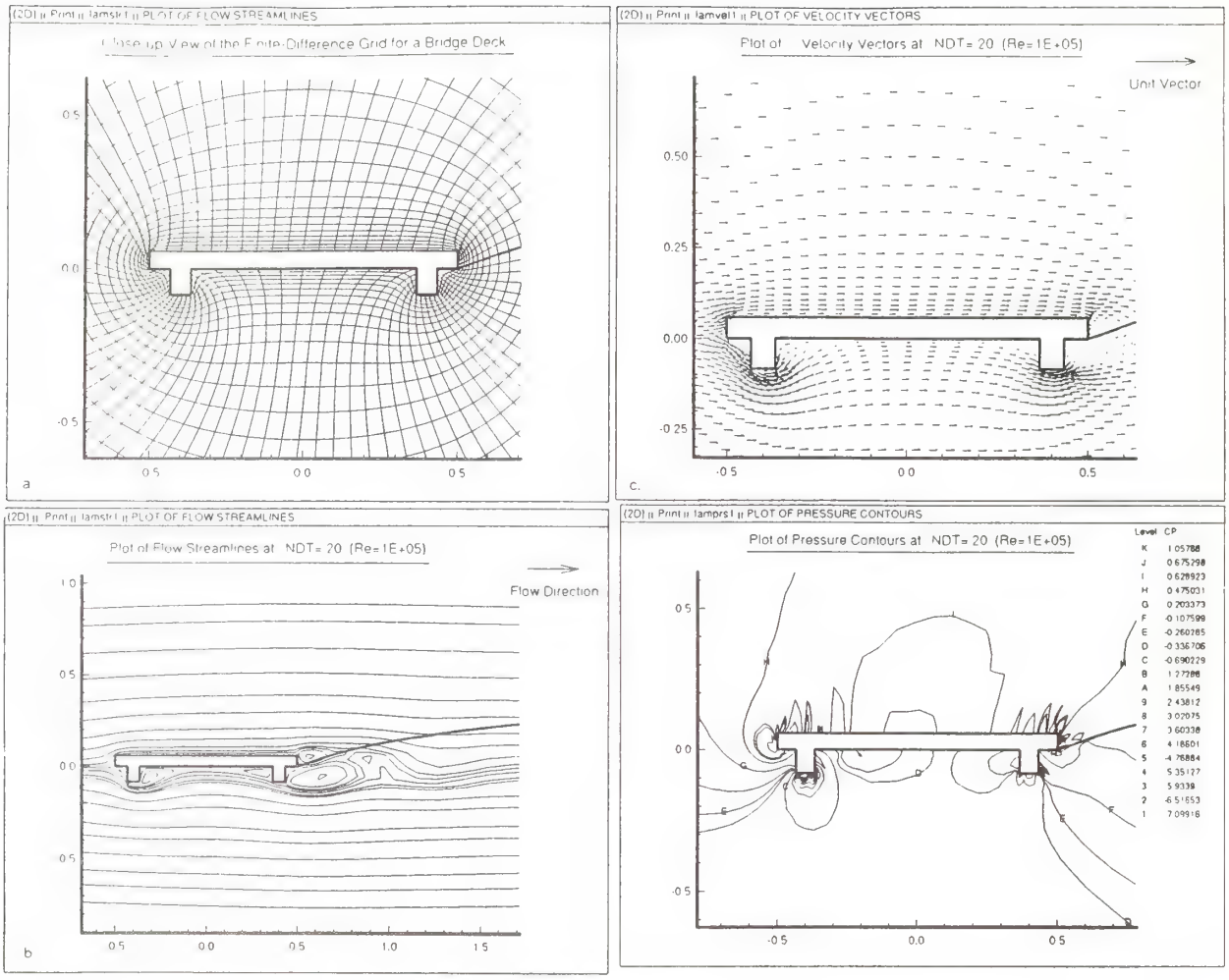

Figure 7. Instantaneous Flow around a typical Bridge Deck Section at NDT= $u_\infty t/L$ = 20

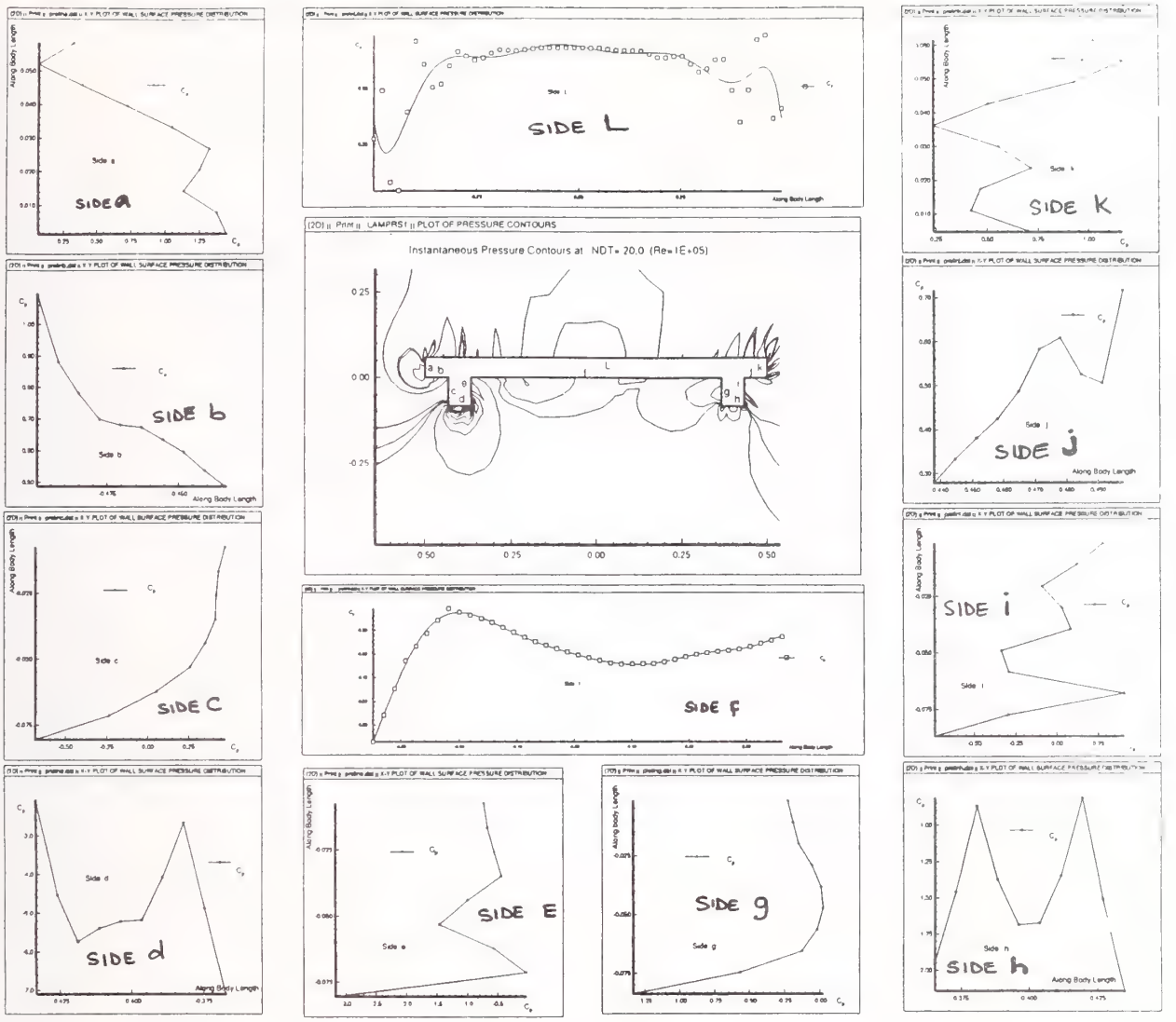

Figure 8. Instantaneous Body Surface Pressure Distribution around a typical Bridge Deck Section at NDT= $u_\infty t/L = 20$

Theme II

Storm Surge and Tsunamis

A Numerical Simulation of the Tsunami Generated by Landslide of Mt. Mayuyama in 1792

by

Chiaki Goto* and Tomotsuka Takayama**

SUMMARY

Through the numerical simulation, tsunami generated by landslide of Mt. Mayuyama in 1792 is investigated. Remarkable characters of landslide tsunami including concentration and divergence of energy by tsunami reflection due to sea topography is clarified.

Key wards : Landslide Tsunami, Numerical simulation, Mt. Mayuyama, Simabara Bay, Ariake Sea

1. INTRODUCTION

By a gigantic collapse of Mt. Mayuyama in Simabara Peninsla in 1792, a grate landslide and tsunami was generated and attacked the coastal area around Simabara bay. The tsunami killed about 15,000 persons and washed away many houses.

Volcanic activity of Mt. Unzen started after 200 years interval since two years ago. Mt. Unzen is a generic name for seven volcanos and was an active volcano up to the end of the 18th century. Because Mt. Mayuyama is a volcano of Mt. Unzen, goverment feels misgivings about generation of landslide and tsunsami same as the event in 1792.

Historical data Near Japan Islands gives an imformation that about 95 percent of tsunamis are generated by sea bottom deformation due to earthquakes and only 5 percent of tsunamis are generated by landeslide or vocanic activity. Characters of landsilde tsunami may be differ from the earthquake tsunami. In this paper, characters of the tsunami in 1792 is investigated by use of numerical simulation model.

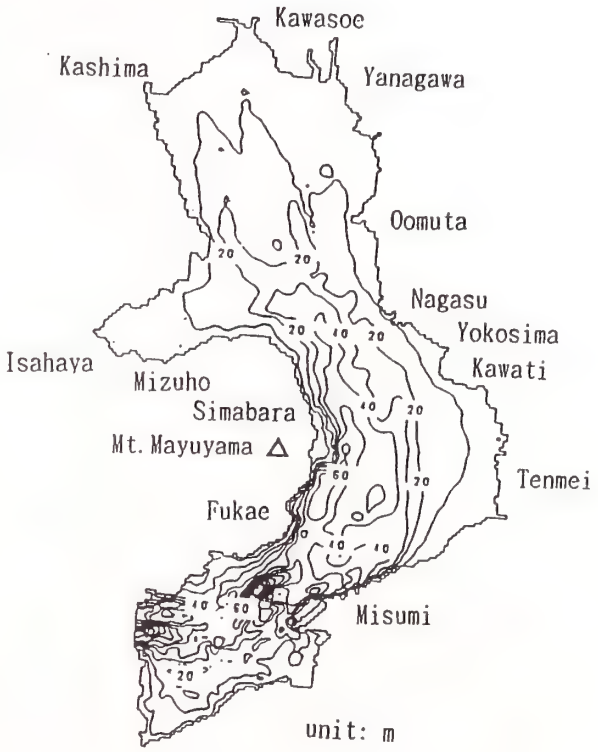

Fig. 1 Water depth of Simabara Bay

* Cheif, Ocean Energy Utilization Lab., PHRI, Ministry of Transport

** Directer, Hydraulic Engineering Division, PHRI, Ministry of Transport

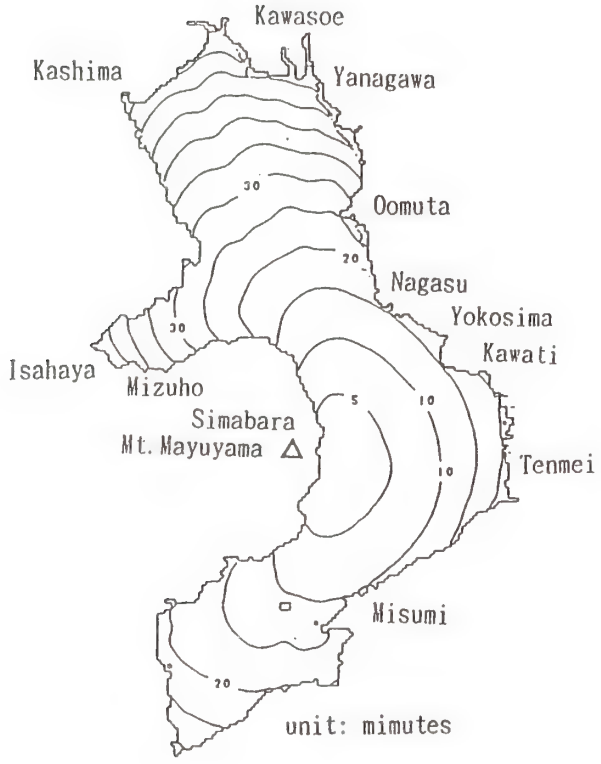

Fig. 2 Arrival time of tsunami front

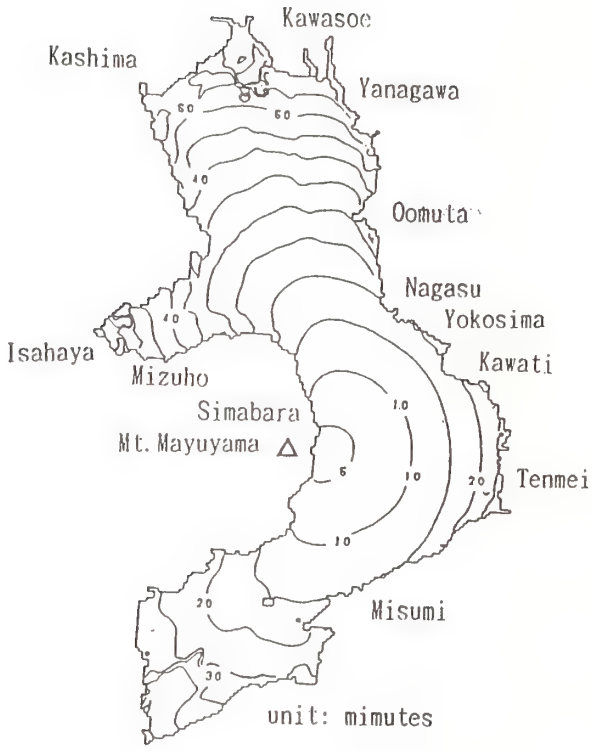

Fig. 3 Arrival time of the first crest of tsunami

2. NUMERICAL SIMULATION MODEL OF TSUNAMI

The governing equations of tsunami numerical simulation are following nonlinear shallow water theory (nonlinear long wave equations) including friction terms.

$$\frac{\partial \eta}{\partial t} + \frac{\partial M}{\partial x} + \frac{\partial N}{\partial y} = 0 \qquad \cdots\cdots (1)$$

$$\frac{\partial M}{\partial t} + \frac{\partial}{\partial x}\left[\frac{M^2}{D}\right] + \frac{\partial}{\partial y}\left[\frac{MN}{D}\right] + gD\frac{\partial \eta}{\partial x} + \frac{g\eta^2}{D^{7/3}}MQ = 0 \qquad \cdots\cdots (2)$$

$$\frac{\partial N}{\partial t} + \frac{\partial}{\partial y}\left[\frac{N^2}{D}\right] + \frac{\partial}{\partial x}\left[\frac{MN}{D}\right] + gD\frac{\partial \eta}{\partial y} + \frac{g\eta^2}{D^{7/3}}NQ = 0 \qquad \cdots\cdots (3)$$

where x and y are the plain coordinates, t the time coordinate, M and N the discharge flux in the x and y direction respectively, η the tsuanmi elevation, g the gravity, h the still water depth, D the total depth and n the Manning's roughness coefficient. In the computation, the finite difference method of the staggard leap frog scheme of equations (1)-(3) is adapted.

The tsunami computation is carried out in

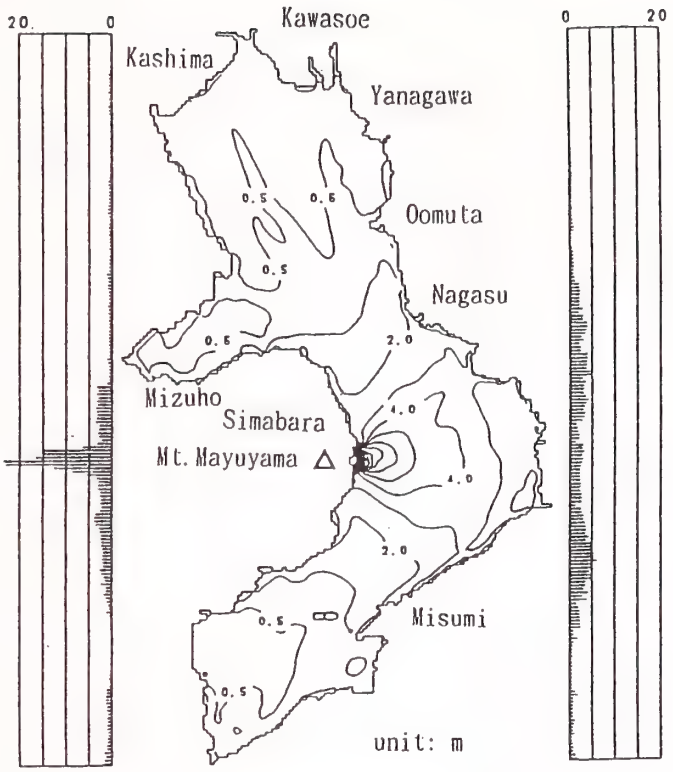

Fig. 4 Distribution of tsunmai maximun height

the whole region of the Ariake sea and Shimabara Bay. Distribution of water depth at the high water level is shown in Fig. 1. In the Ariake sea, averaged tidal amplitude is observed as 2.5 m. As the point view for tsunami defence, the high tide condision is adapted in the computation.

As a grid length of numerical simulation, 400 m mesh is used. Accuracy of the numerical simulation depends on mesh size because the trancated error of computation is growth in case of rough grid length. It is known that more than 20 grid points are necessary within one wave length in the tsunami numerical simulation. In the case of tsunami simulation in Ariake Sea and Simabara Bay, averaged water depth is about 30 m. And the tsunami wave length generated in landslide of Mt. Mayuyama can be estimated about 10 km. Therefore, the ratio of wave length to grid size is about 25 so that the condision for accurate computation is satisfied.

As a open boundary and sea shore condisions, the ragiative and the reflective condisions are adapted respectively in the computation.

The landslide of Mt. Mayuyama is assumed earth and sand of 4.6×10^7 m^3 flows into the sea during 4 minites the same as Aida's[1] model. The area which earth and sand flows is also the same region as Oota's[2] estimation.

3. RESULTS OF SIMULATION

3.1 Arrival time of tsunami front

Figure 2 shows arrival time of tsunami front in computational region. The figure is

drawed by the assumption of time that sea surface changes more than 1 cm.

At the opposite side of sea, Tenmei, tsunami arrives at about 20 minutes after tsunami occured. At Misumi, it takes about 15 minutes. On the other hand, at the inner part of sea, Kashima and Kawasoe, tsunami arrives at 55 minutes.

Figure 3 shows the arrival time of the first crest. The first crest of tsunami reaches for coast at the time after 5 minutes since the front arrive.

3.2 tsunami height

Figure 4 shows the distribution of maximum tsunami height. The contour lines indicate equi-height and numerials are tsuanmi height. The lines at right and left sides of figure also show the maximum tsunami height along the east and west sea shore lines of Ariake Sea and Smabara Bay, respectively.

At tsunami source region, near Simabara, the maximum tsunami height is computed more than 20 m. At the opposite coast, the averaged height is about 5 m and the distribution of the maximum height has a tendancy that the height of the center coast is relatively low but both sides are high. This resion can be think that main part of tsunami propagates both side coast because of tsnami reflection related to sea bottom topography. And the characters of numerical results coincide with tsunami historical data.

3.3 Wave profile of tsunmai

Near the tsunami source area, the first wave is the most dengerous tsunami. But the second and third waves are almost same height. On the other hand, the first wave is the biggest in the opposite coast. The second and third wave are relatively small compared with the height of the first wave. In the inner are of Ariake Sea, tsunami height is very small.

4. CONCLUSION

The paper reports a numerical simulation of tsunami generated by landslide of Mt. Mayuyama in 1792 and discusses a few remarkable tsunami behaviour in Simabara Bay and Ariake Sea. In a future, more detail tsunami numerical simulation includinig run-up on land should be carried out for tsunami defence works.

REFERENCES

1) Aida, I.: Numerical Simulation of tsunami generated by lindslide of Mt. Mayuyama in 1792, Earthquake II, Vol. 28, pp. 449-460, 1970.

2) Oota, K.: A study of gigantic collapse of Mt. Mayuyama, Report of Simabara Volcanic-thermal spring Institute, No. 5, pp. 6-35, 1970.

Empirical Simulation of Storm Histories for Coastal Design

by

Martin C. Miller[1] and Robin D. Reinhard[2]

ABSTRACT

Coastal erosion and flooding caused by hurricanes have tremendous potential for economic damage and loss of life in populated areas. The U.S. Army Corps of Engineers is frequently asked to determine the feasibility of coastal protection projects through evaluation of the economic benefits of project alternatives. The development of design criteria for water level, waves, and beach profile change require the evaluation of data collected over long time periods, or the generation of data using tested computer models. A methodology has been developed at the U.S. Army Engineer, Waterways Experiment Station, Coastal Engineering Research Center for determining project feasibility by the application of several environmental models. The economic evaluation depends on the application of a statistical resampling technique known as the "bootstrap" which allows calculation of expected values of an outcome by sampling, with replacement, from a limited historical data set. This method has been applied to a potential project at Panama City Beach, Florida.

KEYWORDS: modeling; water level; simulation; "bootstrap"

1. INTRODUCTION

Many coastal engineering design problems require estimates of extreme events such as wave height and water levels. Estimates of normal and extreme conditions are also required to justify projects that protect coastal property. Comparisons are made between the consequences of the occurrence of the design storm with and without the protection project in place. The economic benefit of a coastal protection project during the design event must exceed the loss that would be experienced if the protection were not in place. In the Gulf of Mexico and along the southeastern U.S. coast, extreme waves and water levels are caused by hurricanes. Along the mid-Atlantic coast, extremes may be caused by either hurricanes or northeasters, and along the northeast coast, northeasters provide the storms of record. The coastal response to these events is extreme shoreline erosion with consequent flooding, property damage and possible loss of life. The U.S. Army Corps of Engineers is often requested to design measures that will protect the coastal property from the effects of these extremes.

The statistical methods used to estimate the extreme value of an environmental variable are well known (Borgman and Resio, 1982; Goda, 1978; Haring, *et al.*, 1976). Data are collected or hindcast over a long period of time and systematic procedures are used to plot the data according to some probability distribution.

---

[1] Chief, Coastal Oceanography Branch, Coastal Engineering Research Center, U.S. Army Engineer Waterways Experiment Station, Vicksburg, MS 39180-6199

[2] Hydraulic Engineer, Coastal Oceanography Branch, Coastal Engineering Research Center, U.S. Army Engineer Waterways Experiment Station, Vicksburg, MS 39180-6199

The resulting curve may be extrapolated to some selected return interval to determine the magnitude of the parameter selected. Though a data record of three to five times the maximum return interval to be estimated is usually recommended, in most U.S. coastal areas the historical database is not adequate to represent the full range of possible occurrences of storm effects at a specified site. Future storms may pass at different coastal crossing locations than are present in the historical database and the storms may have different characteristics of central pressure, radius to maximum winds, forward speed, duration, etc. It may, therefore, be necessary to augment the historical data set with additional storms that could have occurred at the site given the random nature of events. This paper briefly describes a statistical procedure which may be applied to augment the historical database of hurricanes with hypothetical storms that could have occurred at the site.

2. BACKGROUND

A study has recently been conducted by the U.S. Army Engineer Waterways Experiment Station (WES), Coastal Engineering Research Center (CERC) for the U.S. Army Corps of Engineers Mobile District to examine the feasibility of providing a protective sand berm along an eighteen mile section of Panama City Beach, Florida (Figure 1). This beach is heavily developed over much of its length, with single family homes and condominiums built along the waters' edge. Inlets at each end of the beach provide access to small boat harbors and quiet coastal lagoons. The beach is susceptible to flooding from hurricane related storm surge, which could result in great loss of life and property. Beach and flood protection is considered necessary, but the recreational and aesthetic value of the area must also be preserved. The protective sand berm concept was determined to be appropriate to provide protection from flooding and to preserve, to the maximum extent, the natural scenic and recreational ambience of the area.

In order to determine the economic justification for the project and to effectively design the berm, it is necessary to evaluate the degree of protection it will provide during storms of various magnitude that may impact the site. From the designer's standpoint, it is desirable to know the return period of the storm that would be protected against for the selected design. From the economic standpoint, project justification requires that the benefit derived from the selected level of protection outweigh the cost.

3. GENERAL APPROACH

The primary goal of this study is to provide an estimate of the economic damages which might occur at the Panama City Beach area due to a tropical storm or hurricane. The methodology used to obtain these estimates consists of a many phased approach which relies on the application of several numerical models. Available data on the historic storms affecting the study area were collected. A subset of storms, called the "training set," was chosen which is representative of the full range of possible storm conditions. Numerical models which estimate the winds, water levels, waves, and beach profiles were run for each member of the training set to produce variables of interest, or "responses." A Gaussian "nearest-neighbor interpolation" relationship was developed which allowed the response for a storm to be determined from the training set storm characteristics without having to simulate the responses of all of the numerical models for every storm. One hundred statistical simulations of 50 years each were produced. For each year of a simulation the number of storms was set using a Poisson process. The responses for each of these storms was determined by the random "nearest-neighbor bootstrap" technique. The simulated sequence of storm responses were used to determine the return period levels of the storm response variables. The simulated sequences were also used in the economic model to determine the storm damages and comparisons

were made between conditions with and without the planned improvement.

4. STORM SELECTION

Tropical storm data used in this study was obtained from the National Hurricane Center (NHC) (Jarvinen, *et al.*, 1984) and CERC's Wave Information Study (WIS) data set (Abel, *et al.*, 1989). The latter contains much of the basic information of the former but has been augmented with additional details in order to hindcast the waves in selected storms. The NHC set covers the years 1886-1989. The significance of this data set is it's completeness, which makes it valuable for determining the frequency of different storm characteristics. The WIS data set covers the years 1956-1975. Hurricanes Juan and Kate, both of which made landfall near Panama City Beach in 1985, were added later. Only storms which exceeded the severity threshold of wind speed of at least 34 knots within 75 nautical miles of Panama City, Florida were selected.

The meteorological database included 34 storms which occurred over the past 105 years. The set of 34 historical storms was expanded by running each of the storms at four random tide phases, to obtain response variables for a total of 136 storms. Meteorologic data for 31 additional storms was also gathered. These 31 hypothetical storms did not actually occur as described but are based on the characteristics of the historical Gulf of Mexico storms. The hypothetical storms were chosen so that the entire range of storms which could impact the Panama City Beaches study area were represented. The total storm set contains 167 events (136 historical and 31 hypothetical storms).

A subset of the total storm database, referred to as the training set, was established to determine the relationship between storm parameters and environmental responses. The range of storm types found in the training set should reflect the likely range of storms to be encountered. Storms were chosen for the training set based on the ability of the set to cover the characteristics of a full range of storm types. This was done by working backward through hurricane records and eliminating storms that were near duplicates of each other. The training set included 24 storms from the set of 136 historical storms plus the 31 hypothetical storms.

Storm parameters were determined both at the time of closest approach and at the time of landfall. The set of storm parameters which was chosen to describe the storms statistically are: (1) the relative phase of high tide and storm surge maximum, (2) the relative phase of tidal change and storm surge maximum, (3) maximum wind speed in knots, (4) central pressure deficit in millibars, (5) radius to maximum wind in nautical miles, (6) forward speed in knots, (7) course angle of the storm track in degrees and (8) closest point of approach distance from the study area in nautical miles.

5. HYDRODYNAMIC MODELING OF STORM EVENTS

Several numerical models were used to establish the design criteria for the Panama City Beach area and to provide the data necessary for the economic evaluation of project feasibility. Most of these were developed by CERC engineers or by contractors under the direct technical supervision of CERC.

The hurricane wind-field was produced using the Standard Project Hurricane Model (SPH). This is a parametric model which represents a steady-state hypothetical hurricane defined by a set of interrelated parameters such as eye location, central pressure deficit, track angle, forward speed, radius to maximum winds, etc. (Cialone, 1991). The model produces wind components and surface atmospheric pressures. This model was run for each storm on a grid covering the Gulf of Mexico. Results of the model were used to determine water level and waves.

Total water level was obtained from ADCIRC

(ADvanced CIRCulation model) (Luettich, *et al.*, 1991; Westerink, *et al.*, 1991). This model is a time-stepping finite-element model containing the effects of tidal forcing, surface wind stress, atmospheric pressure variation, and bottom friction. A major advantage of the finite-element method is that the computational mesh can be refined to represent the details of local topography in the area of interest. Figure 2 shows the grid for the area of the entrance to St. Andrew's Bay. The ADCIRC model was tested against tidal data and against the measured storm surge produced by two hurricanes (Kate and Juan) impacting Panama City Beach (Miller, *et al.*, 1991). No tuning was done to the surge model, though some adjustments were required for the SPH to correct for landfall effects.

The waves were determined using the SHALlow water WaVe model, SHALWV, which is a time-dependent, spectral hurricane wave-field model. It has been previously tested against a large number of hurricane wave measurements and used to model sixty-five hurricanes along the Gulf and East coasts of the U.S. (Jensen, *et al.*, 1983). The wave spectrum at a point is represented by an array of discrete frequency and direction components. At each time step of the model, the wave energy is first propagated in the grid, taking into account refraction, diffraction and dispersion. The wave energy in each frequency-direction component at each grid point is then recalculated, taking into account energy input by winds, energy dissipation by breaking, and energy transfers within the spectrum through wave-wave interaction processes.

The results of the wave and surge stage frequency analysis were used as input for the numerical simulation model Storm-Induced Beach Change (SBEACH) (Larson and Kraus, 1989; Larson, *et al.*, 1990). SBEACH was used to evaluate the cross-shore transport of beach and dune materials exposed to varying waves and water levels under hurricane storm conditions. The model calculates sand transport produced by breaking waves, simulates erosion of dune and berm beach fills, and develops the evolution of the equilibrium beach profile including the offshore bar formation. Longshore transport was not modeled. Four representative beach profile lines along the 18 miles of beach were evaluated using the SBEACH model. The selection of the representative surveys were based on property structural value, beach profile shape, dune elevation and shape, longterm erosion rates, and grain size. Four responses (1) maximum linear feet of recession during the storm event measured from zero National Geodetic Vertical Datum (NGVD), (2) maximum water level above NGVD, (3) wave height at a depth of 49 feet, and (4) wave period were obtained from SBEACH to be used in the economic analysis.

6. DEVELOPMENT OF RETURN PERIOD FOR COASTAL STORM IMPACTS

The purpose of running a training set of storms was to determine a relationship between the storm parameters and the response variables, which are values for the storm determined using the numerical models for waves, water level, and beach erosion. Determination of this relationship removes the need for further runs of the numerical model by allowing determination of the water level, waves, erosion, etc. for a given site directly from the storm parameters.

The responses for the 112 storms which were not run through the numerical models are estimated from the responses of the training set storms with a Gaussian Nearest-Neighbor Interpolation. The Gaussian interpolation determines a weighted average of the responses of the training set of storms. For the purposes of determining the relationship, a measure of similarity between storms is required. This measure, called "distance" in this study, should possess the quality that the responses of storms converge as the distance between them decreases. The n storm parameters used can be considered the coordinates of an n-dimensional space in which storm i is represented by a vector, c_{ik} , where k = 1, n.

The difference, or distance, between vectors i and j , d_{ij} is the sum of the squares of the difference between each component of each vector

$$d_{ij} = \sum_k (c_{ik} - c_{jk})^2 \qquad (1)$$

This is the square of the usual Cartesian difference of two vectors.

For this study, different storm parameters are weighted differently for evaluating the distance between two storms. For instance, storms with similar distances and maximum wind speed will produce effects more alike than would storms similar only in radius to maximum wind and tide phase. Therefore, each parameter can be normalized by its root mean square (RMS) value, and assigned a scaling radius, R_k , and weight, W_k , based on the importance of the parameter. The RMS values are used as a scale factor around the mean value to normalize the range of the parameters due to differences in units. The distance then becomes

$$d_{ij} = \frac{\sum_k W_k \left[(\tilde{c}_{ik} - \tilde{c}_{jk}) / R_k \right]^2}{\sum_k W_k} \qquad (2)$$

where the tilde indicates optional norming. For this study, all parameters were normalized, and all R_k were set to unity (Borgman 1991). All W_k were set to unity for most parameters. The W_k were set to ten for maximum wind speed at closest approach and distance of closest approach, set to five for relative phase of high tide and storm surge maximum, and set to three for relative phase of tidal change and storm surge maximum. The values were chosen so the parameters that better describe the similarities between storms are given higher weights. Thus, wind speed of the storm, its distance, and its tidal phase of arrival are considered most important in this study.

The response values, r_{ik} , for the k-th response of the i-th historic storm, not part of the training set, are then given a weighted average value of all training set storms

$$r_{ik} = \frac{\sum_{j_t} w_{ij} r_{jk}}{\sum_{j_t} w_{ij}} \qquad (3)$$

where the j_t are the j-s of training set storms only. The weights w_{ij} are set by a bell-shaped ("Gaussian") curve

$$w_{ij} = \exp\left[-\frac{\pi d_{ij}^2}{D_i^2} \right] \qquad (4)$$

where D_i is an effective width of the bell equal to twice the average distance of the four nearest training set storms to storm i .

If the mean frequency of storms is known, the Poisson distribution can be used to determine the number of storms in a given period. The Poisson distribution is given by

$$\Pr(s;\lambda) = \frac{\lambda^s e^{-\lambda}}{s!} \qquad (5)$$

where $\Pr(s;\lambda)$ is the probability of having s events in a period in which λ is the mean frequency of events per period. For this study, the interval is 1 year and $\lambda = 0.3238$ year^{-1} (34 historic storms / 105 years). As a result, the most likely event for a given year is no storms ($\Pr(0; 0.3238) = 0.7234$). The number of storms in a given year of a simulation is chosen using a random number generator combined with a Poisson probability distribution.

Once the number of storms in a year of a simulation has been found, it is necessary to determine the characteristics of each of those storms. This is done by a nearest-neighbor bootstrap method developed by Borgman (1990 and 1991). Bootstrap methods are based on resampling of observed data (Efron 1982). Multiple sequences of events can be developed

from a single sequence of observed data by drawing random samples (with replacement) from the observed data using the program HBOOT. The multiple sequences can then be used to estimate various statistics of the population of which the observed data is a sample.

To determine the responses of a simulated storm, one historic storm is selected at random from the total storm set. Since all historic storms have equal historic probability (each occurred once), storms selected at random will have the same probability density function (pdf). The responses of the new simulation storm are set to a weighted average of the selected storm and its four nearest neighbors, with the weights determined at random. This averaging procedure makes it possible for the simulation to have storms which have never occurred, but which are relatively similar to the storms which have occurred. It also allows an almost infinite number of hypothetical storms to be generated since storms with different responses will be simulated using the same reference storm.

The results from the statistical model are then used as input for the economic damages model. Data for the determination of the cost-benefit ratio for the proposed project were developed from 100 simulations of 50 years each of the model HBOOT, which is based on the nearest-neighbor bootstrap technique described above and elaborated upon in the references. The rationale for the use of multiple simulations is that tropical storms (including hurricanes) are relatively rare and have varied characteristics so no single 50-year simulation would be adequate to determine the risks, costs, and benefits associated with the project. By determining the cost-benefit ratios for multiple 50-year simulations using the bootstrap, one can determine the expected value of the 50-year cost-benefit ratio, as well as obtain a measure of the uncertainty of the calculations.

Since the economic model used must be given the year of occurrence of each event in a 50-year simulation to allow discounting of damages to a reference year, the 100, 50-year simulations give the number of storms each year and the magnitude of the response variables for each. For a given 50-year simulation, the economic damages can be found for each storm, discounted to the reference year, and summed to give a damage value for that simulation. The hurricane and storm damages were evaluated using a time series simulation combined with a composite damage reduction analysis. The composite damages method computes the damages of a storm to each structure for the three basic categories: inundation, wave attack, and storm recession.

Once the structure and content damages from inundation, storm-induced recession and wave attack were computed, the maximum, or critical, damage was chosen for each. Beginning in the first year of the project life, the model determines if any storms occurred, calculates the damages for each structure and each storm, increments the shoreline by one year of long term change, then begins the calculations for the second year. When the model completes the calculations for one 50 year period, it begins again for the next 50 year period. Other factors that are considered are long-term erosion, rebuilding constraints, back bay flooding, downdrift impacts, existing structural impediments to erosion such as seawalls and bulkheads, and individual actions to protect against erosion.

7. ACKNOWLEDGEMENTS:

The research presented in this paper, unless otherwise noted, was sponsored by the Office of the Chief of Engineers, U. S. Army, and is published by its permission. Panama City Beach studies were conducted for the Mobile District, U. S. Army Corps of Engineers.

8. REFERENCES

1. Abel, C. E., B. A. Tracy, C. L. Vincent and R. E. Jensen, "Hurricane Hindcast

Methodology and Wave Statistics for Atlantic and Gulf Hurricanes from 1956-1975," Wave Information Studies of U.S. Coastlines, WIS Report No. 19, Coastal Engineering Research Center, U.S. Army Engineer Waterways Experiment Station, Vicksburg, MS, March 1989.

2. Borgman, L. E., "An Algorithm for Optimal Efficiency in Selecting Storms for Finite Element Modeling of Surge," Contractor Report, Coastal Engineering Research Center, U.S. Army Engineer Waterways Experiment Station, Vicksburg, MS, 18 November 1990.

3. Borgman, L. E., "A Method for Calculating Statistical Reliability of Estimates of Future Hurricane Damages and Effects," Contractor Report, Coastal Engineering Research Center, U.S. Army Engineer Waterways Experiment Station, Vicksburg, MS, 29 April 1991.

4. Borgman, L. E. and D. T. Resio, "Extremal Statistics in Wave Climatology," in A. R. Osborn and P. M. Rizzoli, Proc. International School of Physics (Enrico Fermi), Topics in Oceanography, North-Holland Publishing Co., New York, 1982, pp 439-471.

5. Cialone, M. A., "The Coastal Modeling System: User's Manual," IR-CERC91-1, Coastal Engineering Research Center, U.S. Army Engineer Waterways Experiment Station, Vicksburg, MS, 1991.

6. Efron, B., "The Jackknife, The Bootstrap, and Other Resampling Plans," Regional Conference Series in Applied Mathematics, No.38, Society for Industrial and Applied Mathematics, Philadelphia, PA, 1982.

7. Goda, Y., "The Observed Joint Distribution of Periods and Heights of Sea Waves," in Proc. 16th Conf. on Coastal Engineering, Hamburg, 1978.

8. Haring, R. A., A. R. Osborne and L. P. Spencer, "Extreme Wave Parameters Based on Continental Shelf Storm Wave Records," in Proc. 15th Conf. on Coastal Engineering, Honolulu, Hawaii, 1976.

9. Jarvinen, B. R., C. J. Neumann and M. A. S. Davis, "A Tropical Cyclone Data Tape for the North Atlantic Basin, 1886-1983: Contents, Limitations, and Uses," NOAA Technical Memorandum, NWS, NHC 22, National Hurricane Center, Miami, FL, March 1984.

10. Jensen, R. E., C. L. Vincent, and C. E. Abel, "A User's Guide to SHALWV: Numerical Model for Simulation of Shallow-Water Wave Growth, Propagation, and Decay; Report 2, SHALWV-Hurricane Wave Modeling and Verification," Instruction Report CERC-86-2, Coastal Engineering Research Center, US Army Engineer Waterways Experiment Station, Vicksburg, MS, June 1983.

11. Larson, M. and N. C. Kraus, "SBEACH: Numerical Model for Simulating Storm-Induced Beach Change, Report 1, Empirical Foundation and Model Development," Technical Report CERC-89-9, Coastal Engineering Research Center, US Army Engineer Waterways Experiment Station, Vicksburg, MS, July 1989.

12. Larson, M., N. C. Kraus, and M. R. Byrnes, "SBEACH: Numerical Model for Simulating Storm-Induced Beach Change, Report 2, Numerical Formulation and Model Tests," Technical Report CERC-89-9, Coastal Engineering Research Center, US Army Engineer Waterways Experiment Station, Vicksburg, MS, May 1990.

13. Luettich, R. A., J. J. Westerink, and N. W. Scheffner, "ADCIRC: An Advanced Three Dimensional Circulation Model for Shelves, Coasts and Estuaries, Report 1: Theory and Methodology of ADCIRC-2DDI and

ADCIRC-3DL," Coastal Engineering Research Center, US Army Engineer Waterways Experiment Station, Vicksburg, MS, In Prep.

14. Miller, M. C., W. E. Roper, L. E. Borgman and J. J. Westerink, "Development of Water Level and Wave Height Design Data," Proc. Panel on Wind and Seismic Effects, UJNR, 23rd Meeting, Tsuduba, Japan, 14-23 May 1991.

15. Westerink, J. J., R. A. Luettich, and N. W. Scheffner, "ADCIRC: An Advanced Three Dimensional Circulation Model for Shelves, Coasts and Estuaries, Report 2: ADCIRC-2DDI Users Manual," Coastal Engineering Research Center, US Army Engineer Waterways Experiment Station, Vicksburg, MS, In Prep.

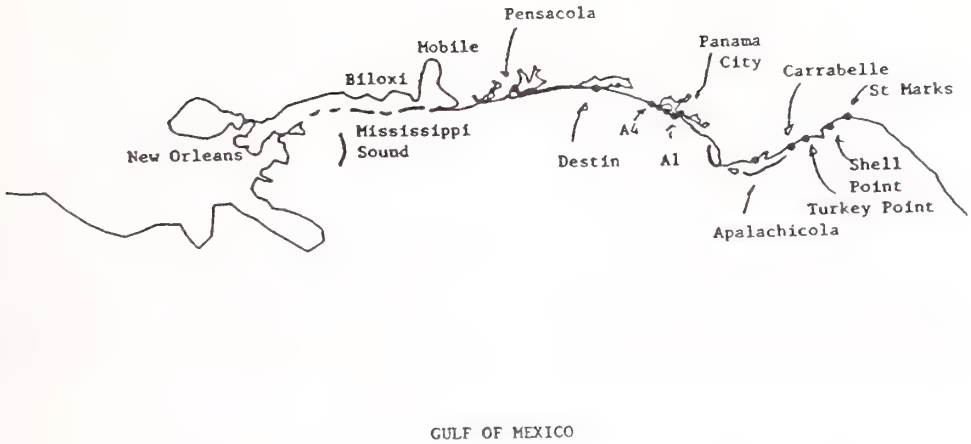

Figure 1. Northern Gulf of Mexico from Louisiana to Florida Bight. Study site is at Panama City.

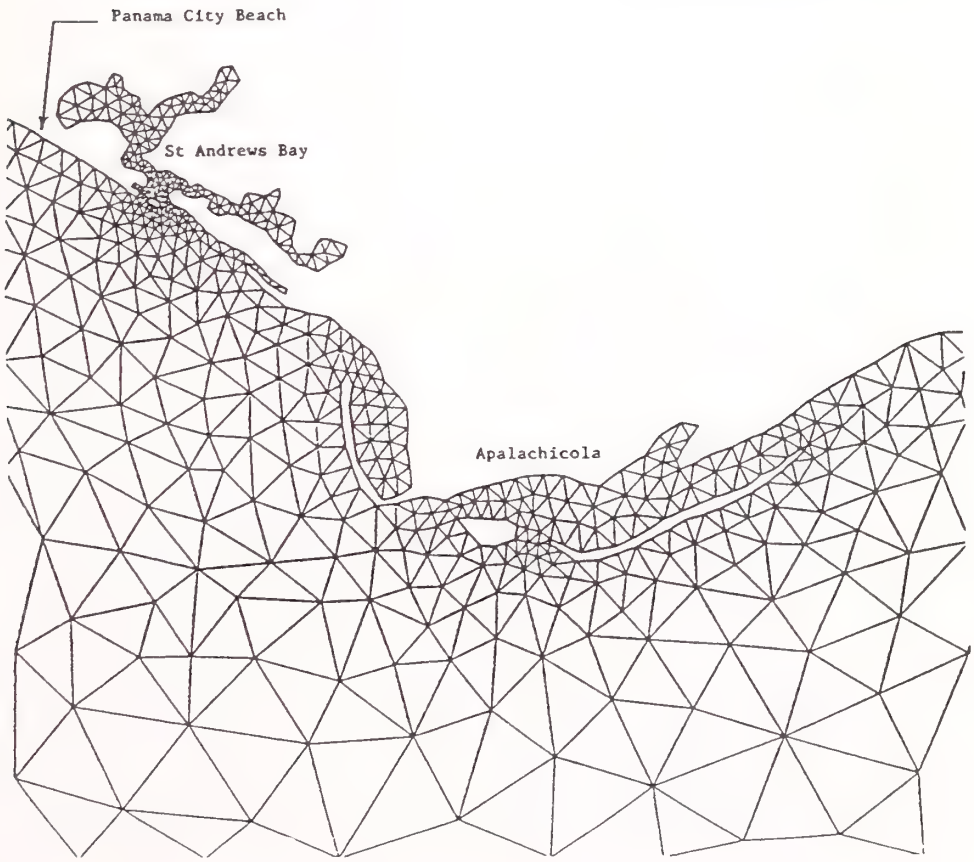

Figure 2. Details of finite element grid near Panama City, FL.

Theme III

Joint Cooperative Research Program

The Japan-PRESSS Program—Analytical Tools in Japan

by

T. Okoshi

Structural Engineering Department
Nihon Sekkei Inc.
Nishi-Shinjuku, Tokyo 163
Japan

S. Nakata

Associate Director for
Composite Structures Research
Structural Engineering Department
Building Research Institute
Ministry of Construction
Tatehara 1, Tsukuba-city, Ibaraki 305
Japan

ABSTRACT

In Japan, it is required the use of nonlinear time-history analysis for the dynamic response analysis of a reinforced high-rise concrete building. There are two models used in the dynamic response analysis, one is the lumped mass model and the other is the frame model. The lumped mass model is formulated distributing the weight as a lumped mass for each story level, and using equivalent flexure-shear springs which are obtained from the static elasto-plastic analysis, and the appropriate damping values. In the static elasto-plastic frame analysis, the distribution of the lateral forces is assumed, and the incremental analysis is used. Each member of the frame is modelled to be elastic with rigid-plastic rotational springs at its ends. The restoring force characteristics of this model are decided considering its flexural cracking and yielding. Usually, the skeleton curve is tri-linear, and the hysteresis rule is degrading tri-linear, like the origin-pointed model or the continuous degrading system (Takeda model), for the case of the restoring force characteristics of the lumped mass model. The same procedure for the static elasto-plastic analysis, and the restoring force characteristics of the lumped mass model can be used for the dynamic response analysis of the frame model.

1. Introduction

The nonlinear time-history analysis is used as a check of responsed story drift of reinforced concrete high-rise buildings in Japan. The modal analysis is not used. This dynamic response analysis is based on the mathematical model of elasto-plastic characteristics of the frame and the reduction of the members stiffness due to flexural cracking and yielding.

Digital acceleration time history records of the following ground motions are used. Standard ground motions are EL CENTRO 1940 NS and TAFT 1952 EW. Local ground motions like Tokyo-101 1952 NS, OSAKA-205 1963 EW, HACHINOHE 1968 NS and others. In this group HACHINOHE 1968 NS and others are ground motions containing long period waves. Three kind of waves are to be used in the dynamic analysis as a rule.

The peak velocities for the earthquake waves are decided according to the earthquake activity at the site. For example, in Tokyo, the peak velocity is greater than 25cm/sec for the ground motion level 1, and its equivalent acceleration value is about 250cm/sec^2; while the peak velocity is greater than 50cm/sec for the ground motion level 2, and its equivalent acceleration value is about 500cm/sec^2.

The dynamic elasto-plastic response analysis is used for level 1, considering the reduction of the members stiffness due to flexural cracking. For level 2, it is used considering the reduction of the members stiffness due to flexural cracking and yielding. However there are many ways to make the mathematical model of restoring force characteristics and damping.

These analysis are quite time consuming and expensive to perform. The use of the dynamic elasto-plastic response analysis is generally justified only for the reinforced concrete building with a height greater than 45m.

2. Static elasto-plastic frame analysis using incremental analysis

The static analysis is the incremental analysis using the stiffness matrix. The restoring force characteristics of all members are difined

independently. The lateral forces are increased step by step, and the stiffness is assumed to be constant for each load increment, which is called " moment stiffness ". The moment stiffness is calculated for each load increment taking into account every load-deflection relationship (skeleton curve). The stress analysis is carried out using these data. Then every story drift, the deformations and stresses at the members ends are obtained for every loading step.

2.1 The distribution of lateral force

The distribution of lateral forces is defined as the modified Ai distribution.
In other cases, it is obtained from the preliminary response analysis.

2.2 Elasto-plastic model of a member

There are two methods to make mathematical model of beam and column, whose flexural characteristics are elasto-plastic. One is an elastic member with plastic hinges at both ends. And the other where the member is divided into many elements, whose restoring force characteristics are defined independently.

There are three models to define plastic hinges at both ends of a member. They are : the hybrid beam model, the model where both ends are rigid plastic rotational springs and the model where both ends are plastic hinge zones.

(1) The Hybrid beam model
In this model the member is composed of an elastic part and a complete elasto-plastic part as shown in Fig.2.1.

(2) The model where both ends are rigid-plastic rotational springs as Fing.2.2.
In this model, rigid-plastic rotational springs are used at both ends of an elastic member. There are two kinds of rigid-plastic rotational springs. One shows the flexural plastic characteristics (Degrading tri-linear). And the other shows an additional deformation due to the slip of the tension bars of a beam-column connection.

(3) The model where both ends are plastic hinge zones in Fig.2.3.
In this case the stiffness of the plastic hinge zone is reduced after yielding.
There are three models to divide a member into many elements with a certain length, whose restoring force characteristics are defined independently.

The model where the member is divided into many parts.
This is shown in Fig. 2.4.

The assumed flexural stiffness distribution model.
This is shown in Fig. 2.5.

The model where two cantilevers are connected.
This is shown in Fig. 2.6.

There are two ways of modelling a shear wall. One is to replace it with a column which is a two - dimensional member. The other is shown in Fig. 2.7.

2.3 Mathematical models

The mathematical model is a two-dimentional frame model, and the degree-of-freedom in the lateral displacement of the same story is one.

The stiffness is fixed at every step. All members are divided into columns, beams and beam-column connections. The shear wall is replaced by a column which is a 2-dimensional member.

2.4 Skeleton curve of a member

Column, Beam : Tri-linear model considering flexural cracking and yielding (Fig.2.8)
Connection panel : Bi-linear model considering shear cracking (Fig.2.9)
Column (axial force) : Tri-linear model for tension and bi-linear model for compression (fig.2.10)

2.5 Analysis procedure

The static elasto-plastic frame analysis is carried out in the following way:
(a) Getting ready for the calculation.
(b) Change the matrix which is in terms of the member end displacements to a matrix in term of node displacements.
(c) Make the moment stiffness matrix of each member.
(d) Make the moment stiffness matrix for every story.
(e) When part of the panels is neglected, the moment stiffness matrix for every story has to be modified.
(f) Make the moment stiffness matrix of the frame.

(g) Make the moment lateral stiffness matrix of the frame (the frame is fixed at the base)

(h) Make the moment stiffness matrix of the frame, considering rocking and sway at the base.
(i) The eigenvalue analysis ..... at first circle.
(j) calculation of the lateral force increment.
(k) Stress analysis ..... Calculation fo the incremental lateral displacement.
(l) Calculation of the incremental displacements and forces of the ends of the members.
(m) The displacement and force at the ends of the member at one step are equal to the displacement and force at the ends of the member at one step before plus the incremental values.
(n) Deciding whether a member is elastic or plastic according to its restoring force characteristics, and then calculating the next moment stiffness.
(o) Go to (c) if the moment stiffness changed. Go to (j) if the moment stiffness did not change.

2.6 Results

Flexural cracking, flexural yielding and ductility factor and forces at each member end are obtained for every load increment step (Fig.2.11). Shear-drift relationship for every story is also obtained. (Fig.2.12). The ultimate lateral shear strength for every story is obtained.

3. Dynamic elasto-plastic response analysis using lumped mass model

3.1 Fundamental mathematical model

(1) Lumped mass
The distribution of weight is defined as a lumped mass for every story level.

(2) Mathematical model
(a) Equivalent flexural-shear model (Fig.3.1)
The shear deformation components of each story are separated from the results of the incremental analysis. They are obtained to subtract the flexural deformation from the story drift. The flexural deformation components are obtained from the axial deformations of the columns. The equivalent flexural and shear springs of each story are obtained from the flexural and shear deformations, where the flexural springs are assumed to be elastic.

(b) Rocking and sway model (Fig.3.2)
Ground or piles are replaced using an equivalent rocking and spring or swaying spring. And the superstructure is replaced using an equivalent flexural and shear model.

(3) Damping

Kind: Viscous damping

$$[c]=\frac{2h_1}{\omega_1}[k]$$

Damping matrix : Proportional to the moment stiffness of proportional to be initial stiffness
Damping factor : 3% for the first mode
The damping factors for the other modes are proportional to the frequencies.

(4) Numerical integration

Linear acceleration method is used.

3.2 Restoring force characteristics

In case of seismic response analysis for reinforced concrete structures, the model used to define the restoring force characteristics is based on the skeleton curves and hysteresis rules based on geometrical rules.

These models can be : Masing type, Slip Type, Degrading type and the combination of these types. The degrading type is used mainly for reinforced concrete structures.

3.3 Skeleton curve

(1) Definition of the skeleton curve

The shear deformation for each story is obtained separating the story drift into shear deformation and bending deformation. The skeleton curve is obtained replacing the shear-deformation relationship in the tri-linear model.

(2) Definition of ductility factor

A story ductility factor is defined as the second yield point in the skeleton curve.

3.4 Hysteresis rule

(1) Tri-linear origin-oriented model
This is shown in Fig. 3.4.

(2) Tri-linear maximum value-oriented model
This is shown in Fig. 3.5.

(3) Degrading Tri-linear model
This is shown in Fig. 3.6.

The hysteresis rule for an amplitude smaller than the yielding point is the same as the normal bi-linear mode. When the unloading starts from the loop point which is over the yielding point, this point is assumed to be the new " yielding point ", the hysteresis rule is the same as in the bi-linear model, but the stiffness is degrading.

(4) Takeda model
This is shown in Fing. 3.7.

(a) $|\delta_{max}| < \delta_{y1}$

The hysteresis rule for an amplitude smaller than δ_{y1}, stiffness K is the same as the linear model.

(b) $\delta_{y1} \leq |\delta_{max}| \ \delta_{y2}$

When δ increases over $\pm\delta_{y1}$ at the first time, or when δ when δ increases over the last maximum deformation point δ_{max}, it goes to the second stiffness K_2. When the unloading starts from this line, it goes in the stiffness K_{e1} or K_{e2} to the horizontal axis. Then it goes to the opposite maximum deformation point from the horizontal axis. THen it goes to the opposite maximum deformation point from the horizontal line.

(c) $\delta_{y^2} \leq |\delta_{max}|$

It is the same as (b). When the unloading starts towards zero, its stiffness is K_{e1} or K_{e2}. Next, when the load starts from zero, is goes to the opposite maximum deformation point.

4. Dynamic elasto-plastic response analysis using frame model

This dynamic analysis is the incremental analysis using stiffness matrix. The restoring force characteristics of all members are defined independently. The time is divided into incremental times. The stiffness is assumed to be constant for every time increment, which is called " moment stiffness ". At each step increment, the moment stiffness is calculated according to each skeleton curve, and the dynamic analysis is carried out using it. In this way each story drift, deformations and forces for every member are obtained successively.

This dynamic analysis requires many iterations and therefore a larger computer capacity is necessary.

4.1 Fundamental mathematical model

(1) Mathematical model
Two-dimensional frame models are shown in Fig. 4.1.

A structure is divided into columns, beams, beam-column panels and shear walls.
The restoring force characteristics are defined independently.

(2) Member model
It is the same as the one used in the static elasto-plastic analysis.

Usually, the elasto-plastic model for column and beam is the model where both ends are rigid-plastic rotational.

(3) Damping

Kind : Viscous damping

$$[c] = \frac{2h_1}{\omega_1}[k]$$

Damping matrix : Proportional to the moment stiffness or Proportional to the initial stiffness

Damping factor : 3% for the first mode
The damping factors for the other modes are proportional to the frequencies.

(4) Numerical integration

Linear acceleration method is used.

4.2 Restoring force characteristics of the members

(1) Skeleton curve
It is the same as in the section 2.4 " Skeleton curve of a member "

(2) Hysteresis rule
It is the same as in the section 3.4 " Hysteresis rule ".
The case for columns in shown in Fig. 4.2.

4.3 Analysis procedure

It is the same as in the section 2.5 " Analysis procedure ".
Only that the item (j) is " incremental acceleration of ground motion ", and (k) is " response analysis"

Reference

1. Materials for Seismic Design in the Building Engineering, AIJ, 1981

2. Recent Advancement of Structural Mechanics in Building Engineering, AIJ, 1987

3. Study of Elasto-Plastic Frame Response Characteristics and Seismic Design of High Rise Reinforced Concrete Buildings, Edo Hiroaki, 1987.

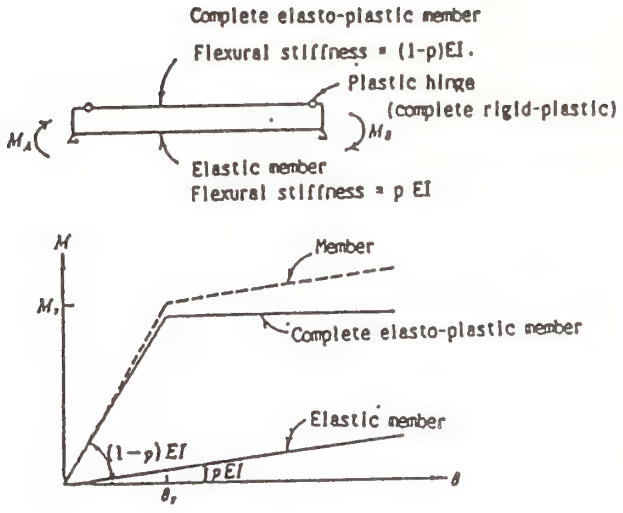

Fig. 2.1 Hybrid beam model

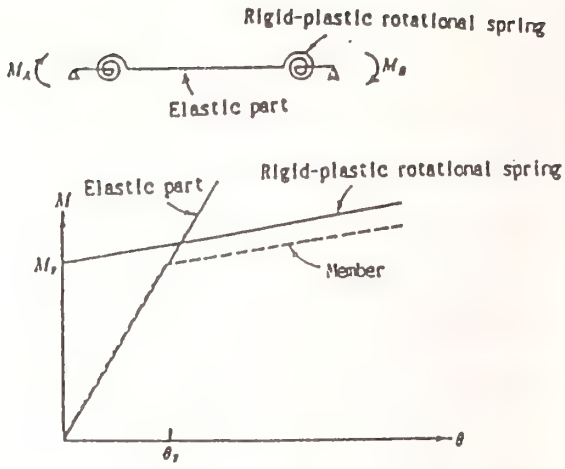

Fig. 2.2 Model where both ends are rigid-plastic rotational springs

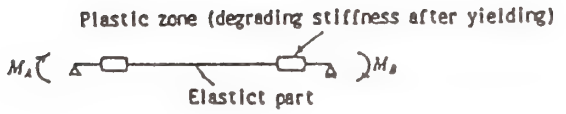

Fig. 2.3 Model where both ends are plastic hinge zones

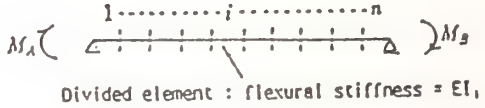

Fig. 2.4 Dividing element method

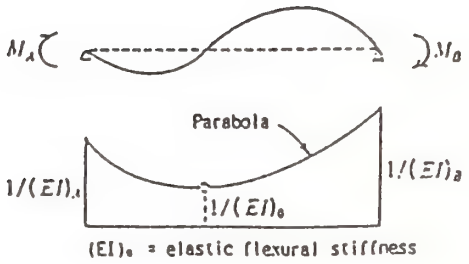

Fig. 2.5 Assumed stiffness distribution method

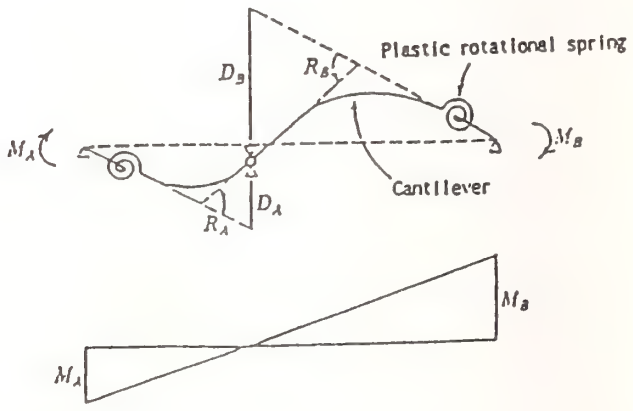

Fig. 2.6 Model where two cantilevers are connected

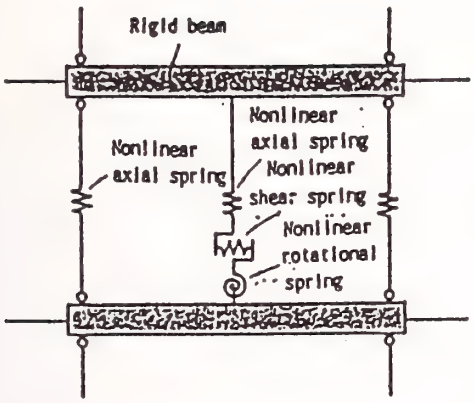

Fig. 2.7 Shear wall model

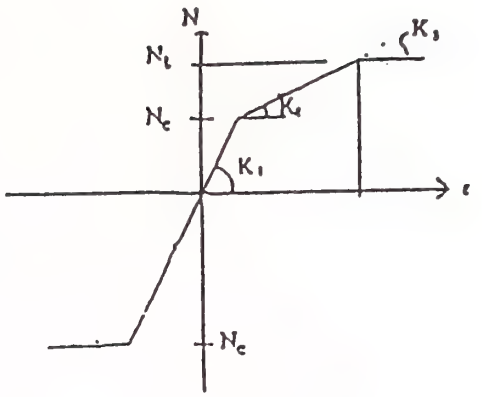

Fig. 2.10 Load-deflection relationship of the column axial force

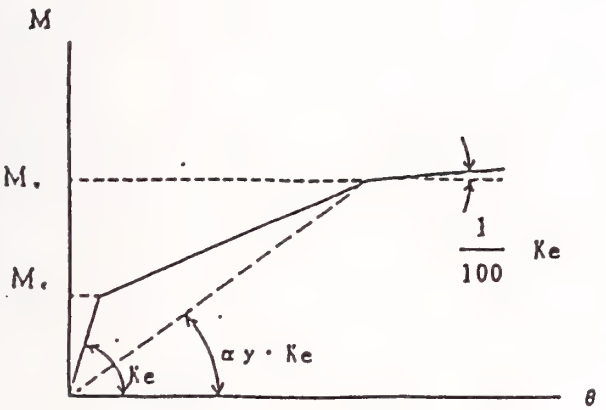

k_θ : elastic stiffness (included slab and re-ber)
α_y : reduction factor of stiffness at yielding point
M_t : flexural cracking moment
M_u : ultimate flexural force

Fig. 2.8 Load-deflection relationship of beam or column

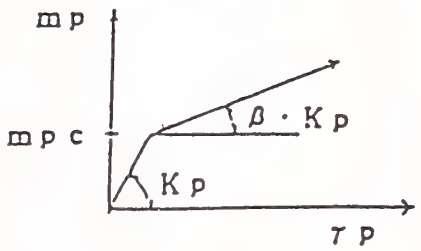

m_p : virtual panel moment
$k_\theta = G_c \times {}_cV_j$ (shear stiffness)
$m_{pc} = \tau_c \times {}_cV_j$
${}_cV_j = j_c \times j_c \times t$, (volume)
$\beta = 0.2$

Fig. 2.9 Load-deflection relationship of beam-column connection

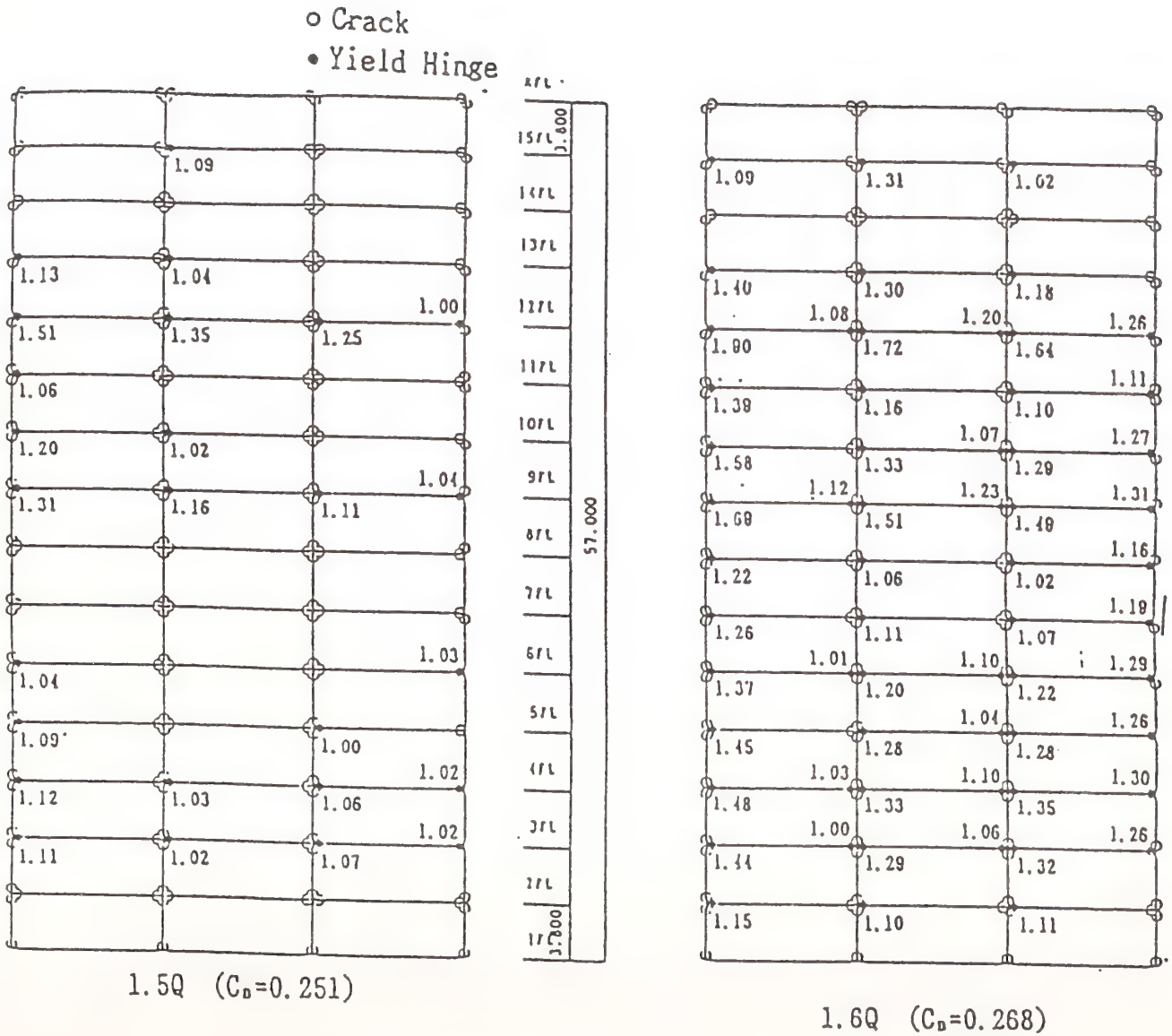

Fig. 2.11 Hinge formation and beam ductility

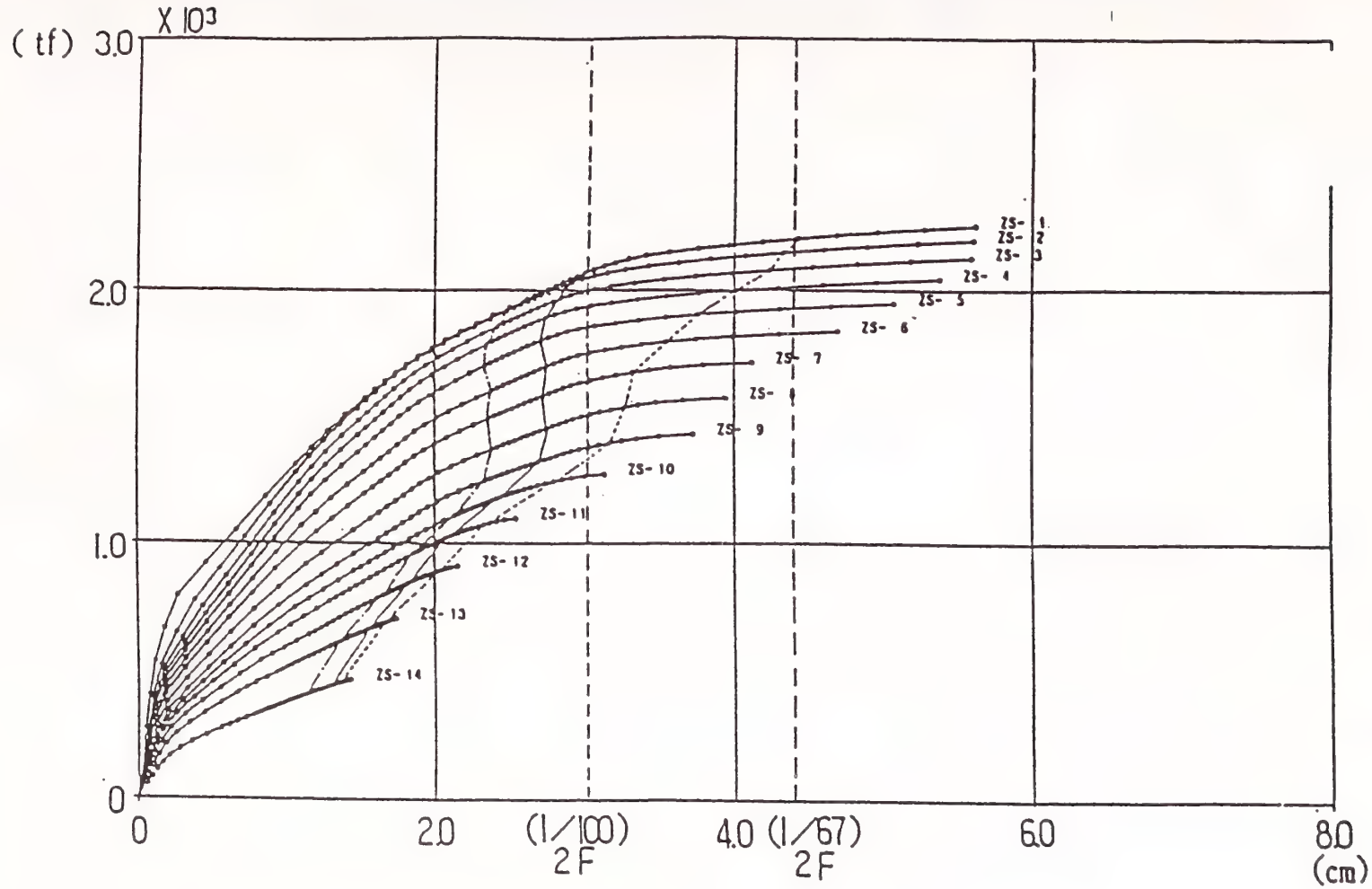

Fig. 2.12 Load-deflection relationship for every story

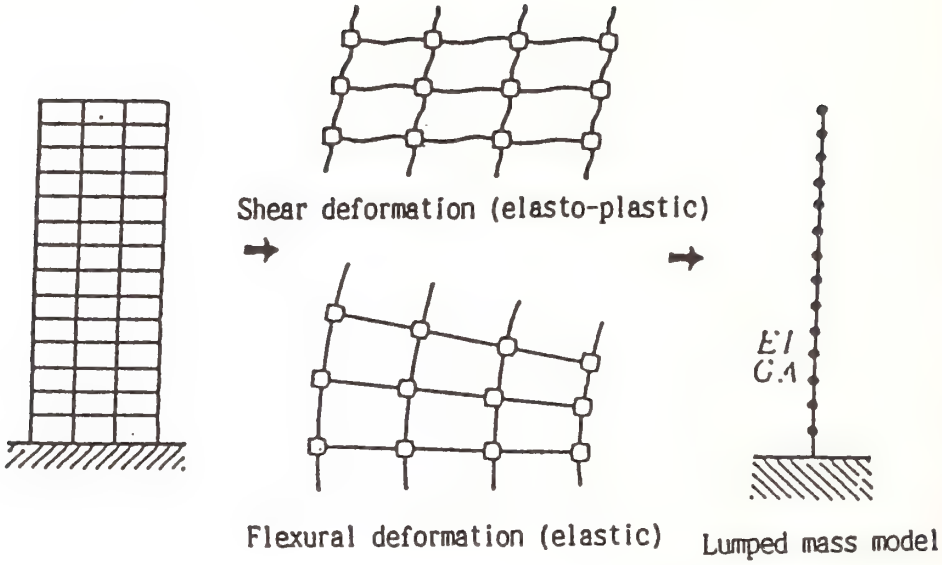

Fig. 3.1 Equivalent flexural-shear model

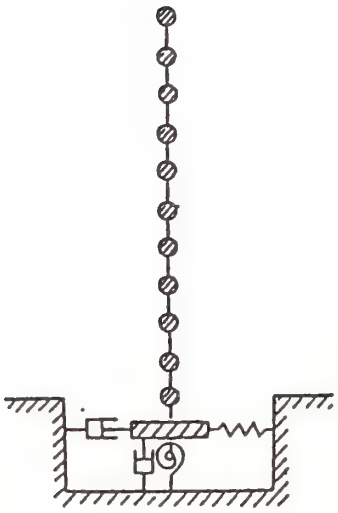

Fig. 3.2 Rocking-sway model

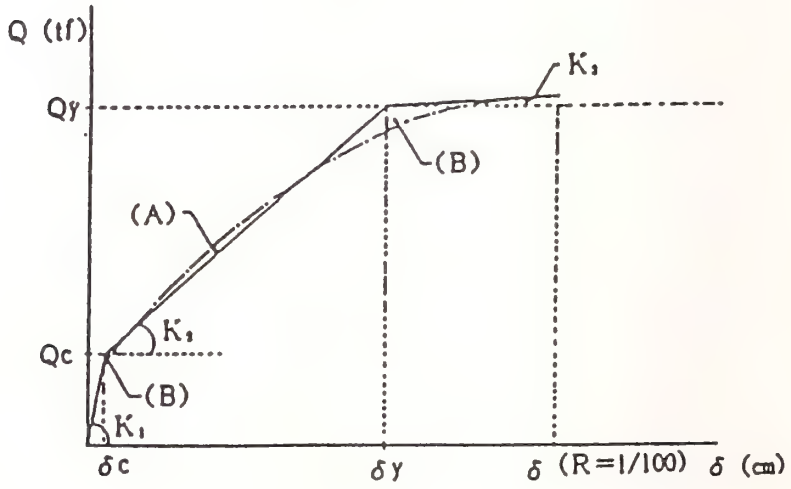

Fig. 3.3 Definition of the skeleton curve

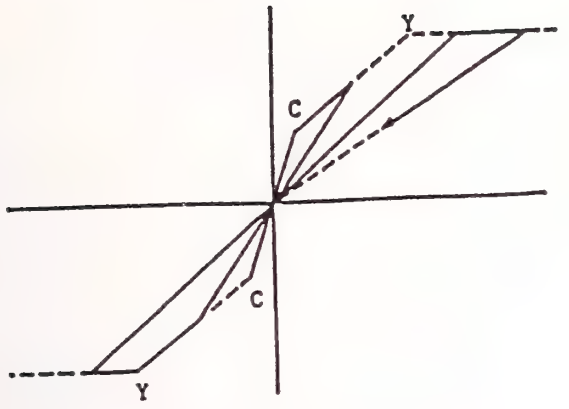

Fig. 3.4 Trilinear origin-oriented model

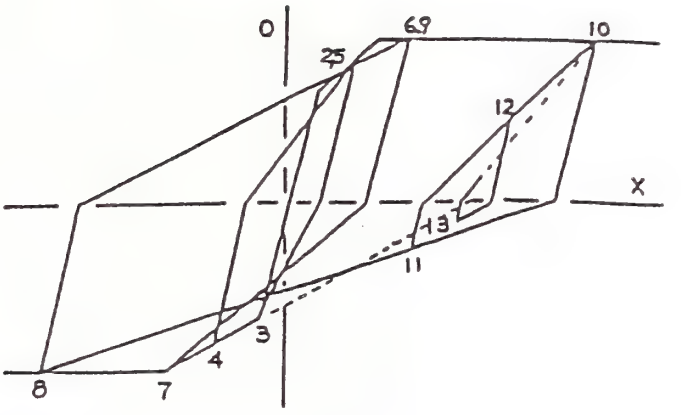

Fig. 3.5 Trilinear maximum value-oriented model

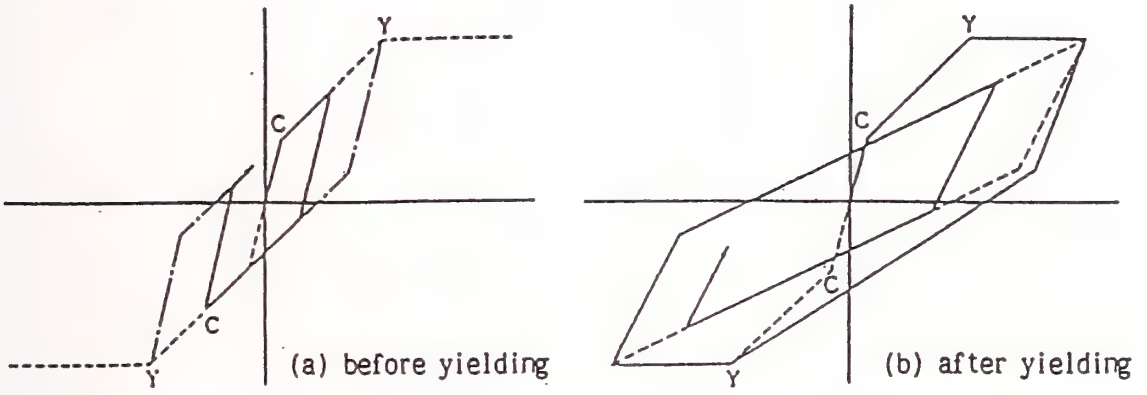

Fig. 3.6 Degrading tri-linear model

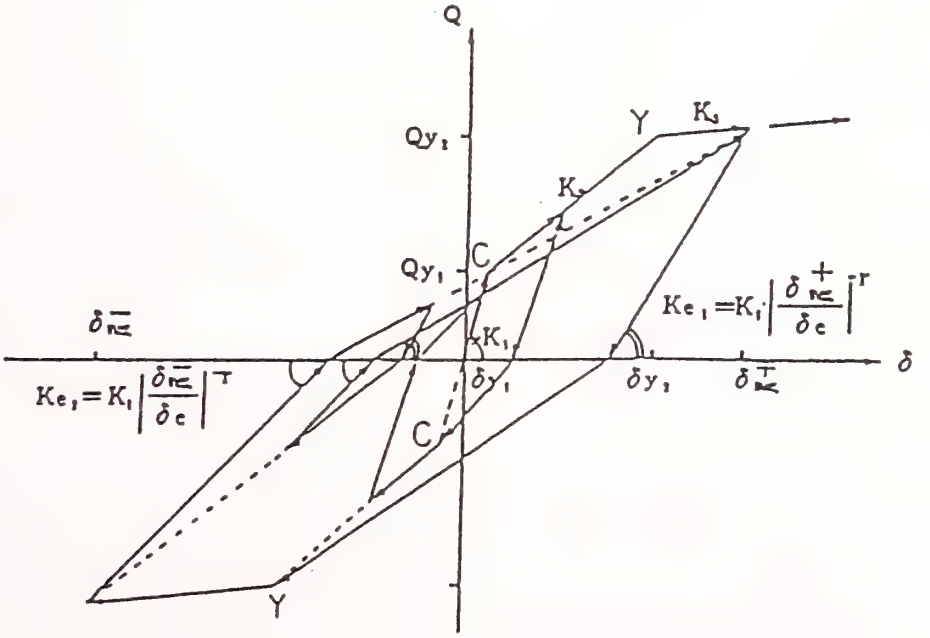

Fig. 3.7 Takeda model

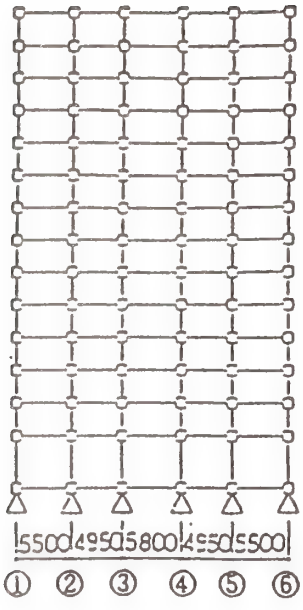

Fig. 4.1 Frame model

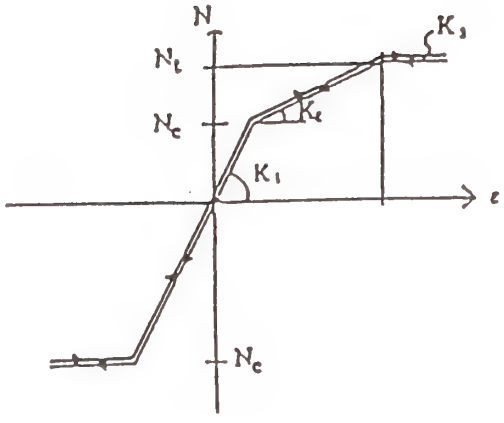

Fig. 4.2 Hysteresis rules for axial forces

U.S. Japan Cooperative Research in Precast Seismic Structural Systems (PRESSS) Program – Status Report

by

Nigel Priestly[1] and H. S. Lew[2]

ABSTRACT

The Precast Seismic Structural Systems (PRESSS) research program was initiated as the fourth topic in the United States - Japan coordinated program on large scale testing for seismic response. The first three topics were reinforced concrete, steel and masonry. The purpose of this coordinated research program is to develop recommendations for the seismic design of buildings constructed of precast concrete systems based on sound analytical and experimental research.

This report describes the scope of the joint program and the current projects being carried out by U.S. researchers.

KEYWORDS:

buildings; concrete; earthquake; precast; research; seismic; structures

1. INTRODUCTION

The fundamental objectives of the U.S.-PRESSS program are two fold:

- To develop comprehensive and rational design recommendations based on fundamental and basic research data which will emphasize the viability of precast construction in the various seismic zones.

- To develop new materials, concepts and technologies for precast construction in the various seismic zones.

The PRESSS program sets out to achieve these objectives by a process of examination and assimilation of existing research and design information, by development and evaluation of new PRESSS concepts in close cooperation with industry, by carefully planned analytical and experimental research, and by formulation of the results within a framework of design recommendations based on state-of-the-art design philosophy.

The program considers only the seismic behavior of building structures where precast construction forms the essence of the structural system. Current precast seismic structural systems can be divided into two categories: precast frame buildings and precast wall panel construction. Both are included in the U.S.-PRESSS program.

2. STRUCTURE OF THE U.S.-PRESSS PROGRAM

The U.S.-PRESSS program was conceived in three phases. Phase I, which is funded by the U.S. National Science Foundation for a three-year period ending in 1993, is focused on identifying and evaluating the most promising structural concepts for precast concrete building systems in seismically active regions.

Phase II involves detailed experimental studies of components and subassemblages of precast systems selected during Phase I for more detailed investigation.

Phase III involves one or more multi-story full-size "superassemblage" experiments and the finalization of the seismic design recommendations for incorporation into the model building codes.

---

[1] University of California, San Diego, La Jolla, California 92093

[2] National Institute of Standards and Technology, Gaithersburg, Maryland 20899

Phase I Program:

- Concept Development

  The project is focused on the development and evaluation of new concepts for precast concrete construction in UBC seismic zones 2, 3, and 4, particularly for low and mid-rise buildings.

- Connection Classification and Modeling

  The project involves a comprehensive review of existing test data and the development of a classification system for PRESSS connections based on type and function.

- Analytical Platform Development

  The widely used DRAIN-2D inelastic time-history analysis program for seismic response is being expanded to three dimensions. In addition, new elements are being developed to model the special characteristics of precast members including joint deformations resulting from slip and ductility.

- Preliminary Design Recommendations

  Current seismic design codes for precast concrete structures are being reviewed and preliminary prescriptive design requirements for "strong connection" precast construction are being developed. In addition, a framework for the final design recommendations, based on structural reliability theory, will be provided. These provisions will include recommendations for ductile connections design.

- Coordination

  This project provides the umbrella under which the four above-mentioned projected are interrelated, and also provides coordination with the Japan-PRESSS research team and the research program at the National Institute of Standards and technology.

Phase II Program:

- Evaluation of Ductile connections for Frame PRESSS

  This project involves the evaluation of the behavior of connecting elements, beam-column subassemblages, and multi-bay subassemblages.

- Evaluation of Wall Panel Building for Moderate Seismic Zones

  This project includes the evaluation of optimal range of connection strength and ductility for a six story building, strength and deformation characteristics required for connection elements, and tests on horizontal panel connections.

3. U.S.-JAPAN COORDINATION

The second meeting of the Joint Technical Coordinating Committee on Precast Seismic Structural Systems was held in Tsukuba, Japan, October 31 - November 2, 1991. The meeting was attended by 21 researchers and 9 observers from Japan, 4 researchers and 3 observers from the U.S., and one observer from New Zealand.

- The need for, and importance of, continuing experimental and analytical research on PRESSS was reaffirmed.
- Analysis of Japanese and U.S. frame buildings have indicated that satisfactory seismic response can be expected from precast frame buildings designed to meet recommendations of both countries.
- The U.S. side will carry out dynamic analysis of the test-design building.
- Both sides will continue to develop and classify new connection concepts.
- The third joint meeting is scheduled to be held in San Diego, October 25 - November 2, 1992.

Seismic Response Control of Highway Bridges by Variable Damper

by

Kazuhiko Kawashima[1], Shigeki Unjoh[2], and Hideyuki Shimizu[3]

ABSTRACT

This paper presents analytical and experimental studies on the dynamic characteristics of a variable damper developed at the Public Works Research Institute. Effectiveness of the variable damper for seismic response control of highway bridges is analytically investigated. A small-size model of the variable damper is developed and the dynamic characteristics through the dynamic loading tests is also presented.

KEY WORDS

Seismic Response Control, Highway Bridges, Variable Damper, Small-Size Model, Dynamic Loading Tests

1. INTRODUCTION

The variable damper[1)2)] is a viscous damper in which the viscous damping force is variable depending on the response of highway bridges as shown in Fig.1. That is:

1) The damping coefficient of the variable damper is taken large during a small deck vibration so that the damper has the same function as a fixed bearing support against the braking load of vehicles. It is movable against actions with low-velocity such as an elongation of deck by temperature change.

2) When the amplitude of deck vibration becomes larger up to a certain level during an earthquake, the damping coefficient is decreased so that the energy dissipation be optimum and the inertia force of a superstructure to substructures be decreased appropriately.

3) Furthermore, when the vibration amplitude of the deck becomes excessive, the damping coefficient is gradually increased in order to suppress the excessive amplitude. Therefore, the damper has a function as a stopper with a shock absorber. This is to prevent the impact response by the sudden operation of the stopper[4)].

Therefore, the variable damper has the advantages of an usual viscous damper stopper[5)-7)], a passive energy dissipator and a stopper with a shock absorber function.

The concept of the variable damper, in which the damping characteristics can be variable dependent on the situation, has been effectively adopted in a field of mechanical engineering, in particular in a suspension system for an aircraft and an automobile. An active suspension to improve driving comfortability and stability of the automobile is one of the examples[8)9)]. However, it is a new idea to apply the variable damper for highway bridges based on the concept of distributing the inertia force of a superstructure to substructures.

Although various types of the variable damper can be made, the simplest one may be as shown in Fig.2. The basic component is an cylinder-type viscous damper. A by-pass pipe is installed between the cylinder-cells divided by the piston. The damping characteristics of the damper can be controlled by varying the amount of flow of viscous material which passes through the by-pass. Since various technology for controlling such material flow has been developed, the variable damper is most promising and near to the practical use. Furthermore, the external energy required for the operation is significantly smaller in the variable damper than in active control devices[10)].

This paper presents analytical and experimental studies on the dynamic characteristics of a variable damper developed. The effectiveness of the variable damper for seismic response control of highway bridges is analytically investigated. A small-size model of the variable damper is developed and the dynamic characteristics through the dynamic loading tests is also presented.

2. SEISMIC RESPONSE ANALYSES OF HIGHWAY BRIDGES WITH VARIABLE DAMPERS

2.1 Seismic Response Analysis Method of Multi-Degree-of-Freedom System with Variable Dampers

The equations of motion for a linear multi-degree-of-freedom system with the variable dampers may be written as

$$\underline{M}\,\ddot{\underline{x}} + (\underline{C} + \underline{C}_v)\,\dot{\underline{x}} + \underline{K}\,\underline{x} = -\underline{M}\,\ddot{x}_0 \qquad (1)$$

in which $\underline{M}$, $\underline{C}$ and $\underline{K}$ represent mass, damping and stiffness matrices of the system, respectively. $\underline{x}$ and x_0 denote displacement vector of the system and an earthquake ground motion, respectively. $\underline{C}_v$ denotes a damping matrix of the variable dampers and is assumed as

1) Head of Earthquake Engineering Division, Earthquake Disaster Prevention Department, Public Works Research Institute, Ministry of Construction

2) Research Engineer, ditto

3) First Research Division, Fukushima Construction Office, Tohoku Regional Construction Bureau, Ministry of Construction (Formerly Assistant Research Engineer of the Earthquake Engineering Division, Public Works Research Institute)

$$\underline{C}_v = \sum_{k=1}^{n_v} \underline{c}_{ij}^{v} \qquad (2)$$

where

$$\underline{c}_{ij}^{v} = \begin{bmatrix} V & -V \\ -V & V \end{bmatrix} \qquad (3)$$

in which $\underline{c}_{ij}^{v}$ and n_v represent damping matrix of the variable damper, which is installed between the i-th node and the j-th node, and a number of the variable dampers installed, respectively. V is the damping coefficient of an each variable damper and is given as a function of relative displacement and relative velocity between the nodes where the variable dampers are installed.

Although there are various methods to prescribe the damping matrix $\underline{C}$, it is assumed here to be written as Eq.(4) assuming that the damping matrix $\underline{C}$ can be diagonalized by the modal matrix.

$$\underline{C} = (\underline{\Phi})^{-1}\ \mathrm{diag}[2h_\kappa \omega_\kappa]\ (\underline{\Phi}^{T})^{-1} \qquad (4)$$

in which, $\underline{\Phi}$ denotes a modal matrix of the system and diag[$2h_\kappa\omega_\kappa$] denotes a diagonal matrix with elements of $2h_\kappa\omega_\kappa$ (κ=1,2,3,$\cdots$; mode number).

Since $\underline{C}_v$ is time-varying, Eq.(1) has to be solved by a direct integration method. According to the above analytical method, a computer program "VDAM" which can analyze earthquake response of a multi-degree-of-freedom system with the variable dampers was developed.

2.2 Highway Bridge Analyzed and Analytical Conditions

In order to investigate the effectiveness of the variable damper, a simple span girder bridge, as shown in Fig.3, with a span length of 30m is analyzed. The response in longitudinal direction is considered. Although the variable damper has better applicability for multi-span continuous girder bridges, the simple span girder bridge is taken as an analytical model here for simplicity. The superstructure of the model is supported by elastic isolators in longitudinal direction and the variable dampers are assumed to be installed between the superstructure and the pier top.

The model can be assumed as a single-degree-of-freedom oscillator if it is assumed that the deformation of the superstructure is negligibly small and that the piers are idealized as a linear spring. Therefore, the damping coefficient of the variable damper, V, can be written as

$$V = \sqrt{m_d\, k_p}\ h_v \qquad (5)$$

in which, m_d, k_p and h_v represent mass of the superstructure, a combined spring stiffness of elastic isolators and piers, and required damping ratio for the variable damper, respectively. The weight of the superstructure and spring stiffness of the isolator are assumed as 241.5tf and 640tf/m, respectively. The flexural stiffness of piers is assumed so that the fundamental natural period of the model be 0.5sec when the both bearing supports are hinged. The stiffness of isolators result in the fundamental natural period of 1 sec for the model with elastic isolators.

Damping ratio of the variable damper h_v defined by Eq.(5) can be variable dependent on both relative velocity and relative displacement between the superstructure and the pier top. Only analytical cases in which the damping ratio is varied with the relative deck displacement are shown here for representing the effectiveness of the variable damper although the velocity-dependent variable damper was also studied.

Six cases in total are analysed as shown in Fig.4. In Case 1, the variable damper is not installed, i.e., no control. In Case 2, the damping coefficient of the damper h_1 is assumed independent on the relative deck displacement. The damping ratio h_1 is varied as a parameter to be investigated. Cases 3 and 4 are cases for investigating the effectiveness of the stopper with a shock absorber for preventing excessive deck displacement. The damping ratio increased from h_1 to h_3 dependent on relative deck displacement. In Case 3, a weak stopper, i.e., a stopper with a shock absorber is assumed and the damping ratio h_3 is assumed to be 3. In Case 4, the strong stopper is assumed and the damping ratio h_3 is assumed to be 500. The displacement at which the stopper initiates to work is assumed as 2/3 of the peak relative deck displacement d_u of Case 2. This displacement is defined hereafter as a design displacement of the variable damper. The design displacement of the variable damper d_u is 7.7cm as will be shown in Case 2. Case 5 is a case for investigating the effectiveness of the stopper for suppressing small deck displacement caused by vehicle loads. The damping ratio is increased from h_1 to h_2 in the range of the relative displacement from $-1/6d_u$ to $1/6d_u$. Case 6 is a combination of Cases 3, 4 and 5.

An acceleration ground motion shown in Fig.5 is used as an input acceleration. The acceleration, recorded on the ground around the Tsugaru Bridge during the Nihonkai-Chubu Earthquake of 1983, was modified so that the response spectrum matches with the target spectrum. The acceleration spectrum, which is specified in "Part V Seismic Design" of the "Design Specifications for Highway Bridges", for the check of bearing capacity of reinforced concrete piers on soft soil site (ground condition III), is assumed as the target spectra.

When the variable damper is not provided, the modal damping ratio of the model bridge is assumed to be 2% of critical in the above cases.

2.3 Effectiveness of the Variable Dampers for Seismic Response Control of Highway Bridges

Fig.6 shows how the peak deck response and force developed at the pier vary in accordance with damping ratio h_1 for constant damping (Case 2). The peak deck displacement monotonously decreases with increasing the damping ratio h_1 and become almost stable for the damping ratio equal or greater than 2. The peak deck acceleration takes minimum at the damping ratio h_1 of about 0.5. This is because the function as a damper stopper becomes predominant rather than an energy dissipator. The shear force and bending moment at the pier bottom with increase of the damping ratio h_1 in a similar manner with the peak deck acceleration.

On the other hand, as the damping ratio increases the maximum damping force developed in the variable damper increases, while stroke of the piston decreases. Total energy dissipated during the excitation takes maximum value at the damping ratio of about 0.2.

Based on the analysis, the most appropriate damping ratio h_1 is considered as 0.5, which makes peak deck displacement and maximum bending moment at the pier bottom decease to 31% and 37% of those with no control, respectively. The damping force and peak stroke of the piston required fro this control are $34.7tf \times 2 = 69.4tf$ and 7.7cm, respectively.

Assuming h_1 as 0.5, the effectiveness of the stopper with a shock absorber was analysed. Fig.7 compares the deck displacement and acceleration as well as damping force of the variable damper for Cases 2 - 4. In Case 4, the pulse-type response developed by strong operation of the stoppers is seen in the damping force of the variable damper. Fig.8 compares the peak response and peak damping force for Case 2 - 4. Comparing Case 3 with Case 2, the peak deck response slightly decreases while maximum forces at the pier bottom increase only 7%. The maximum damping force of Case 3 developed in the variable damper becomes 1.73 times that of Case 2, and the peak stroke decreases by about 10%. The decrease of the stroke of the variable damper means that the function of the stopper operates effectively.

On the other hand, when the stopper operates strongly (Case 4) the responses become larger, and deck acceleration and forces at the pier bottom becomes about 2 times those in Case 3. Although the stroke of the variable damper decrease to the displacement at which the strong stopper operates, the peak damping force increase to about 4.3 times that in Case 3.

Fig.9 shows the effect of the stopper at the small deck displacement. The damping ratio of the damper, h_1, is assumed to be 0.5 and h_2 is varied as a parameter. Although the peak deck displacement decrease monotonously as the damping ratio h_2 of the variable damper increases up to 8, it increases for the damping ratio h_2 greater than 8. This is because that the function as a damper stopper becomes more predominant rather than an energy dissipator when the damping ratio h_2 becomes larger. The peak deck acceleration takes a minimum value when the damping ratio h_2 is about 1, and it increases monotonously for the damping ratio h_2 greater than 1. The forces at the pier bottom vary with h_2 in a similar manner with the deck acceleration.

On the other hand, as the damping ratio h_2 increases the damping force of the variable damper increases and the stroke and the total energy absorbed decrease. Therefore, damper at the small deck displacement which is for suppressing the deck motion caused by the vehicle loads has contrary effects to make seismic response smaller. Therefore, it is necessary to determine damping ratio h_2 in consideration with the function of bridges for normal loads.

Table 1 summarizes the peak responses in Case 1 to 6. If the variable damper with $h_1 = 0.5$ and $h_2 = h_3 = 3$ is provided, peak deck displacement and peak deck acceleration decrease 25% and 43% of those with no control, respectively. The maximum bending moment at the pier bottom decreases to 46% of that. The required damping force and peak stroke of the variable damper are $62.6tf \times 2 = 125tf$ and 5.78cm, respectively. The variable damper with this specification can be designed within the current scope of damper technology.

3. DEVELOPMENT OF A SMALL-SIZE MODEL OF THE VARIABLE DAMPER

3.1 Outline of A Small-Size Model of the Variable Damper

Fig.10 shows a design plan of the variable damper developed. The model is designed so that the damping force be variable in the range of 20kgf to 200kgf, maximum relative displacement of damper piston be within $\pm$ 2.5cm. The control of the damping ratio is arbitrarily made by a personal computer dependent on relative displacement and velocity developed between deck and substructures.

The piston-cylinder has the total length of 394mm, the pressure area of the piston is $12.56cm^2$ and the stroke of the piston is $\pm$ 2.5cm. A steel pipe by-pass is installed between the cylinder-cells divided by the piston and the oil tank through two servo-valves. The servo-valve is called as a D.C. proportional magnetic valve, and the width of the valve is adjusted by the magnetic force of the D.C. proportional solenoid. The return spring is installed at the spool as shown in Fig.11. The differential transformer is installed at the servo-valve for the position detection of the spool so that the accurate control can be made. The input voltage from a servo amplifier to the servo valve is set in the range of 0 to 5V. The valve is closed at the input voltage of 0V and the valve is fully opened at

5V. The viscous material used for the variable damper is an usual oil for a dynamic loading actuator.

Fig.12 shows the flow of the viscous material in the variable damper. The damper piston can move in the left and right directions accompanying with the deck response. When the piston moves in the left side the viscous material flows from the left cell of the cylinder to the oil tank through the servo-valve 1, and from the tank to the right cell through the check valve 2 which can pass the oil only in one direction. At this time the servo-valve 2 is closed. When the piston moves in the opposite direction the oil passes through from cylinder to the tank through the servo-valve 2 and check valve 1. Therefore, the damping characteristics of the variable damper is controlled by the servo valve 1 when the piston moves in the left side, and by the servo-valve 2 when the piston moves in the right side.

3.2 Dynamic Loading Tests of the Small-Size Model of the Variable Damper

The variable damper can vary the damping characteristics depending on the displacement and/or velocity of the structures. Therefore, in order to provide the variable damper with the required damping characteristics it is necessary to know the basic dynamic characteristics of the variable damper. The damping characteristics of the variable damper is controlled by the amount of opening of the servo-valve and it is controlled by the input voltage to the servo-valve. Therefore, to know the characteristics of the variable damper developed, the relation between the input voltage to the servo-valve and damping characteristics of the variable damper is essential.

Fig.13 and Photo 1 show the set-up of the dynamic loading tests. The opening of the servo valve is kept to be constant under the condition that the input voltage is set to be a constant value, i.e., the damping ratio of the variable damper is set to be constant, the load is applied to the model by a dynamic actuator under the displacement control. The input voltage to the servo amplifier, reaction force and stroke of the piston are measured. The loading is harmonic and 10 cycle were repeated for each loading displacement.

Table 2 shows the experimental cases. Case 1 is to measure the friction force of the damper piston and static loading was made with loading frequency of 0.05Hz and loading displacement of 20mm. The input voltage of the variable damper is assumed to be 5V so as to open the valve fully. Case 2 is to obtain the input voltage to the servo-valve vs. damping force of the variable damper relation. Loading frequency, loading displacement and input voltage are varied.

3.3 Performance of the Small-Size Model of the Variable Damper

(1) Friction force of the damper-piston

Fig.14 shows a hysteresis loop of the load-displacement relation when the damper is loaded with the loading frequency of 0.05Hz and loading displacement of 20mm to obtain the friction force of the damper-piston. The load-displacement relation shows almost rectangular shape. This represents the typical type energy dissipation. The hysteresis is stable for a number of loading cycles. The average friction force was obtained as about 7kgf.

(2) Hysteresis Loops of the Load-displacement Relation

Fig.15 shows hysteresis loops of the load-displacement relation. In the loading displacement of 2mm, the time-lag was found in the peak damping force for the input voltage lower than 1.5V. This is developed due to compressibility and friction between the pipes and the viscous material. To compensate the effect it is required to make the pressure area greater for obtaining enough flow even if the displacement is small. In the loading displacement of 6mm and 10mm, the hysteresis loop seems as expected.

(3) The relation between the input voltage and damping force

Fig.16 shows the relation between the loading displacement and damping force dependent on the input voltage. The empirical equations obtained by a least square method are also shown in Fig.16. The relation between the damping force and loading velocity shows a function of the power of the loading velocity as an usual cylinder-type viscous damper. Therefore, the empirical equation is assumed as

$$F = F_0 + C(V) \cdot v^{n(V)} \qquad (6)$$

where

- F : damping force (kgf)
- F_0 : friction force of the damper-piston (7kgf)
- $C(V)$: damping coefficient (function of the input voltage V)
- v : velocity of the damper-piston
- $n(V)$: power coefficient of velocity term (function of the input voltage V)

In Eq.(6), damping coefficient C(V), and power coefficient of velocity term n(V), are unknown factors. They are computed by a least square method based on the tests results. The damping coefficient C(V) thus obtained are almost constant in the range of the input voltage of 0 to 5V, and averaged value of C(V) is 0.8. The relation between the input voltage and the power coefficient of the velocity term obtained is shown in Fig.17. The power coefficient increases with decrease of the input voltage. When the

input voltage is larger than 2.5V, the power coefficient becomes almost constant (n(V) = 1.4), and when the input voltage is lower than 2.5V the value takes larger. The relation obtained by a linear approximation is shown in Fig.17.

5. CONCLUDING REMARKS

The effectiveness of the variable damper developed for seismic response control of highway bridges was analytically investigated. The small-size model of the variable damper was developed and the performance was studied through the dynamic loading tests. According to the above investigations the following conclusions may be deduced:

1) In order to provide functions as damper stopper, energy dissipator and stopper with shock absorber for the variable damper, the damping ratio of $h_1 = 0.5$ and $h_2 \doteq h_3 = 3$ is the most favorable.

2) By providing the variable damper with damping ratio shown in 1), the peak deck displacement and the peak deck acceleration of the model highway bridge were reduced to 25% and 43%, respectively. The peak bending moment decreased to 46%. The required peak damping force and peak stroke of the variable damper were 62.6tf × 2=125tf and 5.78cm, respectively. The peak damping force is equivalent with 52% of the deck weight. These capability of the damper can be designed within the current scope of damper technology.

3) Based on the dynamic loading tests of the small-size model of the variable damper, the load-displacement relation was obtained as expected. A proto-type model of the variable damper is now under development for further improving the performance.

REFERENCES

1) Taguchi, J., Iwasaki, T., Adachi, Y., Sasaki, Y. and Kawashima, K. : U.S.-Japan Cooperative Research Program on Hybrid Control of Seismic Response of Bridge Structures, 22nd Joint Meeting, U.S.-Japan Panel on Wind and Seismic Effects, UJNR, Gaithersburg, Maryland, USA, May, 1990
2) Kawashima, K., Unjoh, S., Nagashima, H. and Shimizu, H. : Current Research Efforts in Japan for Passive and Active Control of Highway Bridges Against Earthquakes, 23rd Joint Meeting, U.S.-Japan Panel on Wind and Seismic Effects, UJNR, Tsukuba, May, 1991
3) Liu, S., C., Lagorio, H., J. and Chong, K., P. : Status of U.S. Research on Structural Control Systems, 23rd Joint Meeting, U.S.-Japan Panel on Wind and Seismic Effects, UJNR, Tsukuba, May, 1991
4) Kawashima, K., Hasegawa, K. and Nagashima, H. : Experiment and Analysis on Seismic Response of Menshin Bridges, Proc. 1st U.S.-Japan Workshop on Earthquake Protective Systems of Highway Bridges, National Center for Earthquake Engineering Research, Buffalo, N.Y., U.S.A., September 1991
5) Fukuoka, S. : Design of Multi-span Continuous Girder Bridge using Viscous Shear Stopper, Bridge, pp.22-29, February, 1980 (in Japanese)
6) Izeki, H. : Viscous Shear Stopper, Proposal to the Multi-Continuous Girder Bridge, Bridge, pp.30-33, February, 1980 (in Japanese)
7) Matsumura, S., Fukuoka, S, Mizumoto, Y. and Nakata, T. : Seismic Design of Multi-Span Continuous Girder Bridge using Damper Stopper, Bridge and Foundation, pp.31-37, May, 1982 (in Japanese)
8) Milliken, Jr., W., F. : Lotus Active Suspension System, Proceedings of 11th International Conference on Experimental Safety Vehicles, pp.467-475, Washington D.C., May, 1987
9) Sugawara, F. : Electronically Controlled Shock Absorber System Used as a Road Sensor which Utilizes Super Sonic Waves, Proceedings of Society of Automotive Engineers, pp.6.15-6.25, 1986
10) Kawashima, K., Unjoh, S. and Shimizu, H. : Optimum Seismic Response Control of Highway Bridges by Active Mass Damper, Civil Engineering Journal, Vol.33, No.9, pp.61-68, November, 1991 (in Japanese)
11) Kawashima, K., Unjoh, S. and Shimizu, H. : Earthquake Response Control of Highway Bridges by Variable Damper, Proceedings of Colloquium on Control of Structures, Japan Society of Civil Engineers, Part. B, pp.221-224, July, 1991 (in Japanese)
12) Feng, Q. and Shinozuka, M. : Use of A Variable Damper for Hybrid Control of Bridge Response Under Earthquake, U.S. National Workshop on Structural Control Research, University of Southern California, CA., U.S.A., October, 1990
13) Shinozuka, M., Feng, Q. and Kawamura, S. : New Perspectives for Sliding Base Isolation Systems, Proceedings of International Workshop on Recent Developments in Base-Isolation Techniques for Buildings, Tokyo, Japan, 27-30 April, 1992
14) Kawashima, K., Unjoh, S. and Shimizu, H. : Earthquake Response Control of Highway Bridges by Variable Damper, Transactions of the Japan National Symposium on Active Structural Response Control, Japan Science Council, pp.311-317, March, 1992 (in Japanese)
15) Kawashima, K., Unjoh, S. and Shimizu, H. : Experimental Study on Dynamic Characteristics of Variable Damper, Transactions of the Japan National Symposium on Active Structural Response Control, Japan Science Council, pp.311-317, March, 1992 (in Japanese)

Table 1 Peak Response of the Bridge and the Variable Damper

	Analyticol Cases	Deck			Pier		Variable Damper			
		Displacement (cm)	Velocity (cm/S)	Acceleration (cm/S^2)	Shear Force (tf)	Bending Moment (tf·m)	Damping Force (tf)	Relative Displacement (cm)	Relative Velocity (cm/S)	Total Energy (tf·m)
1	No Control	33.04	189.0	1300	166.9	3297	——	——	——	——
2	Constant Damping 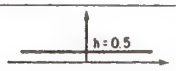	10.28	60.2	478	63.4	1223	34.7	7.67	44.9	93.9
3	Displacement Dependent Damping with Weak Stopper for Excessive Deck Response Displacement 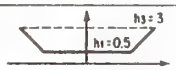	9.94	54.2	538	72.0	1395	60.2	6.90	68.1	94.4
4	Displacement Dependent Damping with Strong Stopper for Excessive Deck Response Displacement 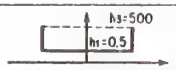	10.90	76.4	965	123.9	2382	151.3	5.54	112.3	94.9
5	Displacement Dependent Damping with Stopper for Small Deck Response Displacement 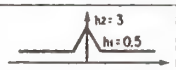	8.50	51.3	567	80.1	1540	64.7	6.34	55.8	74.5
6	Displacement Dependent Damping (Combination of Case 3 and Case 4)	8.38	47.5	555	81.2	1528	62.6	5.78	60.7	77.4

Table 2 Experiment for Small-Size model of Variable Damper

Case	Objective	Loading Frequency (Hz)	Loading Displacement (mm)	Input Voltage (V)
1	Measurement of Friction Force of Damper Piston	0.05	20	5
2	Relation between Damping Force and Input Voltage	1, 2, 3, 4	2, 6, 10, 15	0~5

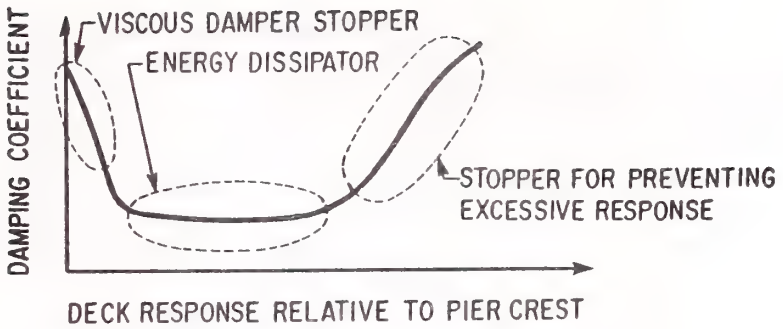

Fig.1 Basic Concept of Variable Dampers

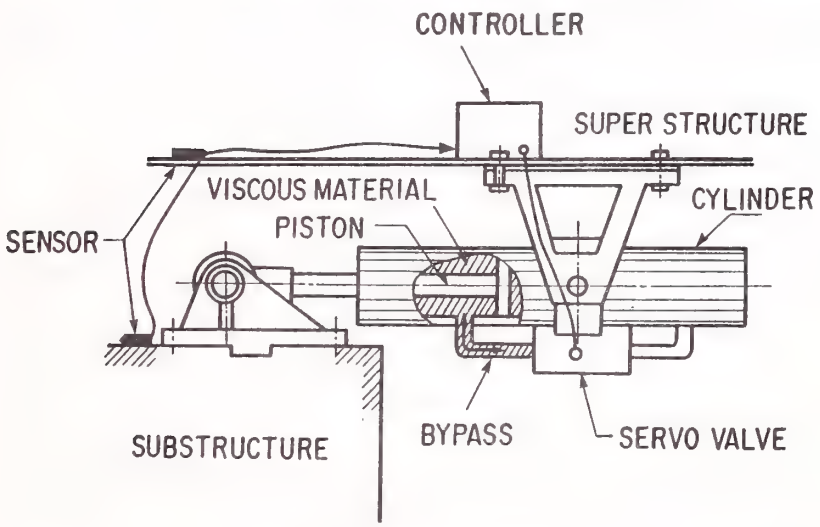

Fig.2 Variable Damper

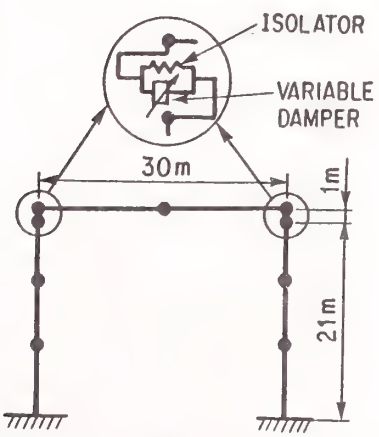

Fig.3 Highway Bridge Analyzed and Analytical Idealization

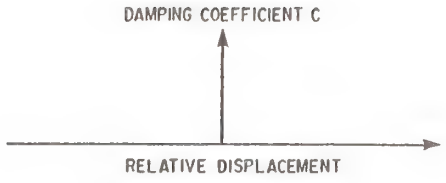

(a) Case 1 : No Control

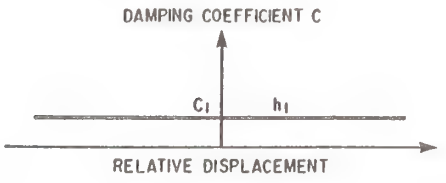

(b) Case 2 : Constant Damping

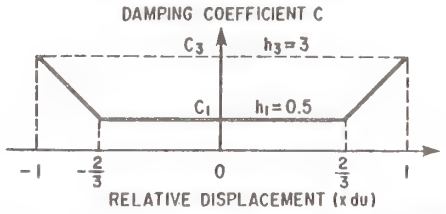

(c) Case 3 : Displacement Dependent Damping with Weak Stopper for Excessive Deck Response Displacement (du=7.67cm)

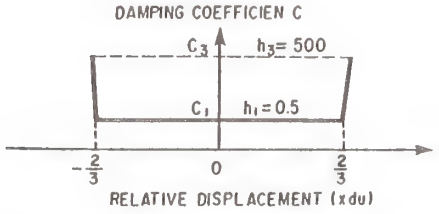

(d) Case 4 : Displacement Dependent Damping with Strong Stopper for Excessive Deck Response Displacement (du=7.67cm)

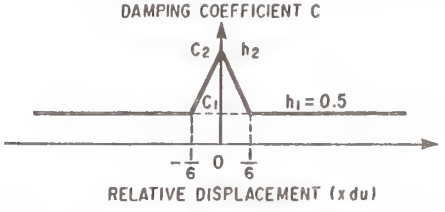

(e) Case 5 : Displacement Dependent Damping with Stopper for Small Deck Response Displacement (du=7.67cm)

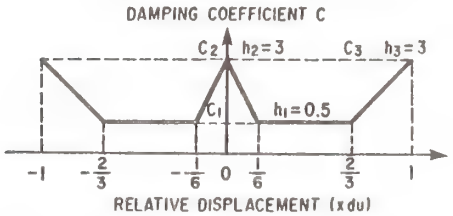

(f) Case 6 : Displacement Dependent Damping (Combination of Case 3 and Case 5) (du=6.34 cm)

Fig.4 Analytical Cases

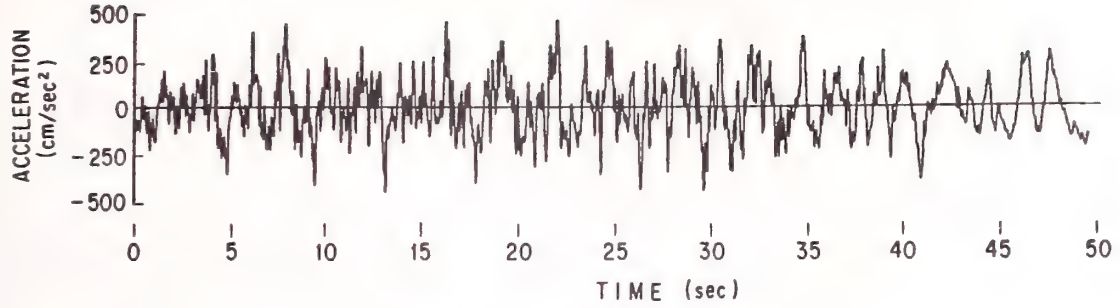

Fig.5 Input Acceleration

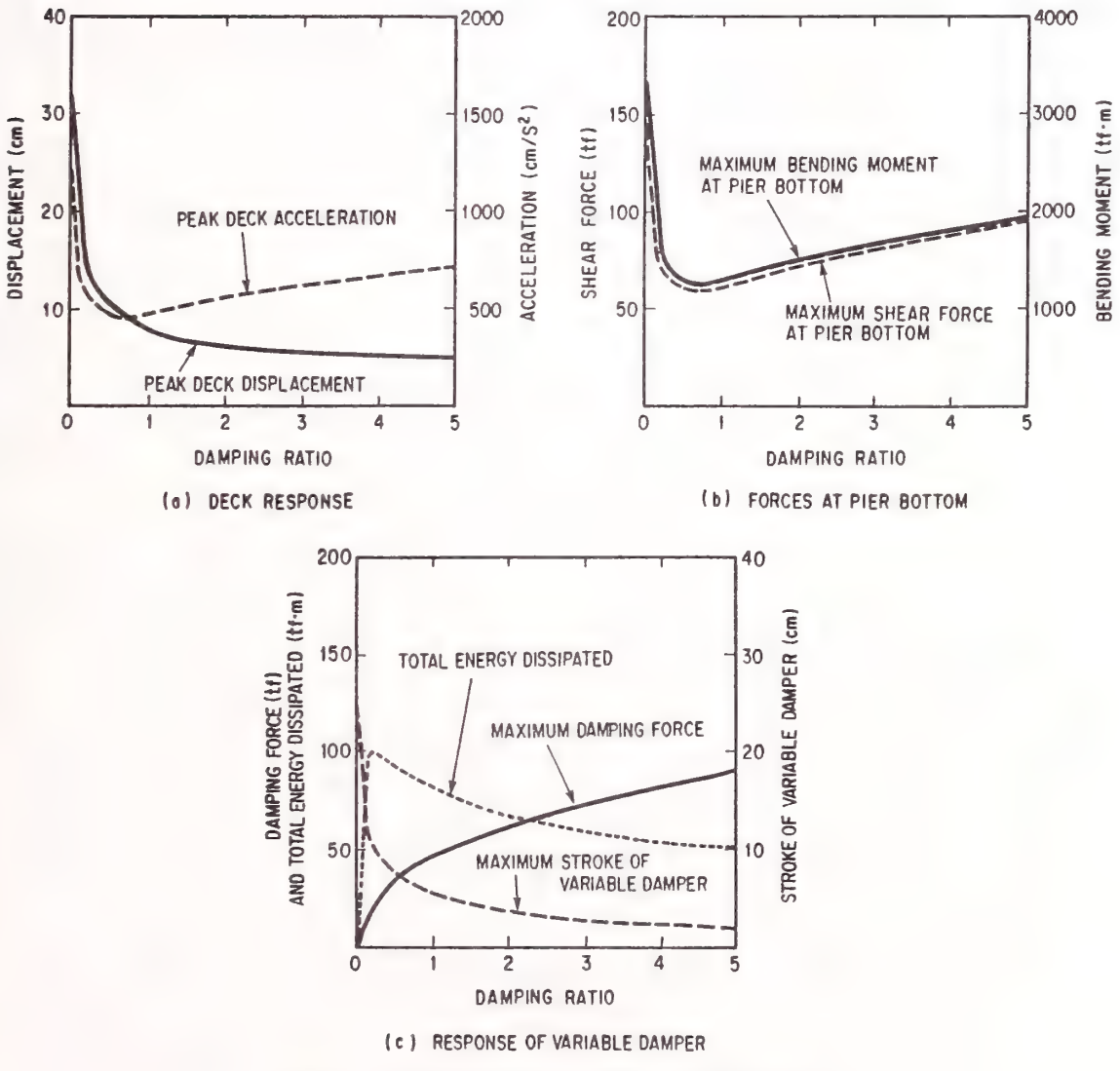

Fig.6 Peak Response of the Bridge and the Variable Damper (Case 2)

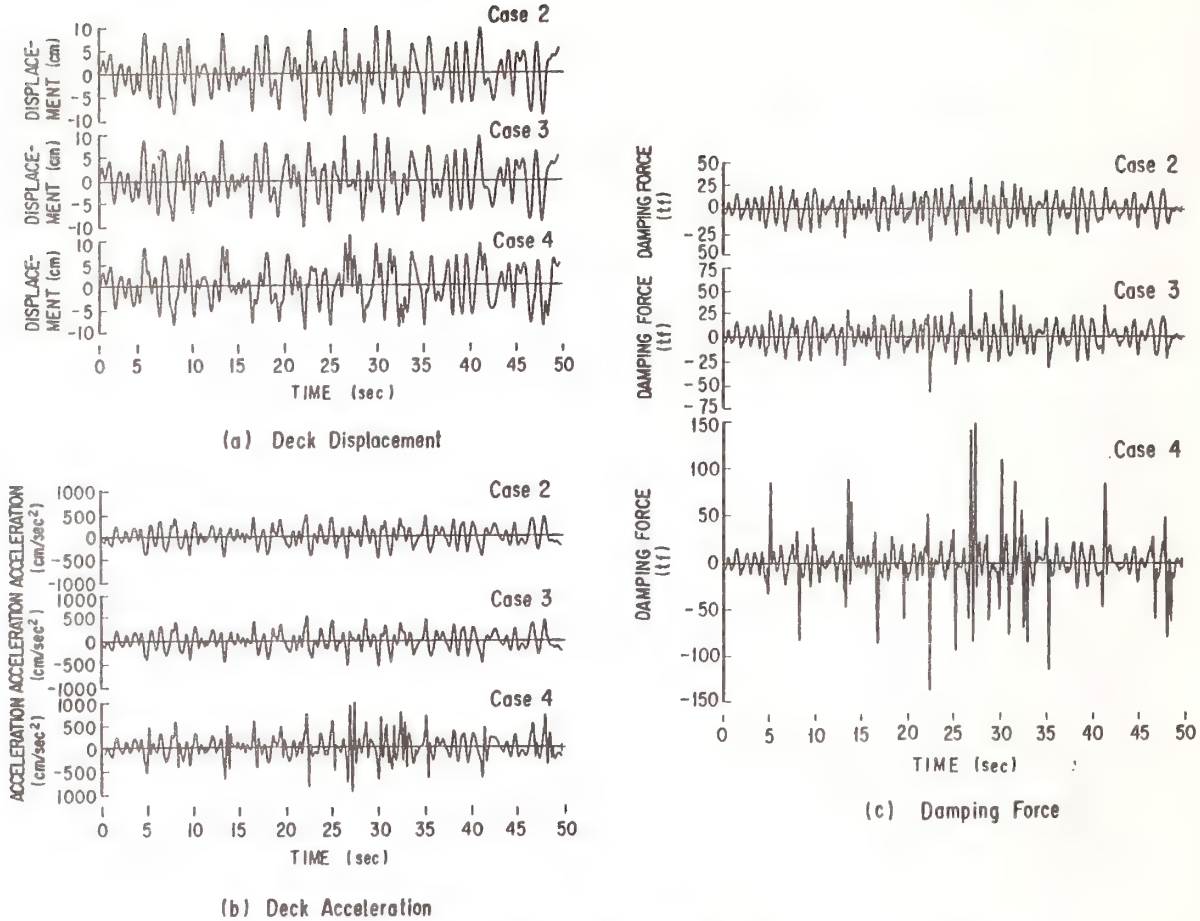

Fig.7 Computed Response of the Bridge and Variable Damper

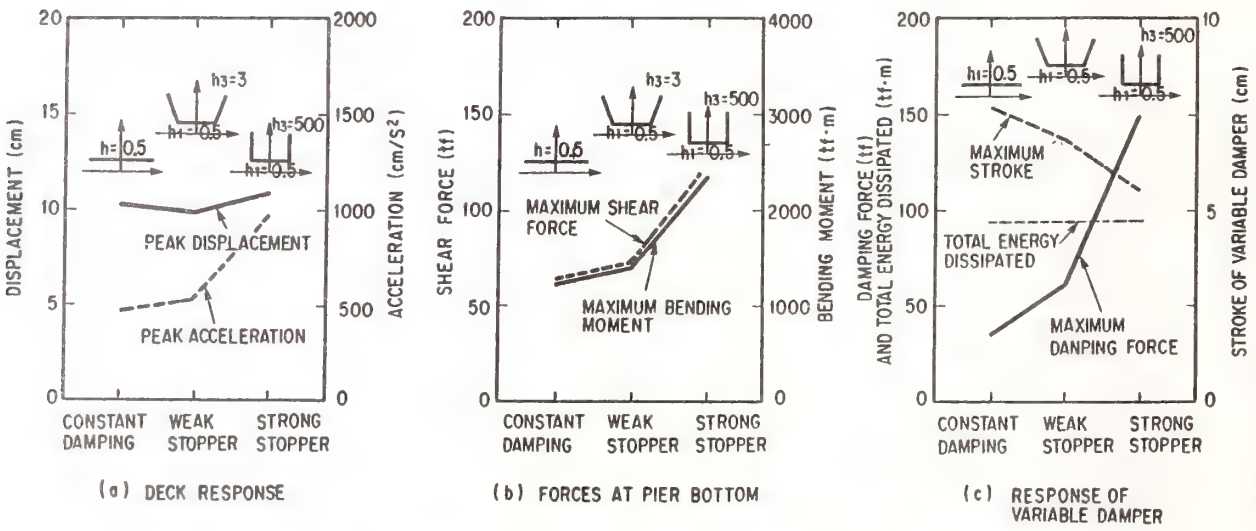

Fig.8 Effect of Weak Stopper (Case 3) and Strong Stopper (Case 4) for Excessive Deck Response Displacement

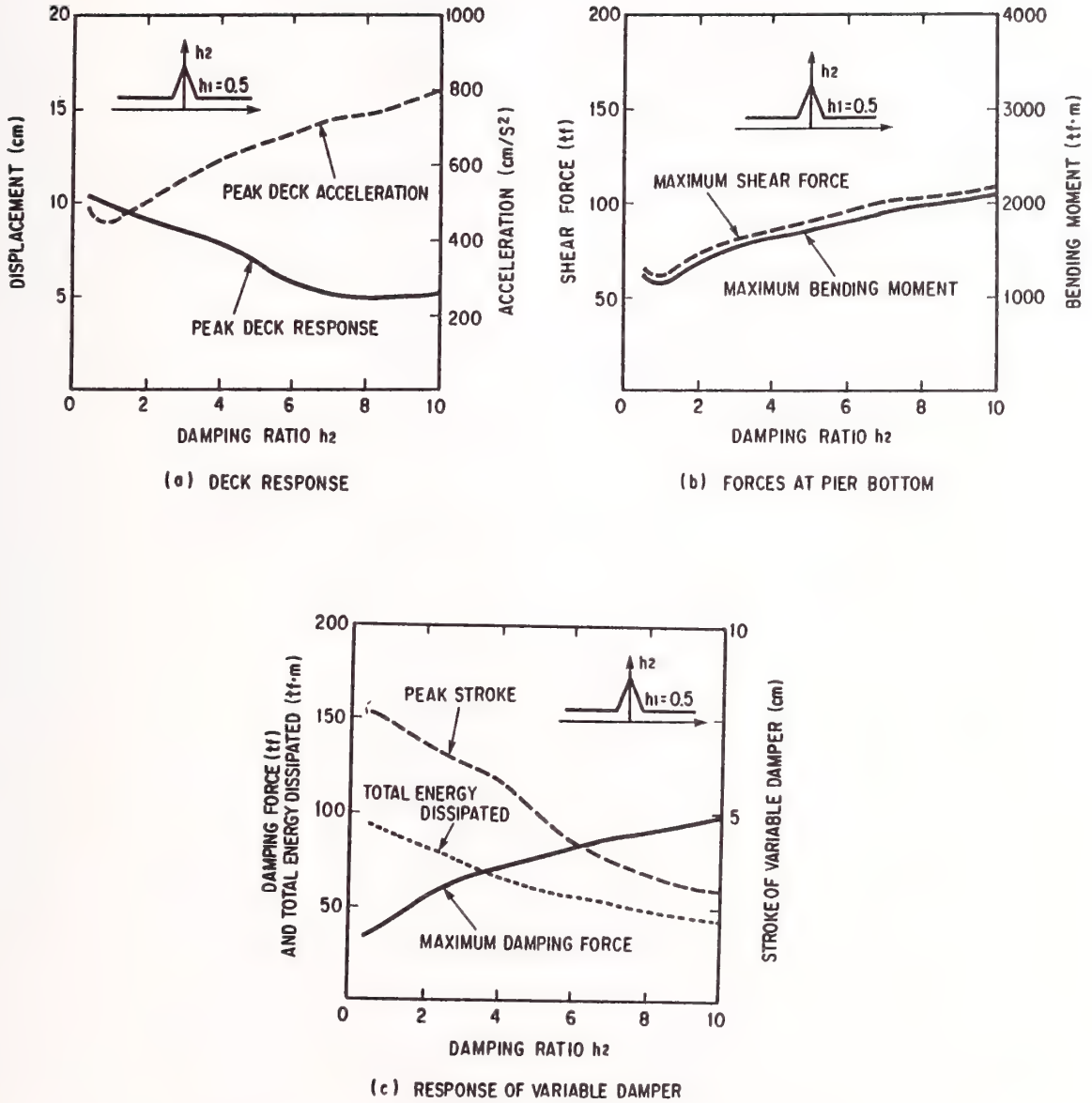

Fig.9 Effect of Stopper for Small Deck Response Displacement (Case 5)

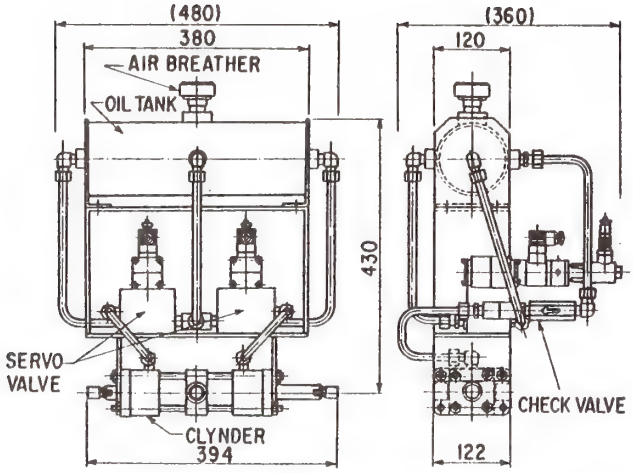

Fig.10 Small-Size Model of Variable Damper

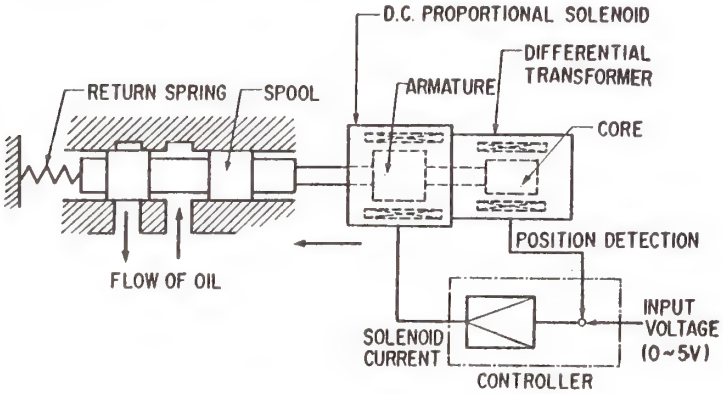

Fig.11 Structure of Servo Valve

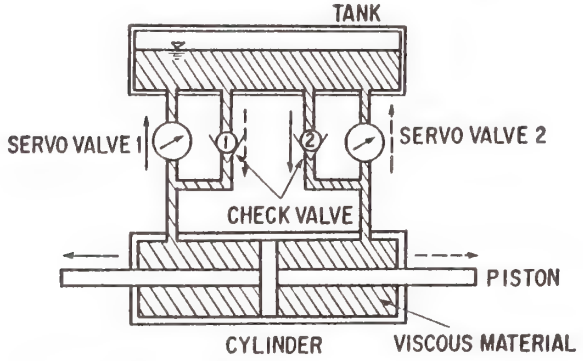

Fig.12 Flow of Viscous Material

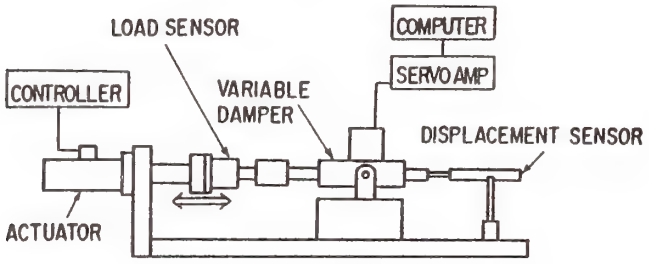

Fig.13 Set Up of Loading Test

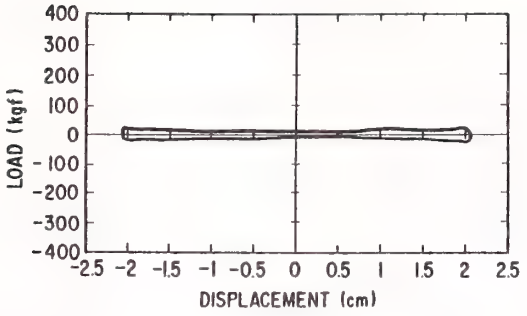

Fig.14 Hysteresis Loops of Load-Displacement Relation (Displacement=20mm, Frequency=0.05Hz)

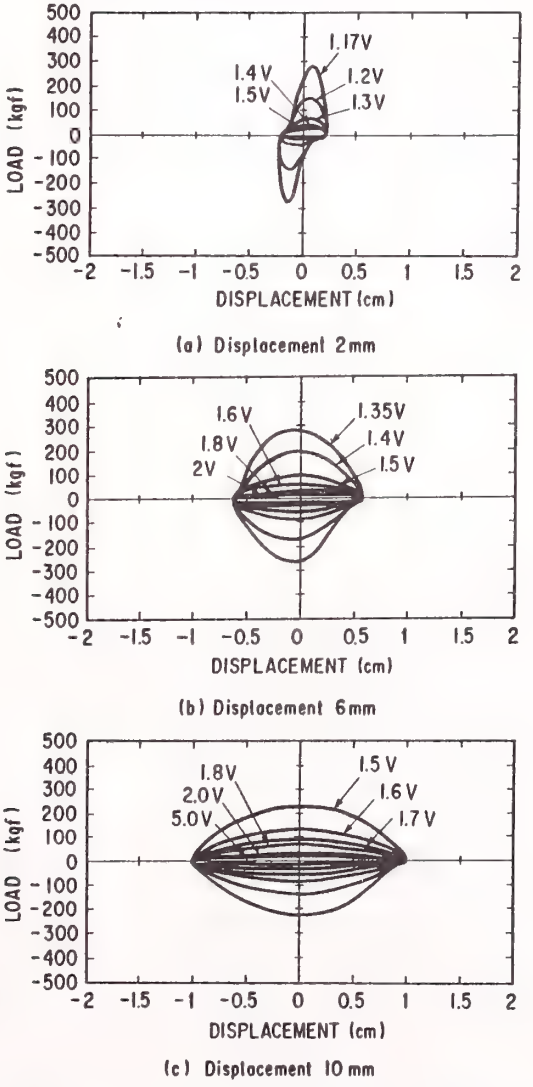

Fig.15 Hysteresis Loops of Load-Displacement Relation (Frequency=1Hz)

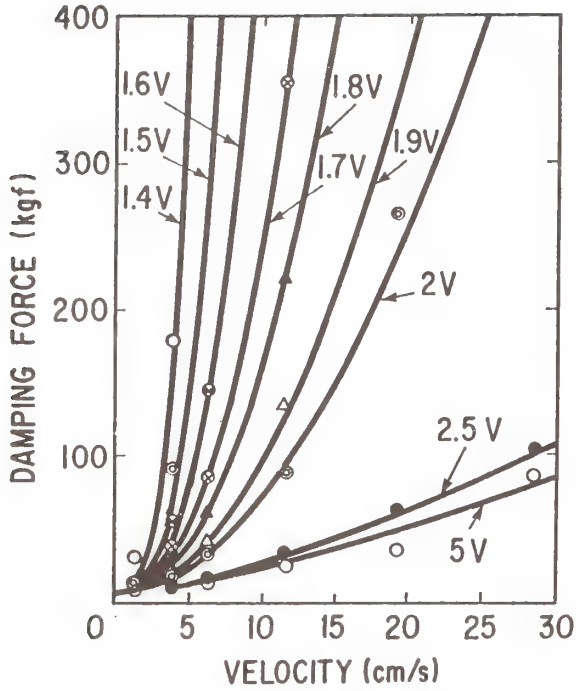

Fig.16 Damping Force vs. Peak Velocity Relation

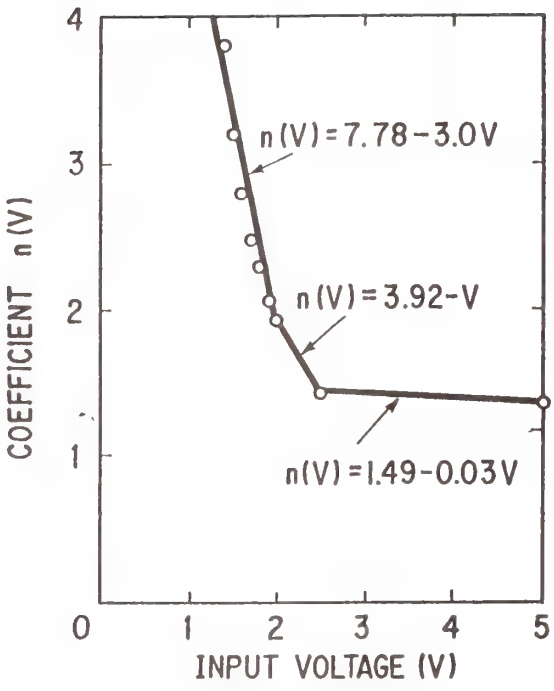

Fig.17 Power Coefficient n(V) vs. Input Voltage Relation

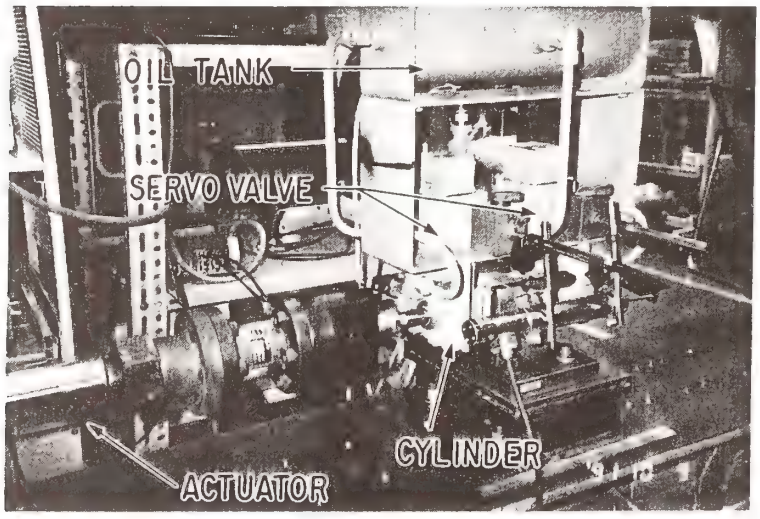

Photo 1 Experimental Set Up

Theme IV

Earthquake Engineering

Seismic Design Considerations for Jordanelle Dam

by

John A. Wilson[1], Perry J. Hensley[1], William O. Engemoen[1], and Francis G. McLean[1]

ABSTRACT

When completed in 1993, Jordanelle Dam will be a compacted, zoned earthfill dam having a sloping core. It is being constructed in northern Utah, USA, an area of significant seismicity. Maximum Credible Earthquakes (MCE) for the damsite were determined to be a magnitude 7.5 at a distance of 19 miles, and a local magnitude 6.0 to 6.5. The dam has been designed to take maximum advantage of the excellent construction materials available at the site. Use of these materials in combination with a sloping core has permitted the use of economical 1-1/2:1 downstream and 2:1 upstream slopes. Seismic analyses confirmed that the structure could withstand seismic loadings with minimal damage. This paper will summarize the design and analysis of the structure, with particular emphasis on seismic design considerations.

KEYWORDS: Embankment; Dam; Stability; Earthquakes; Slopes; Seismicity; Analysis; Design

1. INTRODUCTION

Jordanelle Dam and Reservoir, located on the Provo River near Heber City, Utah, are an important feature of the United States Bureau of Reclamation's Central Utah Project. Its primary function is to store and deliver municipal and industrial water to the growing Salt Lake City/Provo-Orem metropolitan areas. The Reservoir will have a total capacity of over 395,000,000 cubic meters (320,000 acre-feet), impounded by constructing Jordanelle Dam to a height of approximately 91 meters (300 feet) above original ground. The dam is a compacted embankment dam containing over 10.7 million cubic meters (14 million cubic yards) of soil and rock material. It has a crest length of 1,125 meters (3,700 feet) and a crest width of 12 meters (40 feet) as shown in Figure 1. Waterways include a fuse plug controlled emergency spillway and a tunnel outlet works, consisting of both low level and multi-level intakes. Jordanelle Dam was designed in two stages between 1986 and 1989, and construction began in 1987. It is anticipated that it will be essentially complete in early 1993, with reservoir filling to commence later that year.

This paper describes the design concepts for Jordanelle Dam, as related to the consideration of seismic loadings anticipated in this location. Additional analyses undertaken during the construction currently in progress are also presented.

2. DESCRIPTION OF EMBANKMENT DESIGN

The embankment cross section is shown on Figure 2. As shown, it consists primarily of compacted zone 4 material, described in Table 1. The upstream slope is 2 horizontal to 1 vertical, and the downstream slope is 1-1/2

[1] U.S. Bureau of Reclamation, Geotechnical Engineering and Embankment Dams Branch, Denver, CO 80225

horizontal to 1 vertical. A relatively thin upstream sloping clay core, zone 1, is the primary impervious element. It is protected by a two-stage filter-drain system (zones 2 and 3) to prevent piping and control seepage. Slope protection upstream consists of a 1 meter (3-foot) thickness of riprap obtained from nearby quarries. Downstream slope protection for the relatively steep 1-1/2:1 slope consists of cobbles and boulders (zone 5) processed from the borrow area.

The upstream sloping core is a key feature in the configuration of the embankment. It was made relatively thin to minimize the amount of foundation preparation and treatment required beneath the zone 1. It was sloped upstream to reduce the potential for differential settlement between the more compressible zone 1 core and the relatively incompressible zone 4 shells. In addition, the inclusion of the core and filter-drain system in the upstream portion of the dam leaves the vast downstream bulk of the embankment in an unsaturated condition. This ensures both static and seismic stability. The filter-drain system immediately downstream of the core serves as a defense mechanism to ensure that any cracking created by earthquake loading is properly protected by a filter and that any resulting seepage is safely conveyed downstream by the drainage system. The ability to keep the downstream shell unsaturated, plus the availability of good quality, strong materials, enabled the construction of a relatively steep 1-1/2:1 downstream slope.

A significant factor in the final configuration of the embankment was the quality and quantity of available materials. Fortunately, the reservoir area contained an abundant supply of both impervious materials (gravelly clays) and pervious materials (sandy gravels with cobbles and boulders) of excellent quality. The pervious materials, zone 4, are particularly desirable due to their low compressibility, high strength, durability and relatively high permeability. Because of these nearly ideal properties, the design utilized this material to the largest extent possible. The high strength made relatively steep slopes possible. This reduced the overall embankment volume and lowered the construction cost significantly.

Although the pervious materials are plentiful, there was little contingency in the design for a possible underrun of available zone 4 materials. For that reason, provision was made for a 1,700,000 cubic meter (2,200,000 cubic yards) zone 4A fill within the downstream zone 4 shell. Pervious materials were the preferred material for the zone; however, the zone was designed to permit the use of other excavated materials, such as gravelly clays. This provides for the use of suitable, but unspecified, materials from the borrow area and excavations. The impact of this zone on embankment stability was evaluated, as discussed later.

3. SEISMOTECTONIC SETTING

Jordanelle damsite is located in the Wasatch Mountains within the Intermountain Seismic Belt (ISB) in north-central Utah (Figure 3). The ISB is a zone of contemporary seismicity extending from Arizona to Montana along the eastern margin of the Basin and Range province. It is considered to have the highest level of earthquake risk in the contiguous United States outside of California and Nevada. Within the ISB, three historical earthquakes with magnitudes ranging from 6.6 to 7.5 have been accompanied by surface rupture on late Quaternary faults.

Potential earthquake sources for damsites in the ISB are considered to be of two types: 1) large-magnitude earthquakes on faults with evidence of late Quaternary surface rupture and 2) a local random earthquake that occurs on "blind" subsurface faults. The most likely sources of significant ground motions in the region that could affect Jordanelle damsite are the Wasatch fault, faults in Round Valley, and the random earthquake. A maximum credible earthquake (MCE) of magnitude 7.5 is assigned to the Wasatch fault at a distance of 30 km (18 mi)

from the damsite. An MCE of magnitude 6.5 to 6.75 is assigned to the faults in Round Valley at a distance of 20 km (12 mi) from the damsite. An MCE of magnitude 6 to 6.5 is assigned to a local random earthquake source.

Geologic investigations have shown that late Quaternary surface displacements have not occurred on faults in the vicinity of the damsite. We have, therefore, concluded that there is no potential for significant coseismic surface rupture in the dam foundation. However, ground deformation has been associated with recent moderate-magnitude earthquakes that have occurred on blind faults in the ISB. Tectonic subsidence accompanying the 1975 Pocatello Valley earthquake of magnitude 6.0 suggests that a similar phenomenon could accompany a magnitude 6 to 6.5 earthquake on a blind fault in the vicinity of the dam. Historic data and model simulations indicate that a tectonic displacement of about 15 cm could occur on favorably oriented faults in association with a moderate-magnitude earthquake.

4. MATERIALS CHARACTERIZATION

Shear strength parameters used for the principal embankment materials in the preconstruction stability analyses are shown in Table 2 for each loading condition.

The strengths shown in Table 2 were determined as follows:

Zone 1 - Core: Unconsolidated Undrained (UU) triaxial tests were performed on specimens compacted to 98 percent Proctor Density. These were performed in order to obtain undrained shear strengths representative of the gravelly clay core material during construction. Consolidated Undrained (CU) triaxial tests (with measured pore pressures subtracted) were used to develop the drained strength used in the steady seepage analysis. The same tests (without measured pore pressure subtracted) were used to develop consolidated undrained strengths representative of undrained strength available in the consolidated clay core during a rapid drawdown loading.

Zone 2 - Filter: Laboratory testing of the well graded sand and gravel filter material was not performed. Drained strength parameters for the well compacted filter materials were conservatively selected from available literature and past Reclamation experience with similar materials.

Zone 3 - Drain: Laboratory testing was not considered practical due to the large particle size (3.8 to 20.3 cm) of this material. Conservative strength parameters, considering the rounded and highly uniform gradation of the material, were also selected from available literature and past Reclamation experience.

Zone 4 - Shell: Initially, the zone 4 material was assumed to behave dilatively during shear. Drained strengths were, therefore, assumed to represent all loading conditions for this material. The zone 4 was assumed to have drained strengths with an effective ϕ of 44° (Marachi, 1972) below a normal stress of 690,000 N/m^2 (100 lb/in^2) and a ϕ of 39° with a cohesion intercept of 107,600 N/m^2 (15.6 lb/in^2) above a normal stress of 690,000 N/m^2 (100 lb/in^2). These strengths are supported by the work of Leps (1970) with large scale triaxial tests on Oroville Dam material.

Zone 4 shell material is placed in two-foot lift thicknesses and compacted using vibrating rollers. Test fills prior to construction were evaluated to establish the optimum procedures for placing and compacting this material. At the beginning of the stage 2 construction, samples of this material were shipped to the University of California, Berkeley for testing in their 30 centimeter (12-inch) diameter triaxial apparatus (Seed, 1990). Tests were performed on samples scalped to a 5-cm (2-inch) maximum particle size and compacted at a density corresponding to material placed in stage 1. The results indicated that the material might not behave as originally anticipated. The tests

indicated that materials compacted during stage 1 could be slightly contractive rather than dilative during shear. As a result of these tests, a heavier vibratory roller (11-ton-per-drum dual-drum) was specified for stage 2, resulting in higher densities than those achieved during stage 1 construction. In addition, a re-evaluation of the design was made to check the impact of these in-place stage 1 materials on embankment performance.

Based on the test results, the zone 4 material placed during stage 1 would be represented by a consolidated stress phi angle of 19° for a post-earthquake analysis. This conclusion is based on the assumption that the total material will contract and build up pore pressure. In reality, though, the oversized material would likely inhibit the increase in pore pressure. Due to the greater densities of the zone 4 material being placed in the upstream shell during stage 2, the strength is conservatively represented by a phi of 30° for a post-earthquake analysis. The downstream zone 4 material is also being placed at the higher densities and will remain unsaturated. An effective friction angle of 39°, as indicated by the Berkeley results (Seed, 1990) was used in the reanalysis.

Zone 4A - Fill: The strength used for the gravelly clays allowed in the Zone 4A mass fill portion of the dam were assumed the same as the drained and undrained strengths obtained from laboratory tests on the zone 1 core materials. This provides for the flexibility of placing materials of lesser strength in this zone.

5. STATIC STABILITY EVALUATION

The static stability was evaluated for three loading conditions. These were: steady-state seepage, rapid drawdown, and end of construction. The analyses were performed using the computer program SSTAB2 (Chugh, 1981), based on the Spencer method, to compute factors of safety for various failure surfaces. The downstream slope was evaluated for a range of zone 4A configurations. For these analyses, it was conservatively assumed that the zone 4A consisted of impervious gravelly clay materials.

The end of construction case was examined using the conservative assumption that pore pressure developed during placement in either the core or the zone 4A portion of the downstream shell would not dissipate prior to completion of the dam. The gravel and cobble zone 4 material placed in the embankment was assumed to be free draining in the analyses. The factors of safety obtained for the end of construction condition are shown on Table 3.

The steady seepage condition was examined with the reservoir water surface at the maximum elevation of 1884.3 m (6182 ft) and the phreatic surface established by the top of joint use water surface elevation of 1879.5 m (6166 ft). The factor of safety was obtained for different circular searches and wedge surfaces for the steady seepage condition assumptions. The minimum factor of safety obtained for a significant failure surface is shown on Table 3 and meets the Reclamation design requirements (USBR, 1987).

For the steady seepage condition, the internal drainage systems were assumed fully functional. The clayey zone 4A placed in the downstream shell was assumed to remain unsaturated at a moisture content near optimum. Pore pressures in the relatively thin sloping core were estimated by assuming full hydrostatic pressures on the upstream face of the core and atmospheric pressures on the downstream underside of the core.

For the rapid drawdown condition, no pore pressure dissipation due to drainage in the zone 1 core material was assumed. The zone 4 gravel and cobble upstream shell was assumed pervious enough to drain completely during the reservoir drawdown. Construction pore pressures in the clayey zone 4A materials were assumed to have dissipated completely.

The rapid drawdown condition was examined for a complete draining of the reservoir. This was assumed to follow the establishment of steady seepage conditions with the reservoir at elevation 1879.5 m (6166 ft). The values of the factor of safety obtained for the different surfaces for the rapid drawdown conditions are shown on Table 3.

6. SEISMIC GROUND MOTIONS

The maximum credible earthquakes (MCE's) derived for the Jordanelle damsite are shown in Table 4 (USBR, 1988). The Wasatch fault event (No. 3, Table 4) is considered to be the more probable event. It has a recurrence interval for a magnitude 7.0 to 7.5, earthquake of 330 ($\pm$ 90) years for the entire fault zone (Youngs, 1987). The two segments of the Wasatch fault nearest to Jordanelle Dam were assigned recurrence intervals of about 2,000 years.

Three separate accelerograms were used to represent potential earthquakes for analysis. The first was a record developed at the University of California, Berkeley, by Professor H. Bolton Seed. It represents a near-field magnitude 7.25 earthquake on the Hayward Fault in the San Francisco Bay area (Seed, 1983, Pike, 1991). It was scaled to a peak acceleration of 0.67g. This was to represent a magnitude 6.5 event in the immediate vicinity, not associated with a specific fault. This resulted in a maximum velocity of 76 cm/s (30 in/s) and a velocity spectrum intensity of 286 cm (113 inches). The latter value is very large in comparison with available data from historical earthquakes (Von Thun, 1988). The record has a total duration of 23.7 seconds and contains a long-period section referred to as a "fling". This fling causes the motion to have a great deal of energy in the 1.0 to 1.5 second period range. Figures 4 and 5 show the acceleration time history and the acceleration response spectrum for this earthquake record.

The second design earthquake record is a synthetically generated accelerogram considered to be representative of a mean magnitude 6.5 local event. It was developed for use in this type of seismic setting, (Munoz, 1986). It is characterized by a peak acceleration of 0.55g, a peak velocity of 35 cm/s (14 in/s), a total duration of 20.5 seconds, and a velocity spectrum intensity of 163 cm (64 in).

The third earthquake record represented a magnitude 7.5 event on the Wasatch fault at a distance of 30 kilometers (19 miles). An accelerogram developed by H. B. Seed and I. M. Idriss to represent the far field of a magnitude 8.25 earthquake was used. It was scaled to a peak acceleration of 0.29g. This resulted in a record with a peak velocity of 25 cm/s (10 in/s), a velocity spectrum intensity of 171 cm (67 inches) and a total duration of 48 seconds.

7. DYNAMIC DEFORMATION ANALYSIS

Seismically induced embankment deformations were evaluated using the computer program DYNDSP (Von Thun, 1981). This program is based on the sliding block procedure by Newmark (1965) for estimating permanent displacements. It is assumed that slide planes develop within the mass and that the material above the slide plane behaves as a rigid body.

The DYNDSP program uses the limit equilibrium method. It computes an incremental permanent displacement along the sliding plane each time the earthquake loading causes the driving forces along the plane to exceed the resisting forces. The effective angle of motion is calculated as the weighted average of the angle of sliding of each individual slice. The computed displacement is, therefore, calculated as the movement of the sliding mass along the failure surface in the downslope direction. Selective incorporation of the effects of horizontal and vertical inertial forces, excess pore pressure development, shear strength reduction, and dilation is included.

The program estimates the relative displacement of a specific failure mass given the applicable time history of both horizontal and vertical accelerations. The critical surfaces for a structure must be found by the examination of many failure surfaces. The total displacement is determined by integration of the results from these individual surfaces.

Several failure surfaces and driving acceleration records were analyzed for determining response to the MCE's. The results are shown in Table 4.

The shear strength parameters used in the original, preconstruction dynamic analysis are shown in Table 2. These strengths reflected no loss in shearing resistance due to dynamic loading conditions. It was assumed that the embankment would be compacted to a density sufficient to preclude significant loss of shear resistance associated with excess pore pressures in the saturated zone 4 material (upstream). The materials within the downstream shell (zone 4 and 4A) were assumed unsaturated. The downstream failure surfaces were, therefore, located primarily in unsaturated material, a planned result of the sloping core design.

The results of the analysis indicate that up to 1.4 m (4.6 ft) of vertical deformation is possible. This occurred on a circle which passes through half of the crest to one-fourth of the distance down the downstream slope (Fig. 6). The remaining material from the crest would be expected to slough into a more stable position. Total loss of crest elevation would not be expected to exceed the 1.4 m (4.6 ft). All of the deeper failure surfaces evaluated resulted in less deformation. Hence, it was concluded that with 5.7 m (18.6 ft) of designed freeboard above normal reservoir elevation, the embankment would not lose its reservoir-impounding capacity.

The first design earthquake record previously discussed caused significantly larger deformations than the synthetic record or the Wasatch fault earthquake (Table 3). Even so, the displacements of up to 1.4 m (4.6 ft) on shallow upper surfaces, if they were to occur, would require repair, but would cause no loss of the reservoir water.

The largest computed vertical displacement from the synthetic earthquake record was 0.55 m (1.8 ft). This is believed to be the largest seismic loading with a reasonable probability of occurrence. Under this earthquake loading the embankment is expected to retain approximately 90 percent of the design freeboard.

The magnitude 7.5 earthquake on the Wasatch fault has a predominance of long period vibrations in the design record. This caused amplification of the motions within the embankment up to a peak acceleration of 1.2 g near the crest of the dam. This, coupled with a total duration of 48 seconds, yielded calculated vertical displacements up to 0.85 m (2.8 ft). The largest displacement was located on the shallow upstream shear surface (Table 3). Over 4.7 m (15.5) ft of freeboard would remain after this seismically induced deformation.

As a check on the reasonableness of the results presented above, a simplified analysis was also performed. The procedure described by Makdisi and Seed (1977) was used to estimate the earthquake-induced deformations of the embankment with and without the clayey zone 4A in the downstream shell. Deformations were computed for potential failure surfaces through the full height of the embankment, the upper half of the embankment, and the upper quarter of the embankment. The analysis was performed using the computer program SEIDAKA (Adhya, 1982), which uses the Makdisi-Seed (1977) procedure. Maximum estimated deformations were:

0.06 m (0.2 ft) through the full height,
0.24 m (0.8 ft) through the upper half, and
2.0 m (6.5 ft) through the upper quarter.

These displacements compare reasonably with the values obtained using the more rigorous DYNDSP procedure, and confirm the acceptable performance of this design.

As a further check on the probable performance under earthquake shaking, literature reports were reviewed. Several gravelfill or rockfill dams, of varying size and design, which have been subjected to severe seismic shaking suffered minimal, or no damage (Bureau, 1986, and Seed, 1977). Two modern, well-instrumented rockfill dams with thin impervious zones survived strong shaking from the 1985 magnitude 8.1 Mexico earthquake with minor cracking and settlement (Bureau, 1986). LaVillita Dam is located about 24 km (15 miles) from the epicenter of the main shock. It recorded about 50 seconds of ground motion with a peak acceleration of 0.13 g. El Infiernillo Dam, about 74 km (46 miles) from the epicenter recorded an estimated peak acceleration of 0.5 g on the dam crest. These two dams have been subjected to 5 other earthquakes of magnitude 6.5 or larger since 1964, as well as a magnitude 7.5 aftershock to the 1985 event, and are continuing to perform well. Jordanelle Dam has been designed to provide seismic behavior comparable to these two dams.

Following the completion of the laboratory testing on the zone 4 soils at the University of California, Berkeley, the deformation analyses were repeated using the reduced shear strengths. Only materials placed during stage 1 were considered capable of experiencing significant loss of effective shear resistance. It was conservatively assumed that widespread pore pressure increase occurred in zone 4 materials placed during stage 1 in the saturated upstream shell. The analysis results indicated that the embankment would retain sufficient strength to remain stable. Seismically induced deformations would still be considerably less than the available freeboard.

8. CONSTRUCTION MONITORING

Construction began in 1987 as stage 1 of a two-stage construction process. It included stripping the abutments and west side of the valley to bedrock, producing zone 2 and 3 filter and drain materials, and placing embankment material on the west side of the valley up to the original ground elevation. Stage 2 construction, which includes all remaining construction activities, began in 1989. It is scheduled to be completed in early 1993. At the time of this writing, construction of the outlet works tunnels is completed, the embankment is complete to approximately elevation 1838 m (6030 ft), or 40 m (130 ft) above original ground, and construction of the emergency spillway is complete.

As anticipated, material placed in the downstream zone 4A portion of the embankment have varied in origin and composition. Much of the material placed to date has been material from required excavations, with a wide range of gradations. In general, the material placed has been superior to the "poorest" material considered during design analyses.

Due to an overabundance of zone 3 drainage material from the stage 1 material processing, several upstream horizontal drainage layers have been incorporated into the design of the embankment. These layers will serve to allow rapid drainage and dissipation of pressures in the event of rapid drawdown or seismic shaking, providing an extra margin of stability.

9. CONCLUSIONS

Testing of the materials being placed in the embankment confirm that the dam is being constructed in accordance with specifications requirements. Close monitoring and inspection of construction activities is being carried out by construction and design personnel. This assures that the design is being properly adapted to site

conditions, and that design concepts and assumptions are valid for the as-built structure.

The availability of excellent materials for embankment dam construction made construction of Jordanelle Dam with a relatively steep 1-1/2:1 downstream slope in a seismically active area feasible. Investigations and analyses indicate that the structure will be stable and perform well for all anticipated static and dynamic loading conditions. The analyses were carried out using commonly available methods to calculate the static factors of safety and anticipated seismic performance of the dam. Careful construction monitoring and reevaluation of the design assumptions during construction have indicated satisfactory conformance to design concepts with regard to both materials and densities in the field.

10. REFERENCES

1. Adhya, K. A. (1982). "A Computer Program for Simplified Earthquake-Induced Deformation Analysis of Homogeneous Embankment Dam," Draft Report, U. S. Department of the Interior, Bureau of Reclamation, Denver, Colorado.

2. Bureau, G. and Campos-Pina, J. M. (1986). "Performance of Mexican Dams, Earthquake of 1985," U.S.C.O.L.D. Newsletter, Issue No. 79, Published by the U.S. Committee on Large Dams, Boston, Massachusetts.

3. Chugh, Ashok K. (1981). "User Information Manual, Slope Stability Analysis Program SSTAB2," (A Modified Version of "SSTAB1" by Stephen G. Wright), U. S. Bureau of Reclamation, Denver, Colorado.

4. Chugh, Ashok K. (1988). "Static Deformation Analysis of Proposed Maximum Section," Technical Memorandum, Division of Dam and Waterway Design, U. S. Department of the Interior, Bureau of Reclamation.

5. Hensley, P. J. (1988). "Static Stability Analysis, Jordanelle Dam, Central Utah Project, Utah," Technical Memorandum No. JD-3620-7, U. S. Department of the Interior, Bureau of Reclamation, Denver, Colorado.

6. Lambe, T. W. and Whitman, R. V. (1969). Soil Mechanics, John Wiley and Sons, Inc.

7. Leps, T. M. (1970). "Review of Shearing Strength of Rockfill," Journal of the Soil Mechanics and Foundations Division, ASCE.

8. Makdisi, F. I., and Seed, H. B. (1972). "A Simplified Procedure for Estimating Earthquake-Induced Deformations in Dams and Embankments," Earthquake Engineering Research Center, Report No. UCB/EERC-77/19, University of California, Berkeley, California.

9. Marachi, P. N., Chan, C. K., and Seed, H. B. (1972). "Evaluation of Properties of Rockfill Materials," Journal of the Soil Mechanics and Foundations Division, ASCE.

10. Munoz, Richard L. and Greg A. Scott (1986). "Preliminary Studies for Conceptual Designs of Monks Hollow Arch Dam," Technical Memorandum No. MH-221-1, U. S. Department of the Interior, Bureau of Reclamation, Denver, Colorado.

11. Newmark, N. M. (1965). "Effects of Earthquakes on Dams and Embankments," Geotechnique, Vol. 15, No. 2.

12. Pyke, Robert (1991). personal communication.

13. Seed, H. B., Makdisi, F. I., and DeAlba, P. (1977). "The Performance of Earth Dams During Earthquakes," Earthquake Engineering Research Center, Report No. UCB/EERC-77/20, University of California, Berkeley, California.

14. Seed, H. B. (1983). personal communication.

15. Seed, R. B. (1990). "Final Report Presenting Results of Large-Scale Triaxial Tests, Zone 4, Area "G" Borrow Material, Jordanelle Dam Project, Utah," U. S. Department of the Interior, Bureau of Reclamation, Denver, Colorado.

16. Sherard, J. L., and Dunnigan, L.P.(1985). "Filters and Leakage Control in Embankment Dam.," Symposium of Seepage and Leakage from Dams and Impoundments, American Society of Civil Engineers, Spring Convention, Denver, Colorado.

17. U. S. Department of the Interior, Bureau of Reclamation (1987). "Design Standards, Embankment Dams, No. 13, Chapter 4, Static Stability Analyses," Denver, Colorado.

18. U. S. Department of the Interior, Bureau of Reclamation (1988). "Seismotectonic Study for Jordanelle Dam, Bonneville Unit, Central Utah Project, Utah," Seismotectonic Report 88-6, Seismotectonic Section, Division of Geology, Denver, Colorado.

19. Von Thun, J. L. and C. W. Harris (1981). "Estimation of Displacements of Rockfill Dams Due to Seismic Shaking," Proceedings of the International Conference on Recent Advances in Geotechnical Earthquake Engineering and Soil Dynamics, St. Louis, Missouri.

20. Von Thun, J. L., L. H. Roehm, G. A. Scott, and J. A. Wilson, (1988). "Earthquake Ground Motions for Design and Analysis of Dams," Proceeding of the ASCE Specialty Conference, Earthquake Engineering and Soil Dynamics II - Recent Advances in Ground Motion Evaluation, Geotechnical Special Publication No. 20, Park City, Utah.

21. Youngs, R. R., F. H. Swan, J. S. Power, D. P. Schwartz, and R. K. Green (1987). "Probabilistic Analysis of Earthquake Ground Shaking Hazard Along the Wasatch Front, Utah," Assessment of Regional Earthquake Hazards and Risk Along the Wasatch Front, Utah, U. S. Geological Survey, Open File Report 87-585.

EMBANKMENT ZONE	TYPE OF MATERIAL
Zone 1	Lean clays, sandy-gravelly clays
Zone 2	Processed sands and gravels, max size 5 cm
Zone 3	Clean gravels and cobbles, max size 20 cm
Zone 4	Well graded sand, gravel, cobbles and boulders, max size 61 cm
Zone 4A	Variable, ranging from lean clays to rockfill
Zone 5	Cobbles and boulders, max size 61 cm

Table 1. Types of Materials in Embankment Zones

Principal Embankment Zone	Loading Conditions			
	End of Const.	Steady Seepage	Rapid Drawdown	Dynamic
Zone 1 Conf. stress <275,000 N/m^2 (40 psi)	c=11 psi ϕ = 21°	c=2.5 psi ϕ = 28°	c=2.5 psi ϕ = 28°	c=2.5 psi ϕ= 28°
Conf. stress >275,000 N/m^2 (40 psi)	c=2.5 psi ϕ = 28°	c=2.5 psi ϕ = 28°	c=16 psi ϕ = 13°	c= 16 psi ϕ = 13°
Zone 2	c=0 ϕ = 35°	c=0 ϕ = 35°	c=0 ϕ = 35°	c=0 ϕ = 35°
Zone 3	c=0 ϕ = 30°	c=0 ϕ = 30°	c=0 ϕ = 30°	c=0 ϕ = 30°
Zone 4	c=0 ϕ = 44°	c=0 ϕ = 44°	c=0 ϕ = 44°	c=0 ϕ = 44°
Zone 4A Full pore press. dissip.	----	c=2.5 psi ϕ = 26°	c=2.5 psi ϕ = 26°	c=2.5 psi ϕ = 26°
No pore press. dissipation				
a) conf. stress < 550,000 N/m^2 (80 psi)	c=11 psi ϕ = 17°	c=11 psi ϕ = 17°	c=11 psi ϕ = 17°	----
b) conf. stress > 550,000 N/m^2 (80 psi)	c=40 psi ϕ = 0	c=40 psi ϕ = 0	c=40 psi ϕ = 0	----

Table 2. Material Strengths Used for Preconstruction Stability Analysis.

		End of Const	Steady Seepage	Rapid Drawdown
Downstream	Infinite slope	1.5	1.5	---
	Circle	1.5	1.5 1.4*	---
	Wedge	---	---	---
Upstream	Infinite slope	1.9	1.9	---
	Circle	2.1	2.0	2.0
	Wedge	2.7	4.5	2.4
*No dissipation of construction pore pressure in zone 4A.				

Table 3. Factors of Safety for Static Stability

EQ.	Magnitude	Distance	Earthquake Record Used	Peak Velocity	Maximum Vertical displacement (m)	
					Clay zone 4A	Gravel zone 4A
No. 1	M_l 6.5	local	Scaled Pacoima-Taft	76 cm/s	0.4 u/s 0.5 d/s	1.3 u/s 1.4 d/s
No. 2	M_l 6.5	local	Synthetic, USBR	35 cm/s	0.3 u/s 0.3 d/s	0.5 u/s 0.5 d/s
No. 3	M_s 7.5	30 km.	Scaled, Seed-Idriss	25 cm/s	0.4 u/s 0.1 d/s	0.9 u/s 0.3 d/s

Table 4. Maximum Credible Earthquakes and Seismically-Induced Deformations.

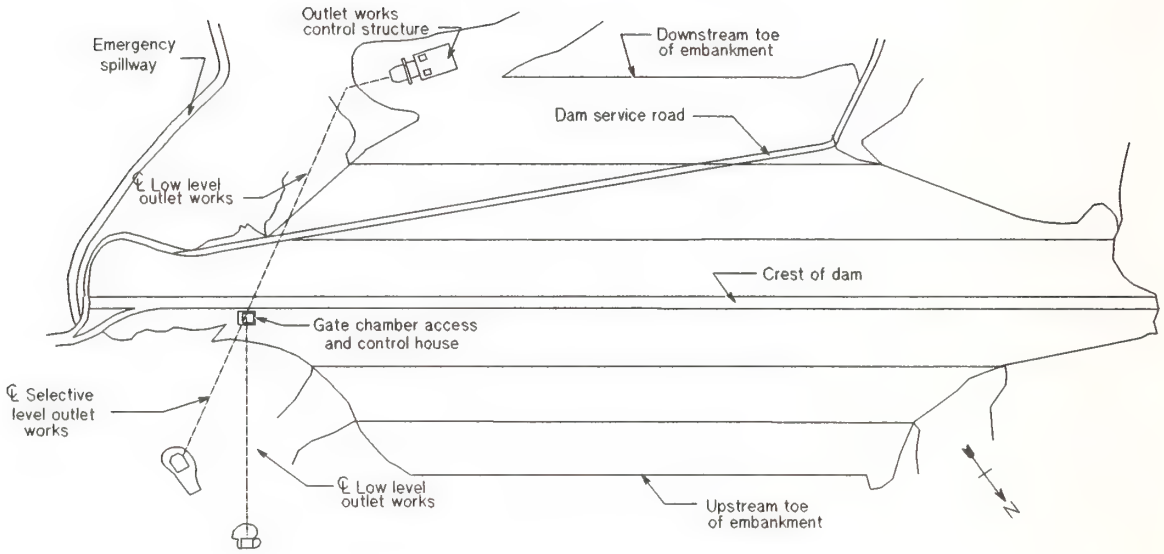

Figure 1 - Jordanelle Dam General Plan

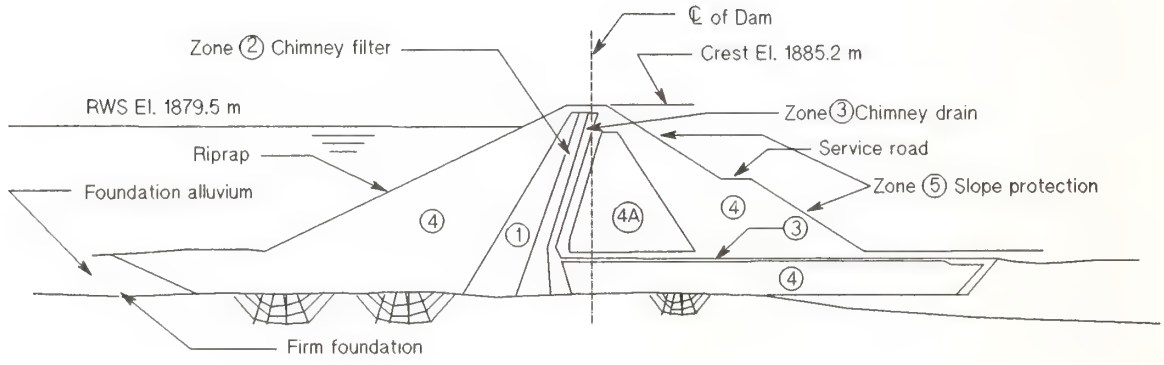

Figure 2 - Jordanelle Dam Embankment Section

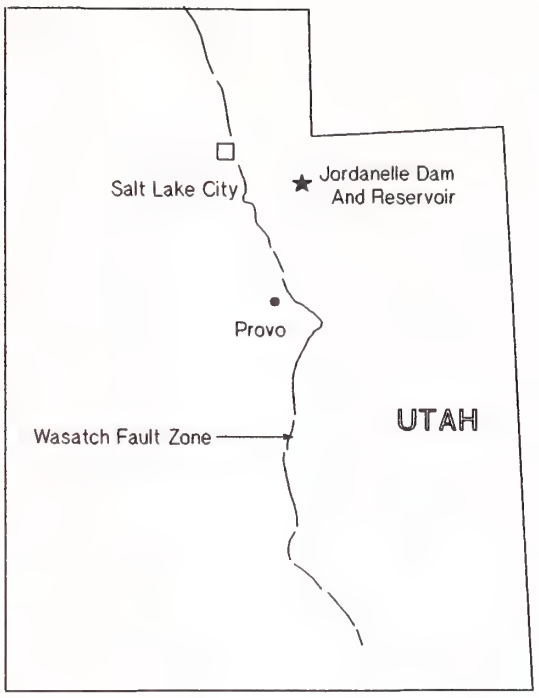

Figure 3 - Location of Jordanelle Dam and Wasatch Fault Zone

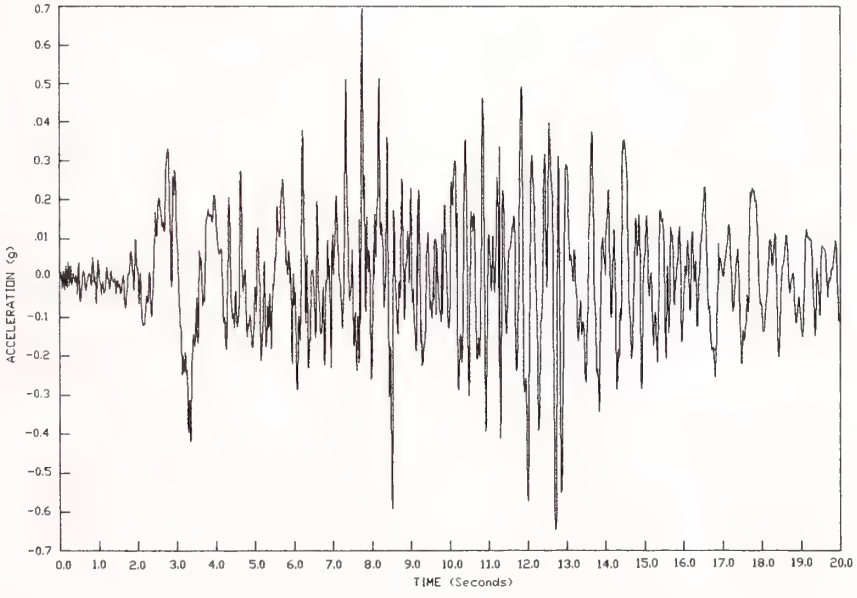

Figure 4 - Jordanelle Dam Design Accelerogram

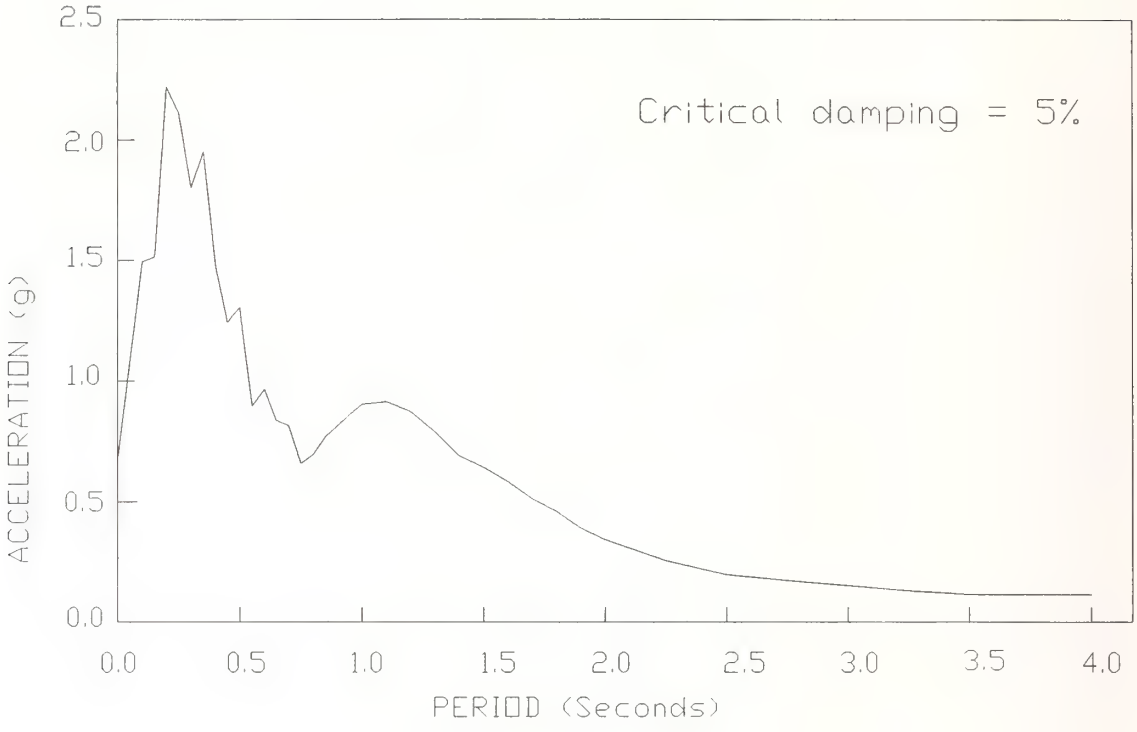

Figure 5 - Jordanelle Dam Acceleration Response Spectrum

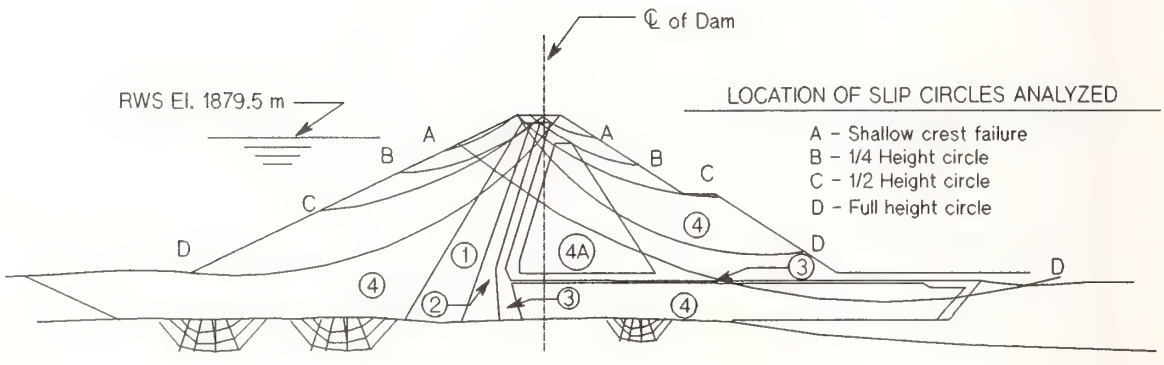

Figure 6 - Jordanelle Dam Deformation Analysis

An Evaluation of Seismic Forces Acting on Embankment Dams and Its Simplified Prediction Procedure

by

Tadahiko Fujisawa[1], Nario Yasuda[2], Norihisa Matsumoto[3], and Kenji Yamabe[4]

Abstract

Seismic force acting on embankment dams is studied using one- and two-dimensional dynamic analyses. In this report, the distribution of seismic acceleration in a typical dam body section is computed using acceleration records of actual earthquakes. On the basis of response computations to different input motions with various frequency characteristics, a relationship for the maximum response acceleration with frequency characteristics of the ground motions is established.

A simplified procedure to estimate the maximum acceleration from the acceleration response spectra of ground earthquake motions is also presented.

Keywords: Embankment dam, maximum acceleration, dynamic analysis, earthquake motion, permanent deformation

1. INTRODUCTION

This paper discusses the relationship between frequency characteristics of earthquake motions on base rock and seismic forces acting on embankment dams. Frequency-dependent characteristics of the seismic force acting on embankment dams were clarified by computing earthquake responses of the dam body to various input motions with different frequency characteristics. In addition, a procedure was developed to easily estimate seismic force from the acceleration response spectra of earthquake ground motions.

A method to estimate the safety of a dam body during earthquakes based on the permanent deformation of the dam has been developed since the prominent research of Newmark(1965) and Seed(1966) for embankment dams with banking materials which do not suffer reduction of strength even when subjected to cyclic loading. The major parameters for computing the amount and extent of such permanent deformation are: 1) average acceleration, $\bar{a}$, which is obtained by dividing the force of inertia acting on a potential sliding soil mass hypothesized in a dam body by the weight of this sliding mass; and 2) maximum average acceleration for the duration of earthquake motions, $\bar{a}_{max}$. If yield acceleration, a_y, is defined as the acceleration when the safety factor of the sliding soil mass becomes 1.0, then the amount of deformation of an embankment dam due to an earthquake is computed based on the concept that the soil mass begins to slide at the moment when average acceleration exceeds a_y. However, the deformation can be approximated simply by the ratio of a_y to $\bar{a}_{max}$. Watanabe *et al.*(1984) calculated the sliding deformation by Newmark's method with 5 sinusoidal waves which periods range from 0.125 sec. to 0.625 sec., and concluded that the permanent deformation at crest is in propotion to the square of the duration of a which exceeds a_y at any location of sliding mass. Makdisi *et al.*(1978) depicted the relationship between $a_y/\bar{a}_{max}$ and permanent deformation at every magnitude of earthquake event, conducting the calculation of sliding deformation by Newmark's method with real earthquakes. In addition, $\bar{a}_{max}$ is closely related to the concept of seismic coefficients pratically used in stability analyses of embankment dams based on the seismic coefficient method, that is, $\bar{a}_{max}$ expresses the seismic force acting on the body of an embankment dam. Considering the strength characteristics of soil, strain in soil materials does not greatly increase when the loading occurs during a short time period of one cycle; it does, however, increase when the soil is subjected to cyclic loading over a certain number of cycles. When $\bar{a}$, which is greater than a specified value, occurs repeatedly more than a certain number of cycles, this $\bar{a}$ is defined as equivalent acceleration, $\bar{a}_{eq}$, and is regarded by Seed *et* al.(1966) as a seismic coefficient for the seismic coefficient method. Initially, Seed *et al.*(1966) and Ambraseys *et al.*(1967) clarified that $\bar{a}_{max}$ for a wedge-shaped potential sliding mass obtained by using a dam body modelled into a homogenious triangle, the sliding surface of which was approximated by a straight line, varied depending on the elevation of the mass and the natural frequency of

*1 Head, Fill-type Dam Division, Public Works Research Institute, Ministry of Construction.
*2 Senior Research Engineer, ditto
*3 Dr. Eng., Senior Research Engineer of Dam Center Incorporated Foundation. (Former Head of Fill-Type Dam Division)
*4 1st Technical Division, the Water and Engineering Headquarters of the Osaka Branch, Research Institute for Construction and Technology, Co., Ltd. (Former visiting researcher)

the dam body. In the numerical analyses conducted in these studies, the procedure for a one-dimensional dynamic analysis based on the shear beam theory proposed by Mononobe *et al.*(1936) was introduced in order to estimate $\bar{a}_{max}$ for the sliding mass. Later, Chopra *et al.*(1967) showed that such values for $\bar{a}_{max}$ computed by the one-dimensional shear beam theory were greater by 10 to 20 % on average than those computed by a two-dimensional dynamic analysis with Finite Element Method. $\bar{a}_{max}$ is represented by a function of y/H, where H denotes the height of a dam and y the difference between the elevation of the dam crest and the minimum elevation of a sliding arc. The curve of normalized $\bar{a}_{max}$ in relation to y/H mentioned above(hereafter referred to as an acceleration curve) can be obtained from devided $\bar{a}_{max}$ by the maximum response acceleration at a dam crest, $\ddot{u}_{max}$. In accordance with the study by Makdisi *et al.*(1979), similar acceleration curves are obtained by both one- and two-dimensional analyses, however, the curve fluctuates to some extent depending on the natural frequency of the dam body, the upper and lower limits of the fluctuation are within the sphere of $\pm$10 to $\pm$20 % for the upper elevation and $\pm$20 to $\pm$30 % for the lower elevation, when average acceleration values are adopted. Thus, it is considered that average acceleration values can be used as a design curve for practical use. When a conservative design is dealt with from the aspect of safety, however, it is recommended that the values employed be 10 to 30 % greater than the average values. $\ddot{u}_{max}$ must be determined when seismic force is computed from an acceleration curve. Makdisi *et al.*(1978) proposed a simplified procedure for determining $\ddot{u}_{max}$ based on the root mean square using the acceleration response spectra of design earthquake motions as well as the modal analysis based on the one-dimensional shear beam theory. Luan *et al.*(1990) studied the effect of the shape of the sliding surface on an acceleration curve; the shape of the sliding surface is determined by the slope gradient of a dam, the damping ratio and the shear strength of soil materials. They demonstrated that the acceleration curve obtained using the procedure by Makdisi *et al.*(1979) resulted in underestimation at an elevation lower than the mid-height of a dam, and that both the slope gradient of a dam and the shear strength of soil materials were almost irrelevant to the curve.

As described above, studies have already been conducted on the relation between $\bar{a}_{max}$ and analytical procedures, dam shapes, the elevation of the sliding soil mass, the dam height and physical properties of dam body. Nevertheless, very few studies have been hitherto conducted on $\bar{a}_{max}$ in relation to the frequency characteristics of input earthquake motions. In this paper, therefore, the relationship between $\bar{a}_{max}$ and the frequency characteristics of input earthquake motions is discussed and a simplified procedure of computing $\bar{a}_{max}$ from an acceleration response spectra is summarized.

2. ANALYTICAL MODEL AND METHODS

2.1. Model Dam

The model dam used in the analysis is a two-dimensional cross section perpendicular to the dam axis. with 63-meter in height and the slope gradients of 1:2.6 on the upstream side and 1:2.0 on the downstream side. The models illustrated in Fig. 1(a) and Fig. 1(b) are employed in one-dimensional and two-dimensional dynamic analyses respectively.

2.2 Physical Properties of the Model Dam

Physical properties of the whole section of the model dam are identical to those of rockfill materials, based on the idea that physical properties of the filter and core materials will have little effect on the results of analyses because a rockfill dam is mostly constited of rockfill materials. Shear modulus of rockfill material was determined from results obtained by cyclic triaxial tests in laboratory; taking into consideration the dependent characteristics with confining stress. The damping ratio for the material has a considerable influence on the response acceleration; therefore, its determination becomes important when an analysis is conducted. The damping ratio is composed of internal damping of the material itself, as well as energy dissipation damping which is related to boundary conditions such as the foundation rock and reservoir. Fig. 2 shows the strain dependent curves of normalized shear modulus and damping ratio of the rockfill material that constitutes the rockfill dam (Matsumoto *et al.*(1990). The internal damping corresponding to a strain level of 10^{-3} is about 10 % as shown in Fig. 2. It has already been verified experimentally that energy dissipation damping increases with the existence of the reservoir water (Matsumoto *et al.* (1983). In addition, Ohmachi *et al.*(1989) pointed out, based on actual measurement, that energy dissipation damping reached about 10 % when the reservoir was full. Therefore, it can be estimated that the damping ratio for rockfill material during large earthquakes when the reservoir is full

maximum acceleration in the base rock, $\ddot{g}_{max}$, except for Case 1. In addition, the value of $\bar{a}_{max}$ is small especially on the dam foundations in Case 6 through Case 8 where predominant frequencies of earthquake ground motions are relatively high. The $\bar{a}_{max}$ of an arbitrary y/H in Case 1, where the predominant frequency is 0.59 Hz, is the greatest of 8 cases, while $\bar{a}_{max}$ at the dam crest is around 3.5 times greater than $\ddot{g}_{max}$. The predominant frequency of earthquake ground motions in Case 4 is the closest to the natural frequency of a dam body. However, the value of $\bar{a}_{max}$ at the dam crest in Case 4 is smaller than that in Case 1 by around 300 gals. Thus, it is proved that the magnitude of acceleration at the dam crest can not be estimated only by the predominant frequency of input ground motions. Fourier spectra for Case 1 illustrate that components of a long period exceeding 0.3 sec. are predominant and the ground motion is close to sinusoidal wave. Furthermore ,comparing the acceleration response spectra in Fig. 4 with $\bar{a}_{max}$ in Fig. 7, it can be seen that the values of $\bar{a}_{max}$ are great in Cases 1, 2, 3 and 5, which have long period components exceeding the natural period of a dam body of 0.6 sec.

Fig. 8 shows the average values of $\bar{a}_{max}$ due to 8 input earthquake motions calculated by the four methods of analysis. As shown in Fig. 8, the values of $\bar{a}_{max}$ obtained by one-dimensional analyses are about 15% greater at the upper elevation than those obtained by two-dimensional analyses; the difference is about 10% at the lower elevation. Thus, it was proved that $\bar{a}_{max}$ from modal analysis, which require the least computation time, were satisfactory comparing with those obtained by other methods. The magnification factors of the maximum response acceleration, $\ddot{u}(y/H)_{max}$, to $\ddot{g}_{max}$ for 8 input earthquake motions were computed at arbitrary y/H corresponding to different elevations. Fig. 9(a) shows distributions of such magnification factors obtained by averaging 8 different cases. The values of responses obtained by a one-dimensional analysis are greater than those obtained by a two-dimensional analysis by about 10 %; however, the difference in responses is entirely small. The magnification factors to $\ddot{g}_{max}$ range around 1.0 for $y/H > 0.5$, and gradually increase along with the increase of elevation, when the elevation is higher than y/H=0.5; finally, they range from 2.2 to 2.5 when y/H reaches 0.0 (the dam crest). Fig. 9(b) shows distributions of $\ddot{u}(y/H)_{max}/\ddot{g}_{max}$ for 8 input earthquake motions computed by QUAD-4.

We compare the computed values as shown in Fig.8 and 9 with the behaviors of actual dams. Fig. 10(a) shows the relationship between maximum acceleration magnifications at dam crests and $\ddot{g}_{max}$ monitored at embankment dams under the jurisdiction of the Ministry of Construction. In accordance with this figure, the magnification ranges from 3 to 6 when $\ddot{g}_{max}$ is equal to or smaller than 20 gals, but it decreases as $\ddot{g}_{max}$ increases, ranging from 2.0 to 2.5 especially when $\ddot{g}_{max}$ is equal to or greater than 100 gals. The first reason for this can be explained by non-lineality in that damping increases as $\ddot{g}_{max}$ increases. The second is based on the fact that the earthquake event with small $\ddot{g}_{max}$ usually has a long epicentral distance and induces earthquake motions with a predominant frequency close to the resonance frequency of the embankment dam, while the earthquake event with $\ddot{g}_{max}$ larger than 100 gals has a short epicentral distance and an inclination to cause earthquake motions with high frequencies. In other words, the frequency characteristics of earthquake motions where $\ddot{g}_{max}$ exceeds 100 gals correspond to that of Cases 6 through 8 in Table 1. The fact that $\bar{a}_{max}$ for y/H=0 in Cases 6 through 8 in Fig. 9 range 1.5 to 2.5 times greater than $\ddot{g}_{max}$ agrees with results obtained by measurement, which indicates that the supposition of material properties used in the dynamic analyses was reasonable. Fig. 10(b) shows the maximum acceleration distribution of embankment dams for each elevation; the figures are arranged in order based on the measured data at embankment dams of the Ministry of Construction, together with the results given in the reference papers (Sawada *et al.*(1979, 1986), Annaka *et al.*(1990), Hasegawa *et al.* (1983)). Fig. 10(b) includes earthquake data where the values of $\ddot{g}_{max}$ are around 5 gals. Since damping is small in such earthquake responses, magnifications in Fig. 10(b) are greater than those in Fig. 9(a). Acceleration distribution at each elevation in Fig. 9(b) ranges between the lowest and average values in Fig. 10(b). In short, if the magnification is considered to be distributed in the middle of the lowest and average values in Fig. 10(b), due to the fact that damping increases when $\ddot{g}_{max}$ is 0.2G, it can be said that the results of analyses shown in Fig. 9 coincide with the measured results. Based on the above examinations, the analyses conducted in this paper are regarded as comparable with measured results. Fig. 11 shows the acceleration curve which was derived by dividing the average values of $\bar{a}_{max}$ by the values of $\ddot{u}_{max}$ with 8 input earthquake motions in Fig. 9 . In addition, Fig. 11 also includes the results of Mak-

is about 20 % in total. In previous analytical studies (Ambraseys *et al.*(1967), Chopra.(1967), Makdisi *et al.*(1978,1979), Luan *et al.*(1990)) a percentage of 20 % was employed as a damping ratio. In this paper, accordingly, the damping ratio is constantly fixed at 20 %, regardless of either the shear strain or the mean principal stress, in consideration of both the intensity of the earthquake expected and the results of these past studies.

2.3. Analytical Methods

The following four methods were used for dynamic analysis: the modal analyses and SHAKEM (Chugh (1985)) for one-dimensional dynamic analysis, as well as QUAD-4 (Idriss *et al.*(1973)) and FLUSH (Lysmer *et al.*(1975)) for the two-dimensional dynamic analysis; a being computed by each method.

The modal analysis is used to conduct earthquake response analyses of a structure during earthquakes, in which the vibration of a structure with multiple degrees of freedom is expressed by superposing several systems of a single degree of freedom by the aid of the orthogonality of normal modes (Okamoto *et al.*(1976)). In adapting the modal analysis to embankment dam , the dam was modelled by a set of masses and stiffness (elastic spring) as illustrated in Fig. 3. The gross mass of a layer, M_i, was set in the center of gravity of each layer and represented by the mass point, while stiffness (elastic springs) were located between each mass point. Subscript i denotes the mass point number. The spring constant, k_i, can be determined by Equation (1) below:

$$k_i = \frac{l_i G_i}{d_i} \qquad .....(1)$$

where l_i = the length of layer i at the mass point (center of gravity); d_i = the distance between mass points; G_i shear modulus of layer;.

$\bar{a}$ for the sliding mass overlying layer i is calculated by the following equation:

$$\bar{a} = \frac{F_i}{\sum_{i=1}^{N} m_s} \qquad .....(2)$$

where F_i = the shearing force acting on the interface between layers i and (i-1), which is expressed by $F_i = k_i \times (y_i - y_{i-1})$ where y_i is the displacement of the mass point in layer;.

SHAKEM, a computer code, is modified version of SHAKE(Schnabel *et al.*(1972)) and was developed so that it could be applied to a finite ground. $\bar{a}$ of the sliding mass determined by SHAKEM was computed from the weighed average acceleration corresponding to the area of each layer within the sliding arc.

In the analyses by QUAD-4 and FLUSH, on the other hand, $\bar{a}$ of the sliding mass was computed from the weighed average acceleration corresponding to the area of each element with nodal points in common within the sliding arc.

2.4. Input Earthquake Motions

As a rule, input ground motions should be determined in accordance with earthquake characteristics set forth as a subject of design. Real earthquake observation records on bedrocks revealed that the frequency characteristics of earthquake ground motions differed with each event, even if the magnitudes were on the same level and the ground motions were recorded at the same dam site. From the viewpoint of conservative design, different earthquake ground motions with various frequency characteristics should be taken into consideration when the input earthquake motions for analyses are selected. Therefore, in the estimation of the seismic force acting on the dam body, earthquake response analyses were conducted using different actual earthquake ground motions with various frequency characteristics as input ground motions. In this paper, 8 earthquake ground motions with various frequency characteristics were selected from numerous actual earthquake records obtained from the base rock of dam foundations, based on the predominant frequencies in the Fourier spectra of earthquake ground motions. Table 1 summarizes the characteristics of the earthquake ground motions. Actual earthquake ground motions were amplified so that the maximum acceleration an input earthquake motion, $\ddot{g}_{max}$, becomes 0.2G (G: gravitational acceleration). Fig. 4 shows the acceleration response spectra for 8 input earthquake ground motions computed at damping ratio of 20 %.

3.PRELIMINARY EXAMINATIONS

3.1. Effect of Vertical Motions

As a preliminary investigation, the effect of the vertical component of response acceleration, on the calculation of a of a potential sliding mass, as well as the effect of the vertical input ground motions was examined. The effects of these vertical components were estimated by the acceleration moment, M_a, of a potential sliding mass given by Equation (3) below:

$$M_a = \sum_{i=1}^{N} \{m_i \times (a_{Hi} \times r_{Vi} + a_{Vi} \times r_{Hi})\} \Big/ \sum_{i=1}^{N} m_i \qquad .....(3)$$

where a_{Hi} and a_{Vi} are horizontal and vertical accelerations respectively, and r_{Hi} and r_{Vi} are horizontal and vertical distances between the center of an arc and the center of the element mass, m_i. In addition, the following 3 cases were established in order to evaluate the influence of vertical ground motions:

(1) M_a is computed using time histories of the horizontal response acceleration obtained through dynamic analyses, where only horizontal ground motions are used as input ground motions (Case ⓐ).

(2) M_a is computed using time histories of the horizontal response acceleration obtained through dynamic analyses, where both the horizontal and vertical ground motions are used as input ground motions (Case ⓑ).

(3) M_a is computed using time histories of both the horizontal and vertical response acceleration obtained through dynamic analyses, where both the horizontal and vertical ground motions are used as input ground motions (Case ⓒ).

Analyses of the model dam in Fig. 1(b) were carried out by QUAD-4, a two-dimensional analysis code, using actual earthquake ground motions. Maximum values of M_a within the time duration of input ground motions at the sliding mass were then determined. The input ground motions used in the analyses were those of Case 5 summarized in Table 1. The maximum acceleration of the vertical ground motions was adjusted to 1/2 of the horizontal maximum acceleration in these analyses, due to the fact that the ratio of horizontal maximum acceleration to vertical one ranges from 1/4 to 1/2 in accordance with the earthquake ground motions recorded at dam foundations.

Fig. 5 depicts the results of the analyses. With respect to the effect of the vertical ground motions, the maximum average acceleration moments obtained in Case ⓐ are greater than those obtained in Case ⓑ by about 4 %, though the shapes of curves obtained in both cases are similar. A comparison of the results of Case ⓐ and Case ⓒ proves that the maximum average acceleration moments in Case ⓒ are smaller than those in Case ⓐ by about 4.0 % at maximum for $y/H < 0.6$; this relationship goes into reverse when y/H reaches 0.7; and the maximum average acceleration moments in Case ⓒ become greater by about 10 % than those in Case ⓐ for $y/H = 1.0$. Judging from these results, the effects of both the vertical input ground motions and the vertical response acceleration on M_a are estimated to be around 10 % at most. Tamura and Okamoto(1987) conducted an evaluation of the effect of vertical input ground motions on the stability of embankment dams through both vibration table tests and dynamic analyses with sinusoidal waves. They concluded that the effect was almost equivalent to an increase of 10 to 20 % at horizontal ground motions, when a dam is vibrated not only by horizontal ground motions but also vertical ground motions, and the maximum acceleration of the latter being a half of that of the former.

Based on the above facts, the effects of vertical ground motions and vertical response acceleration are estimated to be negligible. In order to simplify computation, Case ⓐ, in which both ground motions and response acceleration are exclusively horizontal, was selected for the following examinations.

3.2. Calculation Method for Average Acceleration, $\bar{a}$

In general, $\bar{a}$ of a potential sliding soil mass is computed from the horizontal force acting on the soil mass; however, it may also be computed from the moment acting on the mass. These two methods may be compared thus:

(1) $\bar{a}$ is computed so as to be equivalent to the moment of a sliding mass around the center of a circular arc of the mass. In other words, $\bar{a}$ is obtained by the equation stated below using the time history of horizontal response acceleration, a_{Hi}, element mass, m_i, and the vertical distance between the center of a circular arc and the center of gravity in each element , r_{vi}(Case ⓓ):

$$\bar{a}=\sum_{i=1}^{N}(m_i \times a_{Hi} \times r_{vi})/\sum_{i=1}^{N}(m_i \times r_{vi}) \quad ....(4)$$

(2) $\bar{a}$ is computed so as to be equivalent to force of a sliding mass. In other words, $\bar{a}$ is obtained by Equation (5) using a_{Hi} and m_i of each element (Case ⓔ).

$$\bar{a}=\sum_{i=1}^{N}(mi \times a_{Hi}) \,/\, \sum_{i=1}^{N} m_i \quad .....(5)$$

As a result of the computation, it was found that the values of $\bar{a}_{max}$ obtained by Equations (4) and (5) were almost identical as illustrated in Fig. 6. Thus, Equation (5) was used to compute $\bar{a}_{max}$ in the following examinations.

4.MAXIMUM AVERAGE ACCELERATION, $\bar{a}_{max}$

Fig. 7 shows the relationship between $\bar{a}_{max}$ for a circular arc sliding mass and y/H concerning each input ground motion (Matsumoto *et al.*(1991)). The more y/H increases, i.e., the deeper the location of a circular arc becomes, the smaller the values of $\bar{a}_{max}$ become, as shown in this figure. The values of $\bar{a}_{max}$ are almost equivalent to or smaller than the

disi *et al.*(1978) and Luan *et al.*(1990). The maximum acceleration curve obtained by the two-dimensional dynamic analyses in this paper coincides with that of Luan *et al.* for the most part, but differs slightly from that of Makdisi *et al.* This is perhaps attributable to the difference in the determination of the shear modulus of the rockfill material, shear modulus was changed depending on the confining stress in the analyses by Luan *et al.*, while it was kept fixed in the analyses by Makdisi *et al.* The acceleration curve obtained by the one-dimensional analyses is on the left of that obtained by the two-dimensional analyses, being roughly parallel when the height of the circular arc is over 0.3. This is a relative discrepancy caused by the fact that the values of $\ddot{u}_{max}$ in the one-dimensional analyses were great.

Makdisi *et al.*(1978) and Luan *et al.*(1990) express the acceleration curves in the forms shown in Fig. 11 in order to estimate the sliding displacement. However, these curves are nothing more than average values; the relationship between the frequency characteristics of input earthquake motions and the natural frequency of a dam body are omitted in their studies. As shown in Fig. 7, $\bar{a}_{max}$ greatly depends on such a relationship; when the curve in Fig. 11 is applied to the earthquake motions in Cases 2 and 3, the values of $\bar{a}_{max}$ at the elevations between the middle and the bottom become subject to underestimation. Therefore, there is a possibility that a noticeble error may result if $\bar{a}_{max}$ at respective elevations are simply estimated using $\ddot{u}_{max}$ without considering the facts mentioned above, despite that the usage of an appropriate method for applying an acceleration curve is valid. The method to estimate the distribution of $\bar{a}_{max}$ at each elevation using an acceleration curve is simple and convenient; however, the above mentioned problems do exist. Therefore, for practical use, a method to compute the distribution of $\bar{a}_{max}$ corresponding to the frequency characteristics of input earthquake motions based on Fig. 7 normalized by $\ddot{g}_{max}$ is considered to work better in minimizing errors.

5. A SIMPLIFIED METHOD TO ESTIMATE MAXIMUM AVERAGE ACCELERATION

$\bar{a}_{max}$ of a circular arc potential sliding mass depends on the frequency characteristics of input earthquake motions, and the response of a mass differs according to the frequency characteristics. A method of evaluating the frequency component, which greatly influences $\bar{a}_{max}$ during actual earthquakes, is examined below:

When a physical property R, such as a displacement or stress at an arbitrary position on a structure, is subjected to sinusoidal waves with frequency f Hz at a unit amplitude, R(f) is, in general, a frequency response function, provided that R(f) is expressed by a function of frequency, f. Accordingly, $\bar{a}_{max}$ corresponding to an arbitrary y/H was computed in relation with numerous frequencies, f. Fig. 12 shows such frequency response functions for the dam shown in Fig. 1 computed by QUAD-4 at three elevations, i.e., y/H = 0.0, 0.4 and 1.0. The peaks of each $\bar{a}_{max}$ of the three potential sliding masses are close to f/f_o=1.0; however, the values of $\bar{a}_{max}$ differ depending on the depth of the potential sliding mass. The frequency component which influences $\bar{a}_{max}$ is defined to be within the range where $\bar{a}_{max}/\ddot{g}_{max}$ is greater than 1.0, although it differs depending on the depth of the potential sliding mass. In order to simplify the computation, however, the frequency range was determined based on Fig. 12, which was expressed by Equation (6), regardless of the depth of the potential sliding mass. Because low natural frequencies up to the 5-th or 6-th mode govern the response of an embankment dam during earthquakes, the upper limit of f/f_o was considered to be sufficiently 2.0, while the lower limit was set at f/f_o=0.8, where the magnification of responses of each sliding mass is reduced to half of that for f/f_o=1.0.

$$0.8 \le f/f_o \le 2.0 \quad .....(6)$$

As described above, Makdisi proposed a method which gives a design value of $\bar{a}_{max}$: when an acceleration response spectrum of the earthquake motion is given as a load condition, it is used to estimate $\ddot{u}_{max}$, which is further combined with the acceleration curve shown in Fig. 11 in order to obtain the value of $\bar{a}_{max}$. On the other hand, when the existence of a frequency response function of $\bar{a}_{max}$ along with its characteristics as shown in Fig. 12 is taken into consideration, $\bar{a}_{max}$ can be estimated directly with high accuracy by the acceleration response spectrum given as the load condition. In short, when the acceleration response spectrum of input earthquake motions is given, the mean value of the acceleration response spectrum within the frequency range given by Equation (6), S_{am}, is computed; should a correlation between $\bar{a}_{max}$ computed by dynamic analyses and S_{am} exist, $\bar{a}_{max}$ can be easily computed by S_{am}. The values of S_{am} were computed based on Fig. 4 using the 8 earthquake motions in Table 1 as input motions. Fig. 13 illustrates the relationship between S_{am} and $\bar{a}_{max}$.

In addition, Fig. 14 shows the

results obtained by modal analysis regarding the effect of dam heights (natural periods) on $\bar{a}_{max}$ of a potential sliding mass. This figure shows that there is only a minor difference in $\bar{a}_{max}/S_{am}$ corresponding to arbitrary y/H, even when the height of a dam varies.

The above results were obtained by analyses under the damping ratio of 20 %. Acceleration response spectra were computed separately for h=10%, and the relationship between $\bar{a}_{max}/S_{am}$ and y/H were obtained and compared with that for h = 20 % as shown in Fig. 15. In this figure, $R_{0.1}$ and $R_{0.2}$ is correlation coefficient of fluctuation of $\bar{a}_{max}$ / $\ddot{g}_{max}$ against regression line at the damping ratio of 10% and 20% respectively. The calculation is conducted for 8 earthquake motions in Table 1. In accordance with the results obtained by two-dimensional analyses using QUAD-4 shown in this figure, there is only a slight difference in the relationships of these cases. The following equation can be derived as an approximation:

$$\bar{a}_{max} = \{2.0 - 1.35(y/H)\} \times S_{am} \quad .....(7)$$

Based on the above results, $\bar{a}_{max}$ of a potential sliding mass can be estimated by the following methods:

(1)The acceleration response spectrum of input earthquake motions is computed, provided that the damping ratio to be used is that of the dam concerned.

(2)The natural frequency of the dam is computed.

(3)The mean value of acceleration response spectra is computed within the range given by Equation (6).

(4)The values of $\bar{a}_{max}$ corresponding to an arbitrary elevation are computed by substituting S_{am} into Equation (7) or by using Fig. 15.

6. ESTIMATION OF PERMANENT DEFORMATION AND LOADING STRESS IN CYCLIC LOADING TESTS

When the critical acceleration of an arbitrary potential sliding mass is a_y and the maximum average acceleration of the sliding mass due to input ground motions is $\bar{a}_{max}$, the amount of permanent deformation, U_p, is not generated when $a_y/\bar{a}_{max} > 1.0$, but when $a_y/\bar{a}_{max} < 1.0$. There is a close correlation between U_p and $a_y/\bar{a}_{max}$. The charts to estimate U_p from $a_y/\bar{a}_{max}$ were proposed by Makdisi *et al.*(1978) and Luan *et al.*(1990). This idea is basically an extension of the method proposed by Newmark (1965). This paper deals with a method to estimate the extents of permanent deformation by laboratory tests using $\bar{a}_{max}$. Ishihara(1980) proposed a method by which the extent of permanent deformation is determined through laboratory tests under a stress condition, which is derived by the static and dynamic shear stresses obtained from the safety factors of a potential sliding mass before and during earthquakes calculated by the simplified slice method. This paper also follows this concept, except for the fact that dynamic shear stresses are estimated directly using $\bar{a}_{max}$. When the moment due to a static load acting on a sliding mass before an earthquake is M_s, the mean shear stress, τ_s, acting on a potential sliding mass due to a static load can be given by the following equation, where r is the radius and l the length of the circular arc:

$$\tau_s = \frac{M_s}{r \times l} \quad .....(8)$$

On the other hand, the moment, M_d, of a dynamic load can be obtained from $\bar{a}_{max}$; the mean shear stress acting on a potential sliding mass, τ_d, is as follows:

$$\tau_d = \frac{M_d}{r \times l} \quad .....(9)$$

The specimen of banking material is consolidated by the average confining stress, σ_m; then σ_s is applied to the specimen under a drained condition. Finally, cyclic shear stress of $\pm\tau_d$ is applied under an undrained condition; then the cumulative shear strain summed up in the specimen is obtained. This cumulative strain enables the estimation of deformation of embankment dam during earthquakes. It is desirable to apply the cyclic shear stress, the wave form of which corresponds to the time history of $\bar{a}$; however, $\bar{a}_{eq}$ is used instead of $\bar{a}_{max}$ when cyclic shear stress with a constant amplitude is applied. Fig. 16 shows the results obtained by computation regarding the relationship between $\bar{a}_{max}$ of a potential sliding mass on the upstream side of the dam model shown in Fig. 2(b) and the shear stress of the sliding surface, $\tau(\tau_s + \tau_d)$. The value of τ for $\bar{a}_{max} = 0$ in Fig. 16 coincides with τ_s calculated by Equation (8); the range of τ_d at $\tau_d < \tau_s$ is shown by a dotted line. From this figure, it is recognized that a stress reverse does not occur, due to the fact that τ_d is smaller than τ_s in the range where $\bar{a}_{max}$ does not exceed 0.2G. By the use of Fig. 16, the load condition for determining permanent strain through laboratory cyclic loading tests can be established with high accuracy.

Fig. 17 shows the relationship between U_p related to 10th cyclic loading and τ_d obtained by the cyclic loading tests for the rockfill material(matsumoto *et al.*(1991)). The permanent strain corresponding to 10 th cyclic loading, U_p, can be evaluated,

by calculating τ_s and τ_d coping to a potential sliding mass using Fig. 16, or Equations (8) and (9) and by applying these τ_s and τ_d to Fig. 17. However, Fig. 17 is obtained for 6.0 kgf/cm^2 of mean confining stress, σ_m. It is necessary that curves in Fig. 17 should be drawn for several kinds of confining stress at the laboratory test, because shear strength of rockfill materials has an inclination to depend on confining stress.

7.CONCLUSIONS

The effect of different earthquake ground motions with various frequency characteristics on the seismic force acting on embankment dams was evaluated by 4 methods of dynamic analysis. In addition, a simplified procedure to estimate $\bar{a}_{max}$ was examined. The conclusions of this paper are summarized below:

(1) Even if $\bar{a}_{max}$ is computed using only horizontal input earthquake motions and the horizontal component of response acceleration of a dam body, the errors in $\bar{a}_{max}$ are around 10 % at most compared with the case where both horizontal and vertical components of motions are taken into consideration in input and response. Thus, $\bar{a}_{max}$ can be computed by the horizontal components alone.

(2) There are two methods to compute $\bar{a}_{max}$: one to compute it from the moment of the potential sliding mass concerned and another to compute it from the horizontal resultant force of the sliding mass. The difference in evaluation of $\bar{a}_{max}$ obtained by these two methods is about 5 % at maximum. Thus, $\bar{a}_{max}$ can be conventionally computed by the horizontal force alone.

(3) Distributions of $\bar{a}_{max}$ due to the 8 different input earthquake motions with various frequency characteristics were computed by 4 analysis methods. As a result, it was pointed out that the one-dimensional analyses, such as modal analysis and SHAKEM, gave values of $\bar{a}_{max}$ at dam crest about 15 % larger than those computed by the two-dimensional analyses on the average of results due to 8 input earthquake motions. In addition, the discrepancy of the values of $\bar{a}_{max}$ due to 4 different analyses was less than 10 % when y/H is greater than 0.3. This discrepancy, attributed to the difference in analytical methods, was entirely small, except for the fact that the responses near the dam crest obtained by one-dimensional analyses were comparatively large.

(4) Even when $\ddot{g}_{max}$ is the same, the value of $\bar{a}_{max}$ fluctuates +50% due to the frequency characteristics of the input ground motions on the basis of the average of 8 different responses. Therefore, the frequency characteristics of earthquake motions expected to occur at a dam site should be taken into consideration when the average values of the acceleration curve proposed by Makdisi *et al.*, which was normalized using $\ddot{u}_{max}$, is employed for practical use.

(5) When an acceleration response spectra of input ground motions are given, $\bar{a}_{max}$ can be easily obtained by the use of either Equation (7) or Fig. 15, based on the computation of the average values, S_{am}, for the Fourier spectrum within the frequency range given by Equation (6) corresponding to y/H.

(6) Laboratory cyclic loading tests for embankment material under the shear stresses derived from static and seismic forces, which are calculated by Equations (8) and (9) using $\bar{a}_{max}$, can contribute to greater precision in estimating the extent of permanent deformation to a dam body due to seismic forces.

REFERENCES

N. M. Newmark, "Effects of Earthquakes on Dams and Embankment," Geotechnique, Vol.5, No.2, pp.139-160, 1965.

H. B. Seed, "A Method for Earthquake-Resistant Design of Earth Dams," Jour. of SMFD, Vol.92, No.SM1, pp.13-41, 1966.

H. B. Seed and G. R. Marin, "The Seismic Coefficient in Earth Dam Design," Jour. of SMFD, ASCE, Vol.92, NO.SM3, pp.25-58, 1966.

N. N. Ambraseys and S. K. Sarma, "The Response of Earth Dams to Strong Earthquakes," Geotechnique, Vol.17, pp.181-213, 1967.

N. Mononobe, A. Tanaka and M. Matsumura, "Seismic Stability of the Earth Dams," 2nd ICOLD, pp.435-444, Vol.4, 1936.

A. K. Chopra, "Earthquake Response of Earth Dams," Jour. of SMFD, ASCE, Vol.93, No.SM2, pp.65-81, 1967.

F. I. Makdisi and H. B. Seed, "Simplified Procedure for Estimating Dam and Embankment Earthquake-Induced Deformations," Jour. of GTD, ASCE, Vol.104, No.GT7, pp.849-867, 1978.

F. I. Makdisi and H. B. Seed, "Simplified Procedure for Evaluating Embankment Response," Jour. of GTD, ASCE, Vol. 105, No.GT12, pp.1427-1434, 1979.

M. T. Luan, C. P. Jin, G. Lin and H. Takemiya, "Parametric Studies on Dynamic Stability and Permanent Deformations of Cohesive Embankment,"

Proceedings of the Eighth Japan Earthquake Engineering Symposium, Vol.2, pp.975-980, 1990.

N. Matsumoto, N. Yasuda, M. Ohkubo and Y. Kinoshita, "Shear Strength and Dynamic Deformation characteristics of gravels", Proc. of JSCE, Vol.424, III-14, pp.95-104, 1990. (in Japanese)

N. Matsumoto, M. Toyota and M. Shiga, "Model Vibration Tests of Rockfill Dams," Civil Engineering Journal, Vol.25, No.6, pp.45-50, 1983. (in Japanese)

T. Ohmachi and N. Nakamoto, "In-Situ Measurement of Radiation Damping of Existing Rockfill Dams," Proceedings of 9th World Conference on Earthquake Engineering, [6], pp.337-342, 1989.

Ashok K. Chugh, "Dynamic Response Analysis of Embankment Dams," International Journal for Numerical and Analytical Methods in Geomechanics, Vol.9, pp.101-124, 1985.

I. M. Idriss, J. Lysmer, R. Wang and H. B. Seed, "QUAD-4, A Computer Program for Evaluating the Seismic Stability of Soil Structures by Variable Damping Finite Element Procedures," EERC-Report No.73-16, University of California, 1973.

J. Lysmer, T. Udaka, C. F. Tsai and H. B. Seed, "FLUSH - A Computer Program for Approximate 3-D Analysis of Soil Structure Interaction Problems," EERC-Report No.75-30, University of California, 1975.

S. Okamoto, "Dynamics for Civil Engineers (Second Edition)," Ohmu-publication, pp.57-66, 1976. (in Japanese)

P. B. Schnabel, J. Lysmer and H. B. Seed, "SHAKE, A Computer Program for Earthquake Response Analysis of Horizontally Layered Sites," EERC-Report No.72-12, University of California, 1972.

N. Matsumoto, S. Kondo, H. Katahira and M. Shiga, "Earthquake Ground Motions on the bedrock of Dam Sites." Technical memorandum of Public Works Research Institute, No.1789, 1982. (in Japanese)

C. Tamura and S. Okamoto, " On effects of vertical ground motions on stability of Fill-type dams," International symposium on earthquakes and dams, ICOLD, pp.486-500, 1987.

N. Matsumoto, N. Yasuda and K. Yamabe, "Evaluation of Seismic Force Acting on Embankment Dams," Technical memorandum of Public Works Research Institute, No.2997, 1991. (in Japanese)

S. Okamoto, "Introduction to Earthquake Engineering," Ohmu-sha, p.385,1971. (in Japanese)

T. Sawada, "Behavior of Fill-type Dam during Earthquakes, Case Study of Namioka Dam," Proc. of Japan Acad. 62, Ser.B, pp.201-204, 1986.

M. Annaka, "Earthquake Observation of Fill-type Dams and 3-D Mode-Superposition Analysis using Three-directional Input Earthquake Motions," Large Dams, No.134, pp.22-34, 1990. (in Japanese)

T. Hasegawa, K. Uchida, M. Kikuchi and A. Murakami, "Analysis on the observed seismic response data of Miyama Dam and estimation of its dynamic response behavior," Trans. of JSIDRE, No.108, pp.55-63, December, 1983. (in Japanese)

T. Sawada, T. Hasegawa and M. Kikuzawa, "An application of the proposed complex damping Model to the dynamic analysis of an actual dam," Trans. of JSIDRE, No.28, pp.58-64, August, 1979. (in Japanese)

K. Ishihara, "Current practice and the problems in the earthquake resistant design of earth structures," Soils and Foundations, No.28-8, pp.3-8, 1980. (in Japanese)

N. Matsumoto, N. Yasuda, M. Ohkubo and R. Yoshioka, "Monotonics and Cyclic Loading Tests of Rockfill Materials," Technical memorandum of Public Works Research Institute, No.2996, 1991. (in Japanese)

H.Watanabe, S.Satoh and K.Murakami, "Evaluation of Earthquake-Induced Sliding in Rockfill Dams," Soils and Foundations, Vol.24, No.3, 1984

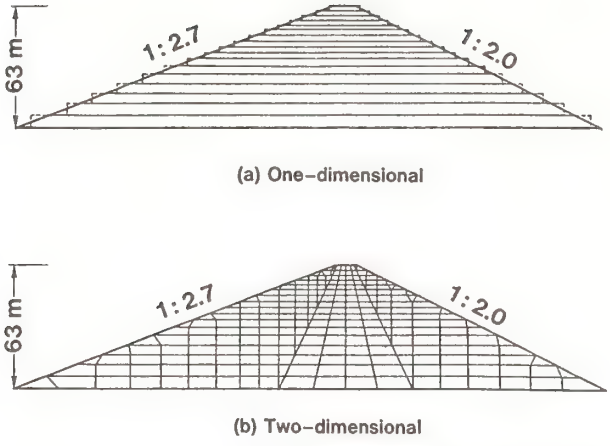

Fig. 1 Finite element idealization used in the analysis

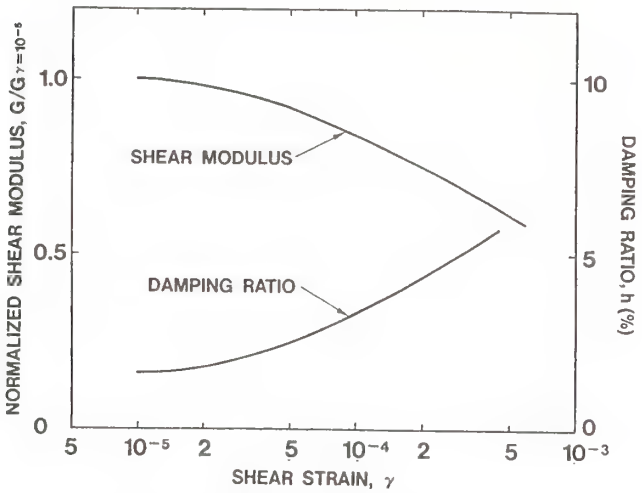

Fig. 2 Strain dependent curves of shear modulus and damping ratio used in response computations

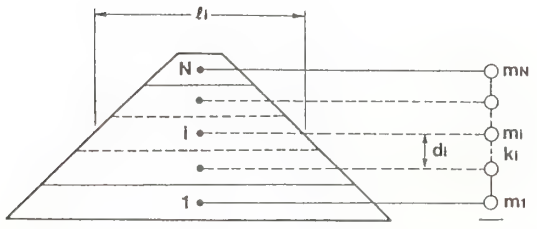

Fig. 3 Shear beam model with lumped mass (Modal Analysis)

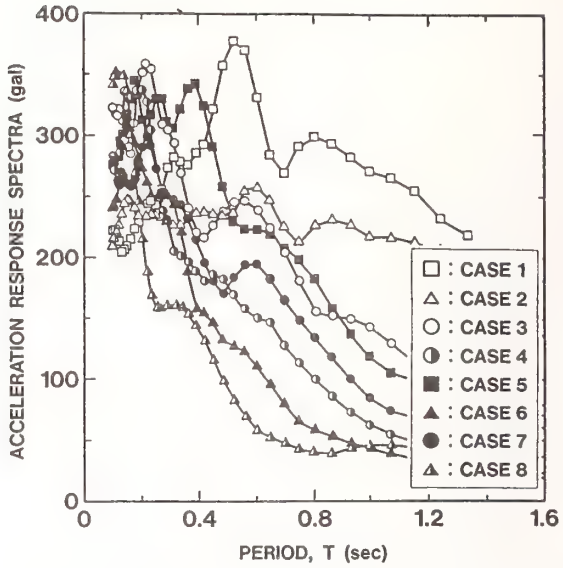

Fig. 4 Acceleration response spectra for input ground motions

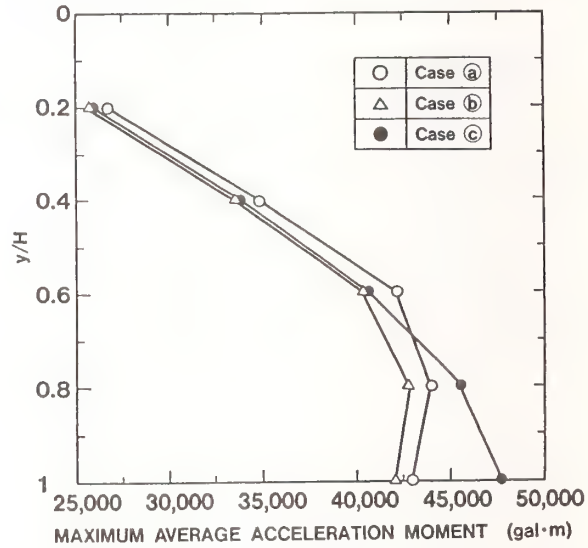

Fig. 5 Maximum average acceleration moment

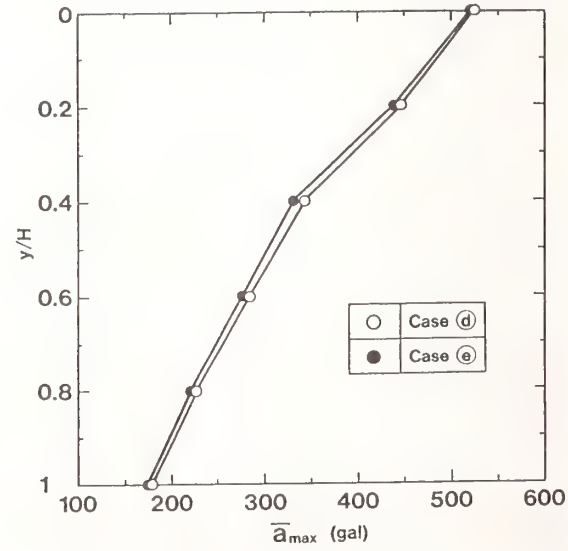

Fig. 6 Maximum average acceleration computed

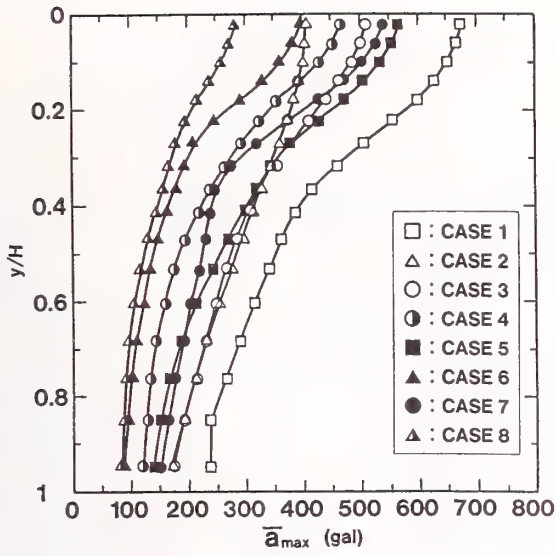

(a) Modal Analysis

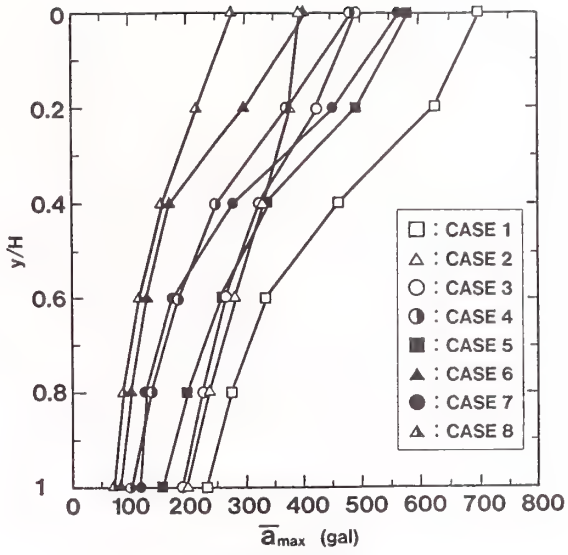

(b) SHAKEM

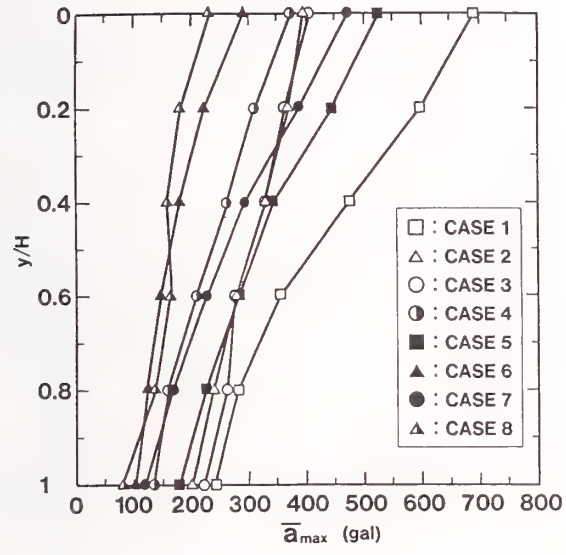

(c) QUAD-4

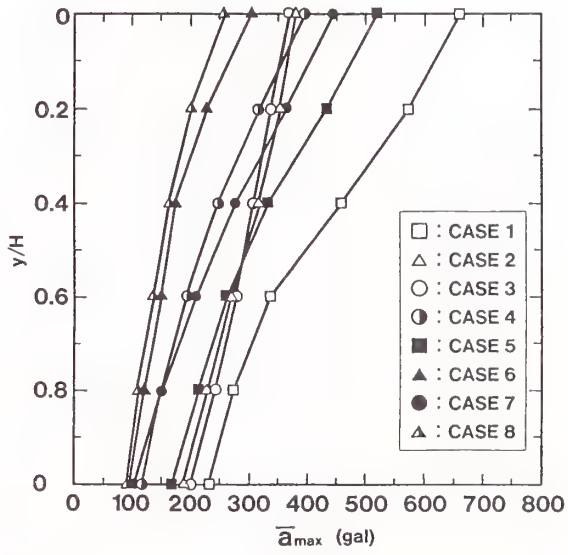

(d) FLUSH

Fig. 7 Maximum average acceleration

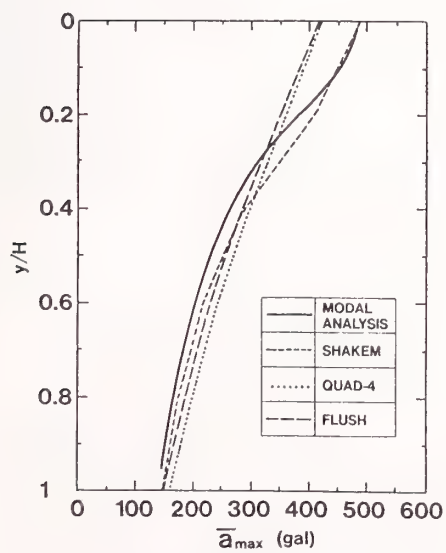

Fig. 8 Relationship between y/H and $\overline{a}_{max}$ for eight input motions

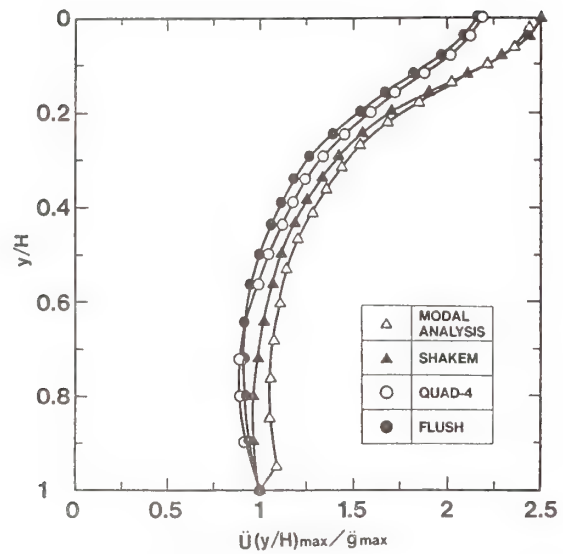

(a) Normalized maximum acceleration from different analytical methods

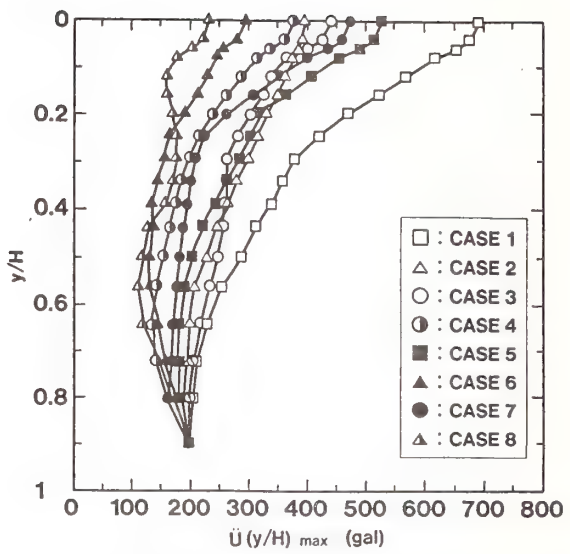

(b) Maximum acceleration from QUAD-4

Fig. 9 Maximum acceleration at various elevations

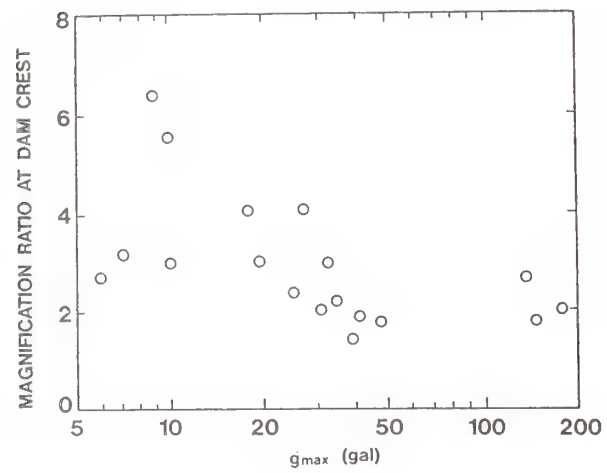

(a) Maximum acceleration magnification ratio at dam crest with maximum ground acceleration

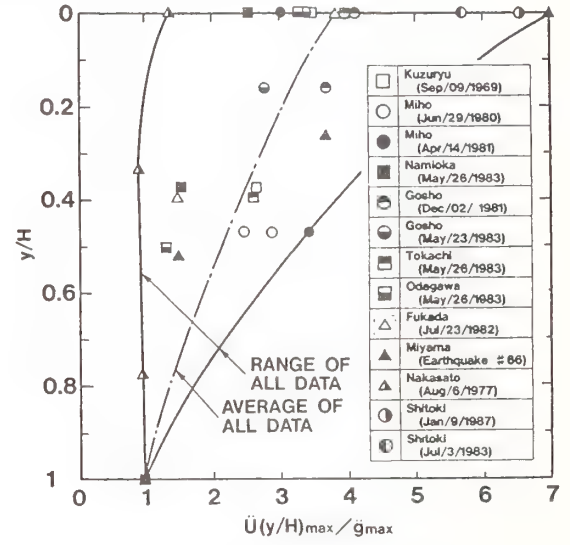

(b) Maximum acceleration distribution with elevations

Fig. 10 Acceleration response measured at rockfill dams

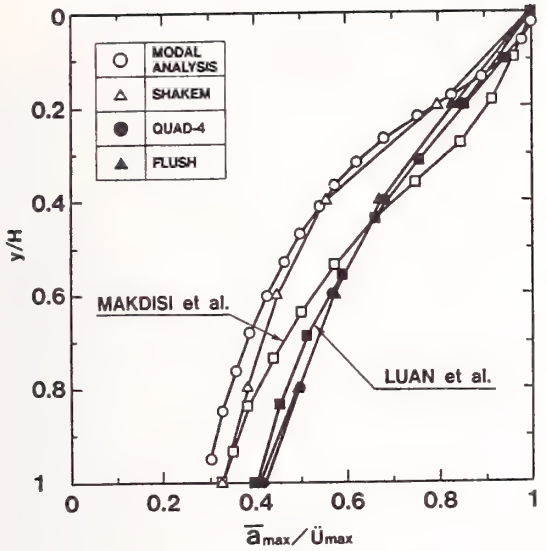

Fig. 11 Comparison of normalized maximum acceleration curve with depth of sliding mass

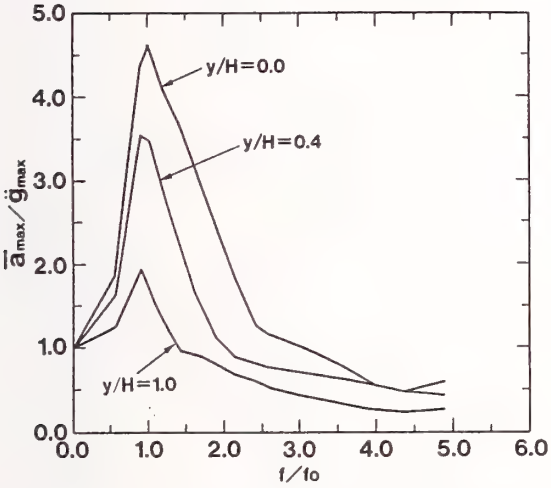

Fig. 12 Frequency response functions of $\bar{a}_{max}$ calculated by QUAD-4

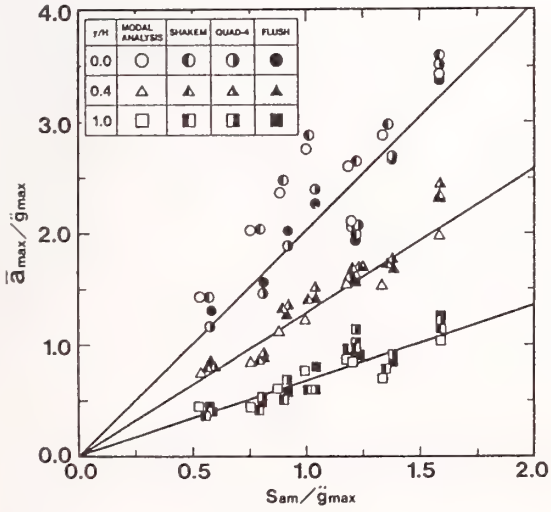

Fig. 13 Relationship between $\bar{a}_{max}/\ddot{g}_{max}$ and $S_{am}/\ddot{g}_{max}$

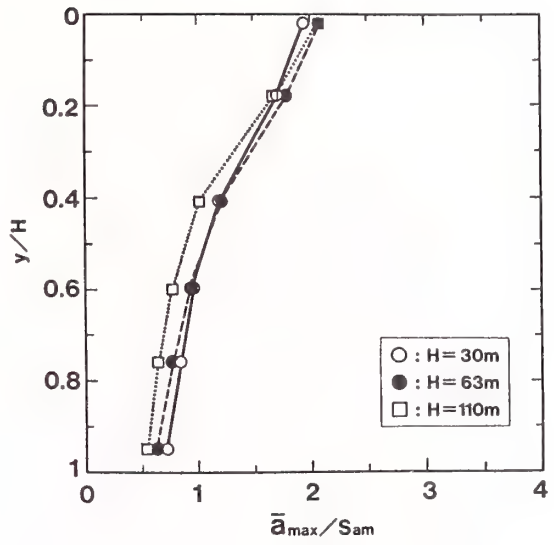

Fig. 14 Relationship between $\bar{a}_{max}/S_{am}$ and y/H for three different dam-heights

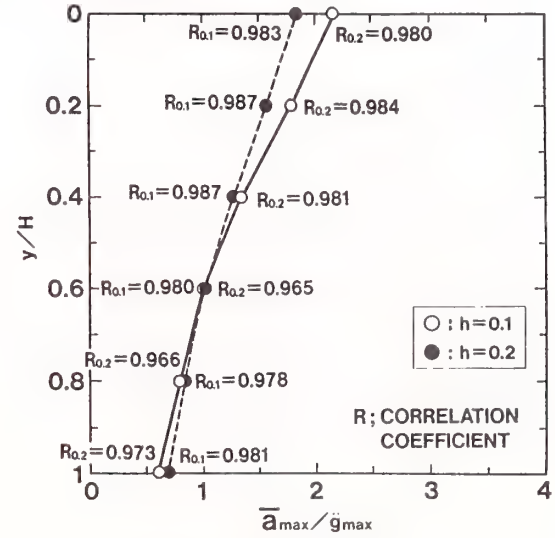

Fig. 15 Relationship between $\bar{a}_{max}/S_{am}$ and y/H for h=10% and 20% (QUAD-4)

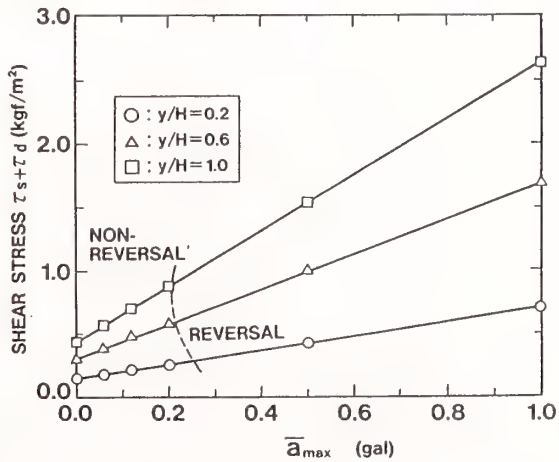

Fig. 16 Shear stresses estimated by using $\bar{a}_{max}$

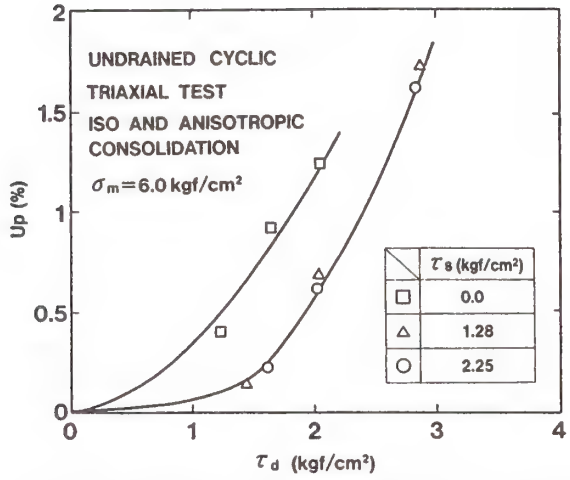

Fig.17 Permanent strain development in undrained cyclic triaxial

Table 1 Characteristics of earthquake motions observed at dam foundation

Case	DAM site	Earthquake	M	L (KM)	f (Hz)	f/fo
1	Gosho	Mid Japan Sea	7.7	198.0	0.59	0.35
2	Minase	Miyagi offshore	7.4	167.0	0.78	0.46
3	Yokoyama	Central Gifu	6.6	60.0	1.07	0.63
4	Tokachi	Northern Hidaka Mts.	7.0	82.0	1.61	0.95
5	Tase	Mid Japan Sea	7.7	264.0	2.39	1.41
6	Gosho	Central Iwate	6.6	69.0	3.20	1.88
7	Miho	Izu peninsula offshore	6.7	56.0	4.15	2.44
8	Miho	Western Kanagawa	5.8	12.0	6.59	3.88

(Note) M: Magnitude L: Epicentral distance
fo: Natural frequency of model dam f: Predominant frequency

Resolving Uncertainties in Seismic Hazard Models

by

J. K. Kimball*

ABSTRACT

This paper describes the types of uncertainties inherent in seismic hazard analysis, and identifies those steps that can be taken to resolve these uncertainties. The focus is on the recent advances that have been made in performing probabilistic seismic hazard studies, with particular emphasis on issues related to identifying uncertainties in the basic seismic hazard models. Comprehensive probabilistic seismic hazard studies have been completed over the past five years by Lawrence Livermore National Laboratory for the United States Nuclear Regulatory Commission and by the Electric Power Research Institute for the commercial utility industry. The United States Department of Energy is actively using these studies to evaluate seismic hazard at Department of Energy sites. Results from these studies can be used to quantify existing uncertainties in seismic source understanding, earthquake occurrence rates, and ground motion attenuation. The resulting uncertainties can then be evaluated to determine those that are reducible with additional study. Additionally, a clear understanding of modeling uncertainties can provide insight into the attributes that future probabilistic seismic hazard analysis should have.

KEYWORDS: seismic hazard; seismicity; seismic sources; uncertainty evaluation; ground motion

1. INTRODUCTION

The purpose of this paper is to provide a summary description of the types of uncertainties inherent in seismic hazard analysis, and to identify those steps that can be taken to resolve these uncertainties. This purpose will be accomplished by describing how the Department of Energy (DOE) is utilizing probabilistic seismic hazard results, including the identification and evaluation of uncertainty. The general purpose of a probabilistic seismic hazard analysis is to evaluate the vibratory ground shaking at a particular site by considering the viable sources of earthquakes, the likelihood of earthquake occurrences for each source, an estimate of the particular ground motion parameter of interest, and an analytical model for estimating the probability of exceeding the ground motion parameter. These general steps are shown on Figure 1. Each of the general steps will be discussed below, in terms of modeling uncertainty.

The DOE currently specifies the loading associated with the Design Basis Earthquake (DBE) based on probabilistic acceptance criteria. Mr. J. Hill, DOE, presented the DOE approach at the twenty-third annual joint meeting of the United States/Japan Panel on Wind and Seismic Effects, May 1991. The DOE facilities range from office buildings to complex

* U.S. Department of Energy, Office of Engineering and Operations Support, Washington, D.C. 20585

nuclear facilities. The design basis earthquake (DBE) acceptance criteria represents a range of probabilistic input levels from those associated with standard building codes (about 1/500 or .002 per year) to those associated with nuclear reactors (about 1/1,000 to 1/10,000 or .001 to .0001 per year). Because the DBE is specified probabilistically, the values selected are associated with mean estimates, to account for uncertainty in seismic hazard.

Because the DBE is probabilistically derived, particular attention has been focused on the types of approaches and inputs that have gone into existing seismic hazard analyses. Separate comprehensive studies were completed by Lawrence Livermore National Laboratory (LLNL) for the U.S. Nuclear Regulatory Commission (NRC) and by the Electric Power Research Institute (EPRI) for the commercial utility industry. These studies have been used at a number of DOE Eastern United States sites to establish the DBE seismic hazard curves. The LLNL and EPRI results can be used to highlight the strength of probabilistic results along with potential shortcomings that must be considered by decisions makers when using such results. Table 1 provides a brief outline of how the LLNL and EPRI studies were developed.

For the reader who is interested in background material regarding probabilistic seismic hazard analysis, two references are particular useful. The first is a National Research Council report from the Panel on Seismic Hazard Analysis (Committee on Seismology) on Probabilistic Seismic Hazard Analysis, 1988. The second is the Probabilistic Safety Analysis Procedures Guide, NUREG/CR-2815, Rev. 1, 1985, which describes how the various types of seismic hazard input should be characterized, including the treatment of uncertainties. The summary references for the LLNL and EPRI studies are D.L. Bernreuter et al, 1987, and Electric Power Research Institute, 1986. Two useful references regarding seismic source characterization are Coppersmith, 1991, and Thenhaus et al, 1987.

2. SOURCES ON UNCERTAINTY IN SEISMIC HAZARD ANALYSIS

It is important in any probabilistic seismic hazard analysis to make an estimate of the confidence in hazard results. In the LLNL and EPRI seismic hazard studies this was accomplished by providing constant percentile seismic hazard curves (such as 15th, 50th and 85th percentiles) and estimates of mean hazard. Figure 2 shows an example of such results for the DOE Savannah River Site in South Carolina. Several observations are noteworthy. First, the median (50th percentile) results are similar between the two studies. Second, the overall estimates of uncertainty are quite different between the two studies, which result in drastic differences between mean estimates of seismic hazard. Because DOE is attempting to use results such as these to establish the DBE, it has been important to understand why the two studies give such divergent estimates of uncertainty.

A convenient way of addressing seismic hazard uncertainty is to segregate uncertainty into two components. For the purpose of this paper these two components are labeled randomness and modeling uncertainty. Randomness represents variability that cannot be reduced with more data or better models. Modeling uncertainty represent variability that can be reduced (in concept) with better data and analysis techniques. The discussion provided below will identify modeling uncertainty issues using the LLNL and EPRI results. The

type of data that could be used to address such modeling uncertainty will also be identified. Such an observation has generic implications for any probabilistic seismic hazard analysis.

2.1 Seismic Source Uncertainty

In the LLNL and EPRI studies each of the experts and expert teams were requested to provide seismic source maps which generally represent areas of uniform earthquake potential. Figure 3 shows examples of such maps from two of the LLNL experts for the southeastern United States. The alternatives shown on the two maps represent very different opinions regarding the identification of seismic sources. Such divergent alternatives represents the ability of earth scientists to identify active seismic features (modeling uncertainty). Presently in intra-plate regions such as the Eastern United States, the identification of specific earthquake causal structure remains elusive. It could be expected that in more active tectonic regions, such as plate margin regions in California and Japan, earth scientists can more readily define the seismic sources. Such an assumption, however, may not be totally warranted given the occurrence of potentially damaging earthquakes such as the 1983 Coalinga, California earthquake. Thus, the current state of practice should recognize the potential large uncertainty in seismic source identification.

Since modeling uncertainty is potentially reducible, it is important to identify the type of data that should be assessed to reduce uncertainty in seismic sources. This data includes:

- Analysis of historic seismicity;
- Accurate instrumental seismic recordings;
- Geologic assessment of paleo-seismic features (such as fault scarps and liquefaction features); and
- Integration of geologic/seismologic/geophysical data to provide a three dimensional picture of the seismogenic crust.

As this type of data evolves, one can expect the uncertainty in seismic sources such as shown on Figure 3 to diminish.

2.2 Earthquake Occurrence Rate Uncertainty

In the LLNL and EPRI studies each of the experts and expert teams were requested to provide estimates of earthquake activity rates (commonly termed the "a" value), slopes of the earthquake occurrence curve (commonly termed the "b" value), and estimates of largest magnitude. Figure 4 displays the earthquake occurrence curves from the LLNL and EPRI studies for the Charleston, South Carolina seismic source, for the best estimate earthquake recurrence parameters ("a" and "b" values). Similar to seismic sources estimation, there is wide divergence in earthquake recurrence estimates. This divergence is even more dramatic if the uncertainty in "a" and "b" values is reviewed. Should such divergence be expected? The answer to this question is not simple considering that the earthquake occurrence information represents both randomness and modeling uncertainty.

In attempting to assess whether the estimates of uncertainty on earthquake occurrence rates are realistic, expert

opinion studies must include sufficient feedback and interaction to assure that input has a scientific basis. Clearly seismicity experts are not necessarily uncertainty experts. To illustrate this problem, the LLNL data for the DOE Savannah River Site has been evaluated in detail. One of the seismicity experts gave a range of recurrence intervals for magnitude 5 earthquakes for the Charleston, South Carolina, seismic source as 20 days to over 2000 years. Such dramatic examples may illustrate more of the problem of expert assessment of uncertainty than true modeling uncertainty.

The modeling uncertainty associated with earthquake occurrence rates, like seismic sources, is potentially reducible. The type of data that should aid this process includes:

- Quantification, on a consistent basis, of the size of historic earthquakes compared to instrumental seismicity;
- Integration of geologic slip rate from paleo-seismic studies with seismicity data; and
- Assessment of short term strain rates in active tectonic regions.

While this type of data should aid in reducing modeling uncertainty in earthquake occurrence rates, it may be more important to ensure that earth scientists better understand the process of uncertainty assessment.

2.3 Ground Motion Attenuation Uncertainty

In the LLNL and EPRI studies separate efforts were completed to develop ground motion attenuation relationships. In the LLNL study five attenuation experts selected attenuation models and provided uncertainty estimates. In the EPRI study one expert selected three attenuation models with one estimate of attenuation uncertainty. Figure 5 displays a comparison of predicted peak ground acceleration from the LLNL and EPRI studies for magnitudes 5 and 7. Figure 5 also shows wide divergence of opinion, similar to other components of seismic hazard input. In a region such as the eastern United States where there are few available strong motion records one might expect relatively large peak acceleration modeling uncertainty. In reviewing Figure 5, however, one sees that the modeling uncertainty predicted by the experts spans over an order of magnitude at the distance of one hundred kilometers. When such divergence exists, the user should require that each model selected be clearly justified. The LLNL seismic hazard is particularly sensitive to one of the attenuation models at rock sites. Much effort has been expended by other experts in an attempt to show that this model is inappropriate. While DOE and the NRC have not agreed with this conclusion, decisions made using the LLNL and EPRI results have had to recognize the sensitivity of this issue.

The type of data that should be used to reduce such modeling uncertainty includes:

- Collection and analysis of strong motion data near damaging earthquakes;
- Assessment of crustal attenuation properties both on a local and regional basis;
- Evaluation of earthquake source characteristics such as stress drop; and

- o Assessment of the effects of local site conditions including the impact of soil consolidation at deep soil sites.

2.4 Overall Summary of LLNL/EPRI Evaluation

Based on the evaluation of the LLNL and EPRI data DOE has reached the following general assessment of these two studies with respect to modeling uncertainty. This assessment provides insight into the types of attributes that any probabilistic seismic hazard should have. There is a high degree of similarity between the LLNL and EPRI seismic hazard studies ranging from overlap of experts used to general overlap in parameter input from the experts. **The key difference between the two studies relates to the topic of uncertainty assessment, particularly modeling uncertainty assessment for all input variables. Identified issues relate to the process of expert opinion elicitation, particularly the issues of how and whether experts assess and understand uncertainty.** This puts increased emphasis on the user or decision maker to fully understand the uncertainties inherent in the probabilistic results.

The DOE review has also found that there are several stable trends in the existing LLNL and EPRI data. These trends include:

- o General consistency in median probabilistic estimates of seismic hazard;
- o General consistency within each study of the ratio of 85th percentile hazard curves to the median hazard curves;
- o General consistency between each study in the ratio of 85th percentile hazard curves to the median hazard curves; and
- o Relative consistency in hazard trends; studies provide similar ranking of high seismic hazard to low seismic hazard sites.

The DOE has used the above trends to develop an interim position regarding how the two studies should be used at DOE sites. This position is built on the stable median hazard curves with a "correction factor" to account for uncertainty. The correction factor will be used to develop mean estimates of seismic hazard. The "correction factor" is based on the above identified trends, and was estimated to have a value of 1.65 for peak ground acceleration at probabilities of about 1/5000 or .0002 per year.

3. ATTRIBUTES OF AN ADEQUATE PROBABILISTIC SEISMIC HAZARD ANALYSIS

Given the types and the order of magnitude of modeling uncertainties described above, it is important to outline the attributes that any probabilistic seismic hazard analysis should contain. It is particularly important that any decision maker who is using a probabilistic seismic hazard analysis require that these attributes be properly addressed. These attributes include:

- o Clear documentation of input including modeling assumptions and how seismicity parameters were selected. It is important to understand the basis for the seismicity parameters (geologic versus seismologic) and attenuation models;
- o Comparison of model input to historic seismicity. While there should not necessarily be an over-reliance on historic seismicity, this type of comparison can identify issues which may otherwise be overlooked;

- o Incorporation of alternative models that represent the current state-of-knowledge. Hazard analyses without this attribute can lead to a false sense of security by not recognizing viable alternatives. It is important, however, that a basis be provided for all models used;

- o An analytical approach that allows the user to understand dominate seismic hazard contributors versus simply showing the bottom-line hazard curve. For many applications it is important to know which sources, magnitudes and distance most contribute to the seismic hazards; and

- o Clear documentation and presentation of uncertainties.

If the above attributes are addressed by a probabilistic seismic hazard analysis, then the hazard results are likely to provide consistent estimates from site to site. Even considering the large absolute differences in results such as LLNL and EPRI, it is at least reassuring to know that both studies provide consistent trends of seismic hazard.

4. CONCLUSIONS

The state-of-knowledge regarding the causes of earthquakes in much of the United States is limited, resulting in large uncertainties in seismic hazard estimates. Probabilistic seismic hazard studies must clearly describe and document this uncertainty to be useful for decision makers. Continued improvements regarding the assessment, quantification and documentation of expert opinion is needed before the actual probabilistic numbers can be used in an absolute sense. At the same time, continued study regarding the seismic and ground motion input should aid in reducing modeling uncertainties. Such efforts fall within the following major areas:

- o Continued geologic, seismologic, and tectonic study of the causes, mechanisms and rates of crustal deformation and the validity of alternative seismicity models;

- o Evaluation of instrumental seismic data including the variability of earthquake occurrence rates; and

- o Enhanced understanding of strong motion characteristics, regional attenuation properties and the effect of local surficial material.

5. REFERENCES

Bernreuter et al, 1987, Seismic Hazard Characterization of 69 Nuclear Plant Sites East of the Rocky Mountains, LLNL, NUREG/CR-5250, Vols. 1-7.

Coppersmith, 1991, Seismic Source Characterization for Engineering Seismic Hazard Analyses, Proceeding Fourth International Conference on Seismic Zonation, Stanford University, Stanford, California

Electric Power Research Institute, 1986, Seismic Hazard Methodology for the Central and Eastern United States, EPRI NO-4726, Project P101-21.

McCann et al, 1985, Probabilistic Safety Analysis Procedures Guide, BNL, NUREG/CR-2815, Sections 8-12.

National Research Council, 1988, Probabilistic Seismic Hazard Analysis, Panel on Seismic Hazard Analysis Committee on Seismology, National Academy Press, Washington, D.C.

Thenhaus, et al, 1987, Earthquake Hazard in the Eastern United States: Consequences of Alternative Seismic Source Zones, Earthquake Spectra, Vol. 3, No. 2.

TABLE 1

Summary of LLNL and EPRI Study

LLNL STUDY:

Used individual expert opinion to evaluate all seismic hazard input.

1. 10 Seismicity experts provided zonation, earthquake occurrence rates and upper magnitude values including estimates of uncertainty.

2. 5 Attenuation experts provided attenuation models and model uncertainty.

3. The LLNL used Monte Carlo methods to evaluate overall seismic hazard uncertainties. Each site included 2750 seismic hazard curves, which were processed into constant percentile seismic hazard curves.

EPRI STUDY:

Used expert teams to evaluate seismic hazard input except for attenuation models.

1. 6 Expert teams provided zonation, earthquake occurrence rates and upper magnitude values including estimates of uncertainty.

2. One expert provided attenuation models and model uncertainty.

3. EPRI used logic trees to evaluate overall seismic hazard uncertainty, which were processed into constant hazard seismic hazard curves.

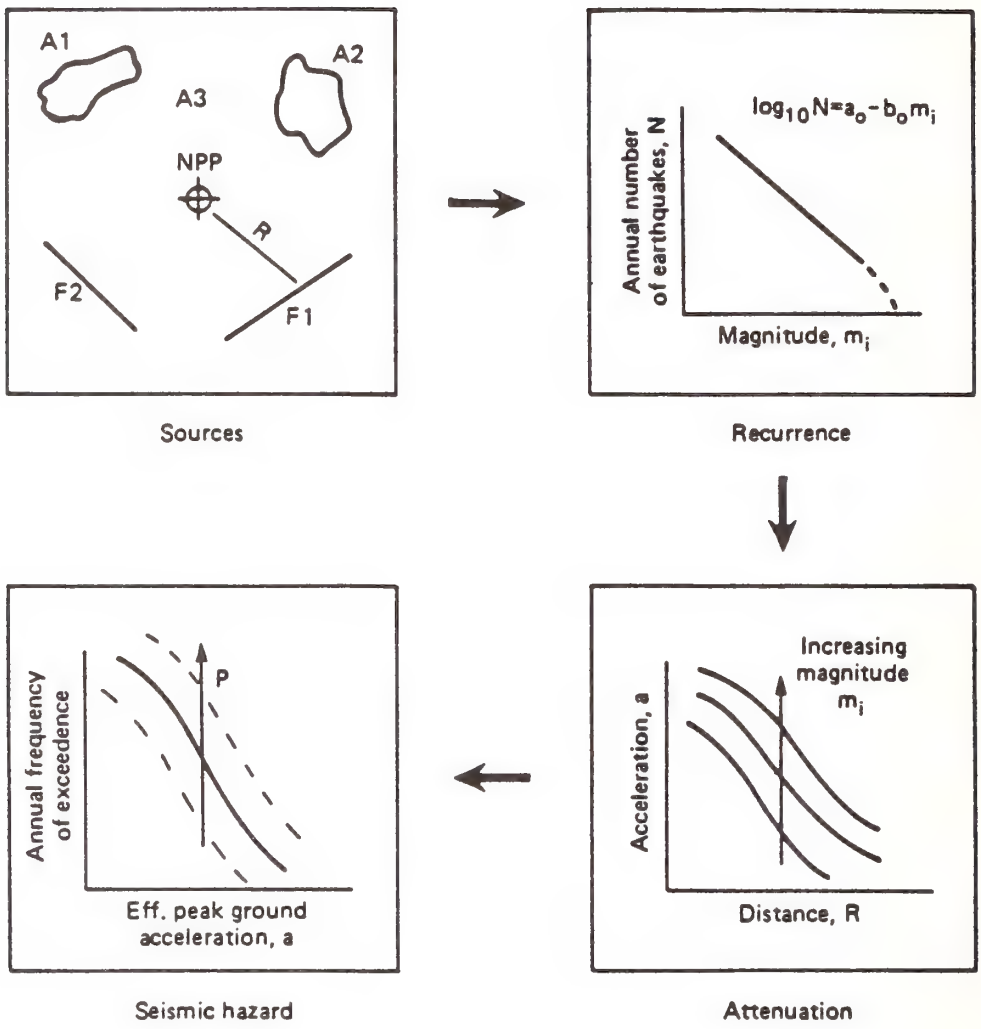

Figure 1

Four steps of a probabilistic seismic hazard analysis: Step 1 Identification of seismic sources; Step 2 Develop earthquake recurrence relationship for each seismic source; Step 3 Develop ground motion attenuation model; Step 4 Use an analytical model to calculate seismic hazard curve including uncertainty.

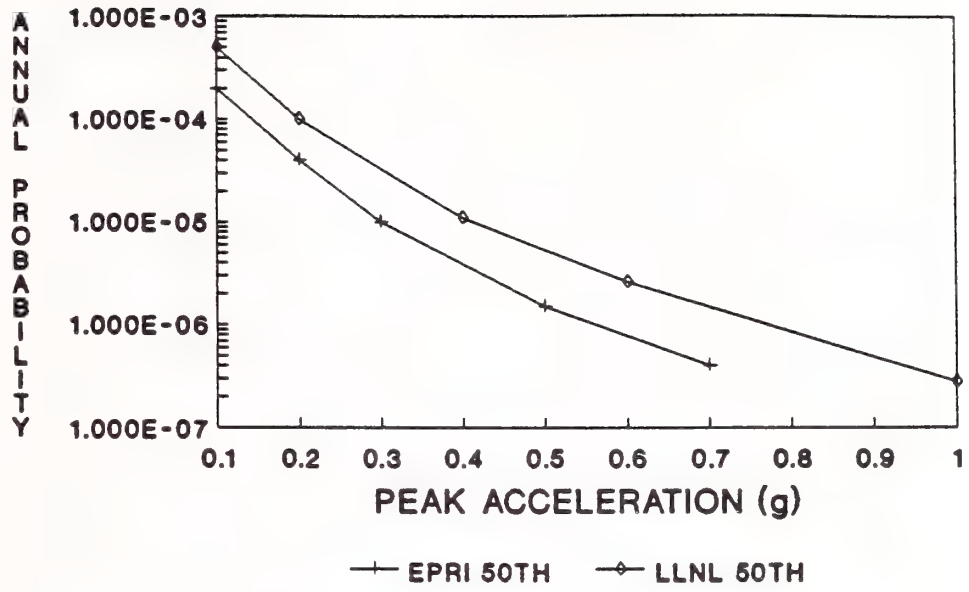

Figure 2a

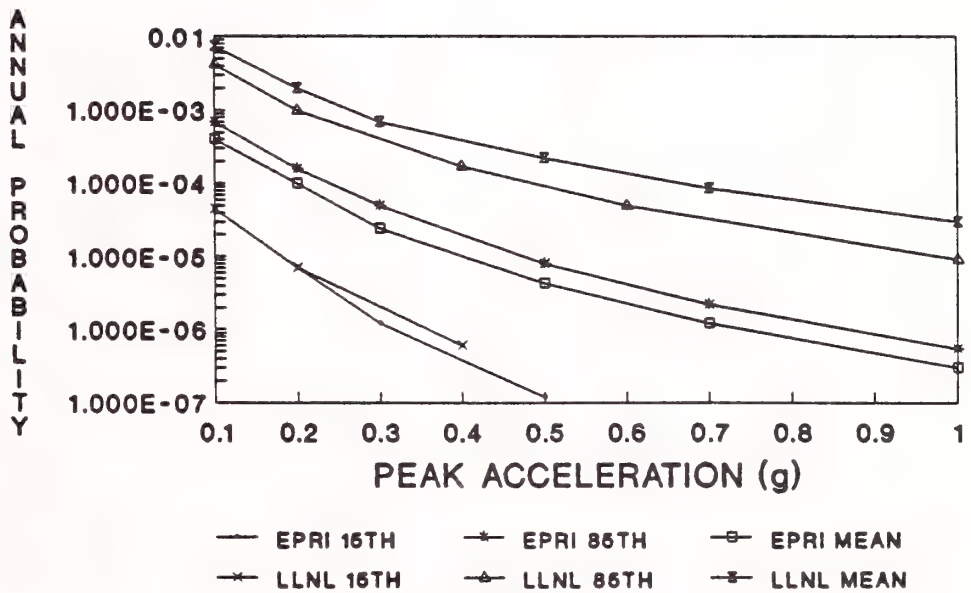

Figure 2b

Figure 2

Probabilistic seismic hazard curves for the DOE Savannah River, South Carolina, site. Figure 2a displays the LLNL and EPRI median seismic hazard curves; Figure 2b displays the LLNL and EPRI 15th percentile, 85th percentile and mean seismic hazard curves

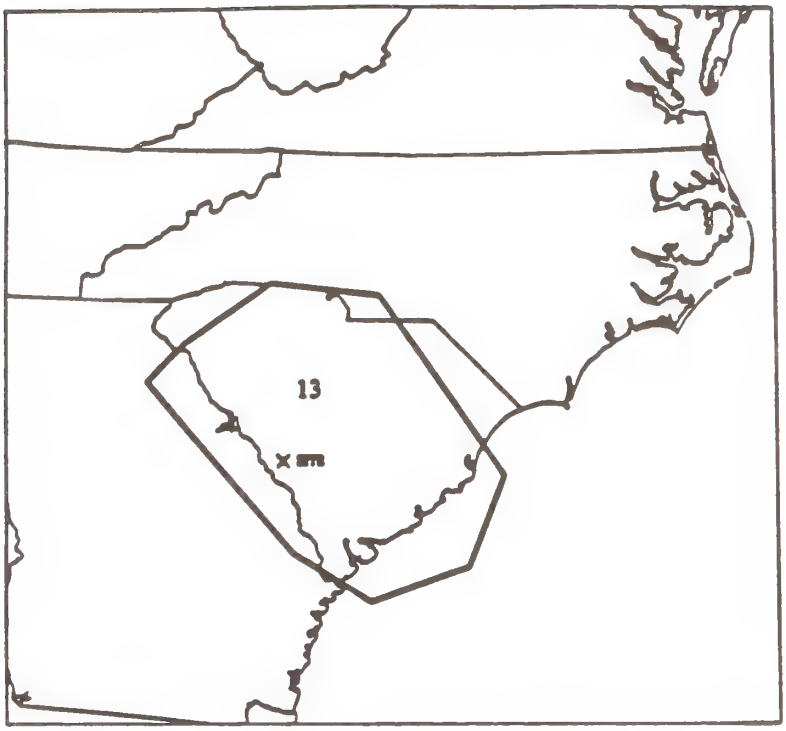

Figure 3a

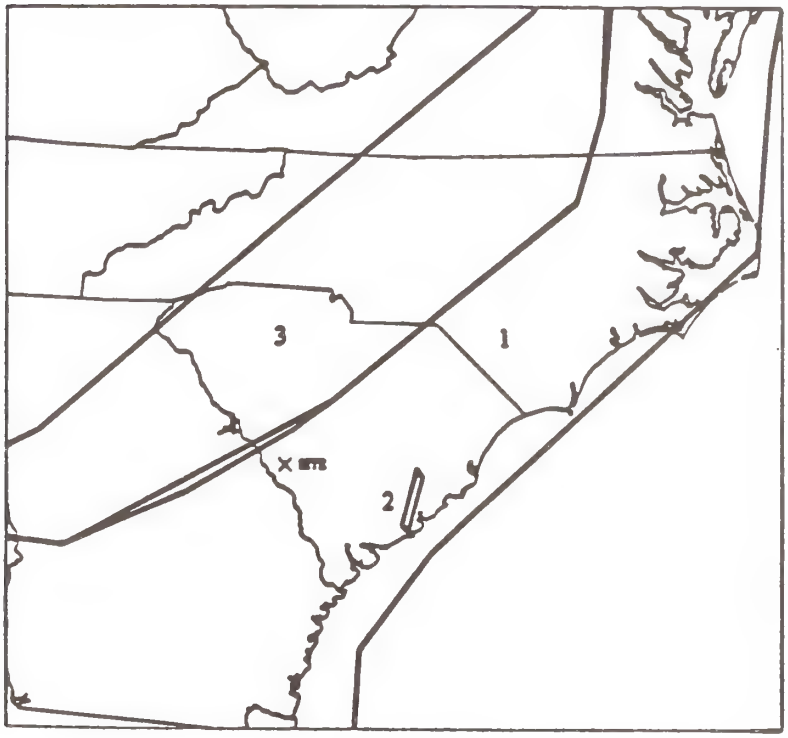

Figure 3b

Figure 3

Seismic source maps for the Southeastern United States from the LLNL study. Figure 3a shows a broad seismic source for the Charleston, seismic zone. Figure 3b shows a very localized seismic source for the Charleston, seismic zone.

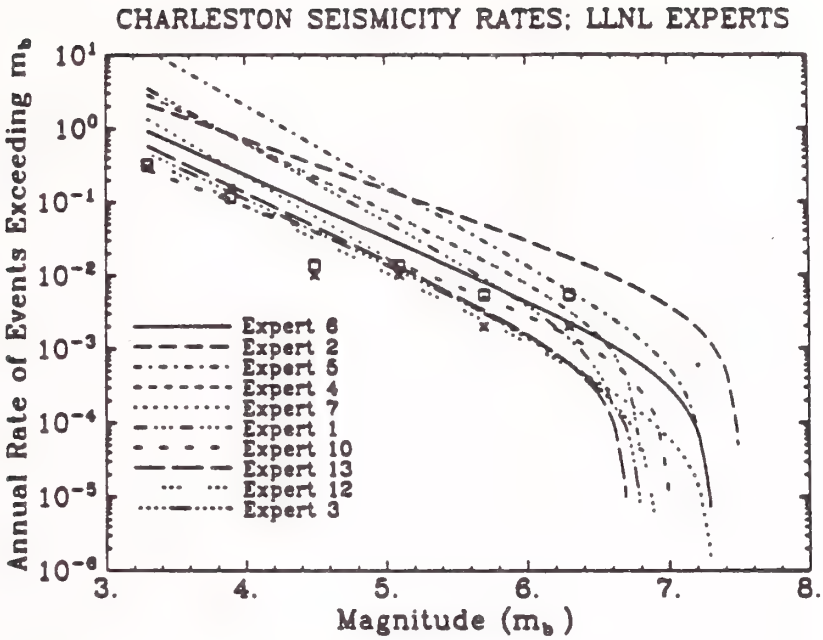

Figure 4a

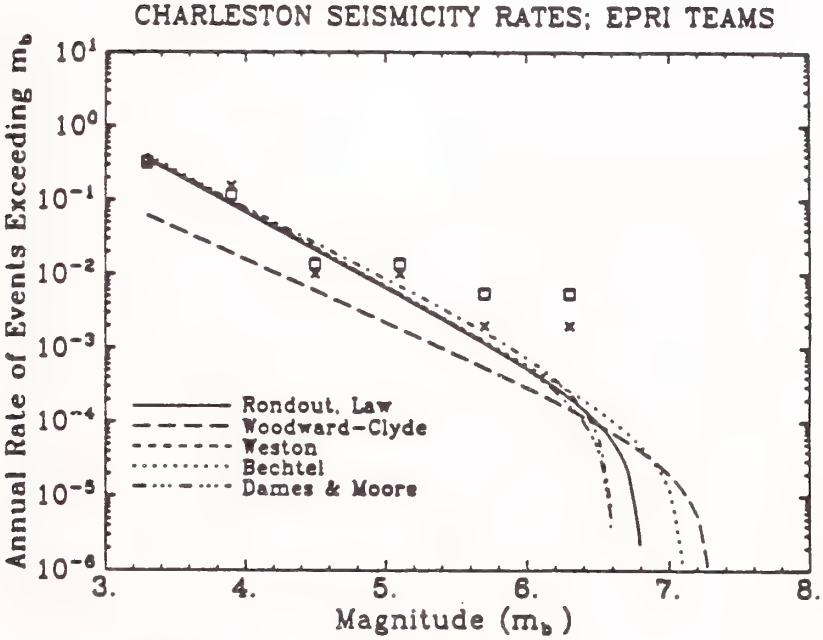

Figure 4b

Figure 4

Earthquake recurrence curves for the Charleston, South Carolina seismic source. Figure 4a displays the range of recurrence curves for the LLNL experts; Figure 4b displays the range of recurrence curves for the EPRI expert teams

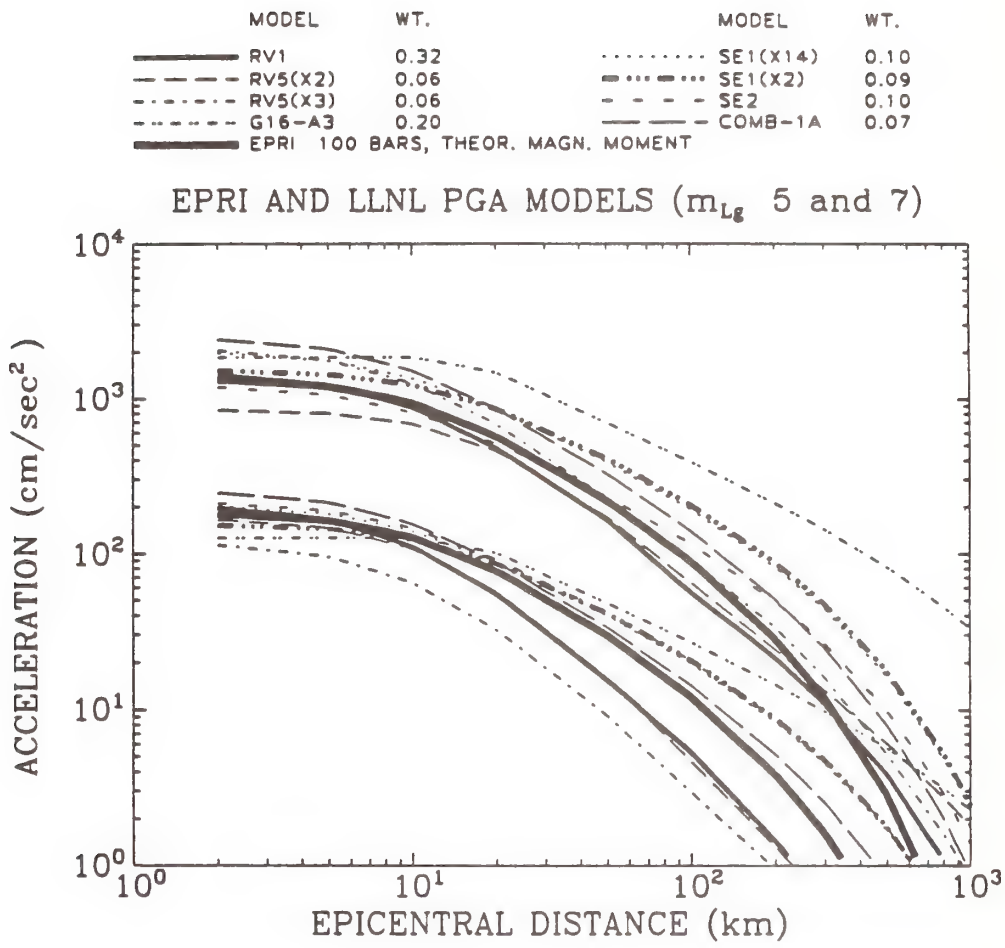

Figure 5

Attenuation relationships from the LLNL and EPRI studies for magnitudes 5 and 7. The figure shows the modeling uncertainty of the combined LLNL and EPRI models which are given weights based on the models selected by the individual experts

Earthquake Alert System Feasibility Study

by

Philip E. Harben*

ABSTRACT

An Earthquake Alert System (EAS) could give several seconds to several tens of seconds warning before the strong motion from a large earthquake arrives. Such a system would include a large network of sensors distributed within an earthquake-prone region. The sensors closest to the epicenter of a particular earthquake would transmit data at the speed of light to a central processing center, which would broadcast an area-wide alarm in advance of the spreading elastic wave energy from the earthquake. This is possible because seismic energy travels relatively slowly (3–6 km/s) when compared with the speed of light. Utilities, public and private institutions, businesses, and the general public could benefit from an EAS.

KEYWORDS: earthquake alert system; microseismic; real time; strong motion

1. INTRODUCTION

The concept of an EAS is not new. It was first proposed in an editorial by J. D. Cooper published in the *San Francisco Daily Evening Bulletin* on November 3, 1868. Although the basic concept for the system is simple, the implementation of a modern EAS requires the use of diverse and fairly sophisticated existing technology in addition to new research and development on a number of operational issues, such as reliability, accuracy, and survivability.

The Japanese have employed a seismic shutdown system for many of their railway lines since the early 1960s and have recently (1990) deployed a five-station Urgent Earthquake Detection and Alarm System (UrEDAS) as part of an earthquake disaster prevention program (Nakamura, 1989). A temporary EAS was deployed by the United States Geological Survey near the epicenter of the Loma Prieta earthquake to give warning to workers on the collapsed Cypress overpass structure in Oakland, California (Bakun, 1990).

The EAS concept discussed here consists of a distributed network of remote seismic stations that measure weak and strong earth motion and transmit the data in real time to a central facility. This facility processes the data and issues warning broadcasts in the form of information packets, containing estimates of earthquake location, zero time (the time the earthquake began), magnitude, and reliability of the predictions. Users of the warning broadcasts have a dedicated receiver that monitors the warning broadcast frequency. The user also has preprogrammed responses that are automatically executed when the warning information packets contain location and magnitude estimates above a facility's tolerance.

The alert signal broadcast is an area-wide transmission and is probably sent via FM radio or television subcarrier communications. Ensuring the survivability of the EAS is addressed with several strategies: hardening the remote stations for strong motion; using redundant widely separated central stations, communications, and warning broadcast transmitters; and noting that strong motion is emergent (i.e., it builds up over a period of several seconds), allowing some period of time in the early evolution of the earthquake, as accelerations build to damaging levels, during which a vulnerable system continues to function.

A low-cost prototype EAS could be developed in some areas by making use of existing dense networks of microseismic monitoring stations. These stations could be inexpensively

* Lawrence Livermore National Laboratory, Livermore, California 94550

upgraded to measure strong motion. When excess communications bandwidth is not available, a strong-motion upgrade could be inexpensively accomplished using the existing communication channel and a switching unit that passes the strong-motion signal during strong-motion conditions and passes the seismometer signal otherwise.

We designed a prototype switching unit and tested it at a surface station in the near-field of an underground nuclear explosion to simulate strong ground motion from an earthquake. This successful test demonstrated that the strong-motion record could be switched into the data stream within 30 ms and that the entire strong-motion record could be reliably switched into the real-time data stream.

About 50 stations distributed relatively uniformly along the major faults of the San Francisco Bay Area could form an effective EAS prototype network. Such a subset of stations could be selected from the U.S. Geological Survey (USGS) CALNET microseismic monitoring network. By upgrading these stations to measure strong motion and by installing a parallel real-time processor at the microseismic central processing facility, a low cost prototype EAS could be developed. The experience to be gained from an operational prototype is very important to help address issues such as false alarm rates, false alarm mechanisms, reliability, earthquake parameter estimation accuracy, and user alert-signal analysis.

In this report, we examine the feasibility of an EAS and attempt to outline some of the features, trade-offs, and technical considerations in implementing such a system. The focus of this report is on the features and design of a low-cost EAS prototype that, to the extent possible, makes use of existing seismic stations, communications, and broadcast facilities.

2. EAS USES

There are numerous potential users who would benefit from an EAS. Table 1 is a partial list of EAS applications; however, automated shutdown and activation are the most common functions. Depending on the application, these two functions vary dramatically in their consequences if action is taken as the result of a false alarm. An activation function such as opening a fire station door has minimal consequences if the door is opened due to an EAS false alarm. An automated shutdown of a nuclear power plant could disrupt the power grid of an entire city and result in expensive power-up procedures to reestablish full-power operation. An EAS false alarm shutdown cannot be tolerated for such an application. Although we will discuss user processing of the EAS alert signal in a later section, it is important to recognize that users of the alert signal have different applications and consequences of their actions. Therefore, the EAS must provide an optimal summary of the current "state of knowledge" for the earthquake parameters transmitted in the alert information so that diverse users can weigh the most recent "state of knowledge" against the consequences of action.

The real-time location and magnitude estimation that an EAS can produce would be very useful in the immediate aftermath of a large damaging earthquake. Emergency services such as fire, ambulance, and rescue could be deployed much more effectively if magnitude and epicenter estimates were immediately available. The communications media would also be much more effective in determining unfolding events related to an earthquake aftermath if estimates of epicenter and magnitude were available. Finally, the strong-motion records obtained from the EAS after a large earthquake would help in fundamental strong-ground-motion seismology investigations. Such investigations could help improve the fundamental understanding of site response and soil amplification during strong ground motion and, thereby, improve acceleration prediction, structural building codes, and structural damage assessment.

3. EAS OVERVIEW

The EAS discussed here was first advanced by Heaton (1985) and is shown in Fig. 1. Strong-motion and seismometer signals from a distributed network of remote seismic stations are transmitted in real time to the EAS processor at the central acquisition facility. The EAS processor estimates earthquake parameters such as location, origin time, magnitude, and the reliability of this information. If the earthquake magnitude estimate exceeds a given threshold, a warning signal is broadcast over an area-wide transmitter. This warning signal contains the earthquake parameter estimates. Each user of the warning signal has a dedicated receiver and processor with preprogrammed responses based on earthquake parameter values. The user's system continuously monitors the warning-signal frequency band. When a user receives a warning signal that has location and magnitude estimates in excess of the user's facility tolerances, the facility's emergency responses are automatically implemented.

3.1 Alert Information Packet

The signal transmitted by an EAS to alert an area must provide estimates of the earthquake's location and magnitude, and an estimate of the reliability of the information since many users of the warning signal would incur significant costs by taking any action based on the alert message. In general, an EAS should produce more reliable estimates of earthquake location and magnitude as the earthquake evolves and as more stations in the network transmit data that can be used in calculating the location and magnitude estimates. It is therefore important for alert information packets to be rapidly updated so that the new, more reliable estimates based on the most recent data can be transmitted to the users. The packet's update rate, however, is limited by the amount of information each packet contains, the communication method employed, and the central processor and alert algorithms used.

An initial alert signal can give the greatest lead time between the warning and the onset of strong motion. By applying a minimal warning algorithm at the central station, an alert signal can be issued shortly after only a few stations have detected strong motion from an earthquake. A very simple algorithm could be used that requires two EAS stations to measure ground accelerations above a predetermined threshold within a specified time window before the initial alert signal is issued.

After the initial alert signal is transmitted, the information transmitted in the subsequent alert packets should contain all of the salient parameters that form the input to any user's preprogrammed response algorithm. An example of a possible alert packet is shown in Fig. 2. This alert packet consists of the following information:

- Update time
- Zero-time estimate
- Location estimate
- Magnitude estimate
- Maximum acceleration
- Number of stations

Including the update time in the packet allows the user to identify the most recent information packet and to determine the time that has elapsed between the most recent information packet transmission and real time. The zero-time estimate refers to the time the earthquake began and is calculated by the earthquake-location algorithm. The location estimate gives the hypocenter coordinates for the earthquake. The magnitude estimate can be an estimate of body wave magnitude, maximum accelerations expected, earthquake moment, or a combination of these. The maximum acceleration gives the value of the maximum seen by any station (or an average of several of the stations reporting the highest accelerations) up to the time that the alert packet is transmitted. It provides the user with a direct measurement (as opposed to processed estimates), which can be compared to the magnitude estimate. Finally, only the

stations reporting strong ground motion above a given threshold are included in the number of stations. This provides the user with some indication of the reliability of the estimates. The more stations reporting strong motion (and therefore included in the estimates), the more likely that the event is a large earthquake.

3.2 Central Processor and Algorithms

The central EAS station acquires the incoming strong- and weak-motion network data for real-time analysis by the central processor. A detector algorithm can monitor the level of strong-motion signals as the data are buffered in memory. When a threshold level is exceeded, an algorithm to pick the time of *P*-wave arrival is repeatedly applied to all weak-motion data channels. When at least four stations have an established first arrival, a location algorithm is repeatedly applied to the first arrival times. As the earthquake evolves, more *P*-arrival times are available to be used in the location algorithm and, therefore, the estimates produced should be more accurate.

In parallel, magnitude and reliability estimates can be made for the data from the strong-motion channels. Several algorithms can be applied to magnitude estimation. Crude estimates can be made by using the maximum accelerations at the stations nearest the estimated earthquake location. The moment estimation method (Toksoz et. al., 1990) uses a relatively dense linear arrangement of sensors along faults to estimate the fault slippage and the length of the rupture in real time. By assuming a fault depth, the moment can then be estimated. The Japanese UrEDAS system estimates magnitude from the predominant period of the initial *P*-wave motion (Nakamura, 1989).

To the extent possible, all magnitude estimation algorithms should be applied to the data from the strong-motion channels to increase the reliability of the estimate. The arrangement of stations forming an EAS could preclude the use of the moment estimation method for earthquakes on some faults or fault segments because of a lack of instrument density.

3.3 User Processing

The extent and specifics of alert information analysis that a particular user may require before executing alert or shutdown functions depends on the user's application. Potential user applications, such as opening a fire station door, do not have a significant cost associated with a false alarm, so minimal or limited processing may be desirable to maximize lead time. However, the shutdown of a nuclear power plant using the alert signal would be high in cost. Consequently, maximum alert information analysis that trades off the time left to execute a safe shutdown against the probability that a shutdown is unnecessary may be desired.

In general, the user's preprogrammed response algorithm can contain a table of precalculated estimates of the ground accelerations expected at their site from earthquakes in a range of magnitudes and at a range of locations on the major faults in the area. When the earthquake location and magnitude estimates provided by the EAS alert packet indicate site accelerations greater than a given shutdown or alert threshold and when the alert packet reliability is sufficient, action is taken. The zero-time estimate of the earthquake can be folded into the user's decision process. A time-of-arrival estimate of strong motion is made by the user's algorithm based on the estimated earthquake location, estimated zero time, and the current time. When there is more lead-time than required for the user to perform alert actions, the user may elect to wait and receive additional alert packets to increase assurance that the estimates are stable and the reliability is high.

3.4 Alert Signal Transmission

A relatively new area-wide communication scheme that has low cost potential is FM radio and television subcarrier communication

(Communications Alternatives, 1991). The information is broadcast on a subcarrier frequency of the main transmission frequency and does not interfere with the main broadcast. Transmission coverage can be up to 100 miles in radius from the transmitter, depending on local terrain. The advantages of FM radio and television subcarrier communications are:

- Low start-up costs
- Wide area coverage
- Low user receiver costs
- Acceptable digital data transmission rate
- High reliability

The start-up equipment cost for a broadcaster to modulate and transmit on a subcarrier is between $5000 and $20,000, depending on existing equipment. The wide-area coverage of a single broadcast station should be reinforced by dual-redundant widely separated broadcast stations to improve area-wide reception owing to terrain limitations and to assure survivability of a transmitter during a large earthquake. User receivers should cost less than $100.

3.5 Survivability

Although a detailed analysis of EAS survivability is beyond the scope of this study, a few comments on this issue are in order. The survivability of an EAS will be driven by the weakest link in the individual components that make up the entire system (i.e., seismic stations, communications system, and the central station and warning transmitter). In general, individual free-field stations should survive during strong motion if proper care is taken in the station design and during station installation. A seismic station running directly on commercial ac power would be vulnerable to the power interruptions likely during a large earthquake. Powering the station by battery and charging the battery with ac power or solar panels assures independence from ac power interruptions. Proper bolting of sensors to a concrete pier, attachment of voltage-controlled oscillators and amplifiers to a rigid structure bolted to a pier, and secure mounting of batteries and charging units will help ensure proper operation during strong motion.

The survival of the EAS communications between the stations and the central processor is a potential weak link. If satellite communications were used, antenna dish alignment during strong ground motion would be a major concern. If dedicated telephone lines or radio telemetry were used, the gathering, repeaters, or central switching stations would be a concern. Direct line-of-sight radio telemetry without repeaters probably would be the least vulnerable, but it is only practical for stations within range and line-of-sight of the central station. However, it is worth noting that in the near-field of a large earthquake, strong ground motion is emergent (Shakal et. al., 1989). This means that there should be some period of time after the onset of ground motion from a large earthquake, as accelerations build to damaging levels, when a vulnerable communications system continues to function.

The survival of the central processing center/warning transmission station is also a potential weak link in an EAS. A large earthquake that occurs near the central processing center could damage or destroy the EAS before any alert warning is transmitted. Hardening all components of this EAS central processing facility may be difficult to accomplish. One possible strategy is to maintain two widely separated EAS centrals in a master-slave relationship. Using identical equipment and algorithms, the slave station issues the alert packets only when the master station fails to do so.

4. A LOW COST PROTOTYPE EAS

Although the conceptual design, technological features, and capabilities of an EAS are important, the cost is the factor that will determine if one is ever built. A California Division of Mines and Geology earthquake-warning feasibility study (Holden et al., 1989) estimates the cost of installing a dedicated 43-station EAS in southern California at $1.4 million for the remote stations, $1.9 million for the central processing facility, and $1.6 million for the annual operation and maintenance costs. Because the benefit of such a system is difficult

to quantify, the study concludes that an EAS cannot be economically justified.

A more recent study by the National Research Council (NRC, 1991) on real-time earthquake monitoring concludes that an EAS is technically feasible and recommends the installation of a prototype system. This recommendation is based, among other considerations, on forming a prototype EAS from existing microseismic monitoring stations to significantly reduce installation and operation costs.

We have examined the characteristics of existing microseismic monitoring networks and have made progress in detailing the modifications necessary to convert them into functioning EAS prototypes. We assumed that each station communicates analog data in real time to a central processing station. Two essential tasks that must be accomplished to create a prototype EAS from such a network are:

- Upgrade the remote seismic stations to measure strong motion.
- Install a real-time central processor and alert algorithms.

4.1 Remote Station Upgrade to Measure Strong Motion

Existing microseismic monitoring stations require adding a strong-motion-measurement instrument for each seismometer component. The strong-motion instruments are commercially available and are typically force-balanced accelerometers. A dramatic reduction in strong-motion instrument cost can be realized by making use of the new silicon microstructure accelerometers as strong-motion instruments. These instruments are now commercially available.

The individual seismic stations of a microseismic monitoring network typically consist of high gain vertical or three-component seismometers, amplifiers, voltage-controlled oscillators (VCOs), telephone or radio telemetry communications, and either ac power or battery power with solar panel charging.

When there is extra bandwidth on the microseismic station real-time communication channel, a strong-motion upgrade can be achieved by adding strong-motion sensors and VCOs: one for each component, and multiplexing these additional data channels on the existing communications channel. The EAS central processing facility would then receive two data streams for each station component: one containing weak-motion data from the seismometer and one containing strong-motion data from the strong-motion sensor. When spare communication bandwidth is not available, additional communication bandwidth can be added by either upgrading the existing link or by adding additional links. Unfortunately, upgrading or installing new communication links (radio or telephone) is expensive.

A low-cost solution to the strong-motion upgrade of microseismic stations that have no spare bandwidth on the existing communication channel is an instrument switch that, using only the existing communication channel, rapidly switches between seismometers and strong-motion sensors at the onset of strong motion. The EAS central processing facility would then receive only one data stream for each station component. The data stream would contain weak-motion data from the seismometer until the onset of strong motion at the station. After that time, the data stream would contain data from the strong-motion sensor. When strong motion at the station subsided, the weak-motion data from the seismometer would be passed to the data stream.

4.2 Prototype Instrument-Switching Unit

We designed a prototype instrument-switching unit and tested it. This switcher concept is shown in Fig. 3. The signals from the seismometer and from the strong-motion instrument are sent through to the instrument switcher. The strong-motion instrument signal is monitored by the switcher and, under normal weak-motion conditions, the seismometer signal is passed to the communications hardware.

When a user-determined threshold is exceeded by the strong-motion instrument (assumed to be set at a level well above the saturation amplitude of the seismometer signal), the strong-motion signal instead of the seismometer's signal is passed to the communication hardware. The switcher has a timer microchip that will perform the switching function for a fixed user-determined time period before switching back to passing the seismometer's signal. The timer chip will continue to extend the switch time by one user-set time period as long as the threshold continues to be exceeded. The unit switches back to the seismometer's signal when one complete user-defined time period has past since the last instant that the threshold was exceeded. It is worth noting that monitoring the strong-motion sensor to determine a switching condition rather than monitoring the seismometer is more reliable since the switching threshold is well within the linear regime of the strong-motion instrument. Furthermore, routine signals transmitted to the seismometers for calibration purposes cannot trigger the switch and are not affected by the prototype EAS.

We tested the prototype switcher in the near field of an underground nuclear test. A Marks Products Inc., model L-4 vertical component seismometer, a Kinemetrics FBA-11 vertical component strong-motion accelerometer, and the switcher output signal were all digitally recorded at 200 samples/s at unity gain. This prototype was set to switch-over at a threshold of 0.01 *g* and the switchover time period was set at 10 s. The results are shown in Fig. 4. The strong-motion recording is shown in the top trace in units of *g*. The middle trace is the L-4 seismometer recording in units of m/s. Note that the L-4 seismometer was physically clipping during the first 8 s or so of strong ground motion. The bottom trace is the switcher output. Since the switcher output is a mix of velocity and acceleration records, the scale was left in raw output voltage units. Clearly, the switcher output is capturing the full strong-motion record before switching back to the seismometer. The initial large negative pulse at about 15 s is actually the L-4 seismometer output. The relative scales of the two instruments is a function of the raw output voltage of the individual instruments. The relative amplitude scales could easily be modified by adding an amplification or attenuation stage to one of the instruments before input to the switcher. Finally, the dc offset evident on the strong-motion part of the switcher record was introduced from an unbalanced voltage supply that was driving the switcher. A dc voltage regulator has since been added to the switcher to eliminate this problem.

Figure 5 zooms in on the switchover time period. All traces and units are as described above. The initial L-4 seismometer signal spike is now evident on the switcher trace. Switchover occurs at about 15.1 s. The strong-motion signal contains a small transient associated with the switching relay but stabilizes quickly. The time between switchover and a stable strong-motion signal is about 30 ms. The switching is fast enough to capture the first peak of the strong ground motion from the nuclear test (Fig. 5). It should be noted that a nuclear test is a worst case test of the switcher performance because the most significant strong motion occurs in the first few cycles of the record. Strong motion from large earthquakes is generally emergent, building to peak levels over many seconds.

4.3 Central Processing Facility Modification

Most existing microseismic monitoring networks telemeter data from remote stations to the central processing facility in real time. The USGS CALNET microseismic network, for example, transmits seismic data in analog form, using radio telemetry or dedicated telephone lines, to a central processing facility. This facility digitizes the incoming data and runs an event detector on the data streams to determine if a small earthquake has occurred. In general, the data are not continuously archived; data are archived when an event is declared by the detector. Although the data are communicated to the central processing facility in real time, the central processor and detector do not run in real time. The data are

buffered in memory so that event processing and data archival can be accomplished after the event has occurred.

Assuming that the remote stations are modified to telemeter strong-motion information, either on new data channels if sufficient spare bandwidth is available, or using the instrument switcher discussed earlier, the EAS requires a real-time processor that performs real-time earthquake parameter estimation on the EAS data channels. An EAS central processing facility that is operated in parallel with the microseismic-network central-processing facility would provide the needed real-time analysis capability without impacting the routine operation of the microseismic network. Figure 6 illustrates this concept. The EAS central processing facility would be collocated with the microseismic central facility. The EAS facility consists of a dedicated real-time central processing unit, digitizers, alert algorithms, and warning communication hardware. The incoming data from the EAS stations, a subnet of the full microseismic network, would be branched off the microseismic central input for digitization and real-time analysis by the central processing facility. The microseismic central processor could also receive the data channels used by the EAS and perform routine event analysis and archiving of those channels. This would eliminate the need for archival capability from the EAS central processing facility. Archived strong-motion events could be "replayed" through the EAS system to test new algorithms or system enhancements.

4.4 A Prototype EAS in the San Francisco Bay Area

The San Francisco Bay Area is an example of a region that has an existing USGS CALNET microseismic network that may be suitable, with modifications, to also function as an EAS. One critical element is the arrangement of sensors; some of them must be located near any expected major earthquake epicenters in the area. Assuming that earthquakes occur with a uniform random distribution of epicenters only on known major faults and neglecting hypocentral depths, Heaton (1989) showed that, for a uniform distribution of n sensors along faults of total length L, the mean travel time for P-waves from the earthquake epicenters on the faults to the closest station is

$$\bar{T} = \frac{L}{4nv},$$

where v is the P-wave velocity. By assuming a fixed hypocentral depth of h for all major earthquakes and, if we also assume that a minimal warning algorithm that issues an initial alert signal would require strong ground motion at two or more stations, then the average time before P-wave arrival at the nearest two stations is

$$\bar{T} = \frac{\sqrt{\left(\frac{3L}{4n}\right)^2 + h^2}}{v}$$

Since the San Francisco Bay Area is known to have three major active faults: the San Andreas, Hayward, and the Calaveras Faults. We can apply Eq. (3) by assuming that the total length of these faults (with instrumentation) is 800 km. Assuming a P-wave velocity of 6 km/s and a hypocentral depth of 10 km (Scheimer, 1985), the mean travel time to the nearest two stations can be calculated as a function of the number of seismic stations along the total length for the three faults. Figure 7 shows the results. There is little improvement in using over 50 stations. The mean P-wave travel time using 50 stations is ~3 s. If we assume that 5 s are required to account for the small delays introduced by radio telemetry or phone line transmission and by the time it takes the alert algorithms to issue a warning and that the P-wave speed is 1.67 times the S-wave speed (Scheimer et. al., 1982), then the damaging S-wave will only have reached an area of 8 km in radius from the earthquake epicenter before the initial alert warning is received by the entire area.

It is worth noting that an EAS is most effective (i.e., gives the longest overall warning times and requires the minimum number of seismic

stations) on shallow faults, which are the sources of most of the major earthquakes in California. Known faults allow the use of a linear distribution of sensors instead of an areal distribution, effectively reducing the number of stations required for the same warning times by about a factor of 10. Shallow focus earthquakes provide the seismic ray path geometry for maximum warning to an area. Japan, for example, has major earthquakes that occur on a myriad of faults without surface expression and at relatively deep focus (Nakamura et. al., 1988), making an EAS much more difficult to implement and of less value because of the very short warning times that could be expected.

The USGS CALNET stations in the Bay Area are shown, along with the major fault traces, in Fig. 8. Clearly, a subset of 50 stations that are located on or near the major faults with an approximately uniform spacing can be selected. A large fraction of the USGS stations consist of a single vertical component seismometer. Some of these stations have fully utilized communication channels and cannot carry additional data on existing communication lines. Such stations could be upgraded to strong motion by adding the switching device described earlier and a single vertical-component strong-motion instrument. When communications are limited to a one component instrument, the vertical component is probably the best axis on which to add a strong-motion instrument since peak accelerations in the near field are generally larger on the vertical component in the early evolution of an earthquake (Shakal et. al., 1987, 1989).

5. CONCLUSIONS

An EAS would provide warning to a diverse community of users, who have applications that range from simply opening a fire station door to shutting down large manufacturing or power-production facilities. Because of the vastly different costs associated with false alarms depending on the application, an EAS must furnish a rapidly updated information packet with estimates of the earthquake's location and magnitude, and an estimate of the reliability of this information so that users can evaluate the data and make independent decisions, depending on their specific needs.

The technology currently exists to develop such an EAS; however, a dedicated system built to all the desired specifications (e.g., number of stations, locations, communications, and hardening) would be very expensive. Furthermore, some operational experience with an EAS is required to define how an optimum system should be constructed. Issues such as false alarm rate, false alarm mechanisms, reliability, earthquake parameter estimation accuracy, and user analysis of the alert information cannot be effectively addressed without the aid of information from an operational EAS. It is therefore very important to establish some prototype systems to serve as test beds for future development.

In some areas, an EAS prototype system can be developed at low cost by upgrading existing dense networks of microseismic monitoring stations so that these stations can also measure strong ground motion; once modified, they could form the nucleus of the EAS network. Strong-motion upgrades can be accomplished without installing any new or expanded communication links. For instance, strong-motion instruments can be added to existing communication links (when unused bandwidth is available) or the instrument switching device that we developed and tested can be added (when spare bandwidth is unavailable). Furthermore, EAS station maintenance can be accomplished during normally scheduled microseismic maintenance visits.

6. ACKNOWLEDGMENTS

First and foremost I wish to thank Bob Murray, Tom Nelson, and Mark Eli for their strong support, encouragement, and helpful criticism. I also thank Jim Hill for supporting the overall effort. I am indebted to Pete Rodgers and Dan Ewert for the design, development, and fielding of the seismic switcher prototype. Special

thanks to Elaine Price for editing this manuscript. Finally, I thank Paul Kasameyer for first introducing me to this topic.

This work was performed under the auspices of the U.S. Department of Energy by Lawrence Livermore National Laboratory under contract No. W-7405-Eng-48.

7. REFERENCES

Bakun, B. (1990), *Early Warning Alert System*, U.S. Geological Survey, Menlo Park, Public Affairs Memo.

Communications Alternatives (1991), Datapro Reports (McGraw-Hill, New York), vol. 2.

Heaton, T. H. (1985), "A Model for a Seismic Computerized Alert Network," *Science* **228**, 987–990.

Holden, R., R. Lee, and M. Reichle (1989), *Technical and Economic Feasibility of an Earthquake Warning System in California*, California Division of Mines and Geology, Special Publ. 101.

Nakamura, Y., and B. E. Tucker (1988), "Japan's Earthquake Warning System: Should it Be Imported To California?" *California Geology*, pp. 33–40

Nakamura, Y. (1989), "Earthquake Alarm System for Japan Railways," *Japanese Railway Engineering* **28**(4), 3–7.

National Research Council of the National Academy of Science (1991), *Real-Time Earthquake Monitoring*, Report from the Committee on Seismology (National Academy Press. Washington, DC).

Scheimer, J., S. R. Taylor, and M. Sharp (1982), *Seismicity of the Livermore Valley Region, 1969–1981*, Lawrence Livermore National Laboratory, Livermore, CA, UCRL-86969.

Scheimer, J. (1985), *Depth Determinations of Seismicity in the East San Francisco Bay Region*, Lawrence Livermore National Laboratory, Livermore, CA, UCID-20522.

Shakal, A. F., M. J. Huang, C. E. Ventura, D. L. Parke, T. Q. Cao, R. W. Sherburne, and R. Blazques (1987), *CSMIP Strong-Motion Records from the Whittier, California Earthquake of 1 October 1987*, California Division of Mines and Geology, OSMS 87-05.

Shakal, A., M. Huang, M. Reichle, C. Ventura, T. Cao, R. Sherburne, M. Savage, R. Darragh, and C. Petersen (1989), *CSMIP Strong-Motion Records From the Santa Cruz Mountains (Loma Prieta), California Earthquake of 17 October 1989*, California Division of Mines and Geology, OSMS 89-06.

Toksoz, M. N., A. M. Dainty, and J. T. Bullitt (1990), "A Prototype Earthquake Warning System for Strike-Slip Earthquakes," *Pure and Applied Geophysics* **133**(3), 475–487.

Table 1. A partial list of potential EAS applications.

Shutdown computers	Reroute electrical power
Shutdown disk drives	Shutdown high precision facilities
Shutdown airport operations	Shutdown manufacturing facilities
Stop trains	Shutdown high energy facilities
Shutdown gas distribution	Alert hospital operating rooms
Open fire station doors	Start emergency generators
Stop elevators in a safe position	Shutoff oil pipelines
Issue audio alarms	Shutdown refineries
Shutdown nuclear power plants	Shutoff water pipelines
Maintain safe-state in nuclear facilities	

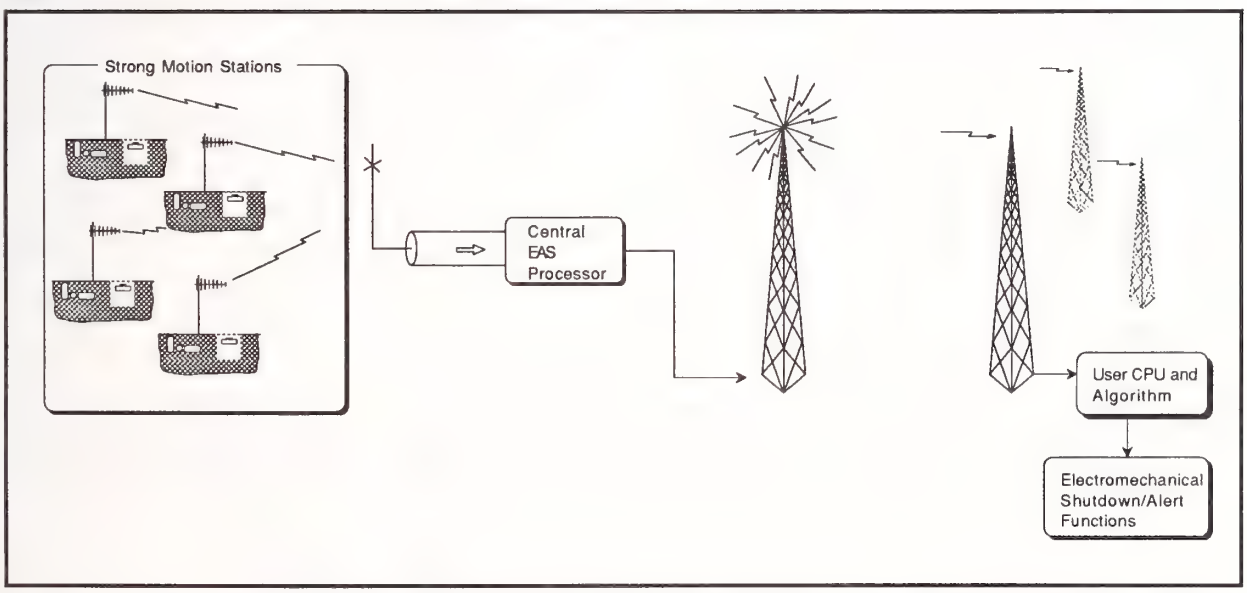

Figure 1. The EAS consists of an area-wide strong-motion network that telemeters real-time data to a central processor. The processor estimates earthquake parameters and issues an alert packet containing these estimated parameters. The user facilities receive the warning packet and execute alert or shutdown functions based on their specific preprogrammed response.

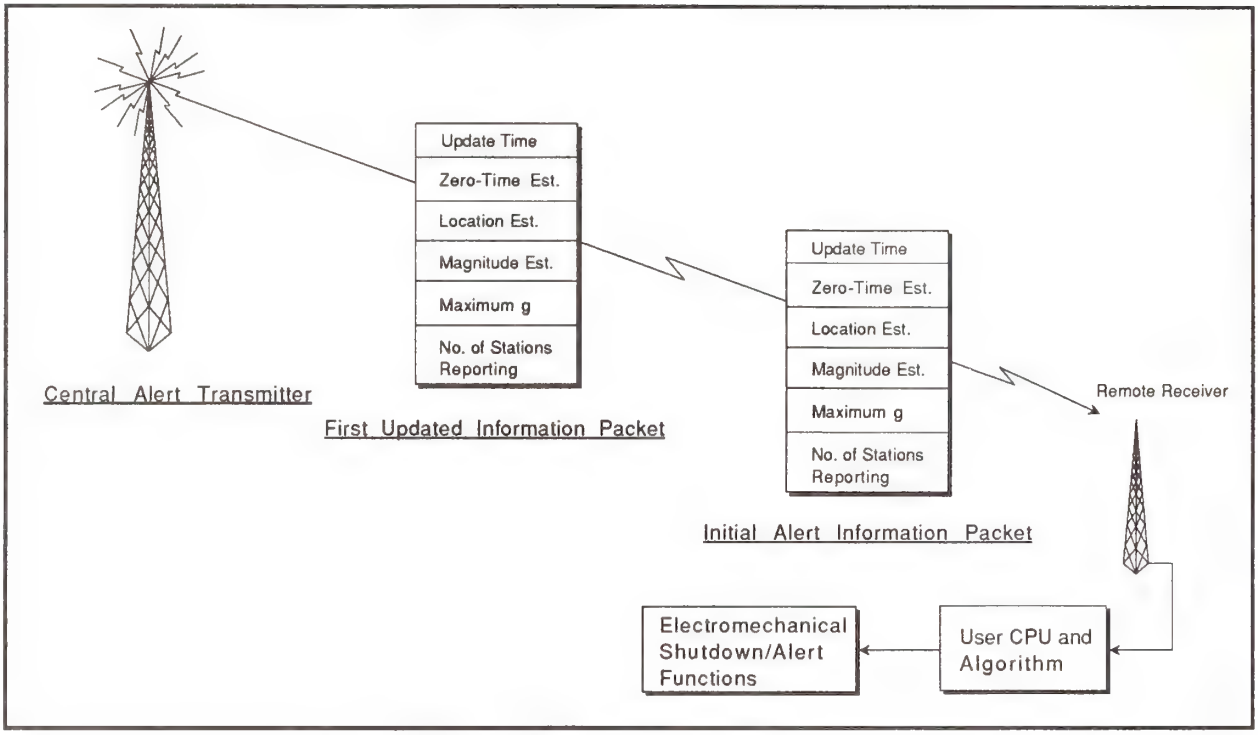

Figure 2. The alert information packet is broadcast and is rapidly updated for user analysis and possible shutdown and alert functions.

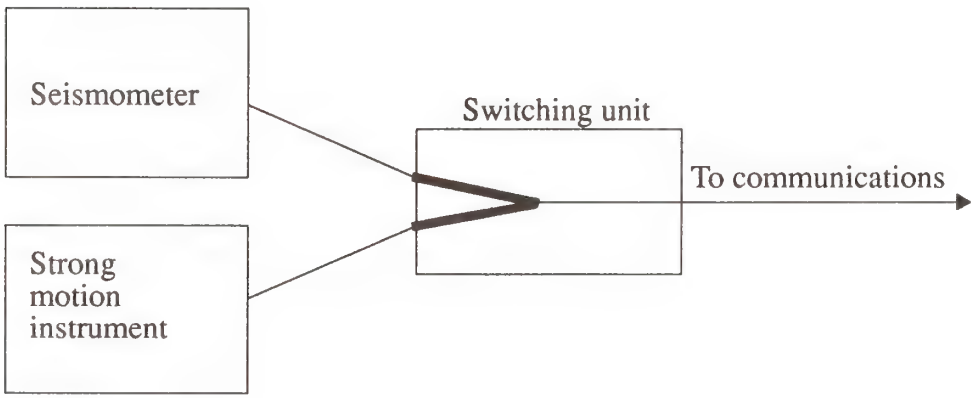

Figure 3. The switching unit receives input data from the strong-motion instrument and the seismometer. The seismometer signal is passed to the station communications under normal seismic conditions. During strong ground motion, the strong-motion instrument data, rather than the seismometer signals, are passed to the station communications.

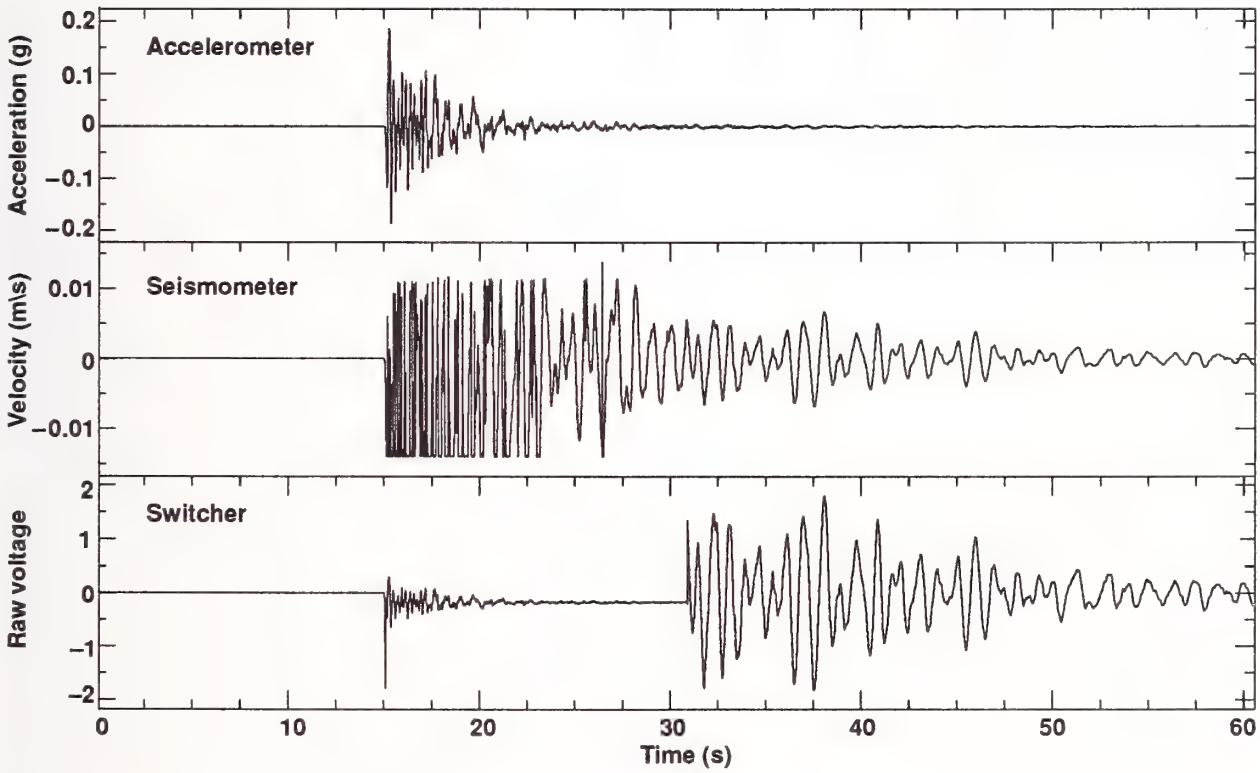

Figure 4. The surface recordings in the near field of an underground nuclear test. The top trace is the strong-motion accelerometer, the middle trace is the seismometer, and the bottom trace is the switcher output.

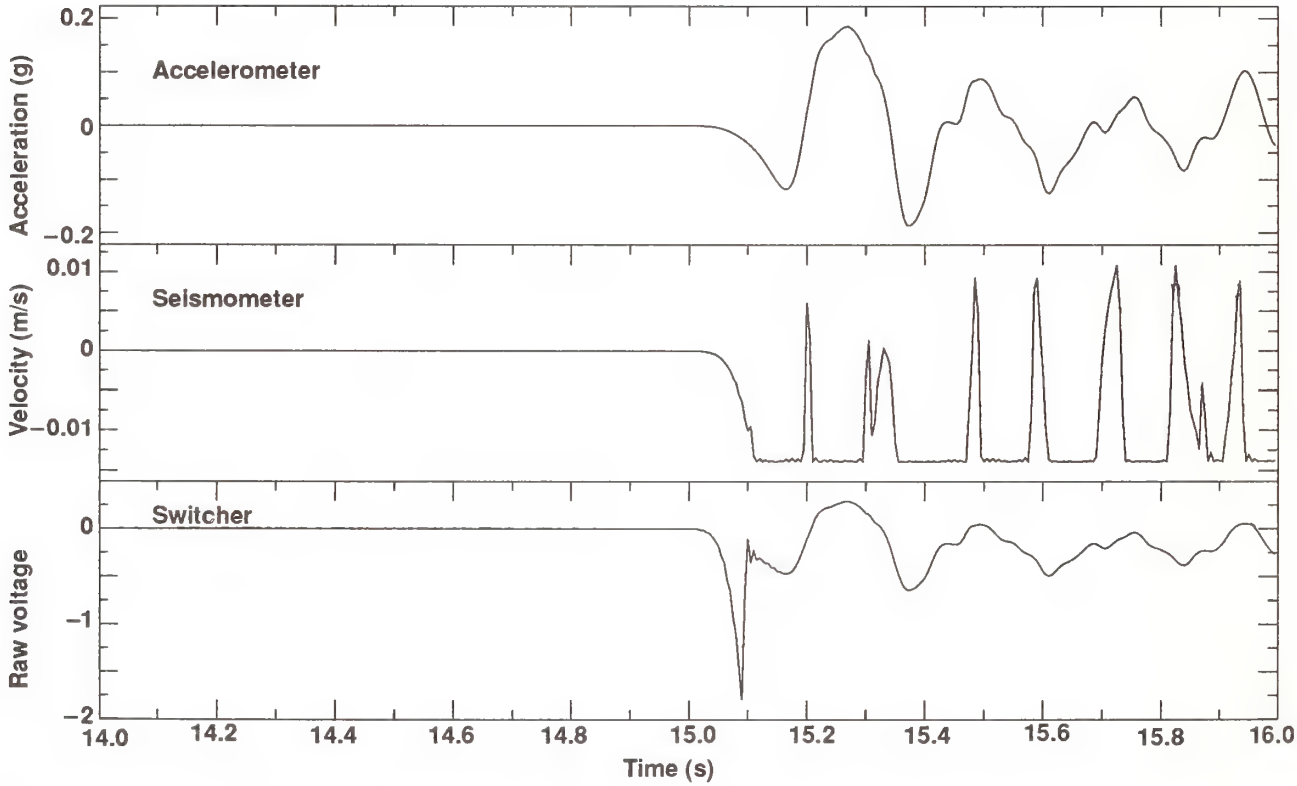

Figure 5. A zoom-in on Fig. 4 at switchover. The switchover time takes place at ~15.1 s, and the stabilization time is ~30 ms. The first major peak of the strong-motion signal is captured in the switched signal.

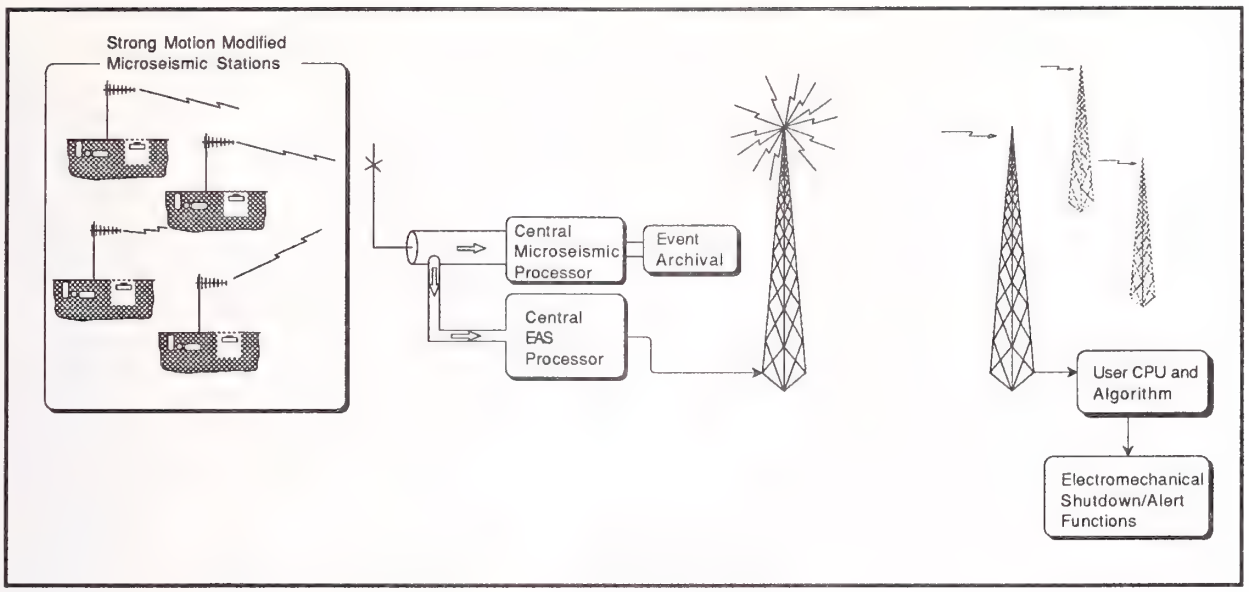

Figure 6. The subnet of a microseismic network that has been modified for strong motion is event-processed by the microseismic processor as usual and is streamed through the EAS central processor for real-time estimation of earthquake parameters and warning broadcasts.

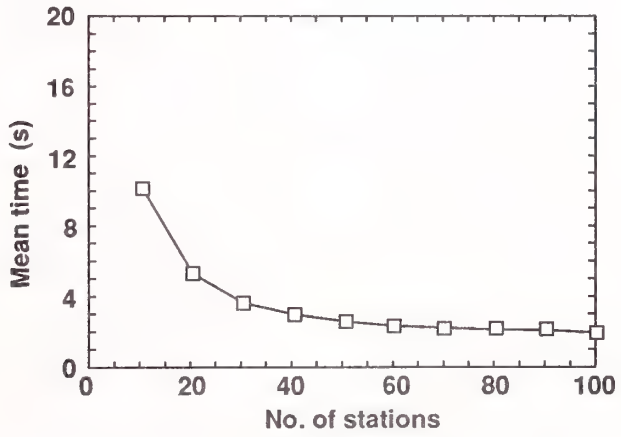

Figure 7. Plot showing the mean *P*-wave travel time to the nearest two stations of a uniformly distributed network of stations along the major faults in the San Francisco Bay Area as a function of the number of stations.

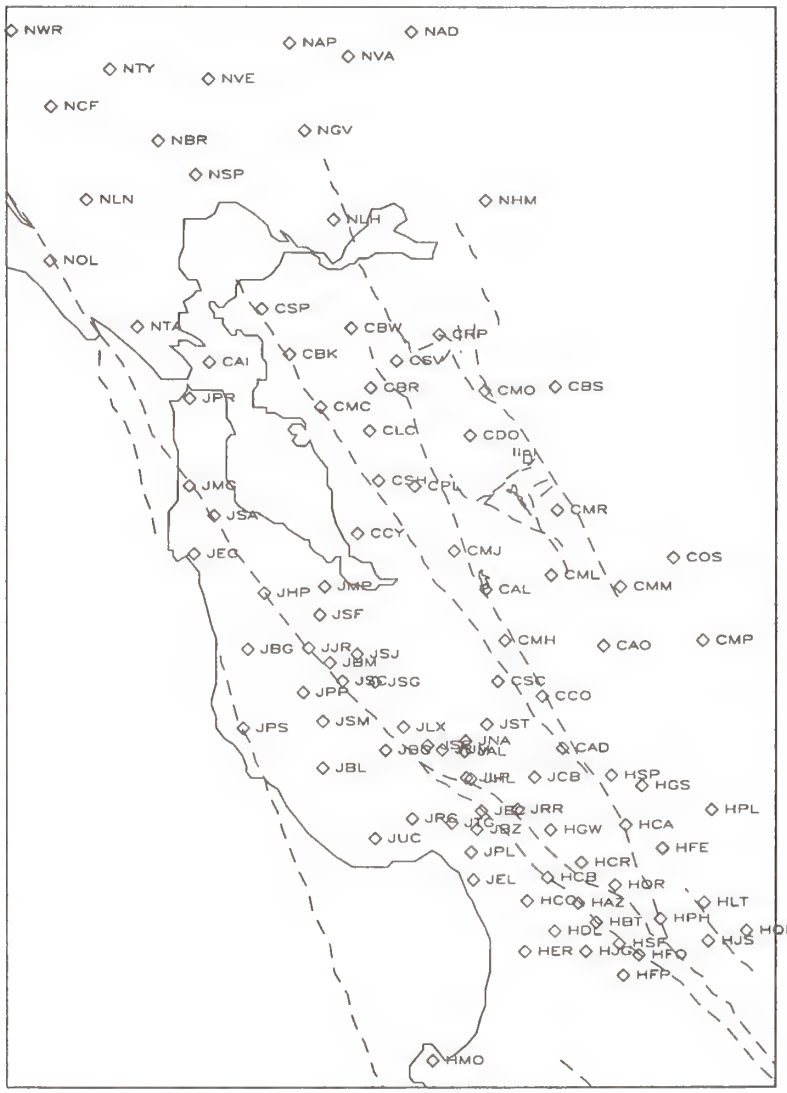

Figure 8. Map showing the location and identifiers of the USGS microseismic network in the San Francisco Bay Area. Major fault traces are also shown.

Guidelines for Seismic Design Methods of Large Underground Structures

by

Hajime Asakura[1], Kazuhiko Kawashima[2], and Hideki Sugita[3]

ABSTRACT

Outline of the Guidelines for Seismic Design Methods of Large Underground Structures is presented. This is one of the final accomplishments of the 5-year Ministrial Research Project on Development of Utilization of Underground Space which was made between 1987 and 1992. Description is given to seismic design methods proposed for the Lateral Long Underground Structures, Laterally Wide Underground Structures and Vertically Long Underground Structures.

KEY WORDS

Underground Structure, Seismic Design, Seismic Deformation Method, Shield Tunnel, Disaster Prevention Systems

1 INTRODUCTION

Utilization of underground space is becoming significant importance in urban area in Japan because of various restrictions for getting open space for new construction. The Ministry of Construction initiated a 5-year Research Project on "Development of Utilization Technic of Underground Space" in 1987. The Public Works Research Institute, Building Research Institute and Geographical Survey Institute worked together in the Research Projects. One of the main research targets of the Project was to develop rational seismic design methods of large underground structures embedded in soft ground.

For executing the Research Projects, joint researches were made between the Public Works Research Institute and Advanced Construction Technology Center. As one of such joint researches, the Joint Research on Development of Seismic Design Method of Underground Structures was conducted between the Earthquake Engineering Division of the Public Works Research Institute, Advanced Construction Technology Center and 8 private firms (Fujita, Kajima, Taisei, Tobishima, Hazama, Okumura, kounoike and simizu).

Including the research results obtained through the joint research[1] with Advanced Construction Technology Center, the final accomplishments of the 5-year Research Project was complied in March 1992. The results of investigations on the seismic design methods of underground structures were complied in the form of "Guidelines for Seismic Design Methods of Underground Structures"[2]. Because the seismic design methods for the underground structures with small diameter such as the petroleum pipes[3] and water pipes[4], and common utility ducts[5] were already in use, the Guidelines show the seismic design methods for larger underground structures than those facilities.

This paper outlines the Guidelines.

2 SCOPES AND CONTENTS OF THE GUIDELINES

The Guidelines present the seismic design methods for large underground structures constructed in soft ground in city area. As shown in Fig. 1, underground structures may be classified, based on their structural response characteristics, into three groups as

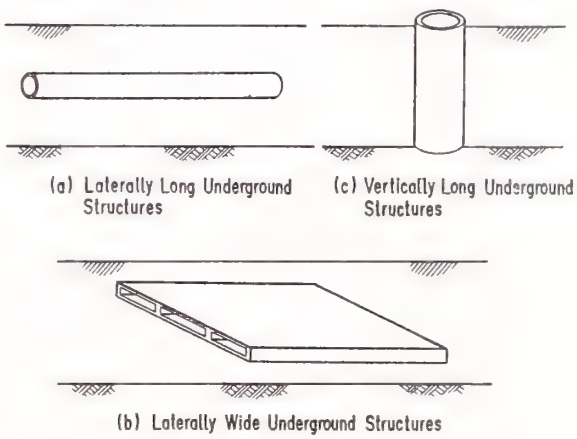

Fig.1 Classification of Underground Structures

1) Laterally Long Underground Structures

Long underground structures embedded laterally along ground surface. Seismic force along their axes is the major effect of an earthquake for such structures.

2) Laterally Wide Underground Structures

Widely spread underground structures along

---

1)Directer, 1st Research Department, Advanced Construction Technology Center
2)Head, Earthquake Engineering Division, Public Works Research Institute
3)Research Engineer, ditto

the ground surface. Shear stress along the surface of structures associated with shear deformation of ground due to an earthquake is the major seismic effect.

3) Vertically Long Underground Structures

Long underground structure in vertical direction. Shear stress along the surface of structures associated with shear deformation of ground due to an earthquake is the major seismic effect.

The seismic safety required for design depends on the type,utilization and importance of the structures. Therefore, seismic design methods which are required for underground structures are presented for the three types in general sense in the Guidelines.
Underground highways, underground parking space and common utility ducts were imaged for developing the Guidelines.

It should be noted that although the description is given in the format of the specifications, it is not the mandate specifications. It merely describes the research results.

The table of contents of the Guidelines is as follows:

1 General
- 1.1 Scopes
- 1.2 Definition of Terms

2 Basic Principle of Seismic Design

3 Loads and Loads Combination for Seismic Design
- 3.1 Loads and Loads Combination
- 3.2 Seismic Effects
- 3.3 Inertia Force
- 3.4 Design Ground Displacement
- 3.5 Dynamic Earth Pressure
- 3.6 Design Shear Stress around Surface
- 3.7 Classification of Soil Condition
- 3.8 Input Ground Motion for Dynamic Response Analysis
- 3.9 Soil Spring Stiffness

4 Seismic Design Method of Shield Tunnels
- 4.1 General
- 4.2 Seismic Design Method in Axial Direction
  - 4.2.1 Basic Principle of Seismic Design
  - 4.2.2 Seismic Design by Seismic Deformation Method
  - 4.2.3 Equivalent Stiffness of Shield Tunnel without Second Lining
  - 4.2.4 Equivalent Stiffness of Shield Tunnel with Second Lining
  - 4.2.5 Evaluation of Seismic Safety
  - 4.2.6 Dynamic Response Analysis
  - 4.2.7 Minimum Reinforcement of Second Lining in Axial Direction
- 4.3 Seismic Design Method in Transverse Direction
  - 4.3.1 Basic Principle of Seismic Design
  - 4.3.2 Seismic Design by Seismic Deformation Method
  - 4.3.3 Dynamic Response Analysis
  - 4.3.4 Evaluation of Seismic Safety

5 Seismic Design Method of Laterally Wide Underground Structures
- 5.1 General
- 5.2 Seismic Design by Seismic Deformation Method
- 5.3Dynamic Response Analysis

6 Seismic Design of Vertically Long Underground Structures
- 6.1 Basic Principle of Seismic Design
- 6.2 Seismic Design by Seismic Deformation Method
- 6.3 Dynamic Response Analysis
- 6.4 Evaluation of Seismic Safety

7 Structures Expecting Reduction of Seismic Effects
- 7.1 General
- 7.2 Flexible Joints
- 7.3 Structures Reducing Stiffness of Ring Joint of Shield Tunnel
- 7.4 Isolation of Underground Structures from Surround Subsoils

8 Earthquake Disaster Prevention Systems for Underground Highways
- 8.1 General
- 8.2 Fear and Anxiety of Drivers against an Earthquake
- 8.3 Factors Causing Fear and Anxiety to Drivers at Underground Highways
- 8.4 Basic Countermeasure against Earthquake Disaster

3 BASIC PRINCIPLE OF SEISMIC DESIGN

Seismic design of underground structures is recommended to be made by the Seismic Deformation Method[6]. In the Seismic Deformation Method, the displacement and deformation developed in the subsurface ground during an earthquake are taken as the major seismic effects to underground structures. The seismic response of underground structures is distinguished by the small mass effect and the large damping ratio from regular structures on ground, i.e.,

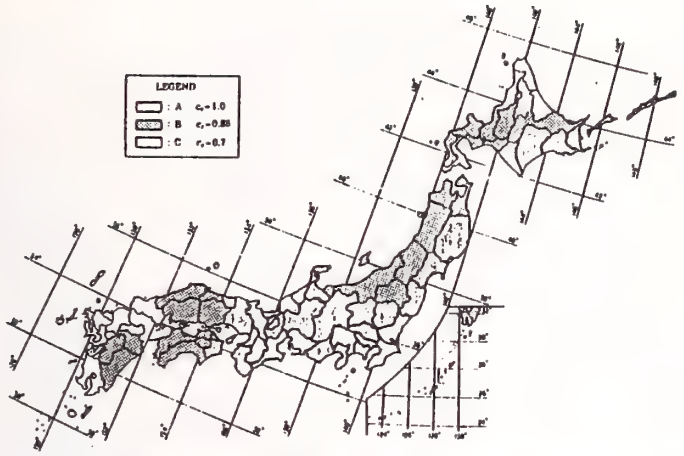

Fig.2 Seismic Zoning Map and Modification Coefficient c_z

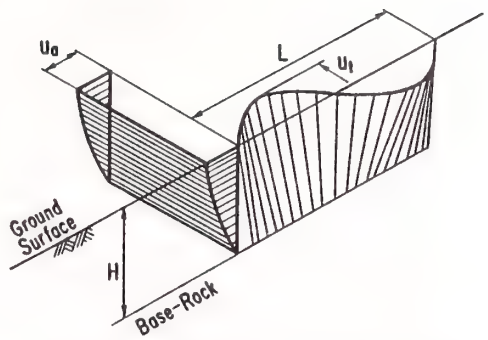

Fig.3 Deformation of Subsurface Ground Assumed in Seismic Deformation Method

a) mass effect is small because unit weight of underground structures is in most cases smaller that that of subsurface ground, and

b) damping is very large because radiational damping due to energy dissipation from underground structures to subsoils is very large.

Therefore, it is assumed in the Seismic Deformation method that during an earthquake underground structures deform following the deformation of subsurface ground. Modelling of underground structures has to be made so that structural response of the underground structures be correctly represented. Because the increase of stress and deformation of underground structures due to seismic effects are evaluated by the Seismic Deformation Method, the stress and deformation actually developed during an earthquake have to be computed by adding them with those developed due to the static loads such as the dead weight.

Evaluation of seismic safety of underground structures can be made by either the Allowable Stress Design Method or the Bearing Capacity Design Method. In the Allowable Stress Design Method the stress and the displacement developed in structual components are required to be less than the allowable stress and allowable displacement. In the Bearing Capacity Design Method the sectional forces developed in structural components are required smaller that those of dynamic bearing capacity of structural systems considering ductility. Displacement of structures are also required to be smaller than the critical displacement.

Table 1 Classification of Ground Condition

GROUND CONDITION	DEFINITION	APPROXIMATE ESTIMATION
GROUP I	$T_G < 0.2$SEC	TERTIARY OR OLDER
GROUP II	$0.2 \leq T_G < 0.6$SEC	ALLUVIUM AND DILUVIUM
GROUP III	0.6SEC$\leq T_G$	SOFT ALLUVIUM

After the design by means of the Seismic Deformation Analysis, dynamic response analysis is recommended for the underground structures with complex structural response.

4 LOADS CONSIDERED FOR SEISMIC DESIGN

In seismic design of underground structures, the dead weight, the earth pressure, the water pressure, the uplift force, the ground settlement and the seismic effects are to be considered. The loads have to be combined so that the most critical stress or displacement be developed. As the seismic effects, the following loads have to be considered:

(1) Inertia Force

The lateral force coefficient has to be evaluated as

$$k_h = c_z \cdot c_G \cdot c_U \cdot k_{h0} \quad (1)$$

where,

k_h : lateral force coefficient

c_z : modification factor for zone (refer to Fig. 2)

c_G : modification factor for ground condition (refer to Table 1)

c_U : modification factor for depth, and is evaluated as

$$c_U = 1.0 - 0.015z \quad (2)$$

z : depth from ground surface (m)

k_{h0} : standard lateral force coefficient

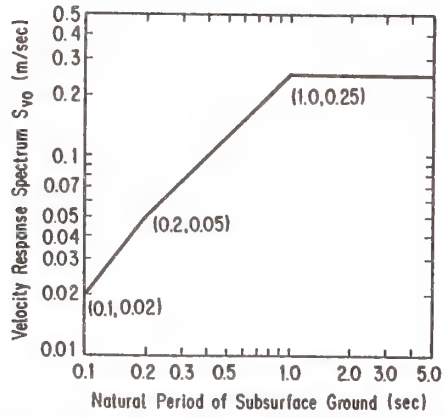

Fig.4 Standard Velocity Response Spectrum (Allowable Stress Design Method)

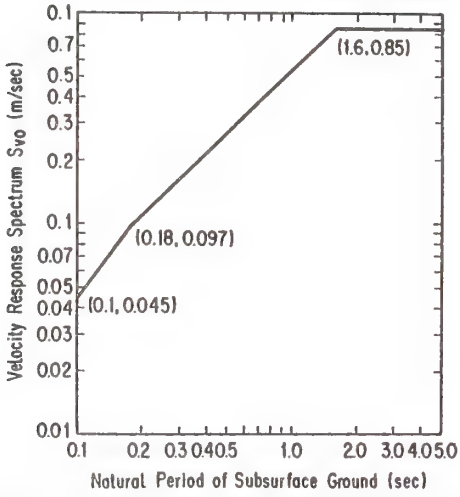

Fig.5 Standard Velocity Response Spectrum (Bearing Capacity Design Method)

(=0.2)

(2) Design Ground Displacement

The design ground displacement is evaluated depending on the depth and the distance as (refer to Fig. 3) :

$$u(z,x)=\frac{1}{\pi^2}S_V \cdot T_S \cdot \cos\left(\frac{\pi z}{2H}\right) \cdot \sin\left(\frac{\pi x}{2L}\right) \quad (3)$$

where,

$u(z,x)$: Design ground displacement (m) at depth z (m) and at distance x (m)

S_V : Design velocity response spectrum at design base rock (cm/sec), and is determined as

$$S_V = c_Z \cdot S_{VO} \quad (4)$$

c_Z : Modification factor for zone (refer to Fig. 2)

S_{VO} : Standard velocity response spectrum (cm/sec) at design base rock, and is given by Fig. 4 for the Allowable Stress Design Method and by Fig.5 for the Bearing Capacity Design Method

T_S : Natural period of subsurface ground (sec), and is evaluated as

$$T_S = 1.25 \cdot T_G \quad (5)$$

$$T_G = 4 \sum \frac{H_i}{V_{Si}} \quad (6)$$

H_i : Thickness of i-th soil layer (m)

V_{Si} : Shear wave velocity of i-th soil layer (m/sec)

L : Design wave length (m) of ground motion

$$L = \frac{2L_1 L_2}{L_1 + L_2} \quad (7)$$

L_1, L_2 : Design wave length (m) at subsurface ground and base rock, respectively, and are determined as

$$L_1 = T_S \cdot V_{SD} \quad (8)$$

$$L_2 = T_S \cdot V_{SDB} \quad (9)$$

V_{SD} : Averaged shear wave velocity of subsurface ground (m/sec)

V_{SDB} : Shear wave velocity at design base rock (m/sec)

(3) Design Shear Stress around Surface

At the surface of underground structures contacting with soils, the design shear stress around surface has to be applied to the underground structures as shown in Fig. 6.

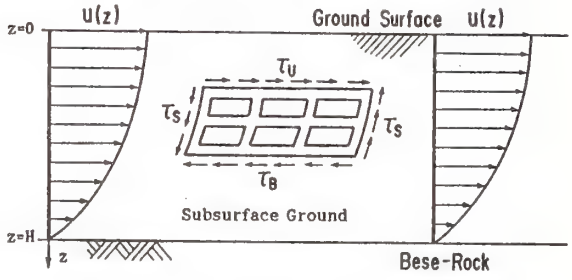

Fig.6 Design Shear Stress around Surface

The design shear stress around surface is given by Eq. (10). If the design shear stress around surface by Eq. (10) is larger than the strength of soils around the underground structure, the design shear stress around surface shall be the strength of soils.

$$\tau = \frac{G_D}{\pi H} S_V \cdot T_S \cdot \sin\left(\frac{\pi z}{2H}\right) \quad (10)$$

where,

τ : Design shear stress around surface (tf/m^2)

S_V : Design velocity response spectrum at design base rock (cm/sec), and is given by Eq. (4)

G_D : Shear modulus of subsurface ground (tf/m^2)

T_S : Natural period of subsurface ground

(sec), and is computed by Eq. (5)

H : Thickness of subsurface ground (m)

(4) Dynamic Earth Pressure

Dynamic earth pressure by Eq. (11) is applied to side wall of underground structures as shown in Fig. 7.

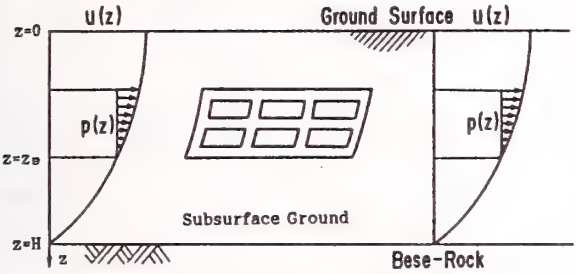

Fig.7 Dynamic Earth Pressure

$$p(z)=k_H \cdot \{u(z)-u(z_B)\} \quad (11)$$

where,

p(z) : dynamic earth pressure per unit area (tf/m^2) at depth z (m)

k_H : spring stiffness of soils per unit area (tf/m^2)

u(z) : Design ground displacement (m), and is given by Eq. (3)

z_B : Depth of base of underground structure (m)

(5) Input Ground Motions for Dynamic Response Analysis

Design acceleration response spectrum at design base rock is given as

$$S=c_Z \cdot c_D \cdot S_0 \quad (12)$$

where,

S : Design acceleration response spectrum (cm/sec) at design base rock

c_Z : Modification factor for zone (refer to Fig. 2)

c_D : Modification factor of damping ratio, and is given as

$$c_D=\frac{1.5}{40h_i+1}+0.5 \quad (13)$$

h_i : modal damping ratio of critical

S_0 : Standard acceleration response spectrum at design base rock, and is given by Fig. 8 for the Allowable Stress Design Method and by Fig. 9 for the Bearing Capacity Design Method

Input accelerations for time response analysis shall be either selected from strong motion records which have the close response spectral characteristics with S by Eq. (12) or

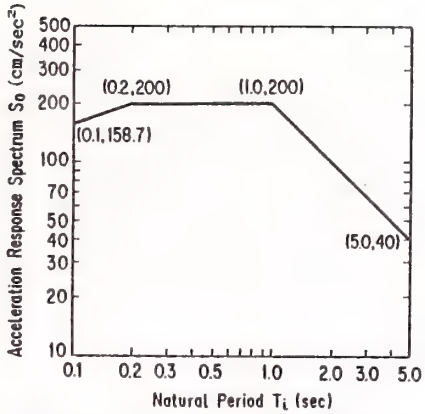

Fig.8 Standard Acceleration Response Spectrum (Allowable Stress Design Method)

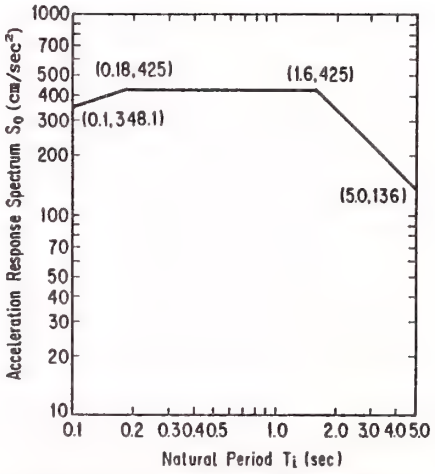

Fig.9 Standard Acceleration Response Spectrum (Bearing Capacity Design Method)

obtained by adjusting the strong motion records in frequency domain so that the acceleration response spectrum be matched with S by Eq. (12).

5 SEISMIC DESIGN METHOD OF LARGE SHIELD TUNNELS

5-1 Seismic Design Method in Axial Direction

(1) Seismic Design by Seismic Deformation Method

Shield tunnels are constructed by assembling a number of segments, ring bolts and segment bolts as shown in Fig. 10. Although there may be various idealizations of shield tunnels as shown in Fig. 11, the idealization of shield tunnels as a beam with equivalent stiffness may be the most appropriate for seismic design. Assuming a shield tunnel as a beam, elastically supported by subsurface ground, with equivalent stiffness as shown in Fig. 12, the seismic forces developed in the shield tunnel are evaluated

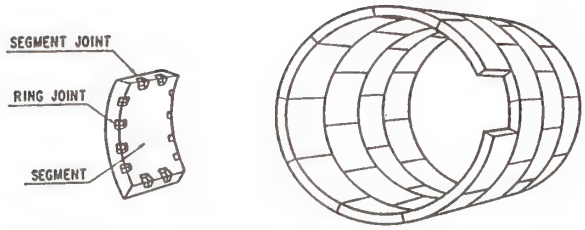

Fig.10 Segments and Joints of Shield Tunnel Lining

by the Seismic Deformation Method as[7] :

$$P_h^C = \alpha_1^C \frac{\pi u_h}{L} (EA)_{eq}^C \quad (14)$$

$$P_h^T = \alpha_1^T \frac{\pi u_h}{L} (EA)_{eq}^T \quad (15)$$

$$P_v^C = \alpha_1^C \frac{\pi (u_h+u_v)}{L} (EA)_{eq}^C \quad (16)$$

$$P_v^T = \alpha_1^T \frac{\pi (u_h+u_v)}{L} (EA)_{eq}^T \quad (17)$$

$$M_h = \alpha_2 \frac{4\pi u_h}{L^2} (EI)_{eq} \quad (18)$$

$$M_v = \alpha_3 \frac{4\pi u_v}{L^2} (EI)_{eq} \quad (19)$$

$$Q_h = \alpha_2 \frac{8\pi u_h}{L^3} (EI)_{eq} \quad (20)$$

$$Q_v = \alpha_3 \frac{8\pi u_v}{L^3} (EI)_{eq} \quad (21)$$

where,

P_h^C, P_h^T : Compression and tension force (tf), respectively, developed due to the design ground displacement in lateral direction

P_v^C, P_v^T: Compression and tension force (tf), respectively, developed due to the design ground displacement in vertical direction

M_h, M_v : Bending moment in horizontal plane and vertical plane (tf·m), respectively

Q_h, Q_v : Shearing force in horizontal plane and vertical plane (tf), respectively

$(EA)_{eq}^C, (EA)_{eq}^T$: Equivalent compression rigidity (tf) and equivalent tension rigidity (tf) of shield tunnel, and is given by Eqs.(31) and (32)

$(EI)_{eq}$: Equivalent flexural rigidity (tf), and is given by Eq. (35)

u_h : Design lateral ground displacement (m) at depth of gravity center of shield tunnel, and is given by Eq. (3)

u_v : Design vertical ground displacement (m) at depth of gravity center of shield tunnel, and is given as 1/2 of u_h

L : Design wave length (m), and is give by Eq. (7)

$\alpha_1^C, \alpha_1^T, \alpha_2, \alpha_3$: Coefficients to represent the degree of transmission of response displacement from the subsurface ground to shield tunnel, and is given by Eqs. (22) ~ (25).

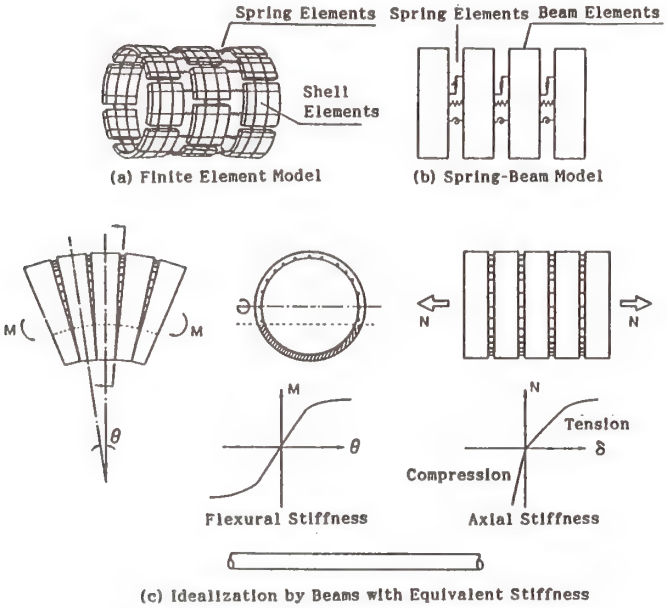

Fig.11 Idealization of Shield Tunnel

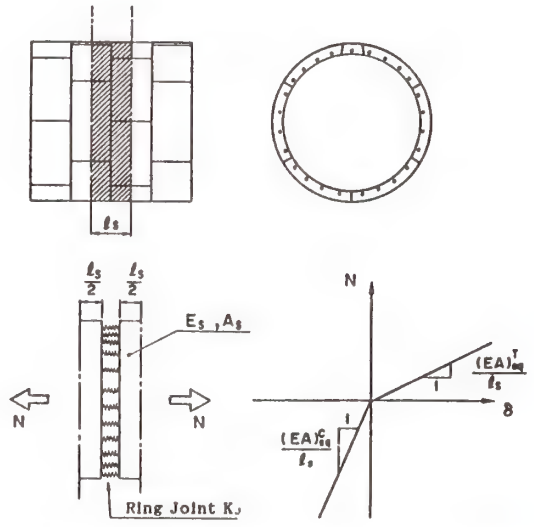

Fig.13 Axial Stiffness of Segments-Ring Joints

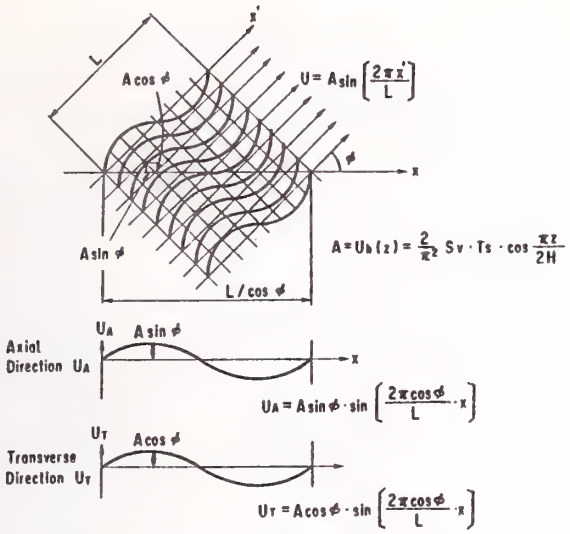

Fig.12 Ground Displacement Assumed in Seismic Deformation Method

$$\alpha_1^{\circ}=\frac{1}{1+(2\pi/\lambda_1^{\circ}L_1)^2} \quad (22)$$

$$\alpha_1^{T}=\frac{1}{1+(2\pi/\lambda_1^{T}L_1)^2} \quad (23)$$

$$\alpha_2=\frac{1}{1+(2\pi/\lambda_2 L)^4} \quad (24)$$

$$\alpha_3=\frac{1}{1+(2\pi/\lambda_3 L)^4} \quad (25)$$

where,

$$\lambda_1^{\circ}=\sqrt{\frac{K_{\sigma 1}}{(EA)_{eq}^{\circ}}} \quad (26)$$

$$\lambda_1^{T}=\sqrt{\frac{K_{\sigma 1}}{(EA)_{eq}^{T}}} \quad (27)$$

$$\lambda_2=\sqrt[4]{\frac{K_{\sigma 2}}{(EI)_{eq}}} \quad (28)$$

$$\lambda_3=\sqrt[4]{\frac{K_{\sigma 3}}{(EI)_{eq}}} \quad (29)$$

$$L_1=\sqrt{2}\cdot L \quad (30)$$

$K_{\sigma 1}$, $K_{\sigma 2}$, $K_{\sigma 3}$: soil spring in longitudinal, transverse and vertical direction, respectively (tf/m^2)

(2) Equivalent Stiffness of Shield Tunnel without Second Lining

1) The equivalent stiffness of shield tunnel is different between tension and compression as shown in Fig. 13. The equivalent rigidity is computed by Eqs. (31) and (32).

$$(EA)_{eq}^{\circ}=E_S A_S \quad (31)$$

$$(EA)_{eq}^{T}=\frac{1}{(K_S/K_J)+1}\cdot E_S A_S \quad (32)$$

where,

$(EA)_{eq}^{\circ}$: Equivalent compression rigidity (tf)

$(EA)_{eq}^{T}$: Equivalent tension rigidity (tf)

E_S : Elastic modulus of shield segments (tf/m^2)

A_S : Sectional area of segment- ring (m^2)

l_S : Length of segment (m) in axial direction

K_S : Stiffness of segment-ring (tf/m), and is given by Eq. (33)

$$K_S=\frac{E_S A_S}{\ell_S} \quad (33)$$

K_J : Tension stiffness of total ring-joints (tf/m), and is given by Eq. (34)

$$K_J = n\cdot k_J \quad (34)$$

k_J : Tension stiffness of a ring-joint (tf/m)

n : number of ring-joint

2) The equivalent flexural rigidity of shield tunnel is computed as shown in Fig. 14, and is given by Eq. (35)[8]

$$(EI)_{eq}=\frac{\cos^3\phi}{\cos\phi+(\pi/2+\phi)\sin\phi}\cdot E_S\cdot I_S \quad (35)$$

where,

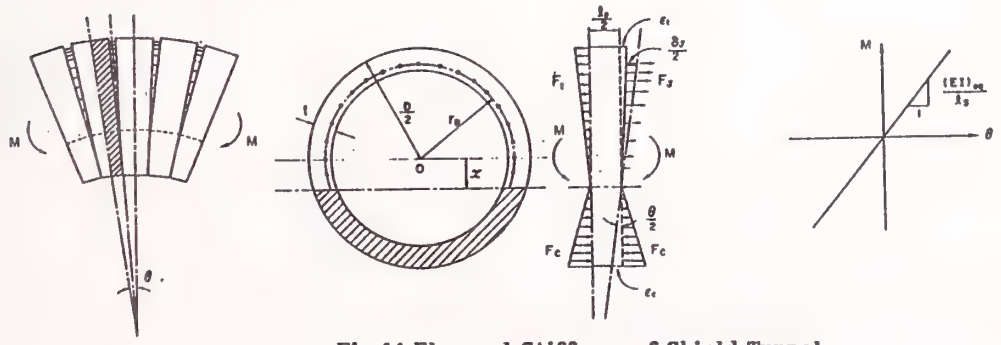

Fig.14 Flexural Stiffness of Shield Tunnel

(a) Experimental Set-up

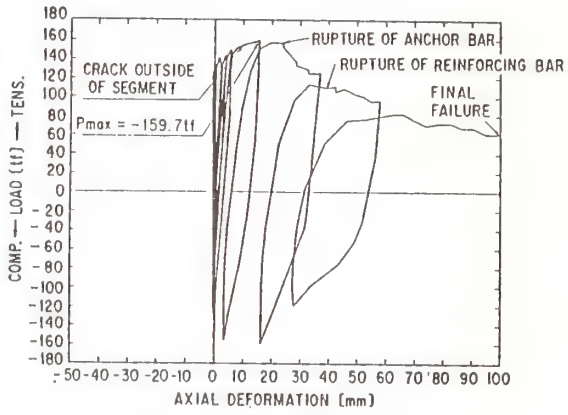

(b) Loading Hysteresis Loop

Fig.15 Effect of Second Lining for Ductility of Flexural Deformation

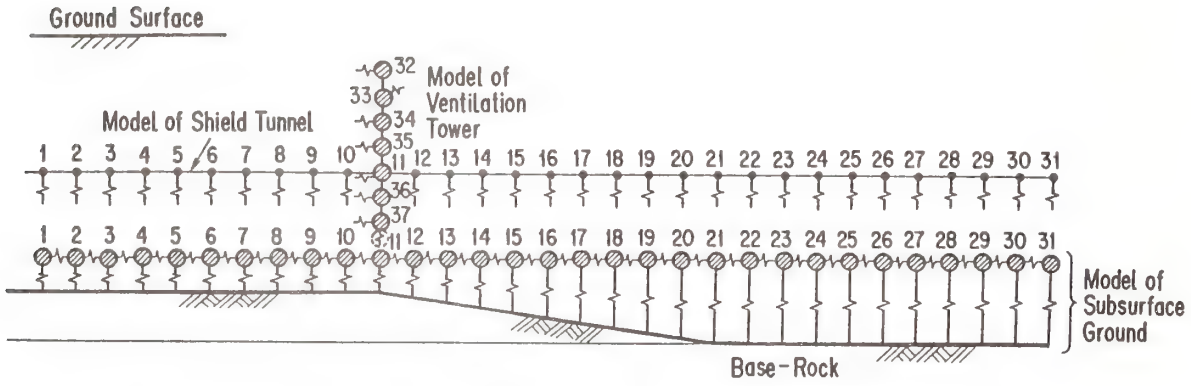

Fig.16 Model of Shield Tunnel, Ventilation Tower and Subsurface ground

$(EI)_{eq}$: Equivalent flexural rigidity of shield tunnel (tfm^2)

E_S : Elastic modulus of segment (tf/m^2)

I_S : Moment of inertia of segment (m^4)

ϕ : angle measured from center line to neutral line (rad), and is given by solving the following equation :

$$\phi + \cot\phi = \pi \left(\frac{1}{2}\frac{K_J}{E_S A_S / l_S}\right) \qquad (36)$$

(3) Equivalent Stiffness of Shield Tunnel with Second Lining

General description for evaluating the equivalent stiffness of shield tunnel with second lining is difficult because it depends on the spring action of axial reinforcements of the second lining. Based on a series of model loading test results at the Public Works Research Institute[9),10)] as shown in Fig. 15, it is known that as well as the segments the second lining resists to the compression force. However, to the tension force the interaction between the segments and the second lining depends significantly on the damage developed in the second lining and at the ring-joints. It may be classified into four steps as shown in Table 2.

(4) Evaluation of Seismic Safety by Dynamic Response Analysis

In the dynamic response analysis, shield tunnel is generally idealized by a elastic beam with the equivalent stiffness as shown in Fig. 16. The subsurface ground is idealized by either finite element model or spring-mass model, and the nonlinearity of soil stiffness is modeled by the equivalent linear method. Input ground motion is prescribed at the base-rock. Evaluation on spatial variation of input motion at the design base-rock is very important.

(5) Minimum Axial Reinforcement in Second Lining

For avoiding the concentration of the damage at only selected ring-joints as shown in

Table 2 Damage Degree of Shield Tunnel with Second Lining

Step	Damage Degree
I	All sections in 1st and 2nd linings are in elastic. No damage.
II	Cracks in 2nd lining around ring only at ring joints.
III	Cracks in 2nd lining around ring occur not only at ring joint but at other sections.
IV	Contact between the 1st lining and 2nd lining is lost. Final failure is to be developed.

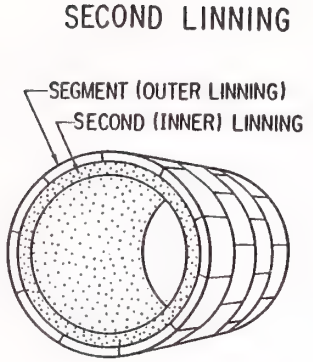

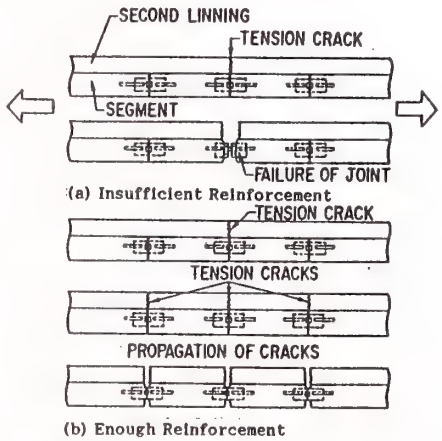

Fig.17 Minimum Reinforcement Required in Second Lining for Preventing Concentration of Damage at only Selected Ring Joints

Fig. 17, it is required to provide the minimum reinforcement in the second lining in tunnel axis as

$$A_S=(A_L\cdot \sigma_L-P_R)/\sigma_{LS} \quad (37)$$

where,

A_S : Minimum reinforcement required for second lining in longitudinal direction (cm^2)

A_L : Sectional area of second lining (cm^2)

σ_L : Tension strength of second lining(kgf/cm^2)

σ_{LS} : Tension strength of reinforcement in second lining (kgf/cm^2)

P_R : Tension strength of ring joint(kgf) ,and takes the smaller value between P_A by Eq.(38) and P_B by Eq.(39).

$$P_A=n\cdot p_A \quad (38)$$

$$P_B=m\cdot p_B \quad (39)$$

where,

P_A : Tension strength of anchor reinforcement(kgf)

P_B : Tension strength of ring bolts(kgf)

n : Number of anchor reinforcements per ring joint

m : Number of ring bolts per ring joint

p_A : Tension strength of an anchor bolt(kgf)

p_B : Tension strength of a ring bolt(kgf)

5-2 Seismic Design Method in Transverse Direction

The seismic design of shield tunnel in transverse direction is generally made as :

1) Idealize the shield tunnel as a ring with equivalent stiffness,

2) Consider soil springs, around the tunnel ring, which represent the soil-structure interaction,

3) Evaluate the design ground displacement, the design shear stress around surface and the inertia force at the center of gravity of the shield tunnel,

4) Divide the design shear stress around surface and the inertia force into the components in tangential and normal directions, and apply them to the shield tunnel. The design ground displacement is also divided into the components in tangential and normal directions, and apply them to the shield tunnel through the soil springs,

5) Compute the increase of force, due to seismic effects, developed in the tunnel rings, and

6) Evaluate the force, developed in the tunnel rings, during an earthquake by adding the force of 4) with the force developed due to static loads

When the following assumptions can be made for the shield tunnel and subsurface ground,

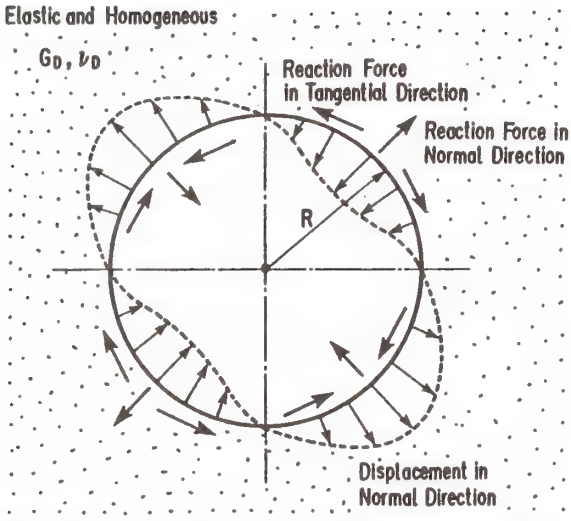

Fig.18 2nd Model Reformation of Fourier Serries assumed for Tunnel Ring

the force increase, due to the seismic effects, developed in the tunnel ring can be easily computed.

1) The subsurface ground is elastic and homogeneous,

2) The fundamental mode is significantly predominant in the subsurface ground,

3) Tunnel ring is elastic,

4) The inertia force to the tunnel ring is negligibly small,

5) Depth of soil to the shield tunnel is large enough, and the shield tunnel is not in close proximity of the design base-rock,

6) Saturation of the design shear stress around surface at the shear strength of soils is disregarded, and

7) The soil spring can be evaluated based on force vs. displacement relation of an elastic ring placed in infinite elastic homogeneous material as shown in Fig. 18.

The assumption 7) require more explanation. Consider an elastic ring which is placed in the infinite elastic material. From the displacement of the ring by applying a distributed load, the soil spring may be evaluated by Eqs. (40) and (41).

$$k_n=\frac{2G_D}{R}\cdot C_n \tag{40}$$

$$k_n'=\frac{2G_D}{R}\cdot C_n' \tag{41}$$

$$C_n=\begin{cases}\frac{1}{2} & :n=0\\ \frac{1}{2} & :n=1\\ \frac{2n+1-2\nu_D(n+1)}{3-4\nu_D} & :n\geq 2\\ 0 & :n=0,1\end{cases} \tag{42}$$

$$C_n'=\begin{cases}\frac{n+2-2\nu_D(n+1)}{3-4\nu_D} & :n\geq 2\end{cases} \tag{43}$$

where,

k_n : Spring stiffness associated with the displacement in normal (or tangential) direction due to the force in normal (or tangential) direction(tf/m^3)

k_n' : Spring stiffness associated with the displacement in normal (or tangential) direction due to the force in tangential (or normal) direction(tf/m^3)

G_D : Elastic modulus of subsurface soils(tf/m^2)

R : Radius of shield tunnel ring(m)

ν_D : Poisson's ratio of subsurface ground

n : mode number in terms of Fourier series

When the soil spring can be represented by Eqs. (40) and (41), the increase of force, developed in shield tunnel ring, due to the seismic effects may be represented as

$$M=\beta\cdot\frac{3\pi\cdot EI}{2R\cdot H_g}\cdot U_n\cdot\sin\left(\frac{\pi\cdot H}{2H_g}\right)\cdot C\cdot\sin 2\theta \tag{45}$$

$$Q=-\beta\cdot\frac{3\pi\cdot EI}{R^2\cdot H_g}\cdot U_n\cdot\sin\left(\frac{\pi\cdot H}{2H_g}\right)\cdot C\cdot\cos 2\theta \tag{46}$$

$$N=-\beta\cdot\frac{3\pi\cdot EI}{R^2\cdot H_g}\cdot U_n\cdot\sin\left(\frac{\pi\cdot H}{2H_g}\right)\cdot\left(1+\frac{G_D\cdot R^3}{6EI}\right)\cdot C\cdot\sin 2\theta \tag{47}$$

$$C=\frac{4(1-\nu_D)\cdot G_D\cdot R^3}{(3-2\nu_D)\cdot G_D\cdot R^3+6(3-4\nu_D)\cdot EI} \tag{45}$$

where,

M : Bending moment of tunnel ring per unit length(tf·m/m)

Q : Shear force developed in tunnel ring per unit length(tf/m)

N : Axial force developed in tunnel ring per unit length(tf/m)

θ : Angle measured from crest of tunnel ring(rad)

Hg : Thickness of subsurface soils(m)

H : Depth of the gravity center of shield tunnel from the ground surface(m)

R : Radius of tunnel ring(m)

EI : Flexural rigidity of tunnel ring per unit length($tf\cdot m^2/m$)

G_D : Shear modulus of subsurface ground(tf/m^2)

ν_D : Poisson's ratio of subsurface ground

u_n : Design ground displacement at the ground surface, and is given by Eq. (3)

β : Modification factor for higher order modes (= 1.3)

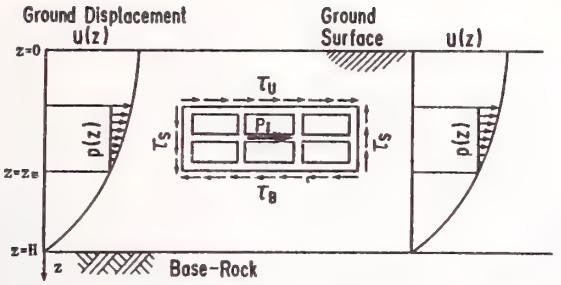

Fig.19 Shear Stress around Surface, Dynamic Earth Pressure and Inertia Force for Seismic Design of Laterally Wide Underground Structures

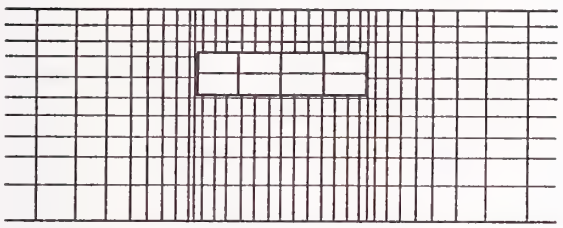

Fig.20 Two Dimensional Finite Element Idealization

6 SEISMIC DESIGN METHOD OF LATERALLY WIDE UNDERGROUND STRUCTURES

The shear stress around surface is significant in seismic design of the Laterally Wide Underground Structures. The increase of force, developed in the structures, due to seismic effects are computed by applying the design shear stress around surface, the dynamic earth pressure and the inertia force as shown in Fig. 19.

Dynamic response analysis is recommended for the Laterally Wide Underground Structures with the following conditions :

1) For the underground structures constructed in subsurface ground with significantly irregular soil condition in either vertical or lateral direction. The condition where irregularity of the surface or the design base-rock is significant is also the one recommended for the dynamic response analysis. Two dimensional finite element idealization as shown in Fig. 20 is recommended for such analyses.

2) For the underground structures with significant out-of-plane deformation. Analytical models as shown in Fig. 21 is recommended for such structures. In the models, the subsurface ground is recommended to be idealized by the mass-spring model with one or two layers in vertical direction and the Laterally Wide Underground Structure is idealized by plate elements, shell and solid elements.

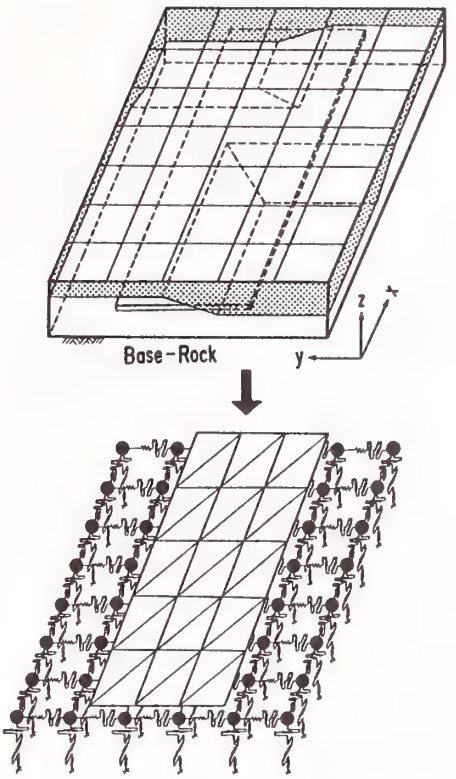

Fig.21 Idealization by Plate Elements and Shell Elements

7 SEISMIC DESIGN METHOD OF VERTICALLY LONG UNDERGROUND STRUCTURES

Because the design shear stress around surface is predominant in the Vertically Long Underground Structures, it is important to evaluate it carefully. Fig. 22 represents how the seismic forces are applied to the structures. There are structures with large section, which shows significant deformation in lateral direction as well. Shell elements and solid elements are recommended for the

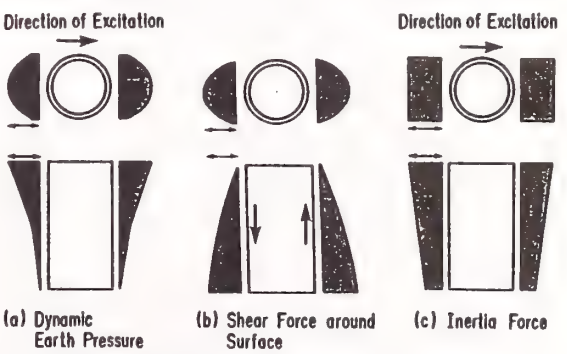

Fig.22 Seismic Effects to Vertically Long Underground Structures

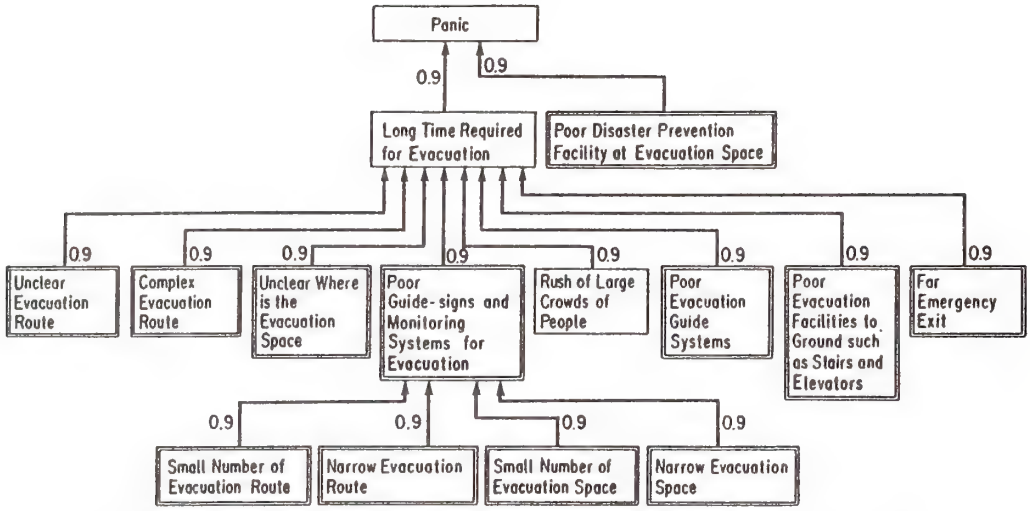

Fig.23 Structural Model predicted by FSM for Fear and Anxiety against Evacuation

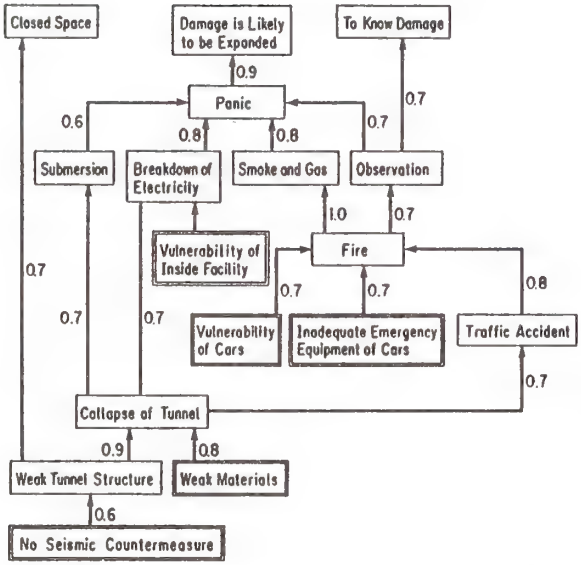

Fig.24 Structural Model Predicted by FSM for Possible Influence of Damage

analysis of such underground structures.

8 EARTHQUAKE DISASTER PREVENTION SYSTEMS FOR UNDERGROUND HIGHWAYS

8-1 General

Although seismic design is, of course, made for constructing underground highways, there are always considerable anxiety for seismic safety. When an earthquake occurs at the situation where drivers have much anxiety about seismic safety, fear is likely to be amplified to cause panic. Therefore although seismic design is of course essential importance for reducing seismic damage, it is also important to mitigate fears and anxiety of drivers against safety during an earthquake.

8-2 Fear and Anxiety of Drivers against an Earthquake

Fear and anxiety which are likely to be induced in drivers when they imagine "underground highways" and "earthquakes" were analyzed by the Value Engineering Method. It was found from the analysis that there are two types of fear and anxiety. The first is the fear and anxiety which are always possessed by drivers against the image of "underground highways", and the second is the fear and anxiety against the accidents which are likely to be developed during an earthquake. Although some of them are infantile imaginations from the professional sense, it is important to know how the drivers feel against "underground highways" and "earthquakes".

(1) Fear and Anxiety Always Possessed by Drivers

a) Fear and anxiety from latent sense to the underground structures

Fear and anxiety come from various latent sense to the underground highways such as darkness, narrowness and dirtiness in comparison with the on-ground highways. They also come from unexperienced driving on underground, unfamiliar sense and insensibility to time and direction.

b) Fear and anxiety against driving

Fear and anxiety are sometimes developed even only anticipating to drive on underground highways. The typical senses are

the difficulty to know where they are driving, limited visibility and possible bad manner of drivers.

c) Fear and anxiety against environment

They come from anticipation that the environment may be worse at underground highway than at on-ground highways, such as insufficient facilities for services and rest room and difficulty for access to other facilities. Little change of scenery and circumstance and possible insufficient maintenance for service facilities also cause the fear and anxiety. Sometimes they are induced even from imaging that there may be few drivers at the underground highways.

(2) Fear and Anxiety against Possible Accidents during an Earthquake

a) Fear and anxiety associated with possible influence of damage

Fear and anxiety are developed against possible influence to drivers due to structural damage, damage of non-structural components and crash of cars. Submergence and fire are the most typical scenario for such fear and anxiety. They are also induced by looking at the occurrence of panic, break-down of electricity and accidents.

b) Fear and anxiety against emergency countermeasures

Some drivers have fear and anxiety because they do not know how to respond to emergent situation, where disaster prevention facilities are and how to operate them due to their inexperience.

c) Fear and anxiety against evacuation

Fear and anxiety are induced by imaging unsuccessful evacuation from underground highways. For example, they have the fear and anxiety against the possible difficulty to know where the evacuation and refuge space are, possible long time required for evacuation, insufficient sign for direction and rush of refugee.

d) Fear and anxiety for insufficient information for damage and refuge

They come from the anxiety for not be able to get enough information on damage situation and evacuation. Drivers at underground highways ancipate that they could not get the information on what damage was developed on ground, and that the information may be incorrect even if they could get the information.

e) Fear and anxiety against traffic accidents

This is not necessarily unique to the underground highways. Fear and anxiety are induced against snake-like driving[1)] and collision of cars due to sudden brake.

8-3 Factors Causing Fear and Anxiety to Drivers at Underground Highways

There are various factors causing fear and anxiety to drivers during an earthquake. Because the factors are complicatedly coupled, their structure was analyzed by the Interpretive Structural Modeling Method and the Fuzzy Structural Modeling Method. Figs. 23 and 24 show some of such analyses. Based on the analyses, the most basic factors (the lowest factors identified from the analyses) causing fear and anxiety to drivers during an earthquake may be represented as :

(1) Fear and anxiety always possessed by drivers
- a) sense of closing and isolation
- b) complex routes
- c) little separation between automobiles and pedestrians
- d) insufficient education for traffic morals
- e) insufficient environmental control
- d) difficulty for access to other facilities

(2) Fear and anxiety against possible accidents during an earthquake
- a) vulnerability of facilities
- b) vulnerability of cars
- c) unexperienced response
- d) insufficient evacuation facilities
- e) insufficient evacuation control systems
- f) insufficient disaster information systems
- g) unexpected obstacles on highways
- h) vibration of tunnel

8-4 Basic Countermeasures against Earthquake Disaster

It is the most important to take countermeasures against the most fundamental factors causing fear and anxiety of drivers during an earthquake. Because the contribution of each factor is different, the countermeasure have to be taken considering their effectiveness. The Analytical Hierarchy Process Analyses were made to identify the predominant factors for causing fear and anxiety of drivers, and it was found from such analyses that the following measures may be effective :

(1) Simulation of environments of on-ground

highways

It is basic to simulate the environments of on-ground highways so as to prevent drivers to have strong feeling to be driving on the underground highways. It is effective to make the space large enough so that mental pressure due to the sense of closing and isolation be small. It is effective to have sun-light at underground.

(2) Positive utilization of advantage of underground

Because ground shaking at underground is smaller than that at the ground surface, positive education of this feature may be important. It is also important to educate that the evacuation to the ground surface is not the only one choice for drivers during an earthquake, because underground structures are sometimes more safe that the on-ground structures.

(3) Disaster education and disaster prevention training

Because there are various fear and anxiety which come from unawareness of disaster prevention systems such as the unawareness of where the disaster prevention facilities are, more efforts are required to educate drivers on disaster prevention systems. Distribution of pamphlet for educating the disaster prevention systems may be essential. Construction of disaster prevention center, which is in most cases constructed at the corner of the underground space difficult to see from drivers, at the place where drivers can see easily may be an effective way for obtaining the trust from drivers. Positive advertisement of such disaster prevention systems may be effective.

(4) Traffic control systems

Nice traffic control systems are important. It is required to shut-down the traffic to enter the underground highways after a significant earthquake.

(5) Emergency Facilities

Reliable access to the ground surface which can be used even after a significant earthquake is required. However as was pointed out in (2), it is not the only one choice for drivers to evacuate to the ground surface. It may be more reliable to construct stable shelter in underground so that drivers could evacuate into the shelter in case of emergency.

(6) Formulation of disaster information system

It is required to provide the disaster information system for showing what are happening on at on-ground soon after the occurrence of an earthquake. Such monitoring system of the on-ground scenery may be also effective at normal time to mitigate the fear and anxiety to be in underground. It should be noted however that the information systems which can provide information by only letters and voice are not sufficient enough, because insufficient amount of information is likely to amplify the fear and anxiety of drivers at underground. Visible monitoring systems is the most effective way.

9 CONCLUDING REMARKS

The preceding pages presented the outline of the Guidelines for Seismic Design Methods of Large Underground Structures. Because it is anticipated that more use of underground space for various purposes such as underground highways and parking is going to be made due to various restrictions of utilization of on-ground land, active use of the Guidelines for designing large underground structures is expected.

ACKNOWLEDGEMENTS

Various supports and guidance were obtained for compiling the Guidelines. The authors express their sincere appreciations to the participants of the Joint Research Program on Development of Seismic Design Method of Underground Structures between the Public Works Research Institute, ACTEC and 8 private firms. The authors also express their appreciation to Professor Kenzo Toki, Disaster Prevention Research Institute of the Kyoto University for his invaluable suggestions throughout the research.

REFERENCES

1) Public Works research Institute and Advanced Construction Technology Center: Investigation on Seismic Design Methods of Large Underground Structures, 1989, 1990, 1991, 1992 (in Japanese)

2) Public Works Research Institute : Guidelines for Seismic Design Methods of Underground Structures, Technical Note, March 1992 (in Japanese)

3)Japan Road Association : Technical Standard for Petroleum Pipeline, June 1971 (in Japanese)

4)Japan Water Supply Association : Seismin

Design Specification for Water Supply Facilities, December 1979 (in Japanese)
5) Japan Road Association : Design Method of Common Utility Ducts, March 1986 (in Japanese)
6) Ministry of Construction : New Seismic Design Methods, Technical Note, No. 1185, Public Works Research Institute, March 1977 (in Japanese)
7)Shiba, Y., Kawashima, K., Obinata, N. and Kanoh, T. : Evaluation Procedure for Seismic Stress Developed in Shield Tunnel Based on Seismic Deformation Method, Proc. Japan Society of Civil Engineers, Vol. 404, April 1989 (in Japanese)
8) Shiba, Y., Kawashima, K., Obinata, N. and Kanoh, T. : An Evaluation Method of Longitudinal Stiffness of Shield Tunnel Lining for Application to Seismic Response Analysis, Proc. Japan Society of Civil Engineers, Vol. 398, October 1988 (in Japanese)
9) Kawashima, K., Sugita, H. and Kanoh, T. : Loading Test of Shield Tunnel Specimens subjected to Alternative Axial Loading, 4th U.S. National Conference on Earthquake Engineering, Palm Springs, CA., U.S.A., May 1990
10) Kawashima, K., Hasegawa, K. and Nagashima, H. : Seismic Behavior of Buried Pipelines through Field Observation, 3rd U.S. National Conference on Lifeline Earthquake Engineering, Los Angeles, CA., U.S.A., August 1991
11)Kawashima, K., Sugita, H. and Kanoh, T. : Effect of Earthquake on Driving of Vehicles Based on Questionnaire Survey, Proc. Japan Society of Civil Engineers, Structural Eng./Earthquake Engineering, Vol. 6, No. 2, October 1989

Seismic Vulnerability and Impact of Disruption of Lifelines in the Conterminous United States—An Overview

by

William S. Bivins

ABSTRACT

The Federal Emergency Management Agency (FEMA) initiated a project to assess the seismic vulnerability and impact of disruption of lifeline systems nationwide. The purpose of the project was to develop a better understanding of the impact of disruption of lifelines from earthquakes and to assist in the identification and prioritization of hazard mitigation measures and policies. FEMA plans to utilize results from the project to promote national awareness of the importance of protecting lifeline systems from earthquakes, and assuring reliability and continued serviceability of lifelines. The project was undertaken by the Applied Technology Council (ATC) and was conducted in several phases. Phase I, which provides the bases for this paper, provides a national overview of lifeline seismic vulnerability and impact of disruption. Lifelines considered include electric systems, water systems, transportation systems, gas and liquid fuel supply systems, and emergency service facilities. The vulnerability estimates and impacts developed are presented in terms of estimated direct damage losses and indirect economic losses. The losses are considered to represent *a first approximation* because of the assumptions and methodology utilized, because several lifelines are not included, and because, in some cases, the available lifeline inventory data lack critical information. This paper is an overview of the project drawn from the full report, *Seismic Vulnerability and Impact of Disruption of Lifelines in the Conterminous United States — ATC-25*, Applied Technology Council, (ATC, 1991).

KEYWORDS: lifelines, earthquake, damage, impacts

1. INTRODUCTION

Lifeline is a term denoting those systems necessary for contemporary life and urban function, without which large urban regions cannot exist. Lifelines basically convey food, water, fuel, energy, information, and other material necessary for modern human existence from the production areas to the consuming areas. Also included are, of course, the transportation of the modern human.

With the advent of more and more advanced technology, the United States has increasingly become dependent on the reliable supply of lifeline-related commodities, such as electric power, fuel, and water. Earthquakes are probably the most likely natural disaster that would lead to major lifeline disruption. Extended disruption of lifelines serving a city or major urban region would lead to major economic losses, deteriorated public health and probable population migration. It clearly became necessary to identify the potential for major disruption to these lifelines, especially at the regional level.

FEMA initiated the study to better understand the impact of disruption of lifelines from earthquakes and to assist in the identification and prioritization of hazard mitigation measures and policies. The study report, Rojahn (1991), from which this paper is extracted, will improve national awareness of the importance of protecting lifeline systems from earthquakes, and of assuring lifeline reliability and continued serviceability.

Lifelines of critical importance at the U.S. national level have been analyzed to estimate overall seismic vulnerability and to identify those lifelines having the greatest economic impact, given large credible earthquakes. The lifelines examined include electric systems; water, gas and oil pipelines; highways and bridges; airports; railroads; ports; and emergency service facilities. The vulnerability estimates and impacts developed are presented in terms of estimated direct damage losses and indirect economic losses. These losses are considered to *represent a first approximation* because of the assumptions and

[a]Federal Emergency Management Agency, Washington, DC 20472

methodology utilized, because several lifelines are not included, and because, in some cases, the available lifeline inventory data lack critical capacity information.

Four basic steps were followed to estimate lifeline damage and subsequent economic disruption for given earthquake scenarios. The steps were:

- Develop a national lifeline inventory database,
- Develop seismic vulnerability functions for each lifeline component/system,
- Characterize and quantify the seismic hazard nationwide, and
- Develop direct damage estimates and indirect economic loss estimates for each scenario earthquake.

Several problems were encountered that could not be resolved because of technical difficulties and lack of available data. For example, telecommunication systems, nuclear and fossil-fuel power plants, dams, and certain water, electric, and transportation facility types at the regional transmission level were excluded from consideration in this project because of the unavailability of inventory data or the need for more in-depth studies.

Interaction effects between lifelines, secondary economic effects, and damage resulting from landslide were also not considered in developing the project report. These, and other limitations, tend to overestimate the losses. Lack of capacity information for most lifelines was also a definite limitation. In aggregate, due primarily to the exclusion of certain systems, the estimates of losses are believed to be quite conservative.

2. NATIONAL LIFELINE INVENTORY

Development of the inventory for all major lifelines in the United States was a major task. Sufficient detail was needed for lifeline seismic vulnerability assessment and impact of disruption at the national level. This required that the inventory be compiled electronically in digital form and dictated the inclusion of lifelines only at the transmission level.

The investigators initially contacted a number of government, utility, trade and professional organizations, and individuals to identify nationwide databases, especially electronic databases. In most cases, these organizations referred the project back to FEMA, since they had either previously furnished the information to FEMA, or know that the data had been furnished to FEMA by others. FEMA's database became a major source of data for several of the lifelines. Unfortunately, much of the inventory data generally date from about 1966.

The network inventory contained in the database is generally at the higher transmission levels, as opposed to lower distribution levels. As an analogy, the inventory contains only the national *arterial* level, and neglects the *capillary* system. For example, all federal and state highways are inventoried, but county and local roads are not.

2.1 Inventory Overview. The inventory data have been compiled into an electronic database consisting of:

- digitized location and type of facility for single-site lifeline facilities (e.g., ports), and
- digitized right-of-way and limited information on facility attributes for network lifelines (e.g., longitude and latitude of each end of a pipeline segment with diameter).

The inventory is only partial, in that important information on a number of facility attributes (e.g., number or length of spans for highway bridges) was unavailable in the FEMA database.

The inventory data include information only on the conterminous United States because lifelines in other regions would not be affected by the scenario earthquakes considered in this study.

2.2 Inventory Summary. The specific lifelines that have been inventoried are:

- Transportation
  - Highways (489,890 km of highways; 144,785 bridges)
  - Railroads (270,611 km of right-of-way)
  - Airports (17,161 civil and general aviation airports)

- Energy
  - Electric Power Transmission (4,551 substations; 441,981 km of transmission lines)
  - Gas and Liquid Fuel Transmission (77,109 km of crude oil pipelines; 85,461 km of refined oil pipelines; 67,898 km of natural gas pipelines)

- Emergency Service Facilities
  - Emergency Broadcast Facilities (29,586 stations)
  - Hospitals (6,973 medical care centers)

- Water Aqueducts and Supply (3,575 km of aqueduct, excluding Utah for which data were unavailable).

Telecommunication, an important lifeline, was excluded because of the unavailability of data. In addition, data on nuclear reactors and dams are excluded because it was believed that such facilities should be the subject of special studies because of the existing regulations relating to seismic safety in many regions and the expected complexity of the performance and impact of these facility types. Thus the losses established by this study will be underestimated to the extent that these facility types are not included.

Also excluded from the inventory, but included in the analysis, are distribution systems at the local level. The number of facility types (water, highway, and electrical systems and police and fire stations) with in each 25-km by 25-km grid cell was estimated on the basis of proxy by population.

3. LIFELINE VULNERABILITY FUNCTIONS

The second step in the project was the development of lifeline vulnerability functions. These functions which describe the expected or assumed earthquake performance characteristics of each lifeline as well as the time required to restore damaged facilities to their pre-earthquake capacity. The development of the vulnerability function for each lifeline considered are too lengthy to detail here but consisted of the following components:

- General information, which comprises (1) a *description* of the structure and its main components, (2) *typical seismic damage* in qualitative terms, and (3) *seismically resistant design* characteristics for the facility and its components. This information was included to define the assumed characteristics and expected performance of each facility and to make the functions more widely applicable.

- Direct damage information, which consists of (1) a description of its basis in terms of structure type and quality of construction, (2) default estimates of the quality of construction for present conditions and corresponding *motion damage curves*, (3) default estimates of the quality of construction for upgraded conditions, and (4) *restoration curves*.

These functions reflect the general consensus among practicing structural engineers that, with few exceptions, only California and portions of Alaska and the Puget Sound region have had seismic requirements incorporated into the design of local facilities for any significant period of time. For all other areas of the United States, present facilities are assumed to have seismic resistance less than or equal to that of equivalent facilities in California.

The two key quantitative vulnerability-function relationships developed under this project—*motion-damage curves* and *restoration curves*—define expected lifeline performance for each of the study regions and for the heart of the quantitative vulnerability analysis. The curves are based on the data and methodology developed on the basis of expert opinion in the ATC-13 project (ATC 1985). The data and methodology of ATC-13 are applicable for California structures only and the data were revised and reformatted to reflect differences in seismic design and construction practices nationwide.

Motion-damage curves developed define estimated lifeline direct damage as a function of seismic intensity (i.e., Modified Mercalli Intensity); direct damage is estimated in terms of repair costs expressed as a fraction or percentage of value. Curves are provided for each study region.

Restoration curves developed for this project define the fraction of initial capacity of the lifeline as a function of elapsed time since the earthquake. Again, curves are defined for each region.

4. SEISMIC HAZARD

Seismic hazard, as used in the study, is the expectation of earthquake effects. It is usually defined in terms of ground shaking parameters (e.g., peak ground acceleration, Modified Mercalli Intensity, peak ground velocity) but, broadly speaking, can include fault rupture, ground failure, or other phenomena resulting from an earthquake. Seismic hazard is a function of the size, or magnitude of an earthquake, distance from the earthquake, local soils, and other factors, and is independent of the buildings or other items of value that could be damaged.

The technical approach for evaluating the seismic hazard of lifeline structures are defined in detail. The approach involves identifying (1) the most appropriate descriptor (parameters) for describing the seismic hazard, (2) regions of high seismic activity, (3) representative potentially damaging, or catastrophic, earthquakes within each of these regions that could be used as scenario events for the investigation of lifeline loss estimation and disruption, and (4) a model for estimating the seismic hazard for each of these scenario events.

Following a review of available parameters for characterizing seismic hazard, the Modified Mercalli Intensity (MMI) Scale was elected for use. The MMI scale is subjective; it is dependent on personal interpretations and is affected by the quality of construction in the affected area. Even though it has these limitations, it is still useful as a general descriptor of damage, especially at the regional level.

The study presents an overview of the seismicity of the United States and representative earthquakes that were selected for the study.

In order to estimate the seismic hazard of the scenario events over the affected area, a model of earthquake magnitude, attenuation, and local site effects is required. For this study the Evernden model (Evernden and Thomson-1985) was selected. The advantages included: (1) verification via comparison with historical events, (2) incorporation of local soil effects and ready availability of a nationwide geologic database, and (3) ready availability of closed-form attenuation relations. An important additional attribute was that the Evernden model would estimate the distribution and intensity of seismic shaking in terms of MMI, the shaking characterization used in the ATC-13 study and the basic parameter, in this study, for lifeline vulnerability functions.

Based on the review of representative earthquakes scenario events were selected for this investigation. These events, presented by Region, Event Name, and Magnitude, are:

- Northeastern, Cape Ann, 7
- Southeastern, Charleston, 7.5
- Central, New Madrid, 7 and 8
- Western Mountain, Wasatch Front, 7.5
- Northwestern, Puget Sound, 7.5
- Southern California, Fort Tejon, 8
- Northern California, Hayward, 7.5.

With the exception of the Cape Ann, Charleston, and Hayward events, all magnitudes are reflective of the representative earthquake for the region. The scenario events for Cape Ann, Charleston, and Hayward have magnitudes one-half unit higher than the representative event. These magnitudes are interpreted as maximum credible for these locations.

5. ESTIMATES OF DIRECT DAMAGE

The analysis of seismic vulnerability of lifeline systems and the economic impact of disruption is based on an assessment of three factors:

- Seismic hazard,
- Lifeline inventory, and
- Vulnerability functions.

In this study these factors are used to quantify vulnerability and impact of disruption in terms of (1) direct damage and (2) economic losses resulting from direct damage and loss of function of damaged facilities.

Direct damage is defined as damage resulting directly from ground shaking or other collateral loss-causes such as liquefaction. For each facility, it is expressed in terms of cost of repair divided by replacement cost and varies from 0 to 1.0 ()% to 100%). It is estimated using (1) estimates of ground shaking intensity provided by the seismic hazard model, (2) inventory data specifying the location and type of facilities affected, and (3) vulnerability functions that

relate seismic intensity and site conditions to expected damage.

The approach to estimate direct damage considers both damage resulting from ground shaking as well as damage resulting from liquefaction. Damage due to other collateral loss causes, such landslide and fire, are not included because of the unavailability of inventory information and the lack of available models for estimating the losses nationwide.

The analysis approach for computing direct damage due to ground shaking proceeded as follows. For each earthquake scenario, MMI levels were assigned to each 25-km grid cell in the affected region, using the Evernden MMI model, assigned magnitude, and assigned fault rupture location. Damage states were then estimated for each affected lifeline component in each grid cell, using the *motion-damage curves*.

Dollar loss estimates are based on the available inventory data, cost per facility assumptions, and other models and assumptions with are described in the report. As a result, the accuracy of these estimates may vary from lifeline to lifeline. Data from the various lifelines are combined to estimate the total direct damage dollar losses for the eight scenario earthquakes as follows:

Earthquake	Direct Dollar Loss (in Billions, 1991)
Cape Ann	$4.2
Charleston	$4.9
Fort Tejon	$4.9
Hayward	$4.6
New Madrid, M=8.0	$11.8
New Madrid, M=7.0	$3.4
Puget Sound	$4.4
Wasatch Front	$1.5

6. ESTIMATION OF INDIRECT ECONOMIC EFFECTS

Earthquakes produce both direct and indirect economic effects. The direct effects, such as loss due to collapsed structures, are obvious and dramatic. However, the indirect effects that these disruptions have on the ability of otherwise undamaged enterprises to conduct business may be quite significant. However, there is very little literature on indirect economic losses.

This study provides a first approximation of the indirect economic effects of lifeline interruption due to earthquakes. A methodology was developed to relate lifeline interruption estimates to economic effects of lifeline interruption in each economic sector. This required a two-step process: (1) development of estimates of interruption of lifelines as a result of direct damage and (2) development of estimates of economic loss as a result of lifeline interruption.

Lifeline interruption resulting from direct damage is quantified in the study in residual capacity plots that define percent of function restored as a function of time. The curves are estimated for each lifeline type and scenario earthquake using (1) the time-to-restoration curves, (2) estimates of ground shaking intensity provided by the seismic hazard model, and (3) inventory data specifying the location and type of facilities affected.

For site-specific systems (i.e., lifelines consisting of individual sited or point facilities) the time-to-restoration curves are used directly. Extended regional networks required special analyses procedures consisting of connectivity analyses and serviceability analyses.

The extensive analyses of the study yields the following estimates of total indict economic losses for the eight scenario earthquakes as follows:

Earthquake	Indirect Loss (in Billions, 1991)
Cape Ann	$9.1
Charleston	$10.2
Fort Tejon	$11.7
Hayward	$11.1
New Madrid, M=8.0	$14.6
New Madrid, M=7.0	$4.9
Puget Sound	$6.1
Wasatch Front	$3.9

7. HAZARD MITIGATION OF CRITICAL LIFELINES

Based on the combined direct and indirect economic losses presented in the study and with consideration

of the assumptions and limitations expressed throughout the report the following relative ranking of the criticality of different lifelines in terms of the estimated impact of damage and disruption:

Rank 1 . . . . . Electric Systems
Rank 2 . . . . . Highways
Rank 3 . . . . . Water Systems
Rank 4 . . . . . Ports
Rank 5 . . . . . Crude Oil.

The study also provides extensive recommendations on measures to reduce the vulnerability of lifeline systems. The recommendations fall into the following categories:

- Damage reduction measures (e.g., strengthening a building, densifying the soil beneath a structure, component improvements)
- Provision of system redundancy
- Operational improvements

9. RECOMMENDATIONS FOR FURTHER WORK

The ATC-25 project has raised a number of questions and indicated areas in which knowledge is inadequate or nonexistent with respect to the impact of lifeline disruption due to earthquake. Following are recommendations for further research and other efforts.

- Lifeline Inventory. Appropriate organizations are encouraged to develop standards for complete lifeline inventories, and coordinate the acquisition of the needed additional updated data from various lifeline owners.
- Lifeline Component Vulnerability. A major effort should be initiated to acquire data on lifeline seismic performance and damage, and conduct analysis towards the development of improved component vulnerability functions. This effort should also investigate lifeline recovery data, and incorporate the extensive experience realized during the October 17, 1989 Loma Prieta, California, earthquake, as well as from other damaging earthquakes.
- Seismic Hazard Data. The U.S. Geological Survey should develop a series of digitized soil/geologic databases.
- Economic Analysis and Impacts Data and Methodology. Further research is recommended in economic areas such as:
  - Economic impacts associated with lifeline disruption,
  - Second-order economic effects (e.g., interaction between lifelines),
  - Elasticities of demand, or substitution of lesser disrupted lifeline for a more disrupted lifeline,
  - Inter-regional impacts, and
  - So-called "benefits," such as increased economic activity associated with repair or replacement of older equipment with new technology.

It should be noted that this study did not address the environmental consequences associated with lifeline disruption, especially the potential for oil spills from broken pipelines in the nations' waterways following, for example, a New Madrid event.

10. REFERENCES

Applied Technology Council (ATC-25), 1991, *Seismic Vulnerability and Impact of Disruption of Lifelines in the Conterminous United States*, Report ATC-25, Redwood City, California.

Applied Technology Council (ATC-13), 1985, *Earthquake Damage Evaluation Data for California*, Report ATC-13, Redwood City, California.

Evernden, J.F., and J.M. Thomson, 1985, *Predicting Seismic Intensities, in Evaluating Hazards in the Los Angeles Region — An Earth Science Perspective*, J.I. Ziony, ed., US Geological Survey Professional Paper 1360, U.S. GPO, Washington D.C.

Design Criteria for Base Isolation of Buildings

by

Harry W. Shenton, III*

ABSTRACT

Presented are the results an investigation in which the performance of "code-designed" fixed-base and base-isolated structures were compared. Two frames, a steel concentrically braced frame and a steel special moment resisting frame were designed as both fixed-base and base-isolated in accordance with the 1991 Uniform Building Code. To establish comparable performance, the base-isolated frames were designed to varying fractions of the code recommended base shear: 100%, 50% and 25%. Non-linear time history analyses were conducted, for three ensembles of earthquakes, to assess the effect of design force level and base-fixity on response and damage level. In general, the base-isolated frames designed to 100% of the code recommended base shear out-performed the fixed-base frames. Based on average values of a number of response quantities, comparable performance could be achieved at design forces lower than currently specified by code for the base-isolated frames.

KEYWORDS: base-isolation; building code; dynamic response; relative performance; steel frame.

1. INTRODUCTION

This paper presents the results of an analytical investigation in which the performance of "code-designed" fixed-base and base-isolated structures are compared. The objective of the study is to determine approximately the design force level for a base-isolated structure which will result in performance comparable to that of a fixed-base structure.

Two simple planar frames, a steel concentrically-braced frame (SBF) and a steel special moment-resisting frame (SMF) have been designed using the static lateral load procedure, in accordance with the 1991 Uniform Building Code(UBC). The frames have been designed as both fixed-base and base-isolated. Design parameters for the frames have been selected to represent a large part of the building inventory: frames are 4-story, 3-bay structures, assumed to be located in Seismic Zone 4 (PGA=0.4g), and founded on dense or stiff soil (UBC soil profile S_2). The base-isolated buildings are assumed to be supported on laminated elastomeric isolation bearings, designed to provide an isolated period of 2.5 s, with equivalent viscous damping equal to 15% of critical.

To establish comparable performance, each base-isolated frame has been designed to 100%, 50% and 25% of the code recommended base shear. The response of the fixed-base design on the isolation system has also been considered (this is equivalent to designing an isolated structure to greater than 100% of the code recommended base shear). To facilitate reference to the various design cases, the following nomenclature has been adopted:

FRAME TYPE - DESIGN CASE

where FRAME TYPE is SBF or SMF, and DESIGN CASE is FB (fixed-base), BI.0 (fixed-base design on isolators), BI.1 (base-isolated, designed to 100% of the code recommended base shear), BI.2 (base-isolated, 50% of code) and BI.3 (base-isolated, 25% of code). Thus, SMF-BI.2 refers to the steel moment frame designed to 50% of the code recommended lateral force.

To evaluate the performance of each design, nonlinear time history analyses have been con-

* Research Structural Engineer
National Institute of Standards and Technology, Gaithersburg, Maryland 20899

ducted, for 3 ensembles of earthquakes, using the computer program DRAIN-2D (Kanaan and Powell, 1973). A number of response quantities have been examined, including, the number of frames that exhibit yielding or collapse, the number of yielded superstructure elements, the maximum total and relative roof displacement of the superstructure, first story drift and the maximum displacement of the base-isolation bearing. Statistical analyses of these quantities have been conducted to determine the approximate design force level for the base-isolated structure which would provide performance comparable to that of the fixed-base structure.

2. FRAME DESIGNS

2.1 Building Configuration

The frames under consideration are assumed to be part of a hypothetical four-story office building, which is rectangular in plan, measuring nominally 45.7 m by 22.9 m with 7.62 m bays in both directions. Story heights are 3.66 m for the first story, and 3.35 m for the second, third, and fourth stories. The roof and floors are assumed to be rigid and to act as diaphragms in the horizontal direction. Alternating frames are designed to carry the lateral load; hence, the tributary width for lateral load is 15.3 m and for gravity load is 7.62 m. The plan and a typical section of the building are shown in Figure 1.

2.2 Dead and Live Load

Frames are designed for a roof dead load of 2.75 kPa and a floor dead load of 3.92 kPa. The corresponding live loads are 0.9 kPa and 2.40 kPa, respectively. The total seismic dead weight (W) is 5190 kN for the fixed base frames and 6570 kN for the base-isolated frames.

2.3 Base Shear, Fixed-Base Design

The design base shear, V, for a fixed-base frame is given by (UBC 1991),

$$V = \frac{Z I C}{R_w} W \qquad (1)$$

in which Z is the seismic zone factor, I is the importance factor, R_W is a reduction factor which is measure of the ability of a structure to sustain inelastic deformations without collapse, W is the seismic dead weight, and C is given by,

$$C = \frac{1.25 S}{T^{2/3}} \leq 2.75 \qquad (2)$$

where S is the site soil coefficient, and T is the fundamental period of the structure, in seconds. T is approximated by

$$T = C_t (h_n)^{3/4} \qquad (3)$$

where h_n is the height of the building in feet and $C_t = 0.02$ for the braced frame and 0.035 for the moment frame.

For the fixed-base frames: Z=0.4, I=1, S=1.2, and $R_W = 12$ for the moment frame and $R_W = 8$ for the braced frame.

2.4 Base Shear, Base-Isolated Design

The design base shear for elements above the isolation plane is given by (UBC, 1991)

$$V = \frac{K_{max} D}{R_{WI}} \qquad (5)$$

in which D is the design displacement of the isolation system, K_{max} is the maximum effective stiffness of the isolation system at the design displacement D, as normally determined by experiment, and R_{WI} is similar to R_W, although not equal in value. The design displacement D, in inches, of the isolation system is given by

$$D = \frac{10 Z N S_i T_i}{B} \qquad (6)$$

in which Z is the seismic zone factor; N is a coefficient related to the proximity of the building to the nearest active fault; S_i is the site soil coefficient for isolated structures; B is a coefficient related to the effective damping of the isolation system, and T_i is the fundamental period of the isolated structure. The fundamental

period of the isolated structure is related to K_{min}, the minimum effective stiffness of the isolation system, by

$$T_i = 2\pi\sqrt{\frac{W}{K_{min}g}} \qquad (6)$$

In this investigation, the isolation bearings are modeled as bi-linear hysteretic elements as shown in Fig. 2. The bi-linear model is fairly general and represents sufficiently well the experimentally observed cyclic load-deformation behavior for many types of bearings. The model is defined by initial stiffness K_1, post-yield stiffness K_2 and yield force F_1. Assuming yielding of the isolation system occurs at 5%W and the post-yield stiffness is equal to 10% of the pre-yield stiffness

$$K_2 = K_E - 0.045\frac{W}{D} \qquad (7)$$

where K_E is the effective stiffness of the isolation system at the design displacement D (Fig-.2). Note that with the assumed bi-linear model, $K_{max}=K_{min}=K_E$ (UBC, 1991).

For the base-isolated frames: Z=0.4, S_i=1.5, N=1, T_i=2.5 s, B=1.35, and R_{WI}=3 for both the braced frame and moment frame. This results in a design displacement for the isolation system of 280 mm.

2.5 Final Designs

A summary of the design specified or computed fundamental period and base shears for the various design cases are listed in Table 1. Note, under current guidelines, the moderate 43% reduction in base shear for the base-isolated braced frame, and the mere 14% reduction for the base-isolated moment frame.

Presented in Table 2 are member sizes for the braced frames, and in Table 3 for the special moment frames. All members are standard structural sections, per the American Institute of Steel Construction. Note, due to a limitation on minimum member sizes, no reduction in member size was achieved for the braced frame designed to 25% of the code recommended base shear, hence, there are only 3 distinct isolated designs for the concentric braced system (BI.0, BI.1 and BI.2).

3. EARTHQUAKE TIME HISTORIES

For the dynamic analysis, 18 recorded earthquakes have been selected from the original 30 used by Seed et al. (1976) to develop the S_2 design spectrum of the design provisions. The 18 have peak ground accelerations ranging from $0.11g$ to $0.28g$, and peak ground velocities ranging from 120 mm/s to 360 mm/s. The original 18 form the "As-recorded" ensemble. To conform to the zone 4 design spectrum PGA of $0.4g$, a second ensemble has been created by scaling each record to a peak ground acceleration of $0.4g$. This is referred to as the "PGA" ensemble. The influence of velocity is examined by scaling each record to a peak velocity of 500 mm/sec, which is the average PGV of the ensemble after it has been scaled to $0.4g$. This is referred to as the PGV ensemble.

4. METHOD OF ANALYSIS

Models were developed for the SBF and SMF for analysis using DRAIN-2D (Kanaan and Powell, 1973). In all cases, nodes are located at the geometric beam-column centerline intersection, seismic mass is lumped at the beam-column joint, joints are assumed to be infinitely rigid and a single element is used to model each story column and each girder span.

In all cases, beams and columns are modeled using a beam/column element with typical A36 steel properties (E=200 GPa, F_y=248 MPa) and nominal section properties. Beams and columns are assumed to exhibit an elastic-plastic moment curvature relation, with no hardening in the SBF, and 2% hardening in the SMF. Braces are modeled using buckling truss elements (Jain and Goel 1978) with typical A46 steel properties (E=200 GPa, F_y=317 MPa). Isolators are modeled using bilinear, elastic-plastic springs located at the base of each first story column. The stiffness of the individual isolators are a fraction of the overall isolation system properties, based on the proportion of dead load carried by each

column. A schematic of the DRAIN-2D model for the SBF is shown in Fig. 3, and for the SMF in Fig. 4.

In the time history analyses, P-Δ effects are considered approximately, the dynamic analysis is performed from the deformed static equilibrium position and original elastic stiffness proportional damping, corresponding to 2% in the fundamental mode, is assumed. Analyses have been conducted for the first 30 seconds of each strong motion record in the 3 ensembles, for the 9 design cases. A total of 486 time history analyses have been conducted.

5. RESULTS

Of the 3 ensembles used in the investigation, the PGA ensemble was the most "damaging"; only the results for the PGA ensemble are presented herein. A compilation of all the results may be found in Lin and Shenton (1992). A summary of response statistics for the steel braced frames are presented in Table 4, and for the steel moment frames in Table 5.

5.1 Braced Frame Designs

The "code-designed" base-isolated frame (BI.1) clearly out-performed the fixed-base frame (FB) in almost every response category, as noted in Table 4. This includes the number of frames which exhibit yield (a measure of the incidence of superstructure yielding for a given frame and ensemble), average number of yielded superstructure elements (a measure of the extent of superstructure yielding), time of first superstructure yield and average relative roof displacement. In only one response category did the SBF-BI.1 not perform better than the SBF-FB, that being first story drift ductility (defined as the first story drift divided by the story drift required to cause first yield in the brace). The average first story drift for SBF-BI.1 was 31 mm, while that for the SBF-FB was 28 mm, resulting in a comparable, but slightly larger drift ductility for the BI.1.

As would be expected, the absolute roof displacement for the isolated structures is greater than that of the fixed base design. The total roof displacement is also seen to be relatively insensitive to design force level. Note that the average relative roof displacement for SBF-BI.1 is roughly 1/3 the total roof displacement, indicating near rigid body behavior in the superstructure.

The results in Table 4 are presented in an alternate format in Fig. 5. Plotted in the figure is the isolated response quantity normalized by the fixed-base response quantity, versus the fraction of code recommended base shear. Comparable performance in this figure corresponds to an ordinate value of 1.0. It is obvious from this figure that the design force level required to provide comparable performance varies with performance criterion. The isolated design BI.2 out-performed the fixed-base design when based on incidence and extent of yield; a design force of approximately 85% of code would be required to provide comparable performance when based on relative roof displacement; the code-designed fixed-base frame performed slightly better than the code-designed base-isolated frame when based on drift ductility.

The average peak isolator displacement for the PGA ensemble was 224 mm, 173 mm and 138 mm, for SBF-BI.0, SBF-BI.1 and SBF-BI.2, respectively. In every case, the average is below the design displacement of 280 mm; however, the design displacement was exceeded in 10 of 54 analyses conducted for the isolated braced frame designs. The largest isolator displacement for SBF-BI.1 and the PGA ensemble was 538 mm, almost twice the design displacement.

5.2 Moment Frame Designs

The "code-designed" base-isolated moment frame (SMF-BI.1) out-performed the fixed-base frame (SMF-FB) in a number of categories; however, performance was only comparable in others. The SMF-BI.1 out-performed the SMF-FB when based on average number of yielded superstructure elements, relative roof displacement and first story drift ductility, as noted in Table 5. The two performed comparably when based on incidence of collapse (defined by an

extreme roof displacement and excessive number of yielded members) and extent of superstructure yielding.

It is interesting to note that in this case the average total roof displacement of SMF-BI.1 is slightly lower than that of the fixed-base design. Also, the average relative roof displacement for SMF-BI.1 is roughly 2/3 the total roof displacement. This, in conjunction with the incidence and extent of superstructure yielding for SMF-BI.1, indicates superstructure behavior which is far from rigid or purely elastic, a common assumption in the analysis of isolated structures.

The results in Table 5 are presented in the alternate normalized format in Fig. 6. In this case it is clear that comparable performance is achieved, for almost all response criteria with the PGA ensemble, with an isolated moment frame designed to between 50% and 75% of the code recommended base shear.

The average peak isolator displacement for the PGA ensemble was 150 mm, 139 mm, 100 mm and 76 mm, for SMF-BI.0, SBF-BI.1, SBF-BI.2 and SMF-BI.3, respectively. Again, the average is below the design displacement of 280 mm; however, the design displacement was exceeded in 9 of 72 analyses conducted for the isolated moment frame designs. The largest isolator displacement for SMF-BI.1 and the PGA ensemble was 394 mm, just 1.4 times the design displacement.

6. CONCLUSIONS

In this study the relative performance of "code-designed" fixed-base and base-isolated steel frames have been compared. Results presented indicate that, based on a number of performance criteria, code-designed base-isolated structures perform better than conventional fixed-base structures. Comparable performance can be achieved with an isolated structure designed to a lateral force level less then that required by the 1991 UBC provisions.

Comparable performance in a braced frame can be achieved with a design force level between 50% and 100% of the code recommended value: the actual level of design force varies with response criterion. Comparable performance in a moment frame can be achieved with a design force level between 50% and 100% of the code recommended value. A lateral force corresponding to 50% of the code specified value provides comparable performance in many cases.

7. REFERENCES

1. Jain, A.K., and Goel, S.C. (1978), "Hysteresis Models for Steel Members Subjected to Cyclic Buckling or Cyclic End Moments and Buckling", University of Michigan Department of Civil Engineering, Report No. UMEE 78R6. Dec.

2. Kanaan, A.E. and Powell, G.H. (1973), **DRAIN-2D User Guide**, EERC Report 73-6 and 73-22, University of California, Berkeley, CA. Apr.

3. Lin, A.N. and Shenton III, H.W. (1992), "Seismic Performance of Fixed-Base and Base-Isolated Steel Frames," ASCE, Journal of Engineering Mechanics, Vol. 118, No. 5, pp 921-941.

4. Seed, H.B., Ugas, C. and Lysmer, J. (1976), "Site-Dependent Spectra for Earthquake-Resistant Design," Bulletin of the Seismological Society of America, Vol. 66, No. 1, pp. 221-243, Feb.

5. *Uniform Building Code* (1991), International Conference of Building Officials, Whittier, Calif.

Table 4. Summary of Steel Braced Frame Results for PGA Ensemble

Design	# of frames that exhibit yield	Average # of Yielded Elements	Average Time of first yield (s)	Average Roof displacement with respect to ground (mm)	Average Roof displacement with respect to isolators (mm)	Average First floor ductility ratio
FB	18	7.3	5.1	106	106	2.2
BI.0	3	1.1	15.4	253	38	1.4
BI.1	6	2.4	9.0	257	89	2.4
BI.2	12	5.1	6.9	246	159	9.4

Table 5. Summary of Steel Moment Frame Results for PGA Ensemble

Design	# of frames that collapse	# of frames that exhibit yield	Average # of Yielded Elements	Average Time of first yield (s)	Average Roof displacement with respect to ground (mm)	Average Roof displacement with respect to isolators (mm)	Average First floor ductility ratio
FB	0	17	34.1	5.1	149	149	2.1
BI.0	0	14	13.1	7.6	129	78	1.0
BI.1	0	17	21.7	5.3	145	96	1.2
BI.2	2	18	33.2	6.1	175	137	2.6
BI.3	5	18	33.5	6.1	184	163	4.3

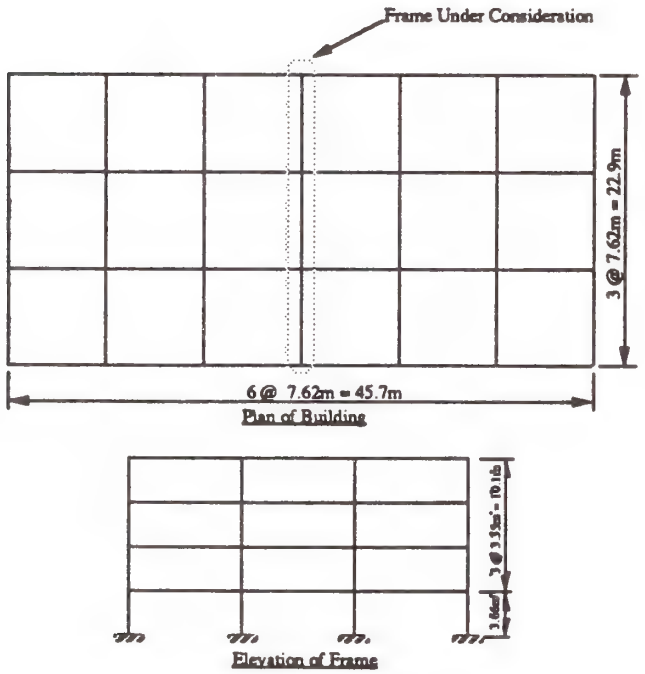

Figure 1. Building Plan and Frame Elevation

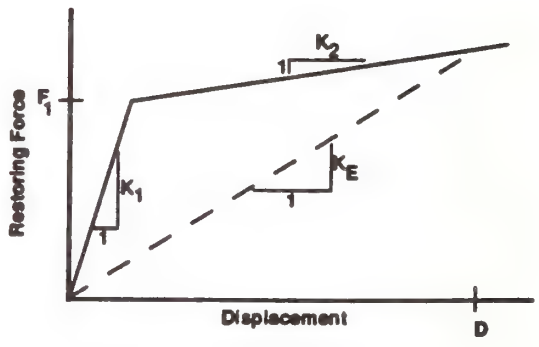

Figure 2. Isolation Bearing Bi-Linear Model

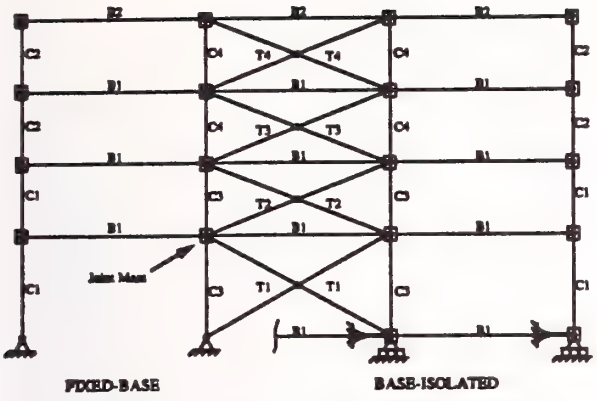

Figure 3. DRAIN-2D Model of Steel Concentric Braced Frame

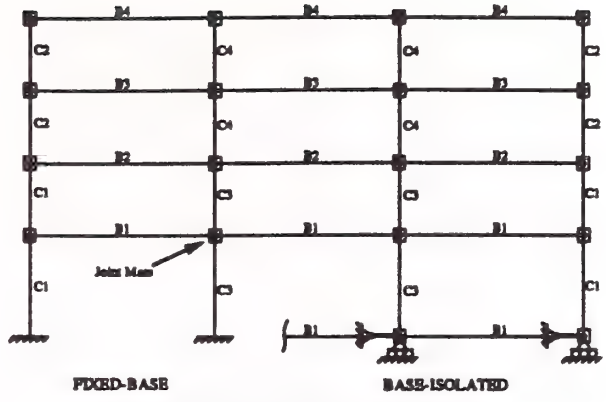

Figure 4. DRAIN-2D Model of Steel Moment Frame

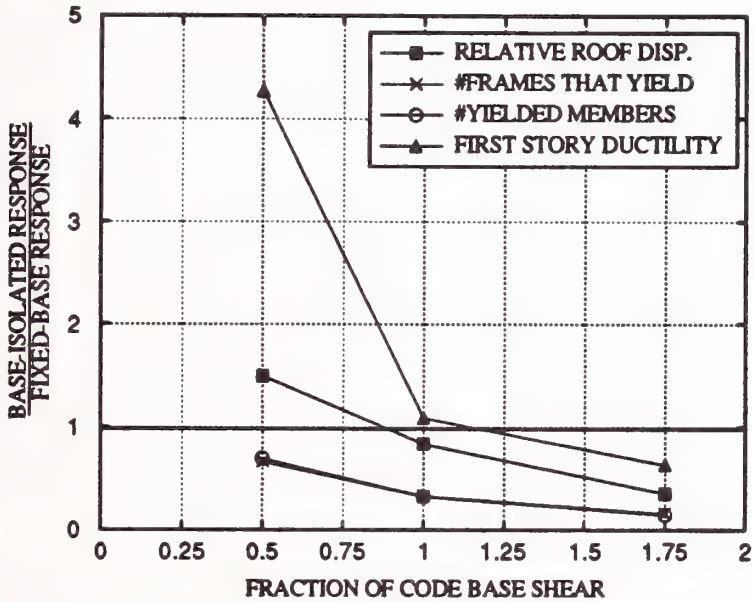

Figure 5. Normalized Results for Steel Braced Frame and PGA Ensemble

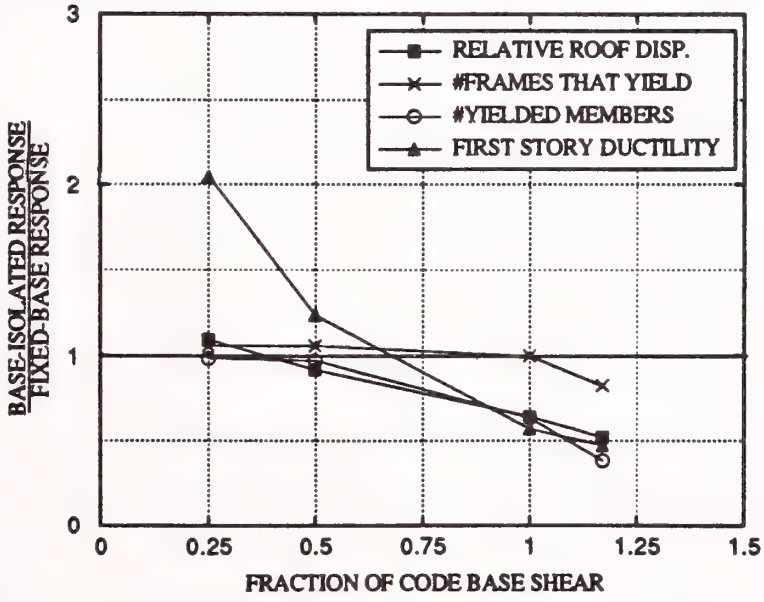

Figure 6. Normalized Results for Steel Moment Frame and PGA Ensemble

Manual for Menshin Design of Highway Bridges

by

Kazuhiko Kawashima[1], Kinji Hasegawa[2], and Hiroyuki Nagashima[3]

ABSTRACT

A three-year research program on "Development of Menshin Design of Highway Bridges" was made from April 1989 to March 1992. Concentrated efforts were paid to develop energy dissipating devices and falling-off prevention devices for bridges. An appropriate design method of highway bridges with energy dissipating devices and favorable application of the menshin design to highway bridges were studied. Final accomplishment of the three-year research was compiled in the form of "Manual for Menshin Design of Highway Bridges" in March 1992. This paper outlines the Manuals.

KEY WORDS
Menshin Design, Highway Bridge, Joint Research Program, Manual for Menshin Design

1. INTRODUCTION

A three-year Joint Research Program between the Public Works Research Institute and 26 groups consisting of 28 private firms on "Development of Menshin Design of Highway Bridges" was made from April 1989 to March 1992. This program intended to develop a rational seismic design method of highway bridges with energy dissipating devices. The highway bridges with span length from 20 m to 100 m were considered as the major target for this Joint Research Program.

As will be discussed later, "menshin" means "reduction of response" in Japanese. Although the menshin design is close with the base-isolation, natural period of bridge is not forcibly elongated in the menshin design, because there are various restrictions for increasing the natural period. Instead of elongating the natural period, emphasis is placed in the menshin design for increasing energy dissipating capability and distribution of lateral force to as many substructures as possible for decreasing lateral force for design of substructures.

As shown in Table 1, concentrated efforts were paid to 1) development of menshin (energy dissipating) devices for highway bridges, 2) development of falling-off prevention devices and expansion joints appropriate for the menshin bridges, 3) development of rational and simple menshin design method and 4) favorable application of menshin design to highway bridges.

In the research project, four high damping rubber bearings, 2 sliding friction dampers, a steel damper, a roller menshin bearing a link bearing and a viscous damper were newly developed for bridges (refer to Fig. 1). The menshin devices for highway bridges have to be more compact and more weather-proof than the base-isolation devices for buildings since the menshin devices are installed at narrow and exposed crest of bridge columns.

The knock-off mechanism at an abutment to ease the impact force induced by the collision between the deck and the abutment (refer to Photo 1), and a finger type expansion joint (refer to Photo 2) which is distinguished from regular finger joints by the transverse movement as well as the longitudinal movement were also developed.

In the research project, a simple but rational menshin design method was developed. A series of shaking table tests were made to study the response of menshin bridges, and to provide realistic data of the seismic response of menshin bridges (refer to Photo 3). Analysis of strong motion records measured at a menshin bridge was also made.

From the study to investigate the favorable application of menshin design, it was found that the menshin design is effective for constructing super-multi-span continuous bridge with total deck length over 1 km. Application of the menshin design for seismic retrofit of exiting bridges and deck connection for making existing simply supported girder bridges continuous was also studied (refer to Photo 4).

The reports of the project were compiled and published by the Public Works Research Institute in the form of the Joint Research Report. As well as these reports, as the final accomplishment of the three-year research program, the Manual for Menshin Design of Highway Bridges was compiled.

This paper presents the outline of the Manual.

2. SCOPES AND CONTENTS OF THE MANUAL

The Manual presents the seismic design method of highway bridges including design details when "the Structures Expecting Reduction of Inertia Force", which is specified in the "Part V Seismic Design" of the "Specifications of Design of Highway Bridges", is adopted. Application of the

1) Head of Earthquake Engineering Division, Earthquake Disaster Prevention Department, Public Works Research Institute, Ministry of Construction
2) Assistant Manager of Planning Division, Road Bureau, Ministry of Construction Proper
3) Technical Research Division, Kantoh Regional Construction Bureau, Ministry of Construction

menshin design to seismic strengthening of substructures and connection of adjacent decks for making existing simply supported girder bridges continuous is also presented.

It should be noted that although the description of the Manual is given in the format of the specifications, it merely represents the accomplishments of the three-year research program, and it is not the mandate specifications.

The table of contents of the Manual is as follows:

1. General
   1.1 Scope of Application
   1.2 Definition of Terms
2. Basic Principle of Menshin Design
3. Menshin Design
   3.1 General
   3.2 Lateral Force Coefficient for Seismic Coefficient Method
   3.3 Lateral Force Coefficient and Equivalent Lateral Force Coefficient for Bearing Capacity Method
   3.4 Characteristics value for Menshin Devices
   3.5 Computation of Natural Period of Bridge
   3.6 Computation of Modal Damping Ratio of Bridges
4. Design of Menshin Devices
   4.1 Basic Principle for Design of Menshin Devices
   4.2 Design of Laminated Rubber Bearings
   4.3 Design of Lead Rubber Bearings
   4.4 Design of High Damping Rubber Bearings
   4.5 Design of Steel Dampers
   4.6 Design of Friction Dampers
   4.7 Design of Viscous Dampers
   4.8 Design of Roller Dampers
5. Dynamic Response Analysis
   5.1 General
   5.2 Dynamic Response Analysis Method
   5.3 Analytical Models
   5.4 Design Seismic Forces
   5.5 Check of Safety
6. Design Details
   6.1 General
   6.2 Gap between Structures
   6.3 Falling-off Prevention Devices
   6.4 Knock-off Devices
   6.5 Details of Expansion Joints
7. Approving Tests of Menshin Devices
   7.1 General
   7.2 Approving Tests for Confirming Requirements for Dynamic Loads
   7.3 Approving Tests for Confirming Requirements for Static Loads
8. Seismic Retrofit of Existing Bridges with Use of Menshin Design
9. Application of Menshin Design for Making Existing Simply Supported Girder Bridges Continuous

Appendices
1. Procedure of Menshin Design
2. Menshin Devices for Highway Bridges
3. References for Dynamic Response Analysis
4. Expansion Joints and Falling-off Prevention Devices for Highway Bridges
5. Design Example of Prestressed Concrete Bridges
6. Design Examples of Steel Girder Bridges
7. Design Examples of Super-multi-span Continuous Bridges
8. Design Examples for Seismic Retrofit
9. Design Examples for Making Existing Simply Supported Girders Continuous
10. Standard Acceleration Ground Motions Recommended for Dynamic Response Analysis

3. BASIC PRINCIPLE OF MENSHIN DESIGN

Whether the menshin design should be adopted or not has to be decided based on the advantages of increasing energy dissipating capability from not only seismic safety but function at normal time.

In general, menshin design can be adopted with advantage for the following conditions:

1) bridges on stiff and stable soils
2) bridges with stiff substructures with short natural period

It is recommended that the natural period of the bridge designed by the menshin design is at least 1.5 times longer than that of the bridge without menshin devices. Such elongation of the natural period of the menshin bridge makes the coupling vibration so small that the deformation of the bridge be concentrated at the menshin devices.

The most important decision of the menshin design is how much increase of the natural period be made. In Japan soils are generally very weak at the bridge construction sites. Significant earthquakes with magnitude over 8, which produce long period ground motions, occur at shorter recurrence period than other countries. Taking account such evidences into account, the design seismic force level is take very high for design of highway bridges in Japan in comparison with the seismic force level adopted in U.S.A., New Zealand and Italy. The natural period at which the design acceleration decrease with increasing the natural period is taken longer, i.e., 1.1 second for type I soils (stiff site), 1.3 second for type II soils (medium site) and 1.5 second for type III soils (soft soils). Therefore, the advantage for reducing deck response can be realized only by elongating the natural period longer than 1.1 ~1.5 second.

However elongation of the natural period brings the increase of the deck response displacement, and this requires the adoption of joints with long legs. This is, however, a crucial requirements difficult to adopt, in particular, for overcrossing in city area because it causes noise and vibration pollution, which is the most serious concern in city area. Furthermore it will have the disadvantage for maintenance because replacement of the damaged expansion joint due to traffic load as well as the pavement adjacent

to the joint has to be frequently made.

Based on these reasons, it is not adopted to forcibly elongate the natural period in order to decrease the deck response acceleration. It is therefore more appropriate to adopt the concept of base isolation not for elongating the natural period but for increasing energy dissipating capability. Distribution of the inertia force to as many substructures as possible, which is the practice adopted in Japan for long time, is also significantly advantageous.

Therefore basic principle recommended for introducing the base isolation to highway bridges in Japan is as follows :

1) Distribute the inertia force to many substructures so intentionally that the inertia force be distributed equally by selecting the spring stiffness of the isolators. Simultaneously, reduce deck response by increasing energy dissipating capability by means of damper.
2) Do not forcible elongate the natural period, but select the natural period so that the resonance of the bridge with soils be avoided.

Such design criteria is no more the "isolation" of the "base". Therefore it is proposed to call the design concept as "menshin". The "menshin" means "reduction of seismic response" in Japanese.

In menshin design, bridges can be designed by following the standard static design method (static frame analysis). More precise approve of the seismic safety can be made by the dynamic response analysis, if required. In such analyses, the menshin devices (isolators and dampers) are idealized by as a set of equivalent linear springs. Equivalent stiffness and the equivalent damping ratio of the isolator and damper are the major parameters used in the analyses. In the static frame analysis, natural period of the bridge can be computed for each seismic design structural unit as :

$$T = 2.01\sqrt{\delta} \qquad (1)$$

$$\delta = \frac{\int w_i \cdot u_i^2}{\int w_i \cdot u_i} \qquad (2)$$

where

T : natural period (sec)

w_i : dead weight (tf/m) of the seismic design structural unit (super structure and substructure above the ground surface assumed in seismic design) at point "i"

u_i : lateral displacement (m) developed in the seismic design structural unit at point "i" when subjected to w_i in the direction considered in design

Damping ratio of the bridges is computed as

$$h = \frac{\Sigma K_{Bi} \cdot u_{Bi}^2 \cdot c_{hi}}{\Sigma K_{Bi} \cdot u_{Bi}^2 \cdot c_i} \qquad (3)$$

$$c_{hi} = h_{Bi} + \frac{h_{Pi}}{K_{Pi}} + \frac{h_{Fui}}{K_{Fui}} + \frac{h_{F\theta i} \cdot H^2}{K_{F\theta i}}$$

$$c_i = 1 + \frac{K_{Bi}}{K_{Pi}} + \frac{K_{Bi}}{K_{Fui}} + \frac{K_{Bi} \cdot H^2}{K_{F\theta i}}$$

where

h : Modal damping ratio of bridge

h_{Bi} : Damping ratio of i-th damper

h_{Pi} : Damping ratio of i-th pier/abutment

h_{Fui} : Damping ratio of i-th foundation associated with translational movement

$h_{F\theta i}$: Damping ratio of i-th foundation associated with rotation

K_{Pi} : Equivalent stiffness of i-th pier/abutment

K_{Fui} : Translational stiffness of i-th foundation

$K_{F\theta i}$: Rotational stiffness of i-th foundation

u_{Bi} : Design displacement of i-th menshin device

H : Height from the bottom of pier to the gravity center of deck

Eq.(3) give the approximate estimation of the damping ratio of bridge assuming that translation and rotation of the foundation are developed only by the inertia force of the deck. When the effect of the inertia force of piers and abutments for evaluating the translation and rotation of the foundation can not be disregarded, it is appropriate to compute the modal damping ratio as

$$h = \frac{\sum_{j=1}^{n} \phi_{ij}^T \cdot h_j \cdot K_j \cdot \phi_{ij}}{\phi_i^T \cdot K \cdot \phi_i} \qquad (4)$$

where

ϕ_{ij} : Mode vector of j-th structural component for i-th mode

h_j : Damping ratio of j-th structural component

K_j : Stiffness matrix of j-th structural component

ϕ_i^T : Mode vector of bridge for i-th mode

K : Stiffness matrix of bridge

Table 2 shows the damping ratio recommended for structural components for Eqs.(3) and (4).

4. DESIGN FORCE FOR MENSHIN DESIGN

In menshin design, the menshin devices are designed by the Seismic Coefficient Method and the Bearing Capacity Method. In both method, the lateral force is statically applied to the bridge, and the seismic safety is examined based on the allowable stress design approach in the Seismic Coefficient Method and bearing capacity basis considering ductility in the Bearing Capacity Method. Bridges are designed by the Seismic

Coefficient Method, and then the ductility is checked for reinforced concrete piers by the Bearing Capacity Method.

In the Seismic Coefficient Method, the design lateral force coefficient k_h is given as

$$k_h = c_Z \cdot c_G \cdot c_I \cdot c_T \cdot c_E \cdot k_{h0} \geq 0.1$$

where

$$c_T \cdot c_E \geq 0.8 \qquad (5)$$

where

k_h : Lateral force coefficient
c_Z : Modification factor for zone (refer to Fig. 2)
c_G : Modification factor for ground condition (refer to Table 3)
c_I : Modification factor for importance (refer to Table 4)
c_T : Modification factor for structural response (refer to Table 5)
c_E : Modification factor for energy dissipation capability (refer to Table 6)
k_{h0} : Standard design horizontal seismic coefficient (= 0.2)

Those factors excluding c_E are the ones specified in the Specifications of Design of Highway Bridges. The modification coefficient c_E takes a value as shown in Table 6 depending on the first modal damping ratio of the bridge. Reduction of the design lateral force as large as 20 % is proposed in the Manual.

In the Bearing Capacity Method, the lateral force coefficient k_{hc} and the equivalent lateral force coefficient k_{he} are given as

$$k_{he} = \frac{k_{hc}}{\sqrt{2\mu - 1}} \geq 0.3 \qquad (6)$$

$$k_{hc} = c_Z \cdot c_I \cdot c_R \cdot c_E \cdot k_{hc0} \qquad (7)$$

where

k_{he} : Equivalent lateral force coefficient for Bearing Capacity Method
k_{hc} : Lateral force coefficient for Bearing Capacity Method
c_Z : Modification factor for zone (refer to Fig. 2)
c_I : Modification factor for importance (refer to Table 4)
c_R : Modification factor for structural response (refer to Table 7)
c_E : Modification factor for energy dissipation capability
k_{hc0} : Standard lateral force coefficient for Bearing Capacity Method (=1.0)
μ : Allowable ductility factor of reinforced concrete piers

The modification factors excluding c_E are the ones specified in the Specifications of Design of Highway Bridges. The modification factor c_E depends on the modal damping ratio of the bridge, and takes a value of Table 8. Reduction of the design force as large as 30 % is proposed.

5. DESIGN OF MENSHIN DEVICES

5.1 Characteristics Value of Menshin Devices

In the menshin design, the displacement assumed in design for the devices u_B (design displacement of menshin device), the equivalent stiffness K_B and the equivalent damping ratio h_B of the menshin device are the key factors. They are evaluated as:

(1) Design Displacement of Menshin Device

The design displacement of menshin device is evaluated as

$$u_B = \frac{k_h \cdot W_u}{K_B} \quad \text{(S. C. Method)} \qquad (8)$$

$$u_B = \frac{k_{hc} \cdot W_u}{K_B} \quad \text{(B. C. Method)} \qquad (9)$$

where

u_B : Design displacement (m) of menshin device
k_h : Lateral force coefficient by Eq.(5) for Seismic Coefficient Method
k_{hc}: Lateral force coefficient by Eq.(6) for Bearing Capacity Method
K_B : Equivalent stiffness (tf/m) of menshin device
W_u : Weight of superstructure (tf) supported by the menshin device

(2) Equivalent Stiffness and Equivalent Damping Ratio

The equivalent stiffness and the equivalent damping ratio of menshin device are evaluated from the hysteresis loops as

$$K_B = \frac{F(u_{BE}) - F(-u_{BE})}{2u_{BE}} \qquad (10)$$

$$h_B = \frac{\Delta W}{2\pi W} \qquad (11)$$

where

K_B : Equivalent stiffness (tf/m) of menshin device
h_B : Equivalent damping ratio of menshin device
u_{BE} : Effective design displacement (m) of menshin device, and is given as
$$u_{BE} = c_B \cdot u_B \qquad (12)$$
u_B : Design displacement (m) of menshin device
c_B : Modification coefficient for evaluating the effective design displacement (=0.7)
$F(u)$: Lateral force required to produce u for the menshin device
W : Strain energy induced in menshin device associated with c_{BE} displacement (refer to Fig. 3)
ΔW : Energy dissipated in menshin device per

cycle (refer to Fig. 3)

5.2 Requirements for Dynamic Load

(1) Menshin devices have to be designed and fabricated so that their equivalent stiffness K_B and equivalent damping ratio h_B be within ± 20 % of the design values. The equivalent stiffness K_B and equivalent damping ratio h_B for this requirement have to be evaluated by Eqs. (10) and (11), and they shall be the ones averaged over K_B and h_B from 4th to 10th loading hysteresis among 10 cyclic loading reversals with harmonic displacement of c_{BE}. This is because deck acceleration and displacement are within tolerable range when the scatter of equivalent stiffness and the equivalent damping ratio are within ± 20 % of the design values. However, the devices which produce unstable hysteretic behavior should not be adopted.
(2) Menshin devices have to be stable against 50 cycles of harmonic loading with displacement of u_B. The number of 50 was determined from the fact that number of load reversals developed during a major earthquake may be about 30. About 50 % tolerance was included in 50.
(3) Deck should return to the rest position even after it was subjected to a large earthquake. Therefore the residual displacement developed in menshin devices after smoothly releasing from the deformed displacement of u_B by Eq. (9) has to satisfy

$$u_{BR} \leqq 0.1 \cdot u_B \qquad (13)$$

where
u_{BR} : Residual displacement (cm)
u_B :
Design displacement(cm) of menshin device by Eq. (9)

(4) The equivalent stiffness and the equivalent damping ratio of menshin devices have to be stable against the change of load condition at normal time, change of natural environment such as the temperature change and cyclic loading developed by an earthquake. Stability has to be examined against the following requirements:

1) cyclic loading due to elongation and shrinkage of deck due to the temperature change and the active load
2) effect of loading hysteresis
3) variation of vertical loading
4) effect of loading rate
5) effect of pre-deformation due to creep and shrinkage
6) direction of excitation
7) change of the equivalent stiffness and the equivalent damping ratio depending on the temperature change

5.3 Requirements for Static Load

(1) Materials and mechanism of menshin devices have to give credit to long term use. They have to be stable against cyclic elongation and shrinkage of deck due to temperature change.
(2) Menshin devices have to be stable against local shear strain. Check of the local shear strain has to be made in accordance of "3.6 Design of Rubber Bearings" of the "Design Guidelines of Bearings".
(3) For rubber-type menshin devices, the creep of rubber in vertical direction due to dead weight of superstructure shall not exceed 5 % of total thickness of the rubber.
(4) The equivalent stiffness of menshin device at -10℃ normalized by the equivalent stiffness at 40 ℃ shall not exceed 1.5. Because the temperatures of -10℃ and 40℃ is for moderate climate area, at cold area they have to be decided based on the appropriate site condition.
(5) Menshin devices have to have appropriate initial stiffness so that harmful displacement of deck due to non-seismic lateral force such as wind effects be avoided.

6. APPROVING TESTS OF MENSHIN DEVICES

6.1 General

Because the menshin device is one of the the important structural components of menshin bridges, their requirements have to be well approved by the tests. There are various types of menshin devices for use of bridges. Based on the mechanism for producing the energy dissipation, the devices may be classified into three groups as

(a) displacement dependent type,
(b) friction force type, and
(c) velocity dependent (viscous) type.

The approving tests for the menshin devices are presented in the Manual for each of the three types.

6.2 Approving Tests for Dynamic Loads

For approving the requirements for dynamic loads presented in 5.2, the following approving tests are provided in the Manual.
(1) Approving test for confirming the equivalent stiffness and the equivalent damping ratio
(2) Approving test for confirming stableness against 50 cycles harmonic load reversals with u_B displacement
(3) Approving test for confirming residual displacement requirement
(4) Approving tests for confirming stableness against variation of load condition at normal time, change of natural environment such as the temperature change and cyclic loading developed by an earthquake. These tests include :

(a) Stableness against Cyclic Load Reversals

Some menshin devices have the dependence of the equivalent stiffness and the equivalent damping ratio on number of cyclic loading. Because considerable change of these parameters during an earthquake produces bridge response significantly different from the one assumed in

design, it is not desirable.

(b) Stableness against Load Hysteresis

In some menshin devices, the equivalent stiffness and the equivalent damping ratio depend on the past experience, in particular, the largest deformation ever experienced. Such dependence of K_B and h_B on the hysteresis ever experienced is significant, it produces different bridge response during an earthquake. Therefore, effect of load hysteresis has to be examined.

(c) Stableness against Change of Compression Force

Compression force applied to the menshin device due to dead weight of superstructure may change associated with the error involved in construction stage and settlement of substructure. If the menshin device shows significantly different stiffness and damping properties due to such change of compression force, it brings different structural response . Therefore, stableness of the equivalent stiffness and the equivalent damping ratio of menshin devices have to be checked.

(d) Stableness against Change of Loading Rate

Because loading rate to the menshin devices is not the same during excitation, dependence of the equivalent stiffness and the equivalent damping ratio on the loading rate has to be examined.

(e) Stableness against Pre-deformation

Menshin devices often start to deform from the displacement drifted to the rest point. This is actually developed if an earthquake occurs when the menshin devices deform due to the deck elongation associated with temperature change and shrinkage of concrete. Because the equivalent stiffness and the equivalent damping ratio depend on the amount of such pre-deformation, their properties have to be checked.

(f) Stableness against Temperature Change

Menshin device have to be stable against daily and yearly change of temperature.

6.3 Approving Tests for Static Loads

For approving the requirements for static loads presented in 5-3, the following tests are required.

(1) Approving test for confirming durability and stableness against cyclic loading associated with the daily and yearly elongation and shrinkage of deck.

(2) Test for evaluating the stiffness of menshin devices subjected to extremely low-rate deformation such as the one encountered due to yearly temperature change and concrete creep. The stiffness of the menshin device during such low-rate deformation is quite important in static design for computing the lateral force developed in substructures due to the temperature change and shrinkage of concrete.

(3) Approving test for confirming the dependence of the equivalent stiffness of menshin device on temperature.

6.4 Two examples of the Approving Test

Approving test methods presented in 6.2 and 6.3 are precisely described in the Manual for each of the displacement dependent type devices, friction force type devices and the velocity dependent type devices. As the example of such approving tests, the test method for confirming stableness against cyclic loading and the test method for confirming the effect of loading rate are briefly described for the displacement dependent type devices in the following.

(1) Approving Test for Confirming Stableness against Cyclic Loads

At the room temperature of 20℃ apply 10 cycles of harmonic lateral load to the menshin device with loading displacement of u_B computed by Eq. (9) or smaller and with the frequency of 0.5 Hz. The vertical load equivalent to the design dead load shall be simultaneously applied. The equivalent stiffness and the equivalent damping ratio from the test have to satisfy Eqs. (14) and (15).

$$R_{KC}=\frac{|K_{Bj}-K_{Bm}|}{K_{Bm}} \quad \begin{matrix}\leqq 0.3\ (j=1.2.3)\\ \leqq 0.1\ (j=4,5\cdots 10)\end{matrix} \tag{14}$$

$$R_{hC}=\frac{|h_{Bj}-h_{Bm}|}{h_{Bm}} \quad \begin{matrix}\leqq 0.3\ (j=1.2.3)\\ \leqq 0.1\ (j=4,5\cdots 10)\end{matrix} \tag{15}$$

where,

R_{KC} : Variation ratio of equivalent stiffness

R_{hC} : Variation ratio of equivalent damping ratio

K_{Bj} : Equivalent stiffness at j-th load reversal(tf/m)

K_{Bm} : Averaged equivalent stiffness by Eq. (16)

h_{Bj} : Equivalent damping ratio at j-th load reversal

h_{Bm} : Averaged damping ratio by Eq. (17)

$$K_{Bm}=\frac{1}{7}\sum_{j=1}^{10}K_{Bj} \tag{16}$$

$$h_{Bm}=\frac{1}{7}\sum_{j=1}^{10}h_{Bj} \tag{17}$$

Being different with Eqs. (10) and (11), the equivalent stiffness and the equivalent damping ratio for the approving tests are defined as

$$K_B=\frac{F(u_B)-F(-u_B)}{2u_B} \tag{18}$$

$$h_B=\frac{\Delta W}{2\pi W} \tag{19}$$

where

K_B : Equivalent stiffness (tf/m) of menshin device

h_B : Equivalent damping ratio of menshin device

u_B : Design displacement (m) of menshin device

$F(u)$: Lateral force (tf) required to produce u displacement for the menshin device

W : Strain energy (tfm) induced in menshin device associated with u_B displacement (refer to Fig. 4)

ΔW : energy dissipated in menshin device per cycle (refer to Fig. 4)

(2) Approving Test for Confirming the Stableness against Loading Rate

At the temperature of 20°C apply 10 cycles of harmonic load with the displacement equivalent to either 100 % of the total thickness of rubber or ± 15 cm. Frequency of the load reversal shall be 0.1 Hz, 0.5 Hz and 1.0 Hz. The equivalent stiffness and the equivalent damping ratio have to satisfy Eqs. (20) and (21).

$$R_{Kf} = \frac{|K_{Bm1} - K_{BmJ}|}{K_{Bm1}} \leqq 0.2 \quad (j=1,2) \qquad (20)$$

$$R_{hf} = \frac{|h_{Bm1} - h_{BmJ}|}{h_{Bm1}} \leqq 0.2 \quad (j=1,2) \qquad (21)$$

where,

R_{Kf} : Variation ratio of equivalent stiffness

R_{hf} : Variation ratio of equivalent damping ratio

K_{Bm1}, K_{Bm2}, K_{Bm3} : Equivalent stiffness by Eq. (16) at frequency of 0.5 Hz, 0.1 Hz and 1.0 Hz, respectively

h_{Bm1}, h_{Bm2}, h_{Bm3} : Equivalent damping ratio by Eq. (17) at frequency of 0.5 Hz, 0.1 Hz and 1.0 Hz, respectively

7. CONCLUDING REMARKS

Excluding specially long-span bridges, it is not easily adopted for highway bridges to reduce the lateral force by forcibly elongating the natural period, because seismic force level is very high even at long natural period, and because the increase of deck response displacement brings various problems such as environmental pollution. Therefore the menshin design, which places emphasis not on the forcible elongation of the natural period but on the increase of energy dissipating capability and distribution of inertia force of superstructure to as many substructures as possible, is proposed. By the menshin design, it is proposed to decrease the lateral force as large as 20 % for the Seismic Coefficient Method and 30 % for the Bearing Capacity Method.

ACKNOWLEDGEMENTS

For executing the three-year joint research project, various supports and encouragement were obtained from many organizations including the Head-quarters of the Ministry of Construction. Without endeavour of more than 100 participants from the 28 private firms, this project could not be successfully made. The authors express their sincere thanks for all who participated in this Joint Research Program.

REFERENCES

1) Public Works Research Institute and 28 Private Firms : Report of the Joint Research on Menshin Systems for Highway Bridges, No. 1, July 1990, No. 2, July 1991 and No. 3, March 1992, Joint Research Report, No. 44, No. 60 and No. 75, Public Works Research Institute (in Japanese)

2) Public Works Research Institute and 28 Private Firms : Manual for Menshin Design of Highway Bridges (Draft), March 1992, Joint Research Report, Public Works Research Institute (in Japanese)

3) Japan Road Association : Part V Seismic Design of the Specifications of the Design of Highway Bridges, February 1990 (in Japanese)

4) Technology Research Center for National Land Development : Guidelines for Base Isolation of Highway Bridges, March 1989 (in Japanese)

5) Japan Road Association : Guide-Specifications of Design of Bearings, July 1991 (in Japanese)

6) Buckle, I. G. and Mayes, R. L. : Seismic Isolation : History, Application and Performance - A World View, Earthquake Spectra, Vol. 6, No. 2, May 1990

7) AASHTO : Guide Specifications for Seismic Isolation Design, June 1991

8) McKay, G. R., Chapman, H. E. and Kirkcaldie, D. K. : Seismic Isolation : New Zealand Application, Earthquake Spectra, Vol. 6, No. 2, May 1990

9) Guidelines for Seismic Design of Bridges with Isolation/Dissipator Devices, Antiseismic Protection of Structures on the Autostrade S.p.A/ Network, October 1991

10) Kawashima, K., Hasegawa, K. and Nagashima, H. : A Perspective of Menshin Design for Highway Bridges in Japan, Proc. 1st U.S.-Japan Workshop on Earthquake Protective Systems of Highway Bridges, National Center for Earthquake Engineering Research, Buffalo, N.Y., U.S.A., September 1991

11) Kawashima, K., Hasegawa, K. and Nagashima, H. : Experiment and Analysis on Seismic Response of Menshin Bridges, Proc. 1st U.S.-Japan Workshop on Earthquake Protective Systems of Highway Bridges, National Center for Earthquake Engineering Research, Buffalo, N.Y., U.S.A., September 1991

Table 2 Damping Ratio Recommended for Structural Components

Structural Components	Steel	Concrete
Superstructures	0.02～0.03	0.03～0.05
Menshin Device	Damping Ratio by Eq.(11)	
Pier/Columns	0.03～0.05	0.05～0.1
Footing	0.1～0.3	

Table 3 Modification Factor for Ground Condition c_G

Ground Group	I	II	III
c_G	0.8	1.0	1.2

Table 4 Modification Factor for Importance c_I

Group	c_I	Definition
1st class	1.0	Bridges on expressway (limited access highways), general national road and principal prefectural road. Important bridges on general prefectural road and municipal road.
2nd class	0.8	Other than the above

Table 5 Modification Factor for Structural Response c_T

Ground Group	Structural Response Coefficient c_T		
Group I	$T < 0.1$ $c_T = 2.69T^{1/3} \geqq 1.00$	$0.1 \leqq T \leqq 1.1$ $c_T = 1.25$	$1.1 < T$ $c_T = 1.33T^{-2/3}$
Group II	$T < 0.2$ $c_T = 2.15T^{1/3} \geqq 1.00$	$0.2 \leqq T \leqq 1.3$ $c_T = 1.25$	$1.3 < T$ $c_T = 1.49T^{-2/3}$
Group III	$T < 0.34$ $c_T = 1.80T^{1/3} \geqq 1.00$	$0.34 \leqq T \leqq 1.5$ $c_T = 1.25$	$1.5 < T$ $c_T = 1.64T^{-2/3}$

Table 6 Modification Factor for Energy Dissipation Capability c_E

Damping Ratio h	Modification Factor c_E
$h < 0.1$	1.0
$h \geqq 0.1$	0.9

Table 7 Modification factor for Structural Response c_R

Ground Group	Structural Response Coefficient c_R		
Group I	$T_{EQ} \leqq 1.4$ $c_R = 0.7$		$1.4 < T_{EQ}$ $c_R = 0.876T_{EQ}^{-2/3}$
Group II	$T_{EQ} < 0.18$ $c_R = 1.51\ T_{EQ}^{1/3} \geqq 0.7$	$0.18 \leqq T_{EQ} \leqq 1.6$ $c_R = 0.85$	$1.6 < T_{EQ}$ $c_R = 1.16T_{EQ}^{-2/3}$
Group III	$T_{EQ} < 0.29$ $c_R = 1.51T_{EQ}^{1/3} \geqq 0.7$	$0.29 \leqq T_{EQ} \leqq 2.0$ $c_R = 1.0$	$2.0 < T_{EQ}$ $c_R = 1.59T_{EQ}^{-2/3}$

Table 8 Modification Factor for Energy Dissipating Capability

Damping Ratio h	Modification Factor c_E
$h < 0.1$	1.0
$0.1 \leqq h < 0.12$	0.9
$0.12 \leqq h < 0.15$	0.8
$0.15 \leqq h$	0.7

Fig. 1 Menshin Devices Developed

TYPE	OUTLINE OF MENSHIN DEVICE
HIGH DAMPING RUBBER BEARING	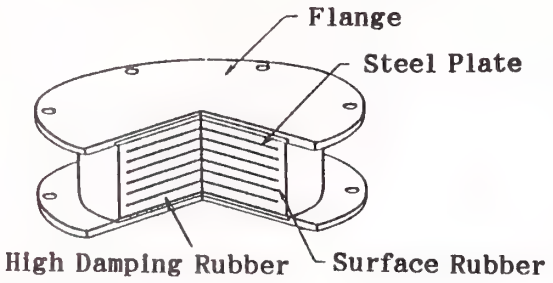
SLIDE FRICTION -RUBBER BEARING	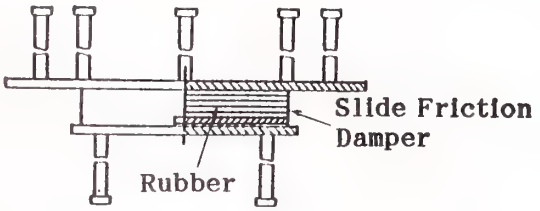
STEEL DAMPER	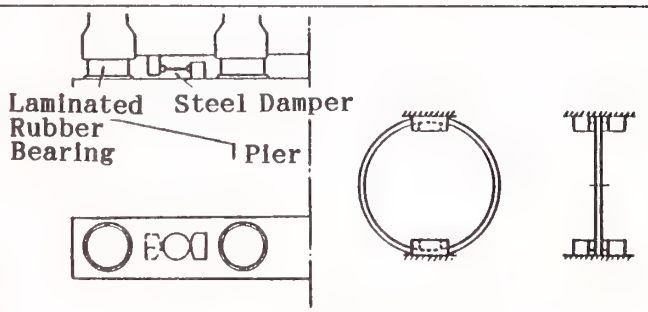
ROLLER MENSHIN BEARING	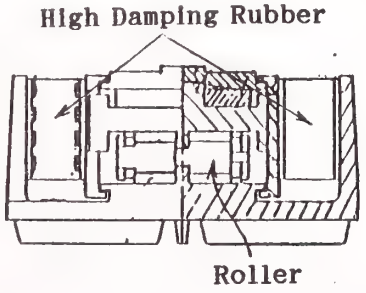
VISCOUS	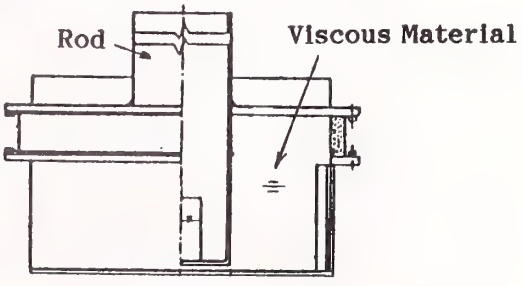

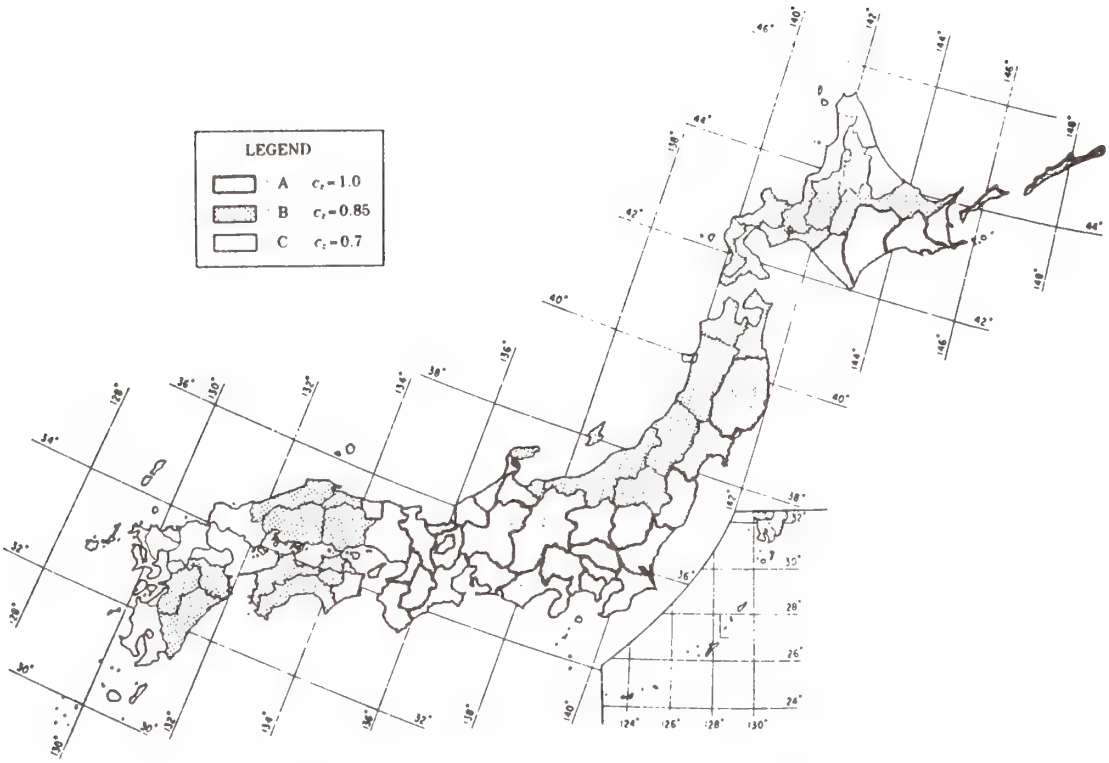

Fig. 2 Modification Factor for Zone c_z

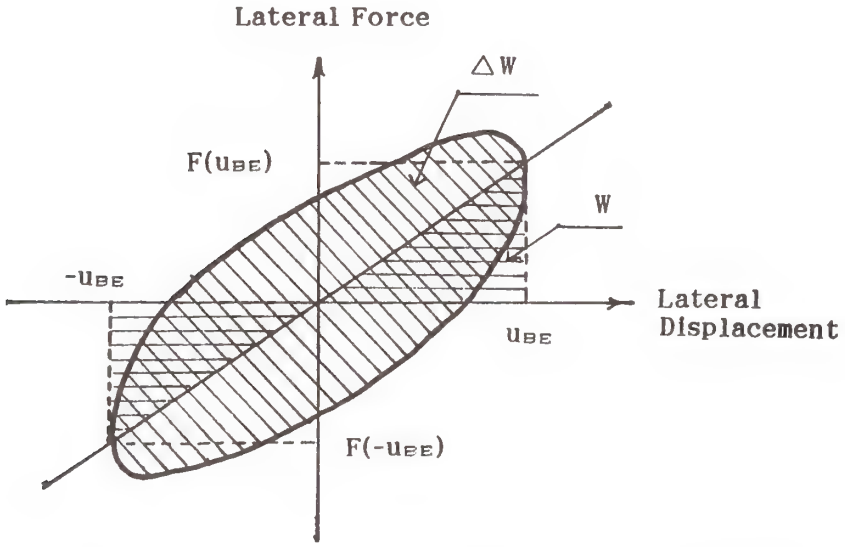

Fig. 3 Definition of Equivalent Stiffness and Equivalent Damping Ratio of Menshin Device for Design of Menshin Device

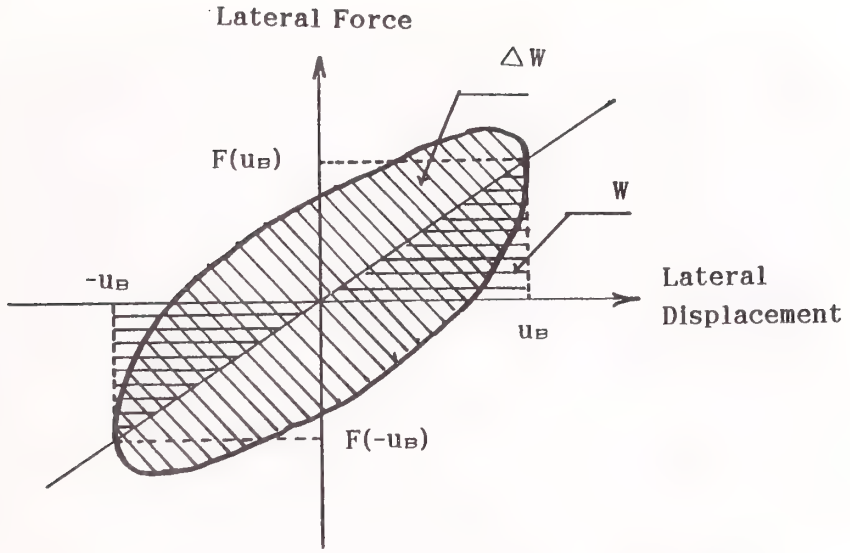

Fig. 4 Definition of Equivalent Stiffness and Equivalent Damping Ratio of Menshin Device for Approving Tests

Photo 1 Knock-off Abutment

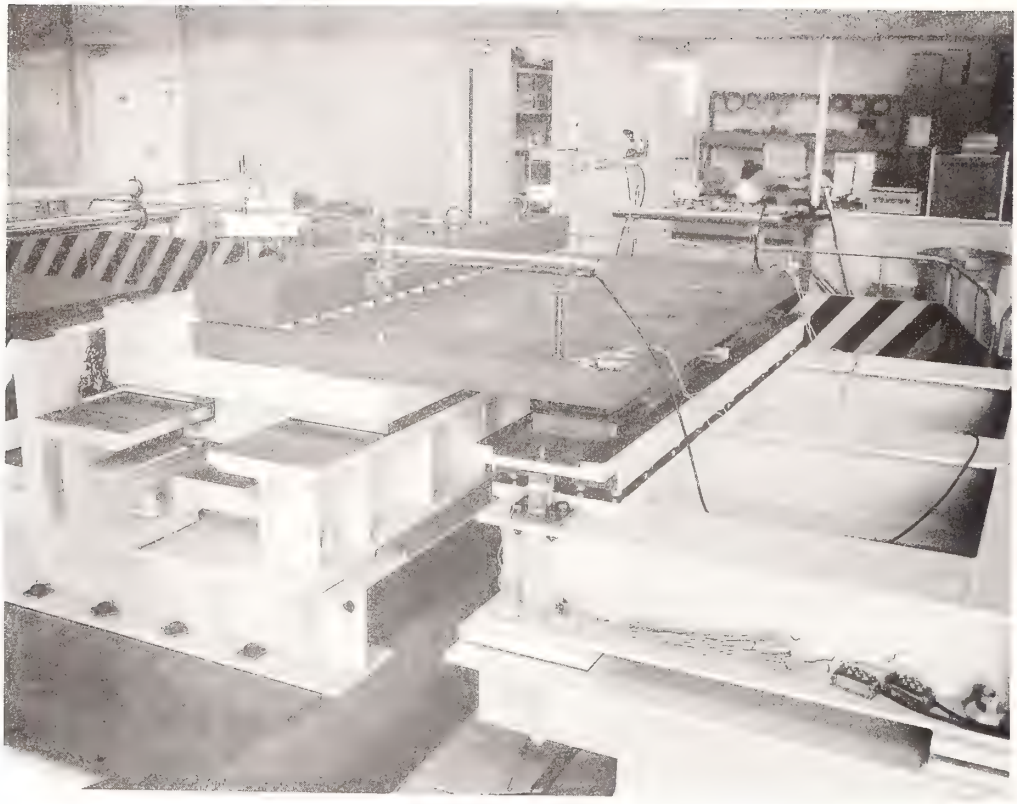

Photo 2 Expansion Joint Movable in Longitudinal and Transverse Directions

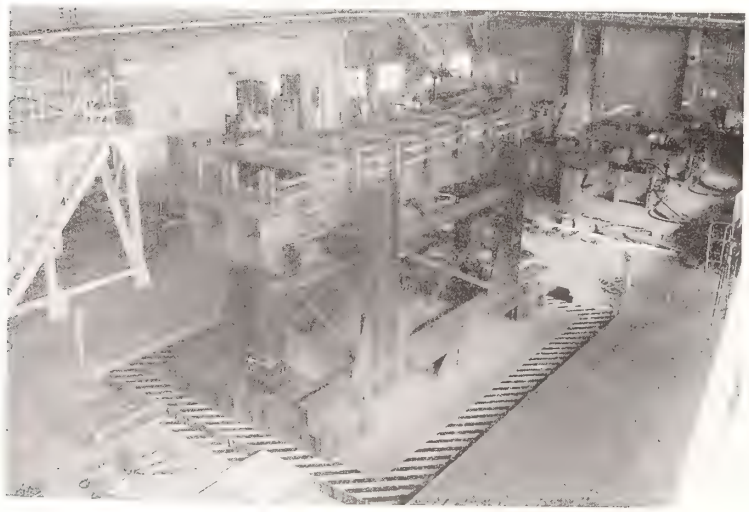

Photo 3 Shaking Table Tests for Studying Structural Response of Menshin Bridges

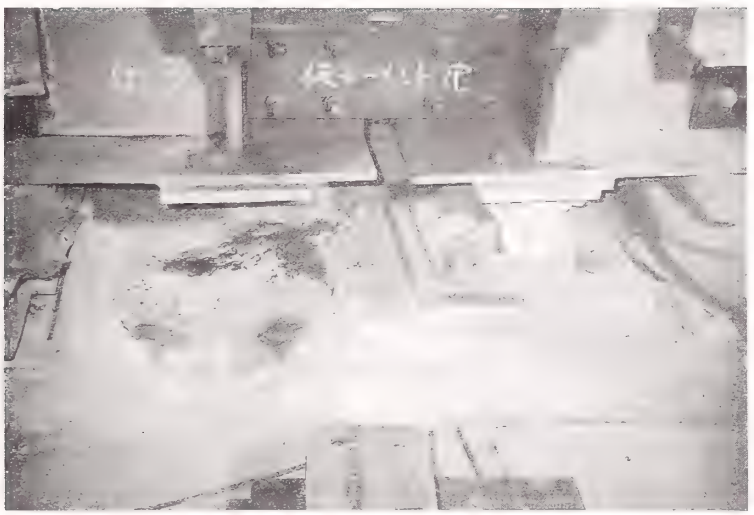

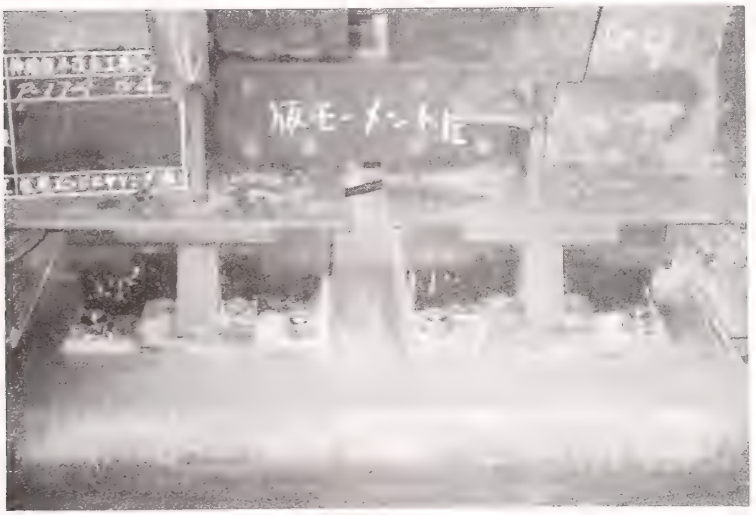

Photo 4 Deck Connection of Existing Bridge

Friction Controllable Bearings for Sliding Base Isolation Systems

by

Maria Qing Feng and Masanobu Shinozuka*

ABSTRACT

Recently, sliding base isolation systems began to be utilized widely in civil and architectural engineering as exemplified by the recent decision on the part of US Federal Government (General Services Administration) to deploy 250-300 spherical sliders to base-isolate the 100 year old, 5-story and 60,000 ton Court of Appeals Building in San Francisco. While the building survived the 1906 San Francisco Earthquake, it was damaged by the Loma Prieta earthquake. Sliding base isolation systems, it is generally perceived, have disadvantages in that they are not effective for small to medium earthquakes, and may not be able to maintain the same value of friction coefficient under a prolonged inactivity and that they may suffer from excessive displacements under strong earthquakes. This paper presents the results of a recent experimental and analytical study jointly performed by Princeton University and Taisei Corporation (Refs. 1 and 2) demonstrating that the use of friciton controllable bearings can not only neutralize the disadvantages indicated above but also make it possible to take full advantage of the beneficial features of sliding base isolation; its inherent effectiveness in limiting the transfer of the ground acceleration to the structure.

KEY WORDS

Hybrid sliding isolation, Friction controllable sliding bearings, Earthquakes, Instantaneous optimal control, Shaking table

*Dept. of Civ. Engrg., Princeton Univ., Princeton, NJ 08544

1 INTRODUCTION

The purpose of this research is to physically develop a sliding bearing that can actively control the friction force on the sliding interface and to demonstrate by shaking table experiments and numerical simulation that the difficulties associated with sliding isolation systems can be significantly alleviated, if not totally eliminated, by such a device. More specifically, the purpose is:

1. to propose and physically develop a friction controllable sliding bearing and a hybrid sliding isolation system using such bearings,

2. to develop control algorithms for controlling the friction force which has nonlinear characteristics, and

3. to analytically and experimentally demonstrate that such a hybrid isolation system can indeed intelligently control the friction force on the sliding interface so as to confine the sliding displacement in an acceptable range, to reduce the residual displacement, and at the same time, to minimize the transfer of seismic force to the structure.

The hybrid isolation system using friction controllable bearings (FCB's) is conceptually depicted in Figs. 1 with a bridge structure resting on the bearings. Each bearing has a fluid chamber which is connected to a pressure control system composed of a servo valve, an accumulator and a computer. The friction on the interface between the bearing and the ground is controlled by adjusting the fluid pressure in the chamber. The computer calculates an appropriate signal to control the fluid pressure based on the observed

structural response, such as response acceleration and sliding displacement, and sends it to the pressure control device as shown in Figs. 1.

The idealized section view of the friction controllable sliding bearing is given in Fig. 2. The bearing made of steel is of disk shape containing a fluid chamber inside which is sealed by a rubber O-ring around the circular perimeter just inside the sliding surface of the bearing. A sliding material such as PTFE plate is placed on the sliding surface.

The word "HYBRID" is used for this system for the following reason. The system can be a paasive sliding isolation system as long as the pressure of the bearing chamber, and thus the friction is kept at a constant value. At the same time, the system can be an active system as long as the pressure is controlled so that the friction is controlled. In the analytical formulatin involving such a hybrid system, the control force does not appear in the equation of motion as an independent term like the force from an actuator. The active control in this case is implemented through the friction term in the equation, and in that sense the system may also be interpreted as "Semi-Active". From the view point of the energy requirement to control the isolation device, the system has a significant advantage since the pressure control does not need as much energy as the common active structural control by actuators would require.

2 ANALYTICAL MODEL

A rigid structure supported by the friction controllable sliding bearings is considered. The motion of the structure can be modeled by a single-degree-of-freedom (SDOF) model as shown in Fig. 3. The equations of motion of the structure under earthquake excitation can then be written as follows.

1. Sticking Phase — Phase I

$$\dot{x} = 0, \quad x = const. \tag{1}$$

2. Sliding Phase — Phase II

$$\ddot{x} = -\ddot{z} - f \ \mathrm{sgn}(\dot{x}), \tag{2}$$

3. Criteria for transition from Phase I to Phase II

$$|\ddot{z}| > f \tag{3}$$

4. Criteria for transition from Phase II to Phase I

$$\dot{x} = 0 \tag{4}$$

$$|\ddot{x}| < 2f \tag{5}$$

where x is the sliding displacement of the mass relative to the ground; $\ddot{z}$ is the input earthquake acceleration; μ is the coefficient of friction on the sliding interface; f is the normalized friction force defined as $f = \mu g$.

In the sticking phase, Eq. 1 governs the motion of the structure until the Eq. 3 becomes true. As soon as the condition in Eq. 3 is met, the sliding phase starts and Eq. 2 governs the sliding motion. During the sliding phase, whenever $\dot{x}$ becomes zero, the criterion, Eq. 4, is checked to determine the subsequent behavior. Validity of the inequality given by Eq. 4 is the condition for entering the sticking phase. That is, if the inequality holds, the structure will stick to the ground and Eq. 1 apply. If the criterion given by Eq. 4 is not satisfied, Eq. 1 will continue to govern the the subsequent sliding motion.

On the other hand, the normalized friction force f on the sliding interface between the structure and the ground is controlled by changing the fluid pressure in the bearing chamber through a pressure control system consisting of a computer, servo valve, amplifier, etc. The dynamic characteristics of the pressure control system are assumed to follow the first order time delay model:

$$T\dot{p} + p = u \tag{6}$$

where, p is the pressure in the fluid chamber of bearing; u is the pressure control signal from computer; T is the time constant

The normalized friction force f is negatively proprtional to the pressure p in the bearing chambe:

$$f = -c_1 p + c_2 \tag{7}$$

where c_1 and c_2 are constants.

3 INSTANTANEOUS OPTIMAL CONTROL

Control theory has not been well developed for the systems in which the control force has the nonlinearity, unique to the friction controllable sliding isolation device. For this reason, an optimal control algorithm for control of the nonlinear friction system is developed on the basis of the instantaneous optimal control theory originally proposed by Yang et al. (Ref. 3).

The optimal pressure control signal $u(t)$ is determined by minimizing the following time dependent objective function $J(t)$ at every time instant t for the entire duration of an earthquake.

$$J(t) = q_d x^2(t) + q_f f^2(t) + r u^2(t) \qquad (8)$$

in which the normalized friction force f equivalently represents the amount of response acceleration and also serves as a measure of the transfer of seismic force to the structure. The weighting coefficient q_d and q_f are non-negative and r is positive. They indicate the relative importance in the control objectives of the sliding displacement, response acceleration and pressure control signal, respectively. The basic objectives of the control is to make the structure slide as much as possible within an acceptable range and at the same time to ensure the transfer of seismic force to a minimum.

With this theory, the following control algorithm is derived under the assumption that the structural motion is always in the sliding phase. The equation of motion given by Eq. 2 should be used as a constraint when minimizing the objective function $J(t)$. The first order time delay relationship between the control singal and the pressure described in Eq. 6, as well as the linear relationship between the friction and the pressure shown in Eq. 7, are also constraints. In the present formulation, however, these equations will be solved numerically using the Newmark's β method with $\beta = 1/6$ as shown below and these numerical solutions will be used as constraints:

$$\begin{aligned} x(t) &= x(t-\Delta t) + \dot{x}(t-\Delta t)\,\Delta t \\ &\quad + \ddot{x}(t-\Delta t)\frac{\Delta t^2}{2} \\ &\quad + [\ddot{x}(t) - \ddot{x}(t-\Delta t)]\,\frac{\Delta t^2}{6} \end{aligned} \qquad (9)$$

$$f(t) = f(t-\Delta t) + \dot{f}(t-\Delta t)\,\Delta t + [\dot{f}(t) - \dot{f}(t-\Delta t)]\frac{\Delta t}{2} \qquad (10)$$

Furthermore,

$$x(t) = a\, f(t)\, \mathrm{sgn}(\dot{x}(t)) + b\ddot{z}(t) + d_{\,1}\,(t-\Delta t) \qquad (11)$$

$$f(t) = -c\, u(t) + d_2(t-\Delta t) \qquad (12)$$

where

$$a = b = -\frac{\Delta t^2}{6}, \quad c = \frac{c_1 \Delta t}{2\,T + \Delta t} \qquad (13)$$

$$\begin{aligned} d_1(t-\Delta t) &= x(t-\Delta t) + \dot{x}(t-\Delta t)\Delta t \\ &\quad + \frac{1}{3}\,\ddot{x}\,(t-\Delta t)\,\Delta t^2 \end{aligned} \qquad (14)$$

$$\begin{aligned} d_2(t-\Delta t) &= \frac{2\,T}{2\,T+\Delta t}\left(\frac{c_2\,\Delta t}{2T} + f(t-\Delta t)\right. \\ &\quad \left. + \frac{1}{2}\dot{f}(t-\Delta t)\Delta t\right) \end{aligned} \qquad (15)$$

Thus, the following generalized objective function is established by introducing the Lagrangian multipliers λ_1 and λ_2:

$$\begin{aligned} H(t) &= q_d\, x^2(t) + q_f\, f^2(t) + r\, u^2(t) \\ &\quad + \lambda_1[x(t) - a\, f(t)\, \mathrm{sgn}(\dot{x}(t)) \\ &\quad - b\, \ddot{z}(t) - d_1\,(t-\Delta t)] \\ &\quad + \lambda_2\,[f(t) + c\, u(t) - d_2\,(t-\Delta t)] \end{aligned} \qquad (16)$$

The necessary conditions for minimizing the objective function $J(t)$ are:

$$\frac{\partial H}{\partial x} = 0, \ \frac{\partial H}{\partial f} = 0, \ \frac{\partial H}{\partial u} = 0, \ \frac{\partial H}{\partial \lambda_1} = 0, \ \frac{\partial H}{\partial \lambda_2} = 0, \qquad (17)$$

Substituting Eq. 16 into Eq. 17 yields the optimal pressure control signal:

$$u(t) = F_f\, f(t) + F_d\, x(t)\, \mathrm{sgn}(\dot{x}(t)) \qquad (18)$$

where, the control feedback gains $F_{\,f}$ and F_d are calculated by

$$F_f = \frac{c\, q_f}{r}, \quad F_d = \frac{c\, a\, q_d}{r} \qquad (19)$$

and the displacement $x(t)$ and friction $f(t)$ are used for feedback purpose. Again, notice that $\mathrm{sgn}(\dot{x})$ can be obtained from the displacement signal without the need to measure the velociy. The friction is difficult to measure by a sensor, but the signal from the acceleration sensor $(\ddot{x}(t)+\ddot{z}(t))$ can be used instead of f. Therefore, the control signal becomes:

$$u(t) = F_f\ |\ddot{x}(t)+\ddot{z}(t)| + F_d\ x(t)\ \mathrm{sgn}(\dot{x}(t)) \quad (20)$$

In the development of the optimal control algorithm shown above, the time delay of control device shown in Eq. 6 has been incorporated. In this case, the control is referred to as "instantaneous optimal control with time delay".

If the response of the control device is so fast that the time delay can be ignored, a similar procedure to the above can be shown to result in the following control signal:

$$u(t) = F + F_d\ x(t)\ \mathrm{sgn}(\dot{x}(t)) \quad (21)$$

where

$$F = \frac{c_1 c_2 q_f}{r + q_f {c_1}^2}, \quad F_d = \frac{c_1 a q_d}{r + q_f {c_1}^2} \quad (22)$$

In this case, only the sliding displacement $x(t)$ needs to be measured and fed back.

4 SHAKING TABLE TEST

4.1 Structure Model and Isolation Device

The structure model used for experiments is shown in Fig. 4. The model, representing a rigid structure, consists of a steel frame and steel weights. The total weight of the model is 12 tonf. The model is supported equally by four friction controllable sliding bearings on the shaking table. The bearing developed for the experiments is shown in Fig. 5. Figure 6 is a photograph of the bearing being used in the experiments. The bearing, with a brass sheet of 1 mm thickness attached to be used as sliding surface, slides on a stainless steel plate fixed on steel I-bars bolted down on the shaking table, as shown in Fig. 4. Furthermore, a rubber O-ring of 5.7 mm in diameter acts as seal for the fluid in the fluid chamber. The area of the sliding surface is 86.0 cm ^{2}, and the vertically projected area of the fluid chamber is 57.7 cm^2. No restoring force device is used in order to study the effect of friction force only. A servo valve is located at the center of the experimental structure from which the pressurized fluid is distributed to each sliding bearings as described in Fig. 4.

4.2 Passive and Hybrid Isolation

Typical experimental results are obtained under the El Centro (NS, 1940) ground acceleration. In the passive isolation results as shown in Fig. 7(a), the pressure in the bearing chamber is kept at 30 kgf/cm^2, corresponding to the coefficient of friction 5.3%. A large residual sliding displacement of 62 mm after the earthquake is observed.

Figure 7(b) shows the results of hybrid isolation experiments using instantaneous optimal control with time delay, in which the feedback gains are set to: F_f = 16.5 kgf/cm^2 and F_d = -16.4 kgf/cm^3 with the pressure control signal confined between u_{max} = 45 kgf/cm^2 and u_{min} = 10 kgf/cm^2.

The performance of the hybrid isolation system is compared to that of the passive isolation system. Figure 8 shows the maximum response acceleration, maximum sliding displacement, and the residual displacement of the structural model with passive or hybrid isolation system under linearly scaled El Centro records of different peak ground acceleration. Hybrid isolation results shown in these figures are those under instantaneous optimal control algorithm without time delay.

In the passive isolation, if a small friction coefficient, for example, 1.6%, is used, a high level of isolation performance is expected since the response acceleration is reduced to a small level. In this case, however, the maximum displacement becomes excessive very rapidly as the input earthquake becomes more intense. On the other hand, if a large friction coefficient, such as 10.2%,

is used, the sliding displacement can be confined within a relatively small range. However the isolation performance in this case is limited in the sense that the acceleration can not be satisfactorily reduced particularly for small to medium earthquakes.

The hybrid isolation system can alleviate these problems associated with passive isolation system; the response acceleration can be considerably reduced even for small to medium earthquakes, while excessive sliding displacement can be prevented for large earthquakes. Another advantage of the hybrid system is clearly seen in Fig. 8 where the residual sliding displacement can be maintained almost at zero level.

In summary, the hybrid isolation system performs better than the passive system in the sense that a reduction of response acceleration is achieved for small to medium earthquakes, and at the same time, the excessive sliding displacement under large earthquakes is prevented. Furthermore, the residual displacement is reduced to zero in most cases.

5 CONCLUSIONS

A systematic study on a hybrid sliding seismic isolation system using friction controllable bearings has been presented in order to significantly improve the base isolation characteristics of sliding systems. For this purpose, a hybrid sliding isolation system using friction controllable bearings has been physically developed, and shaking table experiments were performed on a rigid structural model equipped with such a hybrid system. A computer code has been developed for real-time on-line control implementation. The dynamic characteristics of the control system between bearing pressure and sliding friction have been identified. The results of hybrid sliding isolation experiments were compared with those of passive isolation.

The following conclusions are obtained:

1. Significant advantage of the proposed hybrid sliding isolation system has been demonstrated: (1) for the small to medium earthquakes, the coefficient of friction is kept at the minimum value to reduce the transfer of the seismic force to the structure to a minimum; (2) As the input earthquake becomes more intense, the friction is controlled to confine the sliding displacement of the structure to an acceptable range, while at the same time to keep the transfer of seismic force as small as possible. Such intelligent features of the hybrid system can not be achieved by the passive sliding isolation system.

2. Control algorithms developed for control of nonlinear friction force proved to be effective in achieving the desired control performances. In addition, they are practical and easy for real-time on-ling control operations.

3. The analytical model of dynamic characteristics between the bearing pressure control signal and the friction on the sliding interface has been identified. Computer simulation results excellently match the experiments. This implies that the analytical model represents the actual system very well, showing the possibility of utilizing the model to perform analytical study on other types of real structures equipped with the hybrid isolation system under different earthquake conditions.

4. The hybrid sliding isolation system proved to be quite robust, demonstrating the high potential for the application of the system to actual structures.

Items 3 and 4 above have not been discussed in this paper. The reader is refered to Ref. 4 for the detail.

6 ACKNOWLEDGEMENT

This work was supported partially by the National Center for Earthquake Engineering Research under Grant Number NCEER 90-2204, and partially by Taisei Corporation, Tokyo, Japan.

References

[1] Feng, Q., Fujii, S., Shinozuka, M., and Fujita, T., "Hybrid isolation system using friction-controllable sliding bearings," *Eighth VPI&SU Symposium on Dynamics and Large Structures,* Blacksburg, VA, 1991.

[2] Feng, Q., Shinozuka, M., Fujii, S., and Fujita, T., "A Hybrid isolation system for bridges," *Proceedings the First US-Japan Workshop on Earthquake Protective Systems for Bridges,* Buffalo, NY, 1991.

[3] Yang, J.N., Long, F. X., and Wong, D., "Optimal control of nonlinear structure," *Journal of Applied Mechanics,* Vol. 110, pp. 931-938, 1988.

[4] Feng, Q., Fujii, S., and Shinozuka, M., "Experimental and analytical study of a hybrid isolation system using friction controllable sliding bearings" *Technical Report NCEER,*, NCEER, SUNY, Buffalo, NY, 1992 (to be published).

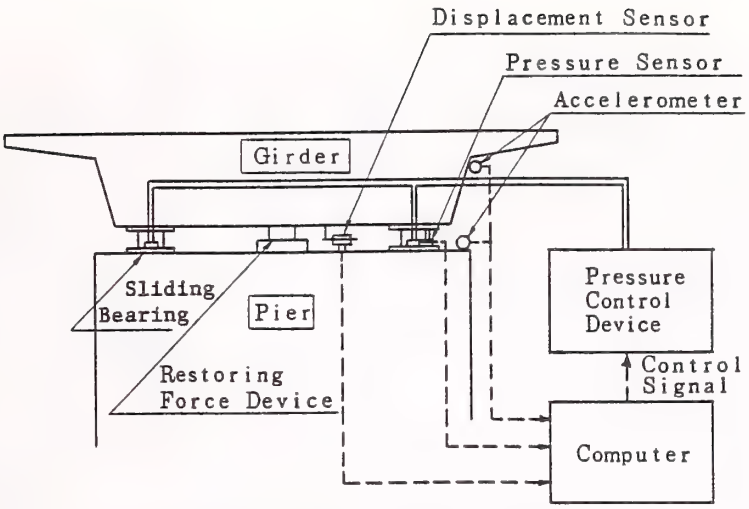

Figure 1: Concept of Hybrid Sliding Isolation System for Bridges

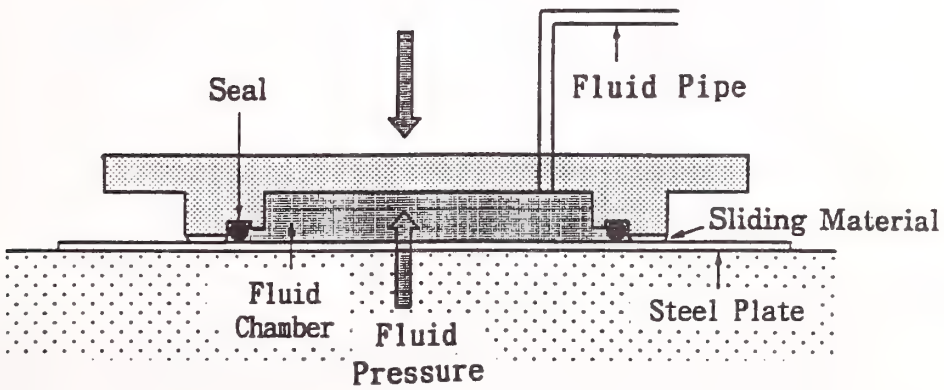

Figure 2: Idealized View of Friction Controllable Sliding Bearing

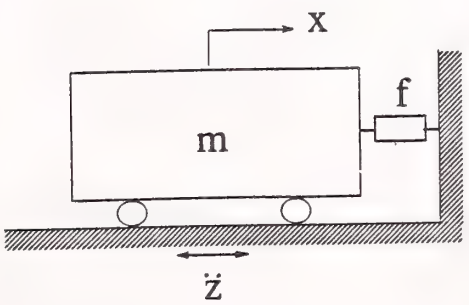

Figure 3: Analytical Model

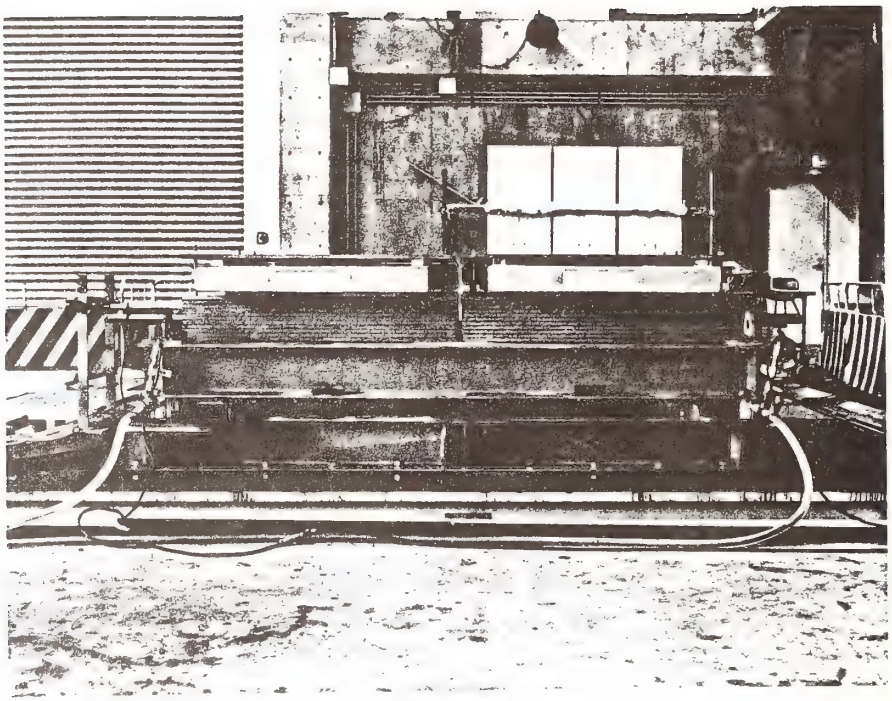

Figure 4: Structure Model with Hybrid Sliding Isolation Device

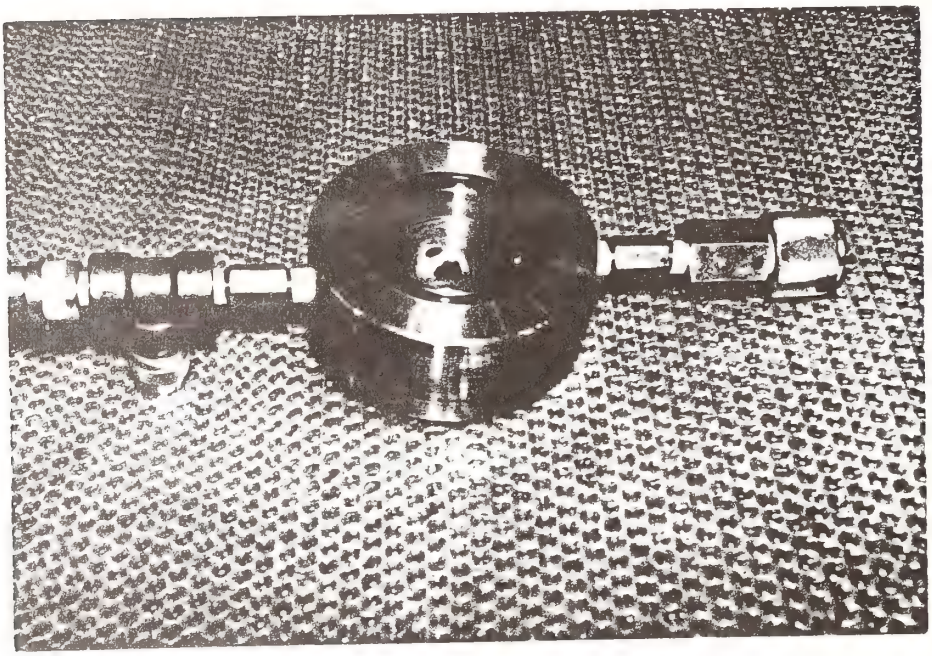

Figure 5: Friction Controllable Sliding Bearing

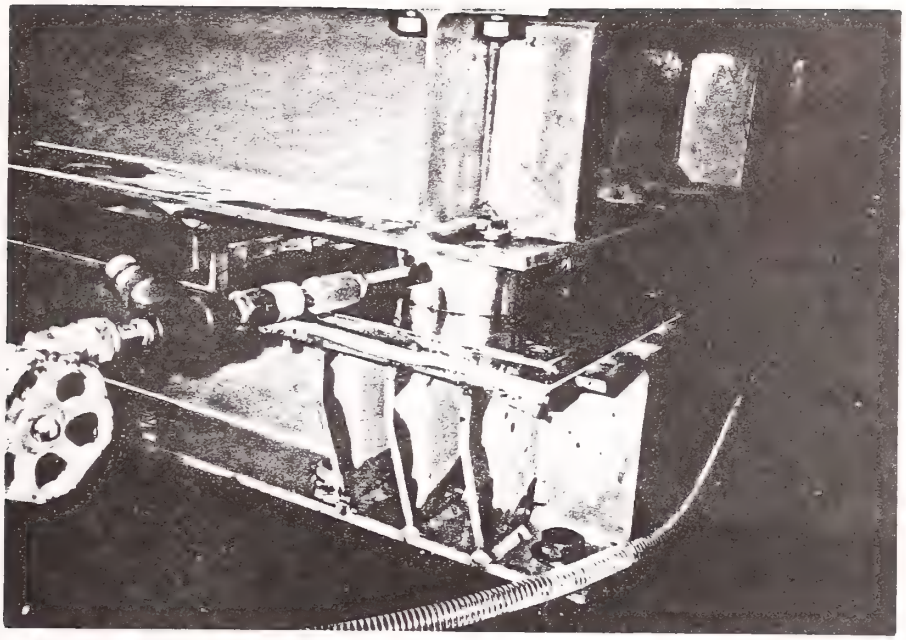

Figure 6: Friction Controllable Sliding Bearing for Experiment

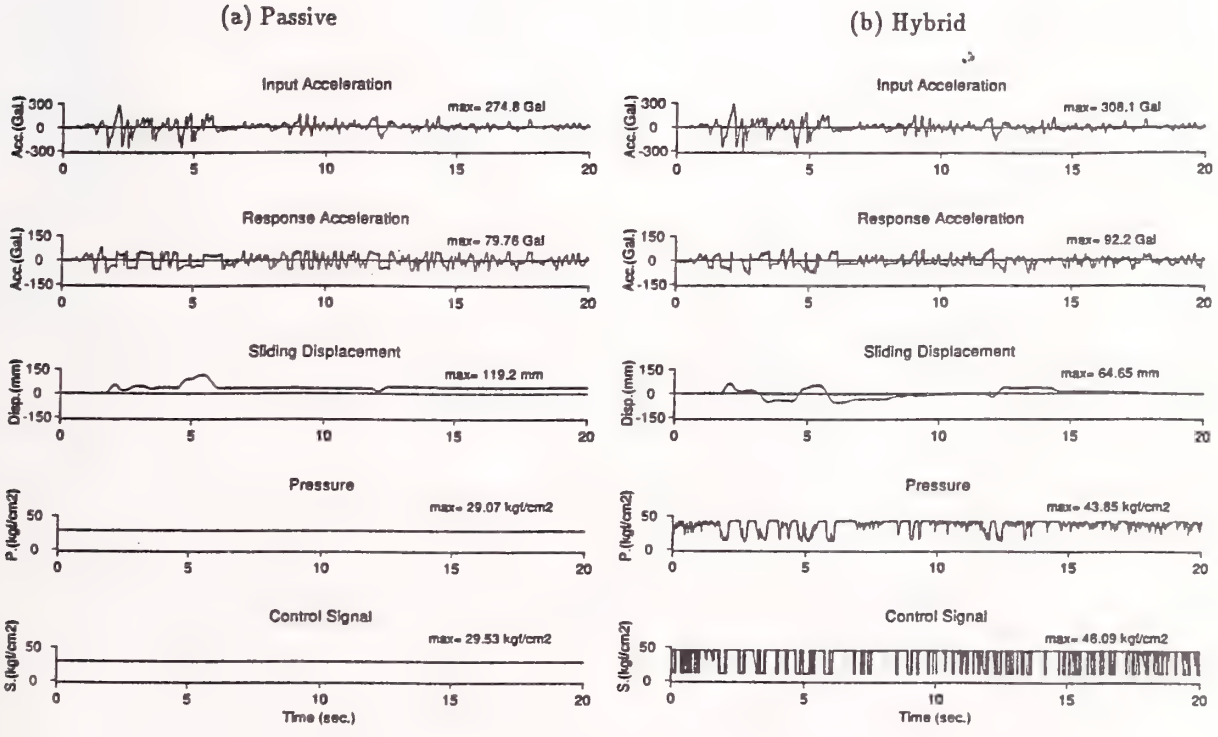

Figure 7: Experimental Results

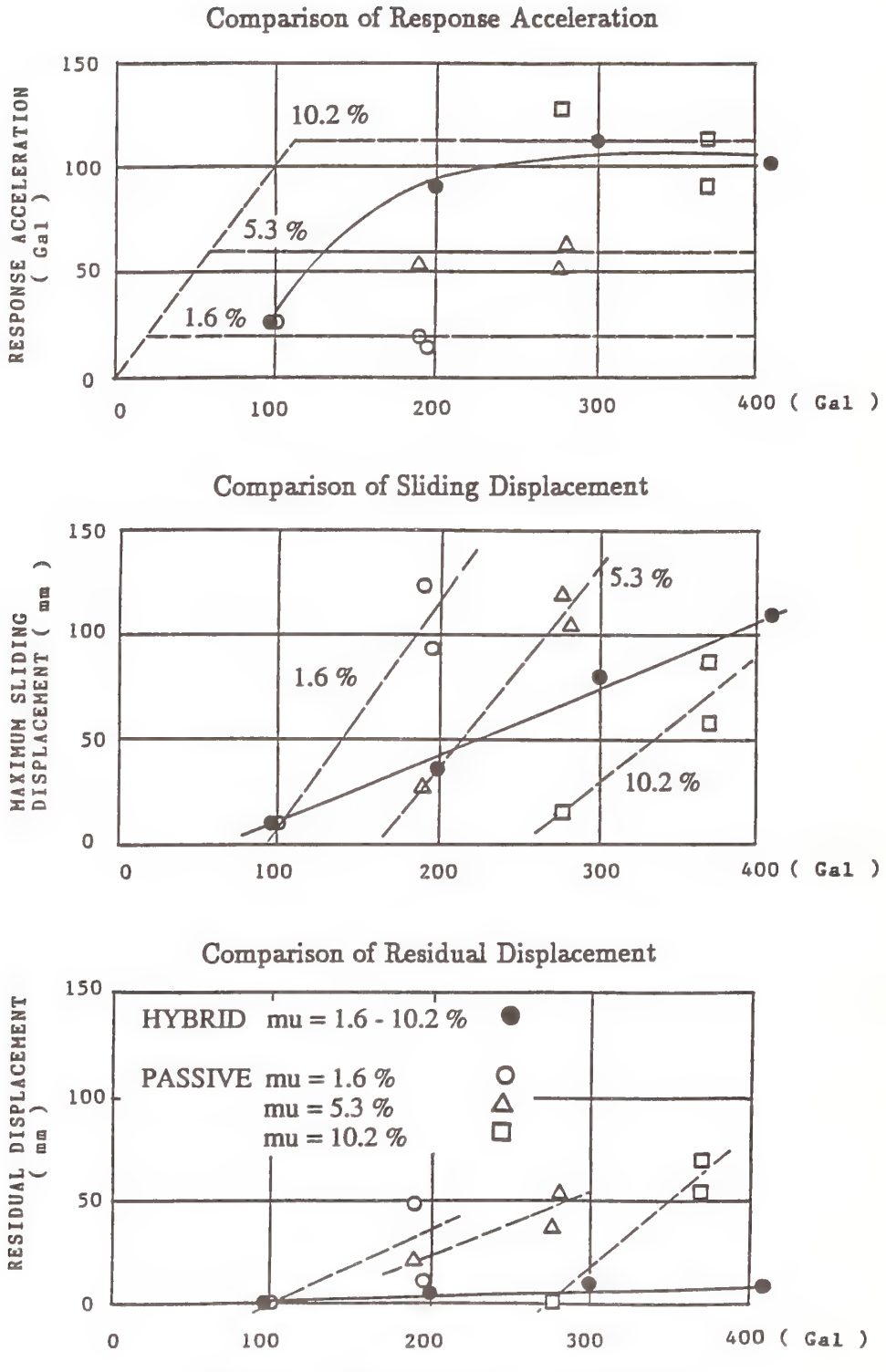

Figure 8: Comparison of Passive and Hybrid Isolation

State-of-the-Arts on Building Structures With Structural Response-Control System in Japan

by

Yosikazu Kitagawa[1] and Mitsumasa Midorikawa[2]

SUMMARY

This paper presents a brief introduction to active/hybrid structural response-control building in Japan. First, classification of seismic response-control system and relationship between control theory and required performance are roughly reviewed. Finally, examples of structural response-control buildings and model structures are given.

KEY WORDS: Classification of Seismic Response-Control Systems, Active and Hybrid Structural Response-Control Building, Control Theory, Required Performance

1. INTRODUCTION

Japan is characteristically subjected to the seismic activity. Therefore, it is a matter of concern how building structures behave under earthquake conditions. Currently the research focus for seismic design methods has changed from static analysis to dynamic analysis. Building structures are also becoming to be taller in height and longer in span with increased demands in living comfort and safety.

In response to these changes, seismic isolation and response-control systems for building structures are becoming important areas in the field of earthquake engineering. The former system includes base and floor isolations, and the latter includes active/passive structural response-control buildings under earthquake and wind excitations.

Many studies and proposals involving active/passive structural response-control system have been conducted. A portion of these projects has resulted in actual and model structures in Japan, USA, and other countries. Recently, structural response-control buildings have been proposed and enthusiastically put into practice in Japan.

In this paper, the structural response-control systems are roughly classified, and the present status of building structures with response-control systems are outlined.

2. CLASSIFICATION AND CHARACTERISTICS OF RESPONSE-CONTROL STRUCTURES

A response-control structure may generally be classified into two groups: one that requires an active response-control system (i.e., some form of applied external energy is required in order to control the response of a building to external turbulence); and one that only needs a passive response-control system (i.e., no such energy is required). Active response-control systems can be classified as either a full-active method in which some form of response control force is applied to resist external turbulence or a semi-active method in which the dynamic characteristics of a structure are controlled. Passive response-control systems can be classified as either a base-isolation method or a tuned-mass damper method. Hybrid methods use a combination of active and passive methods.

In an active response-control structure, the vibrations of a building are reduced through an active method using the signals sensed in and around the building. From the standpoint of signal processing, an active response-control system can be classified in two ways: a forward control in which the necessary control is introduced using signals from the outside sensors before external turbulence can reach the building; and a feedback control in which control is introduced after response of a building are sensed by measurement instruments installed in the building. A flow chart of an active structural response-control system is shown in Fig. 1.

The resultant motion of a building, when it is subjected to external dynamic forces

1) Dr. Engrg., Director of International Institute of Seismology & Earthquake Engineering, Building Research Institute, Ministry of Construction.
2) Dr. Engrg., Head of Earthquake Engineering Div. I, IISEE, BRI, MOC.

such as earthquakes or winds, can be represented by the following equation:

$$m \cdot \ddot{x} + c \cdot \dot{x} + k \cdot x = f + p \quad (1)$$

where,

m = mass of the vibrational system;
c = viscous damping coefficient;
k = stiffness of the vibrational system;
f = external force acting on the vibrational system;
$\ddot{x}$ = response acceleration with respect to the ground;
$\dot{x}$ = response velocity with respect to the ground;
x = response displacement with respect to the ground; and
p = response control force.

Each term in this equation is expressed by a matrix or vector. The object of a response-control structure is to reduce the response acceleration $\ddot{x}$, response velocity $\dot{x}$, and response displacement x. The reduction is done by controlling and adjusting the mass m, the viscous damping coefficient c, the stiffness k, and/or external force f, or by applying a control force p.

According to the basic principles of dynamics briefly outlined above, any structural response-control method can be classified as follows: 1) the method based on control and adjustment of mass, such as rigid mass dampers and liquid mass dampers; 2) the method based on control and adjustment of damping, such as variable-damping mechanisms and building-to-building connecting mechanisms; 3) the method based on control and adjustment of restoring force characteristics, such as variable-stiffness mechanisms and flexible base mechanisms; and 4) the method based on applying control forces using equipment such as jet or injection devices, or using reaction walls.

Theoretically, the structural response-control concepts differ from conventional techniques for earthquake or wind resistant structures in only the method introducing control forces. The difference is that the restoring force characteristics or energy absorption properties depend on structural elements such as columns, girders, walls, and braces in conventional systems, but on mechanical equipment or mechanisms in response-control systems.

3. CONTROL THEORIES

At present, a feedback control system using responses such as acceleration, velocity, and displacement is mainly adopted in an active response-control structure, whose target is to suppress the vibration of the structure induced by external turbulence.

Using old control theory, control effect is attained by avoiding resonance in a structure during external turbulence or by increasing the damping capacity of a structure. In modern control theory, the quantity-of-state is used for the feedback control, even though question remains concerning controllability and sensing ability. If this point is solved, then adjusting dynamic characteristics of a modern control system can put into practice. Optimal control theory is the one mainly adopted in modern control methods.

Control theories may be classified into the following four groups: 1) the self-organizing/structuring control in which the structure of a control system is determined by the control system itself to achieve the target of an entire structure system; 2) the adaptive control in which the evaluation function and the parameters to be optimized are determined adaptively in a given structure; 3) the optimal control in which the operational quantities are determined so as to optimize a given evaluation function; and 4) the direct control in which the operational quantities are directly determined to match the process variables with target values. These classifications are made based on two factors: the degree of complexity or simplicity of a system; and the degree of certainty of information. A mapping of these classifications is shown in Fig. 2.

In the design of a structural response-control system, it is important to identify the dynamic characteristics of the controlled structure. It is also necessary to include fail-safe mechanisms to improve the reliability of an entire structure system. Therefore, it is desirable to develop a fail-safe system with adaptive control in which the control parameters can be adjusted in response to environmental effects.

In building structures, it is generally difficult to construct a control system since there are many unknown variables such as the type of structure, material, and construction, and the deterioration of the structural performance with passage of time. In case of controlling the vibration of a structure subjected to earthquakes, it is critical that the response of a control system be quick enough to include time from sensing external turbulence to putting actuators in operation. There are, however, uncertainties in input signals to a control system caused by many factors such as the direction of input ground

motions and the location of sensors. For dealing with these vague and uncertain problems, further development and application are needed on an intelligent control system that uses fuzzy logic or neural networks. Figure 3 shows an example of the relationship between system requirements and control theories for structural safety evaluation of a response-control structure. Figure 4 shows an example of a control system that uses a fuzzy optimal method. The features of this system are: 1) real time prediction of earthquake ground motions, 2) real time structural identification, and 3) maximizing decision using fuzzy logic. This fuzzy optimal method is basically different from fuzzy control method that uses the proportional, integral, and differential (PID) control.

4. PRESENT STATUS OF STRUCTURAL RESPONSE-CONTROL BUILDINGS

Table 1 shows an outline of active and passive structural response-control buildings in Japan. Many studies and proposals involving active/passive structural response-control systems have been conducted. A portion of these has resulted in actual buildings or model structures in Japan. The KS Building which is actual building structure with an active structural control system was reviewed by the Board of Technical Members of A Special Committee in the Building Center of Japan. This committee inspected the technical aspect of structural safety, vulnerability, and maintenance of the KS Building and its structural control system.

4.1 KS Building (Ref. 6, Figs 5, 6, and 7)

This eleven-story, steel structure office building was constructed in Chuo-ku, Tokyo, in 1989. An active mass damper (AMD) device with an auxiliary weight of about 1% of the total weight of the building was installed on the top floor of the building. Because the building shape is very slender and the damping factor of this structure is small, the aim of the AMD is to control the lateral and torsional vibrations and to satisfy the serviceability condition during earthquakes and strong winds. To do this, the AMD system reduces the maximum response quantities of the uncontrolled structure to about one-half to two-third during earthquakes and strong winds. The AMD system is also designed to function within the device capacity if an excessively large load is applied. After completion of the building, both free and forced vibration tests were carried out. Seismographs and an anemometer have also been installed for carrying out observations.

4.2 K Laboratory Building (Ref. 7, Figs 8, 9, and 10)

A three-story, actual, steel structure for a large-scale shaking table facility was constructed in Chofu, Tokyo, in 1990. To control the vibration characteristics of the building, an active variable-stiffness (AVS) system was installed. A variable-stiffness device was installed on each floor at both end frames, at the joint of the braces and beam to change the connecting condition at the joint using control computer. The resonance with continuously arriving earthquake motions can be avoided, and the building response can be suppressed with a small power energy supply. After completion of the building, the forced vibration test was carried out. An earthquake observation system was also installed in this building to confirm the actual control effect.

4.3 S Building (Ref. 8, Figs 11, 12, and 13)

An eleven-story, actual, reinforced concrete structure office building was constructed in Shibuya-ku, Tokyo, in 1991. The control mechanism is an AMD system used to control translational and torsional motion of the building, and to satisfy serviceability for living comfort during earthquakes and strong winds. The AMD device was installed on the top floor of the building with an auxiliary weight of 1.1% of the total building weight. The purpose of installation is to reduce the maximum response quantities of the uncontrolled structure to about 0.4 to 0.8 times. After building construction was completed, an earthquake observation system was installed.

4.4 MM Tower Structure (Ref. 9, Figs 14 ,15, and 16)

A seventy-story, S/SRC tower structure, for an office and hotel, is under construction in Yokohama, Kanagawa Prefecture, and will be completed in 1993. The control mechanism is a tuned active mass damper (TAMD) system with a multi-stage pendulum to suppress structural response to an occasional strong wind force. The TAMD device will be installed on the first floor of the penthouse (282.3 meters above the ground), with an auxiliary weight of 0.13% of the total building weight. The goal of the TAMD device is to reduce the maximum response quantities of the uncontrolled structure to

about 0.4 times. This control system incorporates the following safety functions: switching to TMD by shutdown of motor electric current in case of abnormality or power failure of the control system; applying a damper brake by switchover of the solenoid valve; and use of malfunction checking system such as turning on warning lamp.

4.5 Full-Scale Model (Ref. 10, Figs 17 ,18 and 19)

A six-story, full-scale, steel model structure was constructed to check the performance of an active structural response-control system in Koto-ku, Tokyo, in 1989. The control mechanism is an AMD system used to reduce the acceleration and displacement response of the uncontrolled structure to one-half to one-third during earthquakes and strong winds. The AMD device is installed on the top floor of the model structure, with an auxiliary weight of 1% of the total model structure weight. A shaking table test to verify the damping effect of the AMD device, the micro-tremor measurements, and a forced vibration test were carried out. An earthquake observation system was also installed in this full-scale model structure. This structural control system was applied to an actual eleven-story, reinforced concrete structure. (See 4.3 S Building).

4.6 Full-Scale Model (Ref. 11, Figs 20, 21 and 22)

A seven-story, full-scale, steel structure was constructed in Koto-ku, Tokyo, in 1991 to check the performance of a hybrid structural control system. The control mechanism is a hybrid mass damper (HMD) system which makes use of its capability to suppress vibration as a tuned mass damper (TMD) system with greater energy efficiency than an AMD system while maintaining the same performance. The HMD device was installed on the seventh floor, and consists of an auxiliary mass supported by multi-stage rubber bearings and actuators driven by AC servo-motors. An auxiliary weight of the HMD system is about 1.2% of the total model structure weight. A shaking table test of the HMD device and a forced vibration test of a full-scale model were conducted to evaluate the dynamic characteristics of the device and the full-scale model. Earthquake and wind observations have also been carried out. In addition, a large-scale genuine HMD system will be installed in an actual fifty-story, steel building (ORC 200 symbol tower for use as office and hotel) at Benten-cho in Osaka.

4.7 Full-Scale Model (Ref. 12, Figs 23, 24 and 25)

A six-story, full-scale, steel model structure was constructed in Tukuba, Ibaraki Prefecture, in 1991 to determine the performance of a structural response-control system. The control mechanism is an active-passive mass damper (APMD) system which exhibits great structural response-control in an active mode during medium and small earthquakes as well as strong winds. When external forces exceed the capacity of the system under strong earthquakes, the APMD system switches over continuously from active to passive mode as a tuned-mass damper system. The APMD device is installed on the top of the structure, with an auxiliary weight of about 1% of the total model structure weight. The control effect is to reduce the maximum response quantities of the uncontrolled structure to about one-half. A forced vibration test was carried out. Earthquake and wind observations have also been carried out.

4.8 Full-Scale Model (Ref. 13, Figs 26, 27 and 28)

A six-story, full-scale, steel model structure was constructed in Tukuba, Ibaraki Prefecture, in 1991 to confirm a structural control system. The control mechanism is a tuned roller-pendulum damper (TRD) system. A free vibration test and forced vibration test were carried out. Earthquake and wind observations have also been carried out. A variable resistance damper (VRD) system as a device for a semi-active structural response-control system was developed, and its effect was confirmed by the shaking table tests. This VRD will be installed inside the earthquake-resistant walls of high-rise buildings or between the base mat and the first floor of seismic isolation building structures with no need for a huge energy supply or backup systems.

4.9 Reduced-Scale Model (Ref. 14, Figs 29, 30 and 31)

An eight-story, reduced-scale, steel model structure was constructed to examine both experimentally and analytically the performance of structural control taking into consideration spillover, robust control, and multi-mode control for high-rise building structures. The control mechanism is an AMD system used to reduce acceleration and to

control vibrations through a wide frequency range that includes higher-order vibration modes of the structure. The AMD device has a ball-screw drive system equipped with an AC servo-motor, and is installed on the top floor of the structure with an auxiliary weight of 0.4% of the total weight of the model structure. The purpose of installation is to reduce the absolute response of the uncontrolled structure to 0.4 to 0.8 times. A plan has been made to install this system in an office and residential building scheduled for construction, in Tokyo, in the near future.

4.10 Reduced-Scale Model (Ref. 15, Figs 32, 33 and 34)

A four-story, steel, reduced-scale model structure was built to confirm the capacity of AMD and ATMD system. These systems involve an auxiliary mass floating on a sliding base, variable friction bearing (VFB). The auxiliary weight of AMD and ATMD systems is about 1% of the total model structure weight. The target of the control effect is to reduce the maximum acceleration and displacement of the uncontrolled structure to about 0.6 times. A shaking table test was carried out. An active control system using gyrostabilizer and a hybrid base isolation system that uses a friction-controlled sliding bearing have been developed, and its effect was confirmed by free vibration and shaking table tests.

4.11 Reduced-Scale Model (Ref. 16, Figs 35, 36 and 37)

A four-story, steel, reduced-scale model was constructed to confirm the effect of structural control. The control mechanism suppresses the vibration of the structure as a hybrid structural control system. An active rolling pendulum (ARP) device is designed to work with a much smaller added mass and to produce a more effective resistive force. This ARP system is installed on the top floor of the model structure. The system works as a passive system, which is made more reliable than an active system by switching the electromagnetic valve when external forces exceed the capacity of the system, and the power supply is disconnected. A shaking table test was carried out.

4.12 Reduced-Scale Model (Ref. 17, Figs 38, 39 and 40)

A ten-story, reduced-scale, steel model structure was built to verify the control effect, the robustness, and the performance of a hybrid structural control system. The control mechanism is a hybrid tuned multi-mass damper (HTMMD) system. This TMMD system consists of three floors unified with braces, and a control device which is composed of levers with an auxiliary mass and actuator driven by an AC servo-motor through a ball screw installed on the ninth floor of the structure. The control effect reduces the maximum response quantities of the uncontrolled structure to about 0.5 to 0.8 times with high robustness, even if the passive TMMD system is not well-tuned. Shaking table tests have been carried out.

5. CONCLUDING REMARKS

This paper presents a brief introduction to active/hybrid structural response-control building in Japan. Response-control devices have been installed in actual building structures, and have been developed, mainly by construction companies, and realized to provide human comfort against excitation such as small and medium earthquakes and strong winds.

It is no exaggeration to say that the performance of structural response-control buildings depends on the control devices which have been developed mainly from a practical use view-point. When we reach a consensus on the structural safety of controlled buildings in view of structural reliability, new structural design systems may be developed. When that occurs, it is important for us to ensure the reliability and to ascertain the vulnerability of a structural response-control system concerning the structural safety as a total system: building structural system, machinery system, and environmental system.

6. ACKNOWLEDGMENTS

The authors express their sincere gratitude to the following people; Mr. M. Sakamoto, Kajima Co.; Mr. S. Aizawa, Takenaka Technical Research Laboratory.; Mr. H. Abiru, Mitsubishi Heavy Industries, Ltd.; Mr. K. Shiba, Shimizu Co.; Mr. O. Chiba, Toda Co.; Mr. I. Abe, Okumura Co.,; Mr. A. Teramura, Obayashi Co.; Mr. S. Kawamura, Taisei Co.; Mr. N. Ogino, Kumagai Gumi Co., Ltd. Appreciation is also expressed to Prof. S. Ishimaru and Mr. T. Niiya, Nihon University for offering the data concerned with Section 4 of this paper.

REFERENCES

1) Y. Kitagawa, M. Hirosawa, "Base-Isolated Building Structure in Japan", 20th UJNR, 1988.
2) Y. Kitagawa, and M. Midorikawa, "Base-Isolated Building and Seismic Safety Evaluation in Japan", 23rd UJNR, 1991.
3) Y. Kitagawa, M. Midorikawa, and et al., "Seismic Response Control System by Fuzzy Optimal Logic (Part 1-4)", AIJ Annual Meeting, 1992, (in Japanese).
4) "Report on R &D to Achieve Active Seismic Control of Building Structure", Cooperative Research with Public Organization and Private Companies, BRI, MOC, 1992.
5) "Seismic Isolation and Response Control for Nuclear and Non-Nuclear Structure", Special Issue, SMiRT 11, 1991.
6) T. Kobori, M. Sakamoto, and et al., "Study on Active Mass Driver (AMD) System (Part 1)", 4th World Congress of Council on Tall Buildings and Urban Habitat, 1990.
7) T. Kobori, M. Takahasi, and et al., "Shaking Table Experiment and Practical Application of Active Variable Stiffness (AVS) System", 2nd Conference on Tall Buildings in Seismic Regions, 1991.
8) M. Higashino, S. Aizawa, and et al., "The Study of Translational-Torsional Control by the Active Mass Damper of Practical Use", Japan National Symposium on Active Structural Response Control, 1992.
9) S. Yamazaki, N. Nagata, and H. Abiru, "Tuned Active Dampers installed in the Minato Mirai (MM) 21 Landmark Tower in Yokohama", 8th International Conference on Wind Engineering, 1991.
10) S. Aizawa, Y. Hayamizu, and et al., "Experimental Study of Dual Axis Active Mass Damper", U.S. National Workshop on Structural Control Research, 1990.
11) K. Maebashi, K. Shiba, and et al., "Hybrid Mass Damper System for Response Control of Building", 10WCEE, 1992.
12) T. Fijita, S. Takahashi, and et al., "Mass Damper with Convertible Active and Passive Modes for Response Control of Building", 10WCEE, 1992.
13) S. Otsuka, Y. Oka, and et al., "Vibration Control of Tall Buildings by Roller Pendulum", AIJ Annual Meeting, 1991, (in Japanese).
14) T. Suzuki, M. Kageyama, and et al., "Active Vibration Control for High-Rise Building using Dynamic Vibration Absorber Driven by Servo Motor", U.S. National Workshop on Structural Control Research, 1990.
15) I. Nagashima, B. Bhartza, and et al., "Experimental Study on Active Mass Damper System", Japan National Symposium on Active Structural Response Control, 1992.
S. Sakamoto, M. Yamada, and et al., "Test on Active Vibration Control System using Gyrostabilizer", Japan National Symposium on Active Structural Response Control, 1992.
S. Kawamura, M. Shinozuka, and et al., "Hybrid Isolation System using Friction Controllable Sliding Bearings", US-Italy-Japan Workshop/Seminar on Intelligent Systems, 1991.
16) K. Hasegawa, Y. Katano, and et al., "Basic Study on Optimal Control Algorithm for Active Vibration Control System", 2nd International Conference on Adaptive Structures, 1991.
17) S. Ishimaru, T. Niiya, and et al., "Experimental Study on Hybrid Tuned Multi-Masses Damper (HTMMD) Structure Controlled by Model-Following-Algorithm", Japan National Symposium on Active Structural Response Control, 1992.

Table 1 List of Seismic Response Control Building Structure (Active/Passive Control Method)[9]

Building Name	Date Completion	Building Structure	Story	Building Uses	Location	Designer/ Construction	Type of Seismic Control Device
Chiba Port Tower	1986	S	(125m)	Observatory	Chiba-shi, Chiba	Nikken Sekkei/ Takenaka	Tuned Mass Damper (TMD)
Yokohama Marine Tower	1987	S	30F	Observatory	Yokohama-shi, Kanagawa	Shimizu/ Shimizu	Tuned Liquid Damper(TLD)
Sonic City	1988	S SRC	31F4B	Office	Omiya-shi, Saitama	Nikkenn Sekkei/ Fujita	Friction Damper
Cold Tower	1988	S	(136m)	Observatory	Utazu-cyo, Kagawa	Mitui/ Mitui	Tuned Liquid Damper(TLD)
Higashiyama Sky Tower	1988	S	7F (134m)	Observatory	Nagoya-shi, Aichi	Nagoya City & Nihon Sogo Arch./ Kajima, Taisei, Tokuso	Tuned Mass Damper (TMD)
Asahi Beer Tower	1989	S	22F2B	Office	Taito-ku, Tokyo	Nikken Sekkei/ Kumagai	Friction Damper
Fukuoka Observatory	1989	S	(148m)	Observatory	Fukuoka-shi, Fukuoka	Nikken Sekkei/ Taisei, Takenaka, Kajima, Shimizu, Obayashi	Tuned Mass Damper (TMD)
Kajima Corp. KI-Building	1989	SRC	5F(A) 9F(B) 1B	Office	Minato-ku, Tokyo	Kajima/ Kajima	Joint Damper(Bell Damper)
Kyobashi Seiwa Building (KS Building)	1989	S SRC	11F1B	Office	Chuo-ku, Tokyo	I & I Architects & Associates Kajima/ Kajima	Active Mass Driver(AMD)
Sky Tower	1989	S	(135m)	Observatory	Nagasaki-shi, Nagasaki	Mitsubishi Heavy Industry/ Mitsubishi Heavy Industry	Tuned Mass Damper (TMD)
Crystal Tower	1990	S SRC RC	37F2B	Office	Osaka-shi, Osaka	Takenaka/ Takenaka	Tuned Mass Damper (TMD)
Control Bldg. of Shaking Table Facility in Kajima Ins. of Construction Technology(K Lab Building)	1990	S	3F	Office	Cyofu-shi, Tokyo	Kajmai/ Kajima	Active Variable Stiffness (AVS)
Fujita Corp. Head Office Bldg.	1990	S SRC	20F4B	Office	Shibuya-ku, Tokyo	Fujita/ Fujita	Lead Damper
Oujiseishi Headquarters Bldg.	1991	S	15F4B	Office	Chuo-ku, Tokyo	Ouji-Kajima JV Design Room/ Kajima+ Takenaka	Honeycomb Damper
Shimizu Head Office Bldg.	1991	S SRC	24F2B	Office	Minato-ku, Tokyo	Shimizu/ Shimizu	Viscous Damper
Hibikiryokuchi Sky Tower	1991	S	(135m)	Observatory	Kitakyushu-shi, Fukuoka	Mitsubishi Heavy Industry/ Mitsubishi Heavy Industry	Tuned Mass Damper (TMD)
Sendagaya INTES (S Building)	1991	S	11F1B (45m) 1B	Office	Shibuya-ku, Tokyo	Takenaka/ Takenaka	Active Mass Driver(AMD)
MM21 Land Mark Tower (MM Tower Building)	1993	S SRC	70F (296m)	Hotel & Office	Yokohama-shi, Kanagawa	Mitsubishi Estate Co./constructor JV	Tuned Active Damper

F: Floor, B: Basement, H: Height(m), — : Active Seismic Control Device

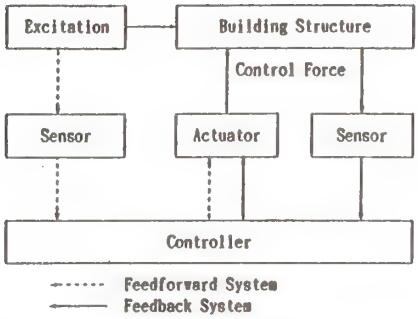

Fig. 1 Flowchart of An Active Structural Control System

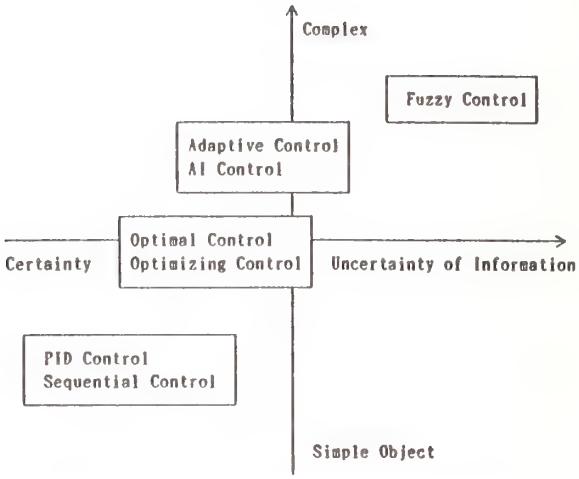

Fig. 2 Mapping of Control Theory Classification

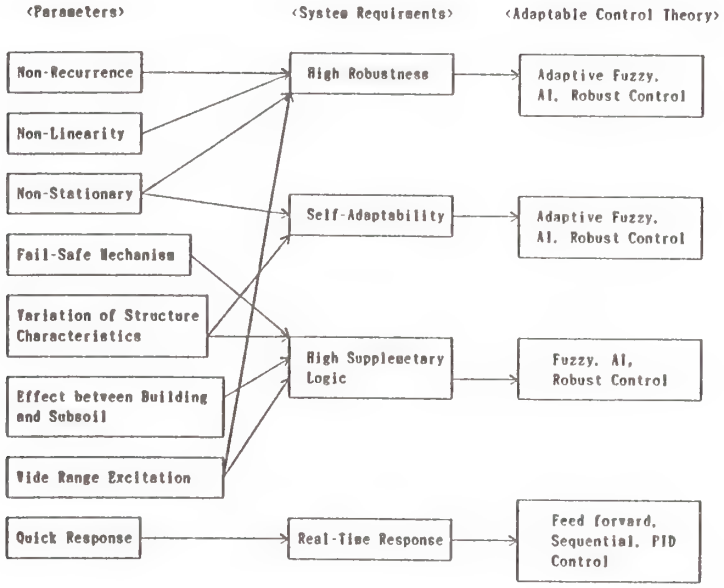

Fig. 3 Relationship between Control Theory and Requirment

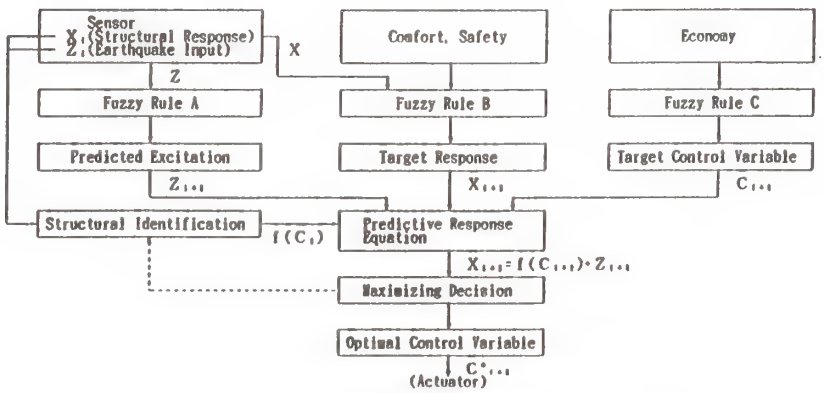

Figure 4 Flow Chart of A Fuzzy Optimal Control System

Fig. 5 Entire View of Building

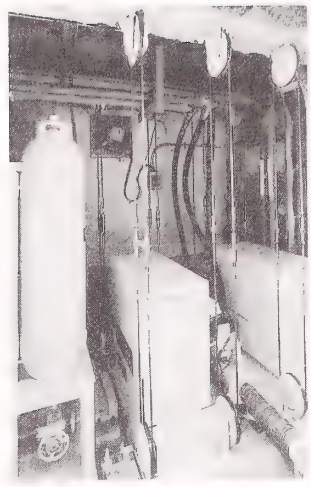

Fig. 6 AMD Device

Realization of Active Mass Driver(AMD) System in 1989 (Kyobashi Seiwa Building in Tokyo)

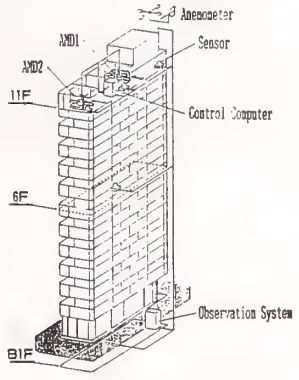

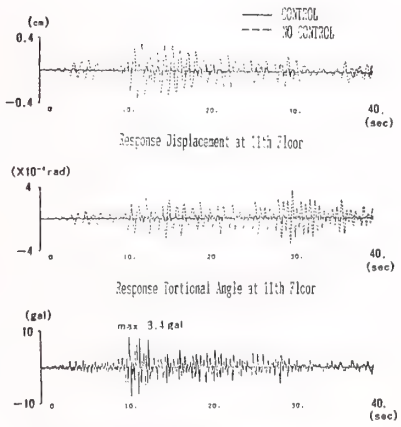

Recorded Ground Acceleration

Epicenter : 10ka north-east of Izu Oshima (Depth 25ka)

Date : Oct. 14, 1989

Magnitude : M 5.2

Fig. 7 AMD System and Earthquake Observation

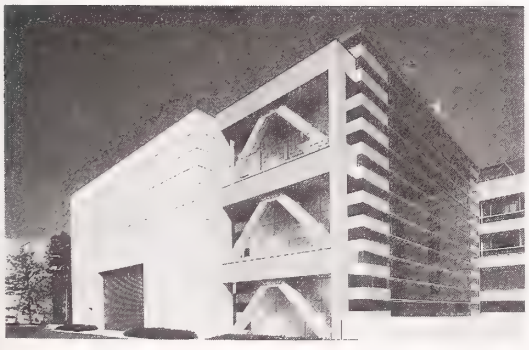

Fig. 8 Entire View of Building

Fig. 9 AVS System

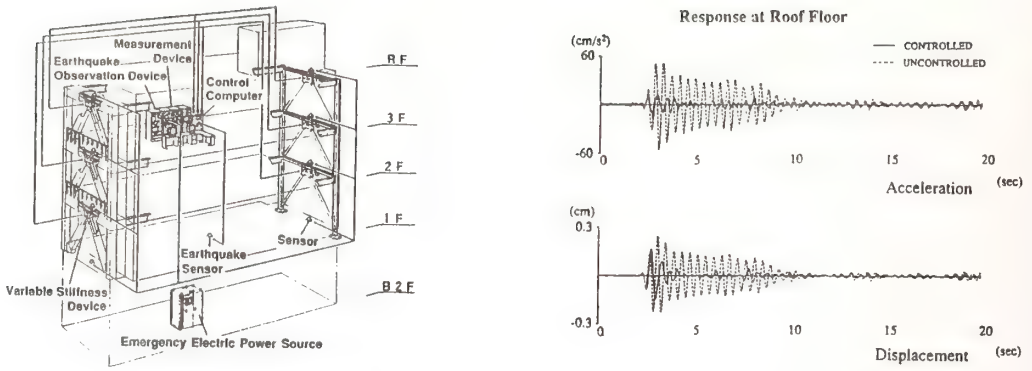

Fig. 10 AVS System and Companison of Response

Fig. 11 Entire View of Building

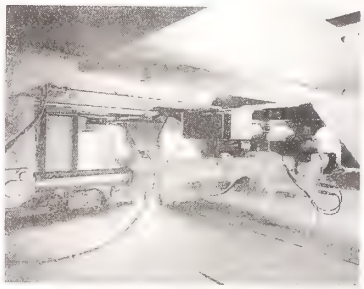

Fig. 12 AMD Device

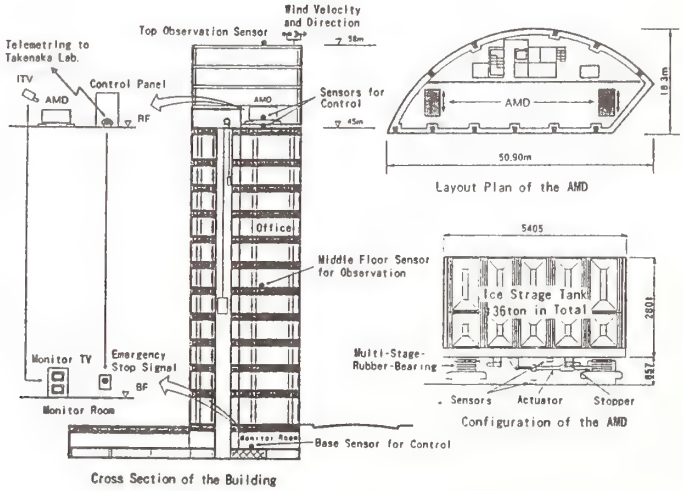

Fig. 13 Outline of AMD System

Fig. 14 Entire View of Building Model

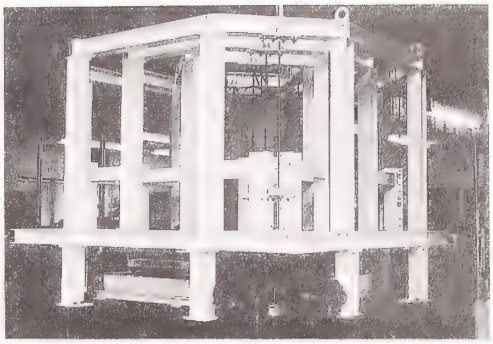

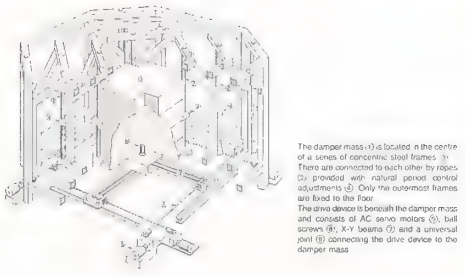

Fig. 15 TAD Divice

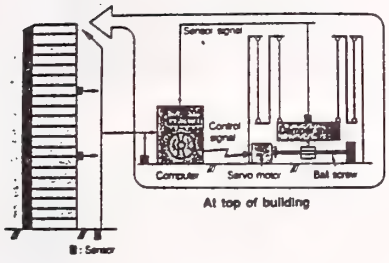

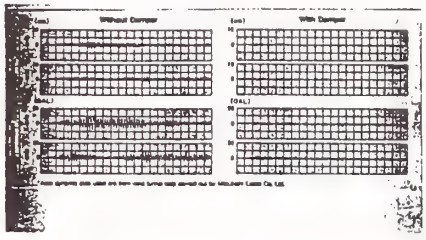

Fig. 16 TAD System and Comparison of Response

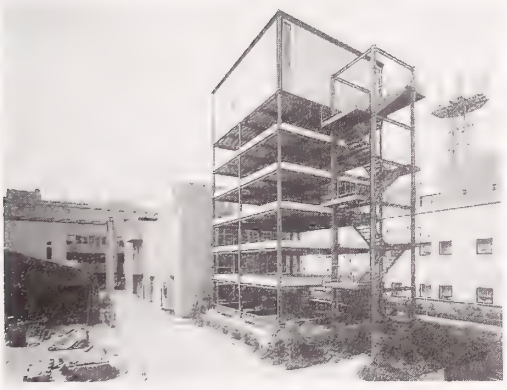

Fig. 17 Entire View of Actual Model

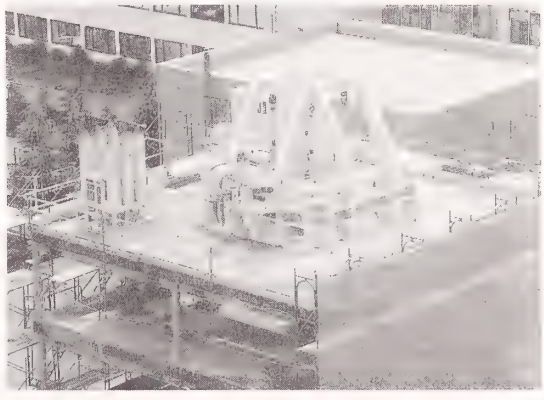

Fig. 18 AMD Device

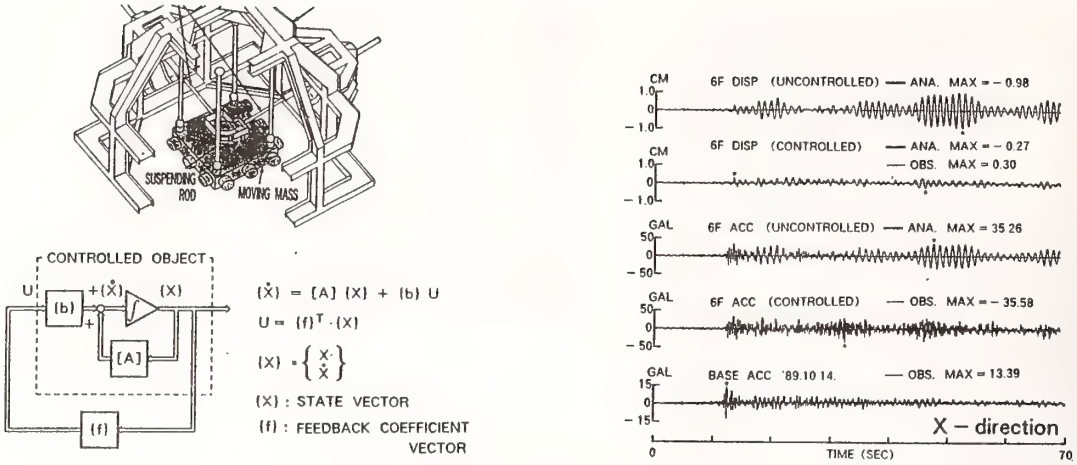

Fig. 19 AMD System and Comparison of Response

Fig. 20 Entire View of Actual Model

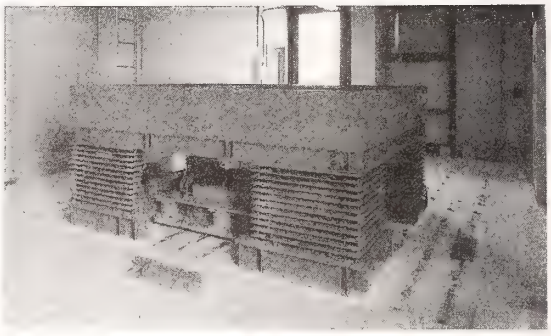

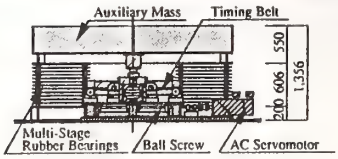

Fig. 21 HMD Device

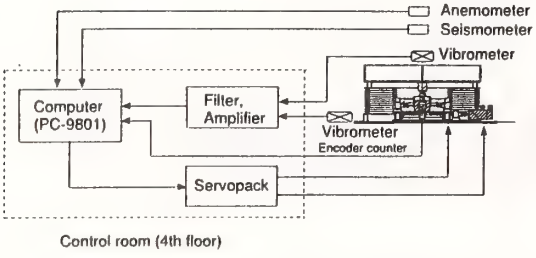

Fig. 22 HMD System and Entire View of Building in Future

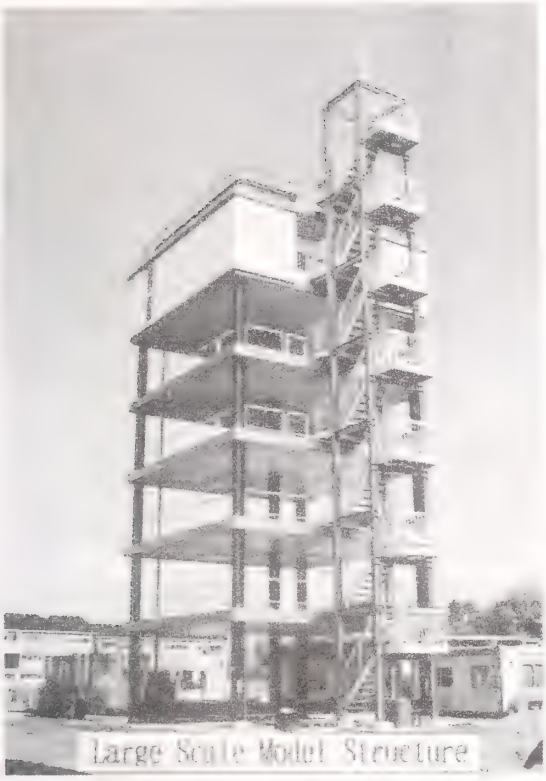

Fig. 23 Entire View of Actual Model

Fig. 24 Active Passive Mass Damper

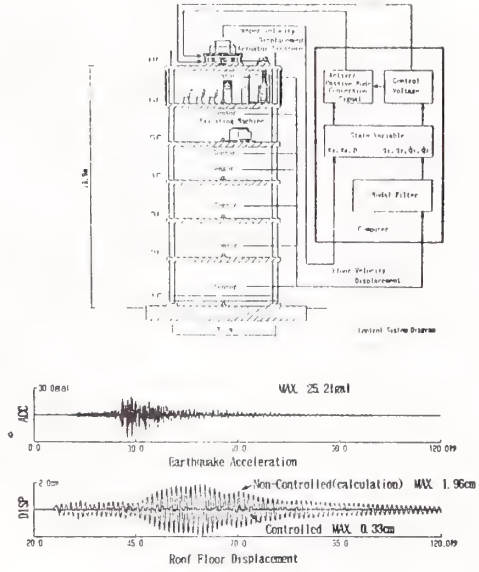

Fig. 25 APMD System and Comparison of Response

Fig. 26 Entire View of Actual Model

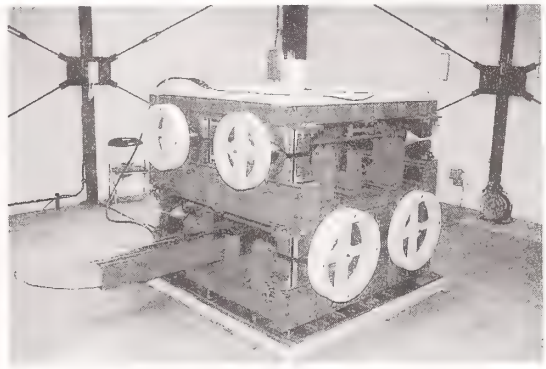

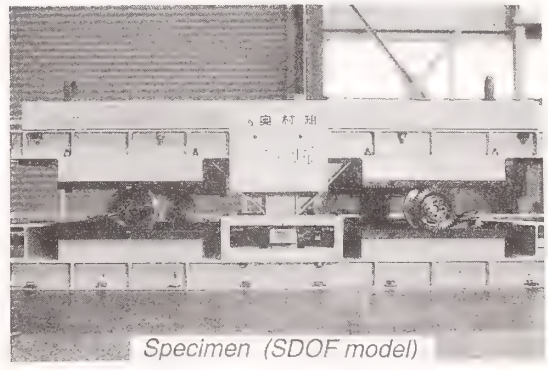

Fig. 27 TMD, VRD Divices

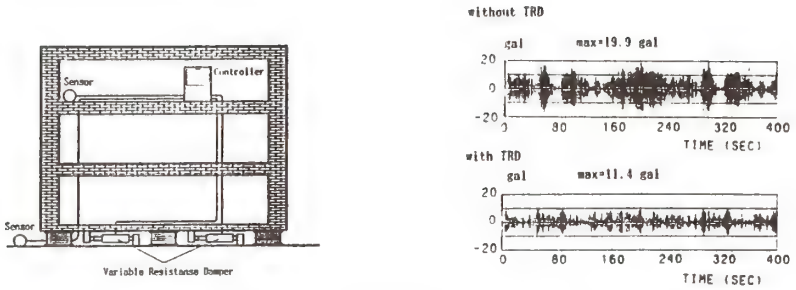

Fig. 28 Application of Semi-Active Vibration Control System and Acceleration Response of TMD System

Fig. 29 Entire View of Reduced Model

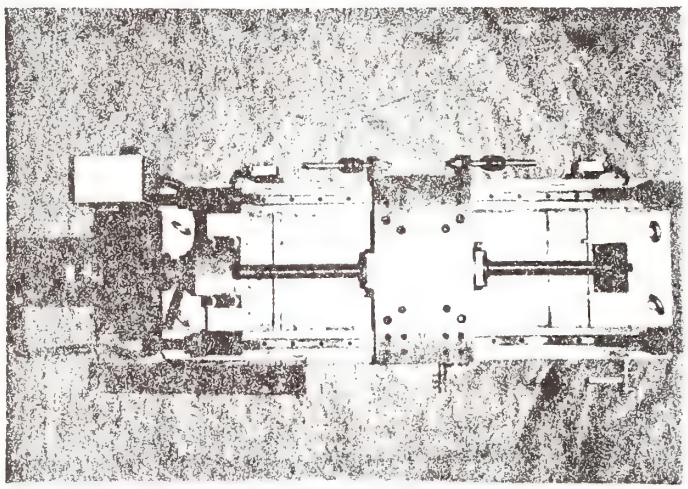

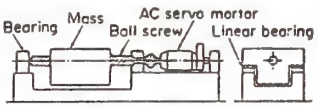

(a) Active vibration absorber

Fig. 30 AMD Device

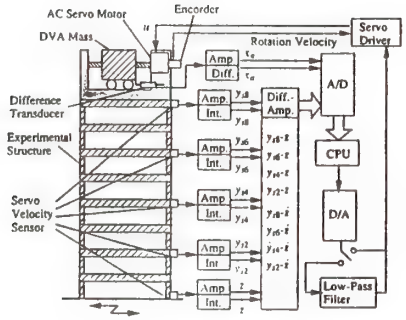

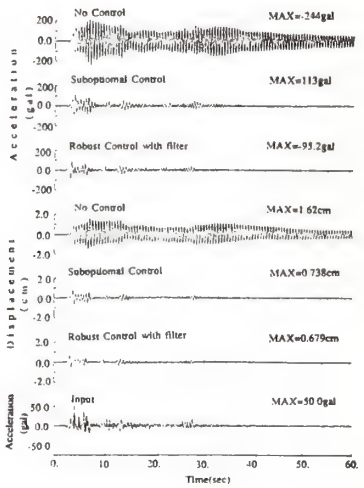

Fig. 31 AMD System and Comparison of Response

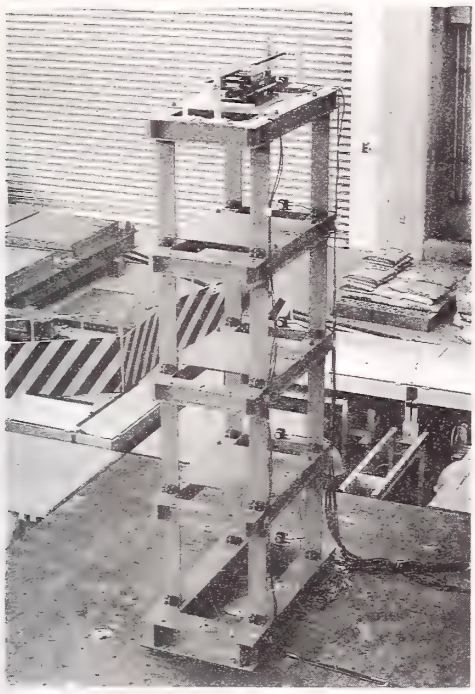

Fig. 32 Entire View of Reduced Model

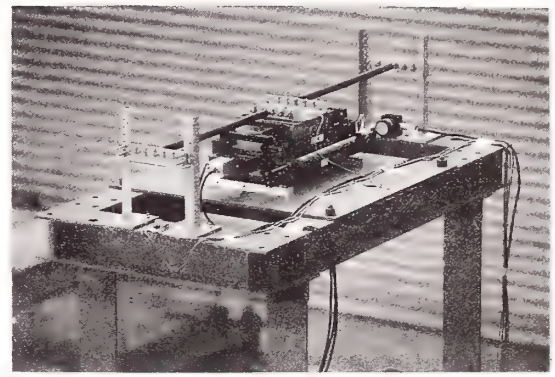

Fig. 33 AMD Device

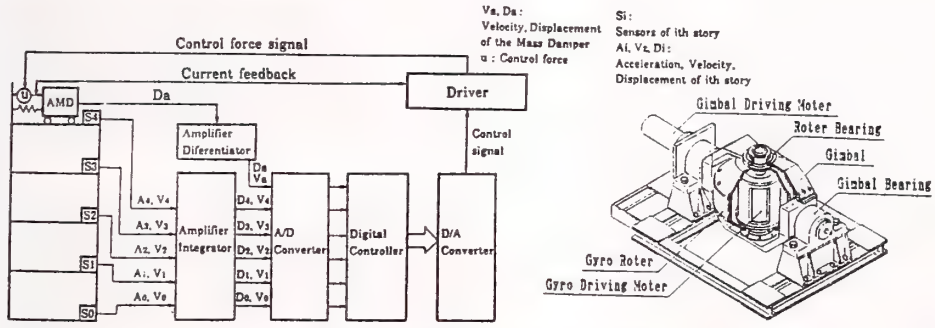

Fig. 34 AMD System and AMD Device using Gyrostabilizer

Fig. 35 Entire View of Reduced Model

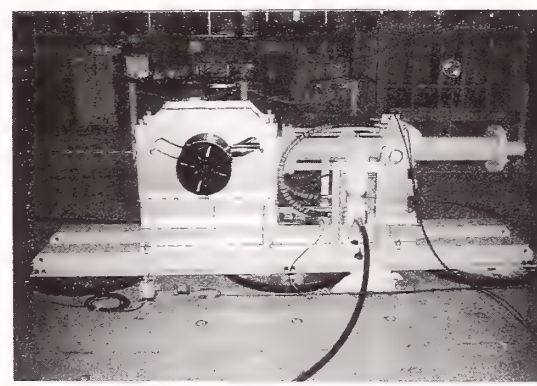

Fig. 36 AMD Device

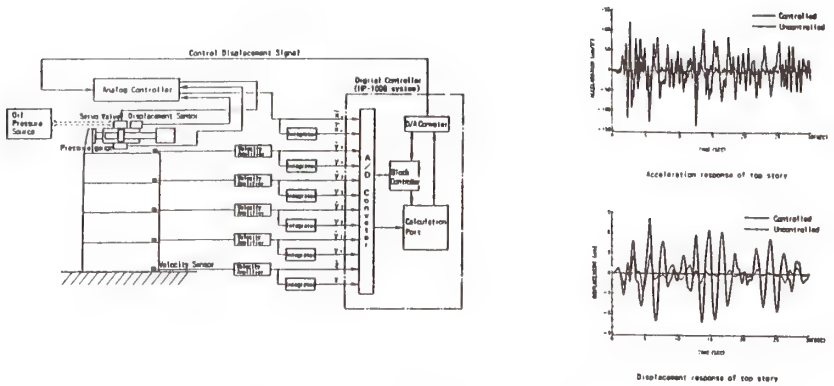

Fig. 37 AMD System and Comparison of Control

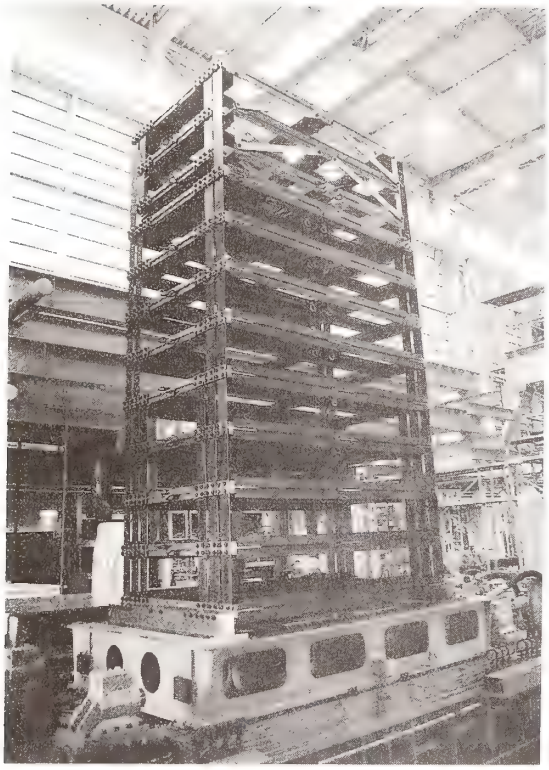

Fig. 38 Entire View of Reduced Model

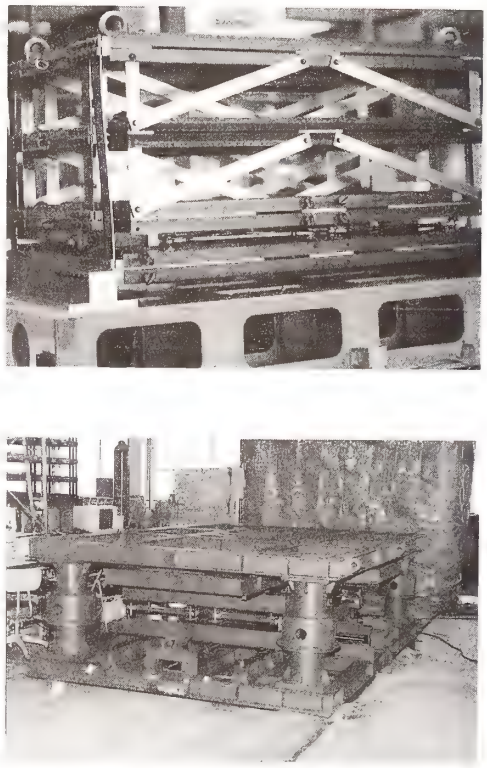

Fig. 39 HTMMD Device

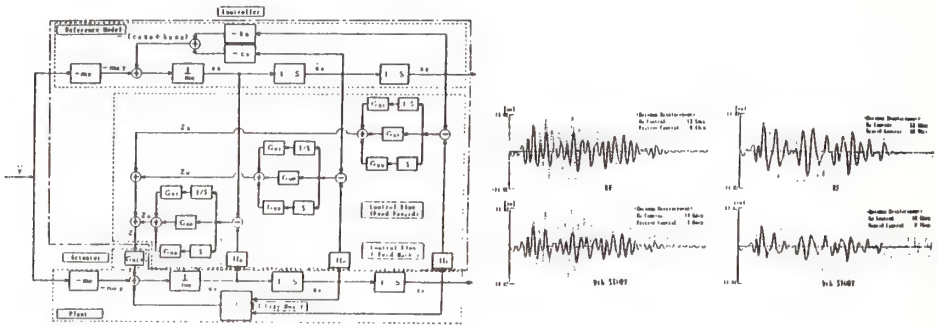

Fig. 40 Bolck Chart and Comparism of Control

Status of NSF Structural Control Research Programs

by

S. C. Liu[1], H. J. Lagorio[1], and K. P. Chong[1]

Washington, DC 20550, USA

ABSTRACT

This paper reports the status of a major research initiative in Structural Control launched in 1991 by NSF. Proposals submitted during the first year (in Fiscal Year 1992) of a 5-year program are analyzed. The proposal review process is described. Technical implications of intelligent control systems and smart materials as applied to civil infrastructure systems are discussed.

KEYWORDS: Structural control, infrastructure systems, smart materials, intelligent structures.

1. INTRODUCTION

Starting from 1989, an intensive effort has been made to develop a long-term national research program in structural control. An important consideration of such a program is to foster, on a coordinated basis, multidisciplinary research and development of passive, active and hybrid control technology for application to structures and nonstructural building systems under dynamic loads. Collaborative efforts among researchers in interdisciplinary areas involving academics, industrial experts and professional practitioners are considered extremely essential.

The important technical events taken place in this program development effort are:

* Establishment of the U.S. Panel on Structural Control Research, 1989.
* International Workshop on Intelligent Structures, Taipei, Taiwan, July 1990.
* NSF-EPRI Joint Workshop on Intelligent Control Systems, October 1990.
* U.S. National Workshop on Structural Control Research, University of Southern California, October 1990.
* NSF Workshop on Sensors and Signal Processing for Structural Control, February 1991.

PROGRAM INITIATION

Following these events, a firm research program base is established. In the summer of 1991, NSF officially announced the "NSF Research Initiative on Structural Control for Safety, Performance, and

---

[1] Program Directors, Engineering Directorate, National Science Foundation,

Hazard Mitigation" - a collaborative effort with the Strategic Highway Research Program (SHRP) of the National Research Council (NRC).

The fundamental objectives of the program initiative are:

- encourage innovations in passive, active, and hybrid control systems.
- advance sensor and actuator technology and signal processing techniques and their applications.
- develop intelligent robots, other devices and computer systems for structural safety.
- develop innovative systems for energy absorption, added damping, and variable stiffness.
- study the robustness and system reliability of control systems.
- develop guidelines, standards and practical approaches and techniques for design, fabrication and field installation.
- investigate emerging technology subjects in innovative structural systems, and smart materials, sensors, and devices for detection, sensing, monitoring, and diagnosis.

In line with the above objectives, the following key research problems are identified:

- New materials.
- Performance evaluation, analytical and experimental verification.
- Standardized test procedures and performance criteria.
- Integrated structural and architectural systems design techniques and standards.
- Control algorithm development, robustness, and reliability, adaptivity, and optimization.
- Sensors, actuators and monitoring system development and optimal deployment.
- Advanced computer technology incorporating artificial intelligence, neural network, fuzzy logic, etc. for on-line targeting, detection, monitoring, diagnosis, and control.
- Intelligent robots and devices.
- Modelling, signal processing, and computer simulations.
- Practical methods and techniques for design, manufacturing, fabrication, and implementation.
- Laboratory and field experiments of systems and devices under actual or simulated dynamic excitations.
- Design and demonstration projects of control systems as applied to new or

existing structures.

- Innovations in base isolation, energy dissipation devices, and other passive techniques.

To carry out the above described research, collaboration among researchers, practicing engineers, and manufacturers is encouraged. It is expected that the research will generate new knowledge, techniques, and a better understanding of the working principles as well as practical limitations inherent in various control systems so that conditions of applicability and design standards and limits of each class of systems can be established and evaluated.

The ultimate goal of the research program is to bring about technological advances through system integration and development innovation so that control technology can be realistically implemented in a timely fashion to provide safety resistance to protect structures such as buildings, bridges, tunnels, and other critical lifeline systems against earthquakes, winds, and other natural or manmade hazard environments, in addition to improving the quality of life.

PROPOSAL EVALUATION

Upon announcing the above-mentioned research initiative, sixty seven (67) proposals were received by the specific proposal submission deadline, i.e., October 30, 1990. Since these proposals cover a wide spectrum of diverse technical subjects, special considerations were given in the review process of such proposals - following the traditional NSF peer review system - to ensure all proposals are evaluated by their technical/scientific merits, relevant factors such as educational and practical values, collaborations between academic and industrial sectors, interfaces among cross-disciplinary subjects, etc.

As a result, a 2-stage review process was adopted by which

(1) Each and every proposal was sent out by mail to peers for disciplinary reviews,

(2) A cross-disciplinary review panel consisting of experts in such areas as control systems, earthquake and wind engineering, sensors and actuator technology, materials and transportation systems was convened to evaluate and rank these proposals.

The panel, after a 1 1/2 day deliberation ranked the proposal into three groups: (1) Highly Recommended, (2) Fundable if Funds are Available and (3) Not Fundable.

Based on the Panel's recommendations, NSF will select by Summer 1992 approximately 7 to 10 proposals for support.

PROPOSAL ANALYSIS

Among proposals submitted, 40 deals with control of earthquake responses of structures in various modes, vs. passive, active, or hybrid. Twenty four (24) proposals study the wind response control and 15 proposals address problems in control of general structural responses and vibrations including one dealing with waves in periodic structures having imperfection and another dealing with random, chaotic motions by active techniques. Among the active control techniques, one proposal investigates the application of active structural members for earthquake and wind resistance.

Several proposals (Table 2) involve development and application of fiber optical sensors in structural control- 4 against earthquake loads, one against winds, and 3 others for general structural motion control. Among proposals which contain the study of actuators and actuation, 6 address earthquake problems, 5 wind problems, and 3 general vibration problems. Types of actuators proposed in these studies include active mass dampers (or drivers), active bracing systems, piezoelectric and electromagnetic actuators, regeneratic actuators, screw jackets, shock absorbers, controlled friction, viscous, or other types of dampers, connectors, or energy dissipators. In terms of processors (i.e., control algorithms, computer software and hardware systems), 3 proposals focus on optimal, robust control against earthquakes, 1 against winds, adaptive control techniques, 6 proposals address earthquake problems, 3 wind problems, and 2 general motion control. Several other proposals employ or involve neural networks techniques in control algorithms and models, 3 for earthquakes and one each for winds and general motion control. Proposals involve material innovations and applications (i.e., high-performance or smart materials) are relatively few. Among them are investigations in using shape memory alloys to provide variable damping and actuation, and self-healing materials for repairing of concrete crack.

Among the proposals described in Tables 1 and 2, there are a few dealing specifically with the systems aspects of the control systems themselves or the structural systems which are under control. These aspects include performance evaluation/requirements/ standards, control systems which are designed for monitoring, detection, and maintenance purposes, and methods for system identification, modelling, and reliability issues involved (Table 3).

These proposals can also be looked at from the application points of view (Table 4). Almost 50% (30 proposals) of the total proposals submitted are attempted to applied to earthquake protection of

various types of buildings structures or their components. Seventeen (17) proposals involve wind-resistant applications and 14 others for other types of motion or response control. In addition, there are a few proposals for applications to non-building types of structures, i.e., bridges (and their components), lifeline systems, industry facilities, and other civil infrastructures. Among these one proposes to investigate control of marine vehicles from impacting to bridge piers, another proposes to use passive approach to control the earthquake damage to wharf structures. It is also interesting to note that while most proposals are formulated for engineering analysis/ design/construction applications in general terms, a few are prepared for more specific purposes, for example, to retrofit a structure under various environmental load conditions, and to retrofit bridges using a vibration isolator controlled in real time.

ENGINEERING RESEARCH IN INTELLIGENT CONTROL SYSTEMS AND SMART MATERIALS

The above analysis indicates an enthusiastic response by the U.S. research community for research in developing and applying intelligent control systems (ICS) to civil engineering structures. It is clear that considerable advance can be made to improve structural safety through research in structural, earthquake, and wind engineering through use of control technology. The possibility of applying control systems to mitigate the structural damage against earthquakes, winds, and other loads open up a wide range of challenging research opportunities for multidisciplinary investigators in the field. In this connection, it is interesting to also note some current engineering research in smart materials under way.

Smart materials is a class of materials which have their own sensors (nervous system), actuators (muscular systems) and control (brain system), mimicking biological systems. Current research activities aim at understanding, developing and synthesizing material systems which behave like biological systems. The U.S., Japan, and industrialized Western European countries are leading in the fundamental research on smart materials and smart systems. To this point, no smart materials, except some that have been biologically synthesized, have been successfully produced beyond laboratories. The Japanese remains at a stage of concept formulation. The U.S. efforts have been focused on development of smart biomaterials and smart systems for control of space structures and mechanical vibrations. Sensors include: optical fibers, strain gages, corrosion sensors (e.g., one developed at Lehigh Engineering Research Center) and other environmental sensors, sensing particles

(e.g., magnetic particles). Examples of actuators are: shape memory alloys (which would return to their original shape), hydraulic systems, piezoelectric devices (which move in an electric field). Microchips, computer software and hardware systems constitute the control aspects.

Smart materials may even heal themselves when cracked, for example, self-healing concrete being investigated in universities of Illinois and Michigan. One idea is to place hollow fibers filled with crack-sealing material into concrete, which if cracked would break the fiber releasing the sealant. Hollow beads filled with sealant (for self-healing), and smart paints, which will release red dye (contained in capsules) when cracked are also being investigated. Concrete may also heal its own cracks under pressure with sufficient humidity. Optical fibers which change in light transmission due to stresses are useful sensors. They can be embedded in concrete or attached to existing structures. Optical fiber sensor systems have been applied for on-line, and real-time monitoring of critical components of structural systems (such as bridges) for detection and warning of imminent structural failures. Fundamentals and dynamics of embedded optical fibers in concrete, electro-rheological (ER) fluids for the vibration control of structures have been investigated. Such ER fluids can stiffen up very rapidly (changing elastic and damping properties) in an electric field.

Several such smart materials are studied to provide sensoring and actuating capabilities, i.e., shape memory alloys, and surface superelastic microalloying as sensors and microactuators; and magnetostrictive active vibration control.

CONCLUDING REMARKS

It is clear that smart materials, smart structures, and control technologies, when sufficiently developed and broadly implemented, possess an excellent potential to impact the safety design and construction of new structures in the future. Furthermore, the dynamic control and intelligent technology also offers a viable, alternative solution to the nation's enormous problems in the construction of new civil infrastructure and rehabilitation of existing structures which are deficient in their functionality, serviceability and in their seismic, wind, or other resistant capacities.

As such it is generally agreed that dynamic control and intelligence technology holds considerable promises in the design applications of civil engineering structures, new and existing. By its interdisciplinary nature, such technology also has the potential impact to the future development of a diverse field of scientific or technical subjects, such as material

science, vibration,
biotechnology, neural network,
and new devices.

Control Technique	No. of Proposals				
	Earthquake	Wind	General Vibration	Waves	Random Chaotic Motion
Passive	12	8	4	1	
Active	18	12	8		1
Hybrid	10	4	1		
Total No. Proposals	40	24	13	1	1

Table 1. Proposal Distribution by Control Techniques

Control Element	No. of Proposals		
	Earthquake	Wind	General Vibration
Sensors	4	1	3
Actuators	6	5	3
Processors (Algorithms, Modelling, etc.)	13	4	3
Materials	2	1	2
Total No. Proposals	25	11	11

Table 2. Proposal Distribution by Control Elements

	Earthquakes	Winds	General Vibrations	Applied to Highway Systems
Performance Evaluation	2	1	2	1
Monitoring Detection Maintenance	4	1	3	4
System Modelling & Identification	1		1	
Reliability	3		2	
Total No. Proposals	10	2	8	5

Table 3. Proposals to Study System Characteristics, Modelling, and Analysis

		Earthquakes	Winds	Others
Elements/Systems Types of Structures	Buildings	30	17	14
	Bridges	4	1	1
	Lifelines, Infrastructures	3	1	
	Wharves	1		
	Traffic Signal Structures		1	
	Claddings	2		
	Nonstructural Elements, Secondary Systems	2		
Special Purposes	Retrofit	3	2	1
	Diagnosis, Monitoring	1	1	4
	NDE			2

Table 4. Proposal Distribution by Applications

Significant Results From Standardization Work on Rubber Bearings for Base-Isolation Buildings

by

Yuji Ohashi[1] and Hiroyuki Yamanouchi[2]

SUMMARY

This paper reports the study on techniques of effective use of the laminated rubber bearings used for base isolation system, the mechanical characters of the bearings and the relation between the mechanical characters and the effective factors of the bearings.

KEY WORDS

base isolation system, rubber bearing, standardization,
Comprehensive Project on New & Advanced Materials by the Ministry of Construction.

1.PREFACE

The Ministry of Construction carries on the Comprehensive Project on New & Advanced Materials. As one part of the study, the laminated rubber bearings used for base isolation system are studied as one of the new material for new structural engineering of buildings.

In this study, some types of laminated rubber bearings, the cracters of the rubber, the mechanical characters of the bearings, the methods of testing, design procedure, production procedure of the bearings, maintenance of the bearings and the base isolated buildings and technical terms are summarized.

The mechanical characters of the bearings and the relation between the mechanical characters and the effective factors of the bearings are studied.

In this project, we intend to provide the guideline of the effective use of the rubber bearings.

In Japan, a lot of studies are already carried out for base isolation systems and rubber bearings. Many research papers which deal with the characters of the materials of the rubber bearings, mechanical characters of the bearings, design, analysis and response of base isolated buildings in case of earthquakes are reported.

The Architectural Institute of Japan issues " the Recommendation of the Base Isolated Buildings "

Some fifty buildings which adopt base is olation system are constructed or under construction in Japan.

In the project, considering these circumstances, we intend to contribute to build base isolated buildings with sufficient safety by providing information and making guideline of laminated rubber bearings.

---

*1 Senior Research Engineer
*2 Senior Research Engineer of International standard
Structural Engineering Department, Building Research Institute, Ministry of Construction
Tatehara-1, Tukuba-City, Ibaraki, Japan

In order to make the guideline, we have been collecting much information on rubber, rubber bearings and mechanical characters of the bearings which the structural engineers should understand and we intend to arrange the condition for the establishment of standards of the bearings.

We set up research committees in Japan Rubber Association. The Ministry of Construction and that association made research corporation contract.

There have been many disastrous earthquakes in the history of Japan. The extreme forces of earthquakes have inflicted great damage on building structures, and it has long been a major task of Japanese building technology to find ways of preventing danger of earthquakes.

Thus, it is highly necessary that buildings in Japan be able to safely withstand attacks of earthquakes. Concept of earthquake proof design of buildings in Japan has been to arrange structural elements appropriately and to maintain sufficient strength, ductility and stiffness for the structural elements.

Several decades of years ago, such kinds of ideas as to isolate the basement of a building from ground were considered. These ideas were called "base isolation systems", and a few researchers studied and developed these ideas, but because of lack of methods of analysis and devices, these ideas were seldom realized.

After the second world war, the development of computer technology also promoted structural analysis methods. Using computerized seismic analysis, construction techno logy of super-high raised buildings, which use the earthquake ground motions recorded in the United States, was developed around 1960.

With these knowledge, we have gotten the behavior of buildings in cases of earthquakes. Laminated rubber bearings were developed. Using the bearings, we became to realize base isolation systems for buildings.

These systems can be adopted not only for buildings but also for other structures such as bridges and machines. This research project focus on base isolation systems of buildings and laminated rubber bearings.

2. Base isolation structure

Advances in response analysis technology had given the knowledge that seismic force could be reduced by lengthening the natural period of a building, and research was carried on how this could be done.

Laminated rubber bearing was invented around 1980. The bearing is made of several alternating layers of rubber sheets and steel plates and can withstand great forces in a vertical direction, such as the self-weight of the building, while horizontally it is flexible in character.

When they are installed in the foundation of a building, or the columns of its lowest floor, they can support the self-weight of the building and at same time, because of horizontal flexibility, can lengthen the building's natural period. That reduces seismic force.

In Japan, it is already beyond the experimental stage and has been introduced gradually into actual construction. Compared with conventional structure it is capable of considerably reducing the effects of seismic force.

Research has also done into other method of absorbing or controlling the response from an earthquake. One of them is to install a "damper". Dampers can be installed independently in the walls or structural braces, or can be used in combination with laminated rubber bearings as part of a base

isolation structure system.

Records of seismic response of the buildings which use base isolation systems using rubber bearings indicate that the acceleration response can be reduced to about 1/2 or 1/3 of the earthquake ground motion. Seismic response of usual buildings usually becomes twice or three times of ground motion. We can understand the effects of the base isolation systems apparently from these records.

3. KINDS AND CHARACTERS OF RUBBER BEARINGS AND DAMPERS

3.1 RUBBER BEARINGS

High strength and stiffness for vertical direction are required for rubber bearings to sustain self weight of buildings. If the stiffness for vertical direction is not sufficient, vertical response will be larger and rocking vibration may occur.

For lateral direction, low stiffness and large deformability are required to have long natural period of building.

Steel plates of the bearings constrain vertical deformation and that gives high strength and stiffness for vertical direction. For lateral direction, deformation is not constrained, soft character of rubber gives low stiffness and large deformability.

Shapes of the rubber bearings are usually flat cylinders. Capacity of load sustain ability, stiffness and deformability depends on the shape, size, thickness and number of rubber sheets. (Fig. 1)

The lower the thickness is and the smaller the number of rubber sheets are, the higher the vertical stiffness of the bearings is.

The lateral stiffness of the bearings is usually about 1/1000 of the vertical stiffness of the bearings. Shape of the bearing relate with the character of deformability.

We use the index which shows shape, "flat ness", of a bearing. We call the index second shape factor, S_2, which means diameter/thickness of the bearing. Usually, bearings S_2 of which are over 2.0 are used. (Fig. 2)

When S_2 is large, namely, the baring is very flat, sheer deformation becomes dominant and the character of deformation for lateral direction becomes stable. When the S^2 is not so large, ratio of bending deformation in total lateral deformation becomes large and the character of deformation for lateral direction becomes unstable.

The role of rubber sheets is to maintain low stiffness and high deformability of the bearings for lateral direction. The role of steel plates is to maintain high strength and stiffness of the bearings for vertical direction by constrain of deformation of rubber sheets.

3.2 KINDS AND CHARACTER OF RUBBER BEARINGS

In Japan, we have four kinds of rubber bearings as showed below.

① bearings of natural rubber
② bearings of high damping rubber
③ bearings of lead and rubber
④ bearings of slip layer and rubber

① bearings of natural rubber

This type of bearings are used most often. Natural rubber is used and have rarely damping. Up to 200% of sheer deformation of rubber itself, character of the deformation of the bearings is usually elastic. When the deformation becomes larger than that, hardening will occur. The sheer deformation of the rubber when the rubber is broken is about or over 400%.

② bearings of high damping rubber

This type of bearings use synthetic rubber which has high damping character.

③ bearings of lead and rubber

This type of bearings use lead and install lead in the center of bearing. Plastic deformation of the lead absorbs energy of vibration and gives damping character. (Fig. 3)

④ bearings of slip layer and rubber

This type of bearings use slip layer of such as fluorine and rubber bearings. In cases of small earthquakes, because of fliction of the layer, rubber bearings act and in cases of large earthquakes because of the slip of the layer seismic force of the earthquake dose not become large. Springs or elastic rubber bearings are used with these types of bearings to return the position of lateral deformation of the building to original position. (Fig. 4)

② and ③ type bearings have damping, so these bearings do not require dampers. But, ① type bearings require dampers to have damping character.

Cover rubber is used for each types of bearings to protect bearing from corrotion and to have durability.

Flange steel plates are installed on the face and bottom of the rubber bearing.

3.3 DESIGN OF RUBBER BEARINGS

It is required for rubber bearings to have below mentioned mechanical characters.

(a) vertical strength to sustain the load of building

(b) lateral stiffness to give suitable natural period

(c) lateral deformability

Design procedure is described below.

1) to settle the design condition such as vertical strength, lateral stiffness and lateral deformability, etc.

2) to settle the kinds of rubber material and characters of rubber

3) to settle the shape of the bearing such as diameter and total thickness

4) to settle the structure of the bearing such as number and thickness of rubber sheets,

5) to certify whether the design meets the design conditions of the bearing

3.4 KINDS OF DAMPERS USED WITH RUBBER B EARINGS

When the rubber bearings do not have enough damping, some kinds of dampers are used for base isolation systems. Kinds of the dampersare followed.

1) viscous damper (Fig. 5)
2) plastic damper (Fig. 6)
3) friction damper (Fig. 7)

4. STRUCTURAL DESIGN PROCEDURE OF BASE ISOLATION SYSTEMS

Usual procedure of structural design of base isolation is followed.

1) to settle design criteria such as allowable response and size of earthquake

2) study and survey of site and character of earthquake which is anticipated at the site

3) to settle the natural period of the building and characters of bearings

4) structural design based on the initial response analysis

5) certification whether the design meets

the design criteria

6) design of details

There is a special approval system by the Minister of Construction for new structures which do not comply with the standards to prevent the building codes from becoming too rigid. The system has provided the way for a lot of new building structure to date.

Before the approval of the Minister, the safety of the buildings shall be evaluated by the committee of the Building Center of Japan under the supervision of the Minister.

Base isolation systems are the newly developed systems and do not comply with the existing building codes.

The construction of base isolation systems requires the approval of the Minister of Construction and evaluation by the committee of the Building Center of Japan before the construction work of the building. In order to evaluate the safety of the buildings which use base isolation systems.

To evaluate the safety of such buildings, adding the allowable stress design, dynamic response analyses are taken using records of the ground motions of past earthquakes, where some typical ground motions such as "El Centro" and the ground motions which were recorded near the construction site of the building are used.

At this time, the scales of the ground motions are normalized and 2 levels of the ground motions are adopted.

Maximum velocity of the ground motions of level 1 is some 25cm/sec and that of level 2 is some 50cm/sec. Response from level 1 ground motions shall not exceed elastic limit of the bearings and that of level 2 ground motions shall be within apt value of deformation.

5. USUAL CHARACTERS OF RUBBER BEARINGS

Mechanical characters of bearings and dampers which are already designed are as followed.

1) vertical load sustain ability for permanent loads - 20 $\sim$ 90 kgf/cm^2

2) natural period of base isolation system - 1.0 $\sim$ 3.0 second

3) damping coefficient - 5 $\sim$ 15 %

These characters are shown in Fig.8 $\sim$ Fig.10

6. CLOSURE

We intend to provide guideline to give effective information for use of rubber bearings by studying above mentioned items

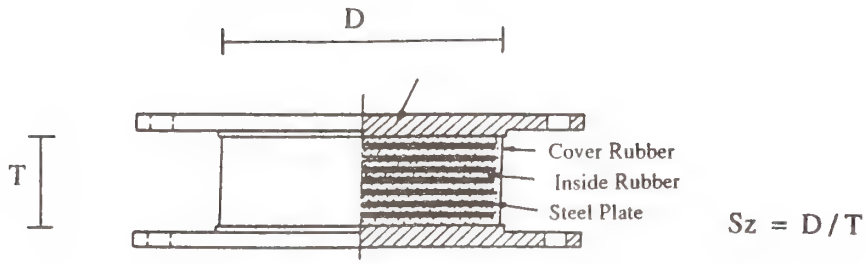

Fig. 1 Rubber bearing

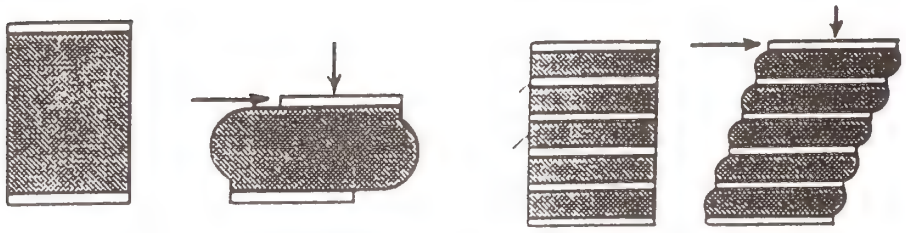

① Single Rubber ② Laminated Rubber

Fig. 2-1 Single rubber and laminated rubber

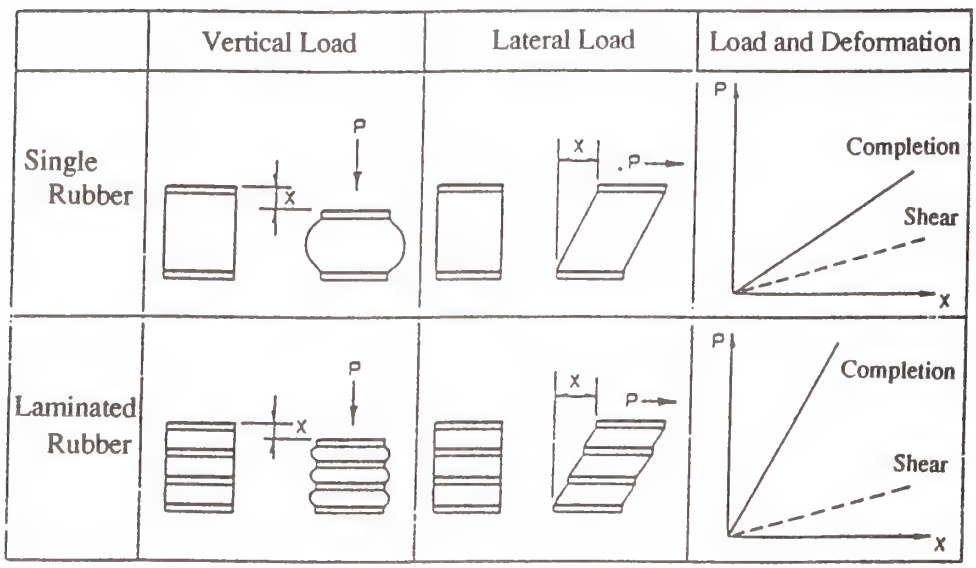

Fig. 2-2 Single rubber and laminated rubber

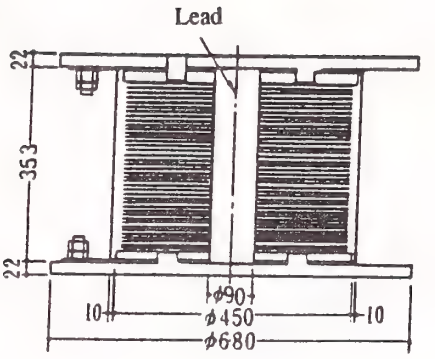

Fig. 3 Lead rubber bearing

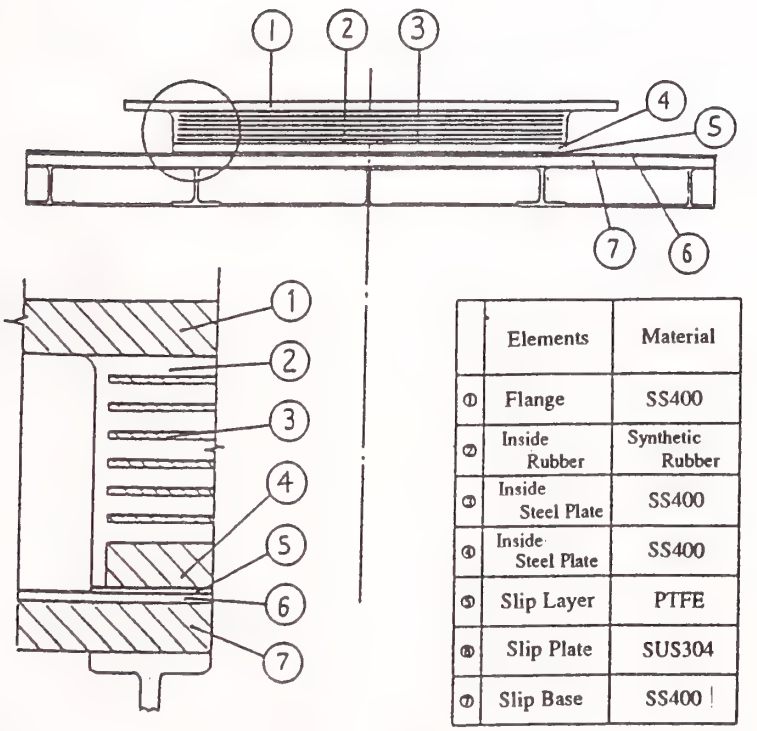

	Elements	Material
①	Flange	SS400
②	Inside Rubber	Synthetic Rubber
③	Inside Steel Plate	SS400
④	Inside Steel Plate	SS400
⑤	Slip Layer	PTFE
⑥	Slip Plate	SUS304
⑦	Slip Base	SS400

Fig. 4 Slip layer and rubber bearing

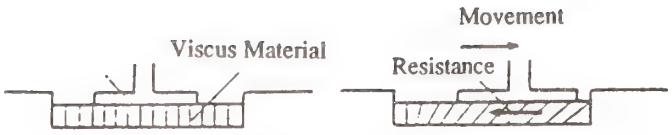

Fig. 5 Viscus damper

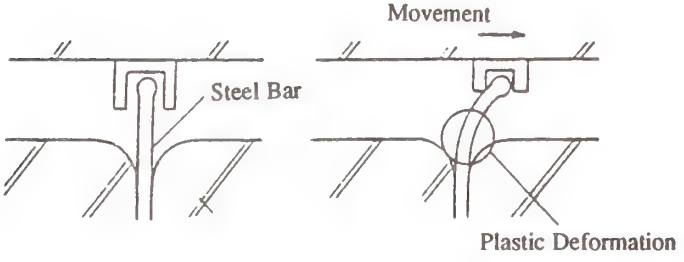

Fig. 6 Plastic damper

Fig. 7 Frictional damper

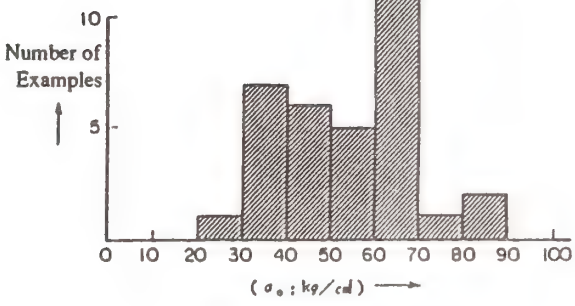

Fig. 8 Stress of bearing

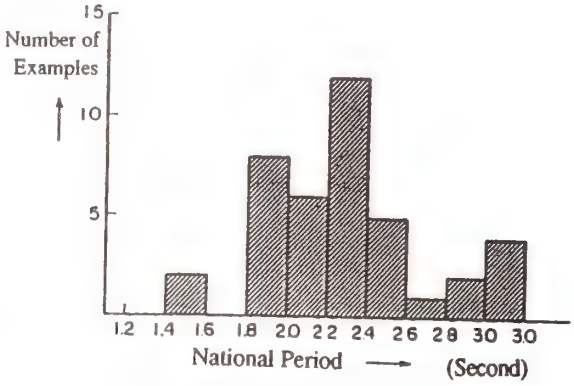

Fig. 9 Natural period of building

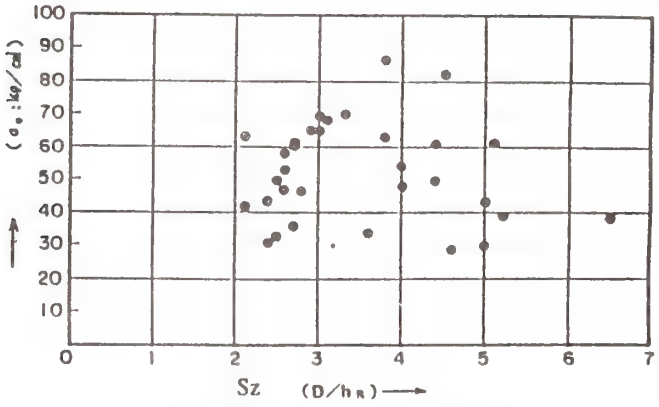

Fig. 10 Sz and stress of bearing

Effect of Temperature on the Dynamic Behavior of Base-Isolated Bearings

by

Osamu Nakano[1], Hideyuki Taniguchi[2], and Hiroaki Nishi[2]

SUMMARY

Our concern is whether the base-isolated bearings, which have recently been introduced to the field of the bridge design in Japan, assume its performance in such cold regions as Hokkaido. For this reason, full-size base-isolated bearing models in accordance with an ongoing bridge construction project were prepared in order to pay attention to their behavior at low temperatures through indoor experiments. As a result, it has been shown that the base-isolated bearing itself has been much effected by temperature, however, it has not been understood that how the change of performance on the base-isolated bearings could influence the response of the entire bridge.

Therefore, further investigation has been made by performing dynamic analysis.

As the result, it was learnt that the bending moment at the base of pier could increase by 40-50% in a certain condition.

KEY WORDS: Base-isolated bearing, Cold region, Effect of temperature variation, Dynamic analysis

1. INTRODUCTION

Generally, the base-isolated bridge is so designed as to decrease the seismic force by making the natural period of the entire bridge longer with a special device called a base-isolated bearing, which supports the superstructure softly on the bearing part in horizontal directions and has a damping characteristic.

The Hokkaido Development Bureau is now constructing the Onnetoh-Oohashi Bridge on National Trunk Road 44 in Nemuro in which side-span on the Kushiro side was selected as such the above-mentioned type of bridge.

As concern about the performance of base-isolated bearings was presented by a regional construction office, that meant the performance might be influenced by temperature drop, indoor experiments in terms of stiffness and damping factor of rubber material properties have been performed for the past three years, which include 50-cycle shear tests, compression tests, shear tests and shear history tests on various temperatures.[1)] Two types of full size models of lead rubber bearing (LRB) and high damping rubber bearing (HDR) are used in the experiments. The models were designed and produced in accordance with the basic design of base-isolated bearings on the Onnetoh-Oohashi Bridge. As the result, it was proved that the base-isolated bearing itself had the strong dependency on temperature with regard to the stiffness, which was not expected before the tests. In this connection, further investigation has been made by conducting dynamic analysis of the entire bridge from the point of view that how the above-mentioned tendency might contribute to the response of the entire bridge.

2. OUTLINE OF THE ONNETOH-OOHASHI BRIDGE

The Hokkaido Development Bureau has decided to plan a special bridge with base-isolated bearings under the schedule of the reconstruction of the existing Onnetoh-Oohashi Bridge on National Trunk Road. In Japan, eight base-isolated bridge projects were planned at the first stage, out of which only the Onnetoh-Oohashi Bridge project is located in a cold region like Hokkaido. The construction site is located at the bottom of the Nemuro Peninsula where the lowest mean temperature is -9.1°C in the past 30 years. The present Onnetoh-Oohashi Bridge is the steel curved-chord Warren truss + steel composite girder bridge with the total span of 99.5 m, built on the Onnetoh in Nemuro, Hokkaido and the new bridge (Fig. 1) after the reconstruction will be 456 m long with the side-span of four-span continuous plate girder and the main span of Nielsen-type Lohse girder with the span of 140 m. The reconstruction is expected to be completed in 1995. Its base-isolated structure is adopted only in the side-span on the Kushiro side and the normal rubber bearings (RB) will be used for both ends A1 and P4.

This year, the side-span bridge with base-isolated bearings is supposed to be erected and the vibration test is scheduled to be done by our laboratory late fall.

3. OUTLINE OF BASE-ISOLATED BEARINGS

The base-isolated device consists of two parts: the isolator softly supporting the structure and the damper with the damping effects by energy absorption. The isolator uses the material called the layered rubber consisting of rubber and steel alternately layered and the damper uses lead or steel bars. The base-isolated devices utilized in bridges are often installed at the bearings part, so that they are especially called base-isolated bearings. Therefore, the base-isolated bearing should be of such a compact design as an integration of isolator and damper. The base-isolated bearings currently available are roughly divided into the following two kinds: those in which lead plugs are inserted so as to provide the layered rubber called lead rubber bearings with damping effects and those using the specially-designed rubber called the high-damping

1. Head, Structure Division, Civil Engineering Research Institute, Hokkaido Development Bureau

2. Research Engineer, Structure Division, Civil Engineering Research Institute, Hokkaido Development Bureau

rubber in which the rubber material itself of the layered rubber called high-damping rubber bearings has the damping effect. Each kind of base-isolated bearing is as shown in Fig. 2.

4. TEMPERATURE DEPENDENCY OF BASE-ISOLATED BEARINGS

The dynamic characteristics of base-isolated bearings are presented by the equivalent stiffness (K_e) and the equivalent viscosity damping factor (h_{eq}) obtained from the shear force - shear displacement curve approximated with the bilinear spring as shown in Fig. 3. K_e and h_{eq} can be defined as the following expressions in general:

$$K_e = \frac{AE}{EC}, \quad h_{eq} = \frac{1}{\pi} \cdot \frac{\Delta W}{W}$$

Where, ΔW: Area of parallelogram ABCD
W: Area of triangle AEC

The shear tests were performed using a full-size model for obtaining the above K_e and h_{eq} from the actual shear force - shear displacement curve[2]. The design displacement of the model can be acquired by the check of ultimate bearing capacity of reinforced concrete piers for lateral force with the resulted value of 15 cm. For details such as the design conditions of the specimen, refer to Bibliography 1). The shear test was performed under a vertical load of 92 tons (= dead-load reaction) as the horizontal displacement is 150 mm (= design displacement) and loading is 40 seconds. For the temperature of specimens it was changed from +30°C to -20°C. The equivalent stiffness and the equivalent viscosity damping factor on each temperature level is as shown in Table 1. The shear force - horizontal displacement curves of LRB, HDR measured at room temperature and -20°C are shown in Fig.4.

For the stability against the temperature change of base-isolated bearings, it is stipulated that the ratio of the equivalent stiffness is within 1.5 between +30°C and -30°C in order to suppress the change of the natural period of the bridge within 20% in the "Guidelines for the base-isolated bearing design method for road bridge (draft)"[3](hereinafter referred to as the guideline).

But, the ratio of the equivalent shear stiffness at -20°C to that at 30°C is 1.63:1 for LRB and 1.59:1 for HDR, where the average of the values of the two specimens were taken for LRB, HDR respectively.

Recently additional experiments have been done at -30°C and room temperature for each bearing under the condition that the loading cycle is 100 seconds due to the limitation of capacity of the test machine.

The following data were obtained from the experiments.

The equivalent stiffness at room temperature are 1391 kg/cm for LRB and 1832 kg/cm for HDR, and those at -30°C are 2089 kg/cm and 3390 kg/cm respectively. The ratio of the stiffness between the two temperature are 1.58, 1.85 for LRB, HDR respectively.

5. ANALYTICAL MODEL AND METHOD

In this analysis, the focal points are placed on the relative displacements of the bearings where relative displacement is defined as the difference between the top and the bottom of the base-isolated bearings and the maximum bending moments at the base of the piers in the case of temperatures between room temperature (approx. 20°C) and -20°C.

For the analytical model, the side-span bridge with the base-isolated bearings was picked up alone due to the simplification. Then, the bridge was replaced by the lumped mass model as shown in Fig. 5. In which, the pile foundations were also replaced by the three-types springs. For the modeling of the base-isolated bearings, which is shown in Fig. 6, a linear-spring model with the equivalent stiffness and the equivalent viscosity damping factor was applied to the equivalent linear analysis and the bi-linear model was adopted in the case of the non-linear analysis.

In the both analysis, the piers and base springs were treated as elastic bodies and the latter was calculated from N value of the ground depth intended for the calculation according to the calculation method described in "Road bridge specifications for seismic design edition"[4]. The time history analysis was adopted as the analytical method. For the both analyses, the computer program "NLDAP"[5] for two dimensional analysis use that was developed in our laboratory, in which calculation was made with the direct integration of Newmark-β method and the Proportional damping was assumed for the viscosity damping. In this case, the analysis has been carried out in the longitudinal direction only, because the Onnetoh-Oohashi bridge is allowed to move toward the above-mentioned direction.

6. DYNAMIC ANALYSIS

6.1 Eigenvalue Analysis

First of all, the eigenvalue analysis was performed in the respective temperatures in order to identify the vibration characteristics of the bridge.

The equivalent stiffness and the equivalent viscosity damping factor for each pier at room temperature and -20°C are listed in Table 2. Fundamental value for each bearing is based on the indoor experiments where the bearing was deformed up to the design displacement (= 150 mm). But, the values in the table are get by multiplying the average of the fundamental values (two specimens for each of LRB and HDR) by the number of bearings (six units).

The normal rubber bearings (RB) will be used in the bearings of A1 and P1, however, because the experimental results are not obtained at room temperature, the design value[6] 363 t/m for the stiffness is adopted as it is, while at -20°C that value is decided as 472 t/m, 1.3 times larger than the design value assuming that the change of the stiffness of normal rubber bearing is similar to that of the base-isolated bearing at this temperature.

Table.3 represents natural periods for the first ten modes by temperatures. The table indicates that the natural period of the first mode on -20°C was decreased

by approx.13 – 14 % compared with that of the room temperature due to the increase of the base-isolated bearing stiffness, however, those of the other modes changed slightly. Since the horizontal displacement of the superstructure dominates in the first mode, it might be considered that the effect appeared strongly. The first mode in the case of LRB at room temperature is shown in Fig. 7.

6.2 Result of time history analysis

6.2.1 Equivalent linear analysis

The strong motion observation has being conducted since 1975 when a analog-type seismograph was installed at the existing Onnetoh Oohashi Bridge.

The strong motion record used in the time history analysis is one of recorded data from the earthquake which took place on January 12, 1978 with magnitude at 5.1. The waveform recorded on the strong motion seismograph and the acceleration response spectrum are shown in Fig. 7 and 8 respectively.

The analysis was performed under the following conditions:

Integral time interval:	$\Delta t = 0.01$ second
Response time:	$T = 10$ seconds
Newmark-β method:	$\beta = 1/4$

The damping factor h of the entire bridge was calculated using the following expression which is indicated in the guideline.

$$h = \frac{\Sigma h_{Bi} K_{Bi} u_{Bi}^2 + \Sigma \frac{h_{pi} K_{Bi}^2 u_{Bi}^2}{K_{pi}}}{\Sigma K_{Bi} u_{Bi}^2 + \Sigma \frac{K_{Bi}^2 u_{Bi}^2}{K_{pi}}}$$

Where, u_{Bi}: Design displacement of the base-isolated device

h_{Bi}: Damping factor of the base-isolated device

h_{pi}: Damping factor of the substructure

K_{Bi}: Equivalent stiffness of the base-isolated device

K_{pi}: Equivalent stiffness of the substructure

For the damping factor of the first and second modes for deciding α and β values of proportional damping, we adopted the damping factor h of the entire bridge for each mode. The h values acquired from the above expression are as shown in Table 5.

As the result of the analysis performed under the above conditions, the comparison between room temperature and -20°C is as shown in Table 6 and 7 on the relative displacement of bearing and on the bending moment of base of pier.

From these tables, it is revealed that the relative displacement of bearing at -20°C is a little larger than that at room temperature in case of LRB, however, in case of HDR, the displacement value varies little even with the change of temperature. With regard to the comparison of the bending moment, it is proved that the bending moment increases only by several percents at -20°C compared to that at room temperature in case of LRB, however, as much as 40 – 50% increase in case of HDR. The reason why the bending moment increased largely according to the temperature drop might be considered as follows .

1, The variation of the equivalent stiffness and the natural period was similar to each other between LRB and HDR .

2, Therefore, it is difficult to consider that the above variation contributes to the increment of the bending moment.

3, Consequently, the increment is supposed to be arose from the relationship between the natural periods of entire bridge and the response characteristic of the inputted seismic wave.

In conclusion, it was proved that the change of temperature didn't always effect the response of the entire bridge.

6.2.2 Non-linear analysis

Since the dependency on temperature of the base-isolated bearings was focused on in the previous section, its influence on the entire bridge was investigated by carrying out the equivalent linear analysis on various temperature. As the results, it was clarified that the change of temperature didn't always contribute to the response of the entire bridge. Therefore, without considering the temperature and the type of the bearing, the following hysteresis curve was assumed, in which a bilinear spring model was adopted, and non-linear analysis was performed in order to compare the results with those of the equivalent linear analysis.

The first stiffness, the second one and the yield displacement of the bilinear spring model (See Fig.3) for each pier are as follows.

The first stiffness : 5550t/m

The second stiffness : 854t/m

The yield displacement : 16.44mm

As the equivalent stiffness is the function of a horizontal displace is calculated to be 1360tf/m in this case because the design displacement is decided to be 150mm.

The bending moment at the base of pier obtained from each analysis, in which the same seismic wave using in the previous section is inputted is listed in Table 8. As a result, the value of bending moment in the non-linear analysis is 4–5 times larger than that of the equivalent linear analysis .

This difference might be arose from the reason why the horizontal displacement was assumed to be 150mm, In other words, the rigidity of the equivalent linear spring was too small.

In fact, the maximum displacement, which was calculated in the equivalent linear analysis, was about 20mm.

Therefore, two additional analysis were carried tout . In the first one, the equivalent stiffness was assumed to be 4714tf/m, which corresponded to the horizontal displacement of 20mm. In the second one, the equivalent stiffness was assumed to be equal to the first stiffness.

These results are shown in Table 9.

However, the values in the non-linear analysis are still 60–90% larger than those of the former, 50–

70% larger in the case of the latter.

In this connection, it could be clarified that the time when the maximum bending moment took place were different in the three cases.

Therefore, careful attention should be paid the equivalent stiffness in the case of the equivalent linear analysis.

7. CONCLUSION

The points clarified from this investigation are listed as follows :

1) The equivalent stiffness on base-isolated bearings of the both, which were tested, increased by approx. 40% due to the change from room temperature to -20°C. It is also shown that in spite of the above fact, the natural period of the bridge is shortened by approx. 14% for both LRB and HDR.

2) As far as natural periods of the bridge was concerned, the influence, which was aroused from the change on the stiffness of the base-isolated bearings due to the temperature drop, appeared only in the first mode.

3) Although the variation on the equivalent stiffness was similar to each other between LRB and HDR, for the base-isolated bearing, with LRB the displacement was larger by around 10% at low varied little even upon the temperature change.

4) For the bending moment at the base of pier, the result by the equivalent linear analysis was different between LRB and HDR, showing only several % increase with LRB, while 40-50% increase with HDR. It is supposed that the main reason why the response was different might be arose from the relationship between the natural period of the entire bridge and the predominant period of the strong motion, because the natural period in the case of HDR is about 10% shorter than that of the LRB and the predominant period of the inputted seismic wave is around 0.6sec.

5) As a result of comparison between the values of the equivalent linear analysis and the non-linear one, it was clarified that careful attention should be paid to the equivalent stiffness in the case of the equivalent linear analysis. It is also indicated that the response might be seriously influenced by the assumed horizontal displacement in the equivalent linear analysis in which time history analysis would be made.

8. POSTSCRIPT

We would like to perform the linear and non-linear analysis using different magnitude seismic waves to compare the both values, to grasp more exact behavior of the base-isolated bridge and to acquire the tendency of the change of sectional force in the future because in this analysis a single inputted seismic wave was only adopted.

Bibliography

1) Structure section, Civil Engineering Research Institute: Experimental Research Reports on Base-Isolated Bearings at Low Temperatures, 1991. 3 (In Japanese)
2) H. Taniguchi, O. Nakano: On the Behavior of Base-Isolated Bearings at Low Temperatures 7th U.S.-Japan Bridge Workshop, 1991. 5
3) Japan Institute of Construction Engineering : Guideline of Base-Isolated Bearing Design Method for Road Bridge (Draft), 1991. 3 (In Japanese)
4) Japan Road Association : Road Bridge Specifications for Seismic Design, 1990. 2 (In Japanese)
5) Structure Division, Civil Engineering Research Institute: Work Reports No.2 on Base-Isolated Bearing-Included Seismic Design program, 1990. 2 (In Japanese)
6) Kushiro Construction Department: Preliminary Report on the Dynamic Analytical Model for the Onnetoh-Oohashi on National Trunk Road 44 in Nemuro, 1990. 3 (In Japanese)

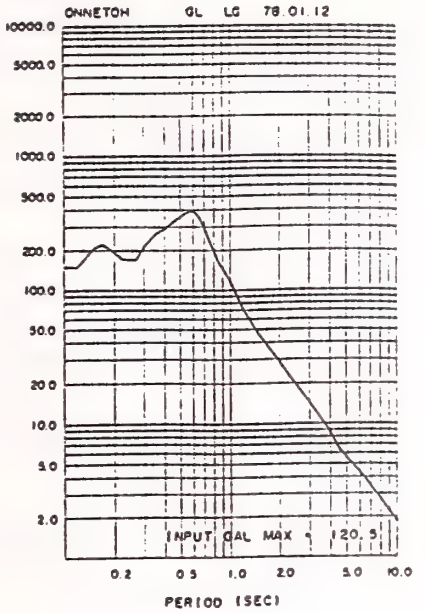

Fig. 9 Acceleration response spectrum

Table.5 Damping factor of the entire bridge:h

	L R B		H D R	
	Room T.	-20℃	Room T	-20℃
h (%)	26	23	10	11

Table.6 Relative displacement of bearing

		A 1		P 1		P 2		P 3		P 4	
L	Temp.	R.T	-20℃	R.T	-20℃	R.T	-20℃	R.T	-20℃	R.T	-20℃
R	δ (mm)	18.5	21.0	18.5	20.6	18.5	20.5	18.7	19.4	26.1	26.6
B	Ratio	1.14		1.11		1.11		1.04		1.02	
H	Temp.	R.T	-20℃	R.T	-20℃	R.T	-20℃	R.T	-20℃	R.T	-20℃
D	δ (mm)	26.7	27.7	26.3	26.8	26.6	26.4	24.5	24.5	40.1	33.1
R	Ratio	1.04		1.02		0.99		1.00		0.83	

Table.7 Bending moment at the base of pier

		P 1		P 2		P 3		P 4	
L	Temp.	Room T.	-20℃	Room T.	-20℃	Room T.	-20℃	Room T.	-20℃
R	M(tf•m)	129.67	134.38	142.00	147.34	197.54	202.68	16627.0	16587.0
B	Ratio	1.04		1.04		1.03		0.998	
H	Temp.	Room T.	-20℃	Room T.	-20℃	Room T.	-20℃	Room T.	-20℃
D	M(tf•m)	156.94	225.07	184.37	281.14	214.36	305.24	23321.0	21248.0
R	Ratio	1.43		1.52		1.42		0.91	

Table.8 Comparison between linear and non-linear analysis
(Bending moment)

	P 1	P 2	P 3
Non-l (tf•m)	655.62	743.86	823.27
A	(0.870)	(0.870)	(0.890)
Linear (tf•m)	128.93	147.38	194.14
B	(0.390)	(0.670)	(0.630)
Ratio (A/B)	5.09	5.05	4.24

The figures in parentheses is a occurrence time.

Table.9 Bending moment at the base of pier in case of changing the equivalent stiffness

	P 1		P 2		P 3	
	20mm	1st. stiff.	20mm	1st. stiff.	20mm	1st. stiff.
M (tf•m)	403.81	444.08	440.75	484.69	434.94	483.2
C	(0.600)	(0.590)	(0.610)	(0.900)	(0.590)	(0.890)
Ratio(A/C)	1.62	1.48	1.69	1.53	1.89	1.70

The figures in parentheses is a occurrence time.

Table.3 Natural period (s)

	LRB		HDR	
Mode	Room T.	-20℃	Room T.	-20℃
1	1.20973	1.05605	1.09633	0.94095
2	0.50958	0.50902	0.50957	0.50902
3	0.48331	0.48258	0.48278	0.48176
4	0.39794	0.39758	0.39775	0.39728
5	0.29420	0.29407	0.29414	0.29397
6	0.23620	0.23618	0.23620	0.23617
7	0.22022	0.21838	0.21863	0.21589
8	0.18659	0.18566	0.18579	0.18440
9	0.17457	0.17385	0.17393	0.17287
10	0.15261	0.15259	0.15259	0.15256

Fig. 7 Figure of First mode (LRB: Room temperature)

Table.4 Strong motion data

Date	1978.1.12
Magnitude	5.1
Depth(km)	40
Epicentral distance(km)	31
Max. acc.(gal)	120.57

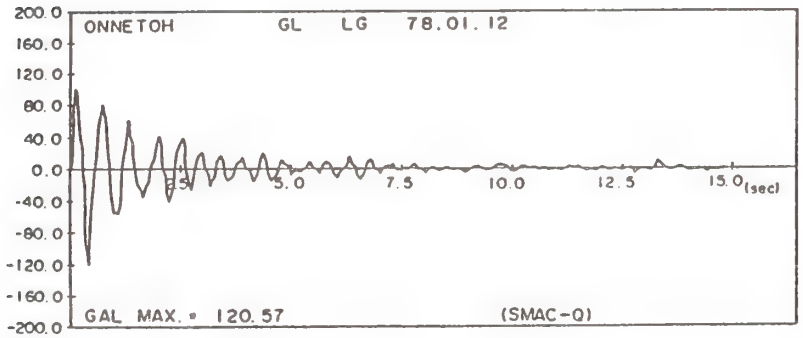

Fig. 8 Inputted seismic wave

Table.1 Equivalent stiffness at each temperature

Specimen	Temp. (℃)	Eq.stiffness(kg/cm)	Damp.factor
LRB1	+30	1332	0.34
	Room temp.	1645	0.34
	0	1832	0.31
	−10	2072	0.31
	−20	2217	0.31
LRB2	+30	1346	0.34
	Room temp.	1619	0.34
	0	1994	0.33
	−10	2005	0.31
	−20	2155	0.30
HDR1	+30	1787	0.13
	Room temp.	2079	0.12
	0	2249	0.12
	−10	2586	0.14
	−20	3044	0.14
HDR2	+30	1944	0.11
	Room temp.	2136	0.12
	0	2340	0.13
	−10	2515	0.13
	−20	2874	0.13

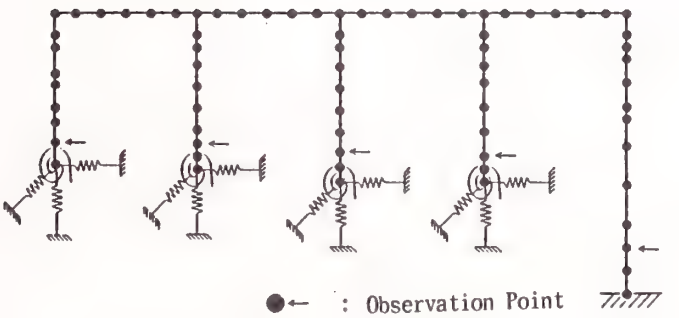

Fig. 5 Analysis model

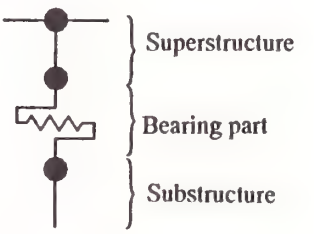

Fig. 6 Magnified bearing part

Table.2 Stiffness and damping factor

	LRB		HDR	
	Room T.	-20℃	Room T.	-20℃
K_e (t/m)	979	1312	1265	1775
h_{eq} (%)	34	31	12	14

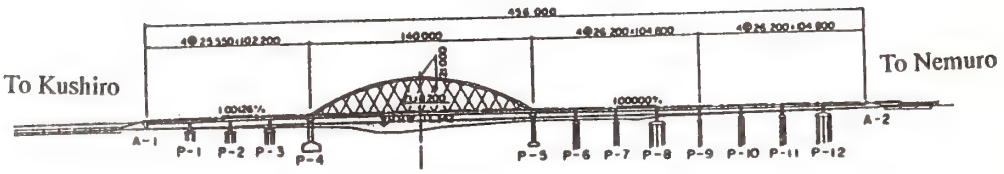

Fig. 1 Onnetoh-Oohashi Bridge

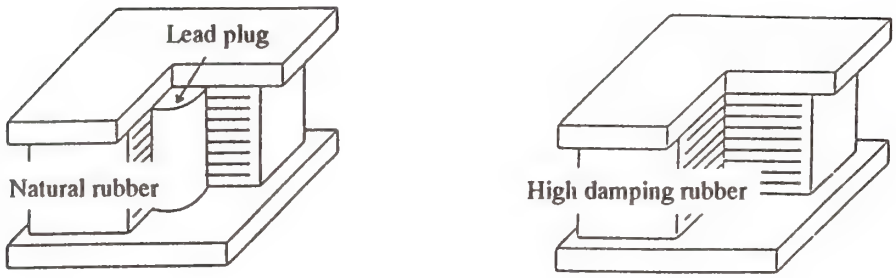

Lead rubber bearing

High damping rubber bearing

Fig. 2 Base-isolated bearings

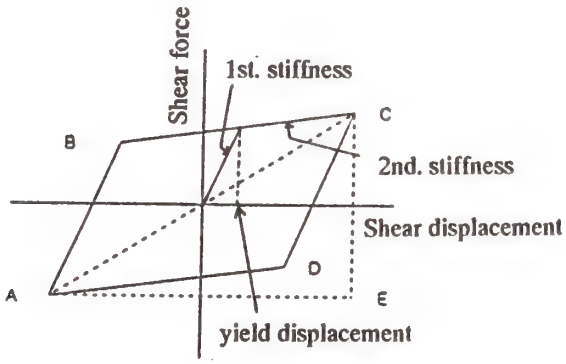

Fig. 3 Bilinear-type spring

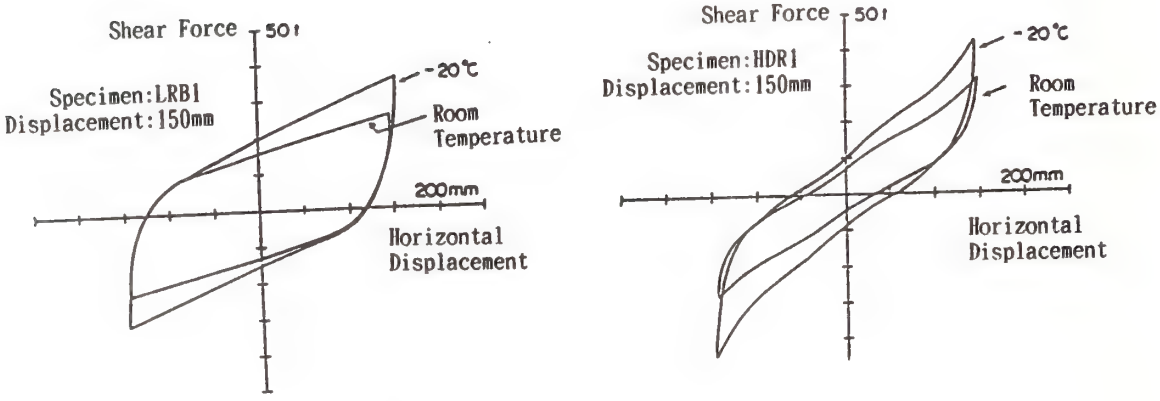

Fig. 4 Hysteresis loop comparison

Dynamic Centrifugal Model Tests of Embankments on Liquefiable Ground (Part 2)

by

Yasuyuki Koga[1], Jun-ichi Koseki[2], and Akihiro Takahashi[3]

ABSTRACT

Dynamic centrifugal model tests were performed to study a seismic behavior of embankments on a liquefiable ground using sinusoidal waves of a different frequency and two kinds of irregular waves as a shaking acceleration. Effects of the shape of the shaking acceleration on the excess pore pressure in the ground and on the settlement of the embankment were investigated, and the applicability of a cumulative damage concept in equalizing the irregular shaking wave was examined.

KEY WORDS: Embankment, Liquefaction, Dynamic Geotechnical Centrifuge, Irregular Wave, Cumulative Damage Concept

1. INTRODUCTION

Liquefaction of a sandy ground causes a settlement of an embankment founded on the ground. A lot of model tests have been executed to reveal the seismic behavior of the embankment, but few of them have been done under a high confining stress.

A centrifugal model test is a test method which can simulate the same stress condition in a scaled model ground as in an actual ground. It has been applied to a dynamic problem using an earthquake simulator[1)2)3)].

The writers have reported dynamic centrifugal model tests[4)] of a horizontal sand layer and an embankment on the layer using a sinusoidal wave of 60Hz as a shaking acceleration. This paper deals with continued tests using a sinusoidal wave of 100Hz and two kinds of irregular waves as well as the above mentioned tests.

2. TEST PROCEDURE

Embankment models and horizontal layer models as shown in Fig.1 were made in a rigid soil container of 80cm in length, 30cm in height and 10cm in width.

A sand layer was prepared by pouring Toyoura sand through air. The surface of the layer was rounded in accordance with a rotational radius. In the embankment models a colored sand mesh was drawn to observe the deformation of the sand layer through a transparent front glass of the container.

After setting the container in a vacuum box the sand layer was saturated with silicone oil which is 30 times as viscous as water. An embankment was made of a mixture of Toyoura sand and a clay-sand which has a ratio of 4:1 in weight and a water content of 15%.

A horizontal shaking was conducted after applying a centrifugal acceleration of 30g. Response accelerations, excess pore pressures and a settlement of the embankment were measured by transducers located as in Fig.1. It was repeated several times increasing an amplitude of the shaking acceleration. A summary of the test condition is shown in Table 1. Sinusoidal waves of 60 Hz and 100Hz, and two kinds of irregular waves were used as the shaking acceleration. The shapes of these shaking waves are shown in Fig.2.

3. METHOD OF DATA ARRANGEMENT AND CALCULATION

The general procedure of the calculation is similar to that of the writers' former study[5)].

3.1 Equivalent Shaking Acceleration

An equivalent shaking acceleration for the cases using irregular waves was calculated based on a cumulative damage concept. The procedure of the calculation is shown in Fig.3.

1) Calculation of Dynamic Shear Stress Ratio

The effective overburden pressure σ_{vo}' and the dynamic shear stress ratio τ_d/σ_{vo}' were calculated one-dimensionally by Eqs (1) and (2) at a point where the pore pressure transducer was installed (P1 to P6).

$$\sigma_{vo}' = \gamma' \cdot z + \gamma_t \cdot H \qquad (1)$$

in which γ' = effective unit weight, z = depth from the ground surface, γ_t = total unit weight, H = height of embankment.

$$\frac{\tau_d}{\sigma_{vo}'} = \frac{1}{\sigma_{vo}'} \sum_i \frac{\gamma i \cdot h i}{g} \cdot Ai \qquad (2)$$

in which σ_{vo}' = initial effective overburden pressure, Ai = response acceleration at the i-th layer, hi = thickness of the i-th layer, γi = unit weight of the i-th layer, g = acceleration of gravity.

Although the response acceleration was

---

[1]Head, Soil Dynamics Division, Construction Equipment and Method Department, Public Works Research Institute, Ministry of Construction, JAPAN.
[2]Researcher, do.
[3]Assistant, do.

amplified or reduced due to liquefaction, it was assumed to be the same as the shaking acceleration for simplicity.

2) Assumption of Liquefaction Resistance Curve

The liquefaction resistance curve was assumed to be given by Eq.(3), which was determined referring to the liquefaction resistance curve of Toyoura sand obtained from cyclic torsion shear tests as shown in Fig.4.

$$\begin{aligned} &\tau_d/\sigma_{mo}' \geqq 0.3 \ ; \\ &\quad \tau_d/\sigma_{mo}' - 0.3 = -1.25 \log (N_C/N') \\ &\tau_d/\sigma_{mo}' < 0.3 \ ; \\ &\quad \tau_d/\sigma_{mo}' - 0.3 = -0.11 \log (N_C/N') \end{aligned} \qquad (3)$$

in which N_C = number of cycles to cause liquefaction when uniform cyclic stress ratio τ_d/σ_{mo}' is applied, N' = parameter to locate the liquefaction resistance curve, σ_{mo}' = effective mean stress, which was calculated from the effective overburden pressure σ_{vo}' by assuming the coefficient of earth pressure at rest Ko = 0.5.

Eq.(3) can be rewritten as

$$N_C/N' = f\ (\tau_d/\sigma_{mo}') \qquad (4)$$

in which f = equation to give the relation between cyclic stress ratio and normalized number of cycles.

3) Calculation of Damage Factor

When the irregular train of the dynamic stress ratio is divided into every half cycle, the damage factor D up to the i-th half cycle is defined in the cumulative damage concept as

$$D = \sum_i \frac{0.5}{(N_C)i} \qquad (5)$$

in which $(N_C)i$ = number of cycles to cause liquefaction when the i-th half cycle stress ratio $(\tau_d/\sigma_{mo}')i$ is repeatedly applied.

The damage factor was calculated from the equation below, which was obtained by substituting Eq.(4) into Eq.(5).

$$D = \frac{1}{N'} \cdot \sum_i \frac{0.5}{f\{(\tau_d/\sigma_{mo}')_i\}} \qquad (6)$$

4) Calculation of Equivalent Shaking Acceleration

If an uniform cyclic shear stress of 20 cycles is applied to give the same cumulative damage as the irregular wave, the amplitude of the equivalent shear stress ratio $(\tau_d/\sigma_{mo}')_{eq}$ can be calculated from the equation below.

$$\begin{aligned} D &= \frac{1}{N'} \cdot \sum_i^{40} \frac{0.5}{f\{(\tau_d/\sigma_{mo}')_{eq}\}} \\ &= \frac{20}{N' \cdot f\{(\tau_d/\sigma_{mo}')_{eq}\}} \end{aligned} \qquad (7)$$

After converting the effective mean stress σ_{mo}' into the effective overburden pressure σ_{vo}', the equivalent shaking acceleration A_{eq} was calculated by substituting the the equivalent shear stress ratio into Eq.(2).

$$(\tau_d/\sigma_{vo}')_{eq} = \frac{1}{\sigma_{vo}'} \cdot A_{eq} \cdot \sum_i \frac{\gamma i \cdot h i}{g} \qquad (8)$$

The coefficient of equalization C_{eq} was defined and calculated as

$$C_{eq} = \frac{A_{eq}}{A_{max}} \qquad (9)$$

in which A_{max} is the maximum amplitude of the shaking acceleration before the equalization.

The relationship between the equivalent shaking acceleration A_{eq} and the settlement of the embankment for the cases using irregular waves was arranged to compare with the ones for the cases using the sinusoidal waves. The relationship between the equivalent shaking acceleration A_{eq} and the excess pore pressure in the ground was also compared in the same way.

3.2 Liquefaction Resistance Factor

The change of the response acceleration due to liquefaction was not considered in the preceding section, but was taken into account in this section in order to evaluate the dynamic shear stress ratio in the ground precisely.

Although the parameter N' to locate the liquefaction resistance curve did not affect the calculated equivalent shaking acceleration A_{eq} in the preceding section, it was estimated in this section in order to evaluate the liquefaction resistance of the ground.

1) Calculation of Liquefaction Resistance

The liquefaction resistance in the free ground was evaluated based on the damage factor D by the following procedure.

When the assumed value of the parameter N' is correct, a value of $D \geq 1.0$ indicates a liquefied condition and $D < 1.0$ a non-liquefied condition. Therefore following equations are obtained for respective conditions.

Liquefaction condition:

$$N' \leq \sum_i \frac{0.5}{f\{(\tau_d/\sigma_{mo}')_i\}} \qquad (10)$$

Non-liquefaction condition:

$$N' > \sum_i \frac{0.5}{f\{(\tau_d/\sigma_{mo}')_i\}} \qquad (11)$$

The liquefaction condition was defined to be the state where the measured excess pore pressure Δu was equal to the effective overburden pressure σ_{vo}' obtained by Eq.(1), which means the excess pore pressure ratio r_u defined in the

following equation was 1.0. The number of cycles required to cause liquefaction was counted at every pore pressure transducer for both the cases using irregular waves and the cases using sinusoidal waves.

$$r_u = \frac{\Delta u}{\sigma_{vo}'} \qquad (12)$$

Substituting the dynamic shear stress ratios up to the cycles to liquefaction into Eq.(9) and those up to one half cycle before the above cycles into Eq.(10), the possible range of the parameter N' which locates the liquefaction resistance curve was estimated.

2) Calculation of Liquefaction Resistance Factor

A liquefaction resistance factor F_L is defined as

$$F_L = \frac{R}{L} \qquad (13)$$

in which R is the dynamic shear resistance ratio, L is the shear stress ratio during earthquakes.

An equivalent liquefaction resistance factor F_{Li} up to the i-th half cycles was defined as well by the following equation.

$$F_{Li} = \frac{R_{20}}{L_i} \qquad (14)$$

in which R_{20} is the dynamic shear resistance ratio corresponding to an uniform wave of 20cycle, L_i is the equivalent shear stress ratio up to the i-th half cycles.

The shear resistance ratio R_{20} was computed by substituting the estimated value of N' and the number of cycles N_C = 20 into Eq.(3) as

$$N' \geq 20: \quad R_{20} = 0.3 - 1.25 \log (20/N')$$
$$N' < 20 \quad R_{20} = 0.3 - 0.11 \log (20/N') \qquad (15)$$

The equivalent shear stress ratio L_i was computed in the same way as was used to derive $(\tau_d/\sigma_{mo}')_{eq}$ in the preceding section using the estimated value of N'.

The relationship between the liquefaction resistance factor F_{Li} and the excess pore pressure ratio r_u was arranged for every pore pressure data to investigate the effect of the embankment on the relationship.

4. RESULTS AND DISCUSSION

4.1 Time Histories

Fig.5 and Fig.6 show time histories of measured data of the embankment models using an irregular wave of a high frequency and a sinusoidal wave of 100Hz as a shaking acceleration respectively. Compared with the result of a sinusoidal shaking, that of an irregular shaking can be characterized as follows:

(1) An increase of an excess pore pressure (P2, P3 and P6) proceeded stepwise at a moment when the amplitude of the shaking acceleration (A0) was large.

(2) A settlement rate of the embankment (DV) was not constant, but increased while the large amplitude of the shaking acceleration was applied.

(3) There were some cases where a rapid response of an acceleration in the free field (A1 and A2) occurred after the acceleration had reduced due to liquefaction.

4.2 Equivalent Shaking Acceleration

Table 2 shows the equivalent shaking accelerations and the coefficient of equalization for the first shaking steps of embankment models using an irregular wave as a shaking acceleration.

The coefficient of equalization below the embankment were mostly larger than in the free field, and it slightly increased as the calculation point below the embankment was shallower. These results may be related with the reduction of the cyclic shear stress ratio below the embankment due to the increase of the effective overburden pressure.

The coefficients of equalization for the cases using an irregular wave of a high frequency were generally larger than those for the cases using an irregular wave of a low frequency, because the number of waves with a large amplitude was larger in the former than in the latter.

In the following the equivalent shaking acceleration at a middle point below the embankment (P5) is used as a representative value.

4.3 Settlement of Embankment

Fig.7 shows the relationship between the settlement of embankment and the shaking acceleration in the first shaking steps, where the shaking acceleration was defined to be a maximum amplitude in the irregular shakings and an average amplitude in the sinusoidal shakings. The settlement for the same shaking acceleration was larger for the cases using the sinusoidal wave than for the cases using the irregular wave.

On the contrary the relationship between the settlement and the equivalent shaking acceleration was almost similar irrespective of the shaking waves as is shown in Fig.8. This result indicates the efficiency of the cumulative damage concept in equalizing the irregular shaking wave.

As for the effect of the frequency, the shaking using a sinusoidal wave of 60Hz caused a larger settlement than the shaking using that of 100Hz . It may be caused by a larger amplitude of a

cyclic displacement and a longer duration for the sinusoidal shaking of a lower frequency. A series of shaking table tests[6] conducted by one of the writers showed a similar result. Such effect of the frequency cannot be considered in the process of the equalization based on the cumulative damage concept except the frequency-dependent characteristics of the responce acceleration.

4.4 Excess Pore Pressure in Ground

Fig.9 shows the relationship between the maximum excess pore pressure ratio in the ground and the equivalent shaking acceleration in the first shaking steps of the embankment models. It was almost similar irrespective of the shaking waves both in the free ground (P1 to P3) and below the embankment (P4 to P6). This result indicates the cumulative damage concept was effective in equalizing the irregular shaking wave not only for the settlement of the embankment, but also for the excess pore pressure in the ground.

4.5 Liquefaction Resistance in Free Ground

Table 3 shows the calculated liquefaction resistance of the horizontal layer models. The estimated N' to locate the liquefaction resistance curve was almost in the range from 1 to 3, and the dynamic shear resistance ratio R_{20} was almost in the range from 0.16 to 0.21. They were not affected by the shaking wave. These results indicate the efficiency of the cumulative damage concept in estimating the liquefaction resistance of the ground.

4.6 Relationship between Liquefaction Resistance Factor and Excess Pore Pressure Ratio

The relationship between the liquefaction resistance factor F_L, and the excess pore pressure ratio r_u of the horizontal layer models is shown in Fig.10, and that of the embankment models is shown in Fig.11. In the calculation the estimated N' was used for the horizontal layer models, and for the embankment models N' was assumed to be 2 which is a representative value of horizontal layer models. In the embankment models the point P4 just below the embankment was excluded from the data arrangement, because the excess pore pressure at the point was negative during the shaking as shown in Figs.5 and 6. The results can be summarized as follows.

(1) In the horizontal layer the excess pore pressure ratio at shallow points P1 and P4 was similar to F_L^{-2}, and the one at the other deep points was similar to F_L^{-7}. The horizontal location of the points did not affect the relationships (Comparison between P1 to P3 and P4 to P6 in Fig.10).

(2) Below the embankment (P5 and P6 in Fig.11) the excess pore pressure ratio for the same value of F_L was smaller than in the free ground (P1 to P3 in Fig.11).

(3) The effect of the shaking history (Comparison between Step 1 and Step 2 in Figs.10 and 11) and that of the shape of the shaking wave on the results of (1) and (2) were small.

Concerning (1) and (2), Fig.12 shows the result of former study[6] based on shaking table tests. The excess pore pressure ratio at the shallow points showed a smaller tendency than that at the deep points for the same value of F_L, and the relationship between the liquefaction resistance factor and the excess pore pressure ratio in the free field was not so different from the one below the embankment as it was in this study. The reason for these disagreements is not known yet, but is a subject of future investigations.

5. CONCLUSIONS

(1) A generation of an excess pore pressure in a sand layer and a settlement of an embankment proceeded while a large amplitude of an irregular shaking acceleration was applied.

(2) The cumulative damage concept was effective in equalizing an irregular shaking wave to evaluate the excess pore pressure in the sand layer and the settlement of the embankment.

(3) The excess pore pressure ratio for the same liquefaction resistance factor was larger in the free field than below the embankment. It was the largest near the surface of the free field.

REFERENCES

1) Koga, Y., Taniguchi, E., Koseki, J. and Morishita, T : Sand Liquefaction Tests Using a Geotechnical Dynamic Centrifuge, Proc. of the 20th Joint Meeting of U.S. -JAPAN Panel on Wind and Seismic Effects, U.S. -JAPAN Conference on Development and Utilization of Natural Resources, 1988.

2) Inatomi, T., Kazama, K., Noda, S. and Tsuchida, H. : Centrifuge Dynamic Model Tests in PHRI, Proc. of the 21st Joint Meeting of U.S. -JAPAN Panel on Wind and Seismic Effects, UJNR, 1989.

3) Ledbetter, R. H. : Modelling of Earthquake Induced Pore Pressure Behavior, Proc. of the 21st Joint Meeting of U.S. -JAPAN Panel on Wind and Seismic Effects, UJNR, 1989.

4) Koga, Y. and Koseki, J. : Dynamic Centrifugal Model Tests of Embankments on Liquefiable Grounds, Proc. of the 22nd Joint Meeting of U.S. -JAPAN Panel on Wind and Seismic Effects, UJNR, 1990.

5) Koga, Y., Koseki, J., Shimazu, T. and Matsuo, O. : Influence of Embankments on the Liquefaction of Ground, Proc. of the 23rd Joint Meeting of U.S. -JAPAN Panel on Wind and Seismic Effects, UJNR, 1991.

6) Koga, Y. and Matsuo, O. : Shaking Table Tests of Embankments Resting on Liquefiable Sandy Ground, Soils and Foundations, Vol.30, No.4, pp.162-174, 1990.

Table 1 Test Cases and Conditions

Model	Case	Type of Model Ground	Shaking Wave	Shaking Acc. (g)*						Dr of Sand Layer (%)
				1st	2nd	3rd	4th	5th	6th	
63-1	63-1-1	Embankment	Sinusoidal	1.2						***
	63-1-2		60Hz,20cycle	2.5	4.1	5.2	7.3	8.7	12.7	***
	63-1-3			3.7	5.6	7.1	8.3	12.5		***
	63-1-4			5.5						***
	63-1-5			7.3						***
	63-1-6			9.0						***
1-3	1-3-1	Horizontal	Sinusoidal	2.3	3.3	4.5	5.6			64
	1-3-2	Layer	60Hz,50cycle	3.4	4.3	5.2				61
	1-3-3			4.5	5.6					59
2-1	2-1-1	Embankment	Sinusoidal	4.0	5.8	9.4				57
	2-1-2		100Hz,20cycle	5.4	8.5	8.6				62
	2-1-3			8.9	9.1					60
	2-1-4	Embankment	Irregular	6.0	8.6	10.8				60
	2-1-5		High Frequency	8.3	10.8					61
	2-1-6			4.3	6.3	7.7	10.6			63
	2-1-7	Embankment	Irregular	5.4	6.9	8.4				63
	2-1-8		Low Frequency	7.0	8.6					65
	2-1-9			8.7						66
2-2	2-2-1	Horizontal	Sinusoidal	3.9	5.0	6.0				66
	2-2-2	Layer	100Hz,50cycle	3.4	4.5	5.6	6.6			68
	2-2-3	Horizontal	Irregular	4.9	6.4	7.1	9.2			66
	2-2-4	Layer	High Frequency	8.1	8.9	11.1				65
	2-2-5	Horizontal	Irregular	**	6.8	8.4				63
	2-2-6	Layer	Low Frequency	6.7	8.4					63

* An average amplitude is shown for sinusoidal shakings, and the maximum amplitude for irregular shakings.

** The shaking acceleration was not known due to mismeasurement.

*** The relative density of the sand layer for model 63-1 was not known due to mismeasurement. It was assumed to be almost the same as others, because the preparation method was the same.

Table 2 Equivalent Shaking Accelerations and Coefficients of Equalization

Case	Shaking Wave	Equiv. Shaking Acc. A_{eq} (g) / Coef. of Equalization C_{eq}			
		Free Ground*	at P4	at P5	at P6
2-1-4	Irregular	3.0 / 0.50	3.8 / 0.64	3.6 / 0.61	3.5 / 0.59
2-1-5	High Frequency	6.8 / 0.82	4.7 / 0.57	5.6 / 0.68	6.2 / 0.75
2-1-6		2.4 / 0.55	2.6 / 0.61	2.6 / 0.61	2.5 / 0.59
2-1-7	Irregular	2.5 / 0.47	3.2 / 0.59	3.0 / 0.56	3.0 / 0.55
2-1-8	Low Frequency	2.8 / 0.40	3.7 / 0.53	3.5 / 0.49	3.3 / 0.48
2-1-9		3.7 / 0.42	4.1 / 0.48	3.9 / 0.44	3.7 / 0.42

* In the free ground A_{eq} and C_{eq} were the same irrespective of the depth, because the water level was equal to the surface of the sand layer.

Table 3 Liquefaction Resistance in Free Ground

Case	Shaking Wave	Shaking Step	Point of Calculation	Liq. Resistance Ratio R_{20}	N' to Locate Liq. Resistance Curve
1-3-1	Sinusoidal 60Hz,50cycle	1st	P1	0.186	1.8
1-3-2	Sinusoidal 60Hz,50cycle	1st	P1	0.235	5.1
			P2	0.195	2.2
			P4	0.271	11.0
			P5	0.264	9.5
			P6	0.258	8.3
		2nd	P2	0.166	1.2
			P5	0.251	7.1
			P6	0.265	9.5
		3rd	P5	0.261	8.8
			P6	0.273	11.3
1-3-3	Sinusoidal 60Hz,50cycle	1st	P3	0.153	0.92
			P6	0.155	0.96
		2nd	P3	0.188	1.9
			P6	0.191	2.0
2-2-1	Sinusoidal 100Hz,50cycle	1st	P1	0.212	3.2
			P2	0.167	1.2
			P3	0.204	2.7
		2nd	P1	0.194	2.2
			P2	0.154	0.95
			P3	0.197	2.3
2-2-2	Sinusoidal 100Hz,50cycle	1st	P1	0.213	3.3
			P2	0.180	1.6
			P3	0.187	1.9
		2nd	P1	0.199	2.4
			P2	0.178	1.6
			P3	0.195	2.2
2-2-4	Irregular High Frequency	1st	P1	0.174	1.4
			P2	0.196	2.3
			P3	0.212	3.2
			P4	0.214	3.3
			P5	0.193	2.1
			P6	0.216	3.5
		2nd	P1	0.152	0.90
			P2	0.189	2.0
			P3	0.202	2.6
			P4	0.200	2.5
			P5	0.218	3.6
			P6	0.233	4.9
2-2-6	Irregular Low Frequency	1st	P1	0.200	2.5
			P2	0.147	0.81
			P3	0.176	1.5
			P4	0.266	9.9
		2nd	P1	0.207	2.8
			P2	0.168	1.3
			P3	0.194	2.2
			P4	0.231	4.7
			P5	0.235	5.2
			P6	0.211	3.1

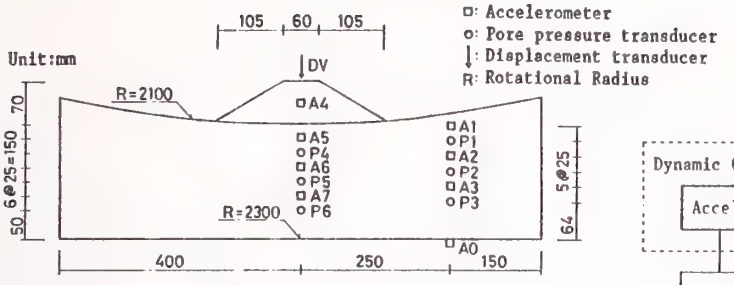

(1) Embankment Model

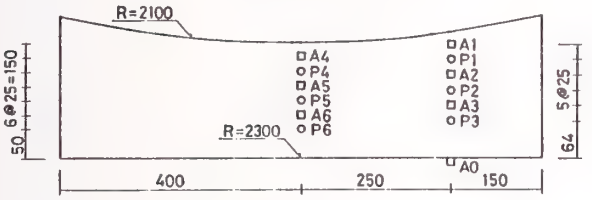

(2) Horizontal Layer Model

Fig.1 Test Models and Location of Transducers

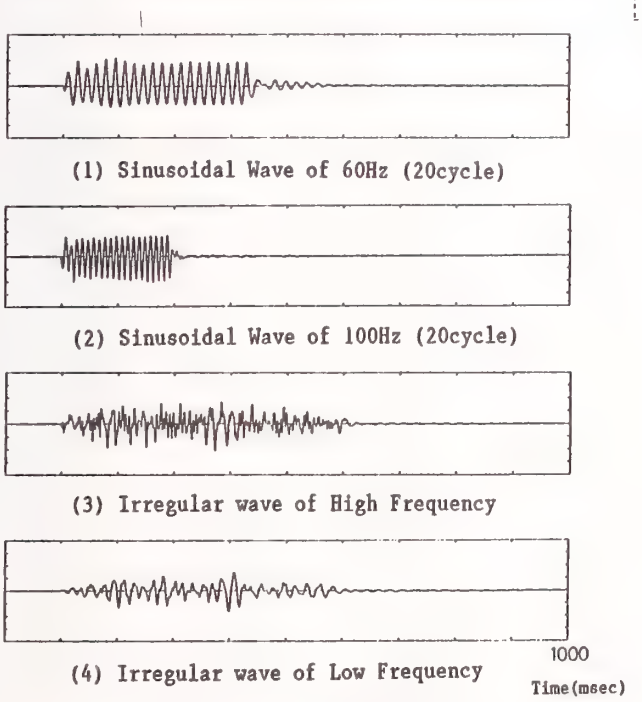

(1) Sinusoidal Wave of 60Hz (20cycle)

(2) Sinusoidal Wave of 100Hz (20cycle)

(3) Irregular wave of High Frequency

(4) Irregular wave of Low Frequency

Fig.2 Shape of Shaking Waves

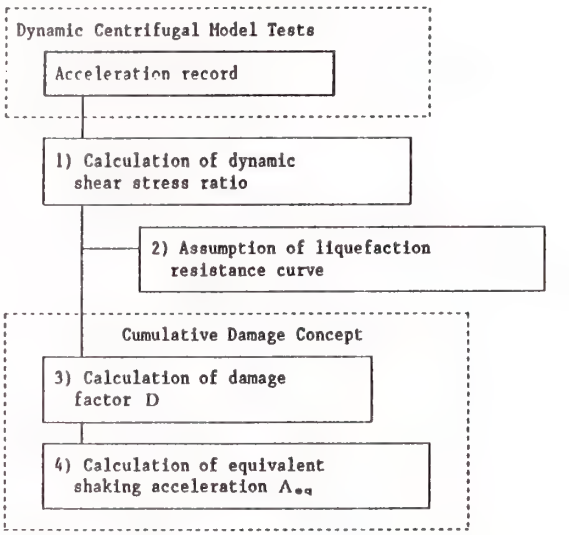

Fig.3 Procedure of Equalization

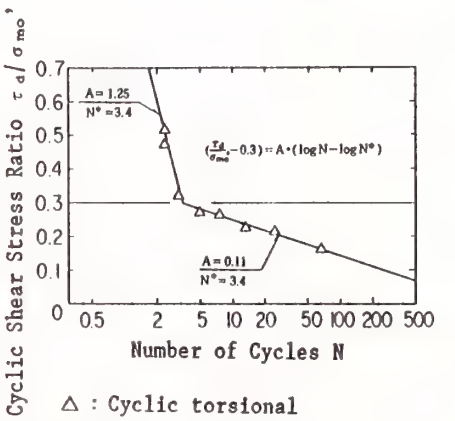

△ : Cyclic torsional shear test results
Toyoura sand, D_r= 55～60%
σ_{vo}'=1.0, σ_{ho}'=0.5(kgf/cm²)
Axial displacement confined
γ_{DA} = 15 %

Fig.4 Assumed Liquefaction Resistance Curve

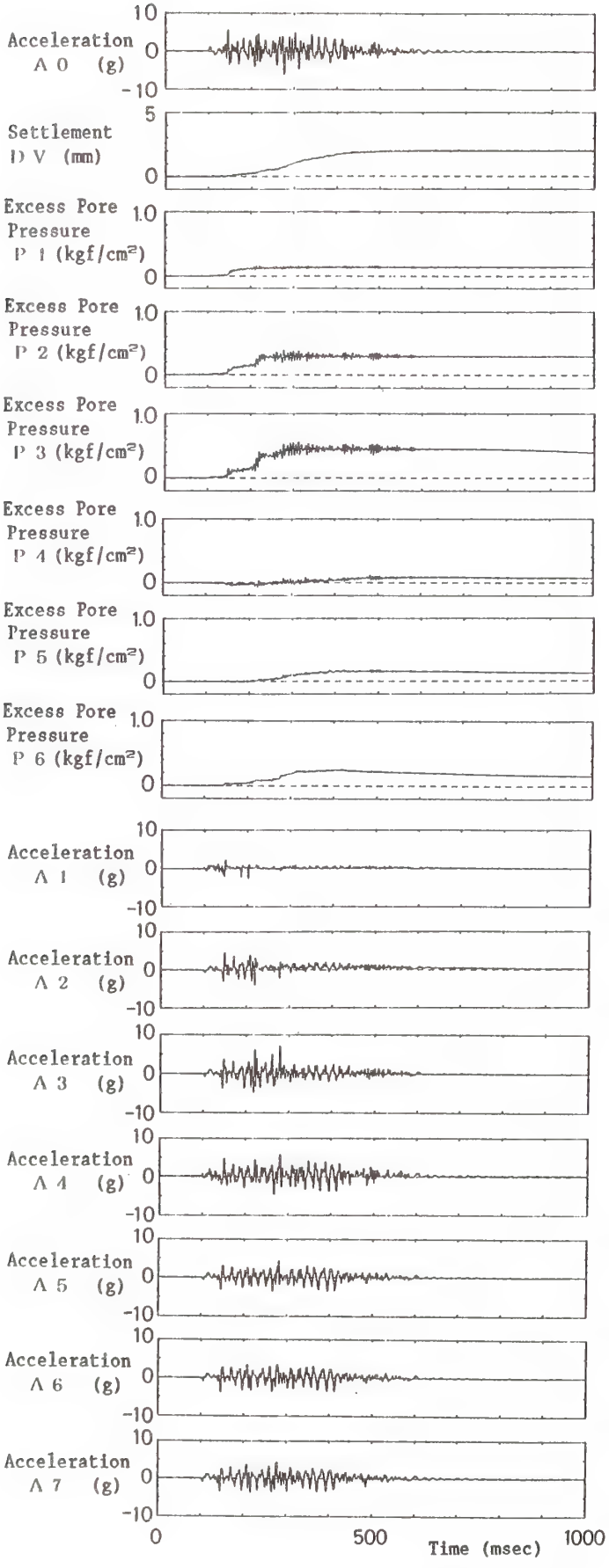

Fig.5 Measured Data of Embankment Models
(Irregular Wave of High Frequency)

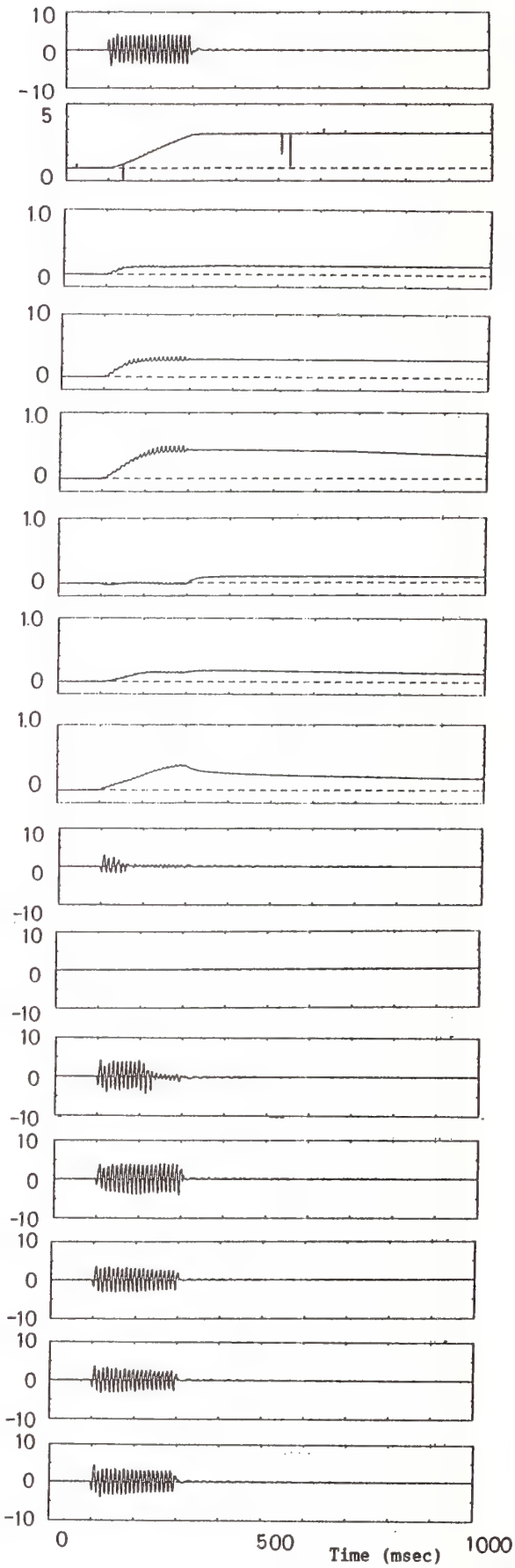

Fig.6 Measured Data of Embankment Models
(Sinusoidal Wave of 100Hz)

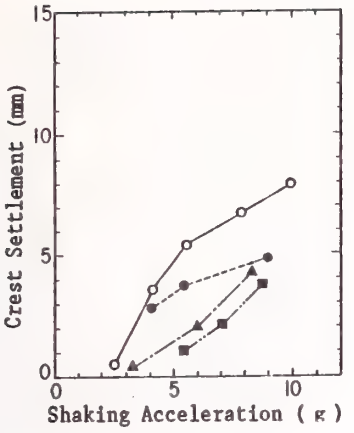

Fig.7 Shaking Acc. vs. Crest Settlement

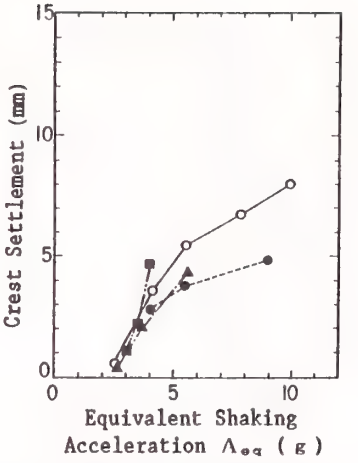

Fig.8 Equivalent Shaking Acc. vs. Crest Settlement

- ○ Sinusoidal wave of 60Hz, 20cycle
- ● Sinusoidal wave of 100Hz, 20cycle
- ▲ Irregular wave of high frequency
- ■ Irregular wave of low frequency

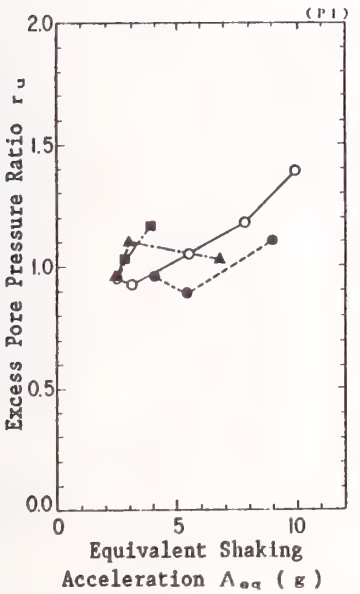

(1) at P1

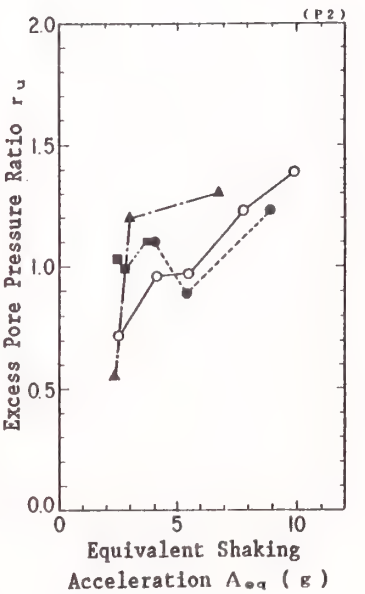

(2) at P2

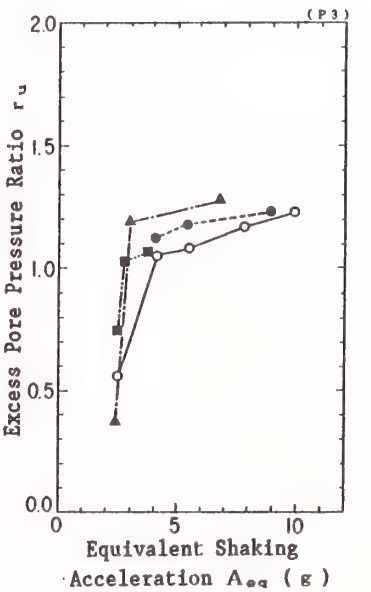

(3) at P3

Fig.9 Equivalent Shaking Acc. vs. Excess Pore Press. Ratio (Embankment Models)

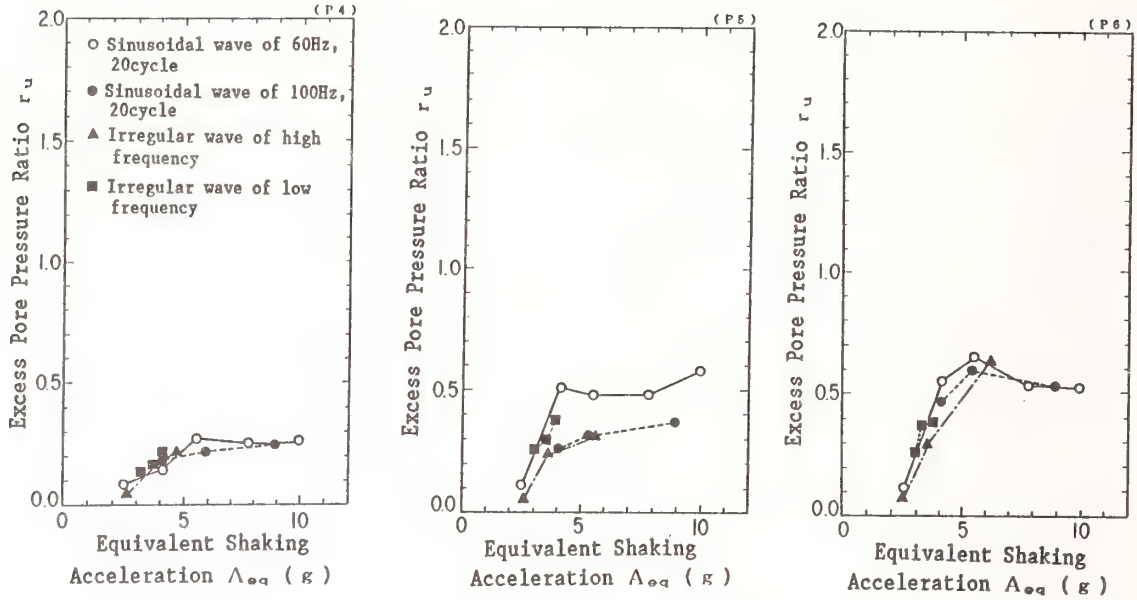

(4) at P4 (5) at P5 (6) at P6

Fig.9 Equivalent Shaking Acc. vs. Excess Pore Press. Ratio (Embankment Models) (continued)

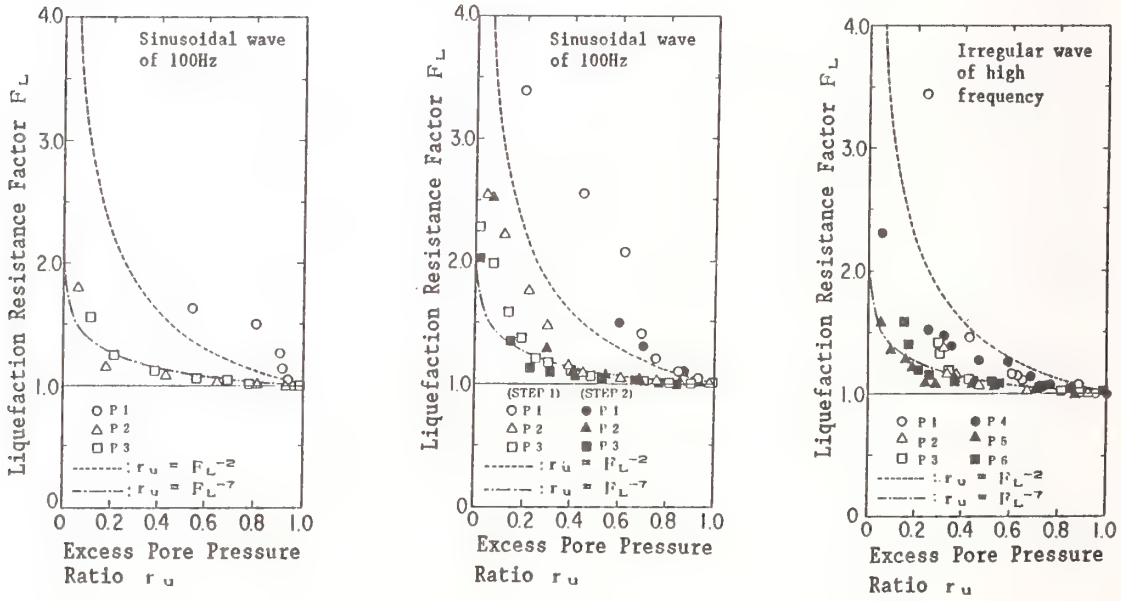

(1) Case 2-2-1, Step1 (2) Case 2-2-2, Step1 and Step2 (3) Case 2-2-4, Step1

Fig.10 Liq. Resistance Factor vs. Excess Pore Press. Ratio (Horizontal Layer Models)

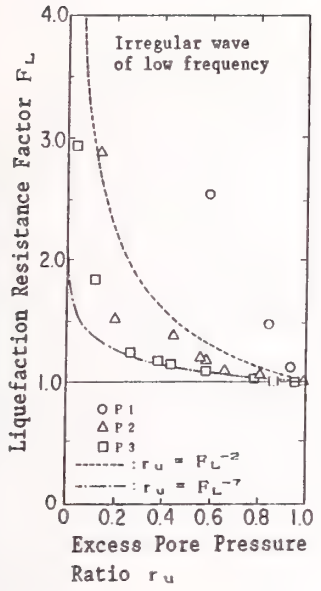

(4) Case 2-2-6, Step1

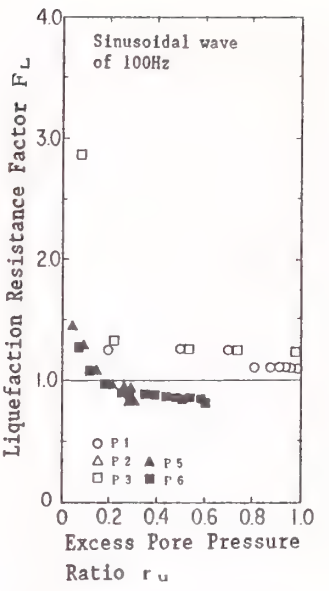

(1) Case 2-1-2, Step1

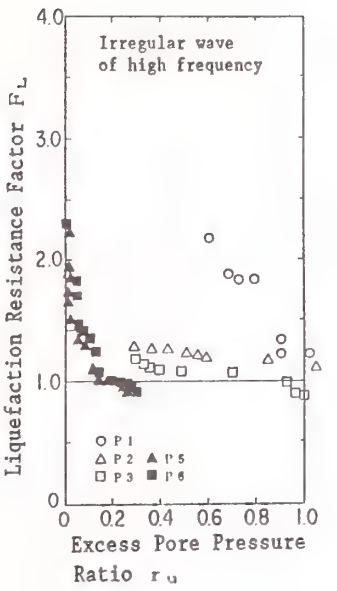

(2) Case 2-1-4, Step1

Fig.10 Liq. Resistance Factor vs. Excess Pore Press. Ratio (Horizontal Layer Models) (continued)

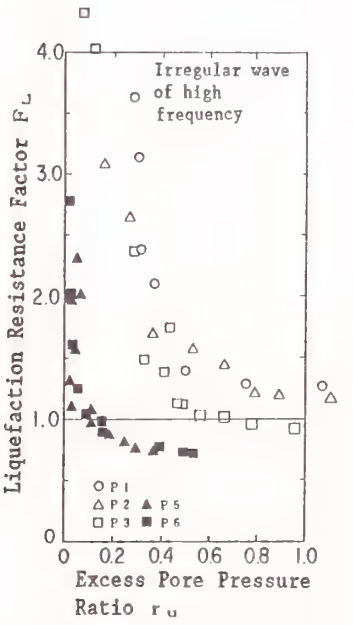

(3) Case 2-1-4, Step2

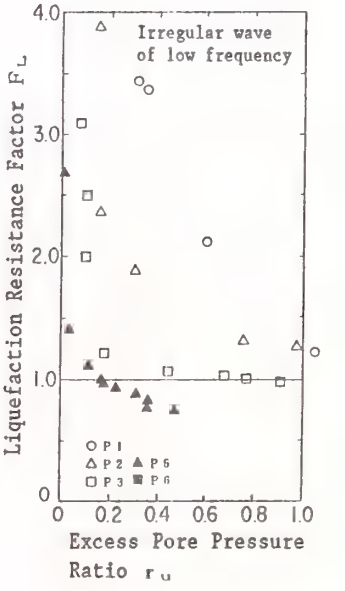

(4) Case 2-1-9, Step1

Fig.11 Liq. Resistance Factor vs. Excess Pore Press. Ratio (Embankment Models)

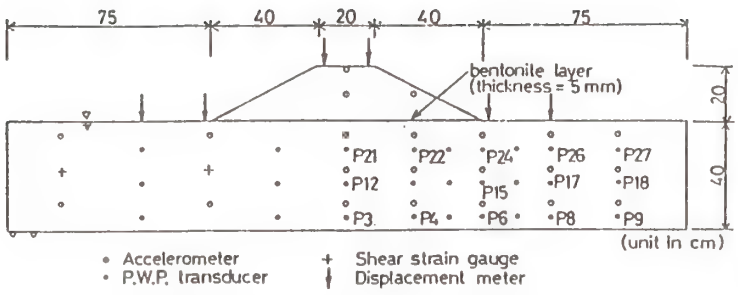

Case	Sinusoidal wave of 20cycle	
	Frequency	Acceleration
1	2.5Hz	190 gal
2	10.0Hz	315 gal
3	5.0Hz	208 gal

(1) Analized Model and Location of Transducers

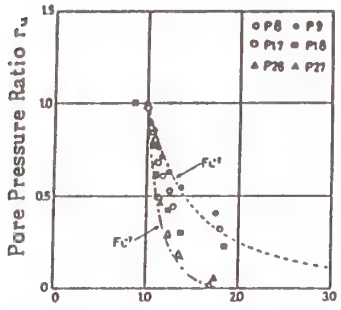

(2) Case 1 Free Field

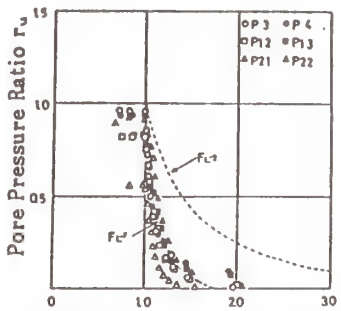

(3) Case 1 Below Crest

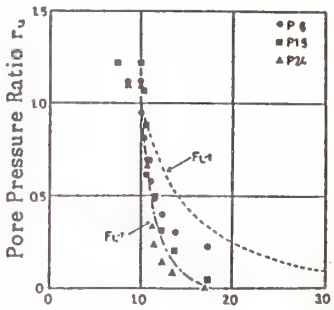

(4) Case 1 Below Slope Toe

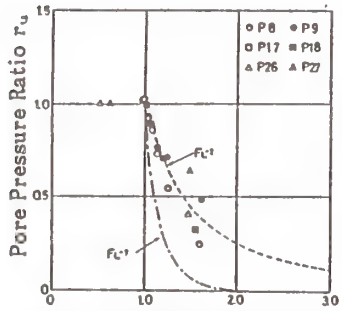

(5) Case 2 Free Field

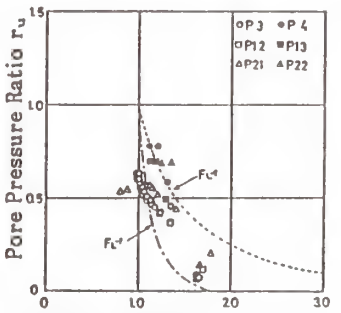

(6) Case 2 Below Crest

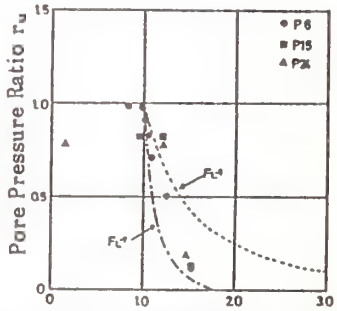

(7) Case 2 Below Slope Toe

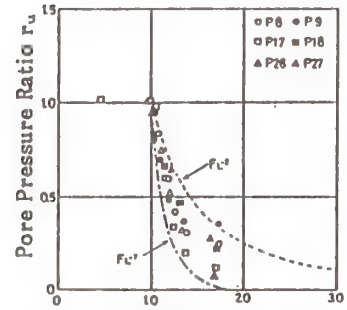

(8) Case 3 Free Field

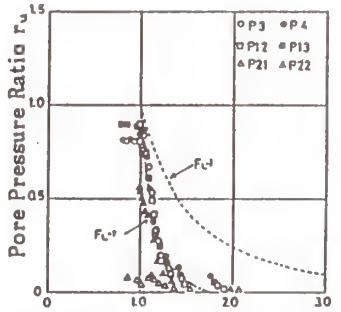

(9) Case 3 Below Crest

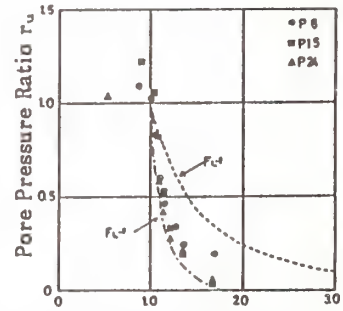

(10) Case 3 Below Slope Toe

Fig.12 Liq. Resistance Factor vs. Excess Pore Press. Ratio (Shaking Table Test[6])

Earthquake-Induced Landslides in the Santa Cruz Mountains

by

M. E. Hynes* and M. Hudson**

ABSTRACT

The magnitude 7.1 Loma Prieta earthquake which occurred at 5:04 p.m on October 17, 1989, ruptured a 25-mile long segment of the San Andreas fault in the Santa Cruz Mountains, California, and caused numerous landslides in the epicentral vicinity. A detailed study of the ground failure in this area is documented by Keefer et al. 1991. This paper summarizes slope stability and deformation analyses of damaged slopes in the Upper Schultheis Road and Villa Del Monte areas that were performed to assess the potential for future movement caused by earthquakes, intensive rainfall, or a combination of the two. The Loma Prieta earthquake and resulting slope movements provided a full scale field test of the strength of the materials in the slope. The stability and deformation analyses were used to back-calculate the mobilized strength of the in situ materials during the earthquake from the observed displacements and estimated ground motions, sliding surface locations, and groundwater conditions. This stability model was then adjusted to simulate intense rainfall conditions with higher groundwater levels, and used to assess static (no earthquake) slope stability for these same sliding surfaces. The resistance to earthquake-induced sliding deformations on postulated surfaces by future seismic events was determined for low groundwater and high groundwater conditions to simulate the relatively dry conditions that existed during the Loma Prieta event and the relatively wet conditions that would result from intense rainfall. It was concluded that (1) the slopes would become marginally stable when the water levels rise to within about 10 ft of the ground surface, and (2) if the Loma Prieta earthquake had occurred during a period of elevated groundwater level, then the maximum landslide displacements could have been three times as large or more; i.e., on the order of at least 25 ft rather than 8 ft.

1. INTRODUCTION

The 1989 Loma Prieta earthquake which occurred at 5:04 p.m on October 17, 1989, ruptured a 25-mile long segment of the San Andreas fault in the Santa Cruz Mountains, California, and caused numerous landslides in the epicentral vicinity. A detailed study of the ground failure in this area is documented by Keefer et al. 1991. This paper summarizes the engineering analyses of two landslide areas in the Santa Cruz Mountains, the Upper Schultheis Road landslide and the Villa Del Monte landslide complex, both of which are located in the epicentral region, about 1000 ft from the trace of the San Andreas fault. Location maps are shown in Figures 1 and 2, and mapped observations of surface cracking are shown in Figures 3 and 4. The geologic materials in the slide areas consist of colluvium and regolith on upturned and folded interbedded shale, sandstone and siltstone that have been complexly sheared and are variably weathered.

The Upper Schultheis Road landslide and the Villa Del Monte landslide complex were modeled in slope stability and deformation analyses first to backcalculate static and dynamic strengths of the slope materials. These backcalculated strengths were then used in the slope stability and deformation analyses to estimate the stability of the slopes under higher groundwater conditions and the displacements that could occur in future earthquakes. In this case history, backcalculated strengths are preferred to laboratory test results because they represent the strength of in situ materials averaged over the entire failure surface, which passes through several types of materials, at full-scale stress conditions. Laboratory tests were performed on selected samples, but these test results represent only point estimates of strength of individual materials in this complex geologic setting.

The slope stability and deformation analyses were calibrated using observed past performance of the slopes. The past performance of the slopes against which the models were calibrated are:

Condition (a): The slopes are generally stable under deep groundwater conditions and static loading as observed during periods of drought and low rainfall before and after the 1989 Loma Prieta earthquake.

Condition (b): Deep basal sliding surfaces of large areal extent are stable to marginally stable under elevated groundwater conditions and static loading, since areally extensive sliding of this type has not been observed during past periods of high rainfall.

Condition (c): Shallow sliding surfaces of limited areal extent are marginally stable to unstable under elevated groundwater conditions and static loading, as observed from localized slope movements experienced in the slopes during past periods of high rainfall.

Condition (d): The severe earthquake ground shaking caused by the 1989 Loma Prieta earthquake triggered instability of deep basal sliding surfaces of large areal extent and resulted in downslope displacements as large as approximately 8 ft. This occurred during a period of drought when the groundwater levels were relatively deep.

The models were developed to reflect condition (a), and then slope stability for conditions (b) and (c) were computed. Thus, it was concluded that the models provided reasonable estimates of averaged static strengths of the slope materials.

---

* U.S. Army Engineer Waterways Experiment Station, Vicksburg, Mississippi

** Department of Civil Engineering, University of California, Davis, California

The slope stability and deformation models were then adjusted to represent the dynamic loading case in condition (d). The computed dynamic strengths from this case were compared to the estimated static strengths, and it was found that the dynamic strengths reflected typical levels of strength degradation associated with dynamic loading and displacements on the order of several feet (Idriss 1985, Seed 1987). Thus it appears that the analytical models provided realistic estimates of both static and dynamic strengths of the slope materials.

The backcalculated static and dynamic strengths were then used to develop charts and procedures from which slope displacements caused by future earthquakes and groundwater conditions could be estimated. For example, the analyses indicated that had the groundwater levels been significantly higher when the 1989 Loma prieta earthquake occurred, then the maximum displacements could have been three times as large or more; i.e., on the order of at least 25 ft rather than 8 ft.

This paper describes the slope stability and displacement models that were developed, and presents the resulting charts and procedures for use in analysis of slope stability for a range of earthquake and groundwater conditions.

2. STABILITY AND DEFORMATION APPROACH

In the Newmark sliding-block deformation analyses adopted for this study, the part of a slope displaced by earthquake shaking was idealized as a rigid block sliding on an inclined plane, as originally proposed by Newmark (1965). Since 1965, a number of researchers (Goodman and Seed 1966, Ambraseys and Sarma 1967, Sarma 1975, Franklin and Chang 1977, Hynes 1979, Makdisi and Seed 1979, Sarma 1979, Wilson and Keefer 1983, Hynes and Franklin 1984, Idriss 1985, Wilson and Keefer 1985) have developed Newmark's conceptual model into a widely used, practical procedure for estimating permanent, earthquake-induced deformation of slopes.

A conventional, limit-equilibrium slope stability analysis with slight modifications was used to determine the shearing resistance along a failure surface. Because the base motions may be amplified upon being propagated upward through a slope, consideration of the dynamic response of the slope was incorporated to account for amplified accelerations in the slope. The shearing resistance determined in the limit-equilibrium slope stability analysis was then used to determine the relative displacement that will accumulate along a slide surface for a representative group of earthquake ground-motion histories. Each of these steps is described in greater detail below.

3. LIMIT-EQUILIBRIUM SLOPE STABILITY ANALYSES

3.1 Method used

A two-dimensional, force-equilibrium solution method using Lowe and Karafiath's side force assumption was used for the slope stability calculations (Lowe and Karafiath 1960). The programs used were UTEXAS2 (Edris and Wright 1987) and UTEXAS3 (Wright 1990). In this method, a pseudo-static horizontal acceleration, k_h, expressed as a fraction of gravity, can be applied to the center of gravity of the sliding mass. The value of k_h that causes the factor of safety against sliding of the slope to equal unity is termed the yield acceleration, k_y. A parametric study was performed to determine values of k_y and static (k_h = 0) safety factors against sliding, FS_S, for a range of shear strength values and groundwater conditions. A unit weight of 134.5 pcf was used as an average estimate for all materials in the slope based on laboratory test results.

3.2 Geometry of Failure Masses

An analysis of the field evidence used to estimate the geometry of the failure masses and locations of the shear surfaces is described by Keefer et al. (1991). Several sliding surface locations were assumed in the slope stability analyses ranging from deep surfaces (greater than approximately 100 ft) to fairly shallow surfaces (approximately 50 ft or less). This range provided (1) insight about the controlling mechanism of failure acting in the slope during sliding caused by the 1989 Loma Prieta earthquake, (2) an indication of the sensitivity of the results to possible slip surface locations, and (3) information about potential slope stability during future rainfall and earthquake events.

A single cross section, denoted SR, was selected through the Schultheis Road landslide area, as shown in Figures 5 (plan) and 6 (section). Two cross sections, denoted DM and SB, were chosen through the Villa Del Monte landslide complex, as shown in Figures 7 (plan) and 8-9 (sections). Estimated deep-seated basal surface locations are shown in Figures 6, 8 and 9 for sections SR, DM and SB, respectively. Additional assumed shear surfaces are shown in Figures 10-12 for sections SR, DM and SB, respectively.

3.3 Groundwater Levels

A range of water-level conditions were assumed in the analyses to simulate the range from the 1989-1990 drought conditions to high groundwater levels, such as may be caused by intense or long-duration rainfall. Monitoring of groundwater levels is discussed in greater detail by Keefer et al. (1991). A key step in the stability analyses is to estimate the pore pressures that existed in the slope just prior to the earthquake; it is estimated that the piezometric levels measured during the spring of 1990 were indicative of those that existed just prior to the earthquake. Since no significant rainfall occurred in the area for several months prior to the earthquake, and the winter and spring months of 1990 had a similar rainfall environment, it is estimated that transient effects related to the earthquake had passed and the groundwater regime had again reached a steady-state condition similar to that before the earthquake. Estimated groundwater levels along the three analyzed sections are shown in Figures 6, 8 and 9. Due to the complex stratigraphy, it was expected that the in situ groundwater pore pressure fields are also complex. However, for the purposes of analysis, hydrostatic pore pressure fields were used as an approximation of the in situ conditions.

In the Upper Schultheis Road landslide, Figure 6, a hydrostatic groundwater level at a depth of 50 ft was used to represent pre-earthquake pore pressure conditions. Analyses were

conducted for hydrostatic groundwater levels ranging from 0 to 50 ft below the ground surface to represent the effects of low to high rainfall.

In the Villa Del Monte area, Figures 8-9, the pre-earthquake groundwater level was assumed to be at a depth of 100 ft, and analyses were conducted for hydrostatic groundwater levels ranging from 0 to 200 ft below the ground surface for sensitivity analyses and to represent groundwater conditions for low to high rainfall.

3.4 Shear Strength

Friction angles represented the shear strength on the stability computations. Friction angles ranging from 10½ to 40½ were used in the parametric studies.

3.5 Parametric Results from Slope Stability Calculations

The sliding masses bounded by deep-seated basal shear surfaces shown in Figures 6, 8 and 9 were analyzed in a detailed parametric study for a wide range of shear strength values and groundwater levels. The resulting relations determined between k_y, mobilized friction angle and groundwater level are shown in Figures 13-18. Minimum values of friction angle required for static stability for the range of groundwater levels correspond to k_y = 0 in these plots and range from 11½ to 24½. These figures were used to estimate the in situ strength mobilized during earthquake-induced sliding and critical levels of groundwater increase, as described later in this paper.

4. ESTIMATED GROUND MOTION AND SLOPE AMPLIFICATION

The next step in the Newmark analysis was to estimate the ground motions (accelerations) that were generated at the base and crest of the mountain by the Loma Prieta event, particularly the peak horizontal ground accelerations. No strong-motion instruments were located in the immediate area. Two California strong-motion instrument stations were close to the epicenter of the earthquake--Corralitos, to the south, at an epicentral distance of approximately 10 km, and Lexington Dam, to the north, at an epicentral distance of approximately 18 km (Shakal and others 1989). For the Loma Prieta event, the peak horizontal ground accelerations at Corralitos were 0.48 and 0.63 g; at Lexington Dam (left abutment), the peak horizontal ground accelerations were 0.41 and 0.44 g.

The Upper Schultheis Road landslide and Villa Del Monte landslide complex are located approximately 10 km north of the earthquake epicenter. The Krinitzsky, Chang and Nuttli (1988) attenuation chart shown in Figure 19 is based on a large body of California data, and indicates a peak horizontal ground acceleration of about 0.63 g would be estimated for a magnitude 7 earthquake occurring at a distance of 10 km; about 0.40 g would be estimated at a distance of 18 km. Since the recorded peak acceleration (maximum of two horizontal records) at Corralitos located at the same distance as the slide areas and the predicted value from a large body of California data both result in a peak acceleration of 0.63 g, it was concluded that the observed values at Corralitos of 0.48 and 0.63 g were realistic estimates of the peak motions at a rock outcrop in the study area.

The possible amplification of the base motions as they propagated upward through the slope to the ridge crest was estimated from consideration of typical values from analytical studies and field observations of natural slopes and embankments, and from a simplified shear-beam numerical model described by Makdisi and Seed (1979).

Typically, analytical studies and field observations indicate that embankments amplify base (toe-of-slope) accelerations, a, by factors ranging from approximately 1 to 4 to obtain peak crest accelerations, u. In special cases, amplification factors greater than 4 have been observed in the field (based on data from Hynes and Franklin 1984, and the Corps of Engineers Strong-Motion network). At high levels of acceleration, embankment amplification factors tend to approach unity, as shown in Figure 20 (from Harder 1991). Simplified shear-beam models tend to yield fairly high amplification factors; values of 4 to 5 were computed in this case. A range of amplification values was used in the sensitivity analysis shown in Table 1 to estimate the pseudo-static acceleration, k_{max}, most appropriate to represent the earthquake motions in the deformation calculations.

The yield acceleration, k_y, from the slope stability analyses is compared to the mass averaged acceleration, k_{max}, induced by the earthquake in the sliding mass. Both shear-beam and finite-element numerical analyses have been used in earlier studies (Sarma 1979, Makdisi and Seed 1979, Hynes and Franklin 1984) to develop generalized charts to compute representative values of k_{max} for a range of sliding mass shapes, slope stiffnesses, and geometries (which affect amplification), and incoming earthquake ground motions.

The value of k_{max} should range from about 0.75 to 1.5 times the base motion on the basis of numerous dynamic finite element analyses of slopes (Idriss 1968, Idriss 1991). The chart for estimating k_{max} from embankment and slope crest peak accelerations developed by Makdisi and Seed (1979) is shown in Figure 21. This chart indicates that deep-seated slides typically have ratios of k_{max} to crest acceleration of about 0.20 to 0.45, depending on the amount of amplification of the accelerations in the mountain. Based on the sensitivity analysis shown in Table 1, values of k_{max} of 0.5 to 0.6 seem to best represent the dynamic load for the 1989 Loma Prieta event. These values were used in the deformation calculations described next.

5. DEFORMATION CALCULATIONS, ESTIMATED FIELD STRENGTHS, AND CALCULATION OF STATIC STABILITY

Charts of the relative displacement, u, that can accumulate between a sliding block and an inclined plane for a range of ratios of k_y/k_{max} have been developed by Franklin and Chang (1977), Seed and Makdisi (1979), and Hynes and Franklin (1984), based on many earthquake accelerograms. The Seed and Makdisi (1979) curves were selected for this study. Generalized displacement curves from Seed and Makdisi (1979) for earthquake magnitudes of 6.5 and 7.5 were averaged to estimate a curve for magnitude 7 earthquakes. This estimated curve used to backcalculate mobilized strength is shown in Figure 22.

The deformations observed in the field were analyzed to estimate the displacement of the center of gravity (CG) of the sliding mass for the various failure surfaces. Both the upper bound and average displacements were used, determined as a sum of observed displacements along each cross section analyzed. The displacements are listed in Table 2 (from Keefer et al. 1991). The total displacement is approximately the cumulative value of downslope displacements observed along the ground surface along and near the limits of a section. Because the sliding mass is compressed during movement, it was estimated that the CG displacement might best be associated with about half of the total displacement (Keefer et al. 1991). Thus, half of the total displacement was defined as the average displacement and represented the best estimate for the backcalculation of strength.

The estimated CG displacements were analyzed with the sliding block model to determine the mobilized shear strength in the field and to estimate the amount of groundwater rise that would lead to static slope instability. The computations are shown in Tables 3 and 4 for upper and lower deep-seated basal shear surfaces identified in Figures 6, 8 and 9. Backcalculated dynamic friction angles for the additional assumed surfaces shown in Figures 10-12 are listed in Tables 5-6.

The computed mobilized friction angles for deep basal sliding surfaces ranged from approximately 16 to 19 for the Upper Schultheis Road landslide and from about 18 to 23 for the Villa Del Monte landslide complex. These backcalculated strengths are from dynamic loading conditions and are typically lower than the strength actually available for static loading conditions. The calculations shown in the last three columns of Table 4 were performed to obtain conservative estimates of the stability of the slopes and the critical rises in groundwater levels for triggering slope instability under static conditions. These conservative results indicated that a groundwater rise of 15 to 30 ft, from a depth of 50 ft to 20 to 35 ft below the ground surface in the Upper Schultheis Road landslide would result in renewed landslide movement without earthquake shaking. At Villa Del Monte, the range of computed critical groundwater levels was broader; the results suggested that some analyzed sliding masses would become statically unstable with a groundwater level increase of as little as 30 ft, while others would remain stable with rises of more than 100 ft (which would require artesian conditions). Computed static factors of safety using dynamic strengths, with estimated pre-earthquake groundwater levels, were in the range of 1.07 to 1.16 for the Upper Schultheis Road landslide and 1.15 to 1.62 for the Villa Del Monte landslide complex. These results are summarized in Table 4. These safety factors for the low 1989-1990 groundwater levels are all quite low, but greater than unity, even when the low dynamic strengths are used in the computations.

The strengths and static stability conditions discussed above are backcalculated from a dynamic loading event. Usually, there is some degradation of strength caused by dynamic loading of geologic materials, especially if they are below the water table. To estimate the amount of strength degradation, the additional assumed sliding masses shown in Figures 10-12 were analyzed. The surfaces were chosen based upon estimated critical locations of slope geometry. Two cases were analyzed to determine (1) the friction angle that would have been mobilized during the Loma Prieta event, and (2) the friction angle required to have a static factor of safety against sliding of unity if the water table is near the surface of the slope, at a depth of approximately 10 ft. These results are listed in Table 5 for shallow (approximately 50 ft or less) surfaces and Table 6 for deep (approximately 100 ft or more) surfaces.

Localized movements have been observed in these slopes after periods of heavy rains. The strengths of the materials in the slope were probably at least as high as the values calculated for static conditions with the water table near the surface and the factor of safety against sliding equal to one. If this were not the case, large failures would have been expected to be seen as the water table rose at times in the past. Instead, localized slope movements have been observed during wet weather, indicating a factor of safety near unity. The strength values in Tables 5 and 6 indicate that the friction angles for the static high-water case are larger than those necessary to produce the observed displacements during the 1989 Loma Prieta event. Therefore, in order to satisfy both conditions, the strength of the slope materials must have degraded due to the shaking of the earthquake.

Degradation of strength is most likely to occur in saturated conditions. The materials along shallow surfaces were not saturated at the time of the earthquake. All of the deep failure surfaces had some of their lengths at or below the water table. Therefore, it is most likely that materials along deep surfaces experienced strength degradation. It was therefore concluded that deep-seated sliding surfaces were more likely to have been responsible for the landslide activity in the Upper Schultheis Road and Villa Del Monte areas, with a reduction in strength occurring in the materials along the deep surfaces due to earthquake shaking.

Another approach was used to estimate the strength of the materials in the slope under static loading conditions. It is known that the slopes were stable before the 1989 Loma Prieta earthquake, with the groundwater table at a depth of about 50 ft in the Upper Schultheis Road area and about 100 ft in the Villa Del Monte area. A factor of safety against sliding of 1.5 was used as a reasonable estimate for the static factor of safety of the slopes for these groundwater conditions. A series of slope stability calculations was performed using these additional slip surfaces to determine the strengths required to have a static factor of safety of 1.5. These strengths were then used to compute the static factor of safety with the water table near the surface. The results of these calculations are shown in Table 7. As can be seen from this table, the friction angles thus generated seem reasonable in that they provide a low factor of safety against sliding after the water table has risen significantly. This correlates well with the observations of localized movements during periods of high water table.

In summary, the strengths backcalculated from the Loma Prieta 1989 event probably

underestimate the available strength of the materials in the slope for the static case of a rise in groundwater levels because of strength degradation of saturated materials due to dynamic loading. The static strengths are likely to be greater than the backcalculated dynamic values and approximately equal to or less than the static values listed in Tables 5-7. Also, if groundwater levels rise, slope movements may involve both shallow and deep surfaces.

6. SLIDING DURING FUTURE EARTHQUAKES WITH HIGHER GROUNDWATER LEVELS

The Newmark sliding block calculation procedure demonstrated in Table 3 can be used in conjunction with the yield accelerations in Figures 13-18 to estimate the potential for further sliding-block displacement in future earthquakes with higher groundwater levels. For example, displacement computations that simulate occurrence of the Loma Prieta-type event with higher groundwater levels indicate that displacements on a deep seated shear surface along cross section SB, in the Villa Del Monte landslide complex, might have been two to three times greater than they actually were if the groundwater level had been at a depth of 50 ft rather than 100 ft during the earthquake. This is determined by observing in the last column in Table 3 that the average mobilized friction angle for the slip surface denoted SB-U was approximately 21 . One then enters Figure 17 at a friction angle of approximately 21 to find the value of k_y corresponding to a water table depth of 50 ft, by intersecting this contour. The corresponding value of k_y is approximately 0.03. Then, one can compute the ratio k_y/k_{max} using a value of k_{max} equal to 0.5 for a nearby magnitude 7 event. The resulting ratio is 0.03/0.5 = 0.06. One then enters the displacement chart in Figure 22 at a ratio value of 0.06. For a magnitude 7 event, this yields a displacement of about 43 inches (110 cm). This displacement value is twice as large as the estimated average observed value of 22 inches (55 cm) during the Loma Prieta event when the water table was at a depth of approximately 100 ft.

If an earthquake occurs when the water table are higher in the slopes, more materials will be saturated and likely to suffer some degradation of strength due to earthquake shaking; consequently, for these conditions, slope instability may not be limited to areally extensive, deep-seated basal shear surfaces, but may also include shallower surfaces and deep surfaces with more limited lateral extents.

The occurrence of an earthquake when the water table is near the surface of the slopes could result in large displacements if the epicenter is close to the landslide areas. The meaning of "close" varies with the magnitude of the earthquake event and the depth to the water table at the time of the event. For the relatively deep water tables that existed during the Loma Prieta event, a magnitude 7 epicenter would need to be as close as approximately 10 miles (16 km) to cause calculated slide displacement on Villa Del Monte slopes of more than a foot; for the Upper Schultheis Road area, the magnitude 7 epicenter could be as far away as about 25 miles (40 km) and still cause this magnitude of displacement. It should be noted that the southern end of the Hayward-Calaveras fault is approximately 25 miles away from the area involved in this study.

7. SUMMARY AND CONCLUSIONS

Slope stability and deformation analyses of the Upper Schultheis Road landslide and Villa Del Monte landslide complex were performed to backcalculate the strengths mobilized in the slopes during the 1989 Loma Prieta earthquake, and to use this and other field performance information to assess the potential for future movement caused by earthquakes, rainfall, or a combination of the two. Both shallow and deep block sliding were analyzed using a limit-equilibrium pseudo-static slope stability procedure (Lowe and Karafiath 1960) and a Newmark sliding-block deformation analysis (Newmark1965). These analyses indicated the following:

(a) It is likely that the saturated slope materials suffered some degradation of shear strength due to earthquake shaking. Strengths backcalculated from observations of the Loma Prieta earthquake can be used to assess future earthquake stability, but are likely to underestimate the available strength for static loading conditions.

(b) The analyses confirm that deep-seated basal shear surfaces were the likely controlling failure mechanism for these landslide areas in the Loma Prieta event, since these deeper materials were saturated and subject to earthquake-induced strength degradation. It is unlikely that the controlling slope failure mechanism for these landslides was shallow slip surface movement since these materials were well above the water table and would not be likely to have suffered earthquake-induced strength degradation.

(c) If there is significant rise in groundwater levels, slope failure mechanisms may include shallower and deeper slip surfaces of limited areal extent. Large slope failures have not been observed in this area during past heavy rainfall events, but rather have involved small movements on sliding masses of limited extent. This past field performance of the slopes and the analyses indicate that the factor of safety against sliding for such surfaces is close to unity when the water table is near the ground surface.

(d) If there is a significant rise in the water table and another earthquake shakes the slopes, the slope failure mechanisms may include deep basal shear surfaces of large areal extent as well as shallow and deep surfaces of limited areal extent. This is because the shallower slope materials would then be saturated and subject to earthquake-induced strength degradation.

(e) If the Loma Prieta event had occurred when the water table was higher, maximum slope displacements might have been on the order of 25 ft rather than 8 ft. This level of displacement was indicated for deep basal shear surfaces as well as the shallow and deep surfaces of limited areal extent for a nearby magnitude 7 seismic event.

Consequently, the analyses indicated that deep-seated basal shear slide masses could become marginally stable when the groundwater rises to within about 20 ft of the ground surface at the Upper Schultheis Road landslide

area and to within about 30 ft of the ground surface at the Villa Del Monte landslide complex. If the groundwater rises to within about 10 ft of the ground surface, the slopes could become marginally stable against deep-seated, large scale, basal shear sliding; the computed safety factors for this case ranged from about 1 to 1.2. The analyses also indicated that shallow and deep surfaces of more limited areal extent may possibly become unstable to marginally stable if the groundwater rises to within 10 ft of the ground surface; the computed safety factors in this case ranged from about 0.8 to 1.1. However, if an earthquake occurs nearby when the water table is high, there may be extensive damage.

8. REFERENCES

Ambraseys, N. N. 1960. "The Seismic Stability of Earth Dams," Proceedings of the Second World Conference on Earthquake Engineering, Japan, Vol. II.

Ambraseys, N. N., and Sarma, S. K. 1967. "The Response of Earth Dams to Strong Earthquakes," Geotechnique, Vol 17, No. 2, pp 181-213.

Edris, E. V., and Wright, S. G. 1987. "User's Guide: UTEXAS2 Slope Stability Package, Vol 1," Instruction Report GL-87-1, U. S. Army Engineer Waterways Experiment Station, Vicksburg, Miss.

Franklin, A. G., and Chang, F. K., 1977. "Earthquake Resistance of Earth and Rockfill Dams; Permanent Displacements of Earth Embankments by Newmark Sliding Block Analysis," Miscellaneous Paper S-71-17, Report 5, U. S. Army Engineer Waterways Experiment Station, CE, Vicksburg, Miss.

Goodman, R. E., and Seed, H. B. 1966. "Earthquake-Induced Displacements in Sand Embankment," Journal of the Soil Mechanics and Foundations Division, American Society of Civil Engineers, Vol 92, No. SM2, pp 125-146.

Hynes, M. E. 1979. "Dynamic Analysis of Earth Embankments for the Richard B. Russell Dam and Lake Project," Final Report Prepared for U. S. Army Engineer District, Savannah, Georgia.

Hynes, M. E., and Franklin, A. G. 1984. "Rationalizing the Seismic Coefficient Method," Miscellaneous Paper GL-84-13, U. S. Army Engineer Waterways Experiment Station, Vicksburg, Miss.

Keefer, D. et al. 1991, "Geologic Hazards in the Summit Ridge Area of the Santa Cruz Mountains, Santa Cruz County, California, Evaluated in Response to the October 17, 1989, Loma Prieta Earthquake: Report of the Technical Advisory Group," U.S. Geological Survey Open-File Report 91-618, Menlo Park, California.

Krinitzsky, E. L., Chang, F. K., and Nuttli, O. W. 1988. "Magnitude-Related Earthquake Ground Motions," Bulletin of the Association of Engineering Geologists, Vol XXV, No. 4, pp 399-423.

Makdisi, F. I., and Seed, H. B. 1979. "Simplified Procedure for Estimating Dam and Embankment Earthquake-Induced Deformations," Journal of the Geotechnical Engineering Division, American Society of Civil Engineers, Vol 104, No. GT7, pp 849-867.

Martin, G. R. 1965. "Response of Earth Dams to Earthquakes," Thesis submitted in partial satisfaction of the requirements for the degree of Doctor of Philosophy, University of California, Berkeley.

Newmark, N. M. 1965. "Effects of Earthquakes on Dams and Embankments," Geotechnique, Vol 15, No. 2, pp 139-160.

Sarma, S. K. 1975. "Seismic Stability of Earth Dams and Embankments," Geotechnique, Vol 25, No. 4, pp 743-761.

_____. 1979. "Response and Stability of Earth Dams During Strong Earthquakes," Miscellaneous Paper GL-79-13, U.S. Army Engineer Waterways Experiment Station, CE, Vicksburg, Miss.

Schnabel, P. B., Lysmer, J., Seed, H. B. 1972. "SHAKE, A Computer Program for Earthquake Response Analysis of Horizontally Layered Sites," Earthquake Engineering Research Center Report No. EERC 72-12, University of California, Berkeley.

William Cotton and Associates 1990. "Villa Del Monte and Schultheis Road Landslides Geotechnical Exploration, Santa Cruz County, California," Draft Contract Report for U. S. Army Engineer District, San Francisco, June 1990.

William Cotton and Associates 1990. "Schultheis Road and Villa Del Monte Areas Geotechnical Exploration, Santa Cruz County, California," Final Contract Report for U. S. Army Engineer District, San Francisco, September 1990.

Wilson, R. C., and Keefer, D. K. 1983. "Dynamic Analysis of a Slope Failure from the 6 August 1979 Coyote Lake, California, Earthquake," Bulletin of the Seismological Society of America, Vol 73, No. 3, pp 863-877.

Wilson, R. C., and Keefer, D. K. 1985. "Predicting Areal Limits of Earthquake-Induced Landsliding," Earthquake Hazards in the Los Angeles Region, Ziony, J. I., ed., USGS Professional Paper 1360, pp 317-494.

Wright, S. G. 1990. UTEXAS32 (UNIVERSITY OF TEXAS ANALYSIS OF SLOPES -- VERSION 3): A Computer Program for Slope Stability Calculations," Geotechnical Engineering Software GS90-1, Geotechnical Engineering Center, The University of Texas at Austin.

Table 1

Sensitivity Analysis of Dynamic Load, K_{max}

Acceleration, g				
Base a	Crest ū	Ratio ū/a	Dynamic Load Ratio K_{max} / ū	Dynamic Load K_{max}, g
0.4	2.4	6	0.20	0.48
0.4	2.0	5	0.25	0.50
0.4	1.6	4	0.30	0.48
0.4	1.2	3	0.35	0.442
0.4	0.8	2	0.40	0.32
0.48	1.44	3	0.35	0.50
0.5	2.5	5	0.25	0.63
0.5	2.0	4	0.30	0.60
0.5	1.5	3	0.35	0.53
0.5	1.0	2	0.40	0.40
0.6	2.4	4	0.30	0.72
0.6	1.8	3	0.35	0.63
0.6	1.2	2	0.40	0.48
0.63	1.26	2	0.40	0.50
0.7	2.1	3	0.35	0.74
0.7	1.4	2	0.40	0.56

Based on sensitivity analysis above,
K_{max} = 0.5 to 0.6 g selected for displacement computations

Table 2

Summary of Slope Displacements
Provided by the T.A.G.

Section	Displacement	
	Total in. cm	Average in. cm
Villa del Monte		
DM	28 72	14 36
SB	44 111	22 36
Schultheis Road		
SR	96 244	48 122

Table 3

Displacement Computations for Villa del Monte Landslide Complex and Upper Schultheis Road Landslide

Section (U-upper, L-lower surfaces)*	Dynamic Load K_{max} g	Total Displacement u in.	Total Displacement u cm	Ratio K_y / K_{max}	Yield Acceleration K_y g	Mobilized Friction ϕ'_{mob} degrees	Average Displacement u in.	Average Displacement u cm	Ratio K_y / K_{max}	Yield Acceleration K_y g	Mobilized Friction ϕ'_{mob} degrees
Villa del Monte											
DM-U	0.5	28	72	0.11	0.055	17.6	14	36	0.21	0.105	20.7
DM-U	0.6	28	72	0.11	0.066	18.3	14	36	0.21	0.126	22
SB-U	0.5	44	111	0.06	0.03	17.8	22	55.5	0.15	0.075	21
SB-U	0.6	44	111	0.06	0.036	18.3	22	55.5	0.15	0.09	22
SB-L	0.5	44	111	0.06	0.03	19.3	22	55.5	0.15	0.075	22.5
SB-L	0.6	44	111	0.06	0.036	19.8	22	55.5	0.15	0.09	23.5
Schultheis Road											
SR-U	0.5	96	244	0.03	0.015	17.6	48	122	0.05	0.025	18.3
SR-U	0.6	96	244	0.03	0.015	17.8	48	122	0.05	0.03	18.6
SR-L	0.5	96	244	0.03	0.015	18.6	48	122	0.05	0.025	19.4
SR-L	0.6	96	244	0.03	0.018	18.9	48	122	0.05	0.03	19.8

* Surfaces identified in Figures 6, 8 and 9

Table 4

Summary of Mobilized Dynamic Friction, Static Stability, and Critical Ground-Water Depths

			Pre-Quake Ground-Water Conditions						
Section*	Estimated Ground-Water Depth at Time of Quake ft	Dynamic Load K_{max} g	Displacement u in.	Displacement u cm	Mobilized Friction ϕ'_{mob} degree	Friction Required for Static Stability $\phi'_{req.}$ degrees	Factor of Safety Against Sliding** FS_a	Ground-Water Depth That Would Trigger Static Instability** ft	Critical Change in Ground-Water Depth** ft
DM-U	100	0.5	28	72	17.6	14	1.27	45	55
DM-U	100	0.6	28	72	18.3	14	1.33	30	70
DM-U	100	0.5	14	36	20.7	14	1.52	10	90
DM-U	100	0.6	14	36	22	14	1.62	>0	>100
SB-U	100	0.5	44	111	17.8	15.5	1.15	70	30
SB-U	100	0.6	44	111	18.3	15.5	1.19	60	40
SB-U	100	0.5	22	55.5	21	15.5	1.38	15	85
SB-U	100	0.6	22	55.5	22	15.5	1.46	5	95
SB-L	100	0.5	44	111	19.3	16.9	1.15	55	45
SB-L	100	0.6	44	111	19.8	16.9	1.19	45	55
SB-L	100	0.5	22	55.5	22.5	16.9	1.36	>0	>100
SB-L	100	0.6	22	55.5	23.5	16.9	1.43	>0	>100
SR-U	50	0.5	96	244	17.6	16.5	1.07	35	15
SR-U	50	0.6	96	244	17.8	16.5	1.08	35	15
SR-U	50	0.5	48	122	18.3	16.5	1.12	30	20
SR-U	50	0.6	48	122	18.6	16.5	1.14	30	20
SR-L	50	0.5	96	244	18.6	17.2	1.09	35	15
SR-L	50	0.6	96	244	18.9	17.2	1.11	30	20
SR-L	50	0.5	48	122	19.4	17.2	1.14	25	25
SR-L	50	0.6	48	122	19.8	17.2	1.16	20	30

* Surfaces identified in Figures 6, 8 and 9
** Based on dynamic strengths

Table 5

Calculated Friction Angles for Shallow Failure Surfaces Shown in Figures 10, 11, 12

Failure Surface Designation	Friction Angle Back-Calculated From Loma Prieta Earthquake (degrees)	Friction Angle Required for Static F.S = 1 With Water Table Near Surface (degrees)
SR-2	19	33
DM-7	33	>40
DM-8	20	22
SB-3	22	26

Table 6

Calculated Friction Angles for Deep Failure Surfaces Shown in Figures 10, 11, 12

Failure Surface Designation	Friction Angle Back-Calculated From Loma Prieta Earthquake (degrees)	Friction Angle Required for Static F.S. = 1 With Water Table Near Surface (degrees)
SR-1	25	32
SR-U	18	22
SR-L	16	22
DM-1	20	29
DM-3	21	27
DM-U	20	23
SB-1	22	29
SB-2	19	22
SB-U	18	22

Table 7

Estimated Static Friction Angles for Deep Surfaces Shown in Figures 10, 11, 12

Failure surface designation	Friction angle required for static F.S. = 1.5 with a deep water table (degrees)	Factor of safety water table at ground Surface
SR-1	35	1.09
SR-U	26	1.18
SR-L	24	1.10
DM-1	24	0.81
DM-3	26	0.94
DM-U	23	1.01
SB-1	28	0.98
SB-2	25	1.16
SB-U	23	1.03

Table 8

Computed Slope Displacements with No Strength Degradation
(Surfaces Identified in Figures 10, 11, 12

Failure Surface Designation	Yield Acceleration Based on Friction Angles Listed in Table 7	K_{max} (g's)	K_y/K_{max}	Calculated Displacement in.	cm
SR-1	0.150	0.5	0.300	24	9
		0.6	0.250	32	13
SR-U	0.100	0.5	0.201	44	17
		0.6	0.167	51	20
SR-L	0.100	0.5	0.199	44	17
		0.6	0.166	51	20
DM-1	0.136	0.5	0.272	38	11
		0.6	0.227	38	15
DM-3	0.147	0.5	0.294	24	9
		0.6	0.245	32	13
DM-U	0.104	0.5	0.209	44	17
		0.6	0.174	51	20
SB-1	0.145	0.5	0.290	24	9
		0.6	0.242	32	13
SB-2	0.138	0.5	0.276	28	11
		0.6	0.230	25	10
SB-U	0.108	0.5	0.217	38	15
		0.6	0.181	48	19

Table 9

Estimated Displacements for Postulated Scenarios
(Surfaces Identified in Figures 10, 11, 12

	Scenario 1:				Scenario 2:			
Failure Surface Designation	Water at 100 ft in.	cm	Water at 50 ft in.	cm	Water at 50 ft in	cm	Water at 25 ft in.	cm
SR-1			76	194			65	165
SR-L			120	306			215	545
SR-U			120	306			194	494
DM-1	80	204			165	419		
DM-3	76	194			144	365		
DM-U	109	278			241	612		
SB-1	76	194			165	419		
SB-2	80	204			157	398		
SB-U	109	278			215	545		

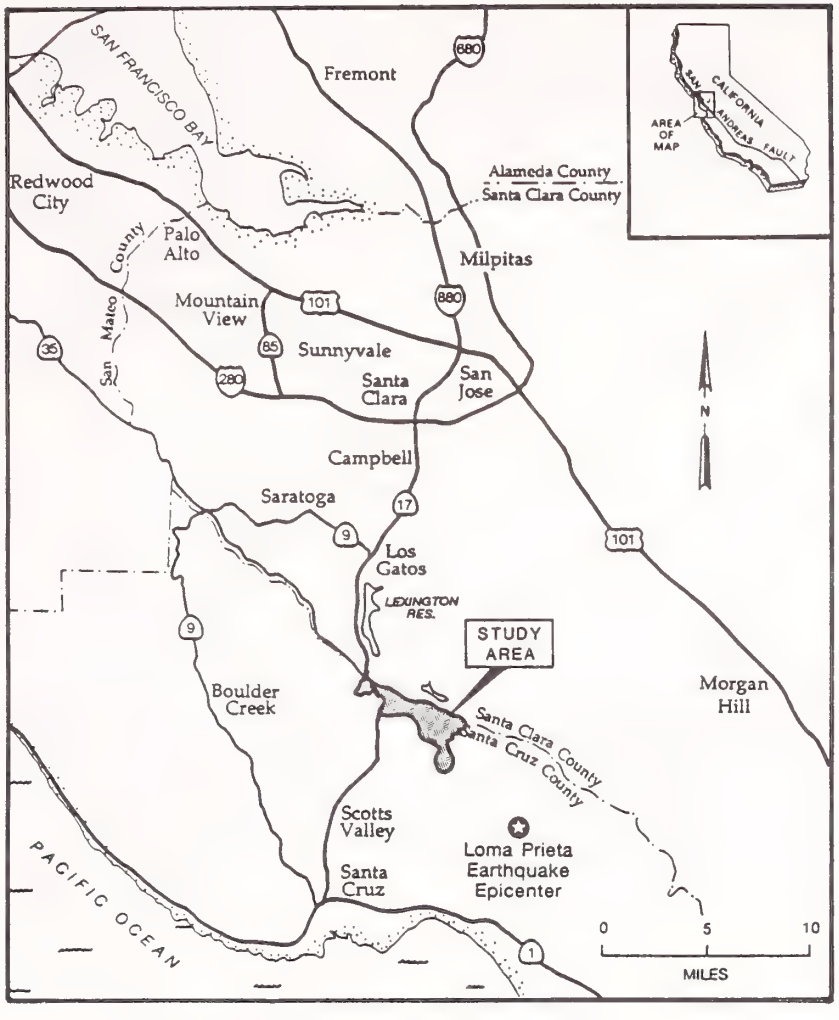

Figure 1. Location of study area
(after Keefer et al. 1991)

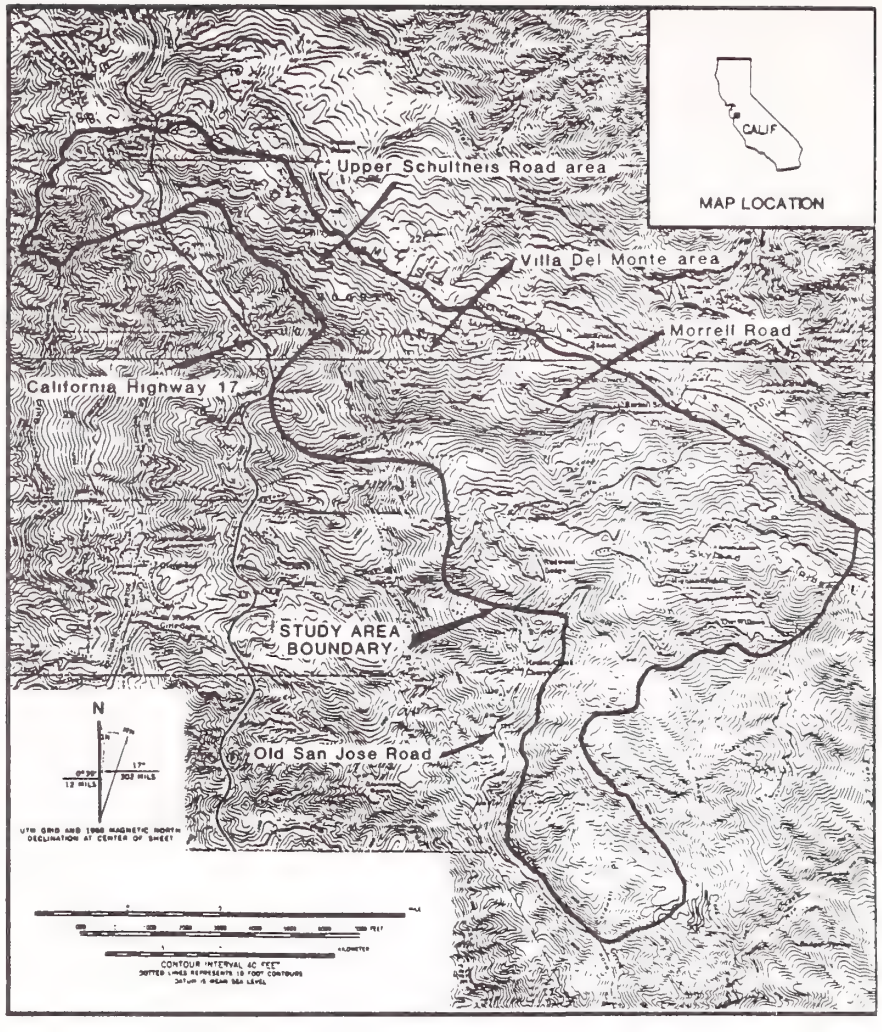

Figure 2. Contour map of study area
(after Keefer et al. 1991)

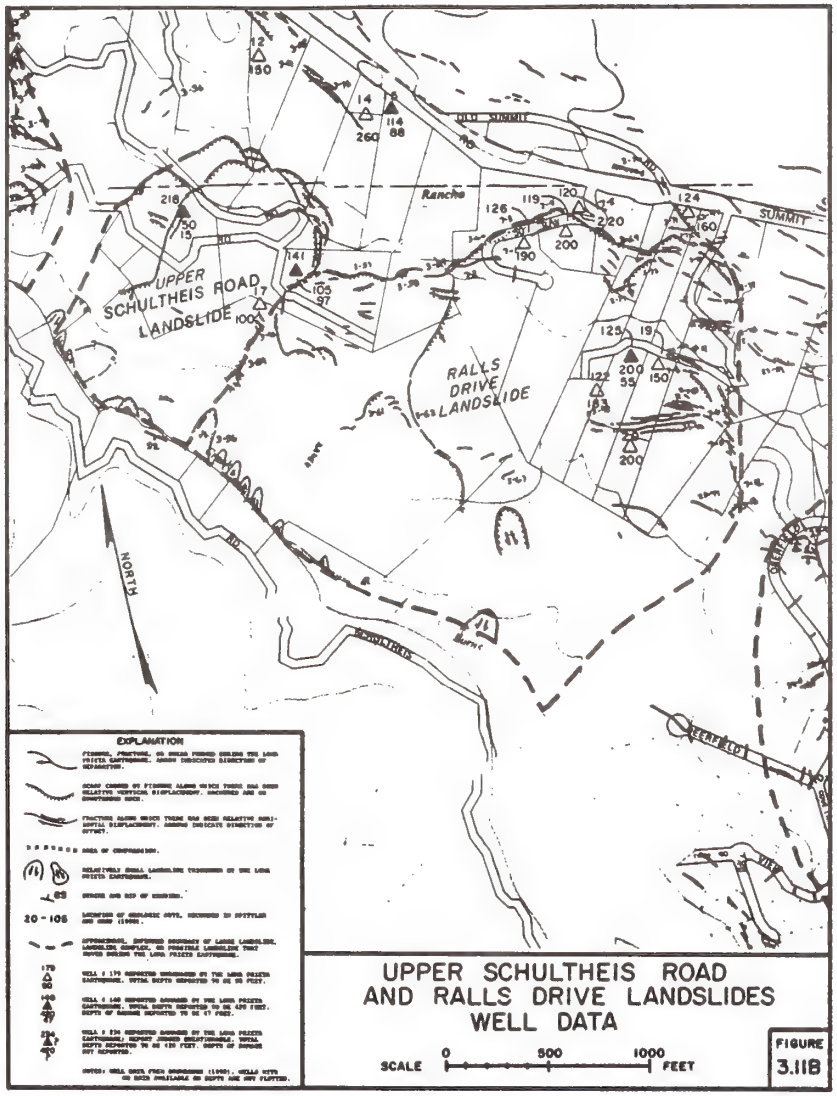

Figure 3. Mapped surface cracks in Upper Schultheis Road area (after Keefer et al. 1991)

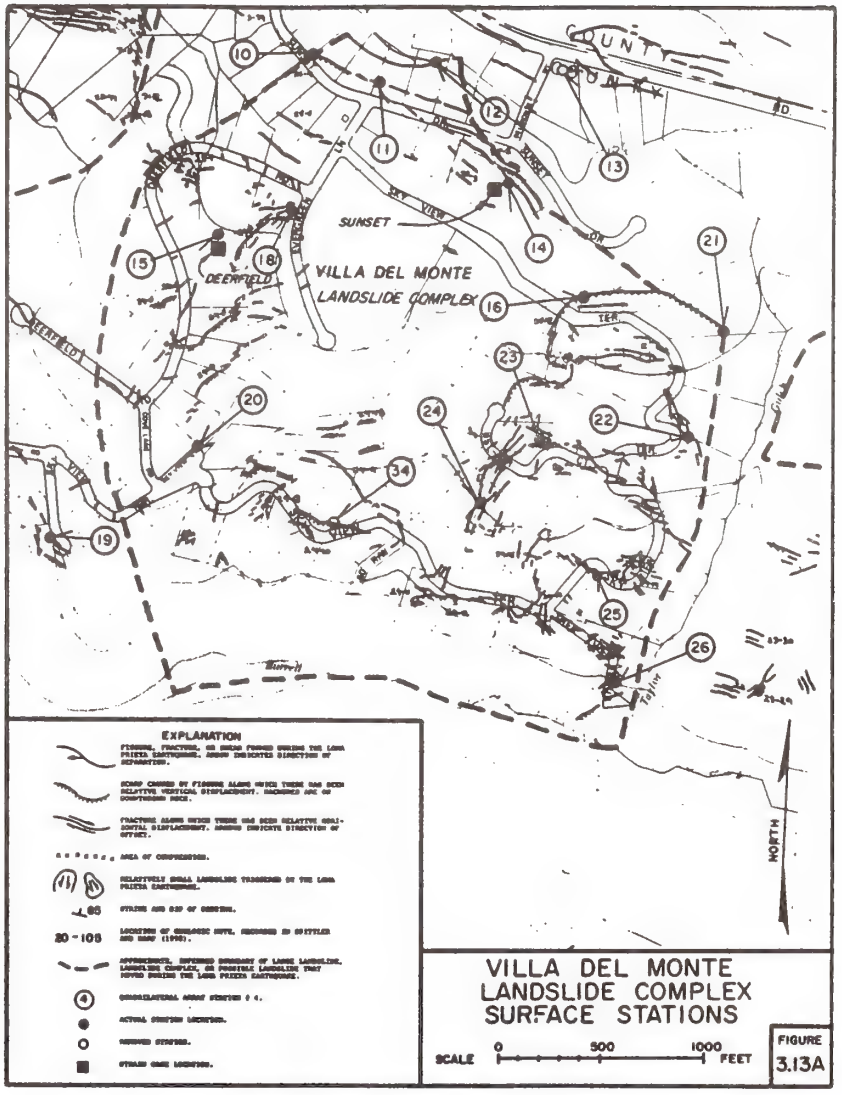

Figure 4. Mapped surface cracks in Villa Del Monte area (after Keefer et al. 1991)

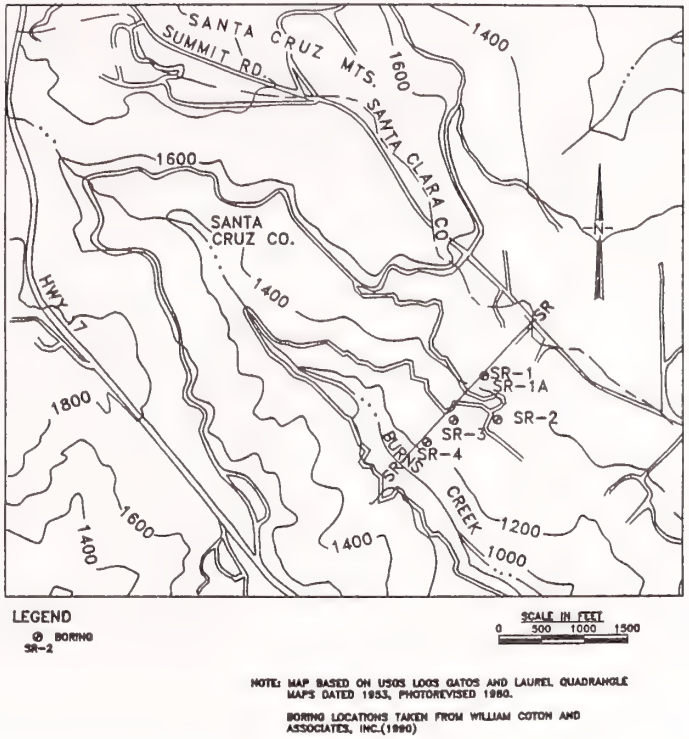

Figure 5. Locations of borings and section SR in Upper Schultheis Road area

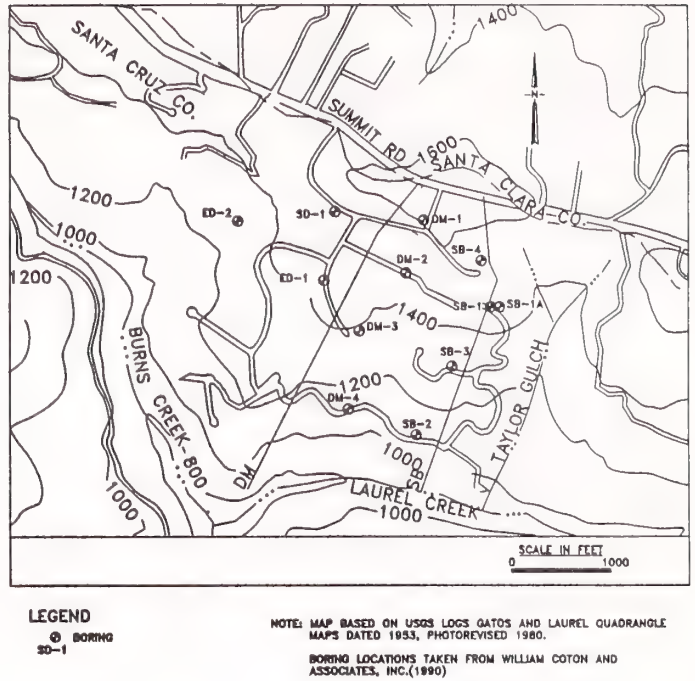

Figure 7. Locations of borings and sections DM and SB in Villa Del Monte area

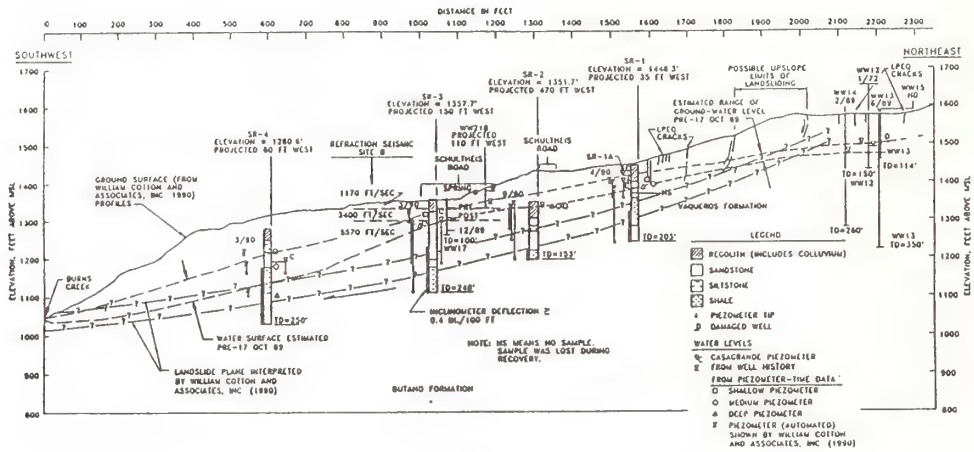

FIGURE 6 Estimated Upper and Lower Locations of Basal Shear Surfaces for Section SR, Upper Schultheis Road Landslide, from William Cotton and Associates, Inc. (1990)

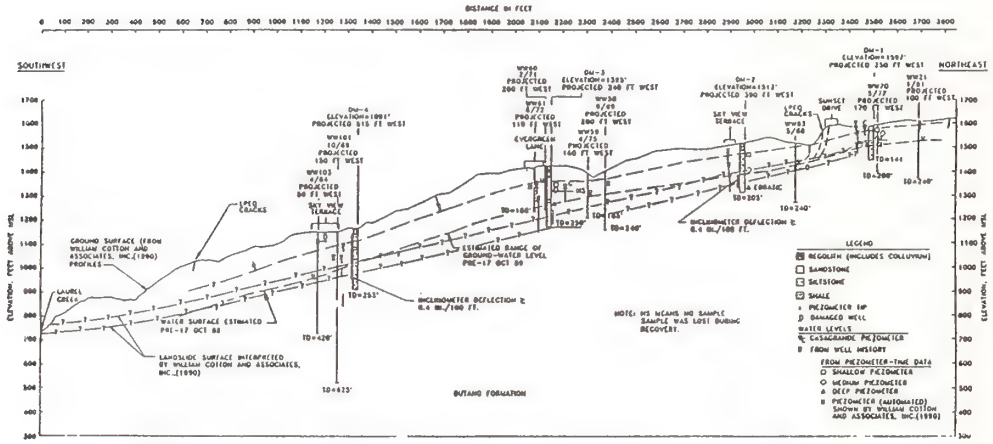

FIGURE 8 Estimated Upper and Lower Locations of Basal Shear Surfaces for Section DM, Villa Del Monte Landslide Complex, from William Cotton and Associates, Inc. (1990)

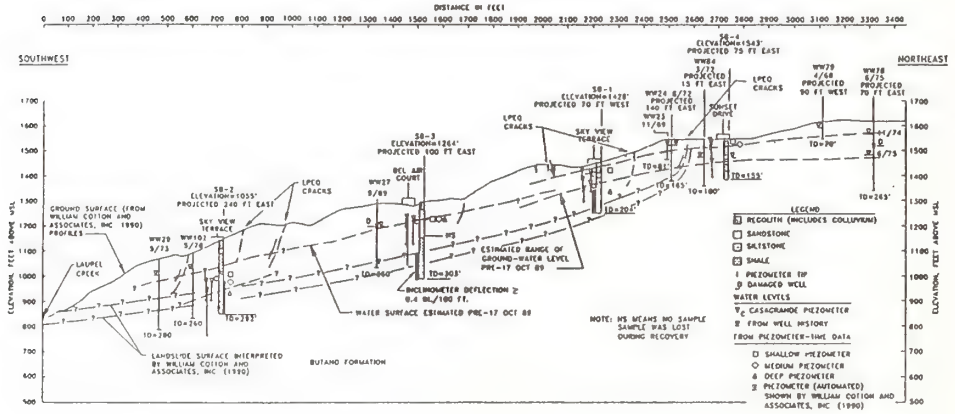

FIGURE 9 Estimated Upper and Lower Locations of Basal Shear Surfaces for Section SB, Villa Del Monte Landslide Complex, from William Cotton and Associates, Inc. (1990)

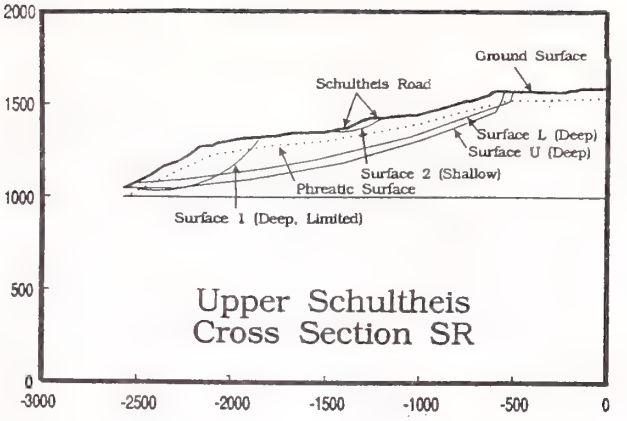

FIGURE 10 Assumed Locations of Shallow and Deep Sliding Surfaces for Section SR, Upper Schultheis Road Landslide

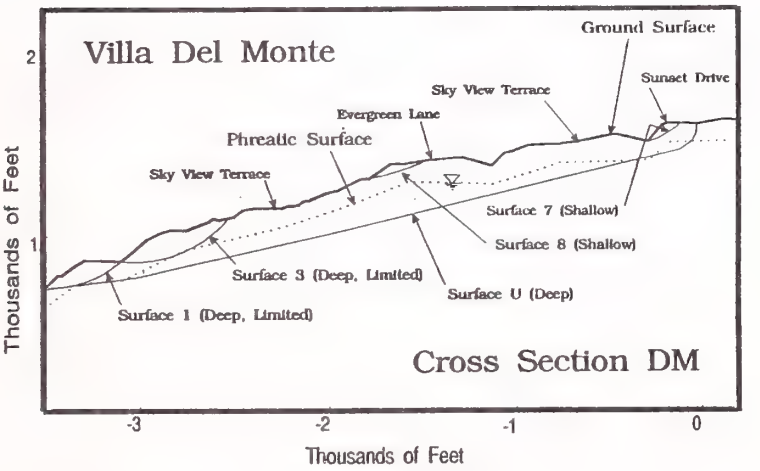

FIGURE 11 Assumed Locations of Shallow and Deep Sliding Surfaces for Section DM, Villa Del Monte Landslide Complex

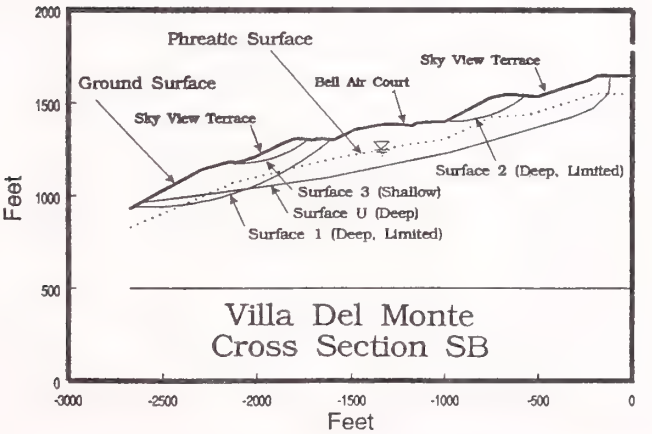

FIGURE 12 Assumed Locations of Shallow and Deep Sliding Surfaces for Section SB, Villa Del Monte Landslide Complex

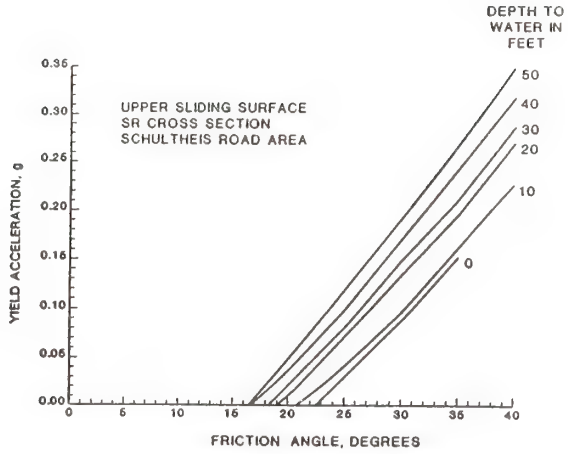

FIGURE 13 Relation Between Mobilized Friction Angle, Depth to Water Table, and Yield Value of Horizontal Acceleration for Upper Basal Shear Surface, Section SR, Upper Schultheis Road Landslide

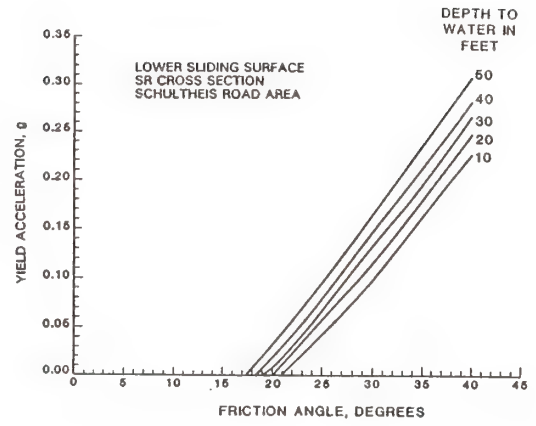

FIGURE 14 Relation Between Mobilized Friction Angle, Depth to Water Table, and Yield Value of Horizontal Acceleration for Lower Basal Shear Surface, Section SR, Upper Schultheis Road Landslide

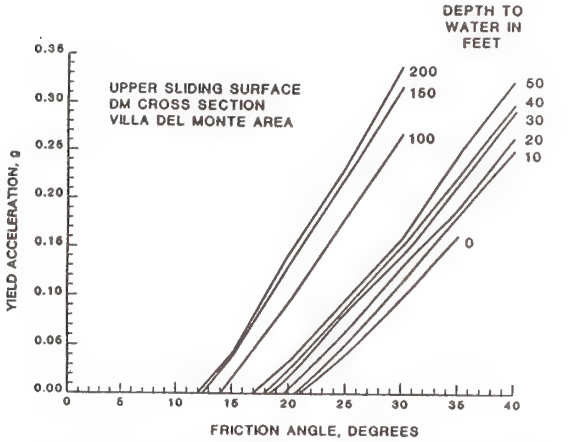

FIGURE 15 Relation Between Mobilized Friction Angle, Depth to Water Table, and Yield Value of Horizontal Acceleration for Upper Basal Shear Surface, Section DM, Villa Del Monte Landslide Complex

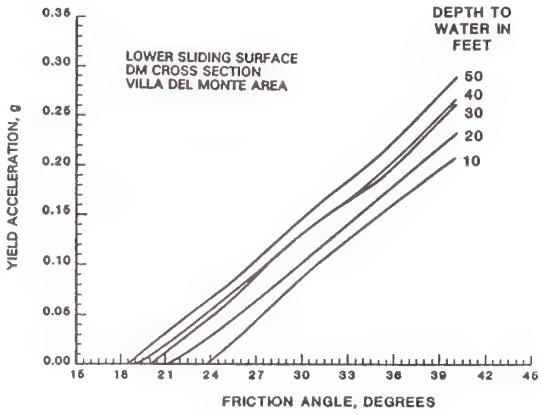

FIGURE 16 Relation Between Mobilized Friction Angle, Depth to Water Table, and Yield Value of Horizontal Acceleration for Lower Basal Shear Surface, Section DM, Villa Del Monte Landslide Complex

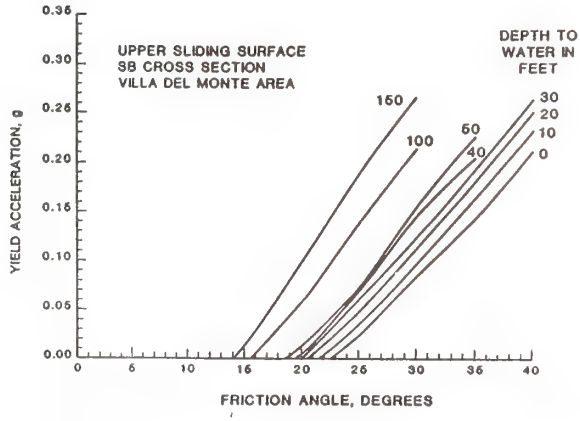

FIGURE 17 Relation Between Mobilized Friction Angle, Depth to Water Table, and Yield Value of Horizontal Acceleration for Upper Basal Shear Surface, Section SB, Villa Del Monte Landslide Complex

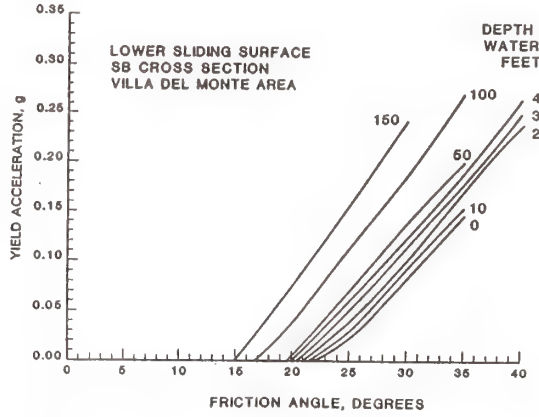

FIGURE 18 Relation Between Mobilized Friction Angle, Depth to Water Table, and Yield Value of Horizontal Acceleration for Lower Basal Shear Surface, Section SB, Villa Del Monte Landslide Complex

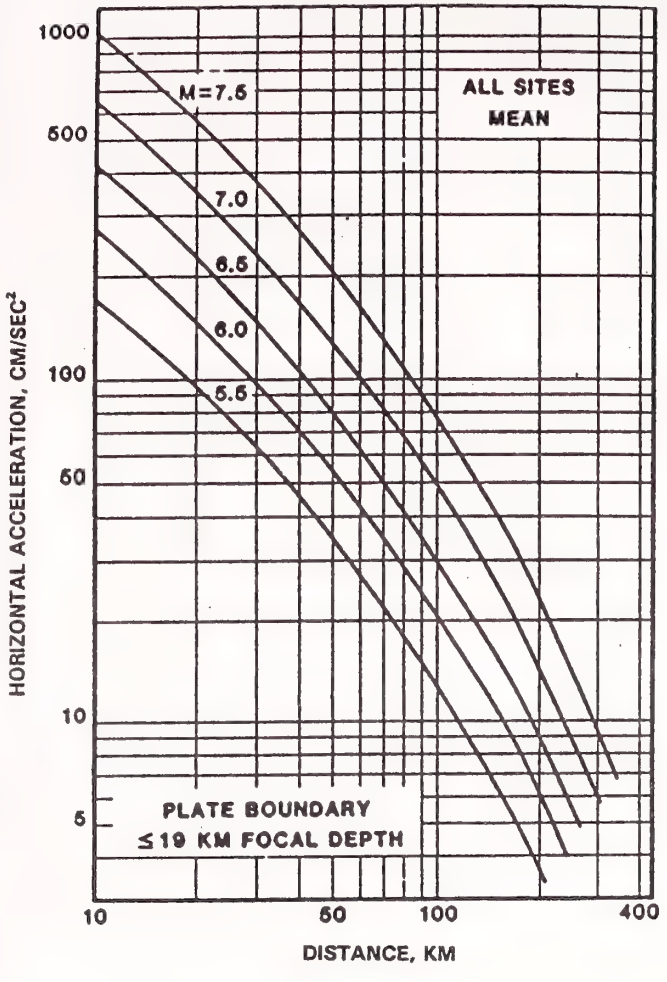

FIGURE 19 Attenuation of Peak Ground Acceleration with Distance. Average Curves for All Site Types for Plate Boundary Seismic Events with Focal Depths Less than 19 km, from Krinitzsky, Chang, and Nuttli (1988)

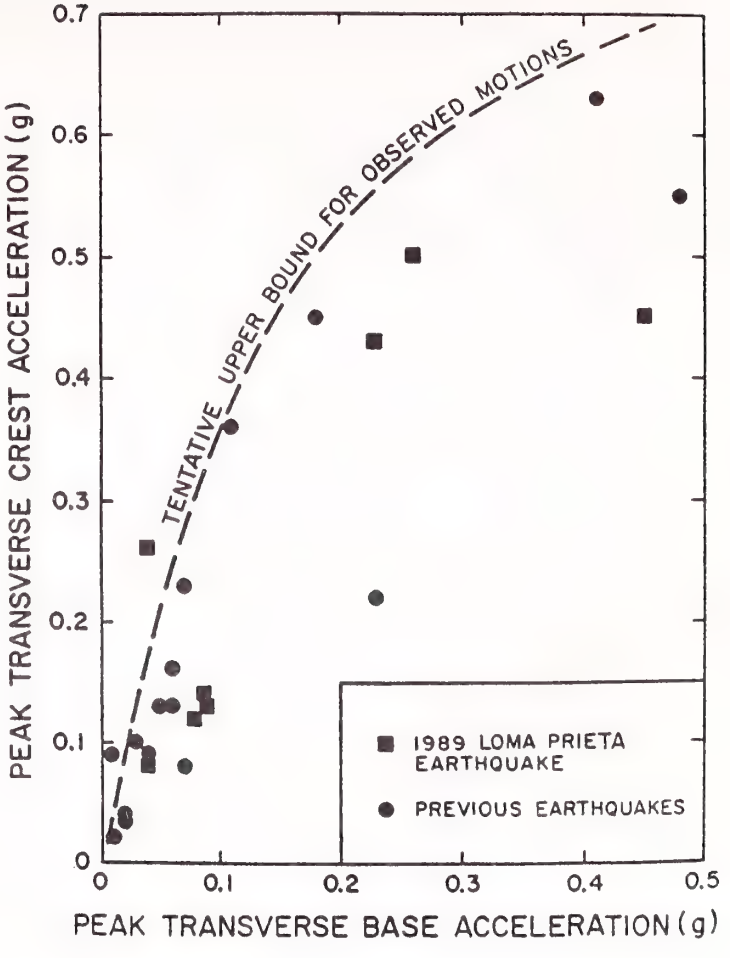

FIGURE 20 Comparison of Peak Base and Crest Transverse Accelerations Measured at Earth Dams (from Harder 1991)

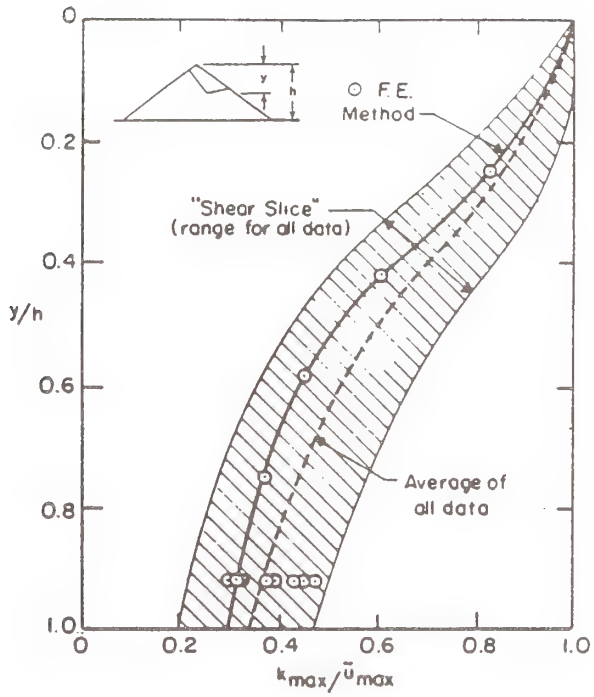

FIGURE 21 Relation between Acceleration Ratio $k_{max} / \ddot{u}_{max}$ (averaged dynamic load to peak crest acceleration) and Relative Height of Sliding Surface (y/h)

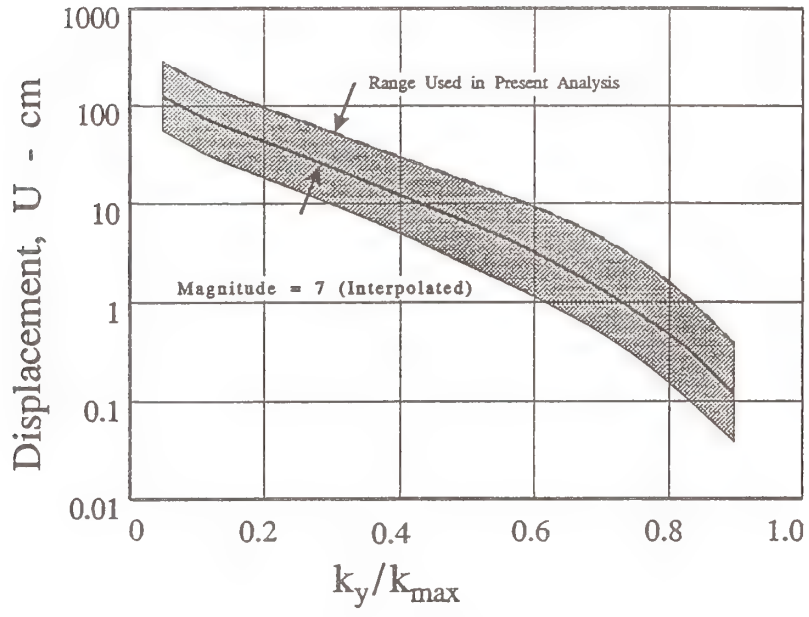

FIGURE 22 Average and Range for Relation Between Accumulated Newmark-Sliding-Block Displacement, U, and Acceleration Ratio, k_y/k_{max}, for Interpolated Magnitude 7 Earthquakes after Makdisi and Seed (1979)

Study on Prediction of Lateral Ground Flow by Soil Liquefaction and Its Influence on Piles

by

Ken-ichi Tokida[1], Hideo Matsumoto[2], Ikuo Towhata[3], and Yasushi Sasaki[4]

SUMMARY

An analytical method based on the minimum potential energy principle is proposed for predicting the permanent lateral displacement of ground due to soil liquefaction. Furthermore, a practical and simplified method obtained by parametric studies with the use of the analytical method proposed is also discussed to predict a maximum lateral displacement of an inclined ground. This was applied to real cases of shaking table tests and case studies in situ for past earthquakes.
Finally, experimental studies were carried out to investigate the external force acting on piles in ground flowed by soil liquefaction.

KEY WORDS :Liquefaction, Lateral Ground Flow, Permanent Displacement, Prediction, Minimum Potential Energy Principle, Parametric Study, Model Test, External Force, Pile

1. FOREWORD

Lateral ground flow induced by soil liquefaction took place apparently in past earthquakes [Refs.1～3]. For establishing a seismic design method of structures considering a lateral ground flow induced by soil liquefaction, essential factors relating to ground flow, a prediction method of permanent displacement and an external force acting on substructures should be investigated. The characteristics of lateral ground flow due to soil liquefaction have been studied by large-scale shaking table tests in the Public Works Research Institute [Refs.4～6]. In these tests, the influence of inclination of the ground surface and thickness of the liquefiable layer were investigated.
This paper presents results of large-scale shaking table tests for investigating the influence of the slope length on ground flow [Ref.7], and an analytical method based on the minimum potential energy principle to predict permanent lateral displacement of inclined ground flowed by soil liquefaction [Refs.8～11]. A practical and simplified procedure obtained by the parametric studies is also proposed to predict maximum lateral ground displacement. Furthermore, shaking table tests on piles in flowed ground [Ref.7] and model tests on piles driven in liquefied soils [Ref.14] were conducted to investigate the external force acting on piles in ground flowed by soil liquefaction.

2. LARGE SCALE SHAKING TABLE TESTS

2.1 METHOD OF EXPERIMENTS

Shaking table tests on four ground models (Model-9 ～ 12) were carried out to investigate the influence of slope length on ground flow induced by soil liquefaction. The conditions of the ground models are shown in Figure 1 and Table 1. A rectangular container used for Model-9～12 was 8.0 m long, 1.0 m wide and 1.0 m high. Six transparent glass windows (each is 0.8 m wide and 0.9 m high) were installed at the one side of the square container. The ground models fundamentally consisted of three layers : a lowermost nonliquefiable layer, a middle liquefiable layer and a uppermost unsaturated layer. However, Model-12 did not have the uppermost unsaturated layer. The materials used for a lowermost nonliquefiable layer and a middle liquefiable layer were mountain sands (Mean diameter of particles: D_{50} = 0.25mm) taken from Mt. Sengen-yama and gravels(D_{50} = 7mm) for the uppermost layer. The detailed method to prepare the ground model is presented in Reference 4. The thickness of liquefiable layer (H_L), the thickness of uppermost unsaturated layer (H_{NL}) and the gradient of ground surface (θ_S) were constant to be 350 mm, 150 mm and 5 %, respectively. The length of Models-9, 10, 11 and 12 was varied to be 2 m, 4 m, 8 m and 8 m, respectively. The water level was set equal to the upper boundary of the liquefiable layer. In each test, a constant sinusoidal acceleration with a frequency of 2 Hz was employed for 20 seconds (40 cycles); and several levels of maximum acceleration were applied stepwise to the shaking table as an input motion. As shown in Figure 1, pore water pressure meters, accelerometers, displacement meters and strain gage meters were installed in and/or on the ground

1) Head, Ground Vibration Division, Earthquake Disaster Prevention Department, Public works Research Institute (PWRI), Ministry of Construction.
2) Research Engineer, ditto.
3) Associate Professor, University of Tokyo.
4) Director, Earthquake · Disaster Prevention Department, PWRI.

models to measure the time histories of pore water pressure, acceleration and displacement/ strain of layers during excitation. Bench mark points were also set on the ground surface to measure manually and photograph the movement of lateral displacement of ground surface.

2.2 RESULTS OF EXPERIMENTS

Figure 2 summarizes the relation between input maximum acceleration of the shaking table and the accumulative lateral displace- ment at the center of the ground surface. As for Models-9, 10 and 11, it can be seen that the lateral ground flow begins to go up at the lower level of input acceleration, according to the increase of length of the ground surface. Because the effect of both end walls of the container is small in the case of Model-11, the liquefiable layer seems to be deformed more easily than Models-9 and 10. On the other hand, the liquefiable ground overburdened by an uppermost unsaturated layer such as Model-11 is less liquefiable than that without an uppermost unsaturated such as Model-12.

3. PREDICTION OF LATERAL GROUND FLOW

3.1 MINIMUM POTENTIAL ENERGY PRINCIPAL

Figure 3 illustrates a ground model which consists of an unliquefiable base layer (Thickness: B), a liquefiable layer (H) and an unsaturated surface layer (T) [Refs.8～11]. The surcharge (P) includes the weight of the surface layer, which is estimated to be moved together with the liquefiable layer (based on the shaking table tests). The horizontal and vertical displacements are denoted by u and w, respectively. The ground configuration varies linearly with the horizontal coordinate , x;

$$B = B_0 + ax, \quad H = H_0 + bx$$
$$T = T_0 + cx, \quad P = P_0 + ex \tag{1}$$

Furthermore, four assumptions were made in the analysis;
1) The lateral displacement is approximated by a sinusoidal distribution function in the z direction;

$$u = F(x)\sin\left[\pi (z-B)/2H\right] \tag{2}$$

where, F is an unknown function of x and stands for the displacement at the surface (z=B+H).
2) Soils flow with a constant volume;

$$\frac{\partial u}{\partial x} + \frac{\partial w}{\partial z} = 0 \tag{3}$$

3) The stress-strain relation of the liquefied sand is simply modeled by equation (4).

$$\tau = G\frac{\partial u}{\partial z} + \tau_r \tag{4}$$

where, τ, G and τ_r are the shear stress, the shear modulus of a liquefied layer and the remained stress. Hereupon, G = 0 and τ_r = 0, because liquefied soils behave as liquid whose flow is governed by the hydraulic gradient.
4) The surface unsaturated layer behaves as a solid bar of Young's modulus E.

Substituting equation (2) into equation (3) and considering zero displacement at the surface of the unliquefiable base layer (z=B), the function w is expressed in terms of F(x). By using u and w, the potential energy of the ground in Figure 3 is calculated [Ref.8～11] and the true F(x) makes this energy minimum. By using the variational principal and theory of Euler's equation,

$$\frac{dF}{dx} = \frac{C_4x^2 + C_5x + A_1}{C_1x^2 + C_2x + C_3} \tag{5}$$

where,

$$C_1 = \frac{4\gamma b^2}{\pi^2}, \quad C_2 = \frac{8\gamma bH_0}{\pi^2} + Ec$$
$$C_3 = \frac{4\gamma H_0^2}{\pi^2} + ET_0,$$
$$C_4 = -\frac{1}{2}\left\{(a+b)\left(c + \frac{2\gamma b}{\pi}\right) + \frac{2eb}{\pi}\right\}$$
$$C_5 = \tau_r - (a+b)\left(P_0 + \frac{2\gamma H_0}{\pi}\right) - \frac{2eH_0}{\pi}$$

A_1 is a constant parameter and γ is the unit weight of the liquefied soil. Thus, equation (5) is solved under relevant boundary conditions at x=0 and x=L, and the solution of Equation (5) is described in References 9～11.

3.2 APPLICATION MINIMUM POTENTIAL ENERGY PRINCIPAL TO REAL CASES

The minimum potential energy method proposed in the former section 3.1 was applied to real cases of shaking table tests conducted at the Public Works Research Institute. Figure 4 shows the results of calculations and measurements of maximum lateral displacement in the case of Model-10 (slope length: 4 m). The analysis was conducted with the estimated values of E = 5 t/m^2, γ = 1.80 t/m^3, and the unit weight of the surface layer of 1.40 t/m^3. Be-

cause the ground model surface neighboring the end of upper side of the container was settled and not cracked, the boundary conditions of F = 0 at both x = 0 and x = L (fixed at both ends of lower and upper sides) were employed in this study. It can be see that the peak value of maximum lateral displacement calculated is about 16 cm at the horizontal coordinate of 3 m. Because the maximum lateral displacement measured ranges from 20 to 25 cm, the calculation is somewhat larger than the measurement.

The minimum potential energy method was also applied to case studies in situ in past earthquakes. Figure 5 shows one of the examples to compare the calculation of lateral displacements at the surface and the measurement at the Maeyama-Hill area in Noshiro City damaged in the 1983 Nihon-Kai Cyubu Earthquake. Since the soil parameters were not known clearly, the analysis was conducted with the fixed values of $E = 1{,}100\ t/m^2$, $\gamma = 1.80\ t/m^3$, and the unit weight of the surface layer of $1.60\ t/m^3$. Boundary conditions of F = 0 at x = 0 (fixed at the end of the lower side) and dF/dx = 0 (free at the end of the upper side) were employed in this study. Although overestimating, the agreement with the observation seems satisfactory.

3.3 PRACTICAL METHOD BY PARAMETRIC STUDIES WITH MINIMUM ENERGY PRINCIPAL

Although the minimum potential energy method can be applied to in situ sites according to each ground condition, a simplified practical method is necessary to be established from the engineering view point. Hamada, M. et al. proposed equation (6) empirically based on case histories in past earthquakes in Japan to estimate the maximum lateral displacement of an inclined ground simply and quantitatively [Ref.12].

$$D = 0.75\sqrt{H \cdot {}^3\sqrt{\theta}} \qquad (6)$$

where, D is the maximum lateral displacement of the ground surface (m), H is the thickness of liquefied layers (m) and θ is the maximum gradient of the ground surface or the lower boundary of the liquefied layer (%).

However, parametric studies were conducted to propose a simplified method to estimate the maximum lateral displacement in this study. As shown in Figure 6, according to experimental studies [Ref.7], four parameters: the length of ground flow area (L), the average thickness of the liquefied layer (H), the average thickness of the unsaturated surface layer (T) and the gradient of the ground surface (θ_g) were employed as important factors against lateral ground displacement induced by soil liquefaction. The values of each parameter to calculate a maximum lateral displacement were selected as follows;

L (m) : 10, 20, 50, 100, 200, 500, 1000
H (m) : 0.1, 0.2, 0.5, 1, 2, 5, 10, 20
T (m) : 1, 2, 5, 10, 19
θ_g(%) : 0.1, 0.2, 0.5, 1, 2, 5, 10, 20

where, total thickness of a unsaturated surface layer and a liquefied layer was limited within 20 m, and the end of lower side and the one of upper side were assumed to be fixed and free, respectively.

Equation (7) is assumed to represent the maximum lateral displacement (D) in this study.

$$D = a \times L^b \times H^c \times T^d \times \theta_g{}^e \qquad (7)$$

The coefficients a, b, c, d and e are obtained by the multiple regression analysis for the maximum displacement at the center of a slope and the end of the upper side, according to the length of the slope as follows;

[$10 \leq L \leq 100$]
Center of slope:
$$D = 1.73 \times 10^{-5} \cdot L^{1.94} \cdot H^{0.298} \cdot T^{-0.275} \cdot \theta_s{}^{0.963} \qquad (8\text{-}1)$$
End of upper side:
$$D = 2.07 \times 10^{-5} \cdot L^{1.90} \cdot H^{0.295} \cdot T^{-0.276} \cdot \theta_s{}^{0.978} \qquad (8\text{-}2)$$
[$100 \leq L \leq 1000$]
Center of slope:
$$D = 1.29 \times 10^{-5} \cdot L^{1.93} \cdot H^{0.280} \cdot T^{-0.243} \cdot \theta_s{}^{0.935} \qquad (8\text{-}3)$$
End of upper side:
$$D = 1.70 \times 10^{-5} \cdot L^{1.93} \cdot H^{0.278} \cdot T^{-0.272} \cdot \theta_s{}^{0.935} \qquad (8\text{-}4)$$

Equation (8) was applied to sites where lateral ground flow due to soil liquefaction occurred in past earthquakes. 12 sites in the 1964 Niigata Earthquake and 27 sites in the 1983 Nihon-Kai Cyubu Earthquake where lateral ground displacement was measured and whose ground profiles were investigated in detail [Ref. 13] were selected. Because the ground conditions in situ were not always clarified to decide the length of ground flow area (L), ground conditions of interest are classified into four types according to the reliability to decide both boundaries of grounds as follows;

Type I : Both boundaries are reliable.
Type II : Only one boundary of upper side is reliable.
Type III : Only one boundary of lower side is reliable.

Type IV: Both boundaries are not reliable.

Figures 7 and 8 present relations between maximum displacements measured in situ and calculated ones with the use of equations (8-3) and (8-4) for ground types I, II, III and IV, respectively. The maximum displacements calculated by equation (6) are also referred. It can be seen that the calculated displacement based on equation (8) has relatively good agreement with the measured one (except for large displacements measured) especially at sites of ground types I, II and III. This also indicates that knowing the ground boundaries is very important and the ground condition should be well understood.

4. EFFECT OF LATERAL GROUND FLOW ON PILES

4.1 LARGE SCALE SHAKING TABLE TEST ON A PILE IN FLOWED GROUND

Shaking table tests on two model grounds Model-1 and Model-12) were also carried out to investigate the influence of ground flow against pile models set in liquefied soils. The conditions of ground models are shown in Figure 1. As shown in Figure 9, a vinyl chloride pipe (ℓ = 790 mm, ϕ = 22 mm) was fixed on the bottom of a container. Strain gages were put on the pipe model to measure the section force. Figures 10 and 11 show time histories of bending moment of the pile model at points of B2 to B6 and bending moment distribution of the pile model at the elapsed time (1, 4, 5, 6, 8 and 10 seconds) respectively. The bending moment of the pile model begins to increase at the elapsed time of about 5 seconds when the ground (liquefied partially) begins to flow. Although points of B2 to B4 are overscaled, the bending moment begins to decrease after the ground liquefied perfectly at the elapsed time of about 11 to 12 seconds. This indicates that the maximum load induced by ground flow due to soil liquefaction doesn't occur in the perfect liquefaction but in partial liquefaction, and the relation between the load acting on piles and the liquefaction potential should be investigated for design of foundations against soil liquefaction.

4.2 TEST ON PILES DRIVEN IN LIQUEFIED SOILS

4.2.1 METHOD OF EXPERIMENTS

Tests on piles forced by lateral ground flow in liquefied soils were conducted with the use of a test apparatus as shown in Figure 12. The container was 1.8 m long, 0.6 m wide and 1.0 m high. At the bottom of the container, a dense sand layer was prepared to arrange the height of liquefiable sand layer and a water supply tank was installed to boil the above layer by supplying water through a water supply pump. In this way, a loose saturated layer was made easily and repeatedly. The material of the liquefiable layer is Toyoura sand. The liquefiable layer was shaken and liquefied by one blow of a hammer against the side wall of the container. Just after the occurrence of liquefaction, a group of pile models fixed by a sliding plate which was supported on a support frame were forced to displace in the liquefied layer by a winch which was driven by hand. As shown in Figure 13, 10 pore water pressure meters (P1 ~ P10) wewe installed at two positions with the horizontal distance of 60 cm. The displacement of a sliding plate and/or pile models and the total load to drive them were measured by a displacement meter and a load cell which were set on the sliding plate, respectively. Three values of constant sliding velocity of the sliding plate were used: 4.5 mm/sec, 2.6 mm/sec and 1.5 mm/sec. The pile models was driven horizontally inside of two positions of pore water pressure meters. A vinyl chloride pipe (ϕ = 18 mm) reinforced inside by a steel bar was used as a pile model. The number of piles and their arrangement (lattice arrangement and zigzag arrangement) were varied as shown in Figure 14. The friction forces between the support frame and a sliding plate measured in advance were 0.9 kgf, 0.8 kgf and 0.75 kgf according to the sliding velocity 4.5 mm/sec, 2.6 mm/sec and 1.5 mm/sec, respectively.

4.2.2 RESULTS OF EXPERIMENTS

Figure 15 shows an example of the time histories: acceleration of the container, total pulling load measured by the load cell, displacement of piles and excess pore water pressure. It can be seen that after shaking by the hammer, the condition of perfect liquefaction at points of P1 and P5 continues for about 4 seconds and it takes about 20 seconds for excess pore water pressure of the whole ground to disappear. Furthermore, the total load increased gradually until the elapsed time of about 6 seconds and rapidly after that.

Figure 16 presents relations between the total load, excess pore water pressure at the points of P1 and P5 and the displacement of pile models. The relation between the total load and the displacement can be classified into two stages: stage I and stage II. Although the displacement of pile models increases at the stage I, the total load is almost constant at a low level. On the other hand, the total load increases according to the increase of the displacement at stage II. It should be noted that

the excess pore water pressure of P1 and P5 at the turning point (D) between stage I and stage II indicates about 20 gf/cm^2.

Figure 17 explains a concept of the distribution of an effective overburden pressure (σ') and/or an excess pore water pressure (ΔU) in liquefied soils. In this paper, the excess pore water pressures measured at the points of P1 and P5 which are 35 cm deep are used to calculate the excess pore pressure ratio (R_U) at the tip of a pile model which is 20 cm deep. Furthermore, the excess pore water pressures (ΔU) of P1 and P5 at the turning point (D) shown in Figure 16(b) are identified as the initial effective overburden pressure at the tip of pile models as shown in Figure 17. Because the average of the excess pore water pressure of P1 and P5 at the turning point (D) for all test cases is 20 gf/cm^2 and the unit weight of soils in the water (γ') is 0.914 gf/cm^3, the initial effective overburden pressure at the tip of pile models is assumed to be 20 gf/cm^2, in other words, the initial depth to calculate the excess pore pressure ratio (R_U) is converted to be 21.9 cm (= 20 / 0.914). The distribution of excess pore water pressures in the cases of R_U = 1.00, 0.90, 0.45 and 0.00 is exemplified in Figure 17.

Sliding/Relative Velocity and External Force Acting on Piles

Figure 18 presents relations between the total loads and the sliding velocity of 9 piles (3 rows × 3 piles) latticed in the cases of R_U = 0.90 and 0.00 (almost perfectly liquefied condition and not liquefied condition) respectively. It can be seen that the total load acting on the piles is almost constant in spite of the sliding velocity of the piles when soil liquefaction does not occur: R_U = 0.00. On the other hand, the total load increases according to the increase of the sliding velocity of the piles when soil liquefaction occurs partially: for example, R_U = 0.90.

Liquefaction Potential and External Force Acting on Piles

Figure 19 presents relations between the total load, the excess pore water pressure at the tip of pile models, the sliding velocity of pile models (4.5 mm/sec, 2.6 mm/sec and 1.5 mm/sec), and the arrangement of them (lattice arrangement of 5 rows × 2 piles, P1-9, and 2 rows × 5 piles, P1-8, and zigzag arrangement of 3-2-3 piles, P2-5, and 2-1-2-1-2 piles, P2-6, see Figure 14) in the sliding direction. From these figures, it can be noted that the total load decreases according to the increase of excess pore water pressure ratio. Furthermore, according to the increase of the sliding velocity of the pile models, the total load increases at each excess pore water pressure ratio. As for pile arrangement, the total loads in the cases of P1-8 and P2-6 are larger than that in the cases of P1-9 and P2-5, respectively. This indicates that the total load is related to the number of piles in the normal direction of a ground flow; in other words, the total load acting on piles or the resistance potential of piles against a lateral ground flow goes up according to an increase in the number of piles in the normal direction of the lateral ground flow.

5. CONCLUSION AND FUTURE REMARKS

Based on the studies in this paper, the following results have been obtained;

(1) From shaking table tests, it can be indicated that a liquefied inclined ground becomes easy to flow laterally according to the increase of slope length and/or the decrease of the thickness of an uppermost unsaturated layer.

(2) A method based on the concept of minimum potential energy is proposed to predict the lateral ground displacement induced by soil liquefaction and applied to real cases of both shaking table tests and case studies in situ in past earthquakes. Although overestimating, the agreement with the observations seems satisfactory.

(3) A simplified method to estimate the maximum lateral displacement due to soil liquefaction is proposed based on a parametric study with the use of the minimum potential energy method proposed in this study. It can be indicated that the calculated displacement has relatively good agreement with the measured one when the ground condition such as boundaries of both sides, area of the slope and soil profile can be understood properly.

(4) From shaking table tests, it can be indicated that the maximum load acting on a pile in the soils flowing due to soil liquefaction doesn't occur in the perfectly liquefied condition but in the partially liquefied one,

(5) Fundamental tests on piles forced by a lateral ground flow in the liquefied soils are conducted: and it can be known that the total load acting on piles by ground flow due to soil liquefaction decreases according to the increase of excess pore water pressure ratio and increases according to the increase of relative velocity between flowing soils and piles in the partially liquefied condition.

(6) The total load acting on piles, in other words, a resistance potential of piles against lateral ground flow, goes up according to the increase of the number of piles in the direction normal to the lateral ground flow.

Further investigation should be carried out in the future to establish a seismic design method to consider the effects of lateral ground flow due to soil liquefaction.

ACKNOWLEDGEMENT

The authors wish to express their sincere gratitude to Professor T. Katayama, University of Tokyo and Professor M. Hamada, University of Tokai, for their invaluable advise and discussion, and to Professor Timothy B. D'Orazio, San Francisco State University, who visited the Ground Vibration Division of Public Works Research Institute as an invited researcher by the STA (Science and Technology Agency) Fellowship and Mr. Takuo Azuma of PWRI for their assistance to present this paper.

REFERENCES

1) Hamada, M., Yasuda, S. and Wakamatsu, K., "Case Study on Liquefaction-Induced Ground Failure During Earthquakes in Japan", Proc. of 1st Japan-United States Workshop on Liquefaction, Large Ground Deformation and Their Effects on Lifeline Facilities, Tokyo, November, 1988.

2) Hamada, M., Yasuda, S., Isoyama, R., and Emoto, K., "Observation of Permanent Ground Displacement Induced by soil Liquefaction", Proc. of JSCE, No.376/III-6, pp211-220(in Japanese).

3)Yasuda, S., Watanabe, H. and Yoshida, N., "Reconnaissance Report on the Valle de la Estrella (Costa Rica) Earthquake of April 22, 1991", Journal of the Japan Society of Soil Mechanics and Foundation Engineering, Vol. 39, No. 8, August 1991(in Japanese).

4) Sasaki, Y., Tokida, K., Matsumoto, H. and Saya, S., "Experimental Study on Lateral Flow of Ground Induced by Soil Liquefaction", 21st U.S.-Japan Panel on Wind and Seismic Effects, UJNR, Tsukuba, May, 1990.

5) Sasaki, Y., Tokida, K., Matsumoto, H. and Saya, S., "Experimental Study on Lateral Flow of Ground Induced by Soil Liquefaction", 8th Japan Earthquake Engineering Symposium 1990, Tokyo, December, 1990.

6) Sasaki, Y., Tokida, K., Matsumoto, H. and Saya, S., "Experimental Study on Lateral Flow of Ground Due to Soil Liquefaction", 2nd International Conference on Recent Advances in Geotechnical Earthquake Engineering and Soil Dynamics, St. Louis, March, 1991.

7) Matsumoto, H., Tokida, K. and Saya, S., "Effects of Boundary Condition on Ground Flow Due to Soil Liquefaction", 21th JSCE Earthquake Engineering Symposium-1991, Tokyo, July, 1991(in Japanese).

8) Towhata, I. and Tamari, Y., "Calculation Method of Permanent Displacement of Liquefied Ground by Variational Theory", 14th Lecture Meeting of Research Society of Civil Engineering, March, 1990(in Japanese).

9) Towhata, I., Tokida, K., Tamari, Y., Matsumoto, H. and Yamada, K., "Prediction of Permanent Lateral Displacement of Liquefied Ground by Means of Variation Principle", 3rd Japan-U.S. Workshop on Earthquake Resistant Design of Lifeline Facilities and Countermeasures for Soil Liquefaction, San Francisco, December, 1990, Technical Report NCEER-91-0001.

10) Towhata, I., Sasaki, Y., Tokida, K., Matsumoto, H. and Tamari, Y., "Permanent Displacement of Liquefied Ground", 9th Asian Regional Conference on Soil Mechanics and Foundation Engineering, Bangkok, December, 1991.

11) Towhata, I., Sasaki, Y., Tokida, K., Matsumoto, H., Tamari, Y., Saya, S. and Yanada, K., "Prediction of Permanent Displacement of Liquefied Ground by Means of Minimum Energy Principle", submitted to Soils and Foundations.

12) Hamada, M., Yasuda, S., Isoyama, R. and Emoto, K., "Study on Liquefaction-Induced Permanent Ground Displacement and Earthquake Damage", Proceedings of Japan Society of Civil Engineers, No.376/III-6, PP.221- 229,December, 1986(in Japanese).

13) Hamada, M., "Large Ground Deformations and Their Effects on Lifelines/1964 Niigata Earthquake/1983 Nihon-Kai Chubu Earthquake, Technical Report NCEER-92-001, National Center for Earthquake Engineering Research, USA, 1992.

14) Tokida, K., Matsumoto, H. and Azuma, T., "Experimental Study on External Force Acting on Pile Induced by Lateral Ground Flow Due to Soil Liquefaction", submitted to the 47th Annual Meeting of Japan Society of Civil Engineering, Sendai, September, 1992(In Japanese).

Table 1. Condition of ground models

Ground Model No.	Gradient of Ground Surface (%)	Length of Ground Model /Slope (m)	Thickness of Liquefiable Layer (cm)	Thickness of Uppermost Non-Liqufied Layer(cm)
9	5	2.0	35	15
10	5	4.0	35	15
11	5	8.0	35	15
12	5	8.0	35	0

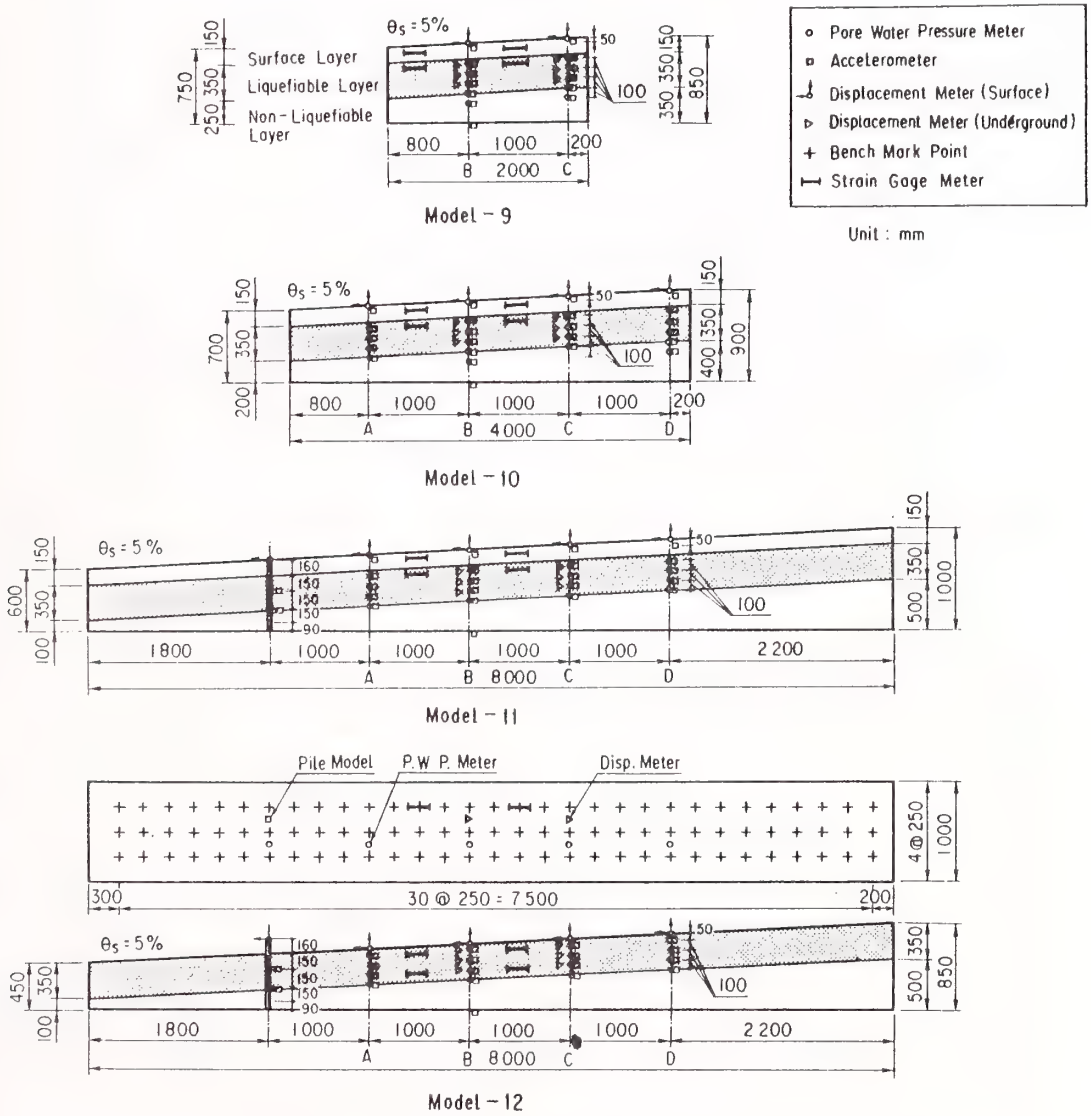

Figure 1. Ground models and measurements for large scale shaking table tests

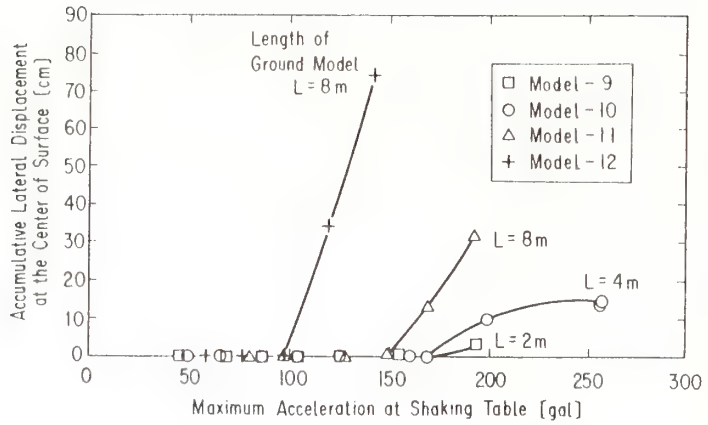

Figure 2. Relation between lateral ground displacement at center of ground surface, input acceleration and length of ground surface

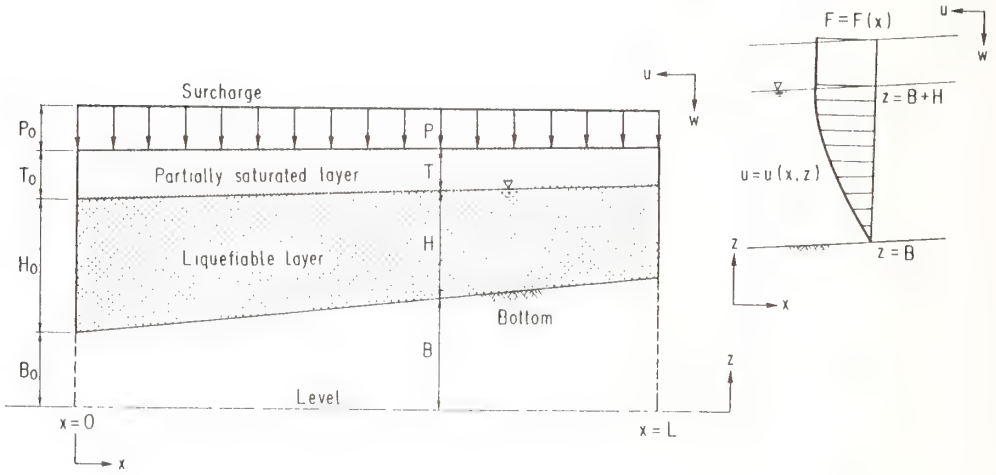

Figure 3. Ground model applied for minimum potential energy method

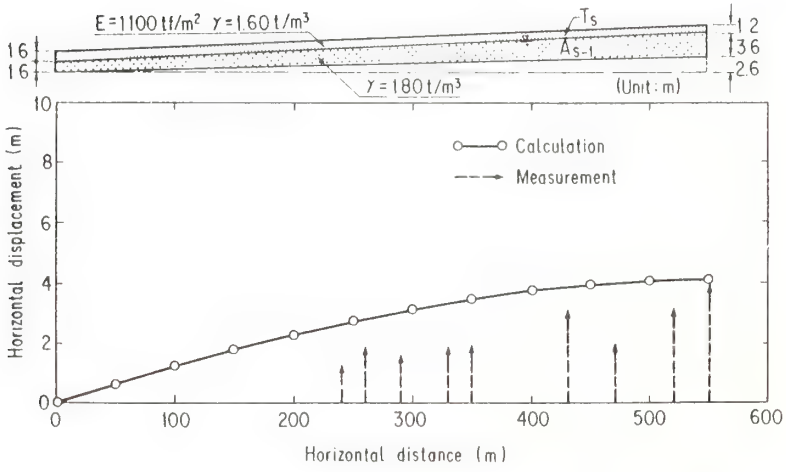

Figure 5. Case history study at Maeyama Area in Noshiro City in the 1983 Nihon-Kai Cyubu Earthquake, Japan

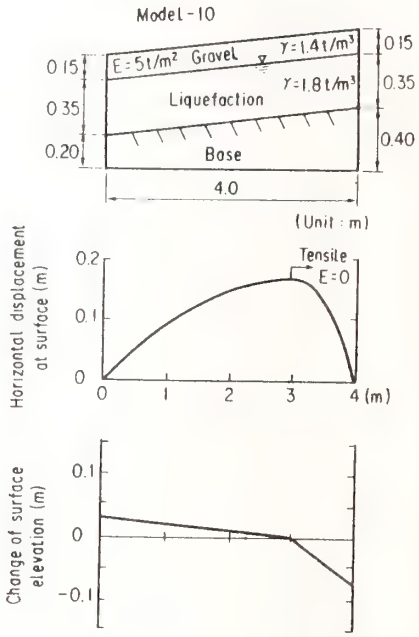

Figure 4. Case study applied for shaking table test: Model-10

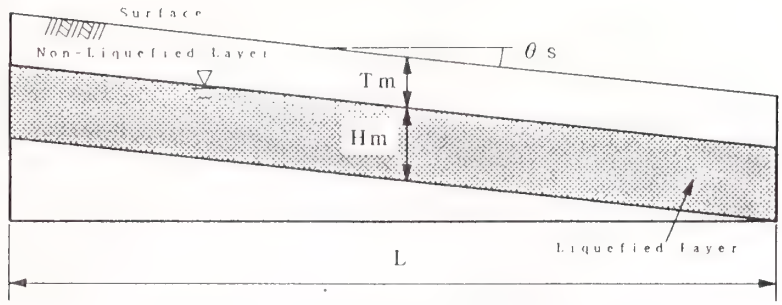

Figure 6. Ground model for parametric study with use of minimum potential energy method

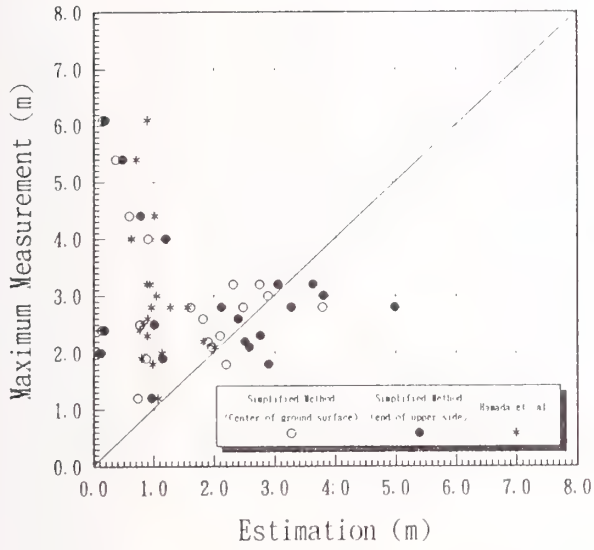

Figure 7. Relation between measured displacement in situ and calculated one (Types Ⅰ, Ⅱ, Ⅲ)

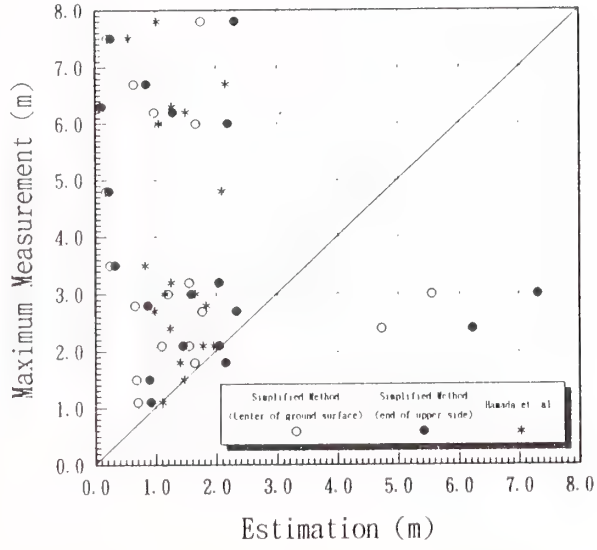

Figure 8. Relation between measured displacement in situ and calculated one (Type Ⅳ)

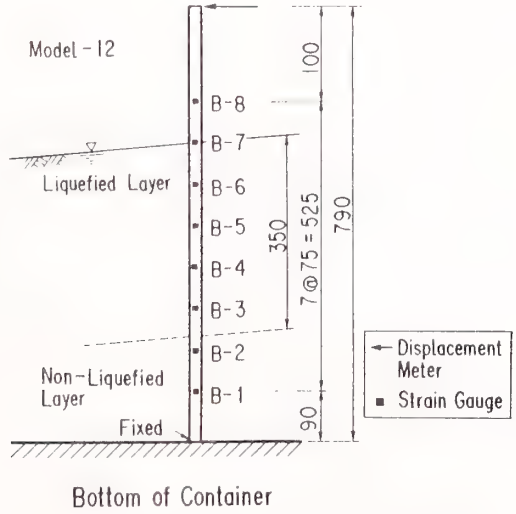

Figure 9. Condition of pile model and measurements

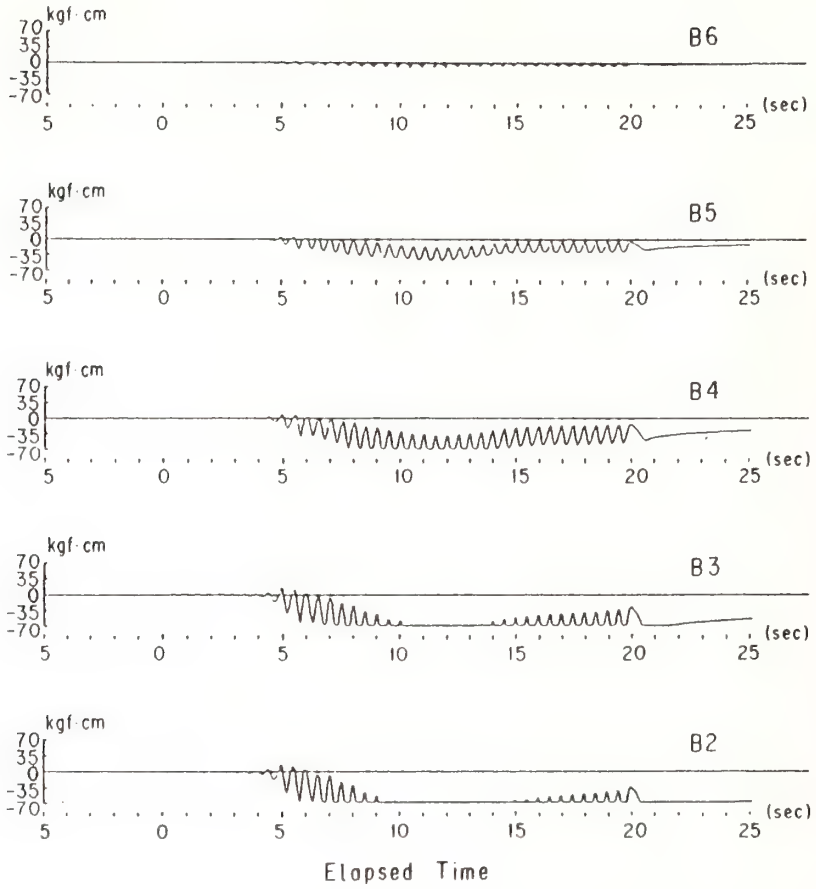

Figure 10. Time histories of bending moment of pile model

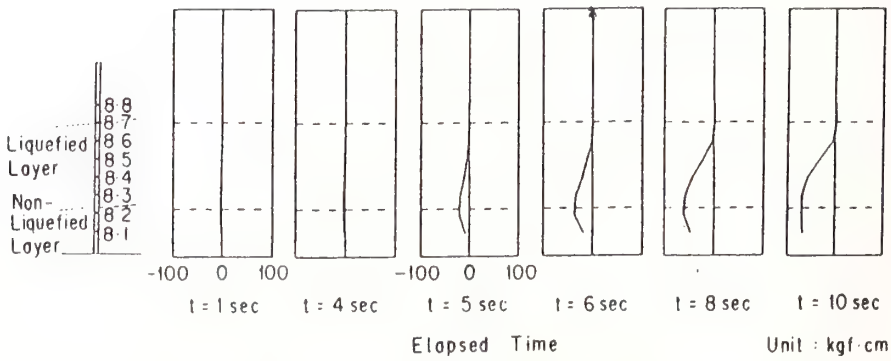

Figure 11. Time history of bending moment distribution of pile model

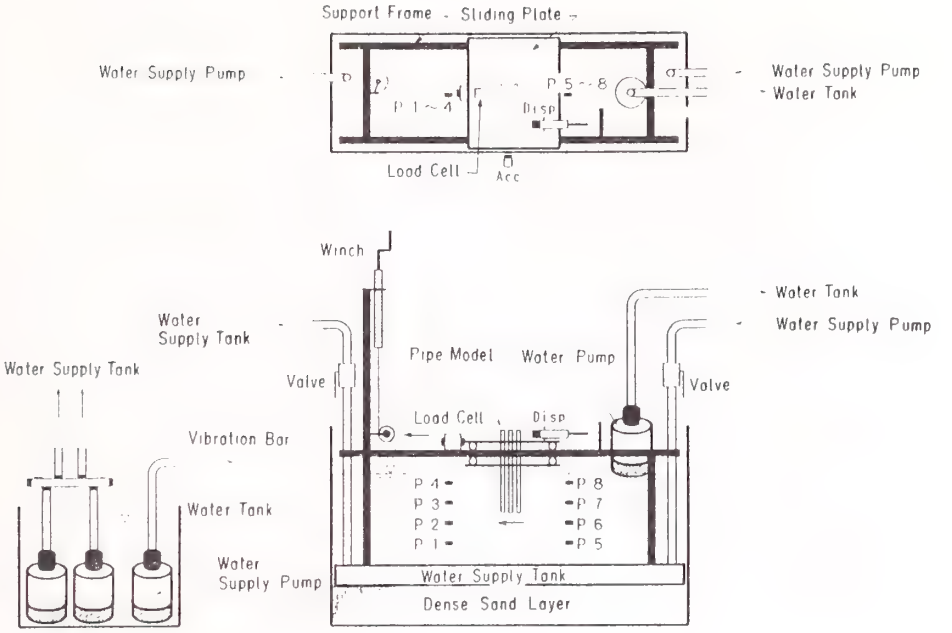

Figure 12. Test apparatus to drive piles in liquefied soils

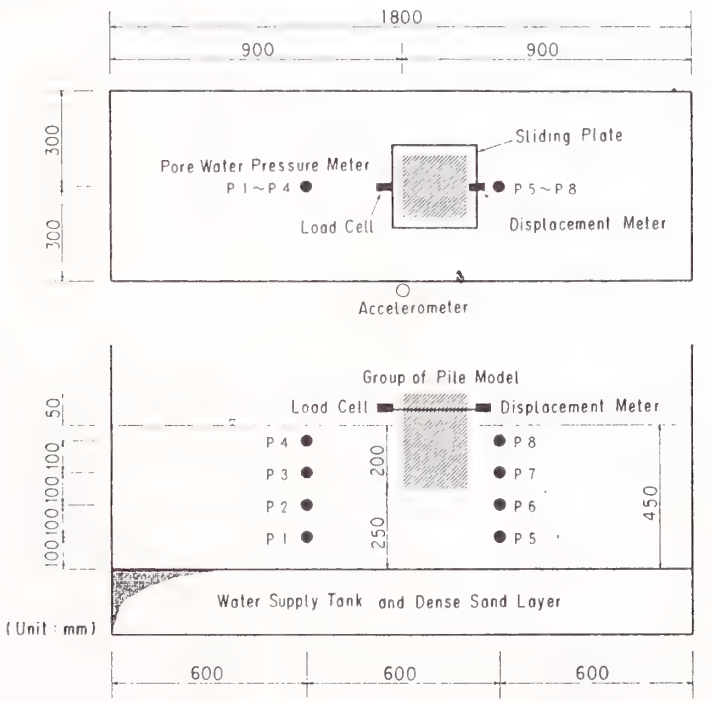

Figure 13. Ground model and measurements

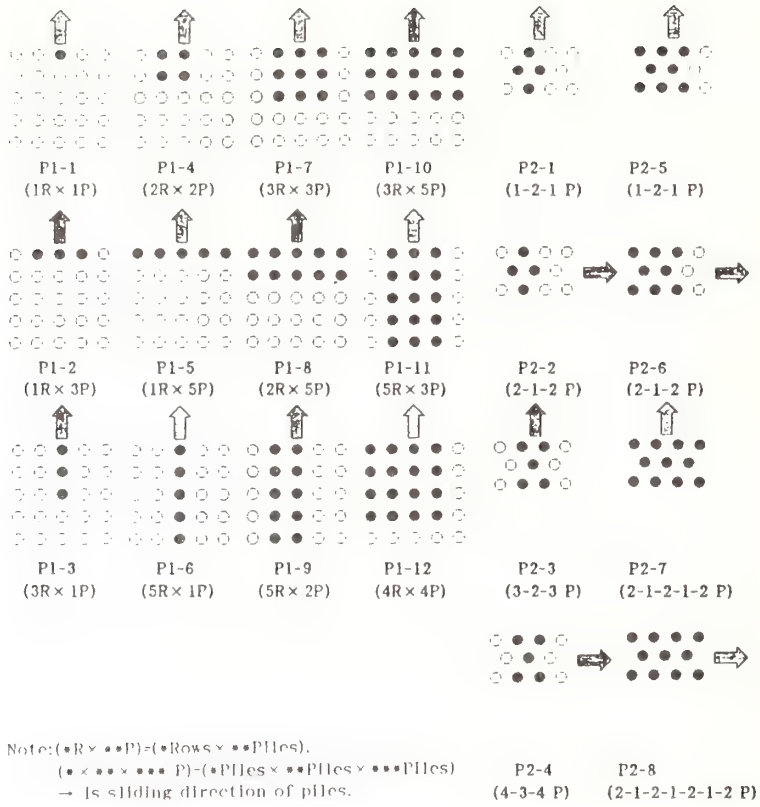

Figure 14. Condition of pile arrangement and sliding direction of piles

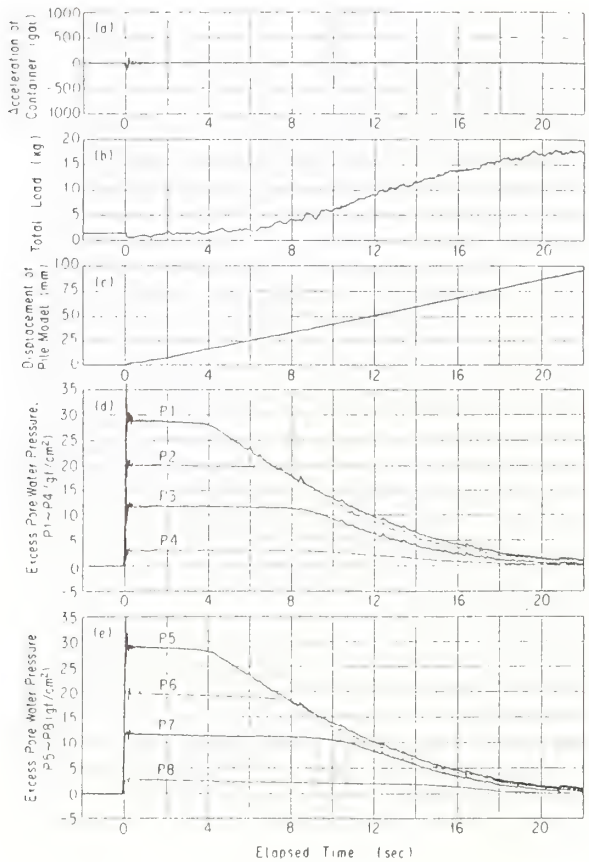

Figure 15.
Example of time histories of dynamic behavior of ground model and pile model

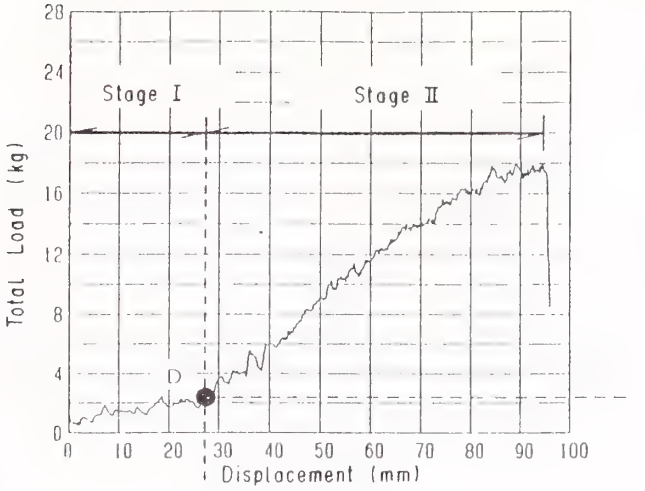

(a) Load~Displacement

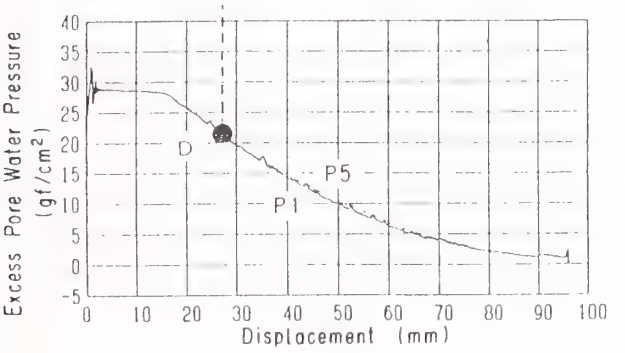

(b) Excess Pore Water Pressure~Displacement

Figure 16. Example of relation between total load, excess pore water pressure and displacement of pile model

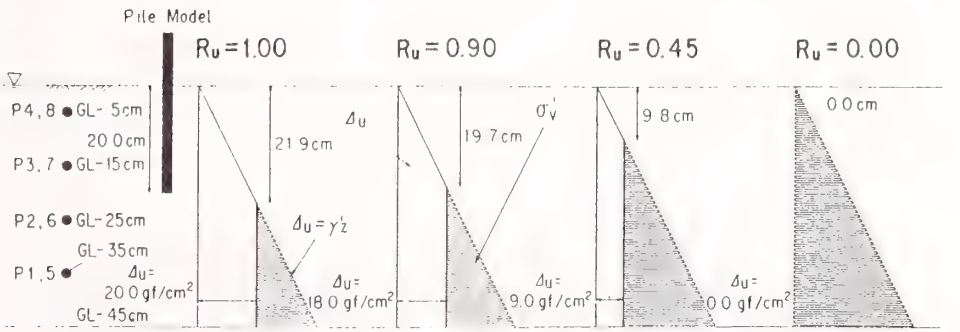

Figure 17. Identification of excess pore water pressure ratio at tip of pile model

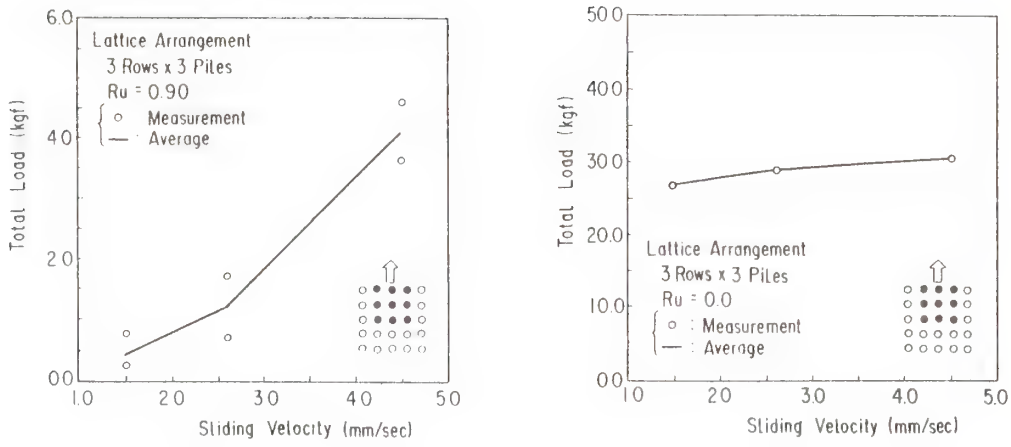

(a) Ru = 0.90 (b) Ru = 0.00

Figure 18. Relation between total load acting on piles and sliding velocity of piles in the case of P1-7

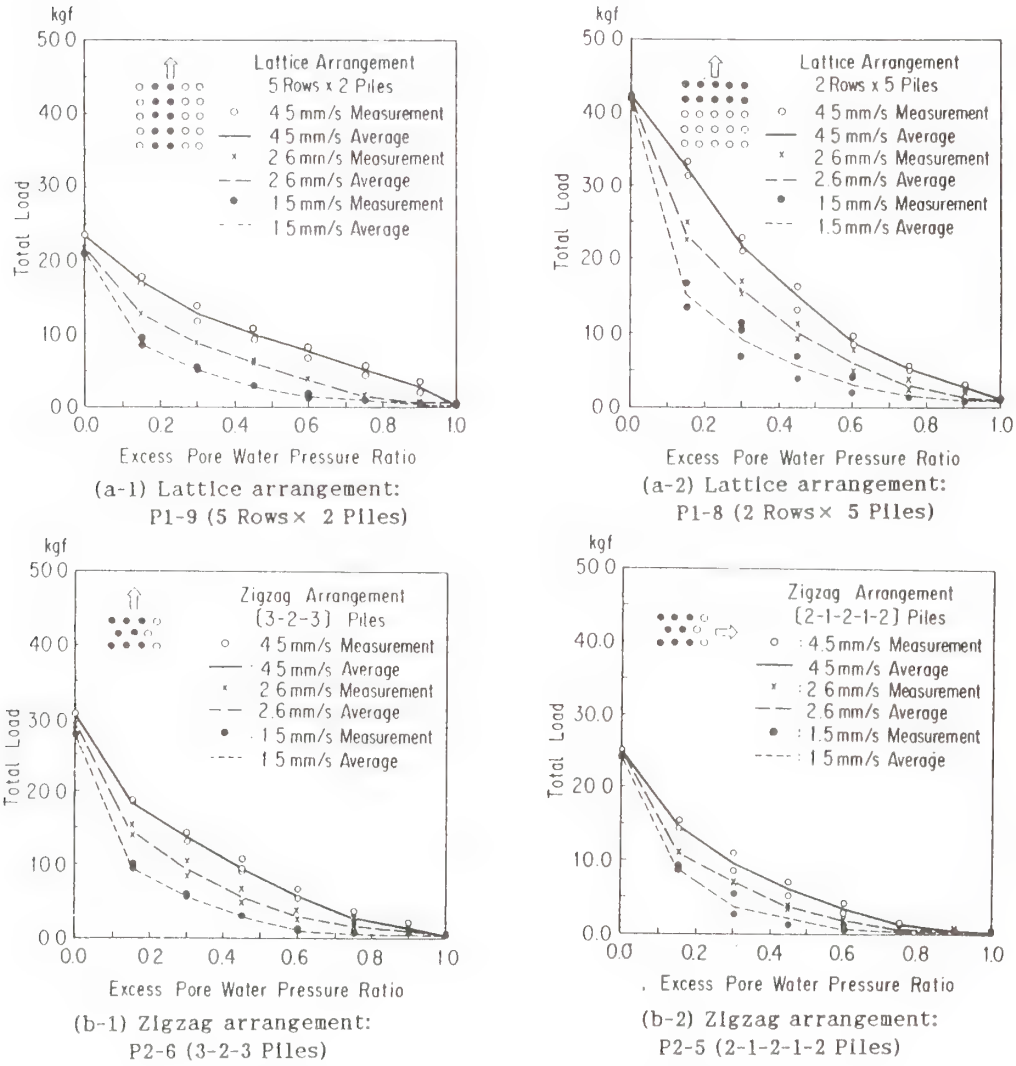

(a-1) Lattice arrangement: P1-9 (5 Rows× 2 Piles)

(a-2) Lattice arrangement: P1-8 (2 Rows× 5 Piles)

(b-1) Zigzag arrangement: P2-6 (3-2-3 Piles)

(b-2) Zigzag arrangement: P2-5 (2-1-2-1-2 Piles)

Figure 19. Relation between pore water pressure at tip of pile and total load acting on pile

Horizontal Bearing Capacity of Pile Foundations Based on Horizontal Loading Tests

by

Minoru Fujiwara[1], Michio Okahara[2], Shoichi Nakatani[3], Yoshitomi Kimura[4], and Shitgeru Takagi[5]

SUMMARY

At present, the design standard used for structures is shifting from the working stress design method hitherto in use to the limit states design method. In accordance with the limit states design method, a limit state is defined so that it can be verified that a structure can maintain required functions; then, it is checked that the structure possesses required safety against external forces such as load and that it doesn't reach limit states during the design's life span. Limit states which are taken into consideration in stability calculations are the elastic limit, which is the reversible limit of the behavior of a foundation, and the ultimate limit, where deformation progresses and reaches a tilting condition. In order to apply the limit states design method to pile foundations, it is necessary to clarify these limit states that must be checked in the design and to establish models for analyses which represent such states.

In this paper, the data of horizontal loading tests of various piles are analyzed in order to elucidate the horizontal elastic limit, and an estimation formula to obtain the coefficient of horizontal ground reaction used for a stability calculation of pile foundations within the elastic limit is proposed. Furthermore, in order to clarify the behavior of pile foundations during large-scale deformation exceeding the elastic limit, ground reaction, effect of pile group, and decrease of flexural rigidity of the pile body are examined by analyzing the results of horizontal loading tests.

KEY WORDS: Pile Foundations, Horizontal Loading Tests, Horizontal Bearing Capacity, Elastic Limit, Coefficient of Horizontal Ground Reaction, Ground Reaction

1. INTRODUCTION

At present the design standard of structures in overseas countries is making a shift from the working stress design method hitherto in use to the limit states design method or the load resistance factor design method[1)2)3)]. Triggered by the revision of "Standard Specifications for Concrete" (Japan Society of Civil Engineers, 1986), various institutions in Japan are also examining adoption of a new design method. In accordance with the limit states design method, a limit state is defined so that it can be verified that a structure can maintain required functions; then, it is checked that the structure possesses required safety against external forces such as load and that it does not reach limit states during the period of design durability. Since the functions that a structure must be equipped with are expressed as the limit state in accordance with this method, design purposes can be clear. In addition, with respect to the safety of structures, this design method is believed to realize more practical designs, due to the fact that various uncertain factors in the design can be evaluated using the theory of reliability, and that the coefficient of load as well as the coefficient of resistance can be employed as coefficients of safety.

In order to introduce this limit states design method to the design of pile foundations, it is necessary to determine the limit state which must be checked in the design stage and to establish a model for stability calculation which can represent the limit state with high precision. Analyses on the horizontal behavior of elastic foundations such as piles can be divided into (1) ultimate ground reaction method, (2) elastic ground reaction method and (3) compound ground reaction method, depending on the treatment of ground resistance (ground reaction, p) surrounding the piles.

(1) Ultimate ground reaction method

This method estimates horizontal resistance only from the balance with external force acting on the piles, supposing the distribution of the ground reaction at the ultimate condition of the ground. Since the given ground reaction is irrelevant with the displacement, and since the flexural deformation of the piles is not taken into consideration, the deformation at the ultimate resistance can not be estimated by this method.

(2) Elastic ground reaction method

This method expresses the ground reaction, p, by the function, p=p(x,y), which represents the relationship between the depth, x, and the amount of deflection of piles, y. Depending on the treatment of p(x,y), this method can be

*1 Director, Structure and Bridge Department, Public Works Research Institute, Ministry of Construction
*2 Head, Foundation Engineering Division, Structure and Bridge Dept., PWRI, MOC.
*3 Engineering Affairs Management Section, Minister's Secretariat, MOC.
*4 Research Engineer, Foundation Engineering Div., Structure and Bridge Dept., PWRI, MOC.
*5 ditto

further divided into the linear elastic ground reaction method, the non-linear elastic ground reaction method, and the p-y curve method. With respect to the constant of ground spring used in the linear elastic ground reaction method, the so-called reverse operation value calculated based on the data obtained from loading tests is used in general. The non-linear elastic ground reaction method unlinearly treats the relationship of ground reaction and displacement in order to take the non-alignment of the resistance of the ground into consideration. The p-y curve method is to estimate the relationship of ground reaction and the amount of displacement based on examinations, etc., and to conduct numerical analyses.

Since these methods are based on the supposition that the ground is elastic, neither the ground reaction at the ultimate state nor the ultimate bearing capacity can be obtained.

(3) Compound ground reaction method

This is a method to conduct analyses on the supposition that the ground near the surface which is largely transformed is in a plastic area and that the lower ground which is less transformed is in an elastic area. Consideration (1) is used for the ground resistance in the plastic area, whereas consideration (2) is used for the ground resistance in an elastic area. Modelization of the ground is still shelved for future examination; however, this method is best able to calculate the actual behavior of foundations with high precision.

As described above, a variety of methods are available for analyses of pile foundations in the horizontal direction. Nevertheless, the choice of method in the design of pile foundations is closely related to the range of amount of displacement that is assumed in each design.

According to the concept of design prescribed in "Specifications for Highway Bridges, Part IV, Specifications for Substructures"[4] (Japan Road Association, 1990) which is used as a technical standard for substructures of highway bridges (herein after referred to as "Specifications"), concerning the level of design load employed at present, a foundation should be sufficiently safe against bearing force, and "any residual displacement that is harmful to the foundation should not occur." In short, pile foundations are designed based on an analysis, in which the pile is converted into linear spring constant, so that both the displacement and the reaction of the pile head obtained by the analysis are controlled within the range where the foundation behaves elastically.

Concerning the limit states design method, on the other hand, it is necessary to keep trying to clarify the limit state that must be checked in the design. In addition to the concept described above, "any residual displacement that is harmful to the foundation should not occur," another concept is also proposed; "foundations should be designed to resist against a load which acts upon it quite rarely during the period of design's lifetime, such as a huge earthquake, so that any destructive damage to the structure, such as a fall of bridge, does not occur." (see Figure 1.1)[5]. Thus, an ideal model for a stability calculation used for the design is a model which can be applied to a large-scale deformation exceeding the range where the foundation behaves elastically, or a model which can be used for a calculation of horizontal durability of the foundation. In this case, the non-linearity of the ground resistance and of the flexural rigidity of piles can not be ignored.

Based on these circumstances, horizontal loading tests were conducted and their data were analyzed in this paper in order to clarify the horizontal behavior and the horizontal bearing capacity of pile foundations. The data obtained from many horizontal loading tests on a single pile were analyzed statistically in order to grasp quantitatively the displacement at the limit where the foundation is considered to behave elastically from a viewpoint of design, and an estimation formula of the coefficient of horizontal ground reaction used for the design within the domain of this displacement was proposed. Furthermore, in order to clarify the behavior of pile foundations in the domain exceeding this displacement, data obtained from horizontal loading tests on both a single pile and pile groups were analyzed; then the non-linearity of the ground resistance and of the rigidity of piles, and the influence of the pile group were examined.

2. LOADING TEST DATA OF PILES USED

The data used for the analyses in this paper are horizontal loading test data filed with prefectural authorities and other institutions such as the four public highway corporations, and which the Public Works Research Institute collected in 1988. The total number of the collected loading test data was 415[6]; however, data used in this paper were selected from these 415 data based on the content of the loading tests and the substantiality of the data. The quantity of data used in this paper is as shown in Table 2.1. In addition, depending on the content of examination, efficient data are selected occasionally from the data shown in Table 2.1.

In order to examine the behavior of pile foundations during large-scale deformation, the data of loading tests which cover large-scale deformation were selected from the above data, and the case with a single pile was analyzed. As for the influence of a pile group, results obtained from model pile tests conducted in the test pit at the Public Works Research Institute as

well as from an in-situ pile foundation test conducted by Metropolitan Expressway Public Corporation were used.

3. HORIZONTAL ELASTIC LIMIT OF PILES

3.1. Definition of Horizontal Elastic Limit

The load-displacement curve of the pile head, when the horizontal load acts upon the pile foundation, shows strong non-linearity. For example, Figure 3.1. shows results of horizontal loading tests[7] on a pile foundation using 9 steel piles (3 x 3 piles) with a diameter of 318mm and length of 1.5m. Figure 3.1. shows that the relationship between load and displacement is non-linear from the initial stage of loading, and that residual displacement remains when loading is removed. This is considered to be attributable to the non-linearity of the deformation characteristic of the earth itself and the consecutive progress of the plastic area of the ground along with the increase of displacement from the surface toward the direction of the depth. Therefore, it is difficult to define the elastic limit in a strict sense,even if the load is controlled at a low level.

Figure 3.2. shows an example of the relationship between the residual displacement of the pile head at every loading cycle in horizontal loading tests of piles and the ratio of displacement of the pile head against the diameter of the pile prior to the removal of loading (strain of the pile head, Sy/D). This figure shows that the residual displacement increases rapidly from a certain level of displacement. If the displacement of the pile head during loading can be controlled within the point, Sry,where the residual displacement makes an abrupt increase, huge residual displacement of the foundation can be prevented. In other words, if the foundation can be designed so that displacement is controlled within this level of displacement even when a short-term loading, such as an earthquake, acts upon the foundation, the foundation is usable without any repair work after the loading is over, since there remains no major residual displacement. Thus, the elastic behavior in an engineering sense, in other words, the limit of displacement which is the amount of residual displacement negligible in the design was defined as the horizontal elastic limit, and its quantitative evaluation was conducted.

The evaluation is conducted based on the various data obtained from horizontal loading tests introduced in Chapter 2. In addition to the point, Sry, where the residual displacement makes a sudden increase, the point, Sy, which is equivalent to the yield load on the distribution curve of the Weibull function defined in Figure 3.3. was studied.

A comparison between the data obtained from horizontal loading tests using a cast-in-place pile and other piles, such as a steel pipe pile, proved that there was peculiarity in the form of load-displacement curve. The following two points stated below are the reasons for this:

(1) In the case with a cast-in-place pile, a bending crack occurs on the pile body at a relatively small load level. Accordingly, the flexural rigidity of the pile body changes and the non-linearity of the pile body appears.

(2) Since a cast-in-place pile loosens the surrounding ground at its placement, the influence of ground slackness appears until the surrounding ground reaches the original stress condition of the natural ground.

Thus, when an analysis is conducted, the displacement index of the Weibull curve formula, m, is made variable without fixing it to 1, in order to improve the conformity of the distribution curve of the Weibull function for cast-in-place piles (in the case of other piles, m = 1 works sufficiently to obtain approximate values).

The point, Sry, where the residual displacement makes a sudden increase and the yield point, Sy, on the Weibull curve were compared using the data obtained from loading tests. Figures 3.4.(a) and 3.4.(b) show the results of this comparison in the cases of a steel pile and a cast-in-place pile, respectively. Since they show a comparatively favorable correlation, there may not be any problem in considering that the point where residual displacement suddenly increases roughly corresponds with the yield point on the Weibull curve.

3.2. Modulus of Deformation of Ground and Yield Displacement

The horizontal elastic limit described above is considered to be related to the flexural rigidity of piles and the modulus of deformation of the ground, Eo, in addition to the diameter and kind of piles. Figure 3.5. shows the relationship between the modulus of deformation of the ground, Eo, and the yield displacement, Sy, which were estimated by approximating the load-displacement curve using the distribution curve of the Weibull function. On the other hand, Figure 3.6. shows the relationship between the yield strain, (Sy/D) and the modulus of deformation of the ground. The modulus of deformation of the ground, Eo, is estimated to be Eo=7N based on the N value of the standard penetration test.

Thus, the following points stand:

(1) The correlations between Sy and Eo, as well as between Sy/D and Eo vary greatly across the board.

(2) There is a general trend that Sy and Sy/D decrease as the modulus of deformation of the ground increases. Nevertheless, this trend is

not apparent in the case of Sy/D .

(3) Values of Sy and Sy/D are large in the case of steel pipe piles, PC piles and PHC piles; however, they are small in the case of cast-in-place piles. This trend is especially remarkable with Sy/D.

3.3. Statistical Characteristics of Yield Displacement

As described above, since Sy and Sy/D do not correlate strongly with the modulus of deformation of the ground, statistical characteristics of Sy and Sy/D are analyzed regardless of the modulus of deformation of the ground.

Figures 3.7. and 3.8. show the distribution of Sy and Sy/D. Both of these figures are in favorable conformity with the logarithmic normal distribution. Figure 3.9. show distribution of Sy and Sy/D of various kinds of piles , which was approximated by the logarithmic normal distribution. Tables 3.1. and 3.2. summarize statistical characteristics of Sy and Sy/D by type of piles.

Thus, the following points stand:

(1) Coefficients of variation of Sy and Sy/D exceed 100%, and they scatter greatly.

(2) The mean value of Sy is 26mm in the case of steel pipe piles and 14mm in the case of PC and PHC piles. On the other hand, the mean value of Sy/D is 4.3% in the case of steel pipe piles and 3.7% in the case of PC and PHC piles.

(3) With respect to cast-in-place piles, values of Sy and Sy/D are small and greatly different from the cases with other piles. For instance, the mean value of Sy/D is 1%. This is not due to the fact that the horizontal resistance of cast-in-place piles is small. This is rather due to the fact that the occurrence of a crack in the pile body influences the determination of an yield point.

3.4. Horizontal Elastic Limit

When piles receive huge horizontal load exceeding the yield load expressed by the load-displacement curve, deformation of piles suddenly increases and the stability of pile foundations is damaged, as mentioned above. Accordingly, one of the states that must be checked in the design is the limit state where the deformation of pile foundations is kept on the side of the so-called elastic area. Nevertheless, since the yield displacement varies a great deal, the problem is to what extent this variation should be taken into consideration in order to reasonably establish the horizontal elastic limit.

The "Specifications" (1990) prescribes that the allowable displacement should be 1% of the pile diameter (minimum 15mm), based on the results analyzed in this paper; however, it might be more reasonable to establish the elastic limit for each one of the piles depending on its respective characteristics. For instance, in the case of steel pipe piles, the allowable displacement can be around 2% to 3% of the pile diameter, since their deformation function is large, while in the case of cast-in-place piles, it can be around 0.7% to 1.0% of the pile diameter, since, in contrast, their deformation function is small.

4. STABILITY CALCULATION METHOD OF PILE FOUNDATIONS WITHIN THE ELASTIC LIMIT

4.1. Model for Stability Calculation

As defined in 3.1., if the displacement of a foundation when load is acting on it is within the elastic limit, the displacement of the foundation is comparatively small and the residual displacement is on the small level. Therefore, within this sphere, no major error arises even if a stability calculation is conducted by replacing the pile with a linear spring. Therefore, the "Specifications" prescribes that a stability calculation of pile foundations should be conducted in accordance with the elastic analysis method which gives consideration to the displacement of the footing (vertical, horizontal and rotary displacement), under the condition that the footing is considered as a rigid body.

On the supposition that a pile is linear elastic when pushed in, pulled out and bended, each pile is modelized into a support spring which is of equivalent value at the pile head as is the case with the analytical model illustrated in Figure 4.1. In short, the stability calculation of pile foundations is replaced with the stability calculation of a rigid body (the footing) supported by many supporting springs which represent a pile group. The supporting springs consist of the spring constant in the direction of the pile axis, Kv, and the spring constant perpendicular to the pile axis, K1-K4, as defined below:

K1, K3: The perpendicular to the axis force (tf/m) and the bending moment (tf m/m) which should act upon the pile head, when the pile head is made to displace by a unit amount in the perpendicular to the pile axis direction without causing the pile head to rotate.

K2, K4: The perpendicular to the axis force (tf/rad) and the bending moment (tf m/rad) which should act upon the pile head, when the pile head is made to rotate by a unit amount without causing any shift to the pile head.

These spring constants of the pile are obtained as summarized in Table 4.1., based on the relationship between the load and displacement calculated using the theory of beams on the elastic foundation which employs the coefficient of horizontal ground reaction, kH. Thus, evaluation of the coefficient of horizontal

ground reaction is an important item in the stability calculation of pile foundations within the elastic limit. Estimation methods of the coefficient of horizontal ground reaction is examined below based on the data obtained from horizontal loading tests.

4.2. Coefficient of Horizontal Ground Reaction Obtained by A Reverse Operation

Coefficient of horizontal ground reaction obtained from horizontal loading tests is referred to as the reverse operation k value. This is calculated in the following manner:

Displacement at pile head, S, in loading tests is obtained by the formula of beam on the elastic foundation, as stated below:

$$S = \frac{P}{2EI\beta^3} \qquad (4.1)$$

where,

P: Load on the pile head (kgf)
S: Horizontal displacement on the pile head (cm)
EI: Bending rigidity of the pile body (kgf cm^2)
β: Characteristic value of the pile (cm^{-1})
$\beta = \sqrt[4]{kH\ D\ /\ 4EI}$
D: Pile diameter (cm)

In short, β is obtained by substituting P obtained from loading tests, where the standard displacement was So, for the formula(4.1). Then kH can be obtained using this β.

4.3. Coefficient of Horizontal Ground Reaction Obtained by Estimation

The estimation formula for the coefficient of the horizontal ground reaction of piles prescribed in the 1980 edition of the "Specifications" was as follows:

$$k = ko\ y^{-1/2} \qquad (4.2)$$
$$ko = \alpha\ Eo\ D^{-3/4} \qquad (4.3)$$

where,

k: Coefficient of horizontal ground reaction of the elastic foundation (kgf/cm^3)
ko: Coefficient of horizontal ground reaction (kgf/cm3) in the case where the displacement on the surface of the design ground is determined to be 1cm
Eo: Modulus of deformation of the ground obtained by the method shown in Table 4.2. (kgf/cm^2)
α: Coefficient shown in Table 4.2.which corresponds to the method to obtain Eo
D: Pile diameter (cm)
y: Displacement on the surface of the design ground that must be taken into consideration in design (cm)

As proved by the formulas (4.2) and (4.3), the coefficient of the horizontal ground reaction is expressed by a function which consists only of ground strength, displacement and pile diameter, in which the influence of the deformation mode in the vertical direction of piles is ignored. As a result, the k values were estimated to be comparatively small in the case of pile foundations using piles of large diameter for their lengths, and this was found to be in adequate when applied to actual cases. Furthermore, the k values did not conform with those of other foundations, such as rigid foundations. Thus, in order to settle these problems, an estimation method of the coefficient of horizontal ground reaction of elastic foundations is proposed as follows:

When the modulus of deformation of the ground is obtained from soil tests, etc., the coefficient of horizontal ground reaction is calculated in the following manner:

$$kH = kHo\ (B_H/30)^{-3/4} \qquad (4.4)$$

where,

kH: Coefficient of horizontal ground reaction (kgf/cm^3)
kHo: Coefficient of horizontal ground reaction (kgf/cm^3) which is equivalent to the value of plate bearing tests using a rigid circular plate with diameter of 30cm. In the case where it is estimated from the modulus of deformation obtained by various soil tests and investigations, the below stated formula is used.

$$kHo = 1/30\ \alpha\ Eo \qquad (4.5)$$

B_H: Equivalent loading width of the foundation (cm) which crosses at right angles with the load direction. With respect to the ground which is involved with the horizontal resistance of the elastic foundation, $1/\beta$ from the design surface of the ground is taken into consideration in general ($= \sqrt{D/\beta}$).
Eo: Modulus of deformation of the ground (kgf/cm^2) in the position taken into consideration in the design, which is measured or estimated by the method shown in Table 4.3.
α: Coefficient used for the estimation of modulus of ground reaction, which is shown in Table 4.3.
β: Characteristic value of the foundation (cm^{-1}).

Although the structure of the calculation formula of the coefficient of horizontal ground reaction of the elastic foundation proposed here is basically the same as the calculation formula of rigid foundations hither to in use, this proposed formula takes into consideration the influence of elastic deformation of the pile body. This is due to the fact that the larger the elastic deformation of the pile body becomes in comparison with the horizontal force acting on the upper part of foundation, the more the ground reaction that contributes to the horizontal resistance concentrates in the upper layer of the ground. Thus, based on both experimental and empirical judgment, the area of

the ground resistance that contributes to the horizontal resistance was determined to be D × $1/\beta$ (D: width of the foundation, $1/\beta$: length of the ground in the direction of depth which is in relation with the horizontal resistance); then the equivalent loading width of the foundation was determined to be $\sqrt{D/\beta}$. This idea can settle the contradiction concerning the calculation of the k values and problems due to difference in the type of foundations.

4.4. Comparison Between k Value Obtained From The Estimation Formula and Reverse Operation k Value Obtained From Loading Test

Estimation precision of formula(4.4) is examined based on the data obtained from loading tests of piles. Figure 4.1. summarizes a comparison between kH which was estimated using formula (4.3) following the 1980 edition of the "Specifications" and the reverse operation kH with standard displacement of 10mm. On the other hand, Figure 4.3. summarizes reverse operation kH obtained under the condition that the standard displacement was 1% of the pile diameter and kH obtained using formula (4.4). In addition, Figures4.4. and 4.5. show the logarithmic normal distribution of the ratio of the reverse operation kH to the estimated kH. Since more than 90% of data used is for piles with less than 1,000mm of pile diameter (about half the data are using piles with a diameter of less than 600mm), precision of the k value obtained using the proposed formula is not very improved in comparison with that obtained in accordance with the 1980 edition of the "Specifications." This is attributable to the fact that the proposed formula improved the adaptability to k values of rigid foundations and pile foundations with large diameter. It is important to recognize that an estimation formula of k values might result in some dispersion to this extent.

5. BEHAVIOR OF PILE FOUNDATIONS DURING LARGE-SCALE DEFORMATION

5.1. Influence of The Non-Linearity of The Ground Resistance

On the supposition that the characteristics of ground reaction are linear elastic when the deformation of pile foundations is small and within the elastic limit, as discussed in 4.1., the characteristics of ground resistance are modelized by using the coefficient of horizontal ground reaction, kH. This supposition is considered to be adequate for the design in the range where the displacement is small; however, the non-linearity of the ground reaction must be taken into consideration, since the errors become great during large-scale deformation.

With respect to the relationship between the ground reaction, p, and the displacement, y, at each depth of the ground, the p-y curve is used by DNV[8] as shown in Figure 5.1. It would be ideal to modelize accurately the characteristics of the ground reaction in order to express the behavior of foundations with high precision. However, when the precision of the ground surveys and simplification of calculations in the stage of design are taken into consideration, it is not necessarily appropriate to apply this idea to general bridges. Thus, in this paper, the characteristics of ground reaction are modelized as a bi-linear model, and the effectiveness of this analysis method was examined based on the data obtained from horizontal loading tests.

As for the data used for analyses, data of piles, the pile was deformed more than 30% of the pile, were selected from the data of loading tests collected in Chapter 2. As for the constant of ground resistance, the coefficient of horizontal ground reaction, kHs, and the maximum ground reaction, pus, obtained by the below-stated formulas are used as parameters, and a combination was selected so that errors of the load-displacement curve and the distribution of bending moment of piles can be minimized.

$$kHs = \alpha_k \times (\text{kH prescribed in the "Specifications"}) \quad (5.1)$$

$$pus = \alpha_p \times (\text{Passive earth pressure strength of Coulomb}) \quad (5.2)$$

The analyses covered the test results in which the horizontal displacement at the ground surface was up to 10% of the pile diameter. Variation was given to the parameters stated above in order to obtain the difference from the analytical results. As an example, figure 5.3. shows a contour map of errors that arise in a test on a steel pipe pile with diameter of 61cm and length of 21m which was placed in the sand ground. In this case, the errors are recognized to be the minimum, the supremum value of the ground reaction being 3.5-fold of the passive earth pressure strength and the coefficient of ground reaction being 1.5-fold of the value obtained in accordance with the "Specifications." As discussed in Chapter 4., the coefficient of horizontal ground reaction, kH, prescribed in the "Specifications" is determined under the condition that the displacement of the pile head is 1% of the pile diameter. On the contrary, the coefficient of horizontal ground reaction used for the elasto-plastic analyses expresses the characteristics on a smaller level of displacement. Thus, the value of α_k exceeds 1. On the other hand, with respect to α_p, the area of ground resistance spreads three-dimensionally; thus, it is presumed that the plastic area became around three times longer than the width of the pile. Figure 5.4. illustrates the load-displacement curve of this situation, while Figure 5.5 shows the distribution of bending moment of piles. These two figures accord with

each other quite favorably; therefore, it was proved that the behavior of piles can be expressed by determining an adequate constant, even when a simplified model is used.

The above result was commonly recognized in the case of other test piles; however, the values of parameters of the ground resistance, α_k and α_p, varied depending on each test, as shown in Table 5.1. Despite the fact that the effectiveness of this analytical method was proved, further studies are needed for better evaluation methods to obtain constants used for the design, and more analytical data are needed for that.

5.2. Influence of The Pile Group

A pile foundation used as a bridge foundation rarely consists of a single pile. In general, many piles are put together by footing to form a pile foundation. When the piles deform greatly due to the horizontal force acting on this footing, each pile interferes with another through the aid of the ground. Therefore, the ground reaction of each pile differs depending of the location of each pile. Nevertheless, the degree of such interference has not been clarified yet since it differs a great deal depending on the kind of piles, pile intervals and the soil condition. The "Specifications" prescribe that the minimum central interval of the piles should be in principle longer than 2.5 times the pile diameter. In this case, the same value of coefficient of horizontal ground reaction for a single pile is used for all the piles which form a pile group. Recently, many institutions have conducted experiments on these problems in order to grasp the mechanisms of the horizontal resistance of piles. In this paper, the influence of a pile group was examined based on horizontal loading tests using steel pipe piles conducted by the Public Works Research Institute and Metropolitan Expressway Public Corporation.

The Public Works Research Institute[9] conducted loading tests of the pile group in a test pit. Piles used for these tests were a single pile, series piles, parallel piles, and a 9 piles group aligned in a square 3*3 (of the model steel pipe piles is 101.6mm) as shown in Figure 5.6. (also see Figure 5.7.). On the other hand, Metropolitan Expressway Public Corporation conducted horizontal loading tests, establishing a 9 piles group in situ using steel pipe piles of natural size (with of 318.5mm) as shown in Figure 5.8.

Figure 5.9. shows the curve of average loading (average load per pile) and footing displacement obtained from the tests conducted by the Public Works Research Institute. The figure shows that the load-displacement curve is located lower than the curve of a single pile when the displacement is great. This is attributable to the influence of the mutual interference of piles. The degree of influence is the greatest for the 9 piles group. It decreases respectively in the order of series piles and parallel piles, then approaches that of the single pile. This is due to the fact that the share of horizontal reaction against the horizontal force of a pile groups different depending on the location of piles within the same footing.

Figure 5.10. shows the share ratio of horizontal reaction carried by the front and rear piles to that carried by the central pile in the case of the 9 piles group. Both of the tests proved that the front piles carry the largest load, and that the load share becomes smaller respectively in the order of the central pile and the rear piles. This trend becomes more apparent as the load becomes larger.

A simulation concerning the difference of the reaction share of each pile in a pile group and the behavior during large-scale deformation was attempted for the purpose of establishing a new design method. In the simulation, the non-linearity of the p-y characteristics of the ground, which becomes an important subject in the case of large-scale deformation, was dealt with bi-linearly as examined in 5.1. In addition, in order to consider the difference of load share of each pile, characteristics of the ground resistance, (pus and kHs), in which α_p and α_k of different values were used as parameters, were established on a trial basis for each position of piles. Then the values of α_p and α_k were selected so that the experimental values and analytical values coincide with each other most favorably in terms of the following four items:

1) load-displacement curve
2) distribution of displacement
3) distribution of bending moment
4) distribution of ground reaction.

The displacement level to be covered by the simulation was until the pile body begins to yield. In this paper, the simulation is carried out until the displacement becomes around 50% of the pile diameter.

Figure 5.11. shows a selection of α_p and α_k which are in conformity with the experimental values concerning the load-displacement curve of the footing part of the 9 piles group. It is proved that a simulation can be conducted with quite high precision if appropriate values can be set up. Figures 5.12. and 5.13. show respectively the distribution of bending moment and the ground reaction in the case of a combination of α_p and α_k that brought about the best conformity in the case of the 9 piles group in Figure 5.11. These values also prove that the experimental values and calculated values are in favorable conformity with each other. In addition, the same level of conformity was obtained for the distribution of pile displacement.

Values of α_p and α_k were also selected by simulation for other cases in order to get such conformity, the result of which is shown in Table

5.2. In the case of series piles, the front piles showed a value of α_p that was on the same level as the case with a single pile, and the values of rear piles decreased gradually. In comparison with the single pile, the values of α_p and α_k of parallel piles decreased as the number of piles in the parallel direction increased. In the case of the vertical and batter pile group using 9 piles, which is a combination of series and parallel piles, the values of α_p and α_k showed a decrease more than with the cases where series piles and parallel piles were used separately. These phenomena are perhaps attributable to the decrease of the coefficient of ground reaction due to the increase of equivalent load width and the decrease of passive resistance due to the mutual overlapping of the area of resistance of each pile.

5.3. Influence of The Non-Linearity of Flexural Rigidity of The Pile Body

Since the piles used for the loading tests which were dealt with by the analyses in 5.1. and 5.2. were commonly steel pipe piles, and since the range of displacement covered by the analyses was until the pile body begins to yield, the pile body itself is treated as an elastic body. On the contrary, with respect to the range exceeding the yield point, the influence of non-linearity of the flexural rigidity of the pile body becomes remarkable in the cases of both cast-in-place piles and steel pipe piles.

In general, the relationship between the bending moment, M, and the curvature, ϕ, when the bending moment acts upon a concrete pile is recognized at the begining of cracks of concrete (C), at the begining of the yield of tensile reinforcement (Y) and at the ultimate phase of section (U). This influence was determined to be taken into consideration in analysis of loading tests, and is modelized by a tri-linear curve which goes through the points obtained for the circular reinforcing concrete section which receives the axial force, N, and the bending moment, M (Figure 5.14.).

For an example, a case analysis[10] concerning loading tests of cast-in-place piles is introduced.

Figure 5.15 shows the load-displacement curves measured during the loading test and obtained by analysis. At the analysis, the characteristics of ground reaction are modelized as a bi-linear model. At small displacement, the calculated values in which the pile body itself is treated as an elastic body, is coincident with experimental values. However, at large displacement these values are different. On the other hand, the calculated values in which the non-linearity of the flexural rigidity of pile body is taken into consideration, is coincident with experimental values at large displacement.

As so far discussed, it was verified that the behavior of pile foundations during large-scale deformation could be simulated if the influence of ground resistance, the non-linearity of the rigidity of the pile body and the effects of a pile group are taken into consideration. With respect to the analytical model used for design calculations of general pile foundations, further studies will be conducted along with the displacement level that must be taken into consideration in the design.

6. CONCLUSION

An attempt was made to introduce the limit states design method to the design of pile foundations. In order to grasp the behavior of piles and to establish an analytical model, analyses were conducted on horizontal loading tests. The results of this study can be summarized as follows:

1) Based on the idea that the elastic limit of pile foundation is the limit where the reversibility is guaranteed, the point where the residual displacement does not make a sudden increase is determined to be the elastic limit in the design. This elastic limit is roughly in conformity with the yield point on the load-displacement curve.
2) The coefficient of fluctuation of the elastic limit described above exceeds 100%, and scatters a great deal. The elastic limit is 3.5% of the pile diameter in the case of the entire average of all piles, 4% in the case of steel pipe piles, and 1% in the case of cast-in-place piles (all these figures are based on the logarithmic normal distribution). In the case of cast-in-place piles, there is a possibility that the occurrence of cracks to the pile body might give influence to the determination of the yield point.
3) A calculation formula of the coefficient of horizontal ground reaction used for stability calculations within the elastic limit was proposed. Giving consideration to the influence of the deformation mode in the direction of the depth of piles, the equivalent load width of the foundation was proposed to be $\sqrt{D/\beta}$. The coefficient of horizontal ground reaction prescribed in the 1980 edition of the "Specifications" was under the condition that the standard displacement was 10mm; however, the coefficient of horizontal ground reaction in this paper was determined to be calculated when it was 1% of the pile diameter following the idea described in 2). It was confirmed that the estimation precision of the coefficient of horizontal ground reaction obtained by these methods was on the same level as the 1980 edition of the "Specifications."
4) It was confirmed that the behavior of pile foundations during large-scale deformation

could be simulated, if the non-linearity of ground resistance, influence of the pile group, and the non-linearity of the flexural rigidity of the pile body are taken into consideration.

While this study was conducted, data of horizontal loading tests of piles were offered by many institutions. A part of this study has been conducted as joint research with the Japanese Association for Steel Pipe Piles. The authors would like to express their gratitude to many researchers who cooperated with this study.

REFERENCES

1) The American Association of State Highway and Transportation Officials: Standard Specifications for Highway Bridges, 1983.
2) Ministry of Transportation and Communications, Ontario: Ontario Highway Bridge Design Code and Commentary, 1983.
3) Canadian Geotechnical Society: Canadian Foundation Engineering Manual (2nd Edition), 1985.
4) Japan Road Association: Specifications for Highway Bridges, Part IV, Specifications for Substructures, 1990. (in Japanese)
5) Technology Research Center for National Land Development: Study on the Limit States Design Method for Highway Bridge Foundation Structures (Part 3). March, 1991. (in Japanese)
6) Okahara, Takagi, Nakatani, Taguchi and Sakamoto, Study on the Characteristics of Horizontal Resistance of Piles Based on Loading Test Data: Technical Memorandum of P.W.R.I., No.2721.January, 1989. (in Japanese)
7) Ogasawara, Hanko, Gose and Kawaguchi: Study on the Yield Strength of Pile Foundations. Journal of Structural Engineering, Vol. 37A. March, 1991. (in Japanese)
8) Det Norske Varitas : Rule for the Design, Construction and Inspection of Offshore Structure, 1977.
9) Okahara, Kimura, Asama, Koyama : Behavior of Laterally Loaded Pile Under Large Deflection, 8th U.S.-Japan Bridge Engineering Workshop, 1922.
10) Kimura, Nakatani, Hamada, Ito: Horizontal Loading Test for Cast-in-place pile in the Field, Proc. of The 46th Annual Conf. of The Japan Society of Civil Engineers, 1992.
11) Okahara, Takagi, Nakatani and Kimura: Study on the Bearing Capacity of A Single Pile and the Design Method of Cylindrical foundations. Technical Memorandum of P.W.R.I., No. 2919. January, 1991. (in Japanese)

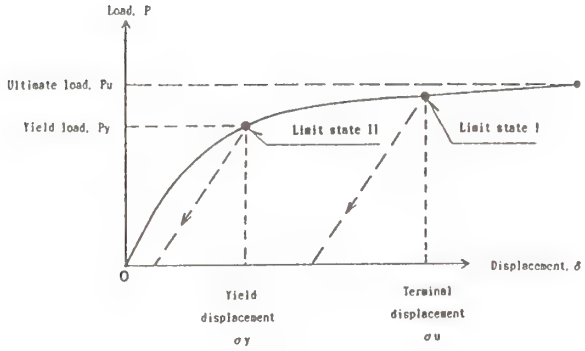

Figure 1.1. Limit states for stability calculations of foundations

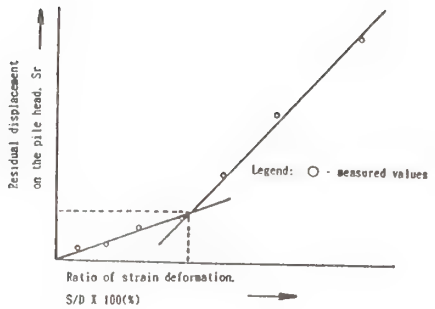

Figure 3.2. A case in which the point where the residual displacement of the ground increases suddenly is defined as the elastic limit

Table 2.1 Data obtained from horizontal loading tests

Type of Pile	Number of date
Steel pipe pile	120
Cast in pile	29
PC pile	31
PHC pile	24
Total	204

(note) Steel pipe piles, PC piles and PHC piles are placed by the driven-pile method.

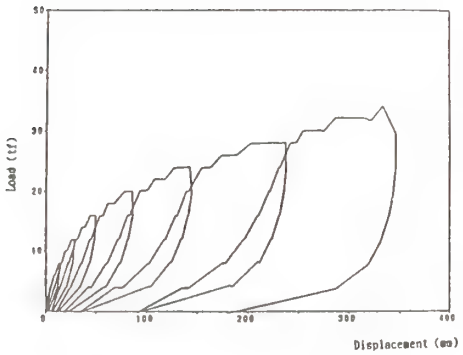

Figure 3.1. Load - head displacement (horizontal loading tests)

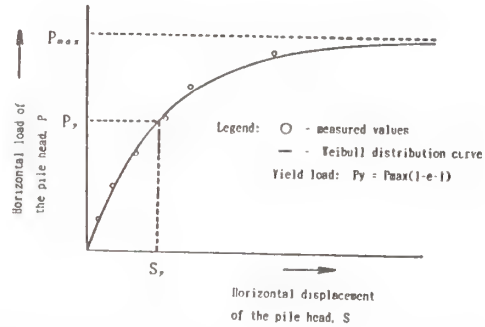

Figure 3.3. A case in which the yield load on the Weibull curve is defined as the elastic limit

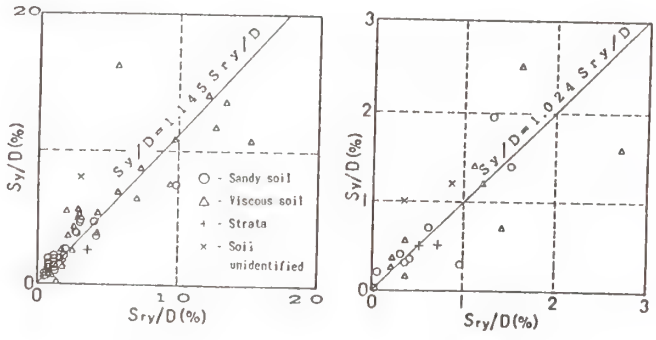

Sy: Yield displacement defined by the Weibull distribution curve, δs(mm)
Sry: Yield displacement obtained from the point where the residual displacement increases suddenly (mm)
D: Pile diameter (mm)

Figure 3.4. Comparison of yield strain deformation obtained from formula of the Weibull distribution curve and the point where the residual displacement increases suddenly

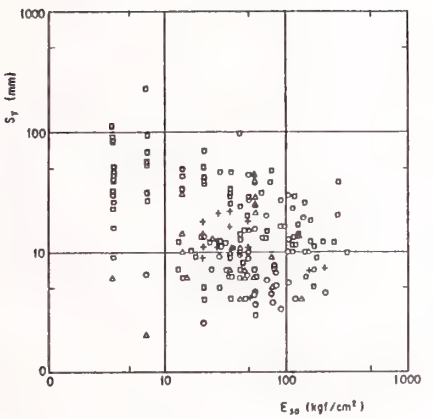

Figure 3.5. Correlation between Sy and E5o

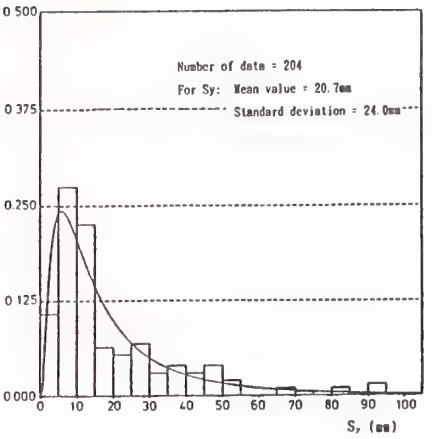

Figure 3.7. Probability density distribution of Sy

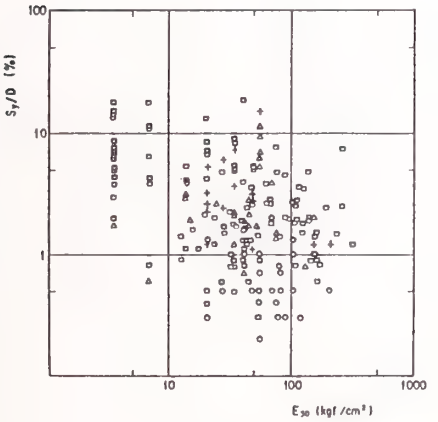

Figure 3.6. Correlation between Sy/D and E5o

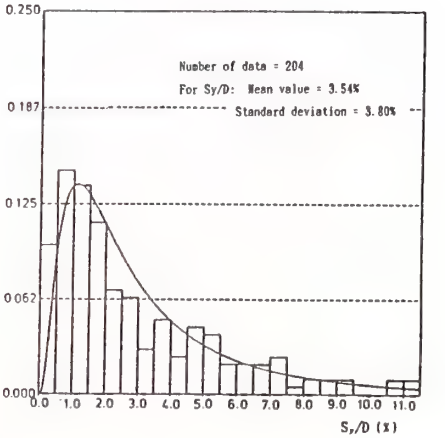

Figure 3.8. Probability density distribution of Sy/D

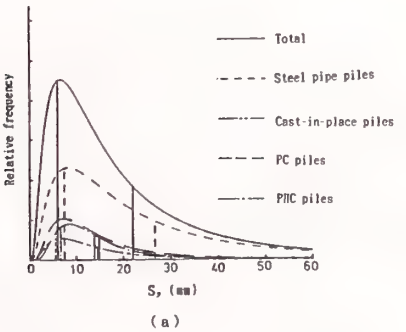

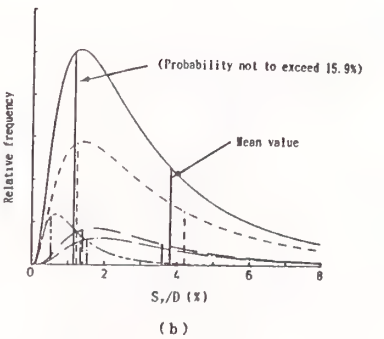

Figure 3.9. Probability density distribution of Sy and Sy/D, expressed by logarithmic normal distribution

Table 3.1 Statistical value of S_y

		Steel pipe pile	Cast in place pile	PC pile	PHC pile	Total
Number of sample		120	29	31	24	204
Extent	(cm)	2.4～224.8	2.5～40.5	1.8～45.3	4.0～44.6	1.8～224.8
Mean value	(cm)	28.1	10.5	14.8	13.8	20.7
Standard deviation	(cm)	28.9	10.1	11.5	8.5	24.0
Coefficient of variation (%)		111	96	78	62	116
S_y (cm)	Non-exceed probability 5 (%)	4.0	2.0	3.8	4.6	3.0
	10 (%)	5.6	3.7	4.9	5.6	4.2
	15.9 (%)	7.2	3.4	5.9	6.6	5.4
	30.0 (%)	11.0	5.8	8.2	8.7	8.4

Table 3.2 Statistical value of S_y /D

		Steel pipe pile	Cast in place pile	PC pile	PHC pile	Total
Number of sample		120	29	31	24	204
Extent	(%)	0.3～22.4	0.2～4.0	0.7～45.3	1.1～14.9	0.2～22.4
Mean value (cm)	(%)	4.1	1.0	14.8	3.8	3.5
Standard deviation	(%)	4.3	0.9	11.5	2.9	3.8
Coefficient of variation(%)		105	90	78	76	109
S_y / D (%)	Non-exceed probability 5 (%)	0.7	0.2	3.8	1.0	0.6
	10 (%)	0.9	0.2	4.9	1.3	0.8
	15.9 (%)	1.2	0.3	5.9	1.5	1.0
	30.0 (%)	1.8	0.5	8.2	2.1	1.5

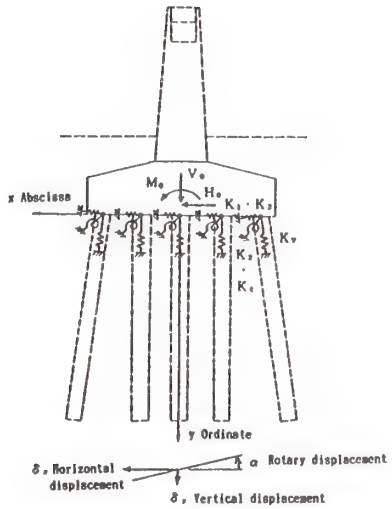

Figure 4.1. Analytical model in the stability calculation of pile foundations

Table 4.1. Spring constant in the vertical direction to the axis of piles ($\beta l \geq 3$)

	Rigidly connected pile heads		Hinge-connected pile heads	
	h = 0	h = 0	h ≒ 0	h = 0
K_1	$\frac{12EI\beta^3}{(1+\beta h)^2+2}$	$4EI\beta^3$	$\frac{3EI\beta^3}{(1+\beta h)^2+0.5}$	$2EI\beta^3$
K_2, K_3	$K_1 \cdot \frac{\lambda}{2}$	$2EI\beta^2$	0	0
K_4	$\frac{4EI\beta}{1+\beta h}\frac{(1+\beta h)^3+0.5}{(1+\beta h)^2+2}$	$2EI\beta$	0	0

where

β : Characteristic value of piles $\quad \beta = \sqrt[4]{\frac{kD}{4EI}}\ (m^{-1})$

λ : $h + \frac{1}{\beta}$ (m)

k : Coefficient of horizontal ground reaction (tf/m2)

D : Pile diameter (m)

EI : Flexural rigidity of piles (tf/m2)

h : Length in the axial direction above the design ground of piles (m)

Table 4.2 Relationships between E_0 and α_p of elastic foundation

	α
Coefficient of variation of the ground E_0 (kgf/cm²)	α
Coefficient of variation of the ground measured inside boring pores	0.8
Coefficient of variation of gained by unconfined or triaxial compression test	0.8
Coefficient of variation of estimated from E_0=28N of N value of standard penetration test	0.2

Table 4.3. E_0 and α

Modulus of deformation E_0 (kg/cm²)	α	
	Ordinary state	During earth-quake
Modulus of deformation obtained from the repetition curve of 30cm diameter plate loading test	1	2
Modulus of deformation measured in a bored hole	4	8
Modulus of deformation obtained from the unconfined compression test or triaxial compression test of specimens	4	8
Modulus of deformation estimated by E_0 = 28N from N value of standard penetration test	1	2

(note) In case of a windstorm, the values of ordinary occasions should be used.

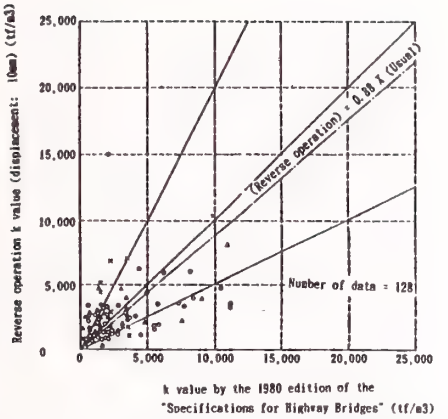

Figure 4.2. Reverse operation k value(displacement:10mm) and estimated k value in the 1980 edition of the "Specifications"

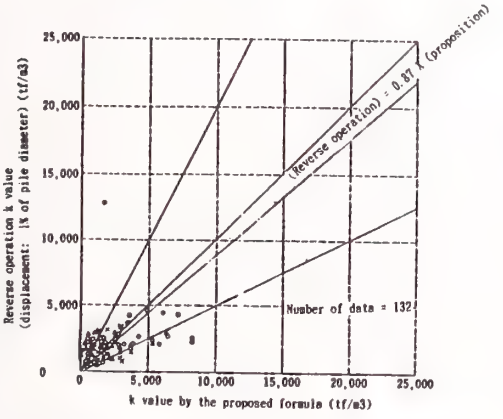

Figure 4.3. Reverse operation k value (displacement: 1% of pile diameter) and estimated k value by the proposed formula

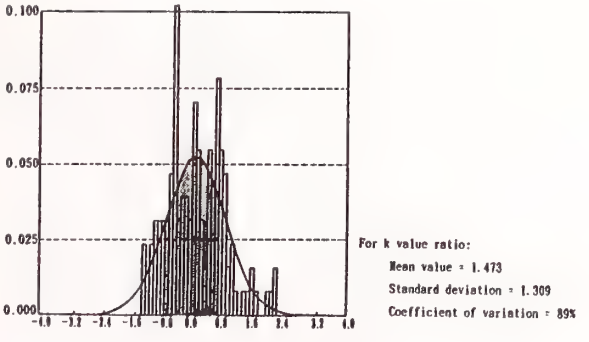

Figure 4.4. Distribution of Log (k value ratio : reverse operation k value (displacement:10mm)) / k value in the 1980 edition of "Specifications"

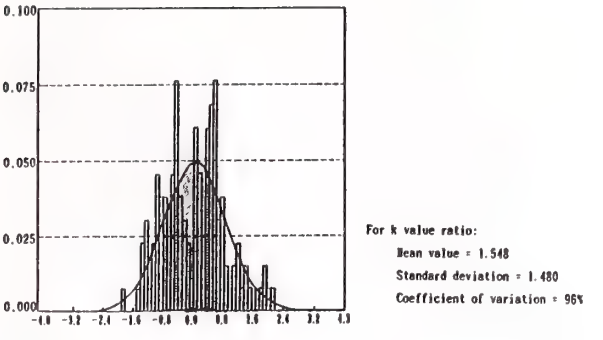

Figure 4.5. Distribution of Log (k value ratio : reverse operation k value (displacement:1% of pile diameter) / k value in proposed formula)

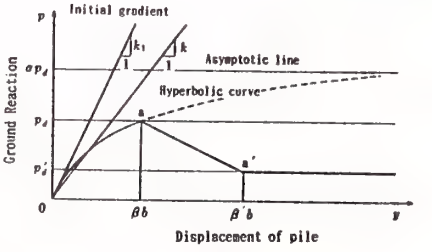

Figure 5.1. Ground resistance characteristics in DNV

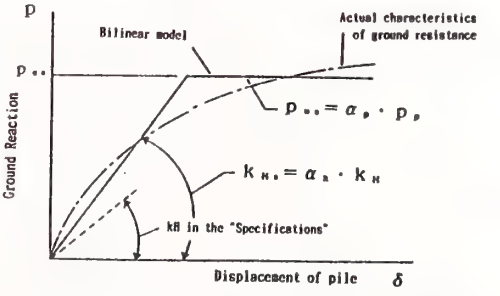

Figure 5.2. Bilinear-type ground resistance characteristics

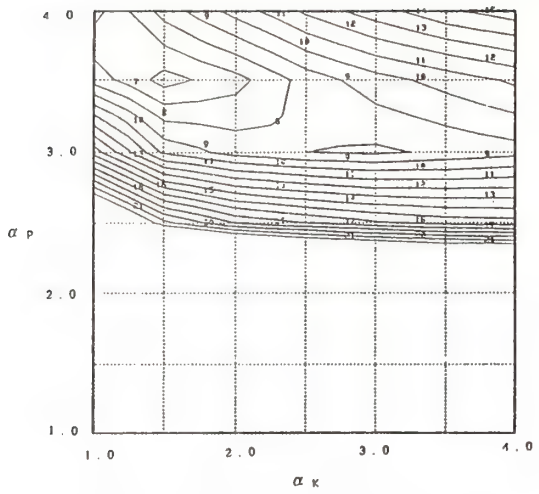

Figure 5.3. Contour map of errors (S3)

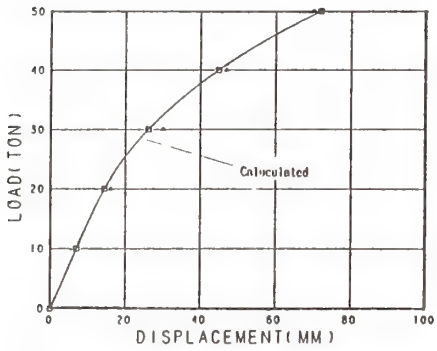

Figure 5.4. Loud-displacement Curve (S3)

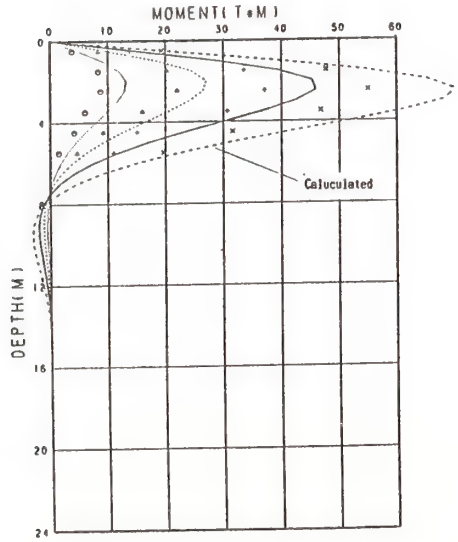

Figure 5.5. Distribution of bending moment of pile (S3)

Table 5.1. Most adequate parameters

Test	Pile		αp	αk	Ground
	D x t(mm)	L(m)			
S 1	φ 191x 5.3	4.5	2.0	1.5	Sand
S 2	φ 319x 6.9	15.0	6.0	6.0	Sand
S 3	φ 610x 9.5	21.0	3.5	1.5	Sand
S 4	φ 610x12.7	36.0	4.0	1.5	Sand
S 5	φ 813x15.0	17.0	4.5	1.5	Sand
C 1	φ 191x 5.3	5.0	0.5	1.0	Soft Clay
C 2	φ 813x14.0	30.7	2.5	1.5	Stiff Clay
C 3	φ1000x27.2	20.0	1.0	2.5	Stiff Clay
C 4	φ1500x13.0	33.1	1.0	1.5	Soft Clay
C 5	φ2000x22.0	51.5	2.0	6.0	Soft Clay

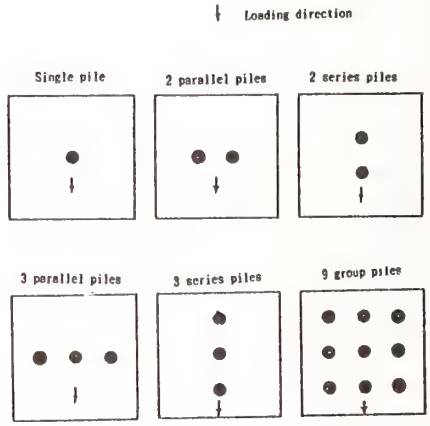

Figure 5.6.

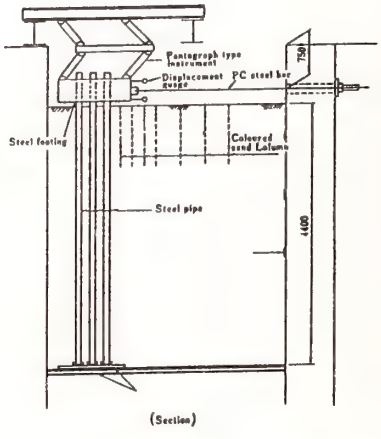

Figure 5.7. Test method for group piles (PWRI)

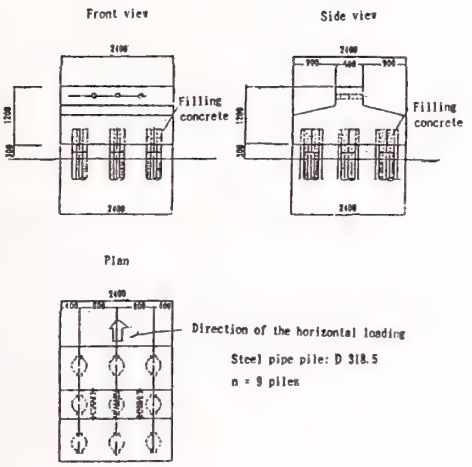

Figure 5.8. Horizontal loading tests of piles (MEPC)

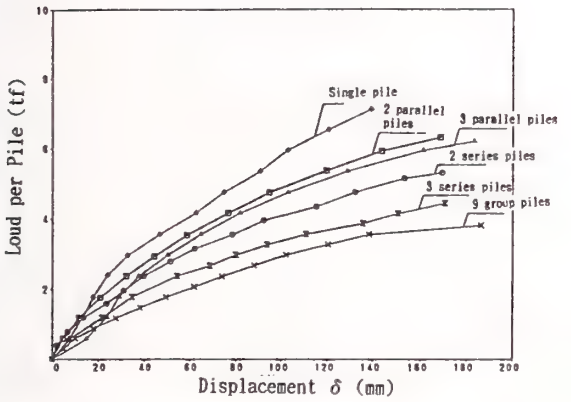

Figure 5.9. Load-displacement curve

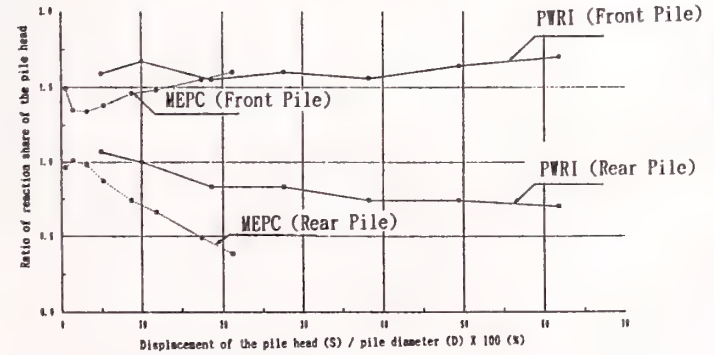

Figure 5.10. Ratio of load share to the central pile (9 piles used)

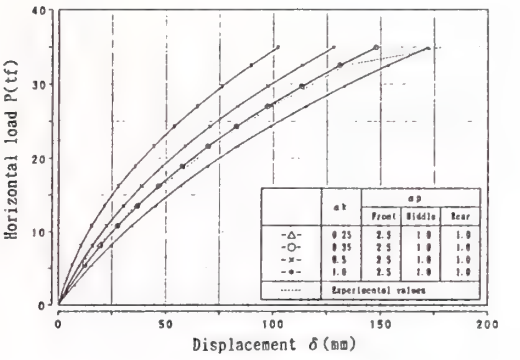

Figure 5.11. Load-displacement curve of the 9 piles

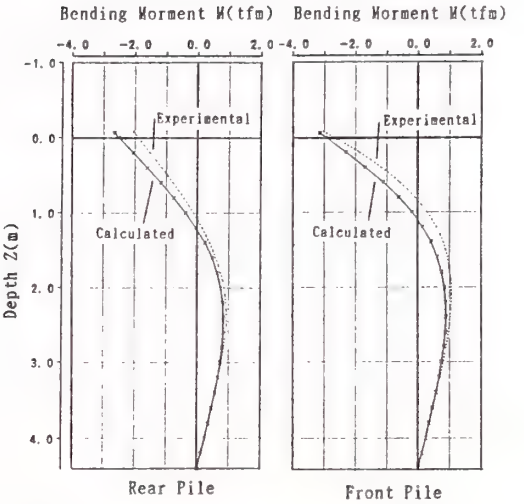

Figure 5.12. Distribution of bending moment of the 9 piles

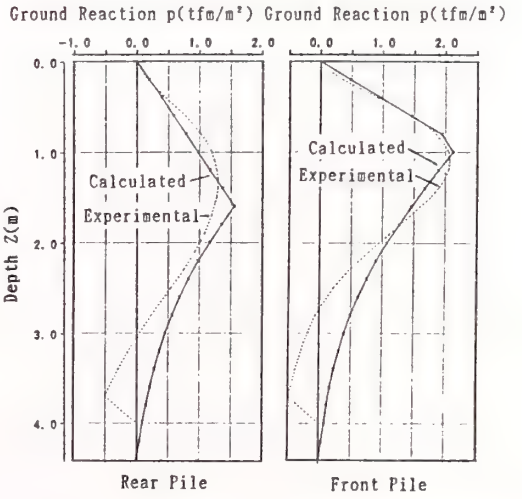

Figure 5.13. Distribution of ground reaction of the 9 piles

Table 5.2. Comparison between experimental values and analytical values

CASE	α_u	α_p		
		Front piles	Middle piles	Rear piles
Single pile	1.5	(3.0) 3.0	-	-
2 series piles	1.5	(3.0) 3.0	(0.8) 1.0	-
3 series piles	1.0	(3.0) 3.0	(1.3) 1.0	(0.8) 0.5
2 parallel piles	1.0	(2.5) 2.5	-	-
3 parallel piles	0.75	(Center 2.8) (Side 3.2) 2.5	-	-
9 group piles	0.35	(Center 2.5) (Side 2.4) 2.5	(Center 1.6) (Side 1.3) 1.0	(center 1.3) (Side 1.2) 1.0

Figures in parenthesis are experimental values

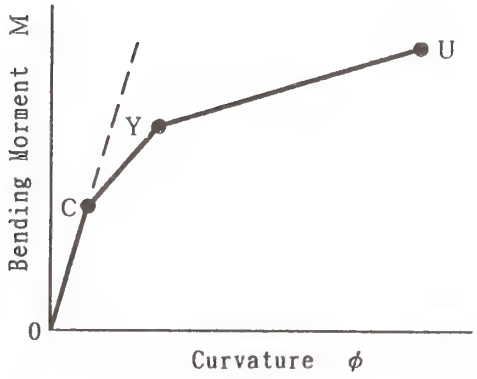

Figure 5.14. M-ϕ of Cast-in-place Pile

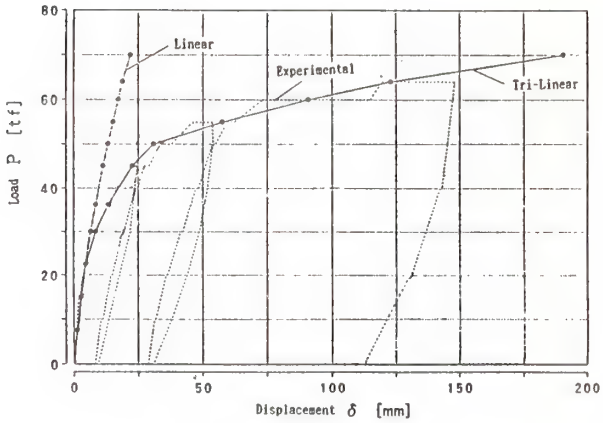

Figure 5.15. Load-displacement curve of Cast-in-place Pile

Seismic Effects on Port and Harbour Structures

by

Hajime Tsuchida[1] and Setsuo Noda[2]

ABSTRACT

In Japan, many port facilities were damaged by the earthquakes. Efforts has been being continued for designing and constructing facilities of larger seismic resistance with less construction cost. Design standards for the earthquake resistant design were proposed and used widely. After earthquakes of large scale, performance of port facilities in a zone of sever shaking were investigated in details. Results of those investigations were reflected to revision of the design standards.

This report presents Japanese experience on earthquake damages, current practice in seismic design and countermeasures against earthquake disaster in connection with port facilities.

KEYWORDS: Earthquake damage, earthquake resistance design, liquefaction of soil, Port and Harbour structures,.

1. DAMAGE EXPERIENCE

1.1 Earthquakes which caused seismic damage

Many of the port facilities in Japan were damaged by earthquakes. The Kanto earthquake in 1923 is well known as one of the earthquakes which caused serious damage to many kinds of structures. Port facilities in Yokohama and Yokosuka were damaged by that earthquake, too. However, none of seismographs recorded peak value of the ground motions in the areas where damage to port facilities took place.

In 1960's, a number of deployed accelerographs increased considerably and since then, more reliable information on ground motions became available. Major earthquakes which caused damage to port facilities since that period are given in Table 1.

The peak acceleration shown in the table were all recorded in port area except Niigata. However, the instrument which recorded the Niigata earthquake was located not much distant from the Niigata Port. In the 1973 Nemuro-Hanto-oki earthquake, the most serious damage took place in Hanasaki Port. Unfortunately, no accelerograph was installed at the port. Although the peak ground acceleration in Kushiro Port is given in the Table 1, the damage in Kushiro Port by this earthquake was not serious.

In the 1987 Chiba-ken-Toho-oki earthquake, there was no damage to port facilities; but liquefaction was observed at many locations in artificially filled land.

Field reconnaissances in detail on seismic performance of port facilities (damaged and undamaged) were carried out after the major earthquakes and reported (Bureau for Ports and Harbours, Ministry of Transport, et al., 1964, 1965, 1968, and 1973; Tsuchida, et al., 1979; Tsuchida, et al., 1985; Iai, et al., 1988).

1.2 Damage examples

1) Liquefaction of ground

During the Niigata earthquake in 1964, seismic damage to large variety of structures took place due to liquefaction of sandy grounds. By this earthquake people started to recognize the importance of liquefaction and very intensive research activities were undertaken by many researchers. Liquefactions were observed in almost all major earthquakes which hit coastal areas in Japan.

2) Gravity Type Quaywall

By the 1983 Nippon-kai-Chubu earthquake, a quaywall using concrete caissons in Akita Port was seriously damaged. Fig. 1 shows the typical cross section and displacements of the quaywall (broken line : after earthquake, solid line : original). The damage was sliding of the caissons towards the sea side more than 1 meter and settlement of backfill was about 1.5 meter in maximum. It was evident that liquefaction had taken place behind the quaywall.

---

1)President, Coastal Development Institute of Technology, 3-16, Hayabusa-cho, Chiyoda-ku, Tokyo, 102 Japan

2) Director, Structural Engineering Division, port and Harbour Research Institute, Ministry of Transport, 3-1-1, Nagase, Yokosuka, 239 Japan

3) Sheet pile bulkhead

Fig. 2 also shows a cross section of the steel sheet pile bulkhead (Ohama No. 2 Wharf) in Akita Port. The sheet piles were broken due to large pressure caused by the liquefied backfill. Adjacent to this bulkhead, there located another sheet pile bulkhead (Ohama No. 1 Wharf) of very similar construction. There was no liquefaction at this site and the structure survived without any damage.

4) Trestle type pier

Since 1960's many trestle type piers with steel pipe piles were constructed. Some of them were subjected to strong ground motions. However, none of them was damaged by the earthquakes. Fig. 3 is a cross section of the trestle type pier in Muroran Port. This pier experienced ground motions of peak acceleration 209 Gal, during the 1968 Tokachi-oki earthquake. The structure was designed for the seismic coefficient 0.10.

5) Cellular bulkhead

The cellular bulkhead in Muroran Port was subjected to the ground motions of 209 Gal, but no damage was seen. Fig. 4 is showing a cross section of the bulkhead.

6) Breakwater

No damage due to the earthquakes listed in Table 1 was seen on the breakwaters. During the Kanto earthquake in 1923, a breakwater in Yokosuka Port settled more than 5 meters. Fig. 5 is a cross section of the breakwater.

7) Warehouse

Many warehouses were damaged by earthquakes in past. The warehouse in Gaiko District of Akita Port was seriously damaged by the 1983 Nippon-kai-Chubu earthquake. The floor slab settled significantly and the foundation piles were broken.

2. OBSERVATION OF STRONG-MOTION EARTHQUAKES

The authors and their colleagues have observed the strong-motion accelerations during earthquakes for 29 years in Japan. As of December 1990, 4802 strong motion earthquake records have been obtained by the observation network of 81 strong-motion accelerographs deployed throughout Japanese port areas (Kurata and Iai, 1991). Fig. 7 shows one of records recovered from this network during the major earthquake. The records were the ground accelerations at Hachinohe Port during the 1968 Tokachi-oki earthquake which caused serious damage to many kinds of engineered structures.

To study seismic wave propagations and strains of ground due to seismic waves, the observation of ground motions at individual points have been found to be insufficient. An array observations have been considered essential. Many research groups started observation of this type. PHRI deployed seismometers three dimensionally in the field of the Tokyo International Airport (Haneda). Fig. 8 is showing the deployment of seismometers of the PHRI array in Haneda.

3. CURRENT PRACTICE IN EARTHQUAKE RESISTANT DESIGN

3.1 Procedure

Structures in ports and harbours in Japan are designed in accordance with the Technical Standard of Port and Harbour Facilities and its Commentary (Japan Port and Harbour Association, 1989). Chronologically, the procedure for earthquake resistant design was compiled as early as in 1950, revised, supplemented or legislated in 1959, 1967, 1971 1975 and 1979. The most recent revision in 1989 aims at assuring, in practice, the greater safety against liquefaction; i.e. the lesson learned from the case history in 1983 Nippon-kai-Chubu Earthquake of magnitude 7.7.

According to the Technical Standard, the steps to be taken for earthquake resistant design are as follows:

(a) take into account the effects of seismic inertia force upon the safety and stability of structures or the effects of seismic displacement upon lifeline facilities and

(b) assess the liquefaction potential of soil due to earthquakes and, if necessary, take measures against liquefaction.

Current procedures taken for these steps will be briefly reviewed in the following sections.

3.2 Stability against seismic inertia force

Seismic inertia force considerably affects the seismic stability of port facilities such as quaywalls, piers and breakwaters. Those effects are, in the routine design practice, treated by a method well known as seismic coefficient method; the seismic inertia force is idealized into a static horizontal load of which magnitude is specified by the seismic coefficient.

The seismic coefficient is determined by taking

1) regional seismicity,
2) condition of foundation soil and
3) importance of structures

into consideration. The regional seismicity in Japan is studied by Kawasumi (1951) with case history data of 343 earthquakes since the year of 599 A.D.. The results obtained by Kawasumi are critically reviewed and idealized, for use in design procedure, into

seismic zoning with three regions, of which regional seismic coefficients are specified as 0.15, 0.10 and 0.05.

Because the results given by Kawasumi are of the alluvial ground, a factor should be multiplied to the regional seismic coefficients for taking variety in soil conditions into account. The factors are given for three kinds of subsoil conditions, specified as 0.8, 1.0 and 1.2.

In addition to the subsoil condition, importance of structures should be considered for determining seismic coefficient. The factors to be multiplied to the seismic coefficients are given for four levels of importance, specified as 1.5, 1.2, 1.0 and 0.5.

Seismic inertia force thus specified will, when loaded, produce increase in the stresses acting in material of structures. Such stresses will be compared with the allowable limits, which are specified as 1.5 times high as those specified for the static stability analysis.

Thus, basically all kinds of structures are designed by seismic coefficient method for the routine practice. Among the various port structures, piers with piles (i.e. trestle type piers) show characteristic dynamic response during earthquakes. For the piers of this type, the validity of the design will be checked by the analysis in which dynamic response of the pier has been taken into consideration (Yamamoto et al, 1970).

4. VALIDATION WITH CASE HISTORY AND STRONG MOTION DATA

4.1 Effect of vertical component on stability

Every fives years or so often the structures designed by the simple procedure presented in the previous section have been exposed to great earthquakes in Japan. With the strong-motion observation network deployed by the Port and Harbour Research Institute since 1963, validity of the simple procedure has been critically evaluated by the research groups of the same research institute.

During the earthquake, structures receive vertical seismic inertia force as well as horizontal one. It is the practice in design, however, that the seismic inertia force is represented by nothing but a horizontal load. Uwabe et al.(1976), using vertical components of 574 strong-motion accelerograms, concluded that ratios of vertical vs. horizontal components in the peak values are less than 1/2 as shown in Fig. 8 and the vertical component has indeed little effect on the stability of gravity type quaywalls.

4.2 Relation between max. acceleration and seismic coefficient

During the earthquake, the peak value of the seismic inertia force is applied instantaneously. The seismic load considered in the design procedure is, however, a continuously applied load. If duration of intense seismic loading is limited to a very short period, nothing but a insignificant deformation will be induced. Besides, if slight deformation is allowed for dense saturated sand (i.e. non-liquefiable sand), dilatant behavior under undrained condition will instantaneously increase the strength of soil. Thus, the instantaneously applied peak value of the seismic inertia force can be higher than the seismic load to be considered in the seismic coefficient method. Noda and Uwabe (1975), using case history data of 129 gravity type quaywalls during 12 earthquakes, studied the relation between the maximum ground acceleration recorded by SMAC-B2 type accelerograph and the seismic coefficient for gravity type quaywall. The results are obtained as shown in Fig. 9 with the relation to be used for the conversion from maximum acceleration to seismic coefficient as follows.

$$k_h = \alpha/g \qquad (\alpha \leq 0.2g) \qquad (1)$$
$$k_h = 1/3(\alpha/g)^{1/3} \qquad (\alpha > 0.2g)$$

in which

k_h: seismic coefficient
α : maximum acceleration (Gal)
g : acceleration of gravity (Gal)

Kitajima and Uwabe (1979) conducted similar study for anchored steel sheet pile quaywalls and, using 110 case history data, concluded that the relation for the gravity type quaywall is also applicable for the steel sheet pile quaywalls.

As shown in Fig. 10, the relation in Eq.(1) contains conservative errors. If an average relation is sought for representing the general correlation between these quantities, it will be given as follows.

$$kh \cong 0.5\ \alpha/g \qquad (2)$$

Obviously the relation by Eq.(2) will not be used in practice for determining the seismic coefficient from maximum acceleration. This relation will, however, be discussed again in the following section in the context of maximum acceleration to be used for assessing liquefaction potential.

4.3 Stability against liquefaction

Soil liquefaction, if occurs, considerably affects the stability of structures. A design criteria to assess liquefaction potential for a sandy ground in coastal areas was originally proposed based on field experiences and laboratory tests (Tsuchida, 1970). Liquefaction potential, in the current practice, is assessed by the following procedure which is a revision of the original one (Iai et al, 1989).

1) Classify the soils by comparing the grain size accumulation curves with the ranges shown in Fig.10;

Soils within the range (A) : very easily liquefiable soil.
Soils within the range (Bf) or (Bc) : easily liquefiable soil but less liquefiable than the soils within the range (A).

Consider that no liquefaction will take place for the soils which do not belong to either the ranges (A), (Bf) or (Bc).

2) Obtain the equivalent N-values from SPT N-values with corrections for effective confining pressures to 0.66 kgf/cm2 and with corrections for fines content. Conduct the earthquake response analysis of ground by equivalent linear method and obtain the equivalent acceleration from the maximum shear stress ratio (the ratio of maximum shear stress over vertical effective stress) by multiplying the factor of 0.7g as a conversion factor.

3) Use the design charts shown in Fig. 11 in accordance with the ranges for grain size accumulation curves. Assess the liquefaction potential in accordance with the regions to which the equivalent N-value and the equivalent acceleration belongs;

Region I : Consider that liquefaction will take place.
Region II : Conduct a further study such as laboratory test of soils if desirable. Otherwise, consider that liquefaction will take place.
Region III : Conduct a further study such as laboratory tests of soils if high reliability is required in the stability of the soil deposit. Otherwise, consider that liquefaction will not take place.
Region IV : Consider that liquefaction will not take place.

Present criterion has evolved from the studies since 1964 Niigata Earthquake (Tsuchida and Hayashi, 1971). Though the evolution process is quite independent from the studies by Tokimatsu and Yoshimi (1983) and Seed et al.(1985), all of these criteria show remarkably good agreement as shown in Fig. 12 (Iai et al, 1989).

In assessing liquefaction potential by the present procedure, maximum accelerations should be specified for the input motions to be given at the base rock for earthquake response analysis. Based on the recent study on seismic zoning (Kitazawa et al, 1984), maximum accelerations as an rock outcrop motions (i.e. double amplitudes of incident waves) are specified for five regions as 300, 250, 200, 150 and 100 Gals.

It is important to assure that the level of safety against liquefaction should be well balanced with the level of safety against seismic inertia force. As partly suggested in the previous section, Eq.(2) shows such balance are indeed assured in the present design procedure.

Based on the assessment of liquefaction potential, adequate measures will, if necessary, be taken against liquefaction. Relevant studies can be referred to on designing the area of ground compaction (Iai et al, 1987) and on designing spacing of gravel drains (Iai et al, 1988).

ACKNOWLEDGEMENTS

The authors express sincere appreciation to Dr. Takamasa Inatomi, Chief of Structural Dynamics Laboratory; Dr. Tatsuo Uwabe, Chief of Earthquake Disaster Prevention Laboratory, Dr. Susumu Iai, Chief of Geotechnical Earthquake Engineering Laboratory, and Mr. Yasuo Matsunaga, Member of Geotechnical Earthquake Engineering Laboratory of Port and Harbour Research Institute for their considerable support to prepare this report.

REFERENCES

Bureau for Ports and Harbours, Port and Harbour Research Institute, and The First District Port Construction Bureau of Ministry of Transport (1964) : "Damage to Harbour Structures by the Niigata Earthquake (Part 1)."

Bureau for Ports and Harbours, Port and Harbour Research Institute, and The First District Port Construction Bureau of Ministry of Transport (1965) : "Damage to Harbour Structures by the Niigata Earthquake (Part 2)."

Bureau for Ports and Harbours, Port and Harbour Research Institute, and The Second District Port Construction Bureau of Ministry of Transport, and Port and Harbour Division of Hokkaido Development Bureau of Hokkaido Development Agency (1968) : "Damage to Harbour Structures by the 1968 Tokachi-Oki Earthquake."

Bureau for Ports and Harbours, and Port and Harbour Research Institute of Ministry of Transport and Port and Harbour Division of Hokkaido Development Bureau of Hokkaido Development Agency (1973) : "The Report on the Damage to Port Structures and the Investigation of the Tsunami Caused by the Nemuro Hanto Oki Earthquake on June 1973."

Iai, S., Koizumi, K. and Kurata, E. (1987) : "Basic Consideration for Designing the Area of the Ground Compaction as a Remedial Measure against Liquefaction," Technical Note of Port and Harbour Research Institute, No.590, 66p.

Iai,S., Koizumi, K., Noda, S. and Tsuchida, H.(1988) : "Large Scale Model Tests and Analysis of Gravel Drains," Proceedings of Ninth World Conference on Earthquake Engineering, Tokyo, Vol.III, pp.261-266.

Iai, S., Urakami, T., Mutoh, Y. and Kikuchi, M.(1988) : "Liquefaction at Coastal Area and Performance of a Quaywall during 1987 Off East Chiba Prefecture Earthquake," Technical Note of Port and Harbour Research Institute, No. 616.

Iai, S., Tsuchida, H. and Koizumi, K. (1989) : "A Liquefaction Criterion Based on Field Performances around Seismograph Stations," Soils and Foundations, Vol.29, No.2, pp.52-68.

Japan Port and Harbour Association (1980) : "Technical Standards for Port and Harbour Facilities in Japan (1989 Edition). "

Japan Port and Harbour Association (1989) : "Technical Standards for Port and Harbour Facilities in Japan (1989 Edition)."

Kawasumi, H. (1951) : "Measures of Earthquake Danger and Expectancy of Maximum Intensity throughout Japan as inferred from the Seismic Activity in Historical Times," Bulletin of Earthquake Research Institute Vol.29, Tokyo University.

Kitajima, S. and Uwabe, T. (1979) : "Analysis on Seismic Damage in Anchored Sheet-piling Bulkheads," Report of Port and Harbour Research Institute, Vol.18, No.1, pp.67-127.

Kitazawa, S., Uwabe T. and Higaki N. (1984) : "Expected Values of Maximum Base Rock Accelerations along Coasts of Japan," Technical Note of Port and Harbour Research Institute, No.486, 137p.

Kurata, E. and Iai, S. (1991) : "Annual Report on Strong-Motion Earthquake Records in Japanese Ports (1990)," Technical Note of the Port and Harbour Research Institute, No.705.

Noda, S., Uwabe, T. and Chiba, T. (1975) : "Relation between Seismic Coefficient and Ground Acceleration for Gravity Quaywall," Report of Port and Harbour Research Institute, Vol.14, No.4, pp.67-111.

Seed, H.B., Tokimatsu, K., Harder, L.F. and Chung, R.M. (1985) : "Influence of SPT Procedures in Soil Liquefaction Resistance Evaluations," Journal of Geotechnical Engineering Division, ASCE, Vol.111, No.12, pp.1425-1445.

Tokimatsu, K. and Yoshimi Y. (1983) : "Empirical Correlation of Soil Liquefaction Based on SPT N-value and Fines content," Soils and Foundations, Vol.23, No.4, pp.56-74.

Tsuchida, H. (1970) : "Design Criteria for assessing Liquefaction Potential of Sandy Ground and Countermeasures," Proceedings of Annual Conference for Research Presentation of Port and Harbour Research Institute, pp.(3)1-33.

Tsuchida, H. and Hayashi, S. (1971) : "Estimation of Liquefaction Potential of Sandy Soils," Third Joint Meeting of U.S. and Japan Panel on Wind and Seismic Effects, UJNR, pp.1-16.

Tsuchida, H., Inatomi, T., Noda, S., Yagiu, T., Tabata, T., Tokunaga, S. and Hirano, T. (1979) : "The Damage to Port Structures by the 1978 Miyagi-ken-oki Earthquake," Technical Note of Port and Harbour Research Institute, No. 325, 50p.

Tsuchida, H., Noda, S., Inatomi, T., Uwabe, T., Iai, S., Ohneda, H. and Toyama, S. (1985) : Damage to Port Structures by the 1983 Nippon-kai-Chubu Earthquake," Technical Note of Port and Harbour Research Institute, No. 511, 447p.

Uwabe, T., Noda, S. and Kurata, E. (1976) : "Characteristics of Vertical Components of Strong-Motion Accelerograms and Effects of Vertical Ground Motion on Stability of Gravity Type QuayWalls," Report of Port and Harbour Research Institute, Vol.15, No.2, pp.239-317.

Yamamoto, R., Hayashi, S., Tsuchida, H., Yamashita, I. and Ogura, K. (1970) : "Evaluation of Seismic Stability of Trestle Type Pier with Vertical Steel Piles," Report of Port and Harbour Research Institute, Vol.9, No.1, pp.179-228.

Table 1 Recent earthquakes which caused damage to port facilities

Date	Name	Mag.	Highest recorded peak acc. in Gal (Location)
1964/06/16	Niigata earthquake	7.5	159 (Niigata)
1968/05/16	1968 Tokachi-oki	7.8	233 (Hachinohe)
1973/06/17	1973 Nemuro-Hannto-oki	7.4	164 (Kushiro)
1978/06/12	1978 Miyagi-ken-oki	7.4	280 (Shiogama)
1982/03/21	1982 Urakawa-oki	7.1	253 (Hiroo)
1983/05/25	1983 Nihonkai-Chubu	7.7	205 (Akita)
1984/08/07	1984 Hyuuganada	7.1	268 (Hososhima)
1987/12/17	1987 Chiba-ken-Toho-oki	6.7	171 (Chiba)

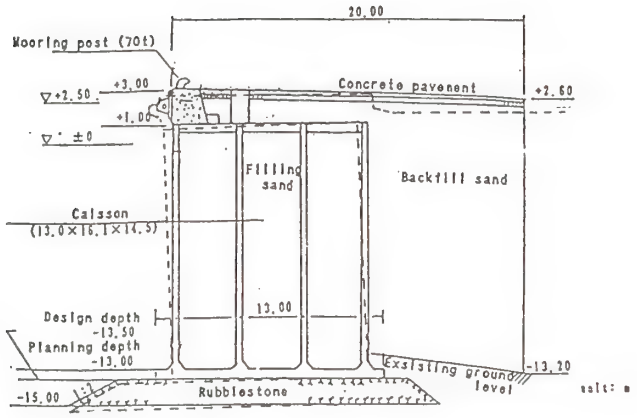

Fig. 1 Cross section of gravity type quaywall (Gaiko Wharf) in Akita Port

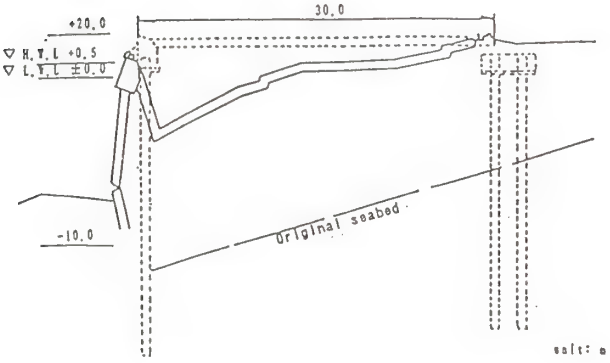

Fig. 2 Cross section of damage to steel sheet pile bulkhead (Ohama No. 2) in Akita Port

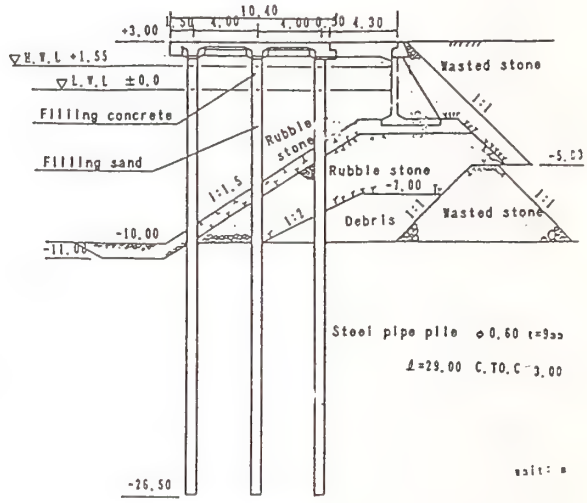

Fig. 3 Trestle type pier (West No. 2 Pier, East Side) in Muroran Port

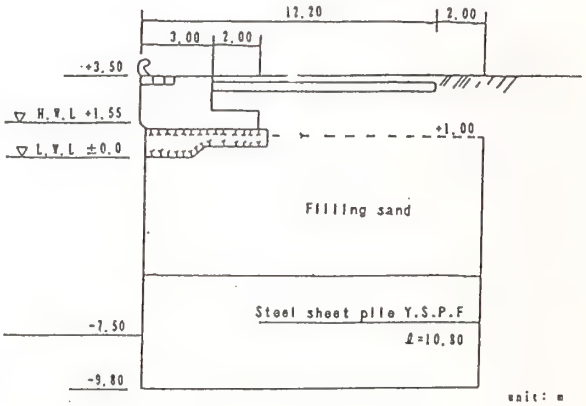

Fig. 4 Cellular bulkhead (Nittsu Wharf) in Muroran Port

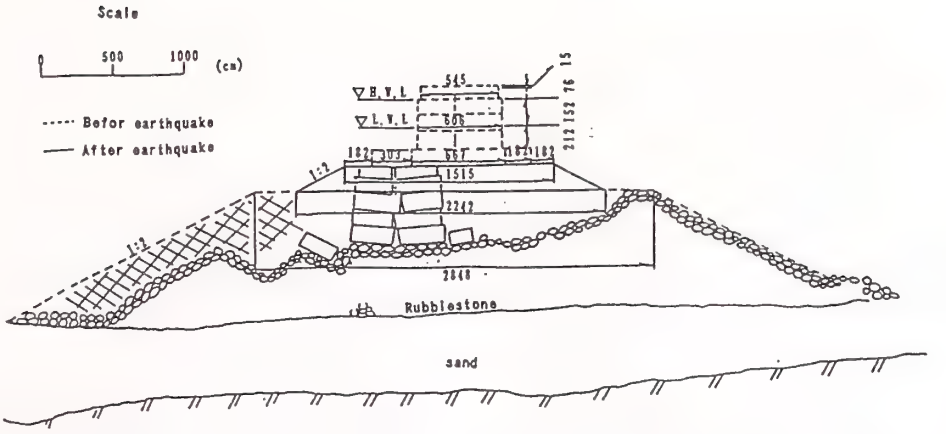

Fig. 5 Breakwater in Yokosuka damaged by Kanto earthquake (1923)

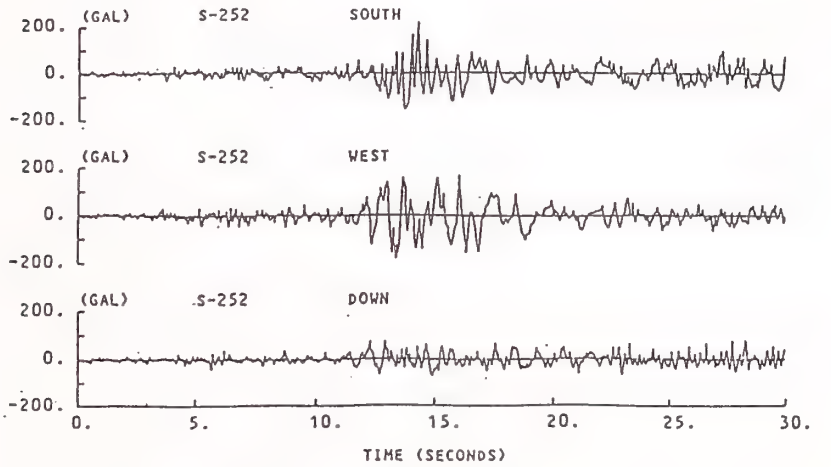

Fig. 6 Accelerations of 1968 Tokachi-oki earthquake at Hachinohe Port

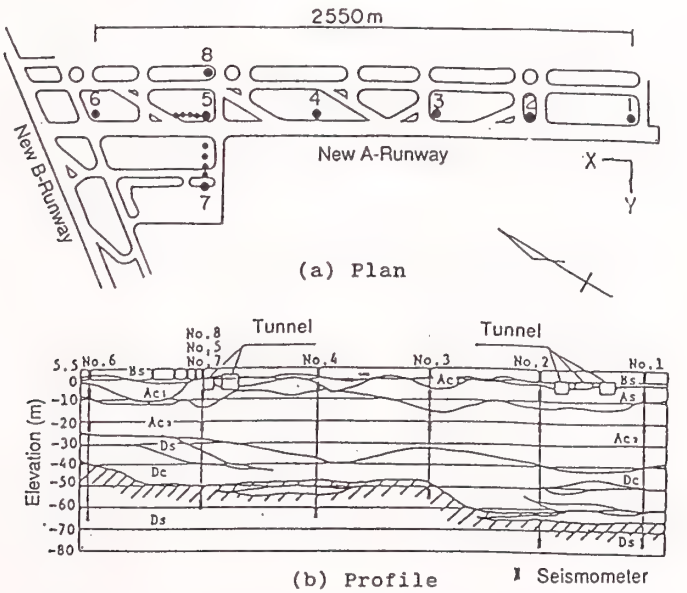

Fig. 7 Deployment of seismometers of array observation system of PHRI(Haneda Airport)

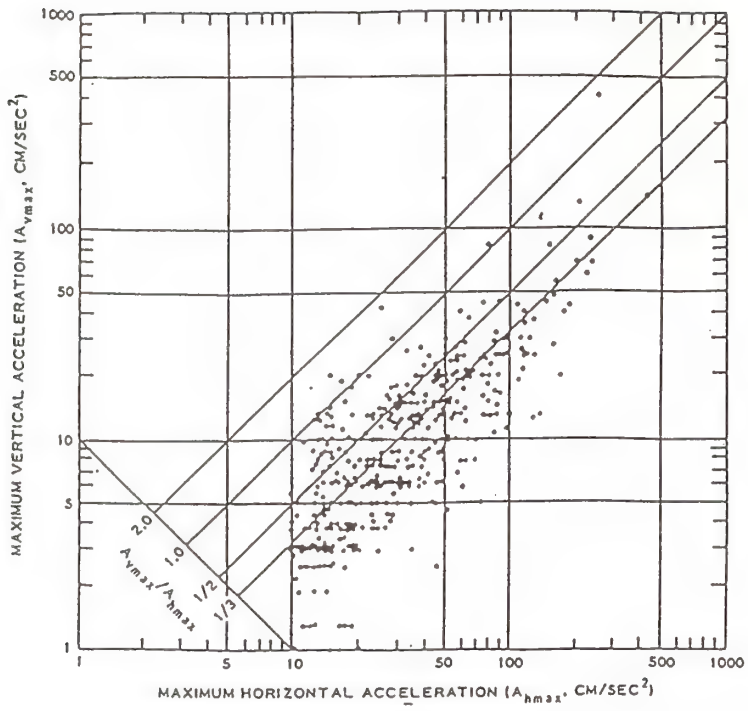

Fig. 8 Maximum vertical vs. horizontal acceleration in Japan (after Uwabe et al, 1976)

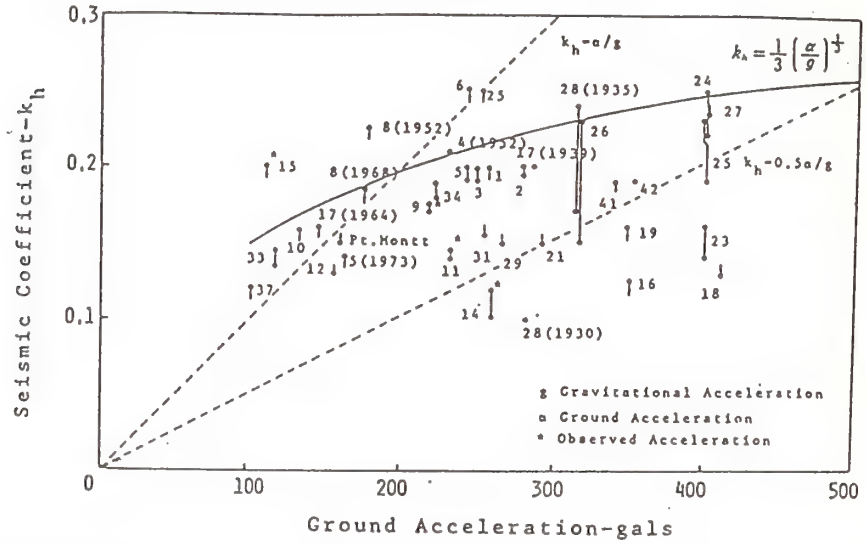

Fig. 9 Relation between seismic coefficient and ground acceleration (after Noda et al, 1975)

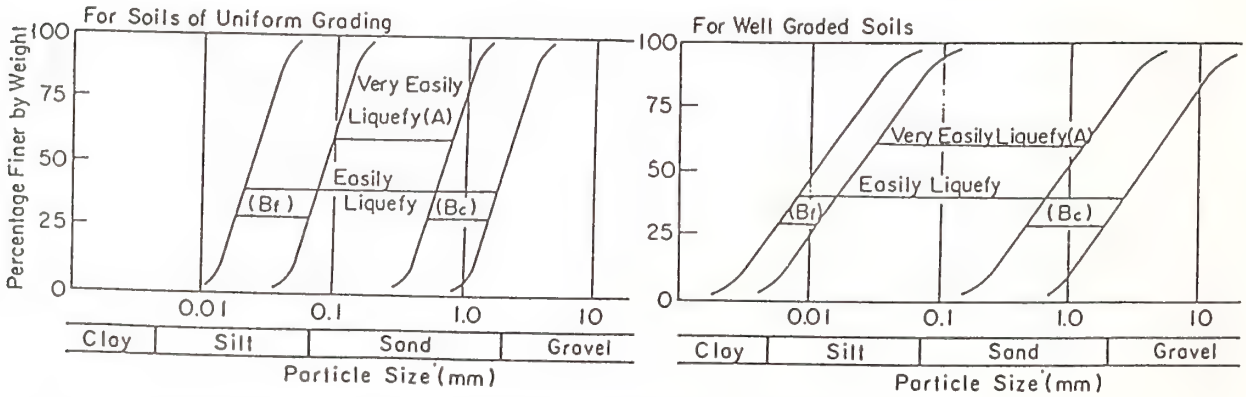

Fig. 10 Ranges of grain size accumulation curves for liquefiable soils (after Iai et al, 1989)

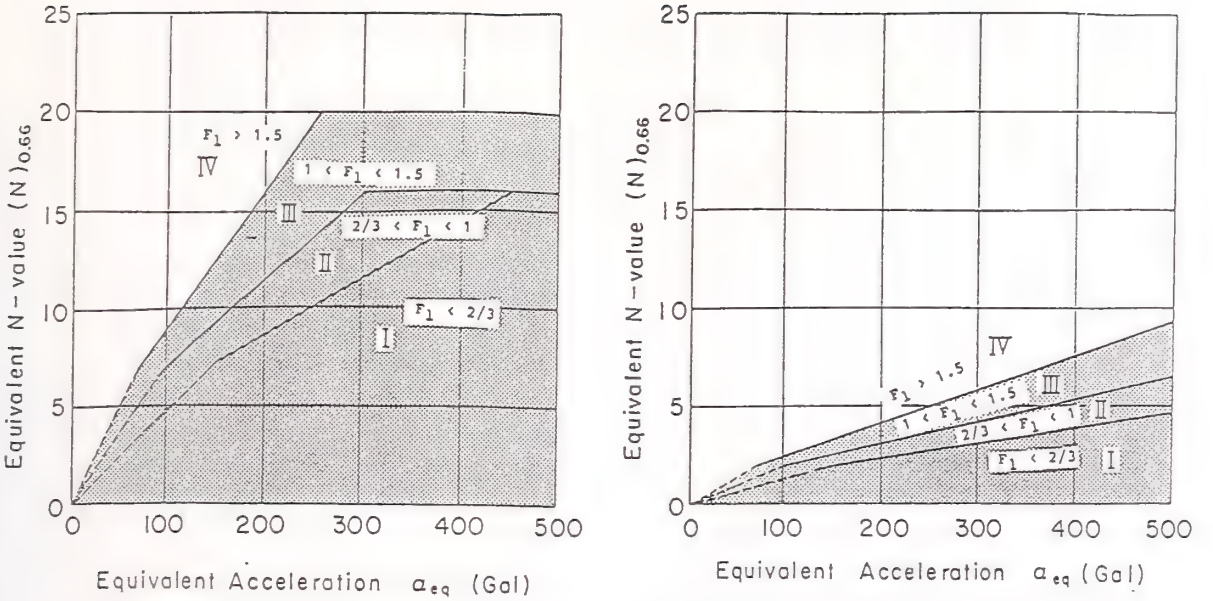

(a) For soils in the range (A)

(b) For soils in the ranges (Bf) or (Bc)

Fig. 11 Design chart for assessing liquefaction potential (after Iai et al., 1989)

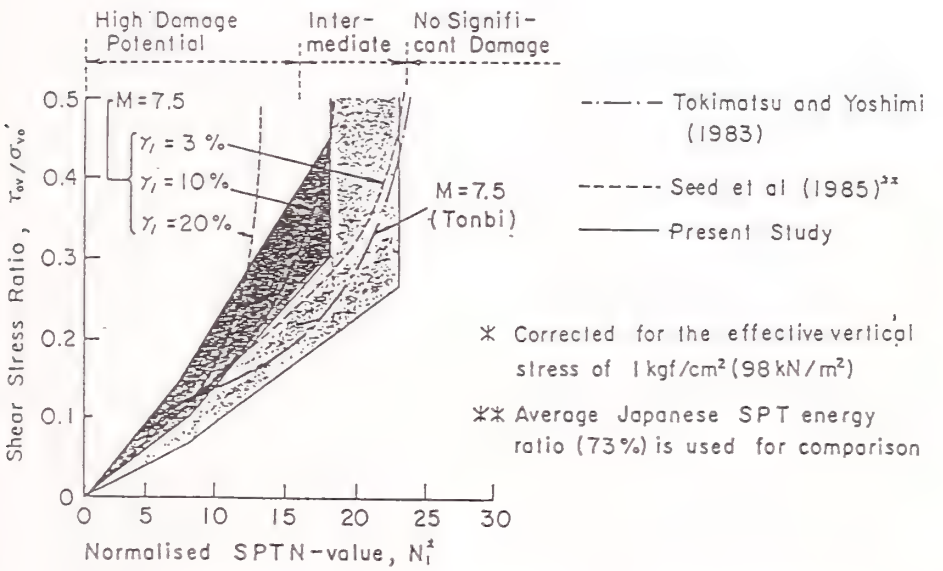

Fig. 12 Comparison with other criteria (after Iai et al, 1989)

Implementation of Executive Order 12699, "Seismic Safety of Federal and Federally Assisted or Regulated New Building Construction "

by

Richard N. Wright*

ABSTRACT

The Interagency Committee on Seismic Safety in Construction (ICSSC) assists federal agencies involved in construction to develop and incorporate earthquake hazards reduction measures in their ongoing programs. ICSSC proposed an executive order for seismic safety in construction that became the basis for Executive Order 12699, "Seismic Safety of Federal and Federally Assisted or Regulated New Building Construction," dated January 5, 1990. ICSSC is working with federal agencies, state and local governments and private sector organizations to implement the Executive Order.

KEYWORDS: building codes; building standards; earthquake hazard reduction; existing buildings; retrofitting buildings; seismic safety

1. THE EARTHQUAKE PROBLEM

Losses of property approaching $10 billion, losses of 62 lives and severe disruption of human activities from the October 17, 1989, Loma Prieta, California, earthquake reminded the United States of the severe threats posed by great earthquakes. In perspective, losses were modest because the earthquake was far from the San Francisco Bay area where the major damages occurred. Unless enhanced efforts are made to reduce earthquake hazards, a large earthquake close to a major metropolitan area can kill tens of thousands of people, cause tens of billions of dollars of direct property losses, and, through consequent losses, severely disrupt economic activity for the whole nation.

It is important to note that earthquake hazards are not only a California problem. Forty-six of our fifty states are vulnerable to strong earthquakes, Figure 1. In the eastern half of the country, the area that will be affected by an earthquake could be 10 times as large as for a similar earthquake in California. Records from historic earthquakes have illustrated this pattern, Figure 2, which is believed to be due to differences in rock and overlaying soil. One or more earthquakes, equal to or larger than that that struck California in 1989, are expected to affect U.S. metropolitan areas in the next ten years.

However, while earthquakes are an inevitable hazard, they are not inevitable disasters. Properly designed and constructed buildings and lifelines (public works and utilities structures) can resist economically the effects of strong earthquake ground shaking.

2. POLICY REQUIREMENTS

The National Earthquake Hazard Reduction Program (NEHRP) was established by the President in 1978 in accord with the Earthquake Hazards Reduction Act of 1977 (P.L. 95-124) to reduce loss of life, injuries, and economic costs resulting from the occurrence of earthquakes in the United

*National Institute of Standards and Technology, Gaithersburg, MD 20899

States. The Interagency Committee on Seismic Safety in Construction was established in 1978 to assist the federal agencies involved in constructions to develop and incorporate earthquake hazard reduction measures in their programs. Twenty-nine agencies participate in ICSSC.

On January 5, 1990, the President issued Executive Order 12699, "Seismic Safety of Federal and Federally Assisted or Regulated New Building Construction." The Executive Order is based on a proposal by the Interagency Committee on Seismic Safety in Construction.

The Executive Order responds to the policy requirements created by the Earthquake Hazards Reduction Act of 1977. The Act requires "the development and promulgation of specifications, building standards, design criteria, and construction practices to achieve appropriate seismic resistance." It calls for "the examination of alternative provisions and requirements for reducing earthquake hazards through federal and federally financed construction, loans, loan guarantees and licenses." The Act requires attention not only to federal facilities, but also to federally assisted or regulated construction. Each agency is responsible for its own actions. Neither the Federal Emergency Management Agency (FEMA) nor ICSSC are given authorities over the agencies' programs.

3. PROVISIONS OF THE EXECUTIVE ORDER

The requirements for the earthquake safety of federal buildings have these purposes: to reduce risks to the lives of occupants; to reduce secondary risks of failures; to improve the capability for important federal buildings to be functional during or after the emergency; and to reduce losses of public buildings. Any new federal buildings entering the detailed design stage after January 5, 1990, shall be designed and constructed in accord with appropriate seismic standards.

For federally leased, assisted or regulated buildings, the purpose of the Executive Order is to reduce risk to lives of occupants of buildings leased for federal uses or purchased or constructed with federal assistance; to reduce risk to the lives of persons potentially affected by earthquake failures of federal assisted or regulated buildings, and to protect public investments. For space constructed and leased for federal occupancy, the Executive Order applies to agreements executed since January 5, 1990.

Federal domestic assistance programs affect most new residential construction because states, municipalities and developers want to be eligible for VA or FHA mortgages. The Executive Order requires agencies, within 3 years, to plan and initiate measures to assure appropriate consideration of seismic safety in domestic assistance programs.

The concurrent requirements are extremely important to the private sector and to the federal agencies. Agencies and ICSSC are not expected to develop federal standards for new building construction. Administration policy in OMB Circular A-119 for the use of nationally recognized standards to the extent possible in federal programs is reflected in the Executive Order. Agencies would use nationally recognized private sector standards unless none are available that meet special agency requirements. The local building code may be used if the agency determines it provides adequate seismic safety. ICSSC is working collectively to provide guidance to the agencies so that each agency doesn't itself have to carry out an assessment of the more than 15,000 local building codes in the country.

Each agency is responsible for issuing its regulations or procedures, planning for implementation through its own budget process and regularly reviewing its regulations and procedures. FEMA is to request from

each agency annually the status of its work and to report on execution of the order annually to Congress.

4. IMPLEMENTATION OF THE EXECUTIVE ORDER

ICSSC is now working on implementation of the Executive Order. Guidelines [1] have been developed for implementation of the Executive Order. ICSSC also is working with the private sector in implementation of the Executive Order. The National Earthquake Hazards Reduction Program has developed, in cooperation with the Building Seismic Safety Council and the Applied Technology Council, "Recommended Provisions for Development of Seismic Regulations for New Buildings." These are being used in the national standards and model codes. The American Society of Civil Engineers is considering the NEHRP Recommended Provisions in revision of its widely used national Standard A7, "Minimum Design Loads for Buildings and Other Structures."

A study with the Council of American Building Officials (CABO) [2] compared model code provisions to NEHRP Recommended Provisions. Based on its review of the CABO assessment, the ICSSC recommended as substantially equivalent to the NEHRP Recommended Provisions:

- 1991 ICBO Uniform Building Code
- 1992 Supplement to the BOCA National Building Code
- 1992 Amendments to the SBCC Standard Building Code

State or local ordinances adopting and enforcing these model codes are deemed adequate for implementing the Executive Order.

These nationally recognized private sector standards will become important resources for new federal buildings. ICSSC also is working with the private sector in preparing guidance documents for the federal agencies to use to assess the adequacy of the local building codes in dealing with the seismic safety of federally assisted or regulated facilities. A study with the National Conference of States on Building Codes and Standards [3] assessed the status in the United States of the adoption and enforcement of adequate seismic provisions.

Considering the strong efforts of the private sector and state and local government to implement seismic design and construction standards for new buildings, and the federal agencies' implementation of the Executive Order, most U.S. new building construction should be appropriately seismically resistant by the mid-1990s.

5. REFERENCES

1. Todd, D. and Bieniawski, A., editors, Guidelines and Procedures for Implementation of the Executive Order on Seismic Safety of New Building Construction, NISTIR, National Institute of Standards and Technology, Gaithersburg, MD, May 1992.

2. Council of American Building Officials, Assessment of the Seismic Provisions of Model Building Codes, NISTGCR 91598, National Institute of Standards and Technology, Gaithersburg, MD, publication pending.

3. National Conference of States on Building Codes and Standards, Seismic Provisions of State and Local Building Codes and Their Enforcement, NISTGCR 91599, National Institute of Standards and Technology, Gaithersburg, MD, publication pending.

Seismic Hazard of the United States

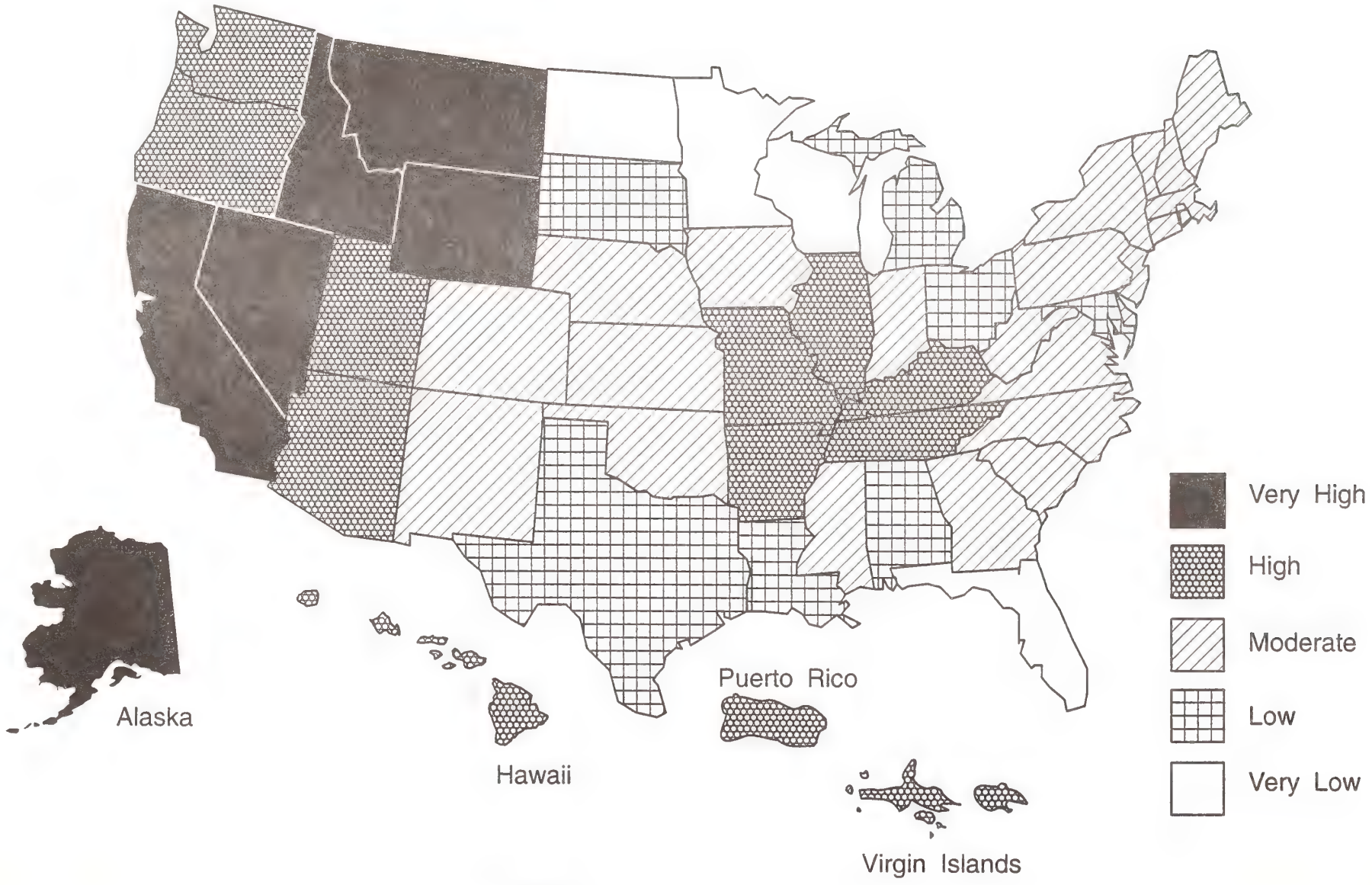

Figure 1

1906 San Francisco
VI-VII
1971 San Fernando
≥ VII
New Madrid
1811
VI-VII
≥ VII
VI-VII
≥ VII
Charleston 1886

Figure 2

U.S. Army Corps of Engineers Earthquake Engineering Research Program

by

W. D. Roper*, M. E. Hynes**, and R. F. Davidson*

ABSTRACT

To ensure the rapid recovery of Corps infrastructure and provide effective, rapid response to earthquake-induced flooding, landslides, and other life threatening emergencies, the Corps has recently organized a focused research and development program, called the Quake Program, to address the primary sources of seismic damage, namely ground shaking and ground failure, and their impact on Corps facilities. Quake Program efforts are prioritized according to the needs of our field engineers who are responsible for the design, construction, operation and maintenance of the Corps' flood control and navigation facilities. The objectives of the program are: (1) to develop practical, more effective seismic design procedures where they are now missing, (2) to reduce the uncertainty in our seismic safety assessments and avoid costly defensive design, (3) to reduce the risk of catastrophic failure of Corps infrastructure, primarily dams, and (4) to save money on new construction and remediation efforts. The Quake studies incorporate the research results of universities and other government agencies in this country and abroad to develop seismic design tools tailored to Corps needs. This paper describes some of the problems we have encountered in our projects which motivated the establishment of the Quake program at this time, the scope of the studies planned for the next few years, and the coordination of these activities with others involved in earthquake-related research.

KEYWORDS: buildings; dams; earthquakes; embankments; foundations; ground motions; liquefaction; locks; outlet works; seismology; walls; lifelines.

1. INTRODUCTION

As part of our Civil Works mission, the Corps of Engineers designs, constructs, operates and maintains approximately 400 flood control dams and reservoirs, and about 150 navigation locks and reservoirs. We have built thousands of miles of levees, and do most of the dredging needed to keep our nation's ports open. In addition, the Corps has been assigned certain emergency responsibilities under the U. S. Federal Response Plan that would be activated after a major earthquake. It is in connection with our Civil Works mission that the Corps is currently organizing an earthquake engineering research program, called the Quake Program.

This paper describes a number of problems we have encountered in our large construction and seismic safety projects which motivated the development of this new research program, the organization and scope of the studies planned for the next few years to address the perceived gaps in our knowledge, and the coordination of these studies with the activities of universities and other government agencies in this country and abroad.

2. THREATENED FACILITIES AND RESEARCH NEEDS

A sudden great earthquake poses the danger of catastrophic failures in major works of the Corps of Engineers including dams, levees, river control structures, navigation channels, harbors, airfields, and hazardous and toxic waste sites, as well as essential military facilities. At least 39 U.S. states are subject to strong earthquakes and more than 20 million people are at risk. In the central United States, where we have little modern experience with earthquakes, at least 20 locks and dams, 51 pumping plants, 19 reservoirs, and 23,000 miles of levees could be impacted by a major seismic event in the New Madrid area.

In spite of major advances over the last 25 years, serious gaps in our knowledge base exist in the areas of earthquake hazard predictions; site characterization for seismically sensitive parameters; constitutive behavior, failure mechanisms and material properties of rock, soils, concrete and composite (reinforced or remediated) materials under seismic loads, and the stress and deformation response of sites and facilities to seismic loading. Cost-efficient remediation and defensive design techniques are needed in addition to careful calibration of fast advancing numerical methods to actual field performance. Part of such calibration includes rapid deployment to sites of earthquake damage to collect and monitor transient data. In addition, some of these same monitoring techniques can be developed for use in immediate urban search and rescue efforts in damaged areas.

It is our experience that every time the Corps is faced with a serious earthquake engineering safety study it becomes a research project because the state of the art in earthquake engineering falls far short of our needs. Thus, earthquake safety studies tend to take a long time since we must perform the research necessary to develop design solutions. These research studies require considerable experimentation in the field, in the laboratory, and on the computer. Each step in this solution process involves a great deal of uncertainty. Once a logical line of reasoning to solve the problem has been developed the results may be tentative because new knowledge provided when earthquakes occur or with a major state-of-the-art advance may necessitate revisions.

This uncertainty combined with disastrous consequences in the event of a failure of one of our critical structures requires diligent

* Headquarters, U. S. Army Corps of Engineers, Washington, D. C. 20314-1000

** U. S. Army Engineer Waterways Experiment Station, Vicksburg, Mississippi 39180-6199

attention to continuously improve our seismic design capabilities and to confirm that our existing designs conform to the highest standards of safety. At this time, we design our structures defensively, to account for the shortcomings in the state of the art to analyze and design efficiently for earthquake problems. Our research is aimed at improving our ability to design effectively, to reduce uncertainty in our end results and reduce the cost of our construction.

3. PROBLEMS ENCOUNTERED IN OUR PROJECTS

The motivating force in all Corps Civil Works research is the need expressed by our field engineering offices for better design procedures and tools. Engineering problems have been encountered in a number of large Corps projects that have highlighted the need for research in earthquake engineering. These problems involve our inability to accurately predict earthquake ground motion levels, our incomplete understanding of materials in situ, material behavior and mechanisms of failure during and after earthquake loading, the need for validation and simplification of our analytical approaches, and the need for more efficient, economical methods of remediation. Three projects are described next to illustrate the knowledge gaps we have been faced with in our efforts to achieve efficient, well engineered designs for seismic loading of these key structures. Two projects are existing dams which have been found to need remediation to withstand their design earthquakes. The other project is a new navigation structure in the design stage.

3.1 Folsom Dam and Reservoir Project

The Folsom Dam and Reservoir Project is located on the American River about 20 miles northeast of the city of Sacramento, California (see location map in Figure 1). The reservoir is retained by about 4.5 miles of earth and rockfill embankment dams and a 1400-ft long concrete gravity section which includes the spillway. At maximum pool, the reservoir retains one million acre-ft of water. The design earthquake for this project is a magnitude 6.5 event occurring 15 km away. Catastrophic failure of this dam is estimated to result in 6,000 deaths, put downtown Sacramento under six ft of water, and cause six billion dollars' worth of property damages. Clearly this is a critical project.

The embankment shells are rolled-fill constructed from gravelly dredge tailings. A portion of one auxiliary embankment dam, Mormon Island Auxiliary Dam, has upstream and downstream shells founded on these loose, gravelly dredge tailings. Figure 2 shows a plan and Figure 3 shows cross sections of this dam. This is the only section of the Folsom Project found to be unsafe. We are now in the process of designing and constructing a remedial measure at this location.

At the time this safety evaluation was started in 1978, there were no established procedures to measure the properties of these gravelly materials, in situ or in the laboratory, and to assess their earthquake behavior. Consequently, we had to perform the research necessary and incorporate the work of others to develop testing and analysis procedures adapted to gravelly soils for which there is little or no earthquake experience -- large-scale in situ density tests, geophysical tests in steel-cased holes, interpretation of geophysical tests in loose gravels and rockfill, laboratory compaction and density tests for gravels, interpretation of Becker Hammer penetration tests and equivalent SPT values, cyclic loading behavior in large-scale laboratory tests and corrections for membrane compliance for extremely loose and moderately dense gravels, and estimation of residual strength for gravels).

For the concrete gravity section, there were also problems, such as realistic ways of determining the adequacy of the complex, three-dimensional connection between the embankment wing dams and the partially embedded concrete gravity dam (see typical section in Figure 4) subjected to seismic loads, procedures for assigning values of reservoir bottom absorption for hydrodynamic response analyses of the concrete dam, and methods of accurately determining the potential for sliding deformation in the dam or in fracture planes in the rock foundation.

Through almost ten years of testing, analysis, and conservative interpretation, we were able to acquire enough information to conclude that only the 800-ft long section of Mormon Island Auxiliary Dam with embankment shells on loose gravels required remedial action. We are now faced with the poor understanding the profession has today concerning the actual behavior of liquefying soils and the design, construction, verification and seismic behavior of remediated (composite) zones. A possible remediation plan under consideration involves a system of drains (shown in Figure 5) to control pore pressures.

We now find that we do not really understand the effective stress states and stress-strain behavior of soils as they are deforming while excess pore pressures increase during seismic loading, and after liquefaction as they develop residual strength. We find we do not fully understand the seismic behavior of improved soils with zones of higher density from dynamic compaction, or with stone columns with higher permeability, or reinforced with piles, and the pore-pressure, stiffness and strength interaction of these relatively loose and dense zones under dynamic loads.

We cannot accurately predict the change in density to be expected with distance from a remedial action. We cannot easily verify that we have indeed achieved the desired results, since the remedial action typically radically increases horizontal stresses which are difficult to measure and for which none of our seismic safety evaluation procedures have been developed and calibrated. For example, SPT blowcounts corrected to one tsf is a widely adopted practice, however, the correction factor C_N was developed for horizontal stress levels typically found in natural deposits, not the high values that result in remediated zones.

This wide range of uncertainty in the design and effectiveness of remedial actions causes us once again to adopt conservative interpretations of our analytical and test results. In this project, our efficiency as engineers is hampered because the design tools were not readily available but had to be developed, and the end results still have considerable uncertainty requiring costly defensive design.

3.2 Sardis Dam and Reservoir Project

Sardis Dam is located in northwestern Mississippi, 70 miles from the southernmost extension of the New Madrid fault zone in the central United States (see location map in Figure 1, project plan in Figure 6, and typical sections in Figure 7). Sardis is a hydraulic fill dam, and study of its seismic safety began right after the near failure of the hydraulic fill Lower San Fernando Dam, Los Angeles, California, in the 1971 San Fernando earthquake. More than once in the process of our seismic safety evaluation we were about to conclude that the dam was safe, only to have new developments in the state of the art of earthquake engineering force us to reconsider.

One of the first issues was the level of shaking to be expected at the site -- early estimates were that it was too small to be of concern. In 1980, Dr. Ellis Krinitzsky of the Waterways Experiment Station at Vicksburg, Mississippi, conducted a survey of 18 individuals and organizations, all of whom were considered to be experts at determining ground motions. All were given the same "hypothetical" sites, one of which was, for practical purposes Sardis Dam. The peak ground accelerations that were recommended ranged from 0.03g to 0.5g -- from imperceptible to very strong. We eventually reached the conclusion that the expected ground motions were sufficiently large to require us to assess the liquefaction potential of the dam and foundation.

After extensive investigations of the sandy portions of the dam and foundation, we had concluded that the dam was safe, when Dr. H. B. Seed (Seed et al. 1983) published data from China indicating that some clays were susceptible to liquefaction -- up to that time clays had generally been assumed to be non-liquefiable. Weak, sensitive clays meeting the Chinese criteria were in fact found in the foundation of Sardis Dam, and in 1988 an upstream berm was completed in the area believed to be most likely to fail. It was recognized at that time that more work was needed to evaluate the safety of the rest of the dam.

The site characterization difficulties for this site and several other complexly stratified alluvial dam sites in the central United States challenged our in situ investigation techniques and consequently we improved our ability to perform and interpret cone penetrometer tests. We pursued laboratory investigations to better understand the behavior of these fine-grained soils under cyclic loading and to better define the criteria indicated by the data from China. These studies helped define additional portions of the dam and foundation that required remedial action. We devoted more than a decade to development and validation of a sophisticated effective stress nonlinear large strain finite element technique to estimate the deformed shape that would result from an earthquake and to develop design parameters for the remediated zones. The deformed shape of the embankment after earthquake shaking using this technique is shown in Figure 8.

In January 1992, nearly 20 years after the San Fernando earthquake that started this reevaluation, the conclusion of the Sardis studies is that additional remedial work is needed at a cost of several million dollars. Design of the proposed solution -- driving several thousand large concrete piles (see Figure 9) -- will be a challenge to the state of the art. Because of the current lack of design tools, we are again forced into a certain amount of concurrent research and design, even though that is not usually a very efficient way to do either.

3.3 Olmsted Locks and Dam Project

Another challenge we now face is to design and construct a new double lock and dam on the Ohio River at Olmsted (see location map in Figure 1). A portion of the dam lies down flat on the river bed so that barge traffic only needs to use the lock in periods of low water. This river carries some of the heaviest barge traffic in the world. Loss of use of this important shipping route would have a serious impact on the economy of our nation as evidenced by the economic damage caused by the severe drought which made shipping impossible on portions of the Mississippi River in 1991. While we believe that the potential for loss of life caused by earthquake-induced failure of this structure is small, the economic losses could be substantial, and failure could shut down navigation on the Ohio River for an extended period.

This important navigation link is located on the northernmost extension of the New Madrid fault zone. Since we have little modern experience with significant earthquakes in the central United States, the earthquake ground motion levels appropriate for design remain controversial, as they were for Sardis Dam. Since the seismic design level this project is largely an economic decision, the many issues that enter into a detailed risk analysis (such as ground motion levels, uncertainty in engineering design aspects, and quantification of consequences) remain controversial because of differences in opinion as to how to define them, and because the construction costs associated with these aspects are substantial.

The design of this massive, complex, rigid structure remains a challenge. The realistic analysis of stiff, rigid, embedded, submerged walls subjected to dynamic loads is a distinct challenge to our dynamic soil-water-structure interaction analysis capability. We have much to learn yet before we have accurate, efficient, practical tools for dynamic design of its pile foundations. Our methods for determining hydrodynamic effects need improvement and validation. To add further geotechnical interest, there is an old landslide on the landside of the locks. The challenge here is to estimate the material strengths in this old landslide and estimate the extent of deformations in an earthquake. Like Sardis and Folsom Dams, the Olmsted Project involves concurrent research and design.

On projects such as Olmsted, we would like to be able to make intelligent decisions concerning the tradeoffs between the cost of providing additional seismic resistance and the expected damage to be avoided -- direct and indirect, tangible and intangible. At the present time, we are not able to define these aspects with sufficient accuracy to be useful. Improvements will require, for example, better estimates of expected ground motions, including recurrence rates, and better methods

of predicting structural damage for a given level of shaking. It has also become clear as we progress in this project and others that the tools for estimating vertical ground motion, empirically and analytically, have not been developed and validated.

The Folsom Dam and Sardis Dam seismic safety evaluations and the Olmsted Locks and Dam design phase are three examples of our field experiences in the shortcomings of the state of the art in earthquake engineering. These and other projects like them lead us to conclude that once we have done the best we can to evaluate the seismic safety of our critical facilities within the current limitation of the state of the art, the remaining uncertainties are large, uncomfortably large, considering the costs and risks involved. These issues have thus motivated us to organize the Quake Program. Our planning process and the current scope of studies in the program are described in more detail in the next section.

4. FOCUS AND SCOPE OF QUAKE PROGRAM

4.1 Program Focus and Planning Process

Since the motivation for Corps-funded research related to Civil Works is primarily driven by needs in the field, it is the nature of Corps Civil Works research programs that they are highly problem-oriented, and generally classify as applied research. These programs are also directly focused on the Corps Civil Works facilities. Thus, the niche that these programs fill, the Quake Program in particular, is a link between the more basic research pursued at universities and the rather unique Corps field engineering needs for practical design of critical flood control and navigational facilities.

The Corps is actually responsible for the enormous capital investment that the United States has made in our system of dams, locks and related facilities. As public servants, it is our mission to protect public safety and to spend public dollars wisely. This serious responsibility sharpens our perspective of research needs for the Corps. Consequently, our selection of research topics is driven by creative ideas that help us solve a real field problem, rather than creative ideas that would be simply intellectually interesting to study. The process by which we formulate our study topics and prioritize them is a combination of (1) needs identified by senior engineers in Corps field offices, (2) knowledge gaps identified by research elements within the Corps, and (3) Corps policy guidance provided by program monitors from Corps Headquarters.

We shape our program based on suggestions provided by a Field Review Group composed of the senior field engineers, who review and prioritize all proposed topics. The Field Review Group provides guidance for the direction of various studies to better meet field needs, and suggests new topics for consideration.

The Corps research elements manage and execute the program, suggest topics to the Field review group for their consideration, provide guidance on technical feasibility, and distinguish between problems actually requiring research and technology transfer (if the needed tools are actually available but have not yet made their way into practice).

Technical Monitors from Corps Headquarters maintain an oversight role throughout the process to provide technical and policy guidance for the program. The proposed program incorporating the field comments and priorities is approved, guided and reviewed by Corps senior policy officials to assure coherent, sensible, productive, cooperative, mission-oriented expenditure of our limited research funds.

4.2 Structure and Scope of Proposed Studies

The program structure follows the solution procedure for an earthquake engineering problem: 1) What are the ground motions? 2) How will they be delivered to the site/facility? 3) Analyze the facility for stress and deformation using appropriate boundary conditions, properties, material behavior and numerical and physical models, 4) Estimate actual performance, and 5) Revise design or implement remedial action if needed.

The program has three primary focus areas (1) earthquake ground motions, (2) geotechnical earthquake engineering, (3) structural earthquake engineering, and one secondary focus area in emergency response. Other Corps civil works related disciplines, such as hydraulics, electrical and mechanical, have indicated that they had no pressing earthquake engineering problems requiring research, and thus are not included in the program at this time.

As recommended by our Field Review Group, the initial efforts are directed toward those areas where greatest loss of life and property would result from an earthquake in conjunction with those structures most likely to fail from earthquakes. That area is unquestionably reservoir dams. Within the arena of reservoir dams, the Field Review Group recommended prioritization of research efforts dealing with liquefaction, followed by nonlinear behavior of concrete dams. Thirdly, they recommended that the next area of emphasis should be navigation locks and dams and other hydraulic structures. In addition, the Field Review Group recommended that additional strong motion instruments be placed in representative structures at sites where earthquake events are likely to occur, to provide additional data for validation of modeling and analysis techniques.

Evaluating the adequate seismic performance of our facilities usually consists of estimating the deformations that we expect and deciding whether the facilities can safely withstand these deformations. There are presently serious limitations in our ability to estimate deformations, and improvements will require (1) better estimates of expected ground motions, (2) improved analytic tools for calculating deformations including better constitutive models, (3) improved site and laboratory investigation methods that provide the information needed to use those analytic tools, and (4) validation of items 2 and 3 with full scale field data, particularly from earthquakes and possibly centrifuge testing.

4.2.1 Earthquake Ground Motions

The greatest uncertainty for all of our projects, be they earth dams, concrete dams, locks, levees, harbors, etc., is by far the level of earthquake ground motion that we should design for. Determining the incoming

ground motions and other possible seismic hazards is common to all design efforts. It is in this step that we define the "loads" we will design for. We find that with each new earthquake we learn a great deal. In this topic area we have planned several work units to improve our procedures for selecting design ground motions for engineering analyses. This effort includes: 1) reconnaissance of earthquake stricken locations world-wide to collect full-scale performance data, 2) continued development of ground motion and response spectra design charts and data bases, 3) development of empirical and analytical procedures to estimate vertical motions in time and frequency domains, 4) investigation of the effects of fault mechanics on vertical motions, 5) two- and three-dimensional boundary effects on ground motions, traveling waves and spacial variation of motions, and 6) instrumentation of a site and structure to capture detailed full scale response data for calibration of analytical procedures.

The continued effort to improve our ability to determine design ground motions is essential since this aspect of earthquake problems typically is a prime controlling factor in the overall cost of a project. Overestimation of ground motions leads to costly overdesign, and underestimation may lead to loss of life and costly, time consuming remediation.

4.2.2 Geotechnical Earthquake Engineering

This portion of the Quake Program is focused on liquefaction and its effects on our facilities. There are four main topic areas addressed:

* Site characterization and material behavior, to include development of innovative methods such as geophysical techniques for in situ identification of potentially liquefiable soils; rapid, less expensive assessment of dynamic material properties in situ; and investigation of the behavior of soils as they approach liquefaction, liquefy, and after liquefaction.

* Seismically-induced deformations to include a series of work units to develop improved methods for estimating deformations, to include the effects of three-dimensional boundary conditions and geometry, and to examine the potential behavior under strong aftershocks.

* Remedial measures and ground improvement to include a series of studies on the fundamental behavior of remediated soils which are now composites; development of procedures for realistically analyzing these composite materials; investigation of the effects of lateral stresses and migration of excess pore pressures into improved ground.

* Dynamic soil-structure-water interaction problems to include design of deep and shallow foundations, walls, tunnels and shafts, and embedded and submerged structures, in cooperation with the structural counterparts.

The best type of data for improving our design procedures is full scale performance data. The above topics are planned to be integrated with data from reconnaissance of earthquake damaged sites and quantitative information from an instrumented structure mentioned in the previous section.

4.2.3 Structural Earthquake Engineering

The structural earthquake engineering studies focus on concrete dams and the outlet works essential for controlled release of the reservoir. In the course of working on these types of projects it has become clear that the output from finite element analyses is not easily translated to the kind of information needed by structural designers; so, another aspect of the proposed studies is to develop such basic tools. The areas for research planned at this time are:

* Seismic structural response of concrete dams to include sliding structural stability, nonlinear material behavior and failure mechanisms, nonlinear behavior of roller-compacted concrete, dynamic uplift pressures, seismically-induced displacements, design earthquake level selection, nonlinear behavior of arch dams, field and model verification tests, reconnaissance of earthquake stricken sites to collect full scale performance data, and instrumentation of a site to collect detailed, quantitative full scale performance data for calibration of analytical procedures.

* Seismic response of outlet works to include overturning stability, nonlinear material behavior, equipment-structure interaction, bridge-tower interaction, and tower-abutment interaction.

* Development of basic engineering tools for extraction of design force information from response spectra analyses, and pre- and post-processors for finite element output.

* Additional soil-structure-water interaction studies for piles, walls, concrete channels, tunnels and shafts, in cooperation with the geotechnical counterparts.

4.2.4 Emergency Response

Another important mission of the Corps is emergency response in the aftermath of a natural disaster. We have certain responsibilities under the Federal Response Plan that would be activated after a major earthquake, such as assisting with removing debris, and restoring transportation routes and utilities. We are also often asked for assistance by others. For example, after the Loma Prieta earthquake, the Corps had more than three hundred engineers in the field supporting the U. S. Federal Emergency Management Agency.

Our plans for this portion of the Quake program are still in the formative stage. At this time we envision (1) periodic review of progress in the general field of earthquake engineering to select information that would impact our emergency response mission, (2) coordination of Quake research and emergency response research, and (3) action to assist transfer of technology to Corps emergency response offices.

5. COORDINATION OF QUAKE PROGRAM WITH OTHERS

For many years, the Corps has exercised well established, existing forums for keeping abreast of current research in earthquake engineering, primarily through national and international, governmental and private professional activities. We typically work with leaders in the field in our earthquake engineering safety evaluation problems, and

perform research in our Corps Laboratories. We learn much from participation, communication and coordination by our headquarters, field and research laboratory staff with:

a. Activities of national and international professional societies such as American Society of Civil Engineers, Earthquake Engineering Research Institute, Seismological Society of America, U. S. Committee on Large Dams, and the International Committee on Large Dams.

b. Activities of national organizations such as the National Research Council Committee on Earthquake Engineering and Transportation Research Board, and the Electric Power Research Institute.

c. Activities of federal agencies, such as the four primary agencies involved in the National Hazards Earthquake Reduction Program, namely the Federal Emergency Management Agency, the U. S. Geological Survey, the National Science Foundation (NSF) which includes the National Center for Earthquake Engineering Research, and the National Institute for Standards and Technology, as well as the many contributing agencies.

d. Activities of university organizations such as the consortium of California Universities for Research in Earthquake Engineering, and the Earthquake Engineering Research Center at the University of California, Berkeley.

e. Activities of international government groups such as the Joint U.S.-Japan Panel on Wind and Seismic Effects.

f. Activities of private companies such as Woodward Clyde and Associates, Dames and Moore and Associates, H. J. Deggenkolb and Associates, and others involved in state-of-the-art earthquake engineering projects.

Through our Field Review Group meetings, close communication with federal agencies, and work with other experts, we develop the perspective needed to plan our research program in earthquake engineering to meet our Civil Works mission.

6. CONCLUSIONS

In the development of a new federally funded research program, it is essential to carefully identify research needs and expected products, coordinate and communicate with other federal agencies, plan and execute the proposed program, and transfer results to the federal field engineers.

We proposed the Quake Program in response to an outcry from our district and division offices who repeatedly encounter the shortcomings in the state-of-the-art in earthquake engineering in their seismic safety evaluations of existing and design of new Civil Works projects, primarily flood control and navigation facilities. The focus of our proposed Quake Program is applied research -- to take fundamental research contributions such as scientific agency and university research, and develop practical design tools tailored to Corps needs for use in Corps offices. At this time, the focus of the program is on the seismic safety of reservoir dams -- the improvements needed in ground motion selection and geotechnical and structural engineering to reduce uncertainties and develop more efficient, effective procedures for assessing dam safety under seismic loading and designing remedial actions if required.

7. REFERENCES

Finn, W. D. L., Ledbetter, R. H., Fleming, R. L., Jr., Templeton, A. E., Forrest, T. W., Stacy, S. T. 1991. "Dam on Liquefiable Foundation: Safety Assessment and Remediation," 17th Congress on Large Dams, Vienna, Austria, June 1991.

Ledbetter, R. H., Finn, W. D. L., Nickell, J. S., Wahl, R. E., Hynes, M. E. 1991. "Liquefaction Induced Behavior and Remediation for Mormon Island Auxiliary Dam," International Workshop on Remedial Treatment of Liquefiable Soils, UJNR, Tsukuba Science City, Japan.

Seed, H. B., Idriss, I. M., Arango, I. 1983. "Evaluation of Liquefaction Potential Using Field Performance Data," Journal of Geotechnical Engineering, American Society of Civil Engineers, Vol. 109, No. 3, pp. 458-482.

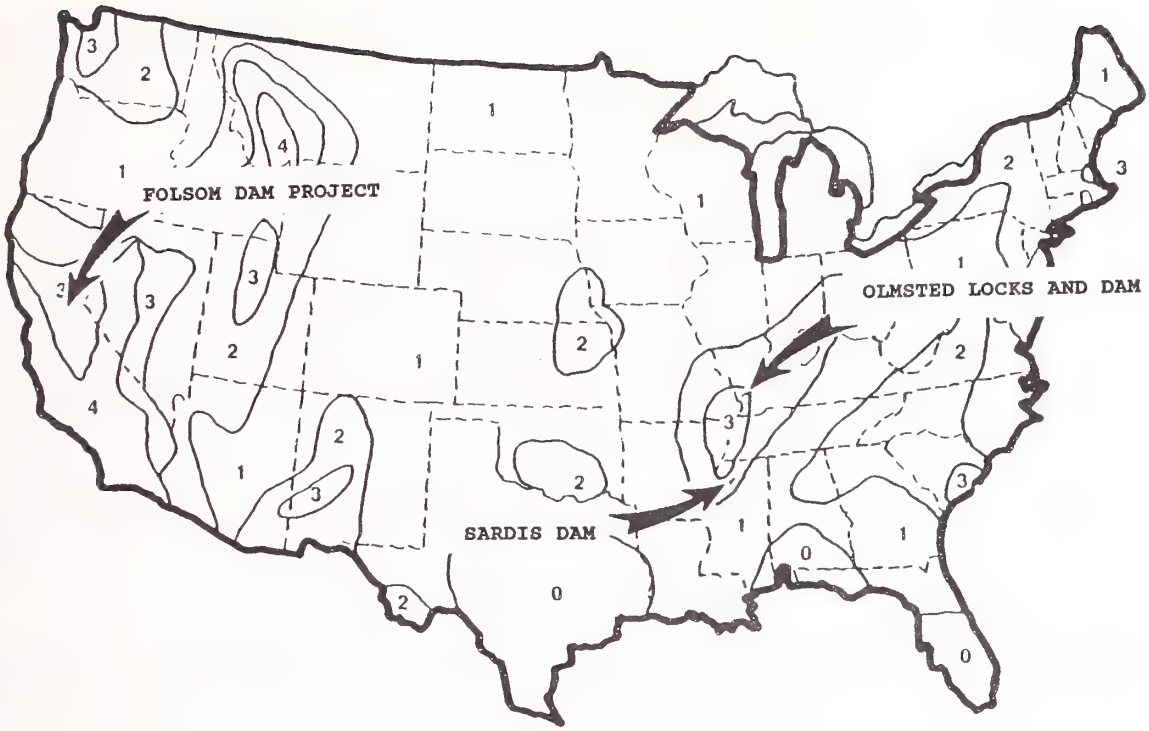

Figure 1. Locations of three Corps projects

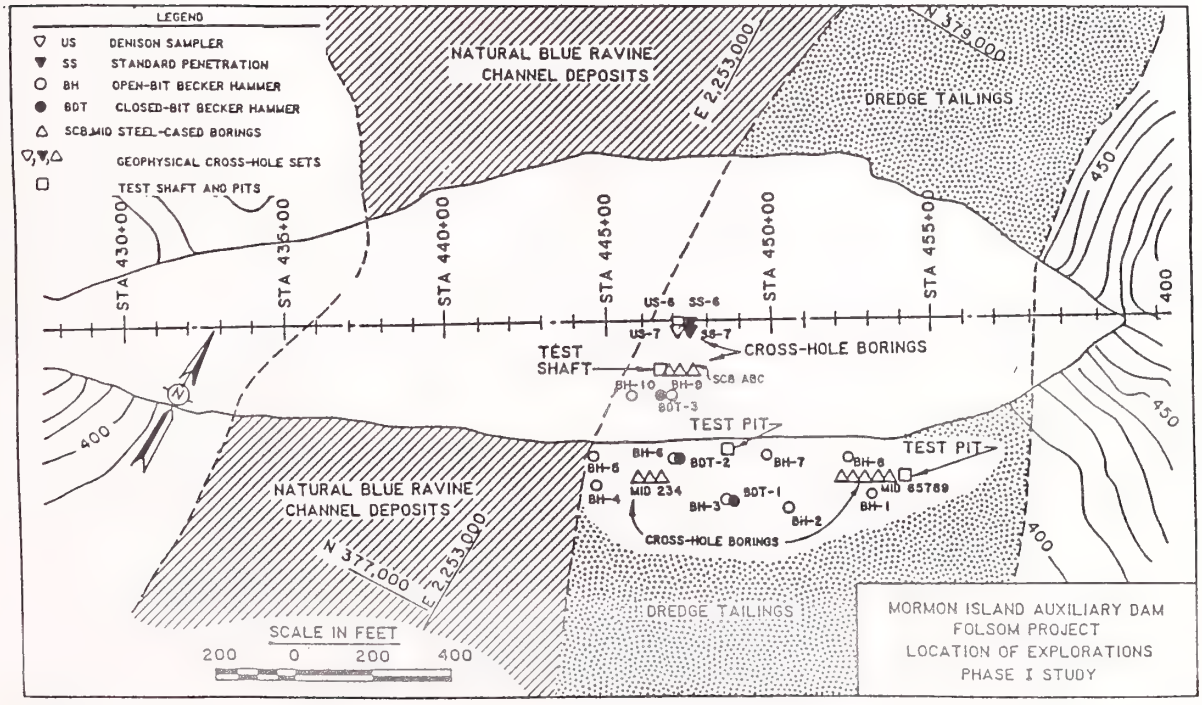

Figure 2. Plan of Mormon Island Auxiliary Dam, Folsom Project, showing locations of field investigations

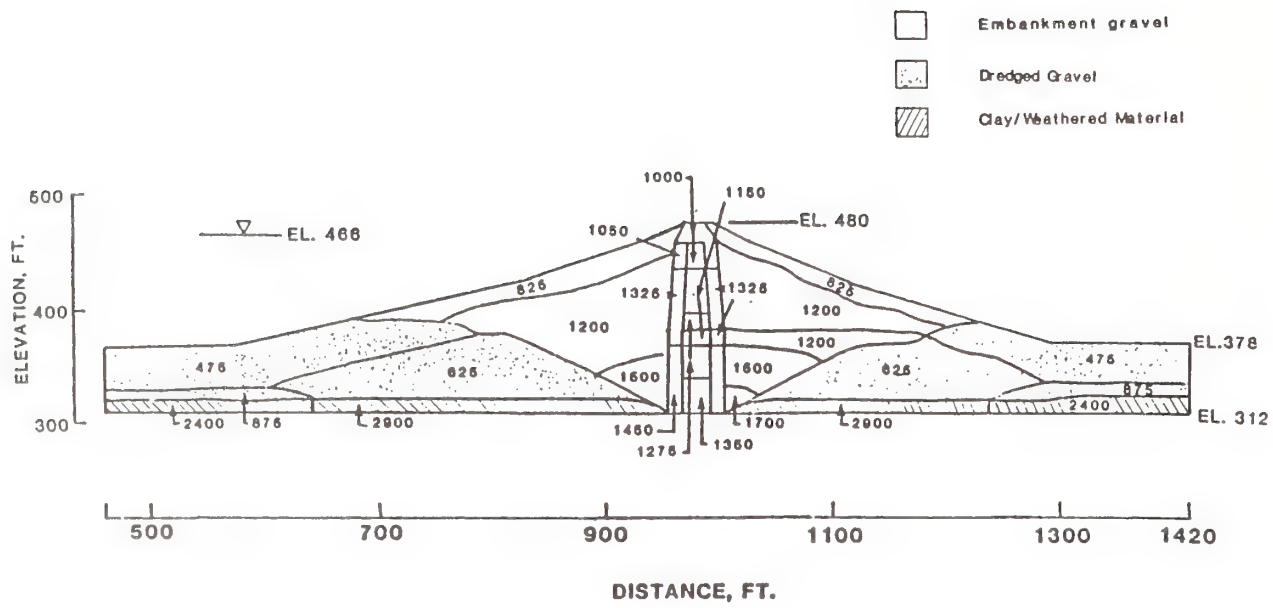

Figure 3. Idealized section of Mormon Island Auxiliary Dam, Folsom Project, showing estimated shear wave velocities in fps

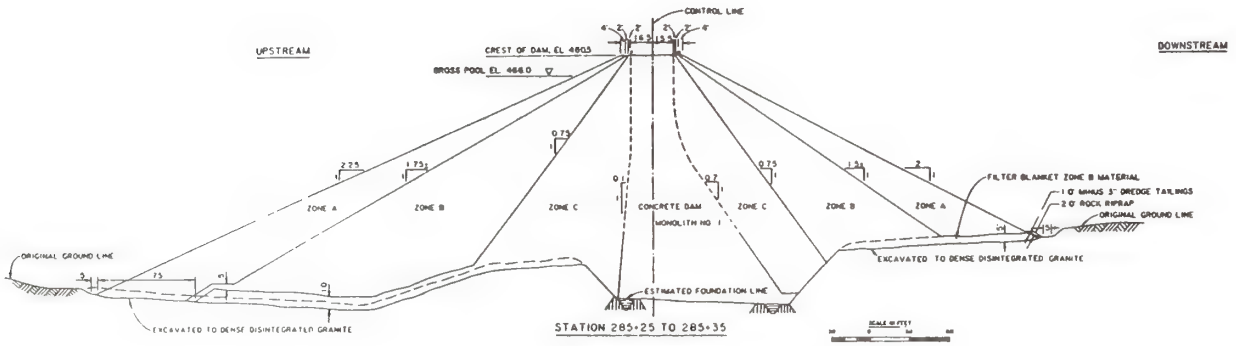

Figure 4. Typical section of Wing Dam, Folsom Project, at interface with Concrete Gravity Dam

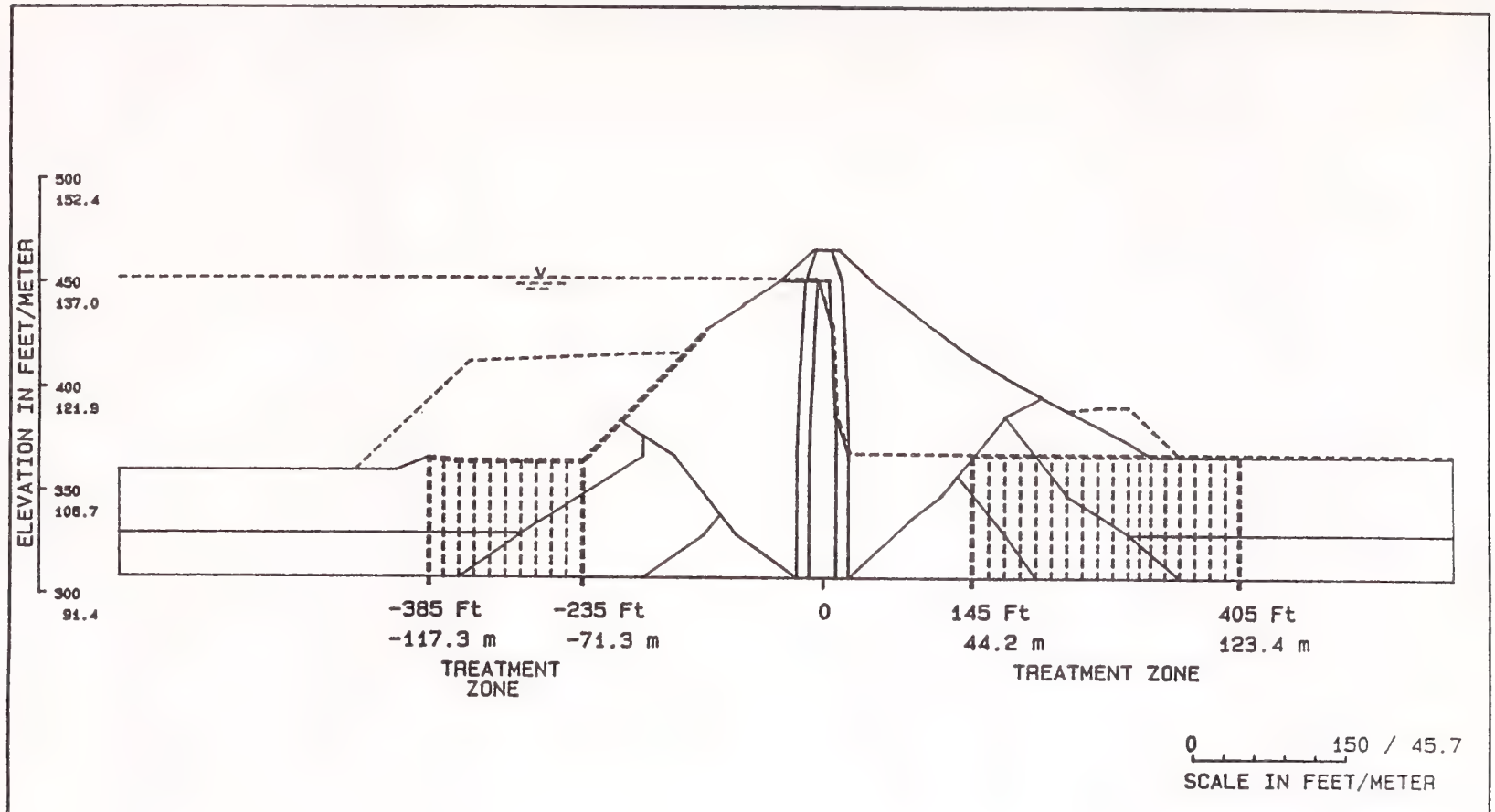

Figure 5. Conceptual plan of pore pressure control alternative for remediation at Mormon Island Auxiliary Dam (after Ledbetter et al. 1991)

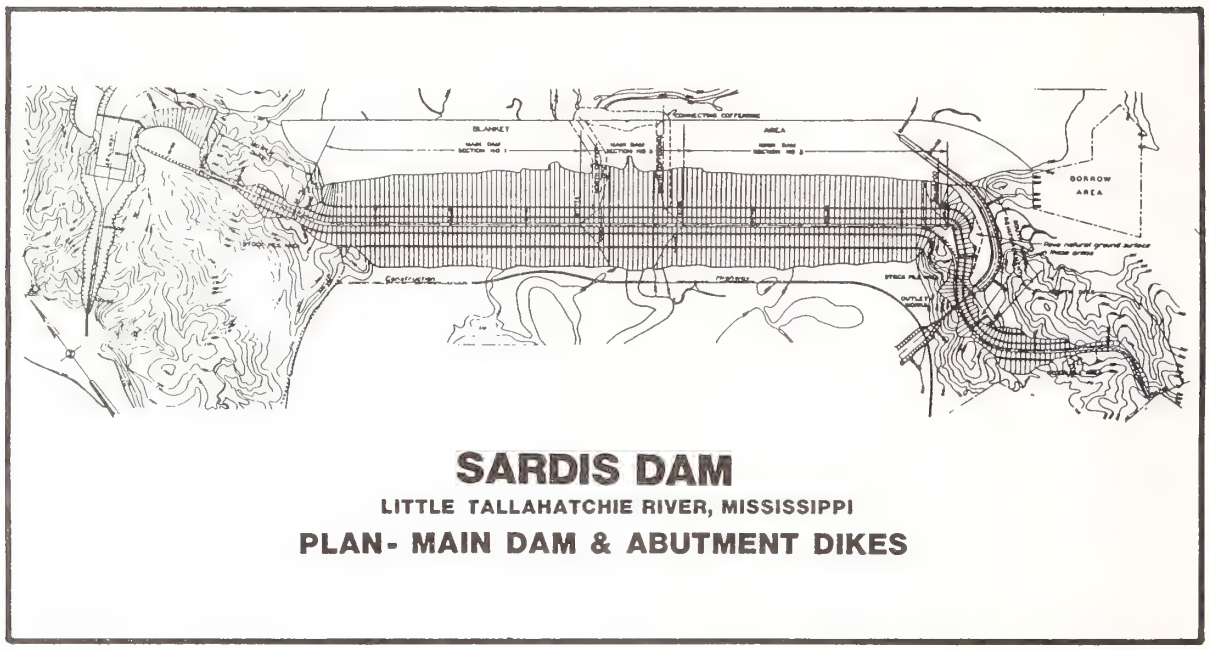

Figure 6. Plan of Sardis Dam, Mississippi

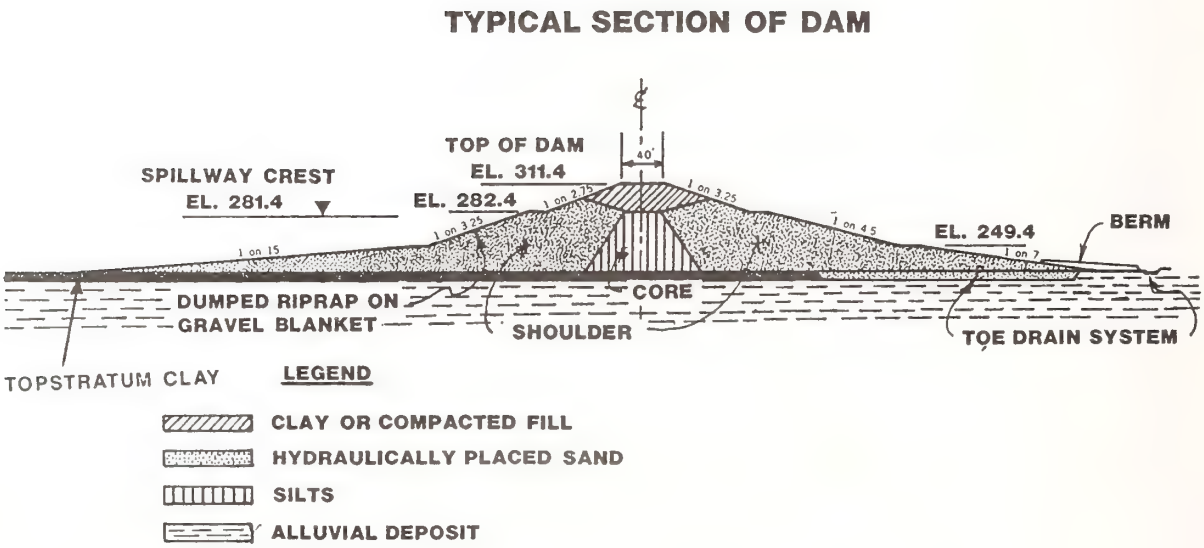

Figure 7. Idealized section of Sardis Dam, Mississippi

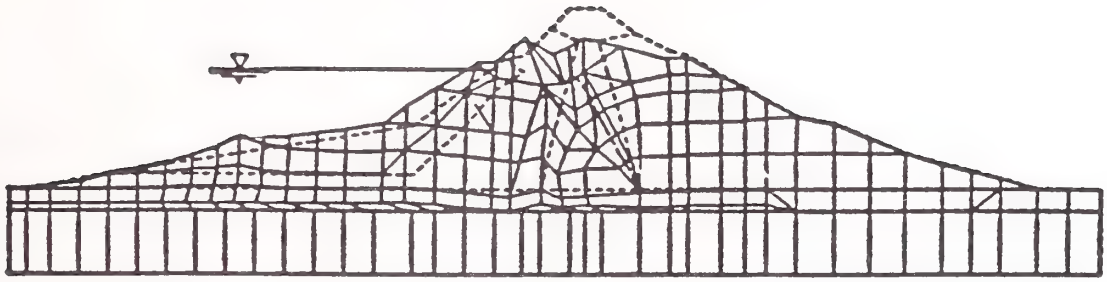

Figure 8. Initial and post-liquefaction estimated shapes for Sardis Dam (without remediation, after Finn et al. 1991)

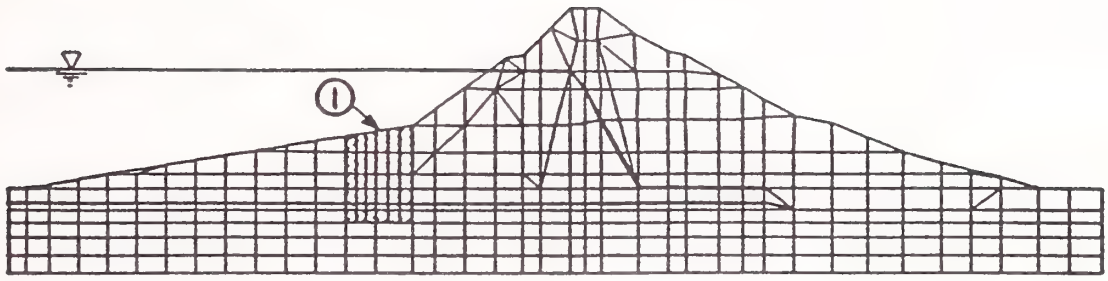

Figure 9. Conceptual plan for remediation of Sardis Dam by strengthening and stiffening upstream foundation materials (after Finn et al. 1991)

A Progress Report on the Worldwide Earthquake Risk Management (WWERM) Program

by

S. T. Algermissen[1], Walter W. Hays[1], and Paul R. Krumpe[2]

ABSTRACT

Considerable progress has been made in the Worldwide Earthquake Risk Management (WWERM) Program since its initiation in late 1989 as a cooperative program of the Agency for International Development (AID), Office of U.S. Foreign Disaster Assistance (OFDA), and the U.S. Geological Survey. Probabilistic peak acceleration and peak Modified Mercalli intensity (MMI) maps have been prepared for Chile and for Sulawesi province in Indonesia. Earthquake risk (loss) studies for dwellings in Gorontalo, North Sulawesi, have been completed and risk studies for dwellings in selected areas of central Chile are underway. A special study of the effect of site response on earthquake ground motion estimation in central Chile has also been completed and indicates that site response may modify the ground shaking by as much as plus or minus two units of MMI. A program for the development of national probabilistic ground motion maps for the Philippines is now underway and pilot studies of earthquake ground motion and risk are being planned for Morocco.

KEYWORDS; Earthquake; hazard; international; risk

1. INTRODUCTION

The WWERM Program was developed as an outgrowth of an Executive Briefing on "Strategic Planning to Reduce Economic Impacts of Earthquake Hazards throughout the World" held at the National Academy of Sciences, Washington, D.C., on March 8 and 9, 1988 (Williams and Hays, 1988). This Executive Briefing established the need for a more quantitative evaluation of the potential for earthquake disasters and for the assessment of the economic impact and casualty loss potential of such disasters. In addition, the need to assess the long-range economic losses associated with destructive earthquakes was also outlined.

Algermissen and others (1991) reported on the WWERM Program from its inception through mid-1991. Here we report on progress in the WWERM Program from mid-1991 through May 1992.

2. OBJECTIVES OF THE PROGRAM

The initial objectives of the program were to develop an action plan and conduct a pilot program in each of three geographic regions to demonstrate the utility, importance, feasibility, and need for uniform

[1]U.S. Geological Survey

[2]Department of Energy

global earthquake hazard mapping and risk assessment/management as a contribution to the International Decade for Natural Disaster Reduction (IDNDR).

The initial three geographic areas for pilot studies were Morocco, Perú/Chile, and Indonesia. Since the initiation of the project in 1990, the scope of the work has been greatly expanded through the funding of additional program in Indonesia and the Philippines by the AID Mission in each country. The supplemental funding from the AID Office in Indonesia has permitted the following additional work: (1) a comprehensive assessment of earthquake ground motion in North Sulawesi Province; and (2) the calculation of estimates of expected future losses to masonry dwellings in Gorontalo, North Sulawesi. Funding from the AID Mission in the Philippines has allowed us to undertake a comprehensive program of earthquake ground-motion assessment for the entire country together with pilot studies of future expected earthquake losses. As in Indonesia, OFDA has provided supplemental funding that has made it possible to purchase and transfer a MacIntosh computer and associated equipment to the Philippine Institute of Volcanology and Seismology (PHIVOLCS) for training and technology transfer for seismic hazard mapping and risk assessment.

As work progresses, we are continuing to expand the technical horizons of WWERM with the hope that the project will eventually become global in scope.

3. PROGRESS

3.1 Chile

Because of funding and technical results available from an earlier OFDA-USGS Project "Seismic Zoning and Implementation of Improved Earthquake Resistant Design in Chile" which in many ways complemented the WWERM Program, it has been possible to develop a considerably broader program in Chile with results and products having widespread application. These products include: (1) probabilistic acceleration and seismic intensity maps of the entire country for an exposure time (period of time of interest) of 50 years and 10 percent chance that the mapped values will be exceeded; (2) comprehensive evaluation of the "site effect" in central Chile, that is, the contribution of the surface geology to the modification of ground shaking during earthquakes; and (3) collection of data for loss assessment.

A probabilistic ground acceleration map for a time period of interest of 50 years is shown in Figure 1. A similar map of seismic intensity for central Chile is shown in Figure 2. These maps are prepared for "average" site conditions in Chile. The primary use of the acceleration maps is to provide the ground motion basis for the earthquake resistant design of structures either for a specific building or as part of the seismic provisions in a building code. The primary use of the intensity maps is to present the expected levels of damage (in descriptive form) for disaster preparedness, mitigation, and land use planning. Figure 3 shows the magnitude of the variation in ground shaking (in units of intensity) associated solely with variations in surface geology. Figure 4 shows how these variations in shaking can be incorporated into probabilistic seismic intensity maps to provide a more realistic estimate of the maximum ground shaking levels that may occur in an area in a specific time period of interest. The level of refinement of estimated ground motion shown in Figure 4 is generally not available, even for most areas of the United States, and represents a state-of-the-art product. The importance of surface geology in controlling ground shaking during earthquakes was first appreciated in Chile after the M_s=7.9, central Chile earthquake of 1985. This is, however, the first study to describe this effect in a

quantitative manner. We anticipate that the intensity maps in this study will be of considerable use in disaster preparedness, mitigation, and land use planning in central Chile.

During October 1991, USGS personnel participated in an international seminar and a separate workshop, both related to the WWERM Project. The first meeting was organized by UNDRO, MAPFRE (a Spanish reinsurance company, ONEMI (the national emergency office in Chile), the Universidad de Chile, the Caja Reaseguradora de Chile (a Chilean insurance company), and the USGS. This "Seminario Internacional" held in Santiago from October 21-24, 1991, was entitled "Disastres Sismicos Urbanos, Codigo de Construccion Sismoresistente y Seguros" (Urban Seismic Disaster, Earthquake Resistant Construction Codes and Insurance).

A workshop entitled "Applicacion de Mapas Probabilisticos de Movimientos Fuertes para la Reduccion del Riesgo Seismico en Chile" (Application of Probabilistic Maps of Strong Motion to the Reduction of Seismic Risk in Chile) was organized by the USGS and the Universidad de Chile during the week following the international seminar. This highly technical workshop was designed to make the results of the two OFDA-USGS projects in Chile available to scientists, engineers, and disaster management specialists in Chile. In particular, scientists and engineers from the major Chilean universities and from major consulting firms involved in the development and revision of the earthquake resistant design provisions of the Chilean National Building Code, together with disaster preparedness and mitigation specialists from ONEMI (the national emergency office in Chile), were invited to attend and participate in the workshop. The papers presented at the USGS-Universidad de Chile workshop are currently being edited. These papers will be published in a special issue of "Revista Geofisica", a professional journal published by the Pan American Institute of Geography and History with wide circulation in Latin America.

3.2 Indonesia

The earthquake hazard and risk study of North Sulawesi, Indonesia, was completed in August 1991, in advance of a workshop held in Bandung in September 1991. Products of the Pilot Study include: (1) synthesis of the geologic structures related to earthquake occurrence in the area; (2) expected peak horizontal ground acceleration on both hard rock and soft soil that have a 90 percent probability of not being exceeded in 50 years; (3) development of inventory and earthquake vulnerability relationships for dwellings; and (4) estimation of both future average annual loss and catastrophe potential for the dwelling stock in Gorontalo, North Sulawesi. Papers on all aspects of the Pilot Study were presented at the workshop in Bandung. A technical paper "Probabilistic Seismic Hazard Estimates in North Sulawesi Province, Indonesia" describing the results of the Pilot Study will be presented at the SECOND-ASIA CONFERENCE on **Engineering for Mitigating Natural Hazards Damage** that is scheduled for Yogyakarta, June 22-26, 1992, (Thenhaus and others, 1992).

3.3 The Philippines

The WWERM Program will begin in the Philippines in June 1992. The intention is to: (1) prepare national probabilistic hazard maps for all of the country; (2) to undertake pilot studies of future earthquake losses in selected areas of the country; and (3) to conduct training and technology transfer in earthquake hazard and risk assessment in conjunction with the Philippine Institute of Volcanology and Seismology (PHIVOLCS).

3.4 Morocco

The Morocco phase of WWERM has been much delayed, first because of the Persian Gulf War, and second, because of the accelerated program of hazard and risk assessment that was undertaken in Indonesia. The work in Morocco will include a demonstration project of earthquake hazard (ground motion) and risk (loss to dwellings) in selected areas. The work will be done cooperatively with the Center for Technical and Scientific Research (CTSR) in Rabat, Morocco. Work in Morocco will begin in August 1992.

4. SUMMARY

Major studies of earthquake ground motion estimation have been completed in Chile and investigations of risk to dwellings in Central Chile are nearing completion. Similar studies have been completed in Sulawesi, Indonesia. Very successful workshops highlighting the technical results have been held in Chile and Indonesia. A major study of earthquake ground motion and pilot studies of seismic risk to dwellings will begin in the Philippines in June 1992 followed by pilot studies of earthquake ground motion and risk in Morocco.

5. REFERENCES

Williams, M.E. and Hays, W.W., 1988, Strategic Planning to Reduce Economic Impacts of Earthquake Hazards throughout the World, Proceedings of the Executive Briefing, National Academy of Sciences, Washington, D.C., March 8-9, 1988, U.S. Geological Survey, Open-File Report 88-361, 149 pps and Appendices

P.C. Thenhaus, I. Effendi and E. Kertapati, Probabilistic Seismic Hazard Estimates in North Sulawesi Province, Indonesia, 1992, to be presented at the SECOND-ASIA CONFERENCE on Engineering for Mitigating Natural Hazards Damage

S.T. Algermissen, Paul R. Krumpe, and Walter W. Hays, 1991, The worldwide earthquake risk management program, Proceedings, 23rd Joint Meeting of the U.S-Japan on Wind and Seismic Effects, Tsukuba, Japan, May 12-17, 1991.

S.T. Algermissen and Paul C. Thenhaus, 1992, The Worldwide Earthquake Risk Management Program: A Program for Global Earthquake Hazard Assessment, presented at the 1992 Joint Spring Meeting, May 12-16, 1992, of the American Geophysical Union in Montreal, Canada

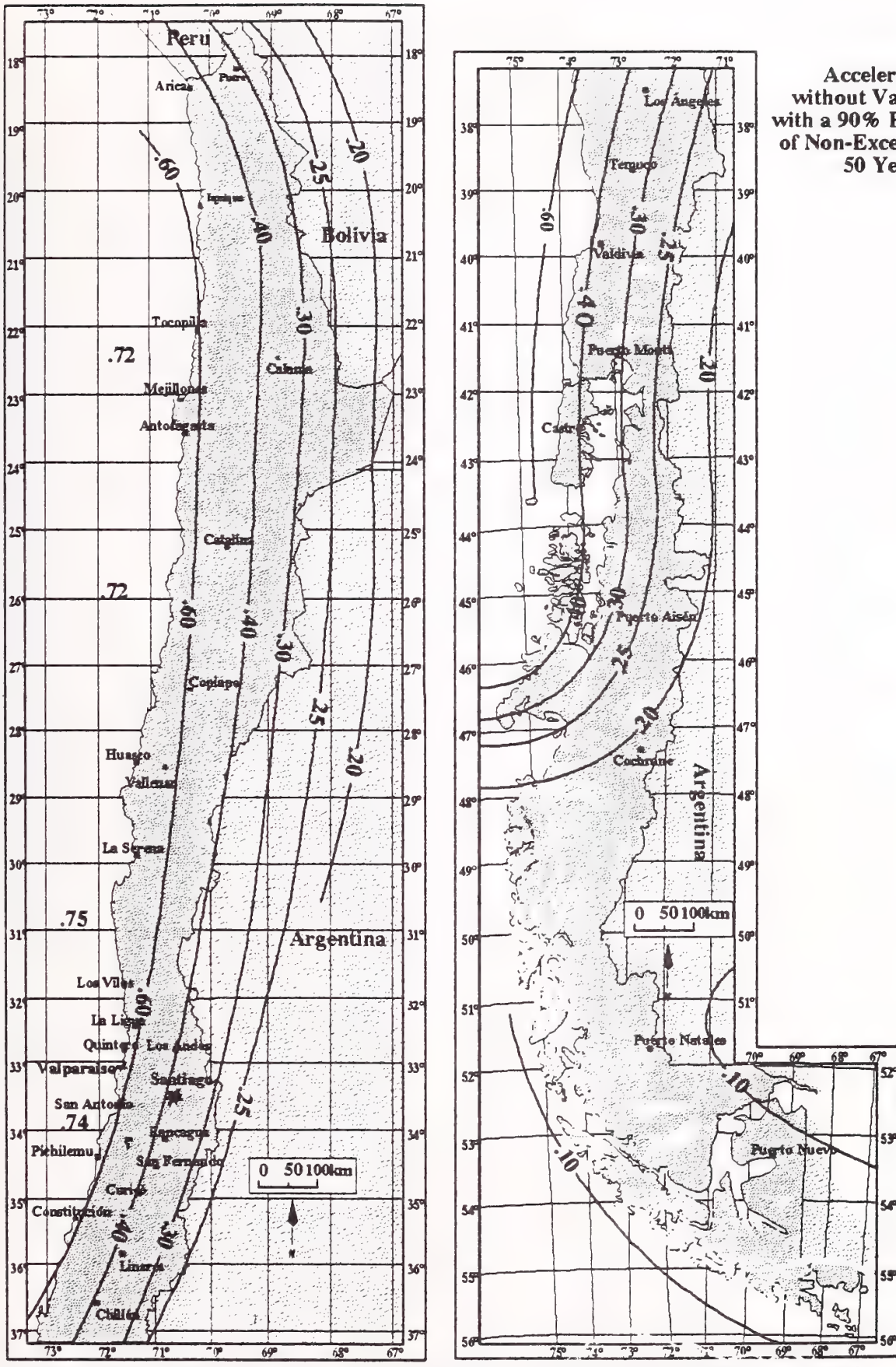

Figure 1. Probabilistic ground motion acceleration map of Chile for a 50 year time period of interest. The ground motions mapped have only an estimated 10% chance of being exceeded in 50 years. Maps of this type are widely used as design maps in the earthquake resistant design provisions of building codes.

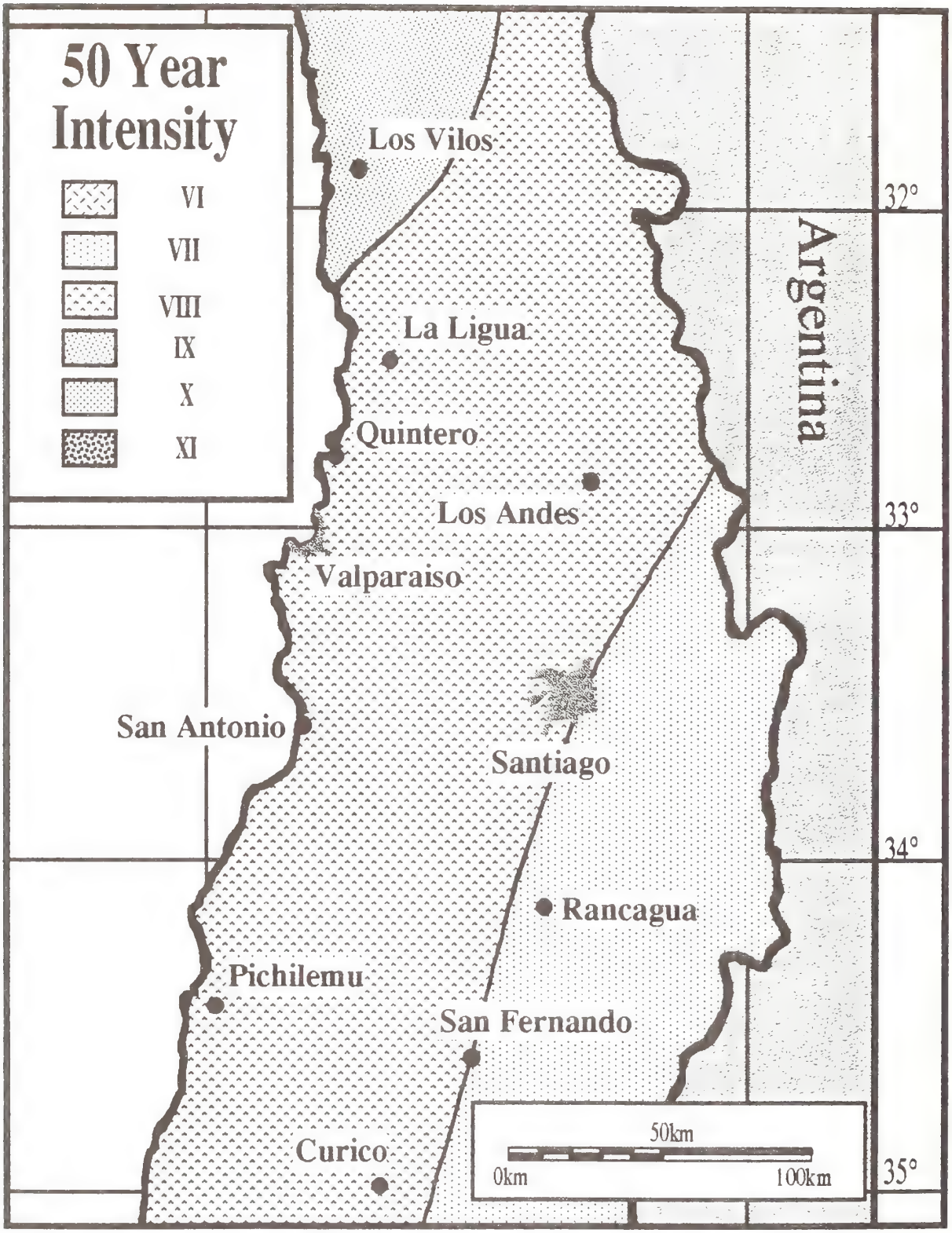

Figure 2. Probabilistic ground intensity map of Chile for a 50 year time period of interest. The ground motions mapped have only an estimated 10% chance of being exceeded in 50 years. Maps of this type are often combined with site specific shaking maps (such as Figure 3) to produce probabilistic ground shaking maps that include the site specific response associated with the near surface materials beneath a site.

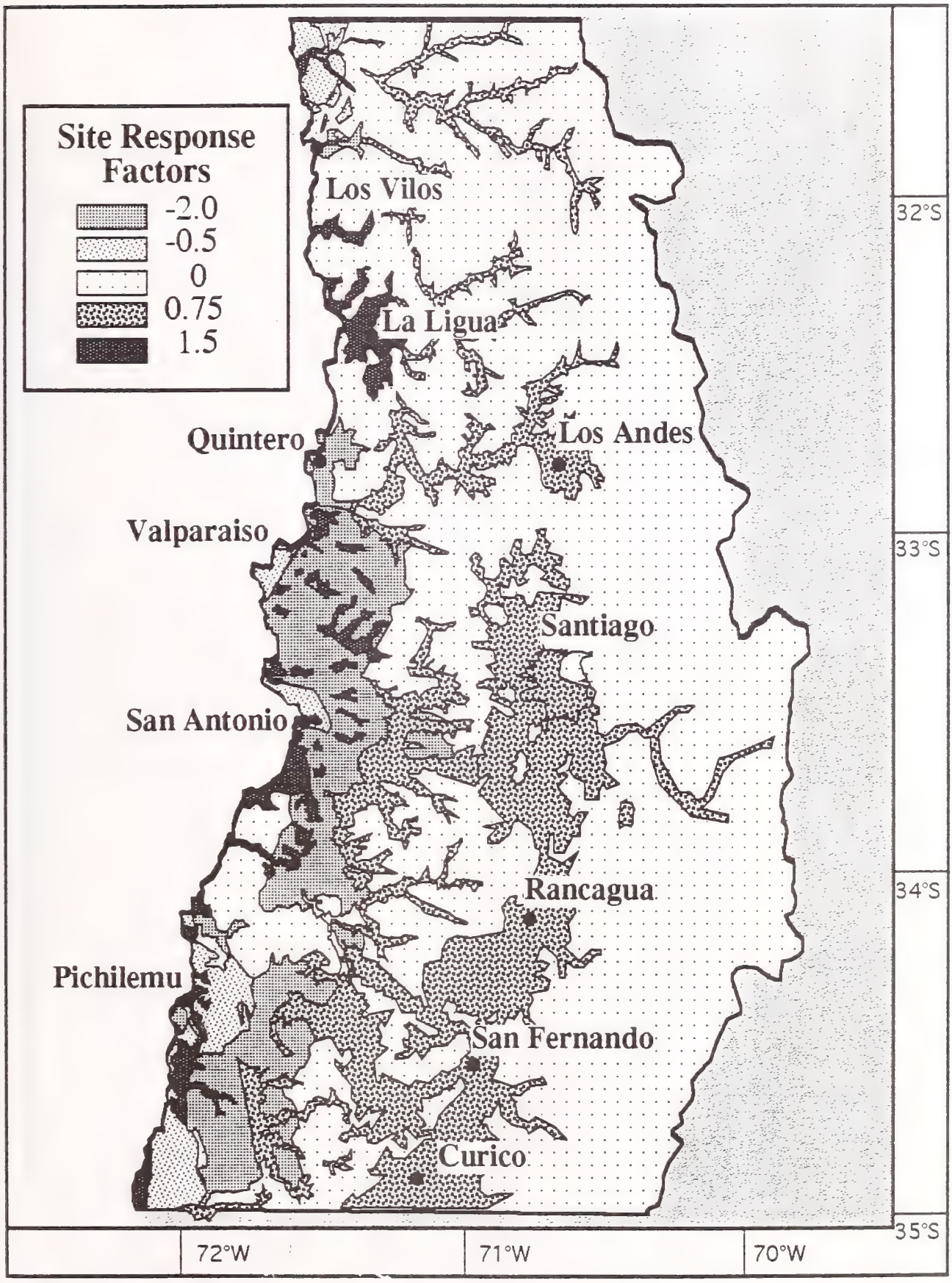

Figure 3. Site specific response factors associated with the near surface materials in central Chile. This map is combined with the regional ground motions shown in Figure 2 to produce the map in Figure 4.

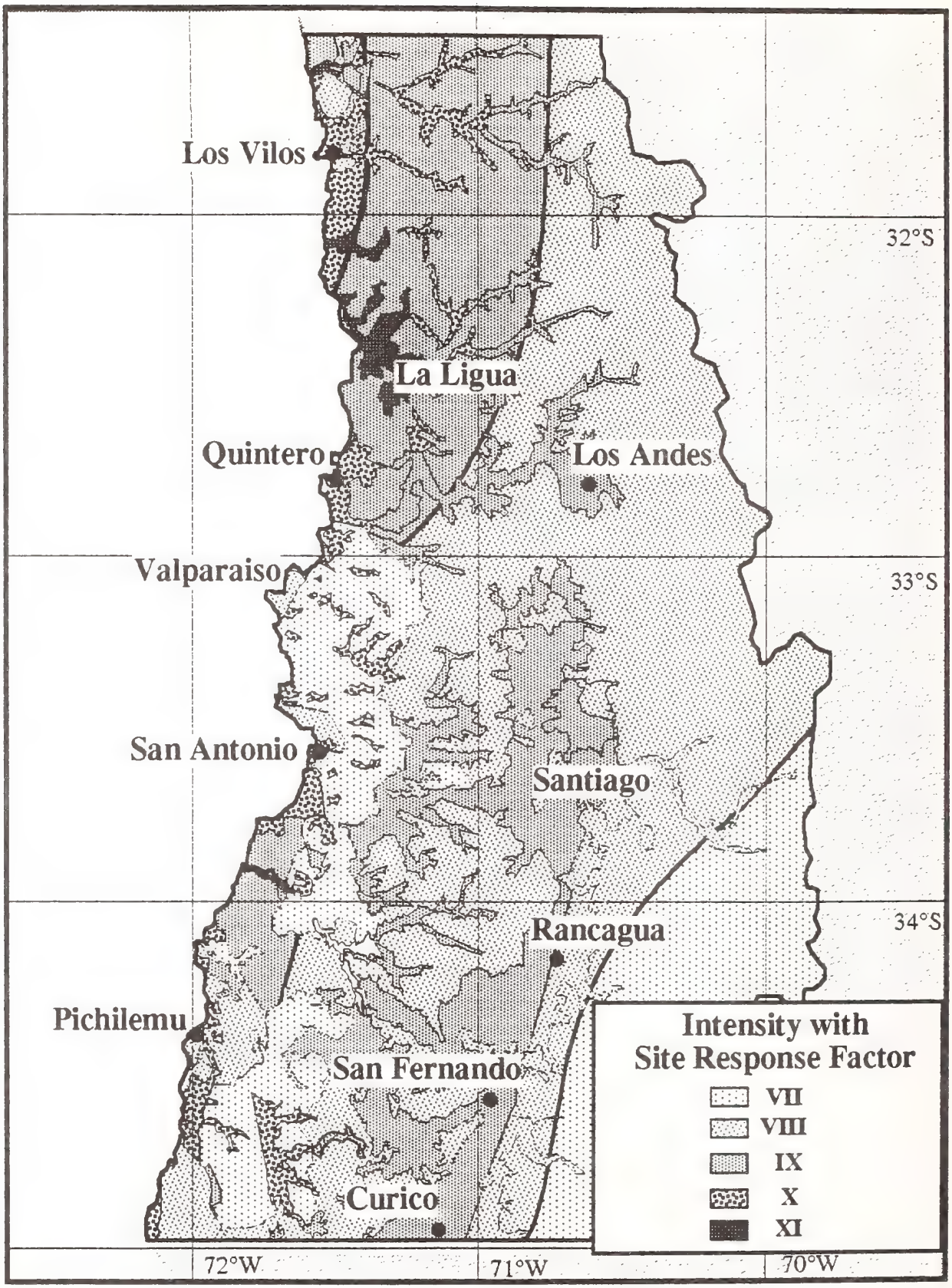

Figure 4. Probabilistic ground motion intensity map of central Chile for a 50 year time period of interest. This map combines the mapped values of Figure 2 with those of Figure 3 to produce a probabilistic ground motion map that includes the effect of near surface materials. These maps are valuable in disaster preparedness, mitigation, land use planning and earthquake risk (loss) studies because they represent an estimate of the maximum damage (and consequently loss) that is expected to occur in the period of time considered in the mapping.

Development of Advanced Reinforced Concrete Buildings Using High-Strength Concrete and Reinforcement Researches on Structural Performance Conducted in 1991

by

Tatsuo Murota[1], Hisahiro Hiraishi[2], Takashi Kaminosono[3], Masaomi Teshigawara[4], Hitoshi Shiohara[5], and Hideo Fujitani[6]

ABSTRACT

A five-year National Project has been promoted by the Ministry of Construction of Japan since 1988 to develop such structures as super high-rise reinforced concrete buildings using high strength and high-quality concrete and reinforcing steel. The project is simply referred as to "New RC". This paper describes the outlines of some research subjects which were conducted in 1991, related to structural performance.

1. INTRODUCTION

Reinforced concrete (hereafter referred as to "RC") has widely been used for medium rise buildings because of the low cost, excellent durability and easy maintenance, so on. However, it is impossible to realize the super high-rise buildings and buildings with long spans which are currently required from the social point of view, if the material strength remains within ordinary ones.

The Project aims to produce high strength concrete of the specified strength of from 300 kgf/cm2 to 1,200 kgf/cm2 (30 to 120 MPa) and high strength and high quality reinforcing steel bars of the yield strength of 4,000 kgf/cm2 to 12,000 kgf/cm2 (400 to 1,200 MPa), and to develop new fields of RC buildings by utilizing them.(Fig. 1)

2. RESEARCHES ON REINFORCING STEEL BARS AND REINFORCED CONCRETE ELEMENTS

2.1 Research Items

2.1.1 Development of High Strength & High quality Reinforcing Steel

a. Development of Technology for Producing High Strength & High Quality Reinforcing Bars, and their Fundamental Mechanical Properties.

b. Weldability of High Strength Reinforcing Bar by Gas Pressure Welding Method

c. Weldability of High Strength Reinforcing Bar by Butt-Welding by Special Process

d. Damage due to Bending and Straightening of High Strength Reinforcing Bars.

e. Strain Aging Property of High Strength Reinforcing Bar

f. Performance of Mechanical Connector for Splicing Reinforcing Bars

g. Performance of Member using Reinforcing Bars with High Yield Ratio and splicing Threaded Couplers

h. Framework of Draft Code for High Strength Reinforcing Bars

2.1.2 Fundamental Mechanical Properties of Reinforced Concrete using High Strength Materials

a. Mechanical Properties of Confined High Strength Concrete

b. Local Buckling of Longitudinal Reinforcing Bars in Flexure Hinge Region

c. Constitutive Model for High Strength Concrete and Reliability of Non-Linear Finite Element Analysis

d. Strength of Plate Anchorage of Beam Longitudinal bar in Exterior Beam-Column-Joint

e. Development of Standard Bond Test Procedure for High Strength Concrete

f. Development of Design Equation for Bond-splitting Strength in Flexure Member

2.2 Results

2.2.1 Development of High Strength & High

1 Director, Structural Engineering Department, Building Research Institute (BRI)

2 Head, Structural Division, Structural Engineering Department, (BRI)

3 Head, Dinamic Division, Structural Engineering Department, (BRI)

4 Senior Research Associate, Large Scale Structure Testing Division, Production Department (BRI)

5 Senior Research Associate, 2-nd Earthquake Engineering Division, IISEE (BRI)

6 Research Associate, Stuructural Division, Structural Engineering Department (BRI)

Quality Reinforcing Steel

a. Development of Technology for producing High Strength & High Quality Reinforcing Bars, and their Fundamental Mechanical Properties

Sample of four different grades of high strength deformed reinforcing bars had been produced. The specified yield strength of the grade USD685 are 685 MPa and designed as high strength mild steel with clear yield plateau. The specified yield strength of the grade USD980 is 980 MPa. It is designed as high-strength steel without yield plateau. Both of these two grades are intended to be used for longitudinal reinforcing bars. The grades USD785 and USD1275 are intended to be used exclusively for transverse reinforcing bar including hoops, stirrups with specified yield strength of 785 MPa and 1275 MPa respectively. Basic mechanical properties including (1) chemical ingredients, (2) yield strength and its scatterings, (3) fracture strain, (4) ratio of yield strength to tensile strength, (5) yield plateau length (6) minimum allowable bend radius were investigated.

b. Weldability of High Strength Reinforcing Bars by Gas Pressure Welding Method

In order to asses the possibility of splicing by gas pressure welding method, tensile tests and bending tests were carried out with respect to grade USD685 D25 reinforcing bars. Gas pressure welding splice could transfer full tensile strength of the reinforcing bars. It was impossible to bend 180 degrees, because they broke during bending due to brittle fracture affected by welding heat.

c. Weldability of High Strength Reinforcing Bars by Butt-Welding by Special Process

High strength welding rod with strength of 1,000 MPa was developed for splicing by butt-welding method. In order to asses the possibility of butt-welding of the grade USD685 D25 reinforcing bars, tensile tests were carried out. Butt welding splice could transfer yield strength but it could not transfer full tensile strength of the reinforcing bars due to brittle fracture of the part affected by welding heat.

d. Damage due to bending and straightening of High Strength Reinforcing Bar

In order to asses the damage caused during bending and straightening, tests of 90 degree bending followed by straightening were carried out with respect to D25 with grade USD685 and USD980. Inside radius of bending was 3.6 db, 4.8 db and 8.0 db; db is nominal diameter of reinforcing bar. Reinforcing bars with normal deformation of grade USD685 and USD980 showed no damage by appearance after 90 degree bend as far as inside radius is equal or larger than 4.8 db. Reinforcing bar with threaded deformation of grade USD685 could be bend if inside radius is equal or larger than 4.8 db, while USD980 needed minimum inside radius of 8.0 db. To get no damage during straightening, minimum inside radius of 8.0 db were needed.

e. Strain Aging Property of High Strength Reinforcing Bar

In order to asses the strain aging property of high strength reinforcing bar, strain aging tests of grade USD685 reinforcing bars were carried out. The reinforcing bars were stretched until the tensile strain attained to 50 % of fracture strain, then strain aging were enhanced by high temperature condition (100 °C * 1 hour). The graded USD685 reinforcing bars produced by "in-line quenched and tempered" process showed no strain aging.

f. Performance of Mechanical Connector for Splicing Reinforcing Bars

High strength threaded sleeves coupler was developed. The mechanical connector was intended to be used for splicing threaded deformed reinforcing bars. In order to asses the reliability of the splicing system, tensile tests of spliced reinforcing bars were carried out. The developed splicing system could transfer full strength of the USD685 reinforcing bar.

g. Performance of Members using reinforcing bars with high yield ratio and Splicing Threaded Couplers

The effect of high-yield ratio and splicing couplers on the strain concentration at flexure critical section are investigated by tests of half-scale three cantilever beam specimens with tensile reinforcement ratio of 0.5 %. Specimens were subjected to statically cyclic load to failure. Figure 2.1 compares the force-deflection relations of specimens using longitudinal reinforcements with yield ratio of 90 % and 75 %. Fracture of longitu-

dinal reinforcements was observed during the test of specimen using the bars whose yield ratio was 90 %. The necessity to limit maximum yield ratio for high strength steel in the code were recommended.

h. Framework of Draft Code for High Strength Reinforcing Bars

Framework of draft code for Reinforcing Bars were proposed.

2.2.2 Fundamental Mechanical Properties of Reinforced Concrete using High Strength Material

a. Mechanical Properties of Confined High Strength Concrete

Analytical models which predict compressive stress-strain relation for confined concrete are surveyed form literature. From the point of view of (1) simplicity, (2) correlation, (3) universal applicability from normal strength concrete to high strength concrete, the effectiveness of existing models are evaluated using test results of uniaxial compressive tests obtained in this research project.

Figure 2.2 shows the comparison of the prediction of ultimate strength by typical existing model and the model proposed. The model proposed showed good correlation for square section column, while the classical model of Richart showed good correlation for circular column.

b. Local Buckling of Longitudinal Reinforcing Bars in Flexural Hinge Region

Twenty four stubbed column specimens using high strength longitudinal bars were subjected to monotonically increasing compressive force, in order to investigate the effect of hoop spacing on the behavior of local plastic buckling of longitudinal reinforcement. Figure 2.3 (a) shows the typical geometry and the dimensions of the specimens. Two slits were made between loading steel plate stabs and longitudinal reinforcement so that the compressive force should be transmitted by steel bars only. All of the specimen showed the local plastic buckling after compressive yield of longitudinal reinforcement. As increasing the spacing of the hoops, ultimate strength decreased and strength degraded suddenly after ultimate strength reached as shown in Figure 2.3 (b).

c. Constitutive Models for High Strength Concrete and Reliability of Non-Linear Finite Element Analysis

Several existing non-linear finite element analysis codes are selected for analytical platforms and were implemented with non-linear constitutive model considering the mechanical properties of high strength material. Figure 2.4 shows the typical model parameters essential for modeling of high strength concrete. Reliability of the programs have been examined by comparison between analytical results and tests results of benchmark specimens selected from member tests carried out in the New RC project.

d. Strength of Plate Anchorage of Beam Longitudinal bars in Exterior Beam-Column-Joint

Pull-out tests of 56 end plate anchorages were carried out, which simulate the beam longitudinal rebars developed in exterior beam-coloumn-joint to investigate the force transfer mechanism and to develop design method of the end plate. Figure 2.5 explains the concept of the tests and the test variables.

e. Development of Standard Bond Test Procedure for High Strength Concrete

The effect of the shape of deformation on the surface of reinforcing bars on tensile splitting bond strength developed in high strength concrete with compressive strength of approximately 100 MPa were investigated by 9 simple bond test specimens.

f. Development of Design Equation for bond-splitting Strength in Flexure Member

Bond-splitting strength tests of 26 high strength concrete beams were carried out to derive empirical design equation for bond strength which takes into accounts the effects of (1) concrete compressive strength (2) bond length (3) amount of transverse reinforcement, (4) number of legs of stirrups or hoops. Design equation was proposed based on the tests.

3. RESEARCHES ON STRUCTURAL PERFORMANCE OF MEMBERS

3.1 Research Items

3.1.1 Flexural Behavior of Columns and Beams

a. Bond splitting failure of columns and beams after flexural yielding
b. Deformation capacity of columns under high-axial force after flexural yielding
c. Minimum reinforcement ratio of beams
d. Numerical analysis using micro models

3.1.2 Shear Behavior of Columns and Beams

a. Shear behavior of columns and beams
b. Bond splitting failure of columns
c. Shear behavior of beams with small openings
d. Numerical analysis using micro models

3.1.3 Shear Behavior of Beam-Column Joints

a. Shear behavior of interior and exterior beam-column joints
b. Anchorage of exterior beam-column joints
c. Shear behavior of interior and exterior beam-column joints under bi-directional loading
d. Numerical analysis using micro models

3.1.4 Shear and Flexural Behavior of Shear Walls

a. Shear capacity of shear walls
b. Flexural deformation capacity of shear walls
c. Deformation capacity of shear walls under bi-directional loading
d. Development of analytical models and parametric studies

3.2 Results

3.2.1 Flexural Behavior of Columns and Beams

a. Experimental study on columns were performed to investigate the relationship between axial stress and deformation capacity. Figure 3.1 shows the results.

   In Figure 3.1, η means axial stress level (η = axial force divided by compressive strength of concrete and cross sectional area of column).

   The specimens S6, S7 and S10 which are subjected to high axial stress (η = 0.5) have smaller deformation capacity than the others (η = 0.35, 0.15).

   Vertical Cracks occurred along the height in the specimen S7 with shear span ratio of 1.5 (η = 0.5) (Fig. 3.2).

b. In case of the beams with double layer longitudinal reinforcement, bond splitting failure of the second layer longitudinal reinforcement occurred early compared with that of the first layer longitudinal reinforcement.

3.2.2 Shear Behavior of Columns and Beams

a. Shear Strength of columns obtained by the test is higher than that calculated by A-method of AIJ [1], but lower than that by B-method of AIJ [1].
b. Shear strength of the shear failure type of beams can be evaluated by A-method of AIJ [1].
c. Two specimens with an opening were tested. Figure 3.3 shows the crack pattern of them. The specimen L1 has reinforcement with long anchorage for the opening, and the specimens S1 has reinforcement with short anchorage for the opening.

3.2.3 Shear Behavior of Beam-Column Joints

a. In the interior beam-column joints of New RC, coefficient for effective compressive strength concrete v decreases rapidly and the joint will fail early compared with the joint by normal strength RC.
b. In the exterior beam-column joints of New RC, anchorage strength of beam reinforcement with double layer arrangement is smaller than that of beam reinforcement with single layer arrangement.

3.2.4 Shear and Flexural Behavior of Shear Walls

Five flexural walls were tested to investigate the ductility under bi-directional lateral loading. Variables in this test are (1) loading hysteresis, (2) ratio of axial stress, (3) concrete strength, and (4) confinement of columns and wall panel.

Figure 3.4 shows the loading system and Fig. 3.5 shows the loading path.

Figure 3.6 shows the horizontal force and displacement relationships. Deformation ductility of the shear wall under bi-directional cyclic loading was influenced by the axial strain of columns and wall panel.

4. DESIGN GUIDELINE

Design guideline committee is in activity to make a design guideline and design criteria for New RC buildings, and to show an example designed buildings. This section shows an outline of a design guideline and related research items to it.

4.1 Scope

This design guideline is adapted to a seismic design for an building which height is not more than 200 meters, and consists of moment resisting frame with/without multi-story structural wall.

Eccentricity of stiffness and mass in the building should be avoided.

Two hundred meters in height is correspond to 60 storied building for residence or 40 storied buildings for office. Up to 200 meters in height, lateral design load is, in general, determined by an earthquake load, not by an wide pressure. Following four types of buildings are temporarily designed and discussed to make a design guideline.

(1) Sixty stories apartment type buildings : Structural systems are a moment resisting frame and moment resisting frame and multi story structural wall.

(2) Forty stories office type buildings : Structural systems are a double tube and tube core wall

(3) Twenty five stories office type buildings : Structural systems is a moment resisting frame

(4) Fifteen stories office type buildings : Structural systems are a moment resisting frame and moment resisting frame and multi story structural wall

4.2 Materials

Materials in Zone I are specified in this design guideline.

Normal strength materials are allowable to be used. Combination of strength of concrete and steel will be provided in Structural Requirement.,

4.3 Design Principles

4.3.1 Design for gravity load

Allowable stress design is adopted.

Allowable compressive stress of concrete is one third of specified concrete strength (Fc), allowable tensile stress of steel is 196 – 215 MPa, and allowable compressive stress of steel is two thirds of its yield strength.

If necessary, cracking width should be checked.

Young modulus ratio of steel to concrete, and creep coefficient should be determined.

4.3.2 Design for seismic load

Against large level earthquake load [1], any members should not reach their yield strength. Against extra large level earthquake load [2], building drift should be within design drift (1/80 at each story [3]).

Against assuring design drift [4] all member should be safe.

In order to satisfy these criteria, following design procedure are proposed.

(1) Standard design base shear coefficient (Co):

By static analysis, yield of members should not be allowed at Co = 0.2. And Co of 0.25 is given to a building at assuring design drift. Design stress for member is derived based on the stress at assuring design drift considering the effect of higher mode, fluctuation of strength, importance factor for members, and accidental torsion. By dynamic analysis, above design criteria is also checked.

(2) Design direction:

In general, a building should be designed to have same safety margin in any direction. In this design guideline, two principle direction and one weak direction of building are discussed. One weak direction may be 45 degree direction. Analytical method in 45 degree direction is now considering and under discussion. It is possible to be proposed as a simple method that flexural and shear

---

Note:

1 earthquake motion with 25 kine of its maximum velocity

2 earthquake motion with 50 kine of its maximum velocity and artificial earthquake motion proposed in New RC project (New RC wave).

3 This story limit is from maintaining of structural performance

4 Considering fluctuation of earthquake characteristics, analytical model, some safety factor is introduced. Assuring design drift is determined as a factored design drift. This factor has not been determined yet.

and axial stress in 45 degree direction is 1.4 times and 2 times stress obtained from analysis in principle directions, respectively.

(3) Estimation of axial load:

Effect of vertical component as well as two directional components of earthquake on axial load is now discussing. But two directional effect will be counted by design in 45 degree direction.

(4) Analytical model and method:

Previous dynamic analysis is necessary to determine the adequate design drift, dimensions of members, and lateral distribution for static design etc.. Simple and convenient dynamic analysis model and method is developed.

Dynamic analysis should be done by more precise model more than a plane frame model.

Static design should be done by the method of non-linear incremental analysis using more precise model more than a plane frame model. Three dimensional analysis is recommended.

(5) Multi story structural wall :

The effect of multi story structural wall on the vibration mode during earthquake motion is now discussing. And three dimensional effect of connecting beam, slab due to the structural wall would be take into the design.

(6) Assuring the deformation capacity of member :

Considering a fluctuation of earthquake characteristics, analytical model, and gravity effect, deformation capacity of member should be assured more than a member deformation at an assuring design drift. Deformation capacity of a member is determined by the minimum estimated value.

(7) Torsion :

Torsion due to the progress of plasticity of members should be taken into the design.

4.3.3 Design for wind pressure

If the lateral load by the wind pressure is smaller than that by the seismic load at Co = 0.2, design for wind pressure would be omitted.

Design for wind pressure is not debating in Design Committee at all.

4.3.4 Design for other loads

Load by temperature, shrinkage, unequal settlement, accident etc. should be considered.

Design for the loads by temperature, shrinkage, unequal settlement, accident etc. is not debating in Design Committee at all.

4.4 Design of member

4.4.1 Flexural strength

Flexural strength should be calculated based on the characteristics of materials. Simple equation will be provided based on experiments.

Equation relating to experiments with mean value and deviation will be proposed from structural performance committee.

4.4.2 Another strength

Strength of shear, bond, beam-column-joint, and structural wall will be provided.

Equation relating to experiments with mean value and deviation will be proposed from structural performance committee.

4.4.3 Deformation capacity

Members should have more deformation capacity than that at an assuring design drift.

In design, flexural yield and failure is supposed. This failure model change to compressive, bond, or shear failure at its final limit. Deformation capacity of a member could be estimated at the point where failure mode changes.

Based on these deformation capacity, assuring design drift is able to be determined. Both assuring drift determined by maintaining a building function and by deformation capacity of members should be adopted.

Balanced steel ratio at ultimate strength should be accounted.

4.5 Earthquake motion for design

As well as recorded earthquake motions, artificial earthquake wave should be used for a

dynamic design.

Artificial earthquake wave would be proposed. As well as recorded motion, this wave should be used for dynamic design. Making method of New RC wave will be explained. New RC wave is proposed as the wave on technical soil. Wave at the base of a building should be translated from the wave on the technical soil considering the interaction between soil and building.

4.6 Foundation

omitted.

4.7 Structural requirements

Expected items for structural requirements are listed. Items that can be determined by design will be omitted. For rest of them structural requirements are determined.

4.7.1 Column and beam

(1) Section (2) Flexural steel (3) Shear reinforcement (4) Openings in beam

4.7.2 Wall

omitted.

5. OTHER RESEARCH ITEMS

5.1 Development of a super high rise flat slab type building

5.1.1 Target buildings

Target buildings are shown in Figure 5.1,5.2 and their structural outlines are tabulated in Table 5.1.

5.1.2 Literature research

On next two items, literature research have been going.

(a) Comparison research on the strength of the joint between experimental results and estimation.

(b) Strength and deformation capacity of a wall.

5.1.3 Experimental work on the behavior of the join of wall or column and slab.

On next four experimental series have been planned.

(a) Inner column and slab joint; 4 specimens

(b) Side column and slab ; 8 specimens

(c) Corner column and slab ; 4 specimens

(d) Wall and slab; 7 specimens

5.2 Feasibility Study on New RC Mega Structures

Trial Designs of Mega-Structures are carried out by using New RC materials. Strength of concrete is from 600 to 1,200 kgf/cm^2 (60 to 120 MPa) and strength of reinforcing steel bar is 7,000 to 12,000 kgf/cm^2 (700 to 1200 MPa). Six trial design models are listed below and Figures 5.3-5.8 show them. The structural design criteria which such mega-structures have to satisfy will be defined.

(1) Frame structure of 200 meters height (Fig. 5.3)

(2) Frame structure of 300 meters height (Fig. 5.4)

(3) Frame structure of 300 meters height (Fig. 5.5)

(4) Frame structure with K-brace of 200 meters height (Fig. 5.6)

(5) Frame structure with one way brace of 200 meters height (Fig. 5.7)

(6) Frame structure with brace of 300 meters height (Fig. 5.8)

REFERENCES

[1] Architectural Institute of Japan : "Design Guideline for Earthquake Resistant Reinforced Concrete Building Based on Ultimate Strength Concept," May 1988 (in Japanese)

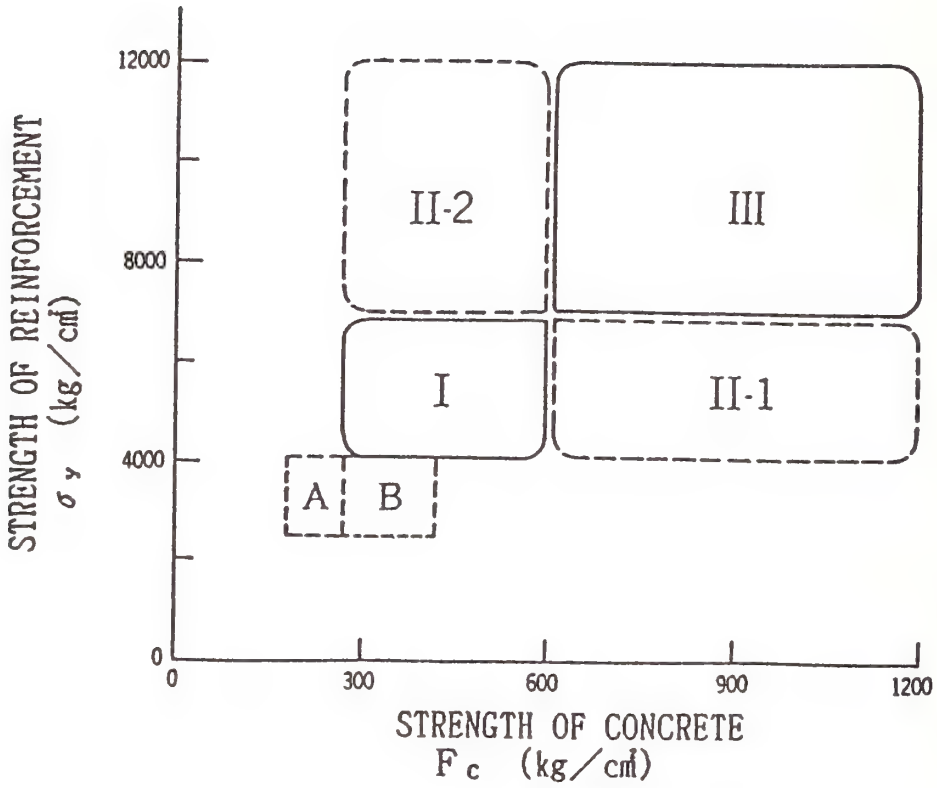

ZONE : TYPE OF RC BUILDINGS & MATERIALS
A: LOW-RISE BUILDINGS IN COMMON
B: HIGH-RISE BUILDINGS CONSTRUCTED IN LAST DECADE
I : HIGH-STRENGTH CONCRETE & REINFORCEMENT
II-1: ULTRA HIGH-STRENGTH CONCRETE & HIGH-STRENGTH REINFORCEMENT
II-2: HIGH-STRENGTH CONCRETE & ULTRA HIGH-STRENGTH REINFORCEMENT
III: ULTRA HIGH-STRENGTH CONCRETE & REINFORCEMENT

Fig.1 Strength of materials and fields of research and development

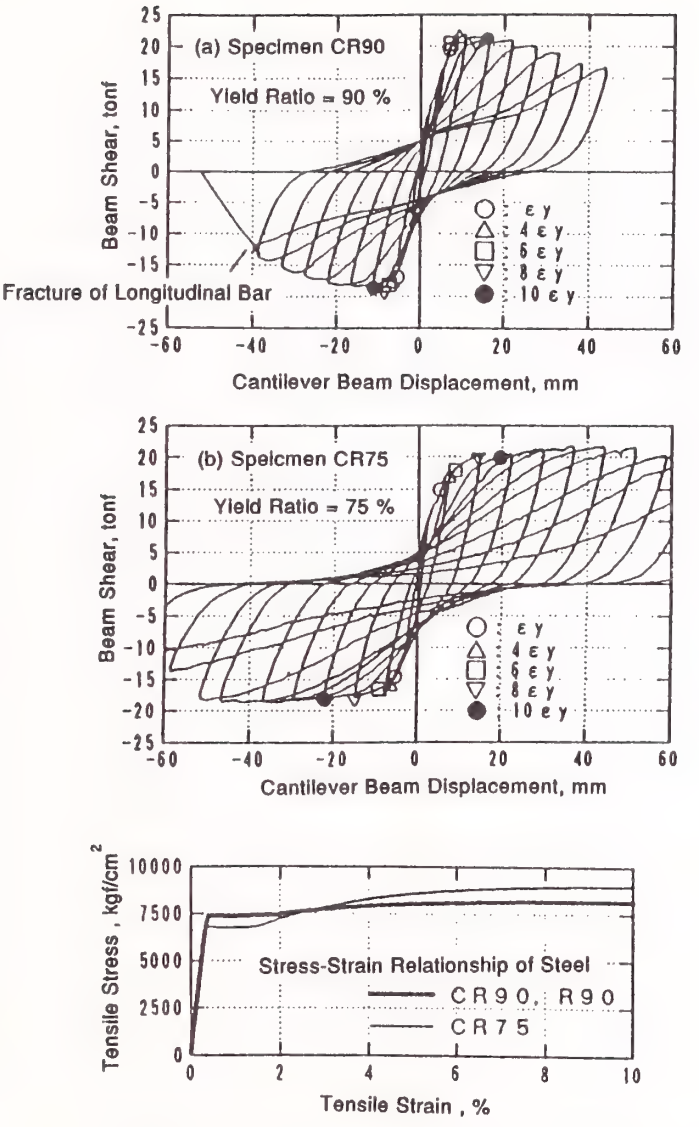

Fig. 2.1 Test of Cantilever Beams using High-yield Ratio Longitudinal Reinforcing Bars

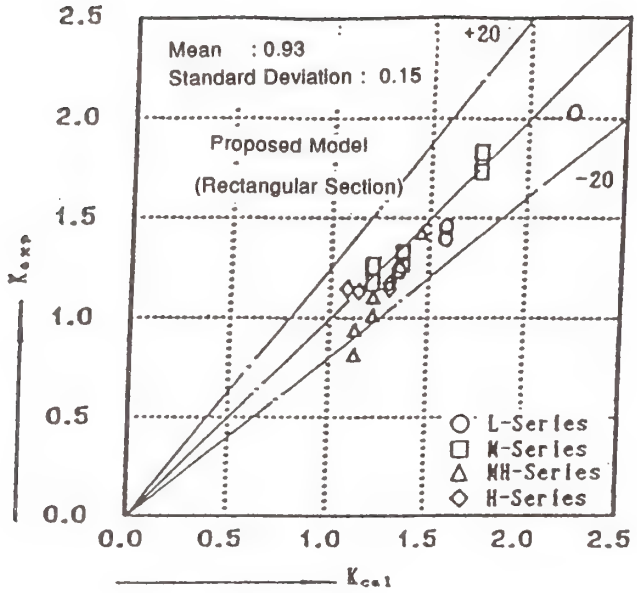

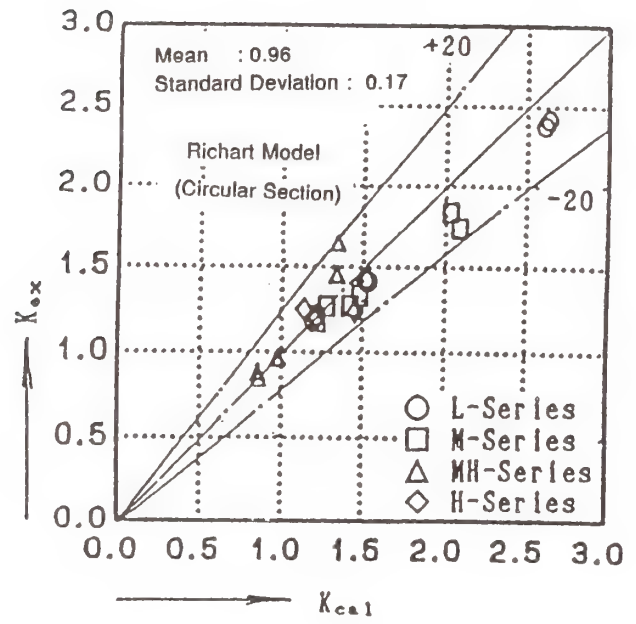

Fig. 2.2 Model Predicting Ultimate Strength Inclease of Confined Concrete

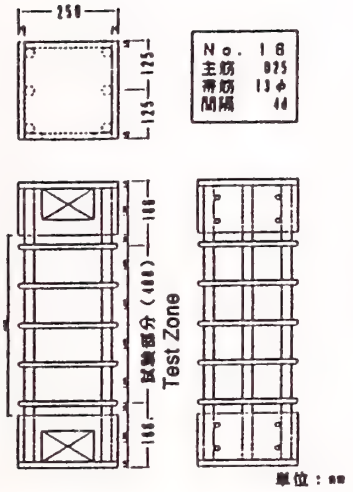

Geometry of Typical Specimen

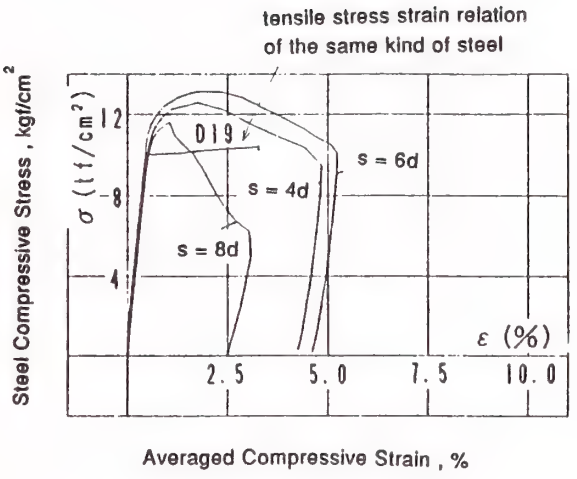

Fig. 2.3 Effect of Hoops Spacing for Preventing from Local Buckling of Longitudinal Bar

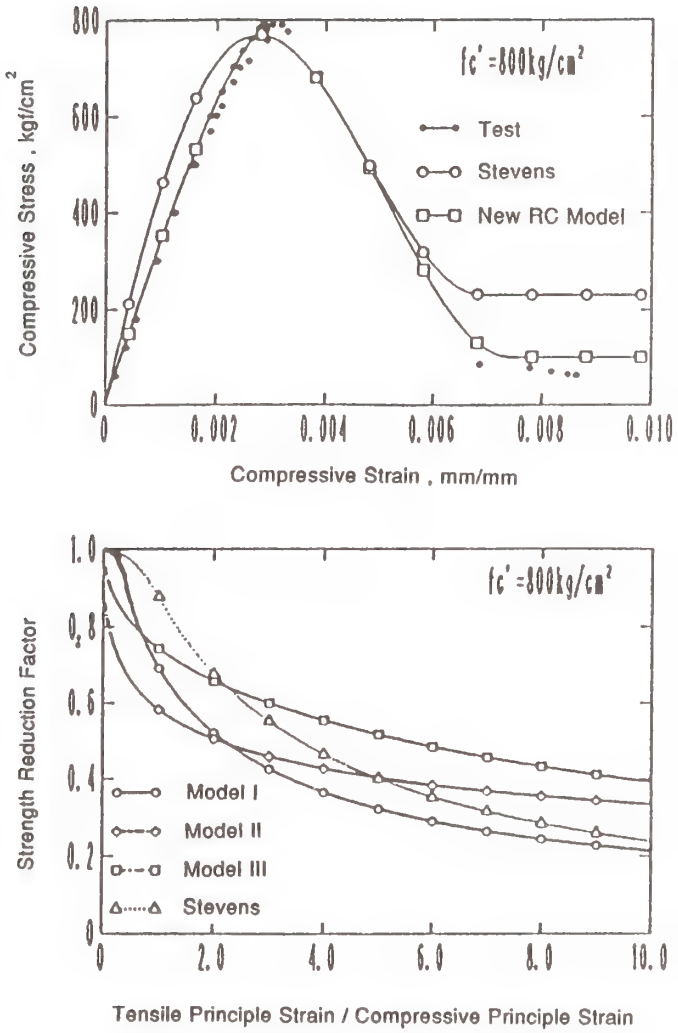

Fig. 2.4 Example of Constitutive Model for Concrete for Non-Linear FEM Analysis

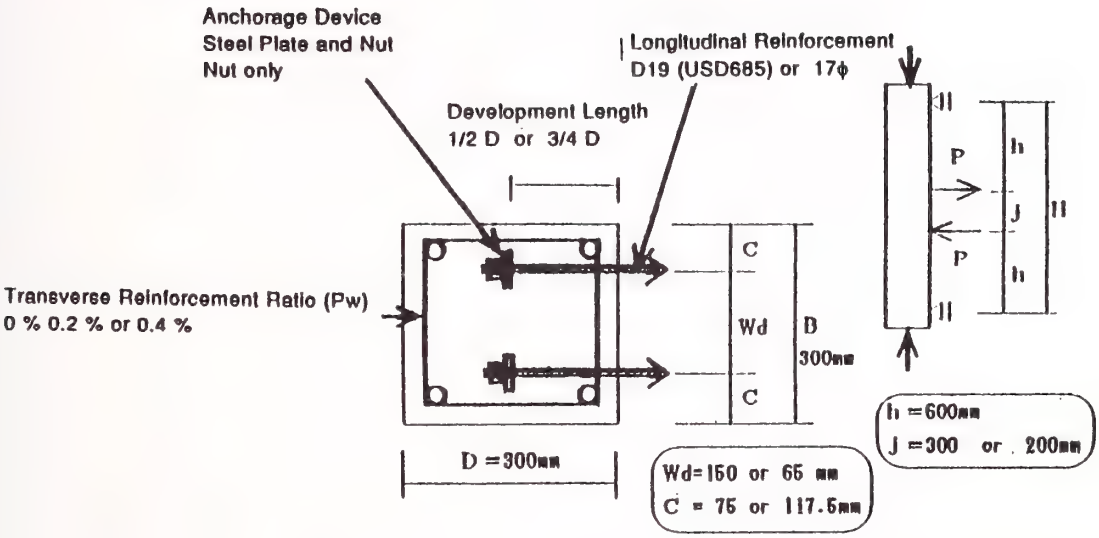

Fig. 2.5 Tensile Strength Test of Plate Anchorage Developed in Exterior Beam Column Joint

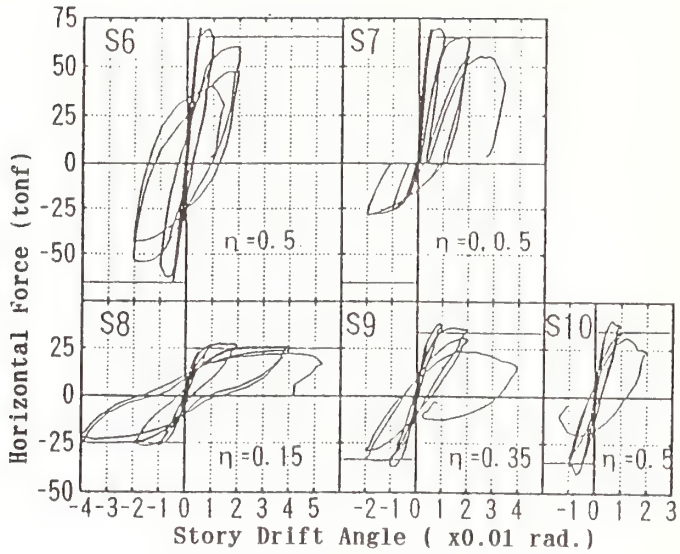

Fig 3.1 Horizontal Force and Story Drift Angle Relationship

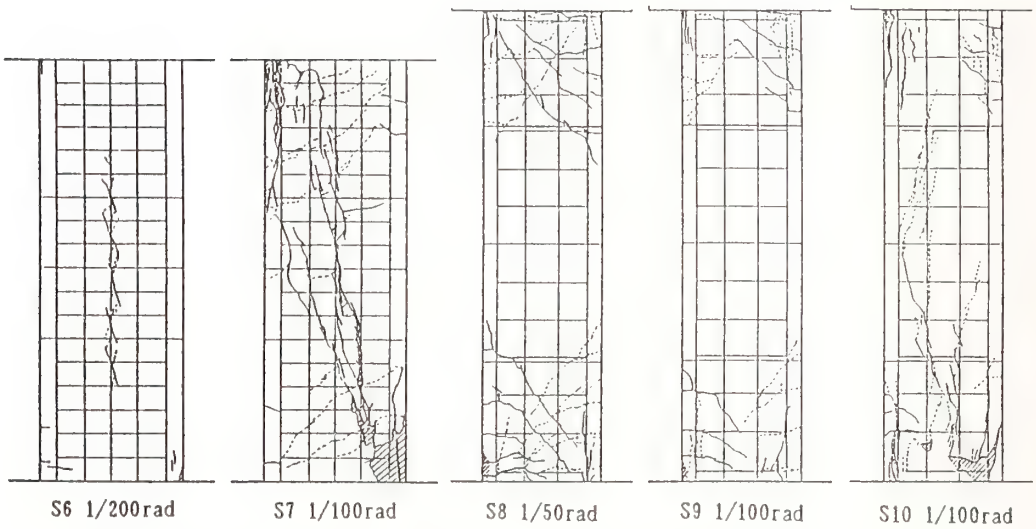

Fig 3.2 Crack pattern of Specimens (at Maximum Horizontal Force)

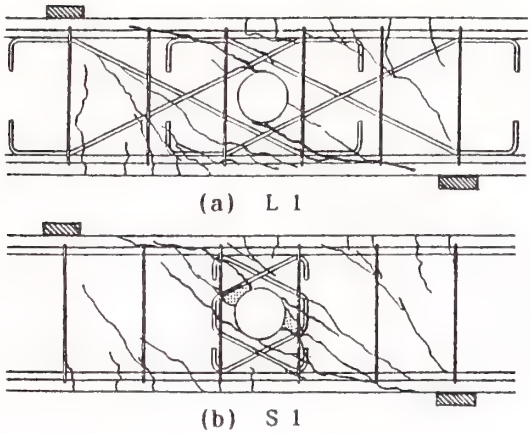

Fig 3.3 Crack pattern of Specimens (at Maximum Horizontal Force)

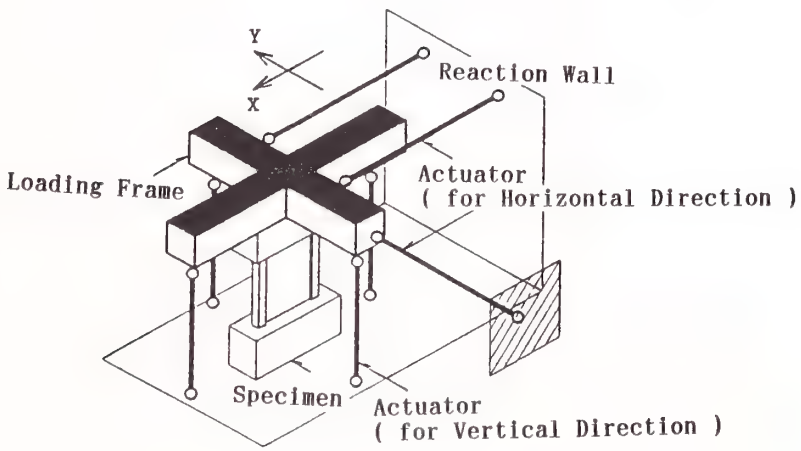

Fig 3.4 Loading System

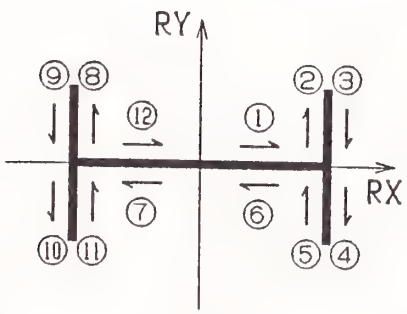

Fig 3.5 Loading Path

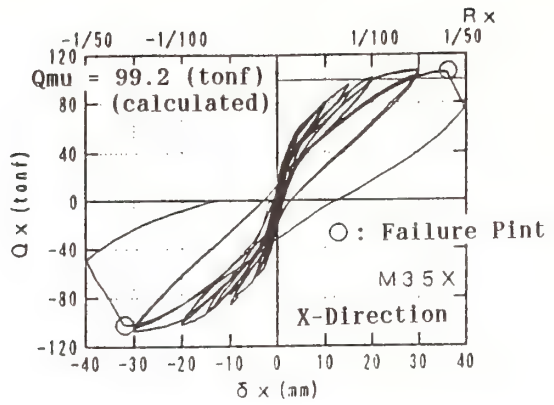

(a) One Directional Loading (X-Direction)

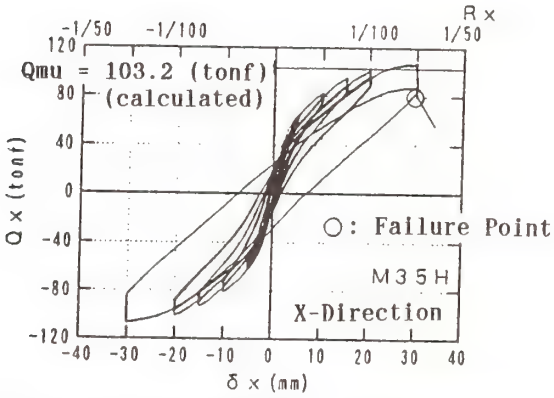

(b) Bi-Directional Loading (X-Direction)

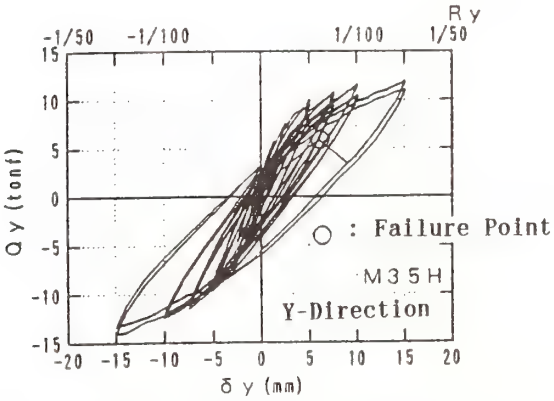

(c) Bi-Directional Loading (Y-Direction)

Fig 3.6 Horizontal Force and Displacement Relationship

Table 5.1 outline of structure

	(1) Core wall type	(2) Wall type
Purpose	Apartment	Resort Hotel
Stories	50F、B－1、P－2	40F
Height	GL＋151.5m	GL＋123m
Story Height	3.0m　1F：4.5m	3.0m　1F：6.0m
Area	41.8×41.8m　(typical floor) 16.2×16.2m　(core arer)	1,090㎡
Concrete	Fc＝98(For slab Fc=56？)MPa	Fc＝98MPa
Steel	σy=980MPa σy=295MPa(for slab)	σy=980MPa
Section	Wall thickness 70cm Boundary beam　70×90cm Column 90×90cm(interior) 80×80cm(exterior) Slab　20or25cm	Wall thickness 40cm Boundary beam　50×300cm Slab　20cm

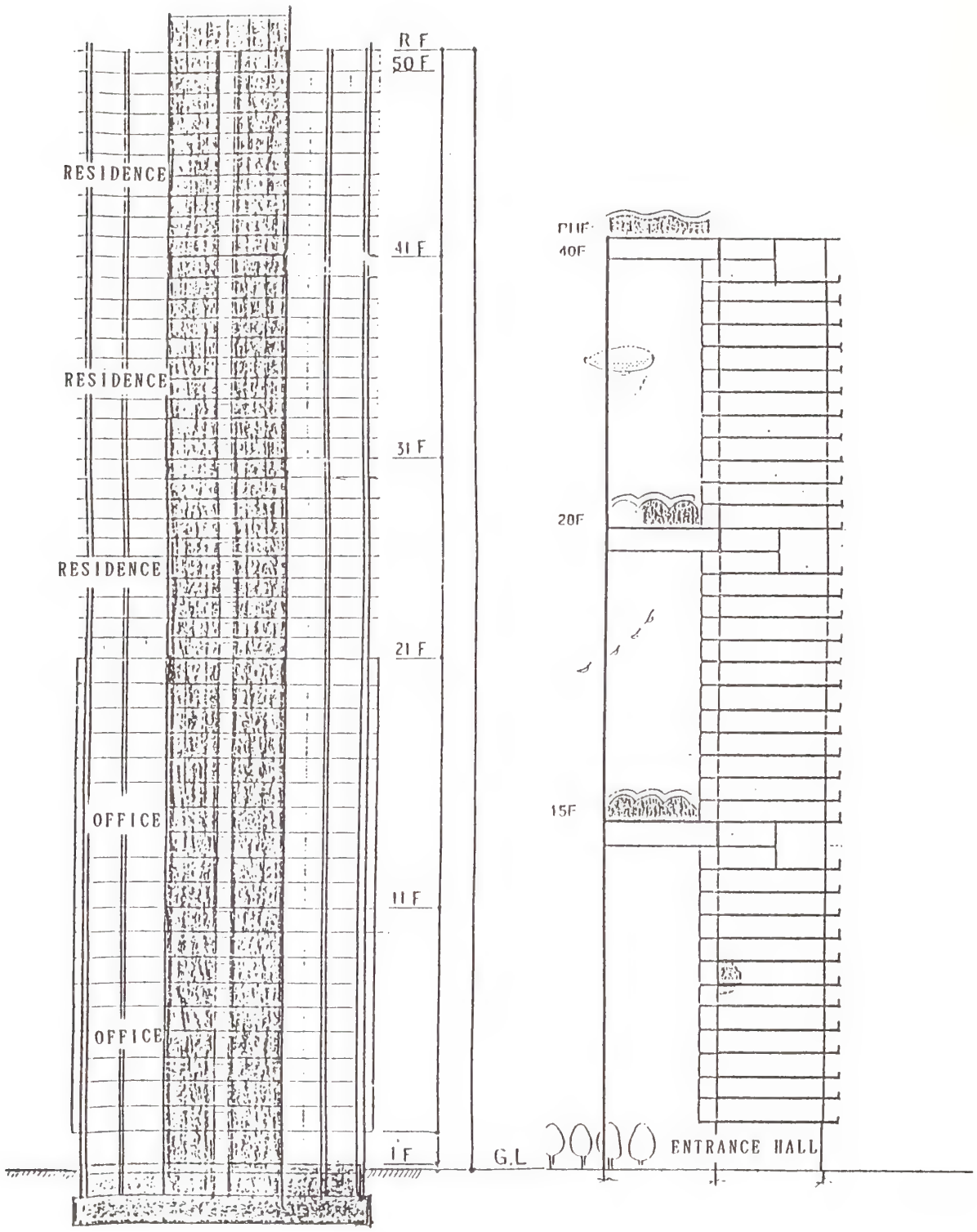

Fig. 5. 1 (b) Section of core wall type Fig. 5. 2 (b) Section of wall type

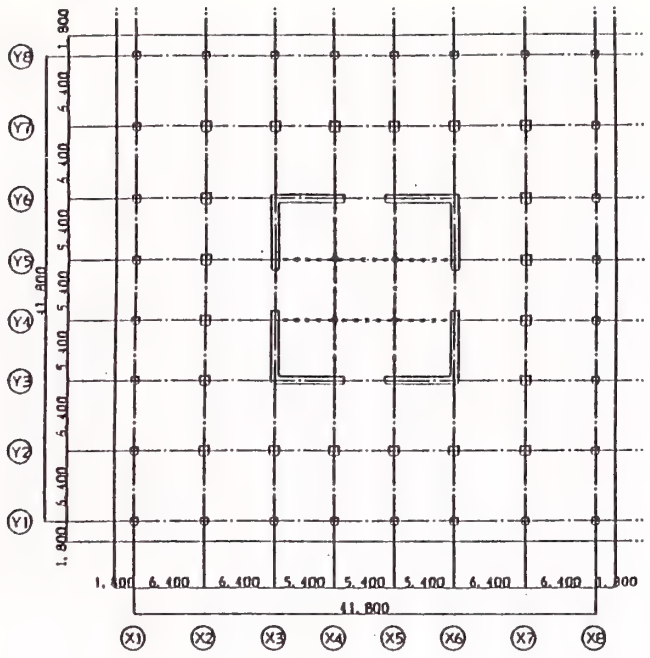

Fig. 5. 1 (a) Plan of core wall type

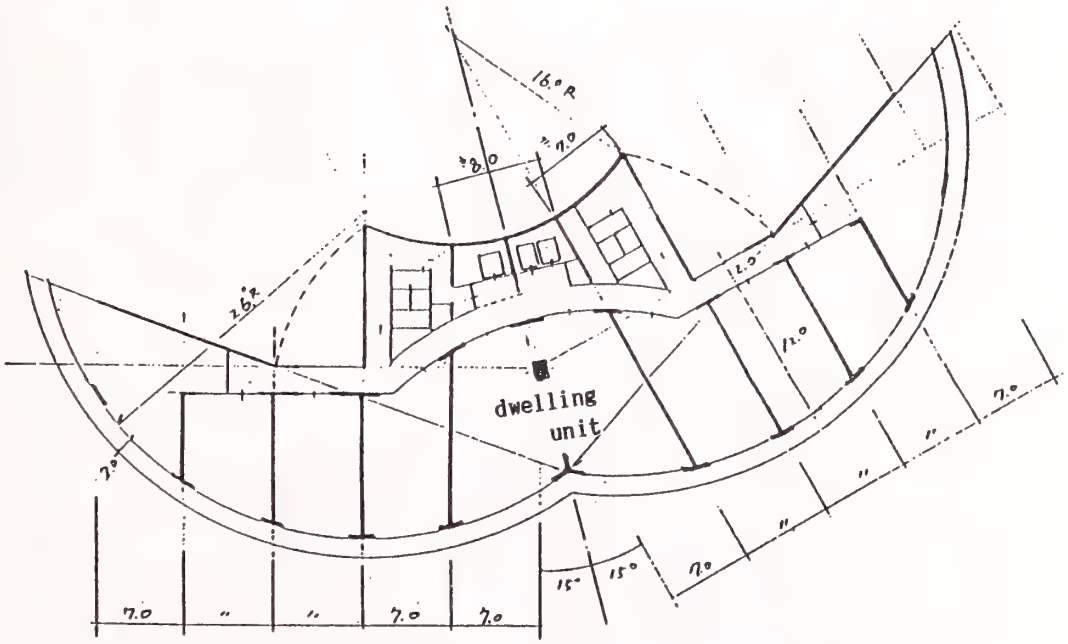

Fig. 5. 2 (a) Plan of wall type

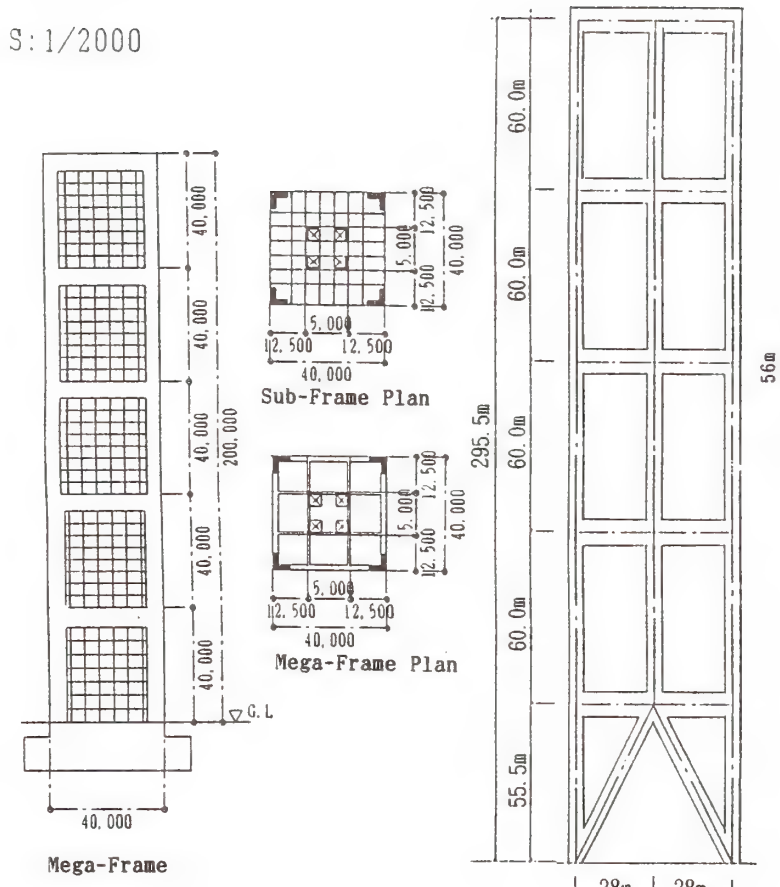

Fig. 5.3. Frame structure of 200 meters height

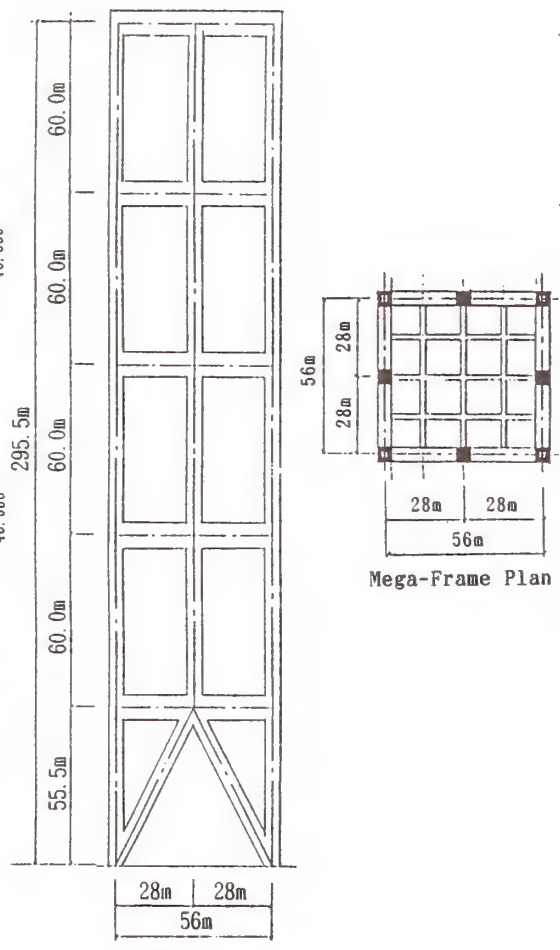

Fig. 5.4. Frame structure of 300 meters height

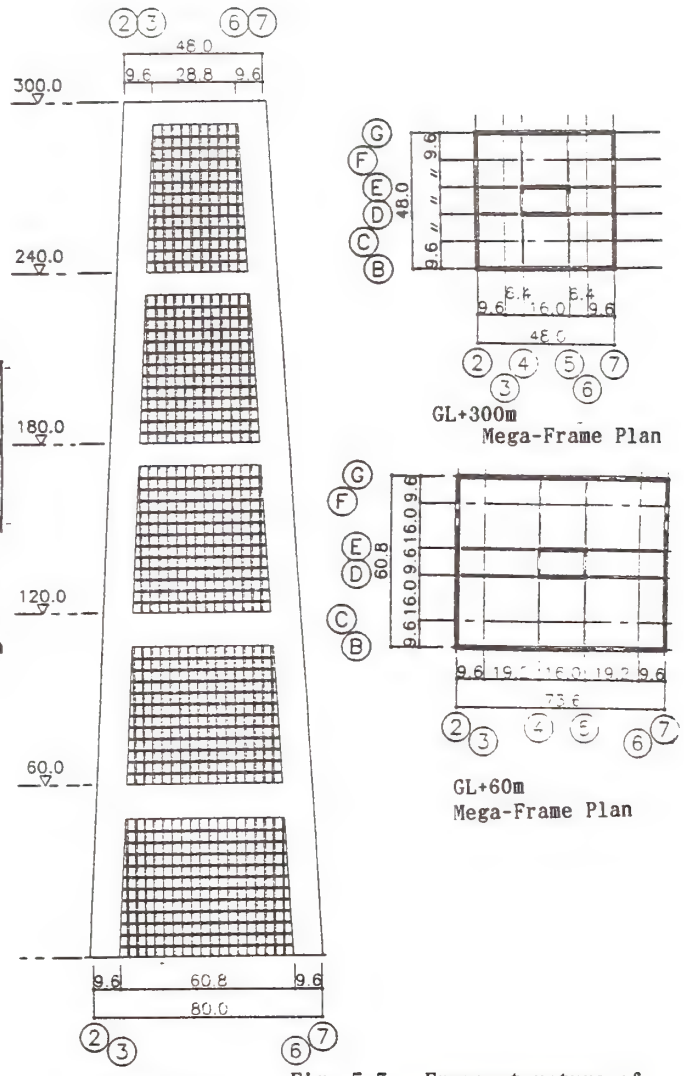

Fig. 5.5. Frame structure of 300 meters height

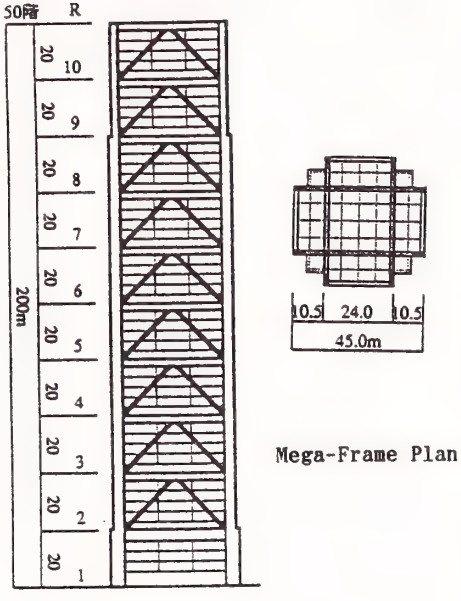

Fig. 5.6. Frame structure with K-brace of 200 meters height

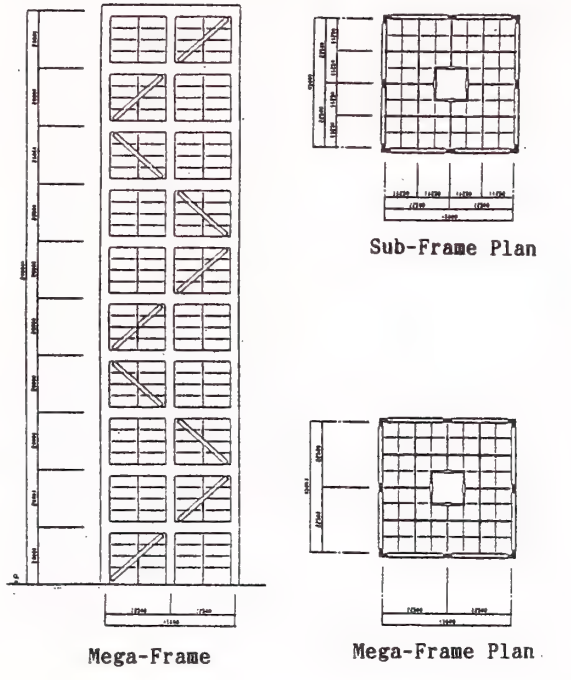

Fig. 5.7. Frame structure with one way brace of 200 meters height

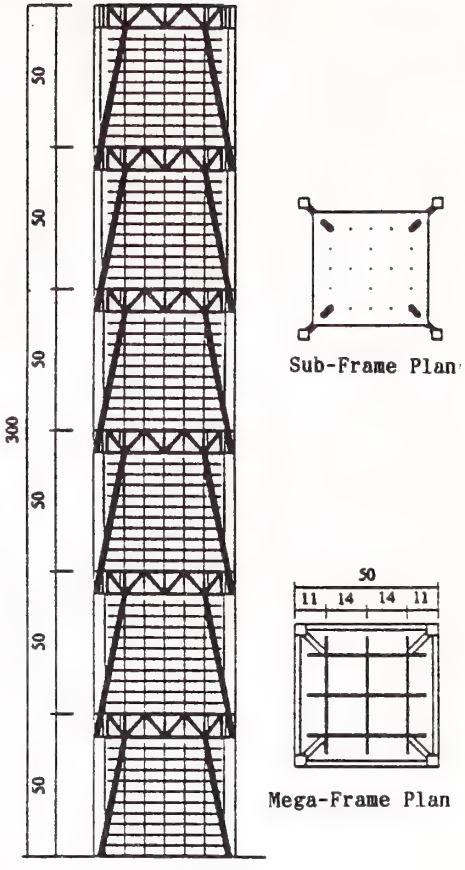

Fig. 5.8. Frame structure with brace of 300 meters heigh

Dynamic Testing of Reinforced Concrete Frames

by

Pamalee Brady[1] and Steven C. Sweeny[2]

ABSTRACT

This paper discusses ongoing research to study the behavior of concrete frame structural systems typical of U.S. military construction, and ways of improving their resistance to seismic loading. One test program focuses on reinforced concrete frames with masonry infill. Frame stiffness and its interaction with the infill is investigated. In-plane and out-of-plane behavior is being studied, including tests on plain infill and infill repaired both before and after damage to the wall has occurred. The second test program focuses on evaluating the capacity of lightly reinforced concrete frames and the feasibility of retrofitting them with viscoelsatic dampers to improve their seismic performance. Both beam/slab/column and slab/column details typical of existing three story concrete frame barracks on the west coast are being tested with and without the dampers to study building response.

KEYWORDS: concrete frames, dynamic testing, non-ductile, repair.

1. INTRODUCTION

Most permanent buildings on Army installations have been constructed, in accordance with seismic criteria applicable during their design, to provide some protection from seismic hazards. However, concern for the seismic safety of these buildings arises from experiences in recent earthquakes, where structures such as hospitals, communications centers, emergency facilities, and other essential and high-loss-potential facilities have been damaged by ground shaking or other seismic hazards. Since the early 1970s the Army has maintained seismic design criteria that are current with national codes and standards. After the 1971 San Fernando Earthquake the Army realized there may be hazards associated with their existing building inventory. Research was initiated to develop methods for evaluating these existing structures. In 1988 technical manual, TM 5-809-10-2, "Seismic Upgrading of Existing Buildings," was published to standardize the procedure for determining building vulnerability analytically.

The large inventory of built structures means that reducing seismic hazards in existing buildings is a complicated and costly issue that must be carefully addressed. The Army alone currently operates and maintains about 164 installations and major activities in the United States. More than 127,000 buildings are located on these installations. A phased plan involving inventory screening, hazard indexing,

[1]Research Structural Engineer, U.S. Army Construction Engineering Research Laboratory, P.O. Box 9005, Champaign, IL, 61826-9005.

[2]Research Structural Engineer, U.S. Army Construction Engineering Research Laboratory, P.O. Box 9005, Champaign, IL, 61826-9005.

preliminary seismic safety evaluations, detailed seismic safety evaluations and development of seismic hazard mitigation plans has been initiated by each of the military services to reduce military seismic hazards. These activities have been accelerated in response to the National Earthquake Hazard Reduction Program Reauthorization Act of 1990.

The U.S. Army Construction Engineering Research Laboratory (USACERL) has performed preliminary seismic evaluations of buildings at several Army and Air Force installations in Seismic Zones 4 and 3. The objective of these evaluations is to determine whether a building provides an acceptable degree of safety, or whether a more extensive detailed investigation is required. At three Air Force bases in Seismic Zone 4, 56 buildings were identified as significant seismic hazards requiring detailed analysis and possible upgrading. Projected cost to bring these buildings up to current seismic standards is $118 M.

Among the vulnerable buildings, we identified several standard barrack designs used by both the Army and Air Force during extensive construction in the 1950s, 1960s and 1970s. Approximately 80 percent of the vulnerable facilities evaluated were of two common structural systems. These systems are 1) concrete frames without infill and 2) concrete frames with full infill, infill with openings, or partial height infill walls. The systems have performed poorly in earthquakes and the American Concrete Institute code requirements changed significantly in 1971 to address the identified problems. Details of the reinforced concrete frames constructed prior to these code changes are the primary reasons for poor behavior of the structural systems and are defined below:

1. Lap splices in columns occur at the base of the columns which for lateral loading is the region of maximum moment. These splices were also not well confined by tie or spiral reinforcing.
2. Positive beam moment reinforcing was discontinuous at the column.
3. Little or no reinforcement was provided in the beam-column joints
4. Construction joints are located above and below the beam column joint.

Additionally, infill walls alter the behavior of the concrete frames. Infills are much stiffer than the surrounding frame and tend to share or resist the lateral loads in the system. Research has shown that partial height walls produce a short column effect in the frames and therefore larger shears in the columns.

Because of the prevalence of these standard designs, the cost benefit of a study to accurately assess the capacity of the existing systems with the goal of developing upgrading solutions to improve their behavior is extremely high. Only recently has research addressed assessing the strength and ductility of existing buildings and dynamic tests have not been performed on these structural system types.

USACERL has undertaken two related research programs to investigate the seismic hazard associated with buildings having these structural systems. The programs evaluate the seismic resistance of the buildings' critical elements to determine the extent of any deficiencies so that practical strengthening concepts can be developed and their effectiveness assessed. One program is directed toward conceptually modelling a prototype structure of concrete frames with masonry infill walls and the other uses scale models of concrete frame prototype structures.

The prototype structures upon which the research is based are three story barrack buildings. There are four prevalent building configurations with similar structural systems; in plan they represent H, rolling pin, hammer head, and T shapes (Figure 1). A typical

building of the H configuration consists of three separate structures each with overall dimensions of 3566.2 cm by 1178.7 cm (117 ft-0 in. by 38 ft-8 in), (Figure 2). Each structure is six bays in the longitudinal direction and two bays in the transverse direction. Bay width is 586.7 cm (19 ft - 3 in.) and story height is 304.8 cm (10 ft). Exterior transverse frames contain full height infill walls. Interior longitudinal frames have no infill and exterior longitudinal frames have partial height infill walls. The balance of this paper discusses the dynamic testing programs to evaluate these reinforced concrete frame systems.

2. Concrete Frames with Masonry Infill

2.1. Objective.

The objective of this project is to conceptually model a transverse frame with masonry infill to study dynamic behavior, failure mechanisms, and the effects of repair and rehabilitation. Two small scale concrete frame models are designed to be used in a multi-year research effort. A strong frame, with larger beam and columns and ductile detailing, and a weak frame with smaller elements and non-ductile detailing will be tested. The test program for each frame is being conducted in three stages. The first stage is determination of the behavior of the bare frame, including the effects of initial cracking and column post-stressing on the behavior of the model. The second phase is determination of the effect of the infill on frame behavior and failure mechanisms of the infill both in-plane and out-of-plane. The final phase is determining the effect of repair and retrofit of the infill on system behavior.

2.2 Test Specimen.

The strong frame is one-half scale of a frame designed in accordance with Chapter 21 of ACI 318-89 (Figure 3). The columns are 15.2 x 15.2 cm (6 in x 6 in), and 88.9 cm (35 in) from base to the center of the beam-column joint. Longitudinal reinforcement consisted of 6 - #3 grade 60 deformed bars. Stirrups are formed from 6 gauge basic wire. A 1.6 cm (5/8 in) brass tube runs down the center of the column to accommodate the post-stressing cable. The beams are 12.7 cm wide by 15.2 cm deep (5 x 6 in), 137.2 cm (54 in) center to center of the beam-column joints. Each beam has 3 - #3 grade 60 deformed bars top and bottom and 6 gauge basic wire stirrups. In addition, the beam has an unsymmetric top flange 5.1 cm (2 in) thick extending 24.1 cm (9.5 in) from the edge of the beam. Both beams and columns extend 15.2 cm (6 in) beyond the joint to provide for continuity of the reinforcement. Concrete is a 2.7 kN/cm^2 (4000 psi) mix with a maximum aggregate size of .95 cm (.375 in). The weak frame has the same clear dimensions for infill as the strong frame with smaller beam and column dimensions and non-ductile reinforcing. The columns will be 12.7 x 12.7 cm (5 x 5 in) with 4 - #3 bars and 6 gauge wire stirrups. Final design of this frame has not been completed.

To facilitate dynamic testing on the shaketable two identical frames in parallel are tested (Figure 4). The two frames are coupled with a reinforced concrete slab. The slab also provides for attachment of 25.4 kN (5.7 kips) additional mass during the in plane tests. Diagonal tension cross bracing is provided at the ends between the two frames to prevent torsion during in plane and to provide all lateral support out of plane. Columns are post-stressed during testing to simulate dead load stresses.

Instrumentation consists of an array of strain gauges, displacement transducers, and accelerometers. One frame is heavily instrumented and the second frame lightly instrumented to verify similar response between the two frames. Strain gauges are mounted on longitudinal bars at the base of the columns and in the beam near the beam-column joints. Two gauges, at 2.5 and 10.2

cm (1 and 4 in) from the base or joint, are mounted at each location. At each strain gauge pair displacement transducers monitor cracking and curvature. Global displacement transducers are attached from a fixed reference frame to the model at the base, mid-height of the column, mid-depth of the beam, and at mid-width of the slab. Displacement transducers within the shake table actuators are used to measure table displacements. Accelerations are measured at the base, mid-height of each column, mid-span of the beam, center of the slab, the top of the mass plates and at the shake table. Accelerations will also be measured at various locations on the infill when tested.

2.3 Test Procedure.

Dynamic testing was conducted on the USACERL Biaxial Shock Test Machine (BSTM). Three tests are used to measure the behavior of the model under dynamic loading; a) a random frequency sine wave, b) free vibration, and c) a time scaled El Centro record. The frame is initially subjected to a low level random sine wave motion to determine the natural frequency and to approximate the dynamic amplification of the base motions. The random input is increased until a significant response is measured. This input level is used for all subsequent random vibration tests. Next, free vibration of the frame is measured. The model is excited with a sine wave at a frequency slightly higher than the natural frequency. Input motions are increased again until significant response is measured. The table motion is then stopped and the structure allowed to oscillate freely. The final test is an El Centro record with a time scale factor of 1.414. For the bare frame only, each of the three tests are conducted at four levels of post-stress applied to the columns. The frames are tested at post-stressing forces of 13.3, 26.7, 40.0, and 53.4 kN (3, 6, 9, and 12 kips). For frames with infill, only the 53.4 kN post-stressing will be used.

The frame or infill are damaged by subjecting the system to increasingly stronger earthquake ground motions until significant cracking develops. It is the intent to destroy the infill, not the frame, and to change the response by cracking the frame or infill without yielding the reinforcement. In order to achieve the necessary forces to crack the system, the time scaled El Centro record had to be filtered to remove the large displacements induced by low frequency motion. A high pass filter with a cutoff frequency of 2 Hz was used to produce the necessary seismic record. This input motion was used at increasing levels until significant damage was observed. Random vibrations are input after each test to measure change in model response. After cracking the bare frame, the model is subjected to the same three tests at each of the four levels of column stress as before cracking to evaluate the effects of cracking on bare frame response.

2.4 Initial Observations.

The Pre-cracking response behavior was as expected for a linear elastic system. The natural frequency for all levels of post-stress remained at approximately 11.6 Hz. The structure showed very good single degree of freedom response. Damping was approximated by both log decrement method from the free vibration curves and the half-power method from the random vibration curves with good agreement. Damping for the uncracked model for all levels of post-stressing averaged of 2.2%. Response to the El Centro record was also consistent for all levels of post-stressing.

The structure was tested with the filtered El Centro record at four levels. The first two tests gave a peak acceleration response of .43g and 1.08g respectively with little indication of damage. The third test showed a peak acceleration of 1.62g and a peak displacement of 3.0 mm (0.12 in). Random vibration and free vibration tests indicated a significant shift in the natural

frequency. The fourth test was performed at an input level 25% higher than test 3. Peak acceleration was measured at 1.72g with a peak displacement of 4.8 mm (0.19 in). Again, random and free vibration tests indicated a significant change in natural frequency as shown by the transfer funcition magnitudes in Figure 5, and the model was considered sufficiently damaged.

Initial cracking on the structure had an effect on both stiffness and damping. Damping calculations by both log decrement and half-power method show that the damping coefficient change from 2.2% to 4.3%. Working backwards through the equations of motion for a damped system using the damping and natural frequencies measured in the tests show that the stiffness of a single frame changed from 82.0 to 44.8 kN/cm (46.8 to 25.6 kips/in).

After cracking, the model was again subjected to the random vibration, free vibration, and unfiltered El Centro tests at the same input level run on the pre-cracked model at the four levels of post-stressing. The post-cracking behavior was much different then the pre-cracked behavior. A slight increase in natural frequency with increasing post-stress was observed. Again, both the log decrement and half-power methods for computing damping give good correlation. While the values for damping of the cracked frame vary, there is no correlation with post-stress values. The average value for the coefficient of damping in the cracked frame is 4.3%. Calculation of frame stiffness gives more consistent results. The drop in stiffness after cracking is significant, and both pre and post-cracked results indicate a slight trend towards increased stiffness with increased post-stressing, which was expected.

Most important for structural engineers is how the shifts in stiffness and damping affect the behavior of the structure during an earthquake. Typically, increased damping is considered beneficial for energy dissipation. In this case however, the effect of the decreased natural frequency caused an undesirable shift towards the predominant frequencies of the El Centro N-S seismic record. The result was a significant increase in peak acceleration and displacement of the cracked model.

3. Lightly Reinforced Concrete Frames

3.1 Objective.

The objective of this research program is to evaluate the effects of the vulnerable details identified above on overall behavior of nonductile concrete frames by experimentally assessing the capacity of scale models drawn from two prototype structural systems. With this knowledge we may better assess the complete capacity of the frame systems. Additionally we will test the effectiveness of viscoelastic (VE) dampers to improve the behavior of concrete frames under earthquake loading. The program is being worked cooperatively with Professors Wood and Foutch at the University of Illinois. It will be conducted in three phases. In the first phase, currently ongoing, tests of scale model frame subassemblages will be conducted to study their behavior and assess their capacities. A test of a scaled three story nonductile structure will be conducted in phase two. The third phase of the project will be devoted to technology transfer. Conventional strengthening schemes will be compared with upgrading using VE damper technology and the cost-effectiveness of different solutions evaluated. The following sections of this paper will focus on the first phase of the program, assessing the capacity of the existing frames through testing of frame subassemblages.

3.2 Test Specimens.

A total of four specimens representing the critical second floor joint of two lightly

reinforced concrete frame systems will be constructed. Two 6/10th-scale models of a typical beam/slab/column joint have been tested on the USACERL Biaxial Shock Test Machine. Two 1/2-scale flat plate/column joint specimens will be tested this summer on the shaketable. Geometric similitude between the prototype and test specimens was maintained. Subassemblage members were reinforced to produce the same demand/capacity ratios as those of the prototype elements.

The beam/slab/column test specimen measures 243.8 cm by 284.5 cm (8 ft-0 in. by 9 ft-4 in.) in plan and is 182.9 cm (6 ft) tall. The column is 18.4 cm (7.25 in.) square. The slab is 7.6 cm (3 in.) thick and the beam extends 16.5 cm (6.5 in.) below the slab. (Figure 6) Reinforcement details of the subassemblage follow ACI 318-51 code provisions. The longitudinal column reinforcement of the model consists of 4 - #5 bars; the bars are spliced 20 d_b at the top of the slab. Transverse reinforcement is provided by #2 ties spaced at 17.8 cm (7 in.) o.c., the minimum column dimension, along the height of the column. The ties have 90 degree hooks. Longitudinal beam reinforcement is 4 - #3 bars top and bottom. Bottom bars were discontinuous and extend 8.9 cm (3-1/2 in.) into the column. This extension provides similitude with the positive moment capacity of the prototype structure based on available bond strength. Where bars were continuous in the prototype structure, such as beam centerlines and midheights of columns, bars were hooked in the test specimen to ensure development. The transverse reinforcement in the beams was provided by #2 bar open stirrups spaced 7.6 cm (3 in.) o.c. arranged typical of gravity load conditions; they did not extend the full length of the beam.

The flat plate/column specimens have nominal dimensions of 304.8 cm by 304.8 cm (10 ft-0 in. by 10 ft-0 in.) and are 182.9 cm (6 ft) high. The column is 18.4 cm (7.25 in.) square and the slab is 9.2 cm (3-5/8 in.) thick. (Figure 7) The reinforcement consists of two mats of #2 perpendicular bars at the top and bottom of the slab. Standard spacing within the column strip was 7.6 cm (3 in.) o.c. and 12.7 cm (5 in.) o.c. in the middle strip. Column reinforcement was the same as that of the beam/slab/column model.

To maintain gravity stresses and produce the appropriate reactive mass in the models their mass was augmented by steel weights. A total of 26.6 kN (6 kips) was added to the beam/slab/column model, 13.3 kN (3 kips) at the top of the column and 13.3 kN (3 kips) on the slab. Inflection points of the columns and beams were assumed to occur at their mid-height and mid length respectively. The test fixture provides for rotation at these points. (Figure 8)

The joint region of each model is instrumented to measure curvature of the beam/slab, curvature of the column above and below the beam/slab and shear in the joint and column. Global displacements are measured from a fixed reference frame at the top of the column, slab and base of the column. Accelerations are measured at the top of the column, slab and base in the direction of load and at the slab in the transverse direction.

3.3 Test Procedure.

White noise and free vibration tests are conducted on each model to determine the characteristic frequency and damping of the model at various points in the test program. The El Centro 1940 N-S record, time scaled by a factor of 2.0, is used to excite the model at increasingly greater magnitudes to produce damage in the model. The specimens are tested to failure. The effects of structure geometry and configuration, yield and collapse capacities and energy dissipation characteristics are evaluated. A viscoelastic damper is incorporated into the second model of each type and the influence of the increased viscous

damping on the elastic and inelastic dynamic response of the structure investigated. Parametric studies will assess the differences in performance of the models with and without dampers.

3.4 Initial Observations.

Tests of the beam/slab/column specimens with and without dampers have been conducted. The failure sequence of the lightly reinforced joint was as expected; first, the discontinuous positive reinforcement slipped from the joint. This was associated with a period shift in the model. As the tests continued a hinge formed at the base of the upper column, indicating slip in the column lap splice, and the joint region of the beam/column deteriorated increasingly. The tests were stopped to prohibit failure of the now unstable upper column. Damage to the joint also made the structure extremely flexible. Capacity of the joint was generally as predicted.

A preliminary review of the data from the tests with the viscoelastic dampers shows reduced accelerations and displacements of the structure as compared with the specimen without dampers for the same input excitation. After testing with the dampers, they were removed from this model and it was tested at the peak excitation of the first model. The failure mode was similar but more dramatic.

Further study of the data from both tests is required to evaluate the response of the subassemblages, the improved response due to dampers and the effect of the test sequence on model response. Similar tests will be conducted this summer on slab/column subassemblages with and without dampers. More detailed analyses will be compared with experimental results. The work summarized above constitutes the first phase in a three phase program. Results of this work will be used to develop a better understanding of the behavior of the structures and to develop simplified design approaches for upgrading lightly reinforced concrete frames to improve their seismic behavior.

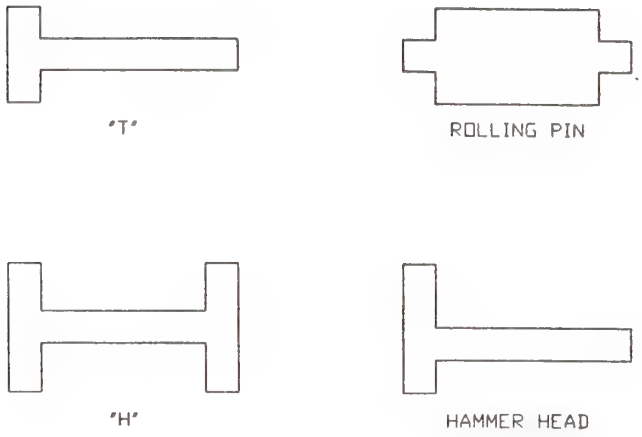

Figure 1. Standard building configurations.

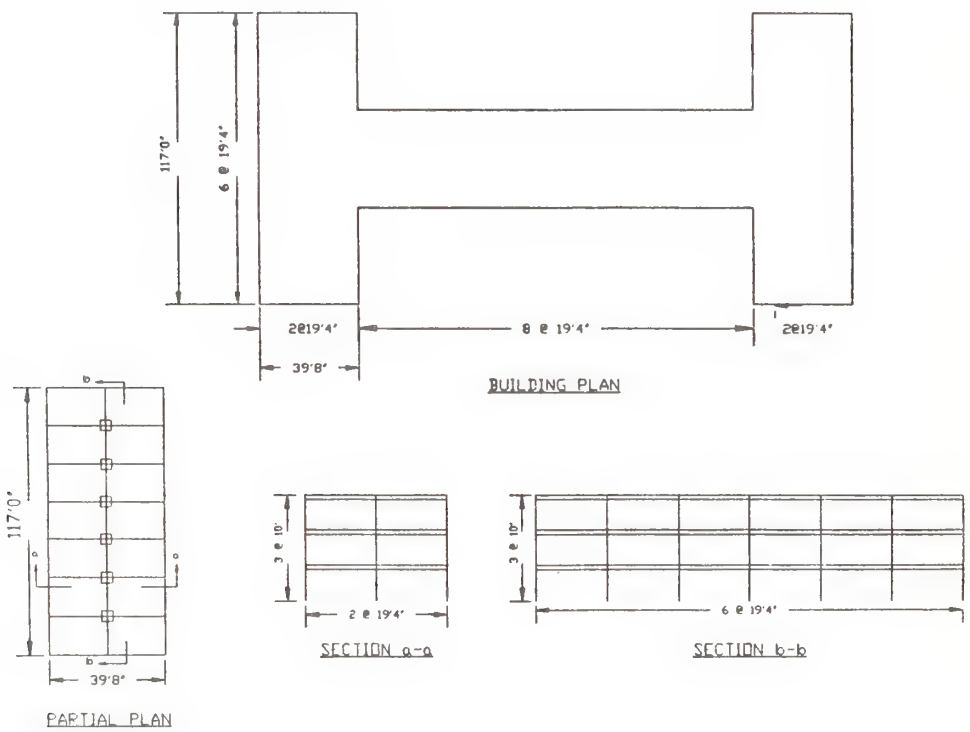

Figure 2. Typical "H" building dimensions.

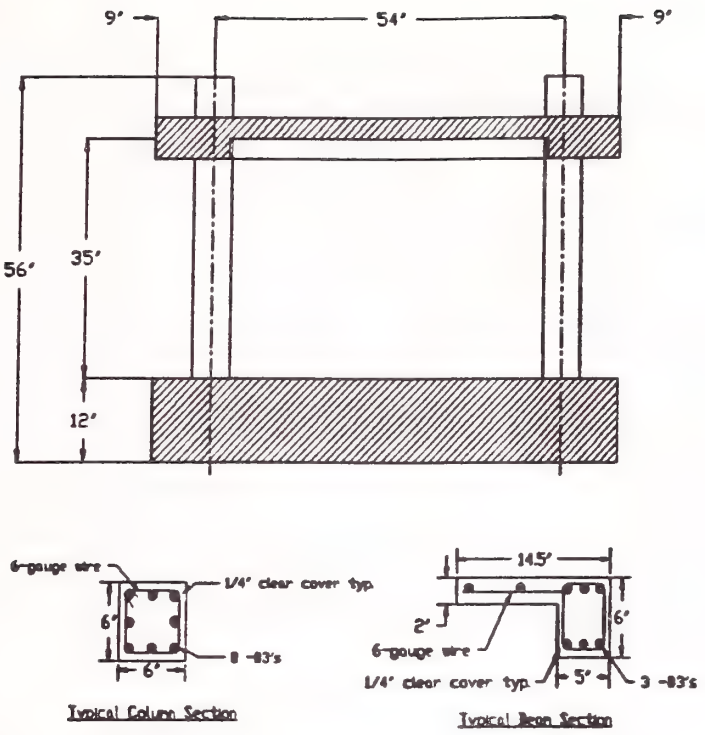

Figure 3. Strong frame dimensions and details.

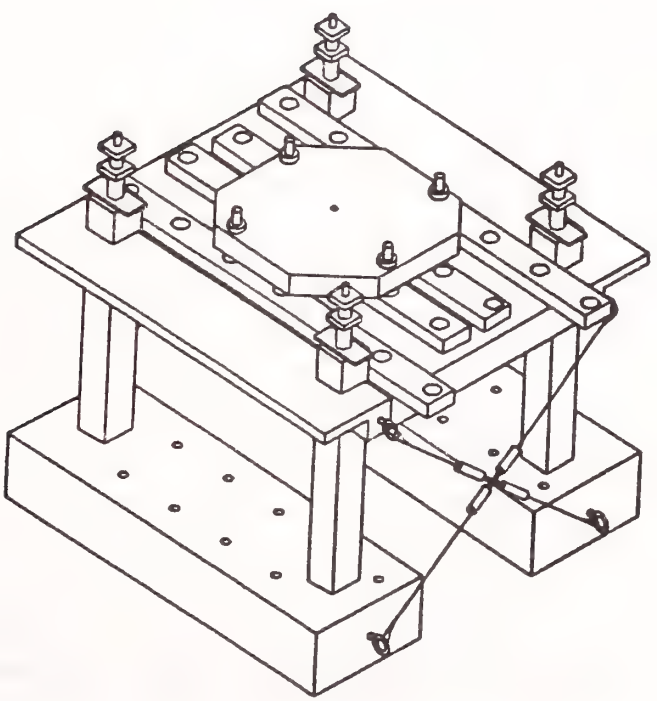

Figure 4. Assembled model with masses and bracing.

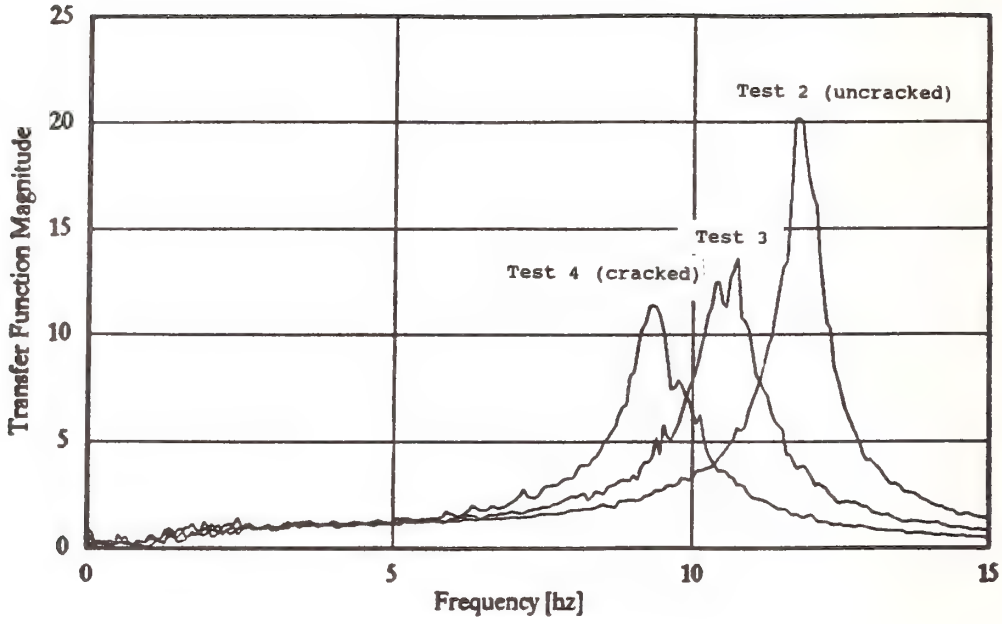

Figure 5. Change in the response due to cracking.

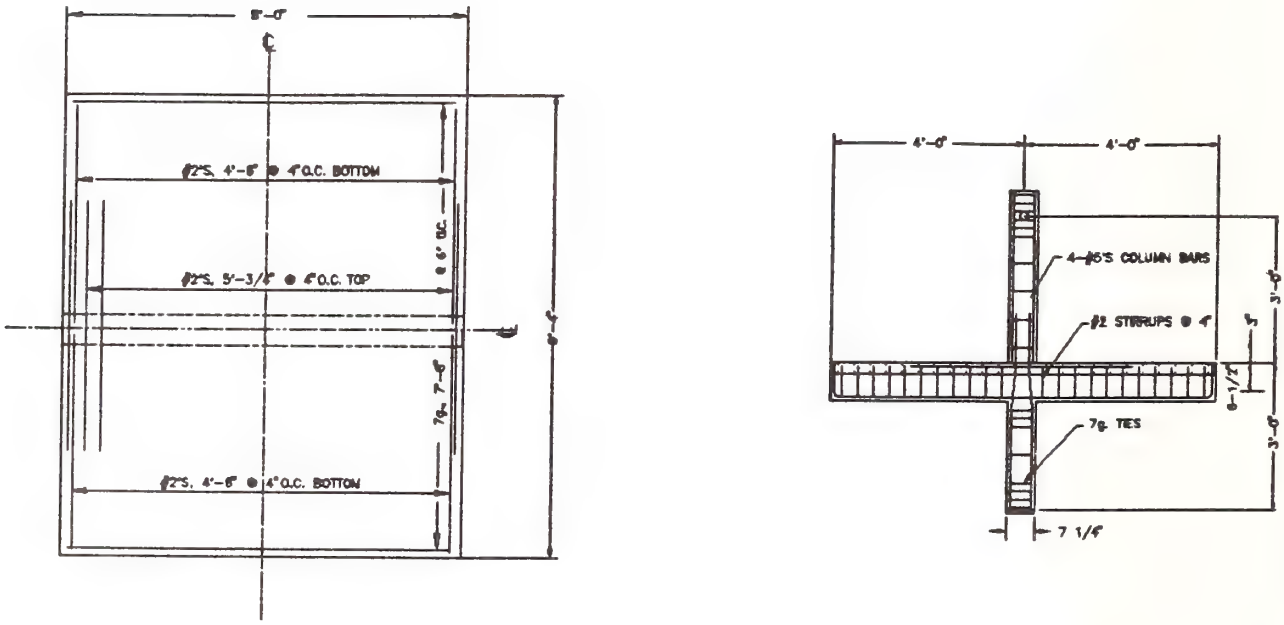

Figure 6. Beam/Slab/Column Subassemblage.

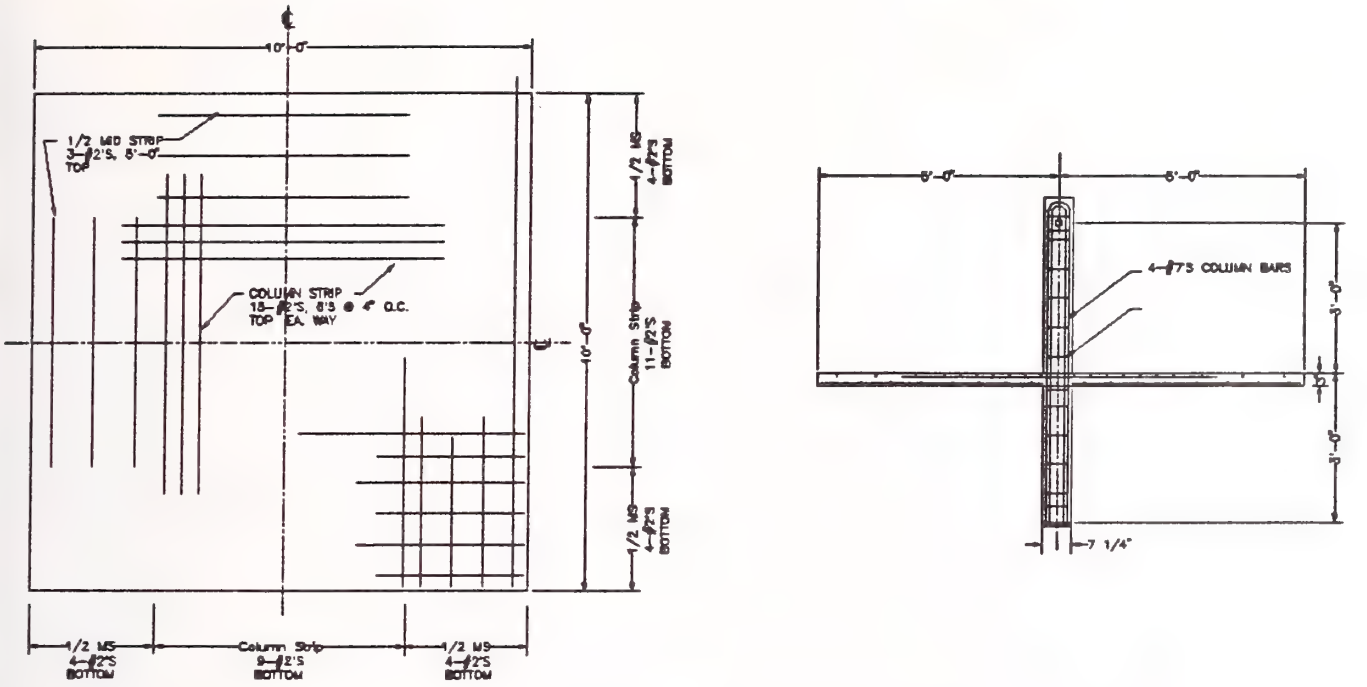

Figure 7. Slab/Column Subassemblage.

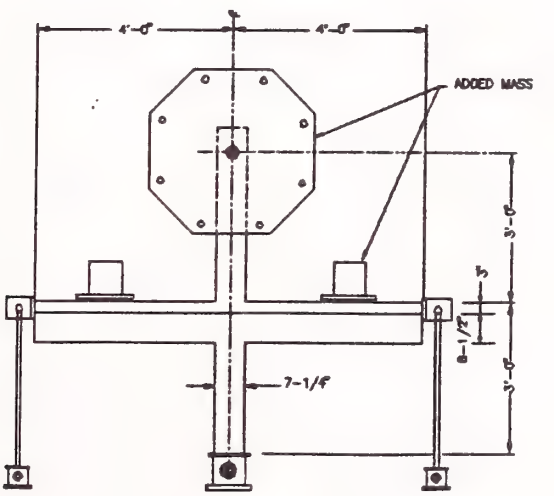

Figure 8. Test Configuration.

Shaking Table Collapse Tests of RC Columns

by

Chikahiro Minowa[3], Nobuyuki Ogawa[2], Tadashi Mikoshiba[4], and Norio Oyagi[1]

SUMMARY

Precise control of shaking table should be desirable for aseismic tests of structures. Large-scale shaking table of National Research Institute for Earth Science and Disaster Prevention (NIED) has employed the digital control system H_2. In order to verify this digital control characteristics, the collapse tests of reinforced concrete columns were conducted.

The reinforced concrete column damage pattern differences between static cyclic loading tests and dynamic shaking table tests were observed. In this study, the spacing of shear reinforcement bars in columns were variable. Four types of spacings of shear reinforcement bar spacing are used. As results of the tests, it was verified that the maximum horizontal strengths of columns, the deformation capacities, and the damage patterns were changed with the shear reinforcement bar spacings, and also with testing method differences between statics and dynamics. Furthermore, P-δ effects were discussed.

KEY WORD: Shaking Table, Digital Control, Analog Control, Reinforced Concrete, Dynamic Collapse Tests, Static Cyclic Loading Tests, P- δ Effects

1 INTRODUCTION

Shaking Tables were used for the tests of base isolation methods, vibration control methods, liquefactions, and verifications of aseismic design codes, and so on. Some of these tests shall require the precise reproduction of earthquake records. Preparatory excitations are permitted for elastic region tests of structures. However, preparatory excitations can not be used for liquefaction tests and structure damage tests. Recently, NEID employed the digital control system using DSP board in order to improve the response properties of the large-scale shaking table. The collapse tests of reinforced concrete columns (model scale:1/3) were carried out so as to verify this digital control method.

Many studies concerning about the ultimate horizontal strengths of columns were already conducted. However, most of these studies were carried out by the static cyclic loadings of one column, or psuedo-dynamic loadings. In this investigation, realistic dynamic loading which would simulate earthquake responses of structures, were done by the use of a shaking table, and the dynamic damage characteristics of columns were observed. A small test structure of one story and one bay had four columns. These columns were made by reinforced concretes. For kind of spacings of shear reinforcement bars were used. In addition to the shaking table test, static cyclic loading test had been done on behalf of the comparisons. The time variations of damage patterns, the ultimate strength and the story deformations were observed.

2 TEST METHODS

Four kinds of reinforced concrete columns were tested on the shaking table. The over view of shaking table tests is shown in Photo 1. Analog control methods were used two times, and also digital control methods were used two times. Additionally, steel column tests were conducted. The new digital control system consists of a personal computer and a digital signal processing (DSP) board. The control methods are selected on a key board. The outline of this control method is shown in Fig. 1. In the case of an analog control, the H_2 controller shall be bypassed, and this system is used as a wave form generator. In this test series, the shaking table were drive by the strong earthquake motion record of 1968 Tokachioki, Hachinohe E-W, which was mode in the use of FFT band pass filter 0.4Hz-50Hz. The real time scale was adopted. Fig. 2 shows the main records of shaking table responses in the analog and digital controls. This digital control methods would give the improvement of gain characteristics and robustness to the shaking table. The control frequency increased from 10Hz to 13Hz with this digital control method. The digital control responses are appeared to be inferior to analog control responses in time domains. It will be necessary to consider the nonlinearity of servo valve in the H_2 controller.

One story X one bay test structure was assembled on the shaking table. Four columns had the section of 13cm X 13cm, and the height of 85cm. The diameters of four main steel bars were 16mm. The columns were fixed in steel roof girder and steel base frames with bolts. The roof of test structure was made by steel frame. On the roof, three concrete mass weight were fixed. Total weight of roof was 27.8ton. The spans of this test structure were 2m in loading direction, and 2m in perpendicular direction. In order to mitigate the shock loads of falling roofs in the shaking table during damage excitations, the roof support frame was installed inside of the test structure.

---

1 Former Director, Disaster Prevention Division,National Research Institute for Earth Science and Disaster Prevention, Science and Technology Agency
2 Head, Earthquake Engineering Laboratory, ditto
3 Senior Researcher, ditto
4 Research Member, Earthquake Engineering Laboratory, ditto

Therefore, the roof of 27.8ton fell about 15cm in damage excitation. The four types of columns with the shear reinforcement bar spacing of 50mm, 105mm, 170mm, and 285mm were tested in the shaking table. The outline of the test structure are shown in Fig. 3. The details of columns are shown in Fig. 4, and the physical properties of columns are concrete compressive strength 230kg/cm^2 - 300kg/cm^2, and steel bar tensile strength 3600kg/cm^2.

In a static cyclic loading test, the pull type oil jacks which were connected in the roof frame, were used. Two jacks were set in right side, the others were set in left side. Cyclic loading level were 1/1000, 1/200, 1/100, 1/50, 1/20 in story deformation angles. After cyclic test, loads increased gradually until column collapses. The one dimensional shaking table of NIED was used in this test. The dimension of shaking table is 12m by 12m. The table weight is 180ton. The maximum power is 360tons. The maximum velocity and displacement are 75cm/s and 24cm. The acceleration levels of these tests were 0.5G and the velocity were 70cm/s approximately. Collapse responses of test columns were observed by video records, and measured by various sensors.

3 STATIC TEST RESULTS

Two kinds of columns were tested. In the static cyclic loading test of column @285mm, the shear cracks appeared in the region between about 10cm and 40cm from two column ends at the cyclic loading of deformation angle 1/100. At the cyclic loading of 1/50, the shear cracks increased diagonally, and, the main steel bars of two columns in X1 frame were buckled at the middle height, with the separation of concrete and main steel bars, at last the roof fell down. In the static cyclic loading test of column @50mm, the bending cracks concentrated in the region from two column ends till 10cm or 20cm positions at cyclic loading of 1/50 and 1/25. At cyclic loading of 1/5, the compressive crushes of two column ends began to grow immediately. At last, the concrete of two column ends were crushed completely, and the main steel bars were buckled. The load-Displacement hysteresis loops of these two static cyclic loading tests are shown in Fig. 5 and 6. The crack sketches of these loadings are shown in Photo 2.

4 DYNAMIC TEST RESULTS

Four kinds of columns were tested in the shaking table. The natural frequencies of the elastic regions of each test structure was 4.5Hz approximately. The damping ratios in elastic regions was estimated 5% - 10% by AR model analysis. Distinct differences between four test structures were not found. The plastic region dominant frequencies of each test structure was about 3Hz at the time just before collapses. Four test structures collapsed at the beginning of main wave. Acceleration-story displacement hysteresis loops of four shaking table tests are shown in Fig. 7. Damaged columns are shown in Photo 3,4,5 and 6.

In the shaking table test of @285mm, initial shear cracks grew immediately, and three columns were cut near column tops, the other one was cut near a column bottom. The main steel bars buckled.

In the test of @170mm, the initial crack types were same to @285 test case. However, the columns collapsed in next opposite acceleration with the separation of concretes and steel bars, and with the crush of core concretes.

In the test of @105mm, the shear bending cracks were appeared near two column ends. These cracks increased and collapsed with the separation of concretes, and with bucklings of main steel bars.

In the test of @50mm, the initial shear bending cracks appeared in two column ends. These cracks grew gradually, and the compressive concretes crushed with main steel bar buckling. The crush region of columns were limited in column ends.

5 P-δ EFFECTS

The Acceleration - story displacement hysteresis loops of Fig. 7 shows the effects of roof weights: that is P-δ effects. The reinforced concrete columns were collapsed without hysteresis loops which would be enough to analysis. Therefore, the data which were recorded in preparatory tests using steel columns(Photo 7), were analyzed. The steel columns have the H shape section of 100mm x 100mm x 6mm x 8mm, and the height of 1m. The frame conditions were same to the reinforced concrete test cases.

A simple model with rigid girders, shown in Fig. 8, is considered. The equations of this model are expressed as follows.

$$m\left(\ddot{v}+\ddot{v}_g\right)-m\left(\ddot{u}+\ddot{u}_g+g\right)\frac{v}{h+u}+k_b v=0$$

$$m\left(\ddot{v}+\ddot{v}_g\right)\frac{v}{h+u}+m\left(\ddot{u}+\ddot{u}_g+g\right)+k_a\left(\sqrt{(h+u)^2+v^2}-h\right)\frac{\sqrt{(h+u)^2+v^2}}{h+u}=0$$

The k_b v term of first equation will be replaced by horizontal restoring force characteristics of columns f(v). The outline of f(v) is indicated in Fig. 9. The responses were calculated with these models. Parameter values were assumed as X1 = 1cm, X2 = 1.3cm, BK1 = 9ton/cm, BK2 = 7ton/cm, BK3 = 0.2ton/cm, BK4 = 5ton/cm, h = 80cm, m = 0.027ton/gal, k_a = 750ton/cm. Damping ratios were assumes as 0.04 for horizontal responses, and 0.01 for vertical responses. Fig. 10 is the simulation responses with the consideration of P-δ effects. Fig. 11 didn't consider the P- effects. Up-down components of input were thought

as noises which were generated by shaking table mechanisms. The comparison of two cases indicates the needs of P-δ analysis for reinforced concrete tests.

6 CONCLUSION

The dynamic maximum horizontal strengths and the dynamic deformation capacities were almost agreed with static ones. However, the damage patterns were changed with the shear reinforcement bar spacing, and also with test method differences between statics and dynamics.

P-δ effects are important for collapse properties of columns.

The shaking table digital control methods improves the shaking table gain characteristics, slightly.

ACKNOWLEDGMENT

This experiment was started with the suggestion of Professor Heki Shibata, University of Tokyo. These tests were carried out with cooperations of Tokyu Construction Co.,LTD. The authors wish to express the appreciations to them.

REFERENCES

Maekawa, A. (1991), Application of H_2 Control to Electric-Hydraulic Shaking Table, JSME D&D Conferences Kobe (In Japanes)

Minowa, C., (1985), One Story Frame Collapse Tests by Using the Two Dimensional Shaking Table (Horizontal and Up-Down), Report of NRCDP No.34

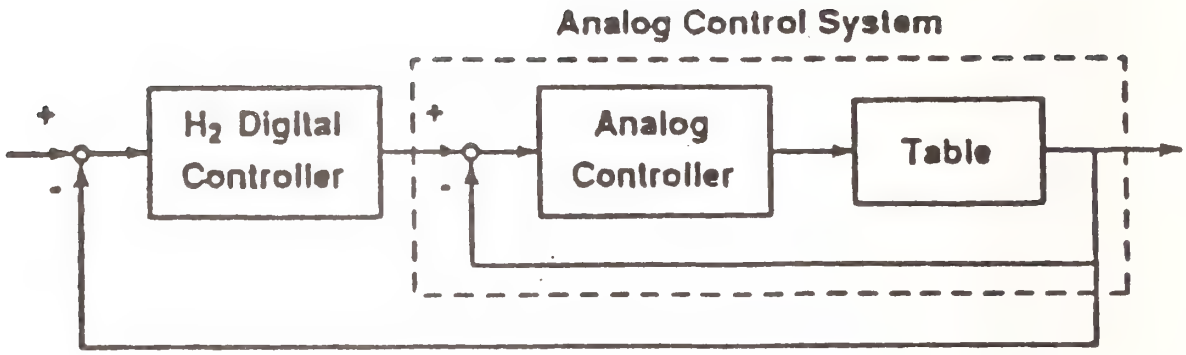

Fig. 1 Outline of Shaking Table Control

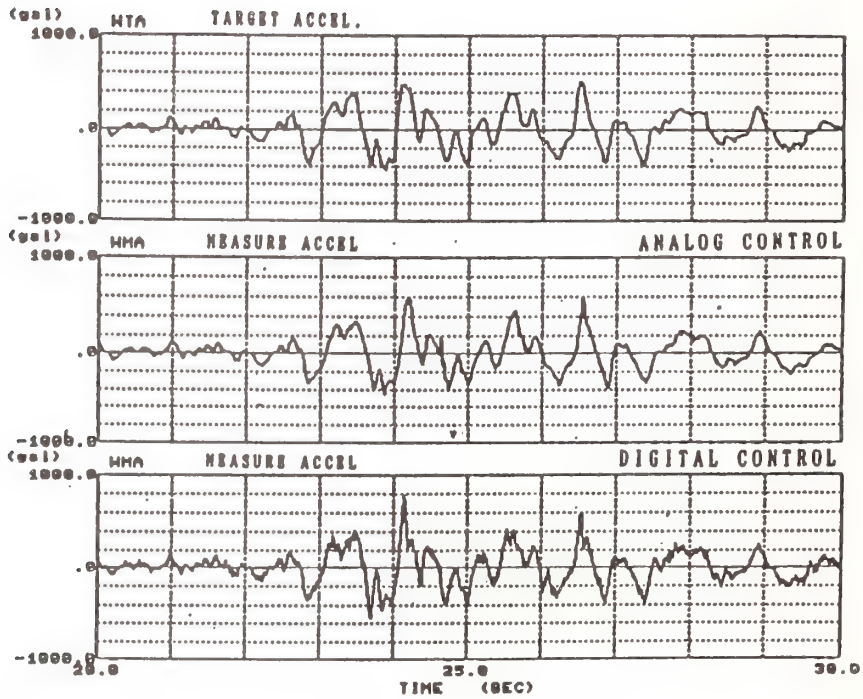

Fig. 2 Shaking Table Responses

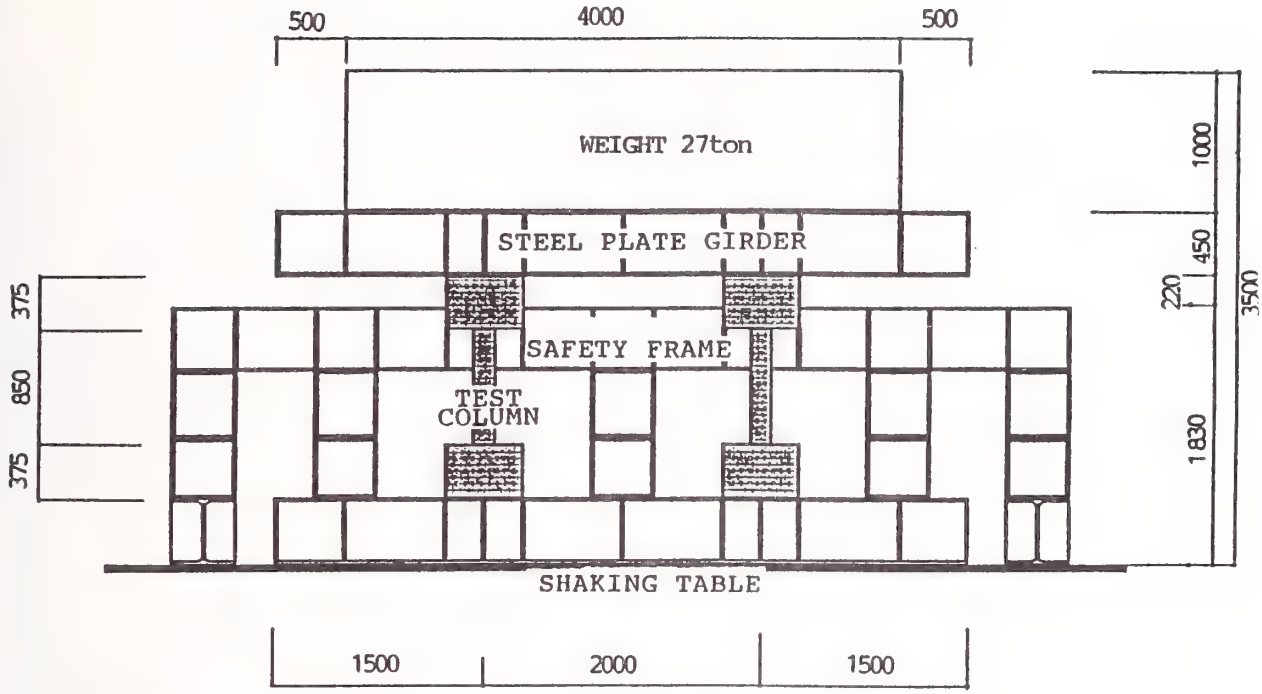

Fig. 3 Outline of Test Structure

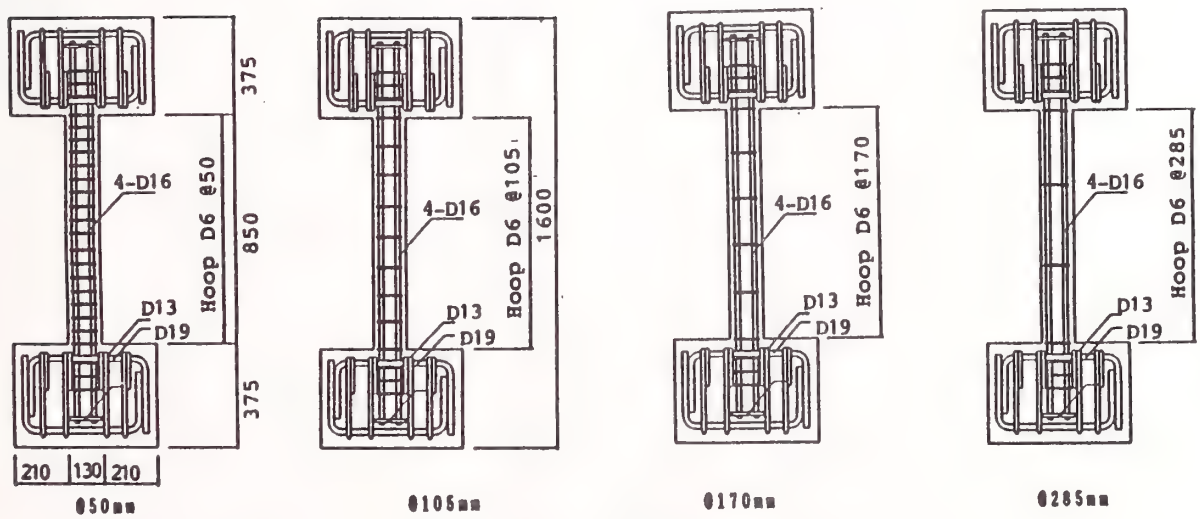

Fig. 4 Reinforcement Bars

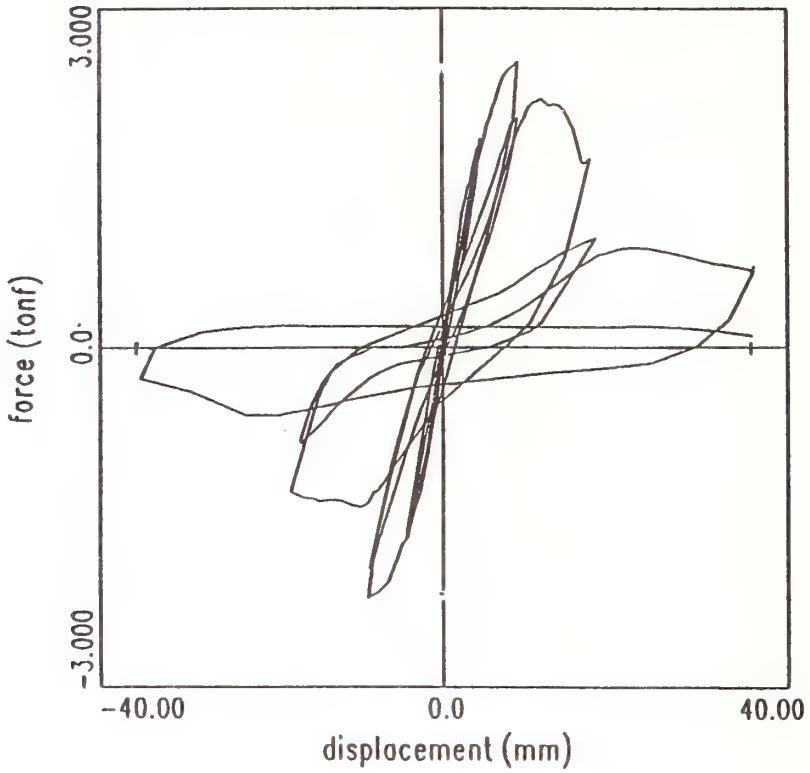

Fig. 5 Ø285mm Static Loops

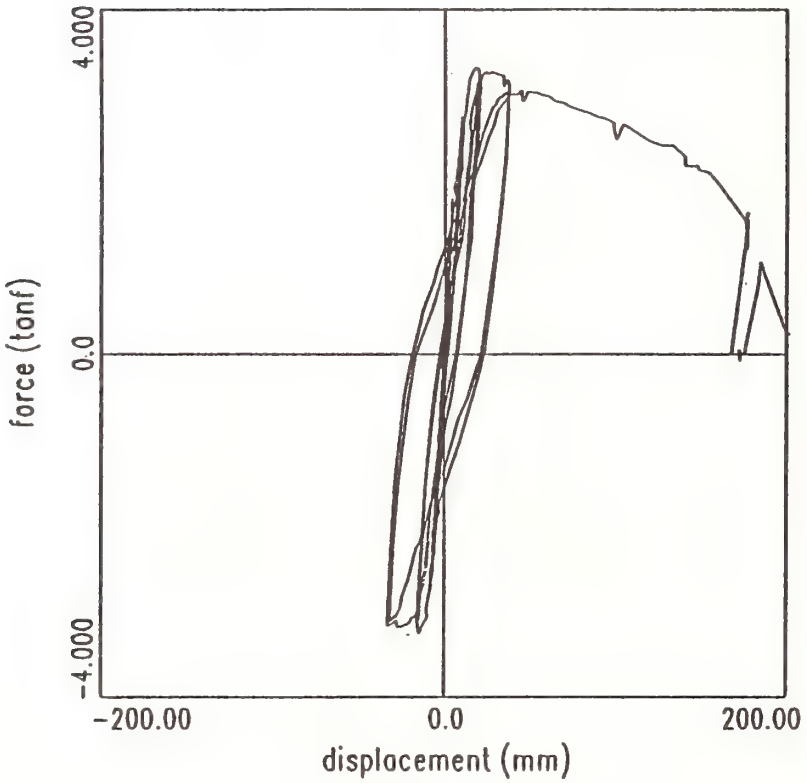

Fig. 6 Ø50mm Static Loops

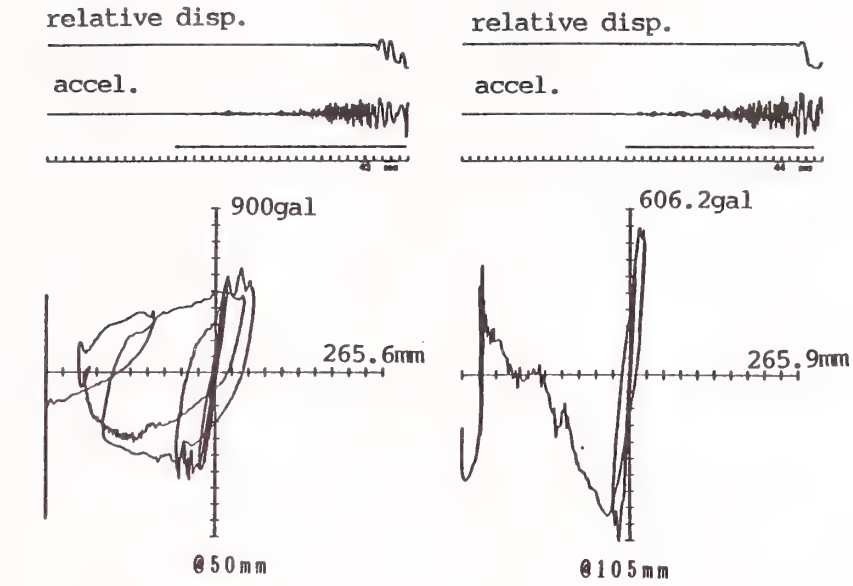

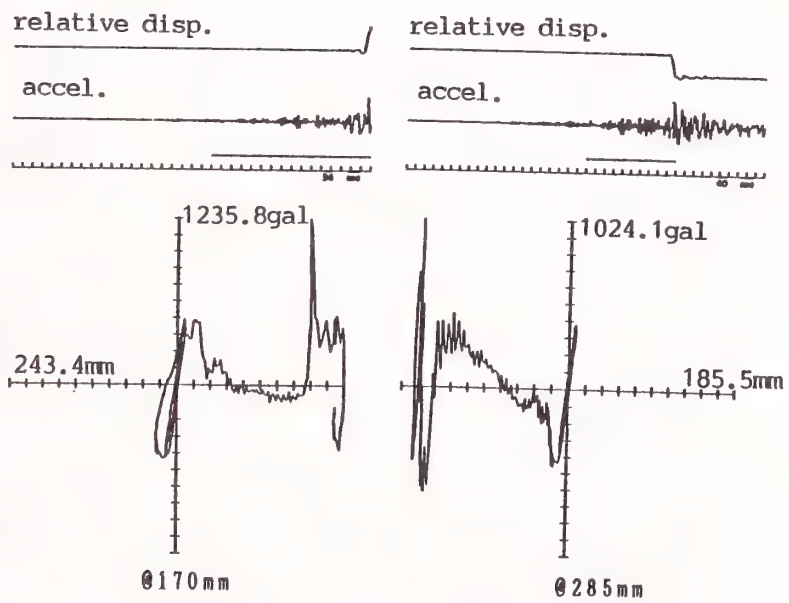

Fig. 7 Dynamic Loops

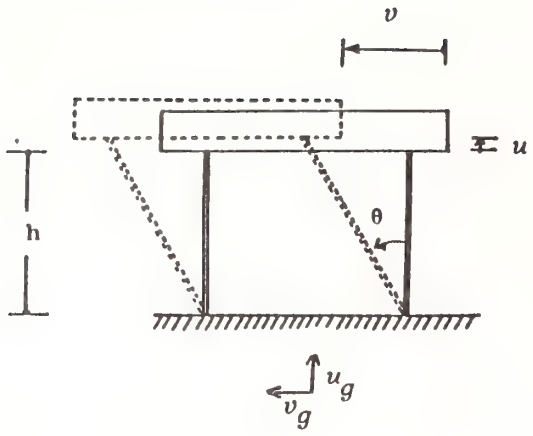

E:YOUNG MODULUS
I:GEOMETRICAL MOMENT OF INTERIA OF COLUMN
m:MASS OF TEST STRUCTURE
A:SECTION AREA OF COLUMN
Q:SHEAR RESISTANCE OF COLUMN
N:AXIAL RESISTANCE OF COLUMN
F_v:HORIZONTAL EXCITATION FORCE
F_u:UP-DOWN EXCITATION FORCE
$k_b=2\cdot12EI/h^3$, $k_a=2\cdot EA/h$

Fig. 8 Analysis Model

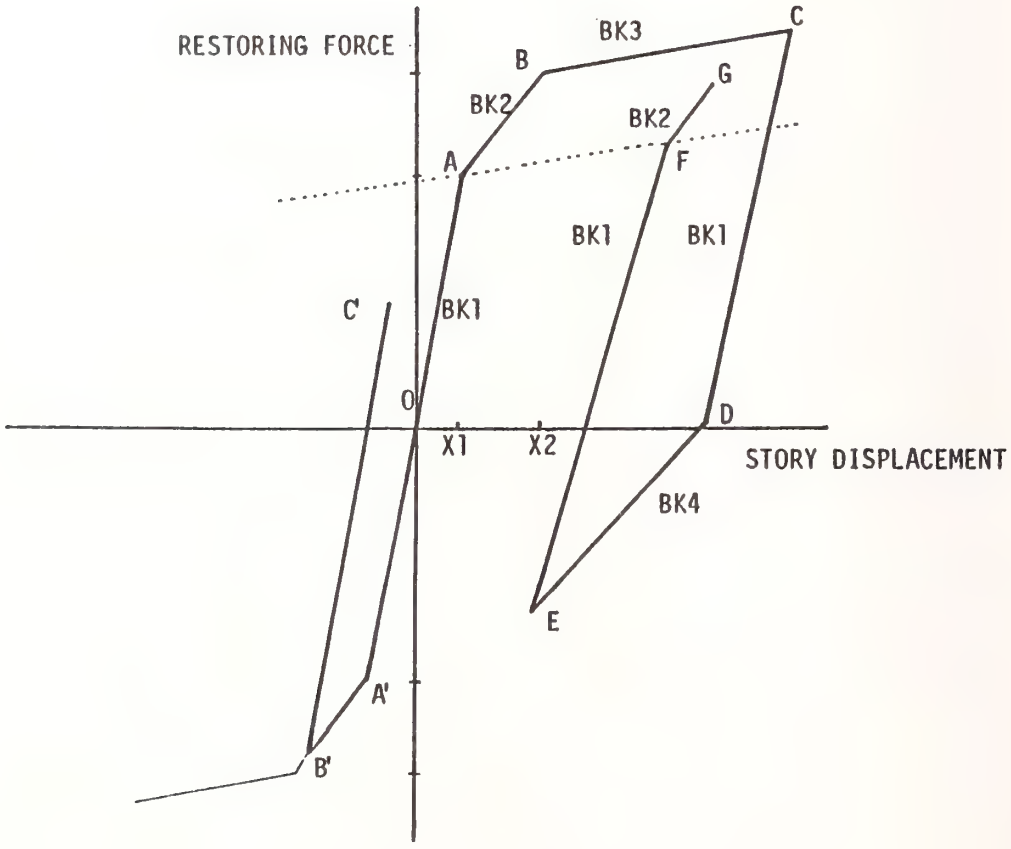

Fig. 9 Restoring Force Model

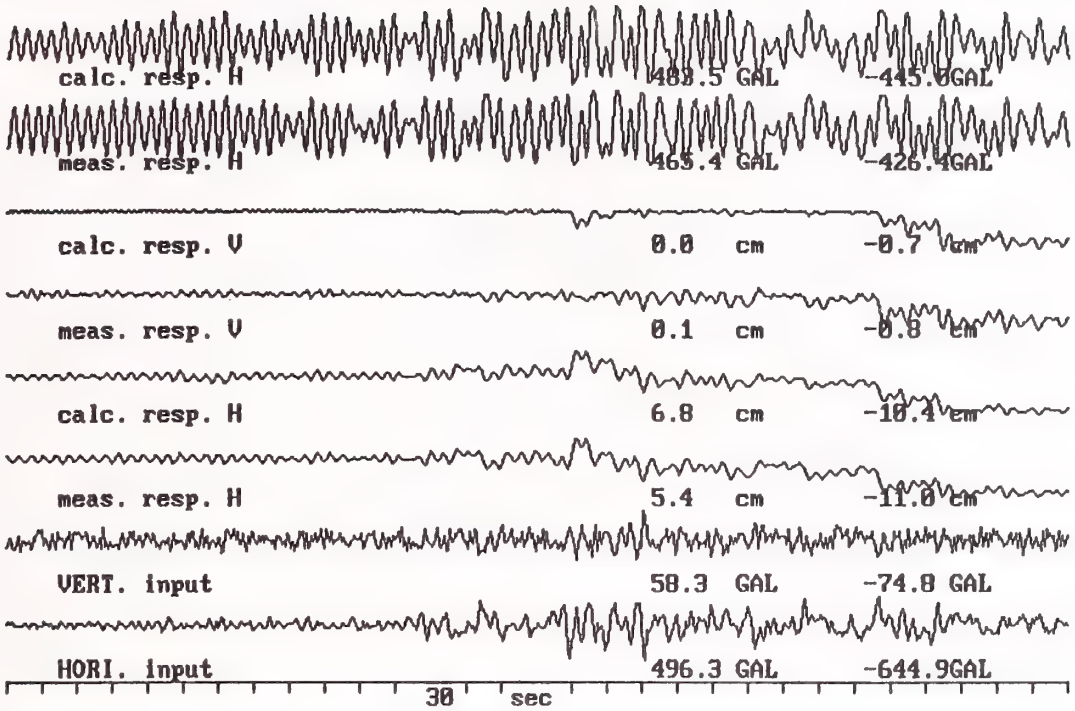

Fig. 10 With P − δ

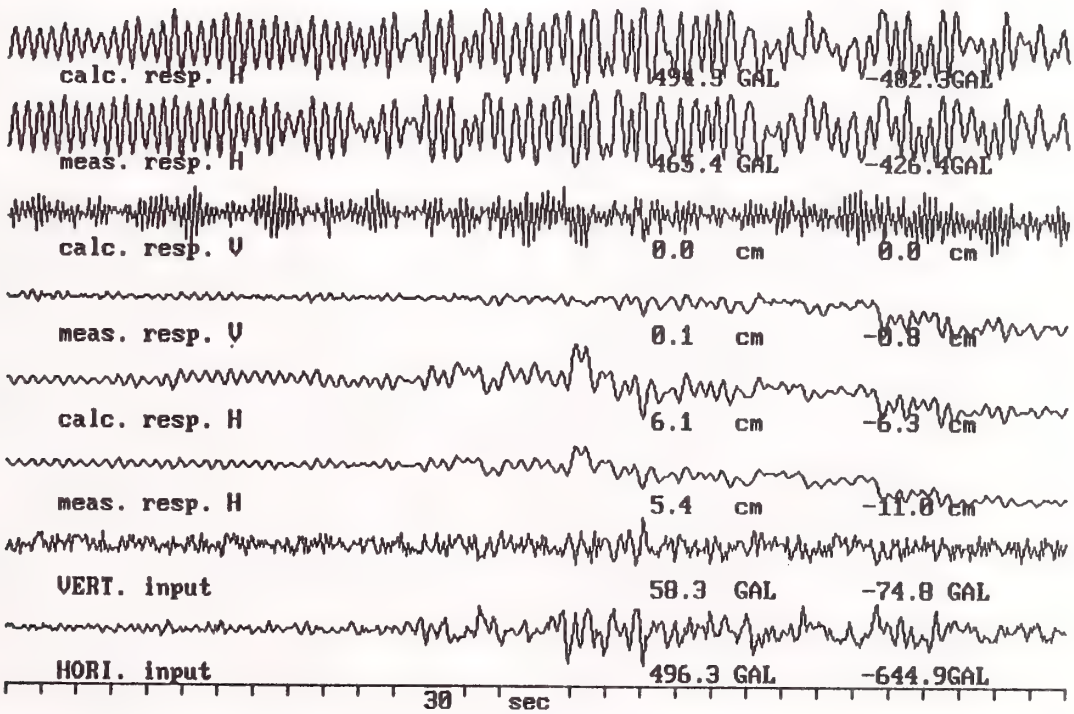

Fig. 11 Without P − δ

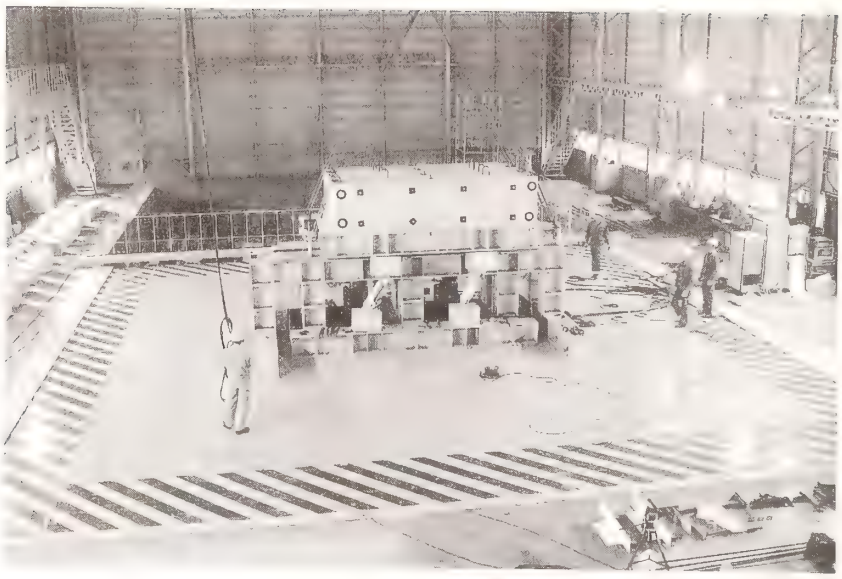

Photo 1 Over view of Test

Photo 2 @285mm (Static)

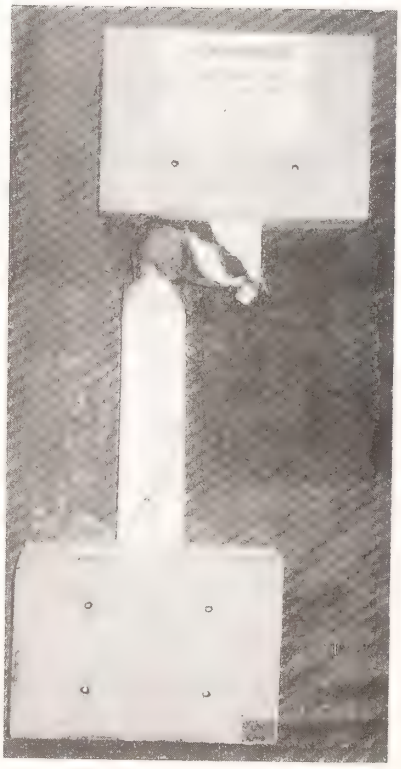

Photo 3 @285mm (Dynamic)

Photo 4 @170mm (Dynamic)

Photo 5 @105mm (Dynamic)

Photo 6 @50mm (Dynamic)

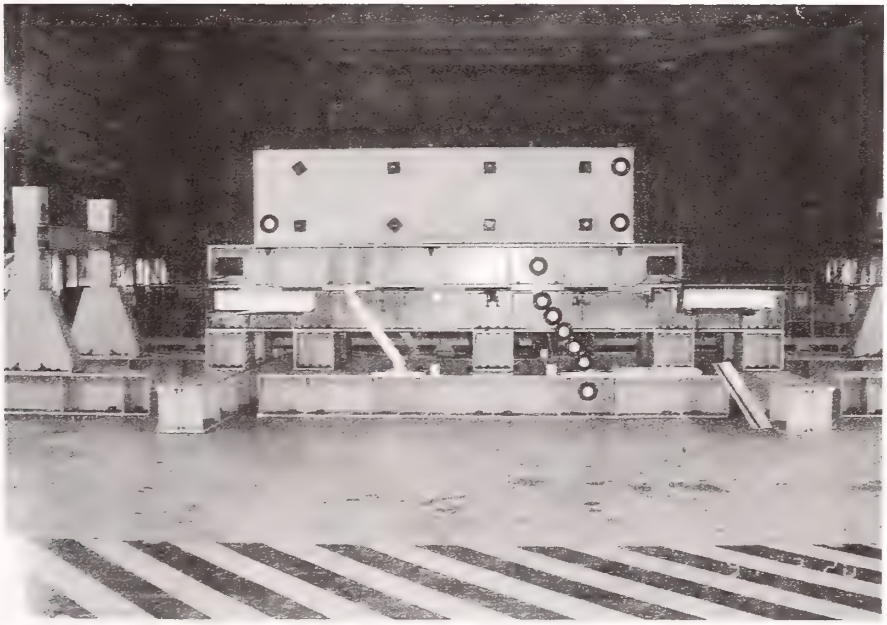

Photo 7 Preparatory Test (Steel Column)

A Hollow Clay Tile Wall Seismic Performance Program Overview

by

J. E. Beavers, W. D. Jones, and W. C. T. Stoddart[2]

ABSTRACT: An overview of a multiyear hollow clay tile wall (HCTW) program being conducted by Martin Marietta Energy Systems, Inc., at the Oak Ridge Y-12 Plant,[3] for the U.S. Department of Energy is presented. The purpose of the HCTW program is to determine the load capacity of unreinforced infilled HCTW buildings when subjected to earthquakes. Progress to date tends to indicate that extensive retrofit of such structures may not be warranted in low-to-moderate seismic zones.

1. INTRODUCTION

Many structures in the United States, especially the central and eastern United States, are constructed of unreinforced masonry. One type of unreinforced masonry, hollow clay tile (HCT), was used extensively as an infill during building construction throughout the United States, especially during the early to middle 1900s. As a result, the U.S. Department of Energy (DOE) has a significant inventory of buildings with infill walls constructed of unreinforced HCT. These buildings do not meet today's seismic standards for new construction.

Bennett and Flanagan (1992) conducted an extensive literature review that revealed no relevant research on the performance of hollow clay tile walls (HCTWs) under seismic loading. To determine the seismic performance of HCT buildings, the Center for Natural Phenomena Engineering (CNPE) of Martin Marietta Energy Systems, Inc. (MMES), is conducting an HCTW testing and analytical program for DOE. The program was initiated in the spring of 1990 and includes in situ, laboratory, full-scale building, and shake table tests; nondestructive evaluation (NDE) development; and analytical studies. The program is focused on the goals of providing information and guidance in the use of this information for assessing the behavior and, if required, identifying cost-effective methodology for retrofitting these buildings.

Nineteen types of in situ and laboratory tests are being performed, ten of which are both in situ and laboratory. The total number of tests to be performed is approximately 110 in situ and 190 laboratory. The NDE program consists of developing techniques to determine HCTW construction quality and infill boundary conditions. The analytical portion of the project consists of research on existing analysis methods and on the development of analytical evaluation techniques for buildings and components.

Building analysis consists of modeling and analyzing entire structures. Potential analysis techniques are either equivalent static analyses

---

[1] Presented at the Tenth World Conference on Earthquake Engineering, July 19–25, 1992, in Madrid, Spain.

[2] Center for Natural Phenomena Engineering Martin Marietta Energy Systems, Inc., Oak Ridge, Tennessee, 37831.

[3] Managed by Martin Marietta Energy Systems, Inc., for the U.S. Department of Energy under contract number DE-AC05-84OR21400.

(such as the UBC code Rw factors) or dynamic methods, such as time history analysis. Modeling of the HCT infills may need to be simplified, using, for example, equivalent struts. Component analysis involves developing an appropriate constitutive model for the HCT and an appropriate idealization. All components that are tested, such as prisms, in-plane infills, and out-of-plane infills (air bag tests), will be analyzed, and parametric studies will be performed. It is expected that this approach will lead to the development of simpler idealizations that can be used in the analysis of entire building structures.

Following the Loma Prieta earthquake of October 18, 1989, a significant number of buildings constructed of HCT in the San Francisco area were found to be damaged, including the city hall of Oakland, California. In addition, those that were not damaged or experienced little damage are being examined for the need for retrofit. The results of this HCTW program will provide significant insight into the performance of such structures and provide a methodology for evaluating HCT buildings that better represents their performance. In fact, in low-to-moderate seismic zones, the results may indicate that, although many such structures were not designed for seismic loads, major retrofit may not be required, as might be indicated from using conventional analysis techniques in the evaluation process.

2. SPECIFIC GOALS AND BUILDING CODES

As noted above, the general goal of the HCTW program is to develop recommendations for assessing the behavior of buildings constructed of infilled, unreinforced HCTWs. The program focuses on HCTW buildings located in zones of low-to-moderate seismicity, although the results are directly applicable to high seismicity zones. If infilled, unreinforced HCTW building construction can be shown to have inherent capacity above that normally assumed by design codes, retrofit may not be required in low-to-moderate seismicity zones if a risk-based approach is adopted. A risk-based approach is based on the principle that, while the building may not meet today's codes and standards requirements, the expected seismic performance is reasonably understood and has sufficient margins of safety. To help accomplish these goals, testing and improved understanding are required.

A second principle that has an impact on the issue of whether or not to retrofit in low-to-moderate seismicity zones is the cost increment for retrofitting. In many cases, the cost for retrofitting a building to a higher seismic capacity rather than to a lower seismic capacity is not much more than the cost for retrofitting to the lower seismic capacity; hence, the incremental cost may be very low. For example, the cost for installing a 1-in.-diameter (25.4-mm) bolt required for the retrofit of a building in a moderate or high seismic zone is basically the same cost as that for installing a 0.5-in.-diameter (12.7-mm) bolt in the same building for retrofit in a low seismic zone. Thus, the most significant cost impact for retrofitting buildings in low-to-moderate seismic zones is not the seismic capacity level of retrofit, but the decision, or requirement, to retrofit.

Building codes in the United States generally specify that the capacity of unreinforced masonry, due to its brittle nature, be limited to a stress less than the stress that causes cracking. However, the overall seismic capacity of an infilled masonry building panel can be an order of magnitude higher than its load capacity when the first crack occurs or as indicated by baseline design codes. This leads to a key proposition in the risk-based approach to a "no retrofit philosophy" for existing construction in low-to-moderate seismic zones. This proposition is that, even though HCTWs may crack when earthquakes occur, overall stability (no collapse) will be maintained. Thus, significant cracking of infilled walls is being

described by the authors as acceptable damage for buildings in low-to-moderate seismic zones. Therefore, the principal basis of the research and development program on HCTWs described in this paper is to investigate and develop understanding and computational methods for determining post-cracking behavior, including ultimate load capacity, of infilled, unreinforced HCTW building construction.

3. HCTW PROGRAM DESCRIPTION

The HCTW program at MMES is divided into four elements of work in a classical engineering work breakdown structure (WBS), shown in Figure 1.

WBS 1.2 is HCTW testing which represents the part of the program that includes static, in situ, and laboratory testing of HCTWs and wall components. WBS 1.3 is analytical modeling and analysis, which consists of research of methodologies, pre- and post-test analyses, and the development of evaluation methodologies that incorporate the results of all research efforts. WBS 1.4 is the seismic shake table facility, which is designed to show that the evaluation methodologies selected, based on static testing, are conservative when tested dynamically. Thus the evaluation methodology selected will provide a better, but still conservative, seismic performance estimate of HCTW buildings. The final element of the HCTW program is WBS 1.8, NDE research and development. For proper evaluation of an existing HCTW building, it is imperative that the existing condition of the HCTWs and the boundary conditions between the HCTWs and the structural framing be determined. Thus, a significant amount of effort in the HCTW program is the establishment of NDE techniques that can correlate controlled laboratory-constructed specimens to in situ wall construction and that can be relied on to properly define key parameter inputs to the evaluation methodologies.

4. DESCRIPTION OF HCTWS

The specific infilled, unreinforced HCTWs studied in this program are constructed of multi- or single-wythe HCT, usually 8 in. (203.2 mm) or 12 in. (304.8 mm) in width, using running bond, with all cores laid horizontally. Double-wythe walls in this program are constructed of 4-in. (101.6-mm) and 8-in. (203.2-mm) HCTs staggered to give overlapping head joints, as shown in Figure 2. The 4-in. (101.6-mm) and 8-in. (203.2-mm) tiles are also staggered from course to course. In this type of construction, no continuous collar joint exists; however, in each row, the 4-in. (101.6-mm) and 8-in. (203.2-mm) tiles are separated by a 0.5 in. (12.7 mm) to 1 in. (25.4 mm) gap. In forming the full wythe bed joint, some mortar has fallen into this gap. There is no vertical or horizontal reinforcement in the walls. The HCTWs are placed within the steel and concrete framing with varying offsets to the framing centerline depending on the particular building. In some cases, HCT pilasters, integrated with the continuous HCTW, are actually framed around a column as the HCTWs transverse the length of a building.

5. PREVIOUS HCTW PROGRAM ACTIVITIES

Aspects of the HCTW program have been going on since 1989; however, the program was not fully developed, as shown in Figure 1, until mid-1990. Beavers, Bennett, and Flanagan (1991) discussed an earlier version of the program and referred to some test results, while Fricke and Jones (1990, 1991) described the results of some of the earlier tests of element WBS 1.2, defined as a subelement WBS 1.2.1, push-test. Nine push-tests to measure the shear strength of the mortar bed joint were reported. The average shear strength was found to be 99 psi (683.1 kPa), with a standard deviation of 32.5 psi (224.3 kPa). Butala, Jones, and Beavers (1991) have described some of the work in WBS 1.3.2,

pre- and post-test analyses in preparation of testing activities of WBS 1.2.14, wall-column bending. By examining analytically the potential implications of story drift on the out-of-plane performance of such walls, they found that building drift in the out-of-plane direction imposed more bending stress on a wall panel than did inertial forces on the wall panel itself. This stress caused horizontal cracking to occur at a "*g*" level less than 5% (5%*g*). They also reported that the cracking would occur along several mortar joints, such that the steel framing would act independently at a frequency of 0.75 Hz; therefore, the inertial forces acting on the wall would be small, and it would remain stable and standing. The question posed here is, How much in-plane strength remains, given the out-of-plane horizontal cracking? This concern will be further addressed by testing in WBS 1.2.14.

Chua (1991), using existing analysis methodologies, conducted a parametric study of boundary conditions, Poisson's ratio, and other parameters to determine a best approach to estimate ultimate out-of-plane behavior of infilled HCTWs. As noted by Beavers, Bennett, and Flanagan, Chua found that for static out-of-plane loads, the modulus of rupture and the modulus of elasticity had the most significant effect on first panel cracking, while Poisson's ratio and shear moduli had little effect.

6. RECENT HCTW PROGRAM RESULTS

Under the HCTW testing element WBS 1.2, one major subelement is the air bag test, identified as WBS 1.2.7. An air bag test is the application of out-of-plane loading to an infilled wall using a pressurized air bag (Dawe and Seah 1989). The first air bag test (Fricke, Huff, and Jones 1992) was conducted in October 1991. The test was conducted on a 8-in. (203.2-mm) single-wythe HCTW 28 ft (8.53 m) wide by 12 ft (3.66 m) tall infilled within a steel frame of W14X142 columns, a W30X108 overhead beam, and a concrete floor slab. This test was conducted on the first floor of a five-story building. A schematic of the test setup is shown in Figure 3, with the actual wall and corresponding reaction frame shown in Figure 4.

For design purposes, conventional methods using code allowables and a static analysis would generally be based on one-way action in the short (vertical) direction. This procedure would predict a uniform loading limit equivalent to an inertial load of approximately 0.1*g*. However, as discussed by Fricke, Huff, and Jones, the test results revealed an equivalent inertial load capacity of around 3*g*, thirty times their results obtained from the conventional approach. These researchers also looked at other alternative conventional evaluation methods and compared the results to their test results. In all cases, the test results revealed a minimum in situ out-of-plane seismic capacity of 13 times the least conservative conventional method. The basic reason for the underestimated capacity resulting from conventional methods is the lack of consideration of two-way arching action that actually occurs in infilled walls. The load deflection curve for the central point of the wall is shown in Figure 5.

More recently, Flanagan, Bennett, and Barclay (1992) conducted three laboratory in-plane tests, on full-scale infilled HCTWs. These tests were part of a sixteen-test program under subelement WBS 1.2.9, designed to study failure mode, shear wall performance, load transfer mechanism, energy absorption, and hysteretic behavior of HCTW infilled frames having various frame to infill stiffness ratios. The walls were 8 ft (2.4 m) in height and width, constructed with single-wythe 8-in. (203.2-mm) HCTs, placed between the flanges and against the column webs, as is much of the construction of DOE facilities. For each test, the overhead beam size was held constant at W12X35 while the column sizes for each test varied (W10X12, W10X30, and W10X45).

For determining the in-plane capacity, conservative conventional analyses usually result in defining that capacity as being the load at which the first shear crack occurs in the infilled wall. The results of the three tests when applied to a first floor interior wall of a typical three-story DOE building showed that the equivalent in-plane seismic capacity was approximately 0.3*g* at first panel cracking. Applying the ultimate capacities of the tests to this typical building indicated an equivalent in-plane seismic capacity of approximately 0.8*g*. A typical failure mode at the completion of each test is shown in Figure 6, while Figure 7 shows a typical hysteretic curve of the in-plane load versus deflection.

Again, the analysis of these tests showed that conventional analysis techniques are inadequate to estimate the ultimate performance of unreinforced HCTW structures of the type described herein.

7. OTHER TEST RESULTS

As shown in Figure 1, unit block tests (WBS 1.2.3), bond wrench tests (WBS 1.2.11), and prism compression tests (WBS 1.2.4) are also being conducted in support of the overall program. Fifteen unit block tests (ten in compression parallel to cores and five splitting tensile strength perpendicular to cores) have been conducted with an average net compression stress of 5539 psi (38,194 kPa) and a standard deviation of 634 psi (4,391 kPa). The average splitting tensile strength was 351 psi (2420 kPa) with a standard deviation of 106 psi (731 kPa). The results of prism compression tests showed an ultimate capacity of 228 psi (1573 kpa) when loaded perpendic-ular to the cores.

Preliminary bond wrench tests on the air-bag-damaged wall have shown an average ultimate tensile capacity of the bed joint mortar to be 16 psi (110 kPa). As the HCTW testing program continues, additional tests and corresponding results will be reported.

8. SUMMARY AND CONCLUSION

The HCTW program is a multiyear testing and analytical effort to address the seismic performance of steel and concrete frame structures with infilled HCTWs. The first year of an approximate three-year program has been completed. Results to date support the assertion that infilled HCTW structures can have significantly more inherent strength than conventional analysis and code allowable stresses would imply, and must be treated as structural systems.

Some progress has been made in developing alternative analytical methods, but more test data are needed to support current results. The program is being documented, with technology transfer as one of its goals. As further testing is conducted and analytical techniques verified and/or developed, results will be published. Based on the preliminary results of the HCTW program, it is believed that many unreinforced HCTW buildings in low and moderate seismic zones may not require retrofit, when evaluated using a risk-based approach. Further testing and analytical development are expected to confirm this assertion.

9. REFERENCES

Beavers, J.E., R.M. Bennett, & R.D. Flanagan. 1991. Research on unreinforced hollow clay tile walls and developments of computational mechanics. *U.S./China Joint Workshop on Computational Mechanics,* September 24-28, Beijing, China.

Bennett, R.M. & R.D. Flanagan. 1992. *Structural Testing of Clay Tile Walls: Testing and Evaluation Program,* Y/EN-4325, Center for Natural Phenomena Engineering, Martin Marietta Energy Systems, Inc., Oak Ridge, Tennessee, USA.

Butala, M.B., W.D. Jones, & J.E. Beavers. 1991. Out-of-plane behavior of hollow clay tile walls infilled between steel frames. *Proc. of the Third Department of Energy Natural Phenomena Hazards Mitigation Conference,* October 15-18, St. Louis, Missouri, USA.

Chua, L.S. 1991. Out-of-plane behavior of unreinforced hollow clay tile masonry infilled wall panels. Thesis presented for the Master of Science degree, University of Tennessee, Knoxville, Tennessee, USA.

Dawe, J.L. & C.K. Seah. 1989. Behavior of masonry infilled steel frames. *Canadian Journal of Civil Engineering,* 16: 865-76.

Flanagan, R.D. & R.M. Bennett. 1991. Analytical modeling of masonry infilled steel frames. *Proc. of the Third Department of Natural Phenomena Hazard Mitigation Conference,* October 15-18, St. Louis, Missouri, USA.

Flanagan, R.D., R.M. Bennett & G. Barclay. 1992. Experimental Testing of Hollow Clay Tile Infilled Frames. *Proc. of the Sixth Canadian Masonry Symposium,* University of Saskatchewan, July 15-17, Saskatoon, Saskatchewan, Canada.

Fricke, K.E. & W.D. Jones. 1990. A test program to determine the structural properties of unreinforced hollow clay tile masonry walls of the DOE Oak Ridge plants. *Proc. of the Fifth North American Masonry Conference,* University of Illinois, Champaign, Illinois, USA: 747-758.

Fricke, K.E. & W. D. Jones. 1991. A test program to determine the structural properties of unreinforced hollow clay tile masonry walls of the DOE Oak Ridge plants. *Masonry Society Journal* 9: 56-63.

Fricke, K.E., T.E. Huff & W.D. Jones. 1992. In situ lateral load testing of an unreinforced masonry hollow clay tile wall. *Proc. of the Sixth Canadian Masonry Symposium,* July 15-17, University of Saskatchewan, Saskatoon, Saskatchewan, Canada.

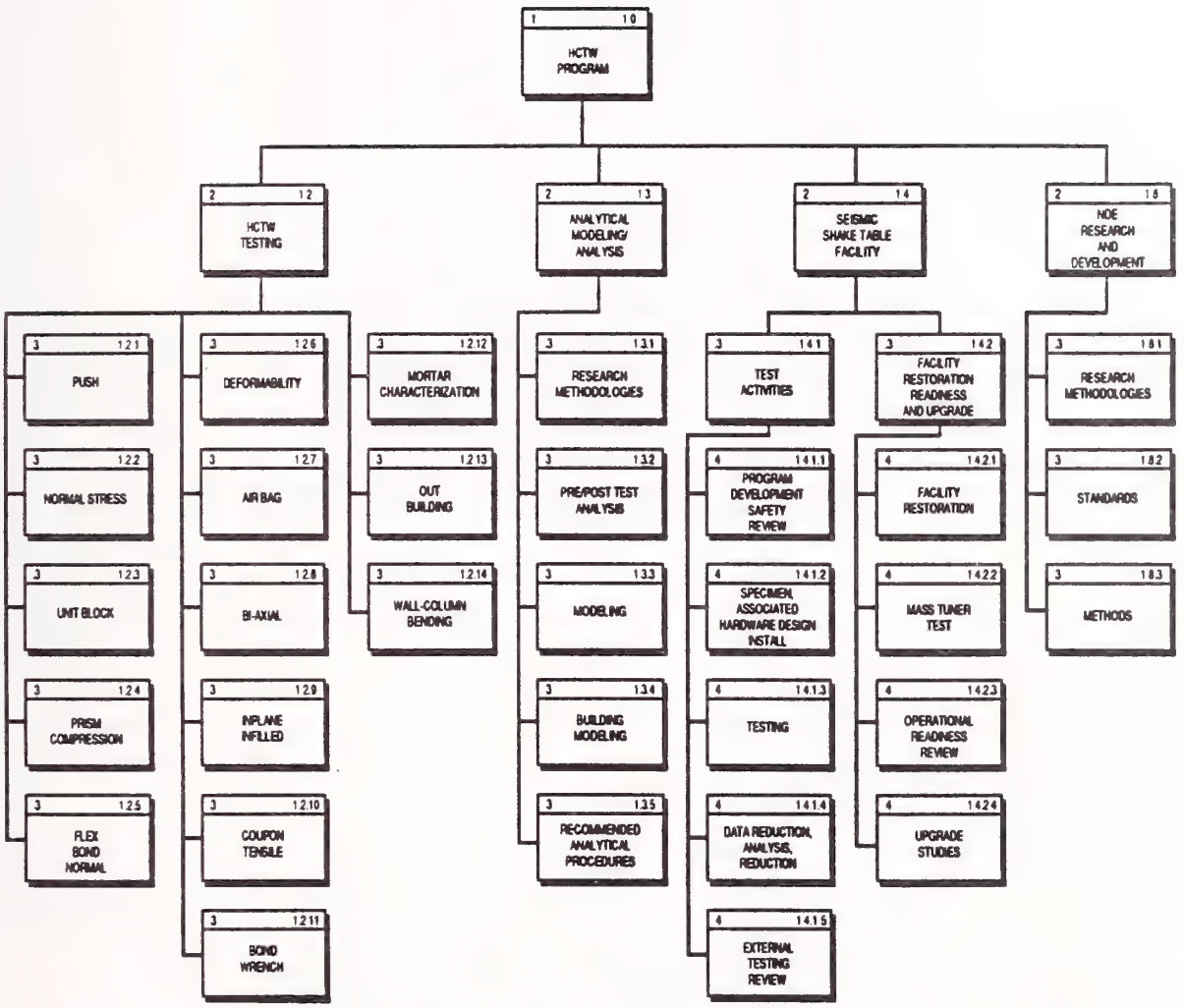

Figure 1. HCTW program work breakdown structure.

Figure 2. Cut-section of an infill HCTW.

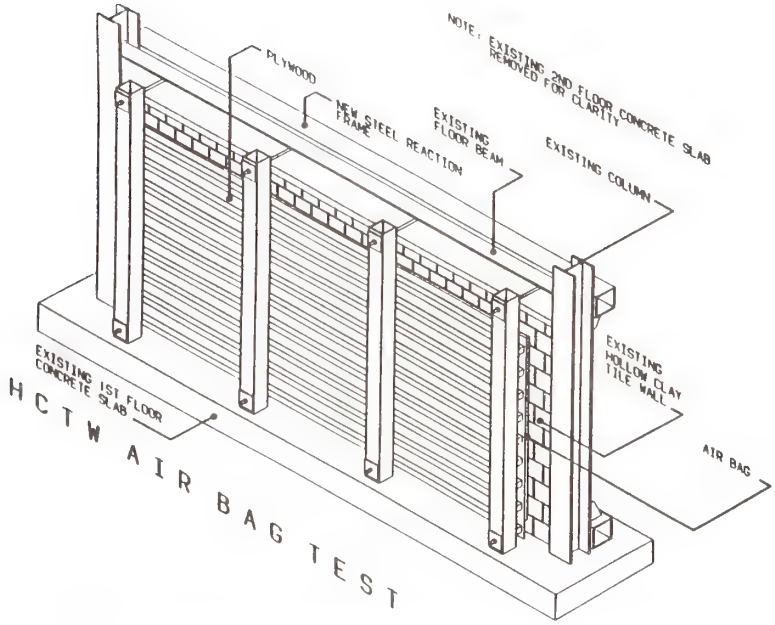

Figure 3. Isometric schematic of HCTW air bag test.

Figure 4. Air bag test HCTW with loading frame.

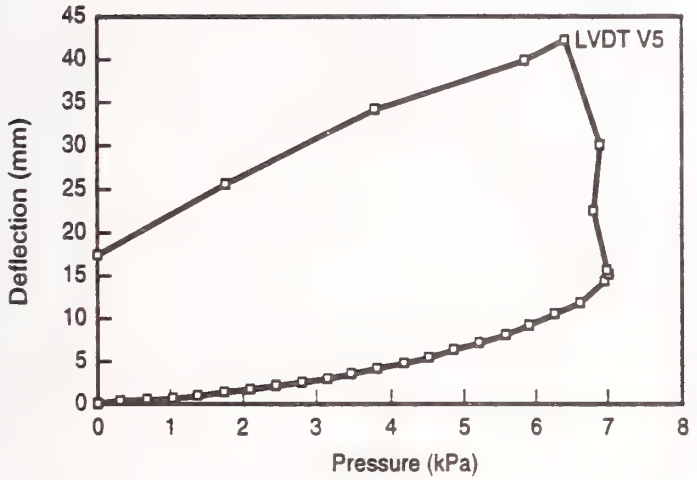

Figure 5. Air bag test HCTW central point load-displacement curve.

Figure 6. In-plane laboratory HCTW test cyclic failure mode.

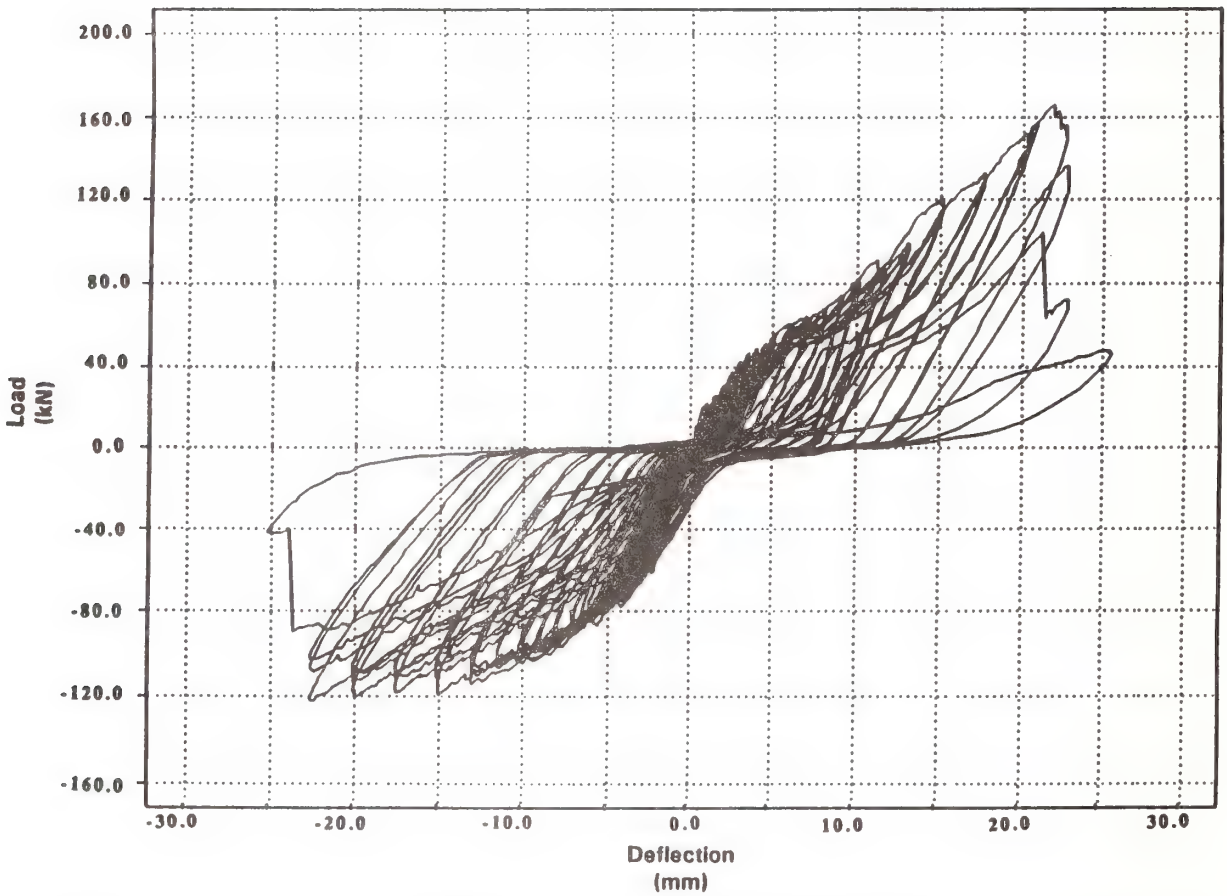

Figure 7. In-plane laboratory HCTW test load-displacement hysteretic curve at top of wall.

The Valuation and Designation Systems for Structural Calculation Programs in Building Engineering

by

Keiichi Ohtani[1]

SUMMARY

In the recent several decades, the computer uses are popularized rapidly to all area of the building world which are involved research, development, design, construction and others. Furthermore, the diffusion of the computer uses will be spread more and more in future. In the background of these situation, the valuation committee for the computer programs was established in the Building Center of Japan in 1974, for the purpose to examine the programs and ensure these quality and reliability. This committee deals with the continuous treatment programs which have general purpose and are used in the structural calculation reports for the approval of requisition. The administration step of the designation by the Minister of Construction for the evaluated programs was started in 1977. This valuation and designation systems are unique without parallel in the rest of the world. By the establishment of this systems, the program maker, user and administrative official are recipient of favours themselves. This report describes the present situation of the above mentioned systems.

KEY WORDS: Valuation of Program, Designation of Program, Structural Calculation Program, System of the Approval of Requisition, Building Standard Law.

1. INTRODUCTION

The computer uses for the all field of the building world, especially the field of structural calculation and sun-shadow calculation, gained experience about 30 years. Hereafter, the computer uses will be increased more and more for all sorts of business.

In the background of these situation, the valuation committee for the computer program of the structural calculation was established in the Building Center of Japan in 1974, for the purpose to maintain the program quality for the structural calculation reports by using the computer and to attempt the convenience of the approval of requisition by the administrative office. Furthermore, the administrative measure of the designation system by the Minister of Construction to the program, which has finished the valuation, was started in 1977.

These valuation and designation systems are epoch-making one and unprecedented one for the foreign countries, then other countries are paid attention to these systems. This report describes the present situation and the contents of the valuation and designation systems for structural calculation program.

2. THE SYSTEM OF THE APPROVAL OF REQUISITION

At the case of design and construction of Building in Japan, we must be according to the rule of "the Building Standard Law". It is the obligation that the designer reports the design specification (drawings, structural calculation report and etc.) to the administrative office for the approval of requisition before the beginning to construct a building. The administrative office is checked the received design specification by the rules of "the Building Standard Law", and given the permission of construction to the designer when he judged that the design proper. However, other system, which is recognized one by one by the Minister of Construction, is set up for the building which is exceed higher than 60 m, and the building which is used the special technique.

It is a characteristic of building administration in Japan that the design specification is recognized by the method of approval of requisition.

3. CIRCUMSTANCES OF THE PROGRAM VALUATION AND DESIGNATION SYSTEMS

1) Director, Disaster Prevention Research Division, National Research Institute for Earth Science and Disaster Prevention, Science and Technology Agency, Tennodai 3-1, Tsukuba-shi, Ibaraki-ken 305 JAPAN

Above-mentioned, the rule of "the Building Standard Law" is decided on the approval of requisition for the designed building. In recent year, the case of structural calculation report for approval made by the using of computer are increased more and more. The building director (administrative official), who is participated in requisition work, is received as the black box as the contents of program, and is judged for the property of structural calculation report. Furthermore, by the data communication in use of computers and telephone lines and the popularization of personal computer, the computer use by the third person, who has no judging ability, is increased more and more. It is a social pressing need to establish the appropriate plan for the computer use of structural technique confusion and maintain the quality of program.

In the background of these situation, Ministry of Construction was established the investigation committee of the program valuation works in the Building Center of Japan in 1971. By the report from this committee (June, 1972), the valuation committee for the computer programs was established in the same center, for the purpose to examine the programs and to ensure these quality and to directly reflect in the administrative management of the valuation results. The activity of the committee was started from January, 1974.

Further, Ministry of Construction was established the designation system by the Minister of Construction for the program which is finished the valuation in 1977. This designation system is enhanced the effect of the valuation system and is reflect to the treatment for the administrative works. And, we were waiting to start this system from beginning the valuation activity.

If the owner who has a valuated program apply for the Minister of Construction by the definite treatment, the Minister will be given the designation to the program. Accordingly, the designated program has tow characteristics; One is the confirm of the applied area and calculation method through the valuation, other is the acceptation of logical accuracy by the Minister. By this measure, the position of the valuation system is defined to the treatment on the building administration. The standpoint of applicant (program owner), administrative official, committee member and user are cleared for each other. Together with immeasurable effects for the the maintain of building safety and for the qualitative improvement of the program.

4. EFFECTS AND CONTENTS OF THE VALUATION AND DESIGNATION SYSTEMS

The considerable effects of these systems are as follows;

1) The program maker need not explain the reliance of the program to the administrative official or user individually.
2) The user use to free from care at the first utilization of the valuated program.
3) The administrative official need not check to reliance of the program, check only the objective building properties.

The proposed reasons by every company is mentioned these effects at the application of the valuation. Now, this valuation system is fixed to work for the public good, and the administrative office estimate the extremely effective system to this valuation.

To reply the expected effects, the following subjects are examined by the committee.

1) Errors affecting the results of structural calculation in the program itself.
2) Misapplication of the program. (protection and caution)
3) Misusages of calculation results. (protection and caution)

In the evaluating of the committee, pertinence of the program is investigated by the explanation of its contents, the test running which is done repeatedly and the other tests. This committee deals with the continuous treatment programs (packaged programs) which have general purpose and are used in the structural calculation reports. It is a big problem to deal with the copyright or know-how of the program at the valuating work, the members of the committee are consisted from university, national research institute and administrative office employs.

5. THE STATE OF THE SYSTEMS

At the early stage, the object of valuation was only limited to the program for wide use computer. The programs for public and private usage were deals with this valuation committee. And also, the committee valuated with appropriateness the

program employment by the different organ with the program maker. The Building Standard Law Enforcement Order, especially the part of structural calculation, was drastic changed in July, 1981. At this moment, 22 programs were valuated (some programs were designated) already. But the according of change of the Building Standard Law Enforcement Order, above mentioned 22 programs were lost effects of the valuation and designation.

After the effectuation of the Building Standard Law Enforcement Order, the new programs (include the above 22 programs with revision) were valuated to the use of wide use computer. The usage of personal computer, which have a good performance, were progressed rapidly more and more. By the considering this condition, the valuation committee, under the auspices of the Ministry of Construction, determined to deal with the programs for personal computer in March, 1982, and was started to this activity in July of same year.

At the present, the 250 matters, in which this number is including with the minor modification or the addendum of function of program, were completed to the valuation work. (Table 1 and Figs. 1, 2) In total, the 101 different programs, include the ones for public use, private use and personal computer, were completed to the valuation, and the 85 organizations had the valuated program for the employment of the structural calculation work. But nowadays, the designation system to the program for the personal computer and the part of program of the calculation of retained horizontal strength were not established. Therefore, the 68 organizations (47 programs) were received the designation from the Minister of Construction.

6. CONCLUSION

The valuation and designation systems for the structural calculation programs in building engineering are fixed to the building world in the background of the popularization of computer uses and the administrative mechanism of the approval of requisition system for building. The number of the valuated program amount to 101 cases and the designated program amount to 68 cases now.

This valuation and designation systems have some problems as follows;
1) To fully equip the corresponding system for change of program.
2) To make the active plan for the more efficiently valuation.

We want to hope that this valuation and designation systems will be developed more and more by the exertion and cooperation of the persons concerned.

Moreover, beside this valuation system for the building, the other organizations were established the similar systems, such as the aseismic design program in high-pressured gas facilities and the analytical program in surveying.

Table 1. THE STATE OF VALUATION AND DESIGNATION SYSTEMS
(February, 1991)

	Valuation		Designation
Public use	17	186	10
Private use	55		37
Personal Computer	29		
Program Employment	85		21
Modification or Addendum	64		
Total	250		68

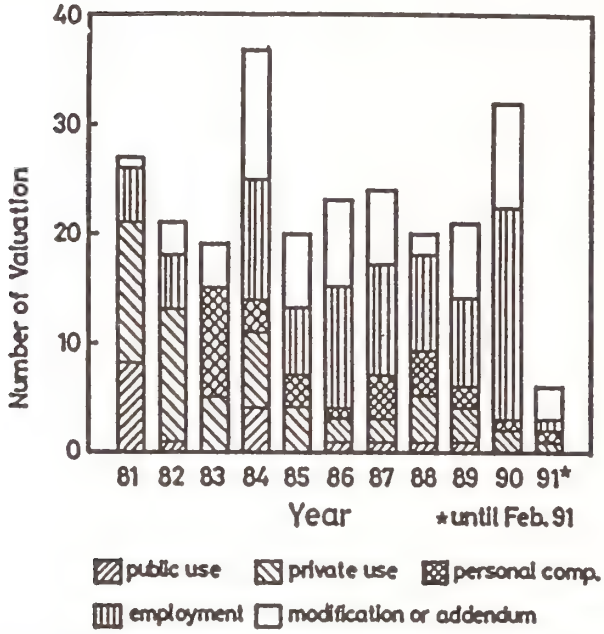

Fig. 1. THE YEAR TREND FOR THE NUMBER OF VALUATED PROGRAMS

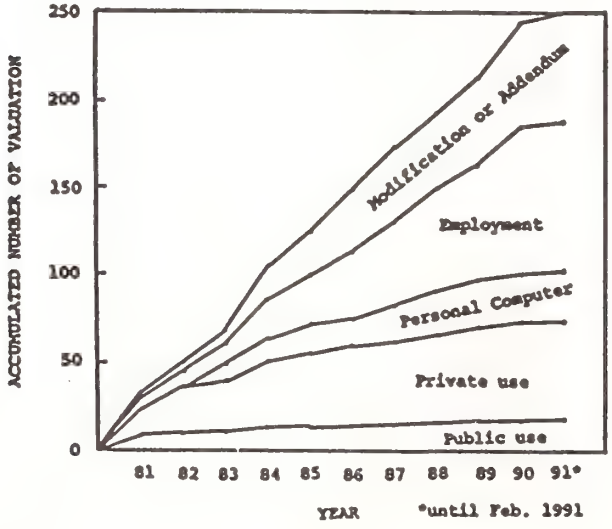

Fig. 2. THE YEAR TREND FOR THE ACCUMULATED NUMBER OF VALUATED PROGRAMS

Highlights of the 13 March 1992 Erzincan (Turkey) Earthquake

by

Mehmet Celebi*

ABSTRACT

The March 13, 1992 M_s = 6.8 Erzincan earthquake in Turkey is highlighted here. The epicenter of this earthquake was located 7.7 km from the eastern end of the North Anatolian fault. The strong motions recorded in Erzincan had peak ground accelerations of approximately 0.5 g, accompanied by a pulse of 2 seconds. The duration of the earthquake was 7 seconds. This earthquake caused collapse of about 150 buildings—mainly to 4–5-story reinforced, concrete-framed buildings with infill walls. This damage, which is discussed, can be attributed to non-compliance with seismic codes.

KEY WORDS: earthquake; North Anatolian fault; magnitude; acceleration, code, spectra.

1. BACKGROUND INFORMATION

At the eastern end of the North Anatolian fault in Turkey, a magnitude 6.8 earthquake occurred on March 13, 1992 at 19:19 local time (17:19 UTC). National Earthquake Information Center (NEIC) reported the depth at 28 km and the epicentral coordinates as 39.706°N and 39.570°E. The epicenter is 7.7 km SE of the center of the City of Erzincan, the coordinates of which, from the Gazetteer (1984), are 39.75°N and 39.50°E. The City of Erzincan has a population of 91,000 plus approximately 30,000 military personnel. Official count of lost lives was 800. However, unofficially, as many as 3,000 persons may have lost their lives during the earthquake.

The City of Erzincan is located on the edge of an alluvium basin lying on an alluvium fan at an elevation of 1,150 m. It is bordered in the north and south by high and steep mountain ranges, some reaching altitudes of 3,800 m. The geology of the basin can be best described as 100 m of interbedded sand and gravel overlying lacustrine sediments. The depth to bedrock in the basin is estimated to be between 1,200–1,500 meters. At Erzincan, the depth to bedrock is estimated to be 300–500 meters. Borehole logs are available only for the top 200–225 meters.

The North Anatolian fault, well known for its similarity to the San Andreas fault in California, is a right-lateral strike-slip fault. The recurrence intervals of large earthquakes are also similar to the San Andreas (California) recurrence intervals. The last large earthquake of 1939 leveled the City of Erzincan of that time, killing 39,000 people. The 1939 earthquake had a magnitude 8.0 and epicentral coordinates of 39.7°N and 39.7°E (Ambraseys, 1970). Since 1939, there have been 60 magnitude 6 and larger earthquakes along the North Anatolian fault

*U.S. Geological Survey MS/977, 345 Middlefield Road Menlo Park, CA 94025-3591 USA

(Ambraseys, 1970). Ambraseys states that historically, there are quiet periods of seismicity of approximately 150 years. A general map showing the North Anatolian fault, the location of the City of Erzincan is provided in Figure 1. The unique topography of the epicentral area and the basin of Erzincan is shown in Figure 2.

As a consequence of the 1939 earthquake, the City of Erzincan was relocated to the north of its original location to its current location (towards the hills) with the idea that the new buildings would be on firmer ground and shallower depth of alluvium. Furthermore, in the new city, the number of stories was limited to 3—a restriction, which, in the 1970s and 80s was slowly forgotten and abandoned. At the time of the 13 March 1992 earthquake, the tallest building in the city was 7 stories. Only 2 engineered buildings (the Railroad Station Building and the Military Headquarters Building) from the pre-1939 era survived the 1939 earthquake and also the recent earthquake.

It was reported that several buildings that collapsed during the 13 March 1992 earthquake were repaired after sustaining severe damage during a smaller (M = 5.6) 1983 earthquake.

TYPICAL CONSTRUCTION

Typical construction in the City of Erzincan is of reinforced concrete frame with infill walls, generally of hollow-tile masonry construction. The infill walls vary in height, sometimes up to window levels and sometimes as piers extending between floor to ceilings. The roofs are generally of wood-truss with clay tiles. Gable end walls, generally not braced, are also constructed with hollow tile masonry. Shear wall construction is seldom used. There is some adobe (mostly single-story) and stone-masonry construction.

The majority of the inventory of buildings in Erzincan is 4–5 stories. A significant percentage of the inventory is single-story houses, although there are many 2–3-story buildings also. Very few of the buildings in the City of Erzincan are 6–7-story buildings.

There are also some typical industrial buildings (steel frame of sugar refinery, saw-tooth, roof-type reinforced concrete cotton textile mill and a new plant of precast gable) in the Erzincan basin.

DAMAGE

The City of Erzincan had most of the engineered structures in the earthquake stricken Erzincan Basin and vicinity and it suffered the most damage. Other population centers that experienced damage were smaller towns and villages where the majority of buildings were not engineered. In a small scale, the basin and the damage patterns in Erzincan due to the earthquake resemble the Mexico City (Michoacoan) earthquake of 1985. Figure 3 shows a typically pancaked four-story building and Figure 4 shows a typical reinforced concrete frame building in the state of collapse, its infill walls spalled out and plastic hinges developed at the column ends due to insufficient and/or incorrectly implemented shear reinforcement. On the other hand, a single-story, partially timber-reinforced adobe

building located in downtown Erzincan (Figure 5) survived the earthquake without any damage.

Typical samples of damage are illustrated in Figures 6 to 10. The general view of Unsan Flour Mill, approximately 10 km east of Erzincan, is seen in Figure 6. The details of the short column clearly indicate insufficient and inappropriately placed shear reinforcement (Figure 7). Similarly, the four-winged Military Hospital, damaged extensively beyond repair, is seen in Figure 8. The hospital lost one of its wings, lost one story in one of the two central wings, and sustained heavy damage to the remaining two wings. This was one of the three hospitals in Erzincan. All three hospitals were out of service as a result of the severe damages during the earthquake. The L-shaped wing of the seven-story Social Security Hospital totally collapsed and the State Hospital was severely damaged.

Some of the very few steel structures in Erzincan, at the Sugar Refinery, were heavily damaged. In Figure 9, the main refinery building is seen. The infill walls of the refinery sustained heavy damage. The stack of the calcination unit of the refinery collapsed (Figure 10) damaging part of the main refinery building in the process.

Approximately 150 buildings either totally collapsed or were damaged beyond repair.

STRONG-MOTIONS RECORDED

The Earthquake Research Center (ERC) of the General Directorate of Disaster Affairs of the Ministry of Public Works and Settlement (Republic of Turkey) operates and maintains the strong ground motion network of Turkey. The network, initiated in 1973, consists of 69 SMA-1 type accelerographs and 36 Wilmot seismoscopes. In the earthquake stricken area, there are three tri-axial strong-motion accelerographs. All three stations recorded the 13 March 1992 main shock. The relative locations of these three stations (Erzincan, Refahiye and Tercan) are seen in Figure 1. The analog films were recovered immediately after the earthquake and processed to be digitized at ERC headquarters in Ankara. These three tri-axial records (as digitized by ERC) are seen in Figure 11.

The record from Refahiye has peak accelerations of 0.07 g (NS), 0.07 g (EW) and 0.04 g (vertical). The records from Tercan have clear peculiarities (no clear P and S waves, etc.) that are not yet clarified; therefore, no discussion of this record will be made. Both records possibly need careful re-digitization and processing.

The record from within the City of Erzincan has peak accelerations of 0.39 g (NS), 0.49 g (EW) and 0.24 g (vertical). The record is significant because (a) it is one of the few near-field recorded strong-motions for a damaging earthquake, and (b) it shows a prominent pulse of approximately 2 seconds duration. Using the ERC digitized uncorrected accelerograms, baseline correction and filtering (high-pass Butterworth filter at 0.125 Hz and order 4) was done at the United States Geological Survey (USGS) offices at Menlo Park, California to obtain the velocity and displacement time-histories seen in Figure 12. From the acceleration time-history, the duration of the earthquake is estimated as approximately 7 seconds calculated on the basis of the 5–95% rule,

applied to the integrated square of the recorded acceleration time-history (Figure 13).

The acceleration response spectra of the (NS, EW and vertical components) of the earthquake for 5% damping are shown in Figure 14. The EW spectrum clearly identifies the predominant peaks at approximately 0.2, 0.3, 0.65 and 2 seconds. Of these, the 2-second period is the source frequency and the others are attributable to the site frequencies, possibly incorporating basin reflection effects. The record shows significant energy at approximately 0.2–0.35 seconds (clearly within the range of the frequencies of the 4–5-story reinforced concrete framed buildings with infill walls).

In Figure 15, the time-histories and the corresponding Fourier amplitude spectra of the dominant direction (and its orthogonal component) of the Erzincan ground accelerations are shown. The dominant direction of 128° is calculated using the recorded NS and EW acceleration records and minimizing their cross-variance. This is accomplished by the relationship:

$$\phi = 0.5 \tan^{-1} \left\{ 2\sigma_{12} / (\sigma_1^2 - \sigma_2^2) \right\}$$

where σ_1^2 and σ_2^2 are the variances of the recorded horizontal orthogonal motions (NS and EW directions) and σ_{12} is their cross-variance. When the NS and EW records are rotated by ϕ, the orthogonal components in the dominant direction of the recorded acceleration time-histories are determined. The significance of the 128° is that the strike of the North Anatolian fault near the Erzincan region is also approximately the same angle. This may possibly be a strong reason as to why the shaking in Erzincan was apparently stronger in the direction of the fault and possibly adversely affected the fate of some of the buildings.

CODES

At the time of the 13 March 1992 Erzincan earthquake, the seismic resistant design code in effect in Turkey was the nationwide code enacted in 1975 entitled "Specifications for Structures to be Built in Disaster Areas." The complete code is included in the previous as well as the latest issue of the "Earthquake Resistant Regulations: A World List," a publication of the International Association for Earthquake Engineering (1988). The basic design philosophy of this code is elastic. This particular code recommended a seismic coefficient of 0.1 for the highly seismic zone. The 1975 code was advanced for its time as it included a spectral coefficient that incorporated the period of vibration of the underlying soil layers. Such a factor entered into the UBC code in 1976.

Since the damages to engineered structures in Erzincan are very much related to the implementation of the code provisions, significant highlights of the 1975 code are summarized below. Also, the new draft code (not yet enacted) will be highlighted to provide a comparison with the 1975 code.

1975 Code

Method of analyses for aseismic design of buildings is based on the equivalent lateral static forces applied at each floor level (as in most other codes including the Uniform Building Code). The code stipulates that, in the absence of rigorous dynamic analyses, the equivalent lateral static force

concept be accepted as the minimum requirement for all reinforced concrete or steel framed structures that are not higher than 75 meters above the foundation level and that have regular load bearing systems. The provisions are also applicable for masonry buildings, chimneys, towers and elevated tanks.

The lateral load is calculated by:

$$F = CW$$

where

C = seismic coefficient $= C_0 K S I$

and

C_0 = seismic zone coefficient,

K = structural type coefficient,

S = spectral coefficient,

I = building importance coefficient.

The structural type coefficient and the building importance coefficient are similar to those in the various versions of the UBC. For one- and two-story buildings, $S = 1$, $K = 1$ and for all masonry buildings $S = 1$.

Some of the significant and unique aspects of the provisions of the 1975 code are:

a) Seismic Zone Coefficients are based on the Seismic Zoning Map. The map divides Turkey into four seismic zones and has been issued in 1972 also by the Ministry of Public Works and Resettlement following a ruling by the Council of Ministers. The map (shown in Figure 16) clearly follows the North Anatolian Fault (Figure 1) as the major Seismic Zone 1 region including the City of Erzincan. The largest coefficient adopted for Zone 1 is 0.1.

b) Spectral Coefficient (with a maximum value of 1.0) is based on the formula:

$$S = 1/[0.8 + T - T_0]$$

where

T = natural period of the structure,

T_0 = predominant period of the underlying soil.

Compared with codes of other countries in 1975, the Turkish Code was one of the first to include the spectral coefficient into the code. UBC included spectral coefficient in 1976.

Reinforced Concrete structures are constructed as "ductile systems." There is no ductility reduction factor (as reflected by the low seismic zone coefficient of 0.1 for Zone 1. Detailing specifics for reinforced concrete structures recommend confinement regions for both the uppermost and lowermost sections of columns and for beam-column joints. One significant deficiency is the lack of provision or recommendation for using deformed reinforcing bars. Again, based on observations of damaged or collapsed buildings, except for a very few cases (less than 10), only undeformed bars were used.

New Draft Code

At the time of the earthquake, a draft of a new version of the code was being circulated for final review. The proposed draft brings significant changes and approaches to the seismic design provisions, particularly in the calculation of the seismic coefficient (C) in the equivalent lateral static force formula $F = CW$:

$$C = C_0 IS/R\,.$$

The coefficient C_0, in the draft code, is proposed to be 0.4 for the seismic Zone 1. The spectral coefficient is revised as:

$$S = 1/[1.0 + T - T_0]^{2/3}$$

The coefficient R is now called the structural type factor and incorporates both the K factor of the 1975 Code and the Reduction Factor of the UBC 1991. For example R is 3.3 for reinforced concrete-framed structures and 5.0 for reinforced concrete-framed structures with "enhanced ductility." Assuming all other coefficients as 1.0, then, $C = C_0$ (new)$/R$ effectively is 0.08–0.12. Comparison with $C = C_0(1975) = 0.1$, indicates that for the structures with the ductility provisions similar to that of the 1975 Code, the coefficient C is increased by 20%. For "enhanced ductility" C is decreased by 20%.

CONCLUSIONS

One of the important factors in the fate of the collapsed buildings during the 13 March 1992 Erzincan earthquake was non-compliance and lack of implementation of the seismic design code rather than significant deficiency in the design code. The 1975 Code provided sufficient and pragmatic detailing provisions for reinforced concrete-framed buildings; if followed, it would probably have prevented the collapse of many of the lost buildings. The damages suffered during this earthquake should be a reminder of the vulnerability of many underreinforced concrete buildings in the mid- and eastern United States.

The repair and retrofitting methods applied in Erzincan and vicinity should be closely monitored to derive lessons about their effectiveness during future earthquakes. During this recent earthquake, such an opportunity was lost because some of the buildings that performed well, that were lightly or heavily damaged or that totally collapsed during the 1992 event had been repaired following the 1983 earthquake. Due to lack of documentation of the various retrofit and repair techniques, many of the lessons that could have been learned were simply missed.

It is imperative that dissemination and outreach of new techniques and modern design details of new construction as well as retrofitting of existing structures must be conveyed to the practicing engineers and contractors.

REFERENCES

Ambraseys, N. N., 1970, Some Characteristic features of the Anatolian Fault Zone, Techtonophysics, v. 9, pp. 143–165.

Anonymous, 1984, Gazetteer of Turkey, v. 1, 2nd ed., Defense Mapping Agency, Washington, D.C., (stock no: GAZGN-TURKEYV1), Sept. 1984.

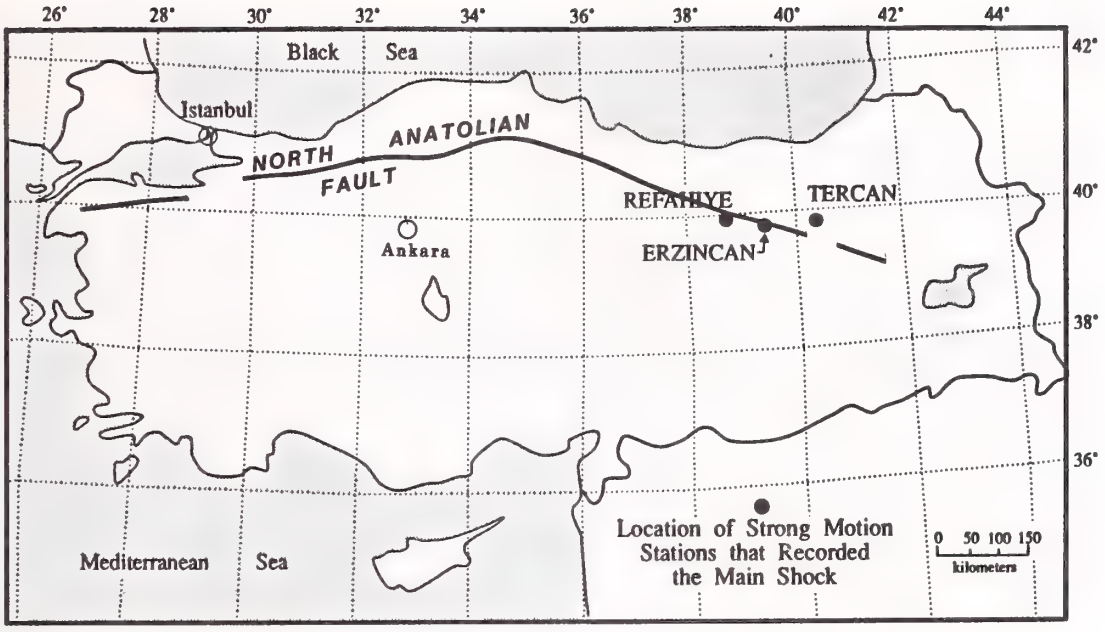

Figure 1. General map of Turkey, the North Anatolian fault and the location of strong-motion stations (at Erzincan, Tercan and Refahiye) that recorded the earthquake.

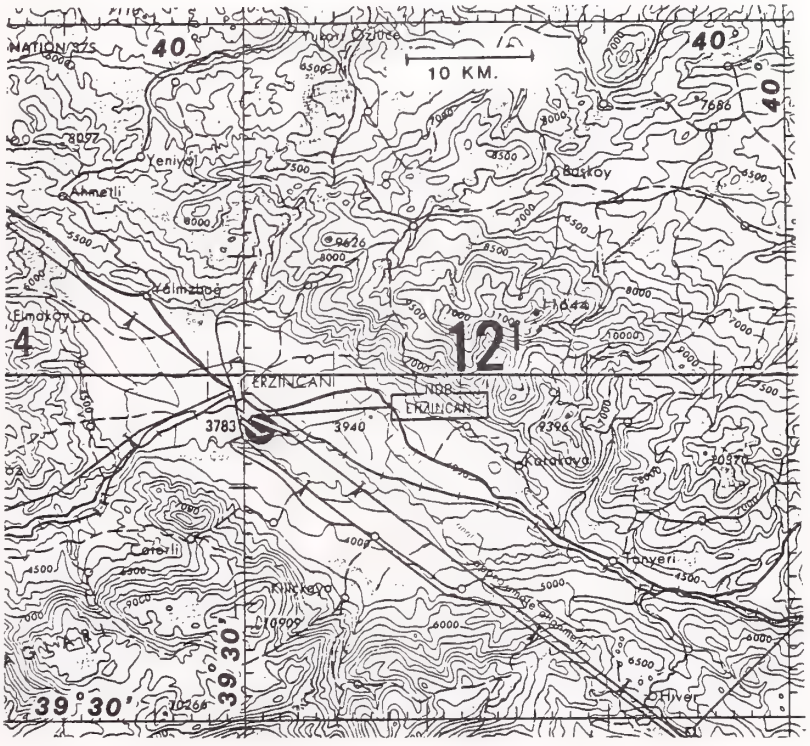

Figure 2. General topographical map of the Erzincan basin (contour intervals 500 ft.) [Source: Defense Mapping Agency, Aerospace Center, St. Louis, Mo., 1989]

Figure 3. Typically pancaked building in Erzincan.

Figure 4. Typical damaged building exhibiting collapse mechanism.

Figure 5. Undamaged single-story adobe building in Erzincan.

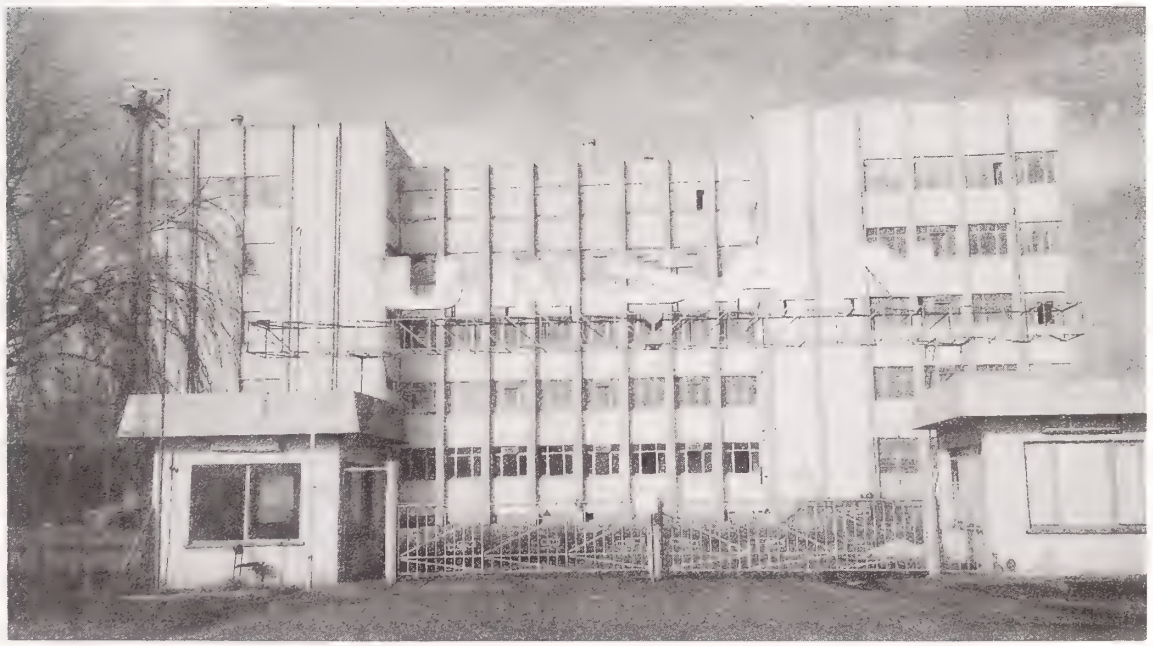

Figure 6. Unsan flour mill.

Figure 7. An external column of Unsan flour mill exhibiting short column and deficient detailing lack of shear reinforcement.

Figure 8. The Military Hospital—lost one wing, lost a story of one of the two middle wings and sustained heavy damage to the remaining two wings.

Figure 9. General view of the main sugar refinery buildings.

Figure 10. Collapsed stack of the calcination unit of the sugar refinery.

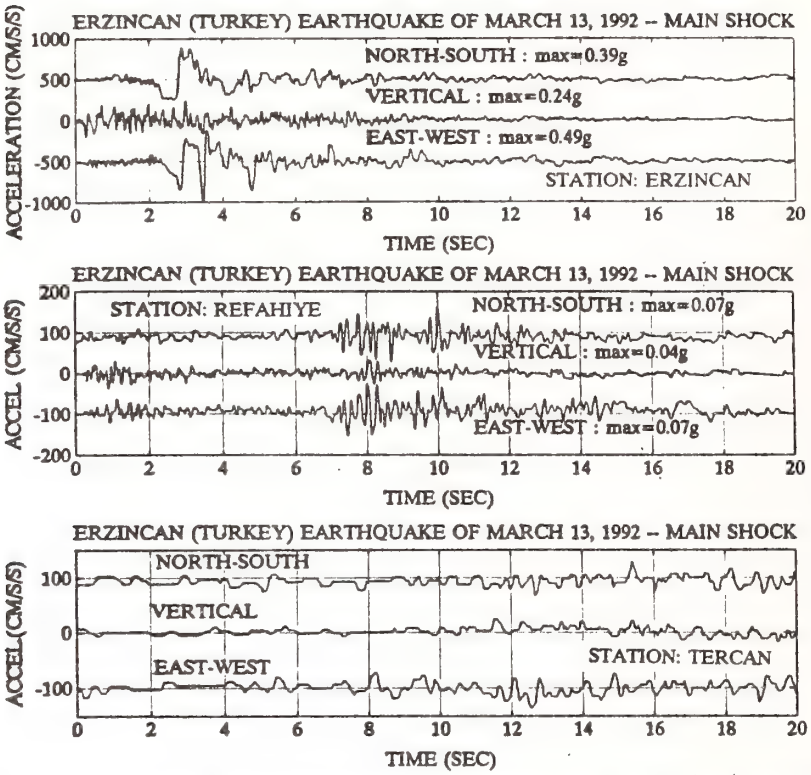

Figure 11. Plots of uncorrected strong-motion acceleration records (courtesy of General Directorate for Disaster Affairs of the Ministry of Public Works and Settlement, Republic of Turkey).

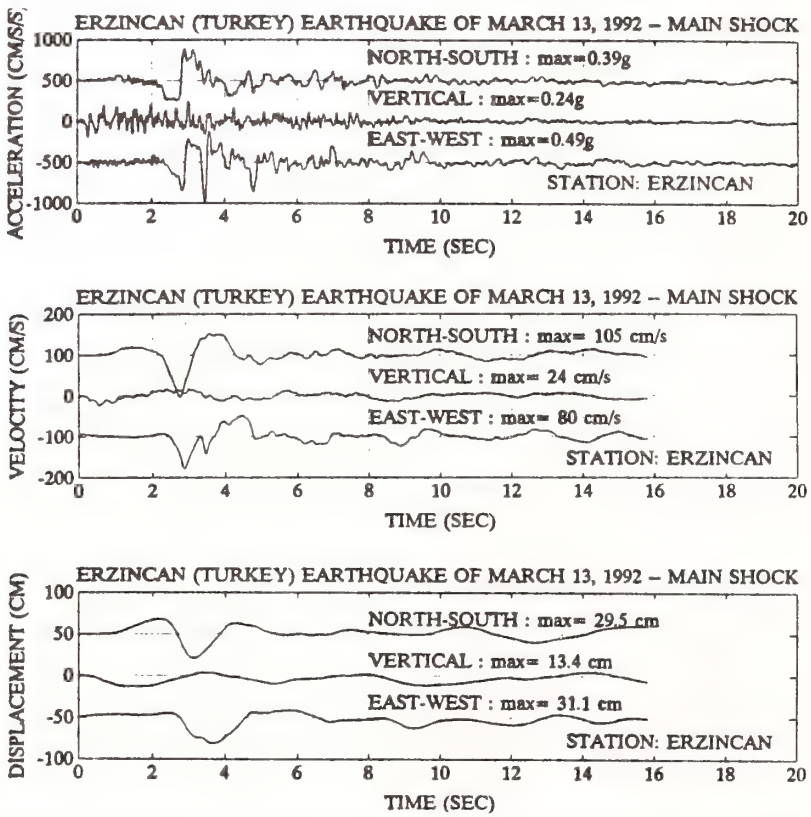

Figure 12. Acceleration, velocity and displacement time-histories of the Erzincan record.

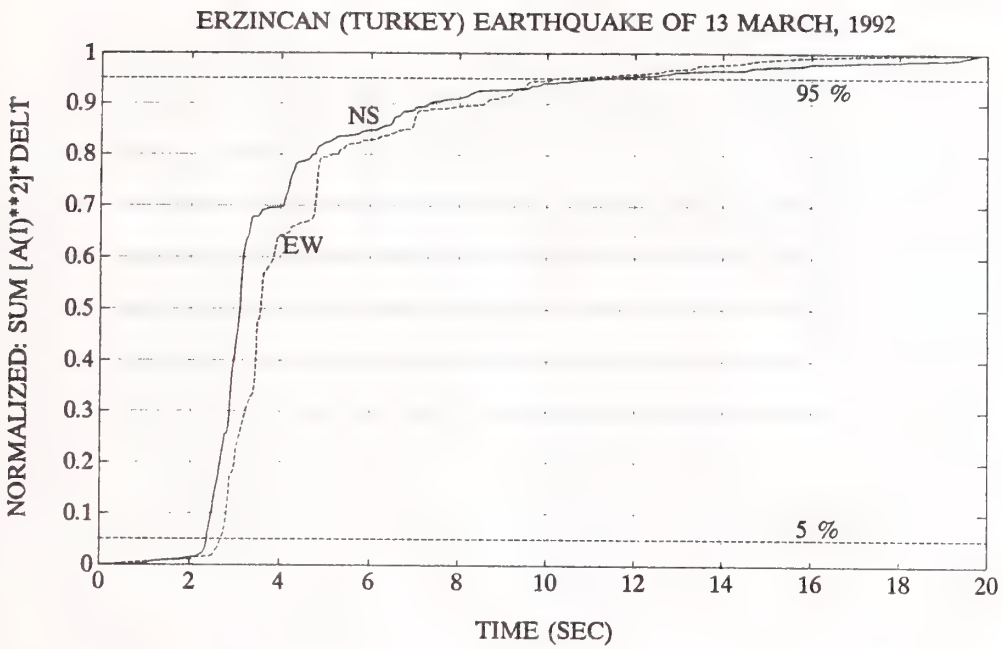

Figure 13. Plot of normalized summed squared (NS and EW) acceleration records.

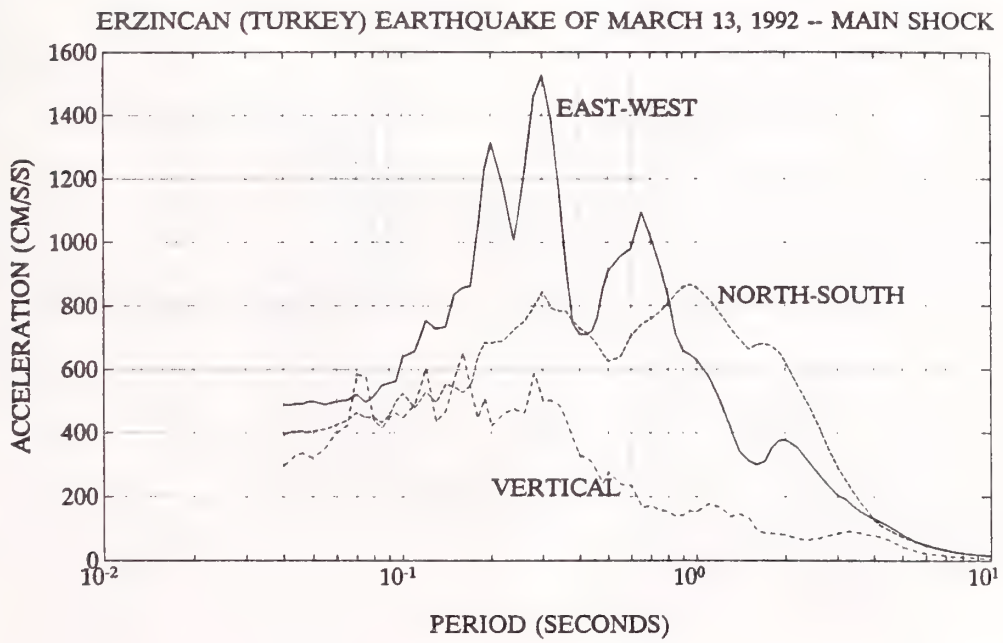

Figure 14. Acceleration response spectra (5% damping) of the Erzincan record.

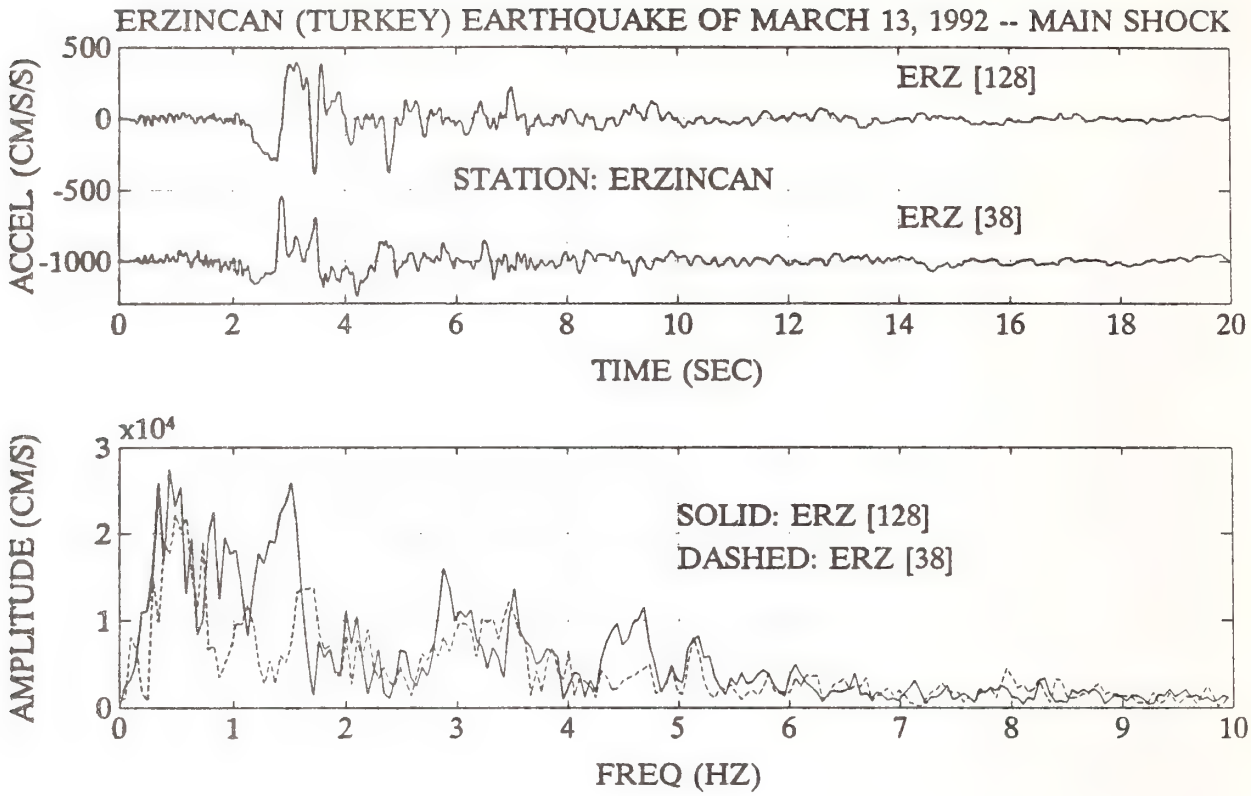

Figure 15. Horizontal components of the Erzincan acceration time-histories rotated to the dominant direction and corresponding amplitude spectra.

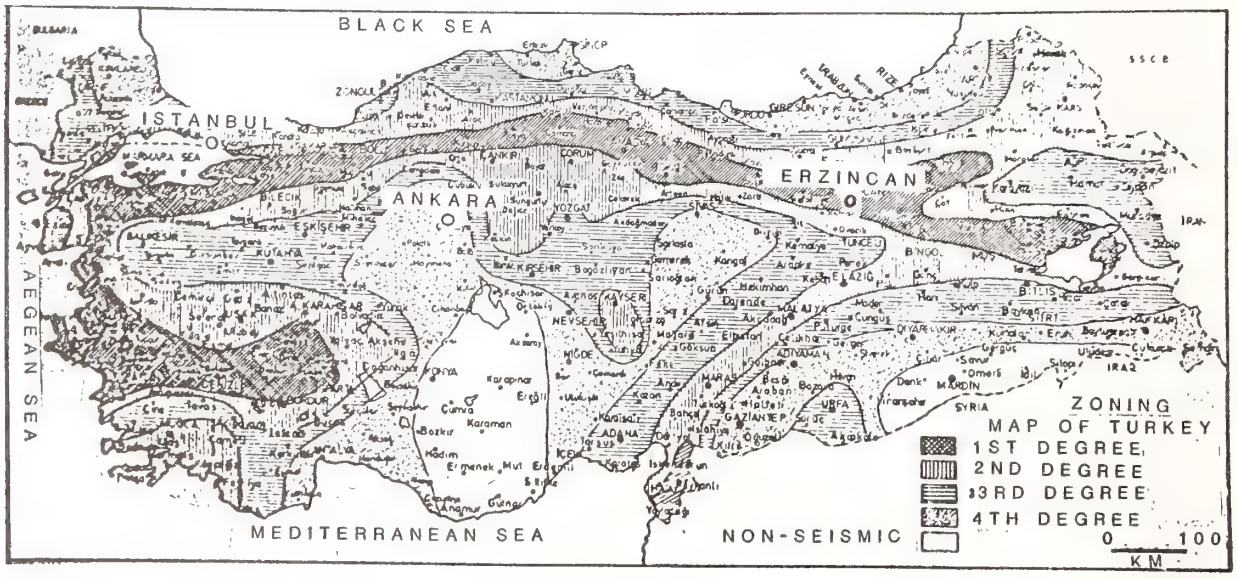

Figure 16. Earthquake zoning map of Turkey.

Beach Profile Response to Storm Surge and Waves

by

Nicholas C. Kraus[1], Magnus Larson[2], Bruce A. Ebersole[3], and Jane McKee Smith[4]

ABSTRACT

The Corps of Engineers interest in storm-induced beach profile change stems from its mission in engineering shore protection projects. Beach fill is a popular method of shore protection, and a major design consideration is the degree of protection the fill provides. Mathematical modeling provides a quantitative tool to evaluate the response of natural beaches and beach fills to storms, and the SBEACH model was developed to fill this engineering need within the Corps. The paper summarizes development and application of the model, and ongoing research aimed at improving it. The SBEACH model simulates many of the important processes that characterize beach profile change during storms, and it has proven to be reasonably accurate as a quantitative predictor. However, applications have demonstrated the need for improving the model, and research efforts are under way to extend model capabilities. The recently completed SUPERTANK data collection project involved use of an extensive and diverse array of instruments to study cross-shore sand transport processes and beach profile change at prototype scale. Analyses of the data collected during SUPERDUCK will improve understanding of the complex storm erosion process and guide development of future model improvements.

KEYWORDS: beach; beach fill; erosion; model; storm.

1. INTRODUCTION

Beach nourishment is becoming the preferred method of shore protection because: (a) it is often the least expensive alternative, (b) use of sand fill provides flexibility, particularly when "hard" engineering structures such as groins, revetments, or seawalls are already in place, (c) some States are now establishing policies against the use of hard shore protection structures, and (d) it is a natural method of protection, providing an aesthetically pleasing environment and recreational benefits. However, recreational benefits can no longer be used to justify Federal participation in a beach nourishment project. Benefits derived from recreational use can be considered, but projects must be justified on the basis of storm-protection benefits, such as prevention of beach erosion and shoreline recession, and reduction in flooding and wave damage.

Reliable engineering methods are needed to aid in the design of protective beach berms and dunes that can withstand the impacts of storms. Mathematical modeling of beach profile and fill change provides a general and quantitative approach for representing the simultaneous influence of hydrodynamic, sediment and geometric factors important in the storm-induced erosion process. Kraus (1989) reviews use of beach change models in the coastal design and engineering process.

[1]Senior Scientist, [3]Supervisory, Research Hydraulic Engineer, [4]Research Hydraulic Engineer, Coastal Engineering Research Center, US Army Engineer Waterways Experiment Station, 3909 Halls Ferry Road, Vicksburg, MS 39180-6199.

[2] Assistant Professor, Department of Water Resources Engineering, Lund Institute of Technology, University of Lund, Box 118, Lund, Sweden S-221 00.

Successful numerical simulations are limited only by the development of the underlying theory and availability of data to refine and validate the model. This paper reviews sand transport processes and beach profile change associated with storms, development and application of a mathematical model to simulate storm-induced beach profile change, and ongoing research aimed at improving both understanding of the governing processes and numerical model accuracy.

2. BEACH CHANGE DURING STORMS

Strong onshore-directed winds that occur during a storm result in the generation of waves that eventually break on the beach. Storm waves usually remove sand from the beach face and transport it both offshore and alongshore. Frequently, a linear bar is created in response to the tendency for offshore transport (linear in the alongshore direction). During the peak of the storm, when breaking wave heights are greatest, most beach erosion occurs and the linear bar is most pronounced. Figures 1a-1c show the evolution of a section of beach at the Coastal Engineering Research Center's (CERC) Field Research Facility (FRF) in Duck, NC, during the period 9-17 September 1985, in response to the passage of a northeaster storm (maximum significant wave height of 2.1 m) (from Howd and Birkemeier, 1987). Figure 1a shows the beach prior to passage of the storm, and Figure 1b shows the beach shape at the time of peak storm intensity. Note the presence and uniformity of the linear bar. During the storm sand can be transported in the alongshore direction at potentially high rates; however, beach profile evolution appears to be dominated by cross-shore processes. Figure 1c shows the same stretch of beach during the latter stages of the storm, as its intensity wanes. The beach begins to assume a very three-dimensional shape. However, the important point is that during the time of greatest beach erosion potential, beach change seems to be dominated by cross-shore processes and transport gradients.

Onshore winds and breaking waves associated with storms also increase the mean level of the water surface near the shore above what would normally be expected due to tidal action. Erosion caused by high-energy breaking waves is exacerbated by abnormally high water levels, which expose the previously subaerial portion of the beach berm and dune system to direct wave attack. As a result, considerable quantities of sand can be removed from the pre-storm berm and dune system and deposited offshore. If water levels remain well below the elevation of the dune crest, scarping of the dune can occur without significant overtopping of the dune. Under these conditions, if wave action persists long enough, severe erosion can occur and impact coastal, commercial, and residential structures (see Figure 2). In areas where no dunes exist, or when rising water levels approach or exceed the elevation of the dune crest, landward overwash of dune sand can occur in addition to offshore transport of foreshore sand. Because dune crest elevation varies considerably along the beach, overwash usually begins at low points in the dune system and overwash fans develop. As the water level rises to the predominant dune crest elevations, large-scale overwash can occur.

As storm wave energy subsides, wave conditions change from very steep wind waves to swell waves with low steepness (ratio of incident wave height to wave length). Swell waves tend to rebuild the beach, and the beach recovery process begins quickly following passage of a storm. Beach recovery is most noticeable in the form of an emergent foreshore berm. The newly formed berm is comprised of sand that was removed from the pre-storm foreshore, transported offshore under the action of storm waves, and then transported onshore under the action of swell

waves. Examples of this process are shown below for two New Jersey beaches.

The aforementioned cross-shore transport processes associated with storms occur over a short period of time (on the order of hours and days), but are of major engineering concern because of the potentially catastrophic nature of foreshore and dune erosion and inundation. Planning and design of shore-protection projects must consider potential damage produced by storms. Major factors that control cross-shore sediment transport and storm-induced beach profile change are: (a) beach profile shape prior to the storm, (b) grain size characteristics of the beach sand, (c) wave and water level climate during the storm, (d) presence of hard shore-protection structures, and (e) longshore non-uniformity in beach conditions.

3. STORM-INDUCED EROSION MODELING

All models of storm-induced beach profile change developed for engineering use have relied on the assumption that the beach profile evolves primarily in response to cross-shore processes. Also, these models have been based on some assumption about the shape of the profile as it evolves in response to varying wave conditions and water level. Early models were effectively time independent in predicting beach profile change from a pre-storm condition to an eroded condition following the storm (Edelman, 1972; Vallianos, 1974; Swart, 1976). Vellinga (1983, 1986) developed a simple mathematical model for estimating severe erosion of protective dunes impacted by storms that might be expected along the Dutch coast. Predictions from these models are independent of the temporal evolution of the storm driving forces (waves and water level); however, erosion is sensitive to the shape and duration of the storm hydrograph, particularly phasing between the storm-induced water level rise and the normal astronomical high tide. Wave properties also change during the storm, as mentioned previously. More reliable estimates of erosion will result if the time-dependent nature of the forcing functions is considered.

Realistic time-dependent simulation of beach and dune erosion was first accomplished by Kriebel (1982, 1986) and Kriebel and Dean (1985), who extended the static equilibrium beach profile concept of Bruun (1954) and Dean (1977). Kriebel and Dean (1985) demonstrated that their model produced reasonable results through comparisons with limited field data on dune erosion. Principal limitations of the model are: (a) weak dependence of predictions on incident wave characteristics (height and period); (b) somewhat unrealistic profile shape, in the sense of not being able to predict bar formation; and (c) limited capability to simulate accretion and berm buildup on the foreshore. Bars are a natural defense mechanism on beaches, and serve as a reservoir for sand that is transported offshore during the storm. It is important to reproduce this type of geomorphic feature.

Larson and Kraus (1989) and Larson et al. (1990) developed a mathematical model called "SBEACH," an acronym for Storm-Induced **BEA**ch Profile **CH**ange model, that overcomes limitations of previous models. A short description of the model follows.

The net direction of sand transport at any time during a storm is defined according to an empirical relationship between the deepwater wave steepness and dimensionless fall speed of the sand particles. These parameters best predicted transport direction observed in large-scale laboratory experiments and in the field, and frequently emerged in empirical correlations of dynamic and morphologic properties of the profile. Figure 3 shows the separation of erosional and accretionary events observed in large-scale wave tank experiments and 99 events in the field, along

with the empirical relationship used to differentiate between the two conditions.

The magnitude of the transport rate is calculated in four distinct zones across the beach profile, as depicted in Figure 4, analogous to zones of different wave properties identified in hydrodynamic studies of the surf zone (e.g., Svendsen et al., 1978; Basco, 1985). Empirical predictive relationships for the transport rate in each zone were developed using sequential measurements of profile change made in the laboratory during large-scale testing conducted by the U.S. Army Corps of Engineers (Saville, 1957; Kraus and Larson 1988) and the Central Research Institute of Electric Power Industry (CRIEPI) in Japan (Kajima et al., 1982). Sand transport rates in the broken wave zone are calculated based on the difference between the amount of local wave energy dissipation and the equilibrium energy dissipation level at which sand movement would cease (the equilibrium beach profile). In other words, the transport rate is proportional to the degree to which the beach profile is out of equilibrium. Available data support use of a linearly increasing transport rate in the swash zone, from zero at the limit of wave runup to the value calculated at the inner limit of the broken wave zone. In the breaker transition zone (between the breaker and plunge points), the rate increases exponentially from the value calculated at the outer limit of the broken wave zone, the plunge point. In the pre-breaking zone, the transport rate decreases exponentially from its maximum value at the break point. Empirical decay coefficients that depend on wave height and grain size were determined based on analysis of the large-scale laboratory data.

Expressions for predicting the position of the break point, the position of the plunge point relative to the break point, and the limit of wave runup are defined using formulations found in the technical literature, and are given in Larson and Kraus (1989). The numerical wave model of Dally et al. (1985) together with the cross-shore momentum equation are used to calculate the wave height needed to define the break point, energy dissipation, set up, and other wave-related quantities at discretized points along the profile.

An explicit finite-difference solution scheme is used to solve the mass conservation equation for sand using the calculated transport rates. The seaward limit of the model domain is set at the location where the calculated transport rate in the pre-breaking zone is negligible during the course of a storm. The shoreward limit is defined to be the limit of wave runup for the case of a sandy beach, or the transport rate is defined to be zero if a seawall or revetment is present. Avalanching is included to limit the steepness of the beach slope at the landward boundary. Typical time and space steps used in model simulations of storms are 5-20 min and 1-5 m, respectively. The water level and offshore wave conditions are input at each time step, and wave height across the shore and profile change are then calculated.

4. MODEL APPLICATION

The empirically based SBEACH model should be calibrated prior to its use in investigating beach fill response to storms, because main model parameters were established for a limited range of wave heights and periods, and grain sizes. Calibration requires high-quality data, including immediately pre- and post-storm beach profile data, grain size data, and the time history of wave and water level conditions during the storm.

Here, an example is given of model calibration using a data set from the Point Pleasant and Manasquan Beaches located on the south and north sides, respectively, of the Manasquan River jetties on the coast of New Jersey. Point Pleasant Beach is a relatively wide sandy beach with no active coastal structures except a 678-m long jetty to the north;

Manasquan Beach is a relatively narrow sandy beach with short groins spaced at approximately 200- to 300-m intervals. Details on the site are given in Larson et al. (1990).

The beach profile was surveyed to wading depth along eight transects spaced at approximate 200-300-m intervals at Point Pleasant and along nine transects midway between groins at Manasquan on March 27-28, 1984. A strong extratropical storm (northeaster) arrived on March 29, halting fathometer surveys that would extend the profile measurements to deeper water. The storm caused significant erosion; and, after the storm passed, profile surveys were repeated along the transects. The post-storm surveys taken on April 2-3, 1984, include 3-4 days of post-storm swell waves with low steepness. Water level changes were recorded hourly by a tide gage located inside the inlet, and wave height and period were calculated from measurements taken by a wave buoy located directly offshore from the inlet in 15 m of water. Water level and wave height and period between the times of profile surveys are shown in Figures 5 and 6.

A mean initial pre-storm profile was developed using an earlier measured subaqueous profile joined to the measured subaerial profile from 27-28 March. The mean subaqueous profile along the two beaches differed substantially, with the water depth along Point Pleasant profiles increasing monotonically with distance offshore, whereas the Manasquan Beach profiles had a subaqueous terrace located near the ends of the groins. A representative grain size of 0.5 mm was estimated from previously collected data. These beach and storm data were used as model input, and beach profile change for the storm was simulated. Calibration was determined based on a least-squares minimization between measured and simulated beach profiles.

Typical results showing measured and simulated profile changes at Point Pleasant and Manasquan are shown in Figures 7 and 8. Because of the small heights and long periods of the waves during the latter stages of the storm (after March 30), partial beach recovery undoubtedly occurred prior to the post-storm survey. This is evidenced by the presence of the foreshore berm in each figure. At elevations above the berm, predicted volumetric erosion is reasonable; and neglecting sand volume in the emergent post-storm berm, total foreshore erosion volume seems to be predicted very well. Bar position is also well-predicted at Point Pleasant but less so at Manasquan, perhaps because of the longshore influence of groins at Manasquan. Predictions of beach recovery following the storm are qualitatively correct, but quantitatively inadequate. Additional discussion of model results for Manasquan and Point Pleasant are discussed in Larson and Kraus (1991).

5. ONGOING RESEARCH

Results from this and many other applications of the SBEACH model have identified areas where further research is needed to improve the model. Better understanding of the relationship between the driving hydrodynamic forces and the entrainment and transport of sediment is needed to reduce the empiricism of the model. Another area of research involves determining the optimal way to include the effects of random wave breaking. The large-scale laboratory tests that produced data used to develop the model only involved generation of monochromatic waves. Monochromatic waves are a simplified representation of waves that impact most beaches. Other areas of much-needed research include study of the dynamics of wave impacts on berms and dunes, dune overwash, swash processes, and the post-storm beach recovery process.

Recently, a major laboratory project called "SUPERTANK" supported by several work

units in the U.S. Army Corps of Engineers Coastal and Dredging Research Programs was completed (Kraus et al., 1992). SUPERTANK focussed on cross-shore hydrodynamic and sand transport processes, and was designed to address the critical research needs outlined above. The 8-week project was conducted in the large wave tank facility of Oregon State University in Corvallis, OR (Figure 9). SUPERTANK drew participation of researchers from 20 Federal agencies, universities, and private companies in the United States, Denmark, Japan, The Netherlands, and Sweden.

SUPERTANK is believed to be the most densely and comprehensively instrumented nearshore processes data collection project ever conducted in the laboratory or the field. At the peak of data collection activities, the wave tank was instrumented with 16 resistance wave gages, ten capacitance wave gages, 18 two-component electromagnetic current meters, 34 optical backscatterence sensors (OBS), ten pore-pressure gages, three acoustic sediment concentration profilers, one acoustic-Doppler current profiler, one four-ring acoustic benthic stress gage, one laser Doppler velocimeter, five video cameras, and two underwater video cameras. Figures 10a and 10b show components of the instrument array (wave gages, current meters, and OBS sensors). These instruments provide detailed measurements of the nearshore hydrodynamics (waves and currents) and sediment concentration needed to quantify sand transport. Numerous fluorescent sand tracer studies were also conducted for the same purpose. During the experiments approximately 350 beach profile surveys were made to record the response of the beach profile to wave action. Surveys were made with an auto-tracking infra-red survey system call a geodimeter, which targeted a prism attached to a survey rod mounted on a moveable carriage. The survey system allowed accurate detailed surveys to be made in minimal time. Sixty-six different wave conditions were run for a total of 129 hours of wave action; 70% of the wave conditions involved random waves.

Test series focussed on the following: (a) beach erosion and accretion due random and monochromatic waves, (b) erosion in front of a seawall, (c) response of offshore subaqueous berms, and (d) dune and berm flooding and erosion. Figures 11 a and b show the condition of a dune before and during tests to investigate the dynamics of dune overtopping and overwash. Data return from the instrument array was remarkably high (99%). Preliminary results support many of the design procedures being used to investigate beach profile and fill response.

6. CONCLUSIONS

Cross-shore sand transport processes during storms are complex, particularly foreshore sand transport and the dynamics of dune erosion and overwash. The SBEACH model has been developed to quantify storm-induced beach profile change, and it successfully simulates many of the major morphologic responses observed during storms, such as foreshore erosion, dune and berm scarping, bar development, and post-storm recovery (with less accuracy). Because of the limited range of wave and beach conditions used to develop the model, calibration of SBEACH is recommended prior to application for project design. However, because of the rapid response of the beach to storm events and short time available to mobilize for data collection, it is usually difficult to obtain accurate data sets that are suitable for calibration purposes. Data from Duck, NC, and Point Pleasant and Manasquan, NJ, illustrate how quickly the beach responds. There are several areas in which the SBEACH model can be improved. For example, better descriptions of the effects of random waves on beach erosion and accretion and their relationship to sand transport are needed, as are improved descriptors of the dynamics of dune and berm inundation,

and subsequent erosion and overwash. Existing technology (laboratory facilities, computers, and instrumentation) allow complex and comprehensive investigations to be undertaken that will improve our understanding of the physics of sand transport and beach profile change. The SUPERTANK data collection project will provide valuable information for improving the SBEACH model and our understanding of storm-induced erosion.

7. ACKNOWLEDGEMENTS

We would like to express our appreciation to Mr. Jeffrey Gebert, Oceanographer, U.S. Army Engineer District, Philadelphia, for providing the beach erosion data set at Point Pleasant and Manasquan, NJ, to Mr. William A. Birkemeier for providing the figures showing storm-induced beach change at the CERC FRF, and to all those who made the SUPERTANK project such a great success.

The contributions of N.C. Kraus, J.M. Smith, and B.A. Ebersole were made as part of the activities of work units in the Coastal and Dredging Research Programs. The contribution of M. Larson was also supported by the Coastal Research Program and funded by the U.S. Army Engineer Waterways Experiment Station's CERC through the U.S. Army Research, Development, and Standardization Group - UK. Permission was granted by the Chief of Engineers to publish this information.

8. REFERENCES

1. Basco, D.R. (1985). "A Qualitative Description of Wave Breaking," *J. Waterway, Port, Coastal and Ocean Engineering*, 111(2), pp. 171-188.

2. Bruun, P. (1954). "Coast Erosion and the Development of Beach Profiles," Technical Memorandum No. 44, Beach Erosion Board, U.S. Army Corps of Engineers.

3. Dally, W.R., Dean, R.G., and Dalrymple, R.A. (1985). "Wave Height Variation Across Beaches of Arbitrary Profile," *J. Geophys. Res.*, 90(C6), pp. 11917-11927.

4. Dean, R.G. (1977). "Equilibrium Beach Profiles: U.S. Atlantic and Gulf Coasts," Dept. Civil Engrg., Ocean Engrg. Rep. No. 12, U. of Delaware, Newark, DE.

5. Edelman, T. (1972). "Dune Erosion During Storm Conditions," *Proc. 13th Coastal Engrg. Conf.*, ASCE, pp. 1305-1311.

6. Howd, P.A., and Birkemeier, W.A. (1987). "Sorm-Induced Morphologic Changes During DUCK85," *Proc. Coastal Sediments '91*, ASCE, pp. 834-847.

7. Kajima, R., Shimizu, T., Maruyama, K., and Saito, S. (1982). "Experiments on Beach Profile Change With a Large Wave Flume," *Proc. 18th Coastal Engrg. Conf.*, ASCE, pp. 1385-1404.

8. Kraus, N.C. (1989). "Beach Change Modeling and the Coastal Planning Process," *Proc. Coastal Zone '89*, ASCE, pp. 553-567.

9. Kraus, N.C., and Larson, M. (1988). "Beach Profile Change Measured in the Tank for Large Waves, 1956-1957, and 1962," Tech. Rep. CERC-88-6, Coastal Engrg. Res. Center, U.S. Army Engr. Waterways Experiment Station, Vicksburg, MS.

10. Kraus, N.C., Smith, J.M., and Sollitt, C.K. (1992). "SUPERTANK Laboratory Data Collection Project," *Proc. 23rd Coastal Engrg. Conf.*, ASCE, in prep.

11. Kriebel, D.L. (1982). "Beach and Dune Response to Hurricanes," Unpublished M.S. Thesis, U. of Delaware, Newark, DE.

12. Kriebel, D.L. (1986). "Verification Study of a Dune Erosion Model," *Shore and Beach*, 54(3), pp. 13-21.

13. Kriebel, D.L., and Dean, R.G. (1985). "Numerical Simulation of Time-Dependent Beach and Dune Erosion," *Coastal Engrg.*, 9, pp. 221-245.

14. Larson, M., and Kraus, N.C. (1989). "SBEACH: Numerical Model for Simulating Storm-Induced Beach Change; Report 1, Empirical Foundation and Model Development," Tech. Rep. CERC-89-9, Coastal Engrg. Res. Center, U.S. Army Engr. Waterways Experiment Station, Vicksburg, MS.

15. Larson, M., and Kraus, N.C. (1991). "Mathematical Modeling of the Fate of Beach Fill," *Coastal Engineering*, 16: 83-114.

16. Larson, M., and Kraus, N.C., and Byrnes, M. R. (1990). "SBEACH: Numerical Model for Simulating Storm Induced Beach Change; Report 2, Numerical Formulation and Model Tests," Tech. Rep., Coastal Engrg. Res. Center, U.S. Army Engr. Waterways Experiment Station, Vicksburg, MS, in press.

17. Saville, T. (1957). "Scale Effects in Two Dimensional Beach Studies," *Trans. 7th General Meeting IAHR*, 1, pp. A3-1-A3-10.

18. Svendsen, I.A., Madsen, P.A., and Buhr Hansen, J. (1978). "Wave Characteristics in the Surf Zone," *Proc. 14th Coastal Engrg. Conf.*, ASCE, pp. 520-539.

19. Swart, D.H. (1976). "Predictive Equations Regarding Coastal Transports," *Proc. 15th Coastal Engrg. Conf.*, ASCE, pp. 1113-1132.

20. Vallianos, L. (1974). "Beach Fill Planning - Brunswick County, North Carolina," *Proc. 14th Coastal Engrg. Conf.*, ASCE, pp. 1350-1369.

21. Vellinga, P. (1983). "Predictive Computational Model for Beach and Dune Erosion During Storm Surges," *Proc. Coastal Structures '83*, ASCE, pp. 806-819.

22. Vellinga, P. (1986). "Beach and Dune Erosion During Storm Surges," Delft Hydraulics Comm. No. 372, Delft Hydraulics Lab.

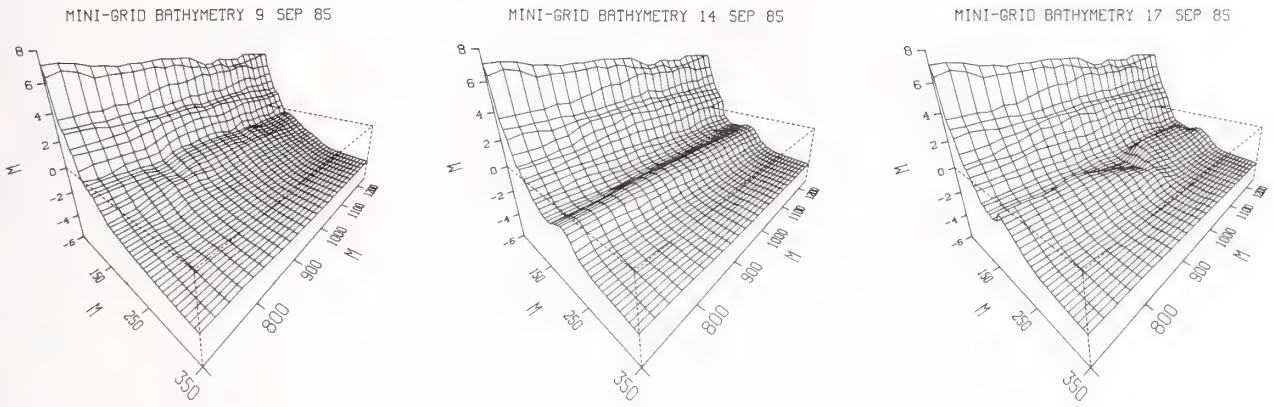

Figure 1. Beach change measured at the CERC FRF during September 1985 storm

Figure 2. Example of severe storm-induced erosion and structural damage

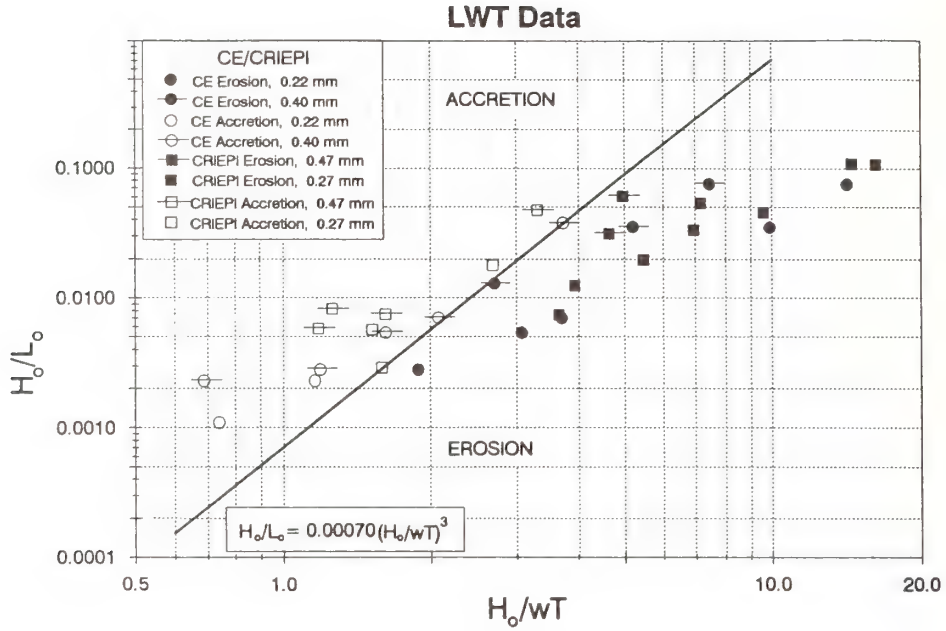

(a) monochromatic laboratory waves

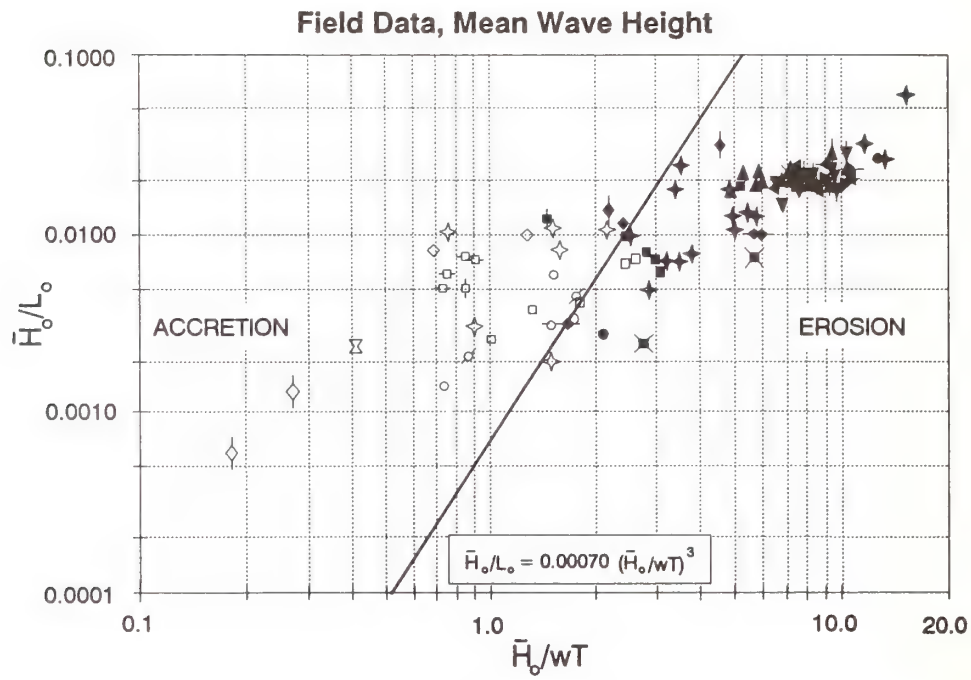

(b) field conditions

Figure 3. Criterion for predicting beach erosion and accretion

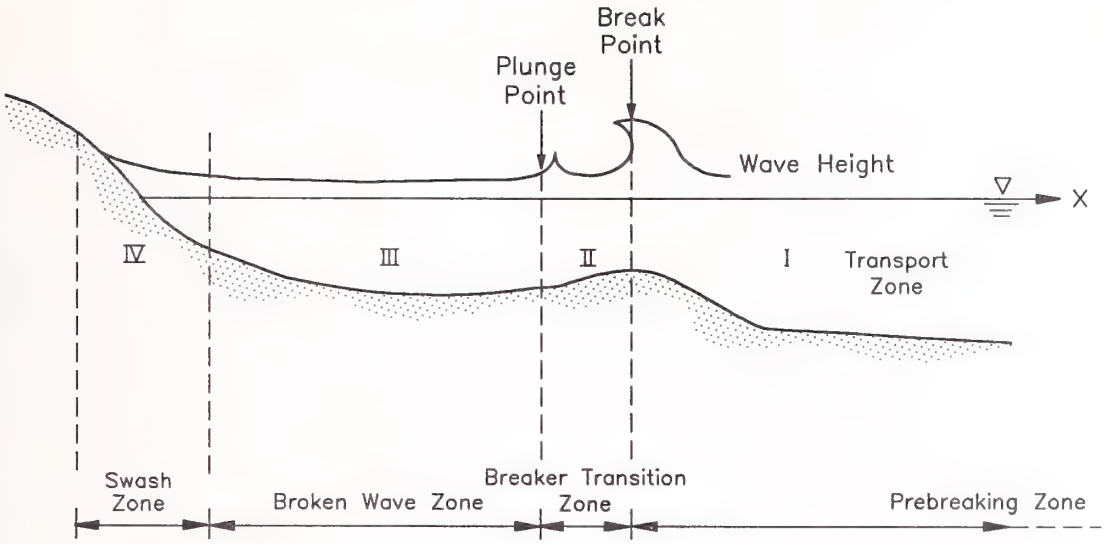

Figure 4. Regions of cross-shore sand transport

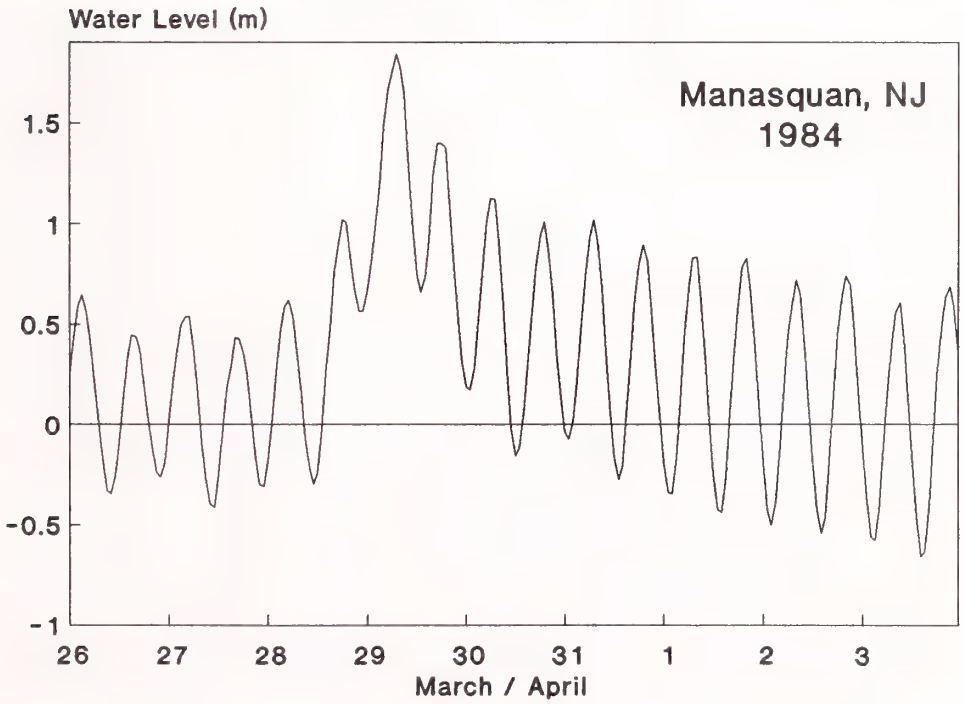

Figure 5. Water level measured at Manasquan Inlet during the March 1984 storm

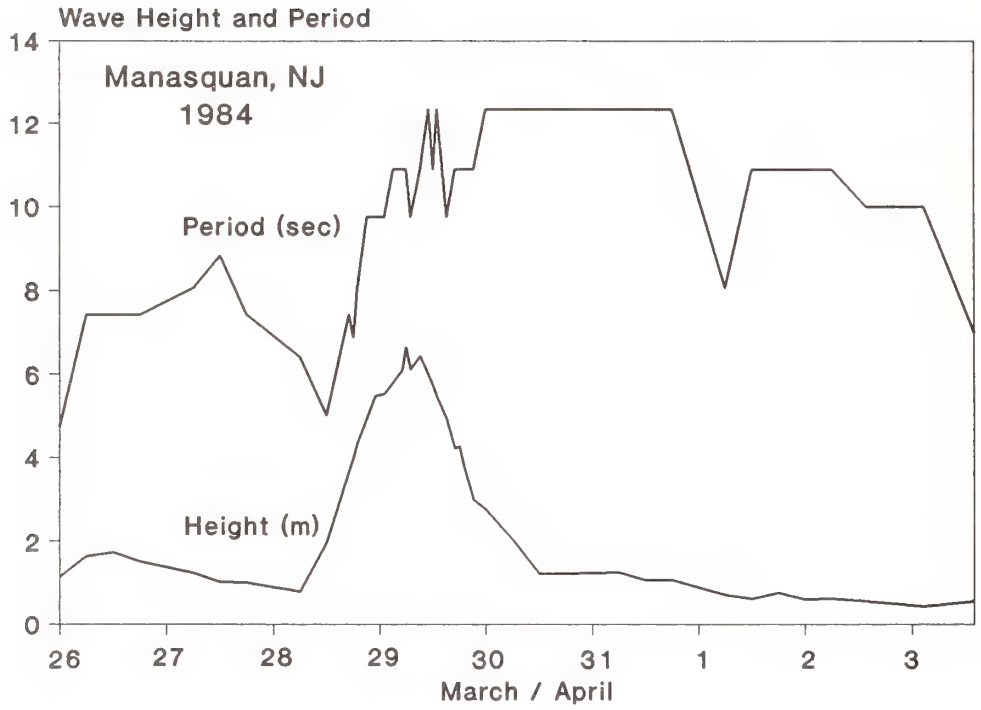

Figure 6. Wave height and period measured at Manasquan Inlet during the March 1984 storm

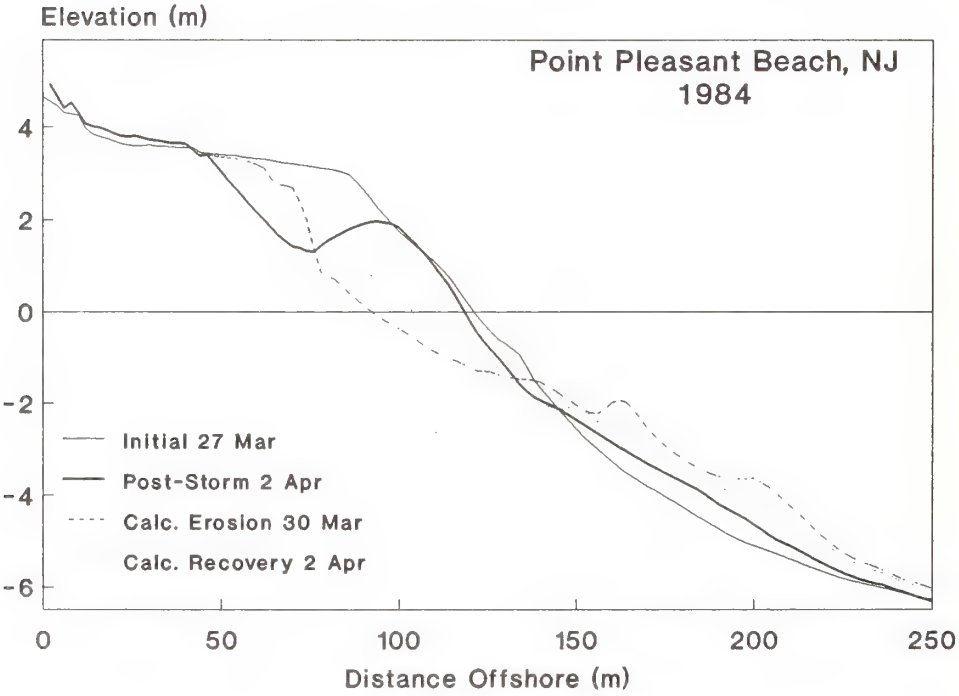

Figure 7. Storm-induced profile change at Point Pleasant Beach, New Jersey

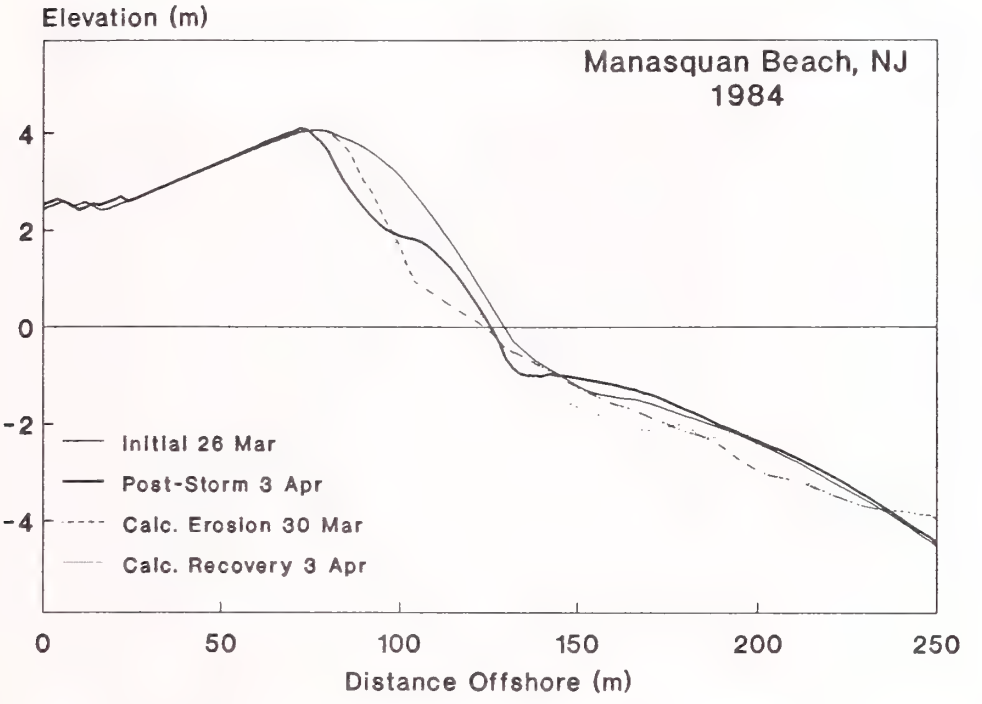

Figure 8. Storm-induced profile change at Manasquan Beach, New Jersey

Figure 9. Large-scale wave tank at Oregon State University

(a) capacitance-type wave gages

(b) electro-magnetic current meters and OBS

Figure 10. Instrumentation deployed in the large wave tank

(a) initial dune shape

(b) eroded dune

Figure 11. Photographs of dune erosion tests

Developing a Seismic Safety Program

by

Donald G. Eagling, P.E.*

ABSTRACT

Although the field of seismic safety is in the domain of the engineering profession, funding to carry out a seismic safety program is normally derived from the budgets that managers (or owners) need to carry out the missions of their organizations. Consequently, it is generally the manager rather than the engineer who must make most of the key decisions which are needed to carry out an effective seismic safety program. It is also the manager who must resolve issues of risk management which accompany seismic hazards and involve life safety, damage control, potential evacuation costs, potential liabilities and cost-benefit considerations. It is therefore very important that facility managers have a broad understanding of the comprehensive nature of an effective earthquake program as well as an awareness of the socio-political, legal and economic risks that often impede the progress and success of such programs.

This paper provides practical guidance for managers who must carry out a seismic safety program including advice for selection of an earthquake safety consultant, the main elements of a balanced program, and risk management techniques for avoiding common pitfalls and achieving expeditious results.

KEYWORDS: risk management; seismic safety.

1. INTRODUCTION

The technical aspects of earthquake safety are normally within the domain and control of the engineering profession and academia. On the other hand, the cost of earthquake safety is a drain on the very budgets that managers (or owners) of facilities need to carry out the missions of their organizations. This is true whether the enterprise is funded privately or by government sources. Consequently, the responsible manager must be heavily involved in the planning, scheduling and funding of an earthquake safety program if it is to be successful. Thus, it is very important that managers receive practical professional advice so they can carry out a cost effective program and properly manage the associated risks. In the end, the responsibility for decision must lie with the manager, but good communication and mutual trust with a practical earthquake engineering consultant is essential to provide the manager with an extension of expertise in this specialized field. On the other hand, the engineering profession has a public obligation to see that earthquake safety is achieved at minimum cost and not lost in the process of lengthy and costly investigation and voluminous reporting.

This paper provides advice for the owner or manager who must carry out an earthquake safety program from the perspective of an engineer who has had such an experience as a facility manager.

The scope, depth and focus required to carry out a satisfactory program will vary considerably with the age of a facility, the risk involved and the quality of design which was applied during its construction history. For a new and growing facility the focus will be on design and construction. For an older facility the need to evaluate existing conditions and prioritize projects for abatement of seismic hazards will receive most attention. For the majority of sites, however, a balanced program will be most effective in preventing further development of new hazards while reducing the backlog of old ones.

Those structural engineers who are experienced in earthquake engineering and have reviewed a number of facilities, both in government and

---

* Retired Plant Manager, University of California, Lawrence Berkeley Laboratory, Berkeley, California 94720

private enterprise, have found a wide variety of serious seismic deficiencies that the owner or manager were unaware existed. This is not unusual even in areas of the country where seismic design provisions have been part of the building code for many years.

East of California, few conventional buildings in the United States have been designed for earthquakes, even where there has been a history of earthquakes of sufficient intensity to damage buildings. At those locations where the potential for seismic destruction exists along with a legacy of hazardous buildings and contents, the prospect of carrying out a comprehensive earthquake safety program is indeed challenging.

The owner or manager who is responsible for a facility is usually unfamiliar with earthquake engineering and may tend to look for answers in techniques that are more sophisticated than are required to solve the actual problems in earthquake safety. The approach to solutions of these problems can become so academic, ponderous, and expensive that abatement of the seismic hazards simply doesn't get done in a timely manner.

In recent years, the state-of-the-art in seismology, geo-technical theory, and the dynamic analysis of structures has progressed tremendously. Spurred on by the need to resolve questions in seismic safety for nuclear power plants, the field has become very compartmentalized and specialized. The great strides made in these specialties have contributed significantly to the field of earthquake engineering and public safety. Unfortunately, it is easy for the responsible manager or plant engineer to "fall into a crack" between these experts who quite naturally tend to resolve seismic questions based on their own specialties.

Often more time and money are expended analyzing the problems in earthquake safety than would be needed to design practical solutions to these same problems. To gain a better perspective it is important to understand that most problems found in existing construction are a result of not implementing what has been known and observed about earthquake-resistant construction for a long time. Structural engineers who have observed and studied earthquake-damaged buildings are able to diagnose hazardous deficiencies in existing buildings rather easily and efficiently, often without complex calculations. They know which building types are hazardous. They also know standard methods for rehabilitating them.

2. SELECTING AN EARTHQUAKE SAFETY CONSULTANT

The most important thing a manager can do to initiate an effective and economical earthquake safety program is to hire an experienced earthquake engineer as an earthquake safety consultant who is strong on design and tends to keep analysis straight-forward and simple. Occasionally, there is good reason to apply structural dynamics to provide a better understanding of a complex problem, but not often. The earthquake engineer, working closely with the manager, should advise on selection of other consultants, define their scope of work, coordinate their work with the overall program and ensure that the owner is not victimized by unnecessary or impractical studies.

Selecting the right structural engineering firm to counsel a practical way through the complexities and pitfalls which can befall earthquake safety programs is the most important decision a manager can make.

This is also true when selecting geo-technical consultants. The level of sophistication in state-of-the-art techniques for predicting the intensity of ground shaking is intimidating. There is a strong tendency for both consultants and clients to believe the predictions to be more accurate than history shows they are. This tendency may lead participants to spend more money and time than the exercise is worth. The illusion of security thus developed is apt to be in direct proportion to the degree of sophistication applied.

Even when structural dynamics is to be employed, the selection of an effective ground-motion input can be a relatively simple matter. There is little to be gained by exhaustive site studies because history shows that the prediction of ground motion is indeed an inaccurate science. The inaccuracies of input often can be accommodated in good structural design.

Potential earthquake engineering and geo-technical consultants should be asked to explain

in simple terms how they expect to approach the project, what techniques will be applied and what they expect to find. They should provide examples of previous work, names of clients, and cost history. The owner should be sure that the lead consultant selected has strong design experience and has made field investigations of earthquake damage.

3. THE BALANCED PROGRAM

An effective earthquake safety program is analogous to an effective lateral-force-resisting system; it should have no weak links. Several basic precautions should be taken in establishing a program; of primary importance are the following five:

First, make certain that planned new buildings are not being inadequately designed while the process of earthquake safety review of existing buildings is underway. This is a profound admonition, but the possibility of its happening is real. It can be avoided by using plan-check or third-party review, prior to construction, to ensure that the calculations and designs of new structures and rehabilitation projects are done properly to resist earthquakes. It is embarrassing for a manager to find that a newly designed and constructed building is worse than an old one, but it happens.

Design criteria should be clearly defined and simple to use. Standards and model codes are readily available and should be used. Complex approaches or criteria should not be applied unless the need is clearly established. Criteria should be practical. At most sites, many building modifications, experimental setups, equipment installations, cabinetry, nonstructural components and other projects are designed regularly by architects, mechanical engineers, designers, and other nonstructural engineers who do not have sufficient background in seismic analysis and design. Nevertheless, if the criteria are simple and straight-forward these minor subprojects will be designed and built with adequate earthquake resistance. The more significant structural problems should be handled by registered structural engineers. Also, research or production facilities using hazardous materials should be carefully reviewed for seismic safety by a structural engineer. A professional engineer's stamp and signature as well as a third-party review should be required.

Second, the site should be reviewed for geologic and seismic hazards. Potential conditions that are inherently hazardous in ground shaking should be identified. These may include the following:

1. Unstable slopes and existing landslides;
2. Areas of low-density saturated granular soils subject to densification and subsidence;
3. Areas of low-density saturated granular soils subject to liquefaction;
4. Areas where sensitive clays may be subject to strength loss under heavy ground shaking;
5. Areas where flooding would occur due to failure of an up-slope levee or dam.

Active faults should be identified and a geologic map of the site developed.

The site review need not be rigorous in detail unless the potential hazards pose a high risk for an existing building or lifeline. If a new building or improvement is planned, the specific siting can be examined in more detail. The main point is to recognize potential hazards and take them into account. For example, it would be folly to permit the typical one-third increase in allowable soil bearing capacity for seismic loading in an area of sensitive clays subject to strength loss under ground shaking. The initial review should be quite broad and superficial in character. It is important that it be carried out by a geologist or soils engineer who understands the nature of soil dynamics, preferably one who has experience with earthquakes. Generally, except for fault rupture, each of the potential hazards that may exist can be mitigated through standard stabilization practices, or by simply avoiding them in the case of new construction. Sometimes fault movement can be accommodated, or the effect of fault movement mitigated, if it is known where surface ruptures are likely to occur.

Third, survey and evaluate all existing buildings and structures to determine their earthquake safety ratings. A structural engineer experienced in earthquake damage investigation should do the job. The assessment should be kept simple. A basic requirement is to find out what has to be done to insure that each building has a predicable lateral-force-resisting system. The job of rehabilitation should be started one step at a time, reducing liability on a priority basis.

Given a limited budget it is important to determine which buildings will have the greatest benefit for the money spent for improvements in life-safety and property damage. Of course, practical risk management must also address those socio-political issues which encompass and plague earthquake safety programs and pose questions of public and personal liability. Practical risk management is discussed in the next section of this paper.

Fourth, make an earthquake-hazards survey of the contents each building including operations, equipment, hazardous materials storage and nonstructural building elements. Obvious hazards, such as loose-item overhead storage, should be corrected by building managers or operations supervisors. Most operational hazards are obvious to one simply observing the scene and imagining an earthquake taking place. Tipping hazards, such as storage cabinets, tall files, library shelving, and similar furnishings, should be braced or anchored. Tie-downs should be installed on plant equipment such as transformers, emergency generators, tanks, elevator drives, fans, motors, and similar units. Apply a simple and judgmental priority system to use limited resources economically.

Fifth, develop an emergency plan to recover from a destructive earthquake. Apply the scenario technique to develop a probable model for the aftermath of an intense earthquake. Use those department heads who will have to handle the recovery to lead the planning effort. Reduce obstacles to recovery by eliminating obvious hazards and ensuring that the supplies and equipment that will be needed in an emergency will in fact be available. Lifelines, such as water supply lines, power systems, storm and sanitary sewers, transportation and communications systems also should be surveyed with earthquakes in mind. The consequences of possible facility losses can be mitigated by careful emergency planning, and the potential for loss of a given facility reduced by "hardening" the lifelines that would likely be in jeopardy during an earthquake.

Self-help planning, preparation, and training should be key elements in any emergency response plan for earthquake safety. Make sure that building managers and operations supervisors understand this fact and let them take part in the preparation of local emergency plans.

In the process of administering an earthquake safety program, a manager will encounter differences of opinion among the engineers and consultants involved. These differences reflect the perspectives of experts and tend to give the managers some insight into the practical state-of-the-art. It also reminds us that there often is more than one answer to a given problem. When a problem is particularly difficult and costs, risks, or liabilities are high, it is unquestionably worthwhile to get more than one opinion.

The question arises, how does a manager resolve technical differences of opinion between two consultants on subject-matter about which the manager feels inadequate.

The best answer lies in the manager's usual role, that of managing the multi-disciplinary functions of a technical complex such as a major research and development laboratory or a sophisticated production facility. The development of good communication and mutual trust with a practical earthquake engineering consultant will provide the manager with an extension of expertise in this specialized field much as it does in any other specialized field under his or her management. In the end the responsibility must lie with the manager and it is important to realize ahead of time that technical differences of opinion are apt to arise about earthquake safety management. A good earthquake engineering consultant will be interested in the goal of practical earthquake safety rather than earthquake engineering for its own sake. This extension of expertise through selection of wise counsel is a challenge that most managers face in other facets of their responsibilities.

When questions regarding technical differences of opinion or criteria persist, it is important that they are resolved by some due process within a technical framework that will stand the test of future technical and legal review. The designer and the manager should be reasonably protected by the due process involved assuming each fulfills his professional responsibilities satisfactorily.

4. RISK MANAGEMENT

Risk management from the manager's point of view is an important part of a comprehensive

earthquake safety program. It is, of course, inherent in the establishment of lateral force criteria for the design of buildings and equipment including research facilities and experimental set-ups. Earthquake codes establish *minimum* requirements for life safety and essentially provide protection against collapse. Damage control is not a prime objective. Many code provisions, such as the prescribed limitations on "drift" (deflection based upon prescribed lateral forces), have the effect of reducing damage, but one must realize that the real earthquake will cause deflections much greater than "code deflections." When damage control is an important consideration, the design must account for these larger deflections. This protection is not inherent in the Code. One approach is to analyze a structure with the objective of predicting or estimating the location and extent of damage that will probably result from a major earthquake. *In this way, additional attention to design detail can be applied specifically in the area of concern to "buy insurance" against damage for little extra cost, an example of good risk management.*

Liability is certainly a legitimate concern in risk management. Often, however, this concern is translated into a legalistic solution, rather than a practical solution which actually mitigates the seismic hazard. For example, the Code is generally not retroactive so it is not legally incumbent upon the "responsible official" to upgrade an existing building to current standards. Nevertheless, some earlier editions of the Code made it "legally" possible to design and construct a hazardous building. A non-ductile reinforced concrete frame building is a good example. A decision not to review an existing building because it was once designed to Code is a legalistic solution to avoid liability, but it does nothing to mitigate any seismic hazard that may exist. This legalistic position under the protective umbrella of the Code is becoming more difficult to assume because the engineering profession is now much more aware of hazardous buildings which have been "built to Code." One cannot be certain to avoid liability by remaining ignorant of the hazard. The legal issue may well be whether or not such a building is commonly known to be hazardous by the profession.

On the other hand, the risk of liability should be managed carefully when structural hazards are revealed as a result of seismic safety surveys and reports. For example, if a building is reported to be a collapse hazard, the official responsible for the safety of the occupants should take steps to mitigate the hazard. It is important to actively seek funds to abate the hazard and to inform the occupants that the building is deficient. While these steps will not guarantee immunity, failure to take them certainly increases liability.

The problems of funding rehabilitation work are unusually difficult and the solutions time consuming. The period during which the hazard may continue to exist increases the risk of liability.

A public agency cannot legally go out of business; therefore, it cannot spend its available funds so heavily for rehabilitation that it cannot fulfill its prescribed mission. This fact weighs against liability, but does not provide immunity. In the event that a damaging earthquake results in litigation, the pertinent issue is: what funds were available to the responsible official and what were they used for? With this in mind, one approach to managing the risk of liability is to take the basic risk-reducing steps which can be identified immediately (assuming the hazard cannot be easily abated in a short item), then follow due process to find a permanent solution to the problem. Examples of emergency steps are: adding temporary supports, reinforcing structural joints, installing epoxy grouting, removing potential hazards, or even reducing the occupancy loading. Normally, some emergency funding can be found for such purposes while the more time-consuming tasks of evolving a permanent solution and developing adequate funding take place. The important point is that responsible action (within constraints) must take place if liability is to be minimized.

It is likely that a seismic safety survey will turn up a number of structurally deficient buildings and facilities. This has been the common result where such reviews have been carried out. For years, many buildings were designed with non-ductile, reinforced-concrete frames that were then permitted by Code, but are now known to have poor seismic resistance. Many older buildings have no formal or predictable lateral force resisting system. Sometimes building alterations have reduced or destroyed the resistance incorporated in the original design. The point is, a seismic safety survey will likely present the responsible official with a multiplicity of hazards and risks to manage.

It is important to mitigate risks on the basis of priority, but it is even more important not to get bogged down in a complex series of studies or a methodology which slows the process of abatement. A simplistic priority system based upon some due process and responsible professional judgment is sufficient. As with the Richter scale for measuring the magnitude of earthquakes, it is not as important that the result is accurate as it is that relative size (or priority) is easily and quickly established.

The same selection principle should be applied when seismic safety surveys are initially carried out. That is, the priority system for the sequence in which buildings and facilities are surveyed should be simplistic and direct. Obvious problems, possible collapse hazards and high risk facilities such as those with toxic dispersible contents, should be reviewed early. Emergency recovery facilities, high occupancy buildings and lifeline facilities should also be early on the list. It is important that the survey should not be held back by an academic approach to the multiplicity of potential hazards and the complexity of the problem. The recommendation is to keep the approach simplistic, rely on good professional judgment and move forward.

One stumbling block to seismic safety is the ever present concern for accurately estimating the intensity of the potential earthquake that a given site might experience. For various reasons, political, academic and psychological, the immediate, basic need to find out whether a brace is indeed missing unfortunately too often becomes secondary to guessing how big the earthquake is going to be. Commonly, the problems uncovered in a seismic survey have less to do with lateral force criteria to be applied than with other design deficiencies such as missing links, brittle members or connections, lack of continuity or just poor construction. When a building or facility is found deficient, the size of potential seismic input is only one of the considerations which may be brought to bear on the corrective measure. Usually there will be ample time to develop detailed lateral force criteria after the real problem is revealed.

The recommendation is: don't delay the seismic survey in order to study the potential seismicity of the site. Experience shows that this approach is not good risk management.

The design criteria for new buildings are rather well established in the latest Codes, but this is not true for rehabilitation work. Here good risk management requires more careful consideration. The lateral force provisions in the Code provide good guidelines for rehabilitation design, but often, lateral force resistance is only part of the problem. As discussed, brittleness, lack of continuity or redundancy, deflections, poor detailing, poor workmanship, and many other possible deficiencies may exist. From the standpoint of risk management, it is even more important than in the design of new facilities that the designer of rehabilitation work give particular attention to a complete seismic diagnosis and criteria development.

Once it is determined that a building has a serious structural deficiency that must be corrected, another kind of problem is often present. The building may have other Code deficiencies by current standards that are not central to the main hazard. That is, the main structural deficiency may be a collapse hazard, but the other Code deficiencies may not present life safety hazards. The question may then arise: will the responsible official (or the engineer who designs the rehabilitation work) be put in a position of liability if the design does not correct all the deficiencies by current Code standards? Often it is not economically feasible or even good risk management to correct everything. For example, funding may be used to correct two collapse hazards rather than spend it all on one building to bring everything up to Code.

The recommendation is to achieve the most life safety for the funding available, but mitigate possible liabilities for the design professional by careful due process. For example: a "criteria board" can be established consisting of professionally knowledgeable members such as the rehabilitation designer, the plan checker (preferably an independent consultant), and the "building official" (the in-house person responsible for design and construction).

The authority to set seismic criteria should then be officially delegated to this "expert" group. Court judgments in the United States have held that the responsible authority will be immune from liability for acting in a discretionary manner if this person has the authority and knowledge to do so. The authority must be properly delegated and

"knowledge" implies professional judgment in the practice involved. The rehabilitation design engineer will be reasonably protected by the due process involved assuming he fulfills his design responsibilities satisfactorily.

High on the list of effective risk management techniques related to seismic safety is the so-called "third party plan check" that has been mentioned earlier in this paper. This independent plan check, together with proper field inspection of construction (whether new or rehabilitation work), is highly recommended as one of the best ways of assuring seismic safety in structural design and construction.

In "earthquake country," engineers generally believe the buildings they design will be subjected to a damaging earthquake during the lifetime of the structure. They don't consider the hazard to be one that in all likelihood will not occur. They are also aware that the earthquake is the real *master inspector.* If there is a gap in the lateral-force-resisting system, the consequences will be more serious than statistical. This point of view has a very positive effect upon risk management as applied to design.

In areas where earthquakes are very rare events, it is difficult for engineers to take them seriously, particularly in the design of conventional structures. It is a fact that few buildings in the midwestern and eastern United States have been designed for earthquake safety, even in those areas where it is well known that damaging earthquakes have occurred in the historic past. Many buildings are constructed of unreinforced unit masonry, one of the building types particularly susceptible to earthquake damage and collapse. A great deal of progress could be made by simply avoiding the use of unreinforced unit masonry in new construction.

In "earthquake country," the choice of criteria for seismic design can be a relatively simple matter, if one believes the great earthquake is imminent. In this case, the design earthquake can be taken relatively close to the maximum credible earthquake. This might correspond to 0.2g base shear using the static equivalent design approach or to 0.8g using ground spectra acceleration for an inelastic dynamic analysis. This design approach is based on what is known as the "minimax decision," since it minimizes the maximum losses in the future.

In areas of the country where the potential for a great earthquake exists, but the probability is extremely low, the choice of criteria can be very difficult. The maximum credible earthquake is not a practical choice for the design of most conventional structures in such areas. *A more fundamental consideration relates to the decision whether or not to design for seismic forces at all. However, considerable seismic resistance can be achieved for very little extra cost by simply applying the principles of equivalent static lateral force design and making sure that the system is continuous and ductile.* The insurance available in such a minimal approach is a true bargain in risk management. The lateral-force factor to be utilized is of secondary importance. However, if *Building Code* values are used, one has some assurance that this choice is properly coordinated with other design provisions of the Code.

5. CONCLUDING COMMENTS

This paper is based upon experience with the earthquake safety program at the Lawrence Berkeley Laboratory (LBL) where 34 buildings were strengthened over a 20 year period following the San Fernando Earthquake in 1971. As a consequence of that experience, LBL published a "Seismic Safety Guide" in 1983 for the U.S. Department of Energy (DOE). It was written for those managers of DOE facilities (and engineers) who had little background in earthquake engineering. Its guidelines include hazard identification and evaluation, site planning, the evaluation and rehabilitation of existing facilities, the design of new facilities, lifelines, operational safety, emergency planning and the management of risks and liabilities.

Since 1983 great progress has taken place in earthquake engineering. Also, a number of damaging earthquakes have taken place where structures were designed to resist them. As a result a wealth of new information has become available. A new edition of the "Seismic Safety Guide" will be published in 1993 to incorporate and interpret this new material so that the managers of DOE facilities can achieve a comfortable level of understanding for the decisions they must make relative to seismic risk management.

The format for the "Guide" will follow the original edition. Each chapter will be written by an experienced professional for an audience composed of managers or engineers with little background in earthquake engineering. Comment and advice from the facility manager's perspective will be provided in the foreword to each author's section. For those interested in a much more detailed treatment of this paper's topic, the new "Seismic Safety Guide" will be published in the Spring of 1993.

6. REFERENCES

1. Eagling, D.G., et al, (1983). "Seismic Safety Guide." LBL-9143, Lawrence Berkeley Laboratory, University of California, Berkeley, CA.

2. Eagling, D.G., (1992). "Seismic Safety Guide, Synoptic Description of the 1993 Edition." Lawrence Berkeley Laboratory, University of California, Berkeley, CA.

Desk-Top Model Buildings for Dynamic Earthquake Response Demonstrations

by

A. Gerald Brady*

ABSTRACT

Models of buildings that illustrate dynamic resonance behavior when excited by hand are designed and built. Two types of buildings are considered, one with columns stronger than floors, the other with columns weaker than floors. Combinations and variations of these two types are possible. Floor masses and column stiffnesses are chosen in order that the frequency of the second mode is approximately five cycles per second, so that first and second modes can be excited manually. The models are expected to be resonated by hand by schoolchildren or persons unfamiliar with the dynamic resonant response of tall buildings, to gain an understanding of structural behavior during earthquakes. Among other things, this experience will develop a level of confidence in the builder and experimenter should they be in a high-rise building during an earthquake, sensing both these resonances and other violent shaking.

KEY WORDS: building models; construction; dynamic; earthquake; resonance; vibration.

1. INTRODUCTION

The physical characteristics and construction of desk-top model structures that demonstrate earthquake shaking effects have probably been described in many research thesis reports. The models here, though, are primarily hands-on displays where the participant provides the shaking input by hand in the form of a sliding to-and-fro motion, of an easily held block of wood acting as the foundation for the structure. The models are suitable for schoolteachers in regions of high seismicity to acquaint children with the kind of motion they might experience if they are in a tall building during an earthquake, rather than a low-rise school building, and to give children a perspective of how the high-rise buildings they are familiar with in their cities shake during earthquakes in ways that are understood, and have therefore been accounted for, by the structural engineering profession. The models are also suitable for showing this behavior in a simple fashion to people outside the seismic engineering profession.

Almost every university or institution with a strong earthquake engineering component will have had, at some time, a motor-driven exhibit shaking a platform in the north-south and east-west directions simultaneously while a structure bolted to the plat-

*U.S. Geological Survey MS/977, 345 Middlefield Road Menlo Park, CA 94025-3591 USA

form illustrates its seismic response. A more current form for this display is a computer program where earthquake magnitude and epicentral distance can be entered, together with structure height and construction material. Detailed structural behavior can be shown on a color screen, and catastrophic collapse provides audience excitement. The models described in this paper, however, are not complicated, and their hands-on feature provide a different experience. It can actually be difficult to find the perfect frequency and thus the perfect timing to excite, slowly and steadily, a flexible or resilient structure into one of its vibrational resonances. Once learned, the ability to excite these model resonances remains, as does the ability to resonate other structures like fishing rods, handrails, and small flagpoles, for example.

The models show how a building resonates in a particular direction when the ground shakes in a steady vibrational to-and-fro motion in the same direction. The frequencies at which this happens have been calculated first, and the models are designed and constructed so that the frequencies are within the range that the operator can readily provide, namely from ½ to 5 cycles per second (cps). This range includes the resonant frequencies of some typical tall buildings (Housner and Brady, 1963). The models show how quickly a resonating mode can be excited and how little input amplitudes are needed to maintain excessive, highly visible, structural amplitudes.

There are two basic models described here, representing the following buildings:

A. Strong column–weak beam (bending beam) buildings: Buildings whose columns are far stronger and stiffer than the floors and floor beams so that the cantilever bending characteristics of the columns are unaffected by the presence of the floors.

B. Weak column–strong beam (shear beam) buildings: Buildings whose floors and floor beams, being far stiffer than the columns, remain flat and horizontal during vibrations. The columns are forced into slight *S*-bends between floors.

There are many versions and combinations of these two that permit modeling:

1. Buildings that are different in height.

2. Buildings which throughout their height, behave as though both types A and B above have an effect.

3. Buildings whose lower stories have such massive columns that type A is in effect there, but whose upper story columns have less strength and type B is in effect.

4. Buildings whose stiffness is increased by the addition of shear walls, sections of exterior wall reaching the entire height, and whose wall direction is the same as the direction of shaking.

5. Buildings that are not symmetric in plan with respect to the shaking direction, and which therefore twist slightly, along a vertical axis, when shaken.

Placing two structural models on the same base can provide an illustration of the pounding of adjacent structures not vibrating in unison.

Although a fundamental structural resonance might have a low resonant frequency, a higher resonance (or overtone or harmonic

in musical terms), can be excited at close to six times (for type A) or three times (for type B) the fundamental frequency, depending on the structural type, and the models are planned to be able to show this.

Construction of the models is based on wood blocks of suitable size to represent horizontal floors, and strips of thin sheet aluminum to represent vertical columns whose flexibility or stiffness can be adjusted by specifying different widths and thicknesses. They have various low amounts of damping, depending on the joint details, but damping is assumed insignificant in the analysis. There is no effort to incorporate specific energy dissipation capability in the models, although some exists in all moving joints. The result is that resonant amplitudes of motion are large, particularly if, by mistake, input amplitudes are maintained at high levels once resonances are achieved. This can lead to damage in the form of weakened screwed joints, permanently bent columns or column fatigue failure unless reasonable care is taken.

2. SPECIFICATIONS

Because these models are hand-held and excited into resonance by shaking of the base with a steady vibrational to-and-fro motion, the highest expected resonant frequency is limited by the highest frequency able to be provided by the user, about 5 cps for most people. The base must be small enough to be grasped between thumb and fingers because the highest frequency resonances require the user to overcome the inertia of the model which builds up in proportion to the square of the frequency, and to overcome the tendency to overturn. For ease of transportation, the height of the tallest models is limited to 2 ft.

Figure 1 illustrates the two basic models and construction details for the joints. Figure 1(A) represents two vertical cantilevers rigidly attached to the base and able to deform by bending under the action of horizontal inertia forces when the base is shaken. Horizontal deflections are representative of the columns of tall buildings whose columns at all elevations are much stronger or stiffer than the floors and floor beams at the same elevations. The floors, where they meet these columns, bend readily, and their contribution to the bending resistance of the joint is insignificant. The column bends, throughout its height, as though the floors have no effect. In the type A model, the floor bending effectively takes place in the joint itself, whereas in real structures it is distributed over the total extent of the floor.

Figure 1(B) illustrates the model of a building with stiff, unbending floors. During vibrations, the floors remain horizontal and the joints do not rotate, forcing the columns in the vicinity of the joints to be vertical. In between floors, the columns bend into very slight S-bends.

The sketches adjacent to the model of Figure 1(A) show two deformed shapes of the basic 2ft-high vertical cantilever model as it vibrates in its first and second modes. The base is shown having zero motion. During an earthquake, or, in this case, during hand excitation, the base is moved at the same frequency that the model exhibits. With models having insignificant damping, the base motion required at resonance has surprisingly low amplitude. The most effective technique, once the resonant frequency is

established, is to vibrate the base slightly ahead of the structure. The second mode of model A has a theoretical frequency 6.27 times faster than the fundamental mode. A model with half the height, also sketched, has a fundamental frequency four times the fundamental mode. Calculations for frequencies, given specific member sizes, may be found in the Appendix.

Adjacent to the model of Figure 1(B) are the deformed shapes of the rigid floor/ flexible column model as it vibrates in its fundamental and second modes. The second mode has a frequency approximately three times the fundamental. A model of half the height has a fundamental frequency two times that of the fundamental mode. Calculations for frequencies may be found in the Appendix.

3. CONSTRUCTION

The construction of these models has been made simple by the selection of hardware that is readily obtainable. The columns are cut from aluminum sheet in thicknesses of 0.031″ (or 1/32″) and 0.010″, obtainable from a metal dealer and cut on a shear at the dealer or local sheet-metal shop. The floors are from 1″ × 2″ pine moulding, smoothed four sides (finished section 3/4″ × 1 1/2″). The bases for those models with no aluminum attached to the longer dimension may be wider, for stability against overturning, for example 1″ × 3″. Models with vertical shear beams for stiffening require bases the same size as the floors above. Short lengths (1/4″) of plastic or rubber hose, inside diameter 1/8″, are required for the hinges of model type A. They hold the floors in position between the columns, threaded on the #8 roundhead wood screws. Washers under the heads of the #8 sheetmetal screws in model type B are built up to an outside diameter of 1/2″ to ensure proper bending of the columns just above and below these connections.

The base of every model is 4″ long, presenting a convenient size to grasp. Floors having hinges are 1/4″ shorter for each end that is hinged, so that the type A model has 3 1/2″ floors. The floors of the Type B model are 4″ long. Column, floor and hinge detail for these and other models listed in the Introduction can be seen in Figure 1.

4. CONCLUSIONS

These models are simple to make and are challenging to excite into resonance. They fulfill the desired goal of providing a hands-on experience for the public in tall building dynamics. Seeing the response of the models to "ground" motion may help allay the fears of persons experiencing an earthquake.

5. APPENDIX

5.1 Buildings with strong columns and weaker floors

Figure 2(a) shows the $x-y$ coordinate system for a cantilever beam, placed vertically, with constant physical characteristics: moment of inertia I, mass density ρ, cross-sectional area A, and Young's modulus E. Neglecting shear distortions and rotary inertia (see, for example, Hurty and Rubinstein, 1964), the deflection $y(x,t)$ satisfies

$$\frac{\partial^4 y}{\partial x^4} + \frac{\rho A}{EI} \cdot \frac{\partial^2 y}{\partial t^2} = 0 \qquad (1)$$

Figure 2(b) shows two such cantilevers representing columns, tied together through floor beams with connections allowing free

rotation of the beams. Representing the floor mass as m_f, total floor mass M_f, and assuming the floor mass is uniformly spread over the height l, equation (1) becomes

$$\frac{\partial^4 y}{\partial x^4} + \left[\frac{2\rho A + M_f/l}{2EI}\right]\frac{\partial^2 y}{\partial t^2} = 0 \quad (2)$$

Looking for a natural mode solution

$$y(x,t) = y(x)\sin\omega t \quad (3)$$

where ω is a modal circular frequency, leads to

$$\frac{d^4 y}{dx^4} - \beta^4 y = 0 \quad (4)$$

where

$$\beta^4 = \left[\frac{2\rho A + M_f/l}{2EI}\right]\omega^2 \quad (5)$$

Looking for a solution of the form

$$y = e^{\lambda x} \quad (6)$$

where λ is complex, and using the boundary conditions

$$y(0) = y'(0) = y''(l) = y'''(l) = 0 \quad (7)$$

yields

$$\cos\beta l \cosh\beta l = -1 \quad (8)$$

Solving numerically, for example by trial and error with a calculator,

$$\beta l = 1\cdot 875\ ,\ 4\cdot 694\ ,\ \ldots \quad (9)$$

Substituting in equation (5),

$$\omega_n = \frac{1}{l^2}\sqrt{\left[\frac{2EI}{2\rho A + M_f/l}\right]}\cdot N_n, n = 1,2,3\ldots \quad (10)$$

where

$$N_1 = 3{\cdot}516, N_2 = 22{\cdot}035, \frac{N_2}{N_1} = 6{\cdot}27 \quad (11)$$

Selecting $l = 24''$, $b = 1.5''$, $d = (1/32)''$, $m_f = 0.1$ $lb./g$, $h = 4''$; and using $E = 10\times 10^6$ psi, $\rho = 0.0975$ $lb./g/in^3$, $g = 386.4$ in/s^2, $I = bd^3/12$, $A = bd$, $M_f/l = m_f/h$, yields

$$f_1 = 0.9 \text{ cps}\ ,\ f_2 = 5.7 \text{ cps} \quad (12)$$

and the frequency of a building of half this height is

$$f_{l/2} = 3\cdot 6 \text{ cps} \quad (13)$$

5.2 Buildings with strong floors and weaker columns

Figure 3(a) and (b) show two structures of height l under the action of a horizontal shearing force F, which displaces the top of the structures a distance y_t. Figure 3(a) is a vertical shear beam with cross-section area A, shear modulus G, and mass density ρ. Figure 3(b) represents an N-story building whose floors are strong and remain horizontal, forcing the weaker columns to be vertical in the vicinity of the beam–column joints. The two columns have Young's modulus E, and each has moment of inertia I. The known wave equation governing the dynamic displacements of (a) can be transferred to the structure (b) provided their stiffnesses under the action of the force F, and densities, are equivalent.

For the vertical shear beam (see, for example, Hurty and Rubinstein, 1964),

$$\frac{F}{A} = G\frac{y_t}{l} \quad (14)$$

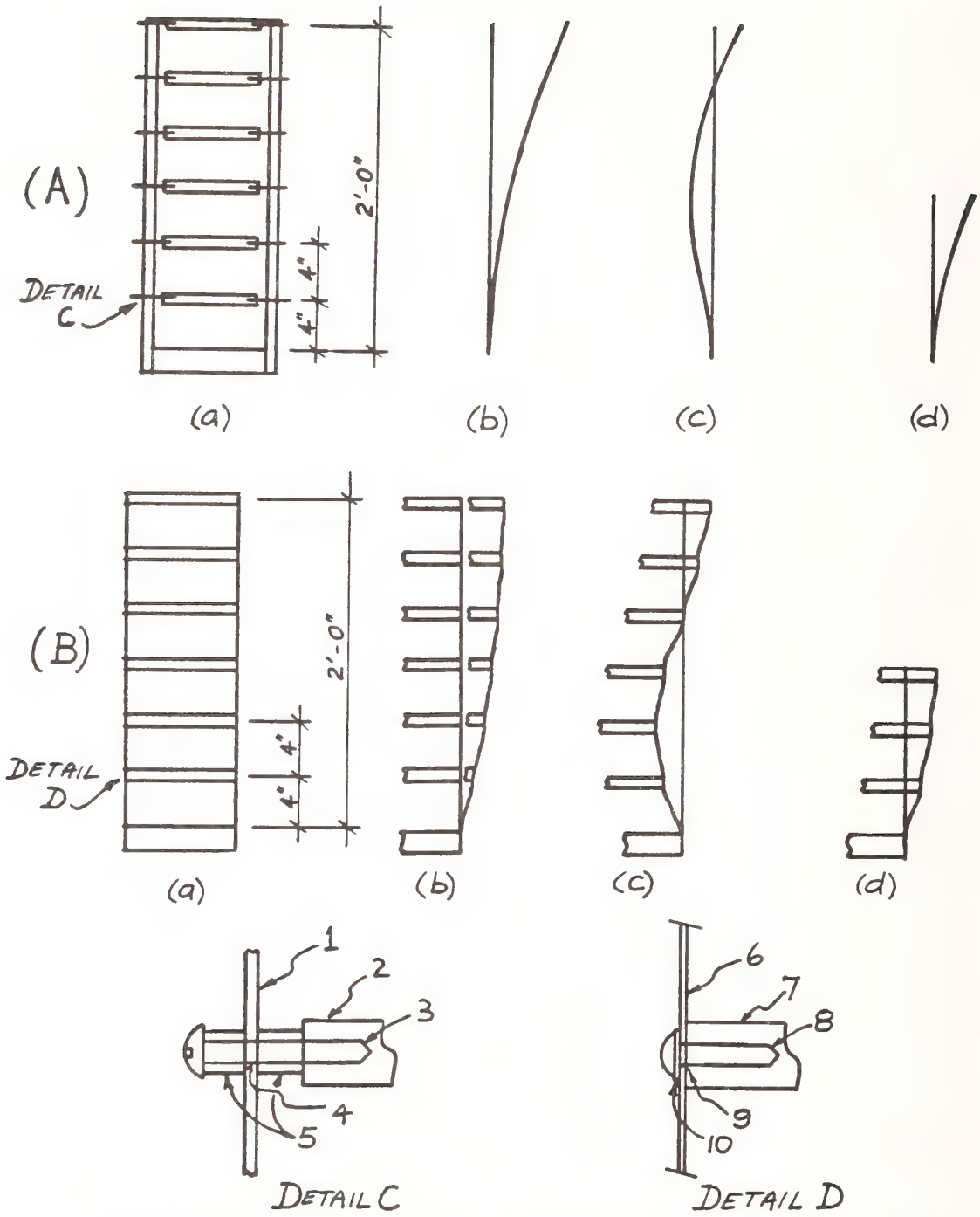

Figure 1. (A) Model type A with wood floors pinned at each end; (B) Type B with floors rigidly connected to weaker columns—(a) general view, (b) first mode shape, (c) second mode shape, (d) first mode shape of half-height model. Details: **1,** 0.031″ × 1½″ aluminum column; **2,** 1″ × 2″ × 3½″-long wood floor; **3,** #8–1¼″ roundhead wood screws, two per hinge, ¾″ apart; **4,** $^{13}/_{64}$″ hole allowing adequate clearance; **5,** ¼″ length of plastic tube, ⅛″ I.D.; **6,** 0.010″ × 1″ aluminum column; **7,** 1″ × 2″ × 4″-long wood floor; **8,** #8–1¼″ roundhead sheetmetal screws, two per joint, ½″ apart; **9,** $^{11}/_{64}$″ hole; 10, #8 and ¼″ washers.

For the N-story building,

$$F = \frac{24EI}{h^3} \cdot \frac{y_t}{N} \qquad (15)$$

Equating stiffnesses,

$$GA = \frac{24EIl}{h^3 N} \qquad (16)$$

Considering free vibrations of the vertical shear beam,

$$\frac{\partial^2 y}{\partial x^2} - \frac{\rho}{G}\frac{\partial^2 y}{\partial t^2} = 0 \qquad (17)$$

Looking for a natural mode solution of the form

$$y(x,t) = y(x)\sin\omega t \qquad (18)$$

leads to

$$y''(x) + k^2 y(x) = 0 \qquad (19)$$

where

$$k^2 = \frac{\rho}{G}\omega^2 \qquad (20)$$

Looking for a solution of the form

$$y = A\cos kx + B\sin kx \qquad (21)$$

with boundary conditions

$$y(0) = y'(l) = 0 \qquad (22)$$

leads to

$$kl = (2n-1)\frac{\pi}{2}\ ,\ n = 1\ ,\ 2\ ,\ \ldots \qquad (23)$$

Substituting equation (23) into (20) yields

$$f_n = \frac{\omega_n}{2\pi} = \frac{1}{4l}\sqrt{\frac{G}{\rho}} \cdot N_n \qquad (24)$$

where

$$N_1 = 1\ ,\ N_2 = 3\ ,\ N_2/N_1 = 3 \qquad (25)$$

Transfer the stiffness from Figure 3(a) to 3(b) using equation (16), and transfer the density by equating the total mass (ignoring the mass of the thin aluminum columns compared with the floors):

$$\rho Al = M_f = Nm_f = \frac{l}{h} \cdot m_f \qquad (26)$$

Selecting $l = 24''$, $b = 1''$, $d = 0.01''$, $m_f = 0.1$ *lb./g*, $h = 4''$; and using $E = 10 \times 10^6$ psi, $g = 386.4$ in/s^2, $I = bd^3/12$; and substituting equations (16) and (26) into (24), yields

$$f_1 = 1 \cdot 4 \text{ cps}\ ,\ f_2 = 4 \cdot 2 \text{ cps} \qquad (27)$$

The frequency of a building of half this height is

$$f_{l/2} = 2 \cdot 8 \text{ cps} \qquad (28)$$

Figure 4 reproduces photos of some of the models and their mode shapes.

6. REFERENCES

1. Housner, G. W., and Brady, A. G., 1963, Natural periods of vibration of buildings: *Jour. Eng. Mech. Div., ASCE*, v. 89, EM4, p. 31–65.

2. Hurty, W. C., and Rubinstein, M. F., 1964, *Dynamics of Structures*, Prentice Hall.

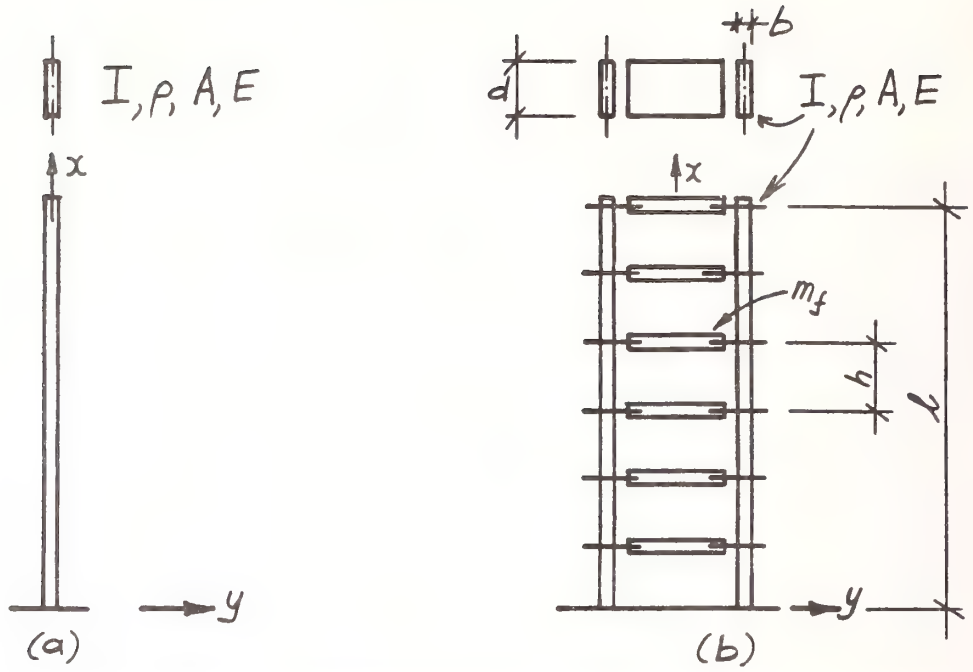

Figure 2. (a) Cantilevered bending beam placed vertically, (b) schematic for analysis of type A model.

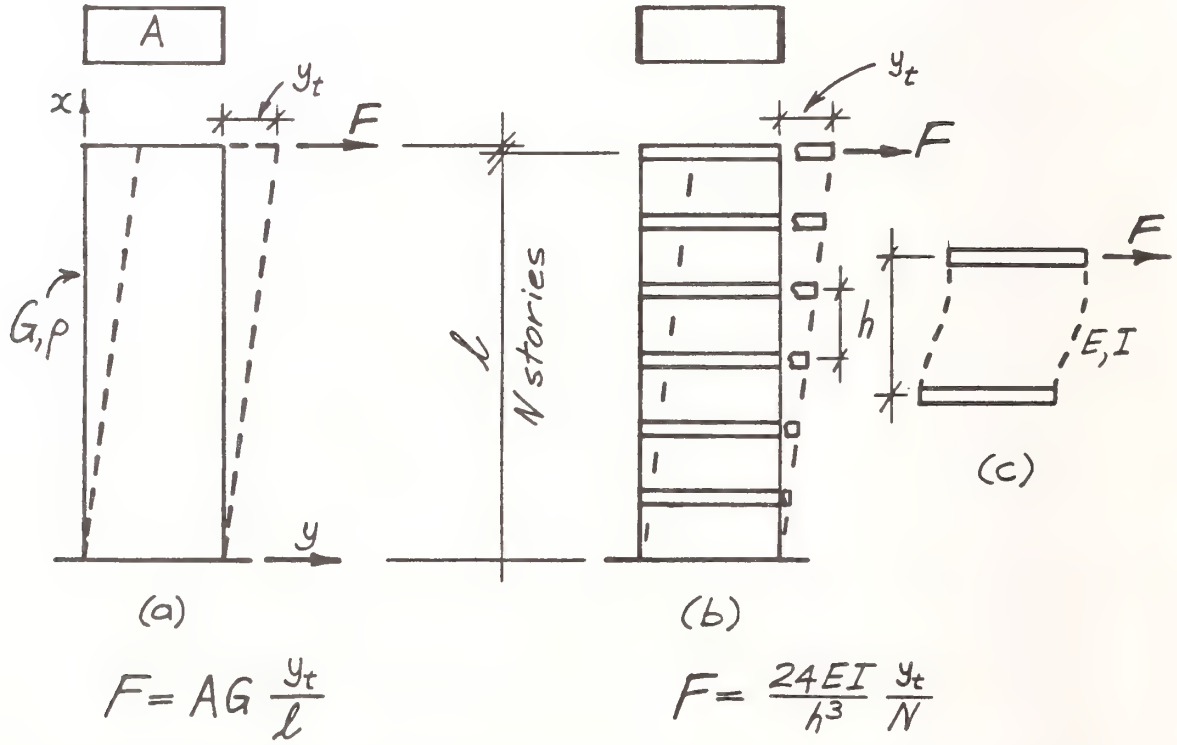

Figure 3. Two structures resisting horizontal forces by shearing action. (a) Cantilevered shear beam placed vertically; (b) schematic for analysis of type B model; (c) interstory detail.

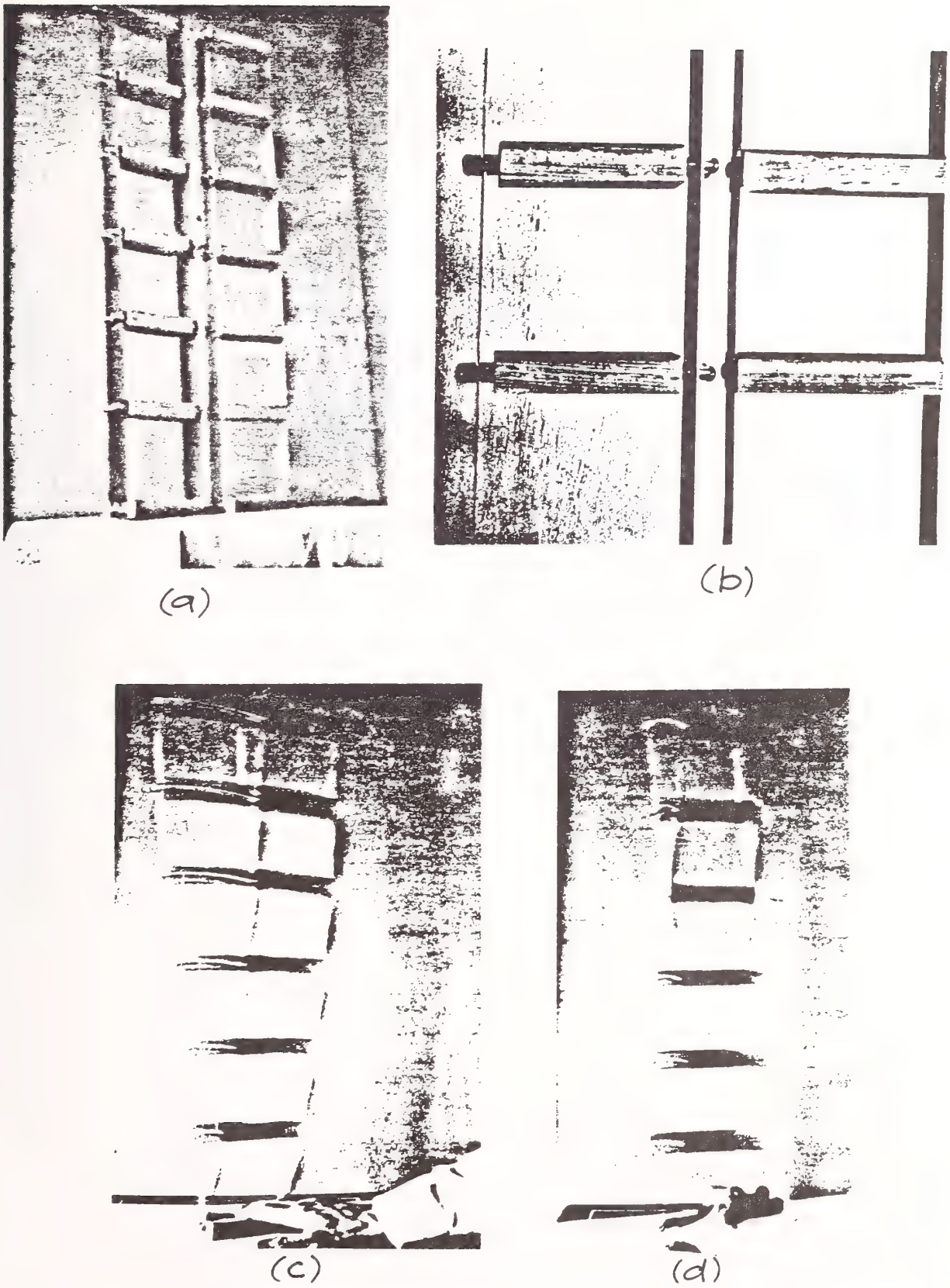

Figure 4. (a) Type A and B models; (b) floor and column detail; (c) first mode of type B model, frequency 1.9 cps; (d) second mode of type B model, frequency 5.6 cps.

Manuscripts Authored for Panel Meeting but Not Presented Orally

Determination of Windborne Missile Design Parameters

by

James R. McDonald*

ABSTRACT

Tornadoes and other high winds pick up and transport objects and debris, which can cause extensive damage to structures. This paper addresses the problem of windborne missile impact on facilities which, if damaged, could result in injury to people or damage to the environment. The problem has two parts: (1) what missiles should be included in the criteria, and (2) what is the impact resistance of different wall and roof panels to the postulated missiles. This paper briefly addresses both issues. The document, *Guidelines for Design and Evaluation of Department of Energy Facilities Subjected to Natural Hazard Phenomena*, (UCRL 15910) specified a missile criteria for moderate and high hazard facilities. The selection of the missiles to be considered and their parameters by the Natural Hazards Phenomena Committee are described in the paper. A series of impact tests were then conducted at Texas Tech University to identify a set of wall and roof panels that could satisfy the UCRL 15910 missile impact criteria. The deterministic criteria is selected to satisfy stated probabilistic performance goals of the DOE facilities.

KEYWORDS: debris; impact; missiles; tornadoes; wind; wind resistant design

1. INTRODUCTION

Model building codes (e.g. SBCCI, 1991) and national wind load standards (e.g., ASCE, 1988) do not require building designs to consider loads produced by tornadoes. The probability of a building at a specific geographic location experiencing a tornado with particular wind speed is considered too small for ordinary buildings. However, there are circumstances where design for tornadoes is necessary or desirable. Facilities that have high dollar value materials or perform critical functions, such as a fur storage warehouse or a corporate computer data center, may need to be designed to be tornado resistant. Facilities that store or process toxic or radioactive materials may also require consideration of tornado effects. Nuclear reactors have traditionally been designed to be tornado resistant. Critical equipment and facilities needed to conduct a safe shut down of the reactor are housed in tornado-hardened buildings or enclosures.

A tornado damages buildings or facilities by three principal mechanisms: (1) wind, (2) atmospheric pressure change (APC), and (3) missile impact. This paper addresses the third damage mechanism: tornado missile impact.

High winds and tornadoes pick up and transport various objects and debris. Under the right set of circumstances, these objects may be accelerated to high speeds, carried to great heights, and travel long distances. Common terms for debris transported by the winds are *wind-generated* or *tornado-generated* missiles. Tornado winds are more efficient in transporting missiles than "straight" winds in hurricanes and thunderstorms.

When a tornado missile strikes the wall or roof of a building, two independent responses are possible: *penetration* or *structural response*. A penetration impact is caused by a long, prismatically-shaped object such as a timber plank, pipe, or pole. When the missile strikes the wall, one of four possible events takes place:

(1) the object strikes the wall at some oblique angle and bounces harmlessly off the wall (oblique strike)

(2) the missile strikes essentially on end, and penetrates some distance into the wall (penetration)

(3) the missile strikes the wall with sufficient force to scab material from back face of wall; it may penetrate but does not perforate the wall (back face scabbing)

(4) the missile passes through the wall and exits at some slower speed (perforation with residual velocity).

---

*Professor of Civil Engineering, Texas Tech University, Box 41023, Lubbock, TX 79409.

Structural response occurs when a large, heavy object strikes a structural component and produces excessive plastic deformations in the material. An example is an automobile striking a reinforced concrete wall panel with sufficient force to produce yielding of the reinforcing steel and crushing of the concrete. If a heavy object strikes a column with sufficient force, the column could collapse and initiate a progressive failure as other columns in the structural system collapse one after the other. Structural response impact is not addressed in this paper.

Many buildings and facilities operated by the U.S. Department of Energy (DOE) house toxic or nuclear materials that present potential danger to plant personnel or the environment should a high wind or tornado damage the facility. Recognizing the potential problem, DOE through Lawrence Livermore National Laboratories, supported the development of *Design and Evaluation Guidelines for DOE Facilities Subjected to Natural Phenomena Hazards*. A committee consisting of wind, earthquake and flood experts produced the guidelines, which are referred to as UCRL 15910. The approach adopted by the Natural Hazards Phenomena (NPH) Committee is to use a deterministic design and evaluation criteria to meet probabilistic performance goals. Hill et al. (1991) describes the treatment of wind and APC loads on DOE facilities. The objective of the study described herein is to establish the basis for the missile criteria and impact-resistant requirements for design or evaluation of DOE facilities.

Four facility-use categories are defined in the current version of UCRL 15910 (DOE, 1990): (1) general use, (2) important or low hazard, (3) moderate hazard, and (4) high hazard facilities. Only the latter two categories require consideration of windborne missiles. A facility will be subject to either high wind or tornado design criteria, depending on its geographic location. Both criteria require consideration of windborne missiles. Tornado missile criteria is more conservative than straight wind.

The remainder of this paper is divided into three sections that present (1) basis for missile trajectory parameters, (2) impact resistance of wall and roof panels, and (3) conclusions and recommendations.

2. BASIS FOR MISSILE PARAMETERS

The principal questions to be answered about tornado missiles are (1) what types are transported by the winds, (2) how fast do they fly, (3) how high, and (4) how far.

2.1 Windborne Missiles

Field damage experience is the best means for identifying the types of missiles that can be picked up and transported by high winds or tornadoes. For purposes of discussion, objects can be classified as lightweight, medium, and heavy missiles (McDonald and Kiesling, 1988). Lightweight missiles include roof gravel, pieces of gypsum board, fiberglass insulation, sheet metal panels, and small tree branches. These missiles primarily break glass or damage building finishes.

Medium weight missiles are, by far, the most common. The category includes pieces of timber plank from damaged or destroyed wood buildings, electrical conduit, plastic pipe, small communication antennas, fence posts, small steel joists, purlins, or girts. These missiles will be picked up by thunderstorm or hurricane winds, but are more likely to achieve the highest trajectory speeds when picked up by tornado winds. They can achieve speeds sufficient to perforate ordinary stud wall construction, walls with brick veneer, unreinforced and ungrouted concrete masonry, and concrete wall panels less than four inches thick.

Heavy missiles include a variety of objects such as large diameter pipes, utility poles, automobiles, trash dumpsters, storage tanks, and railroad cars. Except for the pipes and poles, these objects tend to roll and tumble on the ground rather than become airborne. The poles and pipes can penetrate or perforate all walls with equivalent resistance less than or equal to a 12 in. thick reinforced concrete wall. Large, heavy objects cause structural response rather than penetration failure.

Field investigations of many windstorms have led to the identification and classification of windborne missiles. Lightweight and medium weight missiles are common in relatively weak tornadoes, hurricanes and straight winds. Transportation of heavy missiles is an indication of high winds in an intense tornado.

Because of the adverse consequences of core damage to nuclear power reactors, the USNRC design criteria requires plants to be designed for a very conservative list of heavy weight missiles (USNRC, 1981). As a result of the USNRC

missile criteria, facilities that house equipment or systems required for safe shutdown of power reactors are required to have 24-in. thick concrete walls and 18-in. roof slabs. This very conservative criteria controls design and contributes to high construction costs. Probabilistic risk assessments (PRAs) of heavy tornado missile events suggest that the probability of reactor core damage from missile impact is of the order of 1×10^{-8}.

The probabilistic performance goals established for DOE facilities in UCRL 15910 can be achieved with much less conservative windborne missile criteria. Because PRAs are time consuming and expensive, a deterministic approach was adopted, which leads to designs that meet the performance goals. The approach is based on post-storm damage data and judgments of experts in wind damage assessments.

2.2. Missile Flight Characteristics

Flight characteristics are the parameters that determine how fast, how high, and how far missiles travel in a windstorm. The important parameters are weight, surface area, drag and lift coefficients, release mechanism and height of missile at release. The weight, area and aerodynamic coefficients determine if a missile, when released, will be transported by the wind or merely fall to the ground under the influence of gravity. The height above ground at release determines how long a missile will remain airborne before striking the ground. Another factor is whether the missile is restrained or unrestrained before being picked up by the wind. If it is unrestrained, it may be simply pushed along the ground by the wind. If it is restrained and the winds suddenly overcome the restraint, the missile is more likely to fly higher and faster than if it were not restrained.

In the case of a tornado, the location within the tornado wind field where the missile is released determines the trajectory it will follow. Missiles that release on the right hand side of the tornado path centerline (looking in direction of tornado travel) will generally travel in the direction of tornado translation with the trajectory converging toward the centerline. Objects picked up on the left side of the path centerline are carried by the tangential winds and may initially move in the opposite direction to tornado tranlation and travel around the back side of the tornado vortex.

In field investigations, the initial location ofthe missile and its final impact location usually can be determined. What happens in between can only be determined if movies or videos of the storm were available. Such films are very rare. Thus, the only feasible approach to understanding missile trajectories is by computer simulation.

2.3 Trajectory Simulation

Two approaches to trajectory simulation have been used in the past: deterministic and probabilistic.

2.3.1 Deterministic

Missile aerodynamics are modeled using flight parameters, injection mechanism, wind field model and dynamic equations of motion (McDonald, 1975). Flight parameters include drag and lift coefficients, area, and weight of missile. Drag and lift coefficients are obtained from wind tunnel tests. The flow of wind in the tornado vortex is modeled as realistically as possible. Photogrammetric analyses of the flow observed in movies or videos of tornado funnels are used to identify the wind flow patterns as well as theoretical considerations. Several tornado wind field models have been published in technical literature. The DBT-77 model by Fujita (1978) is based on photogrammetric analysis and extensive field observations of damage patterns by Dr. Fujita. Other models include Hoecker (1960) and Simiu and Cordes (1976).

Injection of the missile into the wind field can be as simple as releasing the missile at some preselected point within the three-dimensional tornado wind field where it will achieve maximum speed, height and/or distance traveled. Another approach is to systematically place the missiles at regular intervals across the tornado path and release them at some predetermined wind speed. Trajectories are then calculated for each missile and the worst conditions are tabulated.

Missiles can be modeled as a three-degree-of-freedom point model or a six-degree-of-freedom rigid model. Calculations are simpler for the point model. The approach was used to successfully predict the impact locations of the steel beams that were picked up by the Bossier City Tornado (McDonald, 1981).

The six-degree-of-freedom model requires a set of drag and lift coefficients for each orientation

of the missile in space relative to the wind direction vector. Such measurements have been made in the wind tunnel for a few objects. The computational effort for the six-degree-of-freedom model is many times larger than for the three-degree-of-freedom model, with no solid evidence that it is more accurate or realistic (Redman et al., 1976). Neither model considers the effects of small scale turbulence in the tornado wind field.

2.3.2 Probabilistic Simulation

The probabilistic approach to trajectory simulation is essentially a Monte Carlo simulation. Tornado wind field characteristics (maximum wind speed, path width and direction) are randomly selected as are certain missile parameters at each time step of the trajectory calculations. The missiles are randomly selected according to some weighted frequency scheme. By simulating many years of tornado missile experience, statistics on the types of missiles and their trajectory characteristics can be obtained. See for example Twisdale and Dunn (1978). The site specific approach, which attempts to model the real situation as accurately as possible, must be applied at each facility being considered for tornado effects. To carefully model a site by this method requires extensive effort and considerable cost.

2.4 UCRL 15910 Missile Criteria

Since UCRL 15910 is based on a deterministic approach to satisfy probabilistic performance goals, the deterministic approach to tornado missile criteria was adopted by the NHP Committee.

Since general use and low hazard facilities are designed by criteria in model codes or national standards, which have no provisions for winborne missiles, UCRL 15910 also does not specify a missile criteria for these facilities. Moderate and high hazard facilities located in areas where tornadoes are not a serious threat have a minimum windborne missile criteria. The minimum missile criteria accounts for objects or debris that could be picked up by straight winds, hurricanes or weak tornadoes.

Moderate and high hazard facilities located in tornado prone areas must satisfy tornado missile criteria. Because the tornado missile trajectory calculations require specialized software and involve considerable time and effort, the NPH Committee established missile criteria that was independent of tornado design wind speed. This was possible because the range of tornado design wind speeds for the 26 DOE sites was relatively narrow. Thus a single criteria for all moderate and high hazard facilities could be established.

Two medium and one heavy weight missiles are considered in the design and evaluation of DOE facilities. A timber missile is typical of debris found in the destruction of office trailers, storage sheds, residences and other light framed timber structures. Hundreds of these missiles can be generated in the destruction of a residential neighborhood. A steel pipe missile represents a class of debris that includes electrical conduit, liquid or gas piping, fence posts and small columns. The pipe missile is less frequently available for transport and does not fly as high or as fast as the timber missile, but is more destructive upon impact. Tornadoes can roll and tumble automobiles, pickup trucks, small vans, forklifts and storage tanks of comparable size and weights. These missiles do not become airborne, but can damage wall panels, frames or columns by excessive structural response.

The three missiles produce varying degrees of damage. A specific type of construction is required to stop each missile. The timber missile is capable of breaking glass and perforating curtain walls or unreinforced masonry walls. Reinforced concrete or masonry walls are required to stop the pipe missile. Timber and pipe missiles can perforate weak exterior walls and emerge with sufficient speed to perforate interior walls and damage HVAC ducts, filter enclosures or control equipment. The impact of a rolling or tumbling automobile produces failure by excess structural response. Bearing walls, rigid frames and exterior columns are particularly susceptible to heavy missile impacts.

Specific missile criteria in UCRL 15910 are summarized in Table 1. Critical missile parameters include (1) material, (2) weight, (3) impact speed and (4) maximum height achieved. Impact speeds are expressed in terms of horizontal and vertical components. They should not be combined vectorially, because the maximum horizontal speed does not occur at the same point in the trajectory as the maximum vertical speed. The maximum horizontal speed generally occurs at maximum height of trajectory above ground, while the maximum vertical speed occurs at impact with the ground.

In general, the maximum horizontal speed is used in the design of walls or other vertical barriers. The maximum vertical speed is used to design roof decks and other horizontal barriers. Both maximum horizontal and vertical speeds should be considered (separately) on sloping surfaces.

The designer or evaluator using UCRL 15910 criteria is not required to determine missile impact speeds. He designs new barriers or assesses existing barriers based on results of impact tests. The impact test results for the timber plank and steel pipe missiles are described in the next section. From the test results, specific wall or roof barriers are known to meet the UCRL 15910 missile criteria.

3. IMPACT RESISTANCE OF WALL AND ROOF PANELS

3.1 Background

Penetration, perforation and scabbing equations used for tornado missile impact design in the 1960s were derived from military applications of ballistic missile impacts. The masses and shapes of the military projectiles were quite different from those generated by tornado winds. Gwaltney (1968) presented a comprehensive review of missile generation and protection in nuclear power plants. A number of penetration formulas are referenced in the Gwaltney paper:

(1) Modified Petry formula

(2) Ballistic Research Laboratory (BRL) formula

(3) National Defense Research Committee (NDRC) equation

(4) Army Corps of Engineers formula

Because none of the ballistic formulas were directly applicable to tornado missile impact design, several agencies and companies initiated impact test programs. Most of the missiles and barriers tested in the 1970s related to the U.S. Nuclear Regulatory Commission (USNRC) criteria for design of commercial nuclear plants. Test results were reported for steel rods (rebar), steel pipes, timber planks, utility poles, and automobiles. Based on test results, a modified version of the NDRC equation was proposed by Kennedy (1975). Rotz (1975) developed an empirical equation based on a series of impact tests sponsored by Bechtel Power Corporation (Velasso, 1975). The NDRC and Rotz equations are applicable to steel pipe missiles for impacting on reinforced concrete panels. The test results were for impact speeds higher and panels much thicker than those required by UCRL 15910.

3.2 Missile Impact Tests

The Tornado Missile Impact Facility (TMIF) at Texas Tech University is capable of testing the resistance of various wall and roof panels to the impact of medium weight missiles. The tests include both the 2x4 timber plank (15 lbs) and the 3-in. diameter steel pipe (75 lbs). A compressed air cannon is capable of propelling the 2x4 plank to 150 mph and the pipe to 75 mph. Figure 1 shows the general arrangement of the facility. Figure 2 is a photo of the cannon. A rigid reaction frame supports the test panels. The speed of the missile just prior to impact is measured by an optical timing gate.

3.2.1 2x4 Timber Plank Missiles

Three series of tests were conducted with the 2x4 plank missile. The first series of tests determined the impact resistance of conventional residential wall construction as defined in *Architectural Graphics Standards* (Packard, ed., 1981). Wall panels 4 ft wide by 8 ft high were constructed with 2x4 Douglas fir studs at 16 in. on center. The inside wall material was 1/2 in. gypsum board. The exterior cladding is described in Table 2. As shown in Table 2, the 2x4 plank perforates the stud walls at speeds of about 55 mph. Missile trajectory simulations of the 2x4 plank suggest that if the missile is transported by the winds, it will most likely achieve speeds greater than 55 mph. Thus, ordinary stud wall construction will be perforated by the 2x4 timber plank missile. Stud walls clad with insulation board and brick veneer are capable of resisting the 2x4 plank missile at speeds less than 120 mph (see Table 2).

The second series of tests involved impact of the timber plank missile on concrete masonry walls (McDonald and Bailey, 1985). Eight-in. and 12-in. concrete masonry unit (CMU) walls with various combinations of reinforcement and grout in the vertical cells were tested. Unreinforced and ungrouted walls offer little resistance to perforation. If the missile strikes the face shell of an 8-in. wall, it perforates at impact speeds as low as 60 mph. The 12-in. CMU wall offers slightly more resistance

because the face shell is thicker. Reinforcing each vertical cell with a 1/2-in. diameter (#4) rebar and filling the cell with a high slump concrete grout produces a wall that is capable of stopping the 2x4 plank at any impact speed. At impact speeds greater than 100 mph, the missile will splinter. Horizontal trussed joist reinforcement at 16 in. on center helps prevent cracking of the masonry panel. Table 3 summarizes the results of the second series of tests on CMU walls.

The third series of tests involved impact of the 2x4 timber plank on unreinforced and reinforced concrete wall and roof panels. The 2x4 timber plank will not perforate a 4-in. unreinforced concrete panel (4000 psi nominal compressive strength), but it will badly crack it. Adding 1/2-in. diameter rebar at 12-in. on center each way on the inside face of the panel will prevent the cracking. Impacts of the plank at speeds greater than 100 mph on slabs thicker than 4 in. will cause the missile to splinter.

3.2.2 Three-In. Diameter Steel Pipe Missiles

A series of impact tests were conducted on reinforced concrete and masonry panels that were designed to satisfy the UCRL 15910 missile impact criteria. Six concrete walls with 6-in., 8-in., 9-in., or 10-in. thicknesses were tested at impact speeds of 50 and 75 mph. All concrete panels performed better than the Modified NDRC equation predicted.

Eight-in. and 12-in. CMU walls that were grouted and reinforced with 1/2 in. diameter rebar were tested. The 3-in. diameter pipe perforated the 8-in. CMU wall at an impact speed of 75 mph. Back-face scabbing occurred at an impact speed of 50 mph. Pieces of material weighing approximately 7.5 lbs came off the back face of the panel. The threshold perforation speed of the 12-in. CMU wall was found to be approximately 60 mph.

Two other masonry panels were tested with the pipe missile. One was a 9 1/2-in. cavity wall consisting of two wyths of clay brick masonry and 2500 psi concrete in the cavity. Number 3 rebar was placed vertically at 8-in. on center. Horizontal joint reinforcement was placed at 16-in. on center. The panel was impacted by the steel pipe at 50 mph. Cracks appeared on both the front and back face, but no perforation on scabbing occurred. This panel was not tested at 75 mph. The second masonry panel was constructed with 8-in. reinforced and grouted CMUs and a 4-in. clay brick veneer. This panel was impacted by the pipe at 50 mph. The impact speed appeared to be near the threshold of back-face scabbing. Table 4 summarizes the results of these tests.

4. CONCLUSIONS AND RECOMMENDATIONS

Several series of impact tests using the 2x4 timber plank and the 3-in. diameter steel pipe have been conducted at the Texas Tech University TMIF. Results of these tests form the basis for the following recommended wall and roof panels for missile protection of moderate and high hazard facilities as defined in UCRL 15910. (See Table 2 for missile criteria.)

4.1 Moderate Hazard - Straight Wind

The 2x4 timber plank impact at 50 mph requires a minimum 8-in. CMU wall with one #3 rebar grouted in each vertical cell and trussed horizontal joint reinforcement at 16 in. on center.

4.2 Moderate Hazard - Tornado

The timber plank impact at 100 mph requires a minimum 8-in. CMU wall with one #3 rebar grouted in each vertical cell and trussed horizontal joint reinforcement at 16 in. on center; 6-in. concrete wall with #3 rebar at 12 in. on center each way 1 1/2-in. from the inside face. The 3-in. pipe impact at 50 mph requires a minimum 12-in. CMU wall with #4 rebar grouted in each vertical cell and trussed horizontal joint reinforcement at 16 in. on center; 8-in. concrete wall with #4 rebar at 12-in. on center, each way 1 1/2-in. from each face.

4.3 High Hazard - Straight Winds

High hazard facilities for straight winds have the same criteria as moderate hazard, except the wall panels are susceptible to impact up to 50 ft above ground level.

4.4 High Hazard - Tornado

The 2x4 timber plank impacting at 150 mph requires a minimum of 8-in. CMU wall with one #4 rebar grouted in each vertical cell and trussed horizontal joint reinforcement at 16-in. on center; 6-in. concrete wall with #4 rebar at 12-in. on center, each way, 1 1/2-in. from each face. The 3-in. diameter pipe impacting at 75 mph requires a minimum 10-in. concrete wall

reinforced with #4 rebar at 12-in. on center, each way, 1 1/2-in. from each face.

4.5 Recommendations

The wall panels described above will satisfy the criteria of UCRL 15910. The criteria will meet the performance goals for the category of facility considered. Additional tests are needed to determine the resistance of doors, grills and other wall cladding systems. The impact resistance of steel plate panels is untested. Additional tests are needed to validate the BRL equation for steel plates.

Considerable additional study is also needed to establish and verify procedures for calculating structural responses to heavy weight missiles.

5. ACKNOWLEDGEMENTS

Financial support for the Texas Tech University missile impact tests from the National Science Foundation and Lawrence Livermore National Laboratory are gratefully acknowledged.

6. REFERENCES

1. ASCE, 1988: *Minimum Design Loads for Buildings and Other Structures*, American Society of Civil Engineers, New York, NY.

2. DOE, 1990: *Design and Evaluation Guidelines for DOE Facilities Subjected to Natural Phenomena Hazards*, UCRL 15910, U.S. Department of Energy, Washington, D.C.

3. Gwaltney, R.C., 1968: *Missile Generation and Protection in Light-Water-Cooled Reactor Plants*, ORNL-NSIC-22, Oak Ridge National Laboratory, Oak Ridge, TN.

4. Fujita, T.T., 1978: *Workbook of Tornadoes and High Winds for Engineering Applications*, SMRP Research Paper No. 165, Department of Geophysical Sciences, the University of Chicago, Chicago, IL.

5. Hill, J.R., McDonald, J.R. and Murray, R.C., 1991: *Probabilistic Performance Goals for Wind and Tornado Design*, 23rd Joint Panel Meeting on Wind and Seismic Effects.

6. Hoecker, W.H., Jr., 1960: "Wind Speed and Air Flow Patterns in the Dallas Tornado of April 2, 1957," *Monthly Weather Review*, Vol. 88, pp. 167-180.

7. Kennedy, R.P., 1975: *A Review of Procedures for Analysis and Design of Concrete Structures to Resist Missile Impact Effects*, Holmes & Narver, Inc., Anaheim, CA.

8. McDonald, J.R., 1975: *Flight Characteristics of Tornado-Generated Missiles*, Institute for Disaster Research, Texas Tech University, Lubbock, TX.

9. McDonald, J.R., 1981: "Incredible Tornado Generated Missiles," *Proceedings*, Fourth U.S. National Conference on Wind Engineering Research, Vol. I, University of Washington, Seattle, WA, pp. 29-36.

10. McDonald, J.R., 1990: "Impact Resistance of Common Building Materials to Tornado Missiles," *Journal of Wind Engineering and Industrial Aerodynamics*, Vol. 36, Elsevier Science Publishers B.V., Amsterdam, pp. 717-724.

11. McDonald, J.R. and Bailey, J.R., 1985: "Impact Resistance of Masonry Walls to Tornado-Generated Missiles," *Proceedings*, Third North American Masonry Conference, The University of Texas at Arlington (June 3-5, 1985), pp. 84-1 through 84-11.

12. McDonald, J.R. and Kiesling, E.W., 1988: "Impact Resistance of Wood and Wood Products to Simulated Tornado Missiles," *Proceedings*, International Conference on Timber Engineering, Seattle, WA (September 19-22, 1988).

13. Redman, G.H. and Associates, 1976: *Wind Field and Trajectory Models for Tornado-Propelled Objects*, EPRI-308, Electric Power Research Institute, Palo Alto, CA.

14. SBCCI, 1991: *Standard Building Code*, Southern Building Code Congress International, Inc., Birmingham, AL.

15. Rotz, J.V., 1975: Summary of Missile Test Results on Concrete Panels, *Proceedings*, ASCE Specialty Conference on Structural Design of Nuclear Plant Facilities, Vol. 1-A, New Orleans, LA.

16. Simiu, E. and Cordes, M., 1976: *Tornado-Borne Missile Speeds*, NBSIR 76-1050, National Bureau of Standards, Washington, D.C.

17. Twisdale, L.A. and Dunn, W.L., 1981: *Tornado Missile Simulation and Design Methodology, Vol. I: Simulation, Methodology, Design Applications and TORMIS Computer Code*, EPRI NP-2005, Electric Power Research Institute, Palo Alto, CA.

18. Twisdale, L.A., Dunn, W.L. and Chin, J., 1978: *Tornado Missile Risk Analysis*, EPRI NP-768, Final Report, Electric Power Research Institute, Palo Alto, CA.

19. USNRC, 1981: *Standard Review Plan 3.5.1.4*, U.S. Nuclear Regulatory Commission, NUREG-08000, Washington, D.C.

20. Vassallo, F.A., 1975: *Missile Impact Testing of Reinforced Concrete Panels*, Report No. HC-5609-D-1, Calspan Corporation, Buffalo, NY.

Table 1. Windborne Missile Criteria in UCRL 15910

	Moderate Hazard	High Hazard
Straight winds	2x4 timber plank, 15 lb @ 50 mph (horiz.); max. height 30 ft.	2x4 timber plank, 15 lb @ 50 mph (horiz.); max. height 50 ft.
Tornadoes	2x4 timber plank, 15 lb @ 100 mph (horiz.); max. height 150 ft; 70 mph (vert.)	2x4 timber plank, 15 lb @ 150 mph (horiz.); max. height 200 ft; 100 mph (vert.)
	3 in. dia. steel pipe, 75 lb @ 50 mph (horiz.); max. height 75 ft; 35 mph (vert.)	3 in. dia. steel pipe, 75 lb @ 75 mph (horiz.); max. height 100 ft; 50 mph (vert.)
		3000 lb automobile @ 25 mph; rolls and tumbles

Table 2. Results of 2x4 Timber Plank Impact Tests on Typical Stud Wall Panels (McDonald, 1990)

Panel Description	Perforation Speed, mph
Masonite Siding	54
Insulation Board and Masonite Siding	54
Plywood (1/2 in.) and Masonite Siding	52
Plywood (1/2 in.)	52
Plywood (3/4 in.)	53
Stucco	53
Lapboard Siding	53
Insulation Board and Lapboard Siding	52
Insulation Board and Brick Veneer	120

Table 3. Estimated Speed for Perforation of CMU Walls by 2x4 Timber Plank Missile (McDonald, 1990)

Wall Construction	Perforation Speed, mph
8-in CMU Wall	
Grout and rebar in every cell	>130[1]
Grout only in every cell	>130[2]
Intermittent vertical reinforcement	65[3]
Horizontal Joint Reinforcement Only	65[3]
Unreinforced	60
12-in. CMU Wall	
Grout and rebar in every cell	>130
Grout only in every cell	>130
Intermittent vertical reinforcement	70[3]
Horizontal Joint Reinforcement Only	70[3]
Unreinforced	65

[1]Missile will splinter.

[2]Missile will not perforate, but wall may crack.

[3]Face shell of ungrouted cell will be perforated.

Table 4. Results of 3-in. Diameter Steel Pipe Impact Tests

Panel Description	Impact speed, mph	Damage
6-in. reinforced concrete panels	35	Small cracks, no perforation or scabbing
8-in. reinforced concrete panels	50	Small cracks, no perforation or scabbing
9-in. reinforced concrete panel	50	No cracks, perforation or scabbing
9-in. reinforced concrete panel	75	Radial cracks on back face, 1 1/2-in. penetration, impending scabbing
10-in. reinforced concrete panel	75	No significant cracks, perforation or scabbing
8-in. CMU panel with vertical cells reinforced and grouted	50	Missile perforated panel; 7.5 lb pieces came off back face
12-in. CMU panel with vertical cells reinforced and grouted	60	Cracks on front and back face; impact speed near threshold for scabbing

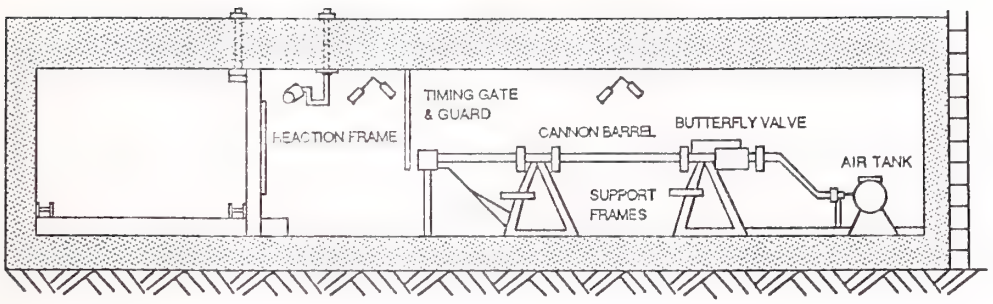

Figure 1. Elevation View of Tornado Missile Impact Facility

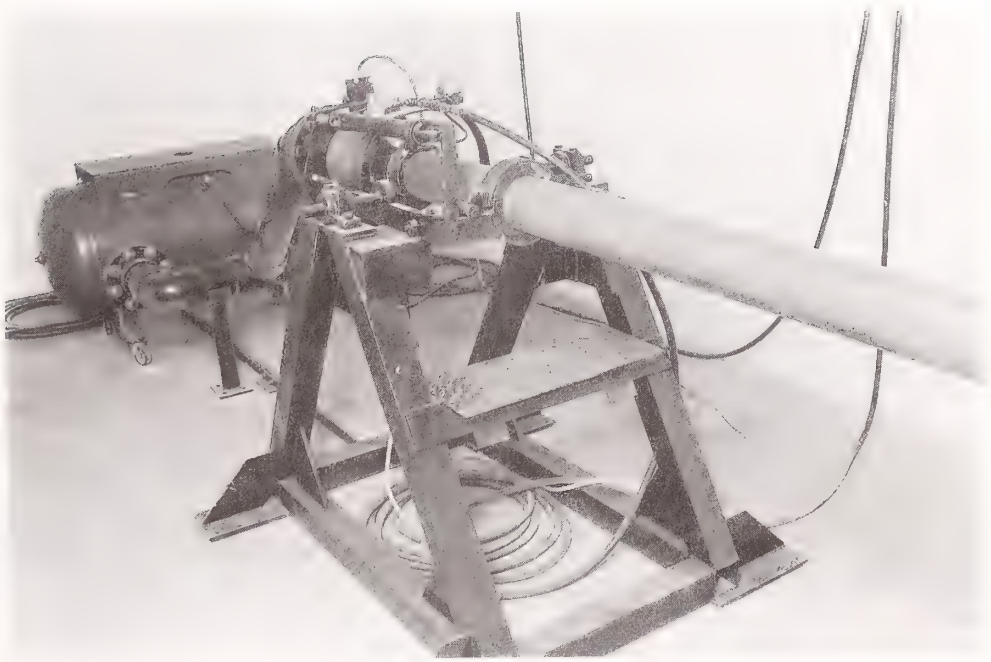

Figure 2. Tornado Missile Cannon

Advances in Wood Engineering and Construction Research

by

Erwin L. Schaffer[1]

ABSTRACT

The Forest Products Laboratory has served the public for nearly 80 years and will continue to serve by providing information on wood-based material properties and advice on how to apply this information to structural products. The audience is broad and our national and international cooperators are many. We welcome your requests for assistance and stand ready to provide help through our many media. The examples of research we've collaborated in over the last 10 to 15 years illustrate that we care about the efficient use of our timber resource and the world's resource, while promoting the durability, economy, and safety of wood products in construction.

KEYWORDS: construction; engineering; design stress; fire endurance; wood assembly.

1. INTRODUCTION

The Forest Service of the U.S. Department of Agriculture supports the largest, most comprehensive forestry research program in the world. The research for utilization of timber—from conversion to lumber and other forest products to recommendations for efficient use in construction—has been focused at the Forest Products Laboratory (FPL) in Madison, Wisconsin, since its establishment in 1910.

Because timber testing was recognized early as both an industrial engineering problem and an important aspect of forest management, the brand-new FPL found its fund of knowledge in engineering already well established. Researchers concentrated on the fundamental problems of determining the mechanical properties of wood and wood products. They evaluated the effects of fire, drying, and preservatives on mechanical properties, and prepared lumber grading rules. Efforts in characterizing the strength properties of structural timbers led to one of the earliest ASTM standards for grading structural timbers. Broadening of the species base in wood utilization by FPL also had a strong and favorable impact on national forest management.

Researchers in the 1920s developed the equipment for testing large structural members, expanding FPL's ability to develop design data for wooden columns used in buildings, bridges, and other such structures.

Large-scale construction research was successful in the design and economics of the laminated arch in the 1930s. Exhaustive screening of appropriate fasteners and joint configurations provided the basis for modern industry standards. The broad public need for information on the engineering properties of wood and FPL's wealth of knowledge complemented each other in the publication of the first edition of the *Wood Handbook* in 1935.

---

[1]Assistant Director, Wood Products Research, USDA Forest Service, Forest Products Laboratory, Madison, Wisconsin 53705-2398. The Forest Products Laboratory is maintained in cooperation with the University of Wisconsin. This article was written and prepared by U.S. Government employees on official time, and it is therefore in the public domain and not subject to copyright.

Expanded fire-testing facilities and the development of the "stressed-skin" or sandwich panel principle, prefabricated wall units, and improved moisture barriers were also part of FPL's contribution in the 1930s. When World War II broke out, FPL engineers sought improved materials and construction for aircraft—first assessing alternate solid-wood species, then experimenting with the Lab's "sandwich" construction. Laminated product strength testing helped fill the need for ship timbers and other military structures.

After the war, renewed research by FPL in housing showed that lighter framing could conserve wood and still meet performance standards. Those principles were supported by a definitive book on construction techniques for the homebuilder. Engineers at FPL developed a series of plans for more affordable housing and studied earthquake and tornado damage to better understand a building's response to natural forces.

As homeowners of the 1970s increased their awareness of ecological concerns and the need for energy conservation, FPL responded with guidelines for thermal insulation, moisture and noise control, and renovation and remodeling techniques. The concerns of economy, strength, and speed in new construction were met in the Truss-Framed System, a prefabricated system suitable for framing houses and small commercial buildings.

In the 1980s, basic work in determining strength properties of members and systems continued, including the assessment of lumber grades and the effects of environmental conditions, loads, constructions, fasteners, and treatments. Building components are increasingly modelled and analyzed to help assess and meet performance standards. A structural test frame subjects an entire house to realistic loads that help measure the performance of materials and construction. Computer-aided modelling of structural behavior, moisture movement,and performance of wood members under fire exposure are opening new opportunities for rational analyses of entire building systems.

2. MEETING USER'S NEEDS

The Forest Products Laboratory has evidenced the ability to meet the needs of a variety of interests. The most popular view of FPL is the traditional one for any R + D laboratory—a producer and disseminator of research results. The FPL is this but much more! We serve a multitude of "users" via many media. Publications—from highly technical reports, to summary compendiums that integrate results in major areas of research, to popular articles for the journalistic press—are a key medium, but other less obvious media are sometimes tools as well (see Appendix).

Whom do we view as "users" of our research, and how do we serve them? Let's deal with answers to these simple questions to illustrate how we relate to our "audience" and might better serve them. Our real challenge is to "package" and "facilitate" the use of our research.

We've attempted to group our national and international research-users as follows:

User group	Specific users
General public	Consumers
Industry	Companies, associations
Legislative bodies	Federal, State
Regulatory groups	Code-making agencies Federal and State agencies
Standards' writers	ASTM, ANSI, ISO, DIN
Professional/Technical groups	ASCE, CIB, RILEM
Educators	Universities
Foresters	Federal, State, Private
Research peers	

As we develop our research planning and conduct, we identify whom we expect to "serve" by conducting the work and through what media we expect to transfer the results to the user. Technology transfer, therefore, is taken seriously as a responsibility of researchers. Of the users cited, providing research results to research peers solely to build a knowledge base is currently considered the weakest use of our resources.

Based upon this variety of users, what are the typical media employed for technology transfer in addition to publications? Media are as many and varied as user groups:

Presentations: Meetings of common interest groups, which provide unique opportunities to pass the word.

Advice: Inquiries or informal meetings regarding a common concern that draw information from completed research.

Committee Participation: Incorporation of research results into appropriate standards, guides, specifications, design criteria, etc.

Cooperation: Cooperation with users who would like to adopt results but require some assistance to do so.

Translation: Interpretation or modification of research results to allow ready adoption and use by educators, consumers, legislators, code-making agencies, and regulators.

Review: Examination of proposed guidelines prepared by others for consistency with completed research.

Extrapolation/Interpolation: Evaluation and guidance on extending research results to similar applications.

Reports: An opportunity for users to interact with researchers and benefit from all stages of research—from planning to performance through review of completed work.

All of these media reflect the variety of roles that FPL researchers satisfy appropriate to the need.

The FPL is a problem-solving R + D laboratory. The above media and users reflect the intense effort to generate useful information. We see ourselves as advisors only. We have no regulator or standards-writing authority, but we will provide assistance to those who have such authority. A typical example is our advisory function to the National Forest Products Association on design procedures, criteria, and procedures for setting allowable properties for structural lumber and fastenings that lead to the National Design Specification.

3. CODE IMPACTING RESEARCH

The Forest Products Laboratory, as a member of the wood resource community, has a long history of providing guidance, solving problems, and generating new concepts and products that have had an impact on codes and standards. Some wood engineering research and technology transfer activity over the last 10 years should be of special interest to this Pacific Rim Group. Following are examples of activities that have resulted in useful products, which may not be familiar to you. We hope that briefly describing the research and results will be informative as well as useful.

3.1 Truss-Framed System

The Truss-Framed System (TFS) is an innovative new building system for residential and light commercial construction. The system offers substantial savings in both materials costs and construction time, with improvement in structural durability and strength. The idea for TFS was conceived at FPL in the late

1970s to meet the need for less costly, high quality home construction.

The system's key structural component is a unitized floor-roof truss, which is joined together by regular wall studs and spaced at 24-in. (610-mm) intervals. The system is a marriage of factory and site-built construction. Trusses are fabricated in a plant under quality conditions and delivered prebuilt to the construction site, where they are erected by a small crew or with light mechanical equipment such as a crane or forklift (Fig. 1). The entire unitized frame is constructed from nominal 2- by 4-in. (38- by 89-mm) dimension lumber rather than the more expensive nominal 2- by 8-in. (38- by 191-mm) or 2- by 10-in. (38- by 184-mm) lumber used in conventionally designed homes (Fig. 2). Because the trusses can be designed to span the width of most homes, supports are not needed in the basement and load-bearing walls are not necessary on the first floor. Once connected with sheathing, the structurally engineered trusses create a strong and durable wood frame building (Fig. 3).

Truss framing was developed after field observations of building damage from high winds or earthquakes showed that roof-to-wall or wall-to-floor joints often failed before the structural members. These observations were confirmed by FPL full-scale house tests. Since the unitized frame assures structural continuity between the critical joints, TFS buildings are often sturdier than those constructed through conventional means.

The innovative system also requires about 30 percent less structural framing lumber than the conventional stick-built home. Because less on-site effort is needed to frame a structure, the average size home can usually be erected in a few hours. As a result, builders have reported savings of about 10 percent of the overall costs by using the TFS building technique.

Since January 1982, U.S. builders have used TFS to construct over 2,000 homes, apartments, and office buildings in 31 states. The TFS has been assigned a public patent and is available to anyone who wishes to use it. A TFS Construction Manual has been published by the National Association of Home Builders Research Foundation (1983) in cooperation with the Forest Products Laboratory. The manual includes sections on the design, detailing, and construction of TFS buildings.

3.2 Calculated Fire Endurance

To improve flexibility in structural wood design, efforts continue to develop models and design procedures for determining the fire endurance ratings of wood members and assemblies. Traditionally, the fire endurance rating has been obtained by testing the assembly in an ASTM E 119 (ASTM, 1983) test furnace. These ratings are published in listings such as the Underwriters Laboratories' *Fire Resistance Directory* (1986), Gypsum Association's *Fire Resistance Design Manual* (1984), and those in the model building codes. These listed ratings are limited to the actual assembly tested. As a result, designers are limited in the type of fire rated assembly that they can use. Modifications such as adding insulation, changing member size, changing or adding interior finish, or changing the spacing between members are generally not permitted. Extrapolation or interpolation of ratings to or for similar assemblies is often questionable. In recent years, two fire endurance design procedures for wood that allow greater flexibility have gained U.S. building code acceptance. Two code-approved calculation procedures have been advanced by the National Forest Products Association to predict fire endurance. These are (1) additive calculation procedure for walls and floors, and (2) procedure for design of 1-h fire-resistive exposed wood members (nominal ≥6 in. (140 mm). In

addition, other procedures have been proposed or are being developed.

The fire endurance of a wood member or assembly depends on the performance of its protective membranes (if any), the charring of the structural wood element, and the structural capacity of the remaining uncharred portions of the structural wood elements. Models have also been proposed for fire-exposed light-frame floor assemblies, fire-exposed glued-laminated beams, and fire-resistive coatings on wood. The first two models emphasize compatibility with reliability-based design for fire exposure performance.

3.2.1 Fire-Exposed Light-Frame Floor Assemblies

Woeste and Schaffer (1981) developed a model for time-to-failure of fire-exposed unprotected wood joist floor assemblies. Replicate ASTM E 119 (ASTM, 1983) tests were run to validate appropriate values for the critical parameters. The model has been extended to floor-truss assemblies. Figures 4 and 5 show how the truss assembly is designed and how time to failure of unprotected truss assemblies theoretically varies with applied load. This model is used as part of a second-moment reliability analysis of the floor assemblies. In the future, reliability analysis will hopefully provide systematic and realistic evaluations of building fire safety.

3.2.2. Fire-Exposed Glued-Laminated Beam

A second approach to evaluating the fire endurance of a wood member is to assume the uncharred region consists of layers (Fig.6). The compressive and tensile strengths and modulus of elasticity of each layer are assumed to be fractions of the room temperature values. Using one 1.5-in. (38-mm) heated layer with reduced properties, Schaffer et al. (1986) analyzed a beam using transformed section analysis. This result was then used to calculate an equivalent zero-strength layer (δ) The δ was estimated to be 0.3 in. (7.6 mm) thick. This zero-strength layer (δ) was added to the char depth (βt) to obtain the total zero-strength layer. The rest of the member was then evaluated using room temperature property values.

Bender et al. (1985) developed a reliability-based model to predict the strength of glued-laminated beams under normal temperature conditions. Using the approach of a $\beta t + \delta$ zero-strength layer, they extended the model to include fire endurance analysis. The char rate (β) and thickness of the zero-strength layer (δ) are assumed to remain constant. The glued-laminated model uses transformed section analysis to determine the stresses within the laminates. In the fire endurance model, the char depth is increased at each time increment until the calculated stresses within the laminates exceed the corresponding tensile strength values. The critical moment permitted by lateral torsional buckling is also calculated. The results compare favorably with tests and allow both a mean time to failure and variability to be calculated. The method allows more flexibility in design for fire performance through the ability to control lumber quality to enhance fire endurance in fabrication of glued-laminated beams, and also provides a basis for reliability-based strength fire design.

3.2.3 Fire-Resistive Coatings

At this time, the fire endurance of wood members needs to be improved. The steel industry improves the fire endurance of steel members by covering them with fire-resistive materials or coatings. Fire-resistive coatings are not available for use on wood. Coatings available for wood are only designed to reduce flame spread. We evaluated the ability of fire-retardant coatings and fire-resistive coatings to improve the fire resistance of plywood

(Figs.7,8). Based on these small-scale tests (White, 1984), we developed empirical equations that can be used to determine the coating thickness needed to increase the time before a given char depth is obtained in the standard fire test. These equations can be combined with fire endurance models for a fire-exposed wood member or assembly to obtain the fire endurance rating of a fire-resistive coated wood member or assembly (White, 1986). Validation of these equations is underway.

3.3 Gypsum Wallboard Protected Wood Assemblies

The rate of heat release (HRR) is increasingly used to assess the overall contribution to fire growth of both individual materials and assemblies. Gypsum panel (0.6 in. (16 mm) thick) protected wall assemblies containing either wood members treated with fire retardants or steel members were exposed to fire using ASTM Method E 119 (1983). The purposes of the test were (1) to obtain additional information on the performance of fire-retardant-treated, wood-based structural assemblies exposed to fire and (2) to extend methods of measuring the rate of heat release in individual construction materials to full-scale structural assemblies.

The results of this study provide information about the fire performance of fire-retardant-treated wood assemblies in terms of HRR. At least 23 min elapsed from the start of the ASTM E 119 test to the time when wall assemblies containing treated wood began to contribute heat (Fig. 9). This result illustrates the effectiveness of gypsum wallboard and fire-retardant-treated studs in restricting contribution of heat from the assembly to fully developed fires within compartments. Two factors contribute to the substantial time delay in HRR: the thermal barrier effect of the gypsum wallboard and the fire-retardant treatment of the wood members. Heat contributions were in the range of up to 80 to 100 Btu/ft^2/min (15,128 to 18,910 W/m^2) near the end of the test. Average HRR values for the assemblies containing treated wood were 20 to 70 Btu/ft^2/min (3,782 to 13,237 W/m^2) over the active period of heat release.

Results of this study demonstrate that current methods used to measure HRR in individual construction materials can be extended to full-scale wall assemblies, and that protection of wood stud assemblies with gypsum wallboard can inhibit stud contribution to fully developed fires for 20 min or more.

3.4 Roof, Floor, and Wall Composite Action

Although the structural performance of a full-scale, light-frame house has not been well-understood, the low incidence of structural failures strongly indicates that the system has been at least adequate and even overbuilt. We have been developing methods to predict the structural characteristics of floor, wall, and roof systems individually. We also endeavor to describe how these components interact when assembled into a structure.

3.4.1 Floors

As a result of extensive research during the past decade, the structural performance of light-frame floors under uniform and concentrated loads is well understood. A comprehensive computer-based analysis program developed by researchers at Colorado State University (CSU) provides a model of the structural interaction of the floor joist, sheathing, and connectors. In a cooperative research project, CSU and FPL used this model to predict the performance characteristic of floors (McCutcheon et al., 1981; Vanderbilt et al., 1983). Research at FPL also showed that a different type of model can closely predict the deflection performance of floors and this model can be

easily adapted to microcomputers (McCutcheon, 1984). The modeled influence of 0.75-in. (19-mm) floor sheathing on assembly deflection as compared to 2 by 8 (38 by 191 mm) joists alone is illustrated in Fig. 10. The joists have high variability in their stiffnesses. As the sheathing bending modulus increases, the variation among joist deflections decreases. Note that much of the variability is eliminated by using a sheathing with a modulus of elasticity of 1×10^6 lb/in^2 (6.89 kPa), which is a realistic value for common floor sheathing materials. Further increases in sheathing stiffness have only a small effect. This example assumes no interaction between the joists and sheathing in the direction of the joist span. Additional work has been aimed at predicting the ultimate strength of floors (Wheat and Moody, 1984).

Most floor analysis has been aimed at predicting performance under stationary or static loads. However, some research indicates that the dynamic or impact performance of floors may often be the critical factor in consumer acceptance. Although some work in this area will soon be completed in Canada, the dynamic performance of floors needs to be better understood—particularly as new products capable of spans beyond the traditional 14- to 16-ft (4.3- to 4.9-m) lengths become more widely available.

3.4.2 Walls

Walls perform several distinct structural functions that require different types of analysis. In a racking or shear mode, walls serve to keep the structure square and prevent cascading failure of other walls ("dominoing"). Analytical methods to predict both the strength and stiffness performance of walls under shear loading take into consideration the nailing between sheathing and studs that provide shear rigidity (McCutcheon, 1985; Tuomi and McCutcheon, 1977). Recently, the significant contribution of gypsum board or "drywall" to the overall shear rigidity was quantified (Wolfe, 1983; Patton-Mallory et al., 1984). Racking loads of 0.5-in. (12.7-mm) gypsum-wallboard single-faced stud walls consistently are 1,100 lb (454 kg) at 0.5-in. (12.7-mm) deflection. Predicting and validating the combined effects of walls sheathed on both sides with dissimilar materials are proving useful to designers and code-making agencies (Patton-Mallory and McCutcheon, 1987).

One function of walls is to transmit roof and/or second-story loads to the foundation through axial loads in the studs. A second function is to resist the bending loads acting perpendicular to the surface. These two functions are satisfied by their combination in an analysis procedure developed by Oregon State University (OSU), which requires as input the properties of interior sheathings, exterior sheathings, studs, and fasteners to predict the strength and stiffness performance of light-frame wall systems. Cooperative work between OSU and FPL has yielded estimates of the effects of the major variables on wall performance (Polensek and Gromala, 1984).

Investigations of wall behavior, similar to research on floors, have primarily considered only static loads. However, dynamic loads produced by earthquake or wind gusts control wall performance in many parts of the United States (Soltis et al., 1981). Thus, new work is underway in the area of dynamic performance of walls under shear loading (e.g., Polensek, 1988).

3.4.3 Roof

The excellent performance of the residential pitched truss roof system confirms that this system adequately resists structural loads. These metal-plate-connected trusses are the most highly engineered component of the wood framing. However, design does not

take into account all the factors that influence overall structural performance of roof systems. An extensive research program at FPL has been underway to better characterize the performance of light-frame roof systems. The objective of the research is to develop a model, similar to the models used in floor and wall research, to predict the load distribution and deflection performance of roof systems (Moody, 1984).

Research on truss modeling has been updated with a modern analysis method for evaluating truss designs (Suddarth and Wolfe, 1984). Work is continuing to improve the methods of predicting the performance of trusses with metal plate connectors. Work reported by Wolfe et al. (1988) has substantially contributed to our understanding of load distribution and composite action in plywood roof sheathed metal-plate truss roof assemblies. The deflection prediction of load-carrying capacity and effect of repetitive members (trusses) on 24-in. (610-mm) centers were evaluated from five full-scale light-frame roof assemblies characteristics and compared to model predictions.

The actual deflection of the assembly is compared with that of loaded pitched trusses (3:12) alone in Fig. 11. This dramatically illustrates the benefit to stiffness of the assembly provided by the composite plywood sheathing-truss assembly compared to the trusses alone.

The distribution of load between adjacent trusses with load applied to one truss in an assembly (truss load influence matrix) is shown in Fig. 12. The National Design Specification currently sets allowed repetitive member increases for lumber joist design stress at 15 percent. This figure indicates that for load distribution from a stiff truss (truss 5) to a less stiff truss (truss 6), the repetitive load-sharing factor is 11/45 or 24 percent—substantially greater than the 15 percent now allowed for floor or roof joists! More detailed analyses and reports are in preparation. We are counting on these results to be used in the development of methodology for reliability-based design of truss roof assemblies.

3.4.4 Full Structure

To better understand the overall structural performance of the entire light-frame structure, investigators at FPL evaluated the structural performance of a conventional full-scale house during progressive stages of construction (Tuomi and McCutcheon, 1974). Wind loads and snow loads were simulated in a large structural test frame (Fig. 13). In wind-load simulation, plywood sheathing on the walls provided more than adequate racking resistance, probably far in excess of normal requirements. In fact, we were unable to really test the walls because the failures in tests first occurred in the connection between the loaded wall and the floor, and later at the connection to the foundation.

Commercially fabricated metal-plate-connected trusses on 24-in. (610-mm) centers were used for the roof system. Tests showed no evidence of distress in the roof system up to 2.5 times the design load. At this point, one member of one roof truss failed, but no collapse occurred. The trusses failed at more than three times the design load; had this been a snow load, the roof would have collapsed.

Of special interest is an assessment of three roof-to-wall plate connections in providing uplift resistance under extreme winds (Conner et al., 1987). The three nailed or nailed/lag-screw connections are shown in Fig. 14. The uplift withdrawal capacities of these connections were compared with probability distributions for occurrence likelihood of extreme winds. Figure 15 shows that 90 percent of severest wind speeds (tornadoes) fall below 157 mph, and a Type-H connection can be expected to

withstand from 110 to 180 mph. Type M appears sufficient for most windspeeds from 70 to 120 mph. Less effective is Type L. Thus, a reliable design for fasteners to withstand expected winds requires a full reliability-based analysis of fastener variability or a function of wind load. Also necessary is an assessment of duration of peak wind speeds to compensate for applying the duration of load factor to the connections.

3.5 Improved Lumber Properties and Design Procedures

Information is available for selecting construction lumber for various applications based on species and characteristics of wood. However, the assignment of strength properties covers a range of values, so selection is based on the lower end of the range. This often results in over-design for much of the material. Research has been conducted to determine the actual strength and stiffness of material as used in the field and how the duration of time loads applied affect the material.

3.5.1 Field Testing

For years, tests of small, clear wood specimens formed the basis for developing engineering stresses for lumber. However, evaluations in the 1970s indicated that this method is inadequate when lumber is used in highly engineered applications. Thus, a very extensive field testing program, called the "In-Grade Testing Program," was conducted in cooperation with representatives of the lumber industry during much of the 1980s (Green, 1983a,b). The program was completed in 1988. The major result of this extensive testing program is currently leading to new standards for assessing structural lumber properties. This will eventually lead to increased quality control and more efficient utilization of lumber when applied during the 1990s.

3.5.2 Duration of Load Adjustment Factor

Historically, a duration of load (DOL) adjustment factor has been used in design to account for a strength reduction of wood members after an elapsed time under load (Gerhards, 1977). The DOL adjustment factor (Fig. 16) is one of the primary factors used to determine allowable design stresses from clear wood strengths, and it has been obtained from bending tests on small clear specimens of only one species. The DOL adjustment factor has been extrapolated to all stress conditions, such as bending, compression, and tension, as well as to all grades, sizes, and species of structural lumber containing a wide range of strength-reducing characteristics. This method of extrapolation is being reassessed. The FPL is conducting an extensive research program in cooperation with the Forintek Corporation in Canada to establish DOL relations for lumber that include the effects of stress condition, species, grade, and size.

Results of the DOL study and of the In-Grade Testing Program will allow comprehensive redefinition of the engineering properties of lumber. The objectives of these study areas are to promote structural designs that use wood efficiently and to form a data-base for future reliability-based design codes.

3.6 Unified Behavior Model for Fasteners

Characterizing the strength of nailed and bolted joints, as previously noted, was among the early investigations conducted at FPL. T.R.C. Wilson initiated nailed joint behavior and design work in 1917. George W. Trayer was responsible for the early study on steel bolts in 1927. These and subsequent studies up to 1980, both at FPL and universities, were the basis for much of our understanding of mechanical joint behavior and for current design procedures and properties in the National Design Specifications. During the last 50 years, a

multitude of studies conducted globally have investigated one or more of the properties that affect connection behavior. Direct comparisons have been difficult because studies have usually differed in measuring more than one connection property or have been unique to the country conducting the tests. In addition, recent failures of bolted joints have raised doubts about our basic understanding of their behavior and the design criteria used.

A general "yield" theory for estimating the ultimate lateral load of nailed or bolted joint was developed by Johansen (1941) and confirmed by experiments in Europe (Aune and Patton-Mallory, 1986). The yield theory assumes the bearing capacity of a bolted or nailed connection is attained when either (1) the compressive strength of the wood beneath the bolt or nail shank is exceeded or (2) one or more yielding plastic "hinges" develop in the shank. A typical joint yield load curve as a function of length of bolt in the center member in a three-member joint is illustrated in Fig. 17. This curve is substantially more conservative for large bolts but more liberal for small bolts, as seen in Fig. 18.

The codes of several European countries (CIB 1983) have adopted allowable load-carrying capacities for bolted and nailed connections based upon this model. A series of studies have been conducted, and more are well underway, to validate yield model theory to design of joints typical in North America (e.g., Aune and Patton-Mallory, 1986; Soltis et al., 1986). Results to date continue to support the flexibility of the method and eventual endorsement of the procedure for assigning bolted and nailed joint properties and design criteria in the National Design Specification. We are grateful to European researchers for publicizing the technique and showing its attractive practical attributes.

4. REFERENCES

AITC (1984). "Calculation of fire resistance of glued laminated timbers." Tech. Note No. 7, American Institute of Timber Construction, Englewood, CO.

ASTM (1983). "Standard methods of fire tests of building construction and materials." ASTM Standard E 119-83, American Society for Testing and Materials, Philadelphia, PA.

Aune, P., and Patton-Mallory, M. (1986). "Lateral load-bearing capacity of nailed joints based upon yield theory." (1) Theoretical development. Res. Pap. FPL 469. (2) Experimental verification, Res. Pap. FPL 470. U.S. Department of Agriculture, Forest Service, Forest Products Laboratory, Madison, WI.

Baechler, R.H., and Gjovik, L.R. (1986). "Looking back at 75 years of research in wood preservation at the U.S. Forest Products Laboratory." In: Proceedings of American Wood-Preservers' Association, Vol. 82, pp. 133-149.

Bender, D.A., Woeste, F.E., Schaffer, E.L., and Marx, C.M. (1985). "Reliability formulation for the strength and fire endurance of glued-laminated beams." Res. Pap. FPL 460, U.S. Department of Agriculture, Forest Service, Forest Products Laboratory, Madison, WI.

Cassens, D.L., and Feist, W.C. (1986). "Finishing wood exteriors." Agric. Handb. 647, U.S. Department of Agriculture, Washington, DC.

CIB (1983). "Structural timber design code." CIB Rep. 66, Intl. Council for Building Research and Documentation, Rotterdam, The Netherlands.

Conner, H.W., Gromala, D.S., and Burgess, D.W. (1987). "Roof connections in houses: Key to wind resistance." J. Struc. Eng. 113(2): 2459-2474.

Forest Products Research Society (1983). "Wall and floor systems: Design and performance of light-frame structures." Proceedings No. 7317, Forest Products Research Society, Madison, WI."

Gerhards, C.C. (1977). "Effect of duration and rate of loading on strength of wood and wood-based materials." Res. Pap. FPL 283, U.S. Department of Agriculture, Forest Service, Forest Products Laboratory, Madison, WI.

Green, D.W. (1983a). "In-grade testing: Impetus for change in the utilization of structural lumber." In: Corcoran, T.V.; Gill, D.R., eds. Proceedings, Recent advances in spruce-fir utilization technology. Soc. Am. Forest. Pub. No. 83-13; Bethesda, MD.

Green, D.W. (1983b). "In-grade testing: Impetus for change in the utilization of structural lumber." Paper presented at the conference "From Stump Thru Mill—Recent Advances in Spruce-Fir Utilization Technology," August 17-19, University of Maine, Orono.

Gypsum Association (1984). Fire resistance design manual. 11th ed. Gypsum Association, Evanston, IL.

ICBO (1985). Uniform building code. International Conference of Building Officials, Whittier, CA.

Johansen, K.W. (1941). "Forsog med Traforbindelser." Danmarks Tekniske Medd No. 10 (in Danish), City Laboratoriet for bygningstekvik.

Lie, T.T. (1977). "A method for assessing the fire resistance of laminated timber beams and columns." Can. J. Civ. Eng. 4: 161-169.

McCutcheon, W.J. (1984). "Deflection of uniformly loaded floors: A beam-spring analog." Res. Pap. FPL 449, U.S. Department of Agriculture, Forest Service, Forest Products Laboratory, Madison, WI.

McCutcheon, W.J. (1985). "Racking deformation in wood shear walls." J. Struct. Eng. 111(2): 257-269.

McCutcheon, W.J., Vanderbilt, M.D., Goodman, J.R., and Criswell, M.E. (1981). "Wood joists floors: Effects of joist variability on floor stiffness." Res. Pap. FPL 405, U.S. Department of Agriculture, Forest Service, Forest Products Laboratory, Madison, WI.

Moody, R.C. (1984). "Improved analysis procedures for roof systems." Wood Truss Council of America. Woodwords. 2(8). 2 p.

Moody, R.C., and McCutcheon, W.J. (1985). "Sheathing properties and component performance in light-frame structures." In: Structural Wood Composites, Proceedings 7339, Forest Products Research Society, Madison, WI, pp. 93-99.

Moody, R.C., and Sherwood, G.E. (1986). "Light-frame construction research at USDA Forest Products Laboratory." A status report, Applied Engineering in Agriculture. 2(2): 167-173.

NAHBF (1983). "Truss-framed construction—A manual of basic practice." National Association of Home Builders Research Foundation, Rockville, MD.

National Evaluation Board (1984). "Design of one-hour fire-resistive exposed wood members (6-inch nominal or greater)." Report No. NRB-250, Council of American Building Officials.

Nelson, C.A. (1971). "History of the U.S. Forest Products Laboratory (1910-1963)." Forest Products Laboratory, Madison, WI.

Patton-Mallory, M., and McCutcheon, W.J. (1987). "Predicting racking performance of walls sheathed on both sides." Forest Prod. J. 37(9): 27-32.

Patton-Mallory, M., Gutkowski, R., and Soltis, L. (1984). "Racking performance of light-framed walls sheathed on two sides." Res. Pap. FPL 448, U.S. Department of Agriculture, Forest Service, Forest Products Laboratory, Madison, WI.

Polensek, A. (1988). "Effects of testing variables on damping and stiffness of nailed wood-to-sheathing joints." J. Testing Eval, Sept., American Society for Testing and Materials, Philadelphia, PA, pp. 474-480.

Polensek, A., and Gromala, D.S. (1984). "Probability distributions for wood walls." J. Struct. Eng. 11(3): 619-636.

River, B.H., and Gillespie, R.H. (1980). "Adhesives in building construction—past, present, and future." In: Proceedings. Adhesive and Sealant Council, Arlington, VA, pp. 31-42.

Schaefer, E.M., and Vanderbilt, M.D. (1983). "Comprehensive analysis methodology for wood floors." J. Struct. Eng. 109(7): 1680-1694.

Schaffer, E.L., and Woeste, F.E. (1981). "Reliability analysis of a fire-exposed unprotected floor truss." In: Proceedings, Metal Plate Wood Truss Conference, Forest Products Research Society, Madison, WI.

Schaffer, E.L., Marx, C.M., Bender, D.A., and Woeste, F.E. (1986). "Strength validation and fire endurance of glued-laminated timber beams." Res. Pap. FPL 467, U.S. Department of Agriculture, Forest Service, Forest Products Laboratory, Madison, WI.

Senft, J.F., Bendtsen, B.A., and Galligan, W.L. (1985). "Weak wood—fast grown tree make problem lumber." J. Forestry, August, pp. 477-484.

Sherwood, G.E. (1975). "New life for old dwellings: Appraisal and rehabilitation." Handbook No. 481, U.S. Department of Agriculture, Washington, DC.

Sherwood, G.E. (1983). "Condensation potential in high performance walls—cold winter climate." Res. Pap. FPL 433, U.S. Department of Agriculture, Forest Products Laboratory, Madison, WI.

Sherwood, G.E. (1985). "Condensation in high thermal performance walls—hot, humid summer climate." Res. Pap. FPL 455, U.S. Department of Agriculture, Forest Service, Forest Products Laboratory, Madison, WI.

Soltis, L., and Wilkinson, T.L. (1987). "Bolted-connection design." Gen. Tech. Rep. FPL-GTR-54, U.S. Department of Agriculture, Forest Service, Forest Products Laboratory, Madison, WI.

Soltis, L.A., Gromala, D.S., and Tuomi, R.L. (1981). "Seismic performance of low-rise wood buildings." In: Proceedings of symposium on seismic performance of low-rise buildings. Am. Soc. Civil Eng. pp. 78-91.

Soltis, L., Hubbard, F.K., and Wilkinson, T.L. (1986). "Bearing strength of bolted timber joints." ASCE J. Struct. Eng. 112(9): 2141-2154.

Southern Building Code Congress International, Inc. (1982). Standard Code, BOCA, Birmingham, AL.

Spelter, H., Maeglin, R., and LeVan, S. (1987). "Status of wood products use in nonresidential construction." Forest Prod. J. 37(1): 7-12.

Stroh, R. (1988). "Wood frame house construction." NAHB Research Foundation, Rockville, MD.

Suddarth, S. K., and Wolfe, R.W. (1984). "Purdue plane structures analyzer II: A computerized wood engineering system." Gen. Tech. Rep. FPL-GTR-40.

TenWolde, A., and Suleski, J.C. (1984). "Controlling moisture in houses." Solar Age, pp. 34-37.

Thompson, E.G., Vanderbilt, M.D., and Goodman, T.R. (1977). "FEAFLO: A program for the analysis of layered wood systems." Computers and Structures VII: 237-248.

Trayer, G.W. (1931). "The bearing strength of wood under bolts." Tech. Bull. 332, U.S. Department of Agriculture, Washington, DC.

Tuomi, R.L., and McCutcheon, W.J. (1974). "Testing of a full-scale house under simulated snowloads and windload." Res. Pap. FPL 284, U.S. Department of Agriculture, Forest Service, Forest Products Laboratory, Madison, WI.

Tuomi, R.L., and McCutcheon, W.J. (1977). "Predicting racking strength of light frame walls." ASCE J. Struct. Div. 104(ST7): 1131-1140.

Underwriters Laboratories, Inc. (1986). Fire resistance directory, Underwriters Laboratories, Inc., Northbrook, IL.

USDA Forest Service. Forest Products Laboratory. Clark C. Heritage Memorial Series on Wood.
(1981). Vol. I, Wood: Its structure and properties.
(1982). Vol. II, Wood as a structural material.
(1983). Vol. III, Adhesive bonding of wood and other structural materials.
(1986). Vol. IV, Wood: Engineering design concepts.
Materials Education Council, Pennsylvania State University, University Park, PA.

USDA Forest Service. (1986). "Wood Handbook: Wood as an engineering material." Ag. Handbook No. 72, Forest Products Laboratory.

Vanderbilt, M.D., Criswell, M.E., Bodig, J., Moody, R.C., and Gromala, D.S. (1983). "Stiffness and strength of uniformly loaded floors with in-grade lumber." Res. Pap. FPL 440, U.S. Department of Agriculture, Forest Service, Forest Products Laboratory, Madison, WI.

Wheat, D.L., and Moody, R.C. (1984). "Predicting the strength of wood-joist floors." Res. Pap. FPL 445, U.S. Department of Agriculture, Forest Service, Forest Products Laboratory, Madison, WI.

White, R.H. (1968). "Modern timber fire protection design." Structures Congress, American Society of Civil Engineers.

White, R.H., Schaffer, E.L., and Woeste, F.E. (1984). "Replicate fire endurance tests of an unprotected wood joist floor assembly." Wood Fiber Sci. 16(3): 374-390.

Woeste, F.E., and Schaffer, E.L. (1979). "Second moment reliability analysis of fire exposed wood joist floor assemblies" Fire and Materials 3(3): 126-131.

Woeste, F.E. and, Schaffer, E.L. (1981). "Reliability analysis of fire-exposed light-frame wood floor assemblies." Res. Pap. FPL 386, U.S. Department of Agriculture, Forest Service, Forest Products Laboratory, Madison, WI.

Wolfe, R.W. 1983. "Contribution of gypsum wallboard to racking resistance of light-frame walls." Res. Pap. FPL 439, U.S. Department of Agriculture, Forest Service, Forest Products Laboratory, Madison, WI.

Wolfe, R.W., LaBissoniere, T., and Cramer, S.M. (1988). "Performance tests of light-frame roof assemblies." In: Proceeding, International Timber Engineering Conference, Seattle, Forest Products Research Society, Madison, WI.

Zahn, J.J. (1977). "Reliability based design procedures for wood structures." Forest Prod. J. 27(3): 21-28.

FIGURE CAPTIONS

Figure 1. Construction of the truss-framed system (TFS) enables a small crew of laborers to frame an average house in only a few hours.

Figure 2. Unitized truss frames are fabricated in a plant to insure maximum quality control and material efficiency.

Figure 3. A simple TFS home after completion

Figure 4. Floor-truss design subjected to test conditions of ASTM E 119. Upper chord was loaded with tanks simulating a uniform load of 55.1 lb/ft^2 (269 kg/m^2) that resulted in a combined live and dead load of 60 lb/ft^2 (293 kg/m^2). 1 ft = 0.3048 m. 1 in. = 25.4 mm.

Figure 5. Relationship of applied load to time-to-failure for floor-truss assembly of Fig. 4.

Figure 6. Illustration of charring and effective residual sections for wood beams and columns.

Figure 7. Coated plywood sheathed stud wall section for fire-resistance test.

Figure 8. Example of intumescent coating for fire-resistance enhancement before and after fire exposure.

Figure 9. Heat release rate (HRR) levels from fire-retardant-treated wood-gypsum wallboard assemblies. 1 BTU/(ft^2 · min) = 189 W/m^2.

Figure 10. Sheathing acts as a beam spanning across floor joists and reduces the variability in floor deflection caused by variation in the stiffness of the floor joists. The floor deflection under uniform load is shown for four different sheathing stiffnesses. Note that the realistic sheathing stiffness of 1 x 10^6 lb/in^2 (6.89 kPa) greatly reduces the variability.

Figure 11. Assembly influence on truss deflection for Group I 3:12 assembly. Trusses individually loaded to their design load value outside the assembly show a larger average deflection as well as greater variability in deflection than when tested as part of an assembly loaded to the same design load value.

Figure 12. Truss load influence matrix. As each truss was loaded in the assembly, loads were distributed to other truss reactions as indicated. The number in each cell is the percentage of the total applied load measured at the reactions of the truss noted on the truss reaction axis. The height of the graphic in each cell is proportional to the load carried by that truss when only the "loaded truss" is loaded directly.

Figure 13. Structural loading frame and test house with partially complete roof.

Figure 14. Joint configurations: Connection details for low, medium, and high strength joints.

Figure 15. Velocity pressure as a function of wind speed with three joint capacities superimposed. 1 mph = 0.447 m/s; 1 psf (lb/ft^2) = 0.042 kg/m^2.

Figure 16. The "Madison" duration of load adjustment factor for design stresses.

Figure 17. Symbolic normalized joint yield load compared to l/d ratio for three-member joint with side members one-half thickness of center member and equal bolt-bearing strength.

Figure 18. Comparison of yield theory and Trayer's (1932) empirical results for (a) parallel-to-grain and (b) perpendicular-to-grain loading. Also included are Trayer's experimental results for Douglas-fir main member with steel side plates (□).

APPENDIX

Information About Publications Available from the USDA Forest Products Laboratory

The Forest Products Laboratory publishes a great number of reports and articles on various aspects of wood utilization and research. To facilitate acquisition, our reports are classified into publication lists. Periodic releases on new publications are provided during the year. Subject areas that may be of special interest are as follows:

Biodegradation and preservation of wood
Economics
Energy from wood
Finishing (exterior only)
Fire performance of wood
Particleboard and panel products
Veneer and plywood
Architects, builders, engineers, and lumber retailers

Detailed instructions for ordering publications in these areas are given in the publication list for each area. If you wish to be placed on our mailing list for one or more of the publication lists, please call or write

Current Information Office
Forest Products Laboratory
USDA Forest Service
One Gifford Pinchot Drive
Madison, WI 53705-2398
(608) 264-5637

Figure 1. Construction of the truss-framed system (TFS) enables a small crew of laborers to frame an average house in only a few hours.

Figure 2. Unitized truss frames are fabricated in a plant to insure maximum quality control and material efficiency.

Figure 3. A simple TFS home after completion

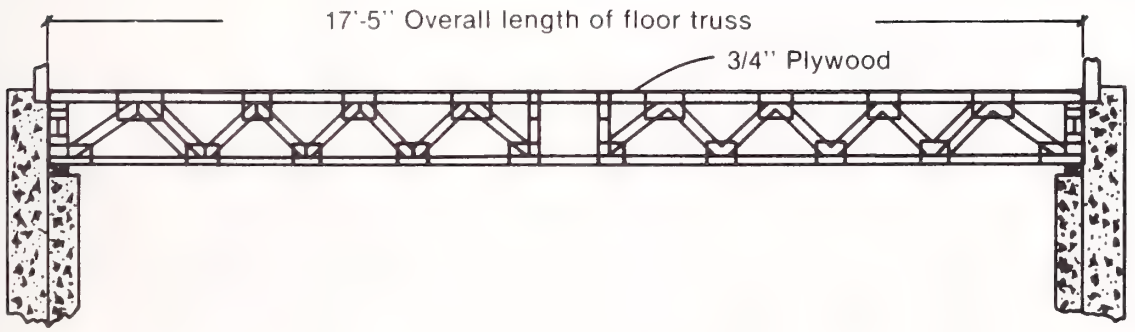

Figure 4. Floor-truss design subjected to test conditions of ASTM E 119. Upper chord was loaded with tanks simulating a uniform load of 55.1 lb/ft^2 (269 kg/m^2) that resulted in a combined live and dead load of 60 lb/ft^2 (293 kg/m^2). 1 ft = 0.3048 m. 1 in. = 25.4 mm.

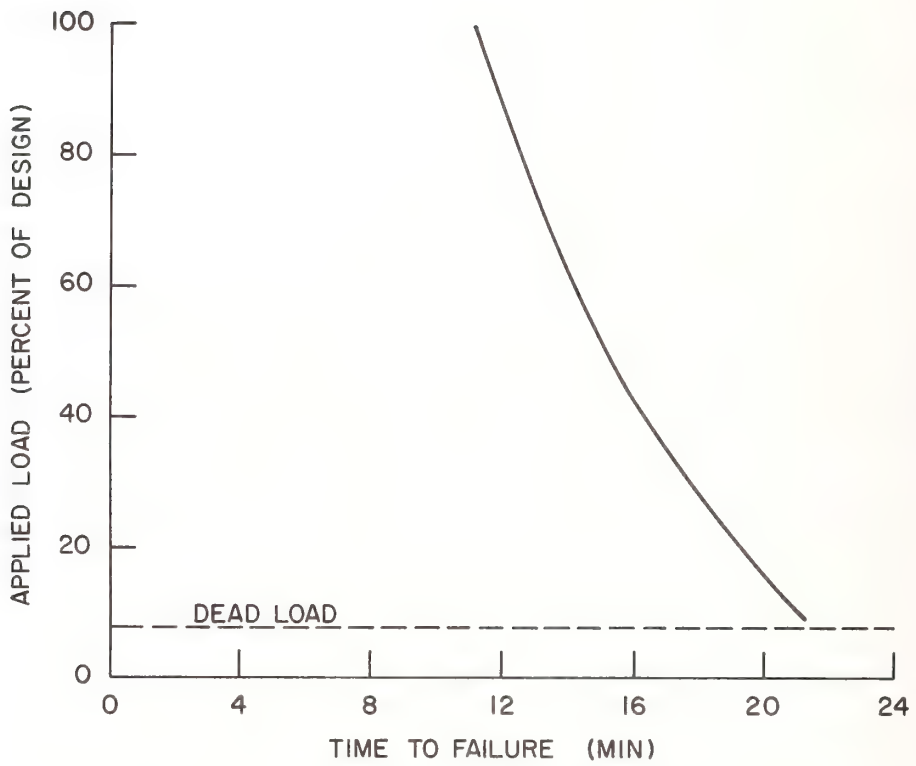

Figure 5. Relationship of applied load to time-to-failure for floor-truss assembly of Fig. 4.

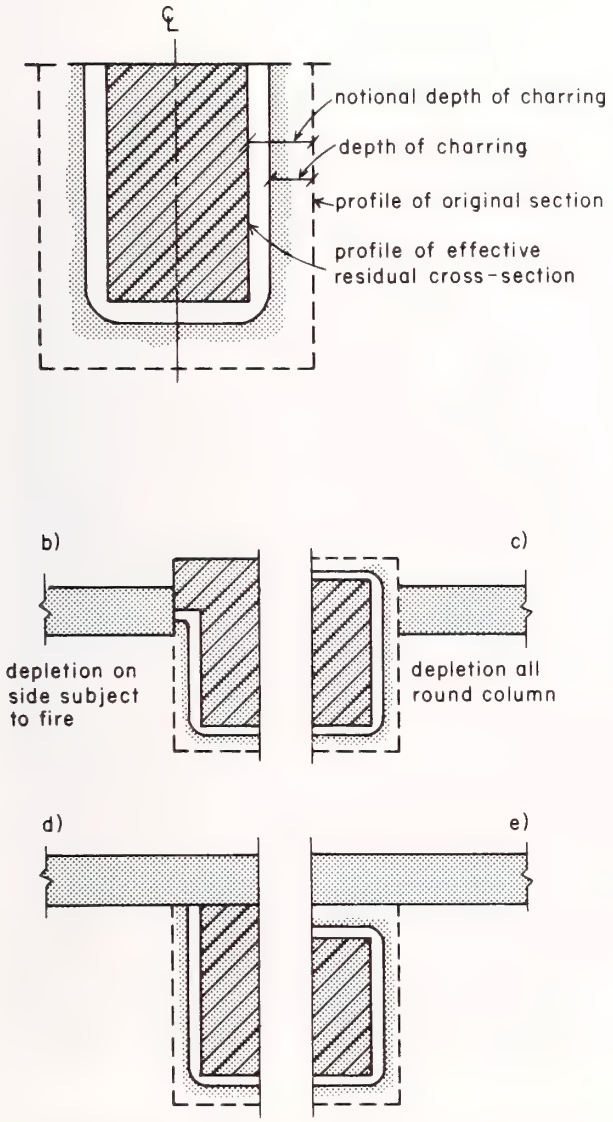

Figure 6. Illustration of charring and effective residual sections for wood beams and columns.

Figure 7. Coated plywood sheathed stud wall section for fire-resistance test.

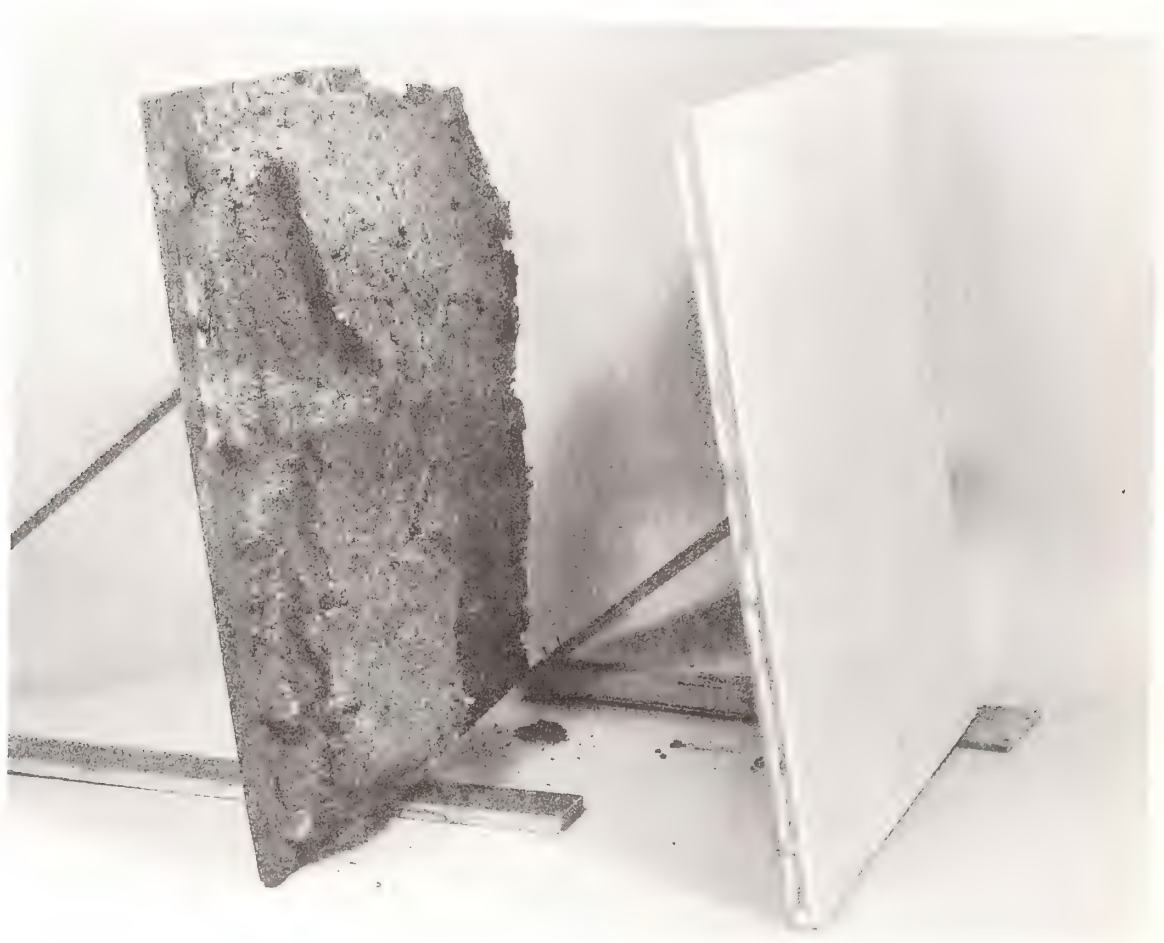

Figure 8. Example of intumescent coating for fire-resistance enhancement before and after fire exposure.

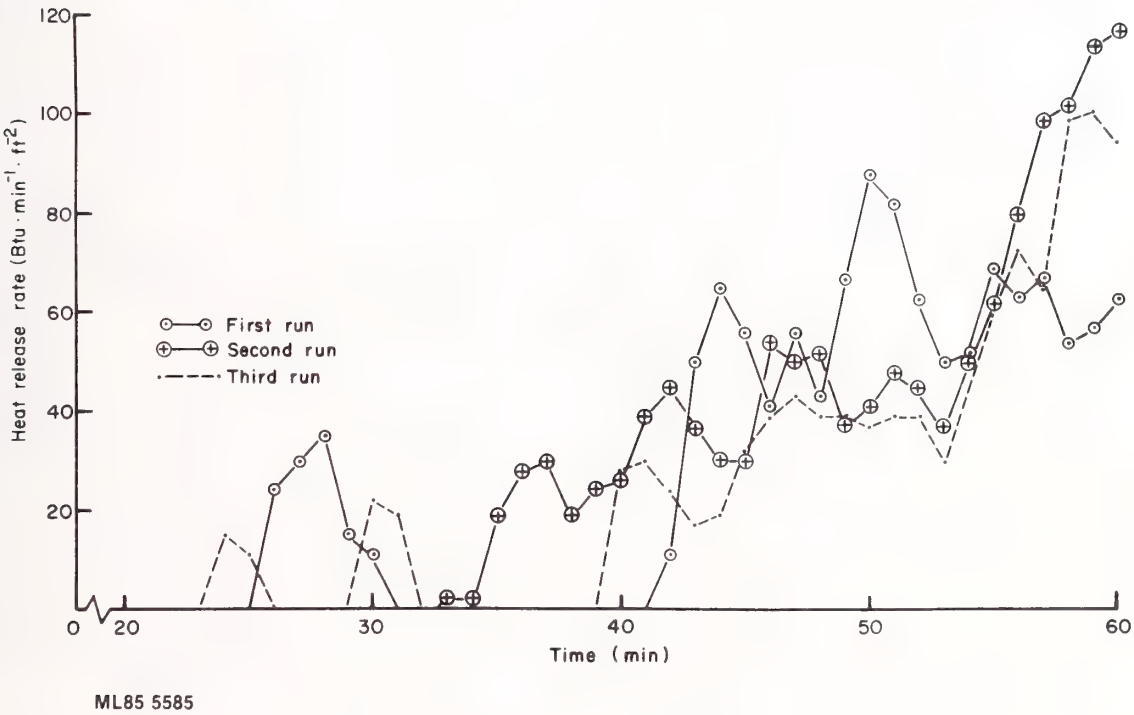

Figure 9. Heat release rate (HRR) levels from fire-retardant-treated wood-gypsum wallboard assemblies. 1 BTU/(ft^2 · min) = 189 W/m^2.

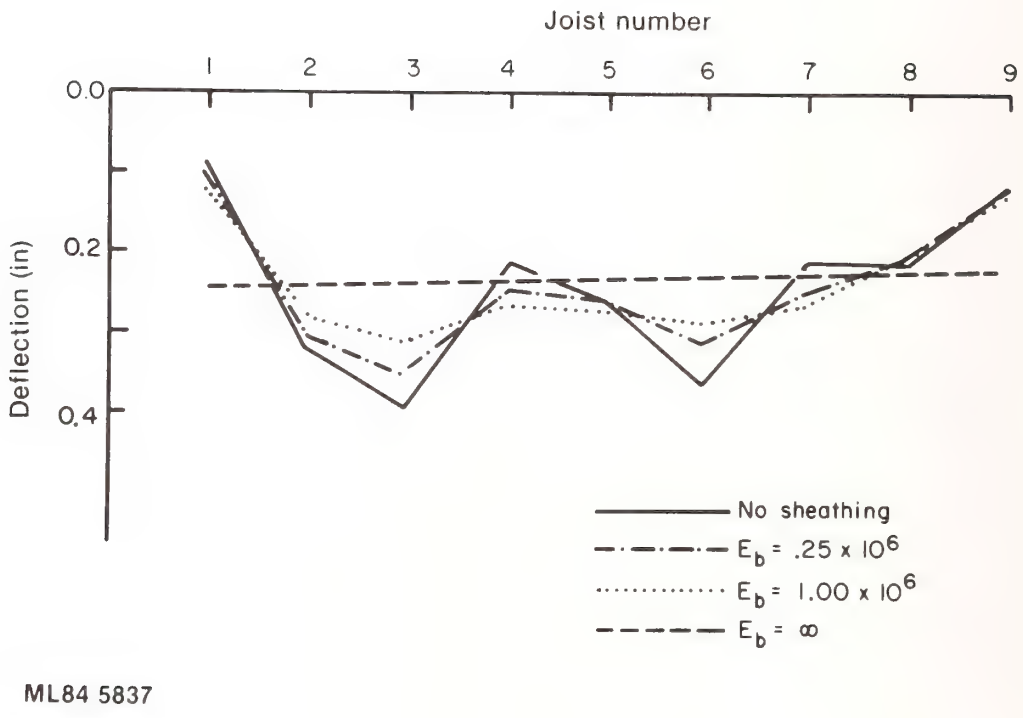

Figure 10. Sheathing acts as a beam spanning across floor joists and reduces the variability in floor deflection caused by variation in the stiffness of the floor joists. The floor deflection under uniform load is shown for four different sheathing stiffnesses. Note that the realistic sheathing stiffness of 1 x 10^6 lb/in^2 (6.89 kPa) greatly reduces the variability.

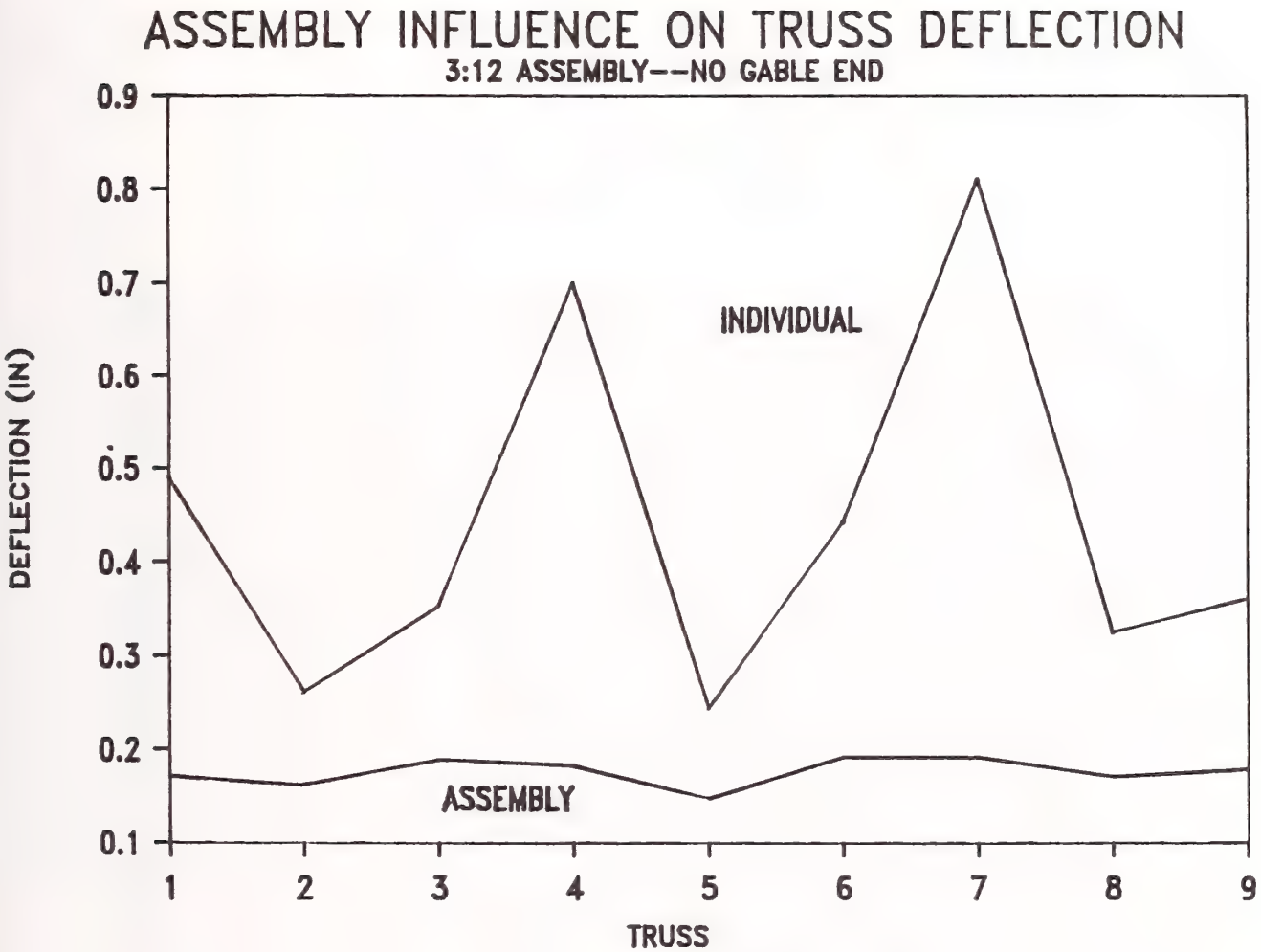

Figure 11. Assembly influence on truss deflection for Group I 3:12 assembly. Trusses individually loaded to their design load value outside the assembly show a larger average deflection as well as greater variability in deflection than when tested as part of an assembly loaded to the same design load value.

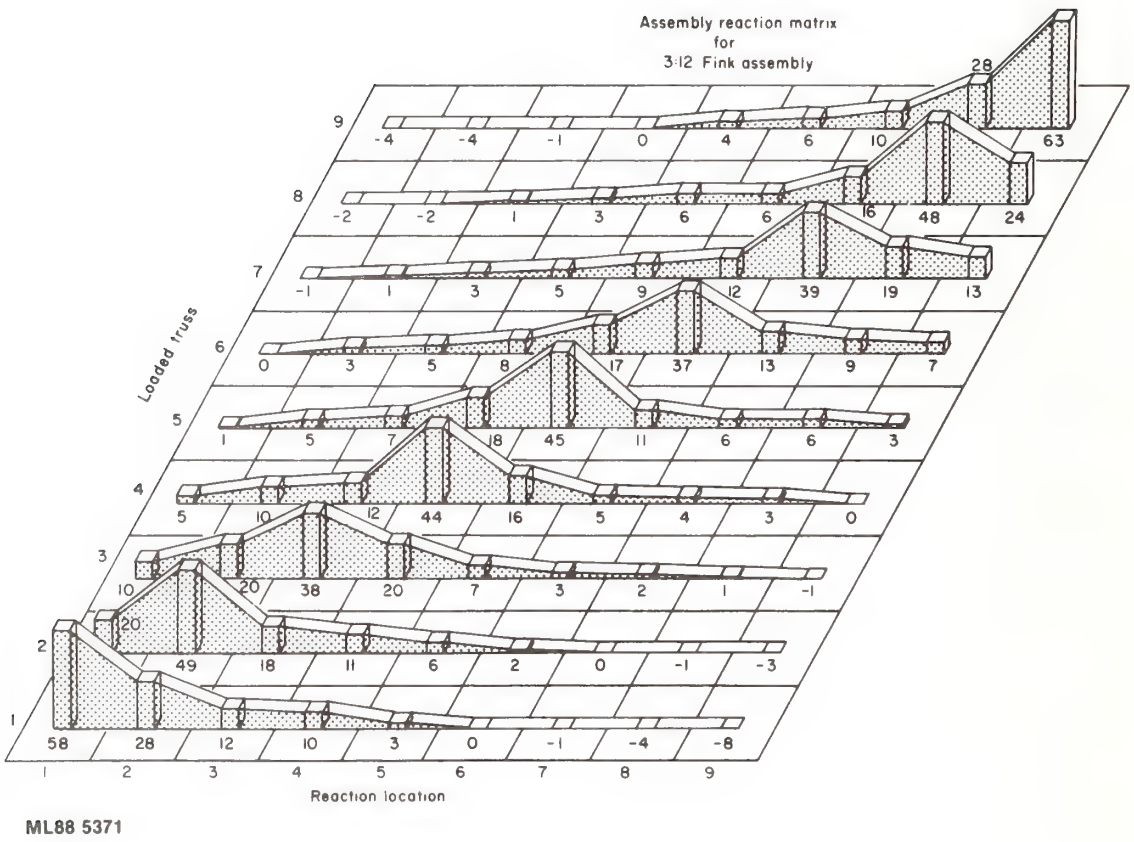

Figure 12. Truss load influence matrix. As each truss was loaded in the assembly, loads were distributed to other truss reactions as indicated. The number in each cell is the percentage of the total applied load measured at the reactions of the truss noted on the truss reaction axis. The height of the graphic in each cell is proportional to the load carried by that truss when only the "

Figure 13. Structural loading frame and test house with partially complete roof.

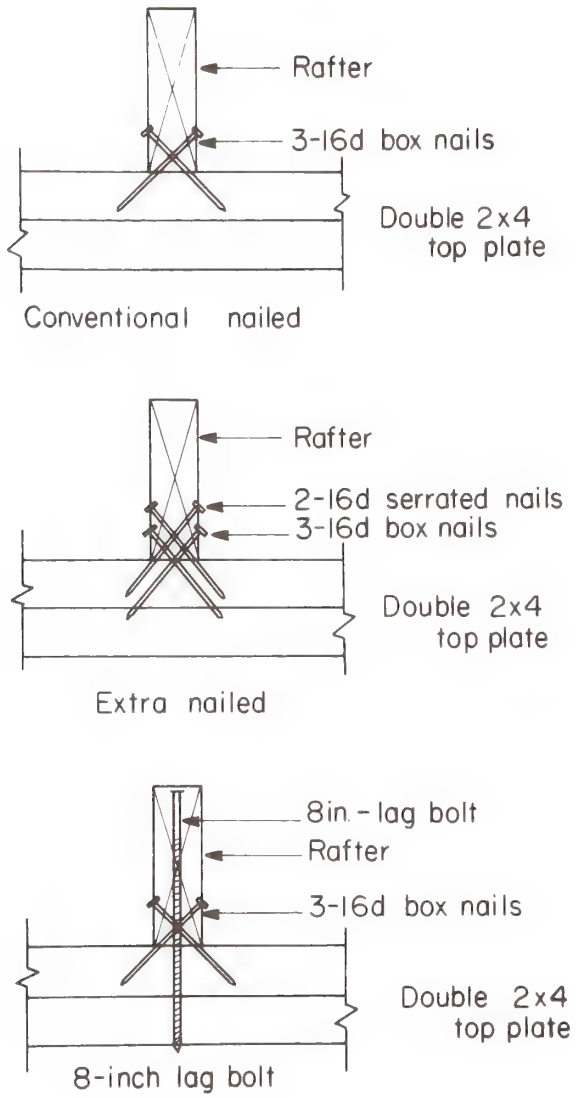

Figure 14. Joint configurations: Connection details for low, medium, and high strength joints.

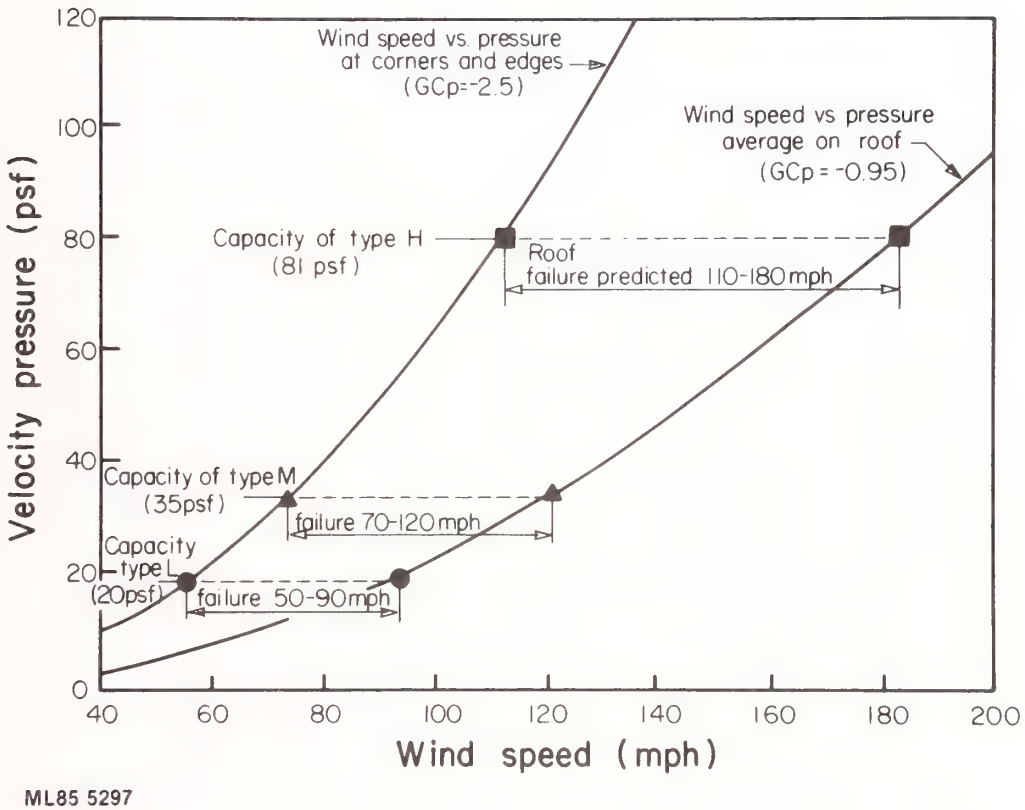

Figure 15. Velocity pressure as a function of wind speed with three joint capacities superimposed. 1 mph = 0.447 m/s; 1 psf (lb/ft^2) = 0.042 kg

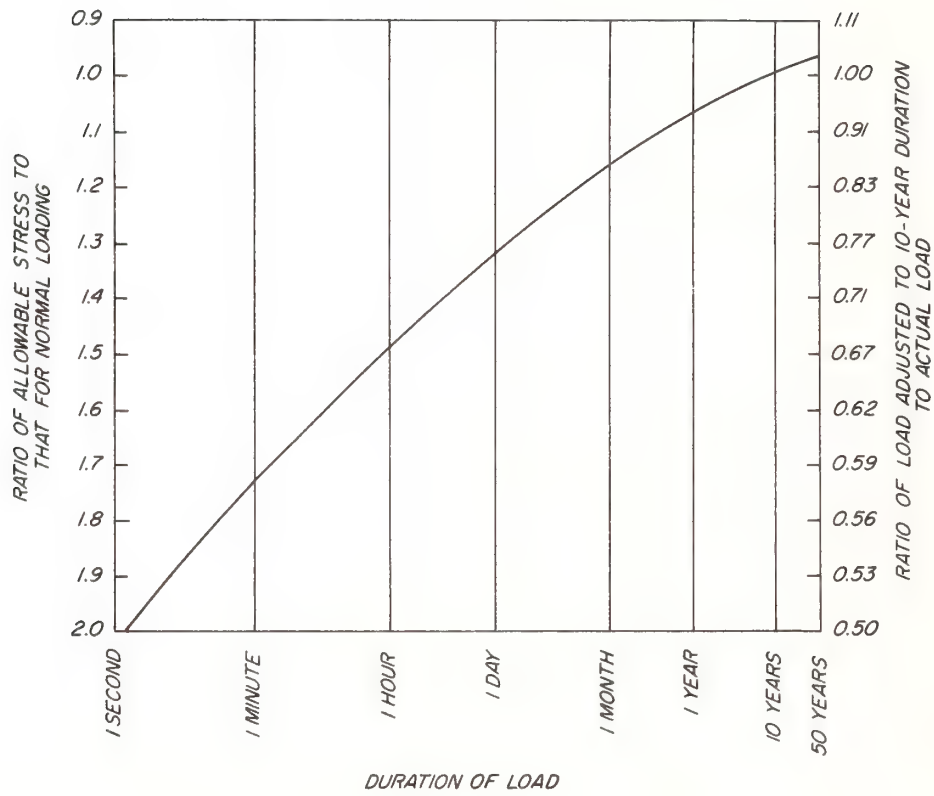

Figure 16. The "Madison" duration of load adjustment factor for design stresses.

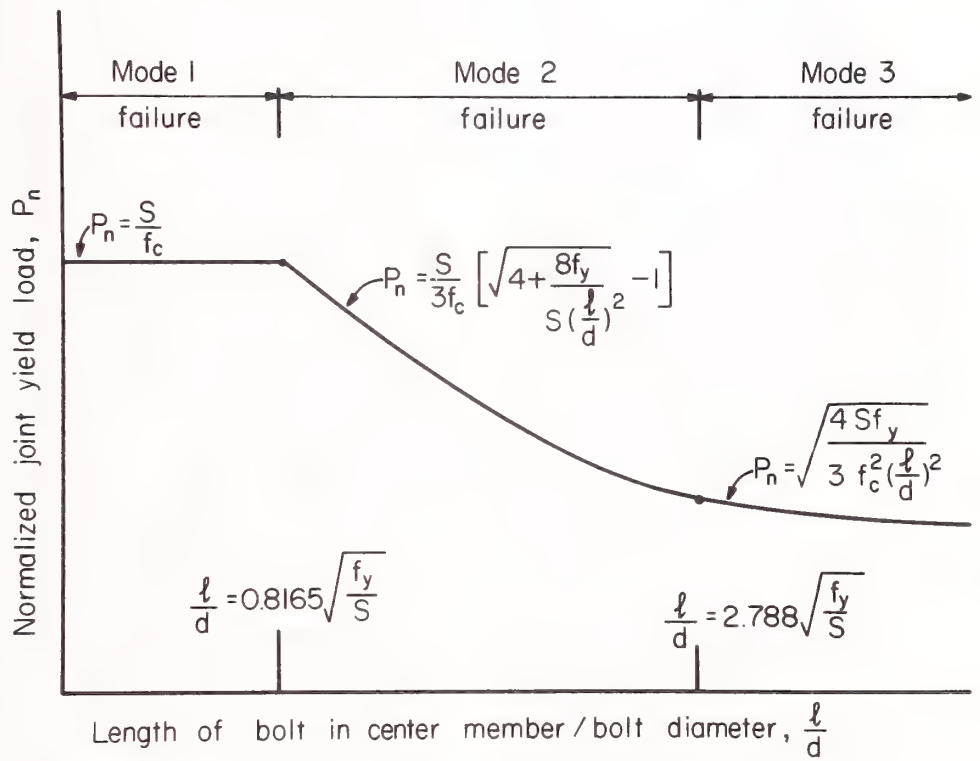

ML85 5515

Figure 17. Symbolic normalized joint yield load compared to l/d ratio for three-member joint with side members one-half thickness of center member and equal bolt-bearing strength.

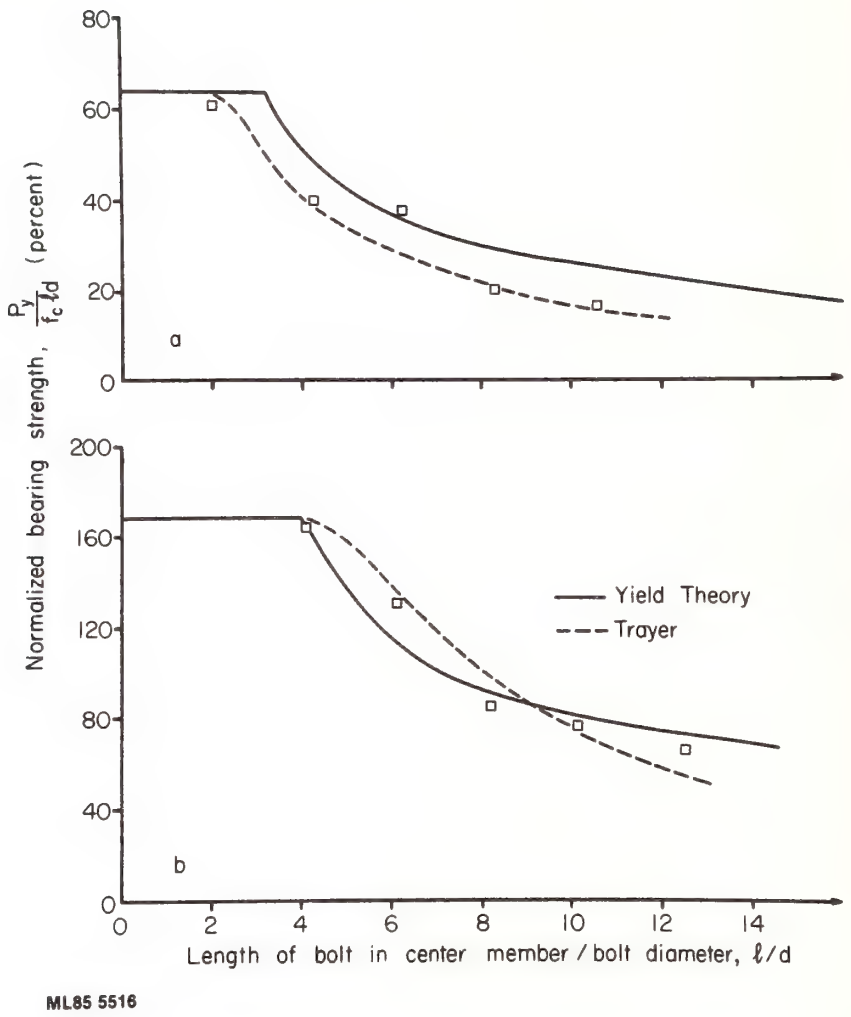

Figure 18. Comparison of yield theory and Trayer's (1932) empirical results for (a) parallel-to-grain and (b) perpendicular-to-grain loading. Also included are Trayer's experimental results for Douglas-fir main member with steel side plates (□).

The Impacts of Siting Lifelines in Close Proximity Upon Their Earthquake Vulnerability

by

William Bivens[a] and Phillip Lowe[b]

ABSTRACT

The Federal Emergency Management Agency (FEMA) has initiated a program to examine the potential increases in lifeline earthquake vulnerability due to their close placement or collocation. To date, the study has focused on developing a practical engineering approach that builds upon available data and analysis techniques for evaluating individual lifelines or lifeline components. The methods have been applied in California at the Cajon Pass, which is located north and east of Los Angeles. The site lifelines analyzed included: highways, railroads, and their bridges; natural gas bulk transmission pipelines; refined petroleum product transmission pipelines; high voltage electric power transmission lines; and fiber optic telephone communication lines. The San Andreas fault crosses at approximately the midpoint of the Cajon Pass canyon. During the study, improved methods to analyze the vulnerability of buried pipelines and bridges were developed. The study found that a fragmented regulatory control system, environmental concerns about disturbing the surface conditions, and the economics of right-of-way acquisition and lifeline construction led to over 100 separate lifeline collocations within the study area. Depending upon the lifeline, collocation impacts were estimated to increase the delay to restore lifeline temporary service from 20 to 60% compared to the restoration time if no collocation were assumed to exist. FEMA now intends to extend the study to examine other locations in the U.S. and to refine the analysis methods.

KEYWORDS: collocation, earthquake, damage, impacts, lifelines

1. INTRODUCTION

In the U.S., lifelines are presently being sited in "utility or transportation corridors" to reduce their right-of-way environmental, aesthetic, and cost impacts on the communities that rely upon them. The individual lifelines are usually designed, constructed, and modified throughout their service life. This results in different standards and siting criteria being applied to segments of the same lifeline, and also to different standards or siting criteria being applied to the separate lifelines systems within a single corridor. Presently, the siting review usually does not consider the impact of proximity or collocation of the lifelines on their individual risk or vulnerability to natural or manmade hazards or disasters.

There have been cases when some lifeline collocations have increased the levels of damage experienced during an accident or an earthquake. For example, water line ruptures during earthquakes have led to washouts which have caused foundation damage to nearby facilities. A transportation lifeline failure has led to the subsequent failure of a collocated fuel pipeline, and the resulting fire caused considerable property damage and loss of life. Loss of electric power has restricted, and sometimes failed, the ability to provide water and sewer services or emergency fire fighting capabilities.

In response to these types of situations, the Federal Emergency Management Agency (FEMA) is examining the use of such corridors, and FEMA has initiated a program to study the impact of siting multiple lifeline systems in confined and at-risk areas.

The overall FEMA project goals are to develop managerial tools that can be used to increase the understanding of the lifeline systems' vulnerabilities and to help identify potential mitigation approaches that could be used to reduce those vulnerabilities. Another program goal is to identify methods to enhance the transfer of the resulting information to lifeline system providers, designers, builders, managers, operators, users, and regulators.

In the initial project of this program[1], a screening tool was developed to identify the critical lifeline

---

[a]Federal Emergency Management Agency, Washington, DC 20472

[b]INTECH Inc, 11316 Rouen Dr., Potomac, MC 20854

collocation locations and the conditions that makes them critical. The probable time required to restore the lifeline service after an earthquake was used to measure the impact of collocation compared to an assumed no collocation situation.

The analysis methods were based on using existing data bases and lifeline vulnerability to earthquake evaluation methods so that a practical, engineering approach could be developed. During the study, improved methods to analyze buried lifelines and to account for soil liquefaction, as well as improved methods to analyze potential bridge vulnerability to an earthquake event were developed. The resulting analysis tools have been successfully applied to the lifelines sited at the Cajon Pass, California. These lifelines included: highways, railroads, and their bridges; natural gas bulk transmission pipelines; refined petroleum product transmission pipelines; high voltage electric power transmission lines; and fiber optic telephone communication lines.

2. CONCLUSIONS

A very useful screening tool has been developed. The tool can be used to identify the critical lifeline collocation locations and the conditions that make them critical. It can be used to identify areas of technical uncertainty and poor siting practices, and its use can identify important research and development opportunities.
At the Cajon Pass it was found that:

- ground movement due to landslides and liquefaction are more important than ground shaking for estimating the vulnerability of most lifelines. Bridges are the exception. For them, ground shaking can be a critical part of the estimation of their vulnerability;

- fuel pipeline failures had the greatest impact on other nearby lifelines during the immediate recovery period after an earthquake;

- current siting practices for fiber optic cables indicates that more severe telephone communication failures than have been experienced in past earthquakes can be anticipated in future earthquakes when fiber optic systems provide the basic telephone service (compared to the current hard wire systems);

- lifeline siting practices do not fully consider the potential impact that other nearby lifelines could have on the lifeline being evaluated;

- communication, electric power, and fuel pipeline lifelines can generally be analyzed as a set of discrete collocation points. The restoration of service at one location is generally not impacted by the restoration work at other collocation points, because the repair equipment and personnel can access the work site from a number of alternative paths. Thus, the critical restoration of service time is the longest time estimated for any one collocation point in those lifelines;

- transportation lifeline restoration of service is highly dependent on sequentially repairing the lifeline damage along the lifeline itself, as heavy equipment access to the next damage location often requires use of the transportation system itself;

- some collocation can produce benefits, as the nearby parallel location of a similar lifeline can provide the detour or access route to the damaged sections of the other lifeline. However, intersecting lifelines generally result in the failure of one lifeline increasing the risk of failure of the lifelines it crosses; and

- additional applications of the analysis methods are needed to assure that the results obtained are not in some way unique to the Cajon Pass and also to see if additional improvements in the analysis methods can be developed.

3. THE ANALYSIS METHODS

The analysis used a four Step approach: 1, data acquisition; 2, calculation of individual lifeline vulnerability; 3, calculation of collocation damage; and 4, interpretation of the collocation impacts on the individual lifeline systems.

3.1 Data Acquisition

In this step all the required information on the lifeline routes, methods of construction, materials of construction, location of the collocation points, collection of the topographic and geologic data, identification of probable landslide and liquefaction locations, performing an earthquake analysis to determine the location of the regions of constant Modified Mercalli Indices (MMI), and the plotting of the data with respect to the lifeline locations are performed. In the first application, the data was

input into a PC computer and analyzed and plotted using commercially available computer aided design (CAD) programs. The MMI isobars were developed using the methods of Evernden[2]. This method was used because it has been verified by comparison with historical earthquakes, it incorporates the local sediment conditions into the model and the sediment conditions are generally available in the U.S. Geological Survey geologic data base, it is easy to use, and it is readily available to other researchers. When this was performed for the Cajon Pass, 103 separate collocation locations that required further analysis were identified in the 220 square kilometer study area (approximately 90% of the collocation locations were found in a 65 square kilometer region along the foot of the Cajon canyon). A number of the lifelines were located in the expected fault zone of the San Andreas fault.

3.2. Calculation of Individual Lifeline Vulnerability

Damage matrices[3] were used to estimate the earthquake damage to each individual lifeline at each collocation point. The analysis was performed as if the lifeline were an isolated lifeline at that location. The damage matrices related the percent damage and the probability of that damage to the MMI index. The analysis also accounted for earthquake-induced landslides, and to a lessor extent earthquake-induced soil liquefaction. In the method applied at the Cajon Pass, improved damage matrices were developed for determining liquefaction impacts on buried lifelines[4]. In addition, an improved screening method to estimate the shaking damage to bridges was developed. It was based on adapting bridge retrofit requirements analysis methods developed by the California Department of Transportation[5].

The important items that are calculated for each lifeline at each collocation point are the estimated damage state (or percent damage) and the estimated time to restore the lifeline to the needed service level. Both of these parameters can be calculated using the matrices and tables of Rojahn[3].

3.3. Calculation of Collocation Damage

This analysis step builds upon the results obtained from the two previous Steps. A lifeline zone of physical influence was defined to describe the physical region in which one lifeline could impact other nearby lifelines. Then, based on the individual lifeline damages calculated in Step 3.2, and the zone of influence, a collocation damage scenario was defined. The damage matrices of step S.2 and the restoration of lifeline service tables of Step 3.2 were used to calculate the percent of damage and lifeline restoration of service time for each lifeline for the assumed collocation damage scenario.

One of the easier direct impacts to hypothesize is that the collocation conditions will lead to an increase in the damage state of one or both of the collocated lifelines (if there are more than two collocated lifelines this applies to all of them). It is easy to understand the damage state, as it relates to a physical condition. Because the individual lifeline damage states assuming no collocation are known, those values can be used to help understand how the lifeline could impact another nearby lifeline. If, for example, light damage of a pipeline had been calculated, it would be expected to cause no direct change in the damage state of a nearby bridge. However, if the bridge had been estimated to collapse, it would be reasonable to estimate that within the bridge's zone of influence it would lead to failure of the pipeline (this example also illustrates that the impacts are not necessarily reciprocal).

As another example of how collocation impacts on damage state can be estimated, consider the condition of a pipeline and a fiber optic conduit hung from a bridge. The earthquake vibration may not be enough to cause serious damage to the bridge or to the pipeline or conduit if they were not collocated with each other. However, the vibrations may cause the anchors holding the heavy pipeline to the bridge to fail. As the pipeline sags (but does not fail) it could fall onto the lower conduit, causing it to fail. The collocation damage state hypothesis would then be: no impact on the bridge; a small increase in damage state of the pipeline to account for the work required to rehang the pipeline; and catastrophic failure of the fiber optic conduit.

Special attention should be given to the collocation of fuel carrying lifelines with other lifelines that have the ability to provide an ignition source. The resulting fire and/or explosion could lead to significant collocation damage. Similarly, broken pipelines which eject fluids could lead to foundation erosion problems that would result in increased damage to nearby lifelines.

3.4. Interpreting the Collocation Impacts on the Individual Lifeline Systems

It was established that the most realistic measure of the impact of collocation was the "most probable incremental change in the restoration of service time" for each lifeline. This is defined as the product of the probability of the collocation damage occurring times the incremental increase in restoration of service time. The incremental increase in restoration of service time is the restoration time calculated for the collocation damage state minus the restoration time calculated for the lifeline at the same location but assuming no collocation existed.

There are several ways to estimate the change in the probability that damage will occur, none are exact and there are no statistics available from the literature on earthquakes. However, there are some insights available to guide the analysts.

If the probabilities for damage to two lifelines, assuming no collocation conditions, are P1 and P2, they represent an upper bound on the probability that a collocation damage would occur. For example, if the probability that lifeline 1 would fail is P1, and it is known that if lifeline 1 fails it will cause, with a 100% probability, damage to lifeline 2, then the probability that lifeline 2 receives collocation damage is also P1 (e.g., P1 x 100%). Similarly, the upper bound on the probability that lifeline 2 has damaged lifeline 1 is P2.

As a practical matter, the collocation damage likely will be less, since there is seldom a 100% chance that the collocation damage scenario will occur. A useful measure of the probability that the collocation event has occurred is the product of the two probabilities that the single independent events that were used to develop the collocation scenario have occurred (the independent events are the estimate of the damage state of each lifeline assuming there was no collocation). In the present case, that is found by multiplying P1 x P2. The product can be interpreted as follows. It represents the increase in probability that the two independent lifeline damages will occur during the same initiating event. If both events must occur before the collocation damage scenario can take place, then it is a measure of the probability of the collocation damage scenario.

The actual probability that the collocation event will occur should be a number between the numerical limits of P1 and (P1 x P2) for having lifeline 1 cause additional damage to lifeline 2, and P2 and (P2 x P1) for having lifeline 2 cause additional damage to lifeline 1. It is recommended that for calculational purposes, the product P1 x P2 be used to characterize the hypothesized collocation damage scenario.

4. REFERENCES

1. Lowe, P., et. al., "Collocation Impacts on the Vulnerability of Lifelines During Earthquakes With Application to the Cajon Pass, California," FEMA 226, February, 1992.

2. Evernden, J., et. al., "Interpretation of Seismic Intensity Data", Bulletin of the Seismological Society of America, V 63, 1973.

   Evernden, J., et. al., "Seismic Intensities of Earthquakes of Conterminous United States - Their Predictions and Interpretations", U.S. Geological Survey Professional Paper 1223, 1983.

3. Rojahn, C. and Sharpe, R., "Earthquake Damage Evaluation Data for California", ATC-13, Applied Technology Council, 1985.

4. See reference 1.

   Lowe, P., et. al., "A New Method to Relate Soil Liquefaction to Pipelines With Applications to Collocated Lifelines", Fourth US/Japan Workshop on Earthquake Resistant Design of Lifeline Facilities and Countermeasures Against Soil Liquefaction", Takai University, Honolulu, May 1992, also to be published as workshop proceedings by the National Center for Earthquake Engineering Research, NCEER.

5. Maroney, B. and Gates, J., "Seismic Risk Identification and Prioritization in the CALTRANS Seismic Retrofit Program", California Department of Transportation, September 1990.

   "CALTRANS Seismic Risk Algorithm for Bridge Structures", SASA Division of Structures, California Department of Transportation, June 30, 1990.

Nonlinear Research Needs for Concrete Gravity Dams

by

Robert L. Hall* and Wayne G. Johnson*

ABSTRACT

The Corps of Engineers' Engineer Technical Letter (ETL) 1110-2-303 outlines a sequence of analyses of concrete gravity dams subjected to the maximum credible earthquake (MCE). The first step is a two-dimensional linear-elastic response spectrum or time-history analysis with five percent damping. This analysis may include the effects of hydrodynamic loads, foundation flexibility, and absorption of the reservoir bottom (Chopra, 1978). For this step, five percent of critical viscous damping is assumed unless tensile stresses exceed fifteen percent of f'_c. If the tensile stresses exceed 0.15 X f'_c, adjustments are made in the damping to account for some cracking of the concrete. These different levels of damping combined with different concrete strengths are assumed to produce a conservative and appropriate procedure.

Nonlinear dynamic calculations were performed to evaluate guidelines of the ETL. The analyses revealed that existing tools generally produce reasonable results; however, the studies demonstrated the need for further development of nonlinear analysis tools. Limitations presently exist in the modeling and assumptions of material properties (Fenves, 1987), damping assumptions, and effects of water cavitation and intrusion into cracks (Dowling, 1987). To ensure the safety of concrete dams subjected to strong ground motions, further research is needed on nonlinear analysis methods and the corresponding parameters that govern these complex geometric and materially nonlinear models.

1. INTRODUCTION

The Corps presently supports the program SDAM (Cole and Cheek, 1988) and an acceleration-time-history program EAGD-84 (Fenves and Chopra, 1984) for the analyses of concrete gravity dams. These codes are supported through the numerical maintenance modeling program. Both codes assume linear-elastic material response and can be used to perform the seismic analyses according to procedures outlined in ETL 1110-2-303.

Mlakar (1986) evaluated the presently accepted procedure by performing a nonlinear analysis of three different dams of different heights subjected to two different earthquake records. The earthquake ground motions and the reservoir-structure dynamic interaction were modeled with the ADINA 84 finite-element code. For the cases investigated, the simpler analytic models seem to be conservative for evaluation of concrete gravity dams.

---

* US Army Engineer Waterways Experiment Station, Vicksburg, MS 39180-6199

However, the elastic procedures incorrectly located the region of maximum cracking (Mlakar, 1986).

Fenves (1987) evaluated this ETL by calculating the nonlinear response of the Pine Flat Dam subjected to a scaled horizontal Taft ground motion for five different load cases. These five load cases considered a full and empty reservoir and peak acceleration varying from 0.18 g to 0.45 g. The results demonstrated that cracks can form but remain stable under low amplitude ground motion; however, under large amplitude ground motion, Fenves found that the cracks propagate across the entire cross-section of the studied monolith.

2. DETAILED STUDIES

Mlakar's research was funded by the U.S. Corps of Engineers' Structural Research Program in order to evaluate the current ETL 1110-2-303. This evaluation was done by performing nonlinear analyses of three nonoverflow-gravity dam cross-sections which were selected to characterize the Corp's population of concrete gravity dams. The N65W and vertical components of the 1966 Parkfield, California earthquake recorded at Temblor No. 2 Station (CIT File Nos. B037-1 and B037-3) were used for each analysis. The records from this earthquake were chosen because the peak ground acceleration and frequency content are representative of strong ground motions. The nonlinear analyses were performed using the general purpose finite-element code ADINA. The constitutive behavior of the concrete was described by Bath and Ramaswamy (1979). The hydrodynamic loading of the reservoir was modeled by adding concentrated nodal masses on the upstream face corresponding to the distribution described by Chopra (1978). All foundations were assumed rigid.

The shortest section analyzed represented the Richard B. Russell Dam on the Savannah River. This structure is 185 ft high and has a modulus of elasticity of three million psi. The finite-element grid contains 65 elements and 247 nodes providing 594 degrees of freedom. The two-dimensional cross-section experienced no nonlinear behavior when subjected to the Parkfield ground motion. The ground motions were then tripled in order to determine the nonlinear response of this gravity dam. Figure 1 shows the cracked regions of the dam due to tripled Parkfield accelerations.

The second gravity dam modeled has a height of 300 ft, but it is not representative of any particular dam and is labeled "Standard Dam." The finite-element model for the dam consists of 594 degrees of freedom. The modulus of elasticity for the mass concrete was assumed to be three million psi. The ADINA analysis showed two cracked zones on the downstream surface at the elevation of slope change and at a slightly lower elevation (Figure 2). These cracks progress to the upstream surface. An examination of the ETL procedure for this situation reveals that no indication of cracking above the base of the dam would be realized.

The third dam analyzed was the Dworshack Dam on the Clearwater River in Idaho. This gravity dam is 638 ft high and it has an estimated modulus of elasticity of five million psi. This structure was chosen to represent the tallest dam owned by the Corps of Engineers. The finite-element model of this dam has 80 elements and 363 nodes with 726 degrees of freedom. The

nonlinear analysis indicates a cracked zone which transect the cross section of the elevation of change in downstream slope. Cracking also initiates at the upstream edge of the base and soon stabilizes (Figure 3). At later times the cracking propagates from the downstream face at the elevation of the slope change. The ETL procedure indicates that cracking is expected through the base of the structure.

Fenves performed a nonlinear seismic analysis of the tallest (400 ft) nonoverflow monolith of the Pine Flat Dam. The finite-element model of the structure consists of 162 nodes comprising 136 quadrilateral elements with a total of 315 degrees of freedom. The finite element model of the impounded reservoir water extends upstream 1,200 ft from the dam and consists of 224 constant-pressure elements. By modeling the reservoir, the analysis accounts for the interaction between the reservoir and dam. Stiffness proportional damping was used to provide five percent critical damping of the fundamental frequency and a modulus of elasticity of 3.25 million psi was used. The S69E component of the 1952 Taft ground motion was taken as a horizontal component acting in the upstream-downstream direction. The peak ground acceleration from these ground motions was 0.18 g.

When the reservoir was empty, the Taft ground motion had to be scaled up by a factor of 2.5 to an acceleration of 0.45 g in order to initiate cracking. However, when the reservoir was assumed full (381 ft), the nonlinear analysis indicates cracking from unscaled Taft ground motions. The cracking occurs at the head of the dam where a stress concentration exists because of the assumed rigid foundation. When ground motions were scaled to 0.27 g, cracks are shown to propagate further along the base. When ground motions were scaled to 0.36 g, cracking also occurs on the downstream slope where the change in the slope occurs. The extensive cracking led to a numerically unstable solution which indicates that stability analyses are needed. Figure 4 gives a summary of these results.

The ETL procedure was followed using the computer program EAGD-84. Five load cases were investigated for the Pine Flat Dam. Table 1 summarizes the five cases and results. For cases 1, 3, and 4 the maximum tensile stresses were less than 638 psi (.15 f'_c), so no cracking of the monolith was presumed. Cases 2 and 5 were performed again assuming 7-percent viscous damping which equates to 14-percent hysteretic damping (Table 2). Case 2 resulted in maximum tensile stress of 563 psi at the downstream face which exceeds 0.10 X f'_c and, according to the ETL, a crack should be assumed at two locations and sliding stability analyses performed for the portion of the dam above this plane. For Case 5, the 0.10 X f'_c criteria was exceeded on the upstream and downstream faces as well as at the heel. The ETL criteria again require stability analysis to be performed.

These nonlinear analyses clearly indicate the importance of the nonlinear response of the Pine Flat Dam to these ground motions. The ETL criteria appeared to be reasonably accurate for these five analyses. However, the procedure needs further investigation because there is no theoretical basis for assuming that tensile cracking results in increased energy

dissipation which is implied by greater damping ratios.

3. NONLINEAR RESEARCH NEEDS

The Panel on Earthquake Engineering for Concrete Dams Committee on Earthquake Engineering, Division of Hazard Mitigation, through the National Research Council has recently completed a publication entitled, "Earthquake Engineering for Concrete Dams: Design, Performance, and Research Needs" (NRC, 1990). This publication presents details for needed research in the nonlinear seismic response of concrete dams. The following are the items which should be addressed in future research programs:

3.1 Material Testing of Mass Concrete

Further testing of mass concrete under dynamic loads is needed. It is needed to determine tensile cracking of the mass concrete under multiaxial stress states which represent the in-situ strain paths in a concrete dam during a seismic event. These tests must quantify the effects of strain rates, concrete mixtures, and aggregate size. Concrete samples should be a mixture of cores from actual dams and carefully prepared laboratory samples.

3.2 Development of Materials Models for Concrete

Once the test data are available, realistic numerical models for tensile cracking under dynamic loads can be developed. These models must allow for multiaxial stress states, strain rate effects, shear transfer by aggregate interlock and criteria for tensile cracking and propagation of cracks. The studies must include smeared-crack approach, fracture mechanics principles, cracking-consistent damping, and the discrete-crack approach.

3.3 Modeling of Other Nonlinear Mechanisms

Since the limiting tensile strength of the concrete is across lift surfaces, it is important to develop construction joint models. These models will redistribute the forces across a joint as the two surfaces open and close. The degradation of the concrete across the joints must be modeled due to the damaging number of loading cycles from an earthquake.

3.4 Numerical Procedures for Computing Nonlinear Response

The numerical material and joint models can then be incorporated into a finite-element program with time integration for the equations of motion or other discretization methods for solving dynamic nonlinear equations. The procedures must also include interaction with the impounded water, flexible foundation rock, and the reservoir-bottom absorption. These procedures will need to be refined to take advantage of vector and parallel processes in the latest computers.

3.5 Parameters and Detailed Response Studies

With the development of accurate numerical procedures, parametric studies can be performed to determine the sensitivity of the nonlinear response to the parameter describing the nonlinear models. These studies would identify the significance of tensile cracking and joint opening with respect to either failure or dynamic response. Finally the following factors should be determined: effects of ground

motion characteristics, water compressibility, foundation flexibility, reservoir bottom absorption, and modeling issues.

3.6 Dynamic Testing of Dam Models

Testing of dam models is essential for verifying nonlinear numerical procedures. These tests may require association with international augmentation testing and use of facilities such as a large earthquake simulator recently installed at the research laboratory of the Ministry for Water Conservancy and Hydroelectric Power in Beijing, China.

3.7 Identification of Design Criteria

Accurate design criteria based on numerical and experimental studies could then be developed. Nonlinear seismic analysis may not become a standard practice in design but will certainly define the tensile strength of the structure and the post-cracking stability.

3.8 Investigation of Earthquake-Resistant Design Measures

These nonlinear capabilities will allow for the investigation of innovative measures for increasing the seismic safety of concrete gravity dams. These tools could be used to study effects in the geometry of dams, jointing schemes, and joint materials to dissipate energy.

4. CONCLUSION

Nonlinear capabilities are important in determining the seismic stability of concrete gravity dams. The capability to develop a complete program as described above is beyond single capability of the Corps of Engineers. However, the Corps can strategically utilize the research being performed through the National Science Foundation and other organizations to answer these complex issues and develop the necessary tools and criteria. Nonlinear analysis will provide the necessary insight for the development of reliable cost saving earthquake resistant designs.

5. ACKNOWLEDGMENT

Acknowledgment is made to Drs. Paul Mlakar and Gregory L. Fenves who conducted the analyses contained in this paper. The paper was prepared under the general supervision of Messrs. Bryant Mather, Chief, Structures Laboratory; and James T. Ballard, Assistant Chief, Structures Laboratory; and under the direct supervision of Dr. Jimmy P. Balsara, Chief, Structural Mechanics Division.

COL Larry B. Fulton, EN, was the Commander and Director of the U.S. Army Engineer Waterways Experiment Station during the preparation of this paper. Dr. Robert W. Whalin was Technical Director.

6. REFERENCES

1. Bathe, K. J. 1979. "On Three-Dimensional Nonlinear Analysis of Concrete Structures," Journal of Nuclear Engineering and Design, Vol 52, pp 385-409.

2. Chopra, A. K. 1978. "Earthquake Resistant Design of Concrete Gravity Dams," Journal of the Structural Division, American Society of Civil Engineers, Vol 104, No. ST6, pp 953-971.

3. Cole, R. A. and Cheek, J. B. 1985. "Seismic Analysis of

Gravity Dams," Technical Report SL-86-44, US Army Engineer Waterways Experiment Station, Vicksburg, MS.

4. Dowling, M. J. 1987. "Nonlinear Seismic Analysis of Arch Dams," Report No. EERL 87-03, Pasadena, CA.

5. Fenves, G. 1987. "Earthquake Induced Cracking in Concrete Gravity Dams," American Society of Civil Engineers.

6. Fenves, G. and Chopra, A. K. 1984. "EAGD-84, A Computer Program for Earthquake Analysis of Concrete Gravity Dams," Report No. UCB/EERC-84/11, Earthquake Engineering Research Center, University of California, Berkeley, CA.

7. Fenves, G. and Chopra, A. K. 1984. "Earthquake Analysis and Response of Concrete Gravity Dams," Report No. UCB/EERC-84/10, Earthquake Engineering Research Center, College of Engineering, University of California, Berkeley, CA.

8. Mlakar, P. F. 1986. "Nonlinear Response of Concrete Gravity Dams to Strong Earthquake-Induced Ground Motion," JAYCOR Report No. J650-86-002/1335, for the US Army Engineer Waterways Experiment Station, under Contract No. DACW39-85-M-4964.

9. National Research Council. 1990. Earthquake Engineering for Concrete Dams: Design, Performance, and Research Needs, National Academy Press, Washington, DC.

10. US Army Corps of Engineers, "Earthquake Analysis and Design of Concrete Gravity Dams," Engineer Technical Letter No. 1110-2-303, Washington, DC

Table 1. Maximum tensile stress in Pine Flat Dam due to scaled horizontal Taft ground motion from first linear dynamic analysis.

Case	Water	a_g	μ_f	Max. Stress (psi)		
				Up	Down	Heel
(1)	(2)	(3)	(4)	(5)	(6)	(7)
1	Empty	0.18	0.10	130	256	4
2	Empty	0.45	0.10	466	666	271
3	Full	0.18	0.10	217	250	361
4	Full	0.27	0.10	415	363	539
5	Full	0.36	0.10	510	580	718

Table 2. Maximum tensile stresses in Pine Flat Dam due to scaled horizontal Taft ground motion from second linear dynamic analysis.

Case	Water	a_g	μ_f	Max. Stress (psi)		
				Up	Down	Heel
(1)	(2)	(3)	(4)	(5)	(6)	(7)
1	Empty	0.18	---	---	---	---
2	Empty	0.45	0.14	383	563	198
3	Full	0.18	---	---	---	---
4	Full	0.27	---	---	---	---
5	Full	0.36	0.14	459	479	642

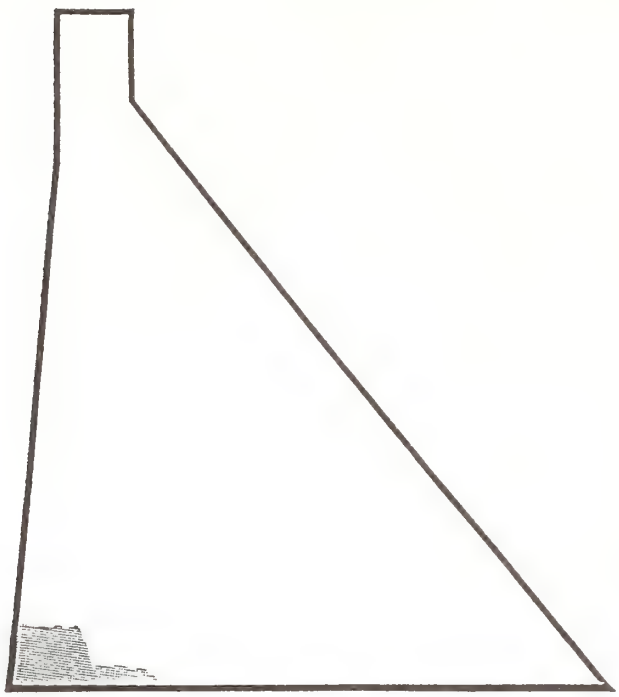

(a) t = 3.84 sec.

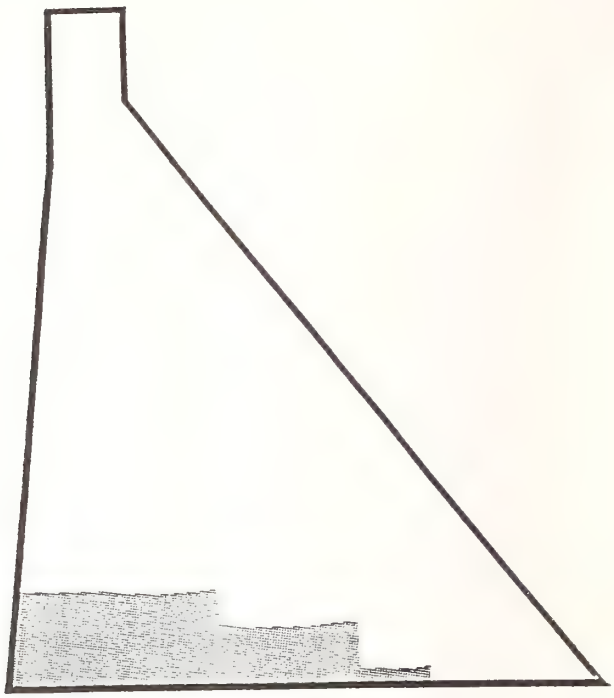

(b) t = 3.92 sec.

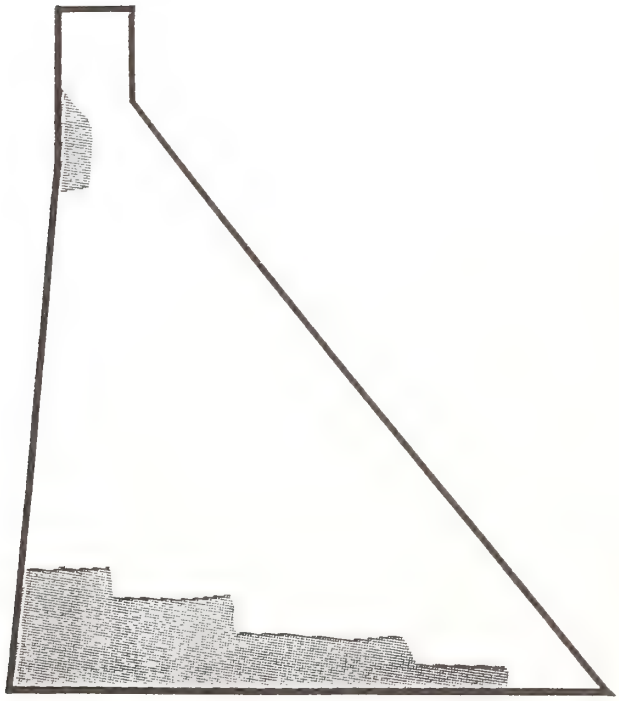

(c) t = 4.02 sec.

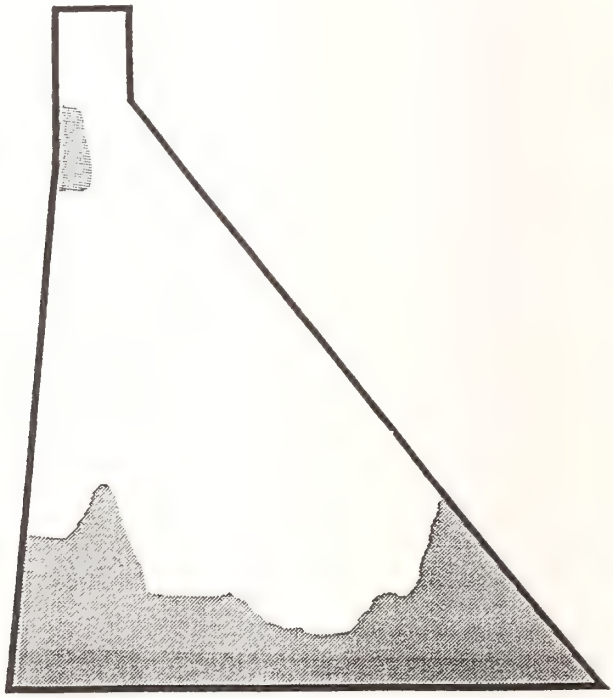

(d) t = 4.04 sec.

Figure 1. Cracked zones of Russell Dam with tripled Parkfield loading.

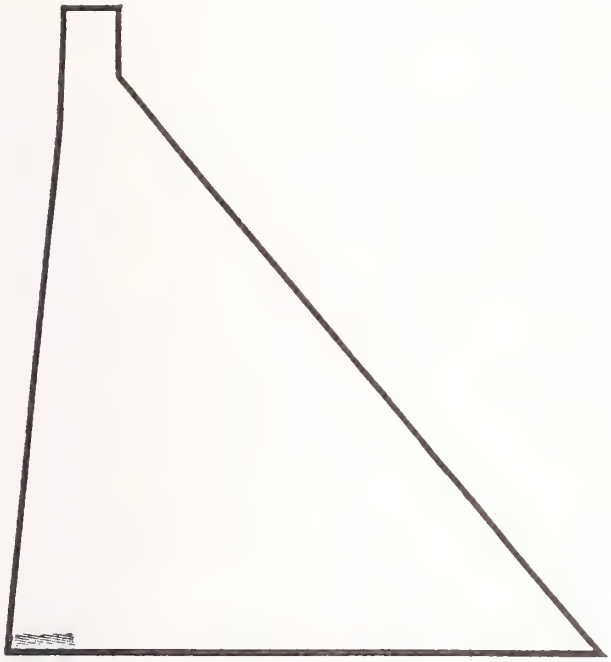

(a) t = 4.00 sec.

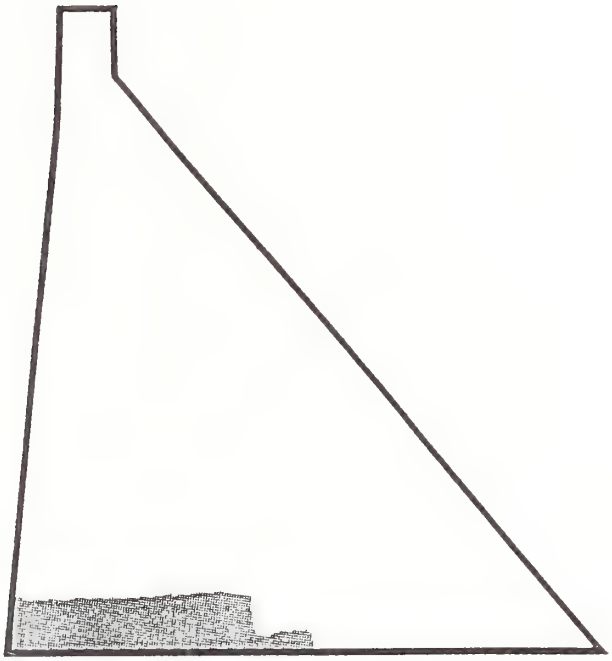

(b) t = 4.40 sec.

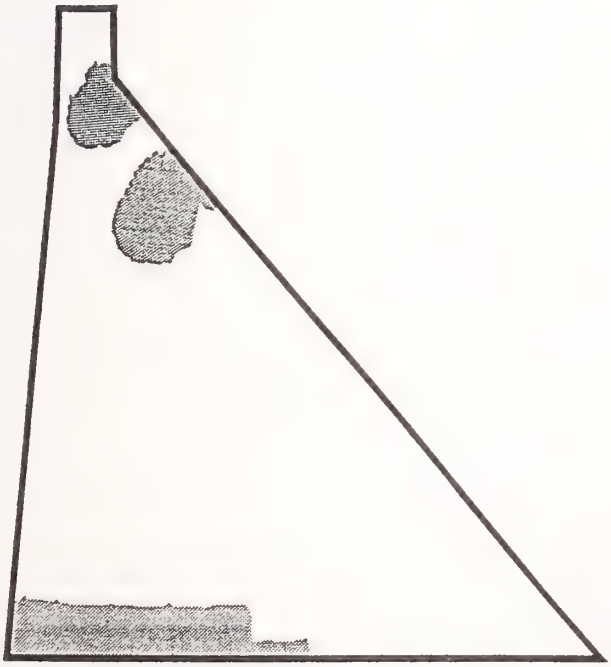

(c) t = 4.48 sec.

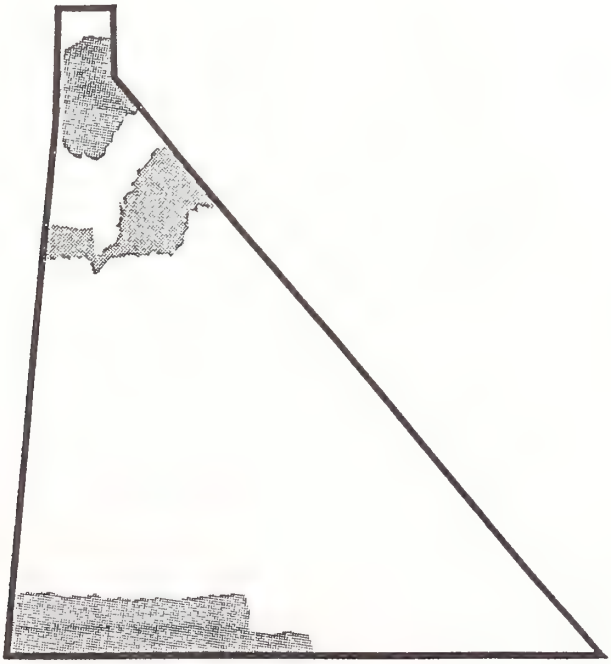

(d) t = 4.56 sec.

Figure 2. Cracked zones of Standard Dam.

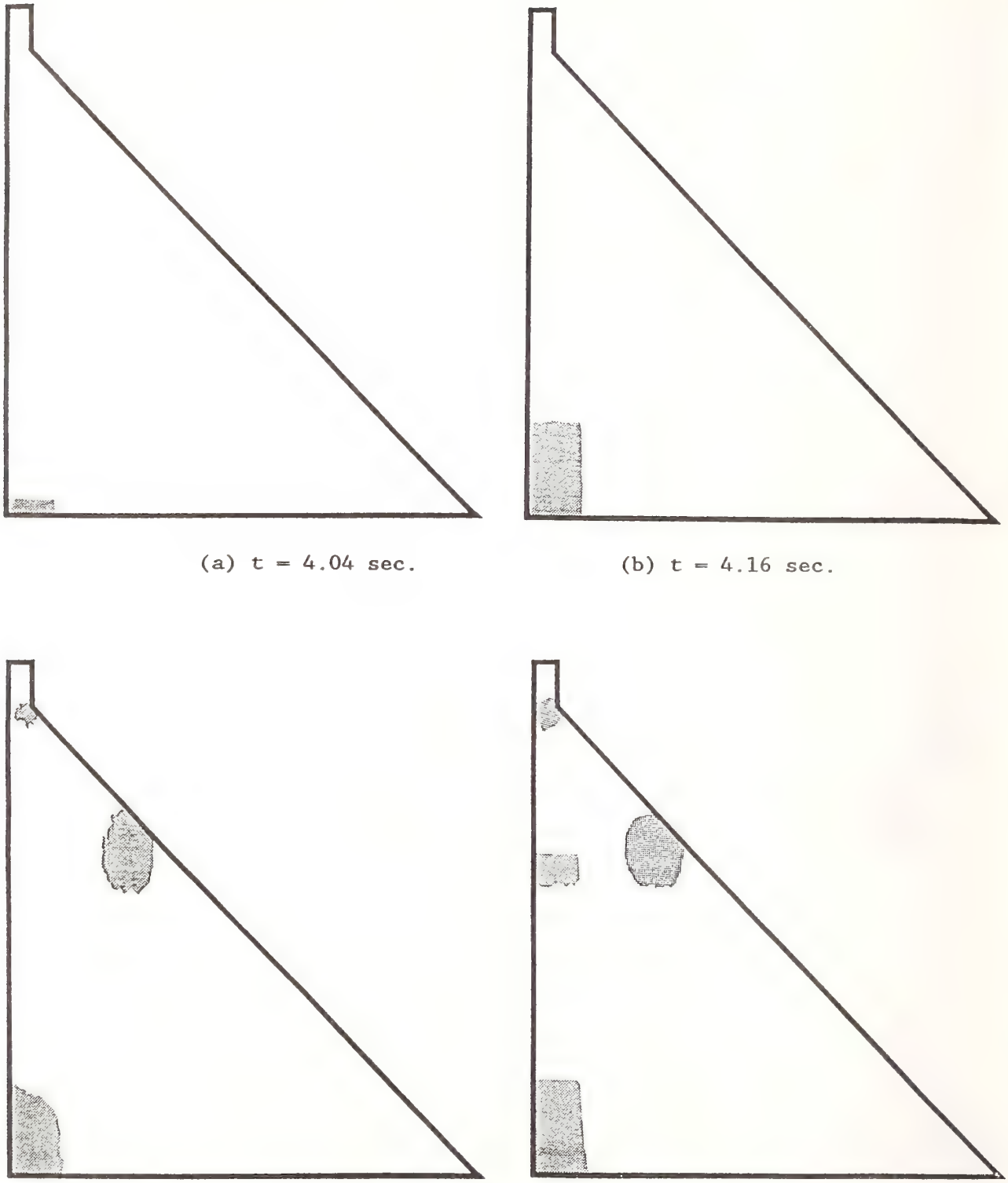

(a) t = 4.04 sec. (b) t = 4.16 sec.

(c) t = 4.24 sec. (d) t = 4.40 sec.

Figure 3. Cracked zones of Dworshak Dam.

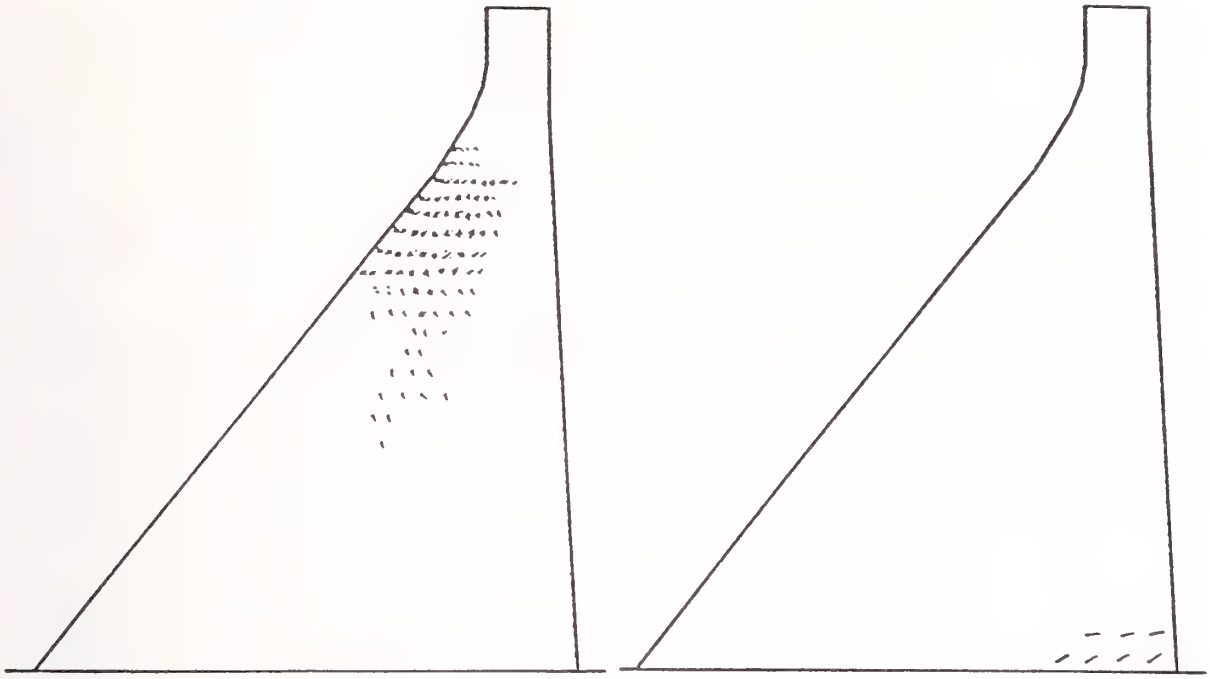

(a) Empty reservoir, a_g = 0.45 g (b) Full reservoir, a_g = 0.18 g

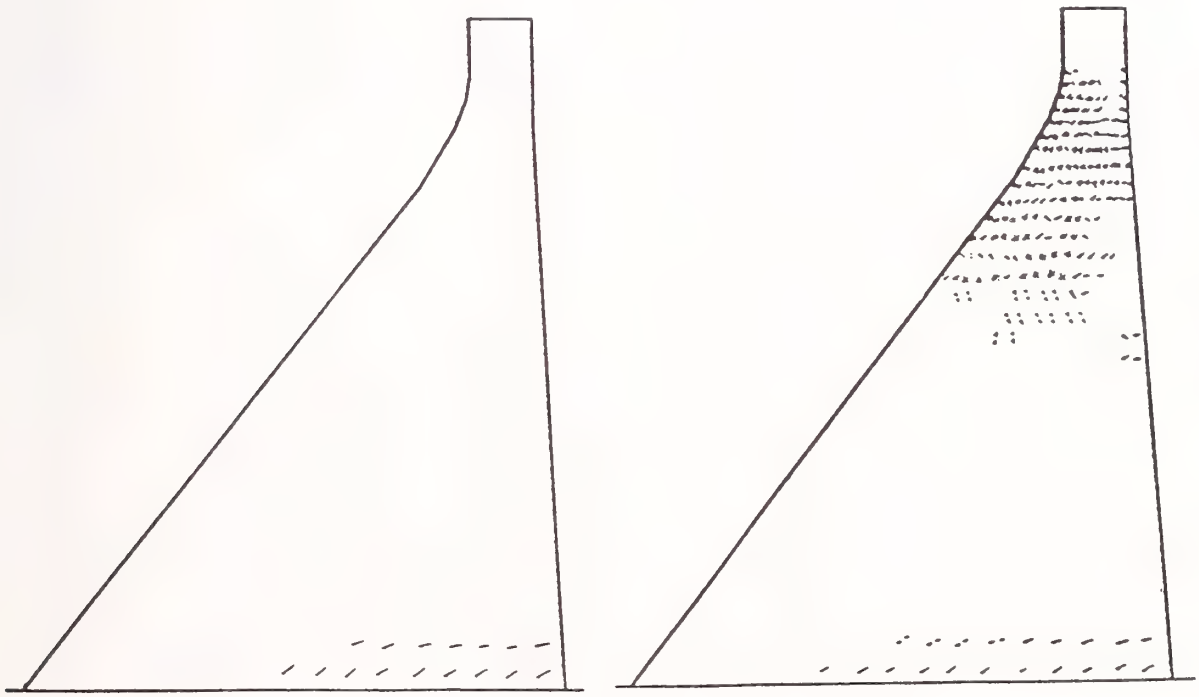

(c) Full reservoir, a_g = 0.27 g (b) Full reservoir, a_g = 0.36 g

Figure 4. Tensile cracks in Pine Flat Dam due to Taft ground motion scaled to peak ground acceleration a_g.

Seismic Risk Assessment Methodology for Water Systems

by

Craig E. Taylor* and Stuart D. Werner**

ABSTRACT

In this paper, we discuss some of the methodological highlights of the five-year voluntary project resulting in the American Society of Civil Engineers (ASCE) monograph entitled Seismic Loss Estimates for a Hypothetical Water System. Highlights of this project include application of the monograph in progress to regional loss studies and discussions of valuation methods, seismic attenuation models, analysis of liquefaction-induced ground failure potential, analytic models for estimating losses from given input earthquake intensities, and probabilistic modeling of earthquake activity and of risks. Based on the results of this project, we make recommendations on future steps to be undertaken in research, the development of a manual, and the integration of earthquake risk methods into system planning.

KEYWORDS:

1. INTRODUCTION

In 1986, the Seismic Risk and the Water and Sewage Committees of the Technical Council on Lifeline Earthquake Engineering (TCLEE) of ASCE undertook a project to demonstrate how direct earthquake loss estimates can be evaluated for a water system. Two years after project inception, a paper on the project progress was presented at the Ninth World Conference on Earthquake Engineering in Tokyo (See Taylor, et al., 1988). Four years after project inception, a paper was delivered on project progress at the annual ASCE convention (see Taylor et al., 1990). Since the state-of-the-art still requires much improvement, this paper explained why the monograph was not designed to be a manual: After five years of effort involving about forty participating engineers, the monograph entitled Seismic Loss Estimates for a Hypothetical Water System was completed (see C. Taylor, ed., 1991).

To develop primary loss estimates, the following steps were undertaken:

- Exposure Definition. The characterization of a hypothetical demonstration water system, including component definition, spatial definition and replacement cost estimation.
- Seismic Hazard Identification and Definition. The characterization of seismic hazards including earthquake sources, regional attenuation patterns, local strong ground motion amplification factors, and local susceptibilities to permanent ground failures.
- Component Loss Algorithm Development. The development of component loss algorithms (or, for other types of studies, component reliability or fragility models), and
- Seismic Risk/Loss Calculation. The calculation of expected direct system losses (or, for other types of studies, the calculation of system reliability and/or secondary losses) and of various breakdowns on these losses (e.g., by

*Dames & Moore, 911 Wilshire Boulevard, Suite 700, Los Angeles, California 90017 USA

**Dames & Moore, 2101 Webster Street, Suite 300, Oakland, California 94612-3011

earthquake source, by component type, by locations in high liquefaction susceptibility zones).

The project implementation began with the assignment of specific project steps to lead engineers, with a group identified for assistance and review. Accomplishment of these tasks was given very wide latitude, with an emphasis on statements of potential difficulties and how potentially innovative approaches can be used to overcome these difficulties. Project coordination made it possible for project steps to be taken so that they fit into an overall framework--a demonstration earthquake loss analysis and resulting monograph being the ultimate goals.

In the remainder of this paper, we first outline some of the highlights of the project and then discuss some future steps that might be taken to improve seismic risk applications to water systems.

2. SELECTED PROJECT HIGHLIGHTS

The highlights of the project result from special efforts made by voluntary participants in for what was many a new context: an earthquake risk analysis. Highlights include:

- The use of the draft monograph in progress as material for regional earthquake loss studies
- The revelation that uniform valuation methods would greatly assist in water system planning as well as in exposure definition for earthquake risk analysis
- The clarification of selection criteria for attenuation functions and of the need for improved modeling of the probability of liquefaction-induced ground failure
- Attempts to overcome the use of subjective estimates of losses through analytic modeling of filtration plants and pipelines, respectively, and
- Use of probabilistic modeling of earthquakes so that potential losses of earthquake scenario selections are overcome.

After reviewing these highlights, we make recommendations on future steps that might be taken.

The aforementioned project highlights will be discussed in turn. Those highlights discussed at length previously will be discussed here only briefly.

2.1 The Benefit to Required Earthquake Loss Studies

When the TCLEE project began, many of the participants were not experienced in all steps needed to perform an earthquake loss analysis for a water system. However, as the project evolved, many participants not only fulfilled their tasks successfully but also became better acquainted with the overall steps needed to undertake a seismic risk analysis. At least three regional earthquake loss studies resulted from the experience of project participants demonstrate the diverse ways how the collaborative TCLEE project has increased the awareness of practitioners of the benefits of the state-of-the-practice methods illustrated in the monograph. These include earthquake loss evaluations of the Seattle water system (Ballantyne et al., 1990), the water system and other utilities in the City of Everett, Washington (Ballantyne et al., 1991), and of the water system in the City of Portland (see Wang et al., 1991).

2.2 The Role of Valuation (Cost Estimation Procedures)

Although technological development and research attention has rightly focused on ways to facilitate inventory development for lifeline networks, the greater emphasis in this project turned out to be the relative absence of uniform valuation methods for water system components. The experience of project participants in water system engineering and planning was

demonstrated in their sensitivity to the uncertainties involved in estimating replacement and repair costs. Often overlooked in scientific and engineering risk studies, these uncertainties can easily yield 30 percent variations in some earthquake loss estimates--at least for specific components. (A more complete discussion of this issue is provided in Taylor et al., 1990.)

2.3 The Role of Ground Attenuation and Liquefaction Probability Models in Seismic Risk Analysis

Although covered elsewhere in the growing earthquake literature, the monograph contains general criteria for the selection of suitable functions for modeling how earthquake ground motions attenuate with distance from the earthquake source. For the specialist as well as the interested engineer, these criteria are expounded in terms of:

- types of variables, including the dependent strong-motion parameter to be used in conjunction with component loss models and the independent parameters such as earthquake magnitude selected, distance from source to site, and local site effects.
- range of variables for application and empirical evaluation (e.g., accuracy of distance estimates, lower and upper earthquakes magnitudes considered, and selection of valid strong-motion records)
- functional form, or form of the equation applied and statistically evaluated.

The models used to assess liquefaction-induced ground failure hazards are based on an extrapolation from standard in-situ methods rather than on general liquefaction probability matrixes. Adaptation of in-situ methods, whether to critical components directly or to microzones through extrapolation from existing boring log and geological data, potentially permits this element of seismic risk analyses to be improved through research designed to examine further these standard methods. As one example, the current problem of how earthquake magnitude (or, somewhat more precisely, the number of strong ground motion cycles) affect liquefaction probabilities is a problem for seismic risk analysis as well as a typical research problem for standard methods.

2.4 The Role of Component-Loss Models in Seismic Risk Analyses

The latitude that was provided task leaders produced noteworthy results with respect to the development of component loss models. These models represent loss (as a percent of replacement value) as a function of some measure of earthquake intensity (e.g., Modified Mercalli intensity, peak ground acceleration, peak ground velocity, etc.). Response to this task typically required clarification of the component-loss model to be developed and, as expected, a lively discussion of what notion of intensity was suitable.

Resulting component loss models were developed from (a) readily-available existing models i.e., the Applied Technology Council (ATC-13) models), (b) empirical data and/or engineering judgment and/or (c) analytic methods. In many cases, as with water filtration plants, past earthquakes provide only scant evidence of potential earthquake damage. Furthermore, this evidence is only rarely documented in terms of dollar loss relative to replacement value, and it is often applicable to filtration plants whose seismic design provisions were very different from those of the plants analyzed in the TCLEE project. In other cases, as with pipelines, investigators have made significant strides in compiling damage data in earthquakes.

Given the dearth of empirical damage or loss data, the uniqueness of some structures, the need to explain damage through analysis, and the subjectivity of readily-available models, task leaders in two topic areas developed analysis methods in order to arrive at component loss models. Those two topic areas were filtration plants and pipelines, respectively. For this

presentation, we shall discuss very briefly the application of analytic methods to filtration plants.

Analytic methods consist of the use of dynamic response calculations, actual earthquake data, and/or experimental data to establish algorithms that interrelate dynamic response with potential earthquake losses. A wide range of dynamic response descriptors and input motion intensity descriptors can be used in these methods as long as (a) the input motion intensity descriptors can be correlated with the potential earthquakes simulated for the water system; and (b) the dynamic response descriptors can be used to establish meaningful relationships between dynamic response and estimated losses.

The TCLEE Monograph contains an example of the application of an approximate analytic method to estimate a loss model for a chemical feed building. This method consists of (a) the development of design spectra for the building, based on empirical compilations of ground response data for different geologic conditions; (b) estimation of a force-deformation relationship for the building that incorporates the building's yield limit and its ultimate capacity; (c) use of these results to obtain approximate dynamic characteristics of the building in terms of its natural period and damping ratios at yield and at ultimate; and (d) estimation of the potential damage to the building as a function of the ground acceleration, by using the design spectra from Step (a), the approximate dynamic characteristics of the building from Step (c), and certain simplifying assumptions that relate the degree of damage to the amount of inelastic deformation estimated for the building at each ground acceleration level.

2.5 Probabilistic Procedures for System-wide Loss Calculation

A major emphasis of the monograph was the use of probabilistic rather than deterministic procedures for calculating potential earthquake-induced losses in geographically dispersed networks. At a minimum, probabilistic modeling incorporates loss estimates from an entire suite of representative earthquakes. In contrast, deterministic modeling considers only a small sample of earthquake scenarios. Whether or not probabilities are somehow assigned to these scenarios, enormous biases enter into the selection. For those who are well-versed in earthquake risk analysis, it becomes possible to select the earthquake scenarios that provide the desired loss result, whether high or low. In the monograph, we avoid these potential biases through the use of probabilistic methods initially developed as recently as the mid-1980's.

3. RECOMMENDATIONS FOR FURTHER RESEARCH AND APPLICATION

The state-of-the-art in assessing the earthquake risks to water systems can still benefit from improvement in a number of areas, as implied for instance by the discussion of highlights. That discussion yields the following research recommendations:

- the need for continuing review and improvement of valuation procedures, especially as the ability to transfer data improves
- the ongoing need for improvements in all geoscience models, including those of earthquake activity sources and rates, attenuation models, and models of the response of sites owing to local soil conditions; the need for improved models to estimate liquefaction probabilities was apparent in this project
- the strong need to replace subjectively derived component loss models with models based on experience and/or analysis.
- the need for a continuing re-examination of how parameter variability affects loss estimates (this includes continuing progress in clarifying the variability of individual parameters).

- compilation of data to assist in the future development of models for calculating secondary losses.

Already earthquake loss and risk estimation procedures have been used in:

- regional earthquake loss estimation studies including water systems
- studies to develop guidelines for state regulatory activities with respect to culinary water facilities, and
- studies designed to assist in developing loss prevention programs for specific systems or subsystems.

Although these earthquake risk studies are clearly providing important insights for planning, design, and retrofit of water systems, there is a need to further develop and refine the current risk modeling and analysis procedure. The monograph itself was designed first for the audience of participants themselves and second for an audience of other potential investigators interested in current methods and difficulties in earthquake loss estimation. Within the limited scope of this paper, only suggestions can be made of how to further this technology transfer. A manual could be a next step, especially if some of the above research issues that outline the step-by-step seismic risk analysis process are addressed. Assignment of a working group to define further possible ways to effectively apply seismic risk analysis to water systems could be another step. Along these lines, earthquake risk methods can be incorporated into current National Institute of Standards (NIST)/Federal Emergency Management Agency (FEMA) efforts to determine how to develop and implement earthquake risk reduction strategies for lifeline networks.

4. REFERENCES

1. Applied Technology Council, ATC-13, 1985. Earthquake Damage Evaluation Data for California. Redwood City, California.

2. Ballantyne, Donald B., E. Berg, J. Kennedy, R. Renau, D. Wu, C. Taylor, C. Crouse, R. Eguchi, and C. Tillman, 1990, "Earthquake Loss Estimation Modeling of the Seattle Water System, "Federal Way, WA: Kennedy/Jenks/Chilton for the United States Geological Survey, October.

3. Ballantyne, Donald B., William F. Heubach, C.B. Crouse, Ronald T. Eguchi, Craig E. Taylor, Craig W. Tillman, Stuart D. Werner, Dennis K. Ostrom, and Felix Wong, 1991, "Earthquake Loss Estimation for the City of Everett, Washington Lifelines," Federal Way, WA: Kennedy/ Jenks/Chilton for the United States Geological Survey, May.

4. Taylor, Craig E. (1991) editor, Seismic Loss Estimates For A Hypothetical Water System New York City: The American Society of Civil Engineers, Technical Council on Lifeline Earthquake Engineering Monograph No. 2, August.

5. Taylor, C.E., W. Elliott, H. Cornell, and D. Ballantyne (1990), "The Demonstration Project on Seismic Loss Estimation for Water Systems," pp. 1-13 in Recent Lifeline Seismic Risk Studies, ed. Anne S. Kiremidjian, New York City: The American Council of Civil Engineers, Technical Council on Lifeline Earthquake Engineering Monograph No. 1, November.

6. Taylor, C.E., R.T. Eguchi, L.R. Wang and J. Isenberg (1988), "Illustrative Methods for Deriving Earthquake Losses Expected to a Water System," Ninth World Conference on Earthquake Engineering, Tokyo.

7. Wang, Leon R.L., Joyce C.C. Wang, Isao Ishibashi, Donald B. Ballantyne, and William M. Elliott, 1990, "Development of Inventory and Seismic Loss Estimation Model for Portland, Oregon Water and Sewer Systems," Norfolk, VA: Old Dominion University, Department of Civil Engineering, for the U.S. Geological Survey, April.

Bridge Scour/An Element of Bridge Management

by

J. Sterling Jones[1] and Stanley R. Davis[2]

ABSTRACT

Several catastrophic bridge failures in the United States were attributed to bridge scour. These events spurred the engineering community to take a hard look at methodologies for evaluating bridges for scour. The Federal Highway Administration (FHWA) took the lead in assembling the technology and State Highway Agencies have taken various approaches for incorporating bridge scour as a major element in existing bridge management programs. A program that is being used by the state of Maryland is described in this paper as an example of how the bridge scour assessments are being handled and as a basis for projecting the magnitude of the program nationwide.

KEYWORDS: bridges; bridge management; bridge scour; hydraulics; waterways.

1. INTRODUCTION

The Federal Highway Administration (FHWA) and the State Highway Agencies in the U.S. are undertaking a major venture to assess the nation's approximately 481,000 bridges over waterways for scour. This venture was prompted in part by two catastrophic failures which resulted in several fatalities and caught the attention of safety officials, news media and legislators. One was the Schoharie Creek bridge in N.Y. which collapsed in April 1987 and caused 10 fatalities. The other was the Hatchie River bridge in Tennessee which collapsed in April 1989 and caused 8 fatalities.

These events were milestones in this nation's concept of bridge scour as a significant component of the overall bridge management program. They spurred the engineering community to take a hard look at existing methods for evaluating new and existing bridges to resist damage from scour. At that time, there was no comprehensive guidance or direction generally acceptable to the engineering community on how to address bridge scour in design and inspection.

To respond to this lack of guidance, FHWA headed up a national cooperative effort among engineers from The National Transportation Safety Board, State Highway Agencies, U.S. Geological Survey, consultant firms and universities to assemble available information and publish what later became Hydraulic Engineering Circulars 18 "Evaluating Scour at Bridges" (Richardson, et. al. 1991) and 20, "Stream Stability at Highway Structures" (LaGasse, et. al. 1991). FHWA and State Highway Agencies updated key items on the National Bridge Inventory to include more information on bridge hydraulics and scour. FHWA developed a demonstration project on underwater inspection and training courses on

---

[1] Hydraulics Research Engineer, Federal Highway Administration, Turner Fairbank Highway Research Center, McLean, VA 22101-2296

[2] Consultant/Hydraulics Engineer, Maryland Department of Transportation, State Highway Administration, Office of Bridge Development, Baltimore, MD 21203-0717; Previously Chief of the FHWA Hydraulics Branch, Washington, D.C.

stream stability and bridge scour. FHWA then set timetables for the State Highway Agencies to assess the susceptibility of bridges to scour and to evaluate and take appropriate action for the bridges that are scour susceptible.

After some discussion with State Highway Agencies, FHWA set two target dates for completion of a bridge scour assessments. April 1992 was set as a target date for completion of a screening to determine which bridges are scour susceptible. January 1997 was set as the target date for completing the more detailed evaluations of the scour susceptible bridges to determine which ones are critical and require remedial action.

State Highway Agencies faced a major bridge management problem in implementing this program. First, scour information was not well documented in the past. Second, there were limited resources both in personnel and in funds to do the scour evaluations. Third, there was a perceived liability and accountability issue that requires a process that is consistent and supportable based on prudent and reasonable judgment. Bridge scour by its nature involves some risk, but State Highway Agencies have to balance the risk against available resources to determine which bridges are evaluated first and what detail of evaluation is appropriate.

Each State Highway Agency has developed some type of management approach that is adaptable to the information available to make prudent and reasonable judgment. This paper describes an approach that was developed by the State of Maryland and relates it to a national perspective.

2. CHARACTERIZATION OF BRIDGES

Bridges in the United States are listed in a National Bridge Inventory (NBI) which is updated by State Highway Agencies and maintained by the FHWA. Elias (1992) studied data in the NBI to establish a profile of bridges in the inventory. Based on his analysis, which reflects a December 1990 inventory, there are 577,000 bridges with approximately 481,000 (or 83%) over waterways. Of the 481,000 bridges over waterways, approximately 90,000 (19%) are actually culverts which are classified as small bridges because they span more than 20 feet.

The remaining 391,000 bridges have the following characteristics:

- Approximately 50% of the bridges in the U.S. have been built within the last 35 years
- Approximately 7% are more than 75 years old
- Approximately 40% of the bridges are simple span construction
- Approximately 40% of the bridges have Average Daily Traffic (ADT) less than 100 vehicles per day
- Approximately 28% have ADT greater than 1,000 vehicles per day.

Based on the nearly complete national screening results, approximately 25% of the bridges are being categorized as scour susceptible and will require more detailed evaluation to determine which ones are scour critical. Based on a relatively small number of the evaluations that have been completed, approximately 11% of the scour susceptible bridges are being categorized as scour critical.

The State of Maryland has 1354 Federal-aid bridges over waterways in The National Bridge Inventory. Four hundred forty of these (32%) are culverts. Two hundred fifty six (19%) of the Maryland bridges are in tidal waterways and will have deferred evaluations for three reasons: (1) there is a general lack of technology to evaluate scour in tidal areas; (2) tidal estuaries tend to dampen the velocity currents for the inland bridges, and (3) the really critical bridges on the coastal waterways are under constant surveillance anyway. Maryland considers that all of the 658 remaining bridges over waterways are scour

susceptible and require a rating. These bridges will be subjected to varying degrees of evaluations depending on the severity of the scour ratings.

3. DEVELOPMENT OF A BRIDGE SCOUR MANAGEMENT PROGRAM

The Maryland Highway Administration recognized the need to draw resources from several different offices and from consultants. A key decision in the use of consultants was that the state must retain the responsibility for assessing the risks involved in the bridge scour management program, and for deciding on the actions necessary to maintain the integrity and safety of the bridge structures.

One of the first things done was to form an interdisplinary team to provide guidance and direction to the team, and to promote coordination and cooperation among the many offices and individuals involved with the general bridge program. Responsibilities of various offices involved in the bridge scour management program were assigned as listed below:

3.1 Bridge Hydraulics Unit

- Technical expertise, guidance and direction
- Overall plan coordination
- Establish agenda for interdisciplinary team
- Prepare bridge scour evaluation reports and review scour reports prepared by others
- Prepare status reports,
- Coordinate program with FHWA, USGS, etc.
- Maintain oversight of research efforts
- Coordinate with other state DOTS, University of Maryland, etc.
- Conduct screening and prioritization studies of bridges for vulnerability to scour damage
- Rate Bridges for Item 113 of The National Bridge Inventory
- Coordinate Training Needs; Conduct In-House Training as Necessary to Meet Program Objectives

3.2 Office of Bridge Development

- Overall management decisions on program approaches and directions, coordination with FHWA and counties, etc.
- Bridge Design Division lead office for designing bridges over waterways; makes decisions on designing foundations to resist scour using guidance and recommendations from Bridge Hydraulics Unit

3.3 Bridge Inspection and Remedial Engineering

- Decisions on what actions to take and relative priorities on bridge needs
- Bridge Inspection Program
- Emergency concerns, closing of bridges, etc.
- Administering Action Plan for scour critical bridges
- Maintaining records on the National Bridge Inventory

3.4 Office of Materials and Research

- Soil borings, stream bed and bank samples, etc.
- Evaluation of foundations in rock; scourability of rock, etc.
- Other guidance on GeoTech matters

The Maryland State Highway Administation then set up two agreements to establish a data base for the program. First, and very important, was an agreement with the U.S.

Geological Survey (USGS) to have two three-man teams conduct a preliminary field survey of non-tidal bridges over waterways that were in the NBI. These crews assigned a USGS rating factor to each bridge based on the following:

- Stability of channel bed and banks
- Approach and "get away" flow conditions to bridge
- Degree of observable scour at bridge
- Susceptibility to damage from scour based on conditions observed at the site.

The USGS teams also rated NBI items 61 (channel), 71 (waterway adequacy) and special state item 321 (scour) for each bridge they surveyed. The fact that there were only two teams gave a degree of uniformity to these ratings that gives them a high weight in a ranking system.

Second, was a contract with a consultant to develop a spread sheet that could be readily managed by state engineers. The spread sheet included the following factors for each bridge:

- Traffic (ADT)
- Superstructure (continuous or simple spans)
- Foundation (spread footing, piles, etc.)
- Waterway area (Item 71)
- Channel Stability (Item 61)
- Observable Bridge Scour (Special State Item 321)
- USGS Rating Factor (from field survey)
- (SHA) Engineer Rating Factor (Based on engineer's evaluation of all available field and office data)

Numbers are assigned to each of these factors and the spread sheet priorities are updated at least monthly as additional information becomes available.

4. SCREENING AND SCOUR ASSESSMENT

The Maryland State Highway Administration uses several levels of screening and assessments to determine which bridges require a full scour evaluation. Advance screening eliminated culverts and tidal bridges for reasons cited previously. The preliminary screening process essentially assigns numbers to the spread sheet factors and ranks bridges from worst to best. The office scour assessment involves some preliminary scour computations, review of foundation information, and special circumstances for the bridge. At this stage some bridges can be categorized as scour critical and others can be categorized as low risk and can be eliminated from further assessment. The office assessment is a relatively low cost effort that requires approximately one person-day per bridge. The spread sheet rating factors, especially the (SHA) engineer rating factor, are revised after this assessment. The field and office scour assessment involves site visits by State Highway engineers, more detailed data gathering, and more precise computations. Again, the spread sheet rating factors are revised after this assessment. Some bridges then will require a full scour evaluation which typically involves taking soil borings, rerunning water surface profile models to get flow and velocity distribution, estimating expected scour depths, and determining structural integrity of bridges with partially exposed foundations. Table 1 shows the expected number of bridges and the relative costs for each process.

5. FACTORS USED TO DEVELOP THE SCOUR PRIORITY NUMBER

A central focus of Maryland's Bridge Scour Program is the spread sheet ranking system which is continuously updated after each process level and whenever new data or better technology becomes available. This system keeps the highest risk bridges at the center of

attention.

The factors used to develop a ranking are of interest and deserve some discussion. Table 2 summarized the spread sheet factors with guidelines used by Maryland for assigning numerical values that calculate a scour priority number for each bridge. Using Maryland's guidelines, the lower the scour priority number, the greater the likelihood that the bridge will be damaged by scour.

ADT reflects primarily on the value of lost time, and traffic running costs if an important bridge fails. It also is a secondary indicator of the probability of fatalities if a bridge does fail, although there are not enough data to establish any correlation between ADT and the probability of fatalities.

Superstructure type is important because continuous spans have more redundancy and less chance of catastrophic failure with little or no warning. This is also an indicator for the probability of fatalities.

Foundation type is definitely one of the most important factors. Historically, most of the scour related failures have been bridges on spread footings.

Waterway adequacy reflects the probability that pressure flow scour is likely to occur. It also may be an indicator of contraction scour. It is an available piece of data that has merit in a ranking system.

Channel stability reflects the tendency for degradation and channel migration. This factor should have a high weight because instable channels generally have more local scour and react to small channel changes.

Bridge Inspection Observations are important because they highlight the bridge inspectors identification of potential scour problem.

The USGS rating factor is especially important in Maryland because of the uniformity of that factor since the same survey crews inspected and rated all of the bridges. The same survey crews also rated the NBI items.

The SHA Engineer rating factor takes into account the accuracy of records and conservatism of engineers at various periods of time. This factor is based on an overview of all of the information in the system, and is the most dynamic factor as the screening and assessment progresses.

The "screamer" factor allows for any bridge to rise to top of the list at any stage of the assessment if anyone reports evidence that a bridge is in danger.

The scour priority number is calculated by multiplying the numerical values assigned to each of these factors. The ratings can be criticized because there is no provision for weighing factors according to importance and reliability of information. It would appear that the wide range of values for some of the less important factors, such as waterway adequacy, would make them have more weight than they are intended to have and lead to erroneous ranking. This was an initial concern with the use of the system, but subsequent testing has satisfied Maryland State Highway Administration engineers that the system, while not perfect, does a reasonable job of prioritization. This success is due to several moderating effects, including the dynamic nature of the program, the flexibility to revise numerical values as more information becomes available, and the central tendency of the NBI rating numbers.

Other State Highway Agencies have developed similar bridge scour management programs. There has been at least one attempt by Elias (1992) to consolidate the best features of the programs into one that can be promoted nationally, but that procedure is still in draft stage and has not been tested by any state.

7. SUMMARY

The Federal Highway Administration took the lead in assembling available information, developing training courses, and providing demonstration projects to deal with an accelerated program to assess the nation's bridges for scour susceptibility. The State Highway Agencies have had to integrate this program into their overall bridge management program with limited resources.

Maryland is a relatively small state with fewer bridges than the average state, but it is a sampling that reflects the magnitude of the overall scour program in the United States. If the average $4,000 per bridge cost for managing the bridge scour program is extrapolated to the total 391,000 bridges (excluding culverts) over waterways, the total cost of this program nationally will exceed $1.5 billion over the next decade.

Maryland has taken a somewhat pragmatic approach in developing its bridge scour program, placing emphasis on engineering judgment to limit the number of bridges requiring full scour evaluation. This approach, coupled with an active bridge inspection program, works for that state. The following considerations were essential to the success of their program:

- Support of top management
- Formation of an interdisciplinary team
- Knowledge of and sensitivity to concerns about scour by the engineers in the bridge management program
- Development of a plan of action to identify the tasks to be addressed
- Assistance of the FHWA and the USGS in training efforts and in developing the program
- Written directives establishing policies and rsponsibility for the scour program
- Importance of the Bridge Inspection Program in identifying and prioritizing potential scour problems
- Use of the Scour Priority Number Spreadsheet as a management tool for evaluating existing bridges

8. REFERENCES:

1. Richardson, E.V., Harrison, L.J., and Davis, S.R. (1991). FHWA Hydraulic Engineering Circular No. 18, "Evaluating Scour at Bridges," Publication No. FHWA-IP-90-017, Washington, D.C.

2. LaGasse, P.F. et. al. (1991). FHWA Hydraulic Engineering Circular No. 20, "Stream Stability at Higway Structures," Publication No. FHWA-IP-90-14, Washington, D.C.

3. Elias, Victor (1992). "Strategies for Managing Unknown Bridge Foundations," Unpublished Draft Publication No. FHWA-RD-92-030, FHWA R&D, McLean, Va. 22101.

Table 1. Maryland Bridge Scour Program

Process	Expected No. of Bridges	Estimated Cost per Bridge	Expected Cost
Preliminary Screening	658	$ 515	$ 340,000
Office Scour Assessment	658	$ 350	$ 230,000
Field & Office Scour Assessment	219 (Approx. 33%)	$ 1600	$ 350,000
Full Scour Evaluation	110 (Approx. 17%)	$ 15,000	$ 1,650,000
Grand Total			$ 2,570,000
Average Cost per Bridge			$ 4,000

Table 2. Maryland Factors used to Rate Bridges for Scour Susceptibility

Factor	Criteria and Numerical Indicators
ADT	> 30,000 veh/day = 1 5 - 30,000 veh/day = 2 < 5,000 veh/day = 3
Superstructure	simple span = 1 continuous = 2
Foundation	Spread footing, erod mat'l. = 1 Unknown = 2 Short Pile = 4 Long Pile > 20' = 6 Found on Solid Rock = 6
Waterway Adequacy NBI Item 71	1 to 9 from Inventory Data
Channel Stability NBI Item 61	1 to 9 from Inventory Data
Bridge Inspection Notes Regarding Scour Special Maryland NBI Item 321	1 to 9 from Inventory Data
USGS Rating Factor	severe = 1 moderate = 2 mild = 3
SHA Engineer Rating Factor	Preliminary = 3 Revised after Office Assessment severe = 1 moderate = 2 mild = 3
"Screamer" Factor	Overrides all others and places a bridge at the top of the list.

U.S. Coordinated Program for Masonry Building Research – Seventh Year Status

by

James L. Noland[1]

ABSTRACT

The U.S. program, which consists of twenty-eight specific research tasks, is coordinated with a parallel program in Japan. Both are conducted under the auspices of the UJNR Panel on Wind and Seismic Effects. The primary purpose of the U.S. program is to support the development of a limit state design procedure for masonry as well as provide experimental data, analytical methods, etc. Several technical accomplishments have been realized in both modeling and experimental areas. The technology transfer plan includes dissemination of research reports, topical reports and a summary report on the specific research areas as well as by presentations and papers. Design and criteria recommendations will be an extremely important mode of technology transfer and are expected to support limit state design standard development. Current status of the program is presented. Completion is expected by July 1993.

KEYWORDS: masonry; progress; structures; technology transfer; UJNR

1. INTRODUCTION

The U.S. Coordinated Program for Masonry Building research is an integrated set of 28 specific research tasks being conducted by the U.S. Technical Coordinating Committee for Masonry Research (TCCMAR/US). The U.S. program is coordinated with a parallel program in Japan to exchange information and concepts for the mutual benefit of both countries. Both programs are conducted under the auspices of the United States - Japan Natural Resources Panel on Wind and Seismic Effects.

2. PROGRAM OBJECTIVES

Primary program objectives are:

1) Development of design and criteria recommendations for limit state design of reinforced masonry buildings and components.

2) Development of a consistent experimental database on the behavior of masonry materials, components and systems.

3) Development of analytical non-linear models for research and design office use for detailed analysis, system analysis, and dynamic loads determination.

4) Improved material and subassemblage experimental procedures for obtaining masonry properties.

5) Improved masonry fabrication procedures and standards.

6) Developing an increased awareness among engineers, architects, code bodies and the public of the capabilities of reinforced masonry in all seismic zones.

7) Interfacing with standards development groups to support development of a consensus limit state standard for masonry.

[1]Atkinson-Noland & Associates, Inc.
2619 Spruce Street
Boulder, CO 80302

3. APPROACH

With NSF support, the Technical Coordinating Committee for Masonry Research/U.S. (TCCMAR/U.S.) was formed in February 1984. TCCMAR/U.S. was and is comprised of researchers from academic and industrial organizations who have strong backgrounds in research into the properties and characteristics of reinforced masonry materials, structural components and systems, analytical techniques, structural dynamics, building codes, and earthquake engineering. TCCMAR researchers are listed in Table 1. TCCMAR participants defined the research program conducted, the research and will analyze and interpret the results.

The U.S. research plan is a phased step-by-step program of separate, but coordinated research tasks. Emphasis is being placed upon intra-task information exchange and consultations so the experimental and analytical efforts are mutually supportive. The research tasks comprising the coordinated program are listed in Table 2.

The program includes both experimental and analytical research tasks. The experimental and analytical efforts are conducted in parallel with each becoming more complex and sophisticated as knowledge and experience accumulate. The U.S. plan is thus a "building block" approach. The program began in October 1985 and will be completed by July 1993.

4. CURRENT STATUS

The program is approximately 90% complete. Remaining work consists of completing experimental efforts on reinforcing bar bond and splicing, experimental and analytical studies of the behavior of a five story research building, development of limit state design and criteria recommendations, and final technology documentation. Research task reports which have been published are listed in Table 3.

Construction of the five story research building has begun. It is expected that it will be completed, instrumented, and checked by June 1992. Testing should be done through the summer.

Funding for the full scale research has been provided by the National Science Foundation, the Department of Energy, and the U.S. masonry industry (organizations such as the Council for Masonry Research, the Masonry Institute of America, the California-Nevada Concrete Masonry Association, and thirty regional masonry associations).

Work on Technology Documentation and Design and Criteria Recommendations will begin formally with a meeting on 10 April 1992. Plans and assignments will be made at that time. TCCMAR Category 2 researchers have done preliminary work to support design and criteria recommendations; this, and a draft of a limit-state design standard previously prepared, will be the starting point.

The Design and Criteria Recommendations project will basically consist of refining the draft limit state design standard, validation of the design standard by trial designs of buildings of different types in different seismic zones, and refinement of the standard as required.

Technology Documentation will involve the preparation of a series of monographs on key topics to clarify and summarize research findings. The documents will be published by the Federal Emergency Management Agency.

Funding for Technology Documentation and Design and Criteria Recommendations has been provided by the National Science Foundation, the U.S. Army Corps of Engineers, and the Federal Emergency Management Agency.

TABLE 1

TCCMAR RESEARCHERS

Daniel Abrams
University of Illinois
Urbana, IL

Samy Adham
Agbabian Associates
El Segundo, CA

Richard Atkinson
Atkinson-Noland & Associates
Boulder, CO

Russell Brown
Clemson University
Clemson, SC

Robert Englekirk
Englekirk,Hart & Sabol
Los Angeles, CA

Robert Ewing
Ewing & Associates
Rancho Palos Verdes, CA

Ahmad Hamid
Drexel University
Philadelphia, PA

Mike Hammons
US Army Corps of Engineers
Vicksburg, MS

Gary Hart
Englekirk,Hart & Sabol/UCLA
Los Angeles, CA

Gilbert Hegemier
Univ. of CA-San Diego
La Jolla, CA

John Kariotis
Kariotis & Associates
South Pasadena, CA

Richard Klingner
Univ. of Texas-Austin
Austin, TX

Ronald Mayes
Computech Engin. Services
Berkley, CA

James L. Noland
Atkinson-Noland & Assoc.
Boulder, CO

Max Porter
Iowa State University
Ames, IA

M.J.N. Priestley
Univ. of CA-San Diego
La Jolla, CA

Freider Seible
Univ. of CA-San Diego
La Jolla, CA

P.B. Shing
University of Colorado
Boulder, CO

Leonard Tulin
University of Colorado
Boulder, CO

TABLE 2

RESEARCH TASKS

SUBJECT	RESEARCHER
Grouted Hollow-Unit Clay & Concrete Masonry in Compression	R. Atkinson
Grouted Hollow-Unit Concrete Masonry Under Combined Compression & Flexure	A. Hamid
Grouted Hollow-Unit Clay Masonry Under Combined Compression & Flexure	R. Brown
Masonry Test Methods for Limit State Design[2]	R. Atkinson
Nonlinear Force-Displacement Models of Reinforced Masonry Components & Systems	R. Englekirk
Nonlinear Finite Element Models for Analysis of Reinforced Masonry	R. Ewing
Nonlinear Lumped Parameter Models for Dynamic Response Analysis of Reinforced Masonry Systems	J. Kariotis
Nonlinear Models of Floor Diaphragms	M. Porter
Nonlinear Models of Reinforced Masonry Walls Acting Out-of-Plane	R. Mayes
Experimental Study of One-Story Reinforced Masonry Shear Walls	B. Shing
Experimental Study of Two-Story Reinforced Masonry Shear Walls	R. Klingner
Experimental Study of Three-Story Reinforced Masonry Shear Walls and Development of Automated Feed-Back Test Method for Stiff Structures	G. Hegemier F. Seible
Experimental Study, Static & Dynamic, of Out-of-Plane Behavior of Reinforced Concrete Masonry Walls	A. Hamid S. Adham

SUBJECT	RESEARCHER
Experimental Study, Static & Dynamic, of Out-of-Plane Behavior of Reinforced Clay Masonry Walls	R. Mayes
Experimental Study, Static & Dynamic, of Flanged Reinforced Masonry Walls	N. Priestley
Analytical Study Based on Prior Tests, of Wall-Floor Intersections[2]	G. Hegemier
Experimental Study (Preliminary) of Reinforcing Bar Bond & Splices in Grouted Masonry	L. Tulin
Experimental Study (continuation) of Reinforcing Bar Bond and Splices in Grouted Masonry[2]	R. Atkinson M. Hammons
Experimental Study, Static & Dynamic Behavior of Scale Model Three-Story Reinforced Masonry Buildings	D. Abrams
Development of Reliability-Based Limit-State Design Methodology for Masonry Buildings	G. Hart
Development of Reliability Factors for Masonry Materials, Components, & Systems	G. Hart
Design of Five-Story Reinforced Masonry Research Building	J. Kariotis
Design and Construction of Large Specimen Research Building[2]	G. Hegemier F. Seible
Experimental Study of Nonlinear Behavior of a Five-Story Building Under Cyclic Lateral Loads[2]	G. Hegemier F. Seible
Design & Criteria Recommendation for Limit State Design and Documentation and Technology Documentation[2]	J. Noland
Overall Program Coordination[2]	J. Noland

[2]Research Tasks to be completed .

TASK REPORTS[3]

Task No.	Author/s - Title
1.1-1:	Atkinson and Kingsley, Comparison of the Behavior of Clay & Concrete Masonry in Compression, September 1985. 151 pgs.
1.2(a)-1:	Hamid A.A., Assis, G.F., Harris, H.G., Material Models for Grouted Block Masonry, August 1988. 67 pgs.
1.2(a)-2:	Assis, G.F., Hamid A.A., Harris, H.G., Material Models for Grouted Block Masonry, August 1989. 134 pgs.
1.2(b)-1:	Young, J.M., Brown, R.H., Compressive Stress Distribution of Grouted Hollow Clay Masonry Under Strain Gradient, May 1988. 170 pgs.
1.3-1:	Atkinson, R.H., An Assessment of Current Material Test Standards for Masonry Limit States Design Methods, June 1991. 38 pgs.
2.1-1:	Hart, G. and Basharkhah, M., Slender Wall Structural Engineering Analysis Computer Program (Shwall, Version 1.01), September 1987. 68 pgs.
2.1-2:	Hart, G. and Basharkhah, M., Shear Wall Structural Engineering Analysis Computer Program (Shwall, Version 1.01). September 1987. 75 pgs.
2.1-3:	Nakaki, D. & Hart, G., Uplifting Response of Structures Subjected to Earthquake Motions, August 1987. 200 pgs.
2.1-4:	Hart, G., Sajjad, N., and Basharkhah, Inelastic Column Analysis Computer Program (INCAP, Version 1.01), March 1988.
2.1-5:	Hong, W.K., Hart, G.C., Englekirk, R.E.,Force-Deflection Evaluation and Models for University of Colorado Flexural Walls, December 1989.
2.1-6:	Hart, G.C. Jaw, J.W., Low, Y.K., SCM Model for University of Colorado Flexural Walls, December 1989. 31 pgs.
2.1-7	Hart, G., Sajjad, N., Basharkhah, M., Inelastic Masonry Flexural Shear Wall Analysis Computer Program, February, 1990. 41 pgs.
2.1-8	Hart, G., Englekirk, R., Srinivasan, M., Huang, S.C., Drag, D.J,., Seismic Performance Study, DPC Gymnasium, Elastic Time History Analysis Using SAP90, February, 1992.
2.1-9	Hart, G., Englekirk, R., Srinivasan, M., Huang, S.C., Drag, D.J., Seismic Performance Study, TMS Shopping Center, Elastic Time History Analysis Using SAP90, February, 1992.
2.1-10	Hart, G., Englekirk, R., Jaw, J.W., Srinivasan, M., Huang, S.C., Drag, D.J., Seismic Performance Study, RCJ Hotel February, 1992.
2.1-11	Hart, G., Englekirk, R., Jaw, J.W., Huang, S.C., Drag, D.J., Seismic Performance Study, 2-Story Masonry Wall-Frame Building, February, 1992.
2.1-12	Hart, G., Englekirk, R., Jaw, J.W., Huang, S.C., Drag, D.J., Seismic Performance Study, 2-Story Masonry Wall-Frame Building Designed by Tentative Limit States Design Standard, February, 1992.

[3]Task Reports are available through the Earthquake Engineering Research Library, Berkley, CA, and The Earthquake Engineering National Center, SUNY, Buffalo, NY.

2.2-1: Ewing, R., El-Mustapha, A., Kariotis, J., FEM/I - A Finite Element Computer Program for the Nonlinear Static Analysis of Reinforced Masonry Building Components, December 1987 (Revised June 1990).

2.2-2: Ewing, R.D., Parametric Studies on Reinforced Masonry Shear Walls Using FEM/I, A Nonlinear Finite Element Analysis Program, March 1992.

2.2-3: Ewing, R.D., Finite Element Analysis of Reinforced Masonry Building Components Designed by a Tentative Masonry Limit States Design Standard, March 1992.

2.3-1: Ewing, R.; Kariotis, J.; El-Mustapha, A., LPM/I, A Computer Program for the Nonlinear, Dynamic Analysis of Lumped Parameter Models, August, 1987. 200 pgs.

2.3-2: Kariotis, J., El-Mustapha, A., Ewing, R., Influence of Foundation Model on the Uplifting of Structures, July 1988. 50 pgs.

2.3-3: Kariotis, J., Rahman, M., El-Mustapha, A., Investigation of Current Seismic Design Provisions for Reinforced Masonry Shear Walls, January 1990. 48 pgs.

2.3-4: Kariotis, J., Rahman, A., Waqfi, O., Ewing, R., Version 1.03 LPM/I - A Computer Program fo the Nonlinear, Dynamic Analysis of Lumped Parameter Models, February 1992.

2.3-5: Kariotis, J., Waqfi, O., Ewing, R., A Computer Program Using Beam Elements for the Nonlinear, Dynamic Analysis of Lumped Parameter Models, February 1992.

2.3-7: Kariotis, J., Waqfi, O., Recommended Procedure for Calculation of the Balanced Reinforcement Ratio, February 1992.

2.4(b)-1: Button, M.R., Mayes, R.L., Out-of-Plane Seismic Response of Reinforced Masonry Walls: Correlation of Full-Scale Test and Analytical Model Results, March 1991. 65 pgs.

3.1(a)-1: Scrivener, J., Summary of Findings of Cyclic Tests on Masonry Piers, June 1986. 7 pgs.

3.1(a)-2: Shing, P.B., Noland, J., Spaeh, H., Klamerus, E., Schuller, M., Response of Single-Story Reinforced Masonry Shear Walls to In-Plane Lateral Loads, January 1991. 136 pgs.

3.1(b)-1: Seible, F. and LaRovere, H., Summary of Pseudo Dynamic Testing, February 1987. 46 pgs.

3.1(c)-1: Merryman, K., Leiva, G., Antrobus, N., Klingner, R., In-Plane Seismic Resistance of Two-Story Concrete Masonry Coupled Shear Walls, September 1989. 176 pgs.

3.1(c)-2: Leiva, G., Klingner, R., In-Plane Seismic Resistance of Two-Story Concrete Masonry Shear Walls with Openings, August 1991.

3.2(a): Hamid, A., Abboud, B., Farah, M., Hatem, K., Harris, H., Response of Reinforced Block Masonry Walls to Out-of-Plane Static Loads, September 1989. 120 pgs.

3.2(b)-1: Agbabian, M., Adham, S., Masri, S., Avanessian, V. Traina, Out-of-Plane Dynamic Testing of Concrete Masonry Walls, Volumes 1 and 2, July 1989. 220 pgs.

4.1-1: Limin, H., Priestley, N., Seismic Behavior of Flanged Masonry Shear Walls, May 1988. 119 pgs.

4.2-1: Hegemier, G. Murakami, H., On the Behavior of Floor-to-Wall Intersections in Concrete Masonry Construction: Part I: Experimental

4.2-2: Hegemier, G., Murakami, H., On the Behavior of Floor-to-Wall Intersections in Concrete Masonry Construction: Part II: Theoretical

5.1-1: Porter, M., Sabri, A., Plank Diaphragm Characteristics, July 1990. 226 pgs.

5.2-1 Porter, M., Yeomans, F., Johns, A., Assembly of Existing Diaphragm Data, July 1990. 142 pgs.

6.2-1: Scrivener, J., Bond of Reinforcement in Grouted Hollow-Unit Masonry: A State-of-the-Art, June 1986. 53 pgs.

6.2-2: Soric, Z. and Tulin, L., Bond Splices in Reinforced Masonry, August 1987. 296 pgs.

7.1-1 Paulson, T., Abrams, D., Measured Inelastic Response of Reinforced Masonry Building Structures to Earthquake Motions, October, 1990. 294 pgs.

8.1-1: Hart, G., A Limit State Design Method for Reinforced Masonry, June 1988.

8.1-2: Hart, G., Expected Value Design in the Context of a Limit Sate Design Methodology, February 1990.

8.2-1: Hart, G., Zorapapel, G.T., Reliability of Concrete Masonry Wall Structures, December 1991.

9.1-1: Kariotis, J.C., Johnson, A.W., Design of Reinforced Masonry Research Building, September, 1987. 42 pgs.

9.1-2: Kariotis, J.C., Waqfi, O.M., Trial Designs Made in Accordance with Tentative Limit States Design Standards for Reinforced Masonry Buildings, February 1992.

9.2-1: Seible, F., Report on Large Structures Testing Facilities in Japan, September 1985. 120 pgs.

9.2.2: Seible, F., Design and Construction of the Charles Lee Powell Structural Systems Laboratory, November 1986. 65 pgs.

9.2.3: Seible, F., The Japanese Five-Story Full Scale Reinforced Masonry Building Test, January 1988. 100 pgs.

11.1-1: TCCMAR, Summary Report: U.S. Coordinated Program for Masonry Building Research, September 1985 to August 1986. 190 pgs.

11.1-2: Status Report: U.S. Coordinated Program for Masonry Building Research, November 1988. 170 pgs.

Appendix

Task Committees A-K Reports

(A) STRONG-MOTION INSTRUMENT ARRAYS AND DATA

Date: May 19, 1992

Place: National Institute of Standards and Technology
Gaithersburg, MD

Attendees:

U.S. Side -	A. G. Brady (Chairman)	(USGS)
	H. Meyers	(NOAA)
	P. E. Harben	(DOE)
Japan Side -	S. Noda (Chairman)	(PHRI)
	K. Ohtani	(NIED)
	K. Shioji	(PWRI)

MISSION STATEMENT

1. Objective:

The objective of the Task Committee is to coordinate the provision of strong-motion earthquake data to researchers and to the practicing engineering community. The Task Committee focuses on instrumentation; recording, processing, and analyzing strong-motion data; research to ensure high-quality data dissemination; and analysis of ground motion and structural motion in dynamic response to earthquakes.

2. Scope of Work

The T/C coordinates strong-motion research, processing strong-motion data, and disseminating information on the recorded behavior of structures. In addition to regular exchange of data and publications, the T/C's technical approach includes:

* Planning and conducting T/C workshops and meetings, held generally in conjunction with UJNR Joint Meetings.

* Conducting related technical sessions at professional society meetings.

* Creating procedures for the dissemination of significant strong-motion digital data with regard for the rights and expectations of (a) the owner, (b) the users of data, and (c) the earthquake engineering community.

* Creating an up-to-date information exchange on computer processing procedures and related research so all users of processed data are aware of valid ranges and practical limitations.

* Coordinating research programs for appropriate instrumentation and dynamic analysis of structures with base isolation or other response-reducing systems, under earthquake excitation.

* Coordinating research programs using both permanent and temporary arrays and data derived to study site response.

3. Accomplishments

* Catalogs of strong-motion earthquake records observed both in the United States and Japan are being exchanged. U.S. data are published in the "Seismic Engineering Program Report", and the Japanese data are published in "Strong-Motion Records in Japan". Digital data is exchanged on tape, floppies, and CDROMs. Many other publications also were exchanged.

* Preliminary Reports of the Southern and Northern California earthquakes, from both the U.S. Geological Survey and California Division of Mines and Geology, were exchanged.

* Prompt report of the Tokyo Bay Earthquake, February 2, 1992, from the Strong-Motion Earthquake Observation Council, NIED, was exchanged.

* From the USGS, a CDROM containing "Digitized Strong-Motion Accelerograms of North and Central American Earthquakes 1933-1986", May, 1992, by Linda Seekins was exchanged, together with a software package for PC processing and a User Manual: "Basic Strong-Motion Accelerogram Processing Software";Version 1.0, May 1992, by April M. Converse.

* From the National Geophysical Data Center, NOAA, disks containing the "Strong-Motion Data Catalog", and software (all records in the global public domain through 1992) were exchanged. The User Manual is "An Earthquake Strong-Motion Data Catalog for PC's, SMCAT" Version 2.0, July 1990, by Lee Wesley Row III).

4. Future Plans

* Coordinate the analysis of records from arrays: downhole 3-D arrays (geophysics and earthquake engineering) and structural arrays (structural engineering).

* The Science and Technology Agency, and the National Science Foundation will be asked to sponsor a joint workshop in Hawaii, in the fall of 1993, on Digital Recording Technologies, for approximately 20

invited participants, including Japanese and US researchers. The workshop will be for 2 days, followed by a technical site visit.

5. Information Exchange

* Performed within the domestic community through technical meetings, conferences, seminars, and workshops.

* Performed through participation in post-earthquake field investigations with concentration in areas where strong-motion stations have recorded data.

* Performed with the counterpart side through T/C workshops; visitor exchanges, seminars, lectures; and participation in annual Joint Panel meetings.

* The most crucial information exchange is rapid description of recovered strong motion records (and subsequently, digital strong-motion data on tape or disk) from significant earthquakes.

6. Impact

* Most managers who process strong-motion recordings use techniques based, or closely associated with, the work of this T/C and its members. Foreign networks fitting this category include:

  AUSTRALIA - Australian Seismological Center, Bureau of Mineral Resources, PO Box 378, Canberra ACT 2601.

  CANADA - Pacific Geoscience Center, PO Box 6000, Sidney, BC. V8L 4B2.

  ITALY - The Italian National Commission for Research and Development on Alternative Energy Sources (ENEA), Rome.

  MEXICO - Japan-Mexico Earthquake and Disaster Prevention Center, Mexico City.

  PERU - Japan-Peru Earthquake and Disaster Prevention Center, Lima.

  TAIWAN - SMART Array

  TURKEY - University of Bogazici, 80815 Bebek, Istanbul.

YUGOSLAVIA - Institute of Earthquake Engineering and Engineering Seismology, Skopje.

* Use of seismological and strong-motion data, in convenient form, is facilitated in seismically active countries having no such data of their own.

* Dissemination of digital data from significant earthquakes, taking into account the conditions of the 3rd paragraph in the Scope of Work, increases the research data base; application of this data in design practice aids in reduction of earthquake hazards.

7. Barriers

* Lack of adequate funding for T/C joint endeavors.

* Establishing joint research efforts and maintaining close interaction between participants are difficult unless visiting research appointments are established. (Funding and staff availability are often barriers).

Report of Task Committee on

(B) LARGE-SCALE TESTING PROGRAM

Date: May 20, 1992

Place: National Institute of Standards and Technology
Gaithersburg, MD

Attendees:

U.S. Side -	H. S. Lew (Chairman)	(NIST)
	W. E. Roper	(COE)
Japan Side -	K. Ohtani (Chairman)	(NIED)
	H. Yamanouchi	(BRI)
	Y. Yamaguchi	(PWRI)

MISSION STATEMENT

1. Objective:

The objective of the Task Committee is to develop performance data of full-scale dynamic properties of structures to better resist wind and seismic loads through both laboratory testing of prototype structures and field testing of structures in situ. Improved full-scale test data will validate the results of small-scale model tests and substantiate the results of computer analyses of structural behavior.

2. Scope of Work

The Task Committee develops its research agenda in coordination with other appropriate T/Cs, such as T/C's "C" and "D", for full-scale evaluation of buildings, and other structures except bridges.

* Plans and conducts workshops and joint meetings to identify research topics and develops joint research programs.

* Coordinates research projects carried out by various laboratories in the U.S. and Japan. Facilitates publication of research results and implementation of findings in codes and standards.

* Facilitates exchange of research personnel, technical information and available testing facilities.

3. Accomplishments

* The second U.S. Technical Coordinating Committee on Precast Seismic Structural Systems Program (PRESSS) was held in June 1991 at San Diego, California.

* The Japan PRESSS Research program is continuing at several institutions including BRI, University of Tokyo, Kyoto University, and Yokohama National University. The Japan TCC Meetings were held during the past fiscal year.

* The second U.S.-Japan Joint Technical Coordinating Committee on PRESSS was held in October 1991 at Tsukuba, Japan.

* The Hybrid structural system is being considered as the fifth topic for the joint research program following PRESSS. In preparation for the joint research, the Japanese Planning Group on hybrid structures met five times since September 1991.

* The first U.S. planning meeting on hybrid structures was held in San Francisco, February 1992. Several Japanese researchers participated in the meeting.

4. Future Plans

* The National Science Foundation (NSF) has funded the third phase(5-story structural test) of the U.S.-side research of the U.S.-Japan Coordinated Program for Masonry Building Research. The testing of a five-story full-scale masonry structure will be carried out at the University of California, San Diego during 1992.

* The third Joint Technical Coordinating Committee (JTCC) on PRESSS will be held in the U.S. in October 1992. The U.S. TCC on PRESSS will meet prior to the third JTCC.

* In support of the International Decade for Natural Disaster Reduction (IDNDR) program, techniques will be explored to disseminate findings of Joint Research Projects carried out under the auspices of T/C "B" to countries with high seismic risks.

* A joint U.S.-Japan workshop on hybrid structural systems is planned to be held in September 1992 in the San Francisco bay area.

* Information exchange of following topics between appropriate U.S. and Japan Organizations will be continued;

a. Application of high strength construction materials, such as concrete and steel, to structures in high seismic zones,

b. Testings of large-scale structures other than buildings and bridges.

* Because the dynamic response of large hydraulic structures is unique, it is recommended that a study be conducted on the feasibility of creating a new task committee on seismic behavior of these structures such as dams, navigation locks and pumping stations (see Appendix). A proposal for creating a new Task Committee will be made to the full panel at the 25th Joint Meeting.

5. Information Exchange

* Technical reports and research documentation were exchanged with participating organizations in both countries.

6. Impact

* The results of the past joint research projects on reinforced concrete, steel and masonry structures have been published in both U.S. and Japanese technical journals. A number of key findings have been incorporated into U.S. and Japanese building codes and design guidelines.

* As a result of joint research projects, the state of practice and understanding in earthquake engineering has been improved in both countries. The results from the joint program above further stimulated research in both countries.

* Facilitate joint research projects utilizing available testing facilities in both countries.

7. Barriers

* There are no major technical barriers for the attainment of the Task Committee mission. However, different building practices and needs require careful planning for effective joint research projects.

* Securing funding to support exchange of research personnel is difficult in both countries. Funding agencies of both countries should be informed about the technical benefits resulting from the joint panel activities and encouraged to participate in researcher exchange and joint research programs.

APPENDIX

The seismic safety issue of large hydraulic structures is important since the risk of a major disaster due to a failure of such structures increases each year with the growth of population downstream.

Experimental and observed measures need to be compared to analytical procedures. For example, the analyses for linear and nonlinear response need to be verified with experimental and observed data. An exchange of details concerning analysis, design, and construction practices can highlight the success and needs for further research.

Report of Task Committee on

(C) REPAIR AND RETROFIT OF EXISTING STRUCTURES

Date: May 19, 1992

Place: National Institute of Standards and Technology
Gaithersburg, MD

Attendees: U.S. Side: Ken Chong (T/C "C", Chair) (NSF)
Bob Fuller (T/C "D", Chair) (HUD)
Jack Scalzi (T/C "D", Incoming Chair) (NSF)
Howard Nickerson (T/C "C") (Naval Facilities Engineering Command)
Kharaiti Lal Abrol (T/C "C") (Department of Veterans Affairs)
Larry Hultengren (DOS)
John R. Hayes, Jr. (USACERL)
Chris Stoddart (Martin Marietta/DOE) (Observer)
Charles E. Anderson (Bureau of Reclamation)
Nicholas J. Carino (Visitor, NIST)
Ugo Morelli (FEMA)

Japan Side: Hajime Asakura (Temporary member) (ACTEC)
Hiroyuki Yamanouchi (Temporary Chairman "C&D") (BRI)
Yoshikazu Kitagawa (BRI)

MISSION STATEMENT

1. Objective:

The objectives of the Task Committee are to encourage research and provide technology transfer activities in materials, components, and whole buildings and structural systems related to the repair and retrofit of existing buildings and other structures. The scope will encompass studies related to materials of construction, structural components as well as prototype structural systems.

2. Scope-of-Work

The T/C work includes information exchanges, planning, and hosting workshops and seminars. Workshops are generally held in conjunction with the annual Panel's meeting. They provide T/C members with an opportunity to review related research and to direct plans for the future, share and implement results. The T/C conducts related technical sessions at professional society's meetings. The T/C studies new materials and methods to accomplish repair and retrofit operations on buildings; e.g., fiberglass reinforced plastics, high performance concrete, post-installed anchor bolts, carbon-fibre wire, structural adhesives, and exploits use of automation and robotics

for repair and retrofit. Work focuses on coordinating research projects in U.S. and Japan to minimize duplication and to maximize benefits.

3. Accomplishments

*Status reports were delivered on recent related NSF initiatives:

- Quantitative Nondestructive Evaluation for Large Structural Systems. This initiative was issued in June 1990. Plans are underway for the second round in 1992. Interdisciplinary research teams are encouraged. Four projects were selected for support in the first round. Details of these projects and a description of the initiative are included in the proceedings of the 23rd UJNR Joint Meeting in Tsukuba, Japan.

- Repair and Rehabilitation Research for The Seismic Resistance of Structures. In early 1990, NSF announced a new 5-year research program that focuses on a coordinated research effort in the seismic repair and rehabilitation of existing structures. During the first year of the research program, FY 1990, NSF funded a total of nine projects.

In addition, cooperation and coordination efforts were initiated with other on-going seismic repair and rehabilitation programs, conducted by the National Center for Earthquake Engineering Research (NCEER), the Earthquake Engineering Research Institute (EERI) through its Existing Building Committee, the Federal Emergency Management Agency (FEMA), the Building and Fire Research Laboratory (NIST), The California Seismic Safety Commission (CSSC), and other organizations. The first coordination meeting of FY 1991 was held in Salt Lake City on February 13, 1991.

* 3 day ASCE seminars on Rehabilitation, Planning and Structural Repair of Concrete and Masonry were held in, Oakland, CA (3/90); Boston (4/90); and Washington D.C. (5/90).

* A workshop on Nondestructive Evaluation, (NDE) of Civil Structures and Materials was held in October 1990, in Boulder, Colorado. Participants came from many disciplines of engineering in academics and industries. A hardcover proceedings (406 pages) is available from the University of Colorado, Department of Civil Engineering.

* A follow-up workshop on NDE was held in May 1992, in Boulder, Colorado.

* Proceeding of the Workshop on Evaluation, Repair, and Retrofit of Structures, (NISTIR 4515), held at NIST in May 1990, was published by NIST and distributed at the 23rd UJNR Joint Meeting in Tsukuba, Japan. Copies of the proceedings were also distributed to authors, workshop participants, and other researchers and practitioners in the U.S. Twenty-two papers were presented

at the NSF sponsored workshop, of which 17 were on repair and retrofit of structures. Delegates totaled 24, 12 were from the U.S. and 12 from Japan.

* In the U.S., FEMA published ATC 21, A Handbook for Seismic Evaluation of Existing Buildings, and ATC 22 Techniques for Seismically Rehabilitating Existing Buildings. The U.S. Department of Energy and U.S. Postal Service are involved in extensive repair and retrofit projects.

* A report on "Retrofitting Buildings for Seismic Safety" was published by the National Academy of Press in 2/91.

* In Japan, the Guidelines for Evaluating and Strengthening Existing Buildings have been revised, and the Guidelines for Evaluation of Earthquake Damage and Repair Methods of Buildings was published. Both guidelines were available in August 1990, and are being implemented.

* Several on-going repair/retrofit projects at the US Army Construction Engineering Research Laboratory (CERL) include:

  o Repair/Retrofit of Non-Ductile Reinforced Concrete Frames. Shake table tests of beam-column subassemblages and scaled frames, both as-built and as upgraded using viscoelastic dampers in frame bracing.

  o Biaxial Response of Reinforced Concrete Frames, shake table tests of in-plane vs out-of-plane response of reinforced concrete frames with masonry in-fills. Future research to retest damaged walls after post-earthquake repair.

  o Strengthening of Precast Concrete Panel Connection Details Planned FY93 new start project.

4. Future Plans

* A second round of related NSF initiatives are planned for FY 92:

  - Quantitative Nondestructive Evaluation for Constructed Facilities.

  - Repair and Rehabilitation Research for the Seismic Resistance of Structures.

  - NSF/SHRP Initiative on Structural Control

  - Advanced Polymeric Materials (NSF/EPRI)

* The feasibility of establishing a Civil Infrastructure Systems Research Program is being studied at NSF.

* Supports NAE/NRC on a study of infrastructure research for 21st century.

* New initiative on innovative steel research for construction, NSF with AISI and AISC.

* Repair and retrofit of existing structures are being studied in association with a possible federal initiative on adaptation due to the global changes (MARS) program.

* New initiatives are being developed by NSF to focus on central and eastern U.S. existing structures/buildings.

* In support of IDNDR activities, T/C "C" plans to participate in task committee activities related to repair and retrofit of damages due to various disasters.

* The T/C "C" will consider joint support of a proposed U.S.-Japan workshop on "Smart and High-performance Material/Systems", by T/C "G". The workshop will possibly be conducted in 1993 in conjunction with the 25th Joint UJNR panel meeting in Tsukuba, Japan.

* A possible session on wind damages will be planned in the future in the U.S.

* The role of testing in support of evaluation of existing structures, characterization of the current conditions and qualification of retrofit approaches should be carefully examined and might be a possible topic for a future workshop.

* In Japan, BRI is considering to propose a new comprehensive research program on new structural design methodology based on the desired structural performance.

* In Japan, state-of-the-art technology for diagnosis, repair and retrofitting of damaged structures will be introduced and discussed at the IDNDR International Symposium on Earthquake Disaster Reduction Technology in commemoration of the 30th Anniversary of IISEE.

5. Information Exchange

* Published workshop reports and individual research papers; they were exchanged with the U.S. and JAPAN-side members.

* Numerous papers presented at the 24th UJNR Joint Panel Meeting are of interest to T/C "C".

6. Impact

* Contributed to development of U.S. and Japan design criteria for repairing and strengthening reinforced concrete, steel, and other buildings.

* T/C recommendations were incorporated into building codes and professional practices, as illustrated by rehabilitation programs used by the City of Los Angeles to upgrade existing masonry buildings to resist earthquake forces.

* Influenced changes to U.S. and Japan design practices to upgrade existing structures.

7. Barriers

* Greater progress needs to be made to implement available research results. Additional funding sources need to be identified to support technical activities to support committee missions and to support participant attendance at Joint Panel Meeting workshops.

Report of Task Committee on

(D) EVALUATION OF STRUCTURAL PERFORMANCE

Date: May 19, 1992 (Joint Meeting with T/C "C")

Place: National Institute of Standards and Technology
Gaithersburg, MD

Attendees: U.S. Side: Ken Chong (T/C "C", Chair) (NSF)
Bob Fuller (T/C "D", Chair) (HUD)
Jack Scalzi (T/C "D", Incoming Chair) (NSF)
Howard Nickerson (T/C "C") (Naval Facilities Engineering Command)
Kharaiti Lal Abrol (T/C "C") (Department of Veterans Affairs)
Larry Hultengren (DOS)
John R. Hayes, Jr. (USACERL)
Chris Stoddart (Martin Marietta/DOE) (Observer)
Charles E. Anderson (Bureau of Reclamation)
Nicholas J. Carino (Visitor, NIST)
Ugo Morelli (FEMA)

Japan Side: Hajime Asakura (Temporary member) (ACTEC)
Hiroyuki Yamanouchi (Temporary Chairman "C&D")(BRI)
Yoshikazu Kitagawa (BRI)

MISSION STATEMENT

1. Objective:

The objectives of this Task Committee are to develop disaster mitigation policies and programs to improve the capacity of existing structures to resist wind and seismic forces. To provide adequate performance evaluation, each country will coordinate development of condition assessment, screening, and structural analysis methodologies. Structures will be analyzed and instrumented, and then evaluated after disasters.

2. Scope of Work

* Develop an inventory of "benchmark" structures that have been analyzed and instrumented to measure wind and seismic responses.

* Develop a uniform system for screening and analyzing wind and seismic resistance capacity of structures in each country.

* Develop sensor technology, instrumentation, and "expert" systems to provide condition assessment of existing structures.

* Evaluate masonry and precast concrete buildings, and seismic base isolation systems; include results in each country's catalog of "benchmark" structures for post-disaster performance evaluation.

* Conduct workshops at future UJNR Joint Panel Meetings, cooperatively with T/C "C".

3. Accomplishments

* TCCMAR Reports by Englekirk and Hart were published in Feb. 1992. Copies were furnished to the Japanese side.

* Further status reports on recent U.S. legislation were presented at the 24th Joint Panel Meeting: 1990 National Affordable Housing Act, Sec. 947 on Seismic Safety Standards. National Earthquake Hazards Reduction Program Reauthorization Act; Public Law 101-614, Nov. 16, 1990. Sec. 8 on Seismic Standards.

* Information was exchanged on the activities of each country in the International Decade on Natural Disaster Reduction (IDNDR), pertaining to winds and earthquakes. A report entitled: Hazard-Proofing the Nation, Strategy to Reduce Natural Disasters was developed by the Subcommittee on Natural Disaster Reduction, a part of the U.S. Federal Coordinating Council for Science and Technology, and printed in June 1992. Included in the research and implementation strategies are risk assessment and mitigation programs. Copies will be mailed to the Japanese members.

* Status reports of several FEMA - ATC projects were discussed, including those on seismic risk assessment of existing structures. FEMA is planning a Loss Assessment Research Project to be conducted over the next several years.

4. Future Plans

* Develop a reporting system and data collection form for building inventory and performance standard, and compile a computer data file for exchange between countries. Report at each Joint Panel Meeting.

* Continue to encourage participation by private industry, consulting engineering firms, universities, funding agencies and State and local government agencies involved in instrumentation, evaluation, and condition assessment of existing buildings.

* Monitor development of sensor technology and instrumentation of structures for condition assessment, and to measure long-term aging effects on building components.

* Participate in coordination of Joint Panel activities in the International Decade for Natural Disaster Reduction (IDNDR), pertaining to structural performance evaluation.

* A workshop on Structural Performance Evaluation was discussed to be held in Japan 1993. The workshop will place emphasis on Non-Destructive Evaluation (NDE).

5. Information Exchange

* Technical documents exchanged, and pertinent Japanese papers delivered at the 24th Joint Panel Meeting.

* Japanese side will send to the U.S. T/C Chairman a copy of the "Design Guidelines for Medium Rise Reinforced Masonry Buildings" developed by TCCMAR-Japan. U.S. Side will explore feasibility of translating this manuscript into English.

6. Impact

* Enables the development of revised standards and building code provisions to prevent destruction from high winds and earthquakes.

* Provides engineers with the capability to conduct condition assessment of existing structures for the purpose of developing cost effective repair, retrofit, strengthening or demolition programs.

* Will increase the confidence level of the public, regulators, policy makers and engineers, to be assured that the majority of major structures will perform adequately to resist high wind and earthquake forces.

7. Barriers

* Insufficient resources to document load-carrying capacity of existing buildings subjected to probable extreme winds and earthquakes.

* Difficulty in developing probability risk maps for tornadoes, typhoons, and hurricanes.

* Limited resources for instrumenting buildings, for conducting post-disaster evaluations, and for participating in foreign travel for coordination of activities.

Report of Task Committee on

(E) GROUND MOTION AND SEISMIC DESIGN FORCE

Date: May 19, 1992

Place: National Institute of Standards and Technology
Gaithersburg, MD

Attendees:	U.S. Side -	Walter Hays, (Acting Chairman)	(USGS)
		Jim Hill	(DOE)
		Jeff Kimball	(DOE)
		Mike Mahoney	(FEMA)
		Mehmet Celebi	(USGS)
	Japan Side -	Kazuhiko Kawashima (Chairman)	(PWRI)
		Keiichi Ohtani	(NIED)

MISSION STATEMENT

1. Objective:

The objectives of this Task Committee are to develop techniques and exchange information and experiences on: 1) engineering characterization of ground motion, 2) mapping techniques for displaying ground motion data, 3) microzonation, 4) siting and design applications, and 5) earthquake hazard risk assessment.

2. Scope of Work

Plan and conduct cooperative research, T/C workshops and meetings, These meetings and workshops are generally held in conjunction with the annual Panel Meeting on Wind and Seismic Effects. Activities include:

- Conduct cooperative research programs

- Exchange research personnel

- Exchange information on a timely basis

- Cooperate in contributing to the goals of the IDNDR

3. Accomplishments

The First U.S.-Japan Workshop on Hazard/Risk Assessment and Design Earthquake Loading was sponsored by the Task Committee E, and was held on May 28-29, 1991

at the Public Works Research Institute, Tsukuba, Japan. Four presentations from U.S. -side and ten presentations from Japan-side were made. During the technical site visits, tours to the sites of large bridge constructions were made and technical discussions on seismic design loading were conducted.

4. Future Plan

Plan the 2nd Workshop on "Ground Motion and Seismic Design Force" with emphasis on subduction zone earthquakes. This Workshop will be held in Japan in May 1993. Three themes will be developed: 1)Data analysis and modeling, 2) Engineering characterization of ground motion and ground strain, and 3) Siting and design applications. Topics will include: attenuation of ground motion with magnitude and distance; linear, nonlinear, and energy response spectra for rock and soil; prediction of strong motion; probabilistic representation; uncertainty; types and importance of structures; soil structure interaction; scenario earthquakes; loss estimation; and zoning maps for siting, design and construction.

5. Information Exchange

Technical reports and research documentation were exchanged with participating organizations in both countries.

6. Impact

Task committee efforts influence the national seismic codes concerning input seismic forces.

7. Barriers

Lack of funding for travel to conduct workshops and related meetings has been the principal barrier in the past. To increase benefits to funding agencies of each country, a study tour is being planned.

Report of Task Committee on

(F) DISASTER PREVENTION METHODS FOR LIFELINE SYSTEMS

Date: May 20, 1992

Place: National Institute of Standards and Technology
Gaithersburg, Maryland

Attendees:	U.S. Side -	R. Dikkers (Chairman)	(NIST)
		H. Bosh	(FHWA)
		J. Cooper	(FHWA)
		R. Chung	(NIST)
		J. Hill	(DOE)
		P. Harben	(LLNL-DOE)
	Japan Side -	K. Kawashima (Acting Chairman)	(PWRI)
		O. Nakano	(HDB)
		H. Asakura	(ACTC)

MISSION STATEMENT

1. Objective

The objectives of Task Committee "F" are to improve: 1) the behavior of lifeline systems during earthquakes and 2) engineering and other seismic countermeasures such as damage estimation techniques and inspection procedures. These technologies provide users with improvements to existing standards of practice for safety and serviceability of lifeline systems. Lifeline systems such as gas, oil, water, and sewage pipelines; and power, communication, and transportation systems are crucial to the survival and health of a city or community. Earthquakes affecting such systems cause severe social and economic disruptions to communities and cause human suffering to the residents.

2. Scope of Work

* Plan and conduct T/C workshops and meetings. The purpose is to exchange the state-of-the-art knowledge and practice, and to identify key cooperative opportunities for exchange and studies which effectively implement research results.

* Conduct related technical sessions at professional society meetings.

* Develop research programs on selected lifeline systems (similar in concept to the Large-Scale Testing Program). For example, through joint demonstration, produce criteria for emergency design and loss evaluation and on-line

monitoring systems for lifeline operation.

* Conduct special activities such as translating, printing, and distributing MOC PWRI's publication Manual for Repair Methods for Civil Engineering Structures Damaged by Earthquakes.

* Develop performance standards and a manual on repair, restoration, and retrofit of lifelines.

3. Accomplishments

* Conducted the 4th Joint Workshop on Earthquake Disaster Prevention for Lifeline Systems on August 19-21, 1991, in Los Angeles, California.

* Contributed technical papers on lifeline systems at the 24th joint panel meeting.

* Participated in promoting the goals of the IDNDR.

* Developed a seismic design manual for underground structures (Japan Side).

4. Future Plan

* Conduct the 5th Joint Workshop on Earthquake Disaster Prevention for Lifeline Systems on October 26 - 27, 1992, in Tsukuba, Japan. A technical study tour will follow the technical sessions.

* Encourage current efforts in both countries to establish seismic design guidelines and standards for lifeline systems. Existing UJNR channels should be fully utilized to facilitate the exchange of relevant information concerning standards development. Possible collaboration of joint development lifeline systems standards and guidelines should be pursued.

* Continue observation of instrumented buried pipes in Parkfield, California, and Chiba, Japan, and exchange data.

5. Information Exchange

* Domestic community: through technical meetings, conference sessions, seminars, and workshops.

* Between U.S. and Japan: through T/C Workshops and annual Joint Panel Meetings.

* Visits by researchers and participation in technical meetings sponsored by organizations such as NCEER, EERI and ASCE.

* Short-term (3 to 12 months) researcher exchanges to participate in on-going lifeline research.

6. Impact

* Contributed to the increase of field engineers' technical knowledge on repair methods, through seminars with lectures by T/C members using the MOC Manual n Japan: more than two thousand participants attended seminars.

* Contributed to the development and assessment of design, construction, and operating standards for lifeline earthquake engineering (TCLEE/ASCE) via T/C members' participation in committee work.

7. Barriers

* Lack of sufficient funds to conduct annual Task Committee Workshops and to publish proceedings and reports.

Report of Task Committee on

(G) PASSIVE, ACTIVE, AND HYBRID CONTROL SYSTEMS

Date: May 20, 1992

Place: National Institute of Standards and Technology
Gaithersburg, MD

Attendees:

U.S. Side -	S. C. Liu (Chairman)	(NSF)
	Jack Hayes	(CERL)
	Chris Stoddart	(Martin Marietta/DOE)
	Richard Sause	(Lehigh Univ.)
Japan Side -	Y. Kitagawa (Chairman)	(BRI)
	M. Fujiwara	(PWRI)
	H. Yamanouchi	(BRI)

MISSION STATEMENT

1. Objective:

The objectives of the Task Committee are to: (1) develop research plans in passive, active, and hybrid control of structures and equipment, (2) implement such control techniques as computerized motion reduction or modification devices/systems in actual design and construction of structural engineering facilities under seismic or wind environments, (3) promote U.S. -Japan cooperation in structural control research (4) bring together governmental, academic, and industrial participants in joint pursuit of such efforts, and (5) contribute to IDNDR by organizing joint research and other technical activities in structural control on the basis of international cooperation.

2. Scope of Work

The UJNR T/C "G" works closely with other organizations to provide the leadership in control research efforts by facilitating the exchange of technical data and information through the established UJNR mechanisms. Work includes:

i) Providing technical assistance, consultation and coordination to UJNR affiliated research agencies in the initiation, development, and execution of their programs in structural control research.

ii) Promoting joint government-university-industry collaborative efforts to facilitate technology transfer and practical implementation.

iii) Sponsoring and conducting multi-disciplinary workshops and meetings to identify key areas of research and opportunities for cooperation, and to exchange new knowledge and experience in practice.

iv) Developing promotional and demonstrative activities to stimulate public awareness and interest in this emerging field of research.

v) Establishing performance standards, design specifications, guidelines and code recommendations for application in new construction as well as retrofit/rehabilitation of existing structures with control systems.

vi) Initiating research in new intelligent materials, high-tech sensors, optimal control systems design, and laboratory and field experiments of prototype and full-scale structures.

3. Accomplishments

i) The U.S. Panel on Structural Control Research worked closely with its counterpart Japanese Panel in exchanging technical information and developing joint research plans.

ii) In cooperation with T/C "J", a "U.S.-Japan Workshop on Earthquake Protective System (Passive Control System)" was held at NCEER, Buffalo, New York, on September 4 and 5, 1991. A study tour to inspect base-isolated bridges across the U.S. was conducted by participants prior to and following the Workshop. I. G. Buckle of NCEER and UJNR Panel members S. C. Liu, M. Shinozuka, K. Kawashima, and 61 researchers from the U.S., Japan, and Taiwan participated in the technical activities. Proceedings of the Workshop is being published by NCEER.

iii) The "Japan National Symposium/Workshop on Active Structural Response Control" was held on March 23-25, 1991, in Tokyo, Japan. The Symposium was organized by Japan National Working Group on Active Structural Response Control, Earthquake Engineering Research Liaison Committee, Science Council of Japan (SCJ). UJNR Panel members S. C. Liu, M. Shinozuka, Y. Kitagawa, and K. Kawashima participated in the Symposium's technical activities. The workshop identified three major areas of research in structural control. They are control theory, devices and systems, and structural design. Preliminary Proceedings of the Symposium was published by SCJ.

iv) The "International Workshop on Recent Development in Base Isolation Techniques for Building" organized by the Architectural Institute of Japan (AIJ) was held in April 1992, in Tokyo, Japan. UJNR panel members Y. Kitagawa and K. Kawashima participated in the Workshop's technical

activities. The Workshop identified four specific topics for future efforts: design concept and code requirements, estimation of seismic input and structural response, behavior of isolators and dampers, and practical applications and field observations. Proceedings of the International Workshop was published by AIJ.

v) A trilateral U.S.-Italy-Japan Workshop/Seminar on Intelligent Systems was held in Perugia, Italy, June 27-29, 1991. Investigators from the U.S., Italy, Japan, and other Western European countries gave presentations of papers and participated in group discussions. UJNR members S. C. Liu, H. J. Lagorio, Ken Chong, William Anderson, etc., contributed papers and H. J. Lagorio participated in the meeting.

vi) Under the NSF initiative on "Structural Control Research for Safety, Performance, and Hazards Mitigation," sixty seven (67) proposals were submitted by the U.S. research community. Approximately ten (10) proposals are being selected for funding during the first year (FY 92) of the 5-year program.

4. Future Plans

i) In cooperation with T/C "J", a "Second U.S.-Japan Workshop on Passive and Active Control of Bridges Against Earthquakes" is scheduled for December 1992 at PWRI, Tsukuba. A study tour to inspect base-isolated bridges across Japan is being planned for the participants prior to and following the Workshop (Workshop Co-Chairmen: Ian Buckle/NCEER and K. Kawashima/PWRI).

ii) In cooperation with T/C "J", support of development and implementation of innovative base-isolation technology for bridge structure will continue.

iii) Specific Task Committee work plans are being developed for coming year (1992-1993) and for the next five years.

iv) Research cooperation between the U.S. and Japan will be pursued using such channels as the UJNR and other inter-governmental mechanisms as the U.S. and Japan Panel on Structural Control. Specific plans to promote "The U.S.-Japan Cooperation Research Project" on active and hybrid control systems are being studied by NSF, BRI, and PWRI.

v) Joint research projects on hybrid control of bridges are on-going by PWRI, NIST, FHWA, NCEER, and University of California, Irvine.

vi) The Construction Engineering Research Laboratory (CERL) will initiative work in July 1992 on active control of building structures using shape memory alloy. UJNR member Jack Hayes is project coordinator of this

research.

vii) A joint U.S.-Japan Workshop on "Smart and High-Performance Materials Systems" will be planned in the near future. If possible this workshop shall be in conjunction with the 25th Joint UJNR panel meeting in Tsukuba, Japan. T/C "C" will be invited to join and help sponsor this Workshop.

viii) Joint research projects on active and hybrid control of buildings are being developed by BRI, NCEER and University of California, Irvine.

ix) At BRI, research programs on structural control of buildings have been developed and implemented under the direction of UJNR member Y. Kitagawa. Shaking-table tests of scaled control models will be carried out in January 1993. Collaborative research program involving possible organizations and private companies are being developed.

5. Information Exchanges

Technical materials on structural response and control systems were exchanged.

6. Impact

The T/C "G" has stimulated research communities from both sides to initiate multi-disciplinary studies and cooperative investigation in structural control.

7. Barriers

No technical barriers are identified at the present time. However, lack of sufficient financial backing from both sides may present difficulties in achieving the objectives of T/C "G".

Report of Task Committee on

(H) SOIL BEHAVIOR AND STABILITY DURING EARTHQUAKES

Date: May 19, 1992

Place: National Institute of Standards and Technology
Gaithersburg, MD

Attendees: U.S. Side - A. G. Franklin (Chairman) (WES)
M. G. Katona (AFCEL)

Japan Side - K. Yokoyama (Temp. Chairman) (PWRI)
Y. Yamaguchi (PWRI)
J. Koseki (PWRI)

MISSION STATEMENT

1. Objective:

Government agencies with responsibility for public works have the need to assure their seismic safety and to provide economical protection against earthquake hazards. The objective of this Task Committee is to assist in meeting those needs by enhancing the available technology for predicting the dynamic behavior of soils, analyzing dynamic soil-structure interaction, and modifying the earthquake behavior of foundations and earth structures in order to assure their safe performance during earthquakes.

2. Scope of Work

* Present technical papers at annual joint panel meetings on technological developments and on state-of-the-art and practice related to soil behavior and stability during earthquakes.

* Exchange information and technical data relating to field performance, research, and methods of practice.

* Plan and conduct T/C workshops in coordination with proposed or on-going cooperative research programs.

* The Task Committee plans and conducts programs of cooperative research, exchange of researchers between U.S. and Japanese research institutions, publication of research results and recommended practice. The benefits realized from available research funds can be amplified by

bringing greater resources to bear on problems of mutual interest, and by coordinating research tasks to make the best use of the respective strengths of the two sides' research capabilities.

* Exchange visiting researchers using mechanisms provided by formal and informal cooperative research programs. Such exchanges promote technical information exchanges, familiarization with methods of practice on the respective sides, and mutual understanding and cooperative relationships between researchers on the two sides.

3. Accomplishments

* U.S. researchers presented 5 papers and Japanese researchers presented 10 papers, on soil behavior and stability during earthquakes, at the 23rd and 24th Joint Panel Meetings. 5/91, 5/92

* The International Workshop on Remedial Treatment of Potentially Liquefiable Soils was conducted at PWRI in Tsukuba from 22 to 25 January 1991. Nineteen papers were presented. 1/91

* Mr. Ken-ichi Tokida, the T/C (H) Japan Chairman, visited St. Louis and met Mr. R. H. Ledbetter of the U.S. Army Engineer Waterways Experiment Station and discussed the Proceedings of the International Workshop held in January and plans for the next Workshop. 3/91

* Proceedings of the International Workshop on Remedial Treatment of Potentially Liquefiable Soils was published and distributed to the members of Task Committee (H) and participants of the Workshop. 3/91, 5/91

* The English language report on the expert team of Japan Disaster Relief Team (JDR) on the earthquake in the Philippines of July 16, 1990, was provided to the U.S. side. 5/91

* T/C (H) has relinquished its responsibility for consideration of marine structures subject to earthquakes and the measurement of sea floor earthquake motions to the new Task Committee (K) on Wind and Earthquake Engineering for Offshore and Coastal Structures, recognized at the 23rd Joint Panel Meeting. 5/91

* Mr. Jun-ichi Koseki of the PWRI is a one-year Guest Researcher at Massachusetts Institute of Technology, working on Liquefaction Risk Analysis. 8/91

* Dr. Richard H. Ledbetter, of the U.S. Army Engineer Waterways Experiment Station, visited Japan in September 1991. Information

exchange and fundamental discussion to start the U.S.-Japan joint research through T/C "H", on remedial treatment of liquefiable soils were conducted, and fundamental subjects were agreed upon. 9/91

* Mr. Yoshikazu Yamaguchi of the PWRI is a one-year Guest Researcher at the U.S. Army Engineer Waterways Experiment Station where he is studying water seepage in dam foundations. 12/91

4. Future Plans:

* The Waterways Experiment Station has initiated a new research project "Repair, Evaluation, Maintenance, and Rehabilitation Research (REMR)" (for the U.S. fiscal-years 1992 - 1996). 10/91

* The Public Works Research Institute and the Building Research Institute have initiated a new research and development project "Research and Development on Earthquake Disaster Prevention in Large Urban Area" (for the Japan-fiscal years 1992 - 1996). 4/92

* The National Research Institute for Earth Science and Disaster Prevention, the Building Research Institute, and Wayne State University have initiated the cooperative research "Research on Earthquake Pile Resistance in Liquefied Soils". 4/92

* Identification of research tasks on preventive measures against soil liquefaction that are of common interest, in accordance with the results of the planning meeting held at Tsukuba in May 1989 and at Yokohama in September 1991. 9/92

* T/C (H) proposes to hold the next U.S.-Japan Workshop on Remedial Treatment of Potentially Liquefiable Soils in Japan, in October 1993. 10/93

* T/C (H) at the 22nd Joint Panel Meeting, discussed the need for technological innovation and research to assist in saving lives following natural disasters caused by earthquakes. The principal areas of need were identified as improved technology for locating survivors and the development of new equipment and systems for safe excavation of debris to remove survivors from collapsed structures. T/C (H) recognizes this subject is outside their area of responsibility but feels it is important and should be discussed by the full Joint Panel.

The Task Committee suggests the following options for implementation:

(1) Explore a new Task Committee which will address this topic area and provide the focal point to share experience and research in this area.

(2) Incorporate this topic into another existing T/C.

T/C (H) will continue to explore methods whereby this topic will receive appropriate attention.

5. Information Exchange:

* T/C workshops, exchange of visitors, participation in annual joint panel meetings, and presenting technical papers.

* Exchange of researchers between U.S. and Japanese government laboratories.

* Visits by researchers and participation in technical activities such as post-earthquake field investigation.

* Fostering professional community contacts in the U.S. and Japan, publication of papers in journals, publication of research reports by the respective agencies, participation in professional society meetings and conferences, and workshops.

6. Impact

* Through the exchange of researchers and the diffusion of earthquake related technical data, experience, and information on methods of practice, the state of technology in geotechnical earthquake engineering has been raised on both sides.

* Through the cooperative research program on in-situ testing of soils which was carried out after the 1983 Nihonkai-Chubu Earthquake, improved and more accurate methods of using in-situ tests for evaluating the liquefaction potential of soils were achieved: these have been in general use in the United States since 1985. The Loma Prieta Earthquake stimulated renewed awareness of the need for further research in soil liquefaction and amplification effects of soft soils.

* Through the workshops on remedial treatment of potentially liquefiable soils held in 1988 and 1991, beneficial information on recent technology were exchanged and contributed to progress future research of both U.S.-and Japan-sides.

7. Barriers

* Insufficient U.S. and Japan Government funds allocated to adequately address earthquake engineering research.

* Department of Army administrative limitation on foreign travel.

Report of Task Committee on

(I) STORM SURGE AND TSUNAMI

Date: May 20, 1992

Place: National Institute of Standards and Technology
Gaithersburg, MD

Attendees: U.S. Side - H. Meyers (Chairman) (NOAA)
W. E. Roper (COE)

Japan Side - K. Yokoyama (Acting Chairman) (PWRI)
K. Shioji (PWRI)

MISSION STATEMENT

1. Objective:

The objective of this Task Committee is to mitigate damages from storm surges and tsunamis through shared technologies, research, information sharing, and cooperative work. Storm surge and tsunami are hazards capable of inflicting damage of disastrous proportions. Storm surges are associated with hurricanes and typhoons where high winds and the mounding of water under the low barometric pressure of the storm's eye can cause extensive flooding and severe wave action. These often can be tracked for days in advance of a landfall but the location of the landfall center is difficult to predict. Tsunamis are predominately caused by underwater earthquakes and, to a lesser extent volcanic and land slide activity. Depending on the distance from the source, tsunamis arrive within minutes to up to a day after generation.

2. Scope of Work:

* Exchange results of research on storm surge and tsunami occurrence, generation, propagation, and coastal effects. This includes observations on historical, current, and theoretical tsunamis. Of particular interest is the effort by U.S. and Japan to acquire deep ocean tsunami measurements.

* Exchange results and status of anti-storm surge and tsunami activities including analysis of the problem, planning, warning, and engineering approaches.

* Exchange information on planned and on-going projects relating to storm surge and tsunamis.

* Exchange information on development of technologies such as computer programs to predict travel times, land-fall locations, run-up heights, and wave characteristics and analysis; improved instrumentation, and use of satellite communications for detection and warning.

* Facilitate dissemination through exchange of literature, technical reports at joint meetings, special workshops, joint projects, and direct interaction among participants.

3. Accomplishments

* Copies of preliminary marigrams from the April 25, 1992 Northern California earthquake and tsunami were distributed to the Japanese side.

* The U.S. side has compiled detailed information on all tsunamis affecting the U.S. and its possessions. The publication, "United States Tsunamis 1690-1989" has been printed and given to the Japanese side.

* A Second Tsunami Workshop was held on November 5-7, 1990 in Honolulu, Hawaii. Nine members participated from the Japanese side and about 20 from the U.S. side. Site visits were made to Hilo as part of the Workshop. Proceedings were published and were sent to all members.

4. Future Plans

* Develop exchanges of data and information on activities related to tsunami measurements including deep ocean measurements. Deep ocean bottom gages will be recovered in June 1992 from the ocean bottom stations which are expected to have recorded the small tsunamis for the April 25, 1992, Northern California earthquake and tsunami. This event was recorded by Hawaiian and U.S. West Coast shore based marigraphs. The seafloor topography of the source area will be re-surveyed. These will be shared with the Japan side.

* Develop activities and information exchanges to support the International Decade of Natural Disaster Reduction.

* Explore and promote joint undertakings such as tsunami gauge testing, scientist exchange, satellite communication for tsunami warning, and assistance in contacts within the U.S. and Japan.

* Increase the participation of storm surge experts in the Panel and T/C meetings.

* The U.S. and Japanese sides agree that there is a need to hold workshops at about 2 or 3 year intervals to exchange the latest research and technology relating to various aspects of storm surge and tsunami hazards. A third workshop including both storm surge and tsunamis is planned for August, 19-20, 1993 in Tskuba, Japan, near the time of the International Union of Geodesy and Geophysics (IUGG) Tsunami Commission Symposium. The Workshop will include about 10 academic researchers and some additional Government Task Committee members from the US side and similar numbers from Japan. There will be about an even split between the storm surge and tsunami problems.

* 1996 will be the 100th anniversary of the great Sanriku Earthquake and tsunami in Japan and the 50th anniversary of the April 1, 1946 Aleutian earthquake and tsunami. These events led to the creation of warning systems and much of the current activity in this field. The Task Committee is beginning to plan for a Joint Commemorative Symposium or other observance.

* The U.S. side is completing a detailed study of tsunamis affecting the US West Coast including copies of all available marigrams. This will be published in the fall of 1992 and shared with the Japan side. Also, at the request of UNESCO-ITSU, the U.S. side will publish a catalog of tsunamis affecting the West Coast of Mexico compiled by Sanchez and Farreras, the Mexican authors.

5. Information Exchange

* Continue exchange of publications, bibliographic data, technical reports, and personal contacts.

6. Impact

* Increased cooperation among scientists and engineers working in these fields.

* Hasten implementation of new modeling and design techniques developed by the U.S. and Japan.

7. Barriers

* Insufficient funding from government and private sector organizations to participate in T/C workshops and the Panel's annual joint meetings.

* The tsunami problem is less severe in the U.S. than in Japan which leads to a smaller community of researchers. There are few U.S. researchers focusing on tsunamis at any specific location; thus highlighting the importance of T/C periodic meetings and workshops.

* There are different approaches and degree of significance in dealing with problems in the U.S. and Japan. For example, in the U.S. much of the hazard is from remote sources which leads the government to emphasize developments of warning and evacuation schemes. In Japan the engineering approach is needed because there are more locally generated tsunamis which often do not provide sufficient times for adequate warning and evacuation. This barrier is partially being addressed by inviting U.S. engineers and non-government specialists to participate during the annual meetings.

* The storm surge research community is less well organized and lacking the specialty societies, journals, and international organizations to define and stimulate work in the field. The Task Committee (I) can help fill this gap.

Report of Task Committee on

(J) WIND AND EARTHQUAKE ENGINEERING FOR TRANSPORTATION SYSTEMS

Date: May 19, 1992

Place: National Institute of Standards and Technology
Gaithersburg, MD

Attendees: U.S. Side - J. D. Cooper (Chairman) (FHWA)
C. Barrientos (NOAA)
R. Dikkers (NIST)
J. Scalzi (NSF)
H. S. Lew (NIST)

Japan side - M. Fujiwara (Chairman) (PWRI)
O. Nakano (Hokaido Development Bureau)

MISSION STATEMENT

1. Objective:

The objectives of this Task Committee are to plan, promote, and foster research on the behavior of highway bridges when subjected to wind and seismic forces and to disseminate research results and provide specifications and guidelines based on the Task Committee's findings. Surface transportation systems play a vital role in the movement of goods and people. Highway bridges are especially influenced by the forces of wind and earthquakes because of their open exposure to those forces.

2. Scope of Work:

The scope of work is applicable mostly to highway bridges without limitation on their size and function including: existing bridge and new bridge designs; whole system of bridges; and/or single components of a bridge.

The mission is performed through:

* Conducting workshops, exchanging researchers, developing methods for design evaluations and test procedures, developing inspection techniques, rehabilitation and maintenance specifications and policies, and performing cooperative research programs and other relevant cooperative administrative activities.

3. Accomplishments (past 2 years)

* The Japanese side hosted the first U.S.-Japan Workshop on Seismic Retrofit for Bridges under the auspices of T/C "J" December 17 to 22, 1990 to discuss and review practical seismic retrofit applications in both countries. Nineteen technical presentations were made by 5 U.S. researchers and 30 Japanese researchers. Technical topics include the history of developing retrofit techniques for bridges; damage assessment from the Loma Prieta earthquake; discussion on condition assessment and prioritization of bridges for seismic retrofit; seismic strengthening methods; and research in progress. Site visits were made to view retrofit technology applied to bridges on Tokyo metropolitan expressways. Workshop Proceedings were disseminated in both countries.

* In cooperation with T/C "G", the U.S. side hosted an Ad Hoc Workshop on Seismic Response Control of Bridge Structures in September 1991 at the National Center for Earthquake Engineering Research to continue discussion and review practical seismic active, passive and hybrid control applications in both countries. Participants toured seismically isolated bridges in the U.S.

* Conducted coordinated research studies on seismic performance of bridge piers and columns. Details of this work involved determining the performance of reinforced concrete piers and columns subjected to dynamic cyclic loading, performing model tests on the failure of reinforced concrete piers, testing full and large-scale concrete columns and for the behavior of concrete filled steel tubes.

* Held the eighth bridge workshop in Chicago, Illinois in May 1992 which was followed by site visits to major bridges along the Mississippi River at Burlington, Iowa; Quincy, Illinois; Alton, Illinois; and St. Louis, Missouri. Main themes of the workshop included: (1) Long-Span Bridges; (2) Wind Effects and Codes; (3) Seismic Issues; (4) Design; (5) Bearings; (6) Foundations; and (7) Evaluation, Rating and Management. Held the seventh bridge workshop in Tsukuba, Japan in May 1991, which was followed by site visits of Higashi Kobe Bridge, Kansai International Airport, and Akashi Kaikyo Bridge.

* Both sides presented technical papers at the 23rd and 24th UJNR Joint Meetings and participated in technical study tours to buildings, bridges, factories, construction sites, and instrumented structures.

4. Future Plans

* Conduct the 9th bridge workshop just prior to the 25th Joint Panel

meeting in Tsukuba, Japan.

* Plan to host a 2nd U.S.-Japan Workshop on Seismic Retrofit of Bridges in the U.S. The Workshop will focus on practical seismic retrofit measures.

* Continue to investigate and exchange technical information on improved seismic retrofit and strengthening procedures for highway bridges based on experimental, analytical, and field studies. This exchange should include information on maintenance of existing bridges.

* Continue experimental research study on the seismic performance of bridge piers and columns, and support emphasis on base isolation and hybrid control of bridges in cooperation with T/C "G". The 2nd Workshop on seismic control is planned for December 1992 in Tsukuba.

* Develop a coordinated research study on seismic, aeroelastic, and aerodynamic response of cable-supported bridges with emphasis on cable inspection, vibration, control and corrosion protection.

* Continue a coordinated research study to compare the seismic design criteria for bridges in Japan and the U.S. and discuss the method and analysis procedures for bridge column design. Information on application of limit state design method continues to be exchanged.

* Encourage a coordinated research study on seismic response and control, system identification techniques, and nondestructive evaluation of bridge structures.

* Encourage a coordinated research study on use and performance of structural materials including new materials.

* Encourage a coordinated study on performance of jointless bridges.

5. Information Exchange

* Exchanged technical reports, research program documentation, construction logs, design plans, and assorted photographs and videos, including technical data appropriate for investigating the Philippine earthquake of 1990.

* FHWA hosted PWRI visitors Messrs. K. Kohno, H. Kanzaki, A. Fujimoto, and J. Inoue. Mr. Inoue studied for five months at the Turner-Fairbank Highway Research Center and visited State highway agencies in Virginia, Maryland, Pennsylvania and California to study bridge maintenance and management. Mr. Inoue prepared a report entitled "Comparison of

Highway Bridge Maintenance Between the U.S. and Japan".

* Mr. Mohsen Sultan, California Department of Transportation conducted a study on the comparison of Seismic Design for U.S. and Japanese bridges during a one year exchange with PWRI in Tsukuba.

6. Impact

* The free exchange of literature, instrumentation technology, and earthquake response data has led to the advancement in design technology, and development of preliminary retrofit guidelines, and to the calibration and verification of specifications.

* Greater uniformity was achieved in wind engineering test procedures and modeling resulting in more efficient solutions to the aerodynamic bridge problem.

* The workshop and study tours in the two countries have facilitated technology transfer. Examples include retrofit technology, cable protection and vibration suppression of cable-stayed bridges.

* A set of priorities for needed research from a more international viewpoint has reduced the conduct of duplicative research efforts.

7. Barriers

There are no major technical barriers to achieve the Task Committee mission. However, financial barriers, especially funding needed to participate in workshops and panel meetings and for conducting actual bridge tests and large-scale model tests, continue to limit the effectiveness of the work in this Task Committee's work.

Report of Task Committee on

(K) WIND AND EARTHQUAKE ENGINEERING FOR OFFSHORE AND COASTAL FACILITIES

Date: May 20, 1992

Place: National Institute of Standards and Technology
Gaithersburg, MD

Attendees:			
	U.S. Side -	C. Smith (Chairman)	(MMS)
		G. Brady	(USGS)
		W. Roper	(COE)
		M. Miller	(WES)
	Japan Side -	S. Noda (Temporary Chairman)	(PHRI)
		K. Yokoyama	(PWRI)
		J. Koseki	(PWRI)

MISSION STATEMENT

1. Objective:

The objective of this Task Committee is to develop technical insights necessary to mitigate damage to offshore and coastal facilities due to extreme wind and seismic effects. The Task Committee will plan, promote, and develop research initiatives to meet this objective, and will disseminate the results of their research for incorporation into future specification or design guidelines.

Criteria for the design of offshore and coastal facilities may differ greatly from their onshore counterparts. These differences can arise due to their unique design or mass distribution, to the fluid/structure or wind/structure interaction, to the placement of foundation elements in or on soft, fully saturated soils that can be subject to large hydrodynamic pressures, and to the lack of specific environmental data or the engineering experience that has been developed for most onshore sites.

2. Scope of Work

The Task Committee's work spans a broad spectrum of scientific and engineering disciplines to include a variety of geoscience, structural, mechanical, and marine topics. Structures of interest include offshore oil and gas facilities, aids to navigation, breakwaters, bulkheads, and other coastal facilities. The Task Committee will provide

the forum for the communication between the above disciplines as they impact the stated objective. Items of specific interest include the following:

* Sponsoring and conducting workshops and meetings to identify key areas of research, opportunities for cooperation, and the exchange of knowledge.

* Predicting strong ground motions for offshore and coastal sites including assessing the effects of basin geometry, linear, and nonlinear local geological effects using actual seafloor response measurements.

* Determining the dynamic response and the interaction of structure/foundation/soil systems to seabed motions and/or extreme wind forces.

* Assessing the dynamic response and behavior of various operational facilities mounted on offshore and coastal structures.

* Developing assessment methodologies for seismicity and other characteristics of potential seismic sources (e.g. faults) for offshore and coastal sites in regards to how these conditions relate to structural design criteria.

* Promoting the implementation of new research results into current design and construction processes.

* Developing research efforts to include laboratory and field programs to obtain data on the response of offshore and coastal facilities to extreme wind and seismic forces.

* Creating performance standards, design specifications, guidelines, and code recommendations for application to new construction as well as remedial action for existing facilities.

3. Accomplishments

* Established T/C scope of work and T/C operational plan.

4. Future Plans

* Hold a U.S./Japan Workshop on Wind and Earthquake Engineering for Offshore and Coastal Facilities the week before the 25th Joint UJNR Meeting at the Port and Harbour Research Institute in Yokosuka, Japan.

* Develop workshop agenda and finalize list of speakers from both the U.S. and Japan Side.

* Coordinate, where possible, on-going research on wind and earthquake engineering for offshore and coastal facilities of interest to the members of the Task Committee.

5. Information Exchange

* With Japan and U.S. members through T/C meetings and annual joint meetings.

* With the Engineering and Scientific community through meetings, conference sessions, seminars, and workshops.

6. Impact

* Increased cooperation among scientists and engineers concerned with the seismic design of offshore and coastal facilities.

* Increased awareness of problems and risks associated with seismic events affecting offshore and coastal facilities.

7. Barriers

* Insufficient funding to sponsor a strong research initiative and to support travel and the exchange of personnel.

* Not enough awareness, especially on the U.S.-side of the importance of investigating the risks associated with seismic concerns for offshore and coastal facilities.

NIST-114A
(REV. 3-90)

U.S. DEPARTMENT OF COMMERCE
NATIONAL INSTITUTE OF STANDARDS AND TECHNOLOGY

BIBLIOGRAPHIC DATA SHEET

1. PUBLICATION OR REPORT NUMBER
NIST/SP-843

2. PERFORMING ORGANIZATION REPORT NUMBER

3. PUBLICATION DATE
September 1992

4. TITLE AND SUBTITLE

Wind and Seismic Effects
Proceedings of the 24th Joint Meeting of the U.S.-Japan Cooperative Program in Natural Resources Panel on Wind and Seismic Effects

5. AUTHOR(S)

Noel J. Raufaste

6. PERFORMING ORGANIZATION (IF JOINT OR OTHER THAN NIST, SEE INSTRUCTIONS)

U.S. DEPARTMENT OF COMMERCE
NATIONAL INSTITUTE OF STANDARDS AND TECHNOLOGY (BFRL)
GAITHERSBURG, MD 20899

7. CONTRACT/GRANT NUMBER

8. TYPE OF REPORT AND PERIOD COVERED
Final

9. SPONSORING ORGANIZATION NAME AND COMPLETE ADDRESS (STREET, CITY, STATE, ZIP)

Same as #6 above

10. SUPPLEMENTARY NOTES

11. ABSTRACT (A 200-WORD OR LESS FACTUAL SUMMARY OF MOST SIGNIFICANT INFORMATION. IF DOCUMENT INCLUDES A SIGNIFICANT BIBLIOGRAPHY OR LITERATURE SURVEY, MENTION IT HERE.)

This publication is the proceedings of the 24th Joint Meeting of the U.S.-Japan Panel on Wind and Seismic Effects. The meeting was held at the National Institute of Standards and Technology, Gaithersburg, Maryland, during May 19–22, 1992. The proceedings include the program, list of members, panel resolutions, task committee reports, and 45 technical papers.

The papers were presented under five themes: (I)—Wind Engineering, (II)—Storm Surge and Tsunamis, (III)—Joint Cooperative Research Program, (IV)—Earthquake Engineering, (V)—Summaries of Task Committee Workshop Reports (oral presentations only).

12. KEY WORDS (6 TO 12 ENTRIES; ALPHABETICAL ORDER; CAPITALIZE ONLY PROPER NAMES; AND SEPARATE KEY WORDS BY SEMICOLONS)

accelerograph; bridges; building technology; concrete; design criteria; disasters; disaster reduction; earthquakes; geotechnical engineering; ground failures; lifelines; liquefaction; masonry; repair and retrofit; risk assessment; seismic; soils; standards; storm surge; structural engineering; tsunamis; and wind loads

13. AVAILABILITY

X	UNLIMITED
	FOR OFFICIAL DISTRIBUTION. DO NOT RELEASE TO NATIONAL TECHNICAL INFORMATION SERVICE (NTIS).
X	ORDER FROM SUPERINTENDENT OF DOCUMENTS, U.S. GOVERNMENT PRINTING OFFICE, WASHINGTON, DC 20402.
X	ORDER FROM NATIONAL TECHNICAL INFORMATION SERVICE (NTIS), SPRINGFIELD, VA 22161.

14. NUMBER OF PRINTED PAGES
594

15. PRICE

ELECTRONIC FORM

* U.S. G.P.O.:1992-311-891:60535

NIST Technical Publications

Periodical

Journal of Research of the National Institute of Standards and Technology—Reports NIST research and development in those disciplines of the physical and engineering sciences in which the Institute is active. These include physics, chemistry, engineering, mathematics, and computer sciences. Papers cover a broad range of subjects, with major emphasis on measurement methodology and the basic technology underlying standardization. Also included from time to time are survey articles on topics closely related to the Institute's technical and scientific programs. Issued six times a year.

Nonperiodicals

Monographs—Major contributions to the technical literature on various subjects related to the Institute's scientific and technical activities.

Handbooks—Recommended codes of engineering and industrial practice (including safety codes) developed in cooperation with interested industries, professional organizations, and regulatory bodies.

Special Publications—Include proceedings of conferences sponsored by NIST, NIST annual reports, and other special publications appropriate to this grouping such as wall charts, pocket cards, and bibliographies.

Applied Mathematics Series—Mathematical tables, manuals, and studies of special interest to physicists, engineers, chemists, biologists, mathematicians, computer programmers, and others engaged in scientific and technical work.

National Standard Reference Data Series—Provides quantitative data on the physical and chemical properties of materials, compiled from the world's literature and critically evaluated. Developed under a worldwide program coordinated by NIST under the authority of the National Standard Data Act (Public Law 90-396). NOTE: The Journal of Physical and Chemical Reference Data (JPCRD) is published bi-monthly for NIST by the American Chemical Society (ACS) and the American Institute of Physics (AIP). Subscriptions, reprints, and supplements are available from ACS, 1155 Sixteenth St., NW., Washington, DC 20056.

Building Science Series—Disseminates technical information developed at the Institute on building materials, components, systems, and whole structures. The series presents research results, test methods, and performance criteria related to the structural and environmental functions and the durability and safety characteristics of building elements and systems.

Technical Notes—Studies or reports which are complete in themselves but restrictive in their treatment of a subject. Analogous to monographs but not so comprehensive in scope or definitive in treatment of the subject area. Often serve as a vehicle for final reports of work performed at NIST under the sponsorship of other government agencies.

Voluntary Product Standards—Developed under procedures published by the Department of Commerce in Part 10, Title 15, of the Code of Federal Regulations. The standards establish nationally recognized requirements for products, and provide all concerned interests with a basis for common understanding of the characteristics of the products. NIST administers this program as a supplement to the activities of the private sector standardizing organizations.

Consumer Information Series—Practical information, based on NIST research and experience, covering areas of interest to the consumer. Easily understandable language and illustrations provide useful background knowledge for shopping in today's technological marketplace.

Order the **above** *NIST publications from: Superintendent of Documents, Government Printing Office, Washington, DC 20402.*

Order the **following** *NIST publications—FIPS and NISTIRs—from the National Technical Information Service, Springfield, VA 22161.*

Federal Information Processing Standards Publications (FIPS PUB)—Publications in this series collectively constitute the Federal Information Processing Standards Register. The Register serves as the official source of information in the Federal Government regarding standards issued by NIST pursuant to the Federal Property and Administrative Services Act of 1949 as amended, Public Law 89-306 (79 Stat. 1127), and as implemented by Executive Order 11717 (38 FR 12315, dated May 11, 1973) and Part 6 of Title 15 CFR (Code of Federal Regulations).

NIST Interagency Reports (NISTIR)—A special series of interim or final reports on work performed by NIST for outside sponsors (both government and non-government). In general, initial distribution is handled by the sponsor; public distribution is by the National Technical Information Service, Springfield, VA 22161, in paper copy or microfiche form.

U.S. Department of Commerce
National Institute of Standards and Technology
Gaithersburg, MD 20899

Official Business
Penalty for Private Use $300